

United States  
Environmental  
Protection Agency

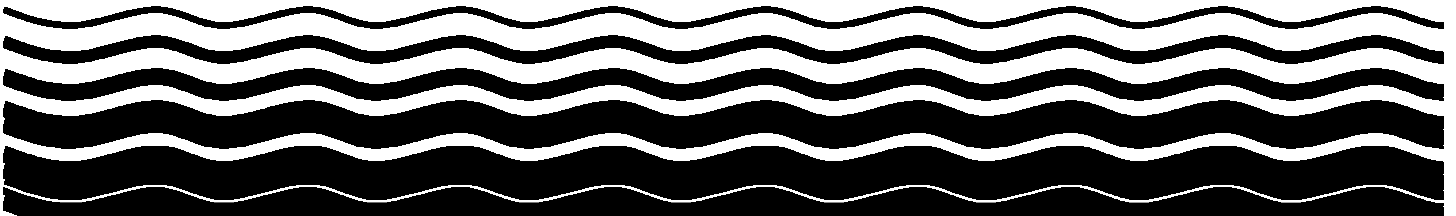
Office of Water  
(4601)

EPA 815-C-99-002  
September 1999

---



# **ANALYSIS OF GAC EFFLUENT BLENDING DURING THE ICR TREATMENT STUDIES**



This page intentionally left blank.

---

## Foreword

Between 1997 and 1999, 98 public water systems conducted treatment studies to evaluate disinfection byproduct (DBP) precursor removal performance of granular activated carbon (GAC) and membranes. The treatment study requirement was a part of the Information Collection Rule (ICR) for Public Water Systems, Subpart M of the National Primary Drinking Water Regulations, § 141.141(e).

Sixty-two public water systems evaluated GAC. The ICR required that DBP precursor removal be evaluated in the effluent of a single contactor as a function of run time, to assess the breakthrough of DBP precursors as the GAC was exhausted. In practice, full-scale plants can reduce carbon usage rates by blending the effluents of multiple parallel contactors prior to disinfection. When the treatment objective is reached in the blended effluent, the contactor with the "oldest" GAC is taken off-line and replaced by a contactor with fresh GAC, and this replacement occurs at regular intervals. GAC effluent blending extends the service life of each contactor because water from contactors that exceed the treatment objective is blended with water from contactors with fresher GAC that have effluent concentrations below the treatment objective. The treatment objective must only be maintained in the blended contactor effluent.

A primary goal during analysis of the treatment study results by the USEPA will be to estimate blended contactor run times to meet target regulatory treatment objectives. This information can be used to estimate GAC treatment costs that reflect full-scale effluent blending. This study provides the background and foundation for the analytical tools used to analyze treatment study data, assessing the applicability and limitations of these tools.

One objective of this study was to evaluate mathematical models for representing single contactor breakthrough data. From a data management perspective, model parameters will be easier to manage than the entire experimental data sets comprising 8,000 to 9,000 breakthrough curves generated by the 62 GAC treatment studies. A best-fit curve also facilitates interpolation and extrapolation of the experimental data. Furthermore, a function that describes the single contactor experimental data set is a prerequisite for calculating the integral breakthrough curve, a tool for predicting blended contactor run times.

A second objective of this study was to evaluate and compare two approaches for predicting the integral breakthrough curve. The first approach, based on application of the average value function to the single contactor breakthrough curve, has been presented by previous researchers. The second approach evaluated was a new computationally-simpler method developed by the treatment study technical work group (TS-TWG).

These two objectives were applied to experimental results from bench-scale GAC runs on eight water sources. Analytes evaluated included DBP surrogates, DBP class sums, and DBP species, yielding an extensive experimental matrix for a thorough evaluation of model results. In addition, GAC effluent blending was assessed experimentally to test model predictions of the integral breakthrough curve.

---

## **Disclaimer**

Mention of trade names or commercial products does not constitute endorsement or recommendation for use.

ANALYSIS OF GAC EFFLUENT BLENDING DURING THE ICR  
TREATMENT STUDIES

Prepared for:

UNITED STATES ENVIRONMENTAL PROTECTION AGENCY  
OFFICE OF GROUND WATER AND DRINKING WATER  
STANDARDS AND RISK MANAGEMENT DIVISION  
Technical Support Center  
26 W. Martin Luther King Drive  
Cincinnati, Ohio 45268

Prepared by:

INTERNATIONAL CONSULTANTS, INC.  
4134 Linden Avenue, Suite 200  
Dayton, Ohio 45432

SUMMERS & HOOPER, INC.  
6 Knollcrest Drive  
Cincinnati, Ohio 45237

*Under ICI Contract 68-C-98-051, Task Order 4*

This page intentionally left blank.

---

## Acknowledgments

This document was prepared by the United States Environmental Protection Agency, Office of Ground Water and Drinking Water, Standards and Risk Management Division, Technical Support Center. The Task Order Project Officer was Steven Allgeier. The Contract Project Officer was Phyllis Branson.

Technical consultants played a significant role in the research performed and the preparation of this document. This task was conducted jointly by International Consultants, Inc. (ICI) and Summers & Hooper, Inc. (S&H), under ICI Contract 68-C-98-051, Task Order 4. Timothy Soward and Christopher Hill acted as Project Managers for ICI. The S&H project team was led by Stuart Hooper, who acted as the Technical Project Leader. Mr. Hooper was responsible for technical direction and led the data analysis effort. Vanessa Hatcher (S&H) led and conducted the associated experimental work, and was assisted by Kristina Trenkamp and Carrie Wyrick. Jeff Welge and Rick Song of ICI performed mathematical modeling and statistical analyses, and provided statistical guidance when necessary. Technical review of the final report was provided by James Westrick (USEPA-TSC), Thomas Speth (USEPA-RREL), and R. Scott Summers (University of Colorado-Boulder).

The experimental portion of this project was performed in conjunction with treatment studies required under the Information Collection Rule. The following public water systems were involved: Charleston Commissioners of Public Works, City of Aurora, City of Escondido, City of Greensboro, City of Topeka, Iowa-American Water Company, Miami-Dade Water and Sewer Department, and Sweetwater Authority. This work could not have been completed without the use of the data generated as part of the treatment studies funded by these public water systems.

This page intentionally left blank.

---

## Executive Summary

When granular activated carbon (GAC) contactors are utilized for disinfection byproduct (DBP) precursor control, multiple contactors can be used more efficiently when operated in parallel with staggered GAC replacement cycles, with the effluents of all contactors blended prior to disinfection. By doing so, individual contactors can be operated past a point at which the effluent exceeds a given treatment objective, because the treatment objective must only be maintained in the blended effluent of all contactors.

The design of this study incorporated two main goals. The primary objectives were to evaluate the ability of the logistic function to model single contactor breakthrough curve data and to evaluate the success and limitations of predictive models used to determine the integral breakthrough curve, a relationship between single contactor run time and blended contactor water quality. The secondary objective of this study was to evaluate the applicability of these models and predictive methods in the context of the Information Collection Rule (ICR) GAC treatment study data analysis.

Full-, pilot-, and bench-scale GAC treatment studies were performed by 62 utilities in fulfillment of ICR requirements. Regardless of scale, the ICR required that the effluent of single GAC contactors be analyzed for DBP surrogate and formed DBP breakthrough as a function of run time, to assess the breakthrough of DBP precursors as the GAC was exhausted. Bench-scale GAC studies typically examined two empty-bed contact times (EBCTs) of 10 and 20 minutes during each of four quarterly studies to account for seasonal variability in source water quality. Pilot-scale GAC studies were typically composed of one to two sessions including 10 and 20 minute EBCT contactors. Thus, a large amount of data was generated and will be analyzed: the 62 GAC treatment studies performed will yield a total of 8,000 to 9,000 individual breakthrough curves.

The logistic function has previously been used to model GAC breakthrough curves and is a suitable model due to the characteristic 'S' shape of most breakthrough curves. Three modifications to the logistic function were developed to improve its performance for modeling single contactor data. Curve fitting involved determining which model was applicable based on characteristics of the breakthrough curve, and applying the appropriate model to the breakthrough curve for each parameter. These enhanced forms of the logistic function model were able to successfully fit single contactor breakthrough curve data for all parameters, including DBP surrogates, DBP sum class parameters, and individual trihalomethane (THM) and haloacetic acid (HAA) species. A method was also employed to detect outlier data points and to limit the influence of these deviant observations on the parameter estimates.

Two predictive approaches were compared for developing determining the integral breakthrough curve, a relationship between operation time of each individual contactor and water quality in the blended contactor effluent: the direct integration (DI) method and the surrogate correlation approach (SCA). The DI method is a time-normalized integration of the logistic function calculated using the average value function that yields the integral breakthrough curve. The SCA method first utilizes the DI method to establish an integral breakthrough curve for total organic carbon (TOC). Then data points on both the single contactor and integral breakthrough curves at a given TOC concentration are mapped, and all other water quality parameters

associated with the single contactor effluent data set at that TOC concentration are applied to the blended effluent curve. The SCA method is especially applicable to the ICR data analysis requirements because it minimizes the computations necessary to estimate blended contactor run times to treatment objectives. An assessment of the concentration of other DBPs at any given treatment objective will be performed as part of the data analysis effort, and the SCA procedure is also suited to this task. The SCA procedure requires that GAC breakthrough curves for all measured parameters be represented by the logistic function model curve fit. By doing so, a smaller amount of data are needed to represent the entire breakthrough curve experimental data set. This procedure inherently relies on the assumption that the relationship between TOC concentration and the other water quality parameters established in the single contactor effluent is maintained in the blended contactor effluent. This study verified this assumption and found that it was valid between TOC and other DBP surrogates, DBP class summation parameters, and individual DBP species. In addition, the correlation between TOC and bromine incorporation factors for THMs and HAAs was shown to be consistent between the single contactor effluent and experimental blended effluent.

The results of the DI and SCA model predictions were compared to experimental data for eight GAC runs performed on eight water sources, with varying pretreatments, influent TOC concentrations, bromide concentrations, and simulated distribution system (SDS) chlorination conditions to evaluate DBP formation. An analysis of the model results across all waters and analytes showed that the prediction error for the two models was equivalent. Both models were biased negative, indicating a tendency to underpredict the experimental data. The SCA model had a slightly higher negative bias than did the DI model. Since the SCA method simplifies and reduces the amount of computations necessary to estimate the integral breakthrough curve, its use is recommended to estimate blended contactor water quality during the ICR treatment study data analysis.

An analysis of model results for individual parameters showed that the SCA method was more successful in predicting the integral breakthrough curve of brominated DBP species, while the DI method was a better predictor of non-brominated DBP species breakthrough. Prediction of the breakthrough of individual DBP species in the blended effluent is important since individual DBPs of potential health concern will be considered during analysis of the ICR treatment study data. For sum parameters such as total THM (TTHM) and the sum of five HAAs (HAA5), the SCA method yielded results that were comparable to or superior to the DI method predictions.

Both predictive methods rely on the assumption that an infinite number of contactors are on-line and operated in parallel-staggered mode. This study examined this assumption and found that the error incurred when applying run time estimates based on the infinite contactor assumption to run times for finite numbers of contactors is impacted by the number of contactors and the magnitude of the treatment objective examined in relation to the asymptotic concentration approached by the single contactor breakthrough curve. Based on the logistic function model of the GAC effluent breakthrough profile, the infinite contactor assumption will yield estimated run times within 10 percent of actual run times for 13 or more contactors operated in parallel-staggered mode. For 10 contactors on-line, the infinite contactor assumption will yield run time estimates within 12 percent of the actual run times. In all cases, run time estimates based on the infinite contactor assumption are longer than those for a finite number of contactors, thus providing a best case scenario for GAC performance. The applicability of the infinite contactor assumption in this model to finite numbers of contactors is especially important for small plants.

Extrapolation of the integral breakthrough curve was also examined during this study. During the ICR treatment study data analysis, extrapolation of some TOC integral breakthrough curves may be necessary to estimate GAC run times when target regulatory values for DBPs or their surrogates are exceeded upon application of the SCA method. Extrapolation of runs performed on two waters were compared to the same runs without extrapolation, yielding a 3 percent error in the predicted blended effluent TOC concentration for a 21 percent run time extrapolation and an 8 percent error in the predicted blended effluent TOC concentration for a 61 percent extrapolation. The impact of extrapolation on the SCA procedure estimates of the integral breakthrough curves for other DBP surrogates and formed DBPs was small: the mean error at the end of the extrapolated integral breakthrough curve was 5 percent for a 21 percent extrapolation and 9 percent for a 61 percent extrapolation. Therefore, based on the waters examined in this study, data sets that do not exceed a given treatment objective may be extrapolated, and the error in predicted blended contactor water quality incurred by extrapolation up to 50 percent of the original run time should average less than 10 percent.

This page intentionally left blank.

---

## Table of Contents

List of Tables .....	xvii
List of Figures.....	xix
List of Abbreviations.....	xxv
1 Background and Method Development.....	1
1.1 Optimization of GAC Operation.....	2
1.2 Modeling the Operation of Multiple Contactors Operated in Parallel-Staggered Mode ....	2
1.3 Single Contactor Breakthrough Curve Models .....	6
1.4 Direct Integration Approach.....	8
1.5 Surrogate Correlation Approach .....	9
1.6 Impact of Bromide Concentration on GAC Effluent Blending Models.....	11
1.7 Effluent Blending Modeling of Fewer than 10 Contactors .....	12
1.8 GAC Breakthrough Curve Extrapolation.....	12
1.9 ICR GAC Treatment Study Data Analysis Context.....	13
1.10 Appropriateness of Model Assumptions to Full-Scale GAC Effluent Blending .....	14
2 Study Objectives and Approach.....	15
3 Materials and Methods .....	17
3.1 Experimental Approach.....	17
3.1.1 Rapid Small-Scale Column Test .....	17
3.1.1.1 GAC Preparation Procedures .....	17
3.1.1.2 RSSCT Column Setup.....	19
3.1.1.3 Batch Influent Preparation .....	20
3.1.1.4 RSSCT Monitoring .....	20
3.1.2 Bench-Scale Blended Water Quality Assessment Approach.....	20
3.1.3 DBP Formation Assessment.....	21
3.1.4 Assessment of the Impact of Sampling on the Integral Breakthrough Curve.....	22
3.2 Data Analysis and Modeling Approach .....	23
3.2.1 Logistic Function Models.....	23

3.2.2	Outlier Methods.....	25
3.2.3	Direct Integration Approach.....	26
3.2.4	Surrogate Correlation Approach .....	27
3.2.5	Comparison of Methods for Predicting the Performance of GAC Contactors Operated in Parallel-Staggered Mode .....	28
3.2.6	Comparison of Single Contactor and Blended Effluent DBP Bromine Incorporation . .....	28
3.2.7	Breakthrough Curve Extrapolation .....	29
3.3	Waters Examined .....	29
3.3.1	Pretreatment and Water Quality .....	29
3.3.2	Simulated Distribution System Chlorination Conditions.....	31
3.4	Analytical Methods .....	31
3.5	Experimental QA/QC Summary .....	32
4	Results and Discussion.....	35
4.1	Overview .....	35
4.2	Correlation between Surrogates and DBPs in Single Contactor and Blended Contactor Effluents .....	37
4.2.1	Correlation between Surrogate Concentration and DBP Formation.....	37
4.2.2	Correlation between Surrogates and DBP Speciation.....	38
4.3	Assessment of Logistic Function Fit to Single Contactor Breakthrough Curve Data .....	67
4.3.1	Surrogates and Class Sum Logistic Function Curve Fits.....	67
4.3.2	DBP Species Logistic Function Curve Fits.....	68
4.4	Comparison of SCA and DI Methods Used to Predict the Blended Contactor Integral Breakthrough Curve .....	89
4.4.1	Surrogates and Class Sums .....	95
4.4.2	DBP Species.....	96
4.5	Analysis of Model Applicability to Finite Number of Contactors.....	113
4.6	Impact of Extrapolation on Integral Breakthrough Curve Prediction.....	121
5	Summary and Conclusions.....	131
6	References .....	135

Appendix A: Breakthrough Curves Corrected for Impact of Sampling.....	137
Appendix B: SAS Code .....	143
Appendix C: Full- and Bench-Scale Pretreatment Schematics.....	147
Appendix D: Single Contactor and Blended Effluent DBP Surrogate and Formed DBP Correlations .....	157
Appendix E: Logistic Function Model Curve Fits .....	223
Appendix F: Comparison of SCA Method to DI Approach for Integral Breakthrough Curve Prediction .....	305
Appendix G: Logistic Function Model Best-Fit Parameters.....	387
Appendix H: Impact of Extrapolation on SCA Prediction of the Integral Breakthrough Curve	393
Appendix I: Impact of Extrapolation on DI Prediction of the Integral Breakthrough Curve ....	415

This page intentionally left blank.

---

## List of Tables

1	Summary of RSSCT design parameters for all runs .....	18
2	Relationship between blended effluent sample number and RSSCT effluent sample number.....	21
3	Summary of pretreatment and water quality .....	30
4	SDS chlorination conditions .....	31
5	Summary of analytical methods and MRLs .....	32
6	Summary of laboratories conducting analyses.....	32
7	Summary of field duplicate precision for single contactor and blended effluent data.....	34
8	Frequency of logistic function model used and $R^2$ values for all parameters and all waters.....	69
9	Summary of DI and SCA integral breakthrough curve prediction RSS values for Waters 1 through 4 .....	90
10	Summary of DI and SCA integral breakthrough curve prediction RSS values for Waters 5 through 8 .....	91
11	Summary of model prediction bias for Waters 1 through 4.....	92
12	Summary of model prediction bias for Waters 5 through 8.....	92
13	Summary of mean RSS, mean bias, normalized mean RSS, and normalized mean bias for all waters .....	93
14	Summary of run times to a 0.35 treatment objective .....	115
15	Summary of run times to a 0.50 treatment objective .....	115
16	Summary of run times to a 0.65 treatment objective .....	116
17	Summary of run times to a 0.80 treatment objective .....	116

This page intentionally left blank.

---

## List of Figures

1	Schematic of blending of multiple GAC contactors operated parallel-staggered mode .....	3
2	Effluent water quality during quasi steady-state operation of multiple contactors in parallel-staggered mode.....	3
3	Operation of multiple contactors in parallel-staggered mode to various single contactor run times: derivation of the blended effluent integral breakthrough curve .....	5
4	Graphical summary of SCA procedure used for base analysis of GAC treatment studies .....	10
5	Logistic function model curves.....	24
6	Correlations based on GAC effluent TOC concentration for single contactor and blended effluents for Water 1 .....	40
7	Correlations based on GAC effluent TOC concentration for single contactor and blended effluents for Water 2 .....	41
8	Correlations based on GAC effluent TOC concentration for single contactor and blended effluents for Water 8 .....	42
9	THM correlations based on GAC effluent TOC concentration for single contactor and blended effluents for Water 2.....	43
10	THM correlations based on GAC effluent TOC concentration for single contactor and blended effluents for Water 3.....	44
11	THM correlations based on GAC effluent TOC concentration for single contactor and blended effluents for Water 8.....	45
12	HAA correlations based on GAC effluent TOC concentration for single contactor and blended effluents for Water 5.....	46
13	HAA correlations based on GAC effluent TOC concentration for single contactor and blended effluents for Water 7.....	47
14	HAA correlations based on GAC effluent TOC concentration for single contactor and blended effluents for Water 2.....	48
15	HAA correlations based on GAC effluent TOC concentration for single contactor and blended effluents for Water 4.....	49
16	HAA correlations based on GAC effluent TOC concentration for single contactor and blended effluents for Water 7.....	50
17	Correlation between single contactor and blended effluent TOC concentration and THM bromine incorporation factor (n) for Water 1.....	51
18	Correlation between single contactor and blended effluent TOC concentration and THM bromine incorporation factor (n) for Water 2.....	51
19	Correlation between single contactor and blended effluent TOC concentration and THM bromine incorporation factor (n) for Water 3.....	52
20	Correlation between single contactor and blended effluent TOC concentration and THM bromine incorporation factor (n) for Water 4.....	52
21	Correlation between single contactor and blended effluent TOC concentration and THM bromine incorporation factor (n) for Water 5.....	53
22	Correlation between single contactor and blended effluent TOC concentration and THM bromine incorporation factor (n) for Water 6.....	53
23	Correlation between single contactor and blended effluent TOC concentration and THM bromine incorporation factor (n) for Water 7.....	54
24	Correlation between single contactor and blended effluent TOC concentration and THM bromine incorporation factor (n) for Water 8.....	54

25	Correlation between single contactor and blended effluent TOC concentration and HAA bromine incorporation factor (n') for Water 1 .....	55
26	Correlation between single contactor and blended effluent TOC concentration and HAA bromine incorporation factor (n') for Water 2 .....	55
27	Correlation between single contactor and blended effluent TOC concentration and HAA bromine incorporation factor (n') for Water 3 .....	56
28	Correlation between single contactor and blended effluent TOC concentration and HAA bromine incorporation factor (n') for Water 4 .....	56
29	Correlation between single contactor and blended effluent TOC concentration and HAA bromine incorporation factor (n') for Water 5 .....	57
30	Correlation between single contactor and blended effluent TOC concentration and HAA bromine incorporation factor (n') for Water 6 .....	57
31	Correlation between single contactor and blended effluent TOC concentration and HAA bromine incorporation factor (n') for Water 7 .....	58
32	Correlation between single contactor and blended effluent TOC concentration and HAA bromine incorporation factor (n') for Water 8 .....	58
33	Correlation between single contactor and blended effluent UV absorbance and THM bromine incorporation factor (n) for Water 1.....	59
34	Correlation between single contactor and blended effluent UV absorbance and THM bromine incorporation factor (n) for Water 2.....	59
35	Correlation between single contactor and blended effluent UV absorbance and THM bromine incorporation factor (n) for Water 3.....	60
36	Correlation between single contactor and blended effluent UV absorbance and THM bromine incorporation factor (n) for Water 4.....	60
37	Correlation between single contactor and blended effluent UV absorbance and THM bromine incorporation factor (n) for Water 5.....	61
38	Correlation between single contactor and blended effluent UV absorbance and THM bromine incorporation factor (n) for Water 6.....	61
39	Correlation between single contactor and blended effluent UV absorbance and THM bromine incorporation factor (n) for Water 7.....	62
40	Correlation between single contactor and blended effluent UV absorbance and THM bromine incorporation factor (n) for Water 8.....	62
41	Correlation between single contactor and blended effluent UV absorbance and HAA bromine incorporation factor (n') for Water 1 .....	63
42	Correlation between single contactor and blended effluent UV absorbance and HAA bromine incorporation factor (n') for Water 2 .....	63
43	Correlation between single contactor and blended effluent UV absorbance and HAA bromine incorporation factor (n') for Water 3 .....	64
44	Correlation between single contactor and blended effluent UV absorbance and HAA bromine incorporation factor (n') for Water 4 .....	64
45	Correlation between single contactor and blended effluent UV absorbance and HAA bromine incorporation factor (n') for Water 5 .....	65
46	Correlation between single contactor and blended effluent UV absorbance and HAA bromine incorporation factor (n') for Water 6 .....	65
47	Correlation between single contactor and blended effluent UV absorbance and HAA bromine incorporation factor (n') for Water 7 .....	66

48	Correlation between single contactor and blended effluent UV absorbance and HAA bromine incorporation factor (n') for Water 8 .....	66
49	Single contactor and blended effluent TOC breakthrough curves for Water 1 .....	71
50	Single contactor and blended effluent TOC breakthrough curves for Water 2.....	71
51	Single contactor and blended effluent TOC breakthrough curves for Water 3.....	72
52	Single contactor and blended effluent TOC breakthrough curves for Water 4.....	72
53	Single contactor and blended effluent TOC breakthrough curves for Water 5.....	73
54	Single contactor and blended effluent TOC breakthrough curves for Water 6.....	73
55	Single contactor and blended effluent TOC breakthrough curves for Water 7.....	74
56	Single contactor and blended effluent TOC breakthrough curves for Water 8.....	74
57	Single contactor and blended effluent UV254 breakthrough curves for Water 5.....	75
58	Single contactor and blended effluent UV254 breakthrough curves for Water 7.....	75
59	Single contactor and blended effluent SDS-TOX breakthrough curves for Water 4.....	76
60	Single contactor and blended effluent SDS-TOX breakthrough curves for Water 8.....	76
61	Single contactor and blended effluent SDS-TTHM breakthrough curves for Water 3.....	77
62	Single contactor and blended effluent SDS-TTHM breakthrough curves for Water 6.....	77
63	Single contactor and blended effluent SDS-HAA9 breakthrough curves for Water 1 .....	78
64	Single contactor and blended effluent SDS-HAA9 breakthrough curves for Water 2 .....	78
65	Single contactor and blended effluent SDS-CF breakthrough curves for Water 4 .....	79
66	Single contactor and blended effluent SDS-BDCM breakthrough curves for Water 6 .....	79
67	Single contactor and blended effluent SDS-BDCM breakthrough curves for Water 7 .....	80
68	Single contactor and blended effluent SDS-BDCM breakthrough curves for Water 4 .....	80
69	Single contactor and blended effluent SDS-BDCM breakthrough curves for Water 8 .....	81
70	Single contactor and blended effluent SDS-BF breakthrough curves for Water 1 .....	81
71	Single contactor and blended effluent SDS-BF breakthrough curves for Water 6.....	82
72	Single contactor and blended effluent SDS-DCAA breakthrough curves for Water 3.....	82
73	Single contactor and blended effluent SDS-TCAA breakthrough curves for Water 5 .....	83
74	Single contactor and blended effluent SDS-DBAA breakthrough curves for Water 6.....	83
75	Single contactor and blended effluent SDS-BCAA breakthrough curves for Water 1 .....	84
76	Single contactor and blended effluent SDS-DCBAA breakthrough curves for Water 2 .....	84
77	Single contactor and blended effluent SDS-CDBAA breakthrough curves for Water 6.....	85
78	Single contactor and blended effluent SDS-TBAA breakthrough curves for Water 7 .....	85
79	Single contactor and blended effluent SDS-BF breakthrough curves for Water 2 .....	86
80	Single contactor and blended effluent SDS-CDBAA breakthrough curves for Water 5 .....	86
81	Single contactor and blended effluent SDS-BF breakthrough curves for Water 3 (original step-lag logistic function model curve fit) .....	87
82	Single contactor and blended effluent SDS-BF breakthrough curves for Water 3 (fit to step-lag-peak logistic function model).....	87
83	Cumulative frequency distribution plot of normalized residual sum-of-squares (RSS) for DI and SCA model predictions.....	100
84	Cumulative frequency distribution plot of normalized bias for DI and SCA model predictions .....	100
85	Comparison of DI and SCA methods for predicting the UV254 integral breakthrough curve for Water 1 .....	101
86	Comparison of DI and SCA methods for predicting the UV254 integral breakthrough curve for Water 3 .....	101

87	Comparison of DI and SCA methods for predicting the SDS-TTHM integral breakthrough curve for Water 1.....	102
88	Comparison of DI and SCA methods for predicting the SDS-TTHM integral breakthrough curve for Water 7.....	102
89	Comparison of DI and SCA methods for predicting the SDS-HAA5 integral breakthrough curve for Water 2.....	103
90	Comparison of DI and SCA methods for predicting the SDS-HAA5 integral breakthrough curve for Water 7.....	103
91	Comparison of DI and SCA methods for predicting the SDS-HAA6 integral breakthrough curve for Water 3.....	104
92	Comparison of DI and SCA methods for predicting the SDS-HAA6 integral breakthrough curve for Water 5.....	104
93	Comparison of DI and SCA methods for predicting the SDS-HAA9 integral breakthrough curve for Water 5.....	105
94	Comparison of DI and SCA methods for predicting the SDS-HAA9 integral breakthrough curve for Water 6.....	105
95	Comparison of DI and SCA methods for predicting the SDS-TOX integral breakthrough curve for Water 6.....	106
96	Comparison of DI and SCA methods for predicting the SDS-TOX integral breakthrough curve for Water 7.....	106
97	Comparison of DI and SCA methods for predicting the SDS-CF integral breakthrough curve for Water 2.....	107
98	Comparison of DI and SCA methods for predicting the SDS-CF integral breakthrough curve for Water 6.....	107
99	Comparison of DI and SCA methods for predicting the SDS-BDCM integral breakthrough curve for Water 1.....	108
100	Comparison of DI and SCA methods for predicting the SDS-BDCM integral breakthrough curve for Water 8.....	108
101	Comparison of DI and SCA methods for predicting the SDS-DBCM integral breakthrough curve for Water 3.....	109
102	Comparison of DI and SCA methods for predicting the SDS-DBCM integral breakthrough curve for Water 7.....	109
103	Comparison of DI and SCA methods for predicting the SDS-BF integral breakthrough curve for Water 1.....	110
104	Comparison of DI and SCA methods for predicting the SDS-BF integral breakthrough curve for Water 5.....	110
105	Comparison of DI and SCA methods for predicting the SDS-DCAA integral breakthrough curve for Water 1.....	111
106	Comparison of DI and SCA methods for predicting the SDS-DCAA integral breakthrough curve for Water 4.....	111
107	Comparison of DI and SCA methods for predicting the SDS-DBAA integral breakthrough curve for Water 2.....	112
108	Comparison of DI and SCA methods for predicting the SDS-BCAA integral breakthrough curve for Water 8.....	112
109	Integral breakthrough curves for varying numbers of contactors operated in parallel-staggered mode (B=30; D=0.1).....	117

110	Integral breakthrough curves for varying numbers of contactors operated in parallel-staggered mode (B=30; D=0.05).....	117
111	Integral breakthrough curves for varying numbers of contactors operated in parallel-staggered mode (B=10; D=0.1).....	118
112	Integral breakthrough curves for varying numbers of contactors operated in parallel-staggered mode (B=10; D=0.05).....	118
113	Integral breakthrough curves for varying numbers of contactors operated in parallel-staggered mode (B=10; D=0.2).....	119
114	Integral breakthrough curves for varying numbers of contactors operated in parallel-staggered mode (B=30; D=0.2).....	119
115	Run time as a function of number of contactors in parallel, expressed as percent of run time for infinite n (B=30; D=0.1).....	120
116	Run time as a function of number of contactors in parallel, expressed as percent of run time for infinite n (B=30; D=0.2).....	120
117	Impact of extrapolation on DI prediction of the TOC integral breakthrough for Water 5.....	124
118	Impact of extrapolation on DI prediction of the TOC integral breakthrough for Water 8.....	124
119	Impact of extrapolation on SCA prediction of the UV254 integral breakthrough for Water 5	125
120	Impact of extrapolation on SCA prediction of the SDS-TOX integral breakthrough for Water 5 .....	125
121	Impact of extrapolation on SCA prediction of the SDS-TTHM integral breakthrough for Water 5 .....	126
122	Impact of extrapolation on SCA prediction of the SDS-HAA5 integral breakthrough for Water 5 .....	126
123	Impact of extrapolation on SCA prediction of the SDS-HAA6 integral breakthrough for Water 5 .....	127
124	Impact of extrapolation on SCA prediction of the SDS-HAA9 integral breakthrough for Water 5 .....	127
125	Impact of extrapolation on SCA prediction of the UV254 integral breakthrough for Water 8	128
126	Impact of extrapolation on SCA prediction of the SDS-TOX integral breakthrough for Water 8 .....	128
127	Impact of extrapolation on SCA prediction of the SDS-TTHM integral breakthrough for Water 8 .....	129
128	Impact of extrapolation on SCA prediction of the SDS-HAA5 integral breakthrough for Water 8 .....	129
129	Impact of extrapolation on SCA prediction of the SDS-HAA6 integral breakthrough for Water 8 .....	130
130	Impact of extrapolation on SCA prediction of the SDS-HAA9 integral breakthrough for Water 8 .....	130

This page intentionally left blank.

---

## List of Abbreviations

BCAA	Bromochloroacetic acid
BDCAA	Bromodichloroacetic acid
BDCM	Bromodichloromethane
BF	Bromoform
BMRL	Below the minimum reporting level
Br:TOC	Bromide to TOC ratio
$C(t)$	Effluent concentration
$\bar{C}(t)$	blended effluent concentration at individual contactor run time, $t$
$C(t_f)$	Last observed data point
$C(t_p)$	Measured peak concentration
$C_0$	Influent concentration
CDBAA	Chlorodibromoacetic acid
CF	Chloroform
$C_p$	Logistic function model best-fit concentration at $t_p$
DBAA	Dibromoacetic acid
DBCM	Dibromochloromethane
DBP	Disinfection byproduct
DCAA	Dichloroacetic acid
DCBAA	Dichlorobromoacetic acid
DI	Direct integration
EBCT	Empty bed contact time

EPA	United States Environmental Protection Agency
$\bar{f}$	Fraction of organic matter remaining in the combined effluent
$f_i$	$C(t)/C_0$
GAC	Granular activated carbon
HAA	Haloacetic acid
HAA5	Sum of five haloacetic acids: MCAA, DCAA, TCAA, MBAA, DBAA
HAA6	Sum of six haloacetic acids: HAA5, BCAA
HAA9	Sum of nine haloacetic acids: HAA6, DCBAA, CDBAA, TBAA
ICR	Information Collection Rule
K	Adsorption rate coefficient
MBAA	Monobromoacetic acid
MCAA	Monochloroacetic acid
MCL	Maximum contaminant level
MRL	Minimum reporting level
$n$	Freundlich isotherm parameter
$N$	Number of contactors
NA	Not applicable
$n_{Br}$	Bromine incorporation factor for THMs
$N_C$	Adsorption capacity coefficient
$n'_{Br}$	Bromine incorporation factor for HAAs
NOM	Natural organic matter
PAS	Polyaluminum sulfate

$q_i$	Throughput of the individual contactor when the treatment objective is exceeded in the single contactor
$q_N$	Throughput of the nth contactor at the time the treatment objective is exceeded in the blended effluent
$R^2$	Coefficient of determination
RSS	Residual sum of squares
RSSCT	Rapid small-scale column test
$RT_{BC}$	Blended contactor run time
$RT_{SC}$	Single contactor run time
SAS	Statistical Analysis Software
SCA	Surrogate correlation approach
SDS	Simulated distribution system
SDS-BCAA	Bromochloroacetic acid evaluated under SDS conditions
SDS-BDCAA	Bromodichloroacetic acid evaluated under SDS conditions
SDS-BDCM	Bromodichloromethane evaluated under SDS conditions
SDS-BF	Bromoform evaluated under SDS conditions
SDS-CDBAA	Chlorodibromoacetic acid evaluated under SDS conditions
SDS-CF	Chloroform evaluated under SDS conditions
SDS-DBAA	Dibromoacetic acid evaluated under SDS conditions
SDS-DBCM	Dibromochloromethane evaluated under SDS conditions
SDS-DBPs	Disinfection byproducts evaluated under SDS conditions
SDS-DCAA	Dichloroacetic acid evaluated under SDS conditions
SDS-HAA5	The sum of five haloacetic acids evaluated under SDS conditions

SDS-HAA6	The sum of six haloacetic acids evaluated under SDS conditions
SDS-HAA9	The sum of nine haloacetic acids evaluated under SDS conditions
SDS-MBAA	Monobromoacetic acid evaluated under SDS conditions
SDS-MCAA	Monochloroacetic acid evaluated under SDS conditions
SDS-TBAA	Tribromoacetic acid evaluated under SDS conditions
SDS-TCAA	Trichloroacetic acid evaluated under SDS conditions
SDS-TOX	Total organic halides evaluated under SDS conditions
SDS-TTHM	Total trihalomethanes evaluated under SDS conditions
SM	Standard Methods
$t$	Service time
$t_b$	Run time at which initial breakthrough above detectable levels occurs
TBAA	Tribromoacetic acid
TCAA	Trichloroacetic acid
THM	Trihalomethane
THMs	Trihalomethanes
TOC	Total organic carbon
TOX	Total organic halide
$t_p$	Run time at which the peak concentration occurs
TSUVA	Specific ultraviolet absorbance based on TOC
TTHM	Total trihalomethane
UV <sub>254</sub>	Ultraviolet absorbance at 254 nm
$v$	Linear velocity

$x$

Bed depth

This page intentionally left blank.

---

# 1 Background and Method Development

Sixty-two public water systems required by the Information Collection Rule (ICR) to perform treatment studies for disinfection byproduct (DBP) precursor removal fulfilled this requirement by evaluating granular activated carbon (GAC), while membranes were examined by 36 utilities. GAC treatment studies included bench-, pilot-, and full-scale studies. Regardless of the scale, the ICR required that GAC treatment studies evaluate DBP precursor removal in the effluent of a single contactor as a function of run time, to assess the breakthrough of DBP precursors as the GAC was exhausted. In practice, full-scale plants can optimize GAC performance and reduce carbon usage rates by blending the effluents of multiple contactors operated in parallel prior to disinfection. To optimize the blending process, replacement of the GAC in each contactor is staggered at regular intervals. By doing so, the service life of each contactor is extended because water from contactors that exceed the treatment objective is blended with water from contactors with fresher GAC that have effluent concentrations below the treatment objective. A cost analysis based on single contactor run times will overestimate the actual treatment costs of full-scale operation of multiple contactors operated in parallel-staggered mode.

Previous researchers have developed mathematical relationships to characterize the water quality in the blended effluent based on single contactor breakthrough curves. These relationships yield a blended contactor effluent or integral "breakthrough" curve that provides a measure of the extended run time for which each contactor can be operated to meet a treatment objective in the blended effluent. The integral breakthrough curve does not directly represent blended effluent water quality, but is a tool for determining the GAC replacement frequency for each individual contactor (of multiple contactors operated in parallel-staggered mode) to maintain the blended effluent below the treatment objective. For example, the results of a GAC study show that based on a single contactor breakthrough curve, GAC effluent formed DBP levels are maintained below the treatment objectives for 80 days of operation. This is the single contactor run time,  $RT_{SC}$ . Since full-scale implementation of GAC will involve multiple contactors operated in parallel-staggered mode, integral breakthrough curves for each parameter are developed based on the single contactor breakthrough curves. The integral breakthrough curves might show that the level of DBPs formed in the GAC blended effluent are maintained below the treatment objectives for 160 days of operation, indicating that each individual contactor can be operated for 160 days while maintaining the plant blended effluent water quality below the treatment objective. The blended contactor run time ( $RT_{BC}$ ) is 160 days.

The basic method utilized to determine the integral breakthrough curve has been a mathematical or numerical integration of the single contactor breakthrough curve. A minimal amount of experimental verification has been performed to verify this approach. Some bench-scale experimental verification data has been presented (Chowdhury et al., 1996; Summers et al., 1998), whereby mathematical integration was simulated experimentally by continuously collecting the effluent from a bench-scale GAC contactor in a large reservoir, and sampling from this reservoir over time. An extensive verification study is needed to thoroughly evaluate the appropriateness of the integration method for predicting the integral breakthrough curve.

## 1.1 Optimization of GAC Operation

The GAC in a contactor has to be replaced when the mass transfer zone begins to exit the column as shown in Figure 1, and the effluent concentration exceeds the treatment objective. However, at this point only part of the GAC bed is saturated and replacement of the GAC will result in high carbon use rates (Snoeyink, 1990). Two common methods of lowering carbon usage rates are to operate contactors in series or to operate multiple contactors in parallel with staggered GAC replacement cycles.

For adsorption of micropollutants, the amount of water treated per mass GAC can be increased by operation of two contactors in series. In this mode of operation, two contactors are operated in series until the treatment objective is exceeded in the second contactor. At this point, the GAC in the first contactor is replaced with virgin or reactivated GAC, and valves are switched so that the second contactor is now operated in-line ahead of the first contactor. This cycle is repeated to maintain effluent levels below the treatment objective. For efficient operation, the mass transfer zone should be contained within the bed length of one contactor. This can be achieved using reasonable bed lengths for adsorption of micropollutants, but the mass transfer zone for TOC removal (and therefore DBP precursor removal) is usually too long. For DBP precursor control, operation of two contactors in series does not result in significantly longer run times over single contactor operation (Sontheimer et al., 1988).

Multiple contactors operated in parallel and staggered in terms of GAC replacement times, as shown in Figure 1, yield blended effluent concentrations as shown in Figure 2. When the lead contactor, which has been in operation the longest, is taken off-line and replaced with a contactor with fresh GAC, the blended effluent concentration decreases as shown in Figure 2. The level of this decrease is dependent on the number of contactors in operation. For two contactors, the concentration will decrease by 50 percent, while for an infinite number of contactors the decrease approaches zero.

Due to the blending of waters from multiple contactors producing varying levels of effluent water quality, individual contactors can be operated past the point at which the effluent water they are producing exceeds the treatment objective, because the treatment objective must be maintained in the blended effluent. Therefore, evaluation of single contactor breakthrough curve data will result in overestimates of the carbon usage rate for a full-scale system operating multiple staggered contactors in parallel-staggered mode. For DBP precursor control, contactor effluents are blended prior to disinfection.

## 1.2 Modeling the Operation of Multiple Contactors Operated in Parallel-Staggered Mode

In modeling the operation of multiple contactors operated in parallel-staggered mode, the goal is not to simulate the actual blended effluent water quality during normal operation (as shown in Figure 2), but to derive the integral breakthrough curve. The integral breakthrough curve is a tool used to determine the GAC replacement frequency for each individual contactor to maintain the blended effluent below the treatment objective: it is a curve that relates single contactor run time to blended contactor effluent water quality. Multiple contactor throughput to a treatment objective can be estimated from the integral breakthrough curve by determining the operation

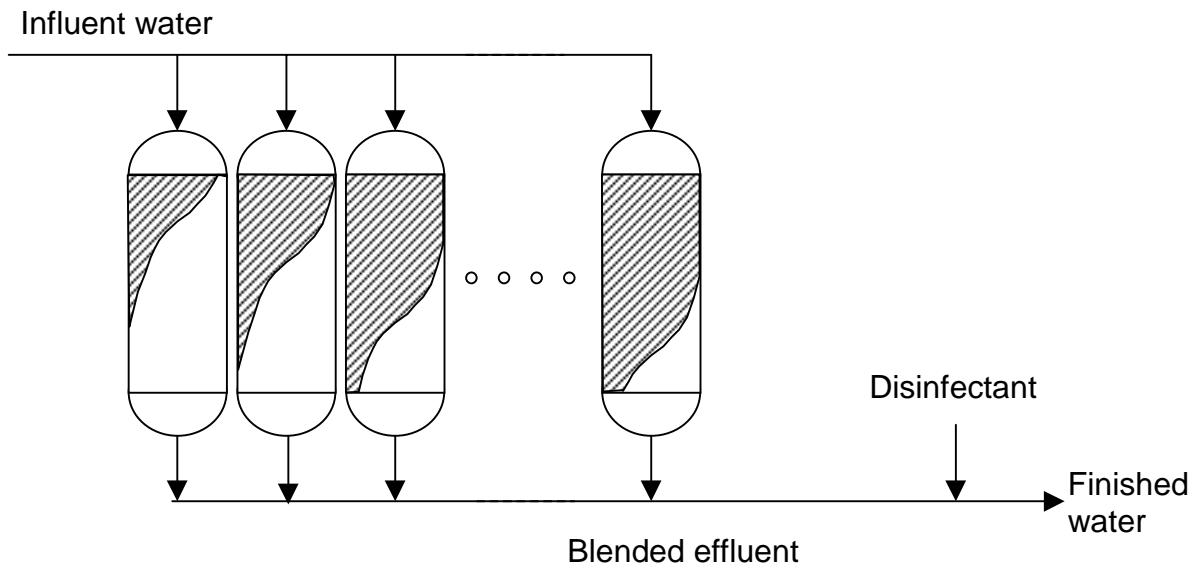


**Figure 1 Schematic of blending of multiple GAC contactors operated in parallel-staggered mode**

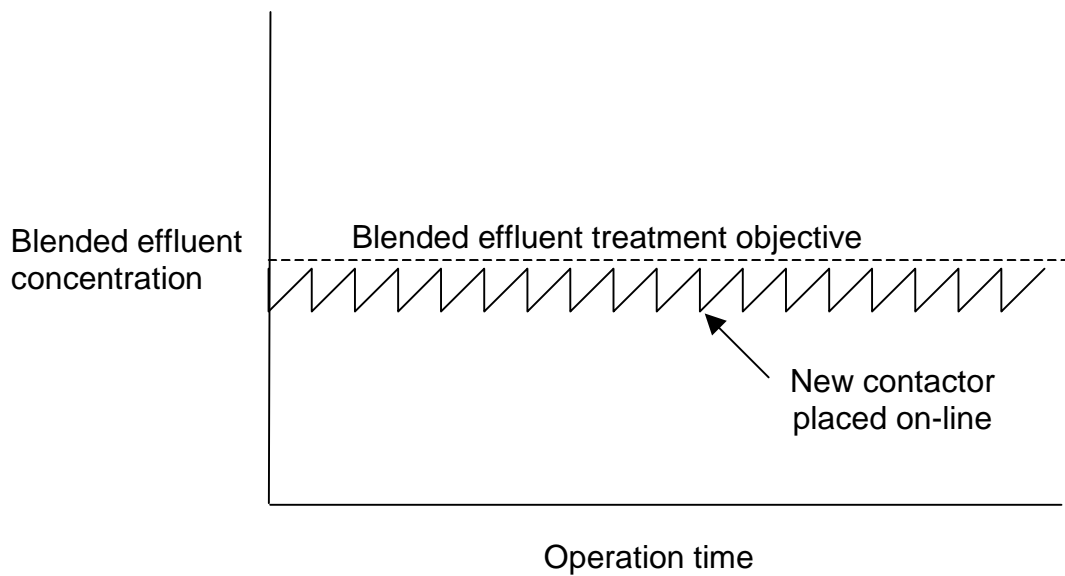


**Figure 2 Blended effluent water quality during quasi steady-state operation of multiple contactors in parallel-staggered mode (adapted from Summers et al., 1998)**

time when the curve intersects the treatment objective, as is done with single contactor breakthrough curves.

Figure 3 shows a series of graphs that describe how the integral breakthrough curve is developed. Graphs A through E depict eight GAC contactors on-line in parallel-staggered mode. For simplification, identical breakthrough curves are assumed for each contactor. The interval between GAC replacement, or the single contactor run time ( $RT_{SC}$ ), is increased from 16 to 99 days over these five graphs. At each  $RT_{SC}$ , the single contactor effluent concentration,  $C(t)$ , is given as well as the blended contactor effluent concentration,  $\bar{C}(t)$ , which is calculated by averaging the effluent water quality of each of the eight contactors at  $RT_{SC}$  (shown as a short dotted line representing the intersection of effluent concentration at  $RT_{SC}$ ). The dashed line breakthrough curve represents the contactor that replaces the first contactor when it has reached the end of its service life. As  $RT_{SC}$  is increased, moving from Graph A through E, the  $\bar{C}(t)$  at  $RT_{SC}$  increases. Therefore, the GAC replacement interval affects the blended contactor effluent water quality. Specifically, as shown graphically by the integral breakthrough curve in Graph E, as  $RT_{SC}$  increases, blended effluent water quality declines. Using the integral breakthrough curve, the single contactor run time at which the treatment objective is exceeded in the blended effluent can be determined.

Assuming a linear breakthrough curve, Westrick and Cohen (1976) modeled the impact of parallel contactor operation on blended effluent water quality, and derived the following equation:

$$q_N = \frac{q_i N}{\frac{N+1}{2}} \quad (1)$$

where  $N$  is the number of parallel contactors,  $q_N$  is the specific throughput of the  $N$ th contactor at the time the treatment objective is exceeded in the blended effluent, and  $q_i$  is the throughput of the individual contactor when the treatment objective is exceeded in that single contactor. For large  $N$ , Equation 1 shows that  $q_N$  approaches twice  $q_i$ : the run time of each contactor when the blended effluent treatment objective is exceeded will approach twice that of a single contactor when the treatment objective is exceeded in the single contactor effluent. For a finite  $N$ , such as 10 contactors,  $q_N$  is a factor of 1.8 times greater than  $q_i$ .

Equation 1 establishes a relationship between the specific throughput of the  $N$ th contactor at the time the treatment objective was exceeded in the blended effluent and the throughput of a single contactor to that same treatment objective, assuming a linear breakthrough curve. For large  $N$ , Equation 1 shows that the run throughput of each contactor approaches twice that for a single contactor:

$$q_\infty = 2q_i \quad (2)$$

where  $q_\infty$  is the throughput of each contactor when an infinite number of contactors are operated in parallel-staggered mode. The relationship between  $q_\infty$  and  $q_i$  expressed in Equation 2 can be substituted into Equation 1:

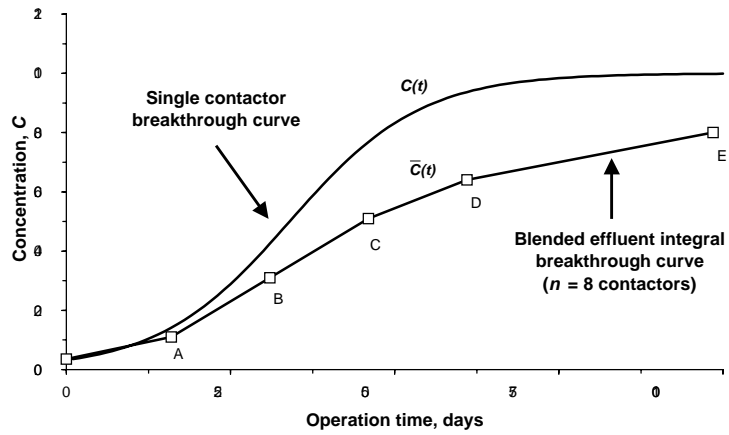
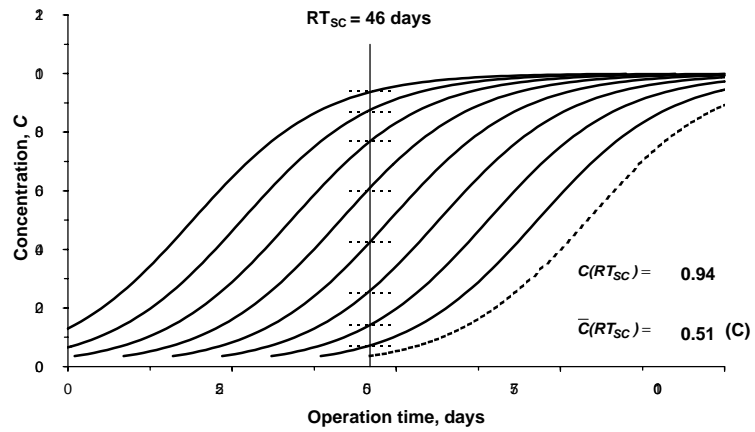
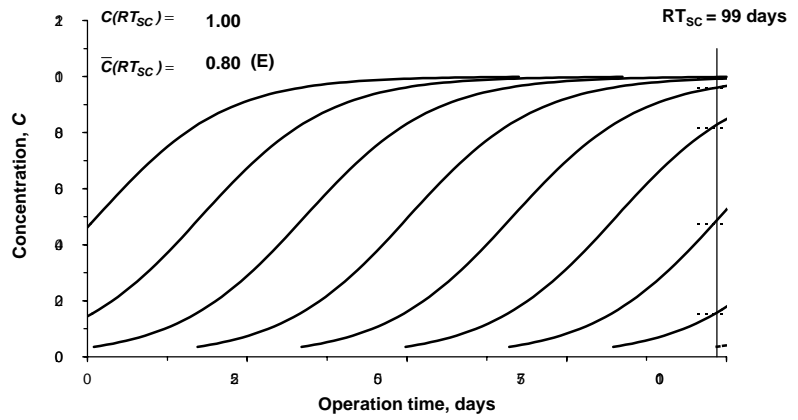
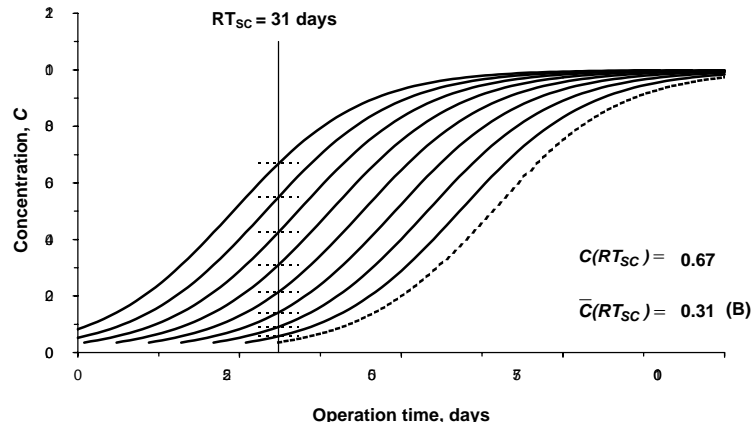
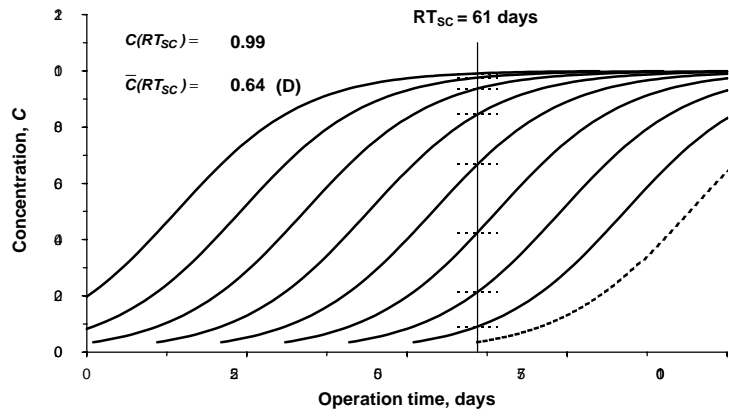
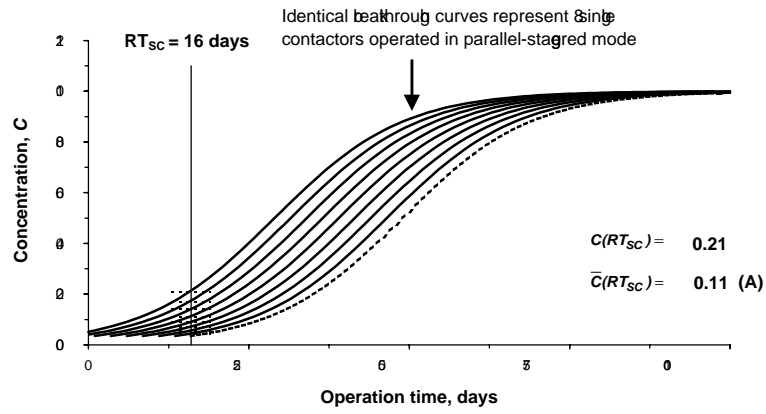


Figure 3 Operation of multiple contactors in parallel staggered mode to various single contactor run times: derivation of the blended effluent integral breakthrough curve

$$q_N = \frac{N}{N+1} q_\infty \quad (3)$$

Therefore, under the linear breakthrough curve assumption, when 9 contactors are operated in parallel-staggered mode, the throughput of each contactor when the blended effluent exceeds the treatment objective will be 90 percent of that for an infinite number of contactors operated in parallel-staggered mode. The analysis assumes a linear breakthrough curve and shows that  $N_{90}$  is independent of the magnitude of the treatment objective.

Roberts and Summers (1982) examined the impact of contactor operation in parallel-staggered mode on the run times of individual contactors. The authors showed that the fraction of organic matter remaining in the combined effluent,  $\bar{f}$ , could be estimated from a single contactor breakthrough curve, assuming regular GAC replacement intervals:

$$\bar{f} = \frac{1}{n} \sum_{i=1}^n f_i \quad (4)$$

where  $N$  is the number of contactors and  $f_i$  is the fraction,  $C(t)/C_0$ , of organic matter remaining in the effluent of the  $i$ th contactor, determined from a breakthrough curve. A plot of the integral breakthrough curve over operation time provides an estimate of the service time of each contactor in a multiple contactor scenario for a treatment objective. This relationship is referred to as the integral breakthrough curve, and the development of this curve is explained graphically in Figure 3.

### 1.3 Single Contactor Breakthrough Curve Models

A model used to describe single contactor effluent experimental data is needed for several reasons. From a data management perspective, best-fit curve parameters that adequately describe experimental data are less memory intensive than storing the entire experimental data set. A best-fit curve also facilitates interpolation and extrapolation necessary to estimate run times for given treatment objectives. Use of a best-fit model curve also provides an estimate of the scatter in the data through the coefficient of determination, and the model minimizes the impact of this scatter on run time estimates. Finally, a function that describes the single contactor breakthrough curve is a prerequisite for calculating the integral breakthrough curve, a curve that relates single contactor run time to blended effluent water quality under the assumption that an infinite number of contactors are operated in parallel-staggered mode. Run time estimates generated by the integral breakthrough curve are more applicable to full-scale GAC operation where multiple contactors are operated in parallel-staggered mode to increase the service time of each individual contactor.

Many researchers have applied various forms of the logistic function to predict GAC breakthrough curves or to fit existing breakthrough curve data. The logistic function is a symmetric S-shaped curve with a midpoint inflection. Oulman (1980) describes the development of the Bohart-Adams equation, published in 1920, which was used to model the service life of activated carbon for the removal of airborne chlorine by gas masks. The Bohart-Adams equation is:

$$\ln\left(\frac{C_0}{C(t)-1}\right) = \frac{KN_c x}{v} - KC_0 t \quad (5)$$

where  $C(t)$  is the effluent concentration at time  $t$ ,  $C_0$  is the influent concentration,  $K$  is an adsorption rate coefficient,  $N_c$  is an adsorption capacity coefficient,  $x$  is the bed depth,  $v$  is the linear velocity, and  $t$  is the service time. The Bohart-Adams equation is a bed depth service model and was derived based on surface reaction theory (Clark, 1987). Equation 5 can be rewritten in the form of the logistic function:

$$\frac{C_0}{C(t)} = \frac{1}{1 + e^{-(a+bt)}} \quad (6)$$

where the variables  $a$  and  $b$  are defined as:

$$a = \frac{-KN_c x}{v} \quad (7)$$

and

$$b = KC_0 \quad (8)$$

If the adsorption coefficients  $K$  and  $N_c$  are known, as well as other operational parameters (velocity and depth), the effluent concentration at time  $t$  can be predicted by Equation 6. Because GAC breakthrough curves are generally not symmetrical, Clark (1987) proposed the use of the generalized logistic function to model GAC breakthrough curves. This generalized model incorporates the Freundlich isotherm parameter and is as follows:

$$C(t) = \left( \frac{C_0^{n-1}}{1 + Ae^{-rt}} \right)^{\frac{1}{n-1}} \quad (9)$$

where  $1/n$  is the Freundlich isotherm parameter,  $r$  is a constant, and  $A$ , a constant, is defined as:

$$A = \left[ \left( \frac{C_0}{C(t)} \right)^{n-1} - 1 \right] e^{-rt} \quad (10)$$

The derivation of this generalized logistic function is described in Clark, Symons, and Ireland (1986). Their approach, which builds on the work of Oulman, is an effort to predict GAC breakthrough curve profiles based on adsorption characteristics and influent concentration.

A predictive approach to single contactor GAC breakthrough curves was not examined as a part of this study. Instead, a model was needed to curve fit experimental breakthrough data. Due to the inherent ability of the logistic function to match the typical S-shaped breakthrough curve, and the previous body of work that has utilized the logistic function to model GAC breakthrough data, the logistic function was chosen as the equation used to fit GAC breakthrough data in this study.

Chowdhury et al. (1996) and Summers et al. (1998) applied the following form of the logistic function to model experimental GAC breakthrough data:

$$C(t) = \frac{A}{1 + Be^{-Dt}} \quad (11)$$

where the values for  $A$ ,  $B$ , and  $D$  are determined experimentally by a best-fit to the breakthrough data. The parameter  $A$  represents the level to which the function approaches asymptotically. Parameters  $B$  and  $D$  affect the shape of the curve. Equation 11 was found to adequately fit GAC breakthrough curves for three water sources and the parameters total organic carbon (TOC) and formed total trihalomethane (TTHM). With a few modifications, as described in Section 3.2.1 below, Equation 11 served as a basis for the single contactor breakthrough curve modeling work contained in this study.

#### 1.4 Direct Integration Approach

The average value function, a mathematical integration, assumes an infinite number of parallel-staggered contactors and replaces the numerical integration required for solving Equation 4. However, it is important to understand the impact of the infinite contactor assumption on model results. Based on Equation 1, nine contactors in parallel will yield  $q_{N=9}$  within 10 percent of  $q_{\infty}$ . Therefore, for 10 contactors or greater, the difference will be less than 10 percent, based on the linear breakthrough curve assumption. Additionally, Westrick and Cohen (1976) found that the carbon usage rate for individual contactors operated in parallel-staggered mode will approach half the carbon usage rate based on meeting the treatment objective using a single contactor. Roberts and Summers (1982) examined integral TOC breakthrough curves applied to eight case studies, and found that GAC run times increased by a factor of two to three over those based on the single contactor breakthrough curve, for a 50 percent TOC breakthrough objective. They concluded that staggered multiple parallel contactor operation will lower carbon usage rates even more than predicted by Westrick and Cohen, whose conclusions were based on a linear breakthrough curve.

Chowdhury et al. (1996) and Summers et al. (1998) applied the average value function to show that the integral breakthrough curve can be represented by:

$$\bar{C}(t) = \frac{1}{t} \int_0^t C(t) dt \quad (12)$$

where  $\bar{C}(t)$  is the blended effluent concentration at individual contactor run time,  $t$ , and  $C(t)$  is an equation that describes the single contactor effluent concentration as a function of time. This time-averaged mathematical integration of the function that describes the breakthrough curve yields the integral breakthrough curve, as it describes the average value of the function at any point in time. This procedure is referred to here as the direct integration (DI) approach. While Equation 4 provides an expression of the average blended concentration of  $N$  contactors in parallel, Equation 12 represents a time-averaged blended effluent concentration of an infinite number of staggered parallel contactors. Therefore, a plot of Equation 12 over operation time represents the run time to any given treatment objective in the blended contactor effluent for

each individual contactor of an infinite number of parallel-staggered contactors. This plot is not a direct representation of blended effluent water quality, but a tool to determine GAC run times of each contactor operated in parallel-staggered mode.

Chowdhury et al. (1996) and Summers et al. (1998) applied Equation 12 to Equation 11 to predict the integral breakthrough curve. Application of the DI approach utilizing different forms of the logistic function (Equation 11) is described below in Section 3.2.3.

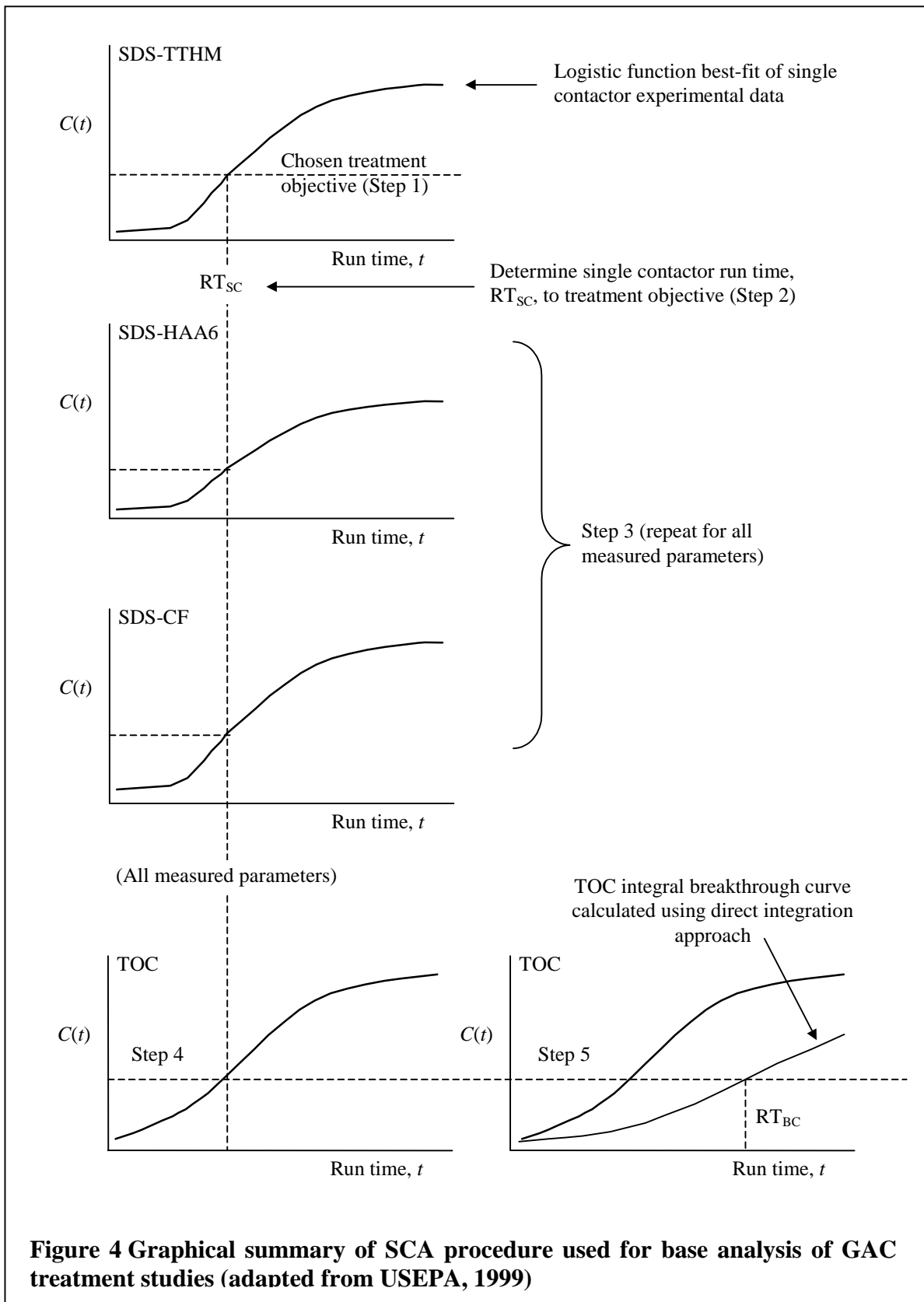
## 1.5 Surrogate Correlation Approach

Theoretically, the direct integration approach is a reliable method for estimating blended effluent water quality. However, during the analysis approach for the ICR GAC treatment study data, the treatment study technical work group (TS-TWG) determined that it would be computationally intensive to apply the DI approach to the large number of breakthrough curves (8,000 to 9,000) comprising the ICR treatment study data set. Furthermore, the DI approach may be less reliable for breakthrough curves that do not follow the typical "S" pattern, such as "peak" curves or sharp "S" shaped curves followed by a plateau. For these reasons, another approach for estimating blended effluent water quality from single contactor data was developed for analysis of the ICR treatment study GAC data.

The surrogate correlation approach (SCA) was developed by the TS-TWG as an alternative to the direct integration approach for calculating the integral breakthrough curve (USEPA, 1999). The SCA is based on the assumption that the relationship between TOC and all other parameters ( $UV_{254}$  and SDS-DBPs) in the single contactor effluent is maintained in the blended effluent of multiple staggered contactors. In other words, the concentration and speciation of DBPs formed after chlorination of the blended effluent of multiple contactors with a given TOC concentration is the same as that formed after chlorination of the single contactor effluent with the same TOC concentration. This method of estimating blended effluent water quality from single contactor data requires that an integral breakthrough curve be determined based on the single contactor TOC breakthrough only. Once this curve is known, along with a relationship between TOC and all other parameters in the single contactor effluent, integral breakthrough curves are estimated for all other parameters. This approach not only allows for the evaluation of blended contactor run times to various breakthrough criteria, but also for the occurrence of other DBPs at that run time. For example, it will be important to evaluate the levels of individual DBPs, such as BDCM, at various regulatory targets under consideration. This will allow EPA to assess whether or not regulating one DBP or DBP group can effectively control the occurrence of other DBPs or DBP groups.

An example of the SCA procedure is described in the steps below and summarized graphically in Figure 4.

1. Select a treatment objective (e.g., TTHM = 32  $\mu\text{g/L}$ ).
2. Use the single contactor breakthrough curve for the parameter of interest and determine the single contactor run time ( $RT_{SC}$ ) at which the treatment objective is exceeded.



3. Use the  $RT_{SC}$  from Step 2 to determine the concentrations of all other parameters from the single contactor breakthrough curves. (In this step, the single contactor effluent concentrations of all parameters are "linked" through the single contactor run time,  $RT_{SC}$ ).
4. Use the  $RT_{SC}$  from Step 2 to determine the single contactor effluent TOC concentration that corresponds to the treatment objective.
5. From the integral TOC breakthrough curve, calculated by the DI approach, determine the blended contactor run time ( $RT_{BC}$ ) to reach the TOC concentration calculated in step 4. This is the only point in the analysis where it is necessary to apply the DI method to establish an integral breakthrough curve, and only the TOC integral breakthrough curve is required. If the integral breakthrough curve does not exceed the TOC concentration calculated in Step 4, extrapolation of the TOC integral breakthrough curve may be required.

This analysis makes the following assumptions:

1. The logistic function model can accurately describe the breakthrough of DBP precursors and DBP precursor surrogates,
2. The relationship between TOC and DBP precursors (concentration and speciation) observed in the single contactor effluent is maintained in the blended effluent,
3. The TOC breakthrough curve can be extrapolated with reasonable results,
4. The TOC integral breakthrough curve accurately predicts the blended water quality of an infinite number of multiple contactors operated in parallel-staggered mode. Furthermore, the TOC integral breakthrough curve based on an infinite number of contactors is a reasonable approximation to a finite numbers of contactors.

All four of these assumptions are verified as a part of this study.

## 1.6 Impact of Bromide Concentration on GAC Effluent Blending Models

The second assumption listed for the SCA procedure is that the relationship between TOC and DBP precursors (concentration and speciation) observed in the single contactor effluent is maintained in the blended effluent. This is an important assumption because the SCA applies DBP formation and speciation at a given single contactor run time and TOC concentration to the blended contactor run time at which an equivalent TOC concentration is achieved. The relative concentrations of TOC and bromide may influence DBP formation and speciation.

A number of researchers have discussed the impact of bromide concentration on DBP formation and speciation. Under constant chlorination conditions, and at a constant TOC concentration, as the bromide concentration increases the bromide to TOC ratio increases and DBP speciation shifts to favor the formation of brominated species (Summers et al., 1993). GAC treatment does not remove bromide, while TOC is adsorbed, resulting in higher GAC effluent bromide to TOC ratios in the GAC effluent as compared to those in the GAC influent. Due to this increase, GAC effluent formed DBPs may undergo shifts in speciation to higher fractions of the more brominated DBP species. In some cases effluent formed DBP species concentrations are measured higher than those formed in the influent. It is important to track the breakthrough

behavior of specific DBP species, because some may be of potential health concern and a MCL could be set for a specific DBP species.

The shift in DBP speciation for THMs can be measured by calculating the bromine incorporation factor for THMs,  $n_{Br}$  (Gould et al., 1983):

$$n_{Br} = \frac{\sum_{i=0}^3 i \cdot CHCl_{3-i}Br_i}{TTHM} \quad (13)$$

where all concentrations (of species and TTHM) are expressed as molar concentrations. The value of  $n_{Br}$  can range from 0 (only chloroform formed) to 3 (only bromoform formed). Based on the bromine incorporation factor for HAA6 (Shukairy et al., 1994), the bromine incorporation factor,  $n'_{Br}$ , for HAA9 is defined as:

$$n'_{Br} = \frac{1 \cdot MBAA + 1 \cdot BCAA + 1 \cdot DCBAA + 2 \cdot DBAA + 2 \cdot CDBAA + 3 \cdot TBAA}{HAA9} \quad (14)$$

where all concentrations (of species and HAA9) are expressed as molar concentrations.

The value of  $n'_{Br}$  can range from 0 (only MCAA, DCAA, or TCAA formed) to 3 (only TBAA formed). Examining and comparing  $n_{Br}$  and  $n'_{Br}$  values between single contactor and blended effluent will help determine whether the second SCA method assumption described in Section 1.5 is valid.

## 1.7 Effluent Blending Modeling of Fewer than 10 Contactors

Both the DI and SCA methods for determining integral breakthrough curves rely on the assumption of an infinite number of contactors operated in parallel-staggered mode. For 10 or more contactors in parallel-staggered operation, the integration presented in Equation 12 approximates blended effluent water quality within 10 percent (Roberts and Summers, 1982). Equation 12 is utilized exclusively for the DI approach, while the SCA approach relies on Equation 12 to establish the integral breakthrough curve for TOC as part of the analysis. Therefore, it is important to examine the impact of the infinite number of contactors assumption on the ability of these methods to predict blended contactor effluent water quality for a finite number of contactors. Furthermore, for smaller plants that operate fewer than 10 contactors in parallel-staggered mode, the approximation given by Equation 12 will be less accurate and actual service lives will be shorter than those predicted by Equation 12.

## 1.8 GAC Breakthrough Curve Extrapolation

The SCA procedure is limited by the highest TOC concentration reached by the TOC integral breakthrough curve, which is typically 40 to 70 percent of the highest single contactor TOC concentration. Therefore, although higher single contactor TOC concentrations are associated with formed DBP concentrations, these cannot be applied to the integral breakthrough curve during application of the SCA procedure unless the TOC integral breakthrough curve is extrapolated. It is therefore important to establish the impact of extrapolation of the TOC

integral breakthrough curve on estimated run times to treatment objectives and blended contactor water quality. The sensitivity of the predicted integral breakthrough curve to extrapolation was evaluated for two waters in this study.

## **1.9 ICR GAC Treatment Study Data Analysis Context**

The design of this study incorporated two main goals. The primary objectives were to evaluate the ability of the logistic function to model single contactor breakthrough curve data and to evaluate the success and limitations of predictive models used to determine the integral breakthrough curve, a relationship between single contactor run time and blended contactor water quality. The secondary objective of this study was to evaluate the applicability of these models and predictive methods in the context of the ICR GAC treatment study data analysis.

A large amount of ICR treatment study data will be analyzed: the 62 GAC treatment studies performed will generate a total of 8,000 to 9,000 individual breakthrough curves. The SCA method is especially applicable to this data analysis procedure because it minimizes the computations necessary to estimate blended contactor run times for treatment objectives. An assessment of the concentration of other DBPs at any given treatment objective will be required as part of the data analysis effort, and the SCA procedure is also suited to this task. The SCA procedure requires that GAC breakthrough curves for all measured parameters be represented by the logistic function model curve fit. By doing so, a smaller amount of data are needed to represent breakthrough curve experimental data. The following steps outline the data analysis procedure to be utilized during the ICR treatment study data analysis effort:

1. The logistic function model will be used to fit all water quality parameters in the GAC effluent.
2. The TOC integral breakthrough curve will be determined using the DI approach. In some cases, this curve may be extrapolated.
3. All logistic function model fit coefficients will be entered into a database to allow different breakthrough criteria to be evaluated and queried across all studies.
4. The SCA procedure will be used to estimate run times for multiple contactors operated in parallel-staggered mode by determining the effluent concentrations of various water quality parameters linked to a common single contactor run time, and calculating the blended effluent run time that corresponds to the TOC concentration. In this manner, simultaneous treatment objectives, such as THM or HAA regulatory target concentrations, can be evaluated to determine which parameter controls the design and operation of the process.
5. Results will be used to evaluate blended contactor run times that meet regulatory target treatment objectives, and this information can be used to estimate costs. Simultaneous treatment objectives will also be evaluated (e.g., HAAs and THMs, TOC and THMs, THMs and BDCM).

## **1.10 Appropriateness of Model Assumptions to Full-Scale GAC Effluent Blending**

Both the DI and SCA methods rely on the assumption that the GAC in each contactor of an array of contactors is replaced at regular intervals, so that the service times of all contactors are equal. They also assume that the breakthrough curve profiles of all single contactors are identical. In a full-scale plant, these idealized conditions will rarely occur. Variability in source water quality may impact the run time of the contactors, depending on when they are placed in service and DBP precursor concentrations in the GAC influent during their service life. Variability in distribution system conditions, especially temperature, may impact the contactor service life, as DBP levels may increase with higher temperatures.

For a plant that operates a fixed number of contactors, water demand changes during the year may directly impact the EBCT of each contactor, or the number of contactors in operation. Under operation of a constant number of contactors, a contactor that is placed on-line at the beginning of the summer high water demand months may be operated under a shorter EBCT as compared to a contactor placed on-line during the winter. Furthermore, it is less desirable to remove contactors from service to replace GAC during high demand periods. Another approach is to increase the number of contactors on-line as water demand increases.

---

## 2 Study Objectives and Approach

This study was performed in conjunction with bench-scale GAC treatment studies that were performed at one laboratory in fulfillment of ICR requirements for eight utilities. It was designed to examine the following experimental objectives:

1. Assess the ability of the logistic function model to fit single contactor breakthrough data for eight GAC runs using eight water sources and all measured parameters, including DBP surrogates, DBP class sum parameters, and DBP species. The water sources represent a range in TOC concentrations, DBP precursor levels, bromide concentrations, and SDS chlorination conditions.
2. Verify through bench-scale experiments the accuracy of the direct integration (DI) method for establishing the integral breakthrough curve, a relationship between single contactor operation time and blended effluent water quality.
3. Examine the accuracy of the computationally-simpler surrogate correlation approach (SCA) to predict the integral breakthrough curves of all measured parameters. Verify a basic assumption of the SCA procedure, that the relationship between DBP formation and TOC concentration in the single contactor effluent and in the blended effluent is maintained.
4. Examine the impact of GAC effluent blending on DBP speciation. Assess the accuracy of models used to predict the integral breakthrough curve for individual THMs and HAAs, and compare bromine incorporation into DBP formation in the single contactor and blended contactor effluents.
5. Evaluate the impact of extrapolation of the integral breakthrough curve on blended effluent water quality.
6. Verify the accuracy of the integral breakthrough curve predictive models, which assume an infinite number of contactors, for the prediction of the service life of finite numbers of contactors.

This page intentionally left blank.

---

## 3 Materials and Methods

### 3.1 Experimental Approach

#### 3.1.1 Rapid Small-Scale Column Test

The performance of full-scale GAC contactors was simulated using the rapid small-scale column test (RSSCT). Previous studies have shown that diffusion of natural organic matter (NOM) to adsorption sites on GAC is proportional to the particle size (Crittenden et al., 1989; Sontheimer et al., 1988). Therefore, by grinding the GAC to a smaller size, rates of adsorption are increased in proportion to the ratio of full-scale to RSSCT GAC particle sizes, or scaling factor. The scaling factor also relates the RSSCT EBCT and superficial velocity to the full-scale contactor. If the RSSCT utilized the full-scale contactor bed length, extremely long columns requiring very high inlet pressures would be required. However, studies have shown that adjustments to the RSSCT Reynold's number utilized (between 0.1 and 1.0) have a negligible impact on results. Therefore, by decreasing the RSSCT Reynold's number, a much shorter column can be designed (with consequently shorter superficial velocities to maintain a constant EBCT). Complete details on the RSSCT design for precursor removal studies can be found in the literature (USEPA, 1996; Summers et al., 1995; Summers et al., 1992; Crittenden et al., 1991).

The RSSCTs designed in this study followed the guidelines outlined in the *GAC Precursor Removal Studies* section of the *ICR Manual for Bench- and Pilot-Scale Treatment Studies* (USEPA, 1996). A summary of the RSSCT design used for each run is given in Table 1. For most waters, a 20 minute full-scale EBCT contactor was simulated. However, 15 minute and 7.2 minute EBCT contactors were simulated for Waters 1 and 8, respectively. The designs were based on the estimated or known GAC influent TOC concentration (which can directly impact the rate of breakthrough), the full-scale water temperature at the time of sampling, the full-scale GAC particle size, and the full-scale EBCT simulated. The full-scale bed porosity was assumed to be 0.45 for all runs. The minimum Reynold's number used ranged from 0.48 to 0.60.

##### 3.1.1.1 GAC Preparation Procedures

Representative batches of Filtrasorb 300 (F-300), and Filtrasorb 400 (F-400), bituminous coal-based GAC, were obtained from the manufacturer, Calgon Carbon Corporation. The representative batch of the reactivated GAC/virgin GAC blend used for Water 4 was obtained directly from the utility. Using a riffle splitter, a small (30 to 50 g) representative sample of the GAC was obtained. Using a jar mill, the GAC was ground to the needed mesh size. Care was taken to frequently remove and sieve the GAC in the jar mill. The GAC was ground until the entire sample passed through the upper mesh size sieve. Usually, a recovery of 25 to 30 percent was obtained, as defined by the amount of GAC retained between the two mesh size sieves and divided by the total amount of GAC prior to grinding.

The ground GAC was transferred to a beaker, and covered with reagent grade (adsorbed-deionized) water. The GAC was washed by repeated additions and decantations of reagent grade

Design parameter	Design value for each water										
	1	2	3	4	5	6	7	8			
GAC manufacturer	Calgn Carbn Co.		Calgn Carbn Co.		Calgn Carbn Co.		Calgn Carbn Co.		Calgn Carbn Co.		
GAC brand name	F-0		F-0		F-0		F-0		F-0		
GAC type	Bituminous		Bituminous		Bituminous		Bituminous		Bituminous		Bituminous
GAC mesh size	0		0		0		0		0		
Particle diameter, $d_p$ (nm)	0		0		0		0		0		
<b>General design parameters</b>											
Minimum Reynolds number, $Re_{s,min}$	0		0		0		0		0		
Full-scale operating temperature (°C)	2		2		2		2		2		
Kinematic viscosity $\nu_c$ (m <sup>2</sup> /s)	0-0		0-0		0-0		0-0		0-0		
Bed porosity $\epsilon_c$	0		0		0		0		0		
Measured dry bed density $\rho_s$ (g/m <sup>3</sup> )	0		0		0		0		0		
<b>RSSCT design parameters</b>											
Mesh size	0		0		0		0		0		
Particle diameter, $d_p$ (nm)	0		0		0		0		0		
Salting factor, $S$	0		0		0		0		0		
Hydraulic loading rate, $v_s$ (m/hr)	6		2		0		0		0		
Column diameter, $D_c$ (m)	0		0		0		0		0		
Flow rate, $Q_s$ (m <sup>3</sup> /min)	0		7		0		0		0		
Full-scale empty bed contact time, EBCT $t_c$ (min)	5		0		0		0		0		2
Estimated full-scale run time, $t_c^T$ (day)	0		2		2		2		0		0
Estimated run time, $t_c^T$ (day)	0		2		2		0		0		0
Volume water required, $V_s$ (L)	0		0		0		0		0		0
Mass GAC required, $m_s$ (g)	0		0		0		0		0		0
Empty bed contact time, EBCT $t_c$ (min)	0		0		0		0		0		0
Bed length, $l_s$ (cm)	2		0		2		0		0		0

Table 1 Summary of RSSCT design parameters for all runs

water. The reagent grade water was added at a high rate and turbulence, to stir up the GAC and release fines. The supernatant water containing GAC fines was decanted after the GAC was allowed to settle. Towards the end of the cleaning procedure, the sample was sonicated twice for 5 to 10 seconds. The sonication step helped loosen fines that were subsequently removed by the addition and decantation of reagent grade water.

The GAC was dried in an oven at 80 to 90°C for 6 to 12 hours. The temperature was then raised to between 100 and 110°C and the sample was dried until it reached a constant weight. The sample was removed and cooled inside a dessicator. Once cooled, if not immediately used, it was stored in a glass vial sealed with a lid with Teflon-lined septum until ready for use.

The dry bed density was measured using a sample of dried and cooled GAC. Stored GAC was dried in an oven as described above prior to the dry bed density measurement. To measure the dry bed density, a sample of the GAC was placed inside a 10-mL glass graduated cylinder to a level of 5 to 9 mL. The cylinder was tapped to pack the GAC. A volume was measured and recorded. This GAC was then weighed on a balance. The volume reading of the graduated cylinder was checked and calibrated if necessary by adding a known volume of water to it using a 10-mL class A graduated pipette. The GAC dry bed density was calculated by dividing the weight by the calibrated volume.

The calculated mass of GAC for each RSSCT was weighed, placed inside a clean beaker, and covered with reagent grade water. The wetted GAC was usually allowed to sit for 12 to 24 hours, followed by placement in a vacuum for at least 1 hour to displace the air within the pores.

### *3.1.1.2 RSSCT Column Setup*

The ground GAC used for the RSSCT was packed in glass chromatography columns. Due to the range of GAC influent TOC concentrations, which correlates to the rate of TOC breakthrough, columns with inner diameters ranging from 8.0 to 12.6 mm were utilized. The 8.0 and 11.0 mm inner diameter columns were standard. Other column diameters (9.0, 10.0, and 12.6 mm) were custom-ordered and the GAC required additional support to ensure the GAC was within the effective length of the column. The GAC support for these special order columns consisted of a stainless steel screen (60 or 100 mesh size), Teflon beads, glass wool, and two stainless steel screens. The support for 8.0 and 11.0 mm inner diameter columns consisted of two stainless steel screens placed on top of the Teflon fitting. The mesh size of the screens utilized were based on the ground GAC mesh size. For 100x200 GAC, a 100 mesh screen and a 200 mesh screen were used. For 140x230 GAC, a 200 mesh screen and a 325 mesh screen were used. For all column inner diameter sizes, a small amount of glass wool was placed inside the Teflon fitting, supported by a 60 mesh size stainless steel screen.

The GAC was added to the columns as a slurry and packed by repeatedly tapping the column sides. The 20 minute full-scale equivalent EBCT RSSCTs were packed into two columns of the same inner diameter placed in series. Only reagent grade water was used during the packing process.

### 3.1.1.3 *Batch Influent Preparation*

Prior to RSSCT testing, all water samples were filtered through a 1.0- $\mu\text{m}$  nominal pore size glass fiber cartridge filter. The cartridge filter was pre-rinsed with deionized water. Dilute solutions of sulfuric acid and sodium hydroxide were used to maintain the influent pH within 0.1 pH units of the target pH during operation of the RSSCTs.

### 3.1.1.4 *RSSCT Monitoring*

The effluent flow rates were monitored constantly to ensure that the flow rates were maintained within 5 percent of the design flow rate. The calibration of the effluent flow rate control system was checked at least three times daily and adjusted when a flow rate differed by more than 3 percent from the design flow rate. The system pressure was monitored daily. The effluent TOC concentration was monitored frequently so that samples could be taken at the required 5 to 8 percent increments of the average influent TOC concentration.

## 3.1.2 Bench-Scale Blended Water Quality Assessment Approach

To simulate the integral breakthrough curve obtained by blending multiple full-scale contactors operated in parallel-staggered mode, the entire effluent from a single GAC contactor was collected in a reservoir and sampled over time. In this study, the entire effluent from the RSSCT was collected in a clean 30 or 55 gallon drum. The only effluent water not collected in the drum was that required for monitoring and sampling of the RSSCT effluent. This included TOC monitoring and sampling, UV<sub>254</sub> sampling, and SDS chlorination. Over time, the blended effluent drum was sampled and analyzed for TOC and UV<sub>254</sub>. Samples were also taken and chlorinated under the same target SDS conditions as those applied to the single contactor study. During every run, TTHM and HAA9 were analyzed, and during two runs, TOX was also analyzed, in addition to TTHM and HAA9. Ten percent of blended effluent samples taken were sampled in duplicate and all analyses were conducted on the duplicate samples (field sample duplicates).

The first discrete sample taken from the RSSCT effluent also constituted the first blended sample. Subsequently, seven samples were taken from the blended effluent drum, evenly spaced over the course of the run. The RSSCTs were operated until at least 70 percent TOC breakthrough was reached, and the last blended effluent sample was taken at that time. Since the ICR required that twelve samples be taken from the RSSCT effluent at even increments of TOC breakthrough, the blended effluent sampling schedule followed the RSSCT sampling. The second blended effluent sample was taken when the third RSSCT effluent sample was taken. The remaining blended effluent sample points were based on the RSSCT effluent sample number as described in Table 2. In practice, the blended effluent samples were taken from the drum just prior to the addition of the RSSCT effluent sample listed in Table 2. This way, the use of the RSSCT effluent sample water for SDS chlorination had a smaller impact on the blended effluent sample. All blended samples were chlorinated under the same SDS conditions as the RSSCT effluent samples. For two of the waters, (Waters 6 and 8) the run was extended for five laboratory days after 70 percent breakthrough had occurred. In these instances, eight blended

effluent samples were taken with the sixth at 70 percent breakthrough, the seventh 2.5 days later, and the eighth five days later.

Blended effluent sample number	RSSCT effluent sample number
1	1
2	3
3	6
4	8
5	9
6	10
7	11
8	12

**Table 2 Relationship between blended effluent sample number and RSSCT effluent sample number**

### 3.1.3 DBP Formation Assessment

The blended effluent samples were chlorinated under the same target conditions as the RSSCT effluent. To minimize the volume of water sampled from the blended effluent reservoir, the chlorine dose used was based on the single column effluent chlorine demand data, by relating chlorine demand to TOC concentration. The sampling volume required was minimized based on the DBPs to be analyzed. For 6 of the 8 waters, the blended effluent sample volume was 800 mL, sufficient for TOC, UV<sub>254</sub>, and SDS chlorination for the analysis of HAA9 and TTHM. When TOX was also analyzed after chlorination, a 1,300 mL sample was required.

For single contactor effluent samples, chlorine demand studies were performed on the first effluent sample and the influent water. For each sample, three 125-mL chlorine demand-free amber glass bottles were used. A combined phosphate/borate buffer solution was added to each bottle (2.0 mL/L) to maintain a constant target pH during incubation. Dilute solutions of sulfuric acid or sodium hydroxide were used to adjust the pH prior to chlorination if necessary. Three chlorine doses were selected based on the TOC concentration of the water and the results of a 5-minute chlorine demand study (providing a relative measure of inorganic chlorine demand). Each bottle was filled to 80 to 90 percent of capacity. Using a pipette, a measured amount of a standardized chlorine solution (using *Standard Methods* 4500-Cl B) was added to each bottle. The bottle was then filled and capped head-space free. The bottles were placed in a constant temperature bath in the dark for the duration of the target incubation period. A titrimetric procedure (*Standard Methods* 4500-Cl F) was used to measure the free chlorine residual after the holding time. The data generated by the chlorine demand study was used to estimate the chlorine dose to achieve the target residual for all effluent samples by correlating TOC

concentration to chlorine demand. When TTHM and HAA9 were analyzed, a clean chlorine demand-free 500 mL amber glass bottle was used. When TOX was also analyzed, a 1000 mL bottle was used. Caps with Teflon-lined septa were used. The order of DBP sampling was THMs, HAAs, and TOX. DBP samples were taken in duplicate in prepared bottles with appropriate preservatives and quenching agents based on the analytical method.

#### 3.1.4 Assessment of the Impact of Sampling on the Integral Breakthrough Curve

Discrete sampling from the RSSCT effluent and sampling from the blended effluent reservoir was required to obtain water quality data to generate single contactor and integral breakthrough curves. However, the impact of both types of sampling on the integral breakthrough curve were unknown. A model was developed to simulate the experimental procedure in an effort to assess the impact of sampling on the integral breakthrough curve. Based on the model results, RSSCT design and sampling procedures were optimized to minimize the impact of sampling on the integral breakthrough curve.

The model was based on sampling the RSSCT effluent continuously in 3-L aliquots. It assumed that these aliquots were sampled for TOC and UV<sub>254</sub> to monitor breakthrough as needed. Based on the TOC concentration of samples taken, effluent samples and duplicates at ICR-required TOC increments were identified and chlorinated under SDS conditions.

All samples were added to the reservoir in the order of sampling, and at even increments over the course of the run, samples were taken from the blended effluent reservoir for TOC and UV<sub>254</sub> analysis and SDS chlorination. The results of these analyses comprised the integral breakthrough curve. The sample volume required was minimized, and any unchlorinated sample remaining after analysis was complete was reintroduced to the reservoir.

Based on these experimental procedures, a model was developed to assess the impact of sampling on the integral breakthrough curve, prior to laboratory experiments. The model inputs were influent TOC concentration, empty-bed contact time (EBCT), column inner diameter, full-scale GAC mesh size, RSSCT GAC mesh size, minimum Reynold's number, and full-scale operating temperature. Based on a correlation between influent TOC concentration and bed volumes to 50 percent TOC breakthrough (Summers et al., 1994; Hooper et al., 1996), and adjustments to the correlation to estimate run times to different levels of TOC breakthrough, a TOC breakthrough curve was predicted.

From the estimated single contactor breakthrough curve, two blended effluent breakthrough curves were generated. A theoretical integral breakthrough curve assumed no column effluent or blended effluent sampling occurred. The experimental integral breakthrough curve assumed typical discrete RSSCT effluent sampling, as described in the *ICR Manual for Bench- and Pilot-Scale Treatment Studies*, and also included the sampling required from the blended effluent reservoir to characterize the blended effluent water quality as described in Section 3.1.2.

Increasing the RSSCT column inner diameter (and thus increasing the ratio of volume water passed to water required for analyses) decreased the impact of RSSCT effluent sampling on the integral breakthrough curve. The model also demonstrated that sampling from the blended effluent reservoir had the greatest impact on the difference between theoretical and experimental integral breakthrough curves. Thus, by increasing the volume of water passed through the

RSSCT (by increasing the column inner diameter or minimum Reynold's number) this effect could be minimized.

After each GAC run was complete, the experimental TOC integral breakthrough curve was compared to an integral curve from which the impact of actual single contactor and blended effluent sampling was subtracted (corrected integral breakthrough curve). For TOC breakthrough of each water, the two curves are compared in Appendix A. Overall, the impact of sampling on the integral breakthrough curve was very small, yielding a mean difference in TOC concentration at the end of the integral breakthrough curve (where the difference between the two curves was typically maximized) of 3 percent. The difference ranged from 1 to 6 percent, with shorter runs yielding higher percent differences. In all cases, the TOC concentration at the end of the experimental integral curve was higher than that in the corrected integral breakthrough curve.

## 3.2 Data Analysis and Modeling Approach

### 3.2.1 Logistic Function Models

In this study, the logistic function was used to fit GAC breakthrough data from 8 water sources and GAC runs, and up to 20 measured GAC effluent parameters (including DBP surrogates, formed DBP class sum parameters, and formed DBP species). In some cases, the logistic function presented in Equation 11 did not satisfactorily fit the breakthrough curve data. Three modifications were made to the logistic function model to enhance the ability of the model to fit breakthrough curve data. The models are described in Figure 5. The first modification was to include an additional parameter, improving the curve fit for breakthrough curves with moderate to high immediate breakthrough levels. The step logistic function is as follows:

$$C(t) = \frac{A}{1 + Be^{-Dt}} + A_0 \quad (15)$$

where  $C(t)$ ,  $B$ ,  $D$ , and  $t$  are as defined previously in Section 1.3, Equation 11. The term  $A_0$  represents the step applied to the logistic function to match moderate to high immediate breakthrough levels. The term  $A$  represents the asymptote to which the logistic function is approaching. In this study, the step logistic function model was used to curve fit all single contactor TOC breakthrough curves. The step logistic function model is also adequate for modeling the GAC effluent chlorine demand breakthrough curve, which typically has relatively high levels of immediate breakthrough. The addition of the step term also allows the curve to have a negative y-intercept, which is necessary for incorporation into the step-lag logistic function model described below.

Because many breakthrough curves (especially for SDS-DBPs) result in a relatively long initial interval where effluent concentrations are below reportable limits prior to breakthrough, a lag was incorporated into the function to shift the logistic function outward, allowing for a better fit of experimental breakthrough data. The run time at which initial breakthrough above detectable levels occurs is termed  $t_b$ , and the step-lag logistic function is as follows:

$$C(t) = 0 \quad t \leq t_b \quad (16)$$

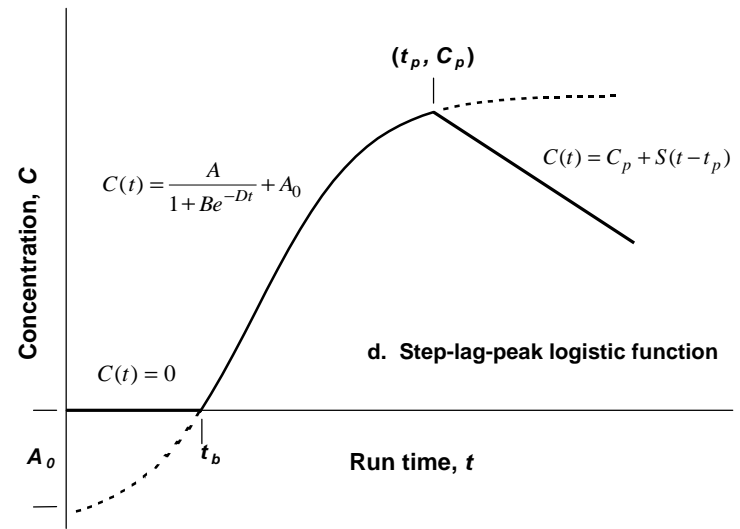
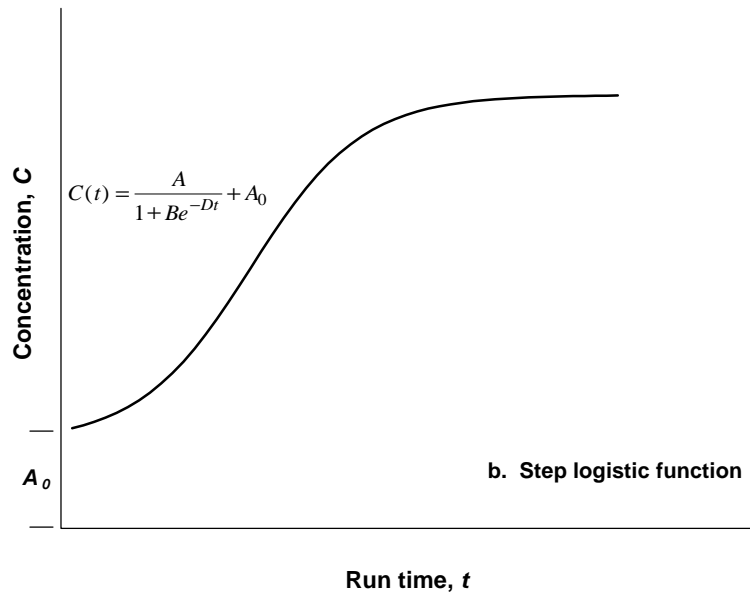
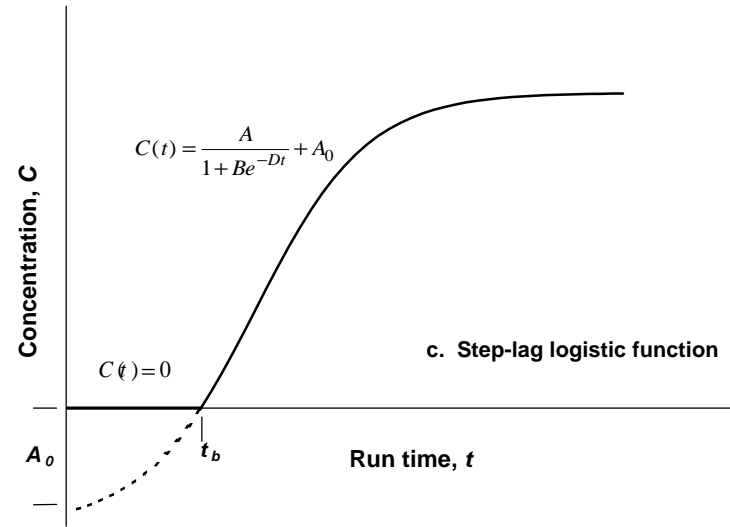
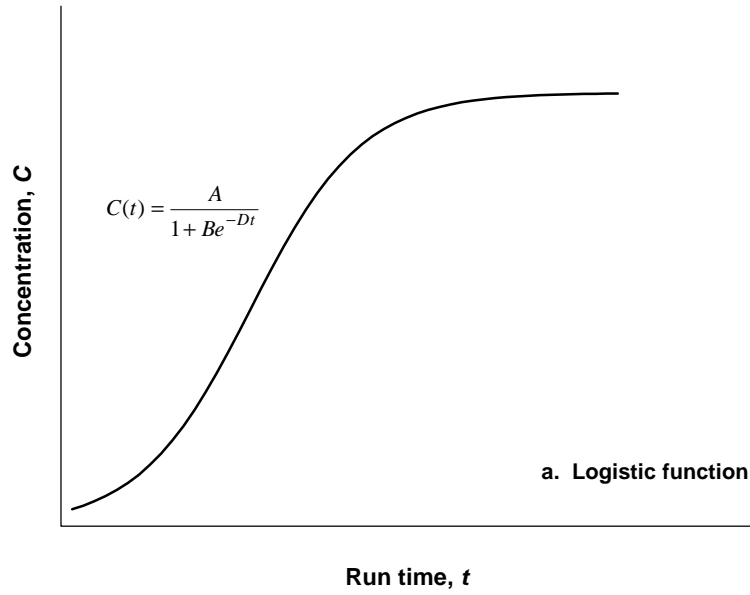


Figure 5 Logistic function model curves

$$C(t) = \frac{A}{1 + Be^{-Dt}} + A_0 \quad t > t_b \quad (17)$$

In many cases, a best-fit of the data will yield a negative value for  $A_0$  (a negative y-intercept). In essence, this shifts the logistic function downward, so that the beginning of the curve is negative (as shown by the dotted line on curve C in Figure 5). However, this occurs when  $t \leq t_b$ , so by Equation 16, the result is set to zero. For ICR treatment study data analysis, the result will be set to 50 percent of the MRL for DBP surrogates and species, and will be set to zero for DBP sum parameters. This modification improves the ability of the logistic function to fit breakthrough data that are not symmetrical.

Under certain conditions, some brominated DBP species exhibit increasing and decreasing breakthrough curves. These "peak" curves can be modeled using the logistic function to the maximum concentration. After this point, effluent concentrations decrease, and this decrease is modeled using a simple linear function. Prior to the point of peak concentration,  $C(t)$  is described by the step-lag logistic function model. The step-lag-peak logistic function model is as follows:

$$C(t) = 0 \quad t \leq t_b \quad (18)$$

$$C(t) = \frac{A}{1 + Be^{-Dt}} + A_0 \quad t_b < t \leq t_p \quad (19)$$

$$C(t) = C_p + S(t - t_p) \quad t > t_p \quad (20)$$

where  $C_p$  is the logistic function model best-fit concentration at  $t_p$ , the run time at which the peak occurs, and  $S$  is the slope of the linear best-fit curve. The following algorithm was used to detect "peak" breakthrough curves:

1. The measured peak concentration,  $C(t_p)$ , is at least 20 percent greater than the concentration at the last observed data point,  $C(t_f)$ .
2. The run time  $t_p$  is less than 80 percent of the run time of the last observed data point,  $t_f$ .
3. The data point corresponding to  $t_p$  is located prior to the penultimate observed data point.

In all cases, a best-fit of the logistic function model to the data was generated by least squares minimization approach. The coefficient of determination,  $R^2$ , was computed for all best-fits. The logistic function models were fit by non-linear least-squares using PROC NLIN in version 6.12 of the SAS system (Littell et al., 1996). Additional details and SAS code are included in Appendix B.

### 3.2.2 Outlier Methods

The large amount of data that will be processed during the ICR treatment studies data analysis necessitates the use of automated curve fitting procedures. To ensure that the fitted models are robust to extreme values, an outlier adjustment methodology that uses all experimental data

points but limits the influence of deviant observations on the parameter estimates was developed and used for this analysis.

Indiscriminate deletion of deviant observations can cause goodness of fit measures (i.e.,  $R^2$ ) to be unrealistically high. Rather than deleting potential outliers, suspect observations were replaced by less extreme values by the following procedure:

1. Fit the logistic function model to the observed data and determine approximate 95 percent prediction limits on the observations.
2. Observations that exceed the threshold Predicted  $\pm (U95 - L95)*K$  are adjusted to Predicted  $\pm (U95 - L95)*K$ , where U95 is the upper 95 percent confidence limit and L95 is the lower 95 percent confidence limit. The constant K determines the magnitude of the adjustment, with larger values of K corresponding to fewer declared outliers and smaller adjustments to those that are detected. The value for the constant K was set to 1/3 based on simulation results that indicated a good balance between false alarms and power to identify substantial outliers ( $>3$  standard deviations from the best-fit prediction). Approximately 2.5 percent of the data in the present study were identified as outliers and adjusted.
3. Refit the logistic function model using adjusted values.

### 3.2.3 Direct Integration Approach

The use of the integrated logistic function model for a given parameter to predict the integral breakthrough curve for that parameter is termed the direct integration (DI) approach. The average value function described by Equation 12 was applied to the expressions used to describe the breakthrough curves presented in Section 3.2.1. An expression for the average value of the step logistic function (Equation 15) is:

$$\bar{C}(t) = A_0 + A + \frac{A}{Dt} \ln \left( \frac{1 + Be^{-Dt}}{1 + B} \right) \quad (21)$$

Application of the average value function to the step-lag logistic function model (Equations 16 and 17) yields the following equations that represent the integral breakthrough curve:

$$\bar{C}(t) = 0 \quad t \leq t_b \quad (22)$$

$$\bar{C}(t) = (A_0 + A) \left( 1 - \frac{t_b}{t} \right) + \frac{A}{Dt} \ln \left( \frac{1 + Be^{-Dt}}{1 + Be^{-Dt_b}} \right) \quad t > t_b \quad (23)$$

Application of the average value function to the step-lag-peak logistic function model at  $t > t_b$  is more complex due to the use of two functions to describe the experimental data. The application of the average value function to the three functions used to describe the experimental data over the range  $[0, t]$  is given by the following equation:

$$\bar{C}(t) = \frac{1}{t} \int_0^t C(t) dt = \frac{1}{t} \left[ \int_0^{t_b} C_1(t) dt + \int_{t_b}^{t_p} C_2(t) dt + \int_{t_p}^t C_3(t) dt \right] \quad (24)$$

where  $C_1(t)$ ,  $C_2(t)$ , and  $C_3(t)$  represent Equations 18, 19, and 20, respectively, the three equations used to model the experimental data. For  $t \leq t_b$ , the integral breakthrough curve is represented by:

$$\bar{C}(t) = 0 \quad t \leq t_b \quad (25)$$

For  $t_b < t \leq t_p$  the function used to predict the integral breakthrough curve reduces to the average value of the step-lag logistic function:

$$\bar{C}(t) = (A_0 + A) \left( 1 - \frac{t_b}{t} \right) + \frac{A}{Dt} \ln \left( \frac{1 + Be^{-Dt}}{1 + Be^{-Dt_b}} \right) \quad t_b < t \leq t_p \quad (26)$$

At  $t > t_p$ , Equation 19 is evaluated from  $t_b$  to  $t_p$ , and Equation 20 is evaluated from  $t_p$  to  $t$ . Combining the two equations yields:

$$\bar{C}(t) = \frac{1}{t} \left[ (A_0 + A)(t_p - t_b) + \frac{A}{D} \ln \left( \frac{1 + Be^{-Dt_p}}{1 + Be^{-Dt_b}} \right) + C_p(t - t_p) + \frac{1}{2} S(t^2 + t_p^2) - S t t_p \right] \quad t > t_p \quad (27)$$

The logistic function integral approach to determine the integral breakthrough curve assumes an infinite number of contactors operated in parallel-staggered mode. This assumption was verified for finite  $N = 2, 3, 4, 6, 10,$  and  $20$  contactors. For finite numbers of contactors, numerical integration of Equations 15 through 20 was performed as described by Equation 4.

### 3.2.4 Surrogate Correlation Approach

The surrogate correlation approach (SCA) is a procedure that simplifies and reduces the amount of computations necessary to estimate DBP formation in the effluent of staggered multiple contactors (blended effluent). The SCA procedure relies on a constant relationship between TOC concentration and DBP formation in both the single contactor effluent and the blended effluent. To apply the SCA method to a GAC run, the single contactor TOC,  $UV_{254}$ , SDS-DBP class sum parameters, and SDS-DBP species breakthrough curves are fit to the appropriate logistic function model. The SCA procedure steps are summarized in Section 1.5 and represented schematically in Figure 4.

Typically, a linear or second order polynomial relationship exists between GAC effluent TOC concentration and any other parameter. The SCA method does not determine or use these correlations directly but instead assumes they exist and are constant in both the single contactor effluent and blended effluent. This relationship is exploited by linking the concentration of all water quality parameters at a common single contactor run time. Using Equation 21, the integral breakthrough curve is calculated for the TOC single contactor breakthrough curve only. Then the single contactor TOC concentration, to which the concentrations of all other water quality

parameters are linked, is applied to the run time at which an equivalent TOC concentration is reached in the TOC integral breakthrough curve.

The SCA procedure can be performed to determine blended contactor run times for a given GAC run and blended effluent treatment objective. In this study, the procedure was verified by comparing the SCA integral breakthrough curve against experimental data.

### 3.2.5 Comparison of Methods for Predicting the Performance of GAC Contactors Operated in Parallel-Staggered Mode

During this study, the methods described in Sections 3.2.3 and 3.2.4 for predicting the integral breakthrough curve were compared to the experimentally derived integral breakthrough curve for eight GAC runs. Using the logistic function models, a best-fit of the experimental blended effluent data was derived. The logistic function models were applied to the integral breakthrough curve data because the blended effluent data curves were similar in shape to those encountered in the single contactor effluent.

Predictions obtained by the SCA method, the DI method, and the best-fitting model were compared using the calculated residual sums of squares (RSS) from the experimental blended effluent data. For each parameter prediction, the prediction bias was determined by averaging the calculated residuals for each model. An evaluation of the bias shows whether the model tended to overpredict or underpredict the observed data. For some parameters, a limited amount of data were measured above the minimum reporting level (MRL). In cases where fewer than six points above the MRL were present, curve fitting was not performed.

### 3.2.6 Comparison of Single Contactor and Blended Effluent DBP Bromine Incorporation

To verify the assumption that the impact of TOC on DBP bromine incorporation would be similar in the single contactor and blended effluents, the bromine incorporation factors  $n_{Br}$  and  $n'_{Br}$  were modeled as a polynomial function of TOC and  $UV_{254}$  concentrations for all waters simultaneously with two regression models:

$$Y = W_i + \beta_1 X + \beta_2 X^2 \quad (28)$$

$$Y = W_i + \beta_1 X + \beta_2 X^2 + \gamma Z, \quad (29)$$

where  $Y$  is  $n_{Br}$  or  $n'_{Br}$  and  $X$  is TOC or  $UV_{254}$ . The intercept  $W_i$  is allowed to be different for each water, to reflect natural differences in bromine incorporation across waters. In the second model, different intercepts are fitted for single contactor ( $Z=0$ ) and blended ( $Z=1$ ) data. The additional parameter  $\gamma$  represents the change in average bromine incorporation associated with blending. Since the first model is a special case of the second with  $\gamma=0$ , the assumption that blending will not impact average bromine incorporation would be supported if the goodness of fit of the two models is similar. Models which allowed the linear and quadratic parameters  $\beta_1$  and  $\beta_2$  to differ for single contactor and blending were considered in order to demonstrate that blended and single contactor scenarios are comparable in terms of the shape of the bromine incorporation profile as well as mean bromine incorporation (i.e., the intercepts). Although these

models make efficient use of all of the data simultaneously in order to reach a general conclusion, the presence of the water-specific random effects  $W_i$  makes ordinary least-squares inappropriate. SAS PROC MIXED was therefore used to estimate the models via general likelihood methods (Littell, et. al., 1996).

### 3.2.7 Breakthrough Curve Extrapolation

For two waters, the sensitivity of blended effluent water quality to a breakthrough curve extrapolation procedure was verified. To verify the extrapolation approach, two GAC runs were operated for five laboratory days beyond 70 percent TOC breakthrough. Based on the scaling factor of each run, the five days were equivalent to 49 and 69 full-scale days for Waters 5 and 8, respectively. The appropriate logistic function model was applied to the abbreviated data set, which reached 70 percent TOC breakthrough. Next, the appropriate logistic function model was applied to the entire available data set for each parameter. The model fit for the abbreviated data set was extrapolated to the total column run time, and the blended effluent water quality predicted based on extrapolation of the abbreviated data set was compared to that using the full experimental data set.

During the ICR treatment studies, only the TOC integral breakthrough curve will be extrapolated. The SCA method relies on projecting water quality data associated with single contactor effluent TOC concentration to the integral TOC breakthrough curve. Since the integral TOC breakthrough curve typically reaches only 40 to 70 percent of the single contactor breakthrough curve, DBP data associated with higher TOC concentrations would not be included. By extrapolating the integral TOC breakthrough curve, the benefit of the data set is increased, because DBP formation associated with higher GAC effluent TOC concentrations will be included in the analysis.

## 3.3 Waters Examined

### 3.3.1 Pretreatment and Water Quality

GAC runs on eight water sources were included in this study. Pretreatment schematics for each water source are shown in Appendix C. The influent to GAC TOC concentration for these water sources ranged from 2.0 to 5.6 mg/L. The specific UV absorbance for TOC (TSUVA, defined as  $100 \cdot UV_{254} / TOC$ ) ranged from 1.6 to 2.3 L/mg-m. A wide range of bromide concentrations were measured, ranging from 28 to 300  $\mu\text{g/L}$ . The GAC influent bromide to TOC ratio (Br:TOC) ranged from 10 to 68. Water 1, received from Miami, Florida, was a groundwater. Water 2, received from Aurora, Illinois, was a mixture of groundwater and surface water. The other 6 waters were all surface waters. A summary of the source water, pretreatment, and treated water quality is shown in Table 3.

Water	Water source	Pretreatment	Treated water quality (GAC influent)							
			TOC (mg/L)	UV <sub>254</sub> (1/cm)	TSUVA (L/mg-m)	pH	Alkalinity (mg/L as CaCO <sub>3</sub> )	Total hardness (mg/L as CaCO <sub>3</sub> )	Bromide (µg/L)	Br:TOC (µg/mg)
1	Miami-Dade County, Florida	Lime-softening	4.5	0.094	2.1	9.2	23	54	115	25
2	Aurora, Illinois	Lime-softening	2.6	0.055	2.1	9.4	58	131	105	40
3	Topeka, Kansas	Two-stage softening	2.4	0.048	2.0	9.0	30	133	160	68
4	Davenport, Iowa	Conventional (PAS*)	3.0	0.065	2.2	7.1	127	217	29	10
5	Escondido, California	Conventional (alum)	3.1	0.051	1.7	7.4	109	225	70	23
6	Charleston, S. Carolina	Conventional (alum)	2.6	0.060	2.3	6.3	9	29	140	53
7	Sweetwater, California	Conventional (ferric)	5.6	0.109	2.0	7.6	138	221	300	54
8	Greensboro, N. Carolina	Conventional (alum)	2.0	0.033	1.6	7.6	23	32	28	14

\* PAS: polyaluminum sulfate

**Table 3 Summary of pretreatment and water quality**

### 3.3.2 Simulated Distribution System Chlorination Conditions

Table 4 summarizes the SDS chlorination conditions for each water. The SDS conditions were chosen to reflect site-specific distribution system conditions at the time the water was sampled. SDS incubation times ranged from 6 to 48 hours; incubation pH ranged from 7.4 to 9.2; target free chlorine residual ranged from 0.75 to 1.50 mg/L; incubation temperatures ranged from 18 to 26°C. All samples were buffered to maintain the target incubation pH constant during the incubation period.

Water	Date sampled	Target SDS chlorination conditions			
		Incubation time (hrs)	Incubation temperature (°C)	Free chlorine residual (mg/L)	pH
1	July 24, 1998	6	26	0.75	9.1
2	September 22, 1998	24	20	0.80	9.1
3	September 1, 1998	48	26	0.80	9.2
4	September 23, 1998	24	20	0.75	7.4
5	January 7, 1999	24	18	0.80	7.4
6	October 12, 1998	28	20	1.50	8.5
7	October 22, 1998	24	24	0.75	8.0
8	October 6, 1998	24	20	1.00	7.7

**Table 4 SDS chlorination conditions**

### 3.4 Analytical Methods

A list of all analytical methods and minimum reporting levels (MRLs) used during the study is shown in Table 5. All analyses were conducted at Summers & Hooper, Inc. or Montgomery Watson Laboratories as outlined in Table 6.

Analyte	Waters	Method	Minimum reporting level (MRL)
Alkalinity	All	SM 2320 B	5 mg/L as CaCO <sub>3</sub>
Bromide	All	EPA 300.0 A	20 µg/L
Calcium hardness	All	EPA 200.7	5 mg/L as CaCO <sub>3</sub>
Chlorine dose (solution standardization)	All	SM 4500-Cl B	NA
Chlorine residual	All	SM 4500-Cl F	0.2 mg/L as Cl <sub>2</sub>
HAA (DCAA, TCAA, MBAA, DBAA, BCAA, BDCAA)	1-4, 6-8	EPA 552.2	1.0 µg/L (each analyte)
HAA (MCAA, CDBAA)	1-4, 6-8	EPA 552.2	2.0 µg/L (each analyte)
HAA (TBAA)	1-4, 6-8	EPA 552.2	4.0 µg/L
HAA (DCAA, TCAA, MBAA, DBAA, BCAA, BDCAA)	5	SM 6251 B	1.0 µg/L (each analyte)
HAA (MCAA, CDBAA)	5	SM 6251 B	2.0 µg/L (each analyte)
HAA (TBAA)	5	SM 6251 B	4.0 µg/L
pH	All	4500-H <sup>+</sup> B	NA
Temperature	All	SM 2550 B	NA
Total hardness	All	SM 2340 B	5 mg/L as CaCO <sub>3</sub>
Total organic carbon (TOC)	All	SM 5310 C	0.50 mg/L
Total organic halide (TOX)	All	SM 5320 B	25 µg/L as Cl <sup>-</sup>
THM (CF, BDCM, DBCM, BF)	All	EPA 551.1	1.0 µg/L (each analyte)
UV absorbance at 254 nm (UV <sub>254</sub> )	All	SM 5910 B	0.009 cm <sup>-1</sup>

SM: *Standard Methods*

NA: Not applicable

**Table 5 Summary of analytical methods and MRLs**

Analyses performed	Waters	Laboratory
Alkalinity, chlorine dose, chlorine residual, pH, temperature, TTHM, TOC, TOX, UV <sub>254</sub>	All	Summers & Hooper, Inc.
HAA9	1-4, 6-8	Summers & Hooper, Inc.
Bromide, calcium hardness, total hardness	All	Montgomery Watson Laboratories
HAA9	5	Montgomery Watson Laboratories

**Table 6 Summary of laboratories conducting analyses**

### 3.5 Experimental QA/QC Summary

As a part of this study, field duplicates were performed on 10 percent of samples analyzed in the blended effluent. The field duplicates for DBPs were generated by duplicate SDS chlorination of split GAC effluent samples. The single contactor effluent samples were duplicated at a higher rate, following ICR guidelines, which required that three field duplicates be collected from the

effluent of each RSSCT (25 percent duplication). The results of all field duplicate analyses are summarized in Table 7.

Analyte	Count	Relative percent difference (RD)		
		50th percentile	Mean	Standard deviation
DC	2	6	0	2
VA	2	0	2	7
SDX	2	2	8	3
SM	2	0	2	6
SHA5	2	3	2	8
SHA6	2	7	6	6
SHA9	2	0	5	6
<b>THM Species</b>				
SCF	2	5	8	0
SDCM	2	3	5	6
SDBCM	2	2	8	6
SBF	2	8	8	7
<b>HAA Species</b>				
SDAA	1	0	0	NA
SDCAA	2	8	8	0
SCAA	8	0	2	8
SBAA	0	NA	NA	NA
SDBAA	2	3	8	6
SDCAA	2	0	0	2
SDDBAA	2	4	6	6
SDCBAA	2	0	0	2
SBAA	4	6	0	0

R: relative percent difference  
NA: not applicable

**Table 7 Summary of field duplicate precision for single contactor and blended effluent data**

---

## 4 Results and Discussion

### 4.1 Overview

A substantial portion of the results presented attempt to verify the underlying assumptions behind the surrogate correlation approach (SCA) and examine the limitations of the application of this method for determining the integral breakthrough curve, a relationship between single contactor run time and blended contactor effluent water quality assuming contactor operation in parallel-staggered mode. The SCA procedure requires that all GAC breakthrough data are fit to a logistic function model. From the perspective of data analysis of the ICR GAC treatment study data, there are several advantages to using a model to fit experimental data. Best-fit curve parameters that adequately describe experimental data are less memory intensive than storing the entire experimental data set. A best-fit curve also facilitates interpolation and extrapolation to estimate run times for given treatment objectives. Use of a best-fit model curve provides an estimate of the scatter in the data through the coefficient of determination, and the model minimizes the impact of this scatter on run time estimates. Finally, a function that describes the single contactor experimental data set is a prerequisite for determining the integral breakthrough curve. Run time estimates generated by the integral breakthrough curve are more applicable to full-scale GAC operation where multiple contactors are operated in parallel-staggered mode to increase the service time of each individual contactor.

The SCA procedure (1) links single contactor TOC concentration to single contactor DBP formation at a given run time ( $RT_{SC}$ ), (2) uses the direct integration (DI) approach to model the integral TOC breakthrough curve, (3) determines the blended contactor effluent run time ( $RT_{BC}$ ) at the TOC concentration used, and (4) applies the linked parameters to estimate DBP formation at  $RT_{BC}$ . This approach allows the blended contactor run time to be determined for all correlated parameters based on the TOC integral breakthrough curve. The SCA procedure assumes that:

1. The correlation between TOC and DBP precursors (concentration and speciation) observed in the single contactor effluent is maintained in the blended effluent. A discussion of comparisons made to evaluate the consistency of these correlations is presented in Section 4.2.
2. The three forms of the logistic function model developed can accurately describe the range of breakthrough of DBP precursors and DBP precursor surrogates evaluated. The results of logistic function model fits applied to all parameters and all GAC runs are discussed in Section 4.3.
3. The TOC integral breakthrough curve calculated by the DI approach is an accurate predictor of blended effluent TOC concentration when multiple contactors are operated in parallel-staggered mode. TOC integral breakthrough curves are compared to experimental data in Section 4.3, while an evaluation of the applicability of the infinite contactor assumption inherent by application of the DI procedure is contained in Section 4.5.
4. The integral TOC breakthrough curve can be extrapolated with reasonable results. This assumption was verified for two GAC runs, as discussed in Section 4.6.

Section 4.4 compares the integral breakthrough curves obtained by both the SCA and DI methods against experimental data for the eight GAC runs and all measured parameters.

## 4.2 Correlation between Surrogates and DBPs in Single Contactor and Blended Contactor Effluents

### 4.2.1 Correlation between Surrogate Concentration and DBP Formation

The correlation assumption is an important underlying foundation for the SCA procedure used to model blended effluent water quality. Verifying the assumption would demonstrate that DBP formation is constant at a given TOC concentration in both the single contactor and blended contactor effluent. Since bromide is not adsorbed by GAC, the bromide to TOC ratio will also be constant, at a given TOC concentration, so DBP speciation should not change between single contactor and blended contactor effluents.

To verify the correlation assumption, plots of paired data were generated between TOC and other parameters, such as SDS-TTHM, SDS-HAA6, SDS-CF, SDS-DCAA, etc. Both summed DBP classes and individual compounds were examined. For each water, two experimental data sets were plotted for comparison: single contactor effluent and blended effluent. The entire graph set is included in Appendix D, which includes correlations based on both TOC and UV<sub>254</sub> as surrogates. Overall, both parameters served well as surrogates for DBP formation, and the correlation between single contactor and blended effluent data was approximately equivalent. A representative sample of the results obtained are discussed in this section.

Overall, the correlations observed between TOC and formed DBPs in the blended effluent were very similar to those observed in the single contactors for each water. Figures 6 and 7 show the correlation of UV<sub>254</sub>, SDS-TTHM, SDS-HAA6, and SDS-TOX to TOC for both the single contactor and blended effluent of Waters 1 and 2 (with the exception of SDS-TOX, for which blended effluent samples were not analyzed in these waters). The correlation between TOC and UV<sub>254</sub> in the blended effluent was very similar to that in the single contactor effluent for these two waters, which was typical of that observed in most cases. The greatest difference in blended effluent and single contactor correlations for TOC and SDS-TTHM occurred for Water 8 (Figure 8) which showed a similar disparity between the blended effluent and single contactor correlations for TOC and UV<sub>254</sub>. Still, at a given TOC concentration, SDS-TTHM formation in the blended effluent was within 5 µg/L of that in the single contactor effluent.

For the THM species, correlations between single contactor and blended effluent TOC and formed concentrations are shown in Figures 9 and 10 for Waters 2 and 3, respectively. For all four species, a very good agreement existed between single contactor and blended effluent TOC correlations. This includes SDS-BF, which yielded a "peak" curve for these two runs. The peak also occurred in the blended effluent, and the single contactor and blended effluent yielded very similar curves when SDS-BF concentrations were plotted against TOC. The correlation of formed THM compounds between single contactor and blended effluent was very good for all waters. The largest difference between correlations seen in the single contactor and blended effluent were observed for Water 8, shown in Figure 11, for which the formed THM species concentrations were low.

Four of the predominant HAA species formed (DCAA, TCAA, DBAA, and BCAA) correlated to TOC concentration for both single contactor and blended effluents are shown in Figures 12 and

13 for Waters 5 and 7, respectively. For Water 5 both single contactor and blended effluent formed HAAs matched very well. For Water 7, the correlations for SDS-DBAA and SDS-BCAA also matched very well. The single contactor and blended effluent correlations between TOC and SDS-DCAA and SDS-TCAA showed slight differences, not exceeding 3 µg/L. The formed levels of these two compounds were low for this water.

Correlations between single contactor and blended effluent for SDS-DCBAA, SDS-CDBAA, SDS-HAA5, and SDS-HAA9 are shown for Waters 2 and 4 in Figures 14 and 15, respectively. Water 2 is shown as it yielded the largest difference in the correlation between single contactor and blended effluent for these parameters, although formed DCBAA and CDBAA levels were low. Water 4 is more representative of what was typically observed, with the correlation between TOC and these parameters in the blended effluent matching that observed in the single contactor very well. For SDS-TBAA, only Water 7 yielded measured levels above the MRL (4 µg/L). The correlation between TOC and formed TBAA in the blended effluent agreed well with that observed in the single contactor effluent, as shown in Figure 16.

The use of UV<sub>254</sub> as a surrogate for these correlations instead of TOC was investigated. In a few cases, UV<sub>254</sub> as a surrogate yielded better correlations between single contactor and blended effluent formed DBPs than did TOC. However, in other instances, and approximately the same number of cases, the correlations using TOC were superior. Because the results for the correlations using UV<sub>254</sub> did not improve over those using TOC, the use of TOC as the surrogate in the SCA procedure was continued. Appendix D also summarizes the correlations observed based on UV<sub>254</sub>.

In summary, this analysis shows that the correlation between DBP formation and TOC concentration in the single contactor and blended contactor effluents is constant. This find is significant because it verifies one of the underlying assumptions behind the SCA procedure, that TOC concentration can be correlated to DBP formation in the single contactor effluent, and that this correlation can then be applied to blended contactor effluent. Section 4.3 will address how single contactor effluent data can be modeled as a function of run time so that this correlation can be utilized to predict blended contactor effluent DBP formation.

#### 4.2.2 Correlation between Surrogates and DBP Speciation

For all four models relating bromine incorporation for THMs and HAA9 ( $n_{Br}$  and  $n'_{Br}$ , respectively) to TOC and UV<sub>254</sub>, the polynomial models described in Section 3.2.6 were found to be appropriate. The model variance over all four combinations of  $n_{Br}$  and  $n'_{Br}$  as a function of TOC and UV<sub>254</sub> yielded R<sup>2</sup> values greater than 0.92 in each case. Although the effect ( $\gamma$ ) of blending on mean bromine incorporation was found to be statistically significant, including this effect improved R<sup>2</sup> values trivially (less than 1 percent for all four cases) by. There was no evidence that different linear or quadratic terms were needed to describe the single contactor and blended effluent data. For THMs, Figures 17 through 24 show the results of fitting second order polynomials to the relationship between  $n_{Br}$  and TOC, combining single and blended contactor data for each water. For HAA9, similar results for the relationship between  $n'_{Br}$  and TOC are shown in Figures 25 through 32. The second order polynomial curve fits for the correlation between  $n_{Br}$  and UV<sub>254</sub> and  $n'_{Br}$  and UV<sub>254</sub> for both single and blended contactor data are shown in Figures 33 through 48.

This analysis shows that there is no significant difference between DBP bromine incorporation between single contactor and blended contactor effluents at equivalent TOC or  $UV_{254}$  values. This conclusion supports the use of the SCA procedure, especially for individual DBP species, because the SCA assumes that DBP formation and speciation in the single contactor effluent at a given TOC concentration is equivalent to that in the blended contactor effluent at the same TOC concentration.

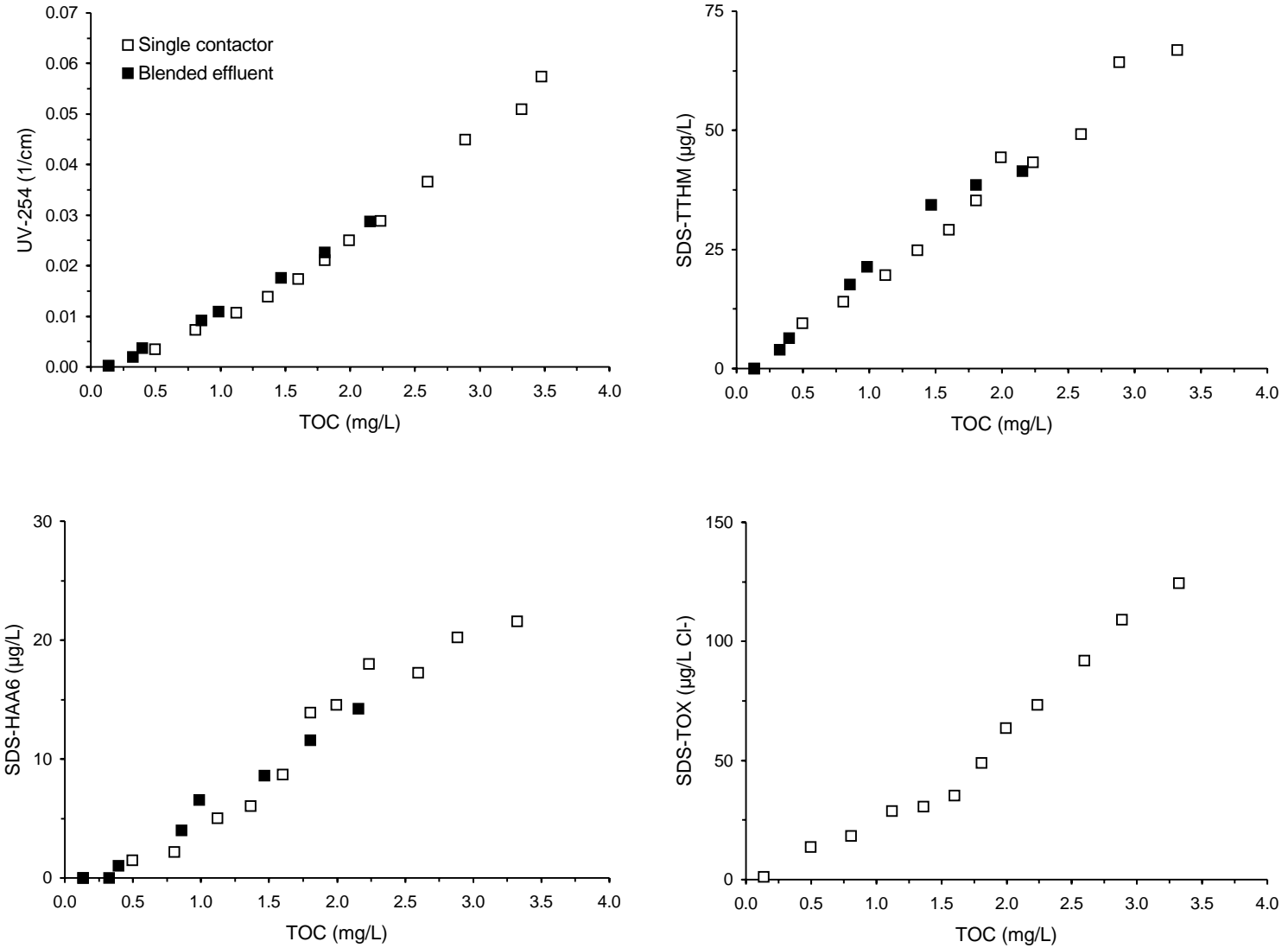


Figure 6 Correlations based on GAC effluent TOC concentration for single contactor and blended effluents for Water 1

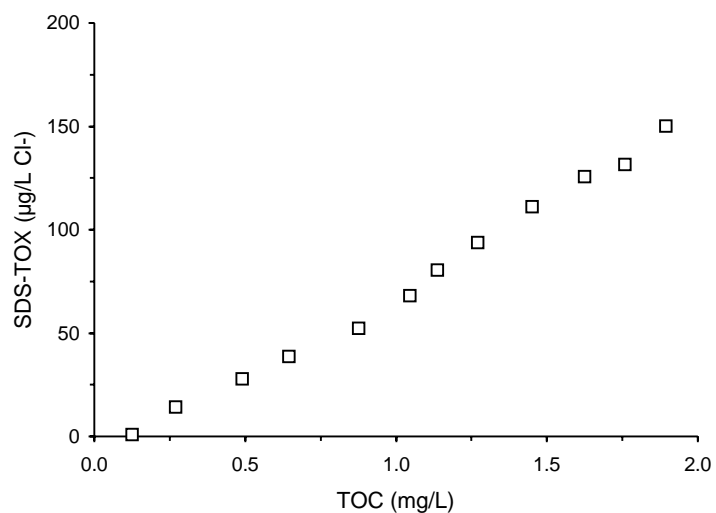
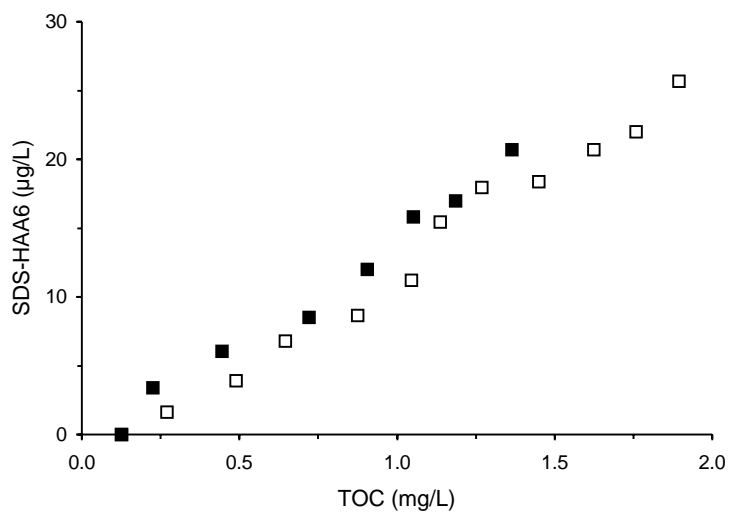
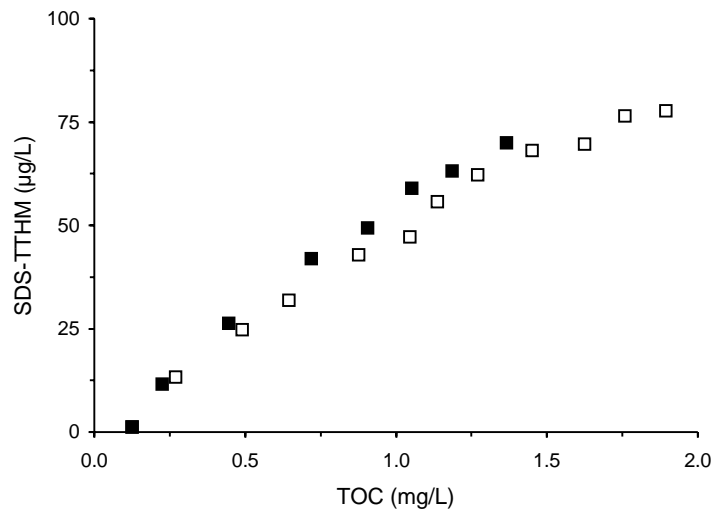
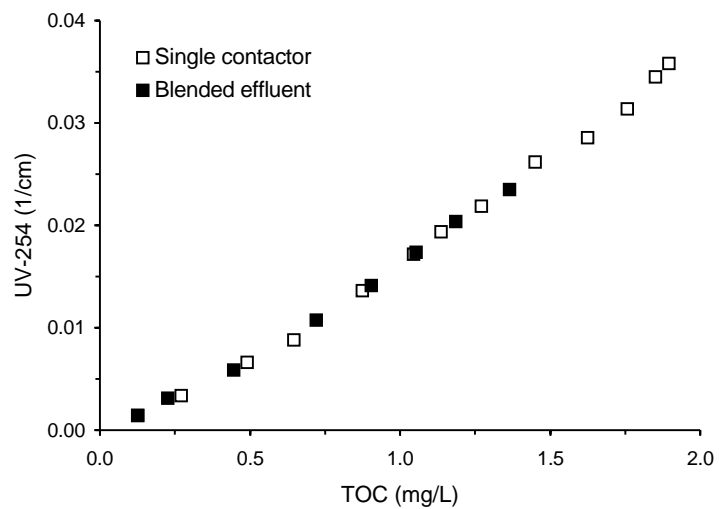


Figure 7 Correlations based on GAC effluent TOC concentration for single contactor and blended effluents for Water 2

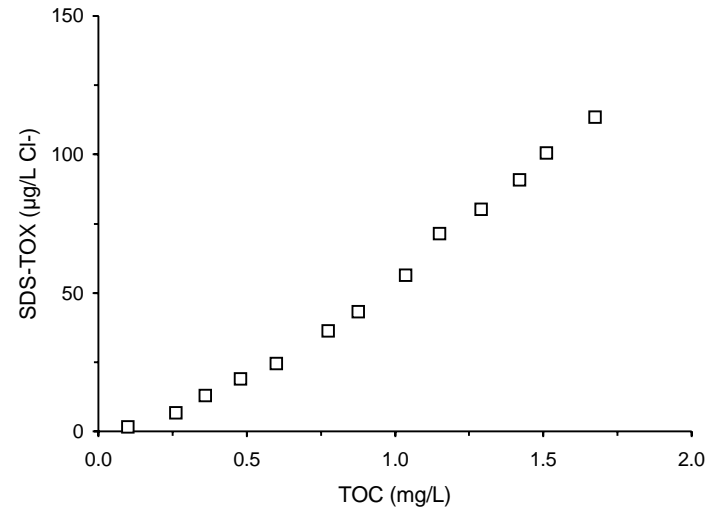
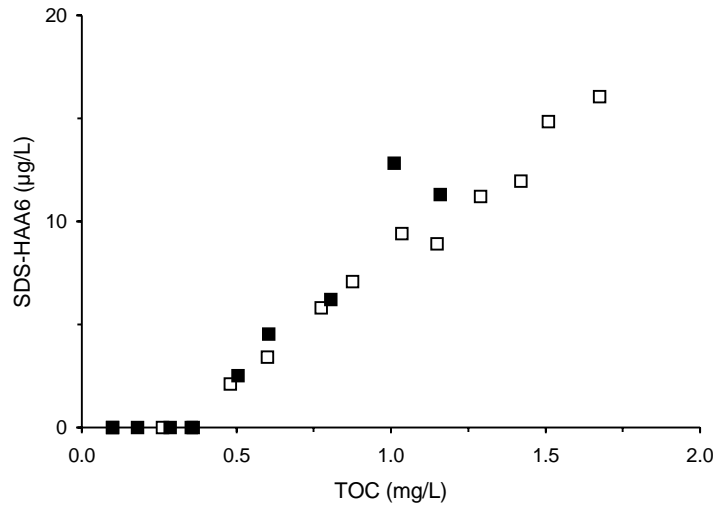
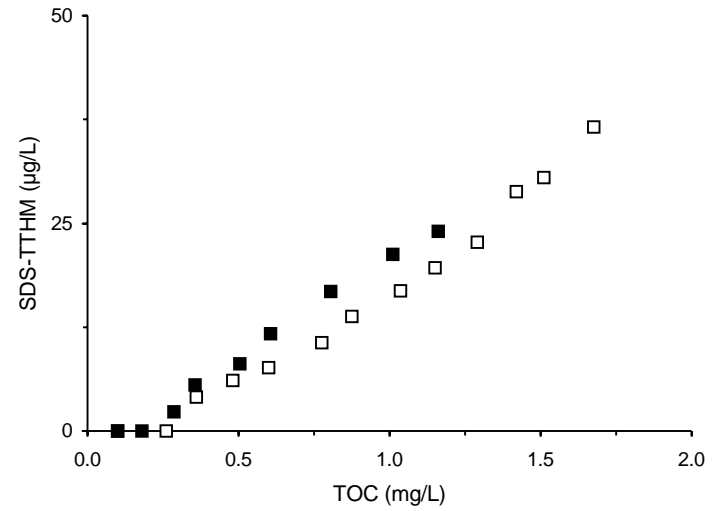
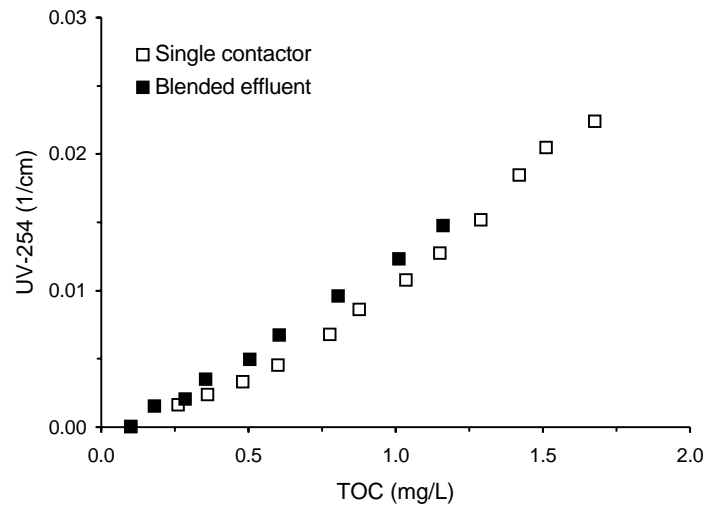


Figure 8 Correlations based on GAC effluent TOC concentration for single contactor and blended effluents for Water 8

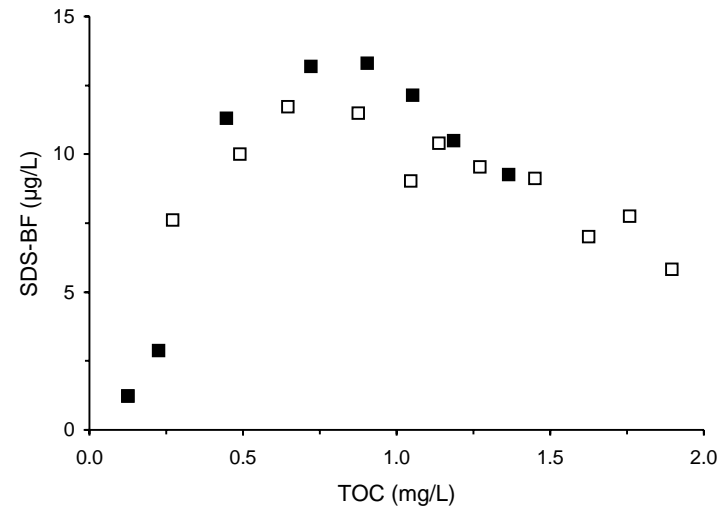
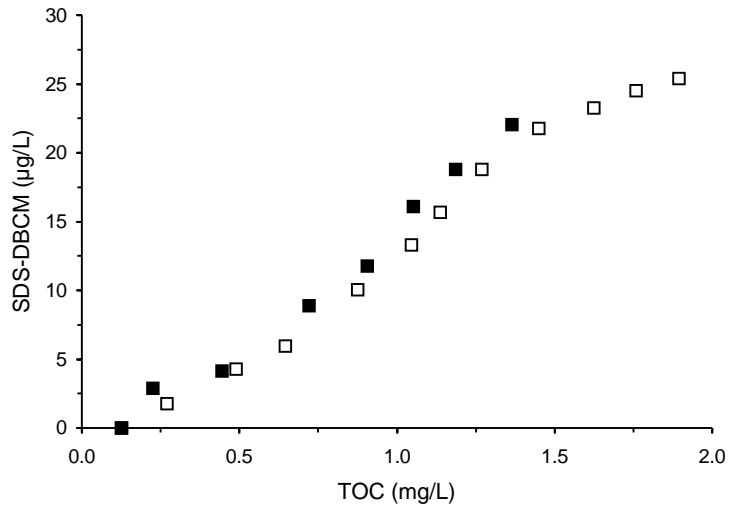
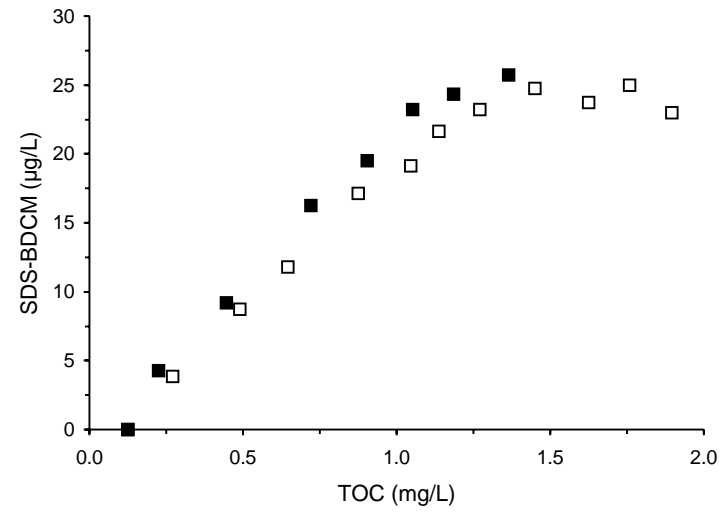
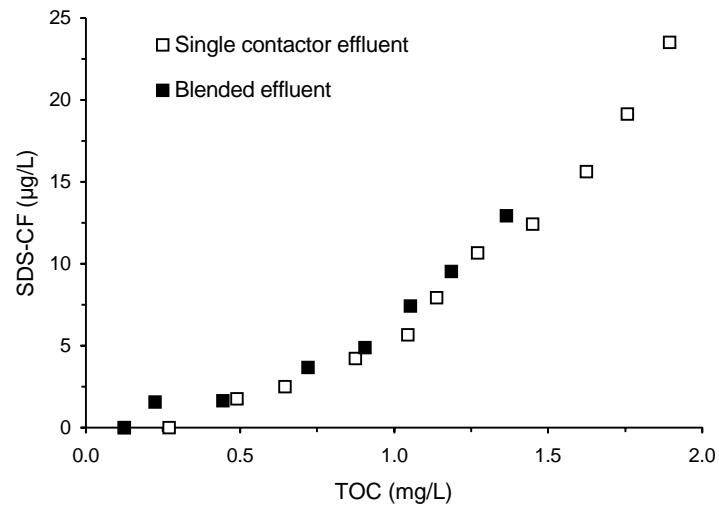


Figure 9 THM correlations based on GAC effluent TOC concentration for single contactor and blended effluents for Water 2

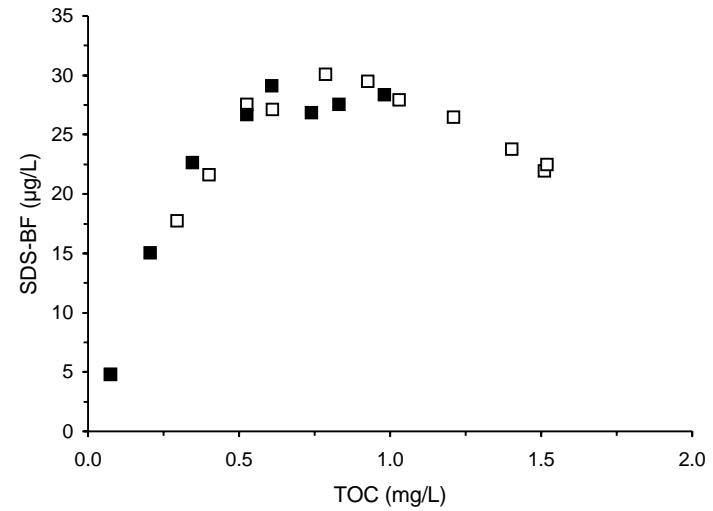
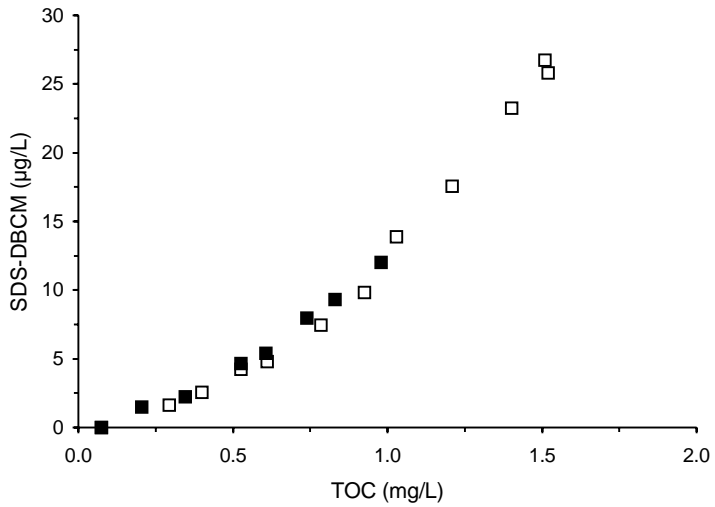
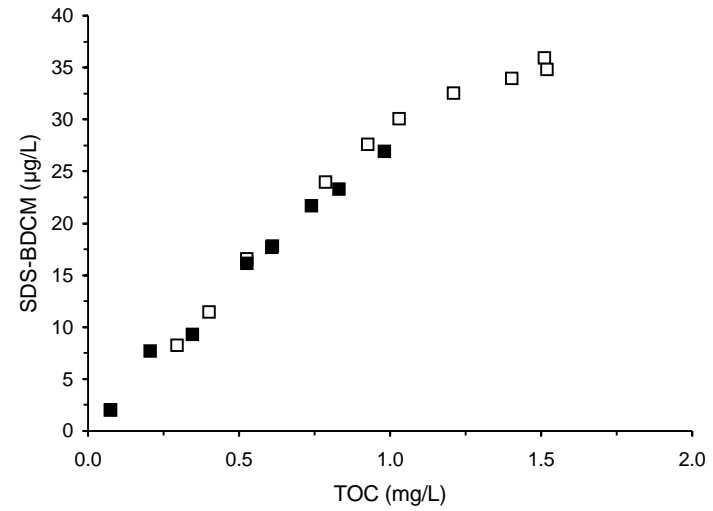
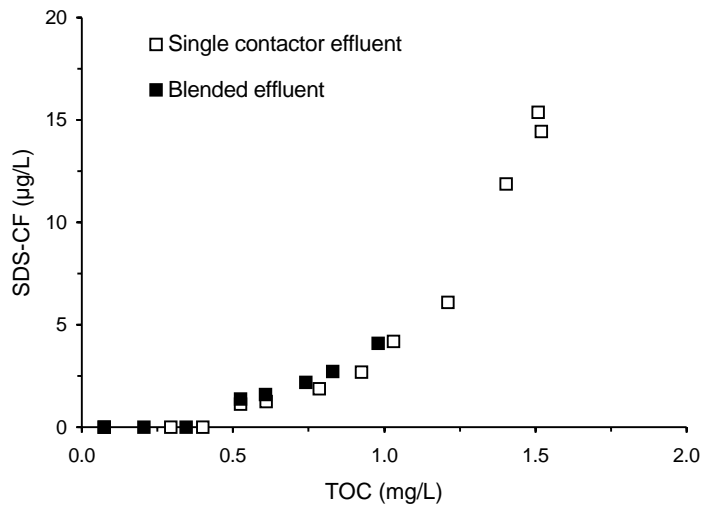


Figure 10 THM correlations based on GAC effluent TOC concentration for single contactor and blended effluents for Water 3

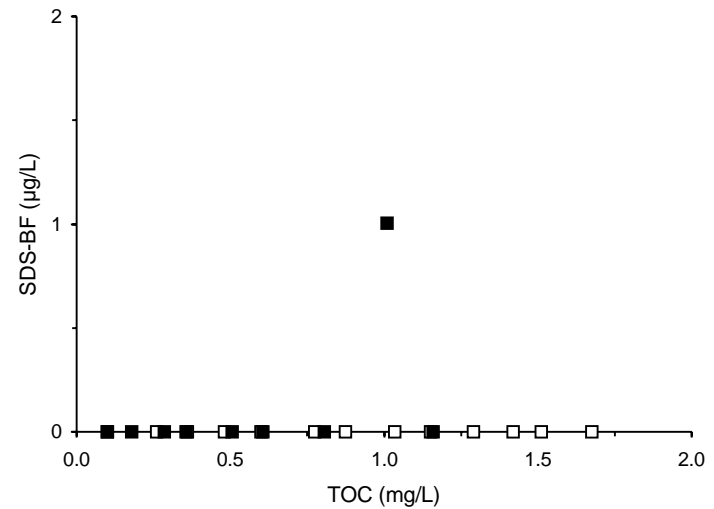
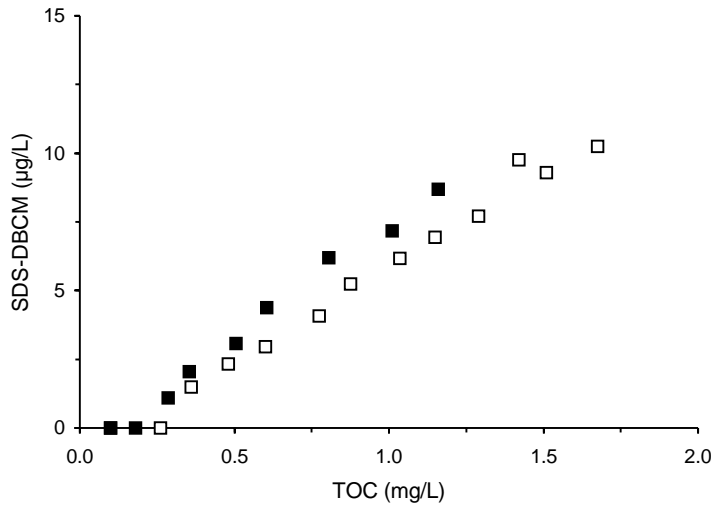
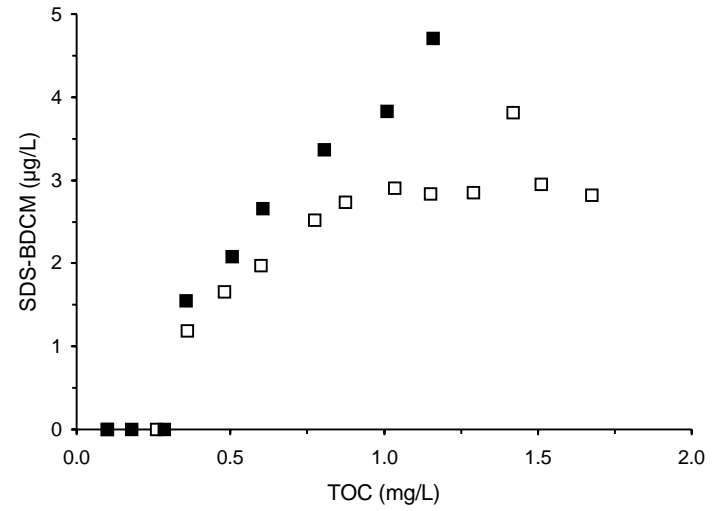
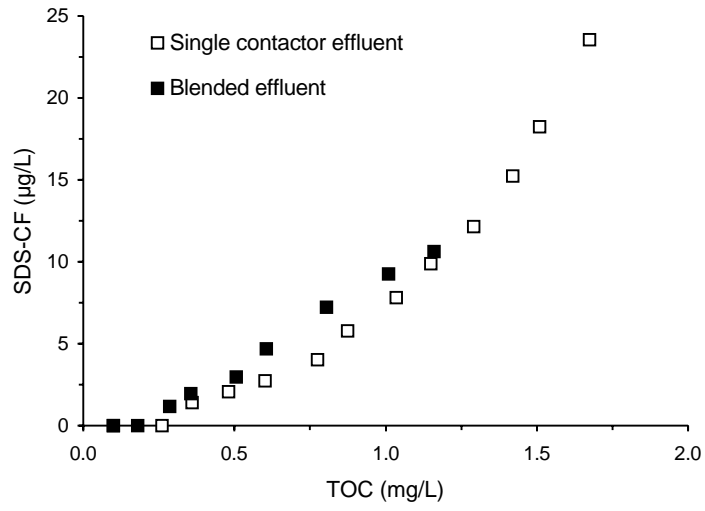


Figure 11 THM correlations based on GAC effluent TOC concentration for single contactor and blended effluents for Water 8

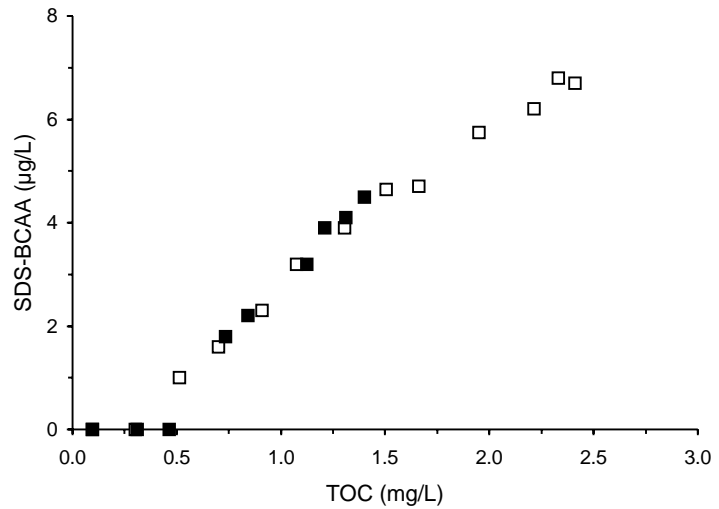
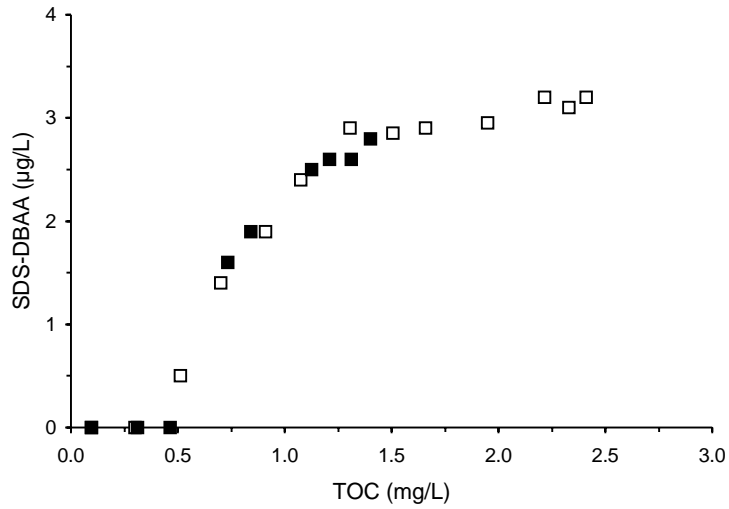
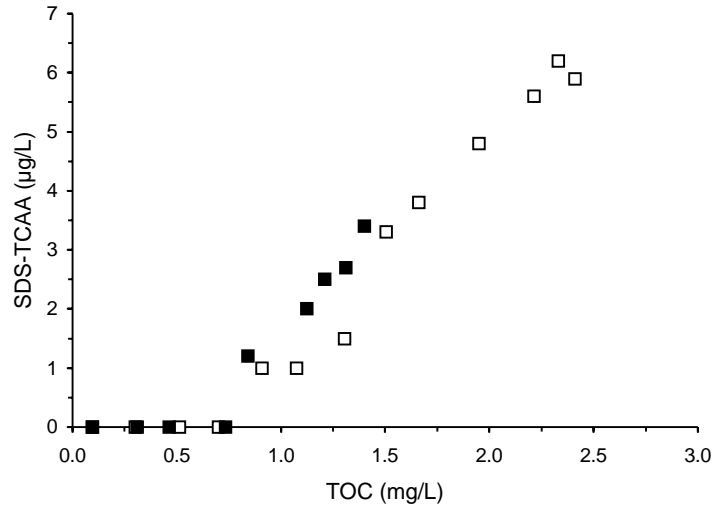
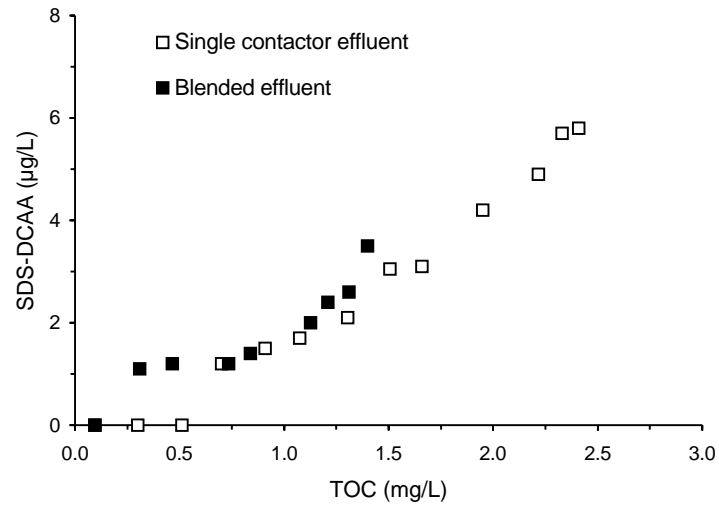


Figure 12 HAA correlations based on GAC effluent TOC concentration for single contactor and blended effluents for Water 5

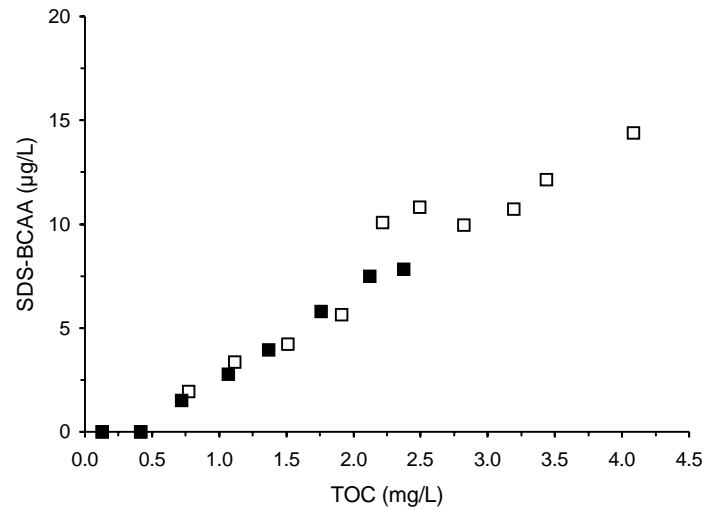
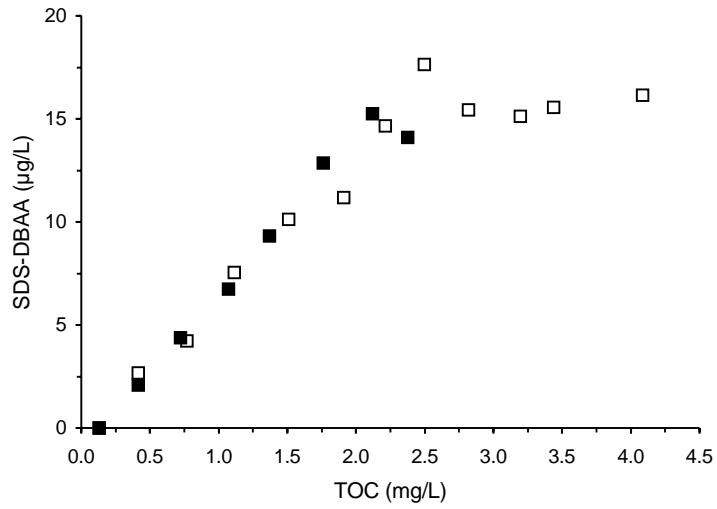
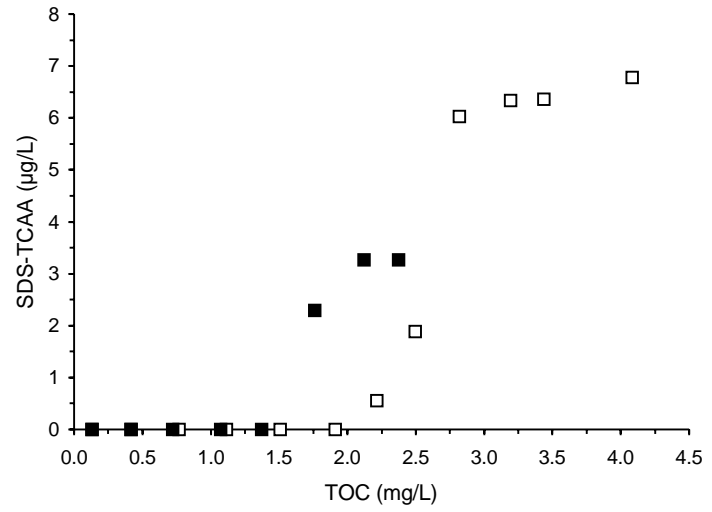
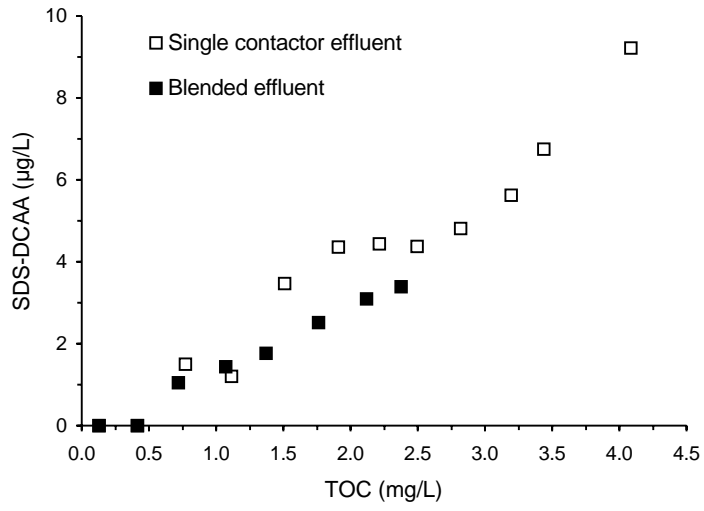


Figure 13 HAA correlations based on GAC effluent TOC concentration for single contactor and blended effluents for Water 7

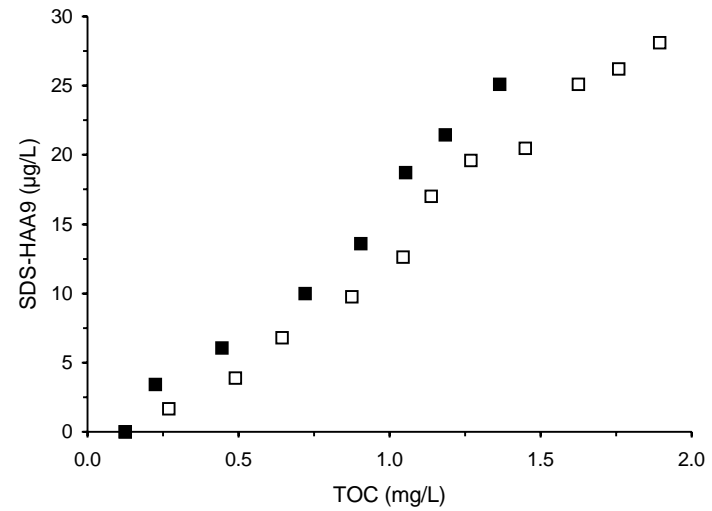
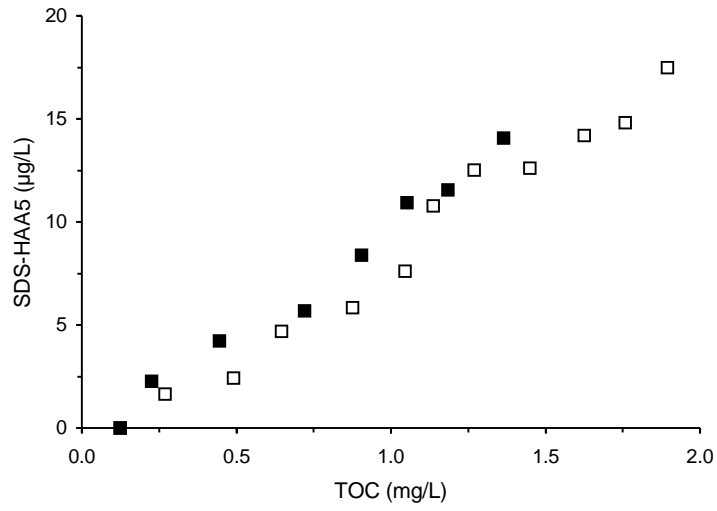
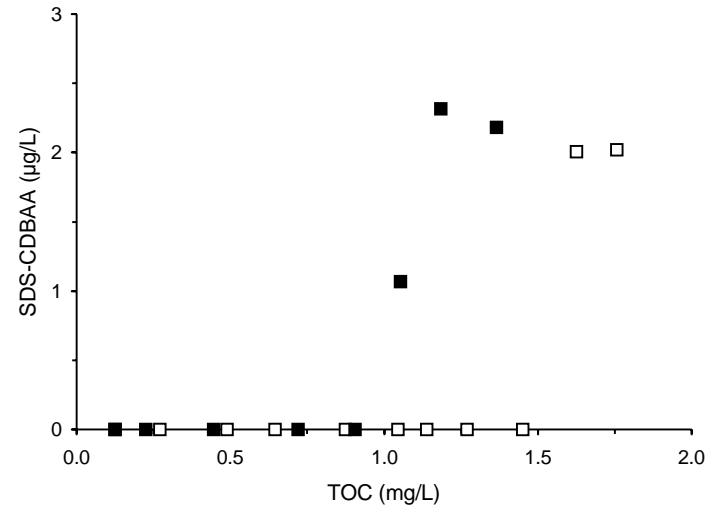
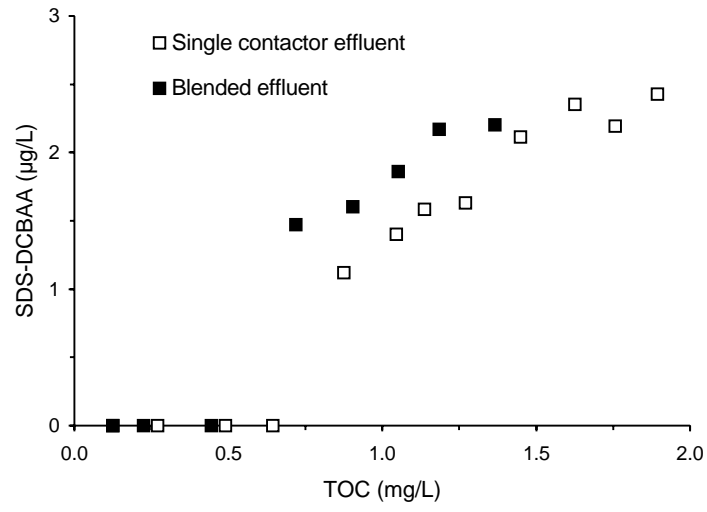


Figure 14 HAA correlations based on GAC effluent TOC concentration for single contactor and blended effluents for Water 2

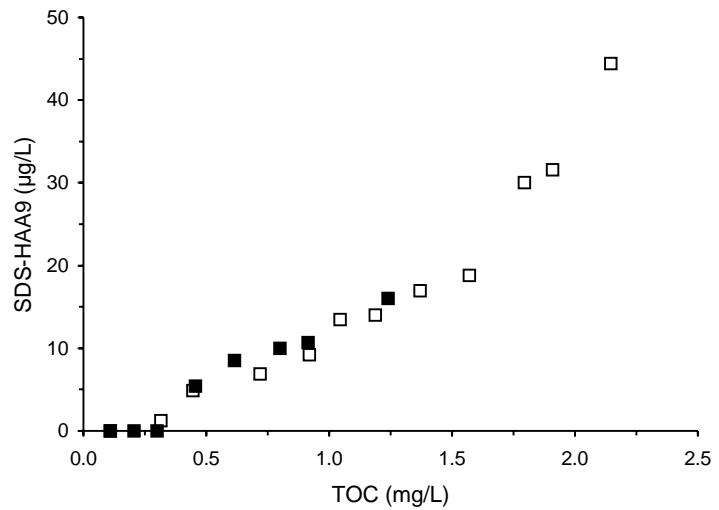
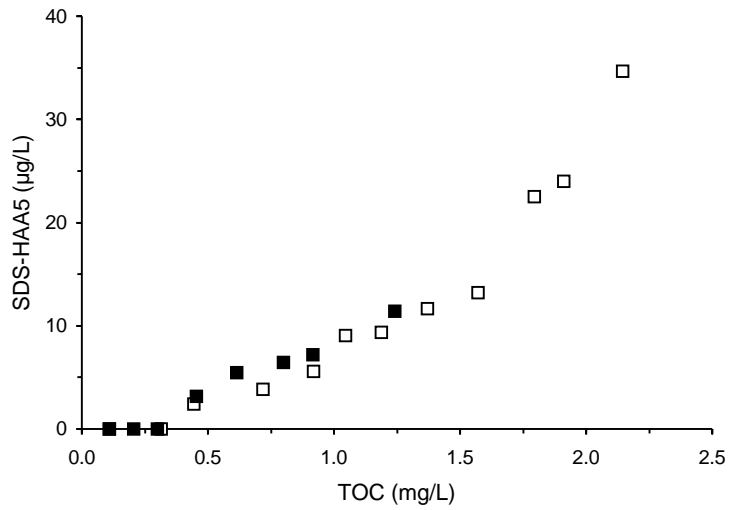
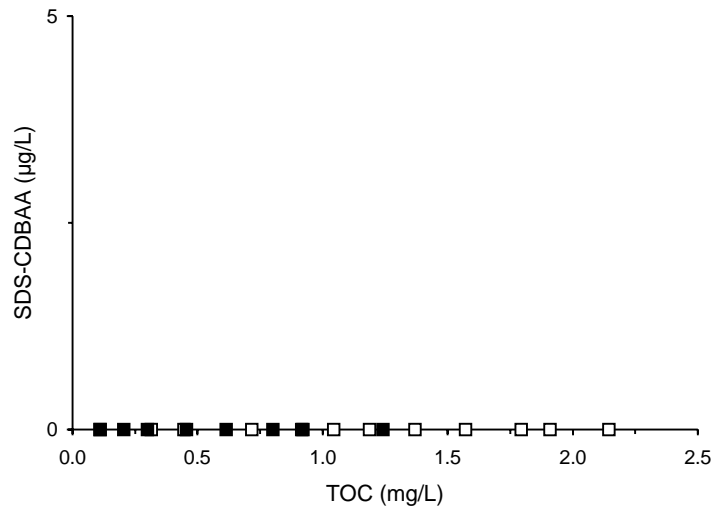
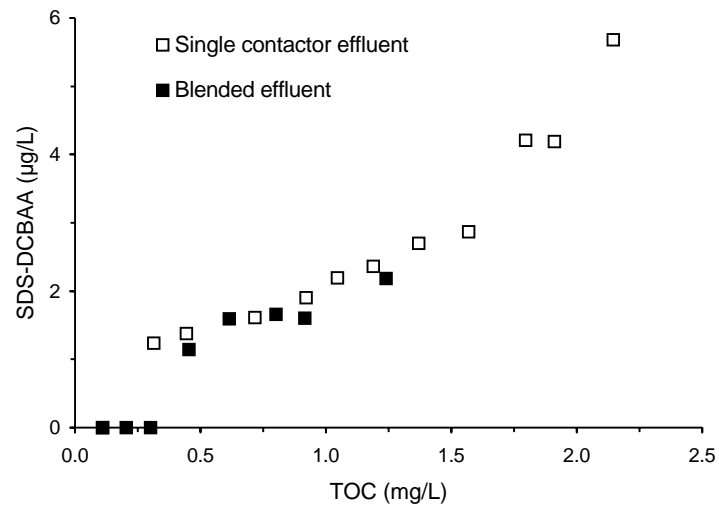


Figure 15 HAA correlations based on GAC effluent TOC concentration for single contactor and blended effluents for Water 4

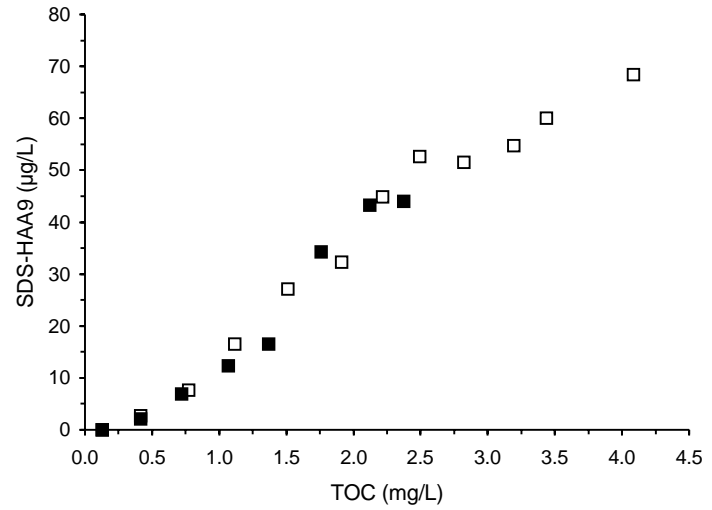
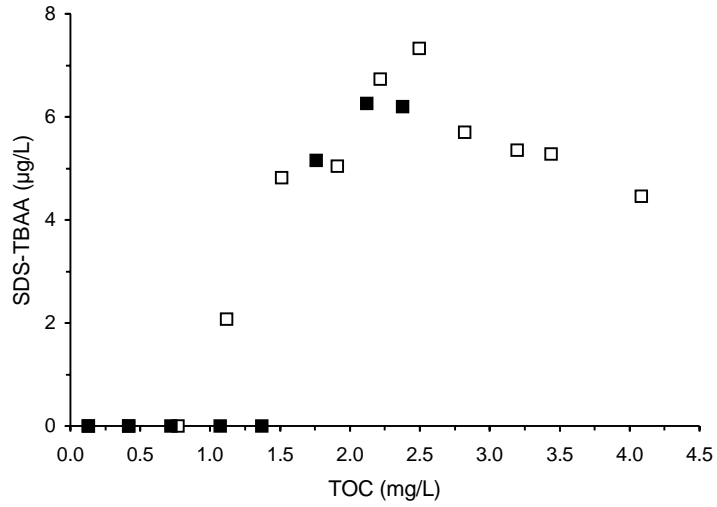
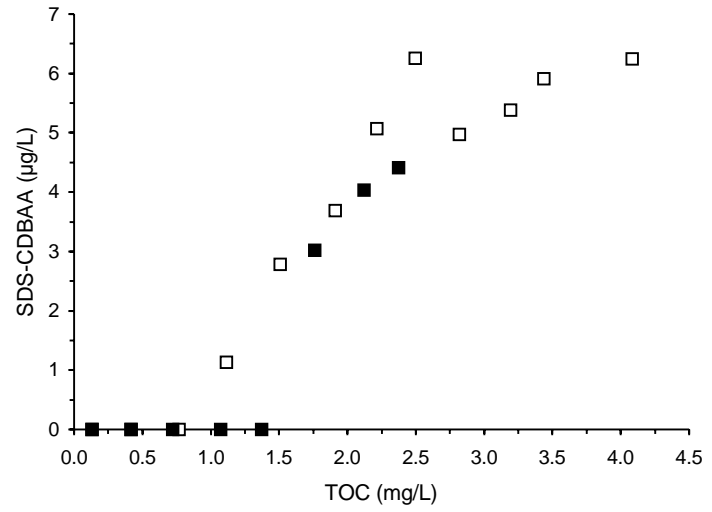
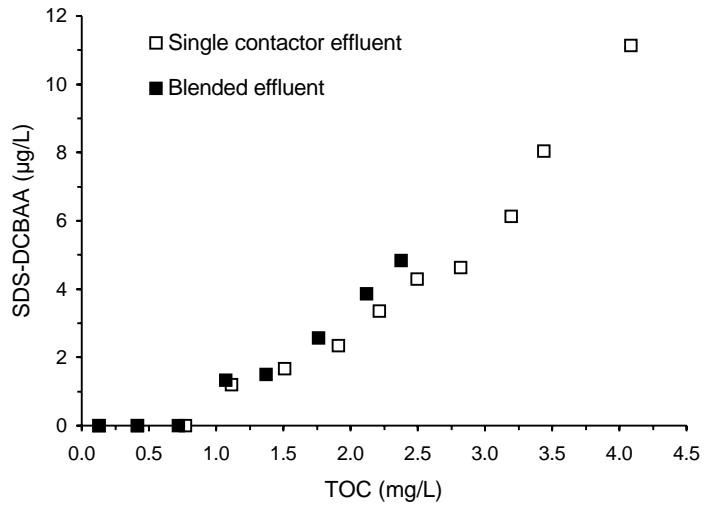
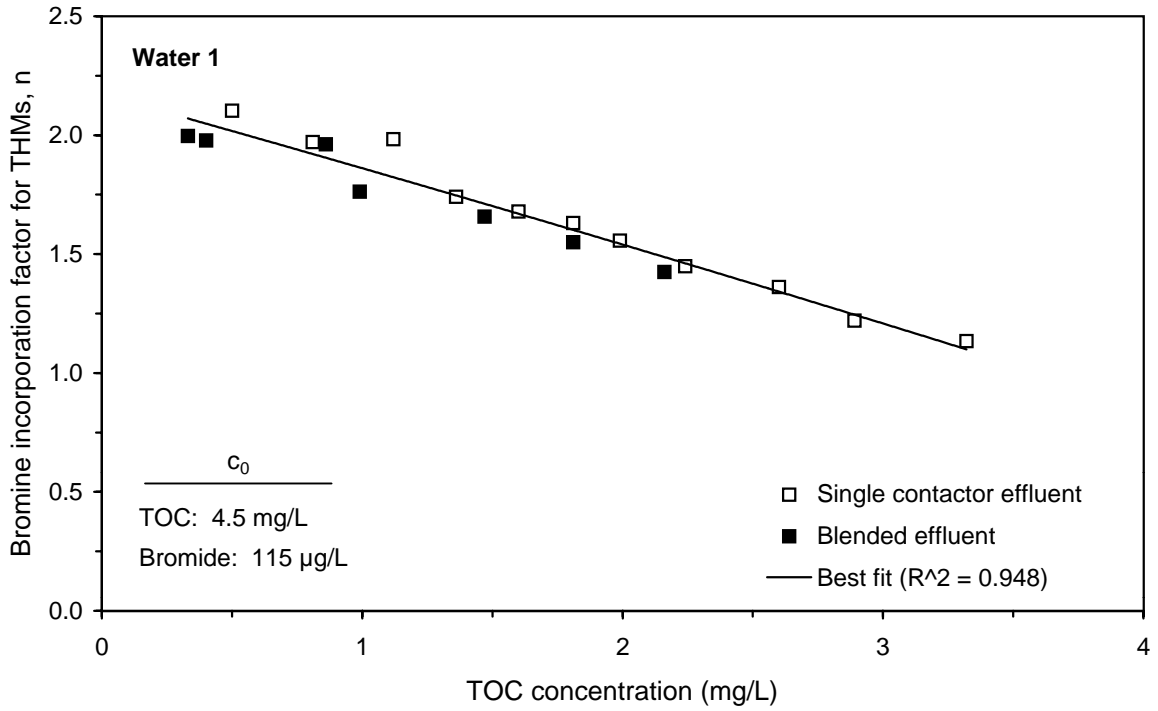
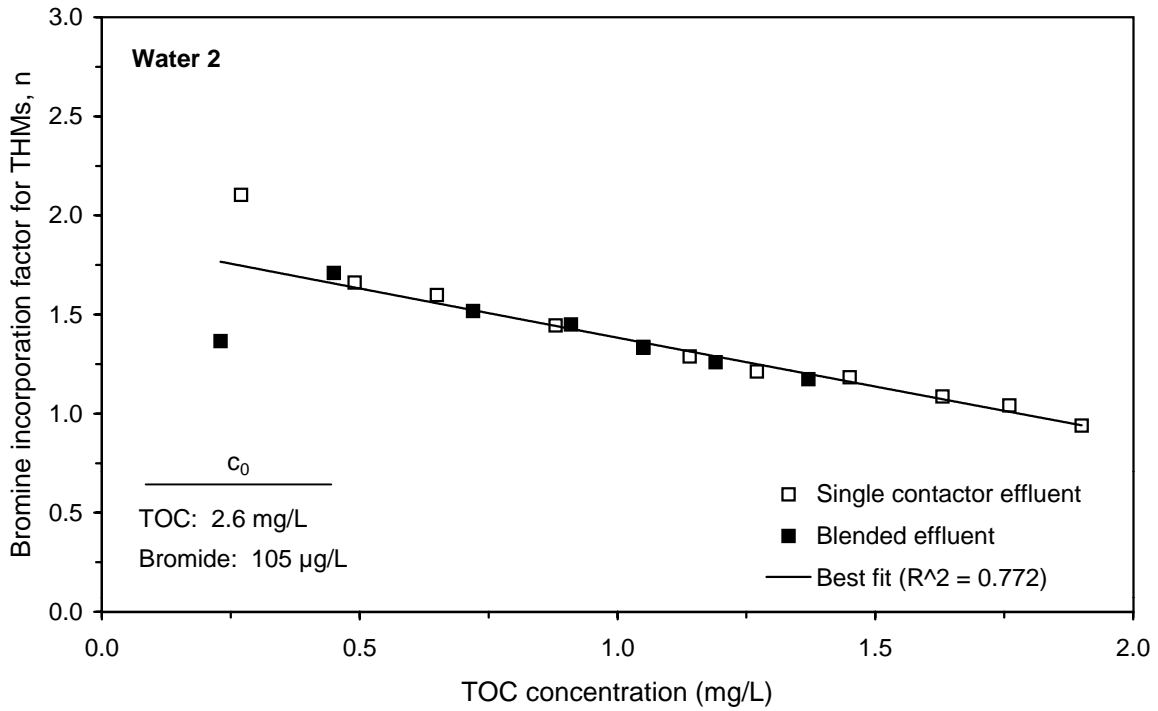


Figure 16 HAA correlations based on GAC effluent TOC concentration for single contactor and blended effluents for Water 7



**Figure 17 Correlation between single contactor and blended effluent TOC concentration and THM bromine incorporation factor (n) for Water 1**



**Figure 18 Correlation between single contactor and blended effluent TOC concentration and THM bromine incorporation factor (n) for Water 2**

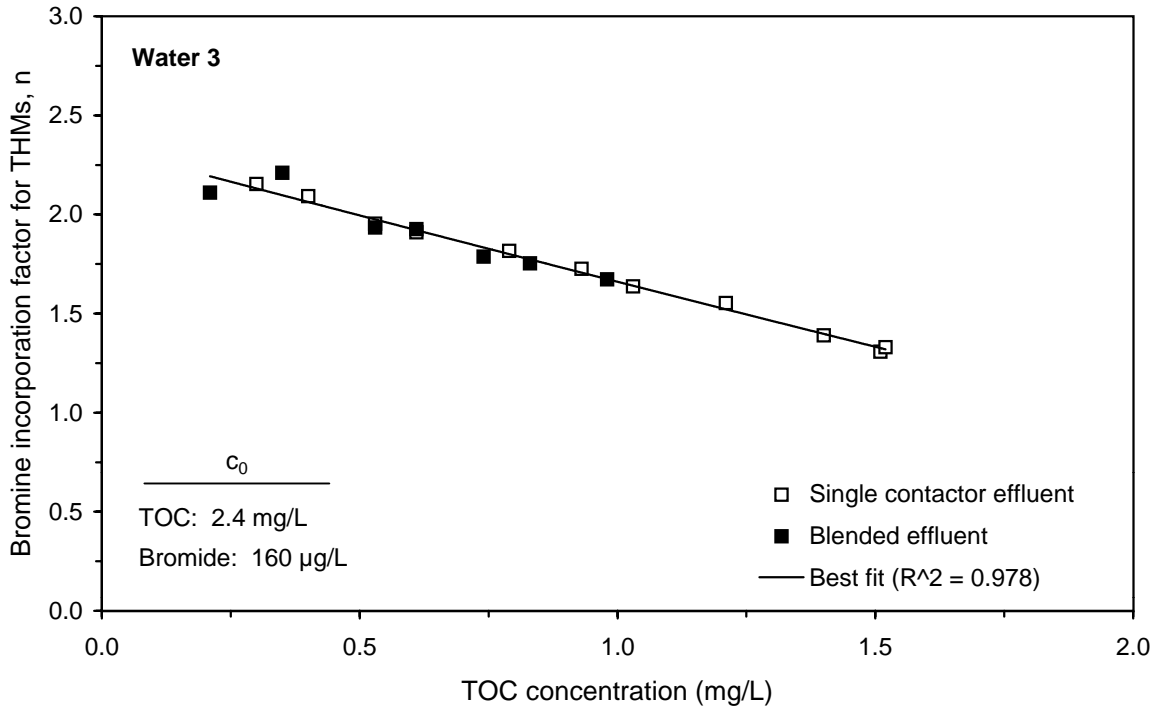


**Figure 19 Correlation between single contactor and blended effluent TOC concentration and THM bromine incorporation factor (n) for Water 3**

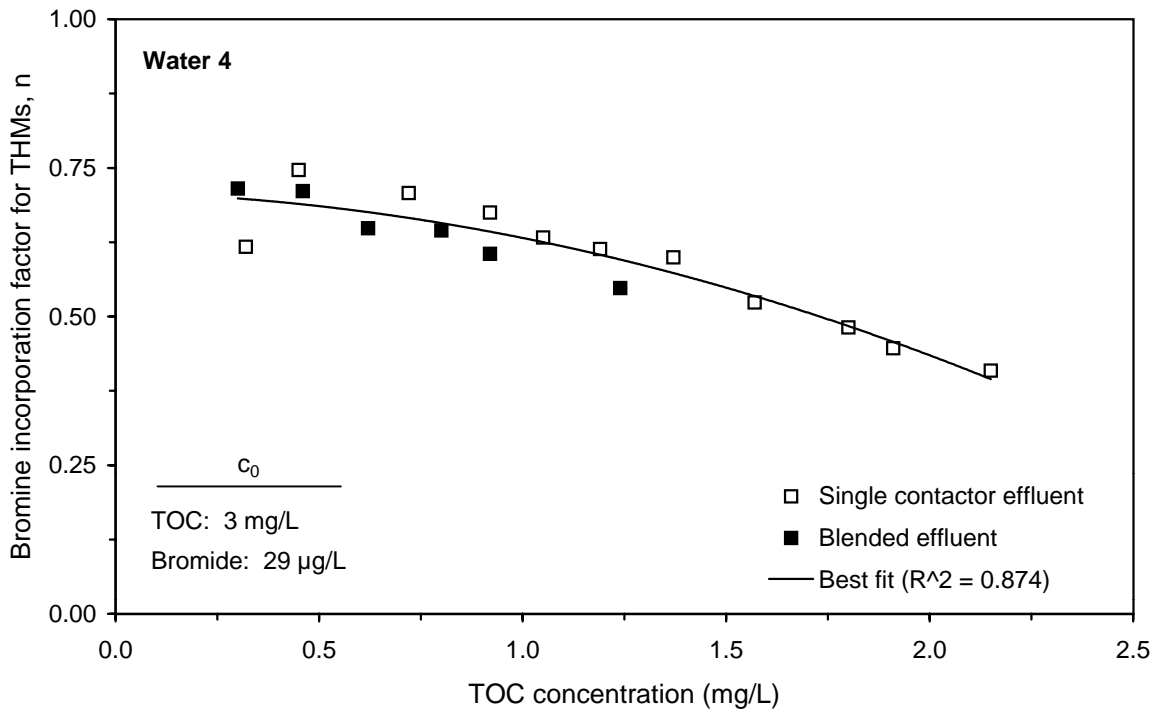


**Figure 20 Correlation between single contactor and blended effluent TOC concentration and THM bromine incorporation factor (n) for Water 4**

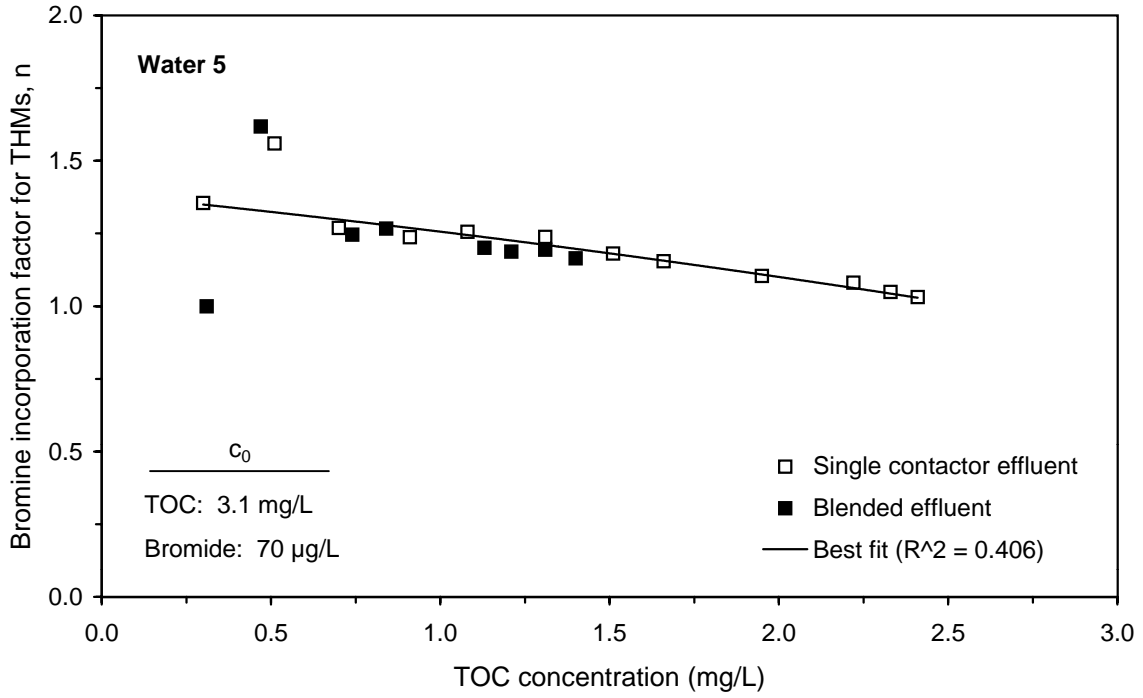


**Figure 21 Correlation between single contactor and blended effluent TOC concentration and THM bromine incorporation factor (n) for Water 5**

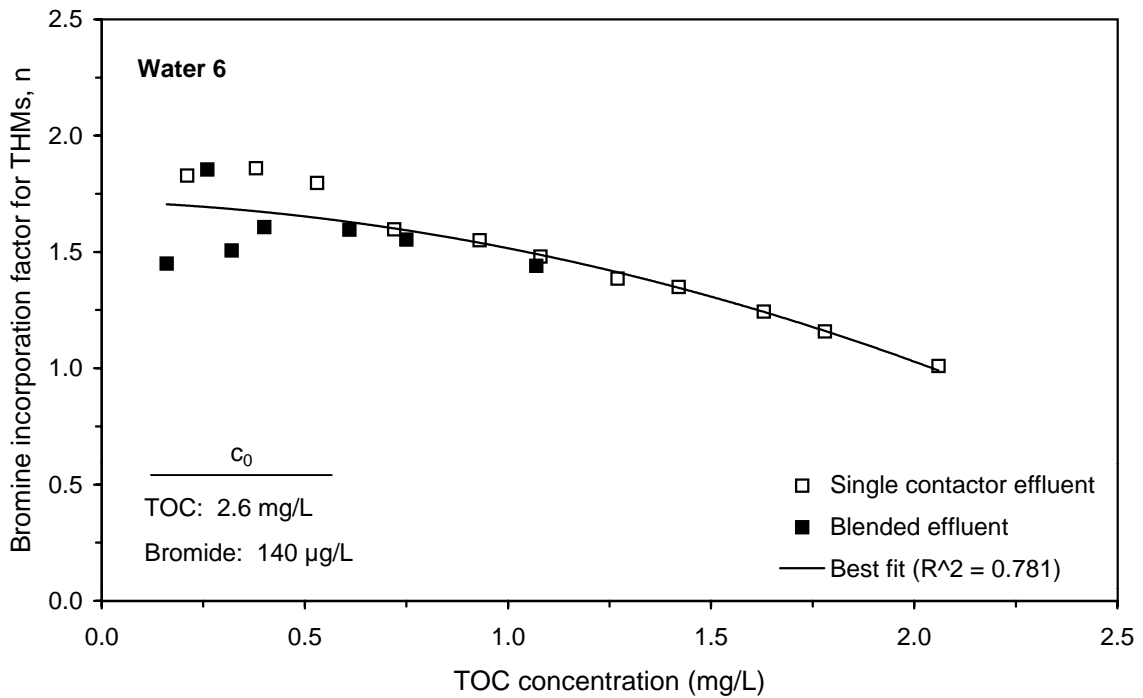


**Figure 22 Correlation between single contactor and blended effluent TOC concentration and THM bromine incorporation factor (n) for Water 6**

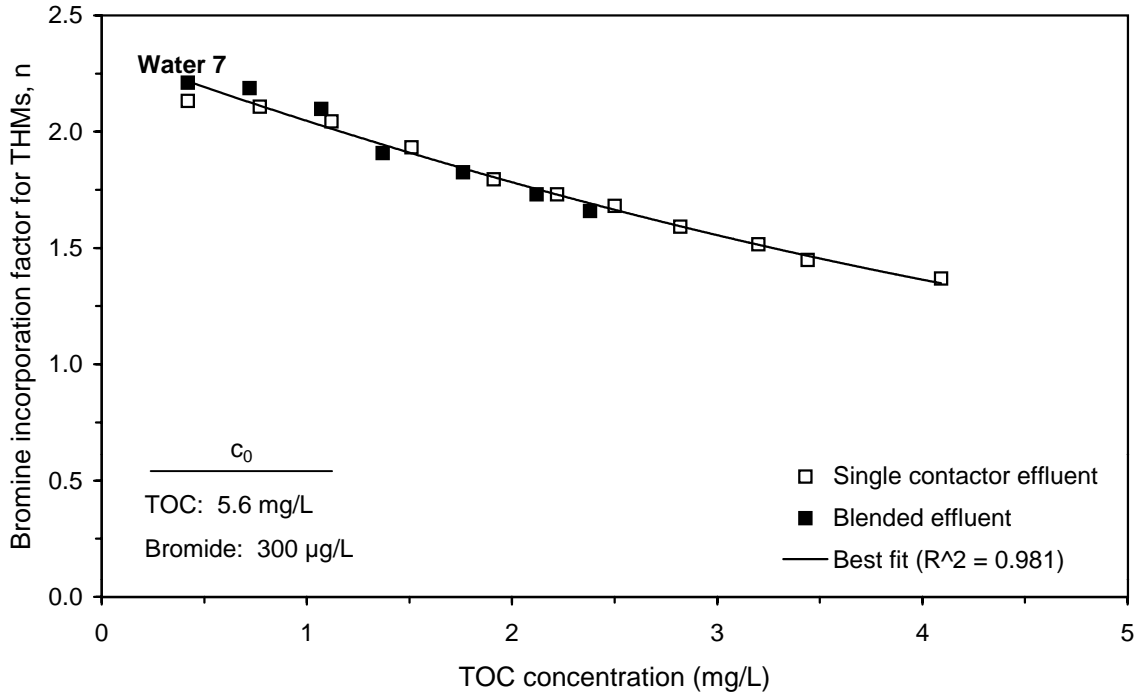


**Figure 23 Correlation between single contactor and blended effluent TOC concentration and THM bromine incorporation factor (n) for Water 7**

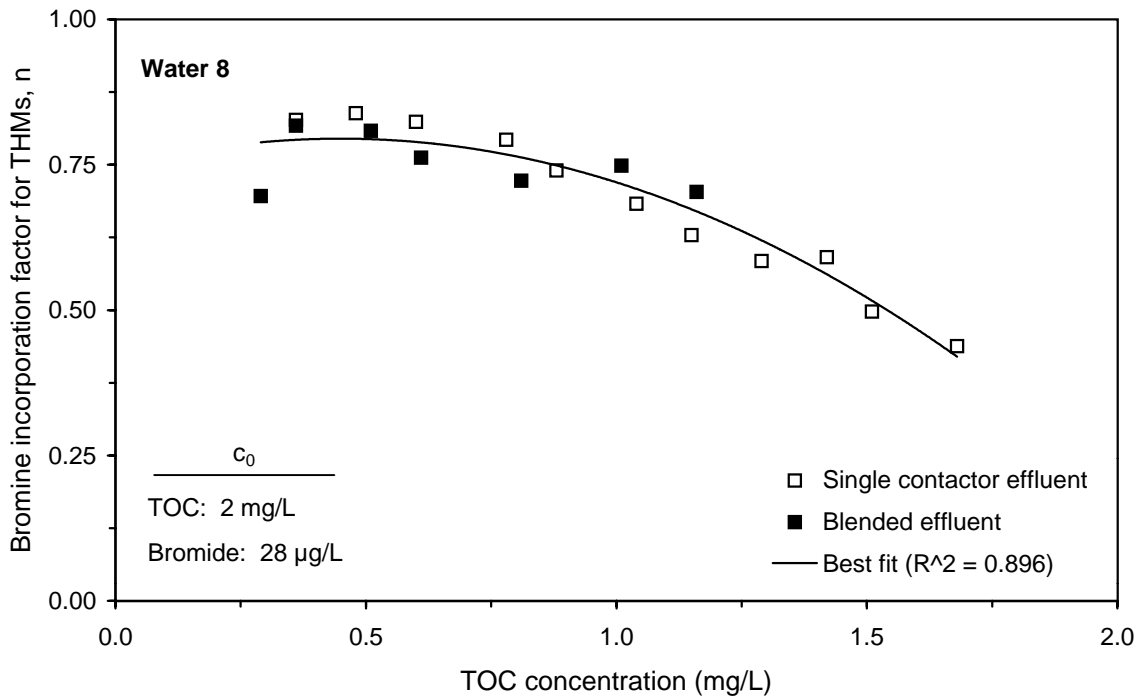


**Figure 24 Correlation between single contactor and blended effluent TOC concentration and THM bromine incorporation factor (n) for Water 8**

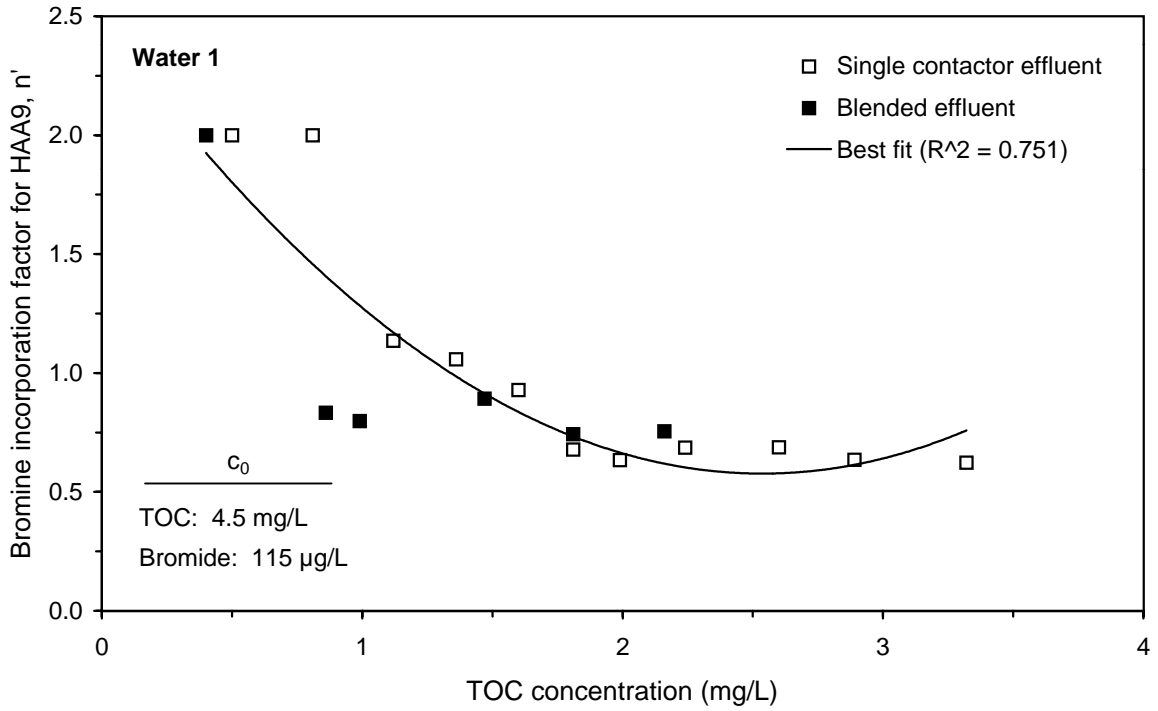


**Figure 25 Correlation between single contactor and blended effluent TOC concentration and HAA9 bromine incorporation factor (n') for Water 1**

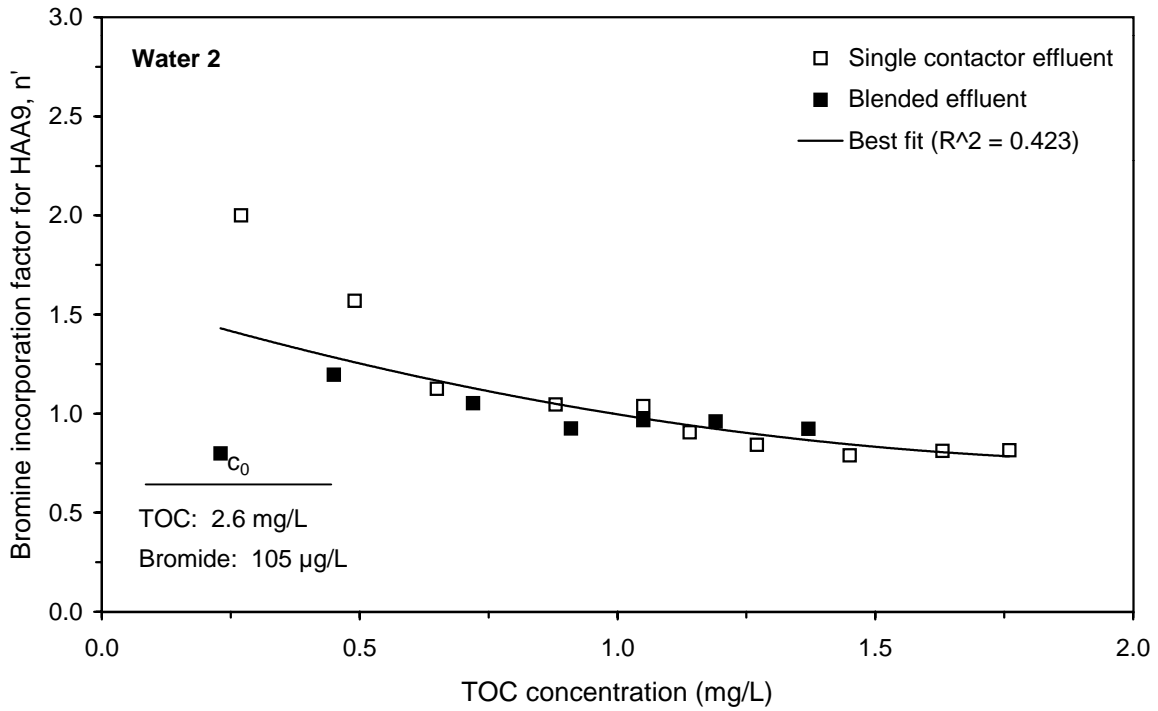


**Figure 26 Correlation between single contactor and blended effluent TOC concentration and HAA9 bromine incorporation factor (n') for Water 2**

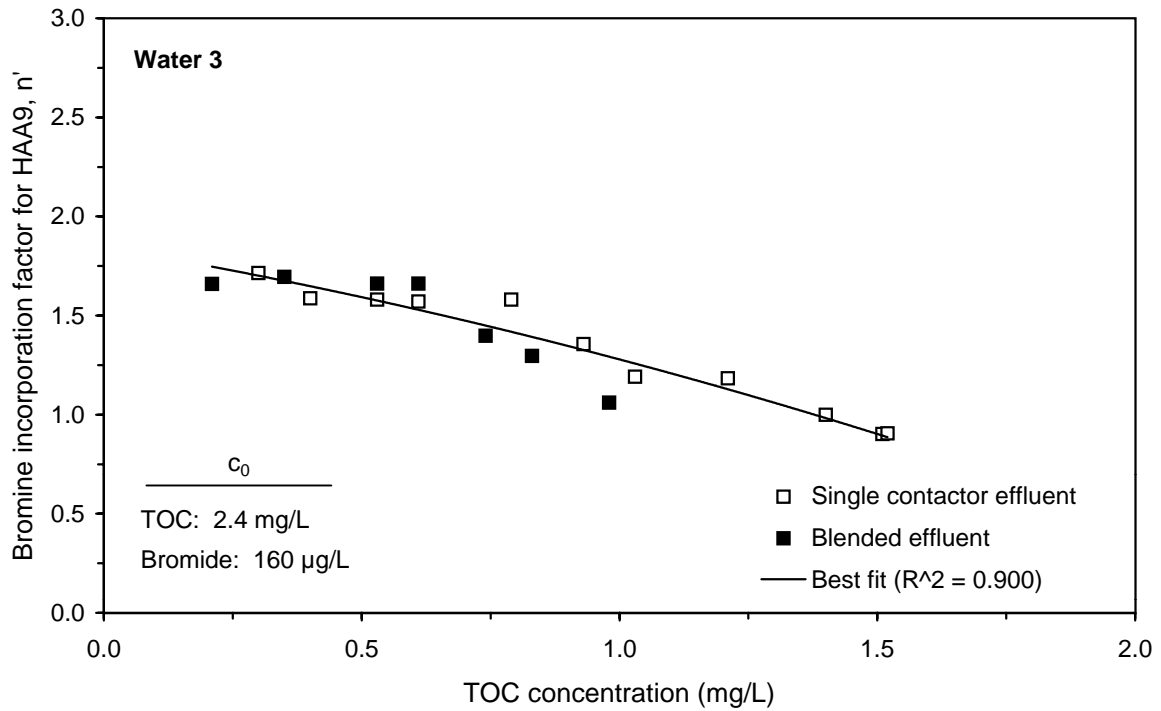


**Figure 27 Correlation between single contactor and blended effluent TOC concentration and HAA9 bromine incorporation factor ( $n'$ ) for Water 3**

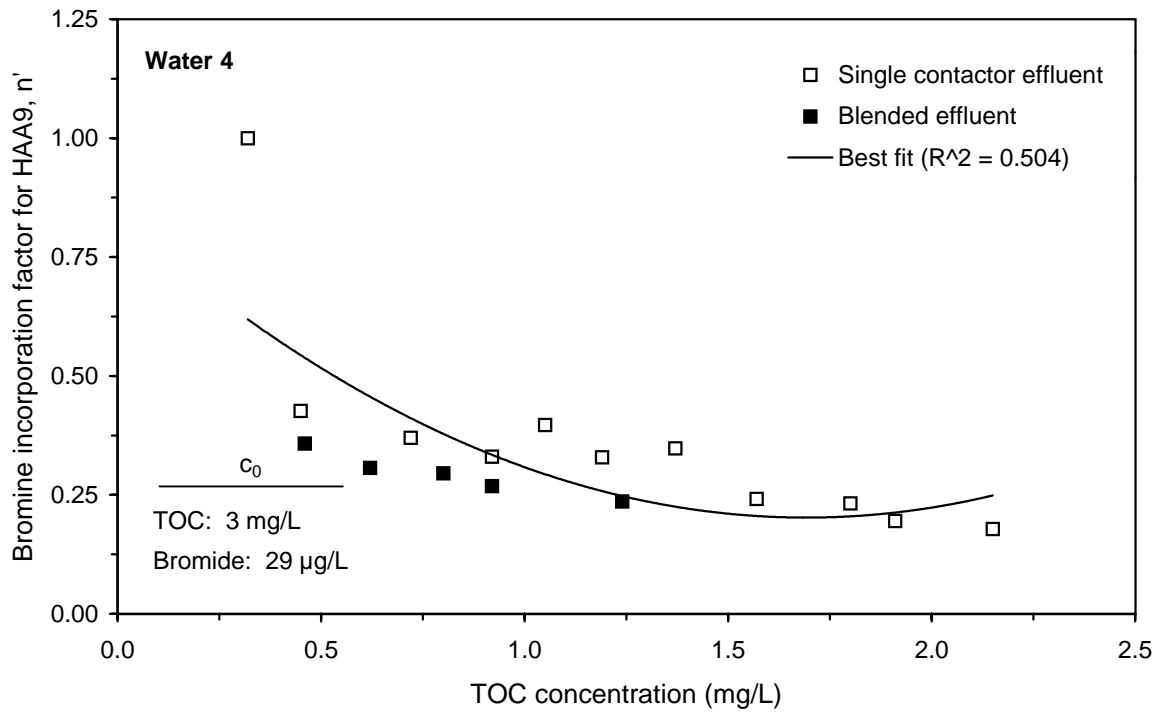


**Figure 28 Correlation between single contactor and blended effluent TOC concentration and HAA9 bromine incorporation factor ( $n'$ ) for Water 4**

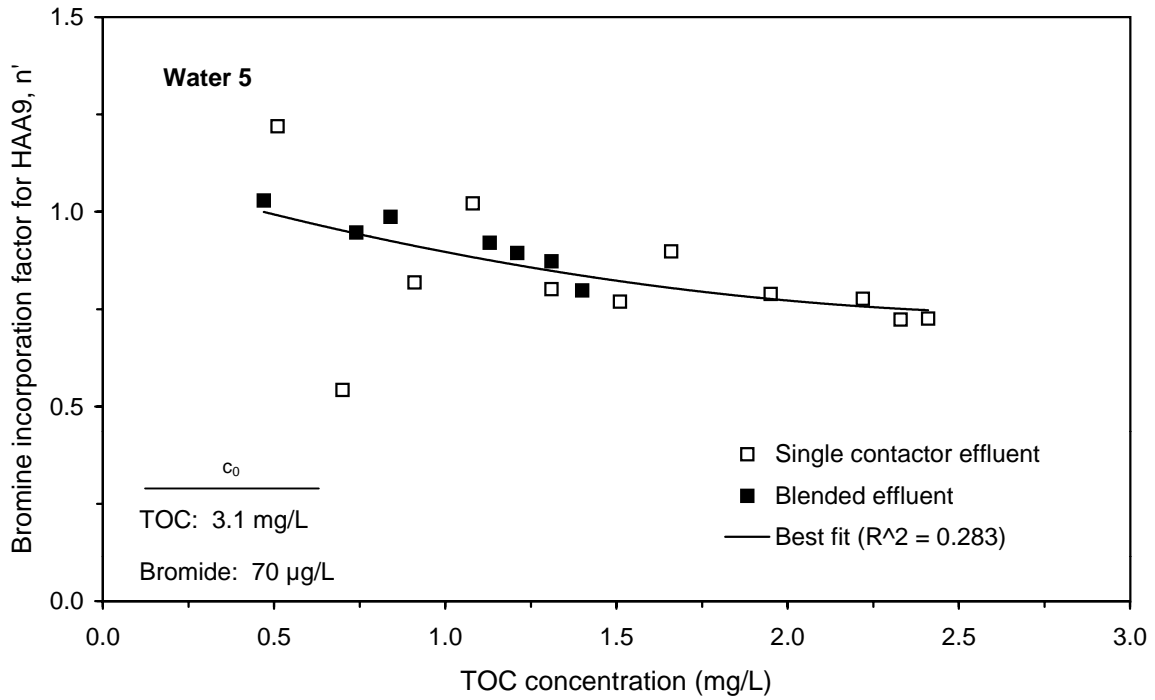


**Figure 29 Correlation between single contactor and blended effluent TOC concentration and bromine incorporation factor ( $n'$ ) for Water 5**

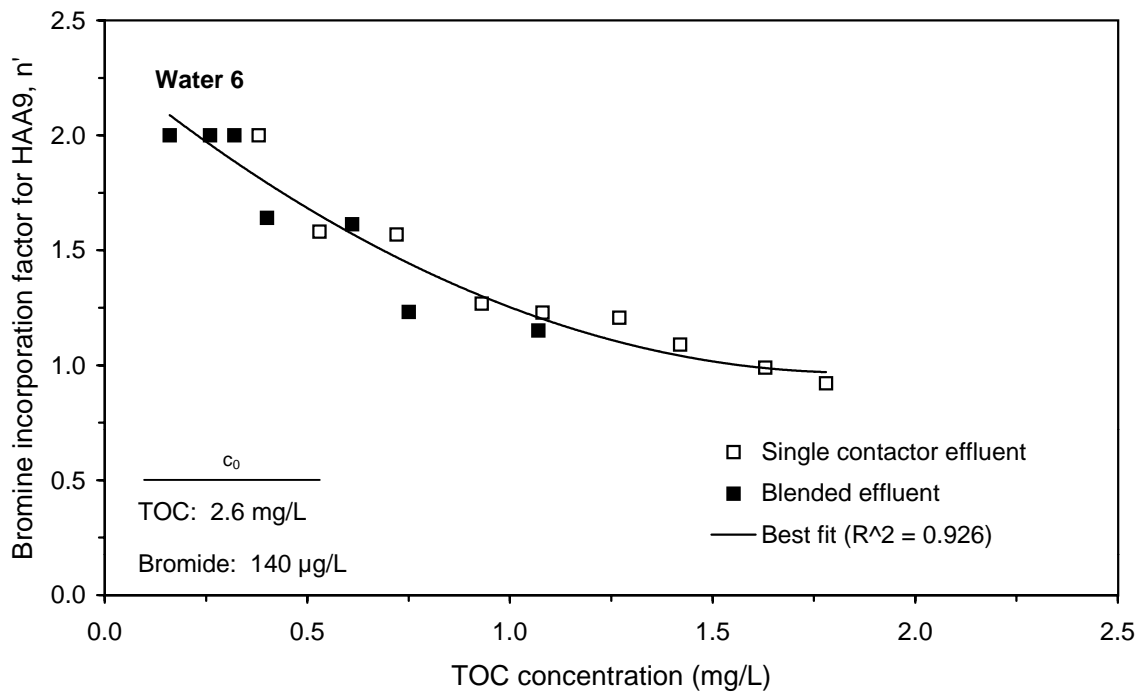


**Figure 30 Correlation between single contactor and blended effluent TOC concentration and bromine incorporation factor ( $n'$ ) for Water 6**

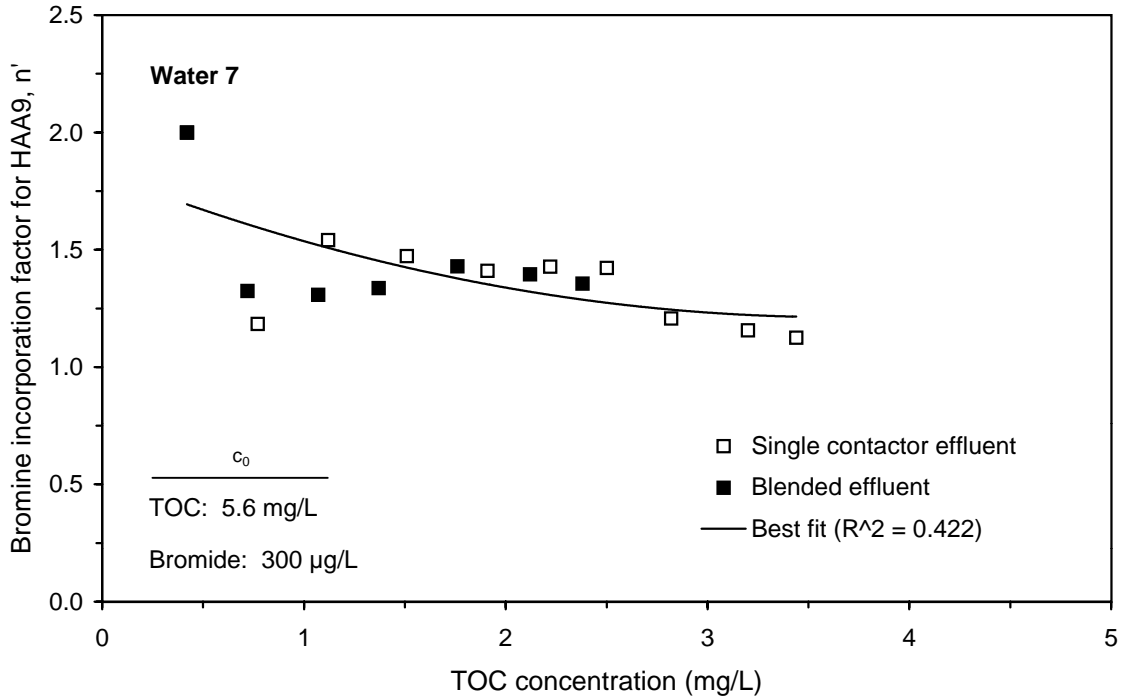


**Figure 31 Correlation between single contactor and blended effluent TOC concentration bromine incorporation factor ( $n'$ ) for Water 7**

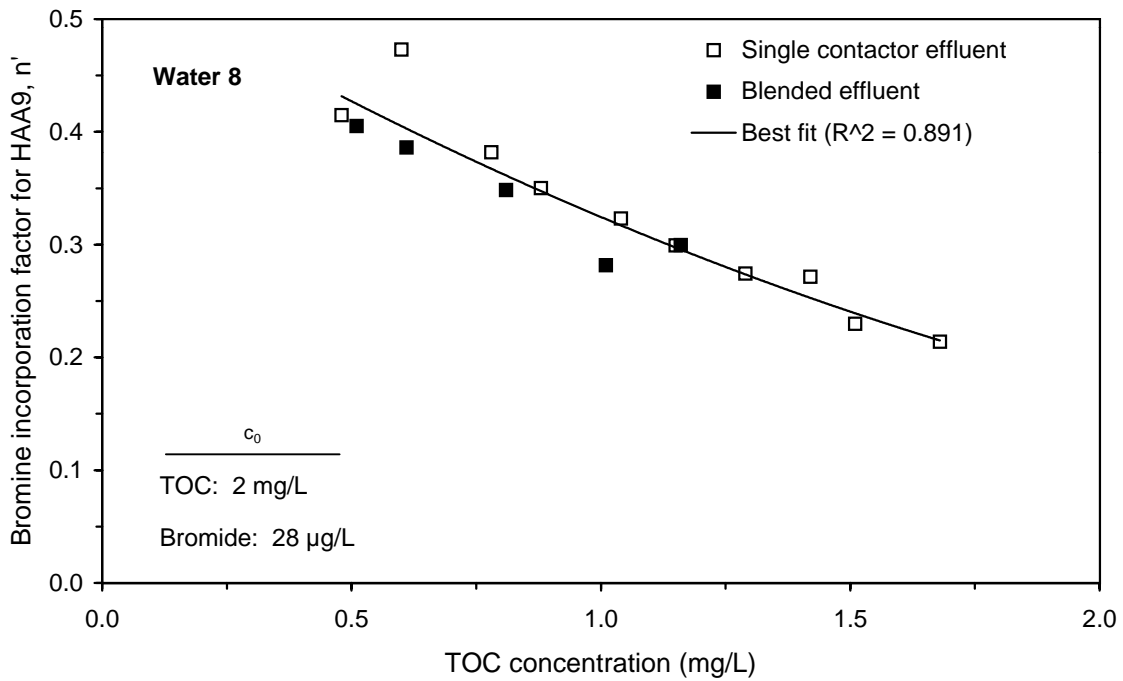


**Figure 32 Correlation between single contactor and blended effluent TOC concentration bromine incorporation factor ( $n'$ ) for Water 8**

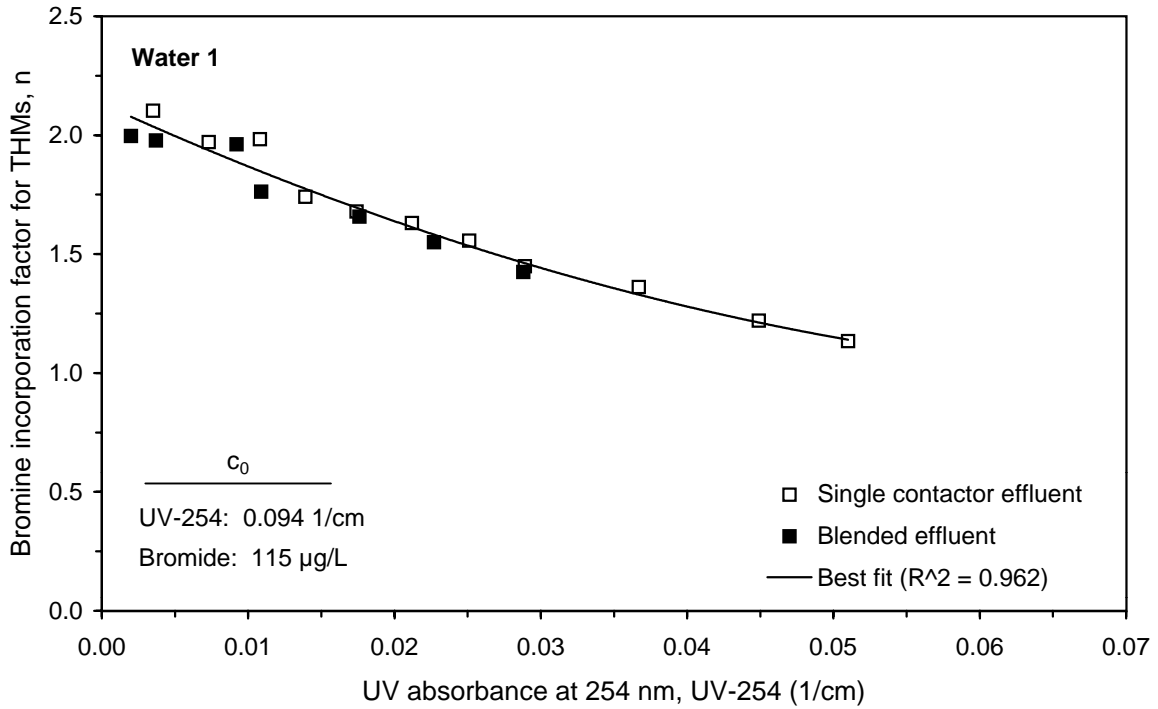


**Figure 33 Correlation between single contactor and blended effluent UV absorbance and THM bromine incorporation factor ( $n$ ) for Water 1**

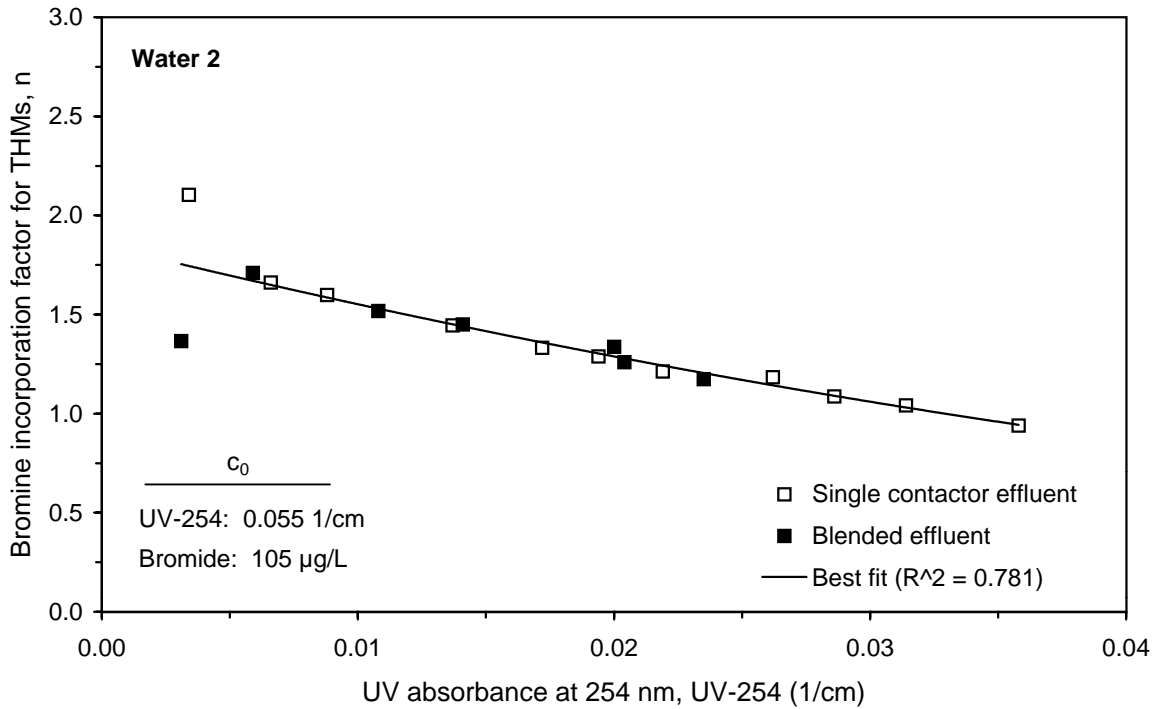


**Figure 34 Correlation between single contactor and blended effluent UV absorbance and THM bromine incorporation factor ( $n$ ) for Water 2**

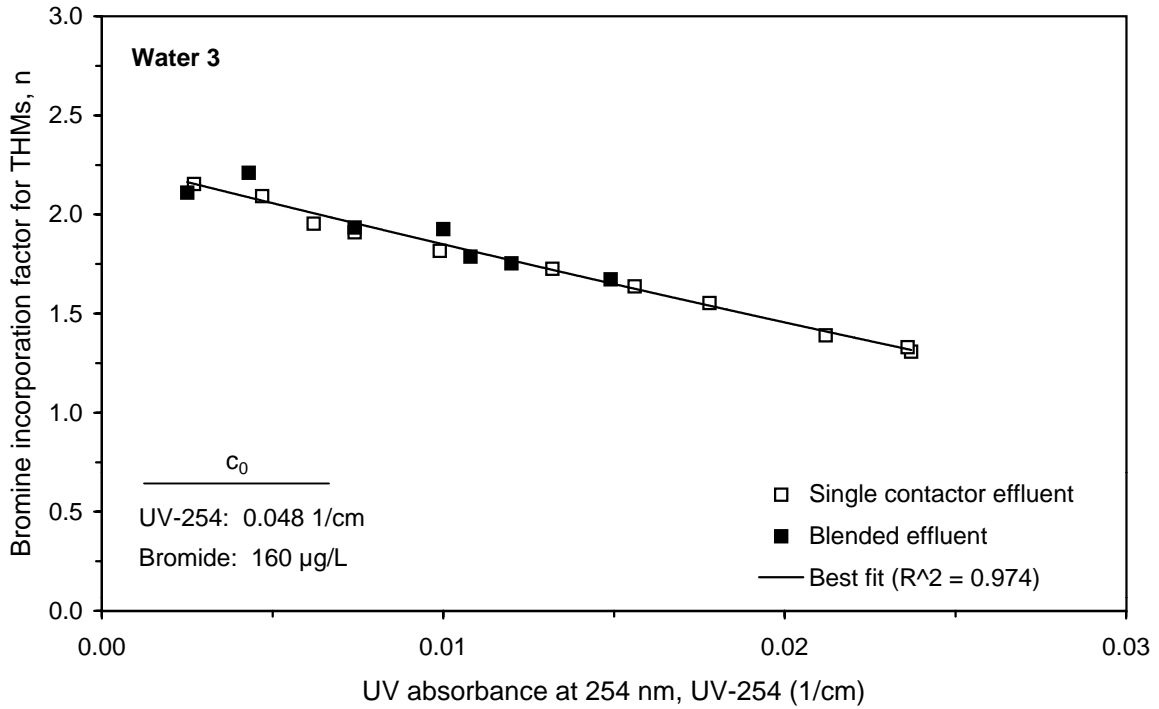


**Figure 35 Correlation between single contactor and blended effluent UV absorbance and THM bromine incorporation factor (n) for Water 3**

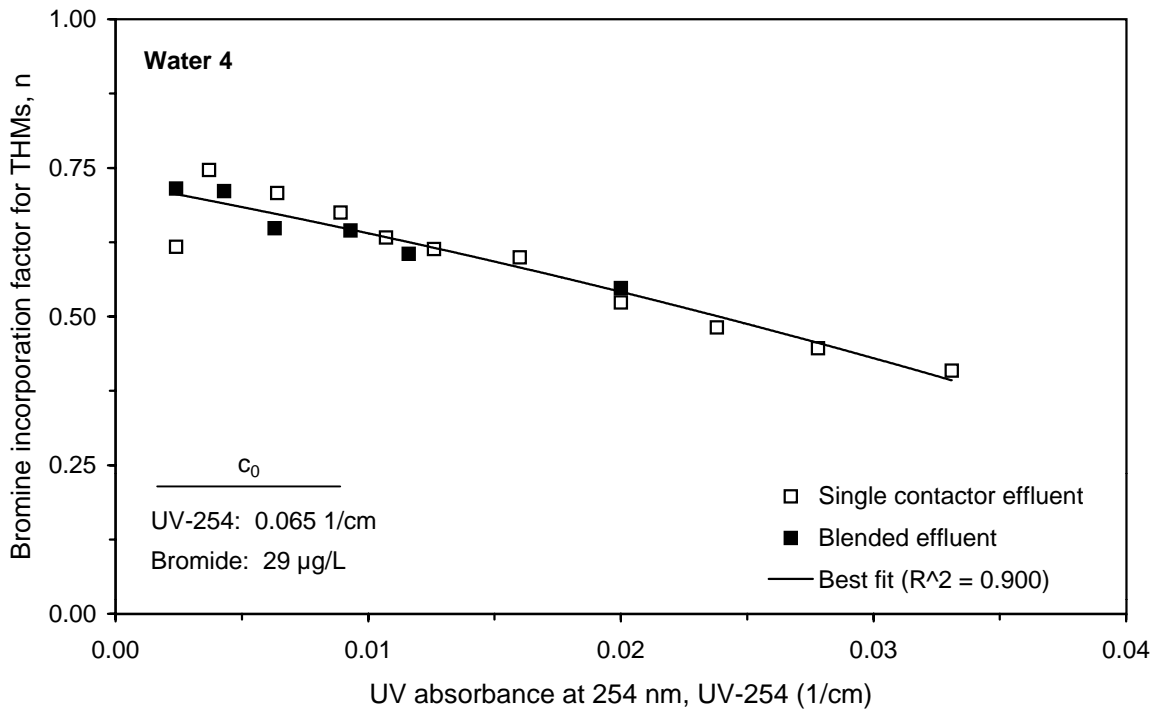


**Figure 36 Correlation between single contactor and blended effluent UV absorbance and THM bromine incorporation factor (n) for Water 4**

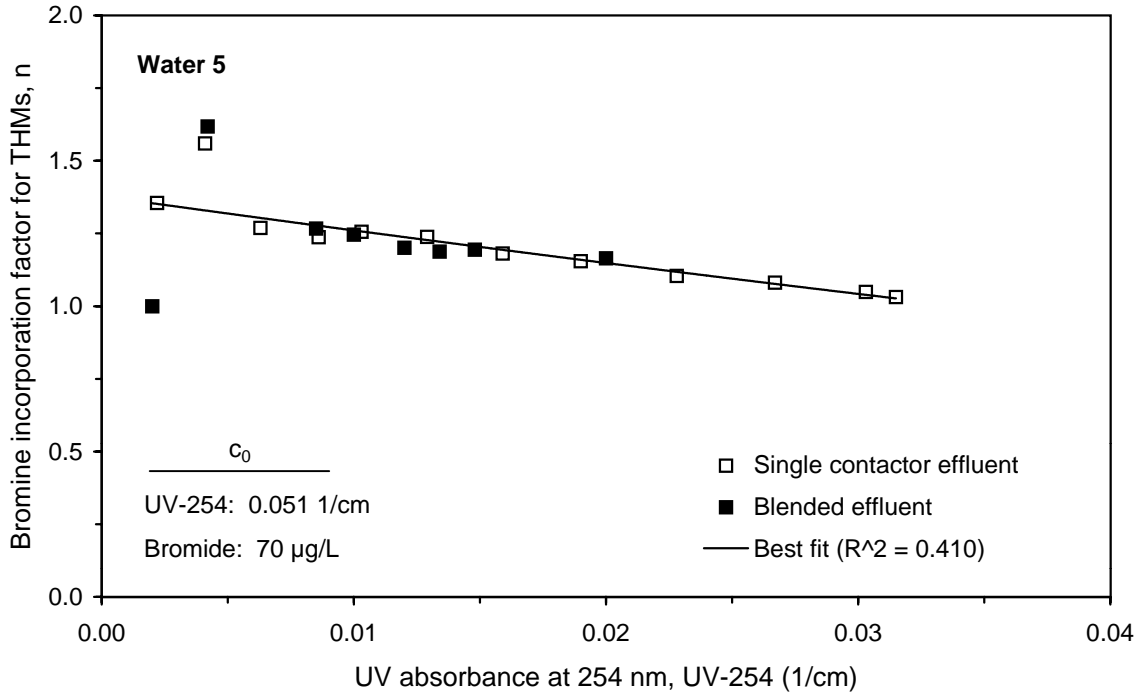


**Figure 37 Correlation between single contactor and blended effluent UV absorbance and THM bromine incorporation factor (n) for Water 5**

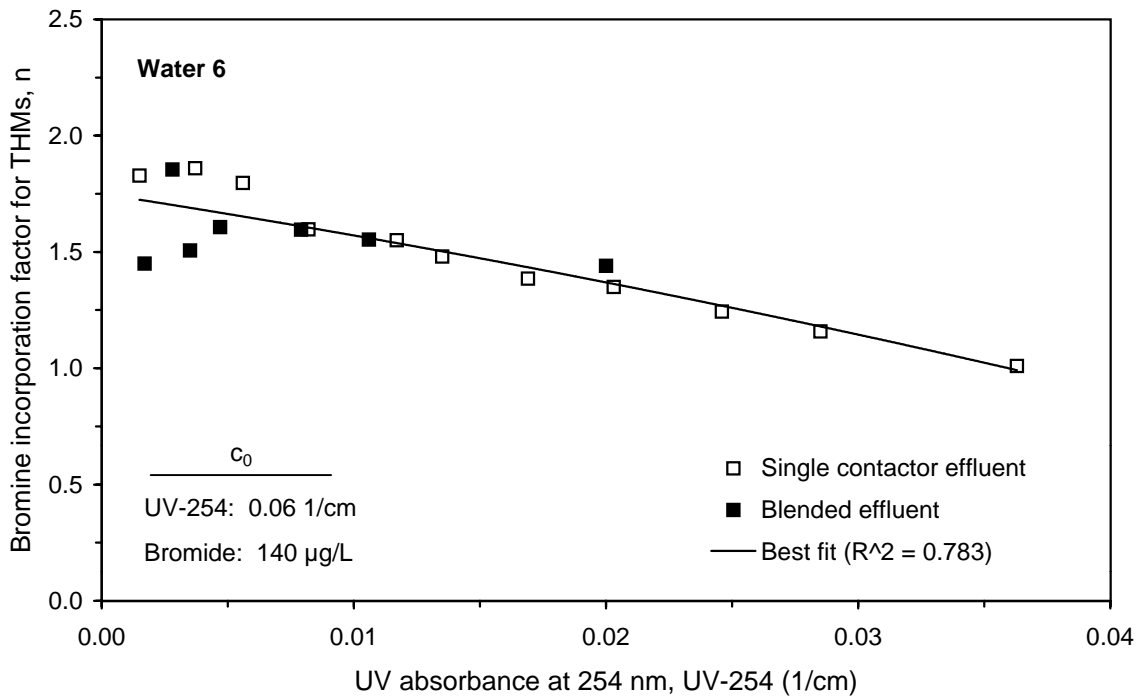


**Figure 38 Correlation between single contactor and blended effluent UV absorbance and THM bromine incorporation factor (n) for Water 6**

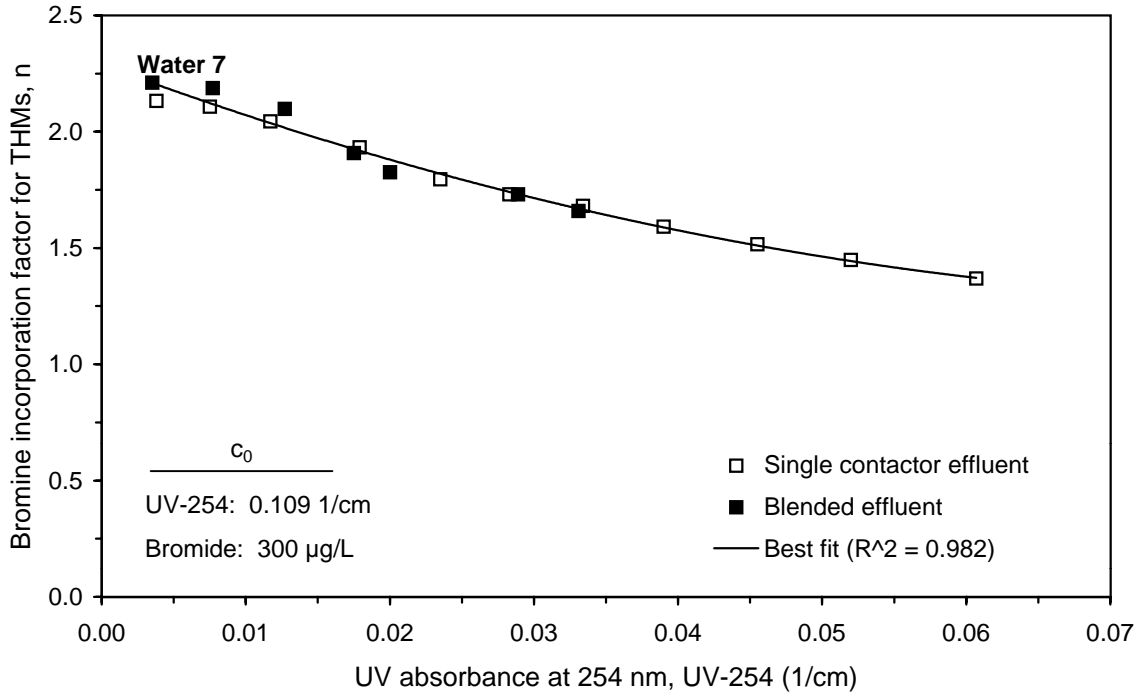


**Figure 39 Correlation between single contactor and blended effluent UV absorbance and THM bromine incorporation factor (n) for Water 7**

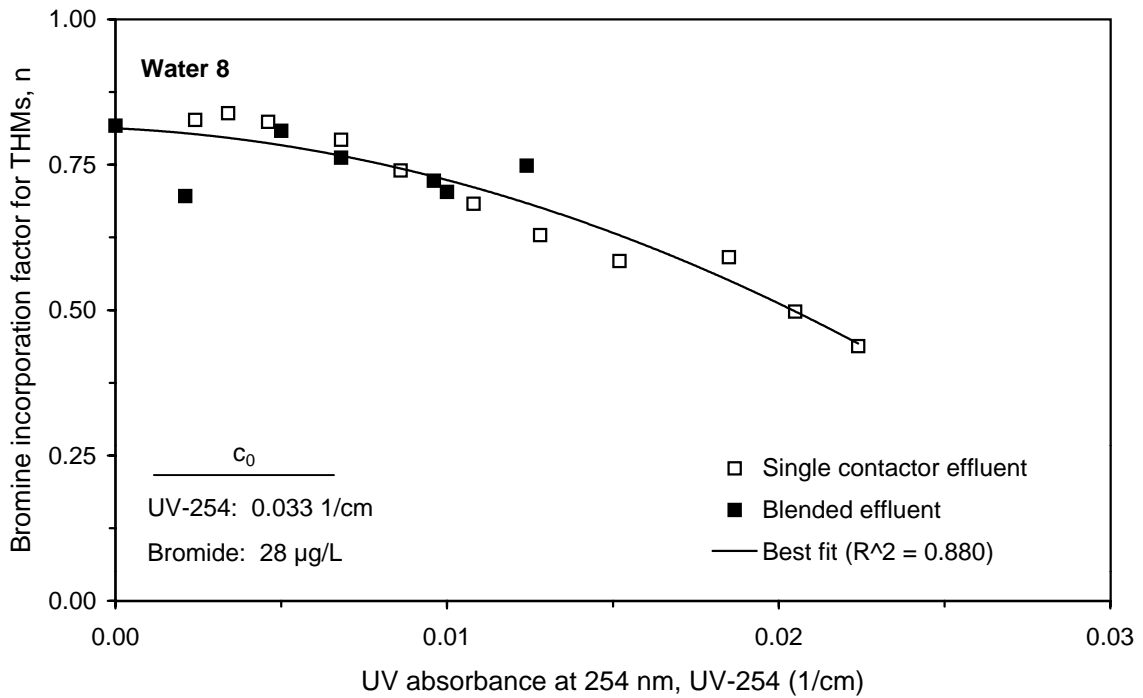


**Figure 40 Correlation between single contactor and blended effluent UV absorbance and THM bromine incorporation factor (n) for Water 8**

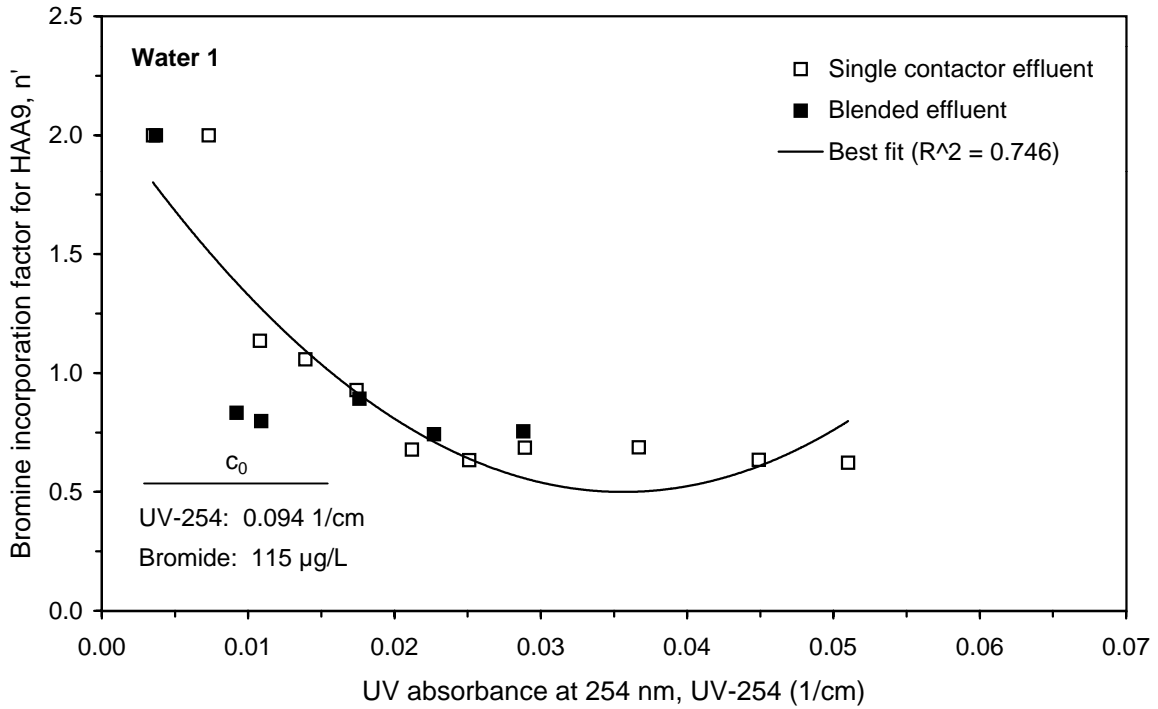


**Figure 41 Correlation between single contactor and blended effluent UV absorbance and HAA9 bromine incorporation factor (n') for Water 1**

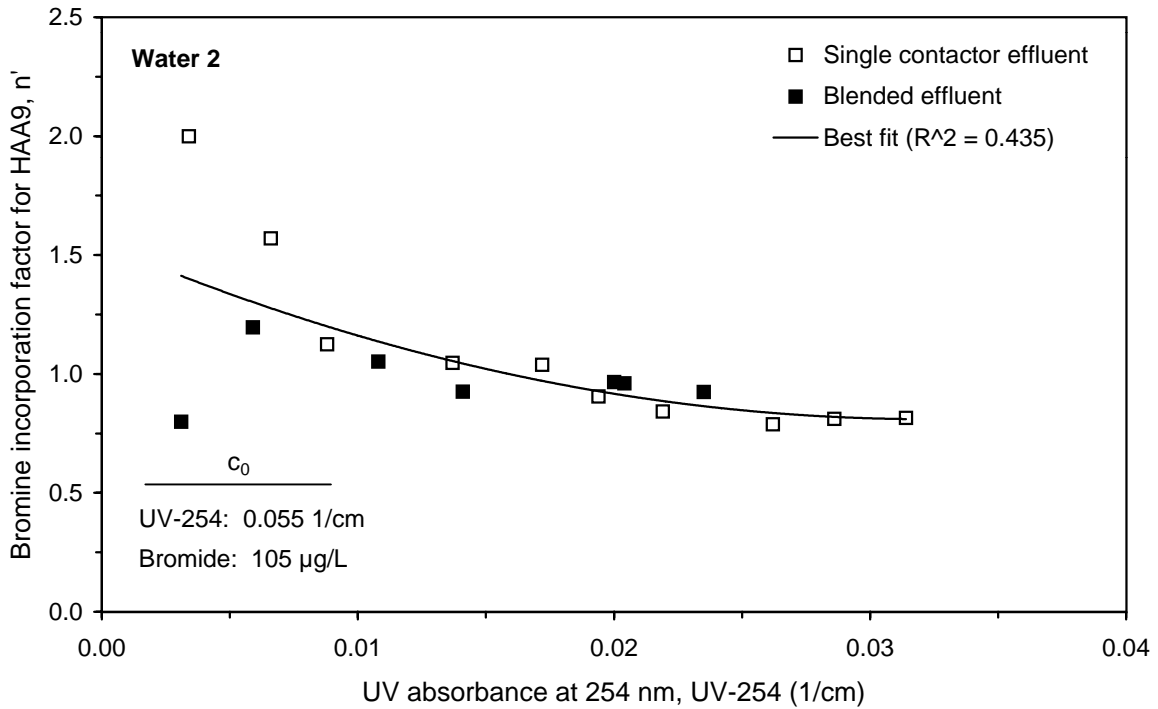


**Figure 42 Correlation between single contactor and blended effluent UV absorbance and HAA9 bromine incorporation factor (n') for Water 2**

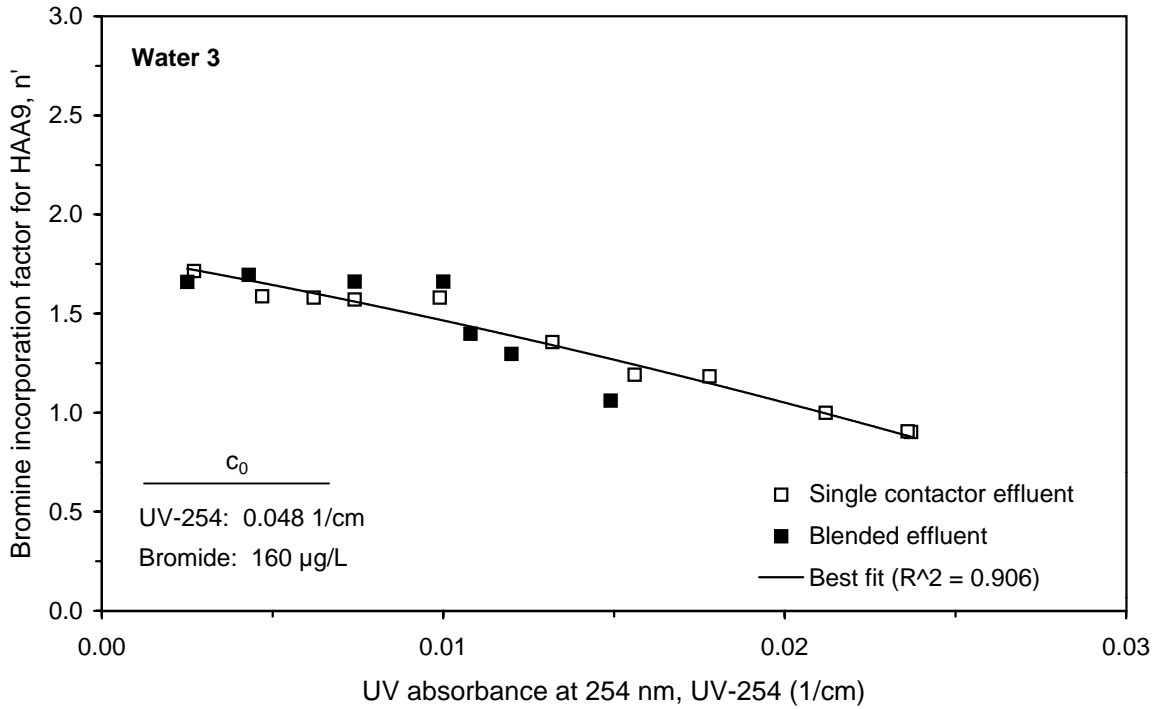


**Figure 43 Correlation between single contactor and blended effluent UV absorbance and HAA9 bromine incorporation factor (n') for Water 3**

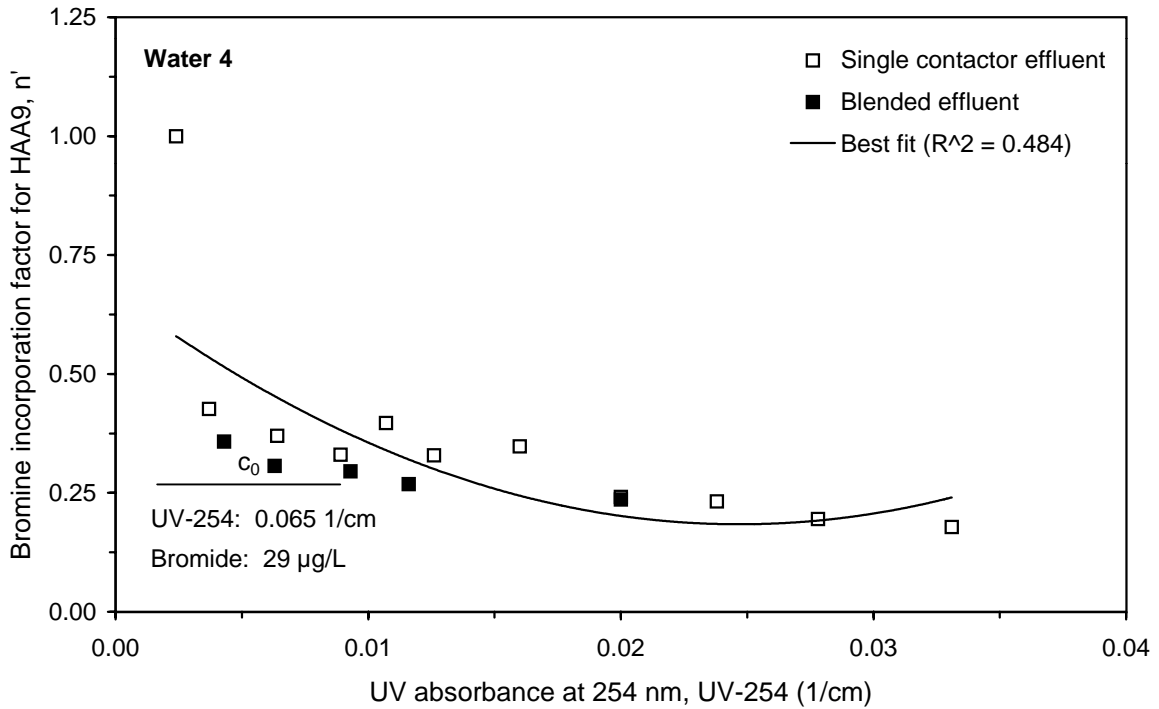


**Figure 44 Correlation between single contactor and blended effluent UV absorbance and HAA9 bromine incorporation factor (n') for Water 4**

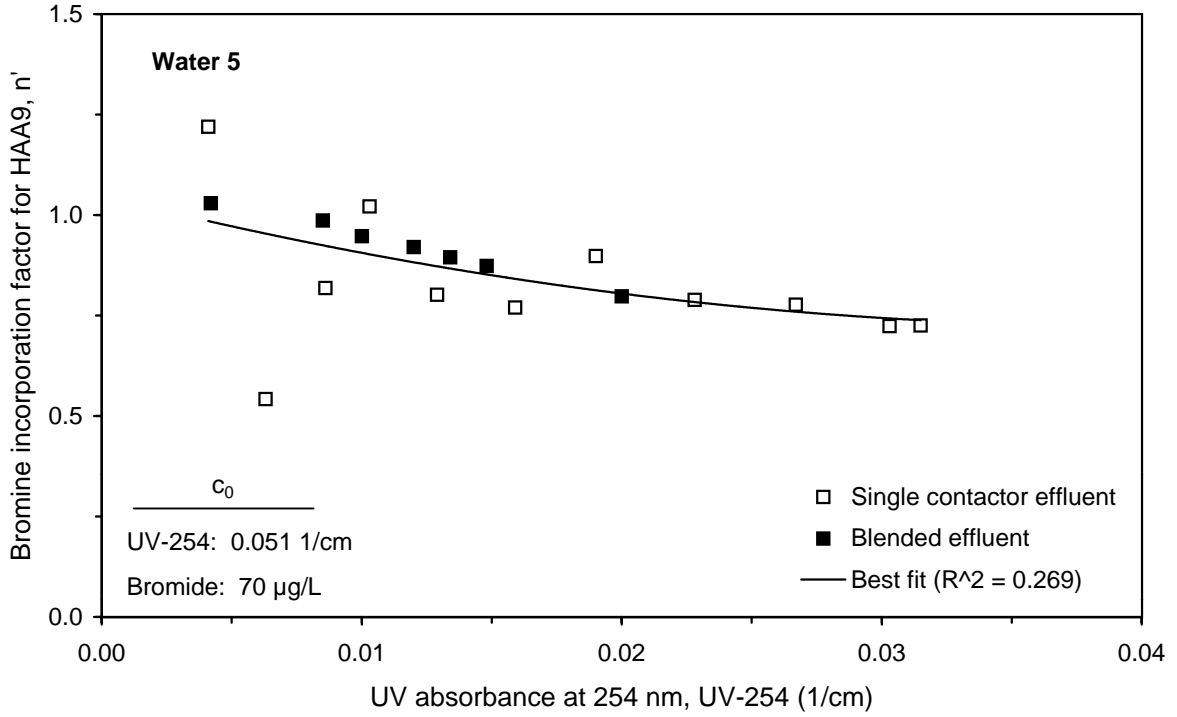


**Figure 45 Correlation between single contactor and blended effluent UV absorbance and HAA9 bromine incorporation factor ( $n'$ ) for Water 5**

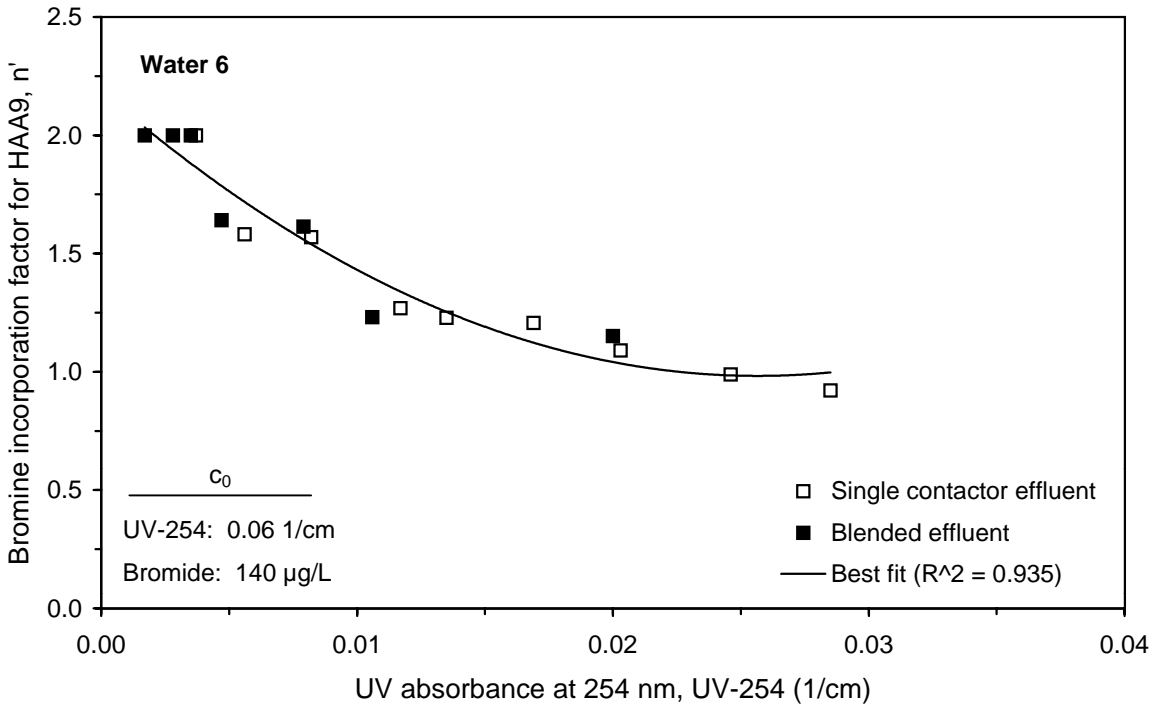


**Figure 46 Correlation between single contactor and blended effluent UV absorbance and HAA9 bromine incorporation factor ( $n'$ ) for Water 6**

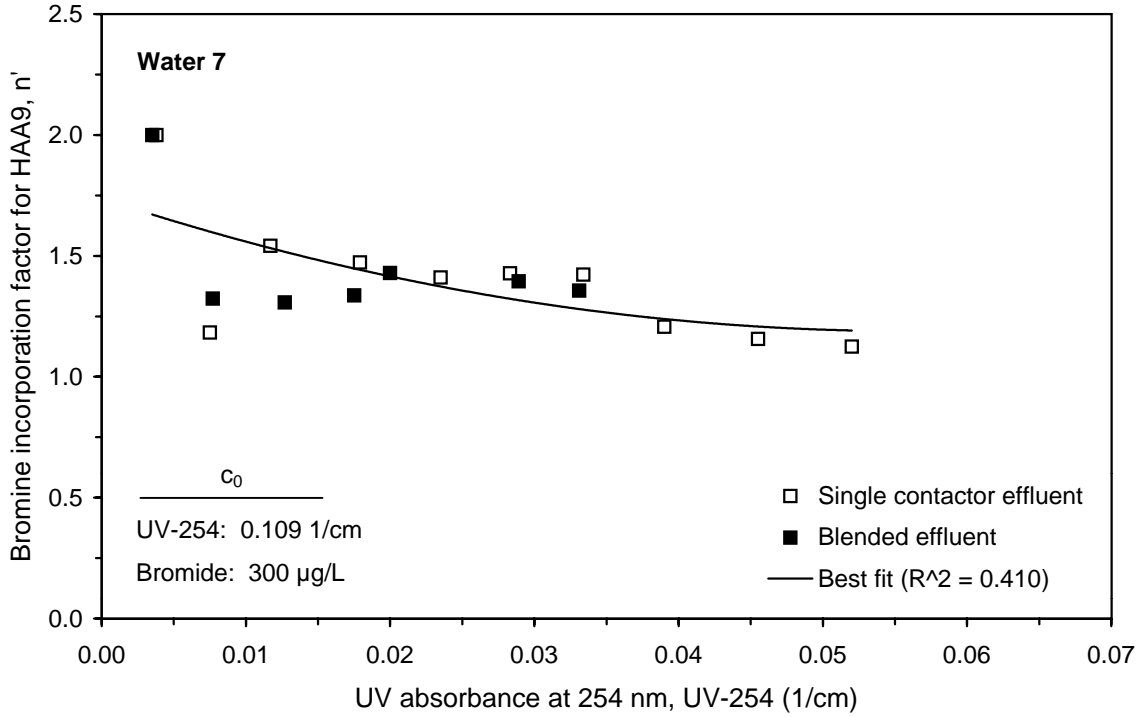


**Figure 47 Correlation between single contactor and blended effluent UV absorbance and HAA9 bromine incorporation factor ( $n'$ ) for Water 7**

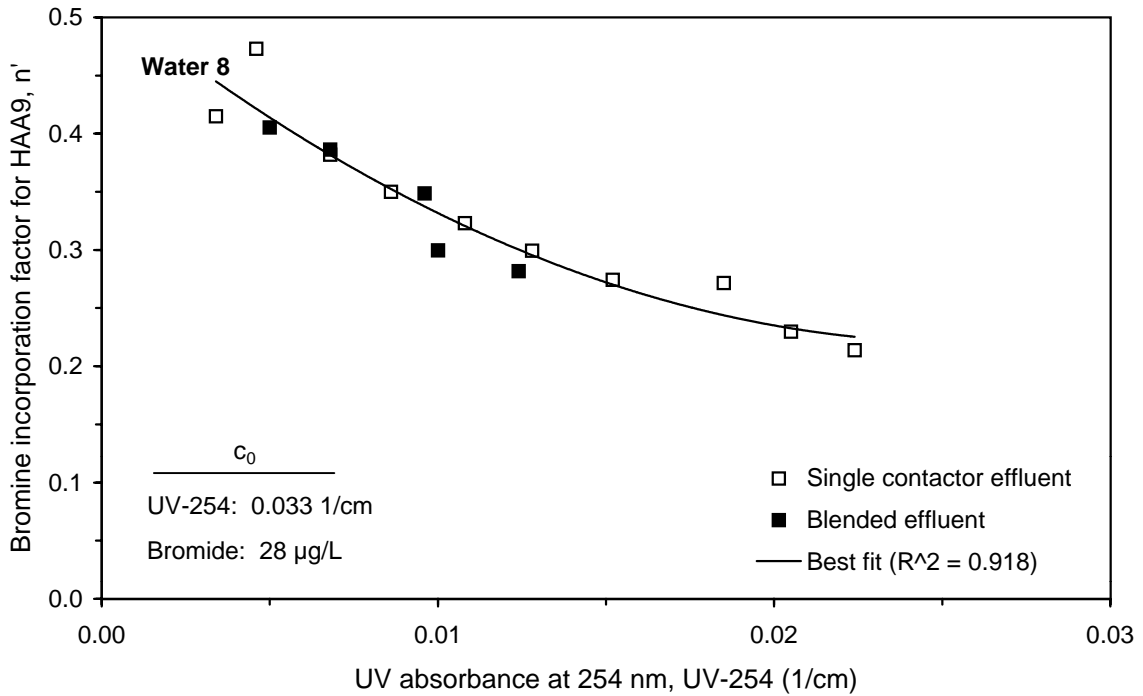


**Figure 48 Correlation between single contactor and blended effluent UV absorbance and HAA9 bromine incorporation factor ( $n'$ ) for Water 8**

### 4.3 Assessment of Logistic Function Fit to Single Contactor Breakthrough Curve Data

A model used to describe single contactor effluent experimental data is needed for several reasons. From a data management perspective, best-fit curve parameters that adequately describe experimental data are less memory intensive than storing the entire experimental data set. A best-fit curve also facilitates interpolation and extrapolation to estimate run times for given treatment objectives. Use of a best-fit model curve provides an estimate of the scatter in the data through the coefficient of determination, and the model minimizes the impact of this scatter on run time estimates. Finally, a function that describes the single contactor experimental data set is a prerequisite for determining the integral breakthrough curve, a curve that relates single contactor run time to blended contactor water quality under the assumption that contactors are operated in parallel-staggered mode. Run time estimates generated by the integral breakthrough curve are more applicable to full-scale GAC operation.

The appropriate logistic curve function model (step, step-lag, or step-lag-peak, as described in Section 3.2.1) was fit to the single contactor effluent data for eight GAC runs comprised of up to 20 parameters each. The GAC runs were performed using conventionally-treated water from eight waters sources, including surface and ground waters. The parameters examined included precursors or surrogates (TOC, UV<sub>254</sub>, and SDS-TOX), DBP class sums (TTHM, HAA5, HAA6, and HAA9), and DBP species (CF, BDCM, DBCM, BF, MCAA, DCAA, TCAA, MBAA, DBAA, BCAA, DCBAA, CDBAA, and TBAA). For some DBP species, samples taken during the initial portion of the breakthrough curve were measured below the MRL. Curve fits were not performed if fewer than six effluent data points were reported above the MRL.

Due to the large amount of graphs generated, all plots are summarized in Appendix E, and a selection of plots are included together with this analysis as examples. The plots contain the single contactor GAC effluent parameter concentration plotted against scaled operation time. A line representing the logistic function model best-fit is included. In addition, the experimental blended effluent data points are included in each plot, along with a dotted line representing the DI method prediction of the integral breakthrough curve, to demonstrate the benefit obtained by blending the effluents of multiple contactors operated in parallel staggered mode. An analysis of the integral breakthrough curve predictive models is deferred until Section 4.4.

#### 4.3.1 Surrogates and Class Sum Logistic Function Curve Fits

The step logistic function model was used to fit single contactor effluent TOC breakthrough curves for all waters, as shown in Figures 49 through 56. GAC run times ranged from 76 to 287 days, and the GAC influent TOC concentration ranged from 2.0 to 5.6 mg/L. For these waters, the step logistic function model provided excellent curve fit approximations: the R<sup>2</sup> values for the curve fits ranged from 0.966 to 0.992.

Using the step-lag logistic function model, excellent curve fits were also obtained for single contactor effluent UV<sub>254</sub> breakthrough curves: the R<sup>2</sup> values for the curve fits ranged from 0.982 to 0.998. The measured GAC influent UV<sub>254</sub> ranged from 0.033 to 0.109 1/cm for the waters

examined. The results for Waters 5 and 7 are shown in Figures 57 and 58. The results for the remaining waters can be found in Appendix E.

SDS-TOX breakthrough curves were also modeled using the step-lag logistic function with excellent results: the  $R^2$  values for the curve fits ranged from 0.990 to 0.999. The GAC influent SDS-TOX ranged from 156 to 486  $\mu\text{g/L}$  as Cl<sup>-</sup>. Figures 59 and 60 show examples of the data obtained for Waters 4 and 8.

Both SDS-TTHM and the SDS-HAA sums (HAA5, HAA6, and HAA9) were modeled using the step-lag logistic function model. Again, single contactor effluent data were well-represented by the model used, as shown for SDS-TTHM in Figures 61 and 62 for Waters 3 and 6. The  $R^2$  values for SDS-TTHM curve fits ranged from 0.977 to 0.995. Overall, the step-lag logistic function model was also successful when used to fit all three SDS-HAA species sums, with  $R^2$  values ranging from 0.952 to 0.994. Figures 63 and 64 show the step-lag logistic function model curve fits applied to single contactor effluent SDS-HAA9 data for Waters 1 and 2.

Table 8 summarizes the  $R^2$  values measured for all curve fits, including DBP surrogates, DBP sum class parameters, and DBP species. For all waters and all parameters the mean  $R^2$  was  $0.973 \pm 0.046$ , indicating that all breakthrough curve data were successfully fit using the logistic function models. For DBP surrogates and DBP sum class parameters only, the mean  $R^2$  value was  $0.982 \pm 0.012$ .

#### 4.3.2 DBP Species Logistic Function Curve Fits

*THM Species.* For all waters, the application of the step-lag logistic function resulted in good curve fits for SDS-CF, as shown by  $R^2$  values ranging between 0.922 and 0.998. Typically, the SDS-CF breakthrough curve shape was similar to that of SDS-TTHM, as shown in the example given for Water 4 in Figure 65. For most SDS-BDCM and SDS-DBCM breakthrough curves, the step-lag logistic function model was used and yielded good results:  $R^2$  values ranged from 0.946 to 0.998. An example of the SDS-BDCM breakthrough curve is shown in Figure 66 for Water 6 and an example of the SDS-DBCM breakthrough curve is shown in Figure 67 for Water 7. The step-lag logistic function model was able to adequately fit the sharp 'S' shape (steep breakthrough followed by flat plateau) observed for the SDS-BDCM experimental data in Figure 66 for Water 6 ( $R^2 = 0.979$ ). Water 2 also exhibited this behavior, as did Waters 1 and 3 to a less pronounced extent, but in all cases the data were successfully fit by the model. For Waters 4 and 8, a peak breakthrough curve for SDS-BDCM was detected by the curve fit algorithm. These curves were fit using the step-lag-peak logistic function model, as shown in Figures 68 and 69. The curve fit procedure successfully fit the single contactor peak curves; the  $R^2$  values were greater than 0.94 for both waters. For 3 out of 6 waters with SDS-BF levels measured above the MRL, a peak curve was detected. The step-lag-peak logistic function model also successfully fit these peak curves, as shown in Figures 70 and 71 for Waters 1 and 6. The  $R^2$  values for SDS-BF curve fits ranged from 0.910 to 0.984. Summary plots of the model fits for all THM species and all waters are included in Appendix E.

*HAA Species.* Of the non-brominated HAA species, no curve fits were applied to SDS-MCAA because only for a few samples was MCAA measured above the MRL (2.0  $\mu\text{g/L}$ ) in the GAC effluent. The experimental breakthrough curves for SDS-DCAA and SDS-TCAA were well

Analyte	Number of each type of curve fit used for all waters				Curve fit R <sup>2</sup> value	
	Step	Step-lag	Step-lag-peak	No fit*	Mean	SD
TOC	8	0	0	0	0.980	0.009
UV-254	0	8	0	0	0.993	0.005
SDS-TOX	0	8	0	0	0.995	0.003
SDS-TTHM	0	8	0	0	0.985	0.007
SDS-HAA5	0	7	1	0	0.975	0.012
SDS-HAA6	0	8	0	0	0.974	0.010
SDS-HAA9	0	7	1	0	0.976	0.013
SDS-CF	1	7	0	0	0.991	0.004
SDS-BDCM	0	6	2	0	0.980	0.016
SDS-DBCM	0	8	0	0	0.992	0.005
SDS-BF	0	2	4	2	0.964	0.027
SDS-MCAA	0	0	0	8	NA	NA
SDS-DCAA	0	8	0	0	0.975	0.023
SDS-TCAA	0	5	0	3	0.973	0.027
SDS-MBAA	0	0	0	8	NA	NA
SDS-DBAA	0	6	0	2	0.957	0.050
SDS-BCAA	0	8	0	0	0.970	0.012
SDS-CDBAA	0	2	1	5	0.946	0.032
SDS-DCBAA	0	7	0	1	0.907	0.167
SDS-TBAA	0	0	1	7	0.976	NA
Total	9	105	10	36		

\*Curve fits were not performed on breakthrough curves with fewer than 6 points measured above the MRL

SD: Standard deviation

NA: Not applicable

**Table 8 Frequency of logistic function model used and R<sup>2</sup> values for all parameters and all waters**

modeled by the step-lag logistic function. Examples of the curve fits are shown in Figure 72 (SDS-DCAA, Water 3) and Figure 73 (SDS-TCAA, Water 5). For all waters,  $R^2$  values ranged from 0.922 to 0.999. SDS-MBAA was not measured above the MRL (1.0  $\mu\text{g/L}$ ) in the GAC effluent during any of the studies. Due to low or BMRL GAC effluent SDS-DBAA levels for Waters 4 and 8 curve fitting procedures were not applied. For the remaining waters, the SDS-DBAA breakthrough curve typically showed a sharp 'S' shape (steep breakthrough followed by flat plateau) and was successfully fit by the step-lag logistic function model ( $R^2$  values ranging from 0.859 to 0.992). An example of SDS-DBAA breakthrough and model fit is shown in Figure 74 for Water 6. The breakthrough curves for SDS-BCAA were also well-fit by the step-lag logistic function model ( $R^2$  values ranging from 0.952 to 0.987), such as that for Water 1, shown in Figure 75. Examples of curve fits for SDS-DCBAA, SDS-CDBAA, and SDS-TBAA are shown in Figures 76, 77, and 78, respectively. For these three compounds,  $R^2$  values ranged from 0.913 to 0.987 except for the curve fit for SDS-DCBAA for Water 3, which yielded an  $R^2$  value of 0.531. For this run, GAC effluent SDS-DCBAA concentrations were low, measured between 1.0 and 2.0  $\mu\text{g/L}$ .

A peak curve was detected in 10 cases out of 126 total curve fits. Every water examined yielded at least one peak curve. In general, the step-lag-peak logistic function model was able to adequately fit the peak curve data. Additional examples of peak curve fits are shown in Figures 79 and 80. Figure 81 (SDS-BF for Water 3) shows an example of single contactor data that qualitatively shows a peak, but the peak curve algorithm did not detect it as such. The logistic function under predicted experimental data at the peak by up to 4  $\mu\text{g/L}$ , and over predicted it at the end of the run by up to 3  $\mu\text{g/L}$ . The  $R^2$  value for this curve fit was 0.856. When refit to the step-lag-peak logistic function model, Figure 82, the  $R^2$  value improved to 0.984.

In general, the logistic function models successfully characterized the variety of breakthrough curves observed in this study. Three logistic function models were utilized: step, step-lag, and step-lag-peak. These models were able to match not only typical S-shaped breakthrough curves but also peak curves observed for some parameters. Table 8 also summarizes the frequency of use for each of the three types of logistic function models used. The step-lag logistic function was the most commonly used, utilized in 66 percent of the curve fits performed. For the DBP surrogates and class sums, the step-lag logistic function model was utilized for 82 percent of curve fits. The step function was almost exclusively utilized for TOC breakthrough curves. For 23 percent of all data sets, no curve fit was performed because fewer than six data points were measured above the MRL. Most of the parameters for which no curve fit was performed were HAA species. For all data sets that were modeled, the mean  $R^2$  was 0.974, indicating that overall, the models were able to successfully fit the GAC breakthrough profiles.

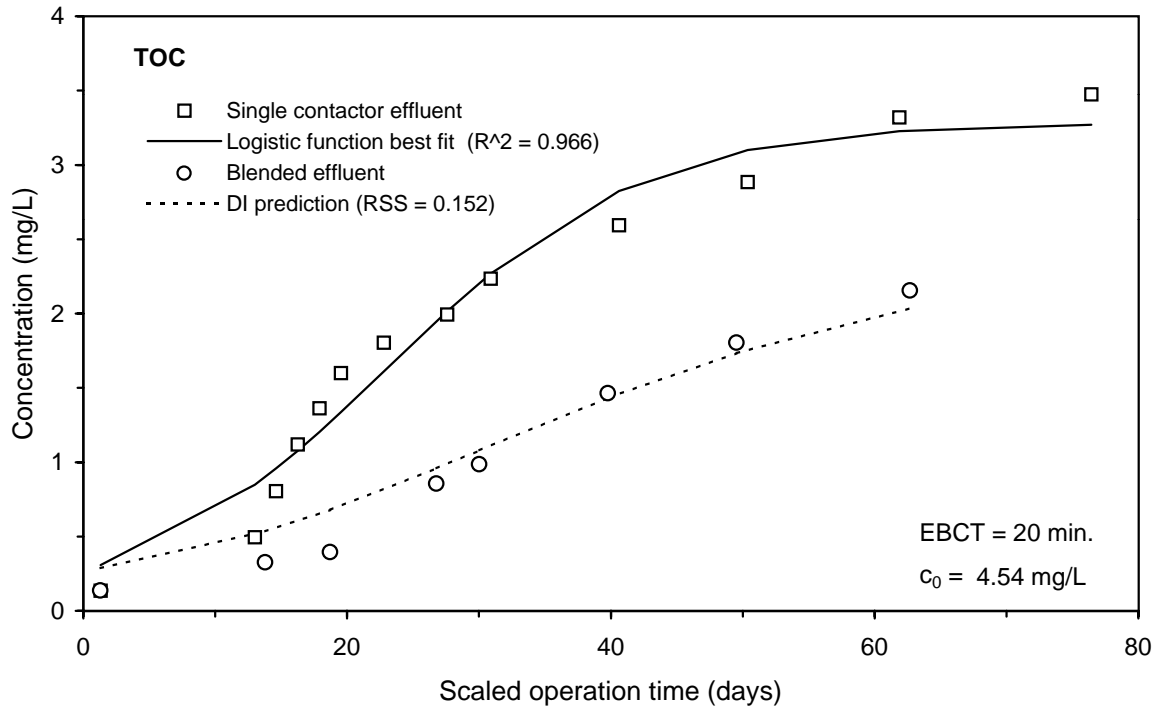


**Figure 49 Single contactor and blended effluent TOC breakthrough curves for Water 1**

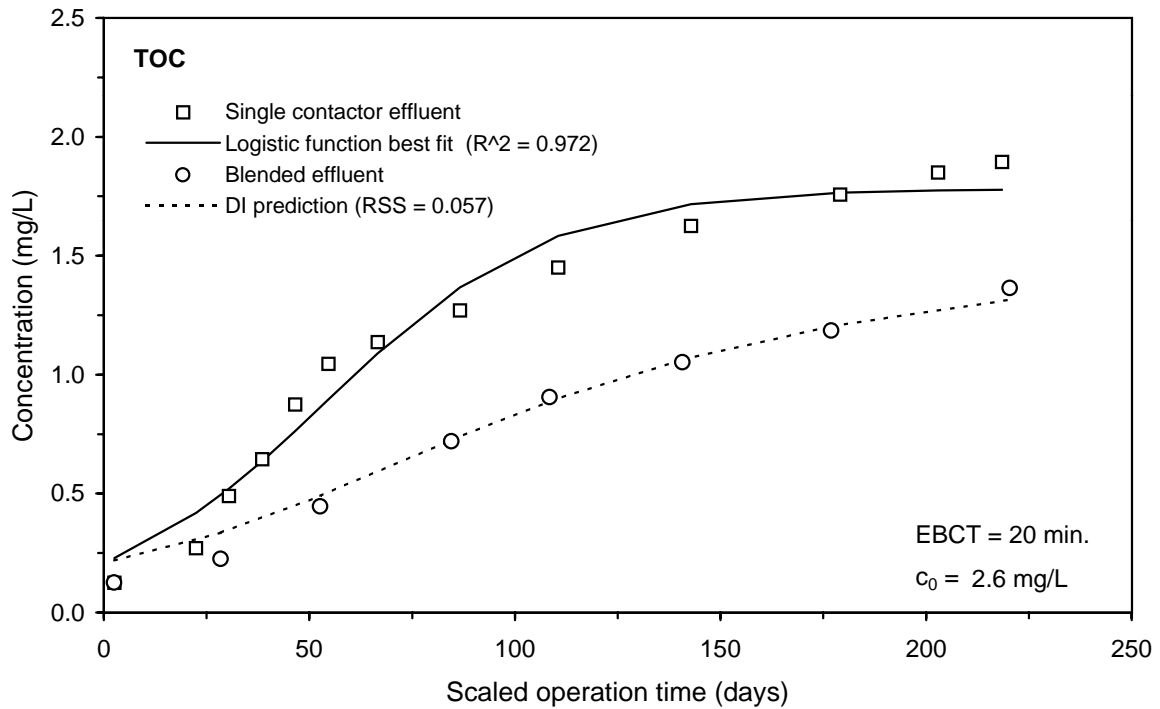


**Figure 50 Single contactor and blended effluent TOC breakthrough curves for Water 2**

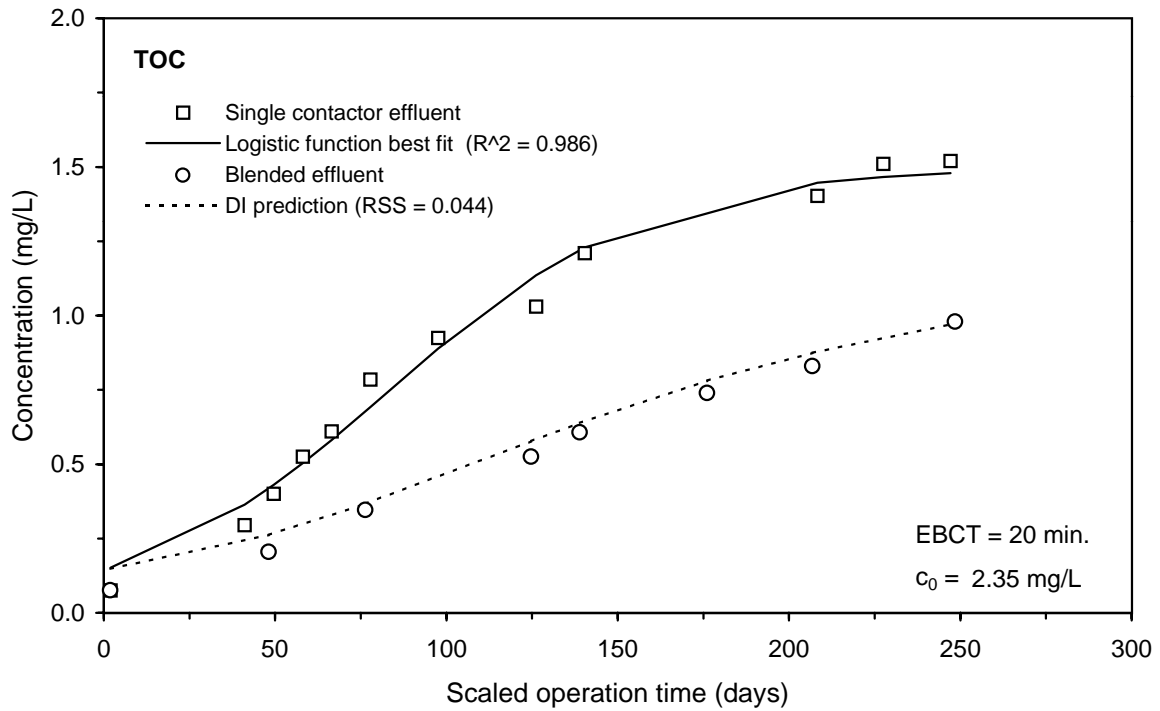


**Figure 51 Single contactor and blended effluent TOC breakthrough curves for Water 3**

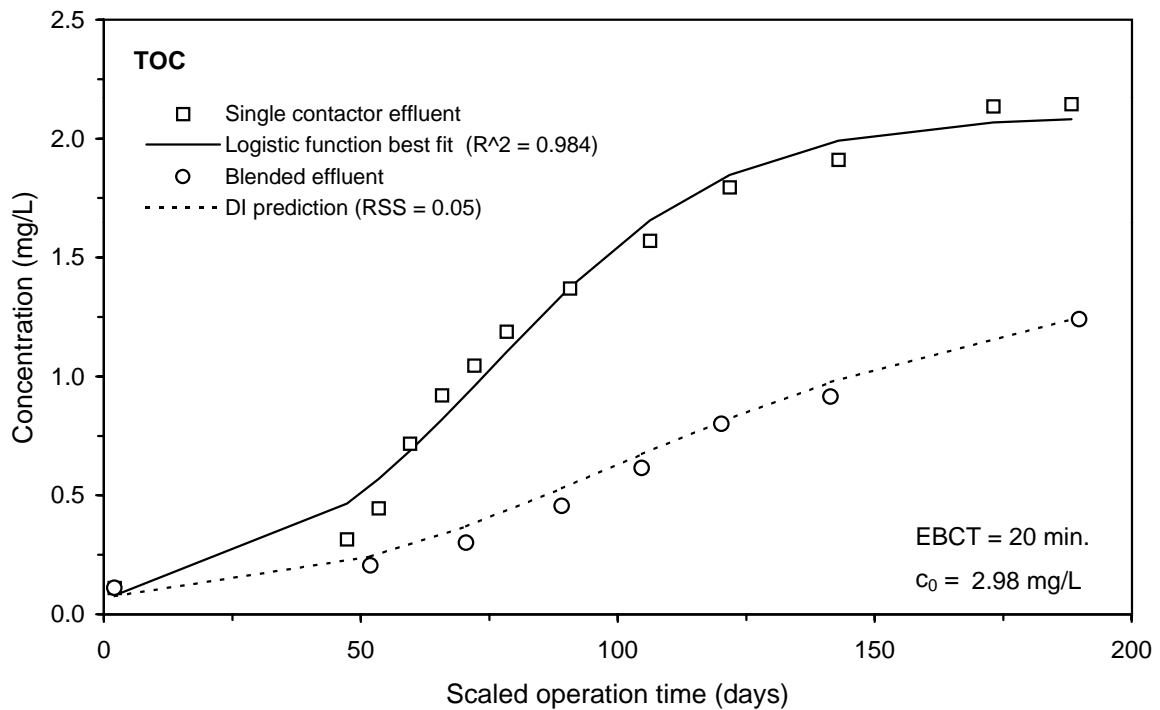


**Figure 52 Single contactor and blended effluent TOC breakthrough curves for Water 4**

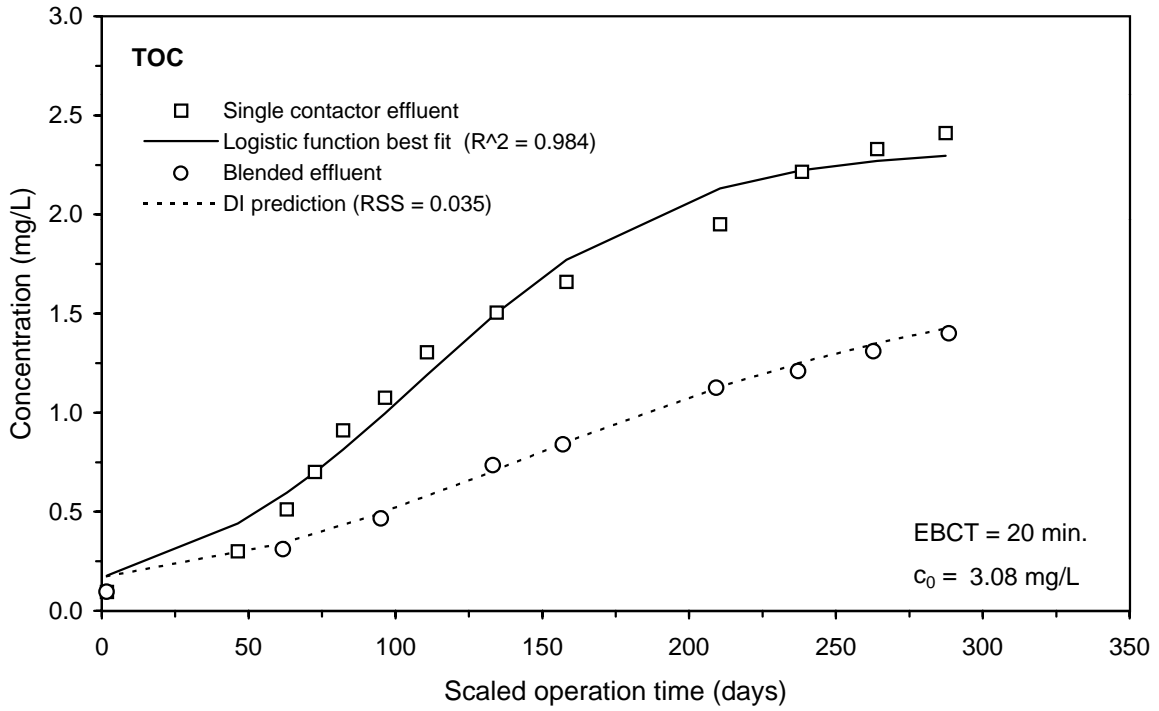


**Figure 53 Single contactor and blended effluent TOC breakthrough curves for Water 5**

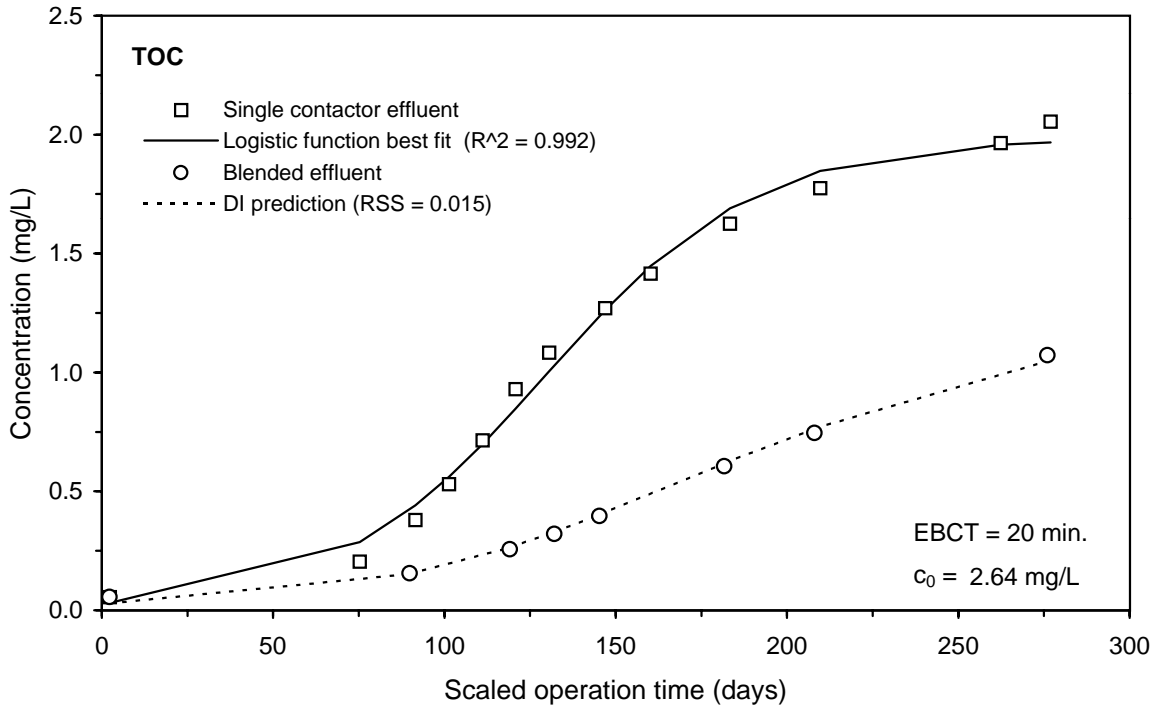


**Figure 54 Single contactor and blended effluent TOC breakthrough curves for Water 6**

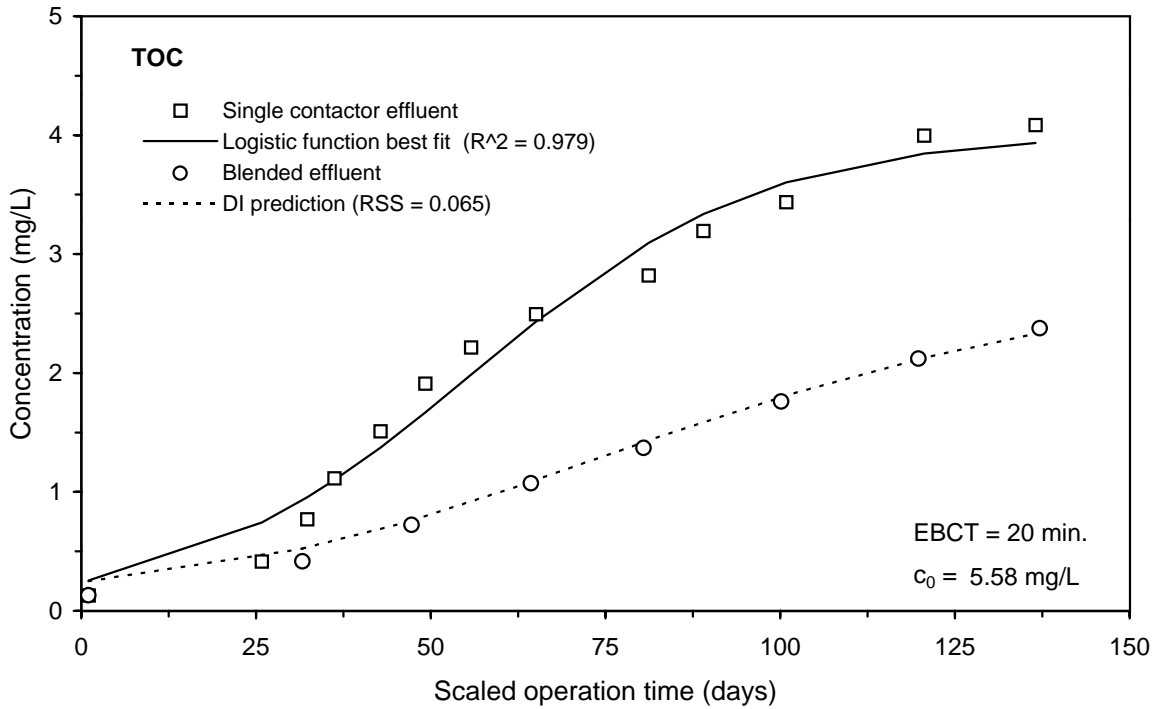


**Figure 55 Single contactor and blended effluent TOC breakthrough curves for Water 7**

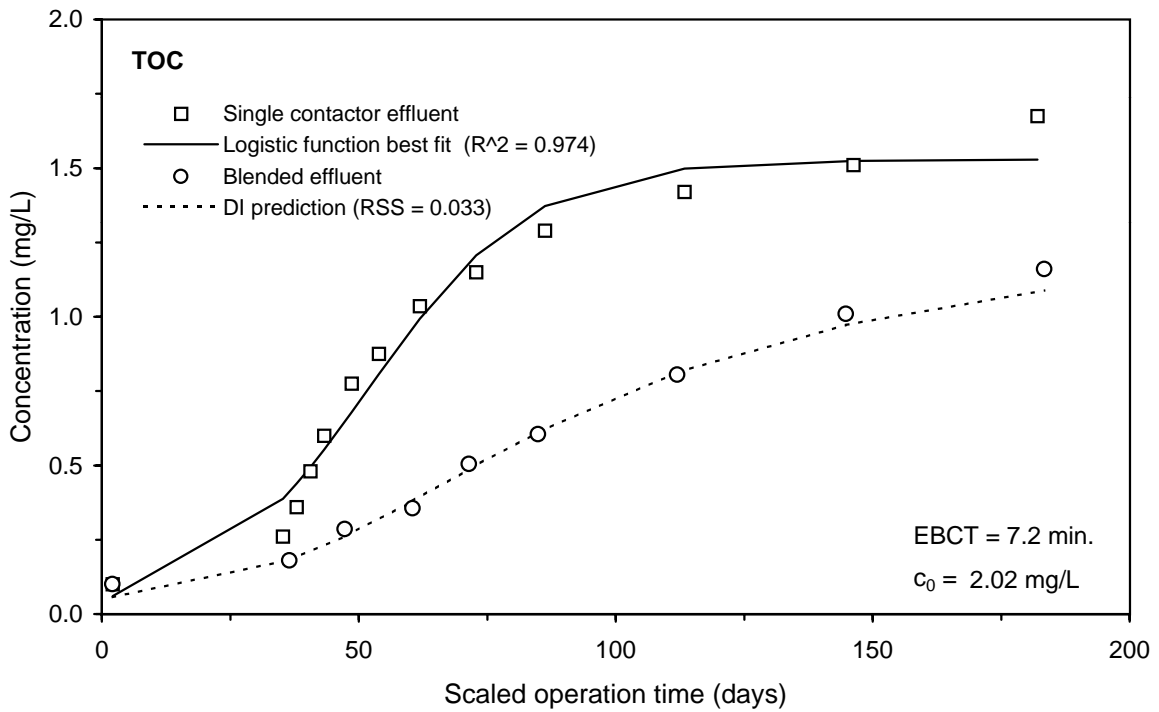


**Figure 56 Single contactor and blended effluent TOC breakthrough curves for Water 8**

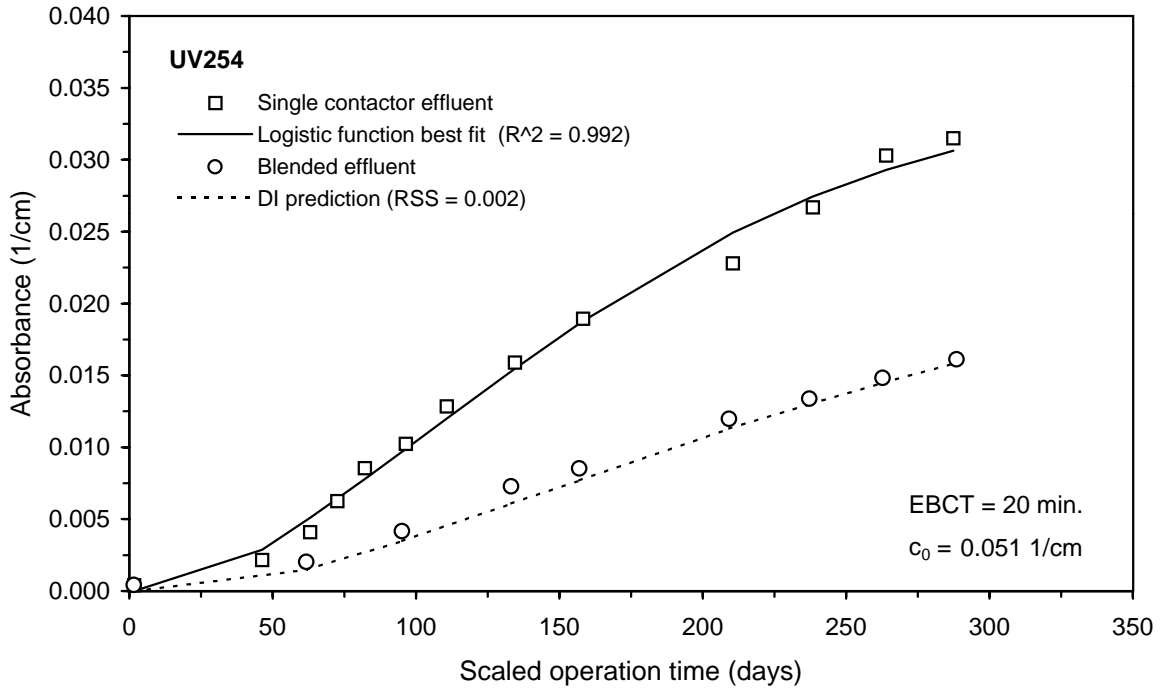


**Figure 57 Single contactor and blended effluent UV254 breakthrough curves for Water 5**

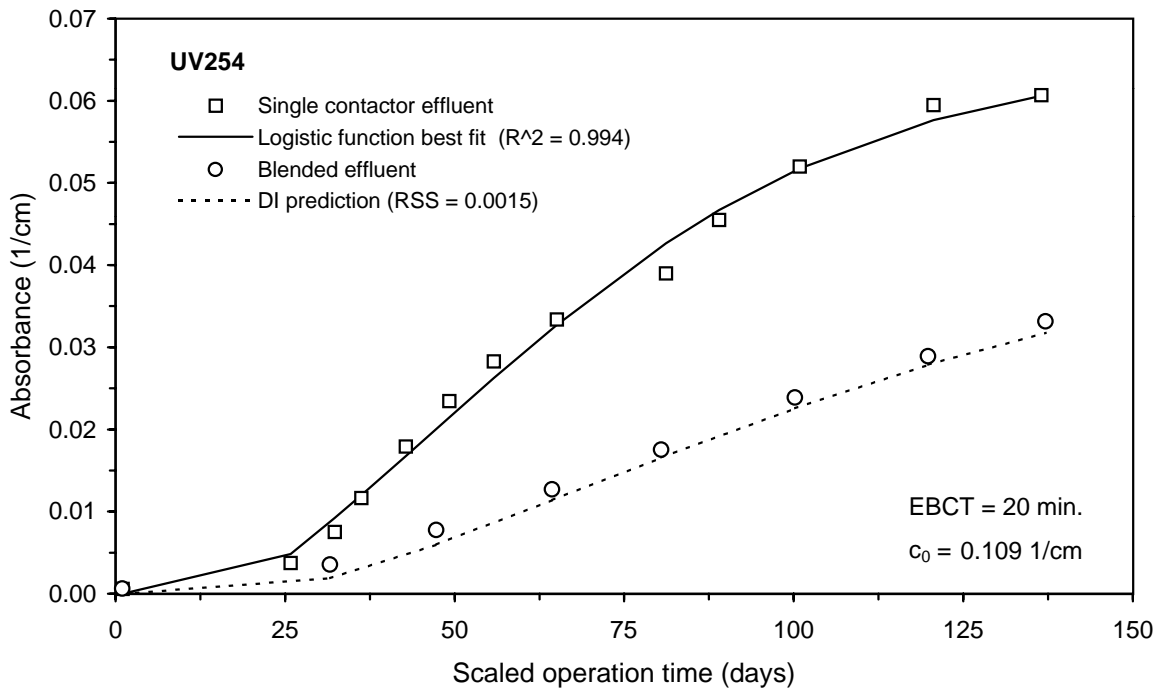


**Figure 58 Single contactor and blended effluent UV254 breakthrough curves for Water 7**

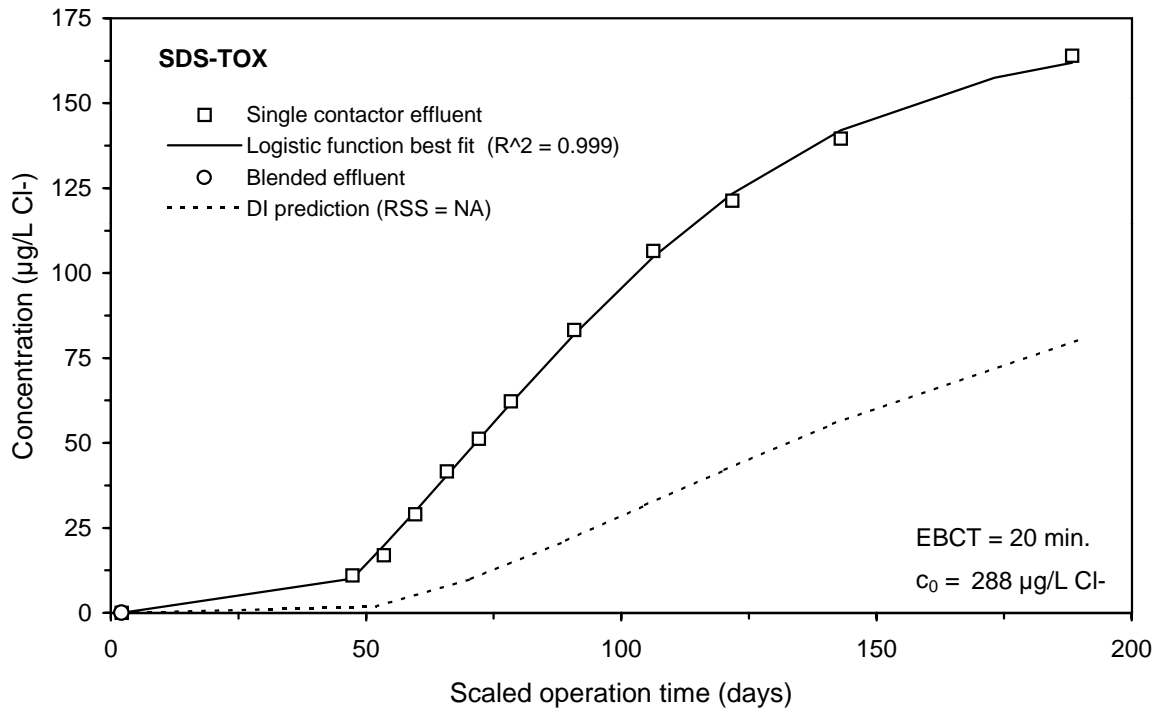


**Figure 59 Single contactor and blended effluent SDS-TOX breakthrough curves for Water 4**

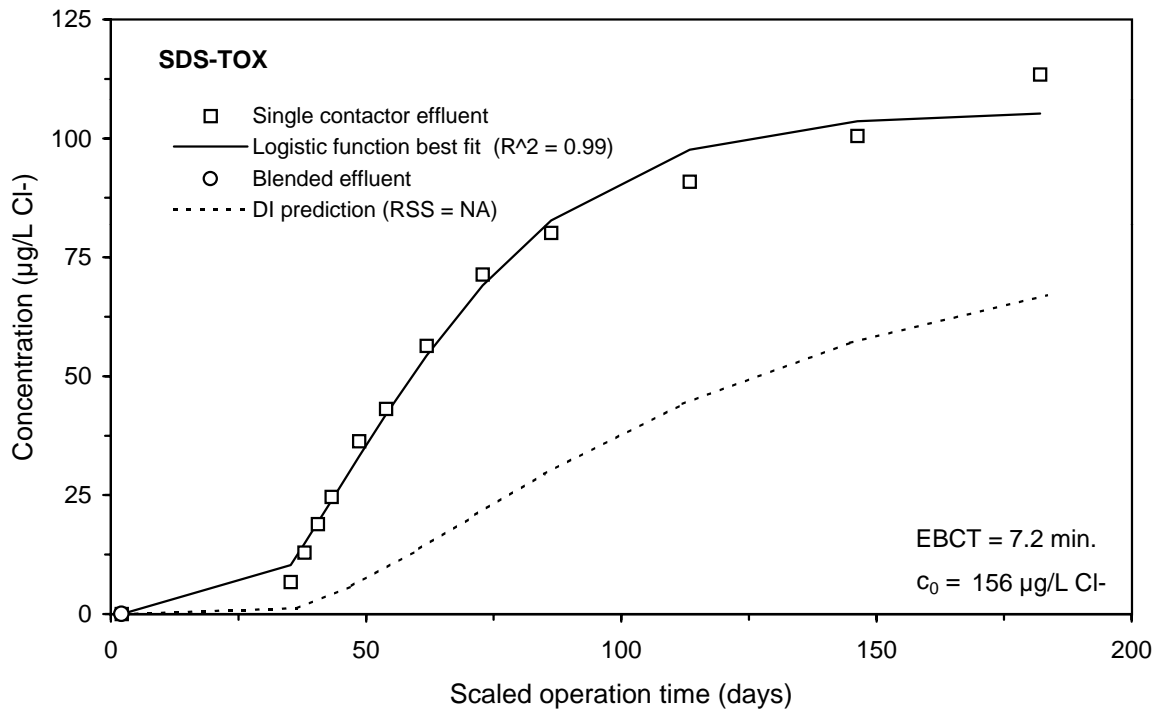


**Figure 60 Single contactor and blended effluent SDS-TOX breakthrough curves for Water 8**

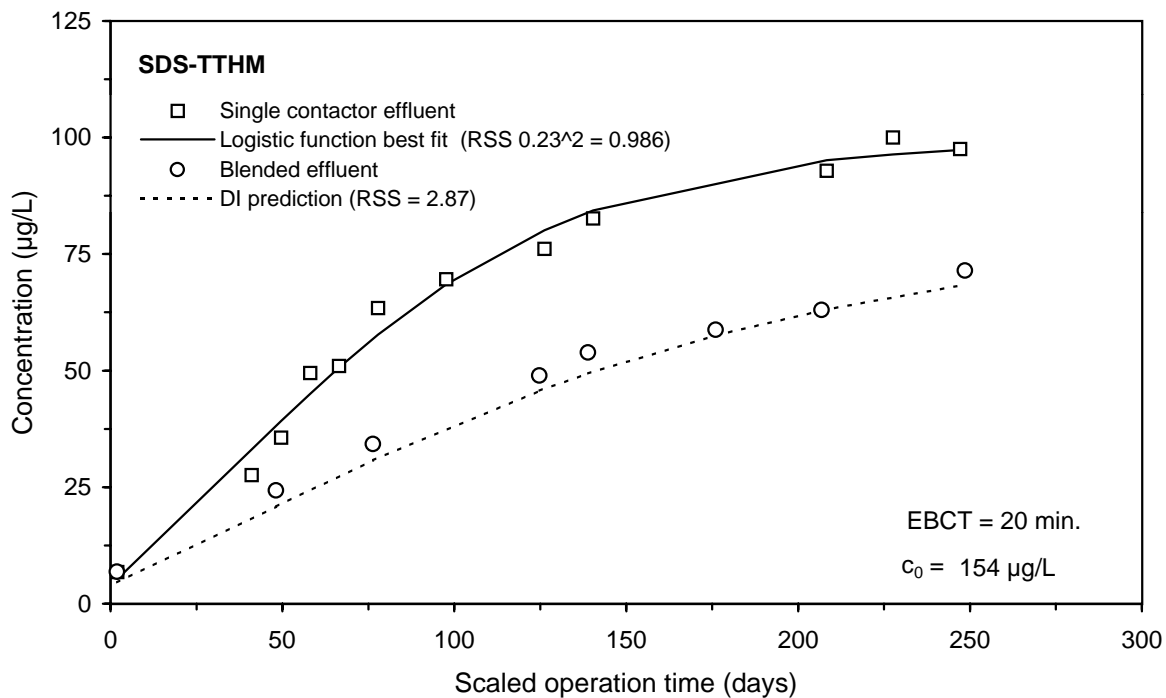


**Figure 61 Single contactor and blended effluent SDS-TTHM breakthrough curves for Water 3**

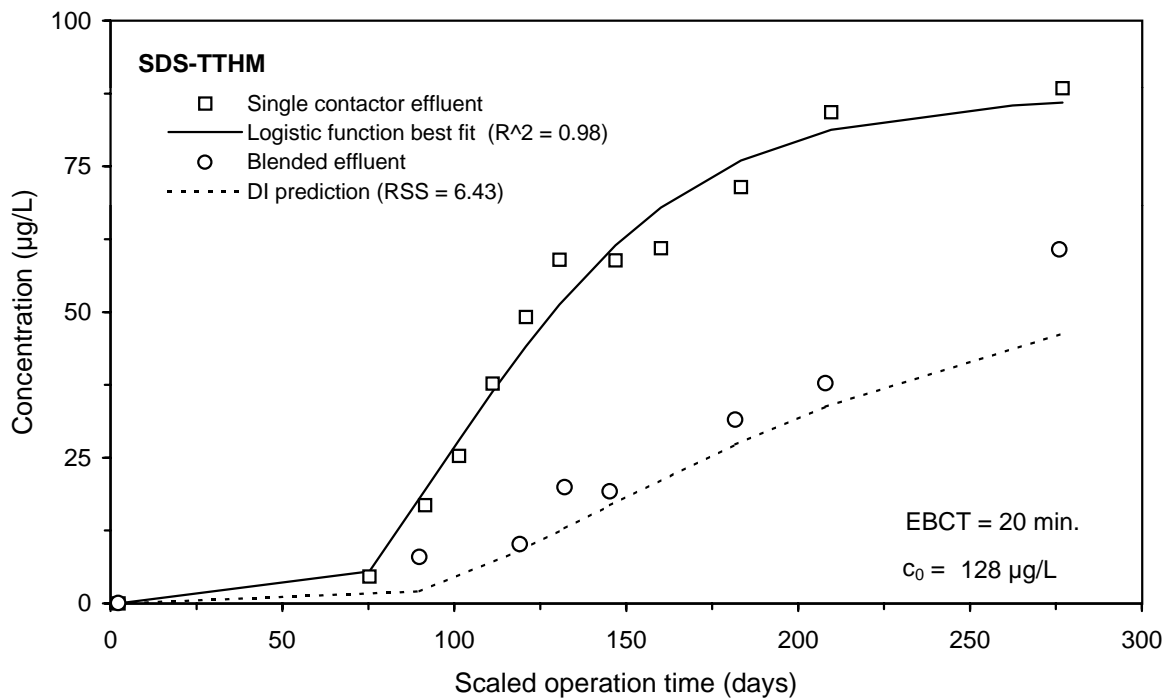


**Figure 62 Single contactor and blended effluent SDS-TTHM breakthrough curves for Water 6**

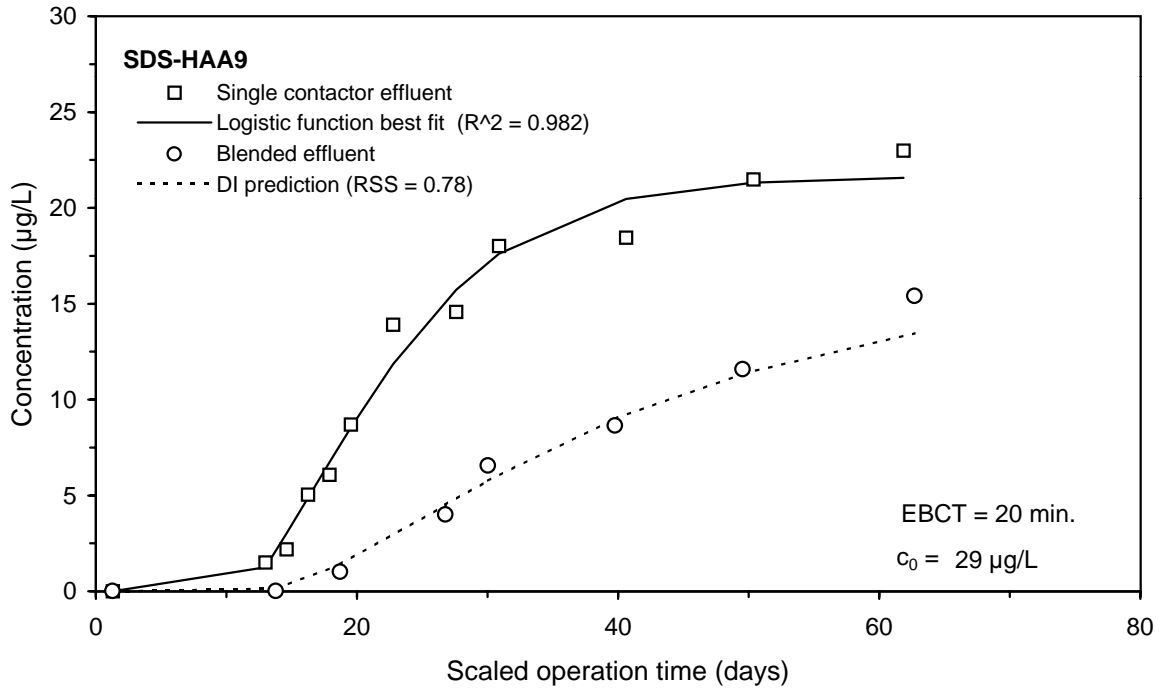


**Figure 63 Single contactor and blended effluent SDS-HAA9 breakthrough curves for Water 1**

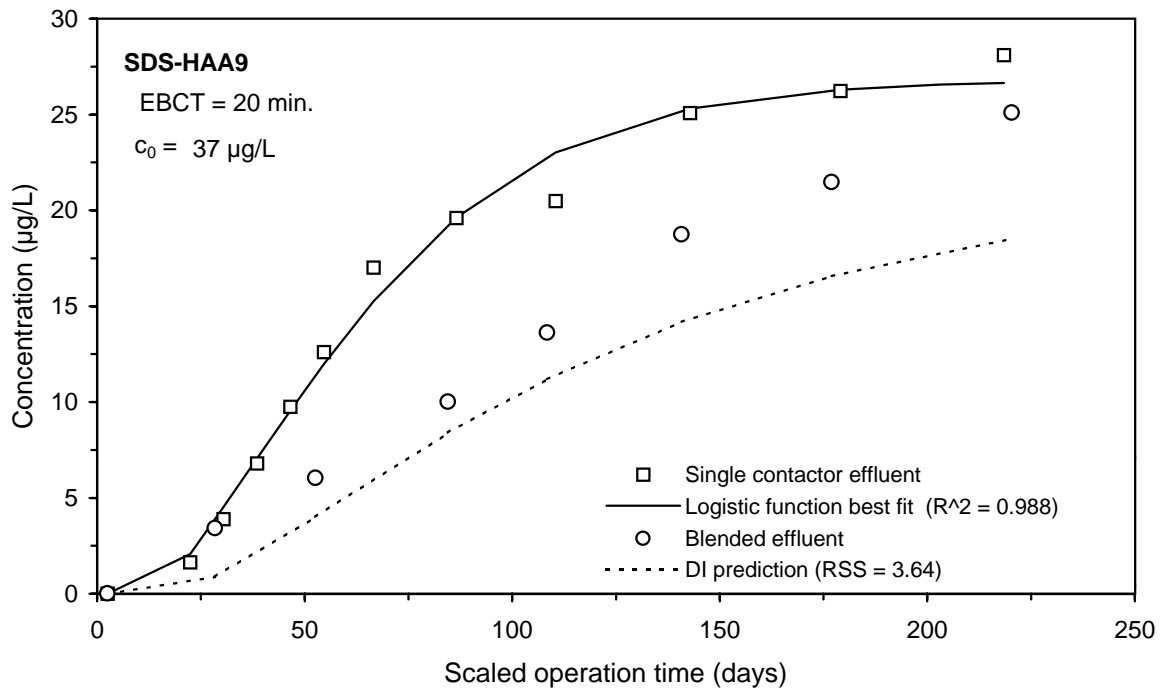


**Figure 64 Single contactor and blended effluent SDS-HAA9 breakthrough curves for Water 2**

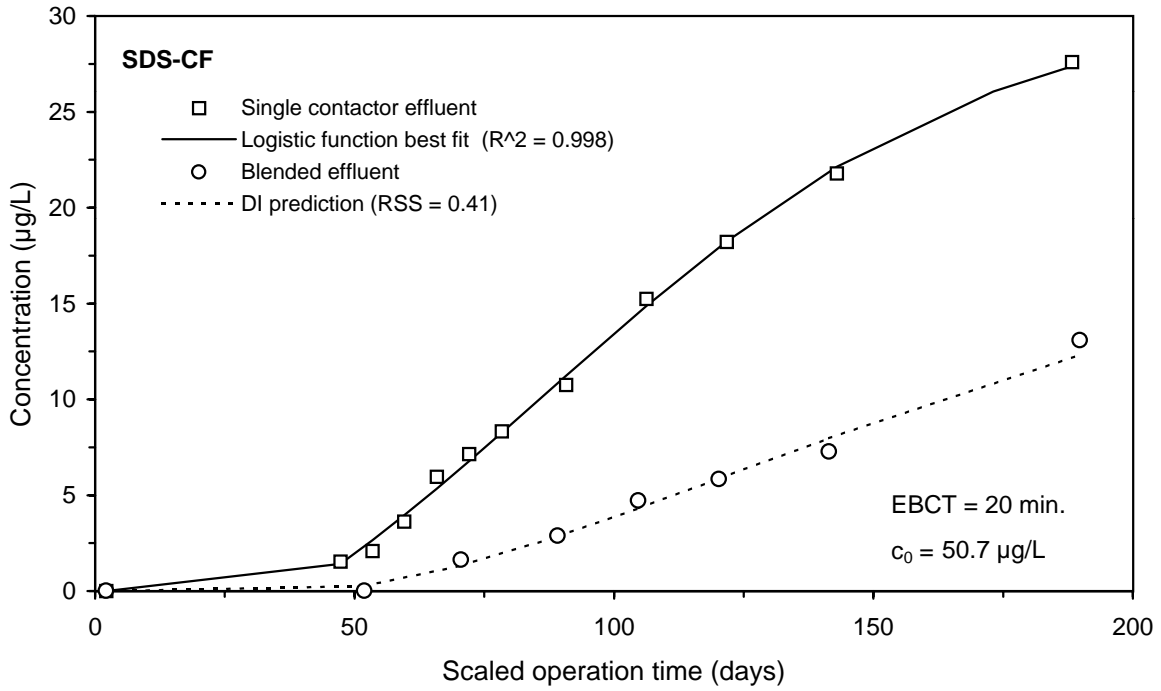


**Figure 65 Single contactor and blended effluent SDS-CF breakthrough curves for Water 4**

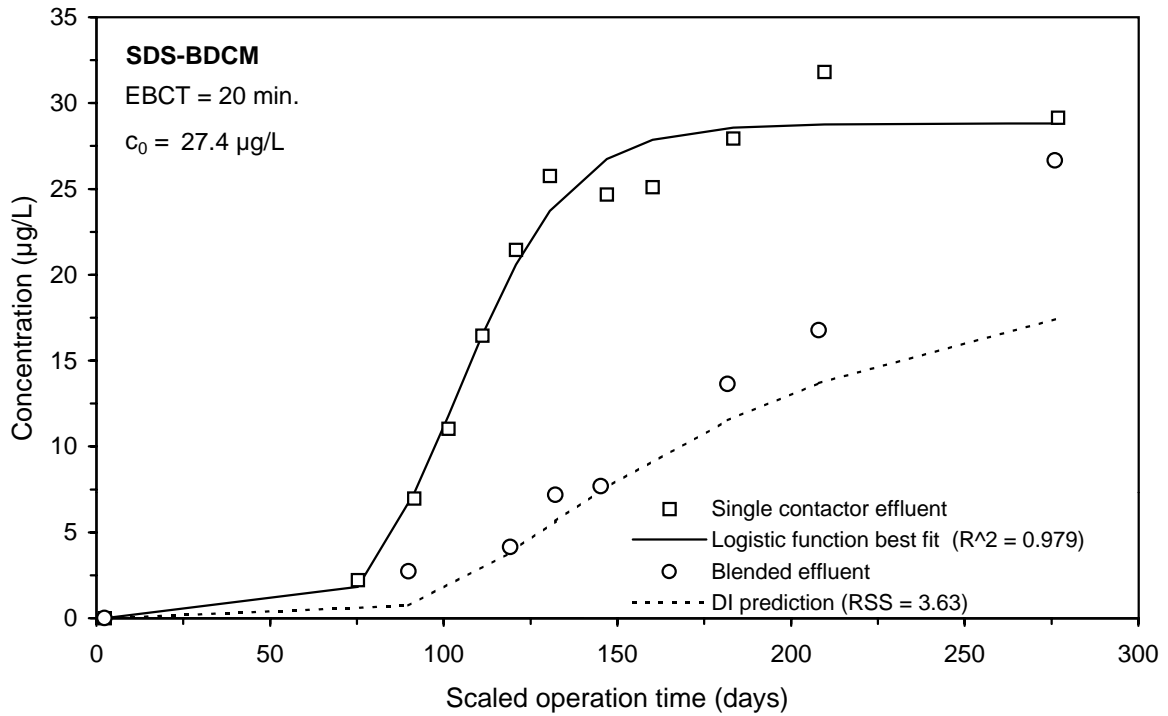


**Figure 66 Single contactor and blended effluent SDS-BDCM breakthrough curves for Water 6**

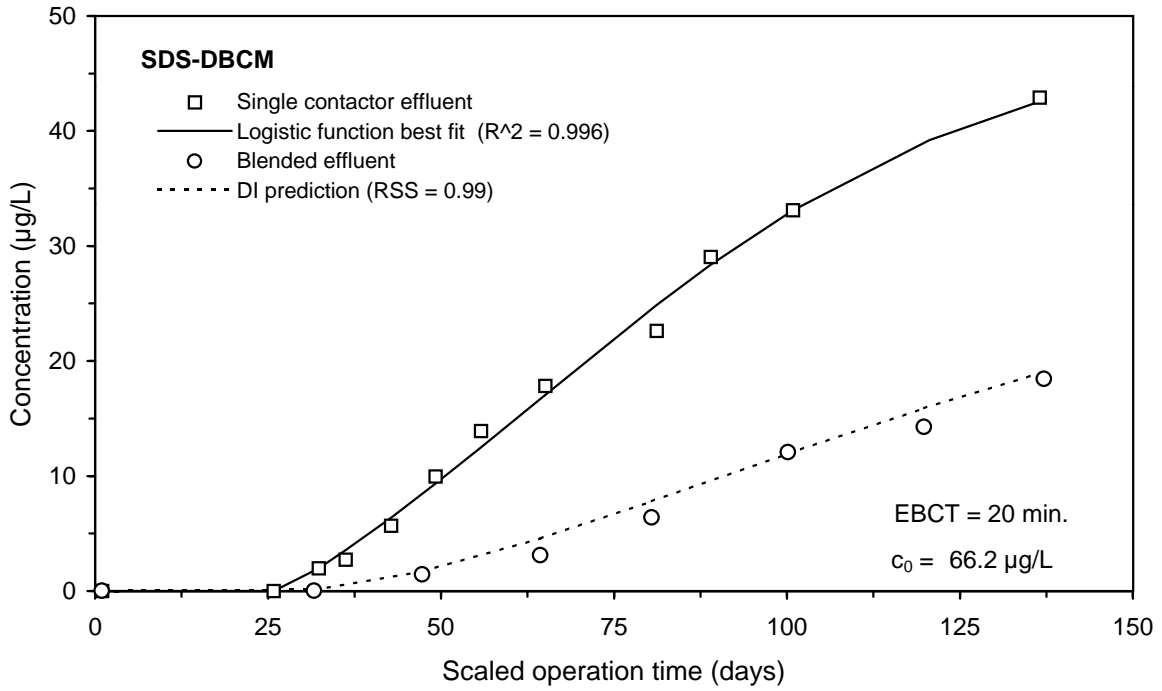


**Figure 67 Single contactor and blended effluent SDS-DBCM breakthrough curves for Water 7**

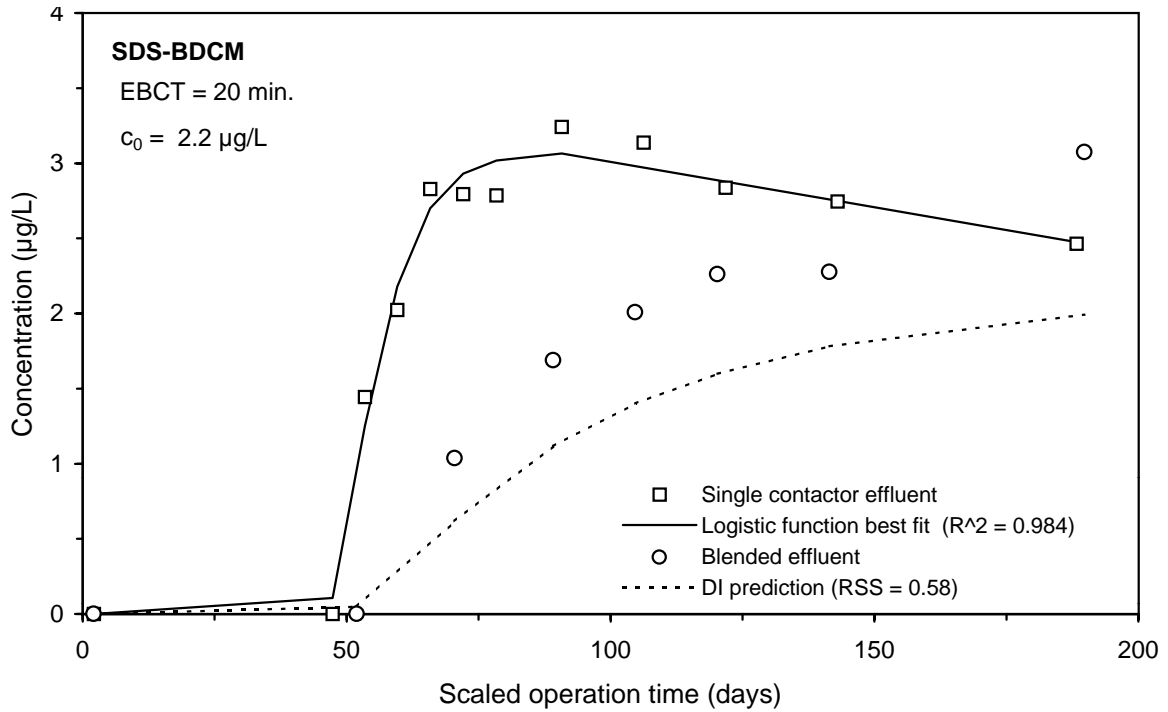


**Figure 68 Single contactor and blended effluent SDS-BDCM breakthrough curves for Water 4**

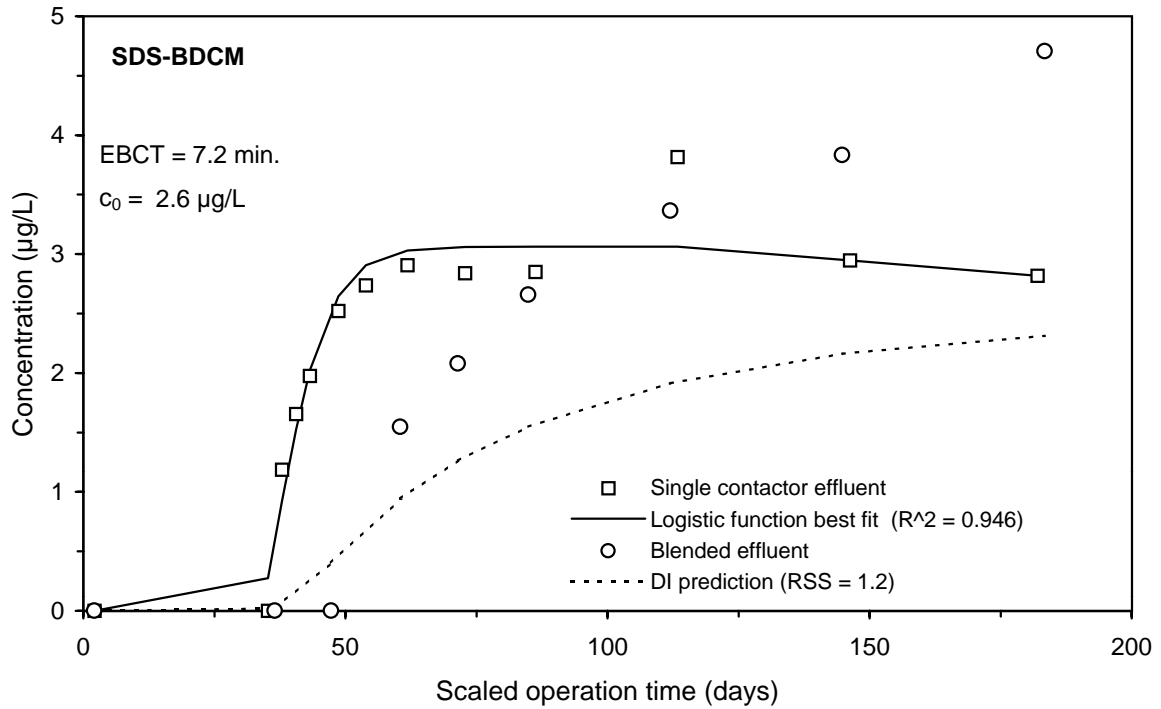


**Figure 69 Single contactor and blended effluent SDS-BDCM breakthrough curves for Water 8**

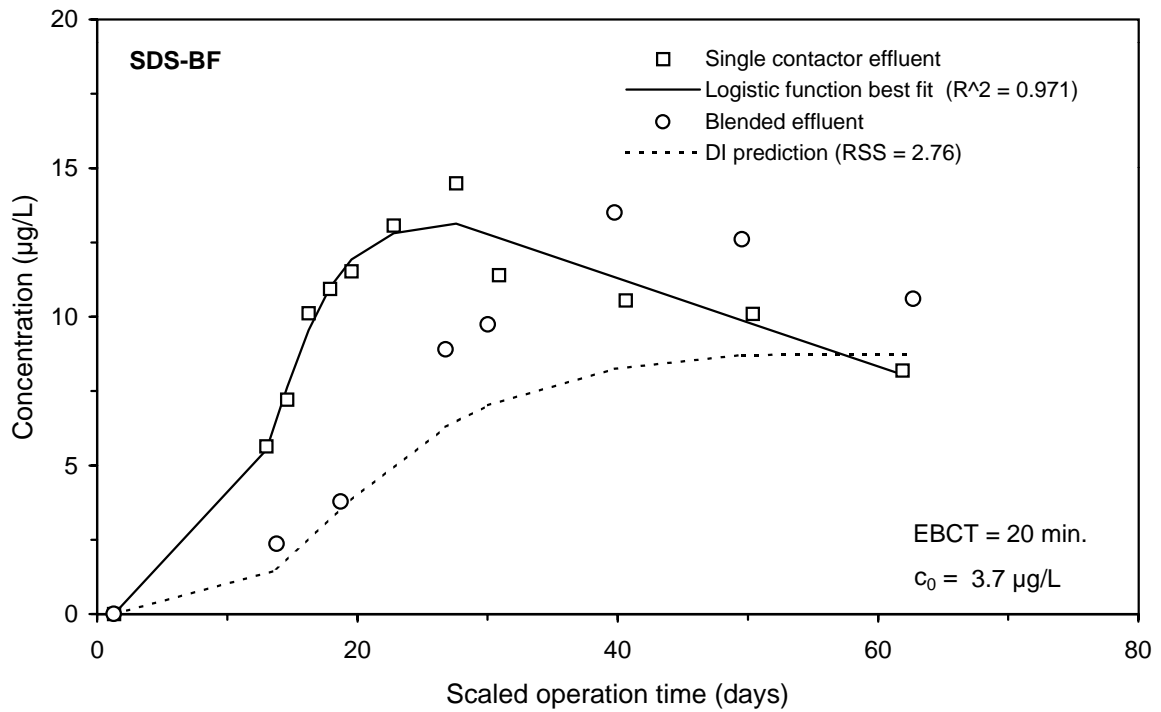


**Figure 70 Single contactor and blended effluent SDS-BF breakthrough curves for Water 1**

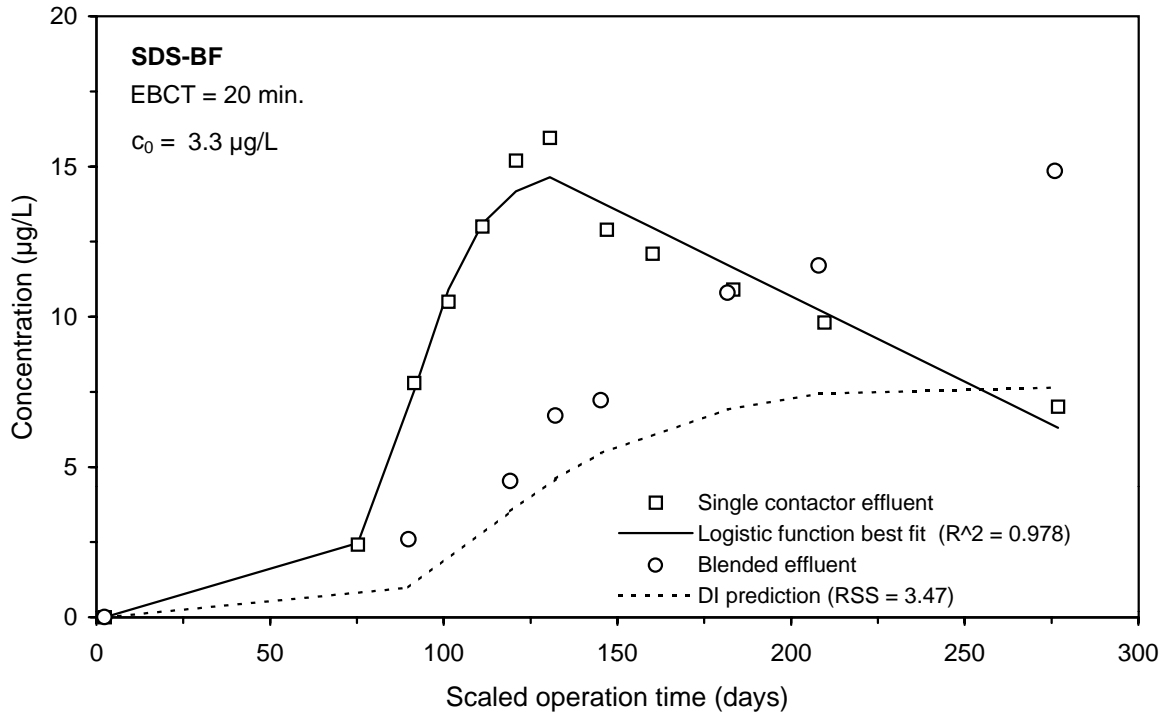


**Figure 71 Single contactor and blended effluent SDS-BF breakthrough curves for Water 6**

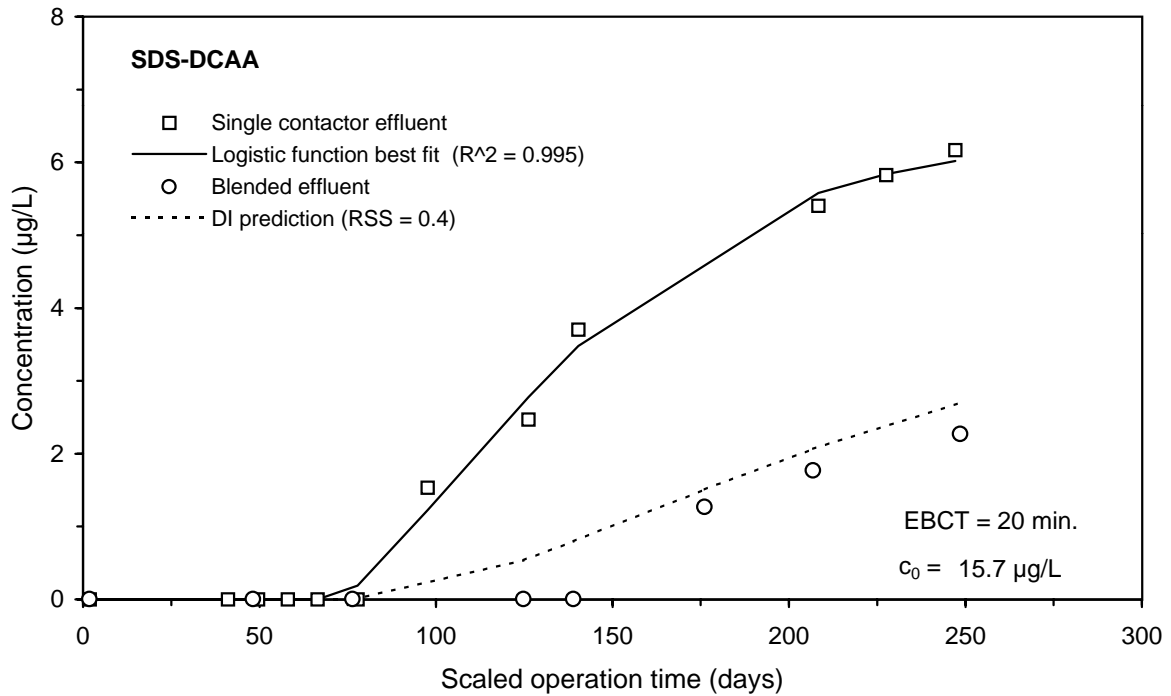


**Figure 72 Single contactor and blended effluent SDS-DCAA breakthrough curves for Water 3**

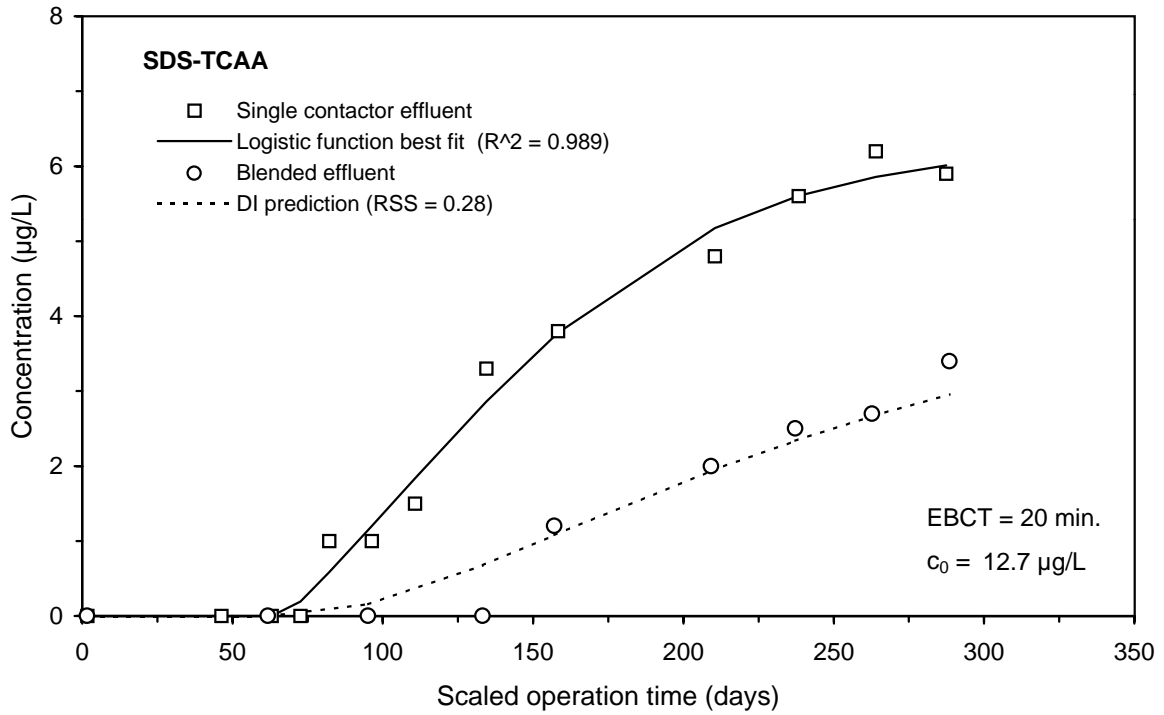


**Figure 73 Single contactor and blended effluent SDS-TCAA breakthrough curves for Water 5**

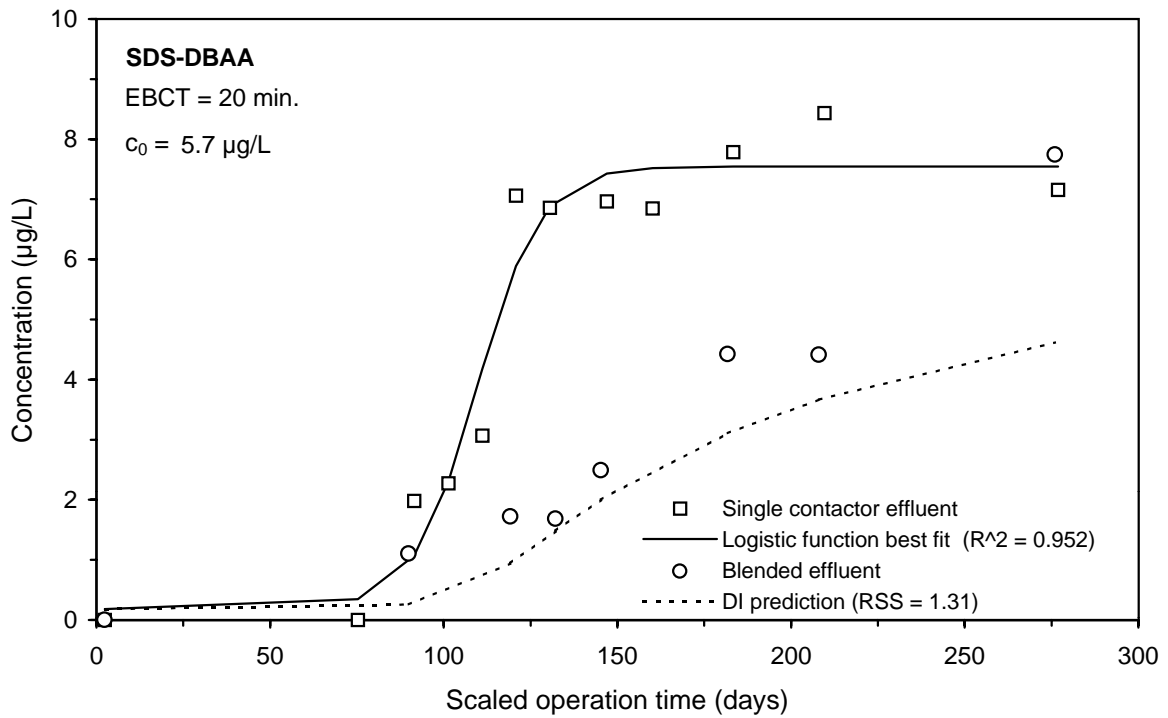


**Figure 74 Single contactor and blended effluent SDS-DBAA breakthrough curves for Water 6**

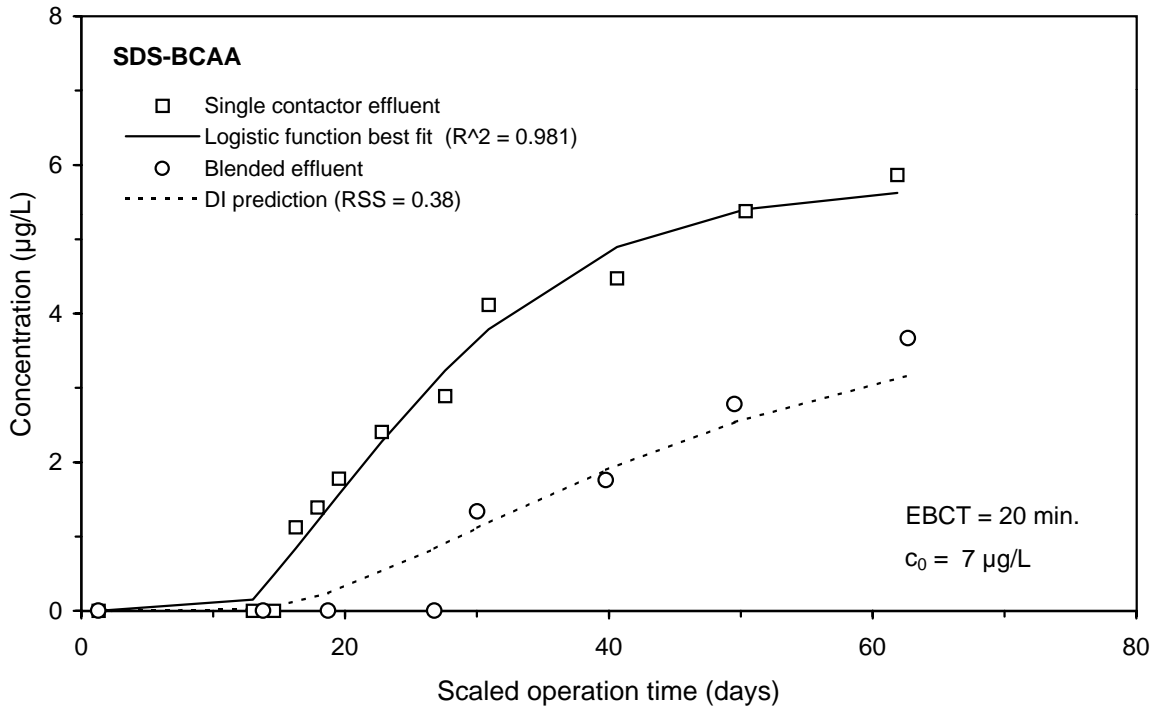


**Figure 75 Single contactor and blended effluent SDS-BCAA breakthrough curves for Water 1**

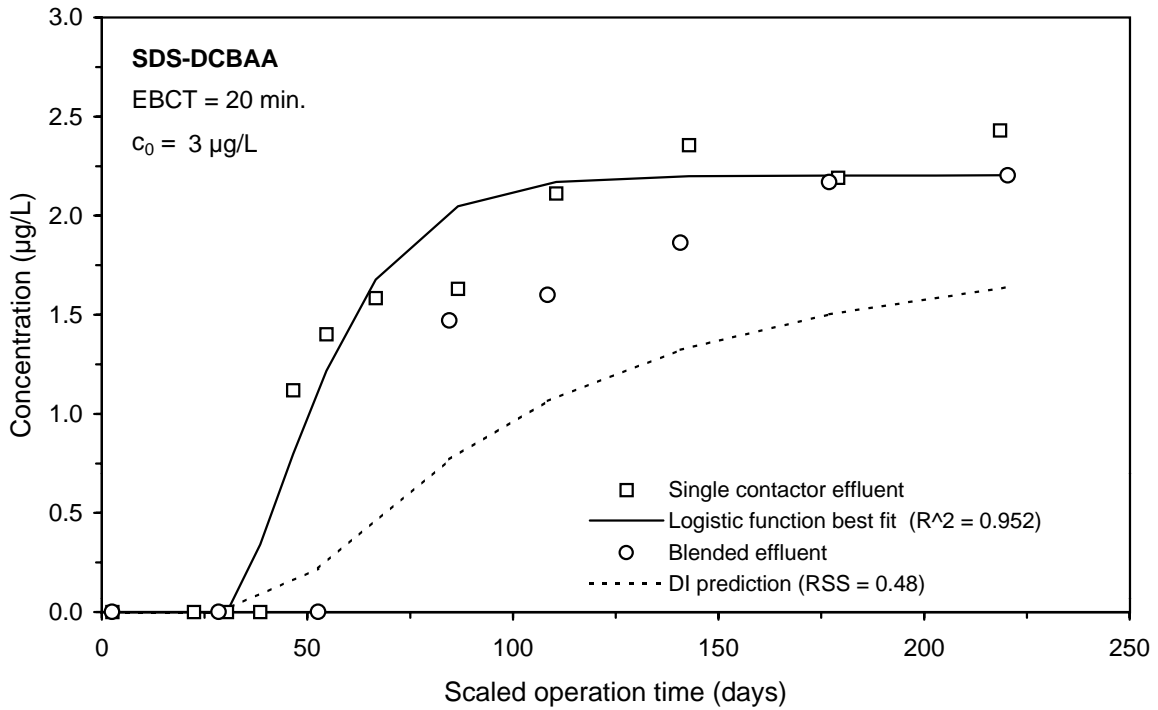


**Figure 76 Single contactor and blended effluent SDS-DCBAA breakthrough curves for Water 2**

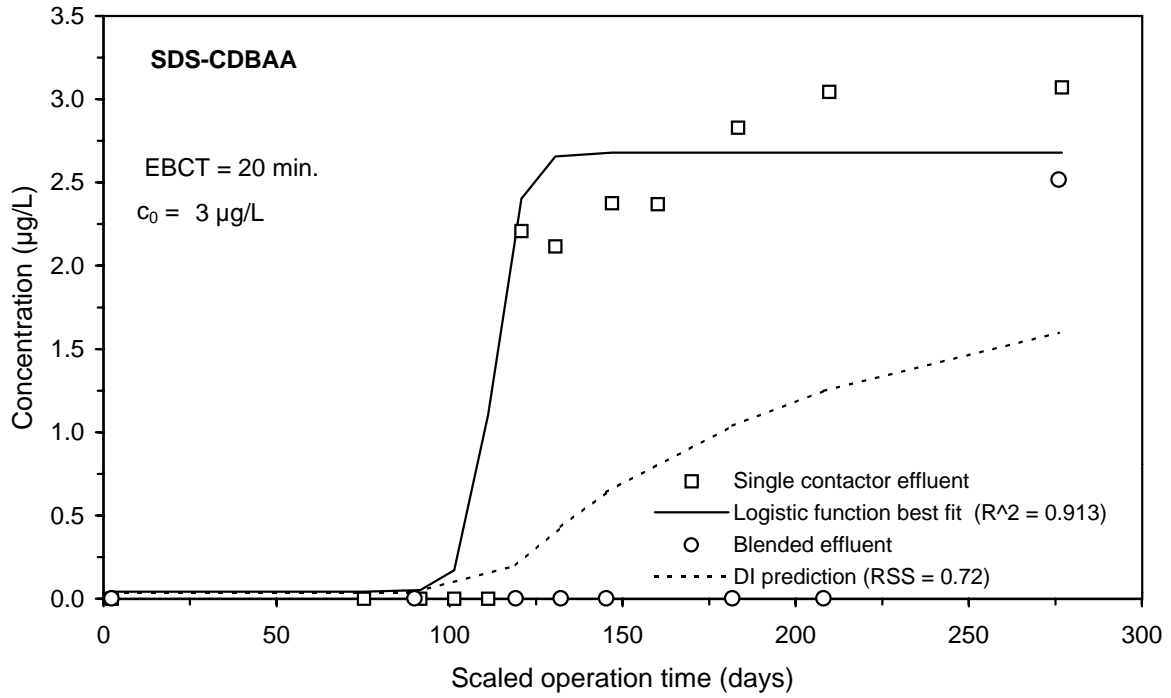


**Figure 77 Single contactor and blended effluent SDS-CDBAA breakthrough curves for Water 6**

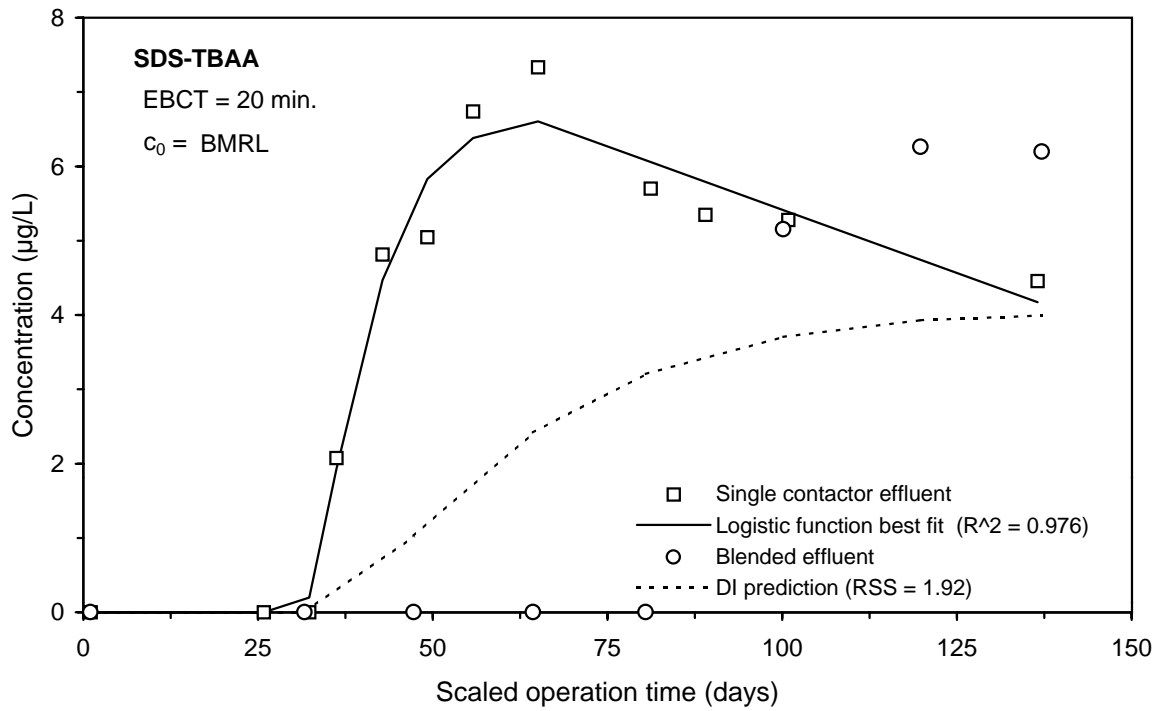


**Figure 78 Single contactor and blended effluent SDS-TBAA breakthrough curves for Water 7**

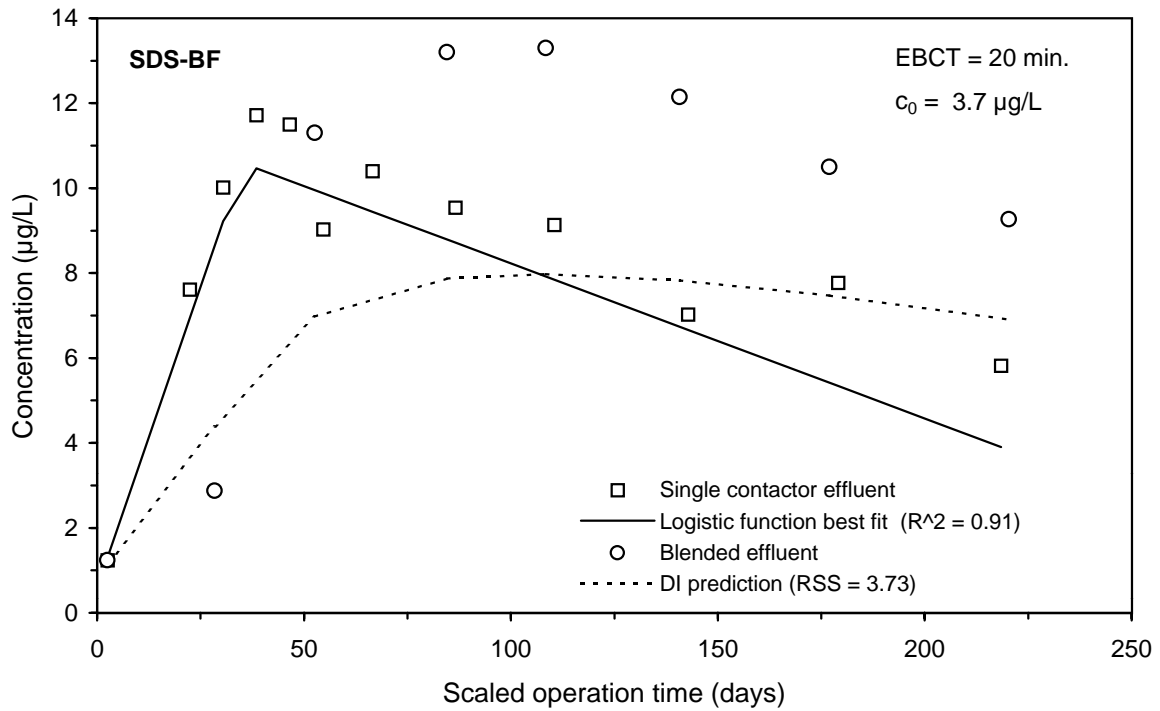


**Figure 79 Single contactor and blended effluent SDS-BF breakthrough curves for Water 2**

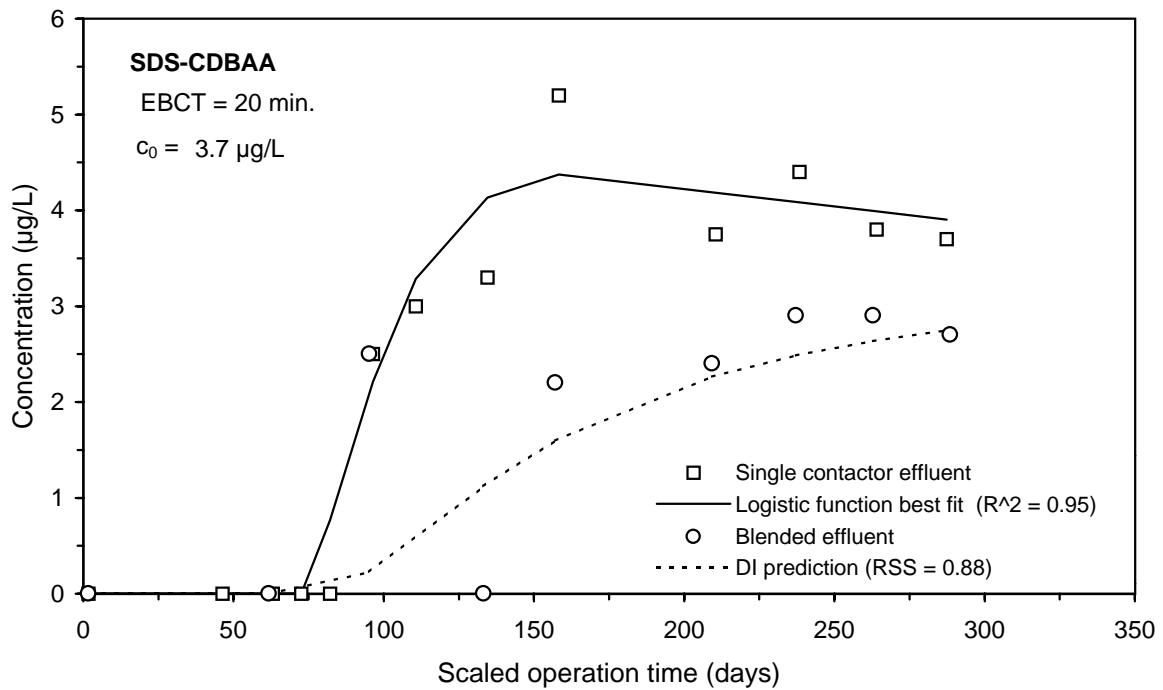


**Figure 80 Single contactor and blended effluent SDS-CDBAA breakthrough curves for Water 5**

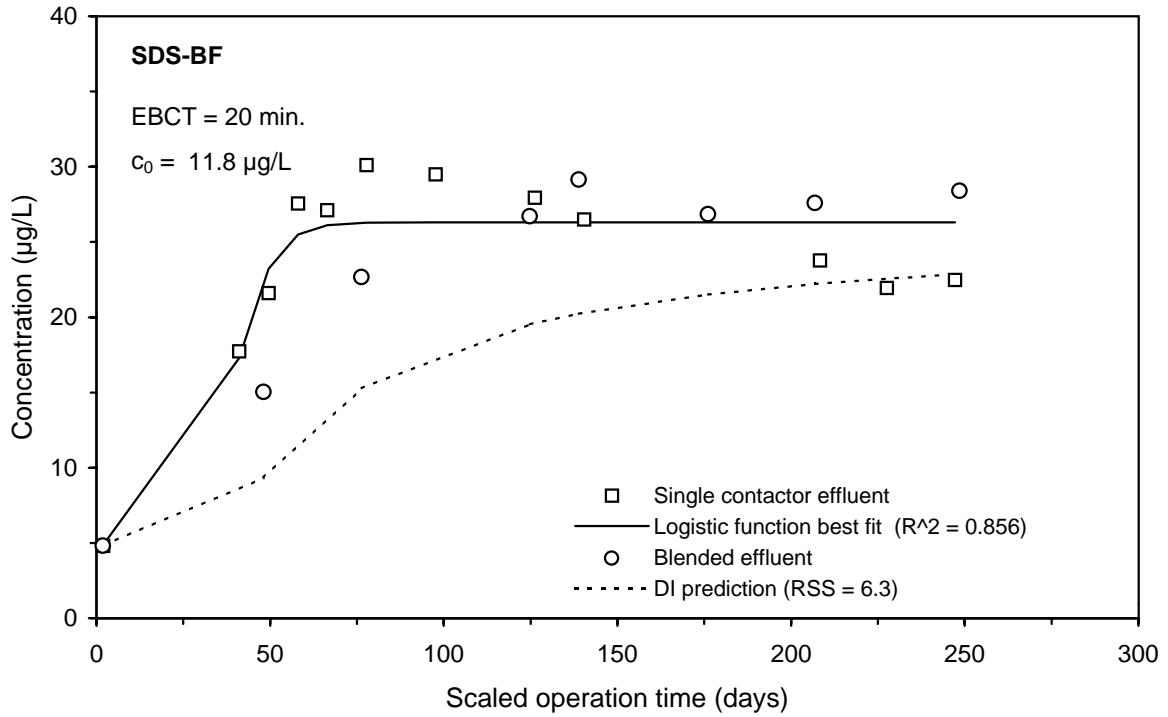


**Figure 81 Single contactor and blended effluent SDS-BF breakthrough curves for Water 3 (original step-lag logistic function model curve fit)**

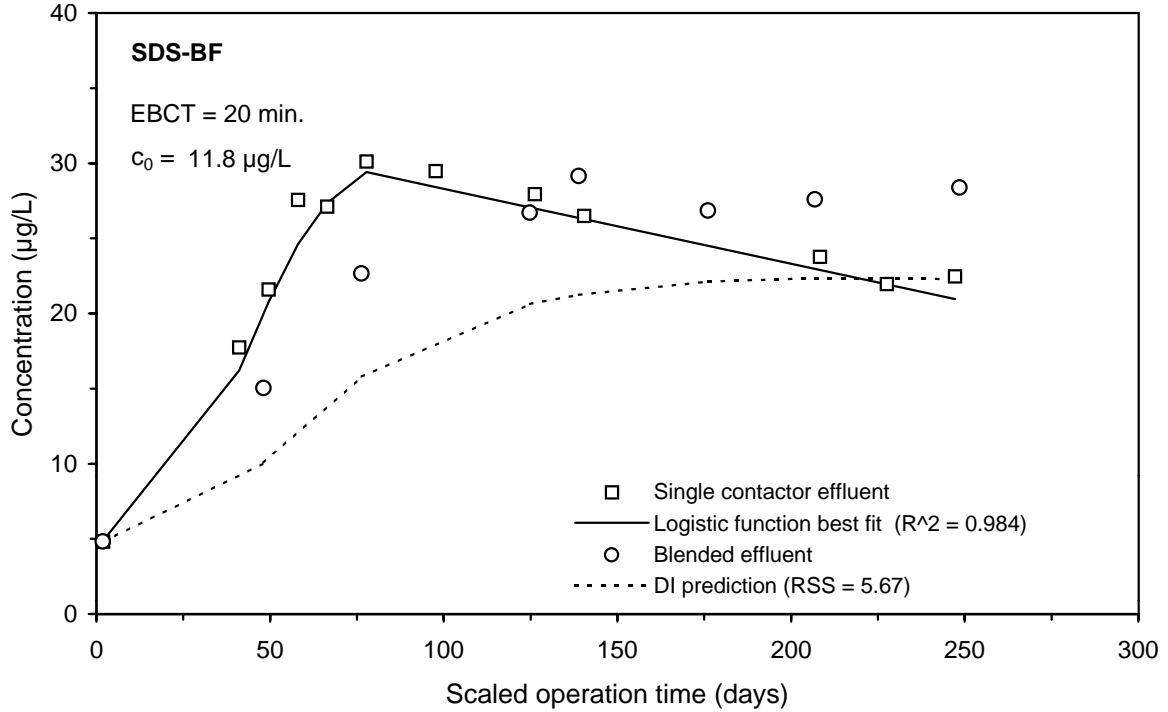


**Figure 82 Single contactor and blended effluent SDS-BF breakthrough curves for Water 3 (fit to step-lag-peak logistic function model)**

This page intentionally left blank.

#### **4.4 Comparison of SCA and DI Methods Used to Predict the Blended Contactor Integral Breakthrough Curve**

Two methods were used to predict the integral breakthrough curve, which is used to estimate blended contactor run times: direct integration (DI) and surrogate correlation approach (SCA). The DI procedure was explained in Sections 1.4 and 3.2.3, while the steps followed by the SCA procedure were described in Sections 1.5 and 3.2.4. The DI method has been presented in the literature and is the traditional method for predicting the integral breakthrough curve, the curve that relates blended contactor effluent water quality to single contactor run time. However, previous verification of the DI method was limited to DBP surrogates and class sums. Verification of the DI method here is expanded to include more GAC runs and water sources, and a larger experimental matrix, including application to DBP species. The SCA method developed in this study is verified against experimental data and compared to results obtained for the DI procedure. The SCA method is computationally simpler than the DI procedure, an important consideration when selecting a predictive method for application to the ICR GAC treatment study data set, which may require 8,000 to 9,000 curve fits.

The results of these predictive models were compared to the experimentally-obtained blended effluent data set. A best-fit curve was used to describe the observed data. The best-fit was derived using the same logistic function models used for the single contactor data, as the shapes observed for many of the blended effluent curves were similar to those encountered during single contactor breakthrough curve analysis. The models were evaluated by comparing the predictions to the experimental data (not the best-fit curve) and calculating the residual sum of squares (RSS) and model bias. The model bias is defined as the mean of the residuals, calculated between the model prediction and experimental results. A summary of the calculated model RSS values is shown in Tables 9 and 10, while a summary of the calculated bias values is shown in Tables 11 and 12. Note that the RSS and bias values have units equivalent to the units of the parameter from which they are calculated; therefore, the magnitudes of these values for different parameters may vary widely and are not directly comparable. A summary of average RSS and bias values is given in Table 13. Based on direct comparisons between the RSS values for each predictive approach, and across all parameters (110 comparisons) the two methods were equally successful in predicting the observed data: for 52 percent of the predictions, the SCA method RSS value was lower than that for the DI method.

To examine the performance of each model for predicting the integral breakthrough curve across all water sources and water quality parameters, cumulative frequency distribution plots were developed for the RSS and bias data. To provide a consistent basis of comparison of RSS and bias data across different parameters, the data was normalized. This was accomplished by dividing the RSS and bias values measured for each parameter and water by the average concentration of that parameter in the blended effluent during each run. This procedure did result in some extremely high normalized values, and overall, the average normalized values were relatively high. However, this is due to the relatively low average effluent concentrations of many parameters, by which the RSS and bias values were normalized. The normalized RSS and bias values are tools that allow comparison of the two predictive models across all available data in this study, and are not intended to provide an indication of model performance outside of

Parameter	Residual sum of squares (RSS)											
	Layer 1			Layer 2			Layer 3			Layer 4		
	DI	SCA	Lower	DI	SCA	Lower	DI	SCA	Lower	DI	SCA	Lower
TOC (ng/L)	0.152	NA	NA	0.057	NA	NA	0.044	NA	NA	0.050	NA	NA
UV-254 (1/cm)	0.0011	0.0017	DI	0.0012	0.0015	DI	0.0010	0.0010	DI	0.0015	0.0023	DI
TOX (µg/L Cl <sup>-</sup> )	NA	NA	NA	NA	NA	NA	NA	NA	NA	NA	NA	NA
TTHM (µg/L)	3.93	2.55	SCA	8.49	4.38	SCA	2.87	2.64	SCA	1.39	2.03	DI
HAA5 (µg/L)	0.38	1.58	DI	1.69	1.48	SCA	2.48	1.13	SCA	1.24	0.87	SCA
HAA6 (µg/L)	0.63	1.26	DI	2.50	2.25	SCA	2.29	2.30	DI	1.34	1.07	SCA
HAA9 (µg/L)	0.78	1.04	DI	3.64	3.43	SCA	4.36	2.20	SCA	1.70	1.12	SCA
CF (µg/L)	0.39	0.65	DI	0.57	1.59	DI	0.85	0.40	SCA	0.41	1.33	DI
BDCM (µg/L)	1.52	1.03	SCA	4.35	1.98	SCA	1.05	2.57	DI	0.58	0.55	SCA
DBCML (µg/L)	0.40	0.73	DI	2.18	1.72	SCA	1.04	0.68	SCA	0.59	0.55	SCA
BF (µg/L)	2.76	1.31	SCA	3.73	2.18	SCA	5.67	3.14	SCA	NA	NA	NA
MCAA (µg/L)	NA	NA	NA	NA	NA	NA	NA	NA	NA	NA	NA	NA
DCAA (µg/L)	0.35	1.46	DI	0.49	0.68	DI	0.40	0.37	SCA	0.32	0.47	DI
TCAA (µg/L)	NA	NA	NA	0.27	0.34	DI	NA	NA	NA	0.96	0.64	SCA
MBAA (µg/L)	NA	NA	NA	NA	NA	NA	NA	NA	NA	NA	NA	NA
DBAA (µg/L)	0.46	0.39	SCA	1.10	0.60	SCA	1.02	1.56	DI	NA	NA	NA
BCAA (µg/L)	0.38	0.29	SCA	0.82	0.78	SCA	0.63	0.63	DI	0.31	0.22	SCA
DCBAA (µg/L)	NA	NA	NA	0.48	0.35	SCA	0.68	0.72	DI	0.49	0.50	DI
CDBAA (µg/L)	NA	NA	NA	NA	NA	NA	NA	NA	NA	NA	NA	NA
TBAA (µg/L)	NA	NA	NA	NA	NA	NA	NA	NA	NA	NA	NA	NA
			DI 7SCA: 5			DI 4SCA: 10			DI 6SCA: 7			DI 5SCA: 7

NA: not applicable

Table 9 Summary of Dland SCA integral breakthrough curve prediction RSS values for Layers 1 through 4

Parameter	Residual sum of squares (RSS)														
	Water 5			Water 6			Water 7			Water 8			All waters lower RSS		
	DI	SCA	Lower	DI	SCA	Lower	DI	SCA	Lower	DI	SCA	Lower	DI	SCA	
TOC (mg/L)	0.035	NA	NA	0.015	NA	NA	0.065	NA	NA	0.033	NA	NA	0	0	
UV-254 (1/cm)	0.0020	0.0022	DI	0.0017	0.0026	DI	0.0015	0.0021	DI	0.0017	0.0017	DI	8	0	
TOX (µg/L Cl <sup>-</sup> )	NA	NA	NA	2.39	6.26	DI	6.92	9.30	DI	NA	NA	NA	2	0	
TTHM (µg/L)	1.89	1.30	SCA	6.43	5.91	SCA	15.22	9.72	SCA	2.59	3.87	DI	2	6	
HAA5 (µg/L)	0.56	0.52	SCA	1.02	1.54	DI	2.02	1.52	SCA	1.35	1.84	DI	3	5	
HAA6 (µg/L)	0.82	0.55	SCA	1.30	1.92	DI	2.09	2.25	DI	1.83	1.86	DI	5	3	
HAA9 (µg/L)	1.19	1.13	SCA	1.88	2.41	DI	4.52	4.70	DI	2.20	1.85	SCA	3	5	
CF (µg/L)	0.31	0.65	DI	1.37	0.74	SCA	0.85	0.46	SCA	0.58	1.62	DI	5	3	
BDCM (µg/L)	0.85	0.34	SCA	3.63	2.31	SCA	5.57	3.38	SCA	1.20	0.81	SCA	1	7	
DBCM (µg/L)	0.54	0.72	DI	1.02	1.84	DI	0.99	1.10	DI	1.15	1.19	DI	5	3	
BF (µg/L)	0.55	0.26	SCA	3.47	1.86	SCA	11.53	5.39	SCA	NA	NA	NA	0	6	
MCAA (µg/L)	NA	NA	NA	NA	NA	NA	NA	NA	NA	NA	NA	NA	0	0	
DCAA (µg/L)	0.49	0.59	DI	0.47	0.31	SCA	0.59	0.63	DI	0.68	0.75	DI	6	2	
TCAA (µg/L)	0.28	0.39	DI	NA	NA	NA	0.40	1.34	DI	0.73	1.00	DI	4	1	
MBAA (µg/L)	NA	NA	NA	NA	NA	NA	NA	NA	NA	NA	NA	NA	0	0	
DBAA (µg/L)	0.47	0.20	SCA	1.31	1.11	SCA	2.21	0.97	SCA	NA	NA	NA	1	5	
BCAA (µg/L)	0.40	0.21	SCA	0.43	0.44	DI	0.35	1.10	DI	0.59	0.31	SCA	3	5	
DCBAA (µg/L)	0.40	0.34	SCA	0.34	0.34	DI	1.13	0.85	SCA	0.46	0.29	SCA	3	4	
CDBAA (µg/L)	0.88	1.10	DI	0.72	0.67	SCA	0.25	1.02	DI	NA	NA	NA	2	1	
TBAA (µg/L)	NA	NA	NA	NA	NA	NA	1.92	1.84	SCA	NA	NA	NA	0	1	
			DI 6SCA: 9			DI 8SCA: 7			DI 9SCA: 8			DI 8SCA: 4	53	57	

NA: not applicable

Table 9 Summary of DI and SCA integral breakthrough curve prediction RSS values for Waters 5 through 8

Parameter	Model Bias							
	Ver 1		Ver 2		Ver 3		Ver 4	
	DI	SCA	DI	SCA	DI	SCA	DI	SCA
TOC (ng/L)	0.074	NA	0.027	NA	0.038	NA	0.037	NA
UV-254 (1/cm)	-0.0007	-0.0012	-0.0004	-0.0005	-0.0008	-0.0007	-0.0009	-0.0016
TOX (µL Cl <sup>-</sup> )	NA	NA	NA	NA	NA	NA	NA	NA
TTHM (µL)	-2.54	-1.65	-7.69	-4.09	-2.55	0.89	-0.81	-1.40
HAA5 (µL)	-0.15	0.29	-1.45	-1.20	4.41	0.22	0.56	-0.57
HAA6 (µL)	-0.16	0.15	-2.16	-1.85	4.48	0.65	0.44	-0.65
HAA9 (µL)	-0.18	-0.03	-3.07	-2.87	4.82	4.23	0.64	-0.36
CF (µL)	0.18	-0.39	-0.15	-0.92	0.57	-0.22	-0.05	-0.89
BDCM (µL)	-1.15	-0.74	-3.83	-1.61	-0.35	4.53	-0.47	-0.09
DBCM (µL)	0.07	-0.48	-1.63	-1.15	0.59	-0.08	-0.36	-0.38
BF (µL)	-2.17	-0.33	-2.91	-1.50	-5.23	-1.17	NA	NA
MCAA (µL)	NA	NA	NA	NA	NA	NA	NA	NA
DCAA (µL)	0.11	0.28	-0.38	-0.57	0.29	-0.22	0.04	-0.33
TCAA (µL)	NA	NA	-0.04	0.00	NA	NA	0.36	-0.44
MBAA (µL)	NA	NA	NA	NA	NA	NA	NA	NA
DBAA (µL)	-0.21	0.22	-0.90	-0.35	-0.03	0.52	NA	NA
BCAA (µL)	0.04	-0.06	-0.72	-0.66	0.36	0.17	-0.13	-0.09
DCBAA (µL)	NA	NA	-0.35	-0.24	0.58	0.62	0.34	0.38
CDBAA (µL)	NA	NA	NA	NA	NA	NA	NA	NA
TBAA (µL)	NA	NA	NA	NA	NA	NA	NA	NA

NA: not applicable

**Table 1** Summary of model prediction bias for Ver 1 through 4

Parameter	Model Bias							
	Ver 5		Ver 6		Ver 7		Ver 8	
	DI	SCA	DI	SCA	DI	SCA	DI	SCA
TOC (ng/L)	0.023	NA	-0.001	NA	0.044	NA	-0.019	NA
UV-254 (1/cm)	-0.0013	-0.0015	-0.0012	-0.0019	-0.0007	-0.0008	-0.0001	-0.0008
TOX (µL Cl <sup>-</sup> )	NA	NA	-1.53	-4.89	-6.24	-5.48	NA	NA
TTHM (µL)	-1.29	-0.89	-4.83	-4.11	-11.39	-7.42	-2.01	-3.15
HAA5 (µL)	-0.22	-0.03	-0.55	-1.14	-1.35	-0.23	-0.20	-0.78
HAA6 (µL)	-0.31	0.03	-0.48	-1.44	-1.20	0.33	-0.43	-0.87
HAA9 (µL)	-0.86	-0.44	-0.10	-1.50	-0.54	4.91	-0.43	-0.79
CF (µL)	-0.04	-0.44	0.55	-0.33	0.59	-0.30	-0.25	-1.29
BDCM (µL)	-0.62	0.04	-2.30	-1.47	-3.28	-1.98	-0.85	-0.58
DBCM (µL)	-0.25	-0.40	-0.21	-1.27	0.71	-0.59	-0.90	-1.03
BF (µL)	-0.45	-0.12	-2.73	-0.76	-9.15	-4.18	NA	NA
MCAA (µL)	NA	NA	NA	NA	NA	NA	NA	NA
DCAA (µL)	-0.35	-0.44	0.34	-0.04	0.48	0.53	-0.13	-0.35
TCAA (µL)	0.00	-0.25	NA	NA	0.03	-0.81	-0.09	-0.39
MBAA (µL)	NA	NA	NA	NA	NA	NA	NA	NA
DBAA (µL)	-0.27	0.10	-0.92	-0.81	-1.65	-0.07	NA	NA
BCAA (µL)	-0.10	0.06	0.07	-0.25	0.17	0.58	-0.25	-0.10
DCBAA (µL)	-0.18	-0.21	0.18	-0.10	0.50	0.05	0.00	0.14
CDBAA (µL)	-0.28	-0.02	0.34	0.32	0.05	0.62	NA	NA
TBAA (µL)	NA	NA	NA	NA	0.08	4.02	NA	NA

NA: not applicable

**Table 2** Summary of model prediction bias for Ver 5 through 8

Parameter	Mean RSS		Mean normalized RSS		Mean bias		Mean normalized bias		Count
			%				%		
	DI	SCA	DI	SCA	DI	SCA	DI	SCA	
TOC (ng/L)	0.06	NA	7.2	NA	0.028	NA	3.7	NA	8
UV-254 (1/cm)	0.0015	0.0019	18	23	-0.0008	-0.0011	-8.2	-12	8
TOX (µg/L Cl <sup>-</sup> )	4.7	7.8	8.5	16	-3.88	-5.19	-7.4	-9.8	2
TTHM (µg/L)	5.4	4.1	19	18	-4.14	-2.73	-15	-10	8
HAA5 (µg/L)	1.3	1.3	26	28	-0.24	-0.43	-4.4	-7.9	8
HAA6 (µg/L)	1.6	1.7	23	25	-0.35	-0.46	-4.7	-6.1	8
HAA9 (µg/L)	2.5	2.2	29	26	-0.22	-0.36	-2.3	-3.9	8
CF (µg/L)	0.7	0.9	36	36	0.17	-0.60	6.5	-22	8
BDCM (µg/L)	2.3	1.6	29	20	-1.61	-0.61	-16	-6.1	8
DBCm (µg/L)	1.0	1.1	19	21	-0.25	-0.67	-4.6	-13	8
BF (µg/L)	4.6	2.4	38	20	-3.77	-1.34	-30	-11	6
MCAA (µg/L)	NA	NA	NA	NA	NA	NA	NA	NA	0
DCAA (µg/L)	0.5	0.7	40	44	0.05	-0.14	3.2	-8.9	8
TCAA (µg/L)	0.5	0.7	39	61	0.05	-0.38	4.1	-29	5
MBAA (µg/L)	NA	NA	NA	NA	NA	NA	NA	NA	0
DBAA (µg/L)	1.1	0.8	28	21	-0.66	-0.07	-17	-1.6	6
BCAA (µg/L)	0.5	0.5	28	24	-0.07	-0.04	-3.5	-2.2	8
DCBAA (µg/L)	0.6	0.5	119	115	0.15	0.09	15	8.4	7
CDBAA (µg/L)	0.6	0.9	98	111	0.04	0.31	2.8	24	3
TBAA (µg/L)	1.9	1.8	87	84	0.08	4.02	3.8	46	1

NA: not applicable

**Table 3** Summary of mean RSS, mean bias, normalized mean RSS, and normalized mean bias for all waters

the context of the actual magnitude of the RSS and bias values. For each parameter, the average normalized RSS and bias across all waters are summarized in Table 13.

The cumulative frequency distribution plot of normalized RSS values is shown in Figure 83. The distribution of normalized RSS values for both predictive approaches is similar, indicating that there was little difference in the relative success of the two methods to predict experimental data over the entire data set. The 25th to 75th percentile range of normalized RSS values for DI predictions was 16 to 39 percent, while that for SCA predictions was similar, 16 to 38 percent. The 10th to 90th percentile range of normalized RSS values for both methods was also similar, at 11 to 57 percent for the SCA method and 12 to 57 percent for the DI method.

Figure 84 shows the cumulative frequency distribution of normalized bias values. Across all waters and water quality parameters, both predictive methods tended to underestimate the experimental data. The median of the distribution for the DI method was -6 percent, while that for the SCA method was -10 percent. The 25th to 75th percentile range of the distribution was -16 to +3 percent for the DI method. The SCA method more often underpredicted the experimental data as indicated by a 25th to 75th percentile range of the distribution of -20 to -1 percent. The 10th to 90th percentile range of the distribution for the DI method was -25 to +30 percent, while that for the SCA method was -28 to +10 percent.

Across all waters and analytes, the distribution of prediction error was shown to be similar based on the cumulative frequency distribution of RSS. However, an evaluation of the results for each parameter is still needed and is addressed below in Sections 4.4.1 and 4.4.2. By comparing the error, as measured by RSS and bias, for each parameter across all waters, the relative performance of each model for each individual analyte can be assessed. A summary of all model predictions for all parameters and all waters is included in Appendix F. For this discussion, examples of DI and SCA model results were selected from the eight runs.

#### 4.4.1 Surrogates and Class Sums

As shown in Figures 49 through 56 (Section 4.3), the DI method was able to successfully predict the integral breakthrough curve for TOC for the eight runs examined. The average DI model RSS for all eight runs was 0.055 mg/L, which compares to a value of 0.025 mg/L for the average of all eight best-fit curves applied to the data. The DI method prediction average RSS was slightly more than twice that for a best curve fit, but both values were very low. Expressed as a fraction of the average TOC concentration of the experimental blended effluent data for each water, the normalized RSS for the DI prediction was low, 7 percent. The average bias for the DI method prediction was low and positive, +0.028 mg/L. The mean normalized bias (bias expressed as a fraction of the average blended effluent experimental data) was also low, 4 percent.

The success of the DI model for predicting the TOC integral breakthrough curve is an important verification prior to the application of the SCA method, as this method relies on the TOC integral breakthrough curve as a basis for predicting the integral breakthrough curves of all other parameters. Although an excellent predictor of the TOC integral breakthrough curve, the DI method was not as successful in predicting the integral breakthrough curve for DBPs, especially brominated DBP species, as shown by the examples given in Section 4.3 (Figures 61 through

82). The results of integral breakthrough curves predicted by the computationally-simpler SCA procedure will be compared to those predicted by the DI method.

Figures 85 and 86 compare the DI and SCA  $UV_{254}$  integral breakthrough predictions against experimental data for Waters 1 and 3. During both these runs, the RSS of the predictions were very low (all less than 0.002 1/cm). For Water 1, the DI method was able to match experimental results early in the run very well, while the SCA method underpredicted the observed data. Later in the run, both methods slightly underpredicted the experimental integral breakthrough curve. The DI method yielded a closer prediction based on RSS values for Water 1. The bias for both predictions was negative (DI: -0.0007 1/cm; SCA: -0.0012 1/cm), indicating quantitatively that the models slightly underpredicted the experimental data. For Water 3, both methods underpredicted blended effluent  $UV_{254}$  early in the run. Beyond the midpoint of the run, both methods matched the experimental results more closely. The RSS values for each predictive approach were equivalent, and the bias values were both slightly negative (DI: -0.0008 1/cm; SCA: -0.0007 1/cm). Overall, the  $UV_{254}$  DI prediction results yielded lower RSS values for seven of the eight runs.

The integral breakthrough curve predictions for SDS-TTHM are given in Figures 87 and 88 for Waters 1 and 7. Based on the calculated RSS values, the SCA method yielded better predictions of the observed data than the DI method (Water 1 DI RSS: 3.9  $\mu\text{g/L}$ ; Water 1 SCA RSS: 2.6  $\mu\text{g/L}$ ; Water 7 DI RSS: 15  $\mu\text{g/L}$ ; Water 7 SCA RSS: 9.7  $\mu\text{g/L}$ ), as was the case with six of the eight runs. Early in the run, at the point of initial breakthrough, the SCA method underpredicted experimental results, while the DI method matched the experimental data more closely. However, later in the run, at higher breakthrough levels, the SCA method was able to better predict the experimental data. This pattern was repeated during most runs. The more pronounced deviation early in the run is preferable over later in the run, because the target treatment objective for SDS-TTHM is usually exceeded later in the run, where the SCA prediction is closest to the experimental data. The prediction bias for Water 1 for both methods was negative (DI: -2.5  $\mu\text{g/L}$ ; SCA: -1.6  $\mu\text{g/L}$ ). Both predictive methods also yielded a negative bias for Water 7 (DI: -11  $\mu\text{g/L}$ ; SCA: -7.4  $\mu\text{g/L}$ ), indicating that the experimental results were underpredicted by both predictive models. The average bias for all runs was negative for both methods.

Neither predictive method was consistently more successful for the prediction of the integral breakthrough curve for SDS-HAA5, SDS-HAA6 and SDS-HAA9. For SDS-HAA5 and SDS-HAA9, the DI method was slightly more successful, with closer matches to experimental data based on RSS values in five out of eight cases for each parameter. For SDS-HAA6, the SCA method was a better predictor in five out of eight cases. The average bias for both model predictions for SDS-HAA5, SDS-HAA6, and SDS-HAA9 for all runs was negative.

Figures 89 and 90 show the model prediction results for SDS-HAA5 for Waters 2 and 7, respectively. For these two waters, the SCA method yielded a better prediction of the observed blended effluent data by comparison of calculated RSS values (Water 2 DI RSS: 1.7  $\mu\text{g/L}$ ; Water 2 SCA RSS: 1.5  $\mu\text{g/L}$ ; Water 7 DI RSS: 2.0  $\mu\text{g/L}$ ; Water 7 SCA RSS: 1.5  $\mu\text{g/L}$ ). For Water 2, both methods underpredicted experimental results throughout the run, while for Water 7, the DI method underpredicted the observed data throughout the run. The SCA method initially underpredicted experimental data, but between the midpoint and end of the run was a close match to the data. The calculated bias for both waters and both methods was negative (Water 2

DI bias: -1.4 µg/L; Water 2 SCA bias: -1.2 µg/L; Water 7 DI bias: -1.3 µg/L; Water 7 SCA bias: -0.2 µg/L).

For Waters 3 and 5, Figures 91 and 92, respectively, compare the model prediction results for SDS-HAA6. For Water 3, both models overpredicted blended effluent concentrations, especially towards the end of the run (DI bias: +1.5 µg/L; SCA bias: +0.7 µg/L), and the RSS values were similar (DI RSS: 2.3 µg/L; SCA RSS: 2.3 µg/L). For Water 5, both models matched the observed results well, with the SCA method resulting in the closest match based on RSS values (DI RSS: 0.8; SCA RSS: 0.6). The bias calculated for the DI prediction was negative (-0.3 µg/L), while that for the SCA prediction was slightly positive (+0.03 µg/L).

For Waters 5 and 6, the model predictions for blended contactor effluent SDS-HAA9 are shown in Figures 93 and 94, respectively. The bias for both model predictions for both waters was negative (Water 5 DI bias: -0.9 µg/L; Water 5 SCA bias: -0.4 µg/L; Water 6 DI bias: -0.1 µg/L; Water 6 SCA bias: -1.5 µg/L). Although the SCA underpredicted blended effluent concentrations early in the run, it yielded a very close match to the experimental data towards the end of the run. For Water 5, the RSS value for the SCA method prediction (1.1 µg/L) was slightly lower than that for the DI method prediction (1.2 µg/L). For Water 6, the DI method yielded a better prediction of the integral breakthrough curve than did the SCA method, based on RSS values (DI RSS: 1.9 µg/L; SCA RSS: 2.4 µg/L).

For two waters (Waters 6 and 7), SDS-TOX was also analyzed in the blended effluent. For these two cases, the DI method was a better predictor of the integral breakthrough curve than the SCA method. For Water 6 (Figure 95), the SCA method underpredicted experimental data throughout most of the run, while for Water 7 (Figure 96), the SCA method underpredicted the experimental results during the initial portion of the run. Later in the run the SCA method resulted in a very good prediction of the integral breakthrough curve. For both waters, the RSS values for the DI method were lower than those for the SCA method (Water 6 DI RSS: 2.4 µg/L Cl<sup>-</sup>; Water 6 SCA RSS: 6.3 µg/L Cl<sup>-</sup>; Water 7 DI RSS: 6.9 µg/L Cl<sup>-</sup>; Water 7 SCA RSS: 9.3 µg/L Cl<sup>-</sup>). The bias values for both runs and both model predictions were negative (Water 6 DI bias: -1.5 µg/L Cl<sup>-</sup>; Water 6 SCA bias: -4.9 µg/L Cl<sup>-</sup>; Water 7 DI bias: -6.2 µg/L Cl<sup>-</sup>; Water 7 SCA bias: -5.5 µg/L Cl<sup>-</sup>).

#### 4.4.2 DBP Species

With a few exceptions, the DI method was able to better predict non-brominated DBP species, while the SCA method was a better predictor of the brominated species. This is due in part to the marginal ability of the DI method to predict blended effluent concentrations that result when the single contactor curve shows a peak, or a steep breakthrough followed by a flat plateau. The influence of the bromide to TOC ratio on the single contactor breakthrough curve is not captured by the DI method, while the SCA method, which inherently correlates DBP formation to TOC concentration, was better able to predict the integral breakthrough curve for brominated DBP species. The relationship between TOC concentration and DBP formation and speciation in both the single and blended contactor effluents is discussed in Section 4.2.

For SDS-CF, the DI method yielded lower RSS values for experimental predictions in five out of eight cases. Figures 97 and 98 show examples of model predictions for Waters 2 and 6,

respectively. For these two examples, the SCA method underpredicted the integral breakthrough curve at the point of initial breakthrough and towards the end of the run. The SCA prediction bias was negative for both runs (Water 2:  $-0.9 \mu\text{g/L}$ ; Water 6:  $-0.3 \mu\text{g/L}$ ). The DI method yielded a better match to the observed for Water 2 (DI RSS:  $0.6 \mu\text{g/L}$ ; SCA RSS:  $1.6 \mu\text{g/L}$ ), but the SCA method was a better predictor of the SDS-CF integral breakthrough curve for Water 6 (DI RSS:  $1.4 \mu\text{g/L}$ ; SCA RSS:  $0.7 \mu\text{g/L}$ ). The DI model bias was negative for Water 2 ( $-0.1 \mu\text{g/L}$ ) and positive for Water 6 ( $+0.5 \mu\text{g/L}$ ). Overall, the average bias for all runs was slightly positive for the DI prediction, while that for the SCA prediction was slightly negative.

Figures 99 and 100 show the DI and SCA method predictions of SDS-BDCM experimental results for Waters 1 and 8, respectively. Overall, the SCA method was a more successful model for predicting observed data, with RSS values lower than those for the DI method for six of the eight runs. In most cases, and as shown in the two examples, the DI method underpredicted the experimental blended effluent concentration throughout the entire run. This was also reflected by the negative bias values for the prediction results. The SDS-BDCM single contactor breakthrough curves typically exhibited sharp breakthrough curves followed by a flat plateau or peak curves. For the two examples given, the SCA method prediction provided a closer match to the experimental data (Water 1 DI RSS:  $1.5 \mu\text{g/L}$ ; Water 1 SCA RSS:  $1.0 \mu\text{g/L}$ ; Water 8 DI RSS:  $1.2 \mu\text{g/L}$ ; Water 8 SCA RSS:  $0.8 \mu\text{g/L}$ ). The SCA prediction bias was negative (Water 1:  $-0.7 \mu\text{g/L}$ ; Water 8:  $-0.6 \mu\text{g/L}$ ), as was that for the DI predictions (Water 1:  $-1.1 \mu\text{g/L}$ ; Water 8:  $-0.8 \mu\text{g/L}$ ). For all runs, the average model bias for both models was negative, although the SCA prediction bias was lower in magnitude as compared to that for the DI method.

For SDS-DBCM, the DI method yielded a better fit to the observed data in five of eight cases. Although a brominated DBP species, the breakthrough of SDS-DBCM was typically shaped similar to that of SDS-CF: a gradual increase in concentration over time, without the "sharp increase and plateau" or "peak" curve shapes observed for other brominated species. Figures 101 and 102 show examples of the results obtained for Waters 3 and 7, respectively. For Water 3 (Figure 101), both methods slightly underpredicted effluent concentrations at the beginning of the run. The DI method overpredicted effluent concentrations towards the end of the run, while the SCA method closely matched experimental data after the first third of the run. The SCA prediction bias was positive ( $+0.6 \mu\text{g/L}$ ), while that for the DI prediction was slightly negative ( $-0.1 \mu\text{g/L}$ ). The RSS value for the SCA prediction ( $0.7 \mu\text{g/L}$ ) was lower than that for the DI prediction ( $1.0 \mu\text{g/L}$ ). For Water 7, shown in Figure 102, the SCA method underpredicted blended effluent SDS-DBCM levels at the point of initial breakthrough and towards the end of the run, while the DI method either overpredicted or matched effluent levels. In this case, the DI prediction RSS value ( $1.0 \mu\text{g/L}$ ) was slightly lower than those for the SCA prediction ( $1.1 \mu\text{g/L}$ ). For these two examples, a positive model bias was measured for the DI prediction ( $+0.7 \mu\text{g/L}$ ), while a negative model bias occurred for the SCA prediction ( $-0.6 \mu\text{g/L}$ ). For all waters, the mean prediction bias for both methods was negative. The magnitude of the mean bias was lower for the DI procedure.

The SCA method resulted in closer matches to the observed data than did the DI method, based on calculated RSS values, for all SDS-BF integral breakthrough curve predictions (six of the eight runs yielded data above the MRL). Several single contactor effluent SDS-BF data formed peak curves, and some of the integral breakthrough curves were also peak curves. The DI method underpredicted blended effluent SDS-BF concentrations. The SCA method was able to better match the peak-shaped integral breakthrough curves that were sometimes observed.

Examples of the model prediction results are given in Figures 103 and 104 for Waters 1 and 5, respectively. The DI method underpredicted the experimental results throughout the entire run for both waters. Although the SCA method initially underpredicted blended effluent concentrations, at higher concentrations the accuracy of the predicted results increased, especially relative to the DI method results. The measured bias values for the SCA prediction (Water 1:  $-0.3 \mu\text{g/L}$ ; Water 5:  $-0.1 \mu\text{g/L}$ ) were lower in magnitude than those for the DI method (Water 1:  $-2.2 \mu\text{g/L}$ ; Water 5:  $-0.5 \mu\text{g/L}$ ), and bias values were negative for both models. The average model bias for the six runs analyzed (DI:  $-3.8 \mu\text{g/L}$ ; SCA:  $-1.3 \mu\text{g/L}$ ) was negative for both methods, and the magnitude of the DI method bias was greater than that for the SCA method by a factor of 2.8.

The DI method continued to perform well for non-brominated HAA species, while the SCA method was superior when predicting the integral breakthrough curve for brominated species. Exceptions to this trend occurred for SDS-CDBAA and SDS-TBAA, for which the DI method more often yielded better predictions. However, only four total cases were available for evaluation of both species, due to concentrations not exceeding the MRLs during many runs. Furthermore, analysis was complicated because formed levels were typically only slightly higher than the MRL. Values below the MRL were assigned a value of zero, which was not the case for the prediction methods. For the one case available to compare SDS-TBAA blended effluent concentrations, the SCA method more closely matched effluent levels (three points) that were measured above the MRL ( $4.0 \mu\text{g/L}$ ). However, the overall calculated RSS for the SCA method was slightly higher than that for the DI method. For SDS-DCBAA, comparisons were possible during only three runs, and the SCA method was a more accurate predictor of the integral breakthrough curve in all three cases. No comparisons were possible for SDS-MCAA or SDS-MBAA.

For SDS-DCAA, the DI method resulted in lower RSS values in six of the eight runs. Examples of the results are shown in Figures 105 and 106 for Waters 1 and 4, respectively. While the DI method well-predicted the data throughout the entire run for Water 1 (RSS:  $0.4 \mu\text{g/L}$ ), the SCA method initially underpredicted and then overpredicted the observed data (RSS:  $1.5 \mu\text{g/L}$ ). For Water 4, the DI method again was a successful predictor of the SDS-DCAA integral breakthrough curve (RSS:  $0.3 \mu\text{g/L}$ ), while the SCA method consistently underpredicted experimental data (RSS:  $0.5 \mu\text{g/L}$ ). For Water 1, both predictions yielded a positive bias (DI:  $+0.1 \mu\text{g/L}$ ; SCA:  $+0.3 \mu\text{g/L}$ ), while for Water 4, the bias for the SCA prediction was negative ( $-0.3 \mu\text{g/L}$ ), and that for the DI prediction was low and positive ( $+0.04 \mu\text{g/L}$ ). Similar results were obtained for SDS-TCAA predictions based on the two methods: for four of five possible comparisons, the RSS value for the DI method was lower than that for the SCA method, indicating a better prediction. The average bias for the DI method prediction ( $+0.1 \mu\text{g/L}$ ) was low and positive, while that for the SCA method was negative ( $-0.4 \mu\text{g/L}$ ).

For SDS-DBAA and SDS-BCAA, whose single contactor breakthrough curve typically exhibit sharp breakthrough curves followed by a flat plateau or peak curves, the SCA method outperformed the DI method for integral breakthrough curve prediction. RSS values for the SCA prediction were lower in four out six cases for SDS-DBAA, and in six out of eight cases for SDS-BCAA. The average model bias was negative for both parameters. For SDS-DBAA, the average bias magnitude was larger for DI predictions (DI:  $-0.7 \mu\text{g/L}$ ; SCA:  $-0.1 \mu\text{g/L}$ ), while for SDS-BCAA, the average bias for both methods was low (DI:  $-0.07 \mu\text{g/L}$ ; SCA:  $-0.04 \mu\text{g/L}$ ). Figure 107 shows the SDS-DBAA results obtained for Water 2 (DI RSS:  $1.1 \mu\text{g/L}$ ; SCA RSS:

0.6 µg/L), while Figure 108 shows the SDS-BCAA results obtained for Water 8 (DI RSS: 0.6 µg/L; SCA RSS: 0.3 µg/L). In both these examples, the SCA prediction was more accurate than the DI prediction based on RSS values. The model bias for these two examples was negative for both models, and lower in magnitude for SCA method predictions as compared to DI method predictions .

This analysis showed that the DI prediction was successful in predicting the integral breakthrough curve for TOC, which is an important step for use of the SCA method. The cumulative frequency distribution comparisons of the SCA and DI model results showed that the two methods were equivalent in their ability to predict the integral breakthrough curve, based on a comparison across all waters and water quality parameters. Over the entire data set, both methods were biased negative in their predictions of the experimental data. Both the DI and SCA predictions agreed well with experimental data for surrogates and class sums. For chlorinated DBP species, the DI method was a better predictor of the integral breakthrough curve than the SCA method. However, SCA method predictions outperformed those determined by the DI procedure for brominated DBP species integral breakthrough curves.

The main advantage of the SCA method over the DI procedure is that predictions using the SCA minimize the number of calculations necessary to predict blended contactor water quality as a function of single contactor run time. Based on the results of this study, use of the SCA procedure for predicting the integral breakthrough curve is recommended during ICR GAC treatment study data analysis.

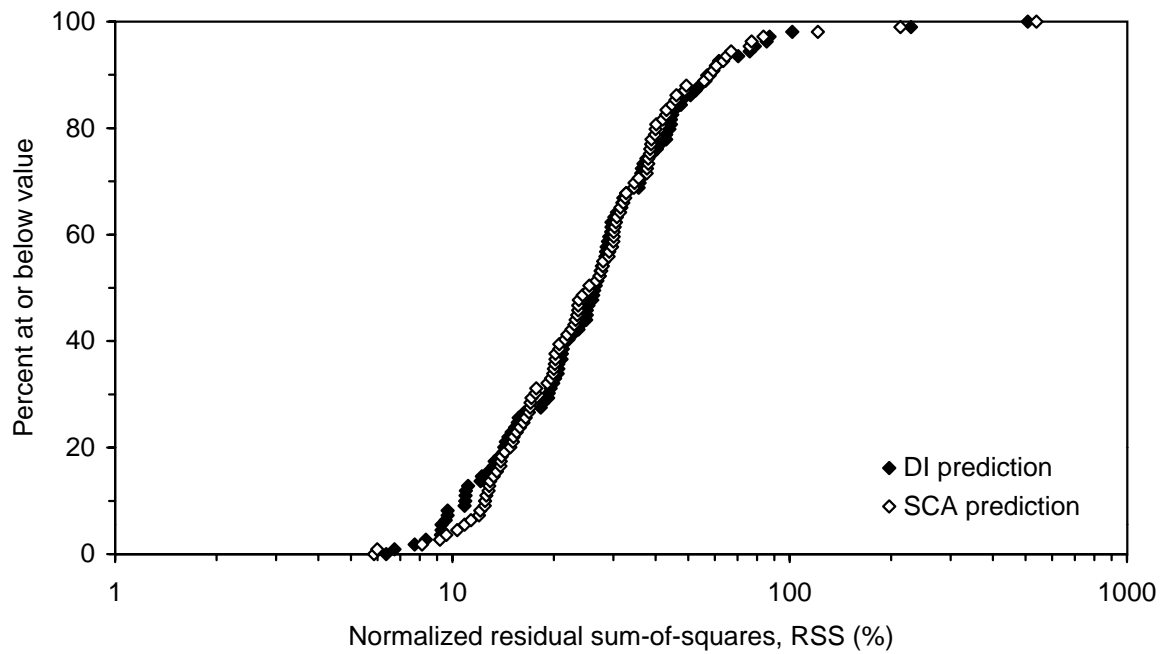


**Figure 83** Cumulative frequency distribution plot of normalized residual sum-of-squares (RSS) for DI and SCA model predictions

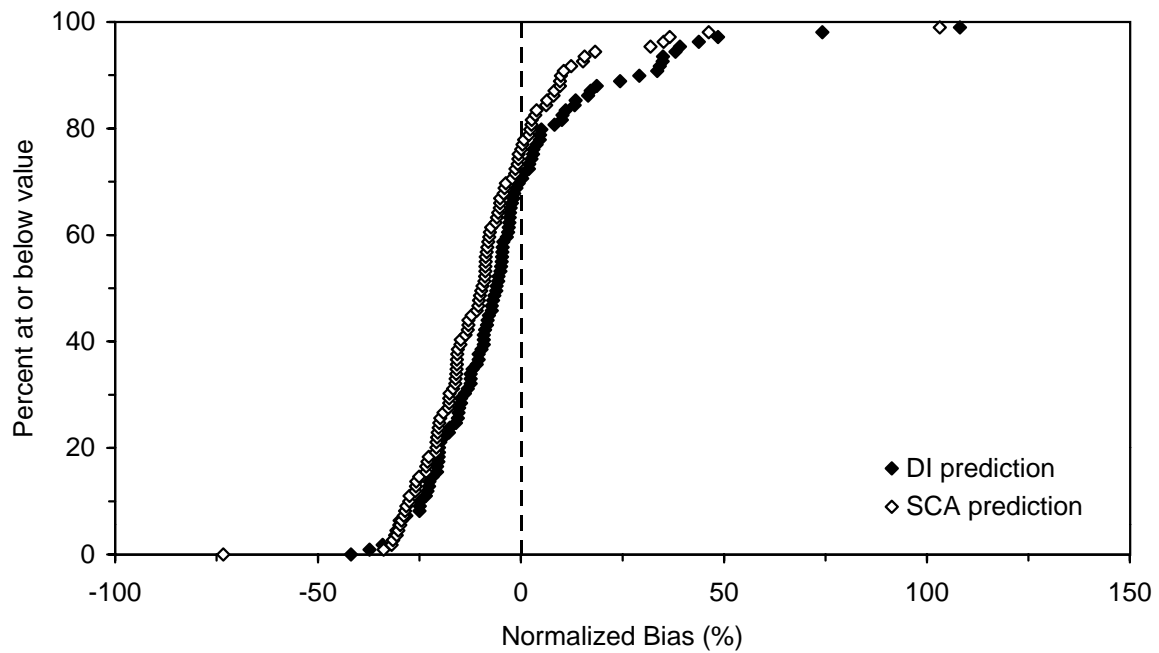


**Figure 84** Cumulative frequency distribution plot of normalized bias for DI and SCA model predictions

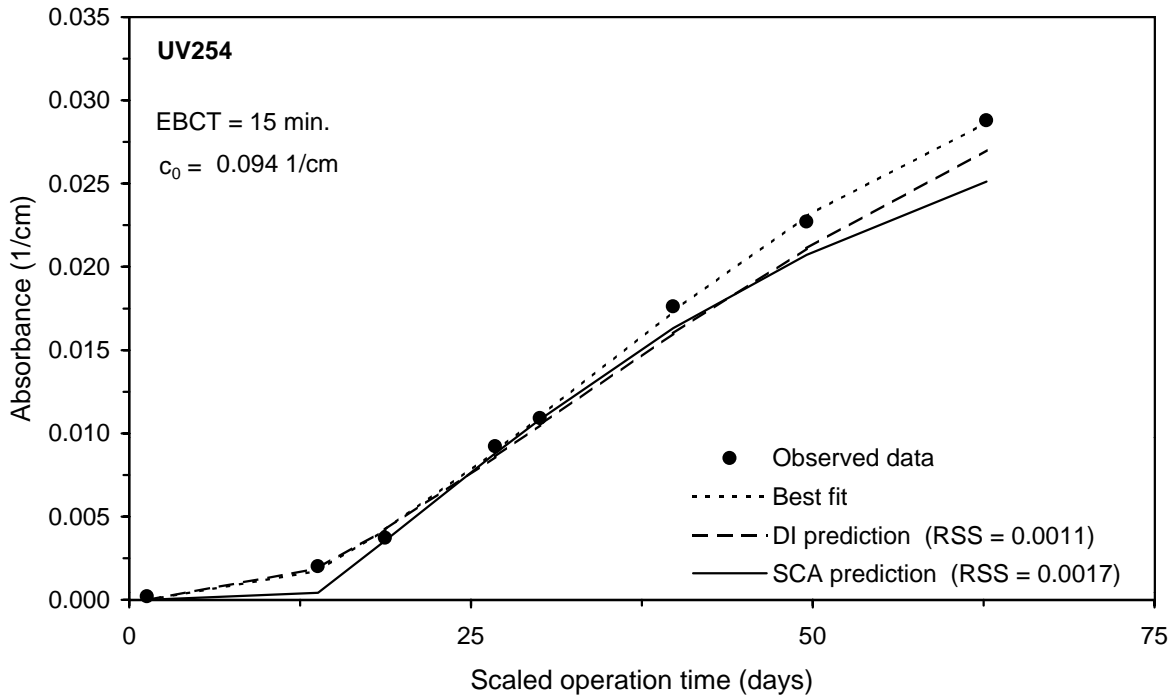


**Figure 85 Comparison of DI and SCA methods for predicting the UV254 integral breakthrough curve for Water 1**

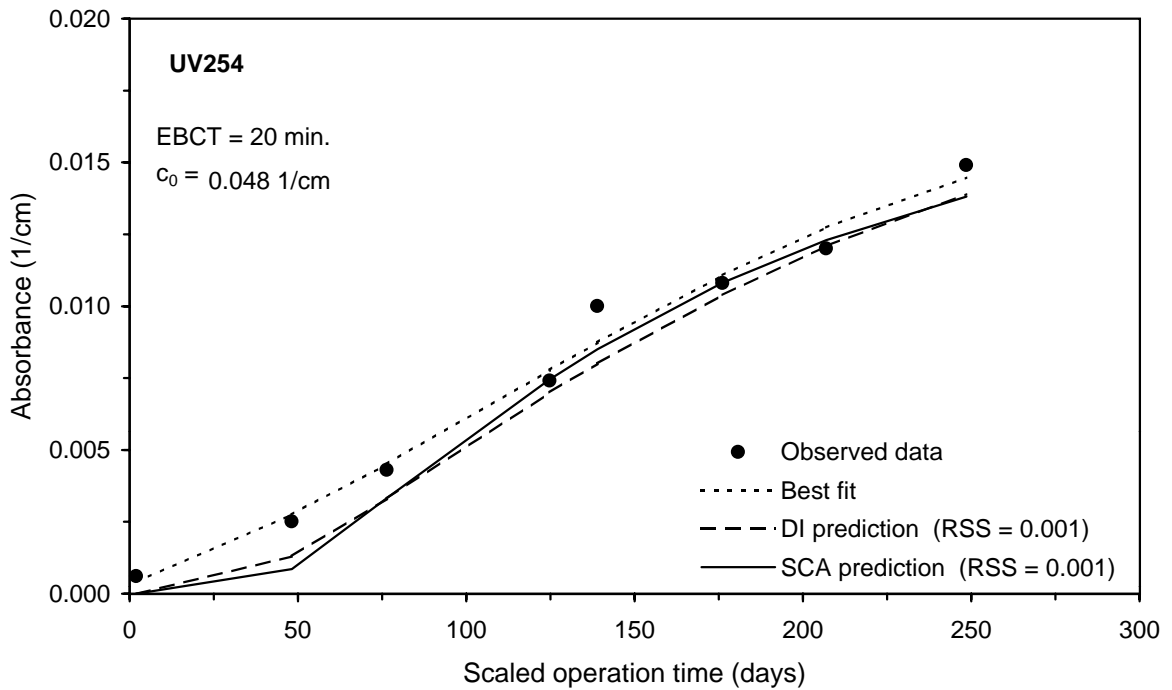


**Figure 86 Comparison of DI and SCA methods for predicting the UV254 integral breakthrough curve for Water 3**

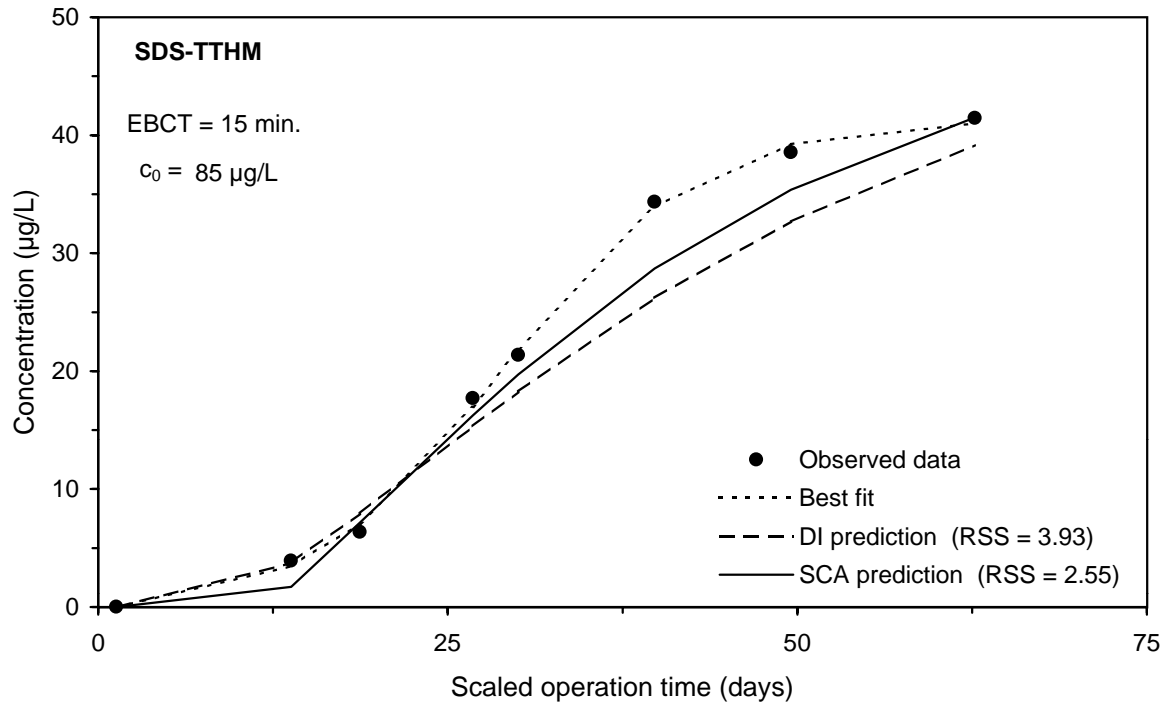


**Figure 87 Comparison of DI and SCA methods for predicting the SDS-TTHM integral breakthrough curve for Water 1**

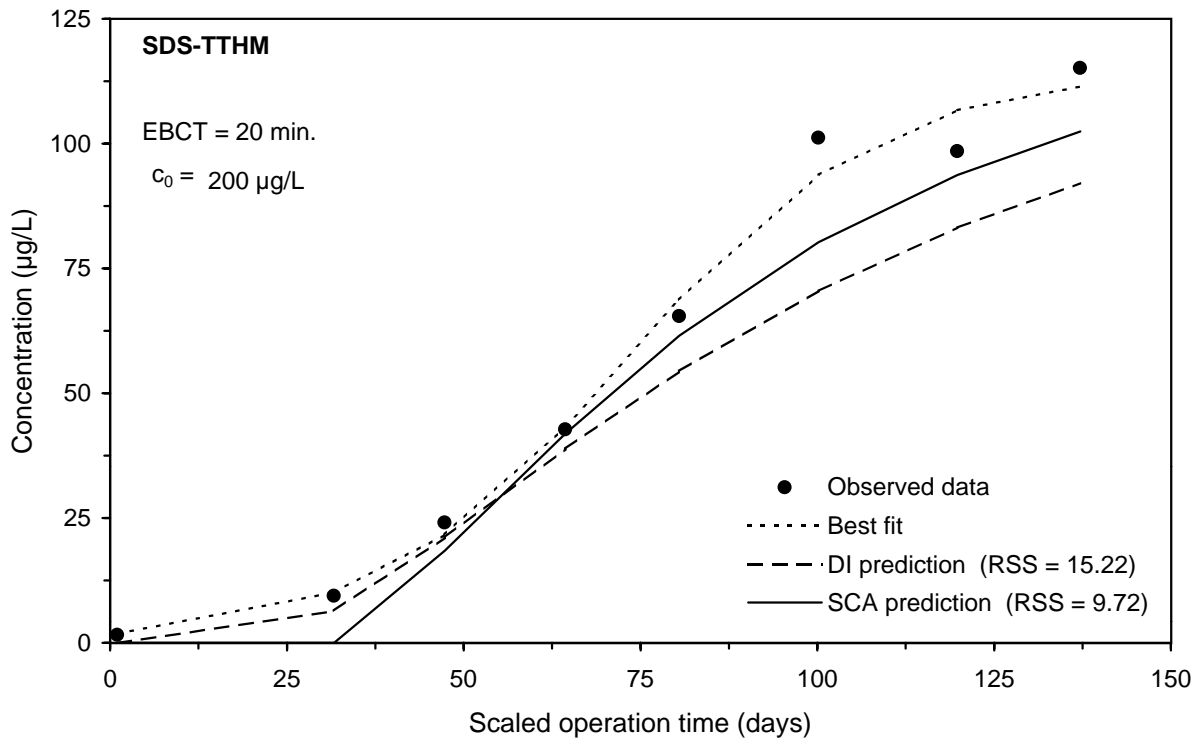


**Figure 88 Comparison of DI and SCA methods for predicting the SDS-TTHM integral breakthrough curve for Water 7**

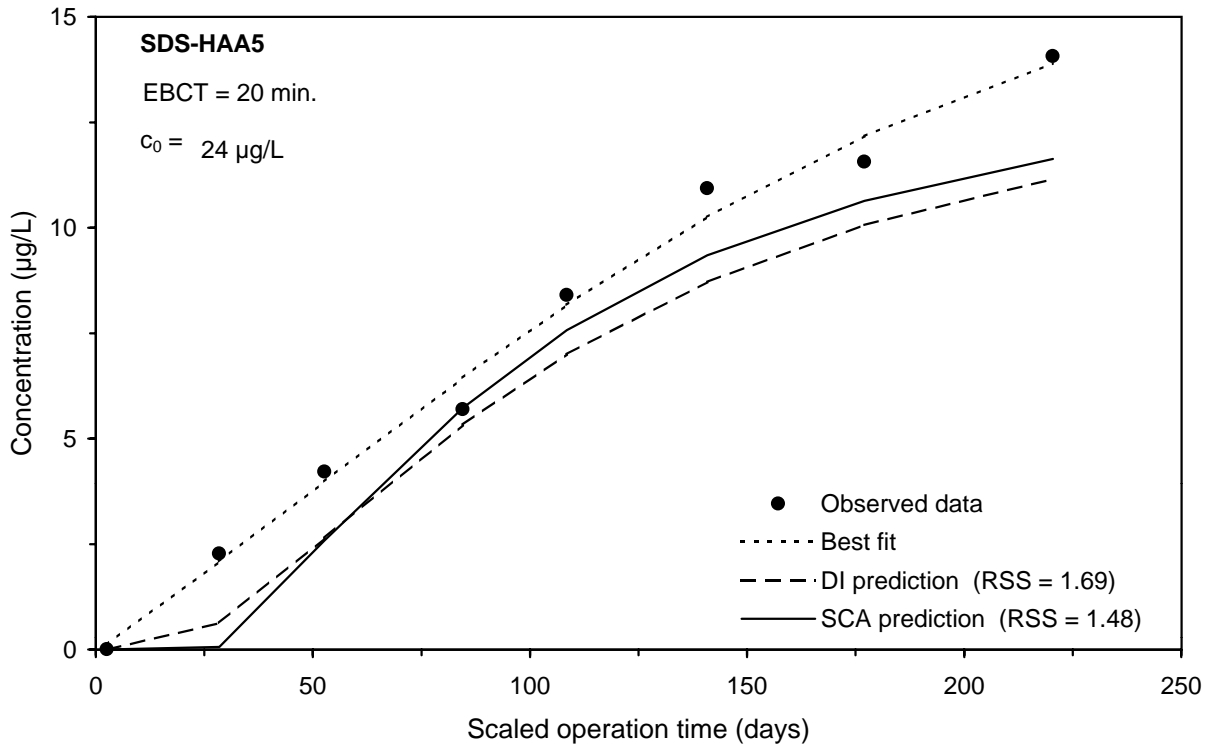


**Figure 89 Comparison of DI and SCA methods for predicting the SDS-HAA5 integral breakthrough curve for Water 2**

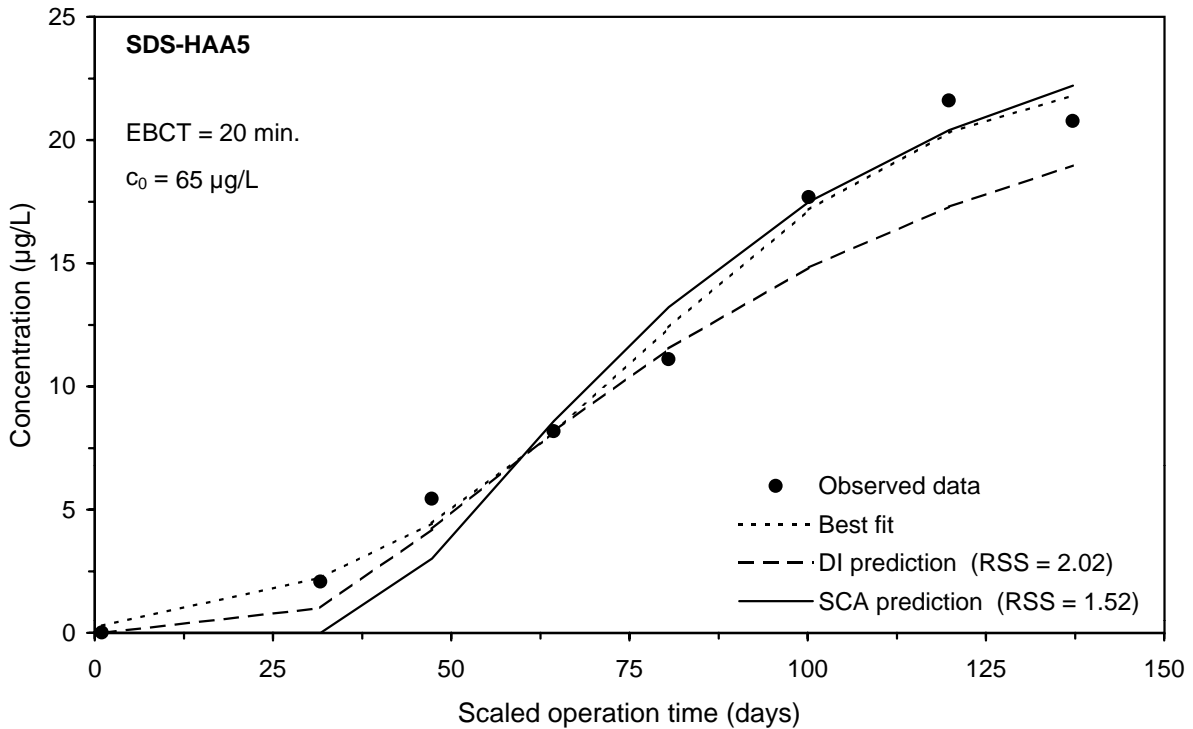


**Figure 90 Comparison of DI and SCA methods for predicting the SDS-HAA5 integral breakthrough curve for Water 7**

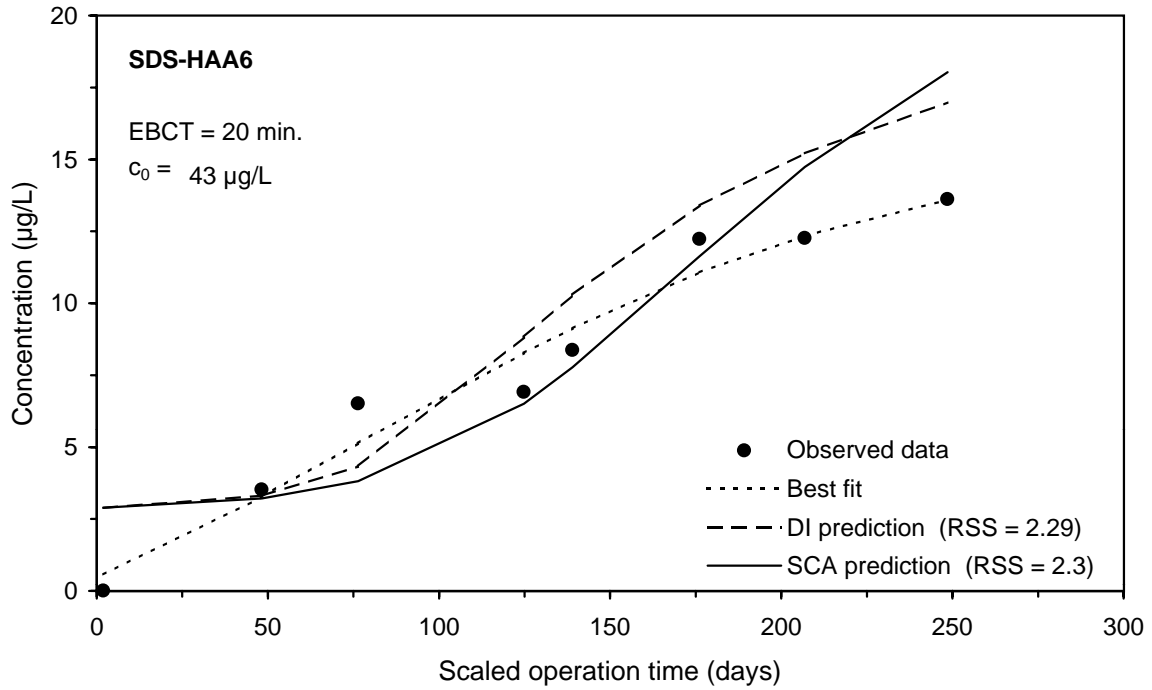


**Figure 91 Comparison of DI and SCA methods for predicting the SDS-HAA6 integral breakthrough curve for Water 3**

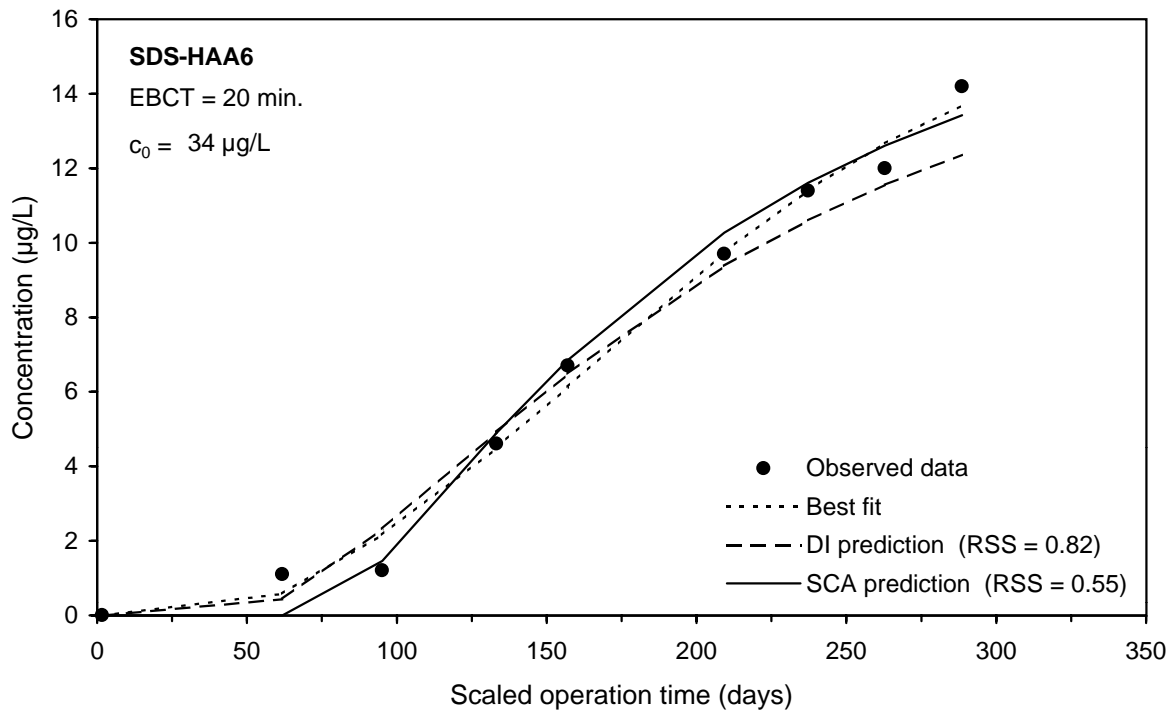


**Figure 92 Comparison of DI and SCA methods for predicting the SDS-HAA6 integral breakthrough curve for Water 5**

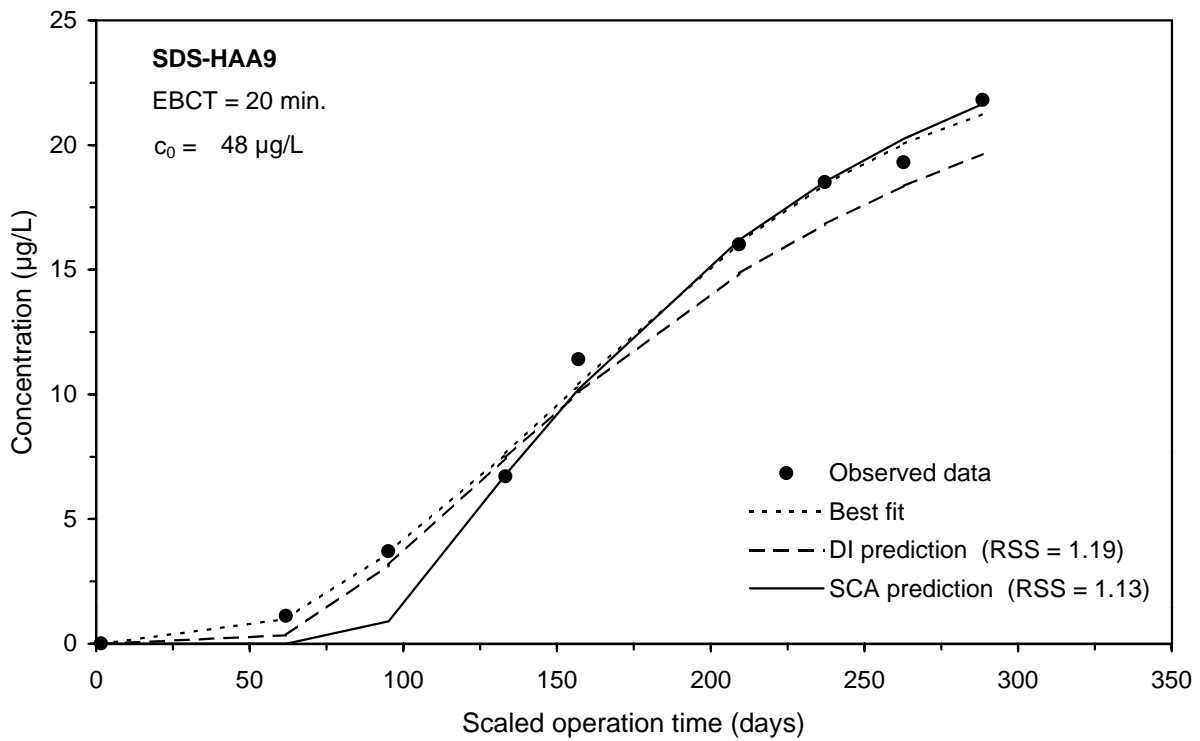


**Figure 93 Comparison of DI and SCA methods for predicting the SDS-HAA9 integral breakthrough curve for Water 5**

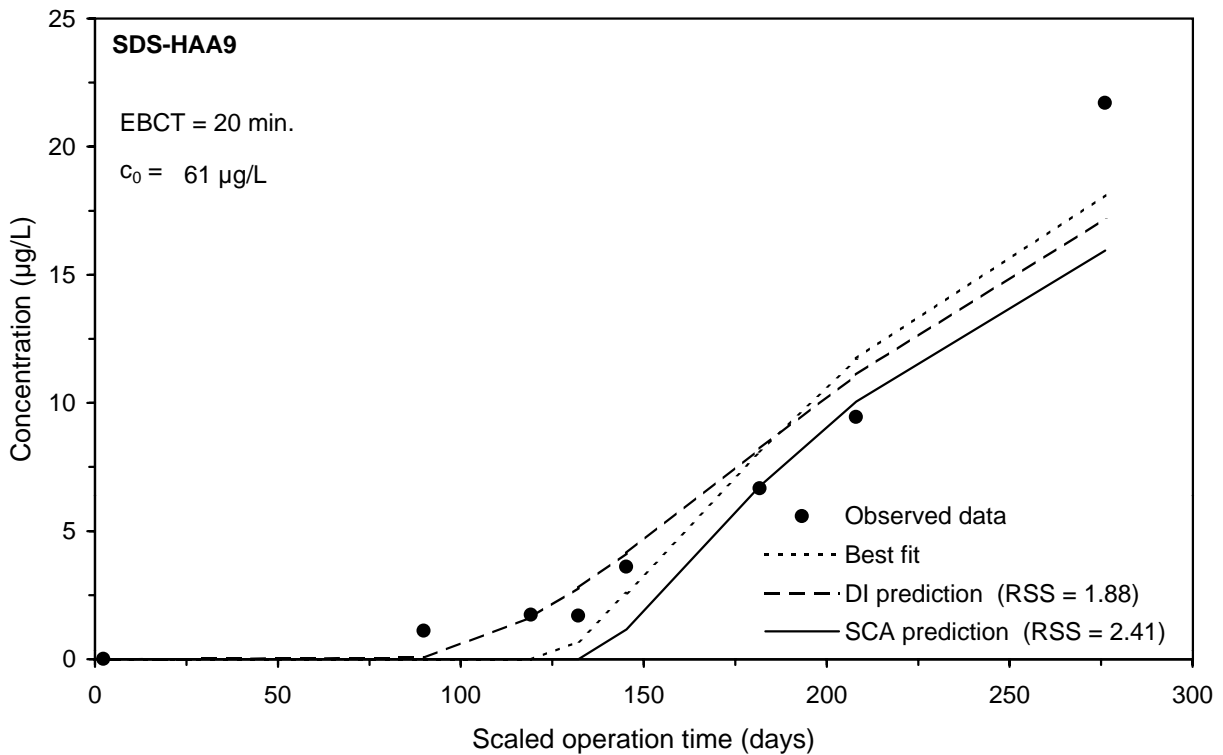


**Figure 94 Comparison of DI and SCA methods for predicting the SDS-HAA9 integral breakthrough curve for Water 6**

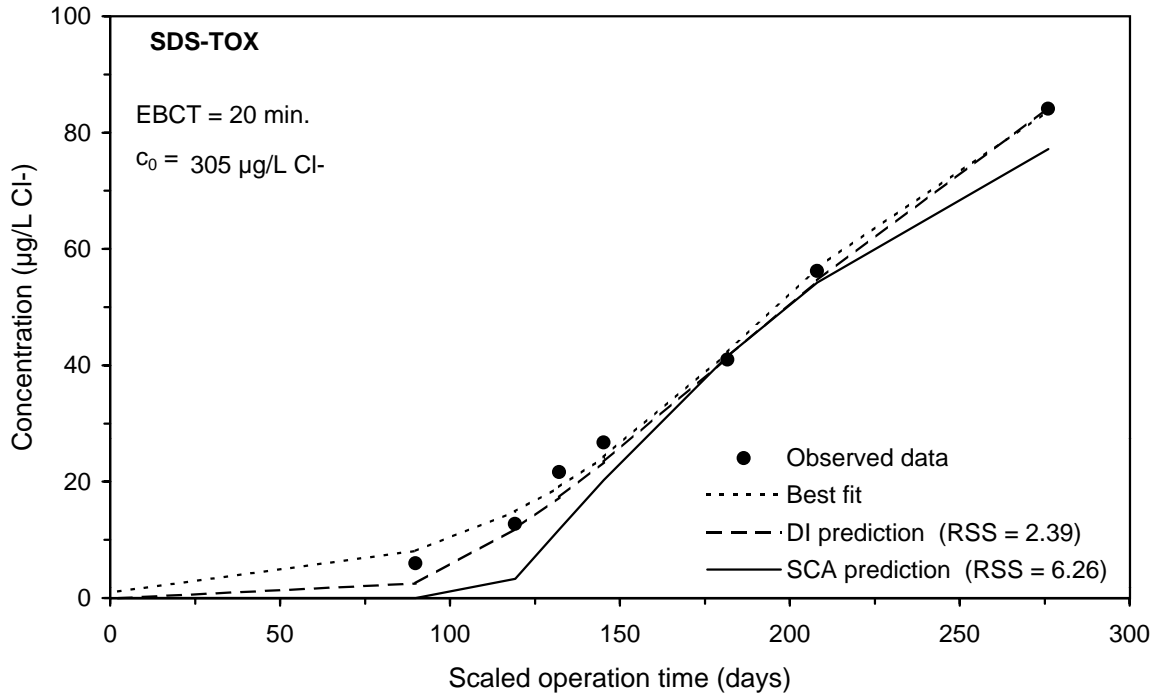


**Figure 95 Comparison of DI and SCA methods for predicting the SDS-TOX integral breakthrough curve for Water 6**

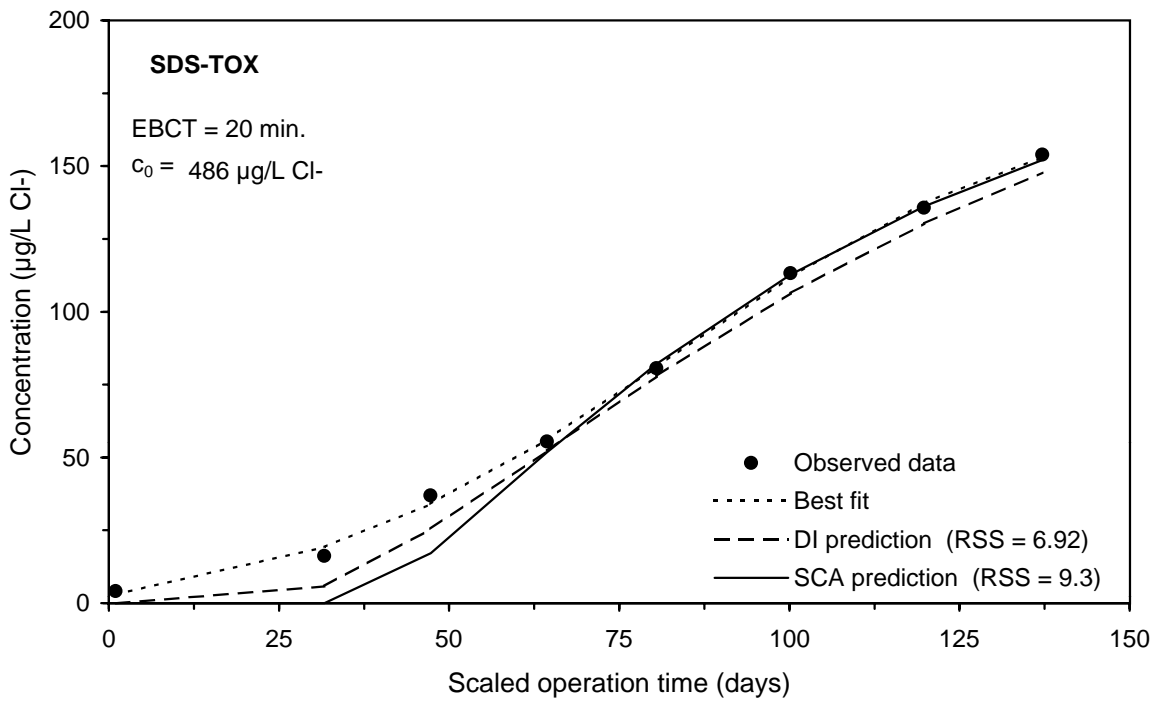


**Figure 96 Comparison of DI and SCA methods for predicting the SDS-TOX integral breakthrough curve for Water 7**

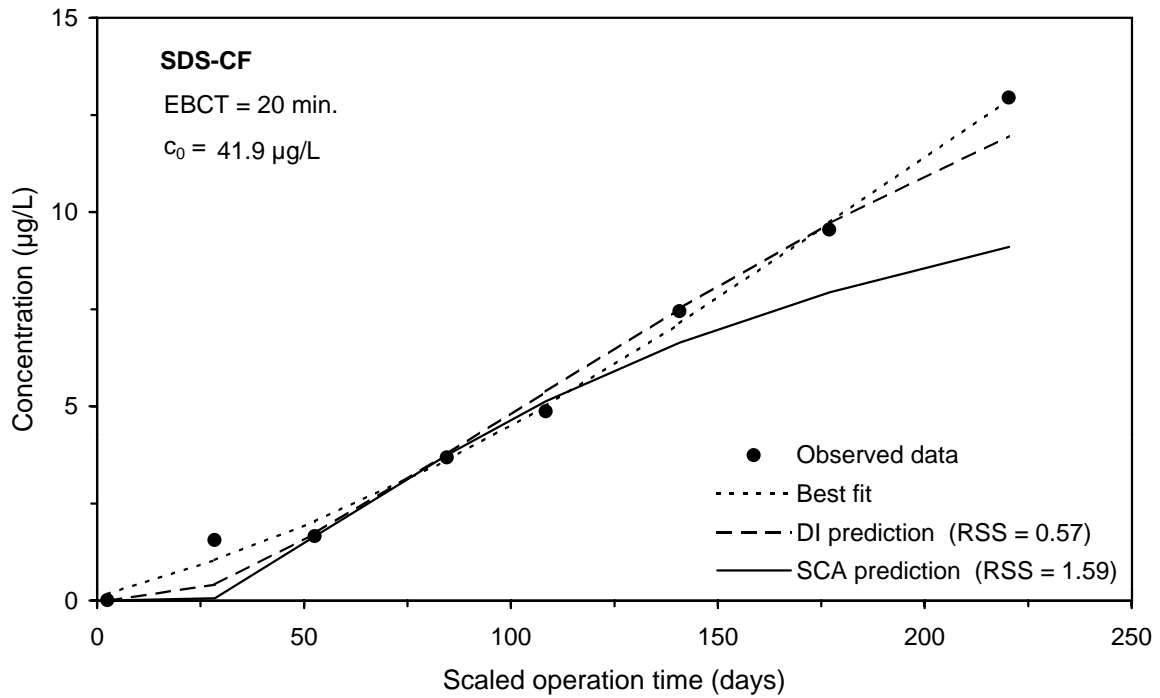


**Figure 97 Comparison of DI and SCA methods for predicting the SDS-CF integral breakthrough curve for Water 2**

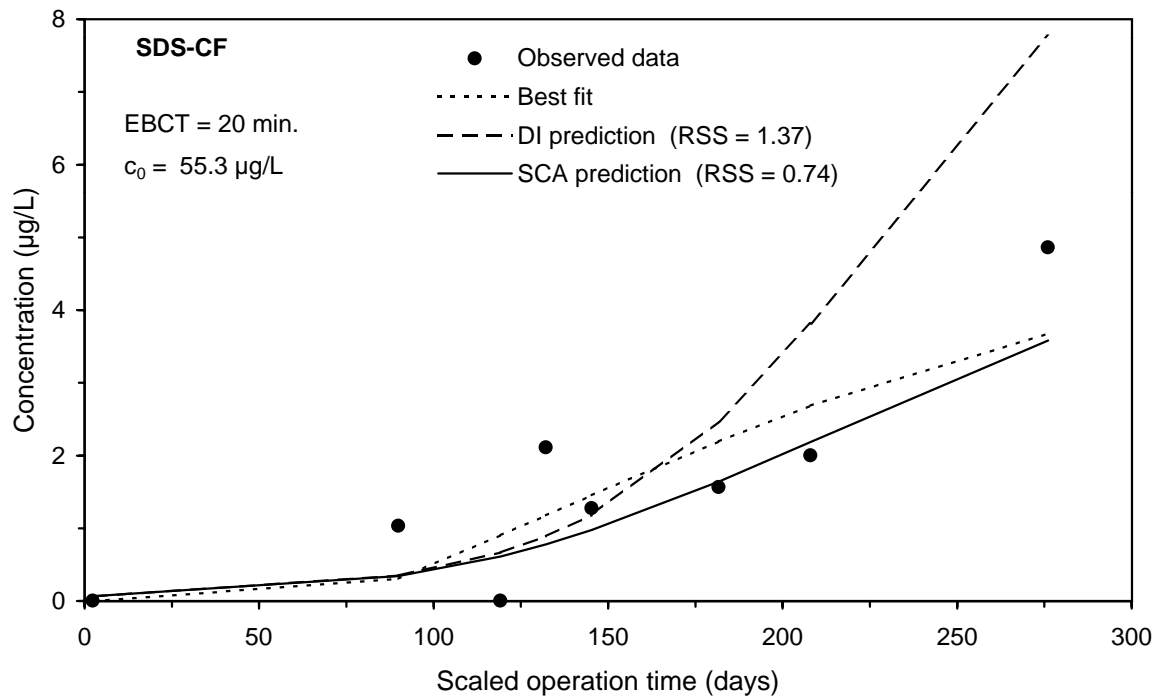


**Figure 98 Comparison of DI and SCA methods for predicting the SDS-CF integral breakthrough curve for Water 6**

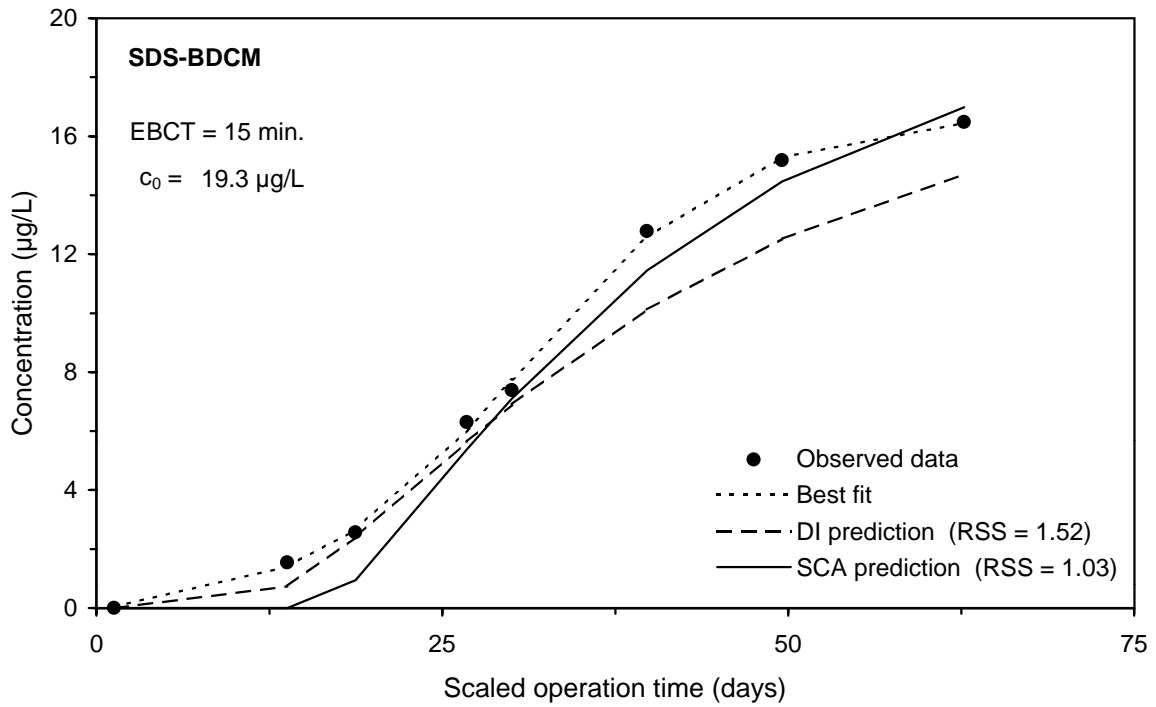


**Figure 99 Comparison of DI and SCA methods for predicting the SDS-BDCM integral breakthrough curve for Water 1**

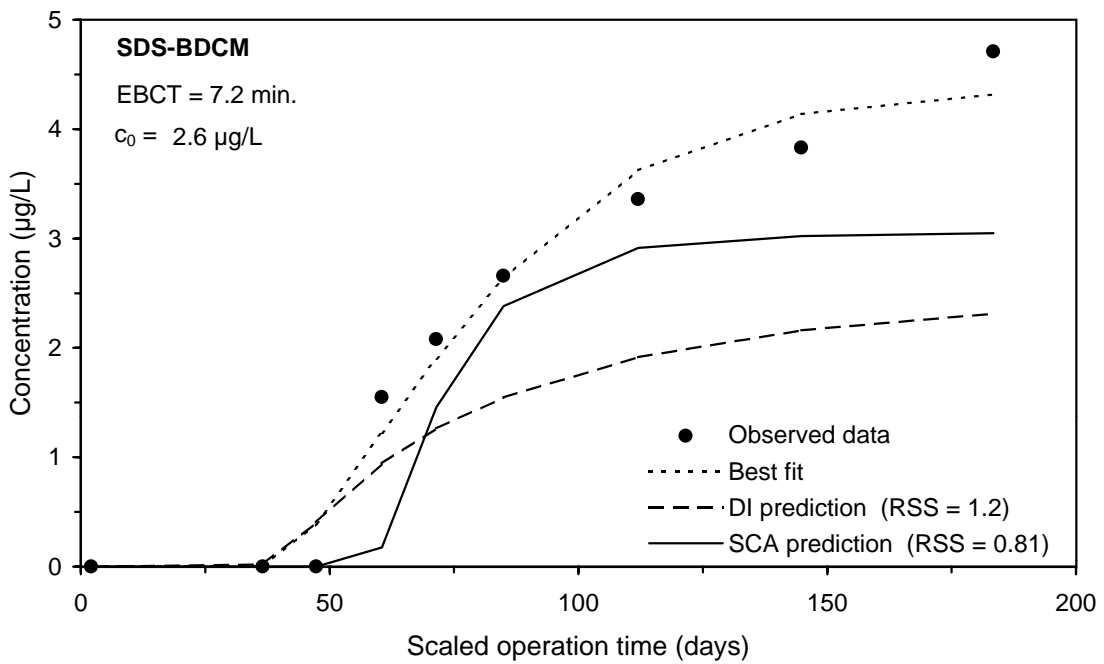


**Figure 100 Comparison of DI and SCA methods for predicting the SDS-BDCM integral breakthrough curve for Water 8**

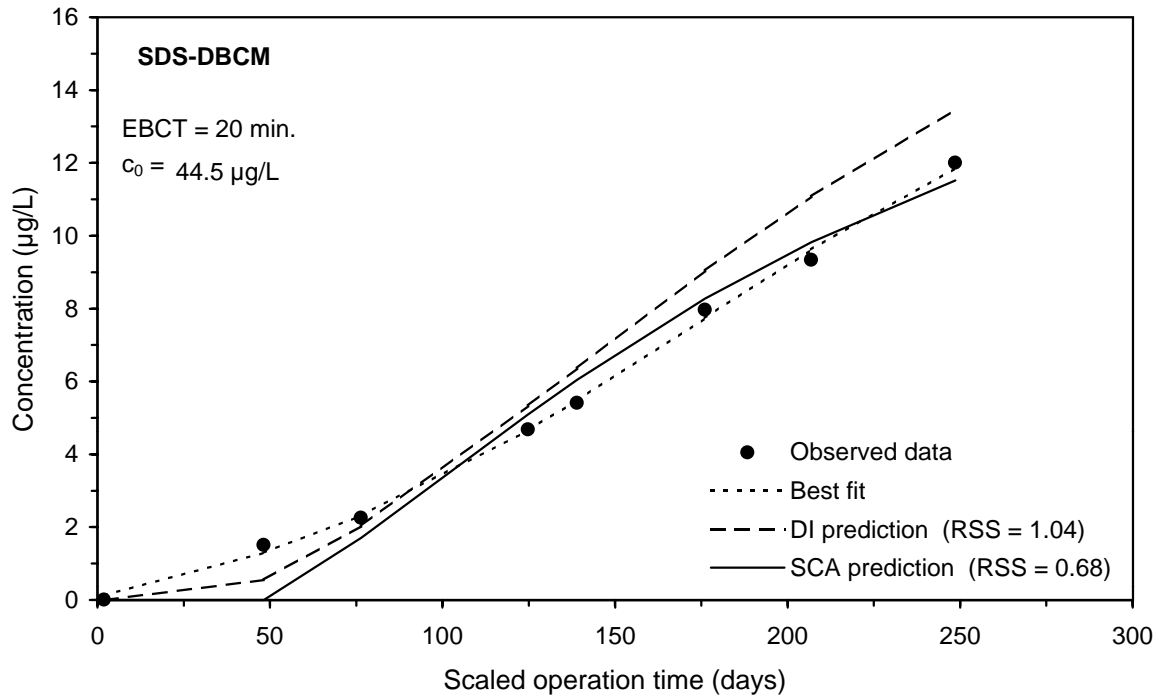


**Figure 101 Comparison of DI and SCA methods for predicting the SDS-DBCM integral breakthrough curve for Water 3**

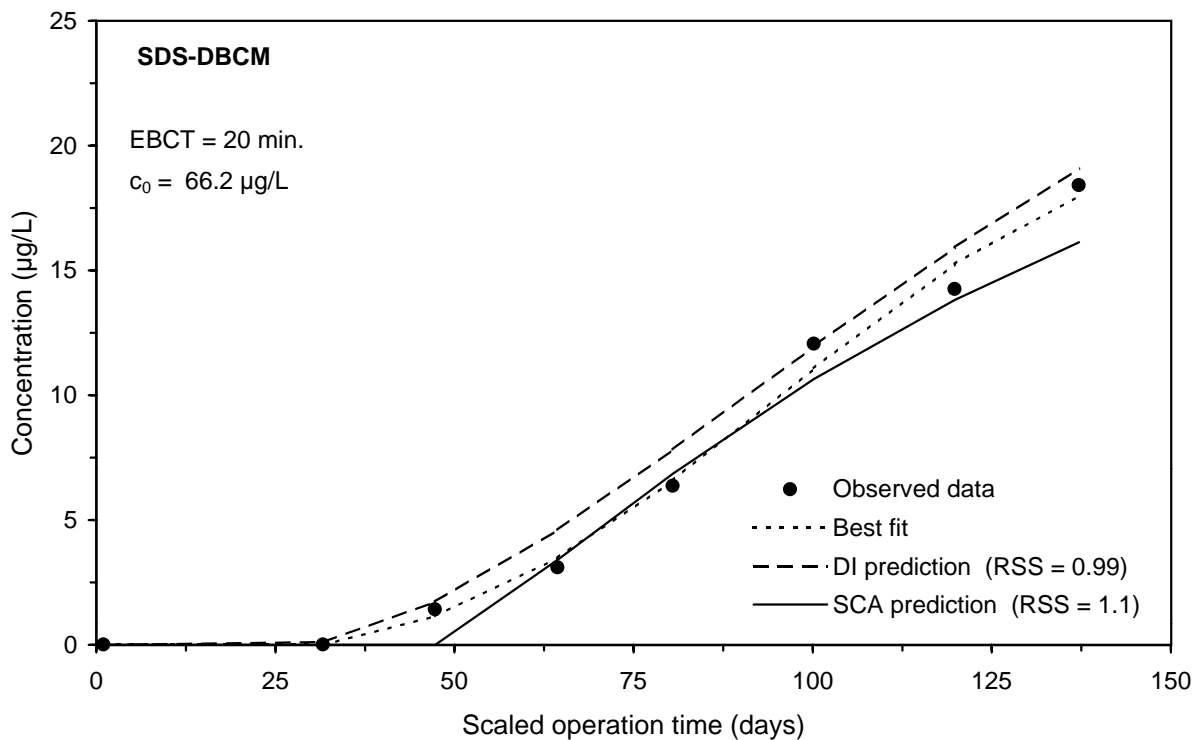


**Figure 102 Comparison of DI and SCA methods for predicting the SDS-DBCM integral breakthrough curve for Water 7**

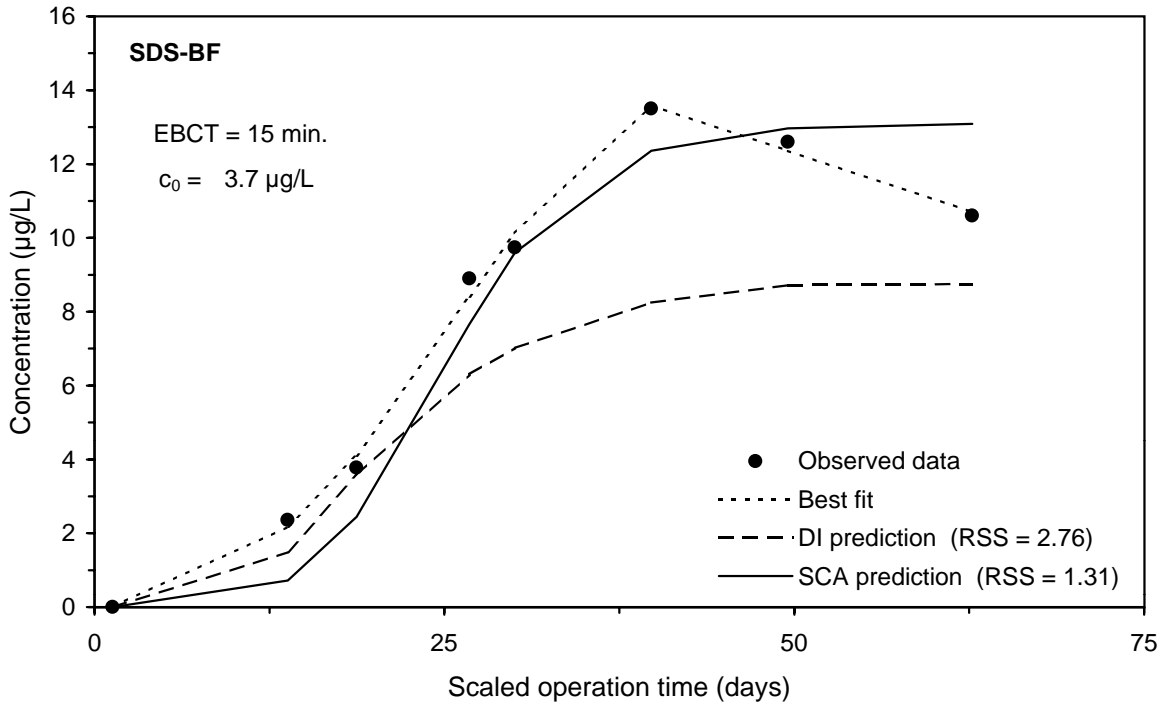


**Figure 103 Comparison of DI and SCA methods for predicting the SDS-BF integral breakthrough curve for Water 1**

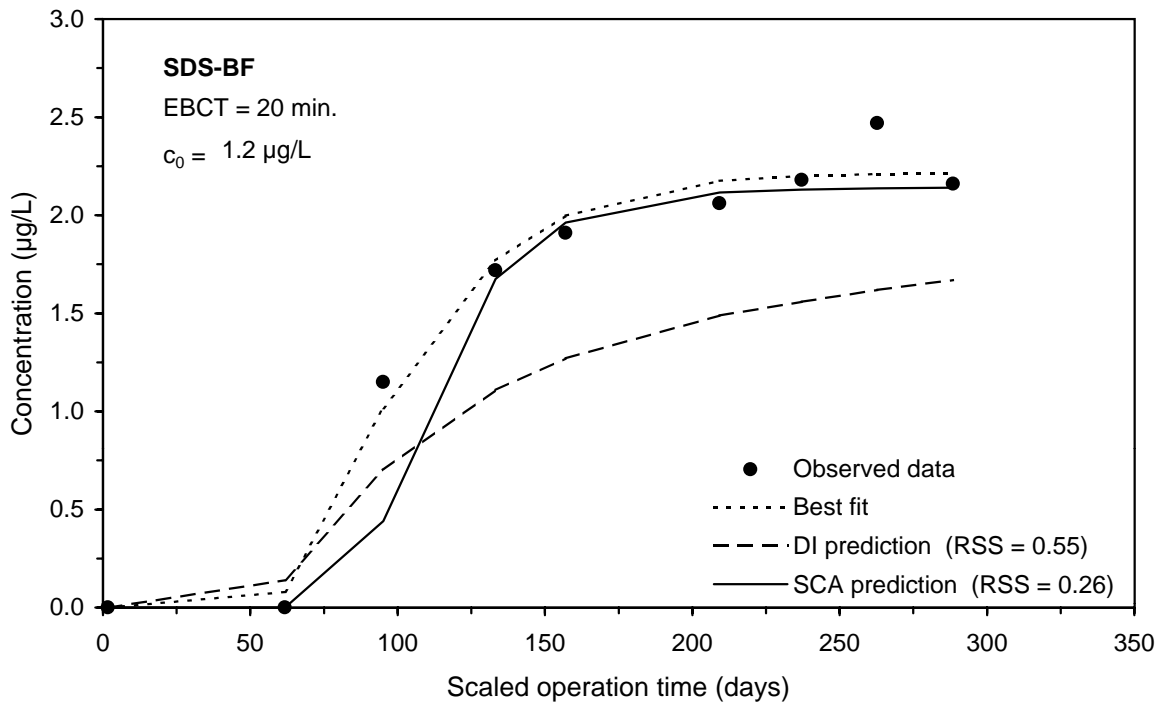


**Figure 104 Comparison of DI and SCA methods for predicting the SDS-BF integral breakthrough curve for Water 5**

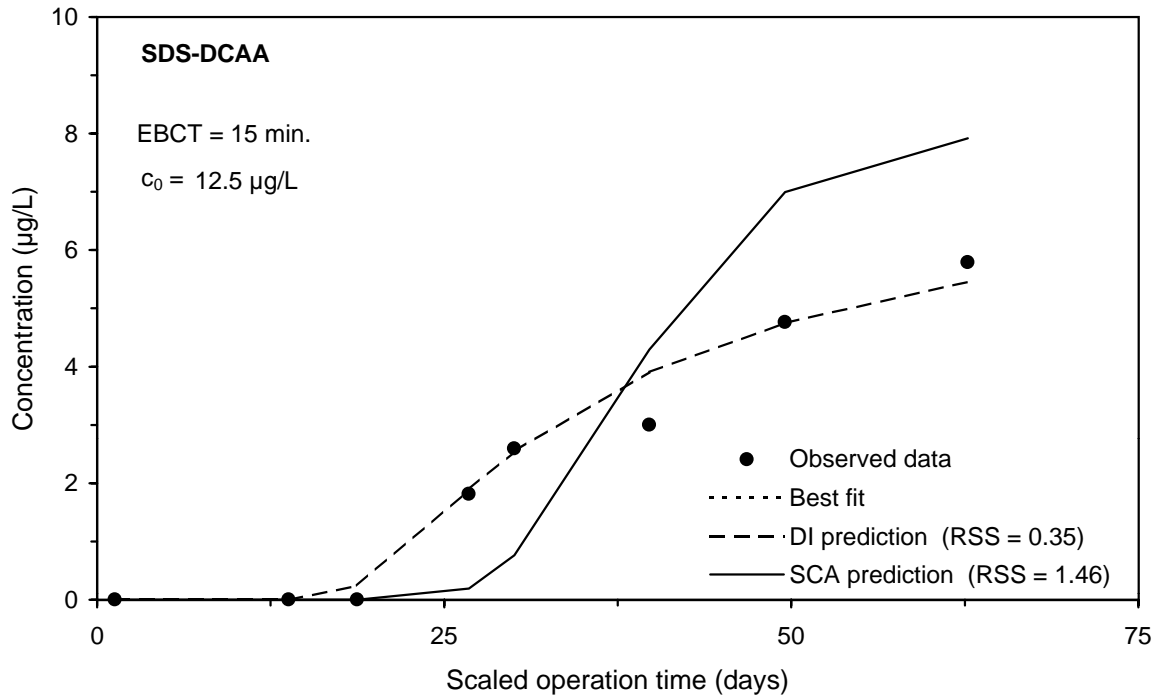


**Figure 105 Comparison of DI and SCA methods for predicting the SDS-DCAA integral breakthrough curve for Water 1**

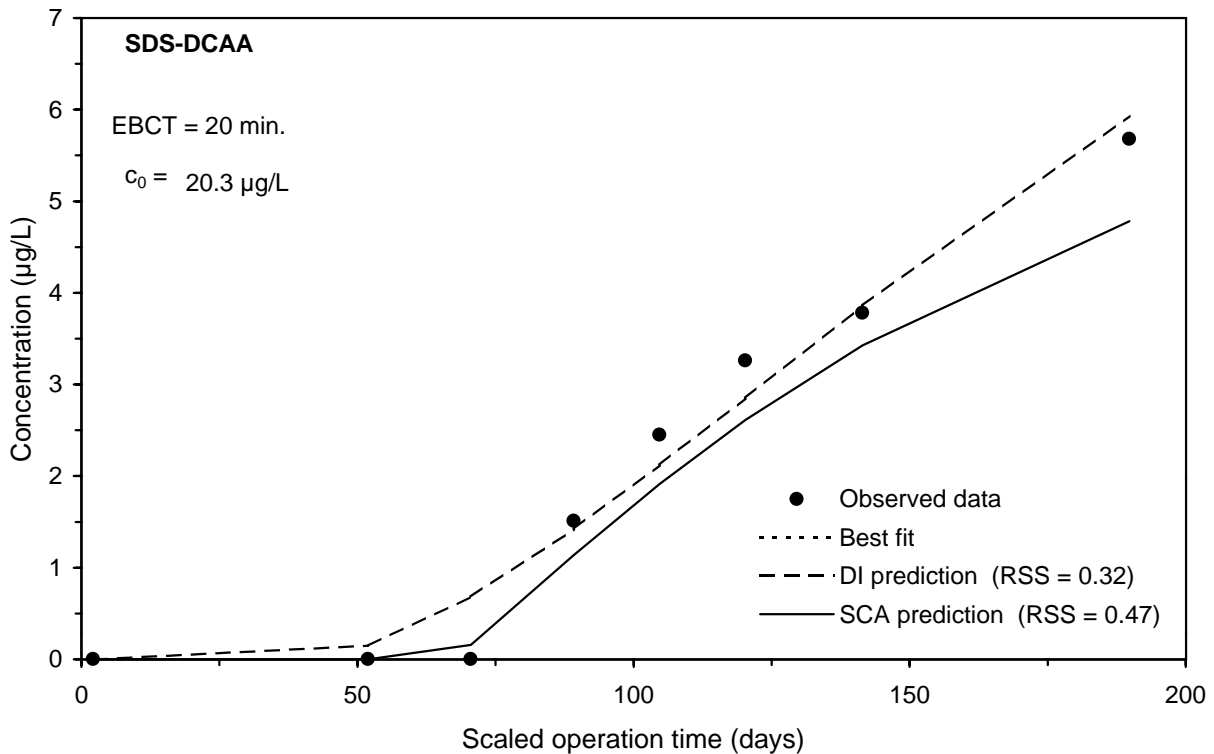


**Figure 106 Comparison of DI and SCA methods for predicting the SDS-DCAA integral breakthrough curve for Water 4**

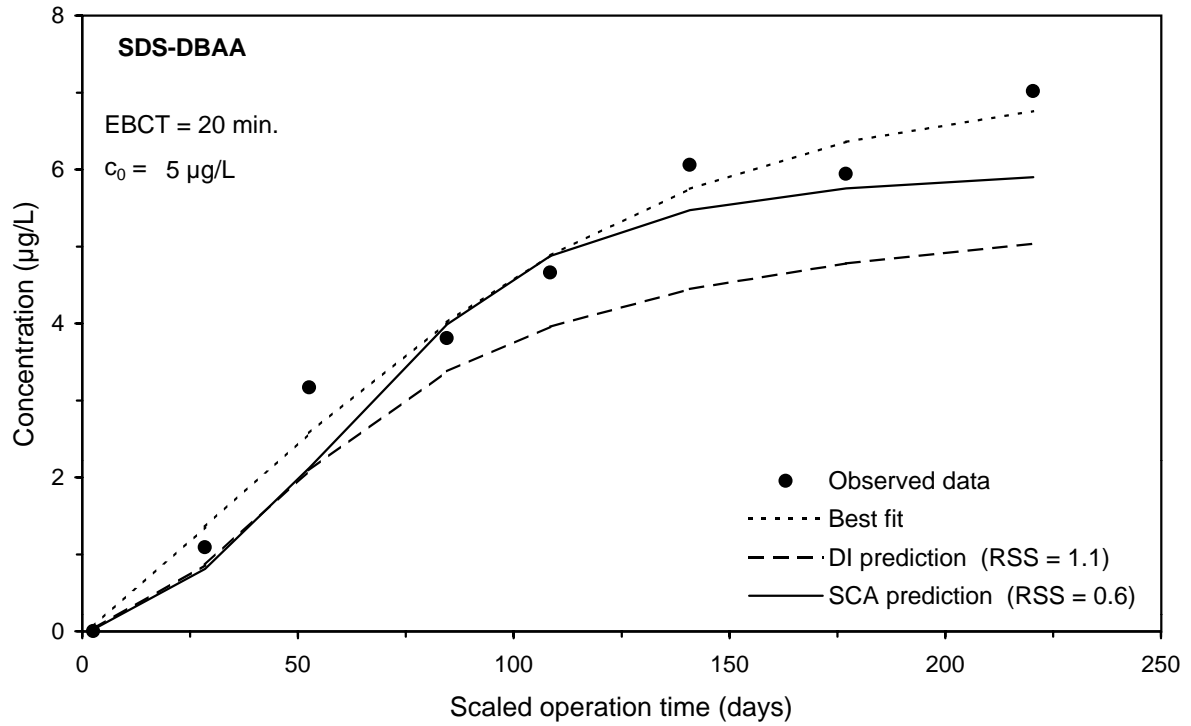


**Figure 107 Comparison of DI and SCA methods for predicting the SDS-DBAA integral breakthrough curve for Water 2**

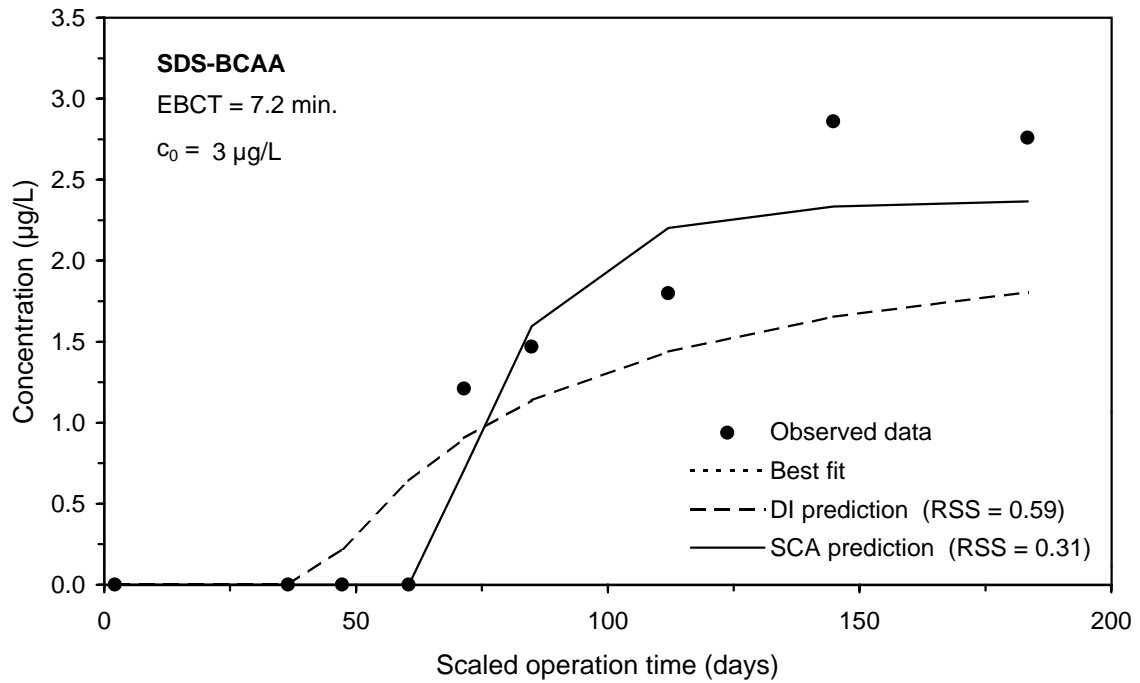


**Figure 108 Comparison of DI and SCA methods for predicting the SDS-BCAA integral breakthrough curve for Water 8**

#### 4.5 Analysis of Model Applicability to Finite Number of Contactors

Both the DI and SCA models for predicting the integral breakthrough curve, a relationship between single contactor run time and blended contactor effluent water quality, rely on the assumption that an infinite number of contactors are operated on-line in parallel-staggered mode. The application of the DI procedure to any parameter relies on the infinite contactor assumption; the DI prediction of the TOC integral breakthrough curve is a preliminary step utilized by the SCA method for predicting the integral breakthrough curves of all other water quality parameters. The application of these methods to situations involving finite numbers of contactors may be limited by this assumption. The following analysis was developed to determine the acceptability of the error incurred by the infinite contactor assumption.

Using the step logistic function model, a series of integral breakthrough curves were developed and plotted for the following numbers of contactors in parallel,  $N$ : 2, 3, 4, 6, 10, 20, and infinite. For the case of an infinite number of contactors Equation 12 (Section 1.4) was used, while in all other cases the numerical integration shown in Equation 4 (Section 1.2) was used. The single contactor breakthrough curve from which the integral curves were developed was also plotted. The results of this modeling are shown in Figures 109 through 114 for varying values of  $B$  and  $D$ , logistic function parameters that affect the shape of the curve. Values used for  $B$  ranged from 10 to 30, while values for  $D$  ranged from 0.05 to 0.20. These value ranges for  $B$  and  $D$  were chosen to reflect the range typically seen for fits of GAC breakthrough curve data. Set values were used instead of experimental data to examine the impact of  $B$  and  $D$  while  $A$  and  $A_0$  were held constant. For the curve fits performed in this study, the 25th and 75th percentiles for the values of  $B$  were 5 and 25, respectively, while the 25th and 75th percentiles for the values of  $D$  were 0.02 and 0.07, respectively. The best-fit parameters for all curve fits performed in this study are included in Appendix G. The parameter values used for  $A_0$  and  $A$  were held constant for all six series of breakthrough curves, at values of 0 and 1, respectively. (The logistic function parameter  $A$  represents the asymptote to which the logistic function is approaching, while  $A_0$  represents a step value given to the function.) All the data were plotted over 100 full-scale operation days.

The graphs in Figures 109 through 114 show that as the number of contactors operated in parallel-staggered mode increases, the integral curve approaches the model results for an infinite number of contactors. The largest incremental benefit afforded by operating contactors in parallel-staggered mode over single contactor operation occurs when two contactors are operated. The benefit realized by adding an additional contactor decreases as the number of contactors on-line increases.

To quantitatively compare the results, the run time to a range of treatment objectives expressed as a fraction of the parameter  $A$ , the value to which the breakthrough curve approaches asymptotically, was estimated based on the curves developed for  $N$  contactors. These are not percent breakthrough values; they represent instead a fraction of the concentration that the single contactor curve approaches asymptotically (asymptotic concentration). Values of 0.35, 0.50, and 0.65 were utilized as treatment objectives. Note that each value corresponds to a lower percent breakthrough value than that calculated based on the GAC influent concentration. An extreme case of a 0.80 treatment objective was also examined. This analysis is summarized in Tables 14 through 17.

The goal of this analysis was to establish what the smallest value for  $N$  was for which the integral curve (derived based on the infinite number of contactors assumption) would yield a maximum 10 percent error in the estimated blended contactor run times, assuming this level of error is acceptable. The parameter  $N_{90}$  will represent this breakpoint and is defined as the minimum  $N$  at which point the throughput of each contactor operated in parallel-staggered mode is 90 percent of that for an infinite number of contactors on-line. This is equivalent to the point at which the run time estimated using an assumption of an infinite number of contactors on-line is within 10 percent of the actual run time of each of  $N$  contactors.

Figures 115 and 116 establish a relationship between integral breakthrough curve run time estimates based on an infinite number of contactors and that based on a finite number of contactors. As shown in Figures 115 and 116, the minimum number of contactors operated in parallel-staggered mode necessary so that the integral breakthrough curve for finite  $N_{90}$  is within 10 percent of the integral breakthrough curve for infinite contactors varies with treatment objective. For  $B = 30$  and  $D = 0.10$  and treatment objectives ranging between 0.35 and 0.65, the  $N_{90}$  ranged from 7 to 13 contactors. As the value used for the treatment objective was increased (a less stringent treatment objective relative to GAC effluent concentration),  $N_{90}$  increased. Similar results were obtained for  $B = 30$  and  $D = 0.20$ . As the treatment objective was varied between 0.35 and 0.65, the  $N_{90}$  ranged from 7 to 13 contactors. The  $N_{90}$  to meet the given treatment objectives did not vary as  $B$  and  $D$  were varied: for treatment objectives between 0.35 and 0.65, the  $N_{90}$  varied from 7 to 13 contactors for both pairs of  $B$  and  $D$  values modeled. Therefore, the error between run times estimated based on an infinite number of contactors and that estimated for  $N$  contactors is independent of the shape of the curve, although it is dependent on the extent of breakthrough achieved. For the extreme asymptotic concentration fraction value of 0.80,  $N_{90}$  was 22 contactors.

The assumption of an infinite number of contactors operated in parallel-staggered mode simplifies the analysis of the integral breakthrough curve, as does the assumption of a linear breakthrough curve. However, the data presented here indicate that for breakthrough profiles that follow the logistic function form,  $N_{90}$  varies between 7 and 13 contactors, as the treatment objective is varied between 35 and 65 percent of the asymptotic concentration. Thus, when using the infinite contactor assumption to model the integral breakthrough curve for less than 14 contactors in parallel, the magnitude of the treatment objective in relation to the single contactor breakthrough curve is important in minimizing the error between  $q_N$ , the specific throughput of a finite number of contactors,  $N$ , and  $q_\infty$ , the specific throughput of each contactor assuming an infinite number of contactors on-line.

Based on the use of the logistic function model and for the range of treatment objectives evaluated in this analysis, the integral breakthrough curve developed from the infinite contactor assumption will yield estimated run times within 10 percent of actual run times for 13 or more contactors operated in parallel-staggered mode. For 10 contactors on-line, the infinite contactor assumption will yield run time estimates within 12 percent of the actual run times. In all cases, run time estimates based on the infinite contactor assumption are longer than those for a finite number of contactors, and thus yields a best case estimate of GAC performance. The relationship developed between integral breakthrough curve run time estimates based on an infinite number of contactors and that based on a finite number of contactors can be applied to

ICR treatment study data to obtain GAC run time estimates that are more applicable to GAC applications with a small number of parallel contactors.

Number of contactors, <i>N</i>	Run time to treatment objective (0.35), expressed as percentage of run time for infinite number of contactors					
	<i>B</i> = 30; <i>D</i> = 0.10	<i>B</i> = 30; <i>D</i> = 0.05	<i>B</i> = 10; <i>D</i> = 0.10	<i>B</i> = 10; <i>D</i> = 0.05	<i>B</i> = 10; <i>D</i> = 0.2	<i>B</i> = 30; <i>D</i> = 0.2
	1	56	56	54	54	54
2	71	71	70	70	70	71
3	78	78	78	78	78	78
4	83	83	82	82	82	83
6	88	88	87	87	87	88
10	92	92	92	92	92	92
20	96	96	96	96	96	96

**Table 14 Summary of run times to a 0.35 treatment objective**

Number of contactors, <i>N</i>	Run time to treatment objective (0.50), expressed as percentage of run time for infinite number of contactors					
	<i>B</i> = 30; <i>D</i> = 0.10	<i>B</i> = 30; <i>D</i> = 0.05	<i>B</i> = 10; <i>D</i> = 0.10	<i>B</i> = 10; <i>D</i> = 0.05	<i>B</i> = 10; <i>D</i> = 0.2	<i>B</i> = 30; <i>D</i> = 0.2
	1	50	NA	50	50	50
2	67	NA	67	67	67	67
3	75	NA	75	75	75	75
4	80	NA	80	80	80	80
6	86	NA	86	86	86	86
10	91	NA	91	91	91	91
20	95	NA	95	95	95	95

NA: not applicable, treatment objective not exceeded

**Table 15 Summary of run times to a 0.50 treatment objective**

Number of contactors, <i>N</i>	Run time to treatment objective (0.65), expressed as percentage of run time for infinite number of contactors					
	<i>B</i> = 30; <i>D</i> = 0.10	<i>B</i> = 30; <i>D</i> = 0.05	<i>B</i> = 10; <i>D</i> = 0.10	<i>B</i> = 10; <i>D</i> = 0.05	<i>B</i> = 10; <i>D</i> = 0.2	<i>B</i> = 30; <i>D</i> = 0.2
1	41	NA	43	NA	43	41
2	59	NA	60	NA	60	59
3	69	NA	70	NA	70	69
4	74	NA	75	NA	75	74
6	81	NA	82	NA	82	81
10	88	NA	88	NA	88	88
20	94	NA	94	NA	94	94

NA: not applicable, treatment objective not exceeded

**Table 16 Summary of run times to a 0.65 treatment objective**

Number of contactors, <i>N</i>	Run time to treatment objective (0.80), expressed as percentage of run time for infinite number of contactors					
	<i>B</i> = 30; <i>D</i> = 0.10	<i>B</i> = 30; <i>D</i> = 0.05	<i>B</i> = 10; <i>D</i> = 0.10	<i>B</i> = 10; <i>D</i> = 0.05	<i>B</i> = 10; <i>D</i> = 0.2	<i>B</i> = 30; <i>D</i> = 0.2
1	NA	NA	NA	NA	31	28
2	NA	NA	NA	NA	48	45
3	NA	NA	NA	NA	58	56
4	NA	NA	NA	NA	64	63
6	NA	NA	NA	NA	73	71
10	NA	NA	NA	NA	82	81
20	NA	NA	NA	NA	90	89

NA: not applicable, treatment objective not exceeded

**Table 17 Summary of run times to a 0.80 treatment objective**

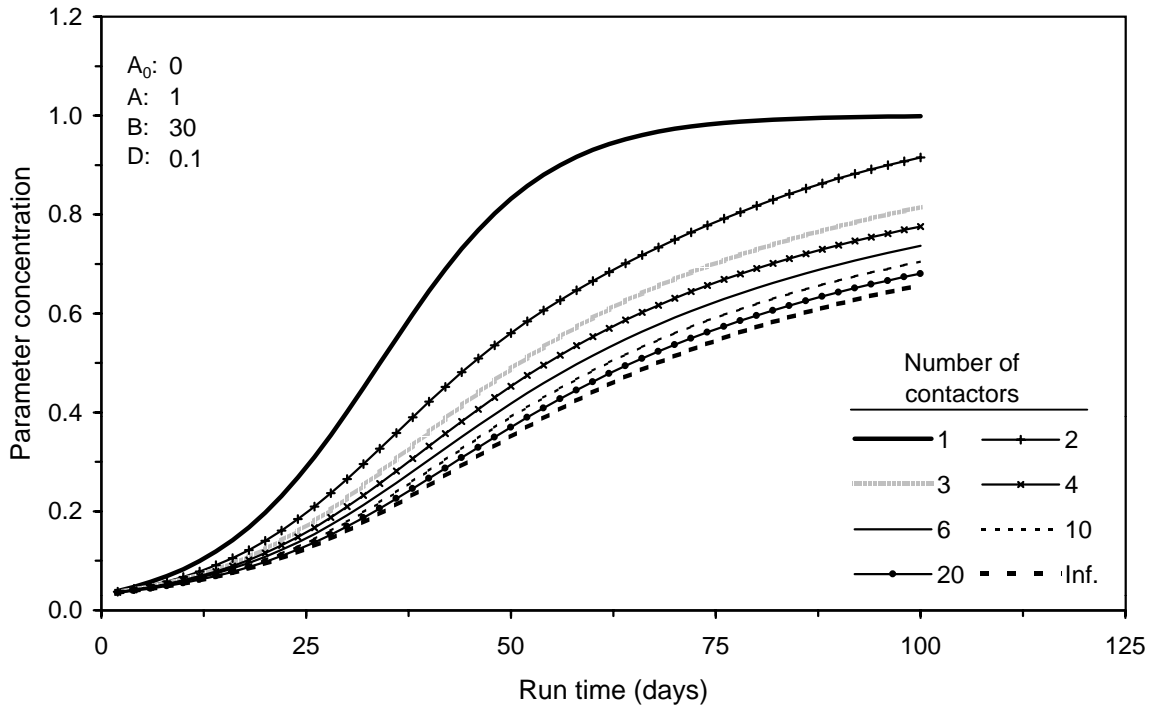


**Figure 109 Integral breakthrough curves for varying numbers of contactors operated in parallel-staggered mode ( $B = 30$ ;  $D = 0.1$ )**

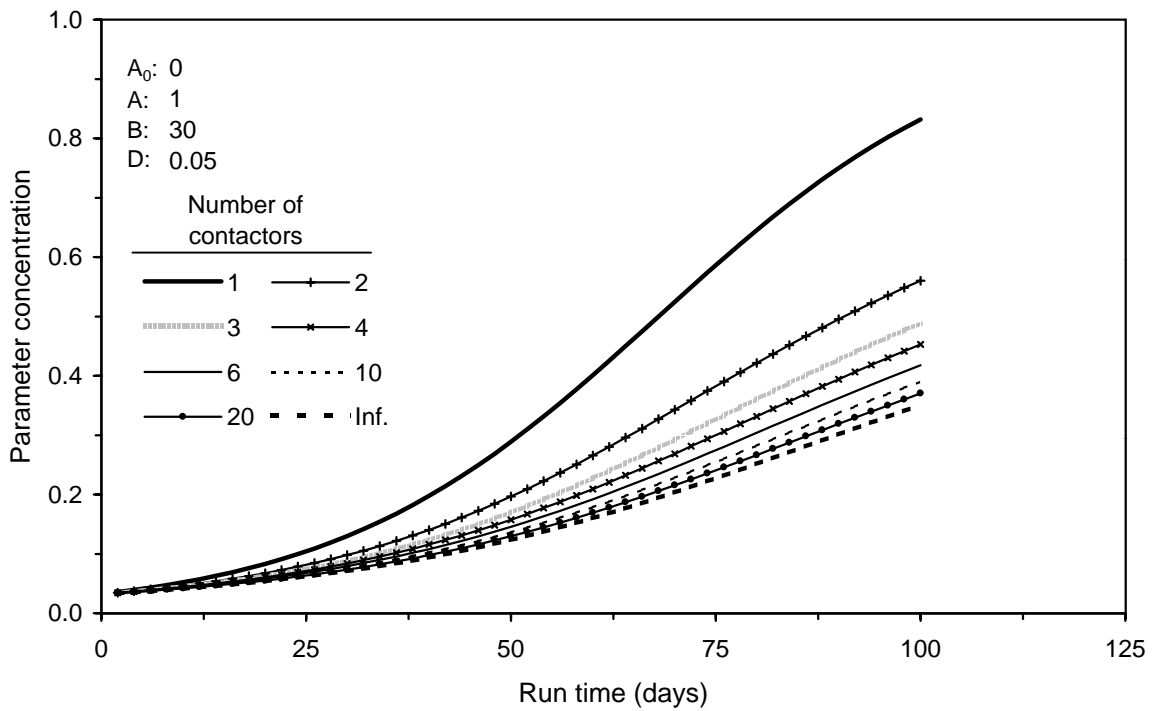


**Figure 110 Integral breakthrough curves for varying numbers of contactors operated in parallel-staggered mode ( $B = 30$ ;  $D = 0.05$ )**

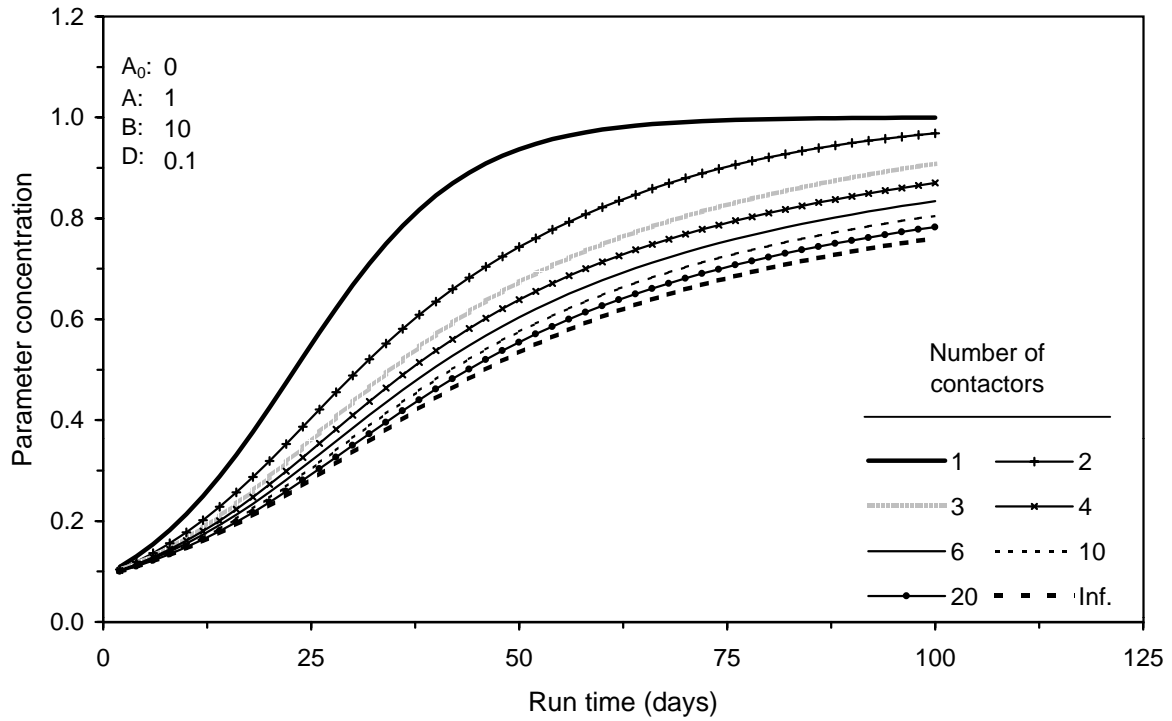


**Figure 111 Integral breakthrough curves for varying numbers of contactors operated in parallel-staggered mode ( $B = 10$ ;  $D = 0.1$ )**

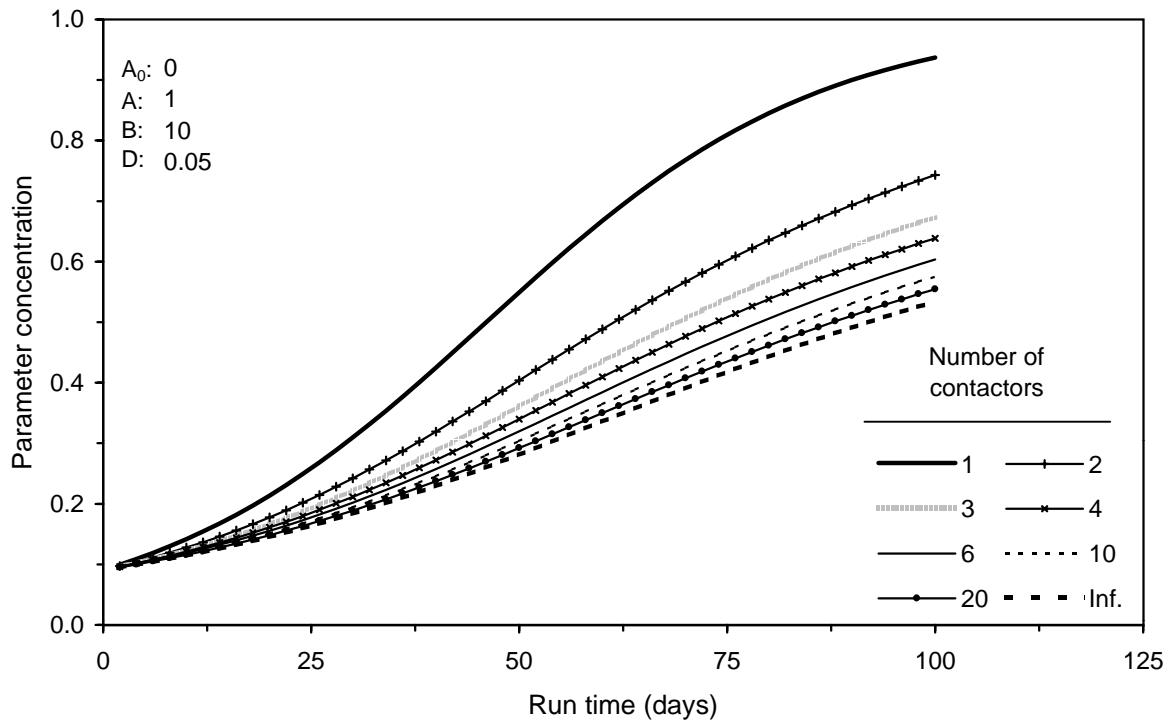


**Figure 112 Integral breakthrough curves for varying numbers of contactors operated in parallel-staggered mode ( $B = 10$ ;  $D = 0.05$ )**

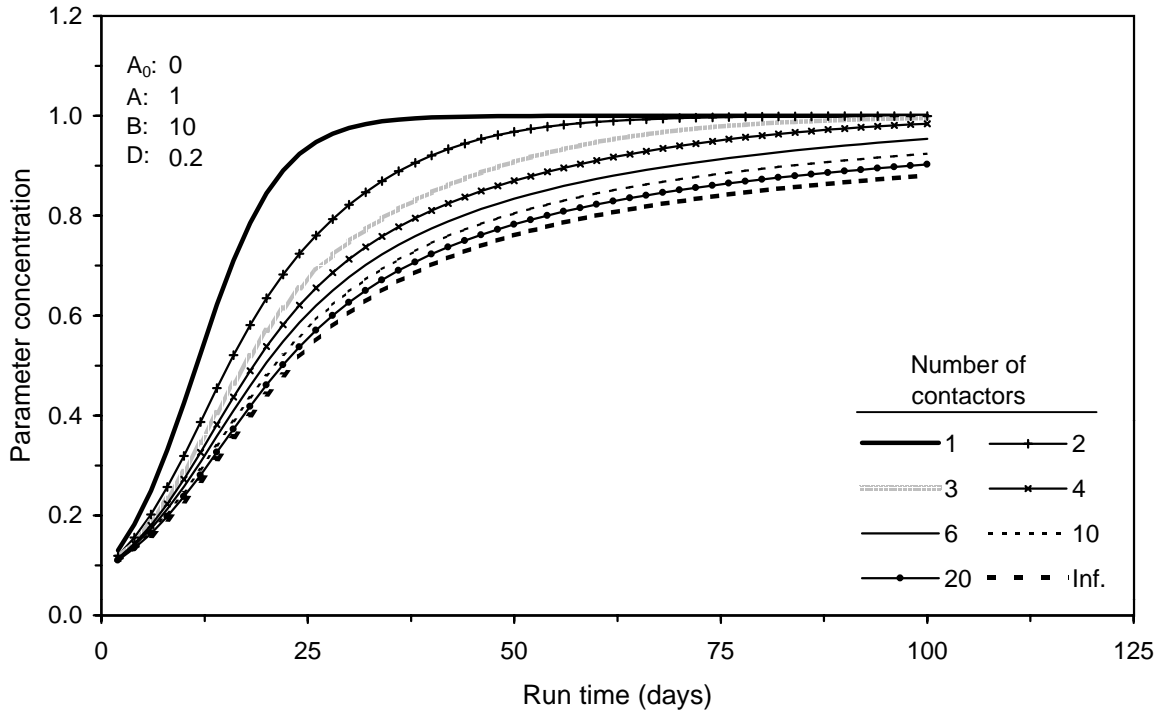


**Figure 113 Integral breakthrough curves for varying numbers of contactors operated in parallel-staggered mode ( $B = 10$ ;  $D = 0.2$ )**

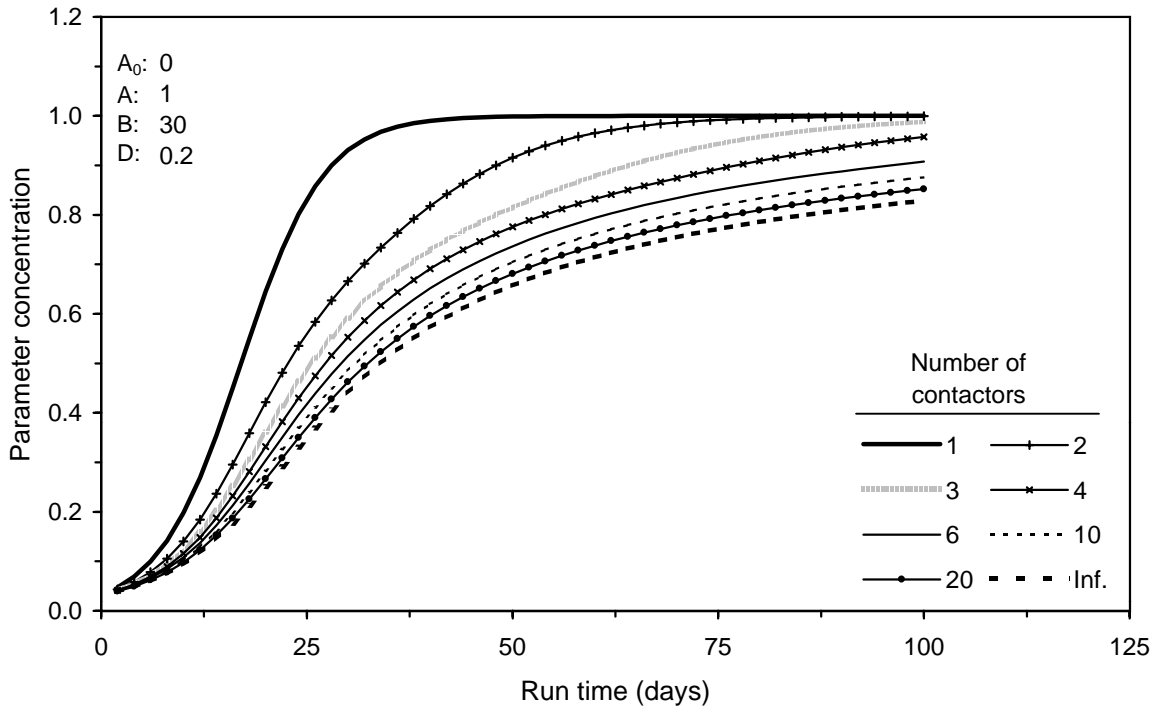


**Figure 114 Integral breakthrough curves for varying numbers of contactors operated in parallel-staggered mode ( $B = 30$ ;  $D = 0.2$ )**

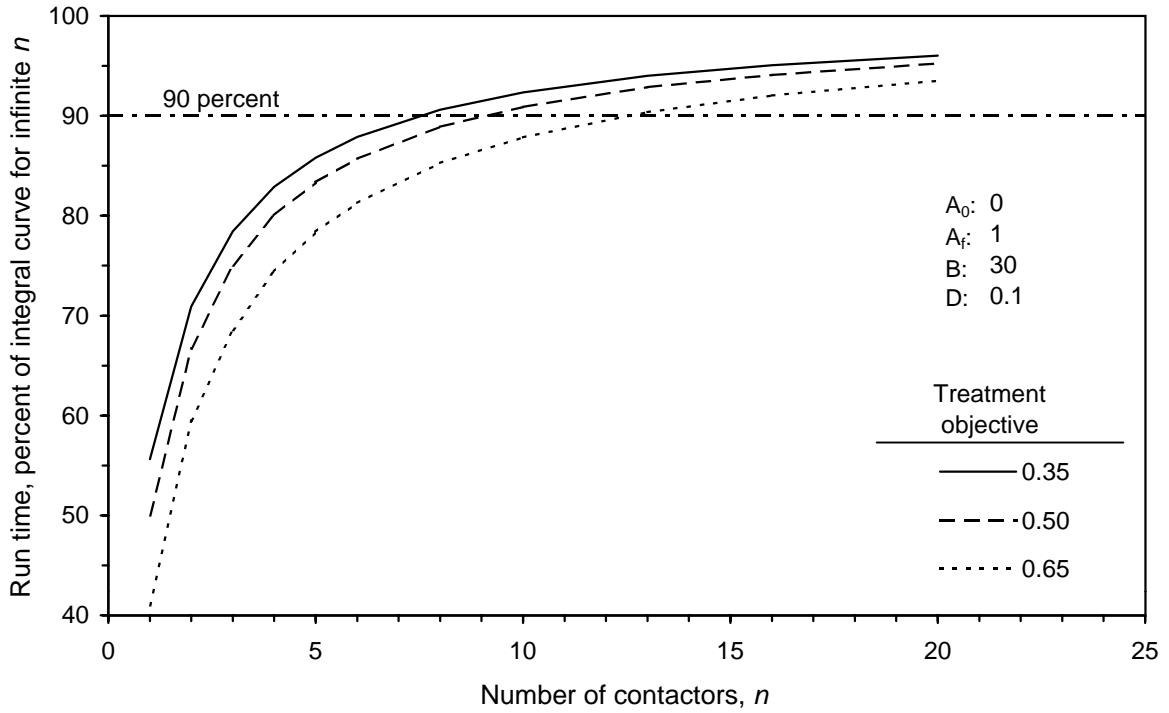


**Figure 115** Run time as a function of number of contactors in parallel, expressed as percent of run time for infinite  $n$  ( $B = 30$ ;  $D = 0.1$ )

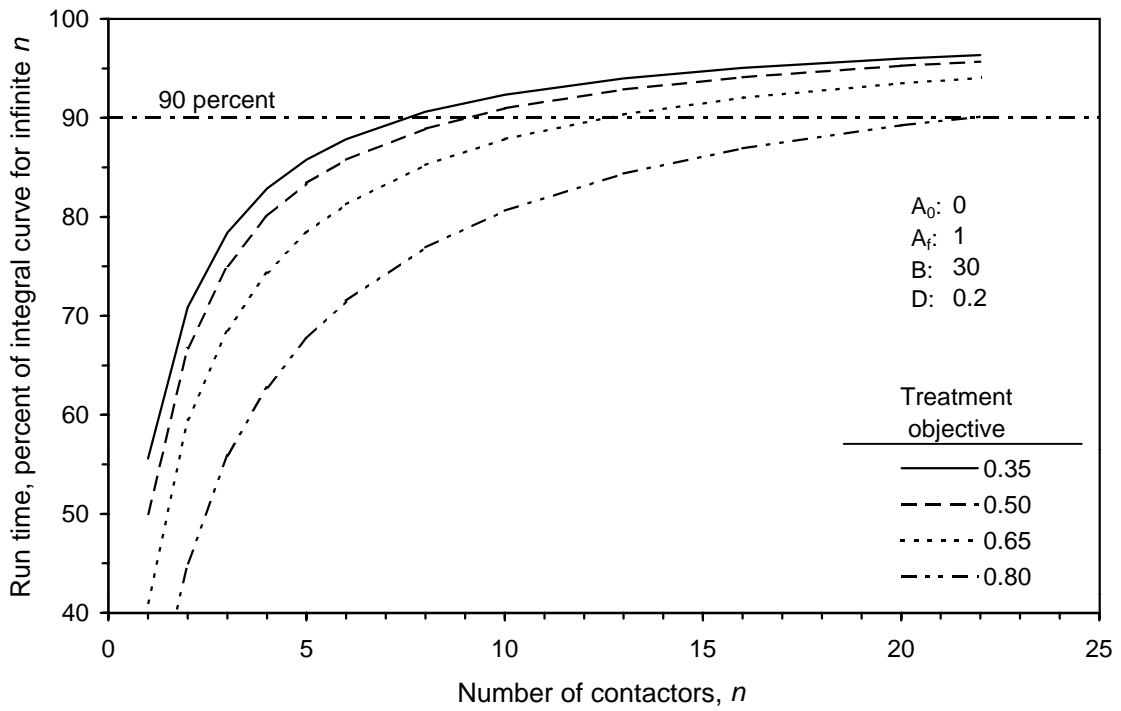


**Figure 116** Run time as a function of number of contactors in parallel, expressed as percent of run time for infinite  $n$  ( $B = 30$ ;  $D = 0.2$ )

#### 4.6 Impact of Extrapolation on Integral Breakthrough Curve Prediction

Extrapolation of the integral TOC breakthrough curve may be necessary during ICR treatment study data analysis because the SCA procedure is limited by the highest TOC concentration estimated from the direct integration of the single contactor TOC breakthrough curve. The highest blended effluent TOC concentration is typically 40 to 70 percent of the highest single contactor TOC concentration. Although higher single contactor TOC concentrations are associated with formed DBP concentrations, these cannot be applied to the integral breakthrough curve during application of the SCA method unless the TOC integral breakthrough curve is extrapolated. The impact of breakthrough curve extrapolation was analyzed for two GAC runs to determine whether the error caused by extrapolation was acceptable for ICR data analysis.

For two water sources (Waters 5 and 8), the RSSCTs were operated longer than required by the ICR. For Water 5, the run was extended 49 full-scale days after 70 percent TOC breakthrough was reached, equivalent to a 21 percent extension of the required run time. For Water 8, the extension beyond the required run time was 69 days, equivalent to a 61 percent increase. During the extended run time, two additional single contactor GAC effluent samples were taken. Two additional blended effluent samples were also taken. The first 11 GAC effluent data points that comprised a normal ICR treatment study run reaching 70 percent TOC breakthrough were modeled separately from the entire 13-point GAC effluent data set. Based on the logistic function model best-fit of the first 11 data points, the water quality at the end of the run (21 or 61 percent extrapolation) was predicted by extending the model fit.

Using the DI method, the TOC integral breakthrough curve was calculated based on the truncated logistic function model fit and then extrapolated to predict water quality at the end of the entire run. The TOC integral breakthrough curve was also calculated based on the logistic function best-fit of the entire single contactor effluent data set. For the other water quality parameters, the SCA prediction of blended contactor effluent water quality based on the extrapolated data set and was compared to that based on the entire data set. The impact of extrapolation on the TOC integral breakthrough curve is of special interest, due to the application of this extrapolation as a part of the SCA procedure during data analysis of the ICR treatment studies.

The impact of extrapolation on integral breakthrough curve predictions is shown in Figures 117 through 130. In these figures, the single contactor and integral breakthrough curves are plotted against scaled operation time. The data points used for the extrapolated single contactor data set are plotted with filled symbols, to differentiate these from the open symbols used for the first 11 data points. For the single contactor data, the solid best-fit line represents the logistic function best-fit using the entire data set, while the dashed line represents the best-fit of the first 11 points and extrapolation to the end of the run. Similarly, a dashed line also represents the extrapolated integral breakthrough curve. The  $R^2$  value is given for both best-fits of the single contactor data.

Figures 117 and 118 show the impact of extrapolation on the TOC single contactor logistic function curve fit and the TOC integral breakthrough curve predicted by the DI method for Waters 5 and 8, respectively. At the end of both runs, the extrapolated logistic function curve fit underpredicted single contactor effluent data. Based on the extrapolated logistic function, the TOC concentration at the end of the run was 8 percent lower than that based on the logistic

function best-fit of all available single contactor data for Water 5. For Water 8, the extrapolated predicted TOC concentration at the end of the run was 12 percent lower.

This underprediction of the single contactor effluent data by the extrapolated logistic function best-fit had a smaller impact on the TOC integral breakthrough curve prediction. The error associated with extrapolation of the TOC integral breakthrough curve at the end of the run was 3 percent (0.05 mg/L) for Water 5. For Water 8, the error was slightly larger, 8 percent (0.08 mg/L).

Application of the SCA procedure to the extrapolated single contactor breakthrough curves for all parameters yielded an average error in the predicted blended contactor concentration at the end of the run of  $5 \pm 3$  percent for Water 5. Figures 119 through 124 show the impact of extrapolation on SCA prediction of the blended contactor effluent for UV<sub>254</sub>, SDS-TOX, SDS-TTHM, SDS-HAA5, SDS-HAA6, and SDS-HAA9. For these DBP surrogates and class sums, the average error in the SCA prediction due to extrapolation was also 5 percent, (the run time was extrapolated by 21 percent) and in all cases, the extrapolated prediction was lower than the prediction using the entire data set. Comparisons of all water quality parameters, including DBP species, are given in Appendix H.

For Water 8, the average error in the predicted blended contactor concentration at the end of the run based on the SCA prediction of the extrapolated integral breakthrough curve was  $9 \pm 5$  percent. This higher mean observed error for Water 8 as compared to Water 5 can be attributed in part to the larger percent extrapolation, 61 percent, performed on Water 8 as compared to that for Water 5, 21 percent. For UV<sub>254</sub>, SDS-TOX, SDS-TTHM, SDS-HAA5, SDS-HAA6, and SDS-HAA9 the average error was 7 percent. Figures 125 through 130 show the impact of extrapolation on the SCA prediction of the blended contactor concentration of these DBP surrogates and class sums. The blended contactor effluent concentration at the end of the run after extrapolation was lower than that based on the entire data set, except for SDS-HAA5.

An analysis of Water 8 was also made using an extrapolation of 29 percent, which is similar to the extrapolation applied to Water 5. For this shorter level of extrapolation, the mean error in the integral breakthrough curve at the end of the run for all parameters was 8 percent, only slightly lower than that observed for an extrapolation of 61 percent. For UV<sub>254</sub>, SDS-TOX, SDS-TTHM, SDS-HAA5, SDS-HAA6, and SDS-HAA9 the average error was 6 percent. Therefore, for Water 8, extending the extrapolation from 29 to 61 percent of the run time did not proportionally increase the mean observed error in the predicted integral breakthrough curve at the end of the run.

Under the SCA procedure, the error in the extrapolated integral breakthrough curve for any parameter (other than TOC) is dependent on the error in the extrapolated DI prediction of the TOC integral breakthrough curve as well as on the difference between the parameter single contactor curve fits using the entire data set and the truncated data set. This difference typically increases over the course of the run, and can be especially large in the extrapolated portion of the curve. However, the error at the end of the single contactor curve may not impact the prediction of the integral breakthrough curve by the SCA method because the maximum TOC concentration at the end of the extrapolated integral breakthrough curve is still less than the maximum TOC concentration at the end of the single contactor curve. This upper bound on TOC limits the

concentrations of all other parameters to the initial and middle portions of the single contactor curves when using the SCA procedure to predict integral breakthrough curves.

Conversely, the DI method prediction of the integral breakthrough curve relies on the entire single contactor breakthrough curve for each parameter. Therefore, the error at the end of the run due to extrapolation may have a larger impact on integral breakthrough curve predictions by the DI method than predictions by the SCA procedure. Appendix I summarizes the integral breakthrough curve predictions after extrapolation based on the DI method for all parameters. The average difference at the end of the run between DI integral breakthrough curve predictions with and without extrapolation was 3 percent for Water 5, which is slightly lower than the average obtained using the SCA method. For Water 8, the average error was slightly higher, 10 percent.

Based on the two runs examined, extrapolation up to 61 percent beyond available experimental data yielded a mean 9 percent error in the predicted water quality based on the extrapolated integral breakthrough curve as compared to that based on the complete data set. For a shorter extrapolation, 21 percent, the mean error was 5 percent. An understanding and acceptance of the error due to breakthrough curve extrapolation is important because extrapolation may be used in many cases during the ICR treatment study data analysis to gain additional information from GAC breakthrough data sets. In particular, data sets that do not exceed a given treatment objective may be extrapolated by up to 50 percent in an attempt to determine a GAC run time for the treatment objective. Based on the two waters examined in this study, the error incurred by extrapolation up to 50 percent of the original run time should average less than 10 percent.

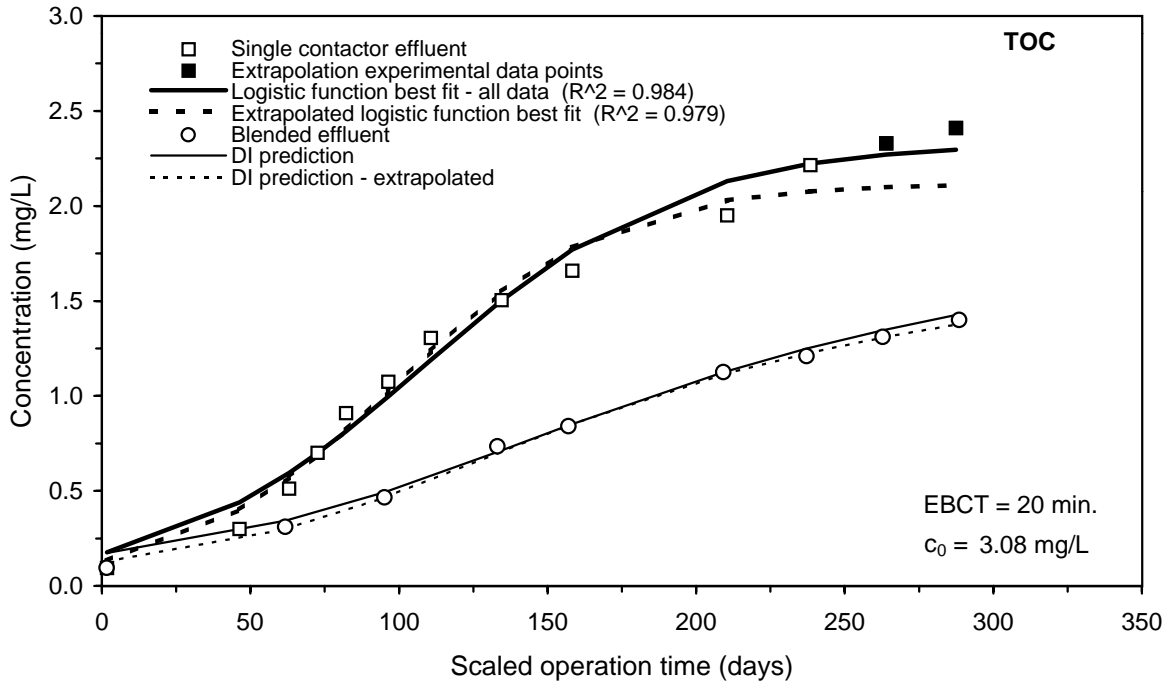


**Figure 117 Impact of extrapolation on DI prediction of the TOC integral breakthrough curve for Water 5**

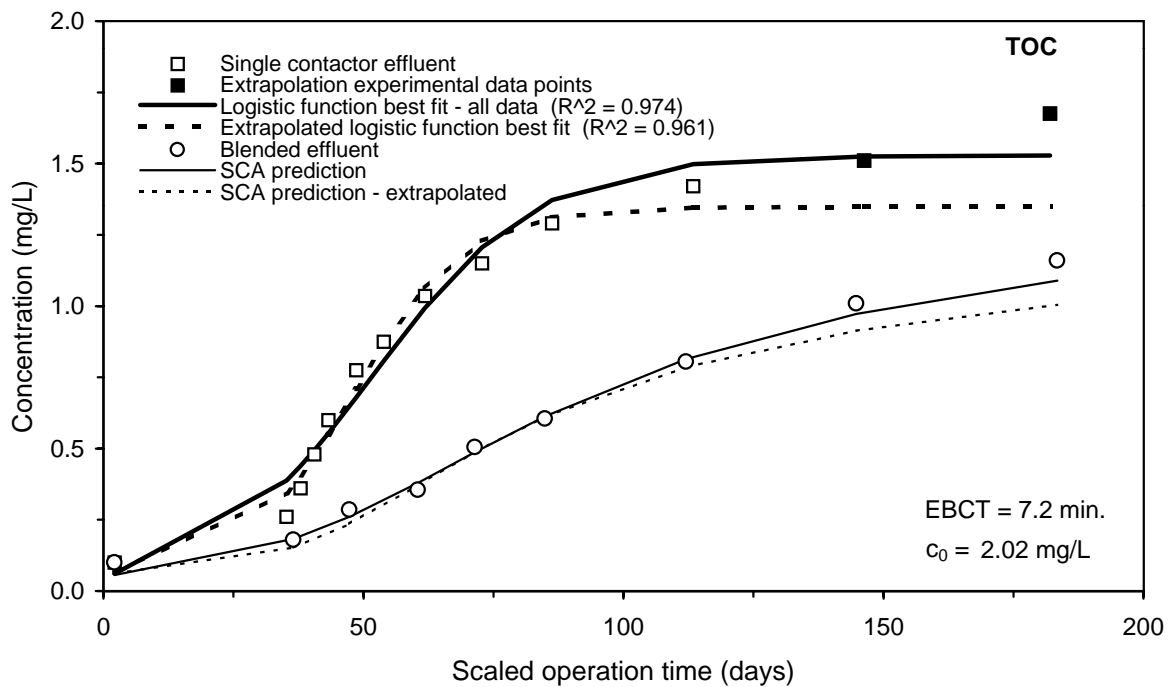


**Figure 118 Impact of extrapolation on DI prediction of the TOC integral breakthrough curve for Water 8**

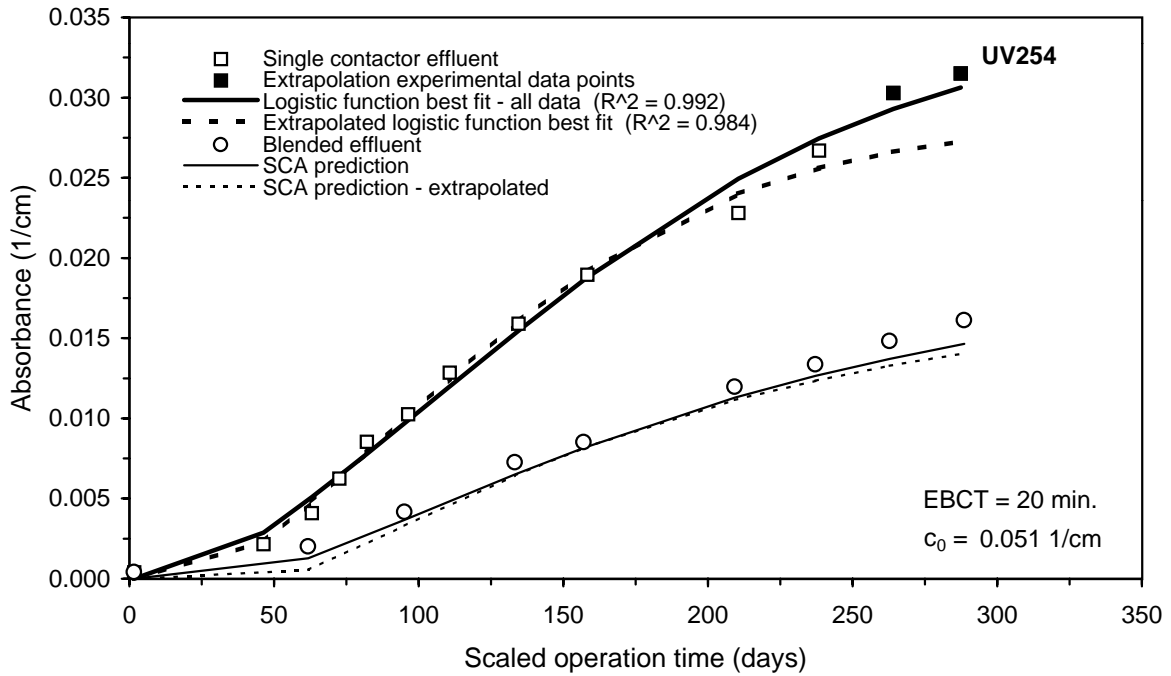


**Figure 119 Impact of extrapolation on SCA prediction of the UV254 integral breakthrough curve for Water 5**

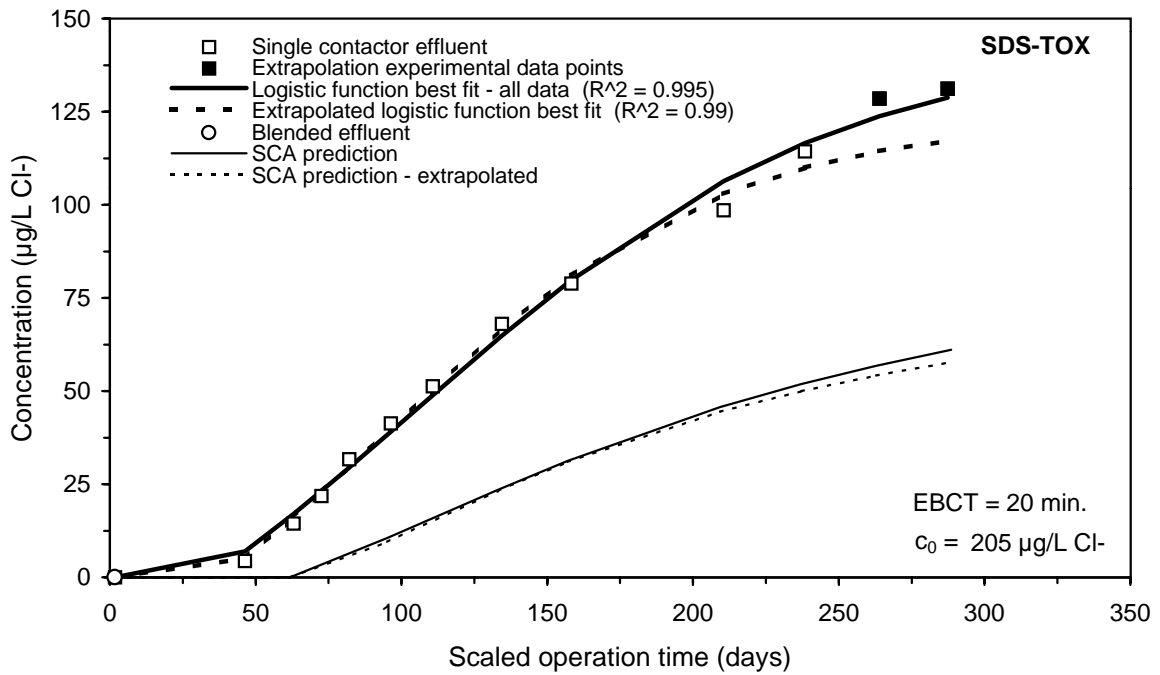


**Figure 120 Impact of extrapolation on SCA prediction of the SDS-TOX integral breakthrough curve for Water 5**

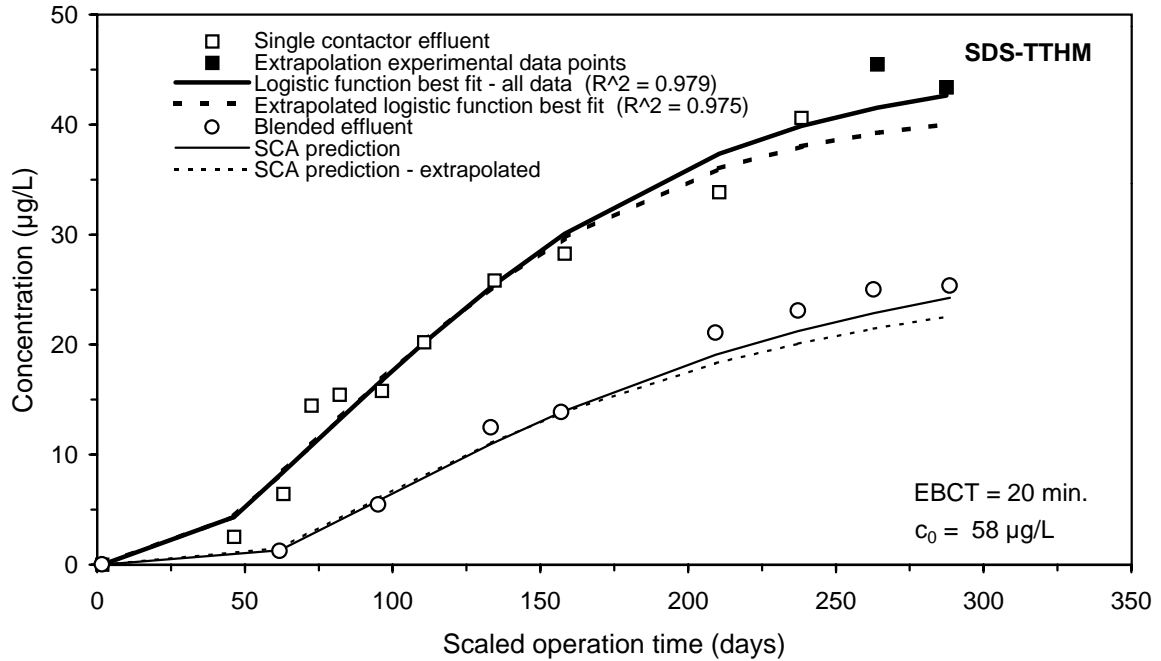


**Figure 121 Impact of extrapolation on SCA prediction of the SDS-TTHM integral breakthrough curve for Water 5**

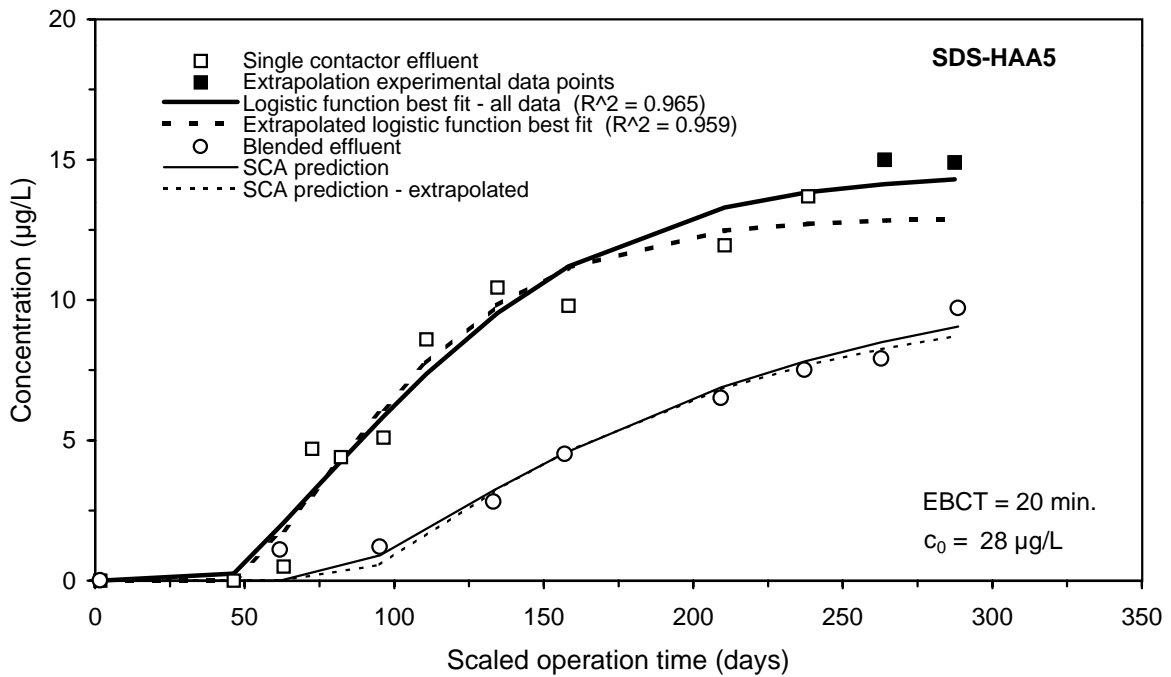


**Figure 122 Impact of extrapolation on SCA prediction of the SDS-HAA5 integral breakthrough curve for Water 5**

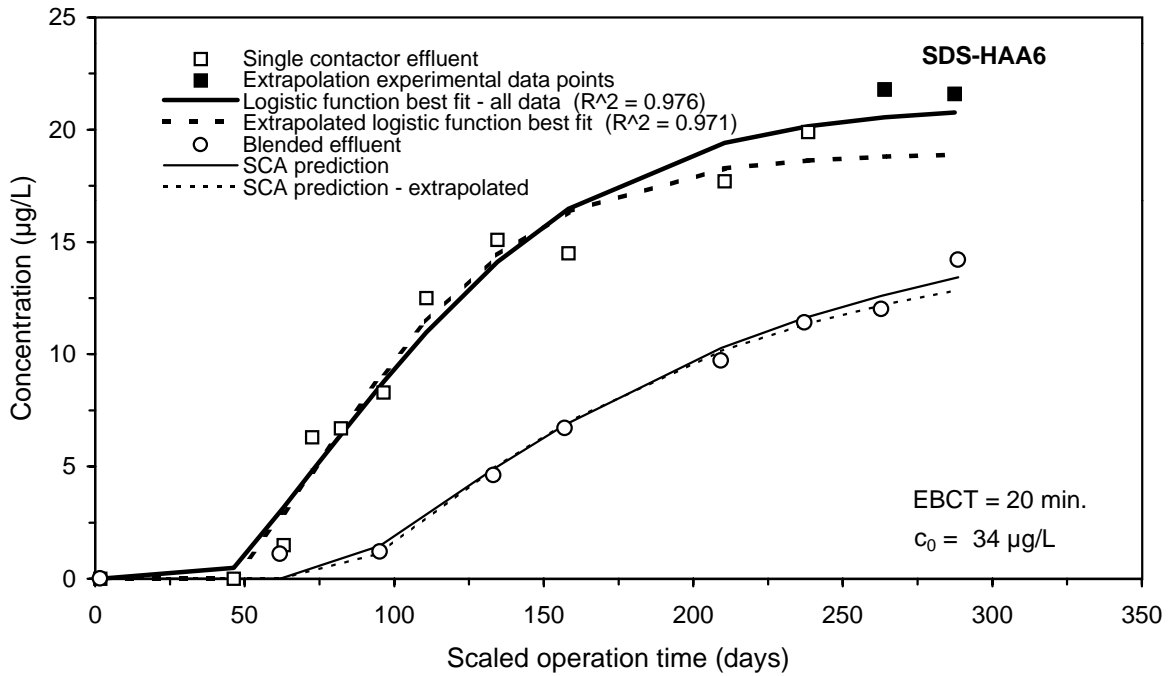


**Figure 123 Impact of extrapolation on SCA prediction of the SDS-HAA6 integral breakthrough curve for Water 5**

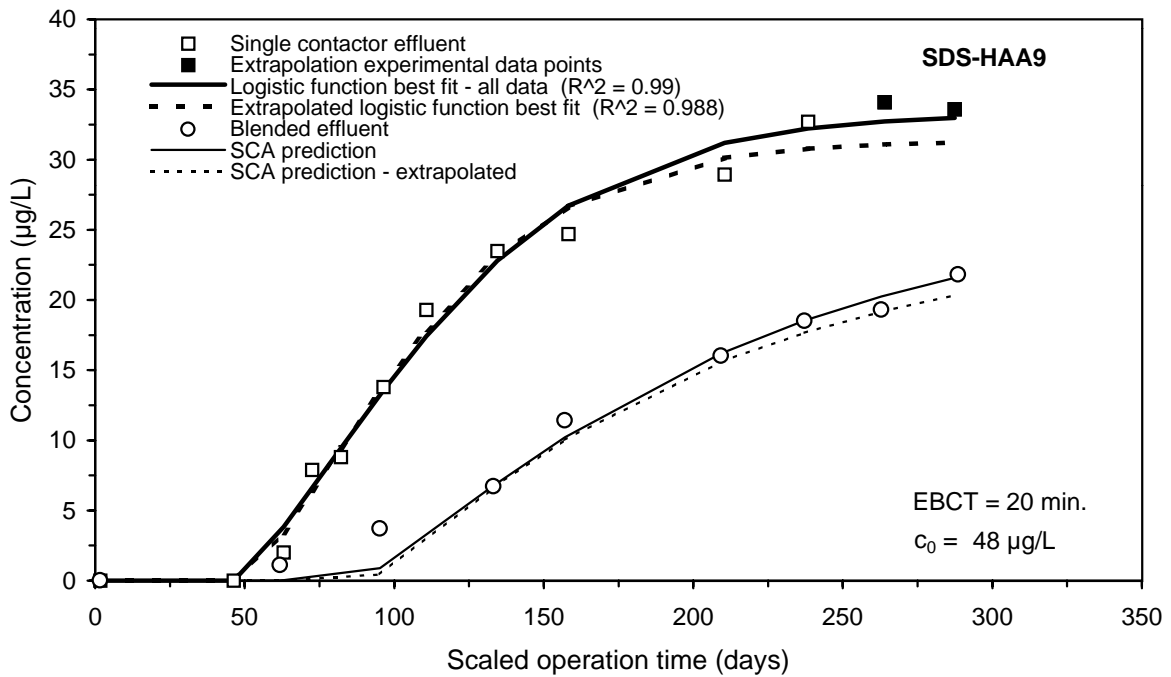


**Figure 124 Impact of extrapolation on SCA prediction of the SDS-HAA9 integral breakthrough curve for Water 5**

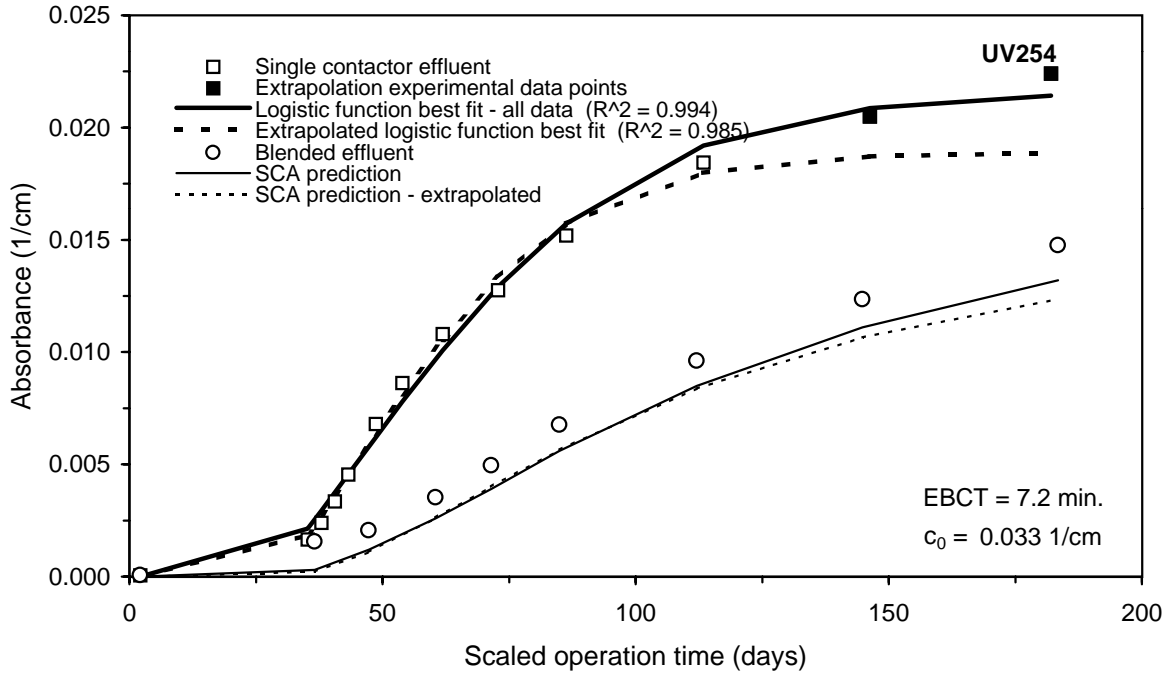


**Figure 125 Impact of extrapolation on SCA prediction of the UV254 integral breakthrough curve for Water 8**

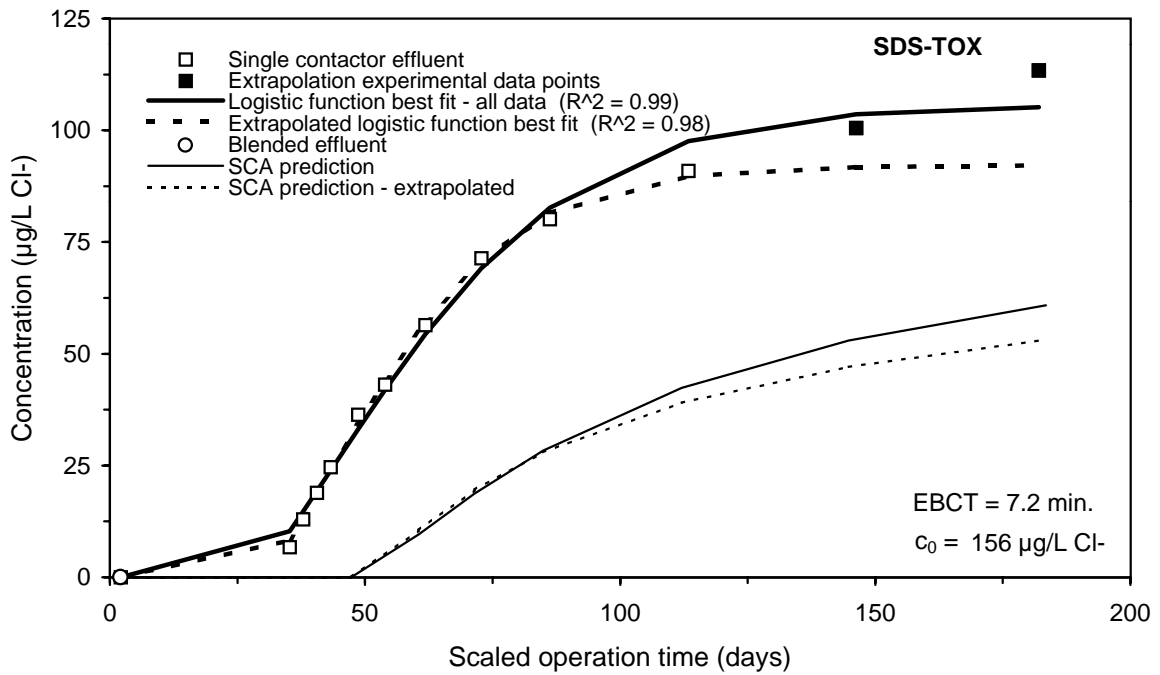


**Figure 126 Impact of extrapolation on SCA prediction of the SDS-TOX integral breakthrough curve for Water 8**

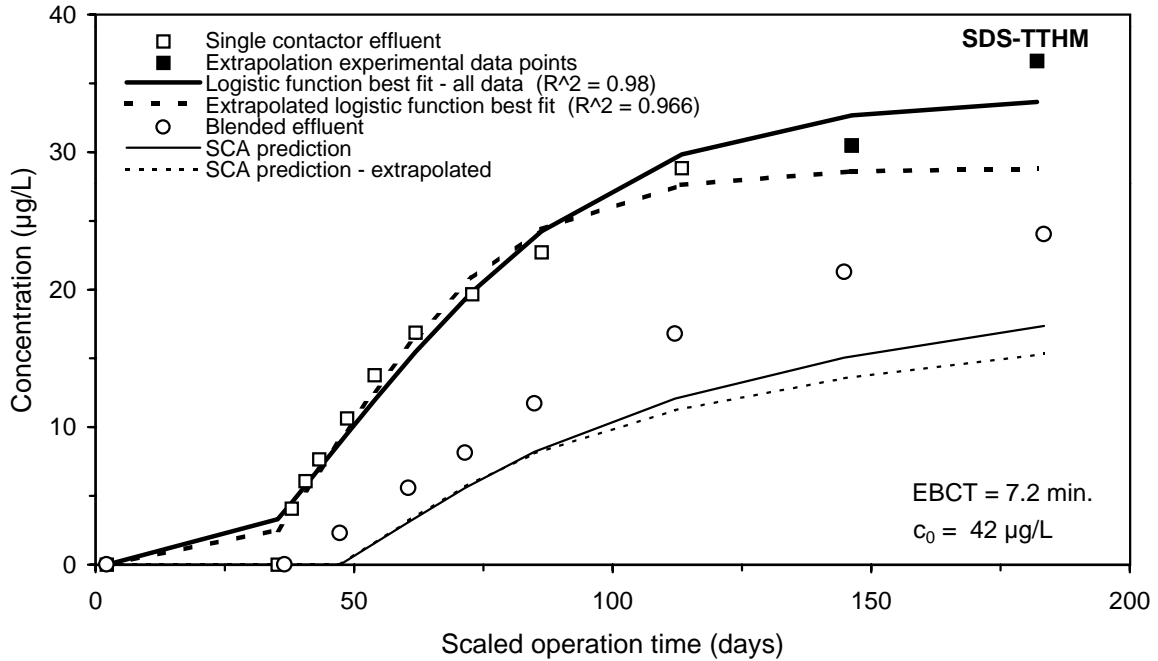


**Figure 127 Impact of extrapolation on SCA prediction of the SDS-TTHM integral breakthrough curve for Water 8**

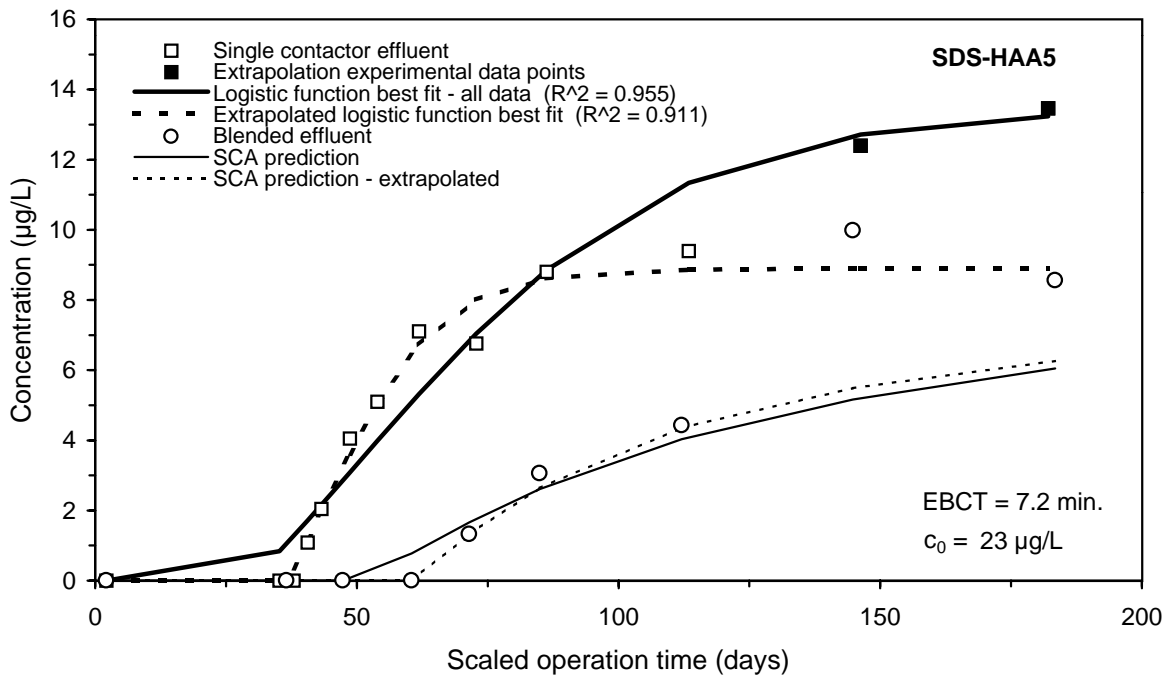


**Figure 128 Impact of extrapolation on SCA prediction of the SDS-HAA5 integral breakthrough curve for Water 8**

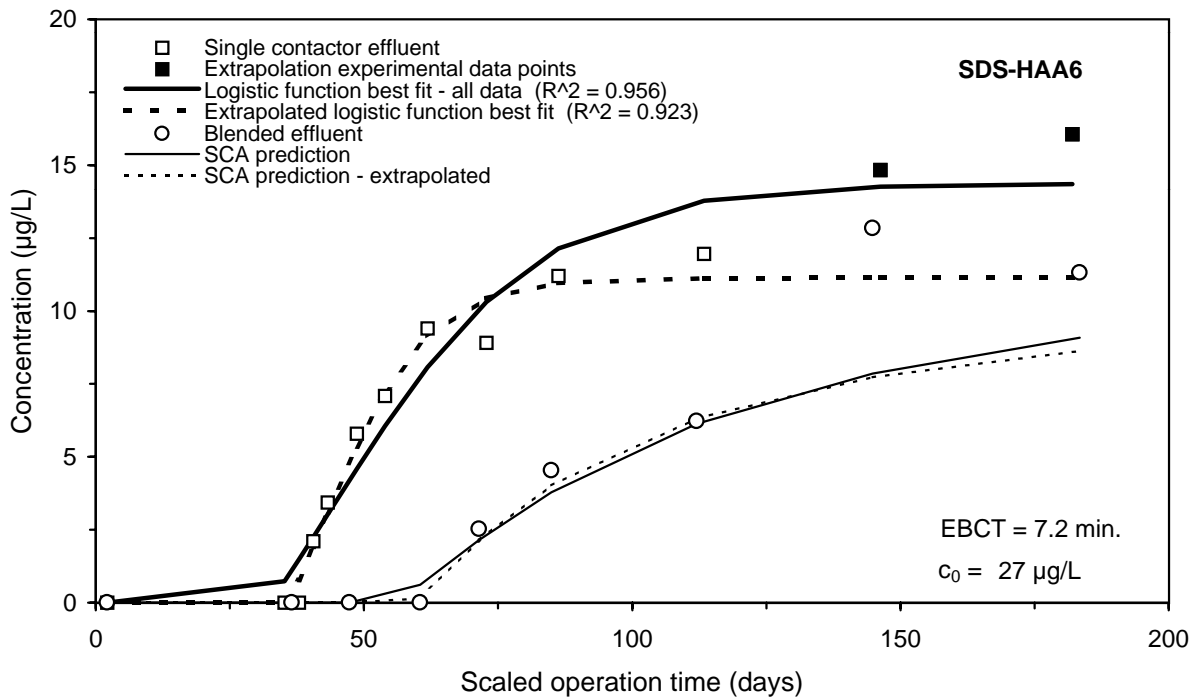


**Figure 129 Impact of extrapolation on SCA prediction of the SDS-HAA6 integral breakthrough curve for Water 8**

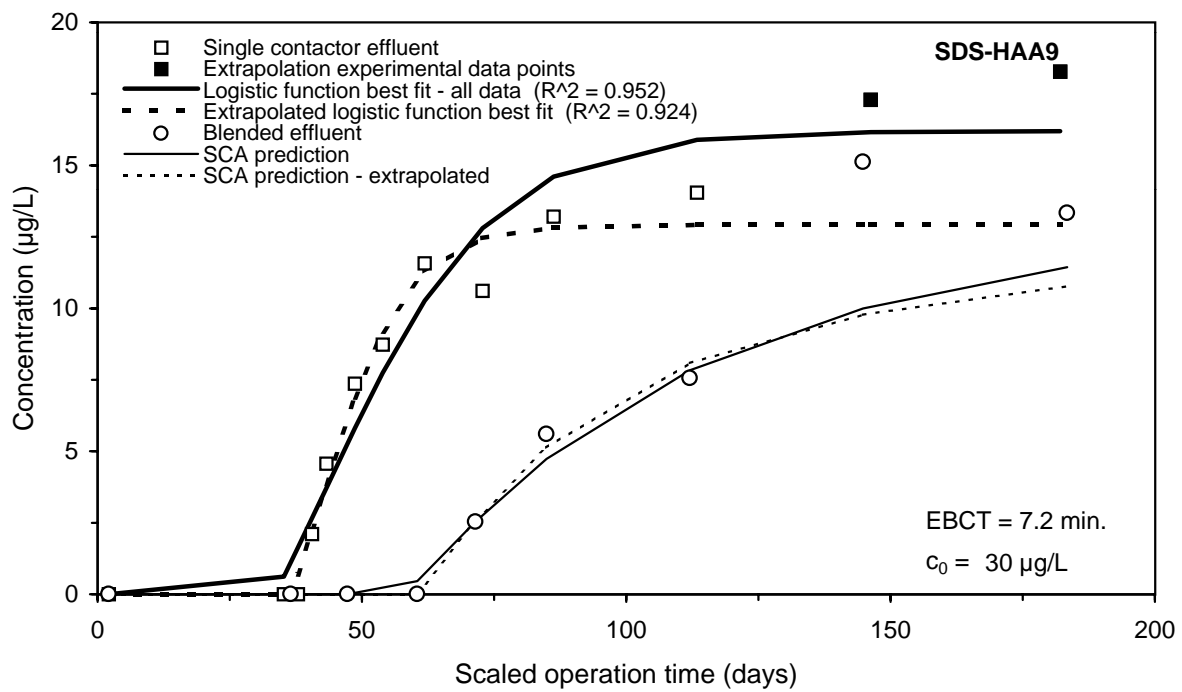


**Figure 130 Impact of extrapolation on SCA prediction of the SDS-HAA9 integral breakthrough curve for Water 8**

---

## 5 Summary and Conclusions

The design of this study incorporated two main goals. The primary objectives were to evaluate the ability of the logistic function to model single contactor breakthrough curve data and to evaluate the success and limitations of predictive models used to determine the integral breakthrough curve, a relationship between single contactor run time and blended contactor water quality. The secondary objective of this study was to evaluate the applicability of these models and predictive methods in the context of the ICR GAC treatment study data analysis. A large amount of data will be analyzed: the 62 GAC treatment studies performed will generate 8,000 to 9,000 individual breakthrough curves. Experimental verification was performed on data from eight bench-scale GAC runs with varying water sources, pretreatments, DBP precursor concentrations, bromide concentrations, and SDS chlorination conditions. The GAC runs utilized the rapid small-scale column test (RSSCT) and were performed according to ICR requirements.

A primary requirement for the ICR GAC treatment study data analysis procedure is to model the single contactor effluent breakthrough data, for all parameters analyzed, including DBP surrogates, DBP class sums, and DBP species. A model used to describe single contactor effluent experimental data is needed for several reasons. From a data management perspective, best-fit curve parameters that adequately describe experimental data are less memory intensive than storing the entire experimental data set. A best-fit curve also facilitates interpolation and extrapolation to estimate run times for given treatment objectives. Use of a best-fit model curve also provides an estimate of the scatter in the data through the coefficient of determination, and the model minimizes the impact of this scatter on run time estimates. Finally, a function that describes the single contactor experimental data set is a prerequisite for determining the integral breakthrough curve, a curve that relates single contactor run time to blended effluent water quality under the assumption that contactors are operated in parallel-staggered mode. Run time estimates generated by the integral breakthrough curve are more applicable to full-scale GAC operation.

Previous researchers have used various forms of the logistic function to predict and model GAC breakthrough curve data, and the logistic function was found to be an adequate model in this study, where it was applied to data from eight GAC runs (160 potential curve fits, but only 126 were performed because concentrations in the GAC effluent were below the MRL for some parameters). However, poor curve fits occurred for some parameters, especially very sharp "S" shaped breakthrough curves, and "peak" curves (breakthrough curves for brominated species that increased and then decreased in concentration over the course of the run due to changes in the bromide to TOC ratio). To improve the performance of the logistic function for modeling single contactor data, three enhancements were made, yielding the step, step-lag, and step-lag-peak logistic function models. The step logistic function model is applicable for GAC breakthrough curves with relatively high levels of immediate breakthrough. The step-lag logistic function model incorporates an initial phase where the model output is set to zero, to better fit DBP breakthrough curves with relatively long initial intervals of effluent concentrations reported as BMRL, prior to breakthrough. The step-lag-peak logistic function model incorporates a linear decay term and is applied to "peak" breakthrough curves, which sometimes occur for brominated DBP species.

Curve fitting involved determining which model was applicable, and applying it to the breakthrough curve for each parameter. These enhanced forms of the logistic function model were able to successfully fit single contactor breakthrough curve data for all parameters. A method was also developed to detect outlier data points that limited the influence of deviant observations on the parameter estimates. In general, the application of the three enhanced forms of the logistic function curve to single contactor effluent breakthrough data was successful, with a mean  $R^2$  of 0.974.

Two predictive approaches for determining the integral breakthrough curve were examined: the direct integration (DI) and the surrogate correlation approach (SCA). The results of these procedures were compared to experimental results. Experimental data were obtained by collecting the entire effluent from each of eight bench-scale GAC experiments in separate reservoirs and sampling from these reservoirs over time. This experimental procedure simulates the integral breakthrough curve for an infinite number of contactors operated in parallel-staggered mode.

The DI procedure applied the average value function to the logistic function model fit of the experimental single contactor data, and is based on the assumption of an infinite number of contactors operated in parallel-staggered mode with regular GAC replacement frequencies. For DBP surrogates (TOC,  $UV_{254}$ , and SDS-TOX), the DI procedure yielded excellent results in comparison to experimental data. For class sums, such as SDS-TTHM and SDS-HAA5, predictions were usually adequate. However, for individual DBP compounds, especially brominated species, the DI approach did not always result in accurate predictions. The inaccuracy of the DI approach for the prediction of some DBP species is problematic since individual DBPs of potential health concern will be considered during analysis of the treatment study data.

The SCA procedure was developed to reduce the computational requirements of estimating blended contactor run times for any given regulatory treatment objective evaluated during the ICR GAC treatment study data analysis. The SCA procedure relies on the DI method to establish an integral breakthrough curve for TOC only. The DI method yielded excellent predictions of the TOC integral breakthrough curve for the waters examined in this study, with a mean error quantified by the residual sum of squares (RSS) of 0.055 mg/L, and a mean bias of +0.028 mg/L. Once the TOC integral breakthrough curve is obtained, data points on both the single contactor and integral breakthrough curves at a constant TOC concentration are mapped, and all other water quality parameters associated with the single contactor effluent data set at that TOC concentration are applied to the blended contactor integral breakthrough curve. The SCA procedure requires that single contactor effluent data be adequately modeled using the logistic function models. For eight GAC runs and eight water sources, this study showed that the enhanced logistic function models successfully simulated a wide variety of GAC breakthrough curve profiles. The SCA procedure inherently relies on the assumption that the relationship between TOC and the other organic precursors, SDS DBP class sums, and SDS DBP species established in the single contactor effluent is maintained in the blended contactor effluent. This study found that this assumption is valid for the eight waters examined. In addition, the correlation between TOC and bromine incorporation factors for THMs and HAAs was shown to be consistent between the single contactor effluent and experimental blended effluent.

Application of the SCA procedure to the experimental GAC breakthrough curves for eight water sources showed that the overall accuracy of the model was equivalent to the DI method for predicting the integral breakthrough curve. This analysis was performed by calculating the RSS and bias between model predictions and experimental data. The cumulative frequency distribution of the normalized RSS showed that across all waters and all analytes, the prediction error for the two models was equivalent. Both models were biased negative, indicating a tendency to underpredict the experimental data. The SCA model had a slightly higher negative bias than did the DI model. Based on these results, application of the computationally-simpler SCA procedure to ICR treatment study data is recommended.

A comparative analysis of the two predictive models was also performed for each individual analyte. The SCA method was more accurate than the DI method when applied to SDS-TTHM, and was equally accurate when applied to SDS-HAA5, SDS-HAA6, and SDS-HAA9. For the two waters that examined SDS-TOX, the DI method was a better predictor of experimental results. For the predominant THM and HAA species (for which comparisons could be made for six or more of the eight runs), the SCA method outperformed the DI method when applied to brominated DBP species, with the exception of SDS-DBCM. The DI method generated more accurate predictions of the non-brominated DBP species (SDS-CF, SDS-DCAA, and SDS-TCAA). The impact of changing bromide to TOC ratio on the shape of the breakthrough curve for brominated DBP species, yielding peak curves or very sharp curves followed by a plateau, typically resulted in underpredictions by the DI method of the observed data. The SCA method was able to better predict the integral breakthrough curves for the brominated species because it relied on the relationship between TOC and DBP formation in the single contactor effluent, which inherently accounts for changing bromide to TOC ratios.

An important limitation of the DI and SCA procedures is that they rely on the assumption of an infinite number of contactors operated in parallel-staggered mode. Previous work has maintained that for 10 or more contactors in operation, actual blended effluent run times are within 10 percent of those estimated based on the infinite contactor assumption. This study found that the error incurred when applying run time estimates based on the infinite contactor assumption to run times for finite numbers of contactors is impacted by the number of contactors and the magnitude of the treatment objective examined in relation to the asymptotic concentration approached by the single contactor breakthrough curve. Based on the logistic function model, the infinite contactor assumption will yield estimated run times within 10 percent of actual run times for 13 or more contactors operated in parallel-staggered mode. For 10 contactors on-line, the infinite contactor assumption will yield run time estimates within 12 percent of the actual run times. In all cases, run time estimates based on the infinite contactor assumption are longer than those for a finite number of contactors, thus providing a best case scenario for GAC performance.

The applicability of the infinite contactor assumption in this model to finite numbers of contactors is especially important for small plants operating fewer than 10 contactors on-line. Also evident was that the largest incremental benefit afforded by operating contactors in parallel-staggered mode occurs when two contactors are operated as compared to a single contactor. The benefit realized by adding an additional contactor decreases as the number of contactors on-line increases. The relationship developed between integral breakthrough curve run time estimates based on an infinite number of contactors and that based on a finite number of contactors can be

applied to ICR treatment study data to estimate the performance of large and small GAC systems.

During the total run time for any given single contactor TOC breakthrough curve, the blended contactor integral breakthrough curve determined by the DI approach will typically reach concentrations ranging from 40 to 70 percent of those measured at the end of the single contactor GAC run. Therefore, when using the SCA procedure, the latter portion of the single contactor breakthrough curve (consisting of higher surrogate and formed DBP levels) will not usually be applied to the blended effluent data set. This may be an issue during ICR treatment study data analysis if a significant number of integral breakthrough curves estimated by the SCA procedure do not reach regulatory treatment objectives. For these runs, extrapolation of the TOC integral breakthrough curve would increase the usefulness of the entire data set.

For two waters, experimental evaluation of the sensitivity predicted water quality to extrapolation of the integral breakthrough curve prediction was performed. For one water, extrapolation by 21 percent yielded a 3 percent error in the predicted integral TOC concentration at the end of the run and a mean 5 percent error at the end of the run for all analytes predicted by the SCA method. For a second water, which was extrapolated by 61 percent, the error in predicted TOC concentration was 8 percent at the end of the run, and the mean error at the end of the extrapolated run was 9 percent for all analytes.

An understanding and acceptance of the error due to breakthrough curve extrapolation is important because extrapolation may be used in many cases during the ICR treatment study data analysis to gain additional information from GAC breakthrough data sets. In particular, data sets that do not exceed a given treatment objective may be extrapolated by a reasonable extent (up to 50 percent) in an attempt to determine a GAC run time for the treatment objective. Based on the two waters examined in this study, the error incurred by extrapolation up to 50 percent of the original run time should average less than 10 percent. This error may be acceptable for ICR treatment study data analysis, given the benefit afforded by the extrapolation.

The models used to simulate GAC operation of multiple contactors in parallel-staggered mode rely on the assumption that the GAC is replaced at regular intervals, so that the service times of all contactors are equal. They also assume that the breakthrough curve profiles of all single contactors are identical. In a full-scale plant, this idealized situation will rarely occur. Variability in source water quality will impact the run time of the contactors, depending on when they are placed in service and the concentration of DBP precursors in the GAC influent during their service life. Variability in distribution system conditions, especially temperature, will impact the contactor service life, as formed DBP levels increase with higher temperatures. Furthermore, for a plant that operates a fixed number of contactors, water demand changes during the year may directly impact the EBCT of each contactor. A contactor that is placed on-line at the beginning of the summer high demand months may be operated under a shorter EBCT as compared to a contactor placed on-line during the winter. Furthermore, it is less desirable to remove contactors from service to replace GAC during high demand periods. Another approach is to increase the number of contactors on-line as water demand increases. These full-scale issues should be considered when interpreting the results of the ICR treatment study data analysis.

---

## 6 References

- Clark, R.M. 1987. Modeling TOC Removal by GAC: The General Logistic Function. *Jour. AWWA.* (79:1:33).
- Chowdhury, Z.K., G. Solarik, D.M. Owen, S.M. Hooper, and R.S. Summers. 1996. NOM Removal by GAC Adsorption: Implications of Blending. In *Proc. of the AWWA Annual Conference*, Toronto, Ontario, Canada.
- Clark, R.M., J.M. Symons, and J.C. Ireland. Evaluating Field Scale GAC Systems for Drinking Water. *Jour. Environ. Engr.* (112:4:744).
- Crittenden, J.C., P.S. Reddy, D.W. Hand and H. Arora. 1989. *Prediction of GAC Performance Using Rapid Small-Scale Column Tests.* AWWARF/AWWA.
- Crittenden, J.C., P.S. Reddy, H. Arora, J. Trynoski, D.W. Hand, D.L. Perram, and R.S. Summers. 1991. Predicting GAC Performance with Rapid Small-Scale Column Tests. *Jour. AWWA.* (83:1:77).
- Gould, J.P., L.E. Fitchorn, and E. Urheim. 1983. Formation of Brominated Trihalomethanes: Extent and Kinetics. *Water Chlorination: Environmental Impact and Health Effects.* Vol. 4 (R.L. Jolley et al., eds.), Ann Arbor Sci. Publ., Ann Arbor, Michigan.
- Hooper, S.M., R.S. Summers, G. Solarik, and S. Hong. 1996. GAC Performance for DBP Control: Effect of Influent Concentration, Seasonal Variation, and Pretreatment. In *Proc. of the AWWA Annual Conference*, Toronto, Ontario, Canada.
- Littell, R.C., G.A. Milliken, W.W. Stroup, and R.D. Wolfinger. 1996. SAS System for Mixed Models. Cary, NC (SAS Institute Inc.)
- Oulman, C.S. 1980. The Logistic Curve as a Model for Carbon Bed Design. *Jour. AWWA* (72:1:50).
- Roberts, P.V. and R.S. Summers. Performance of Granular Activated Carbon for Total Organic Carbon Removal. *Jour. AWWA.* (74:2:113).
- Shukairy, H.M., Miltner, R.J., and Summers, R.S. 1994. Bromide's Effect on DBP Formation, Speciation and Control: Part 1, Ozonation. *Jour. AWWA.* (86:6:72).
- Snoeyink, V.L. 1990. Adsorption of Organic Compounds. *Water Quality and Treatment: A Handbook for Community Supplies.* 4th ed. (F.W. Pontius, ed.), AWWA and McGraw-Hill, Inc.
- Sontheimer, H., J.C. Crittenden, and R.S. Summers. 1988. *Activated Carbon for Water Treatment.* 2nd ed., DVGW-Forschungsstelle, Universitat Karlsruhe, Karlsruhe, Germany.
- Standard Methods for the Examination of Water and Wastewater.* 1998. APHA, AWWA, and WEF. Washington D.C. (20th ed.)

- Summers, R.S., D.M. Owen, Z.K. Chowdhury, S.M. Hooper, G. Solarik, and K. Gray. 1998. *Removal of DBP Precursors by GAC Adsorption*. AWWARF and AWWA, Denver, Colorado.
- Summers, R.S., S.M. Hooper, G. Solarik, D.M. Owen, and S. Hong. 1995. Bench-Scale Evaluation of GAC for NOM Control. *Jour. AWWA*. (87:8:69).
- Summers, R.S., S. Hong, S.M. Hooper, and G. Solarik. 1994. Adsorption of Natural Organic Matter and Disinfection By-Product Precursors. In *Proc. of the AWWA Annual Conference*, New York, NY.
- Summers, R.S., M.A. Benz, H.M. Shukairy, and L. Cummings. 1993. Effect of Separation Processes on the Formation of Brominated THMs. *Jour. AWWA*. (85:1:88).
- Summers, R.S., L. Cummings, J. DeMarco, D.J. Hartman, D.H. Metz, E. Howe, B. MacLeod, and M. Simpson. 1992. *Standardized Protocol for the Evaluation of GAC*. AWWARF and AWWA, Denver, Colorado.
- USEPA. 1999. *GAC Base Analysis Approach for the ICR Treatment Study Database*.
- USEPA. 1996. *ICR Manual for Bench- and Pilot-Scale Treatment Studies*. EPA 814-B-96-003. Technical Support Division, Office of Ground Water and Drinking Water, Cincinnati, Ohio.
- Westrick, J.J. and J.M. Cohen. 1976. Comparative Effects of Chemical Pretreatment on Carbon Adsorption.

---

**Appendix A: Breakthrough Curves Corrected for Impact of Sampling**

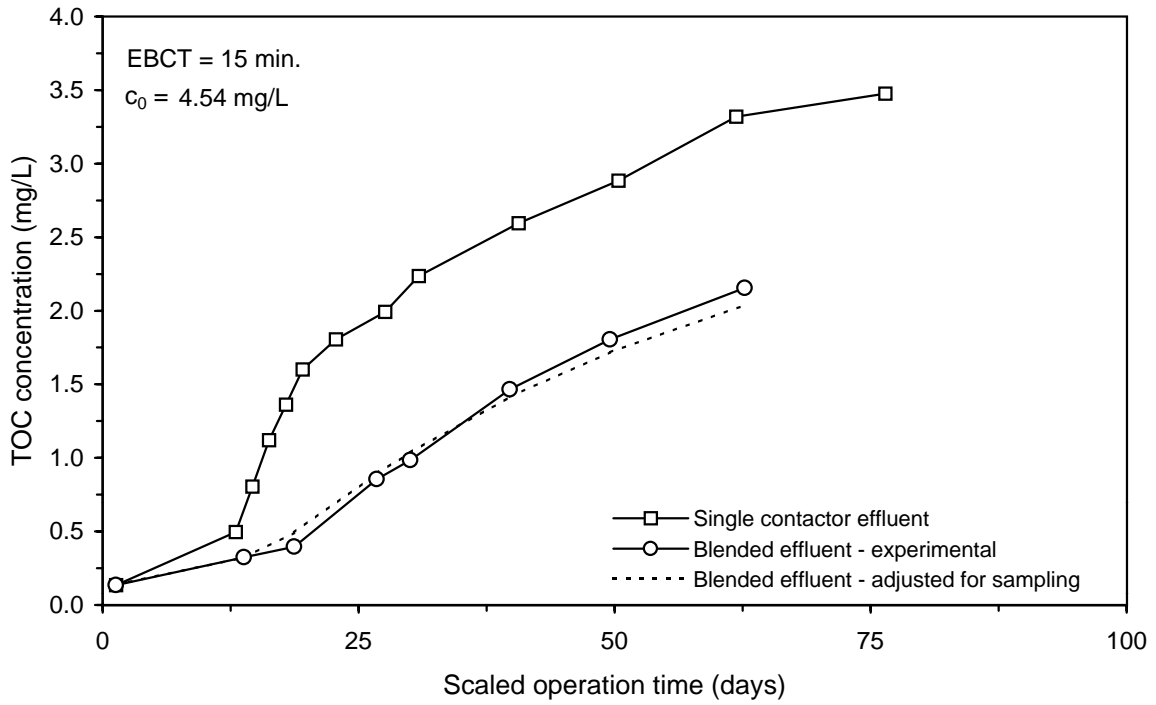


**Figure A-1 Comparison of blended effluent TOC adjusted for experimental sampling to blended effluent experimental results for Water 1**

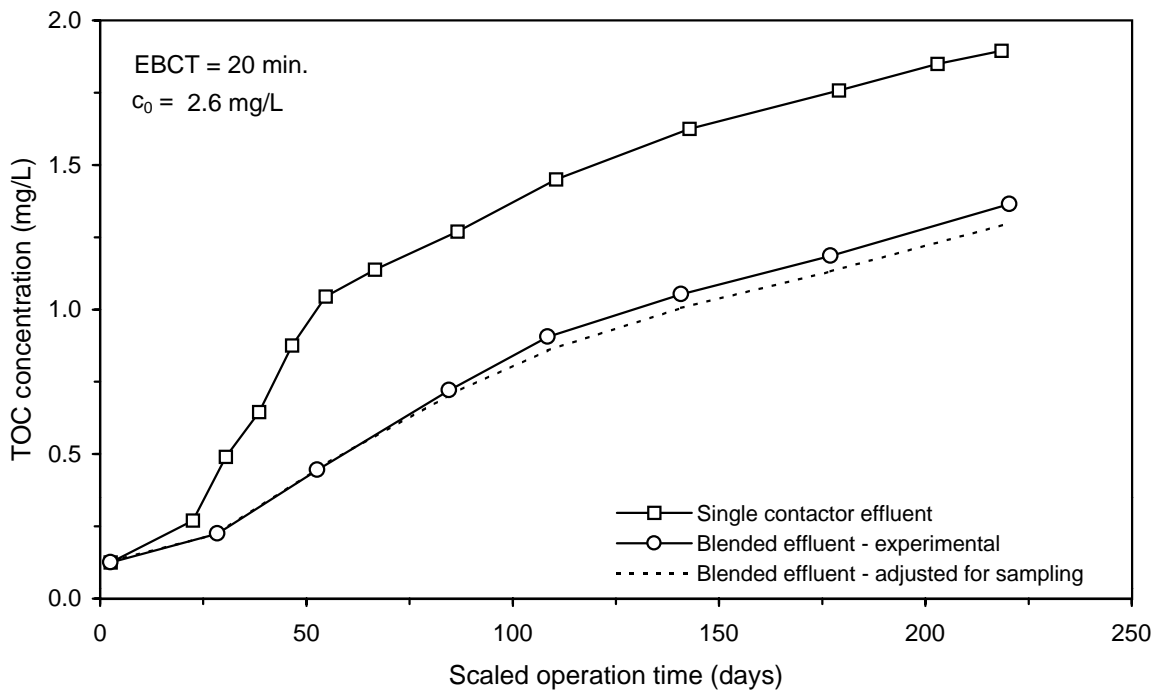


**Figure A-2 Comparison of blended effluent TOC adjusted for experimental sampling to blended effluent experimental results for Water 2**

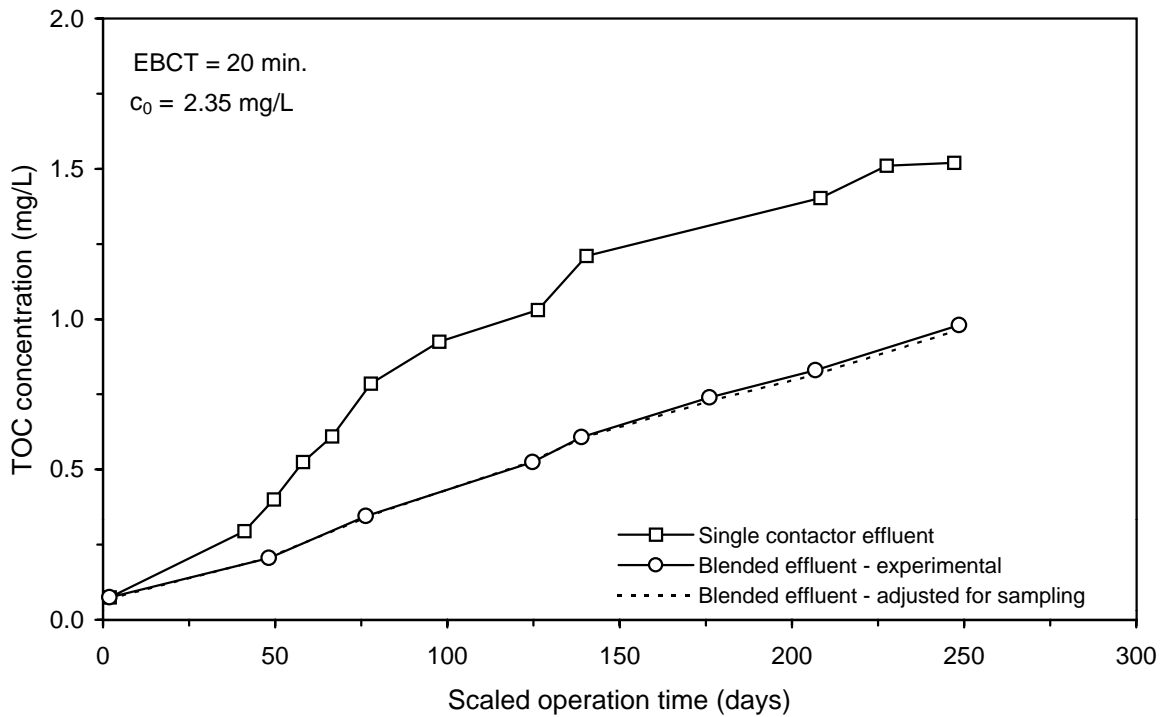


**Figure A-3 Comparison of blended effluent TOC adjusted for experimental sampling to blended effluent experimental results for Water 3**

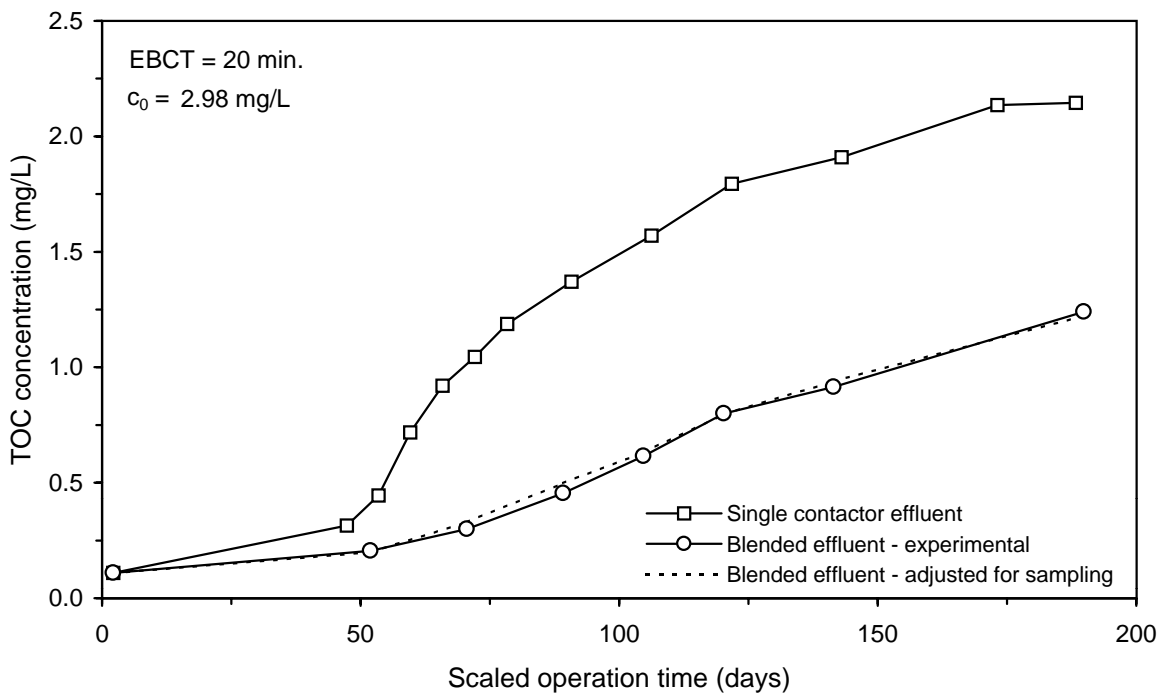


**Figure A-4 Comparison of blended effluent TOC adjusted for experimental sampling to blended effluent experimental results for Water 4**

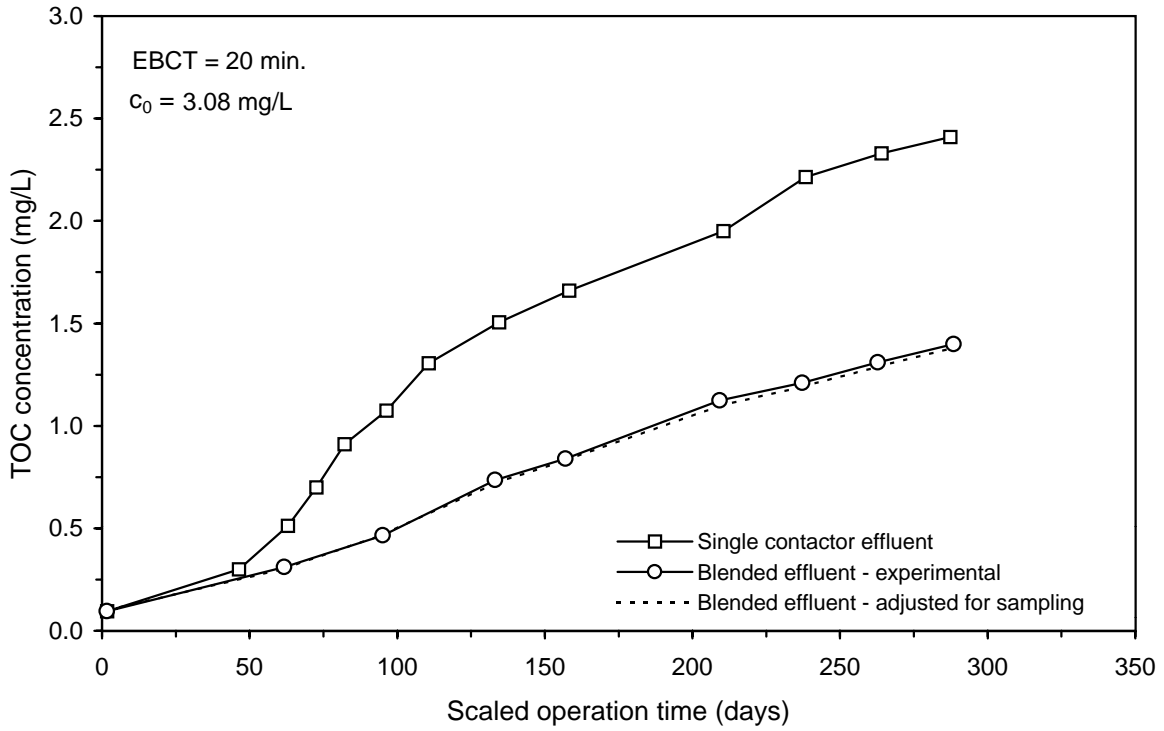


**Figure A-5 Comparison of blended effluent TOC adjusted for experimental sampling to blended effluent experimental results for Water 5**

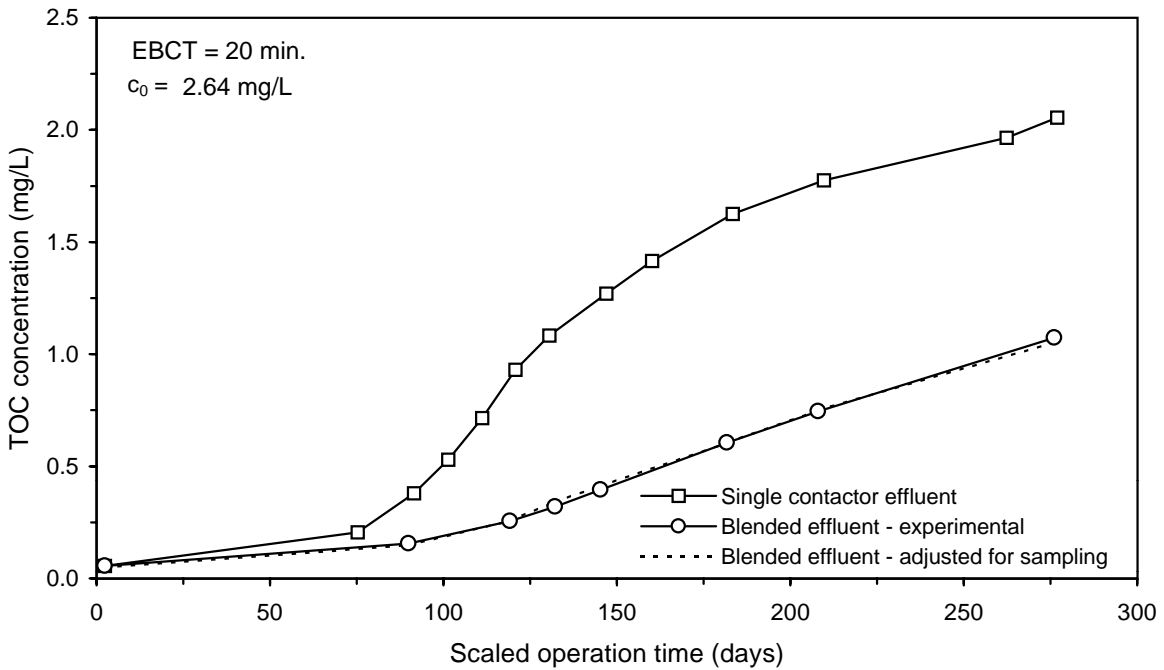


**Figure A-6 Comparison of blended effluent TOC adjusted for experimental sampling to blended effluent experimental results for Water 6**

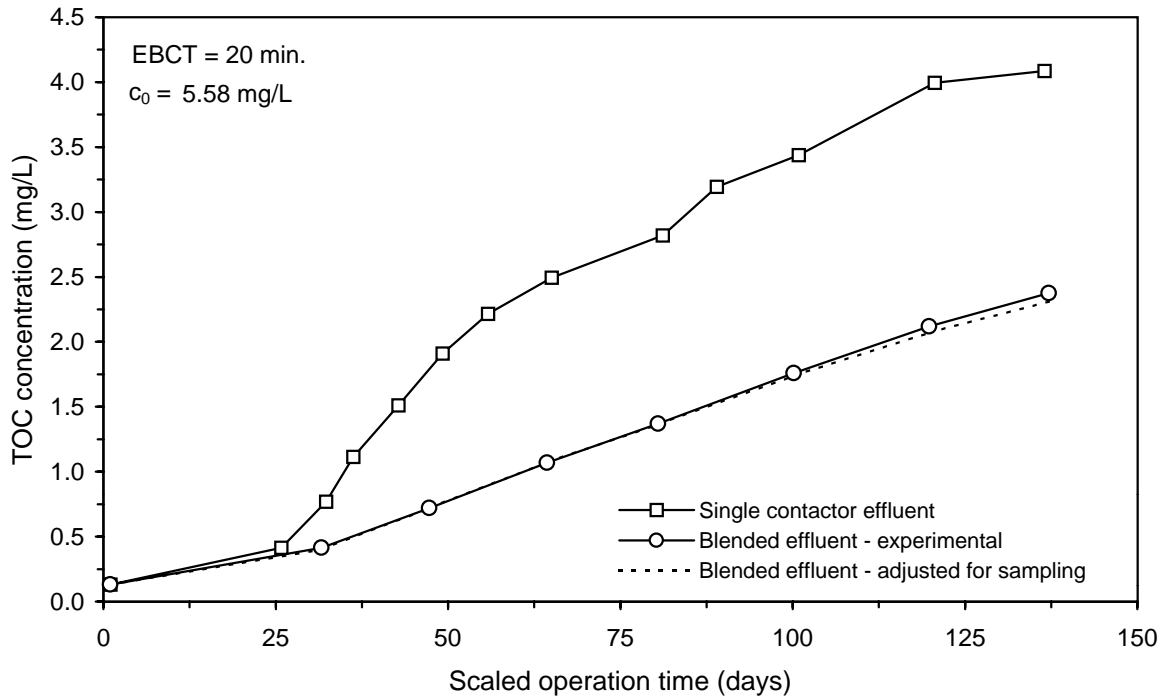


**Figure A-7 Comparison of blended effluent TOC adjusted for experimental sampling to blended effluent experimental results for Water 7**

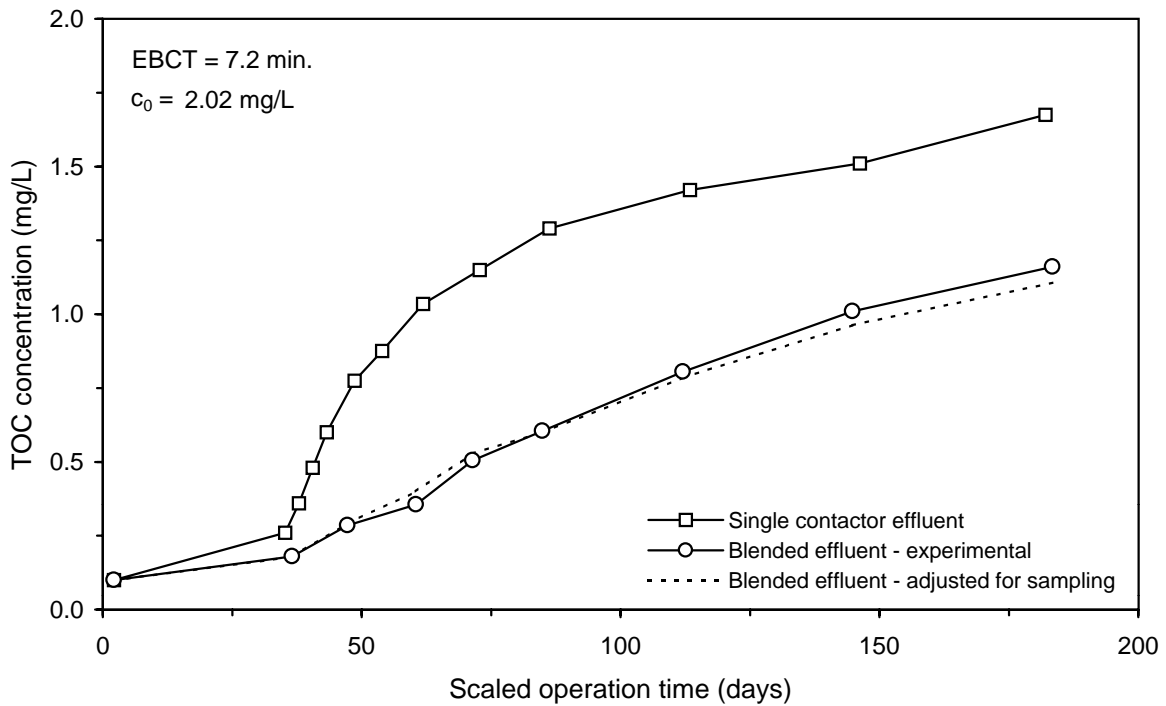


**Figure A-8 Comparison of blended effluent TOC adjusted for experimental sampling to blended effluent experimental results for Water 8**

This page intentionally left blank.

---

## Appendix B: SAS Code

SAS code to fit the step-lag-peak logistic model and perform outlier adjustment.

```
/******  
This program fits data with the following functions:  
  
1. Cs(t) = 0 for t <= t0  
2. Cs(t) = A0+A/(1+B*exp(-D*t)) for t0 < t <= Tmax  
3. Cs(t) = Cmax+S*(t-Tmax) for Tmax < t  
  
where t0 = (1/D)*LN(-A0*B/(A0+A)), Cmax = Cs(Tmax),  
Tmax is the runtime at which effluent reaches its maximum.  
Bounds: -Cmax/2 <= A0 <= Cmax/2, 0 < A <= 1.5*Cmax, 0<B, 0<D, S <= 0  
  
Input parameters:  
RawData - the input data set name, the data set contains  
the x variable time (ordered and no duplicates)  
and the y variable analyte (concentration).  
BasInfo - the input data set name, the data set contains  
Tmax and Cmax used to set bounds and the initial value  
Analyte - the y variable name of the NLIN regression  
PlotData- name of the data set containing data for curve fit plot  
FitInfo - name of the output data set containing curve fit information  
;  
*****/  
  
%macro FitF012(RawData=, BasInfo=, Analyte=, FitInfo=);  
data _null_; set &BasInfo;  
if analyte="&Analyte";  
Cmax05 = Cmax/2;  
Cmax15 = Cmax*1.5;  
call symput('xCmax', Cmax);  
call symput('xCmax05', Cmax05);  
call symput('xCmax15', Cmax15);  
call symput('xTmax', Tmax);  
run;  
  
PROC NLIN DATA=&RawData NOPRINT;  
parms A0=0 A=&xCmax B=10 to 50 by 10 D=0.05 to 0.15 by 0.02 S=0;  
bounds -&xCmax05 <= A0 <= &xCmax05, 0< A <= &xCmax15, 0<B, 0<D, S<=0;  
if A0<-A/(1+B) then  
t0=log(-A0*B/(A0+A))/D;  
else t0=0;  
if time < t0 then do;  
dA0= A/(D*A0*(A0+A));  
dA =-1/D/(A0+A);  
dB = 1/(B*D);  
dD =-t0/D;  
  
BEXP =B*exp(-D*t0);  
BEXP2=(1+BEXP)**2;  
model &Analyte = A0+A/(1+BEXP);  
der.A0= 1+A*BEXP*D*dA0/BEXP2;
```

```

    der.A = (1+BEXP+A*BEXP*D*dA)/BEXP2;
    der.B = -A*BEXP*(1/B-D*dB)/BEXP2;
    der.D = A*BEXP*(t0+D*dD)/BEXP2;
    end;
else if time < &xTmax then do;
    BEXP = B*exp(-D*time);
    model &Analyte = A0+A/(1+BEXP);
    der.A0= 1;
    der.A = 1/(1+BEXP);
    der.B = -A*BEXP/(B*(1+BEXP)**2);
    der.D = A*BEXP*time/(1+BEXP)**2;
    end;
else do;
    BEXPmax = B*exp(-D*&xTmax);
    model &Analyte = A0+A/(1+BEXPmax)+S*(time-&xTmax);
    der.A0= 1;
    der.A = 1/(1+BEXPmax);
    der.B = -A*BEXPmax/(B*(1+BEXPmax)**2);
    der.D = A*BEXPmax*time/(1+BEXPmax)**2;
    der.S = time-&xTmax;
    end;
    output out=outp p=pred u95=u95 l95=l95;
*proc print;
data outp; set outp;
    winsor=&Analyte;
    delta=(u95-l95)/3;
    low=0;
    high=0;
    if &Analyte ne . and &Analyte<pred-delta then do;
        outlier=&Analyte; winsor=pred-delta; low=1; end;
    if &Analyte ne . and &Analyte>pred+delta then do;
        outlier=&Analyte; winsor=pred+delta; high=1; end;
    keep time &Analyte winsor outlier low high;
proc means data=outp noprint;
    var low high;
    output out=outout sum=outlow outhigh;
data outout; set outout;
    keep outlow outhigh;
*proc print;

PROC NLIN DATA=outp outest=outest NOPRINT;
    parms A0=0 A=&xCmax B=10 to 50 by 10 D=0.05 to 0.15 by 0.02 S=0;
    bounds -&xCmax05 <= A0 <= &xCmax05, 0 < A <= &xCmax15, 0 < B, 0 < D, S <= 0;
    if A0 < -A/(1+B) then
        t0=log(-A0*B/(A0+A))/D;
    else t0=0;
    if time < t0 then do;
        dA0= A/(D*A0*(A0+A));
        dA = -1/D/(A0+A);
        dB = 1/(B*D);
        dD = -t0/D;

        BEXP =B*exp(-D*t0);
        BEXP2=(1+BEXP)**2;
        model &Analyte = A0+A/(1+BEXP);
        der.A0= 1+A*BEXP*D*dA0/BEXP2;
        der.A = (1+BEXP+A*BEXP*D*dA)/BEXP2;

```

```

    der.B = -A*BEXP*(1/B-D*dB)/BEXP2;
    der.D = A*BEXP*(t0+D*dD)/BEXP2;
    end;
else if time < &xTmax then do;
    BEXP = B*exp(-D*time);
    model &Analyte = A0+A/(1+BEXP);
    der.A0= 1;
    der.A = 1/(1+BEXP);
    der.B = -A*BEXP/(B*(1+BEXP)**2);
    der.D = A*BEXP*time/(1+BEXP)**2;
    end;
else do;
    BEXPmax = B*exp(-D*&xTmax);
    model &Analyte = A0+A/(1+BEXPmax)+S*(time-&xTmax);
    der.A0= 1;
    der.A = 1/(1+BEXPmax);
    der.B = -A*BEXPmax/(B*(1+BEXPmax)**2);
    der.D = A*BEXPmax*time/(1+BEXPmax)**2;
    der.S = time-&xTmax;
    end;
output out=outq p=pred r=redis u95m=u95m l95m=l95m;

*proc print data=outest;
proc reg data=outq outest=r2 adjrsq noprint;
    model winsor = pred / noint;
data r2; set r2;
    keep _rsq_ _adjrsq_;

data outq; set outq;
    keep time pred redis l95m u95m;
data &Analyte; merge outp outq; by time;
    if &Analyte=. then missing=pred;
    if outlier=. then winsor=.;
    if l95m<0 then l95m=0;
RUN;

data std; set outest;
    if _type_='COVB';
    retain std_a0 std_a std_b std_d std_s;
    if _name_='A0' then std_a0=sqrt(a0);
    if _name_='A' then std_a=sqrt(a);
    if _name_='B' then std_b=sqrt(b);
    if _name_='D' then std_d=sqrt(d);
    if _name_='S' then std_s=sqrt(s);
    if _name_='S';
    keep std_a0 std_a std_b std_d std_s;

data estimate; set outest;
    if _type_='ITER' or _type_='FINAL';
proc sort data=estimate; by _type_;
data estimate; set estimate; by _type_;
    if last._type_;
proc means data=estimate noprint;
    var _iter_ _sse_ a0 a b d s;
    output out=outest mean=iter sse a0 a b d s;

data &FitInfo; merge outest std r2 outout;

```

```

analyte("&Analyte");
if _freq_=1 then converge='NO ';
            else converge='YES';
if std_a0=0 or std_a=0 or std_b=0 or std_d=0 or std_s=0 then
singular='YES';
                                else singular='NO ';
if A0+A/(1+B) >= 0 then t0=0; else t0=(1/D)*log(-A0*B/(A0+A));
keep analyte a0 a b d s t0 std_a0 std_a std_b std_d std_s
    _rsq_ converge singular outlow outhigh;
run;
%mend;

/*
%FitF012(RawData=Raw, BasInfo=BasInfo, Analyte=BDCM, FitInfo=FitInfo);
proc print data=FitInfo;
run;
*/

```

---

## Appendix C: Full- and Bench-Scale Pretreatment Schematics

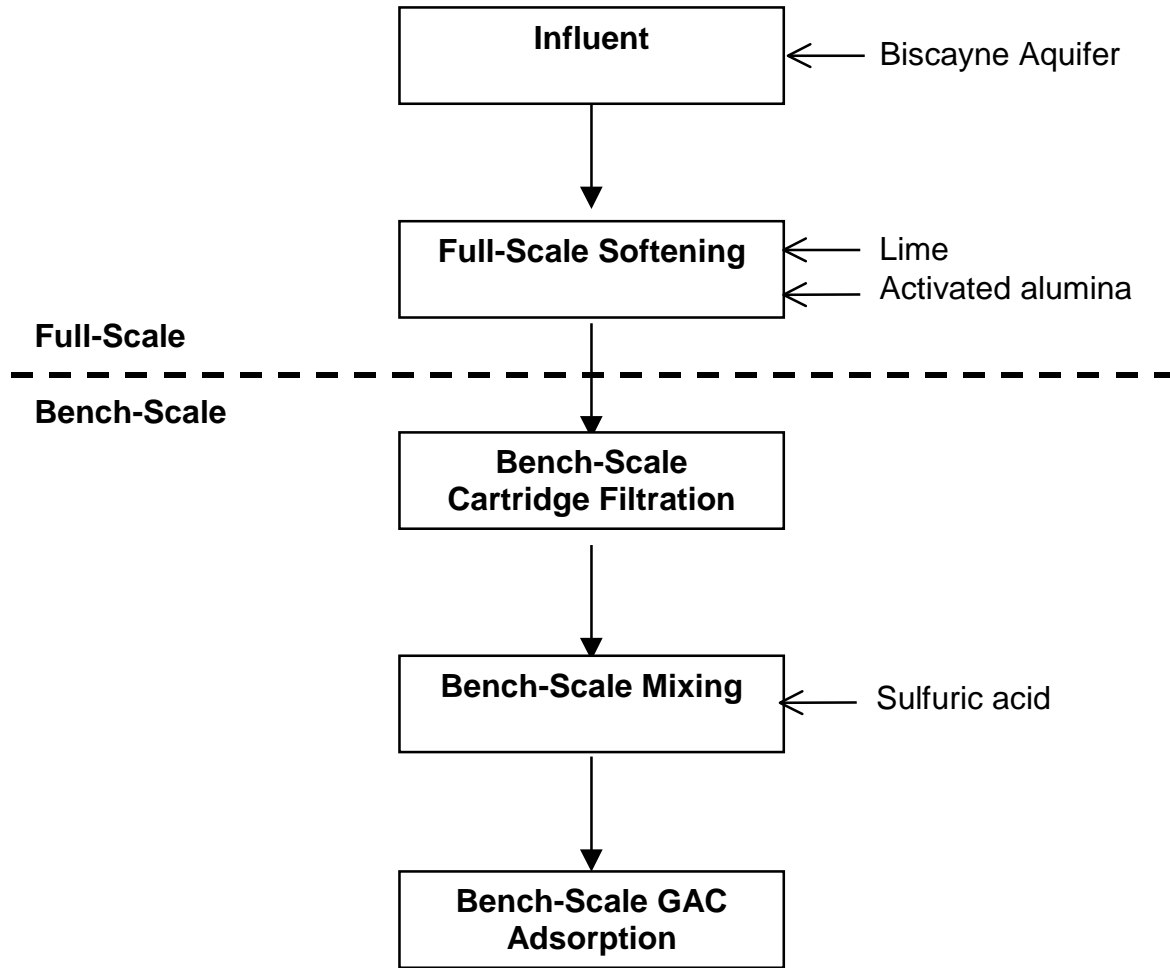


Figure C-1 Full- and bench-scale pretreatment schematic for Water 1

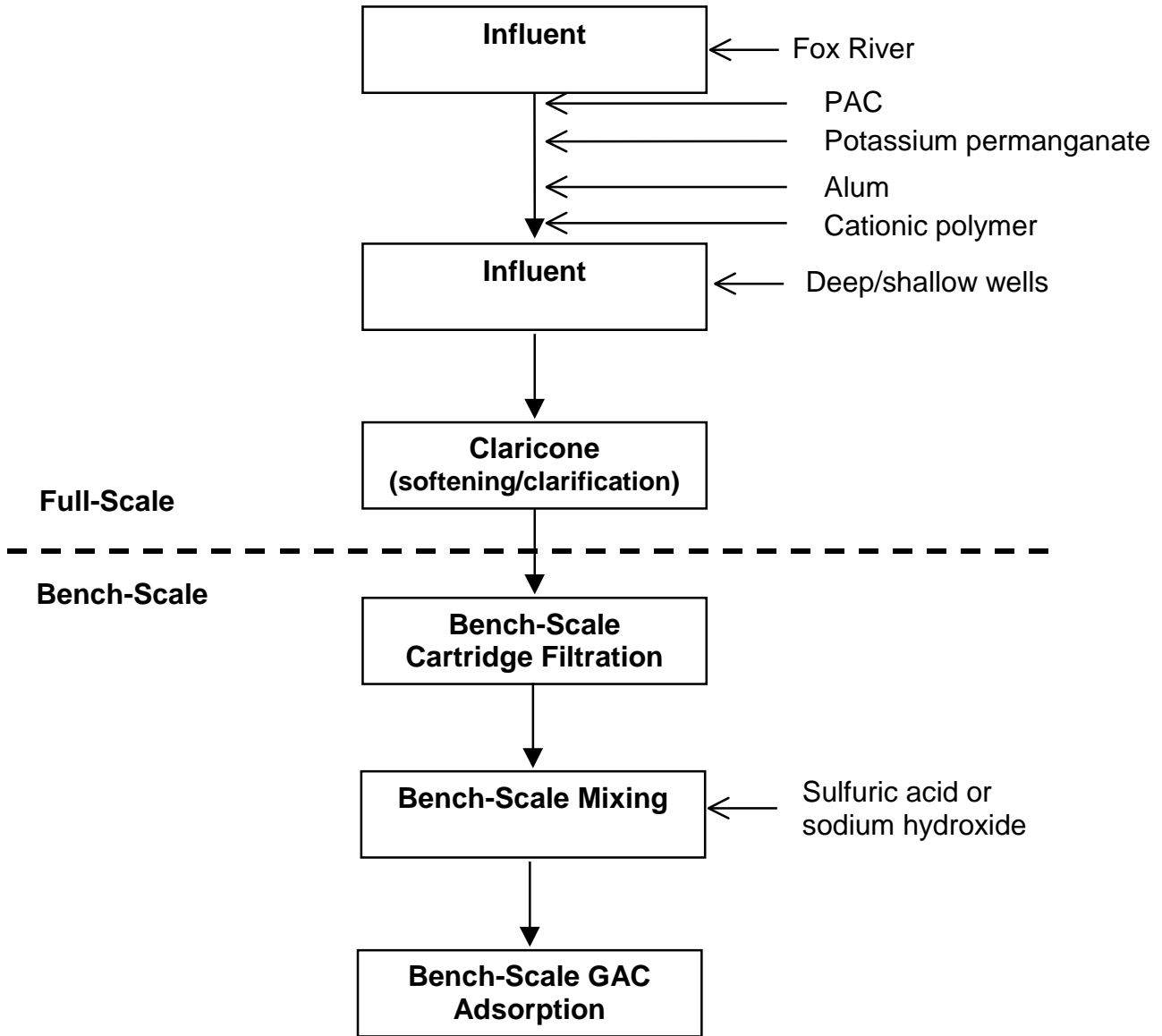


Figure C-2 Full- and bench-scale pretreatment schematic for Water 2

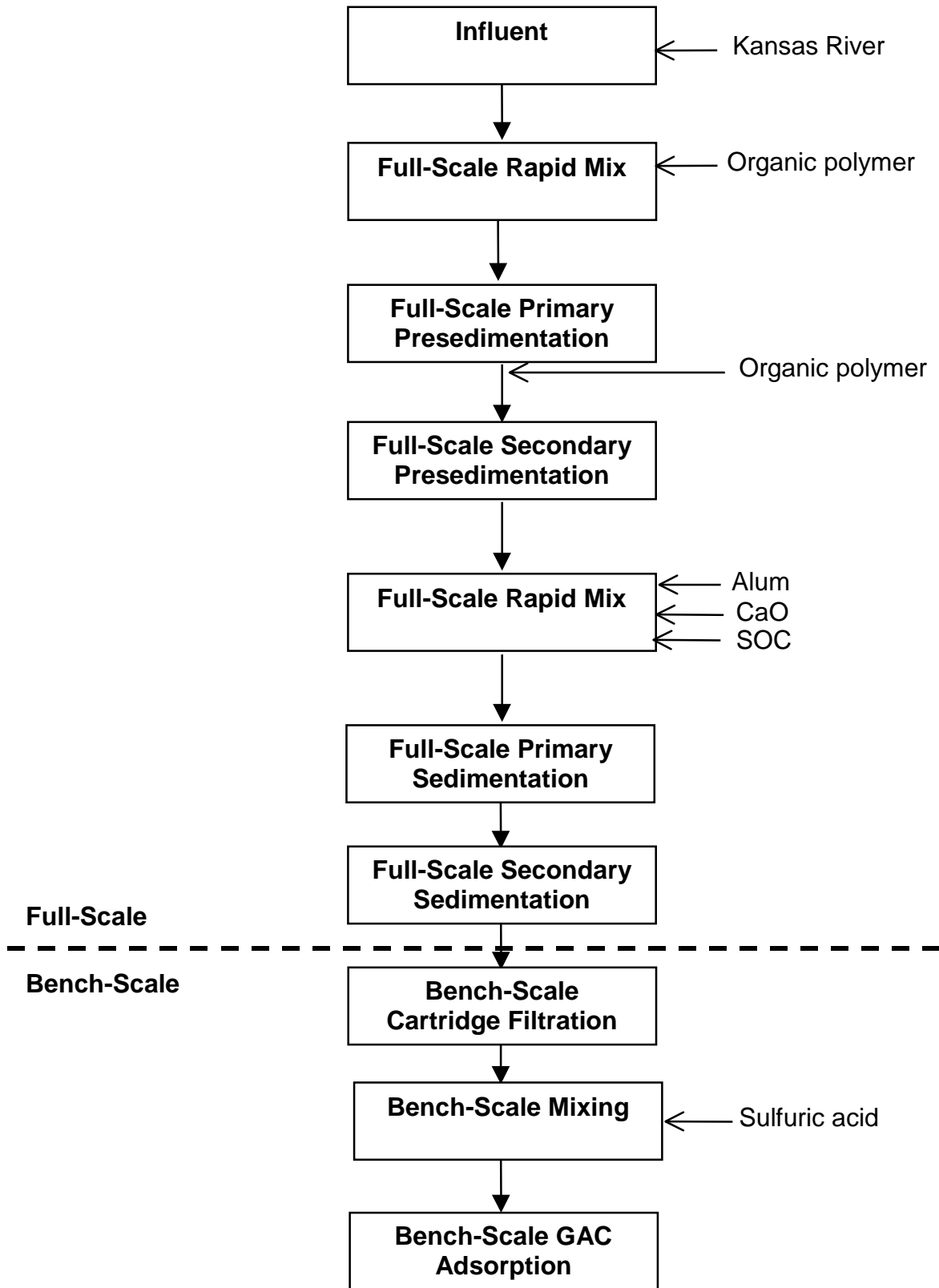


Figure C-3 Full- and bench-scale pretreatment schematic for Water 3

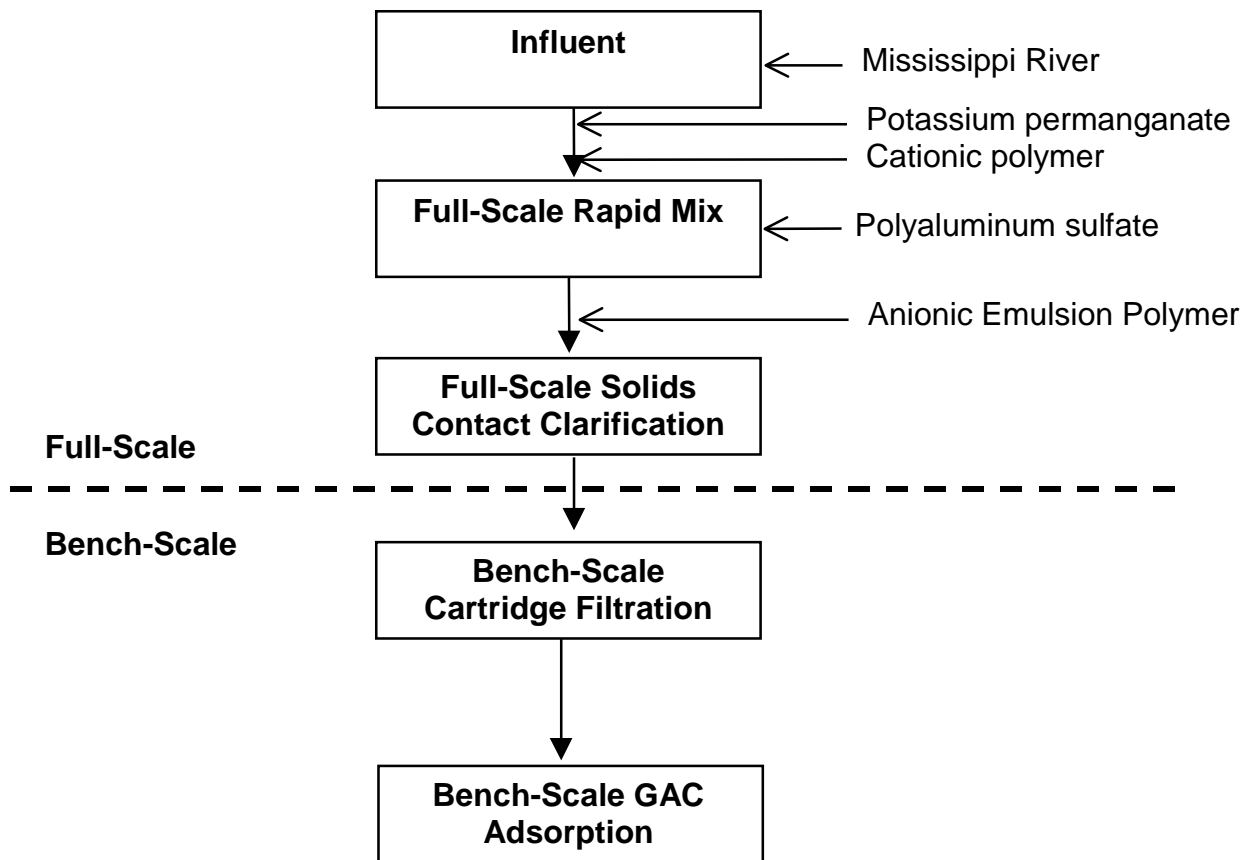


Figure C-4 Full- and bench-scale pretreatment schematic for Water 4

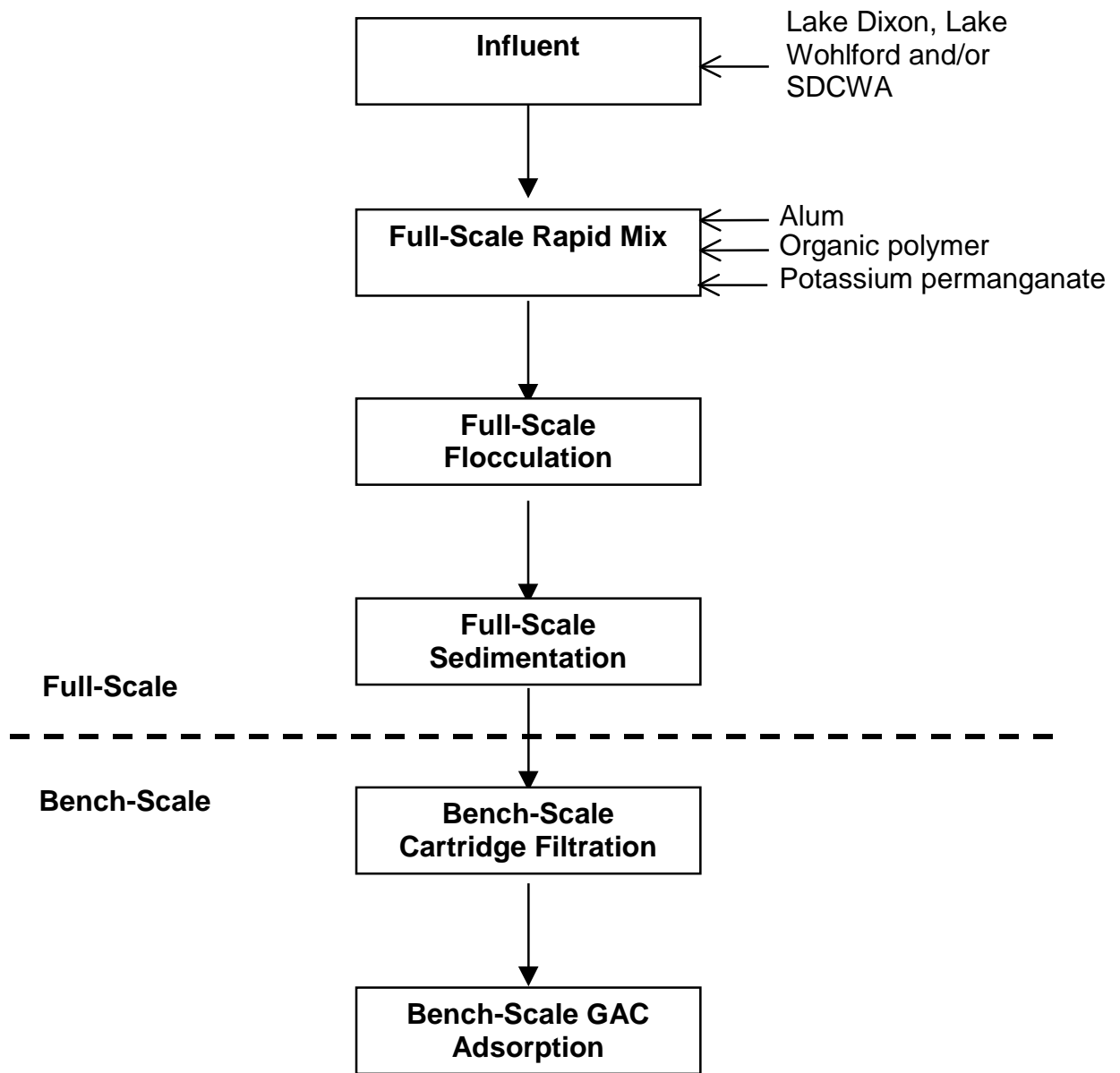


Figure C-5 Full- and bench-scale pretreatment schematic for Water 5

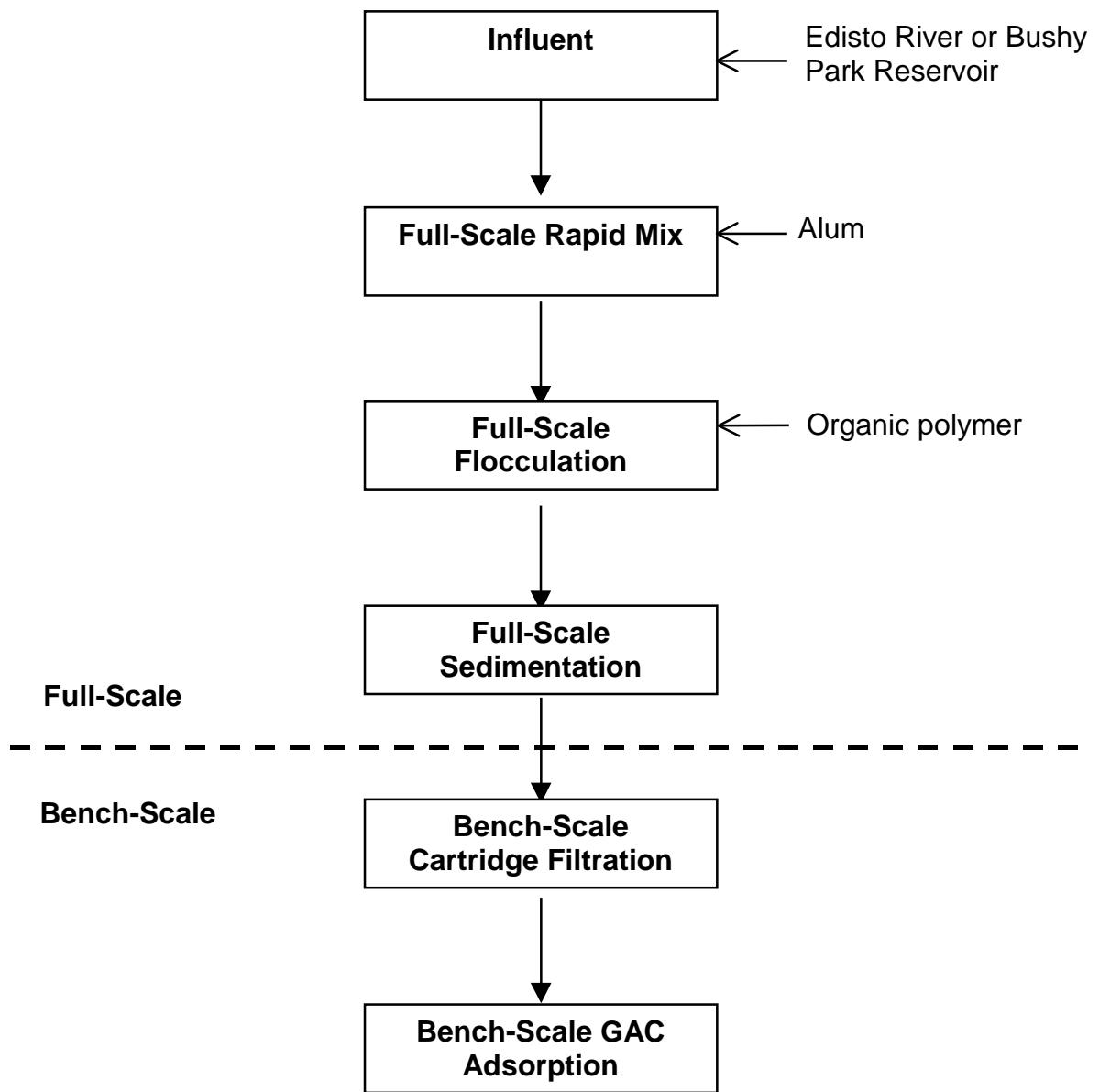


Figure C-6 Full- and bench-scale pretreatment schematic for Water 6

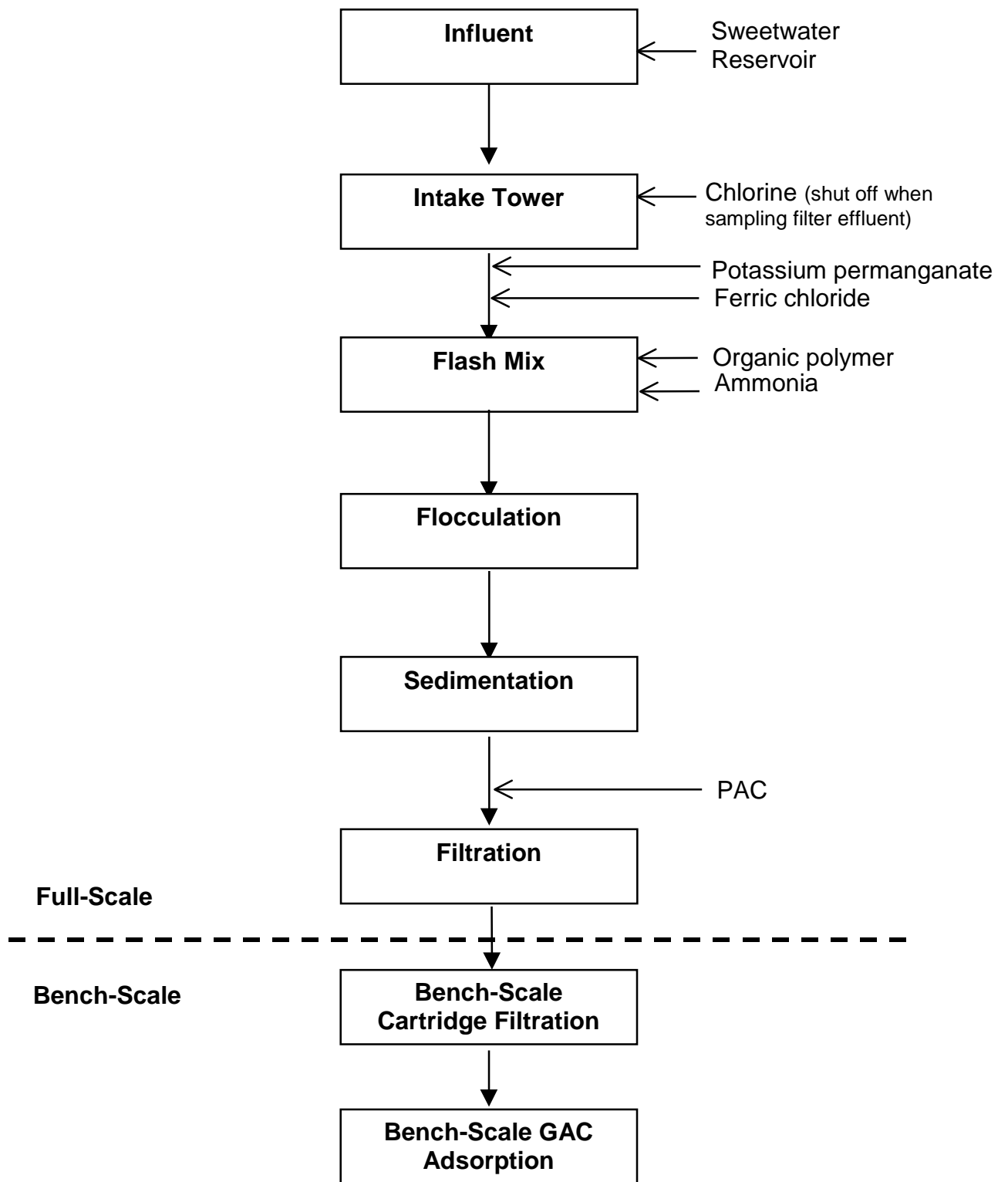


Figure C-7 Full- and bench-scale pretreatment schematic for Water 7

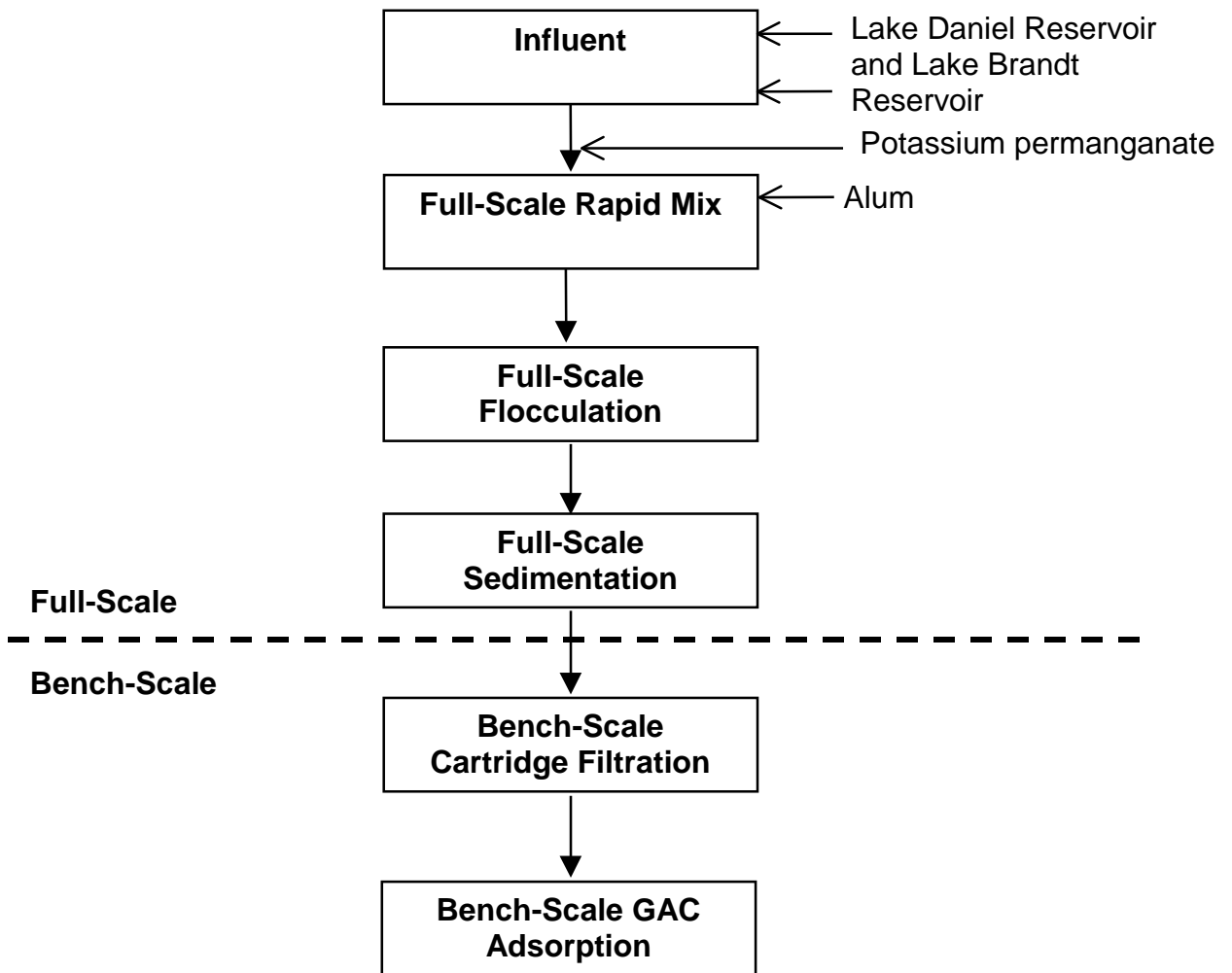


Figure C-8 Full- and bench-scale pretreatment schematic for Water 8

This page intentionally left blank.

---

**Appendix D: Single Contactor and Blended Effluent DBP Surrogate  
and Formed DBP Correlations**

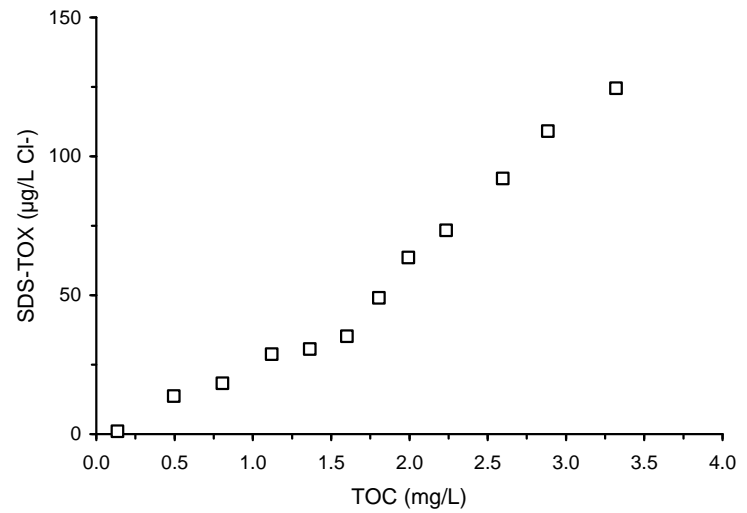
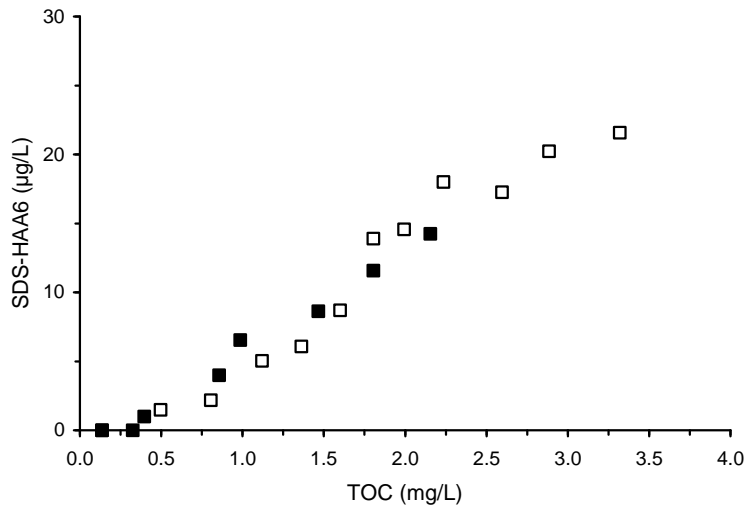
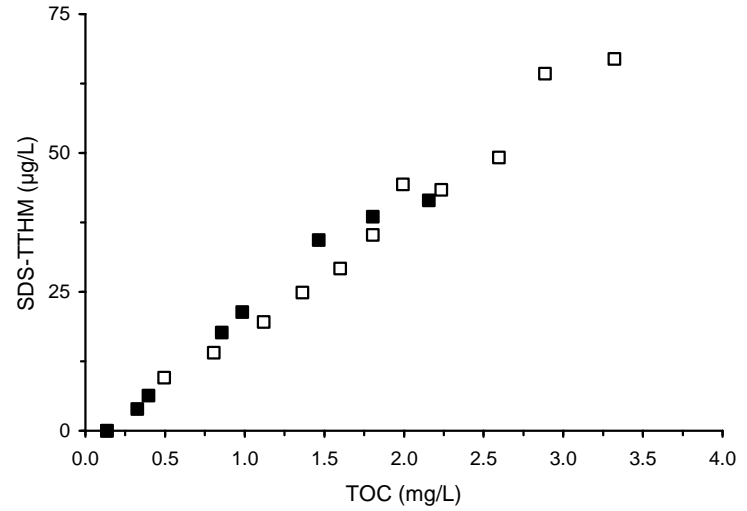
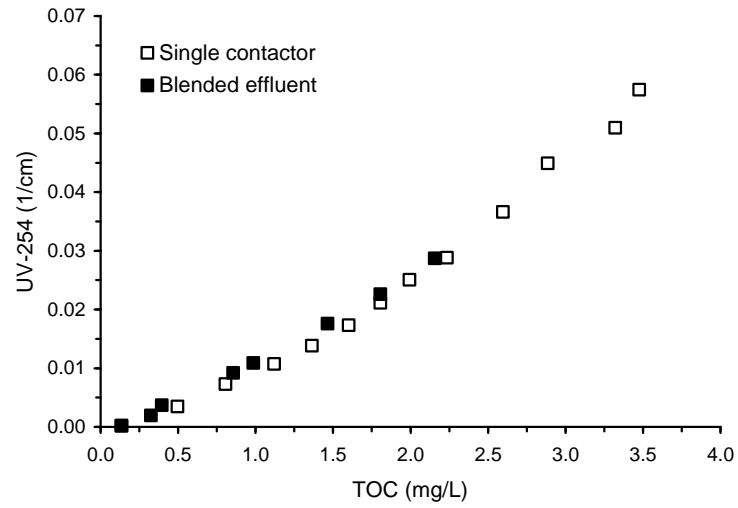


Figure D-1 Correlations based on GAC effluent TOC concentration for single contactor and blended effluents for Water 1

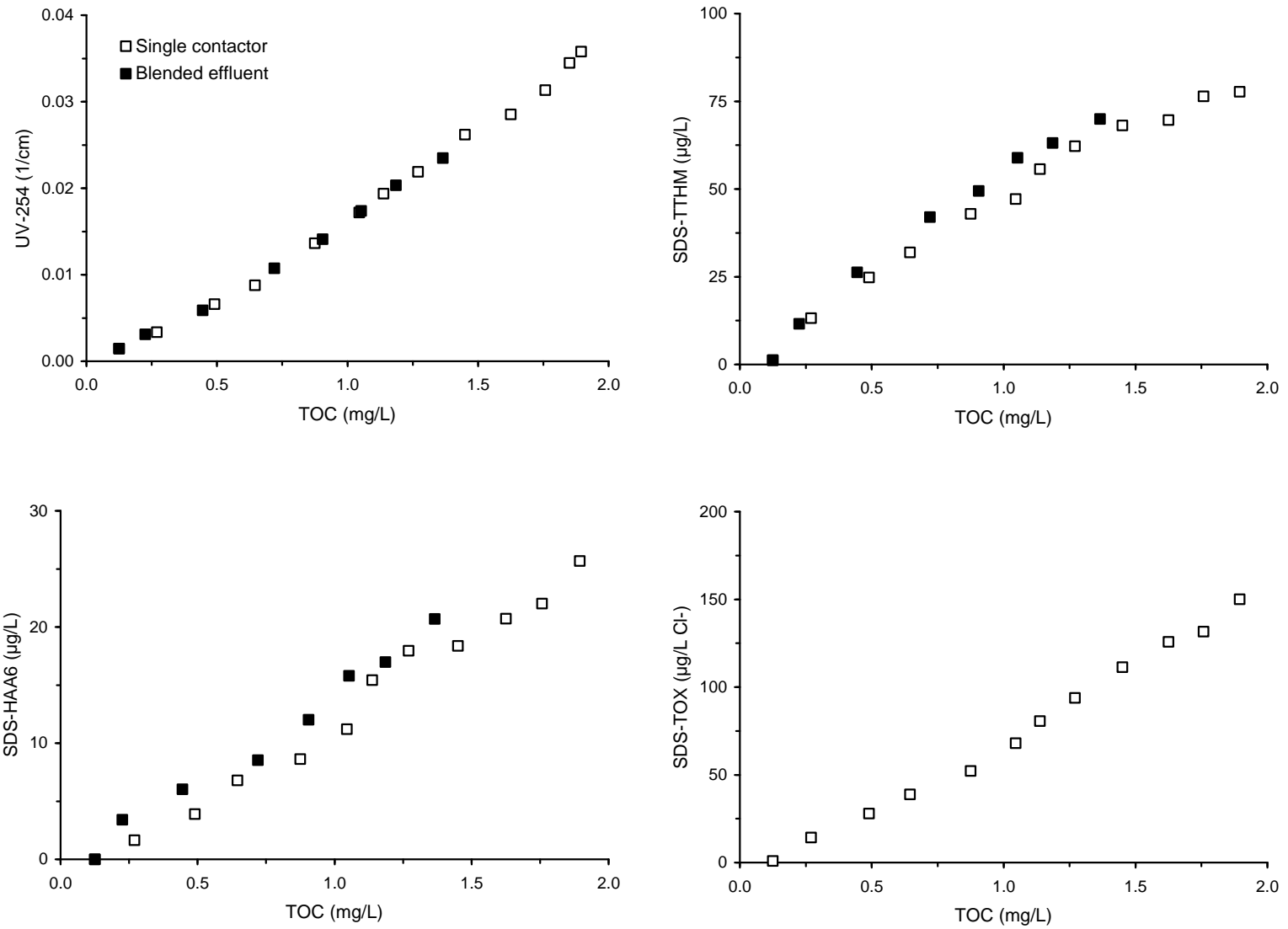


Figure D-2 Correlations based on GAC effluent TOC concentration for single contactor and blended effluents for Water 2

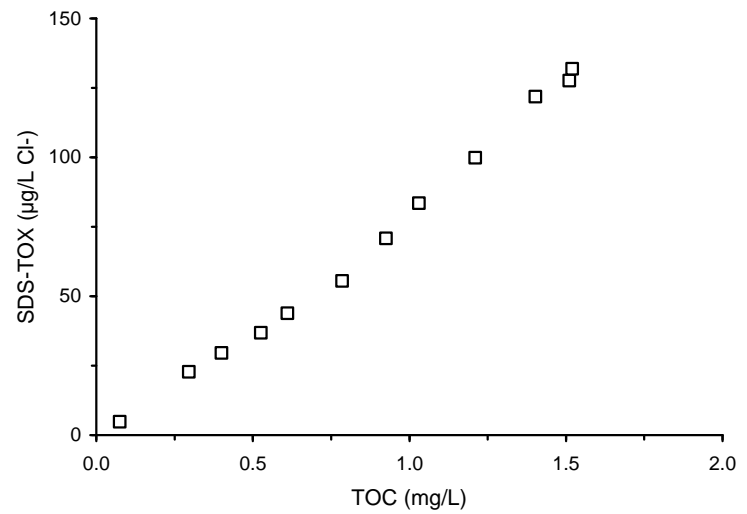
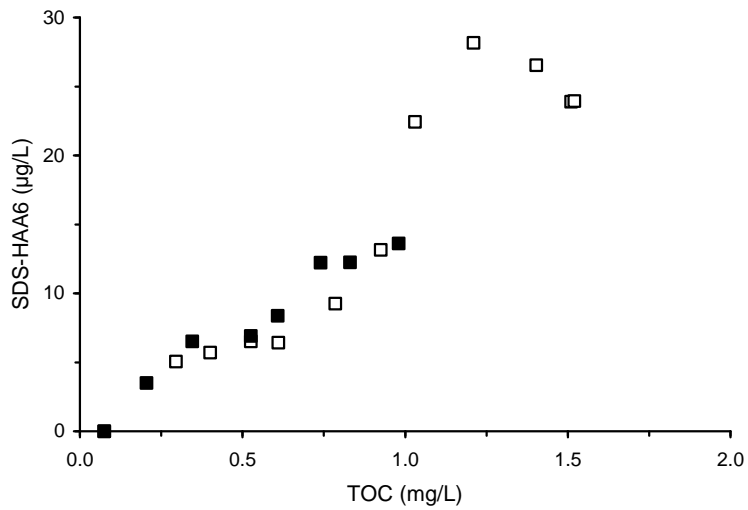
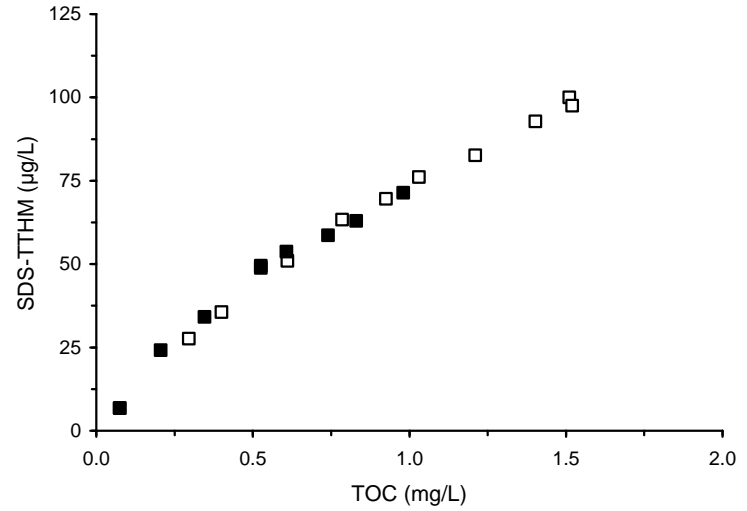
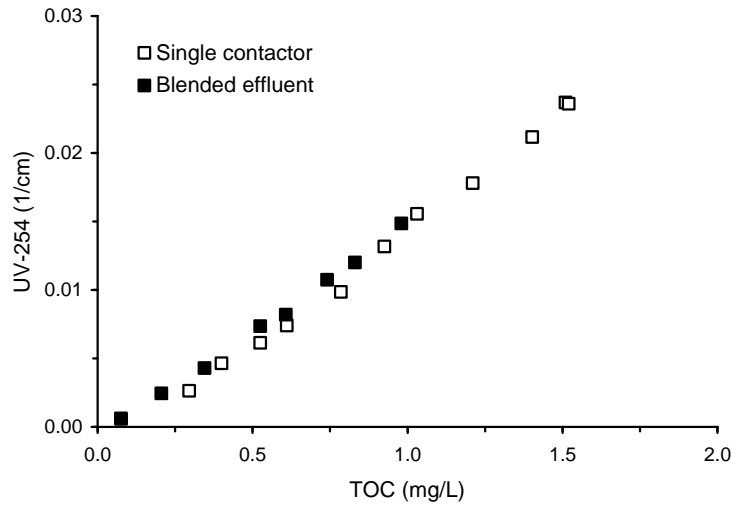


Figure D-3 Correlations based on GAC effluent TOC concentration for single contactor and blended effluents for Water 3

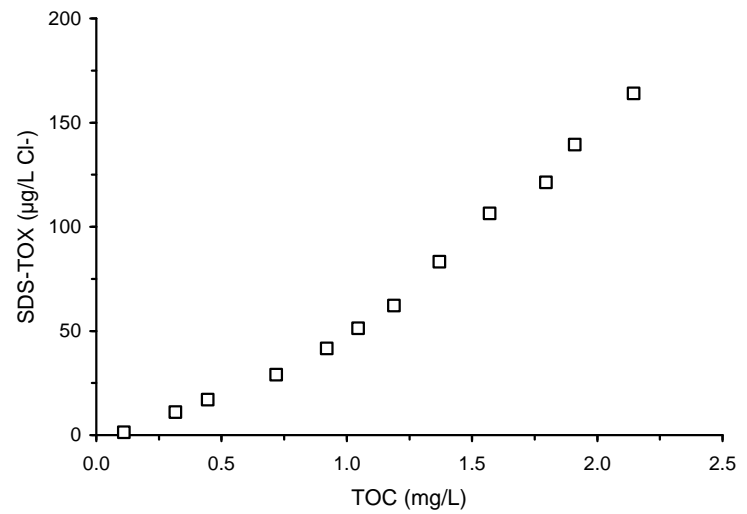
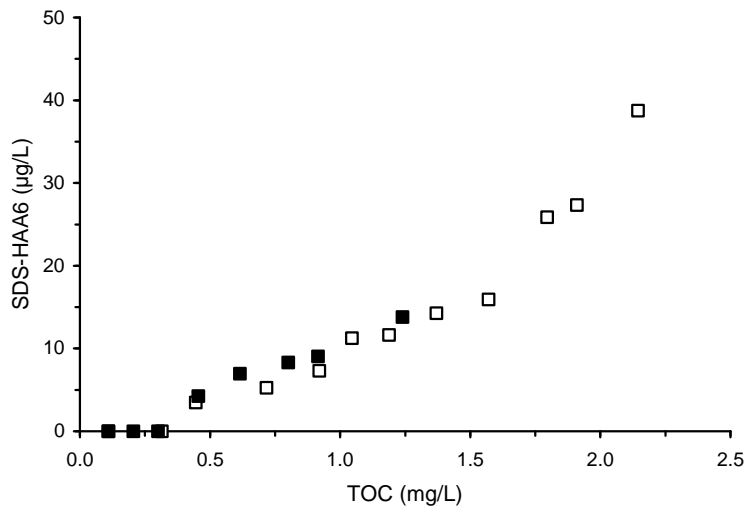
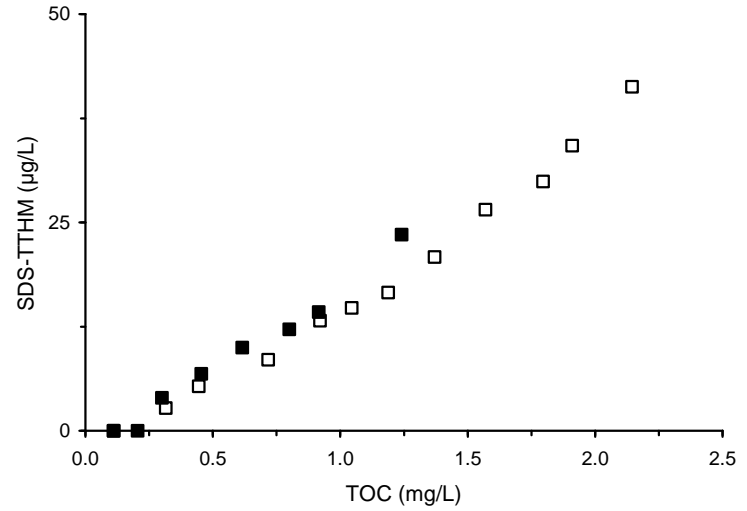
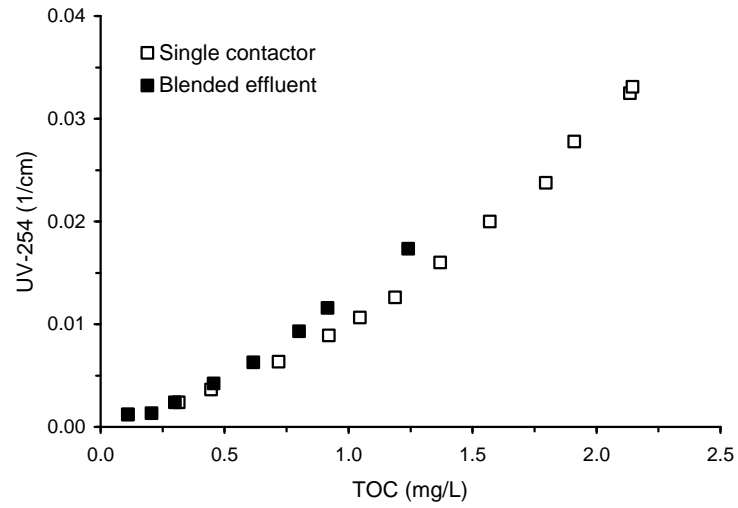


Figure D-4 Correlations based on GAC effluent TOC concentration for single contactor and blended effluents for Water 4

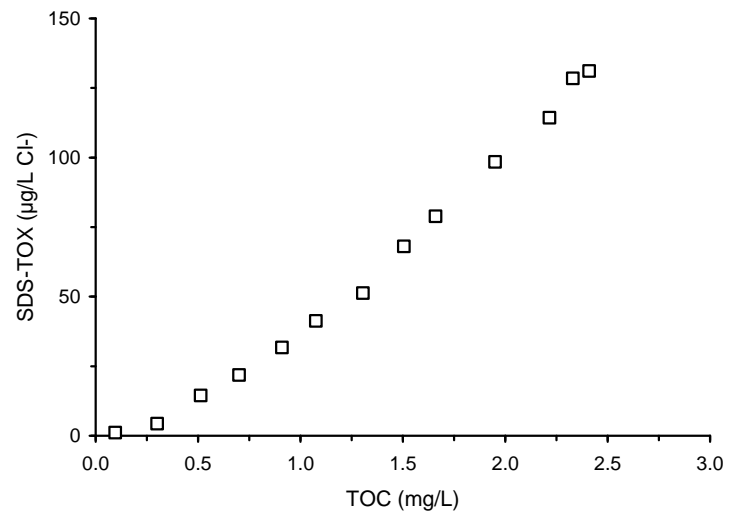
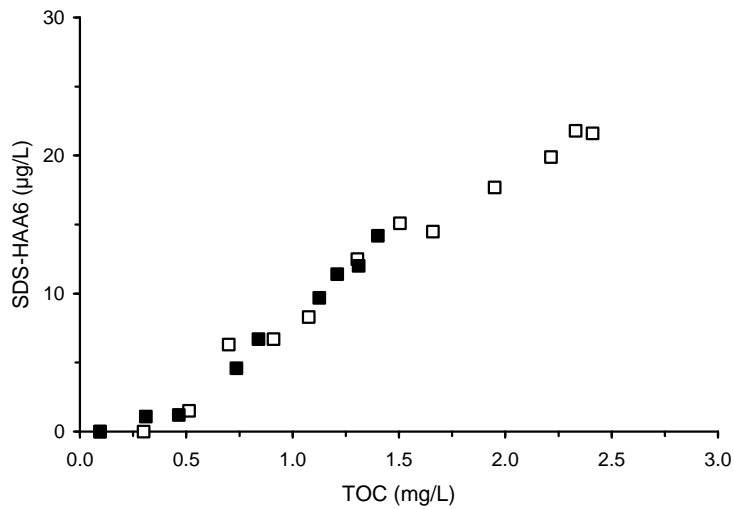
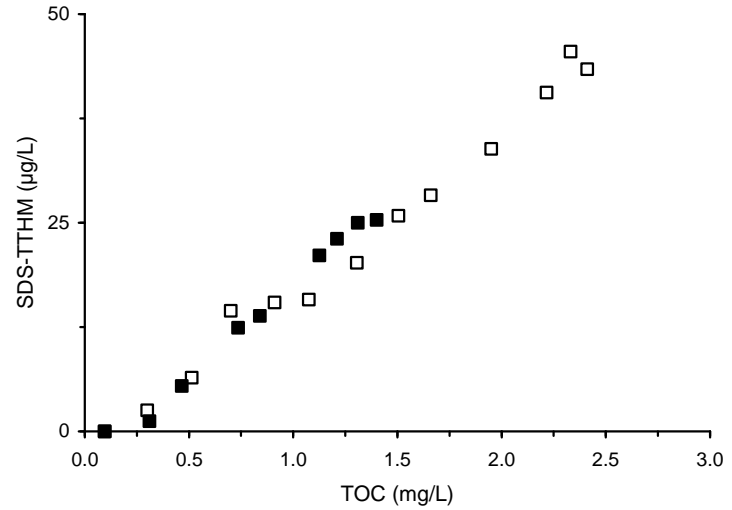
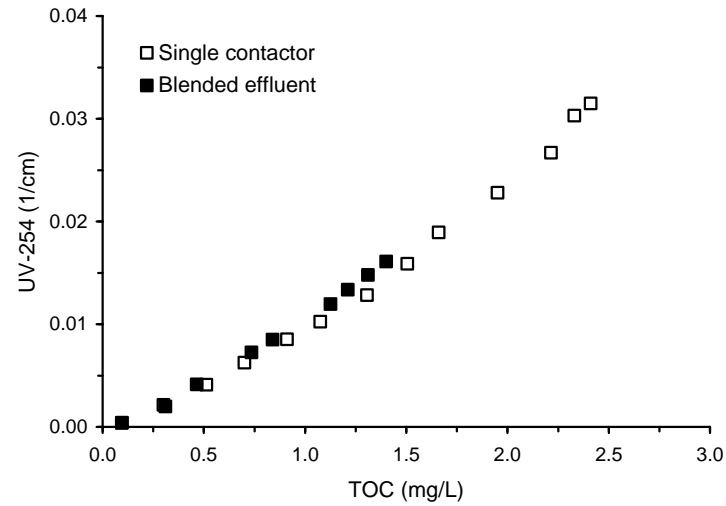


Figure D-5 Correlations based on GAC effluent TOC concentration for single contactor and blended effluents for Water 5

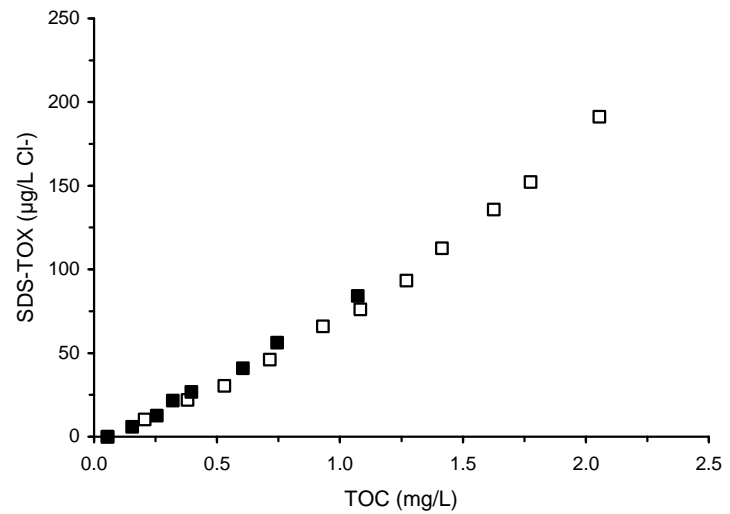
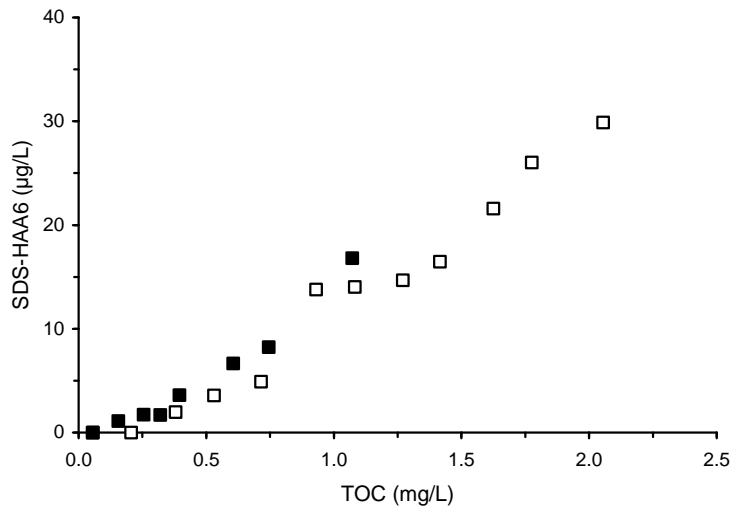
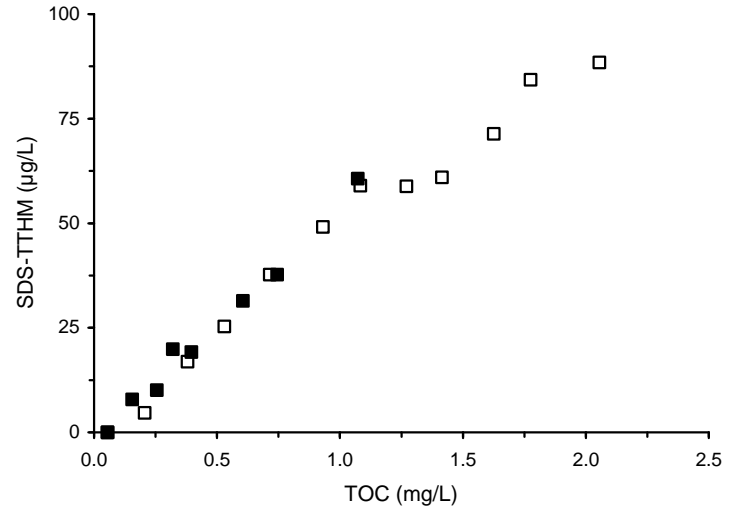
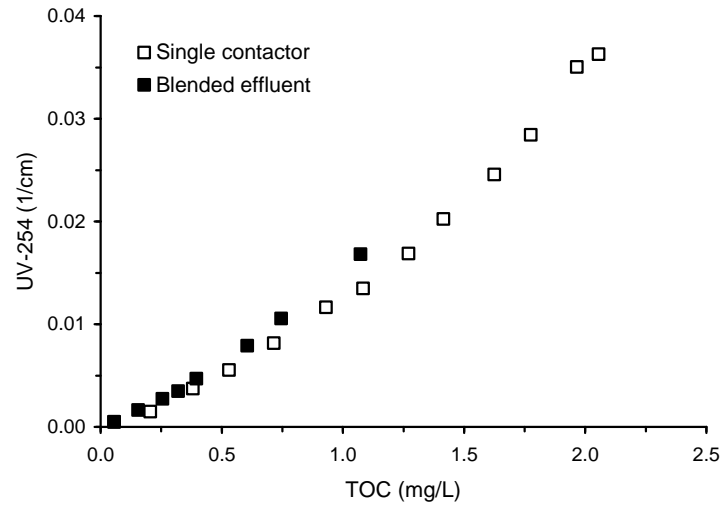


Figure D-6 Correlations based on GAC effluent TOC concentration for single contactor and blended effluents for Water 6

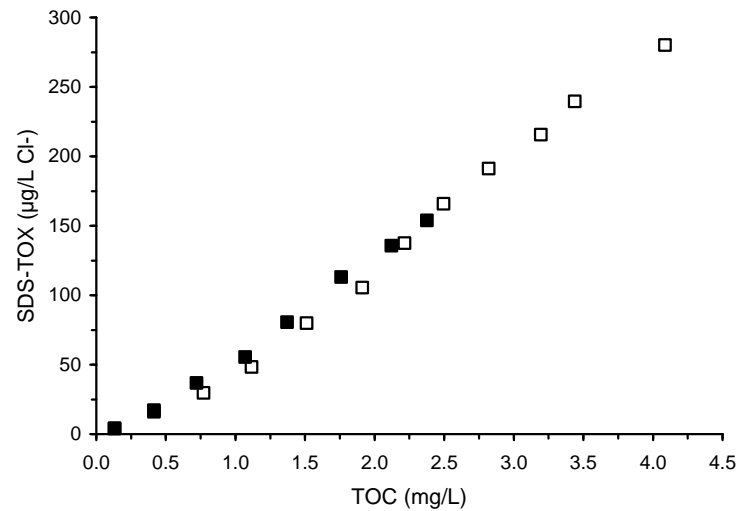
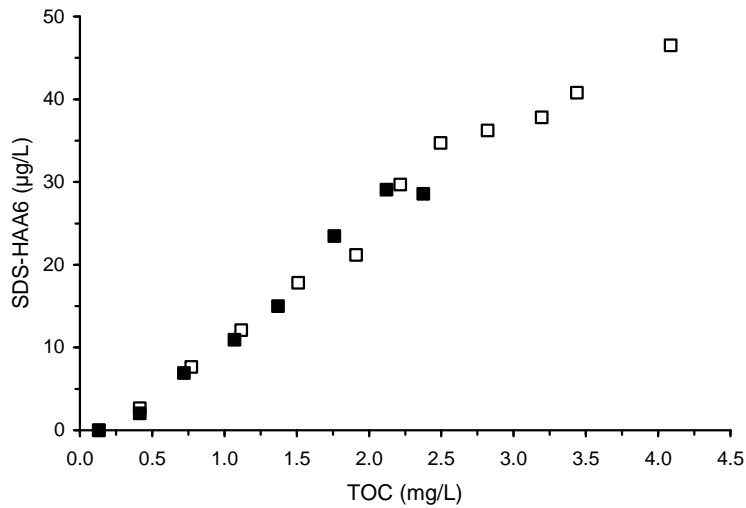
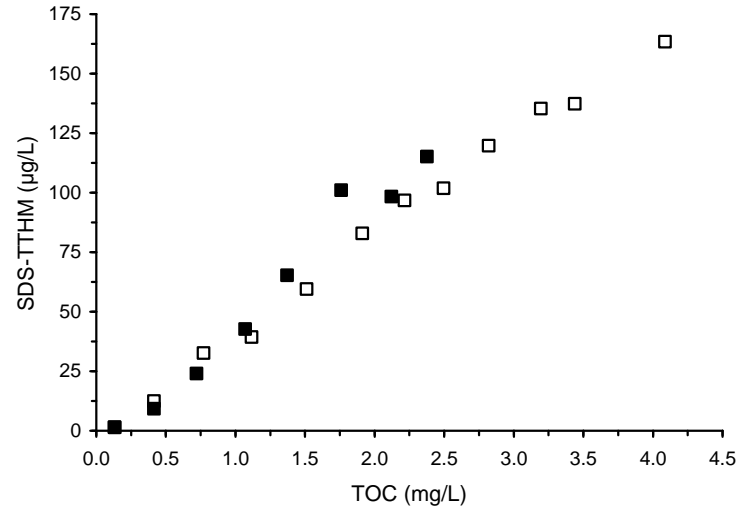
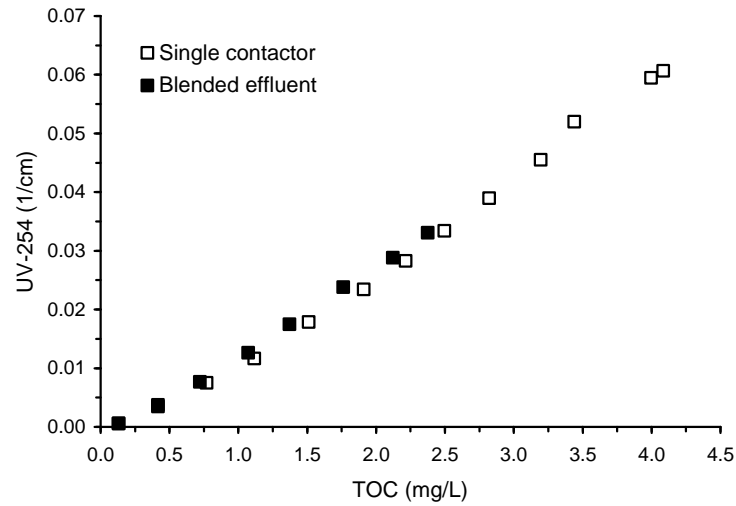


Figure D-7 Correlations based on GAC effluent TOC concentration for single contactor and blended effluents for Water 7

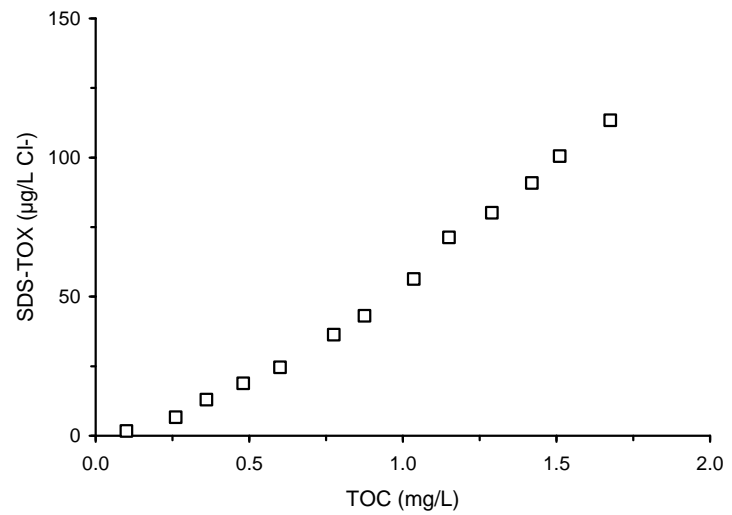
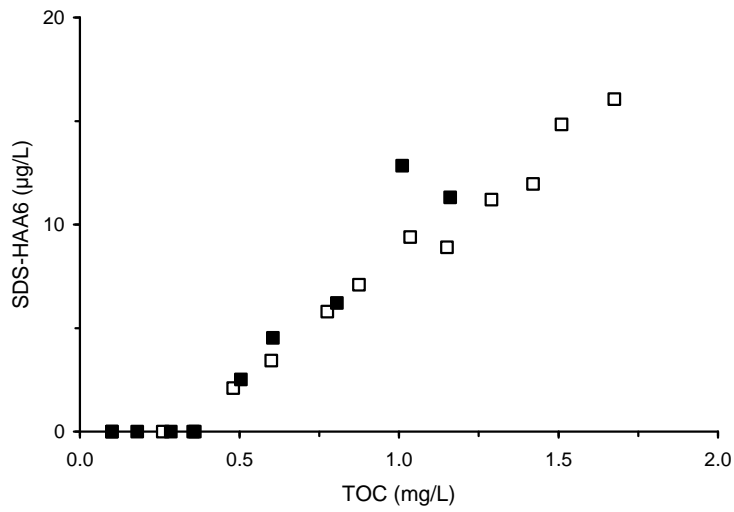
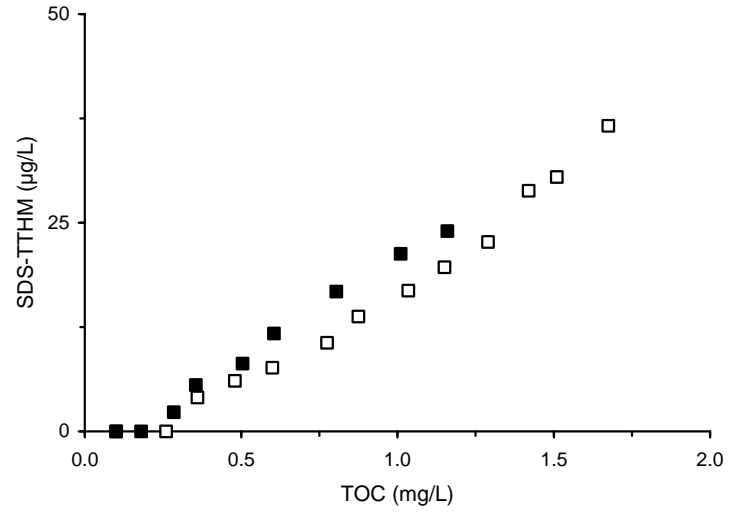
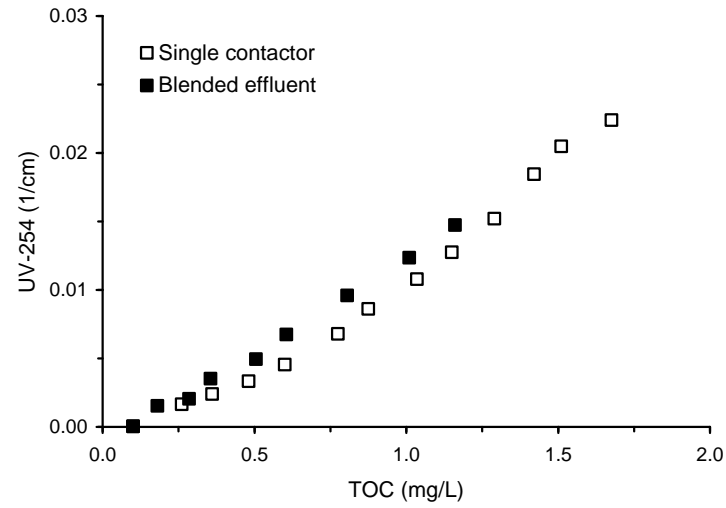


Figure D-8 Correlations based on GAC effluent TOC concentration for single contactor and blended effluents for Water 8

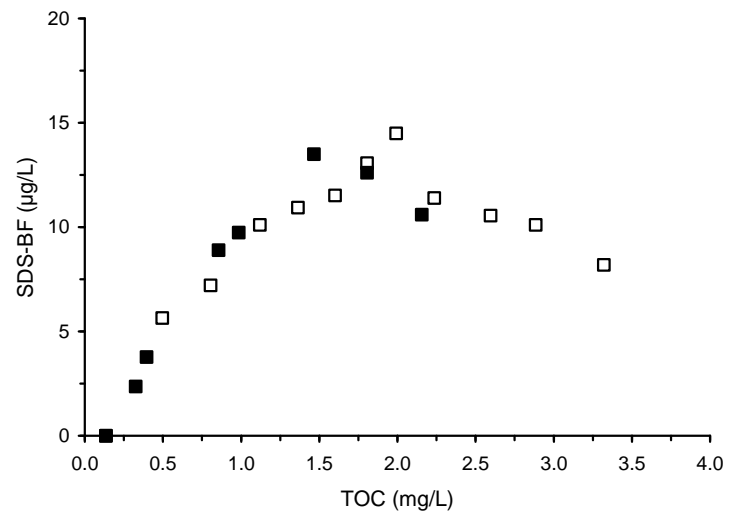
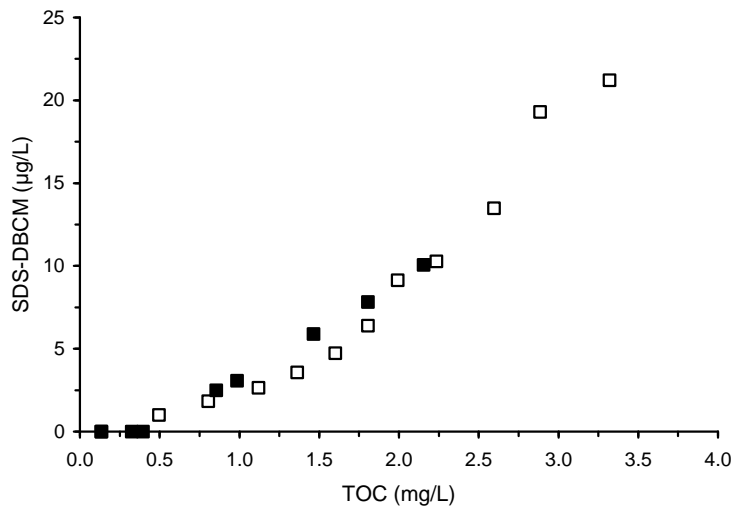
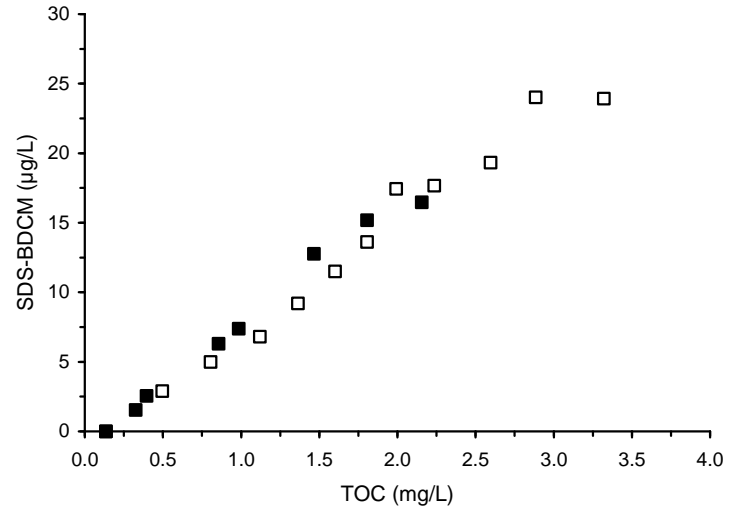
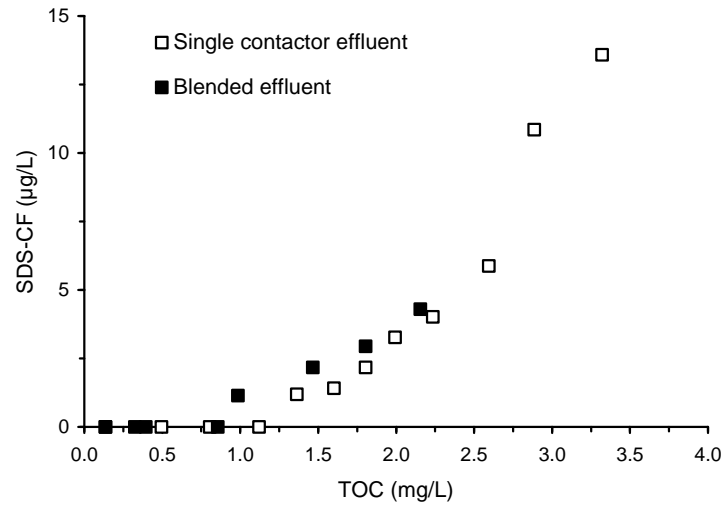


Figure D-9 THM correlations based on GAC effluent TOC concentration for single contactor and blended effluents for Water 1

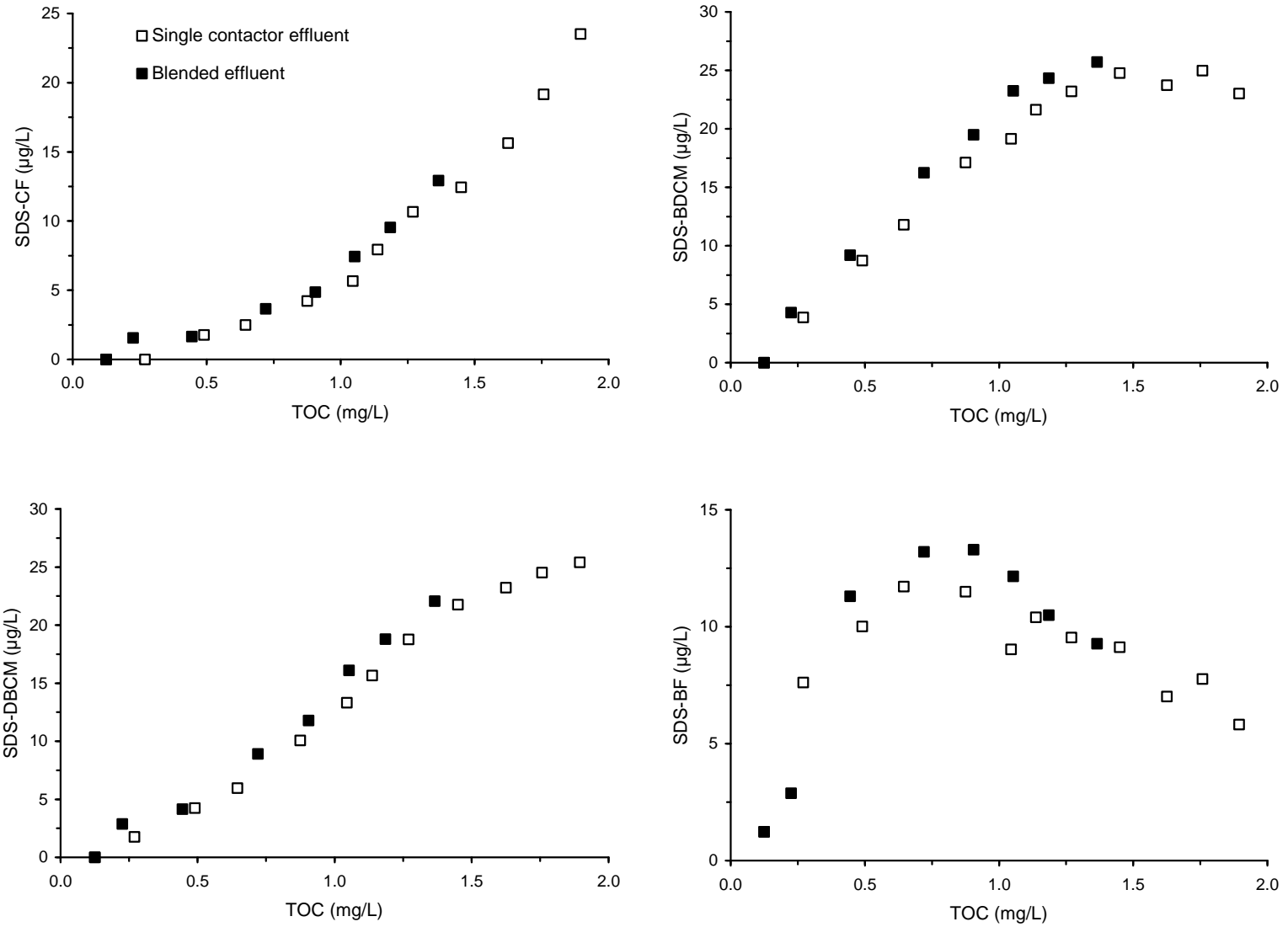


Figure D-10 THM correlations based on GAC effluent TOC concentration for single contactor and blended effluents for Water 2

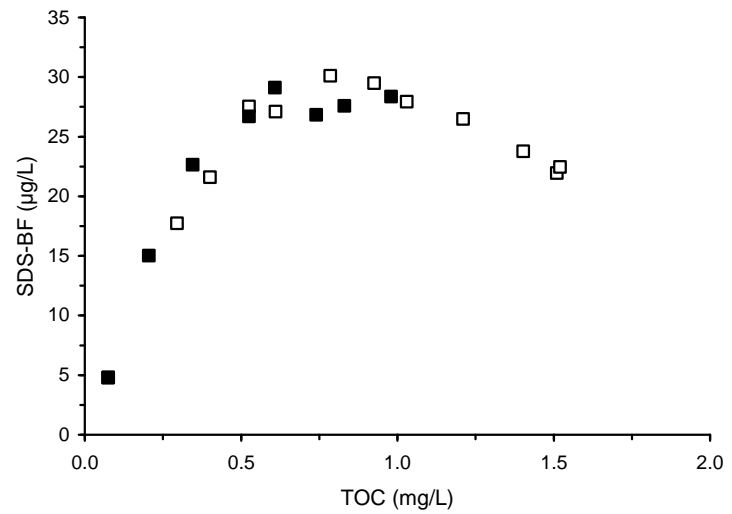
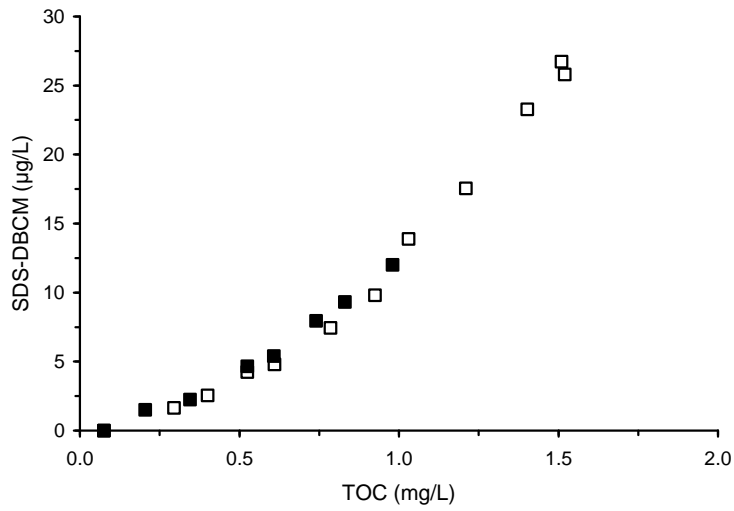
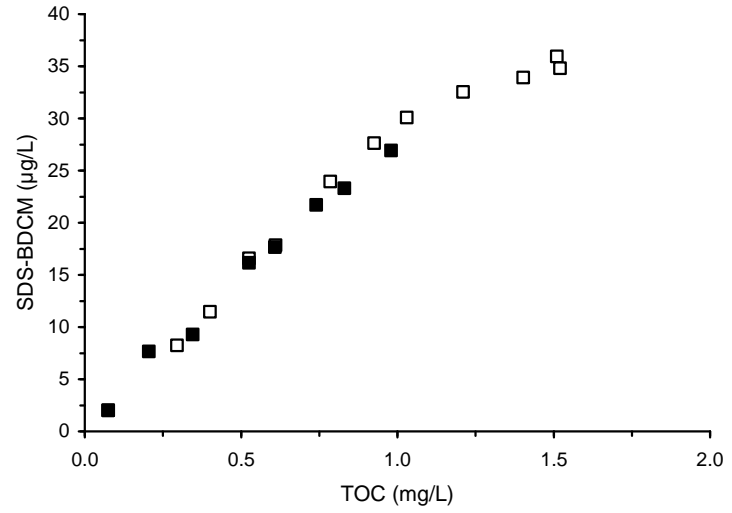
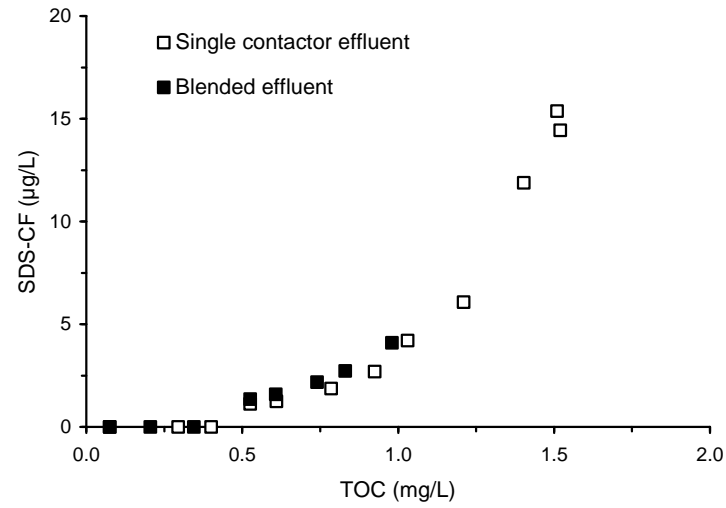


Figure D-11 THM correlations based on GAC effluent TOC concentration for single contactor and blended effluents for Water 3

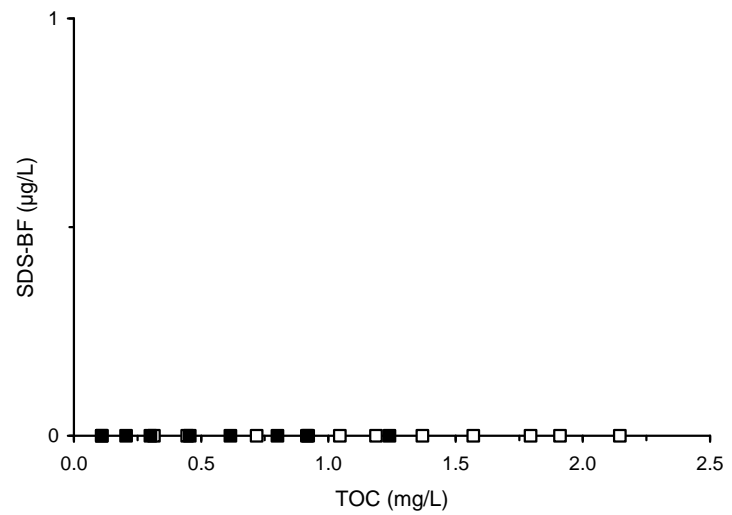
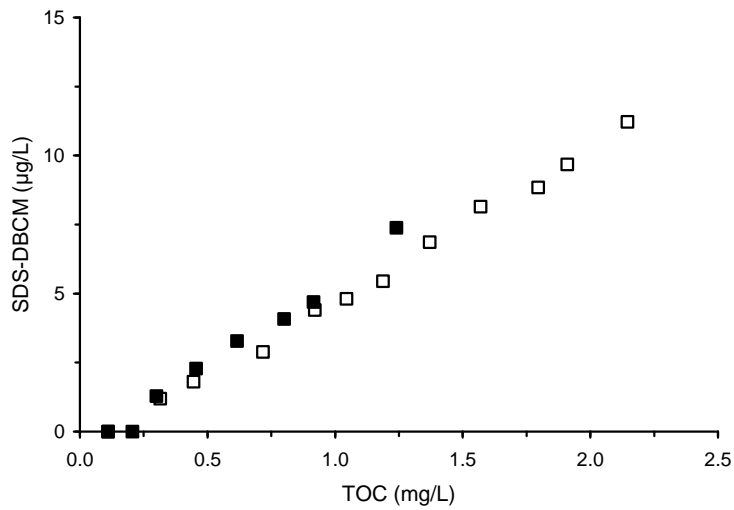
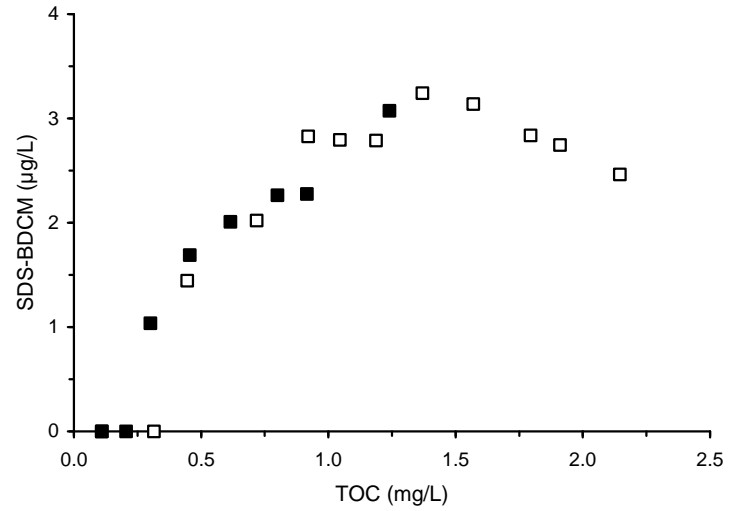
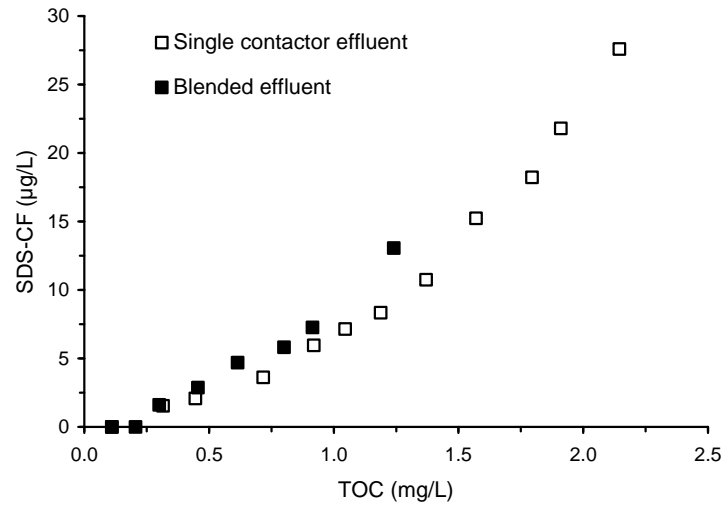


Figure D-12 THM correlations based on GAC effluent TOC concentration for single contactor and blended effluents for Water 4

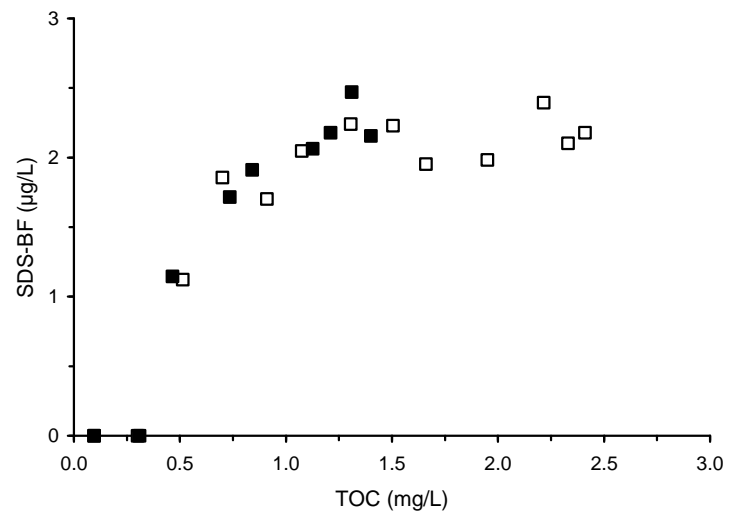
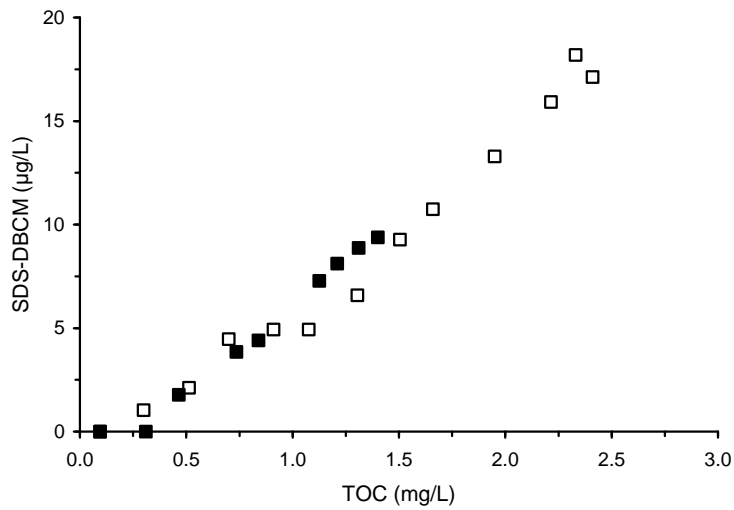
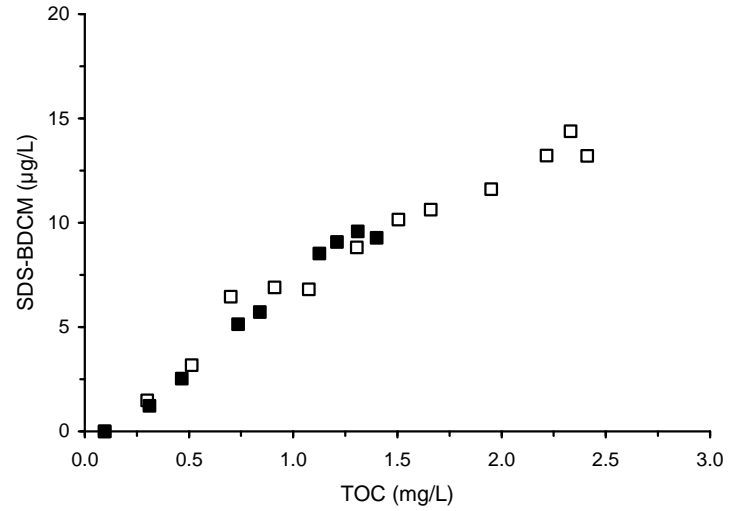
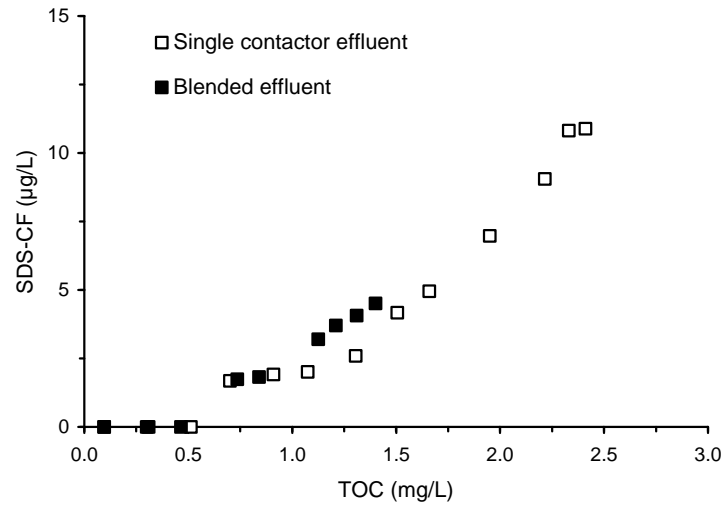


Figure D-13 THM correlations based on GAC effluent TOC concentration for single contactor and blended effluents for Water 5

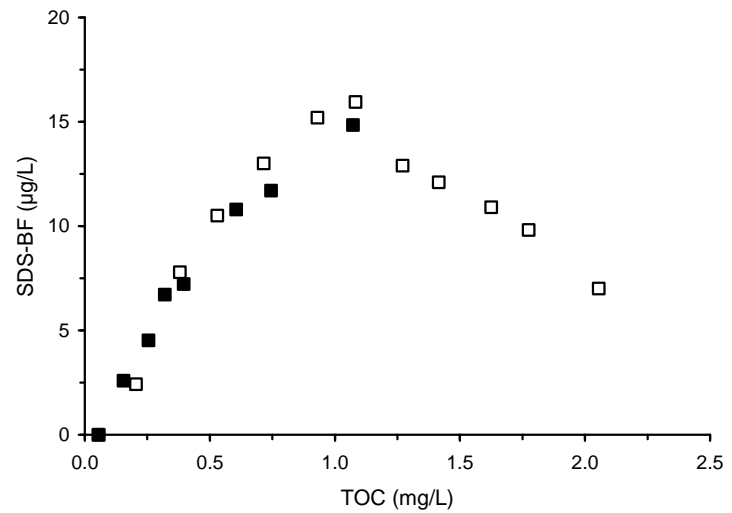
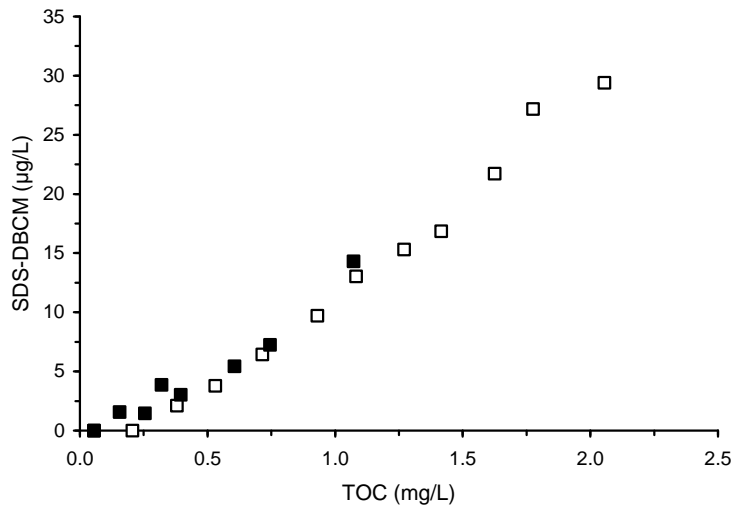
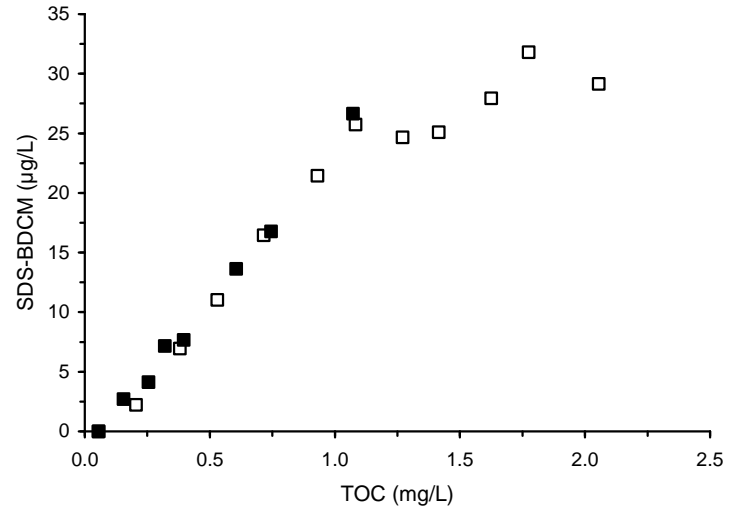
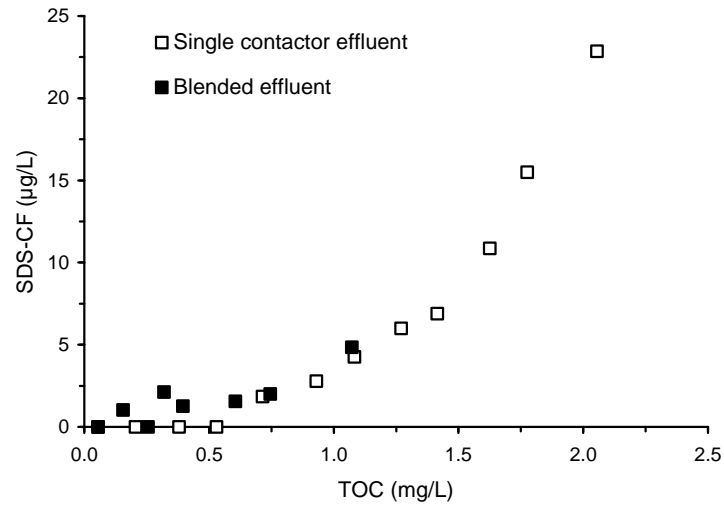


Figure D-14 THM correlations based on GAC effluent TOC concentration for single contactor and blended effluents for Water 6

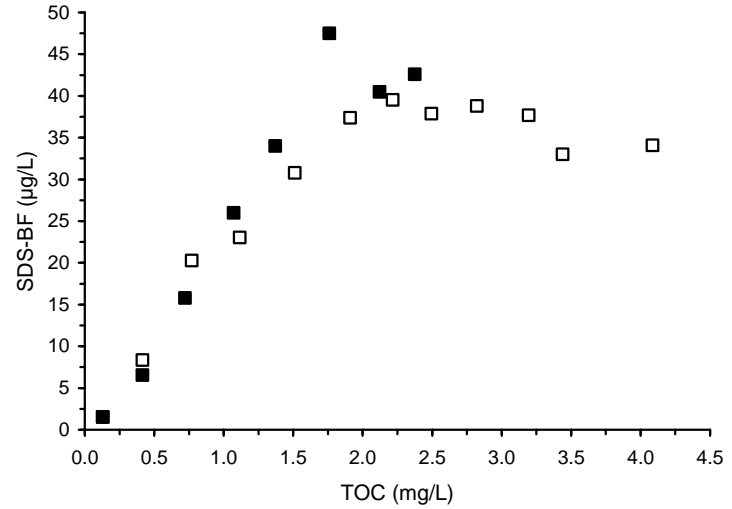
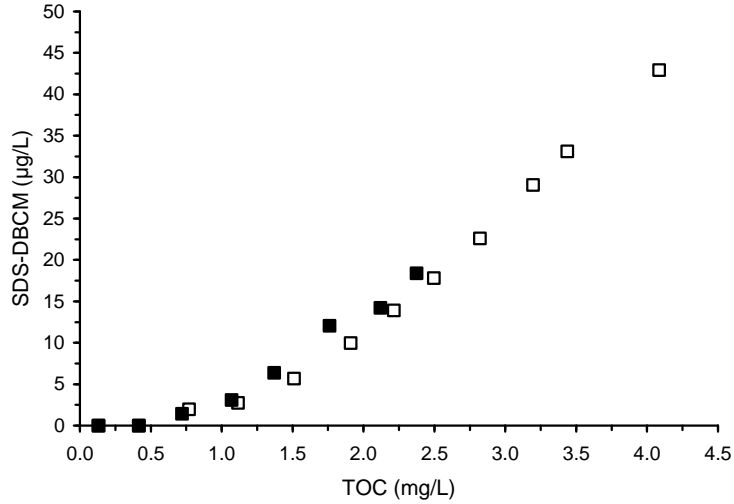
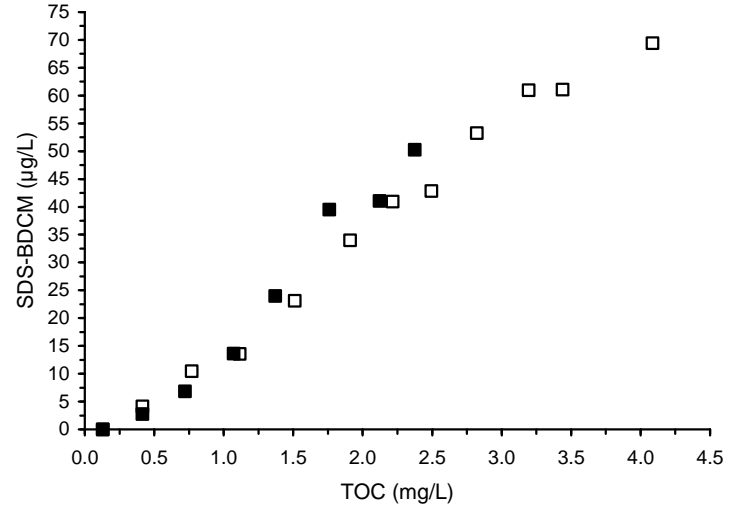
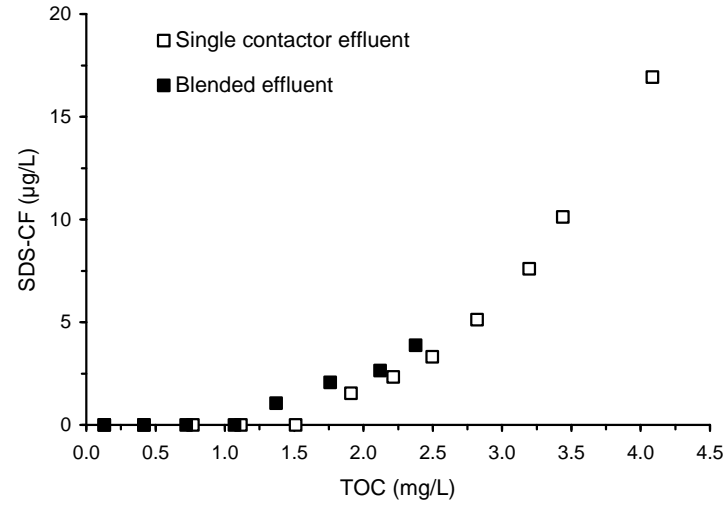


Figure D-15 THM correlations based on GAC effluent TOC concentration for single contactor and blended effluents for Water 7

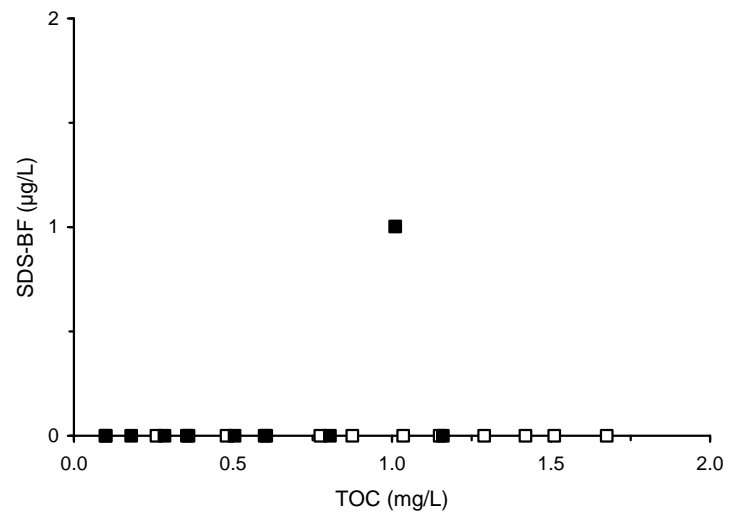
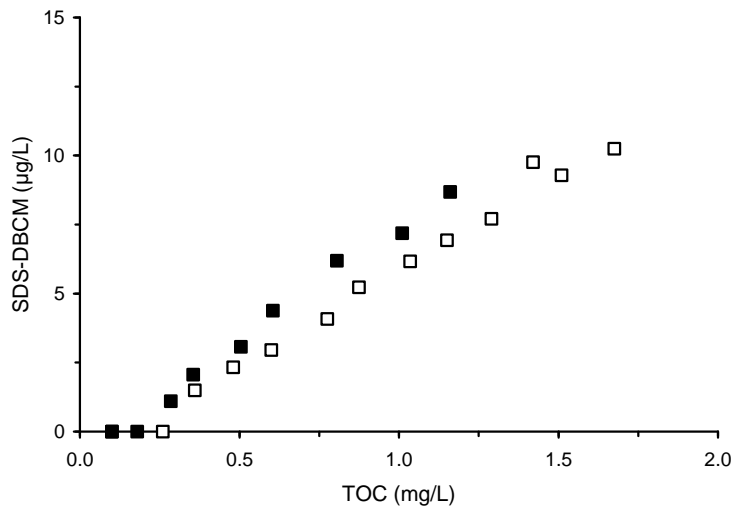
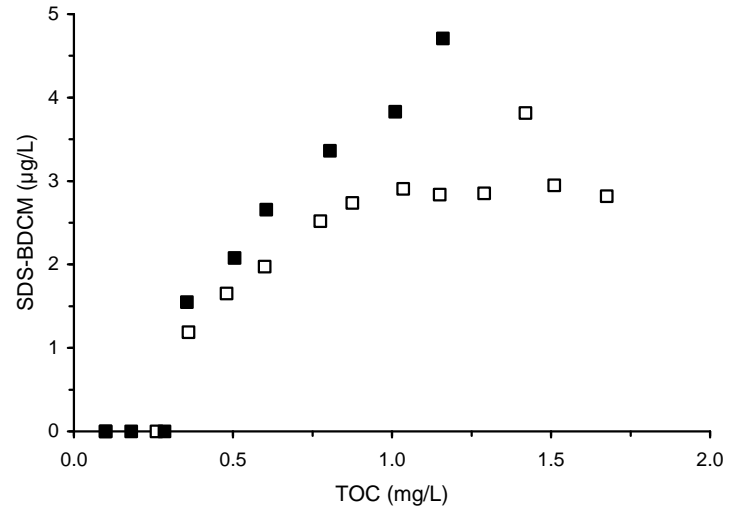
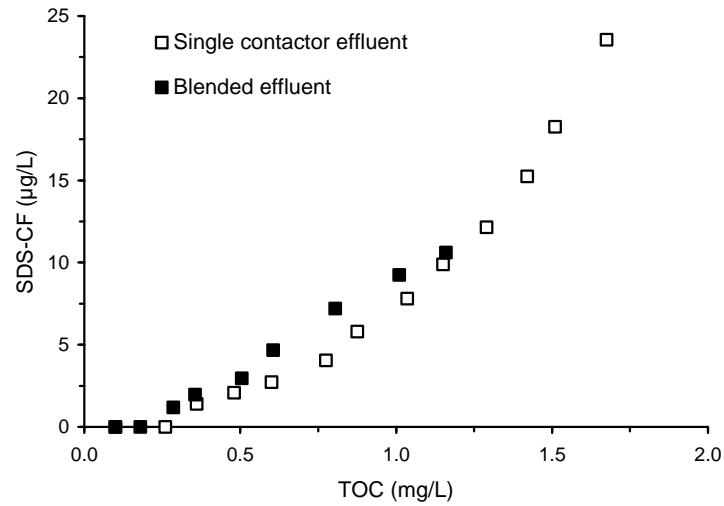


Figure D-16 THM correlations based on GAC effluent TOC concentration for single contactor and blended effluents for Water 8

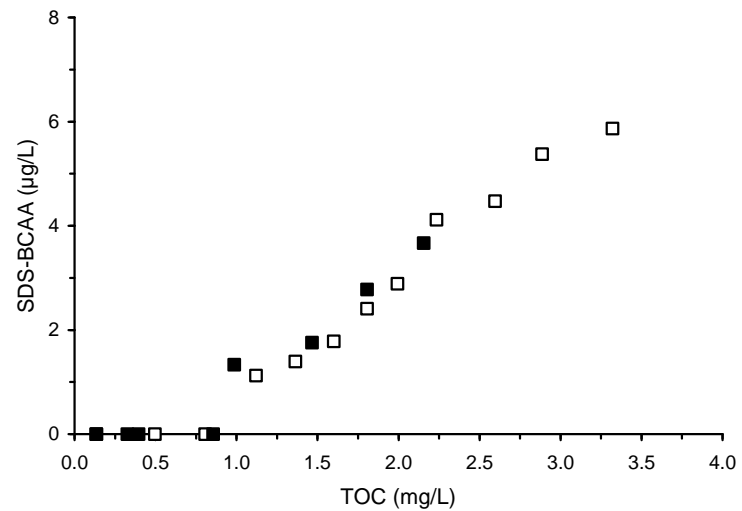
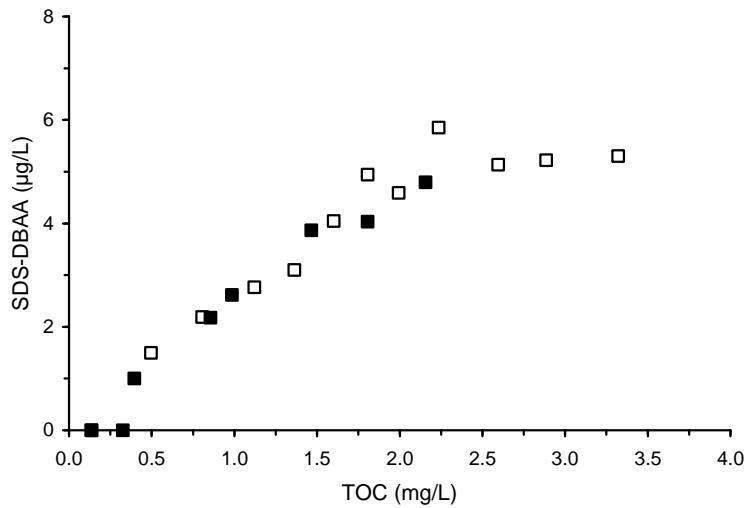
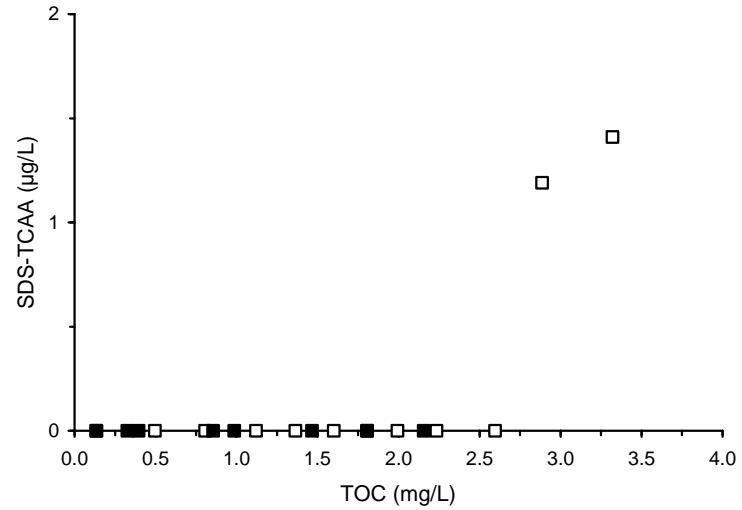
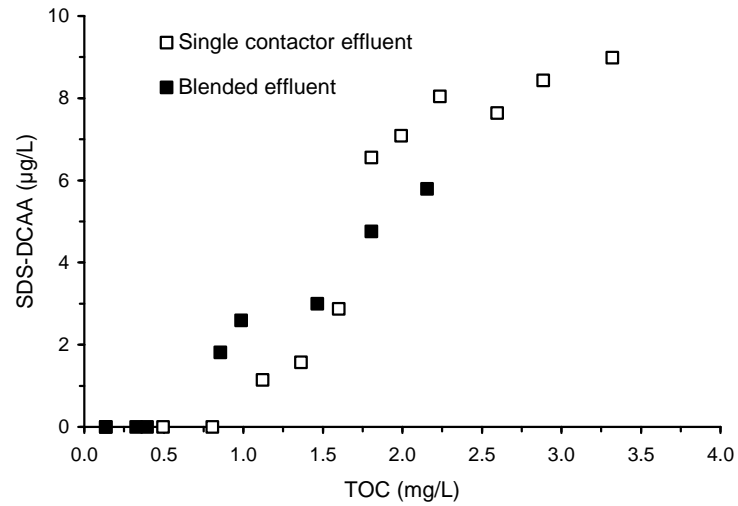


Figure D-17 HAA correlations based on GAC effluent TOC concentration for single contactor and blended effluents for Water 1

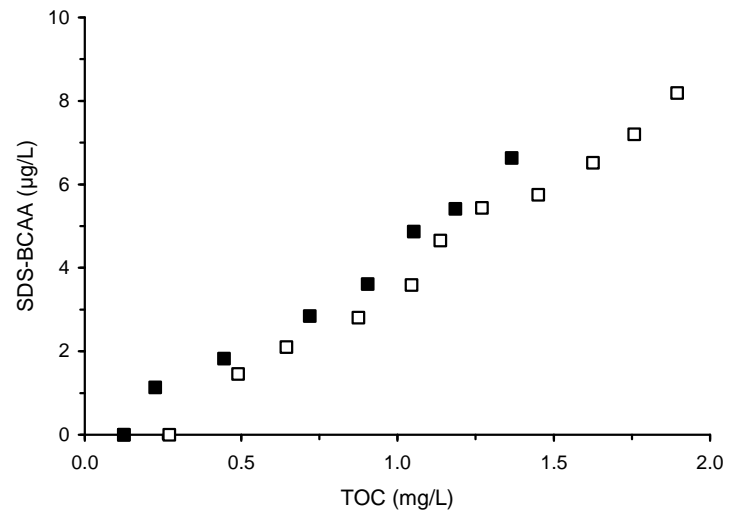
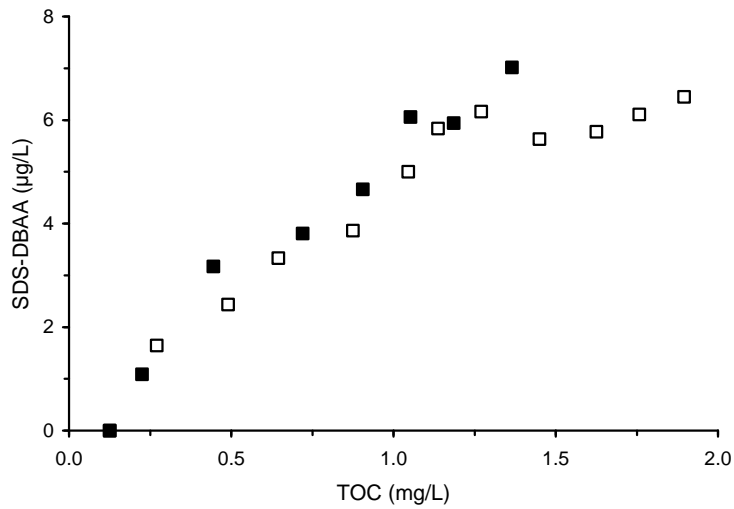
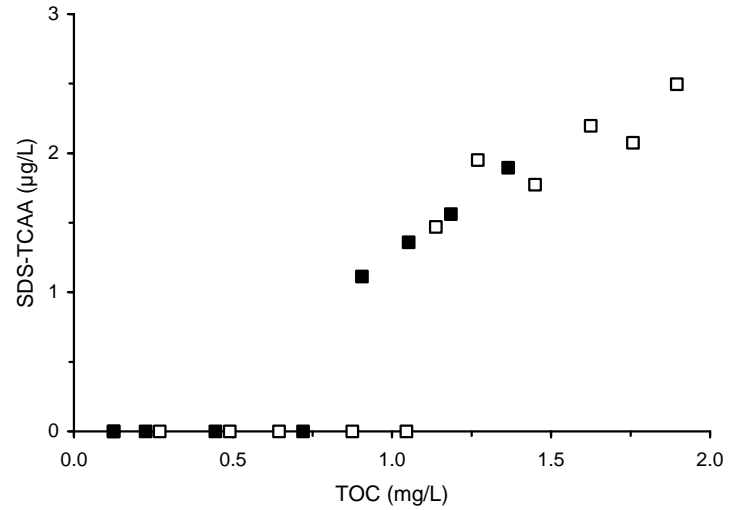
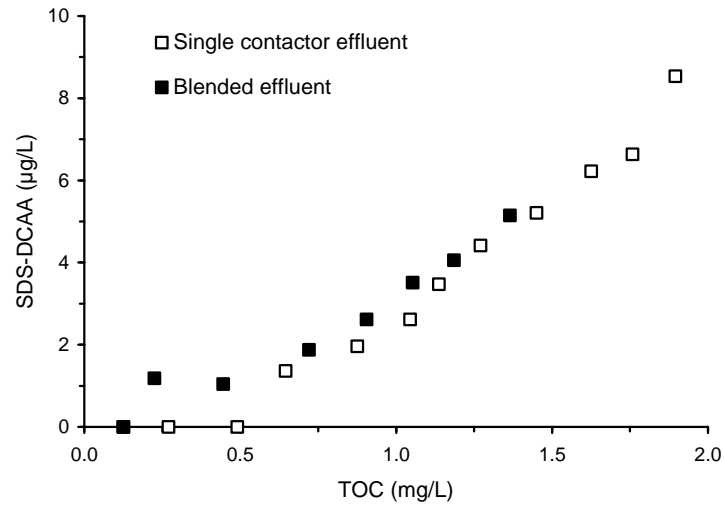


Figure D-18 HAA correlations based on GAC effluent TOC concentration for single contactor and blended effluents for Water 2

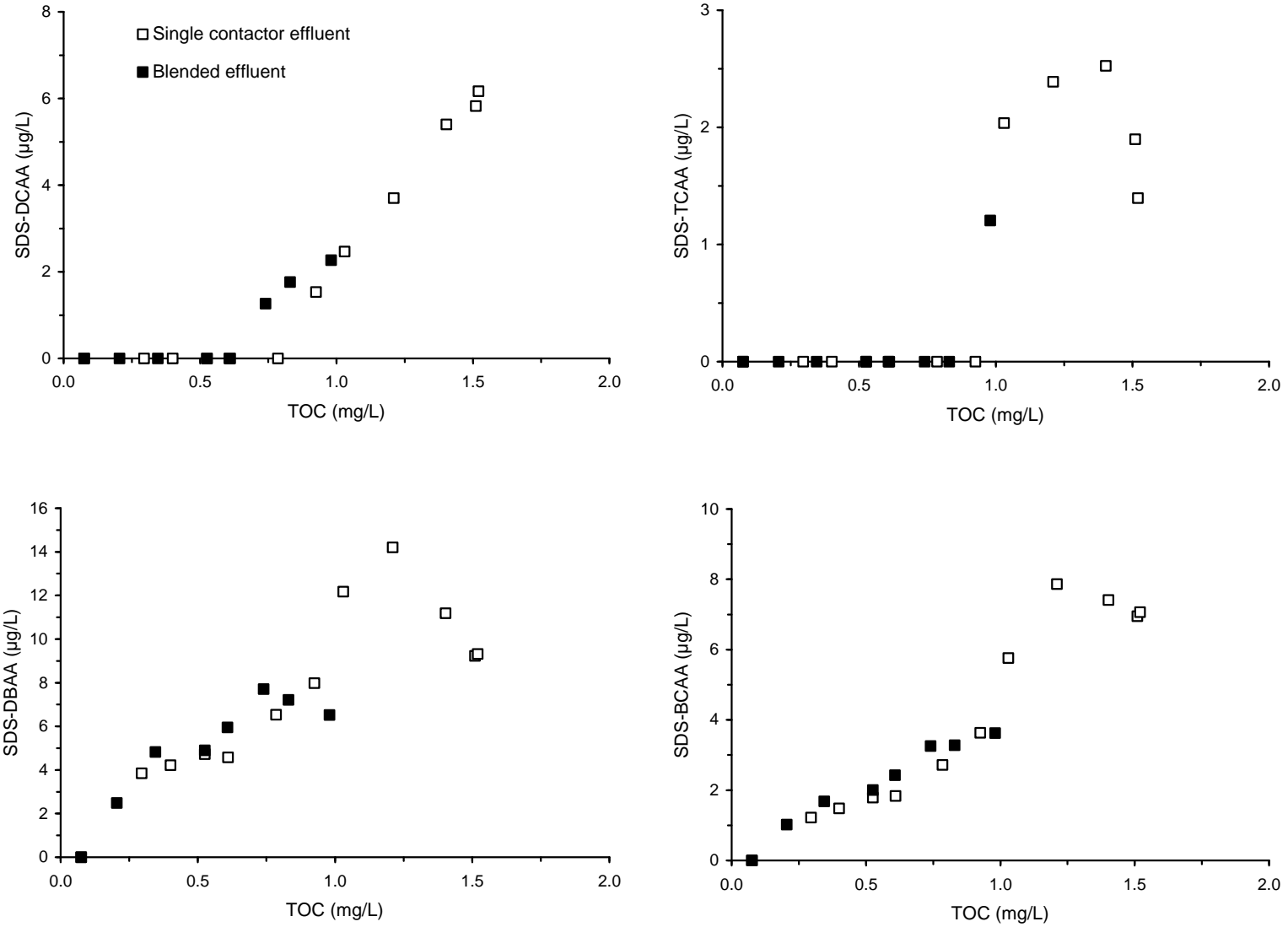


Figure D-19 HAA correlations based on GAC effluent TOC concentration for single contactor and blended effluents for Water 3

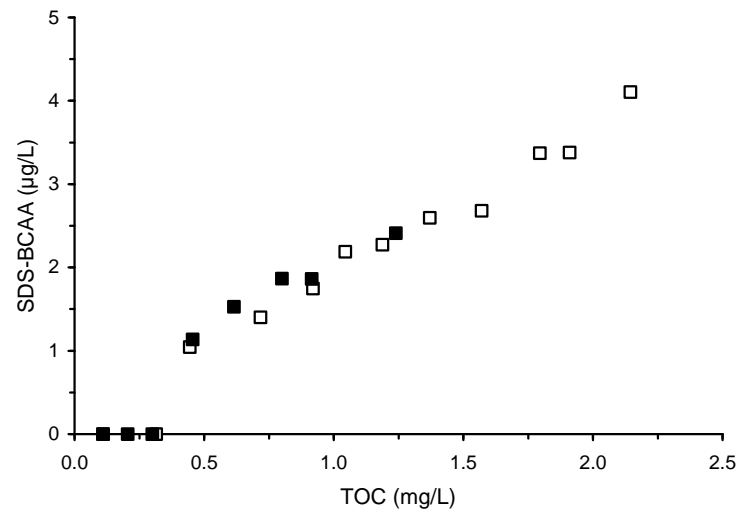
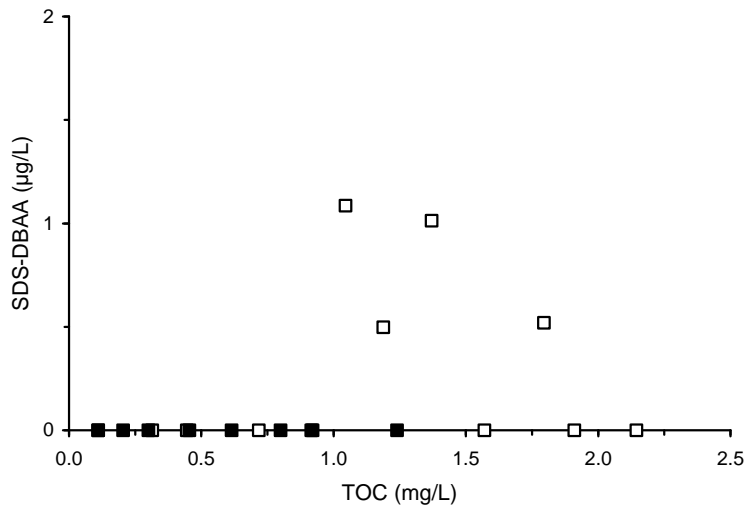
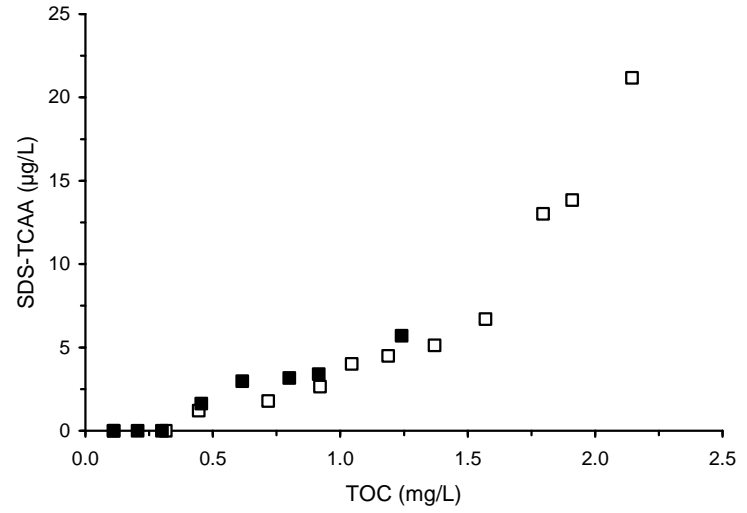
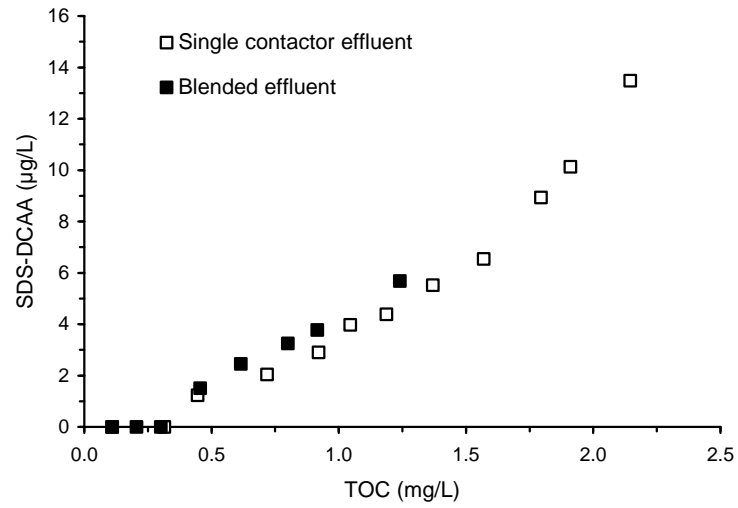


Figure D-20 HAA correlations based on GAC effluent TOC concentration for single contactor and blended effluents for Water 4

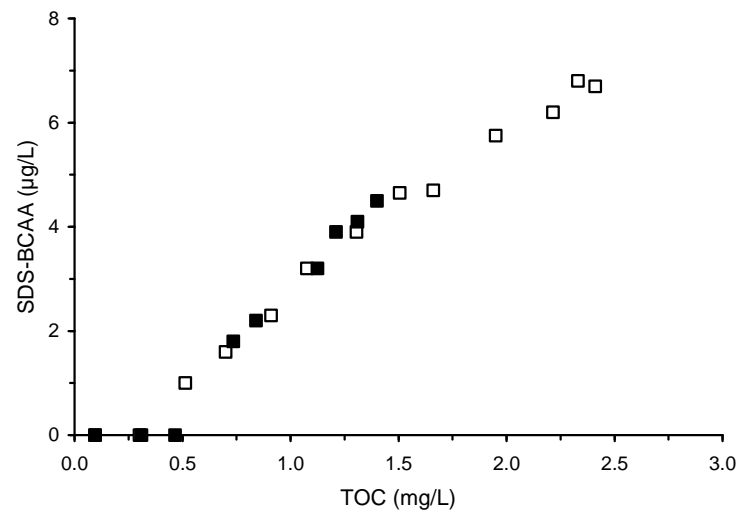
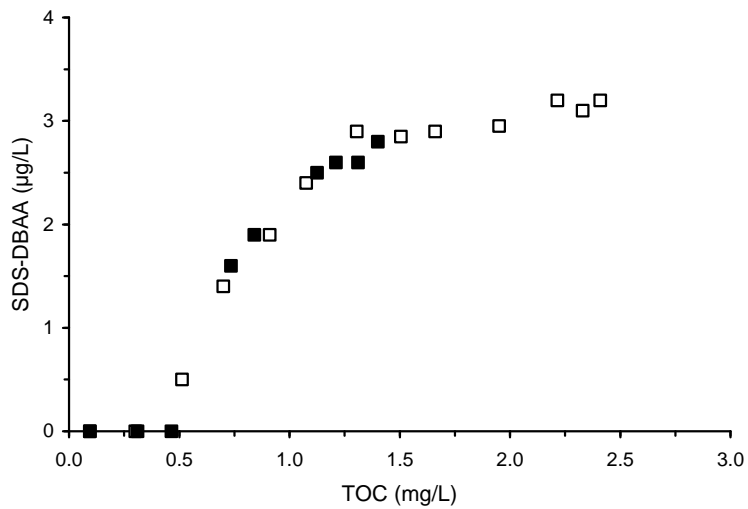
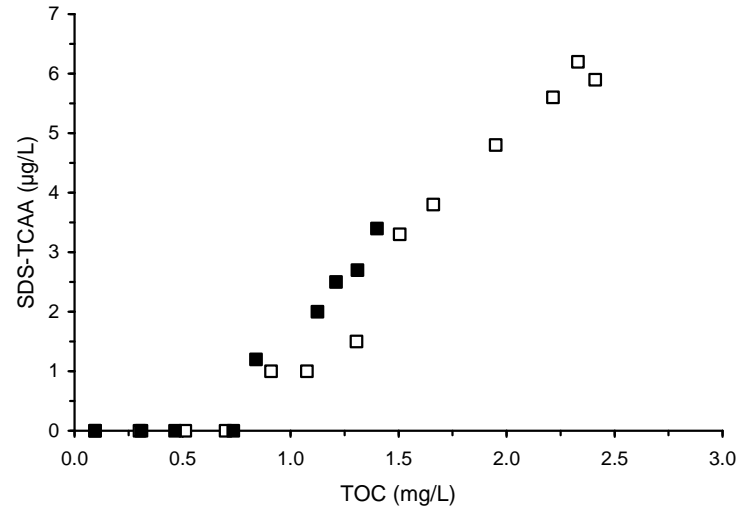
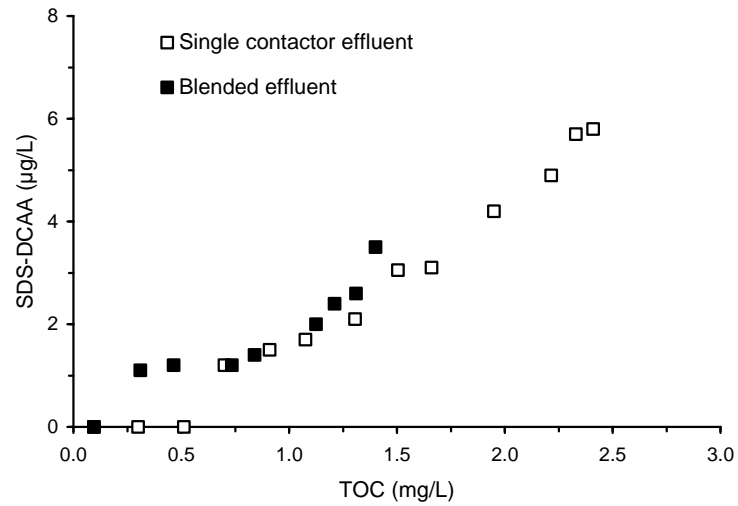


Figure D-21 HAA correlations based on GAC effluent TOC concentration for single contactor and blended effluents for Water 5

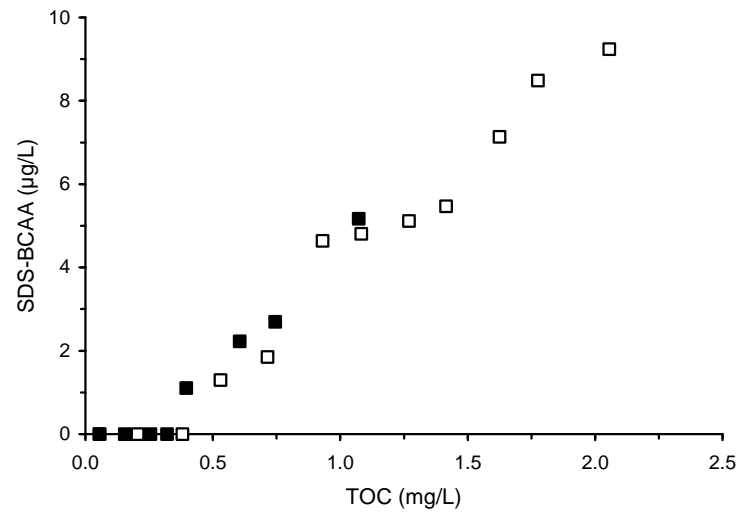
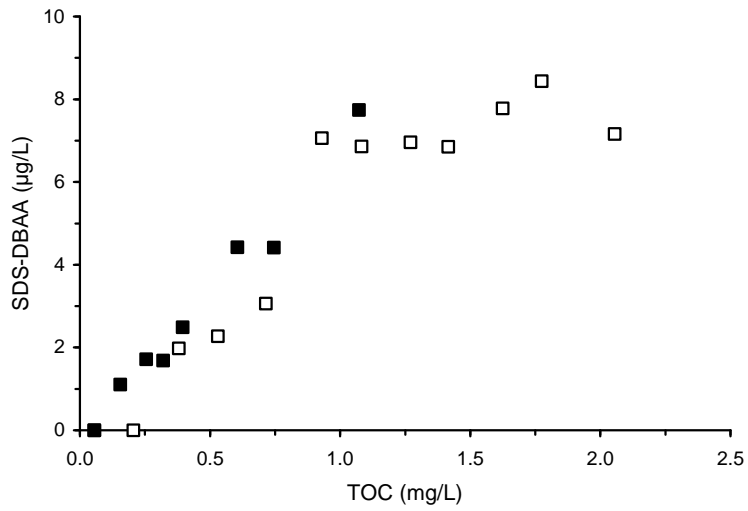
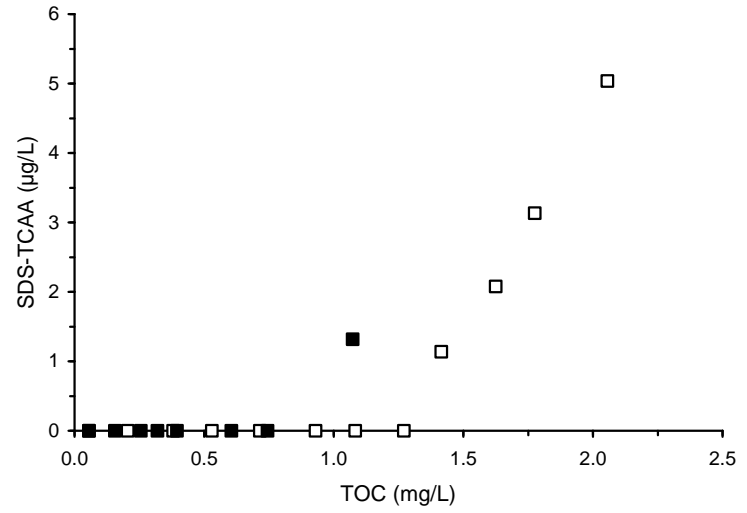
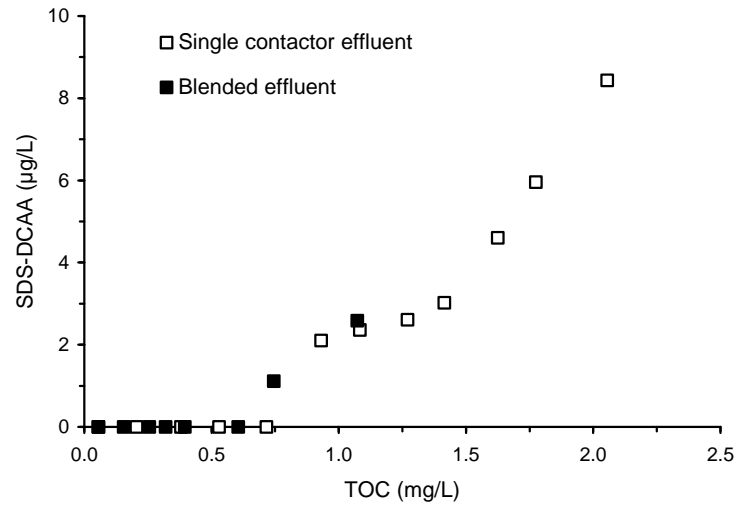


Figure D-22 HAA correlations based on GAC effluent TOC concentration for single contactor and blended effluents for Water 6

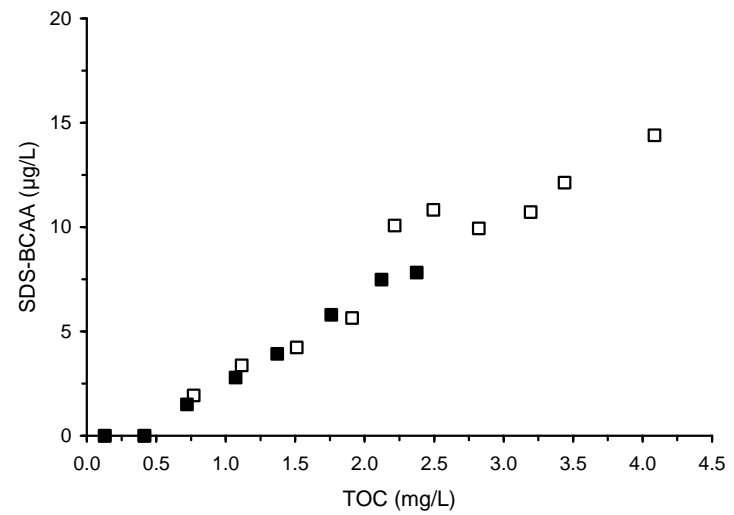
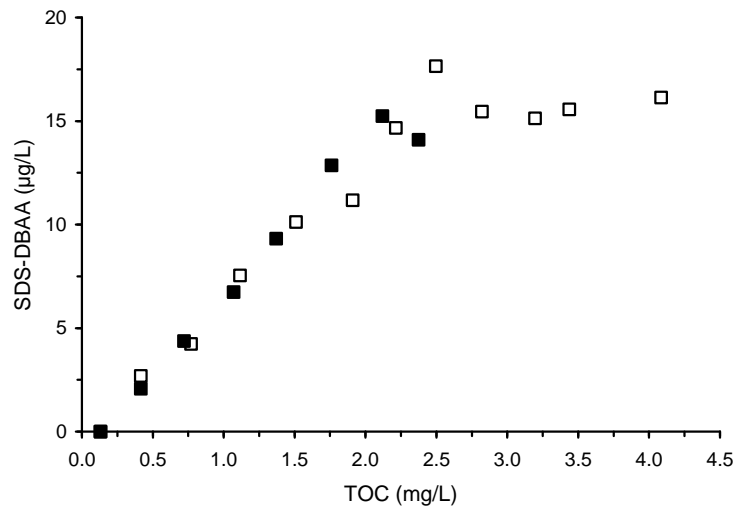
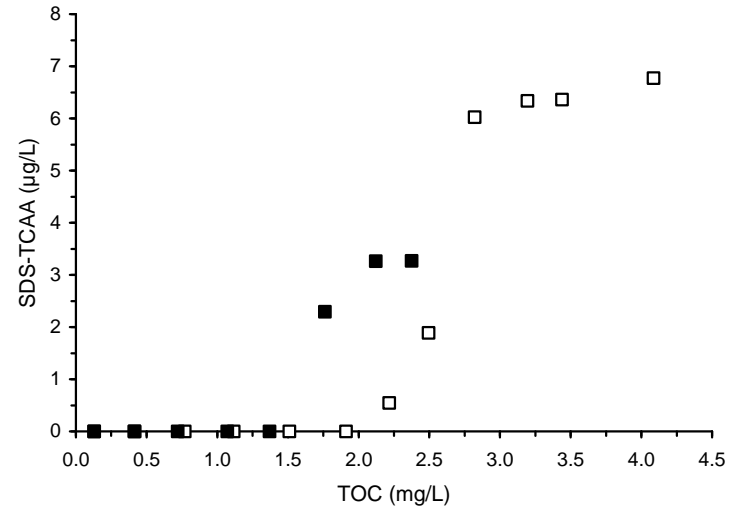
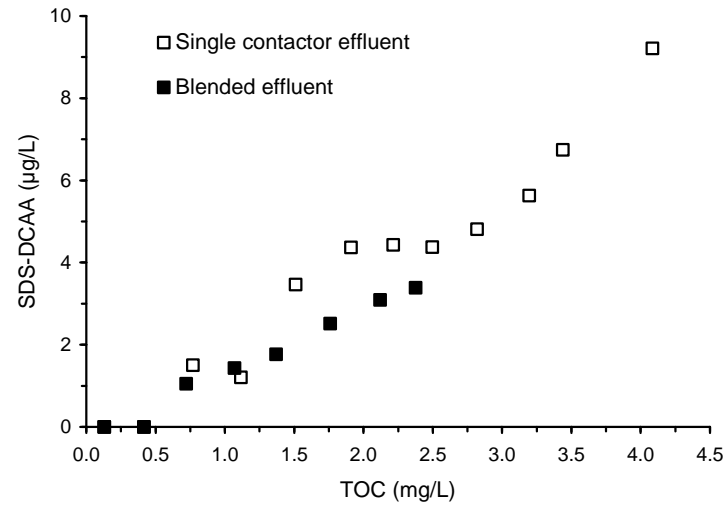


Figure D-23 HAA correlations based on GAC effluent TOC concentration for single contactor and blended effluents for Water 7

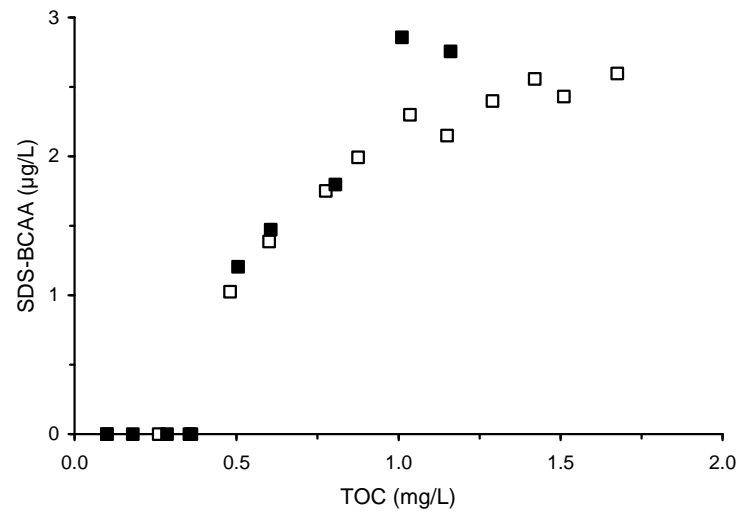
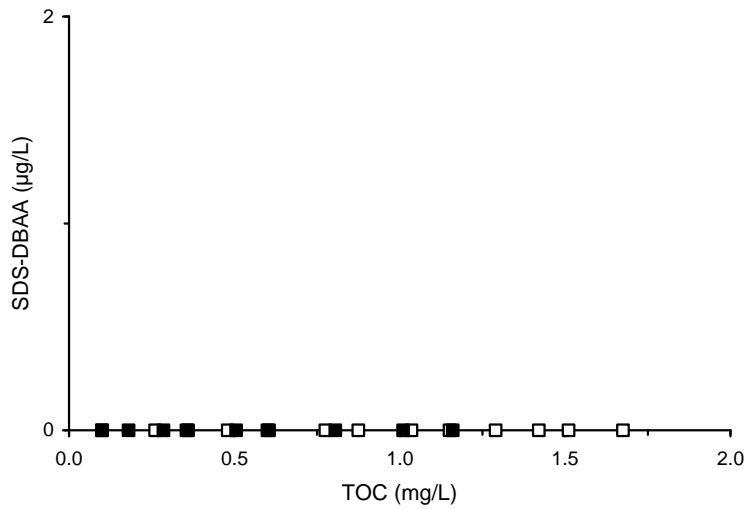
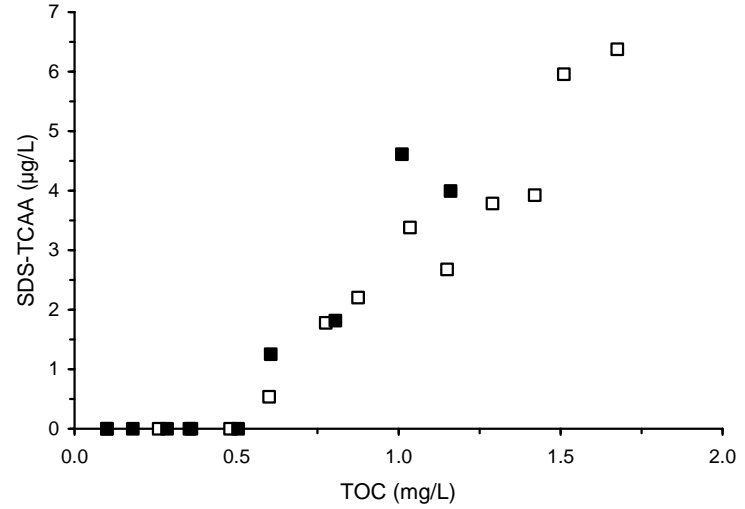
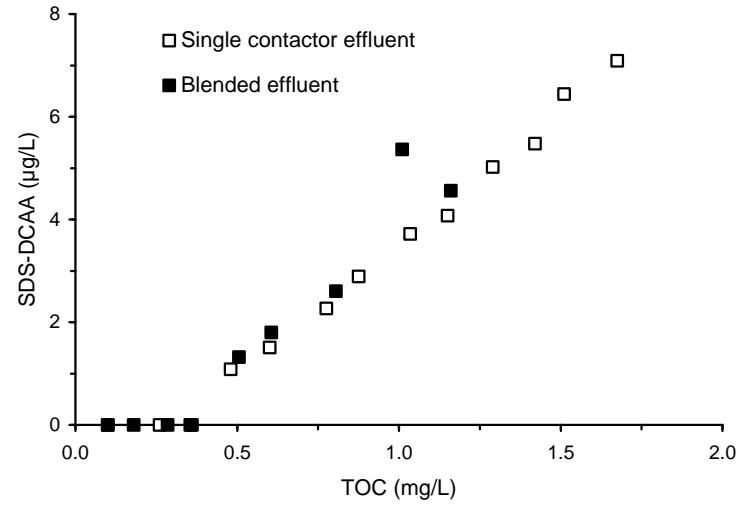


Figure D-24 HAA correlations based on GAC effluent TOC concentration for single contactor and blended effluents for Water 8

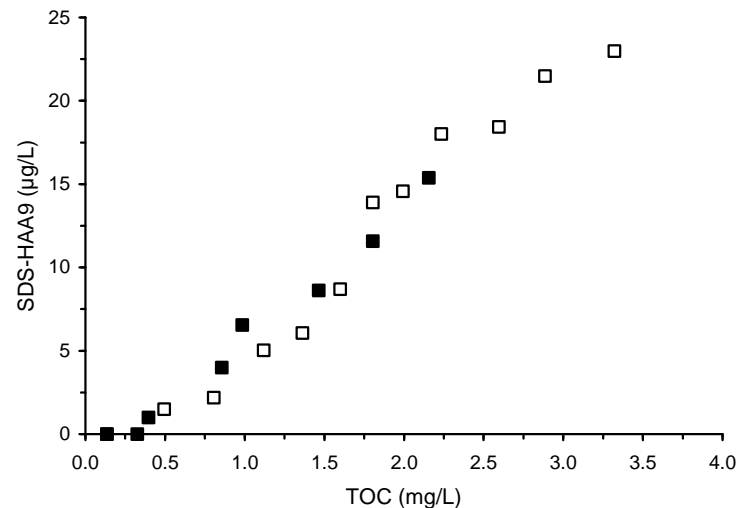
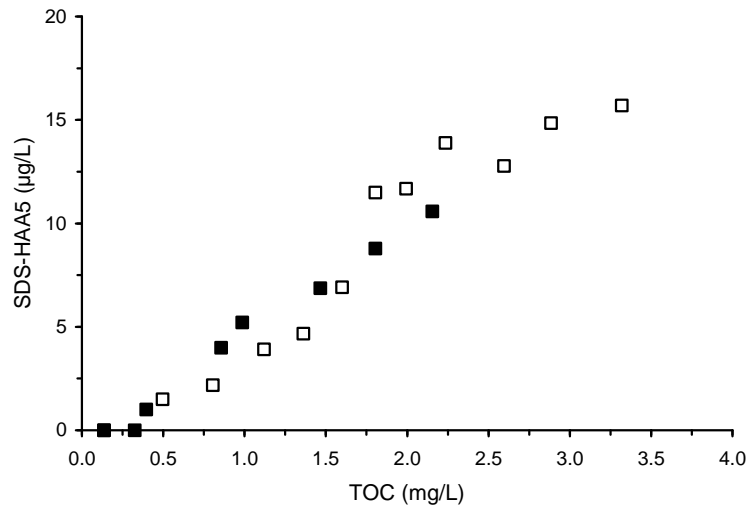
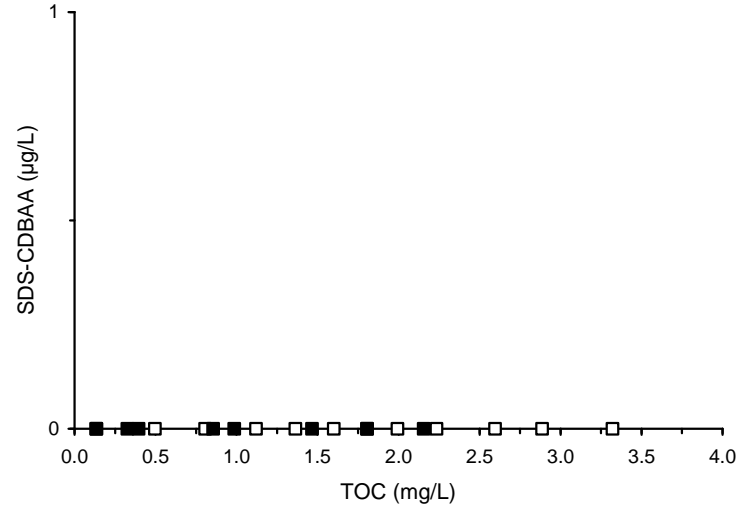
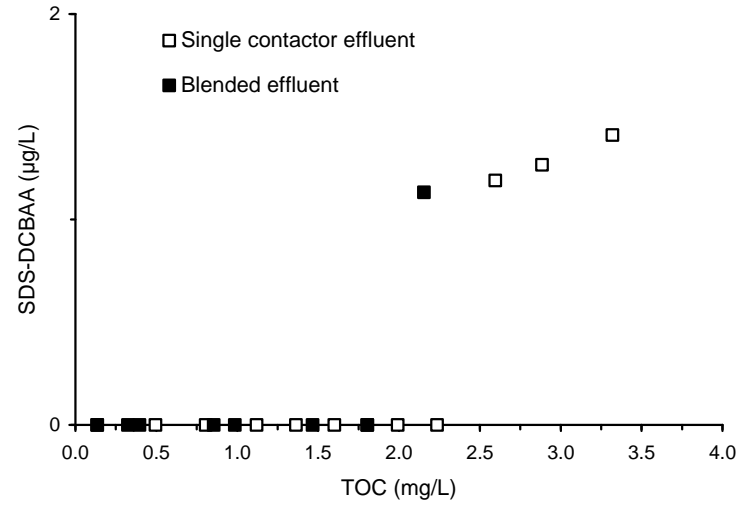


Figure D-25 HAA correlations based on GAC effluent TOC concentration for single contactor and blended effluents for Water 1

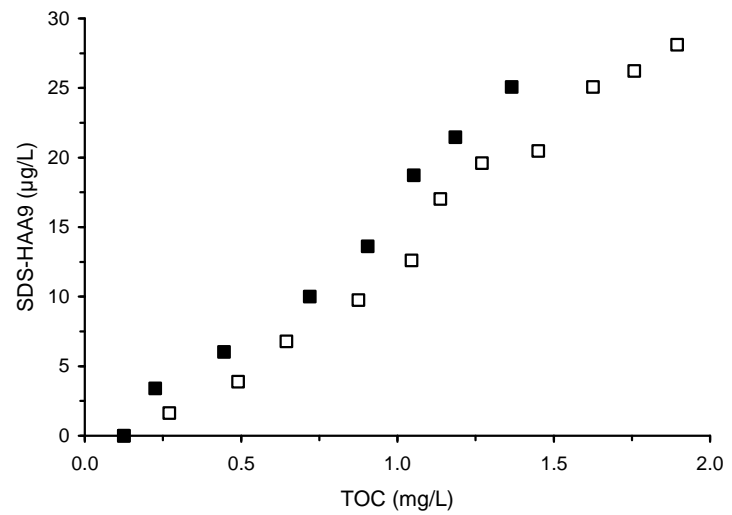
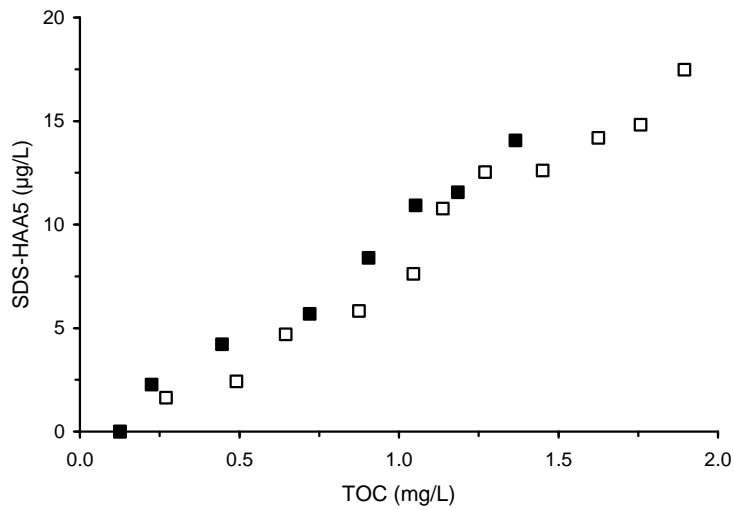
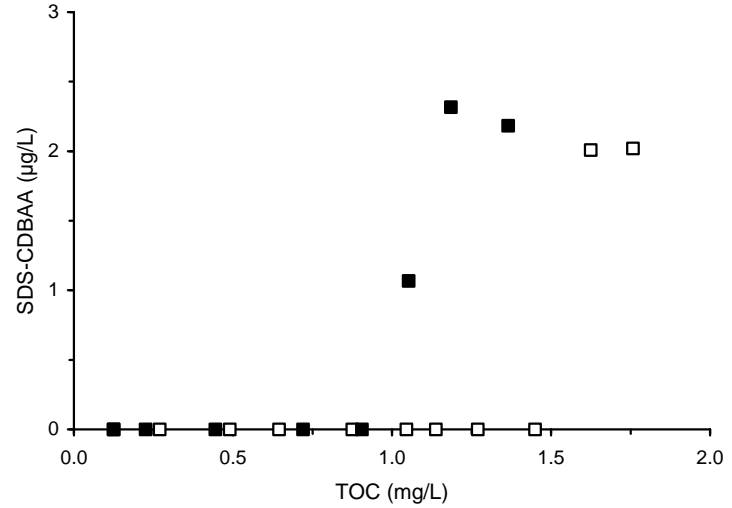
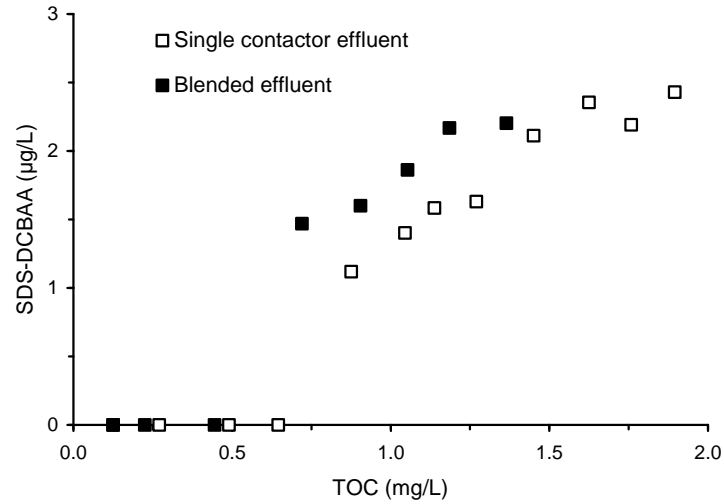


Figure D-26 HAA correlations based on GAC effluent TOC concentration for single contactor and blended effluents for Water 2

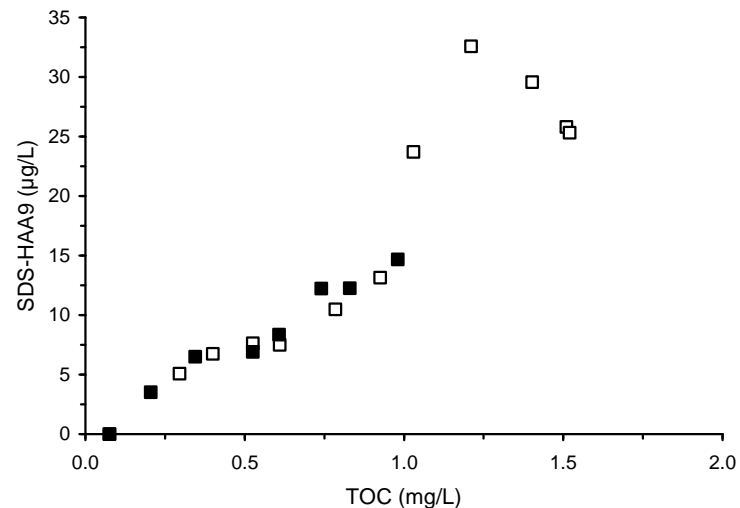
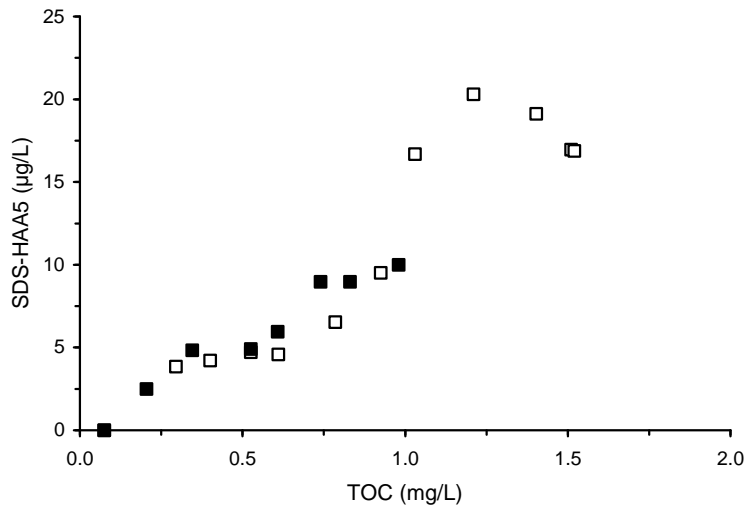
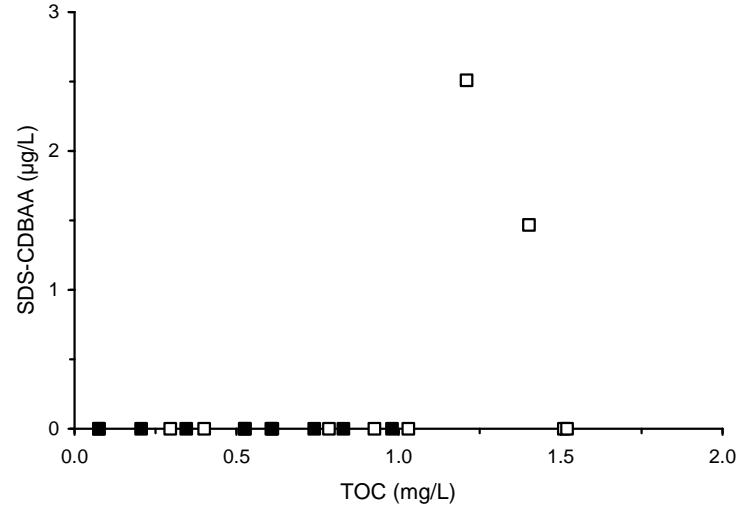
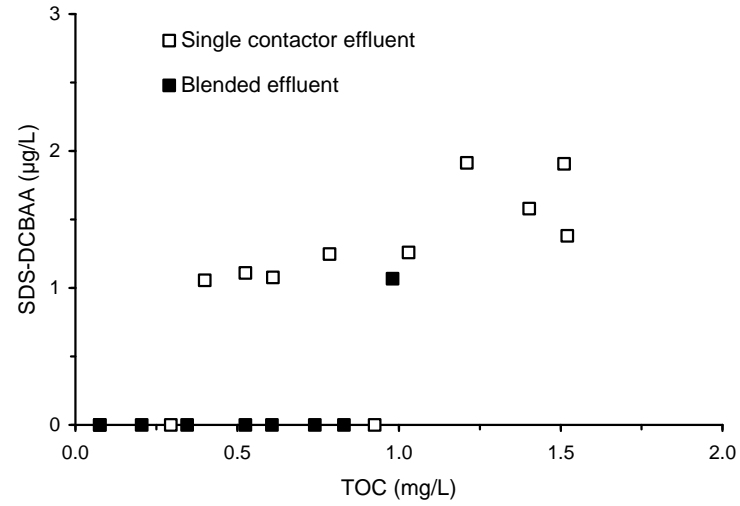


Figure D-27 HAA correlations based on GAC effluent TOC concentration for single contactor and blended effluents for Water 3

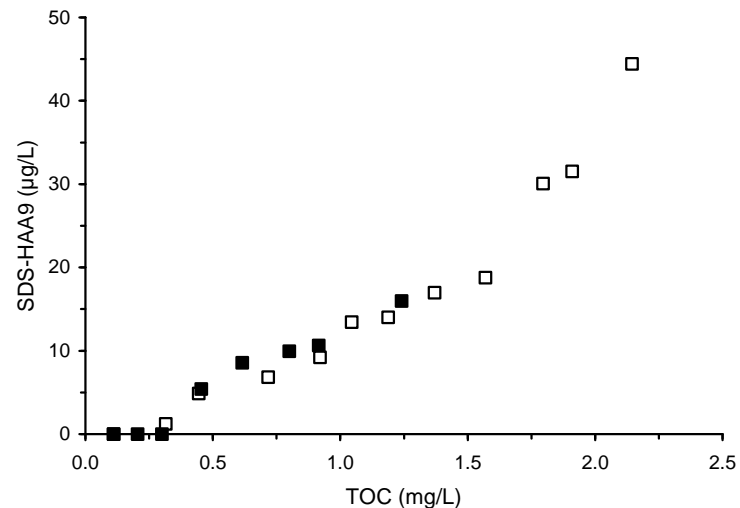
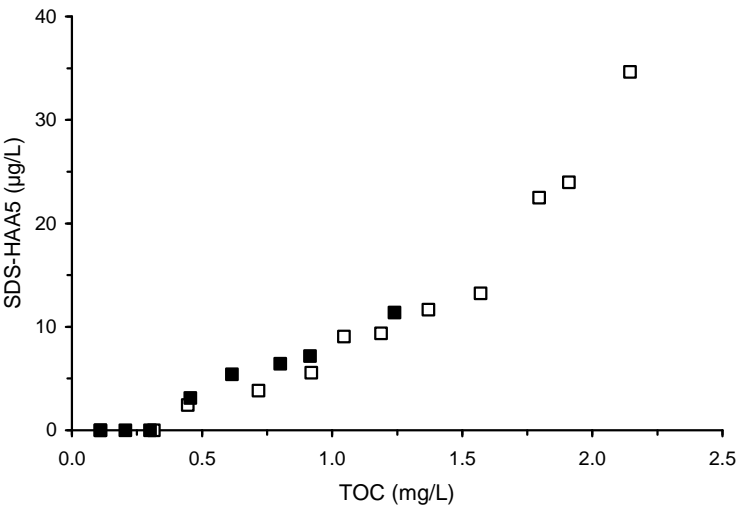
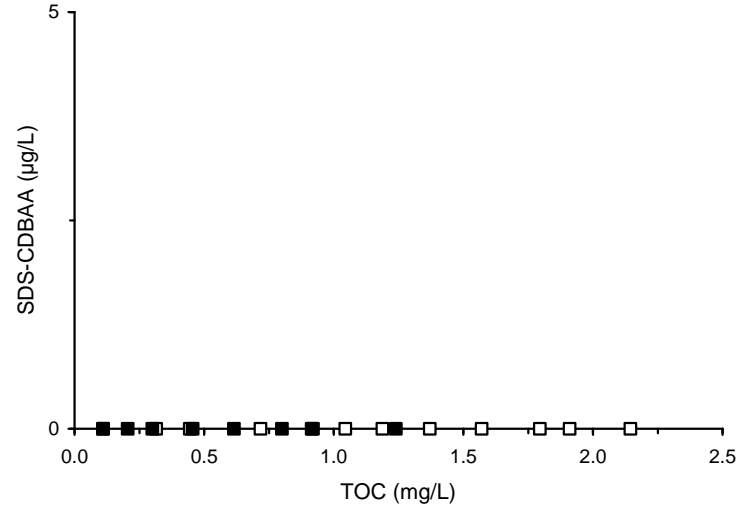
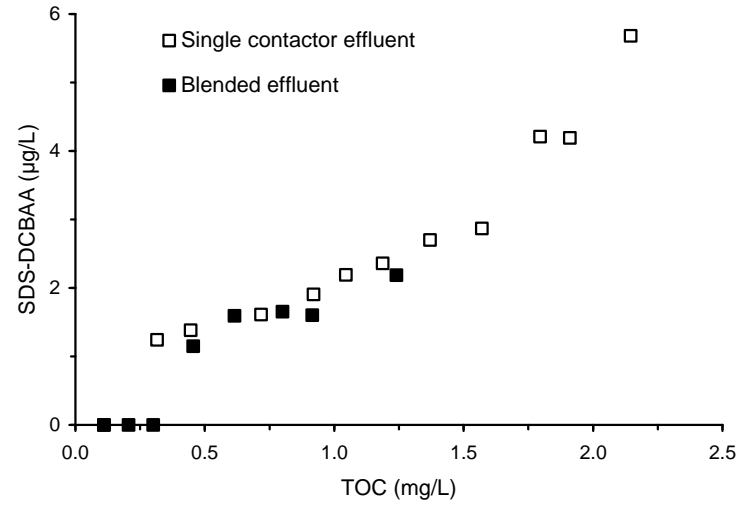


Figure D-28 HAA correlations based on GAC effluent TOC concentration for single contactor and blended effluents for Water 4

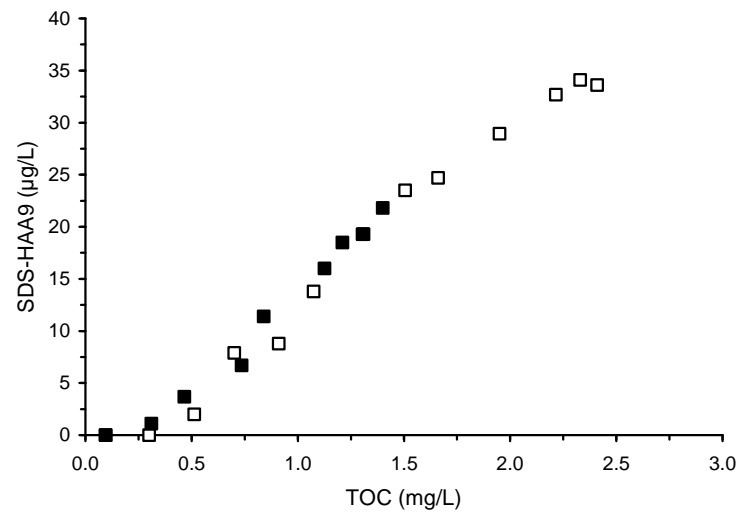
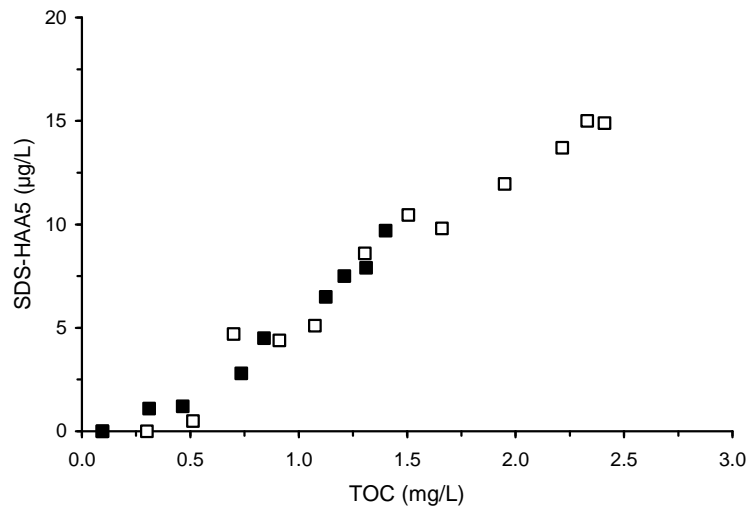
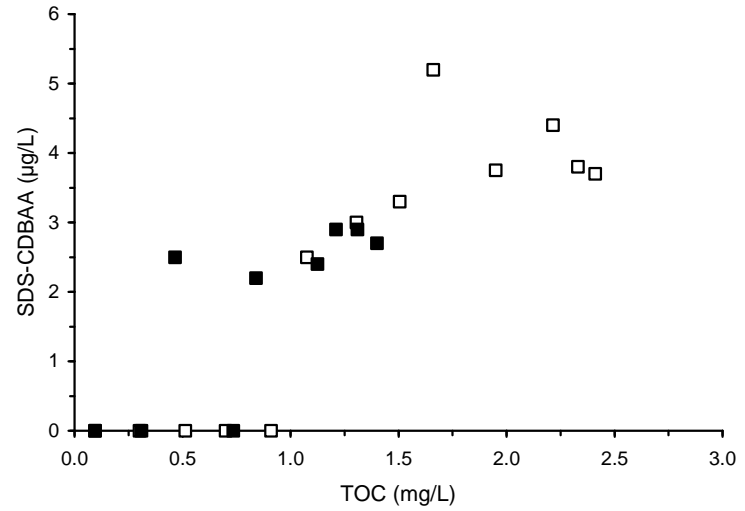
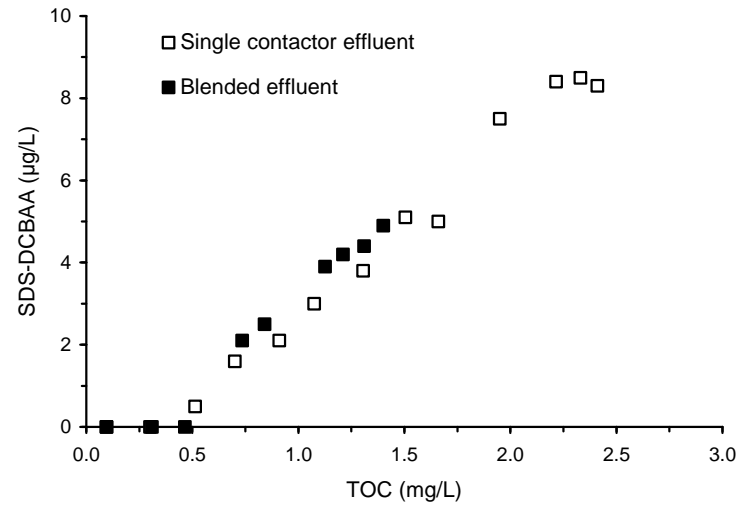


Figure D-29 HAA correlations based on GAC effluent TOC concentration for single contactor and blended effluents for Water 5

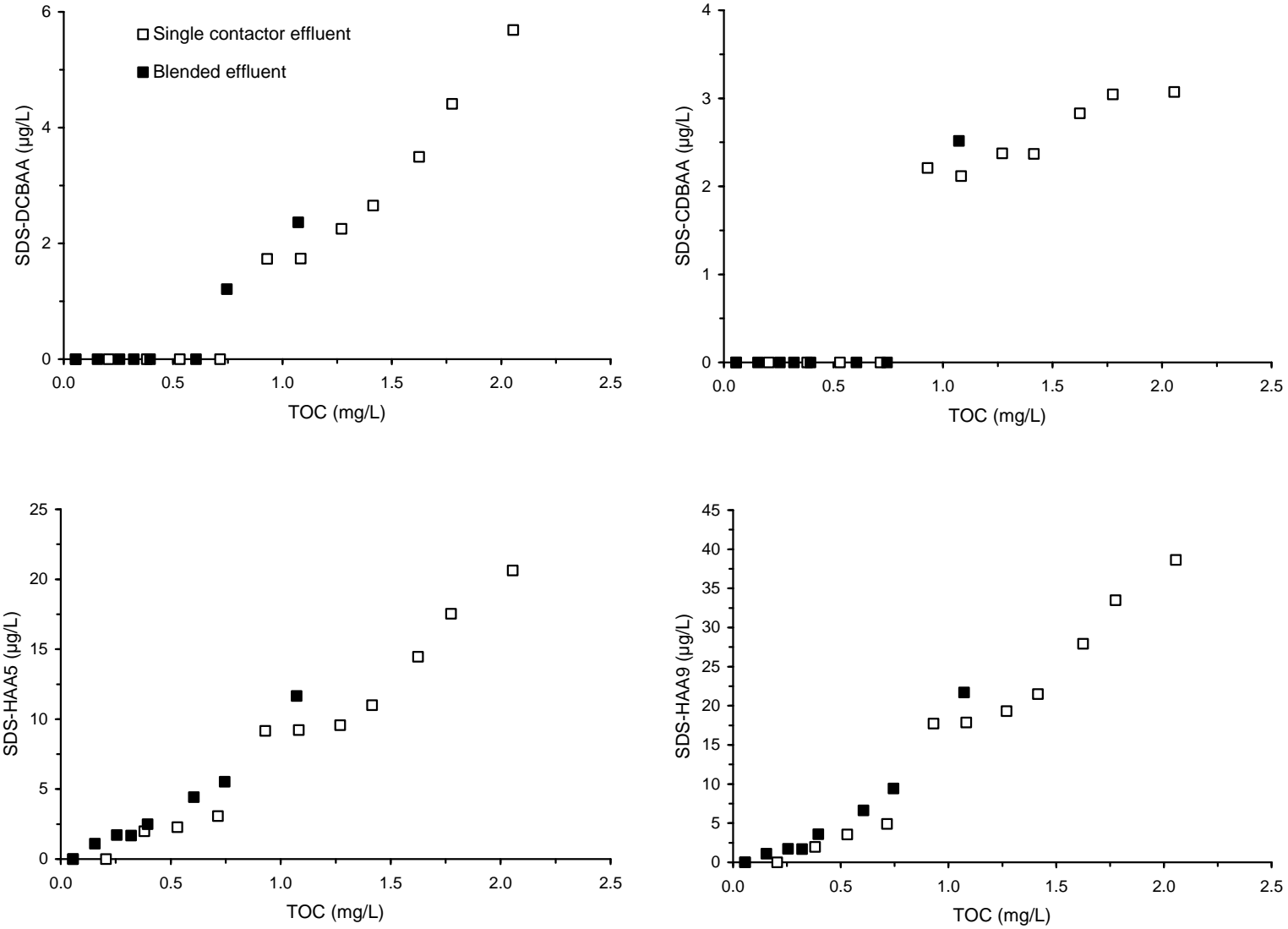


Figure D-30 HAA correlations based on GAC effluent TOC concentration for single contactor and blended effluents for Water 6

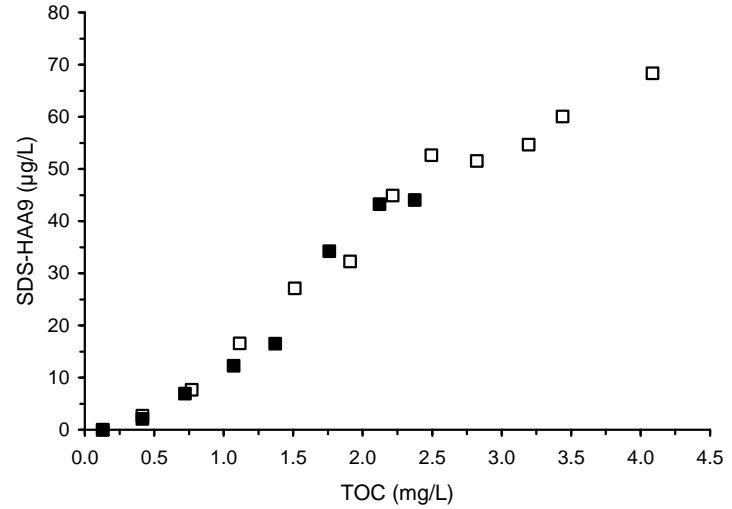
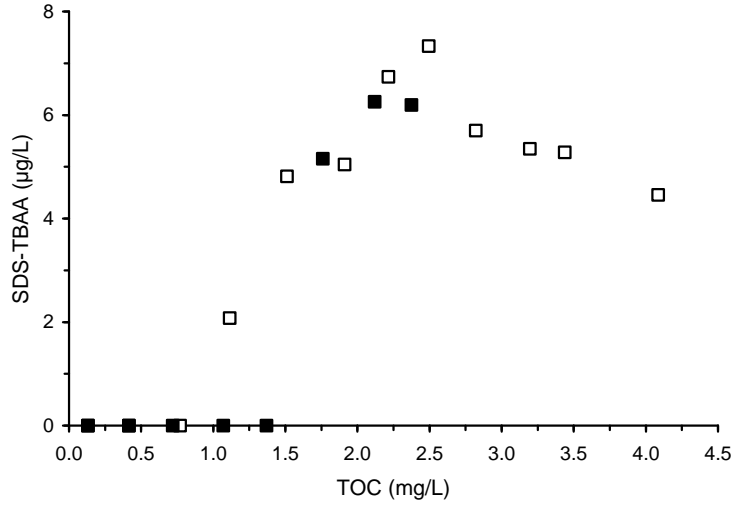
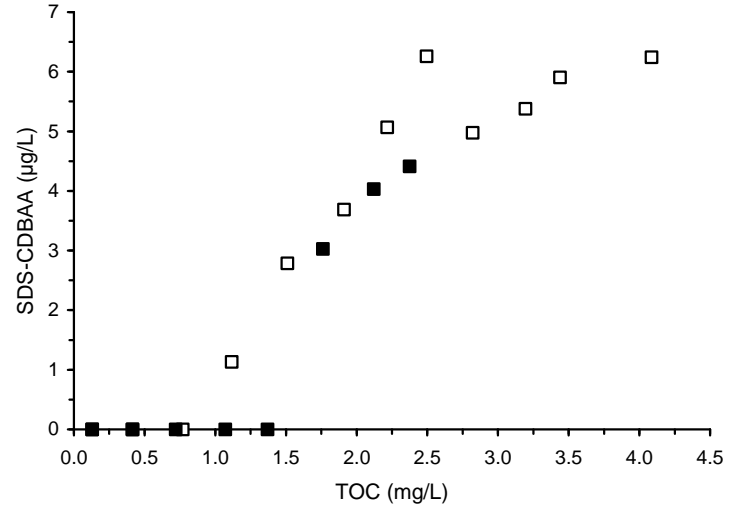
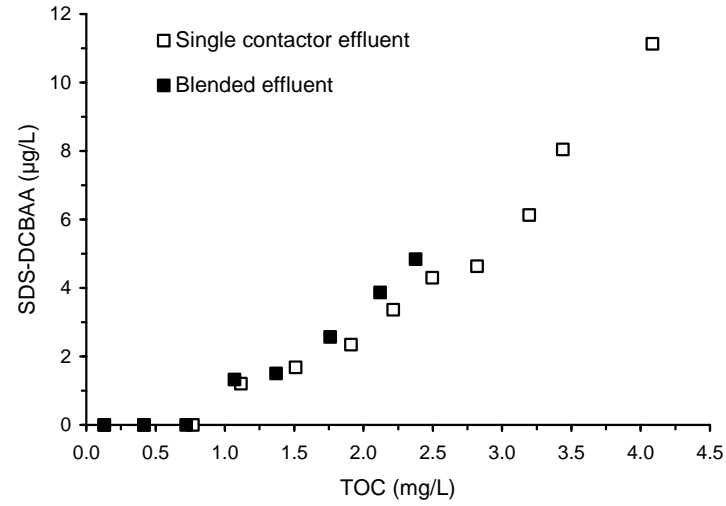


Figure D-31 HAA correlations based on GAC effluent TOC concentration for single contactor and blended effluents for Water 7

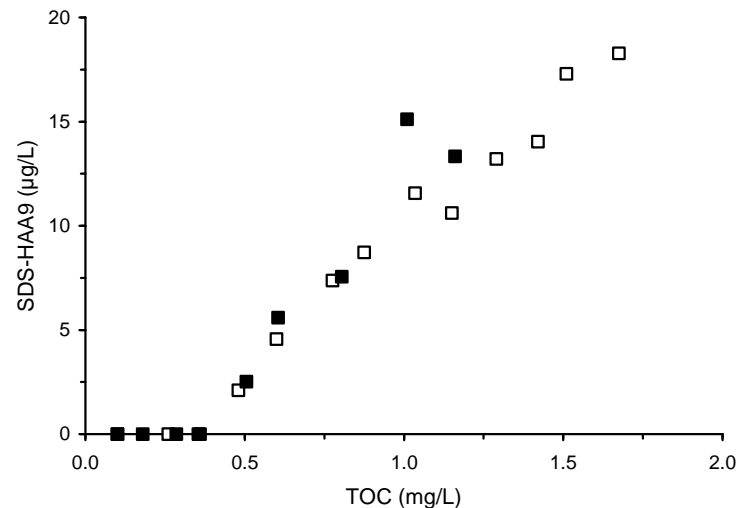
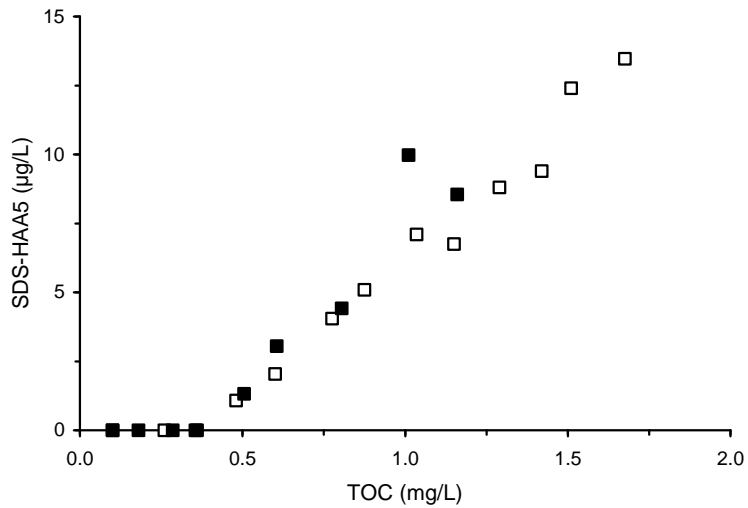
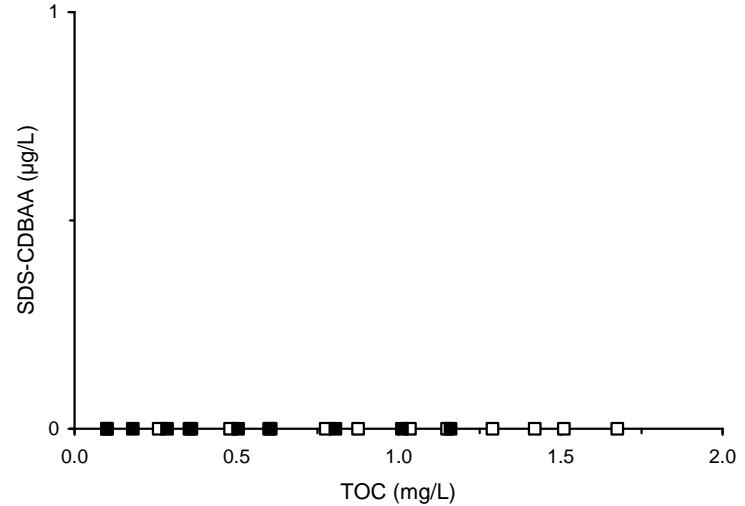
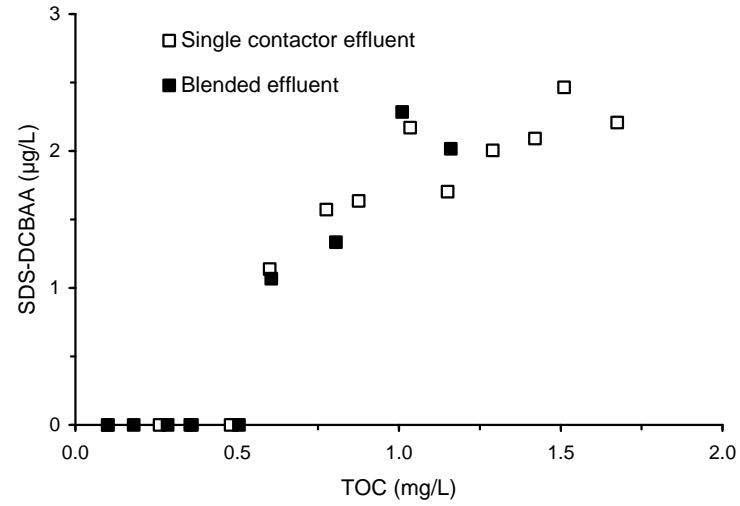


Figure D-32 HAA correlations based on GAC effluent TOC concentration for single contactor and blended effluents for Water 8

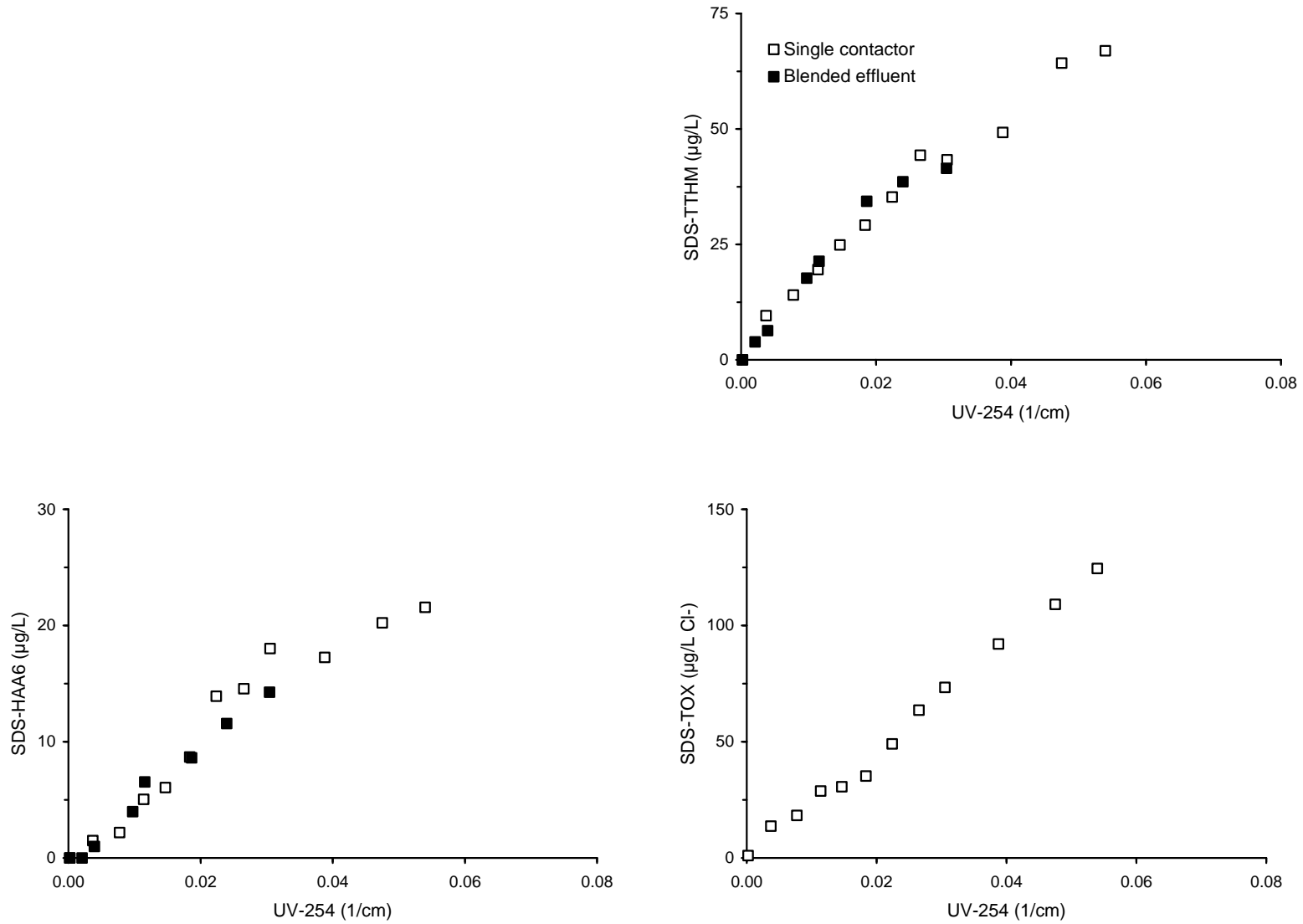


Figure D-33 Correlations based on GAC effluent UV-254 absorbance for single contactor and blended effluents for Water 1

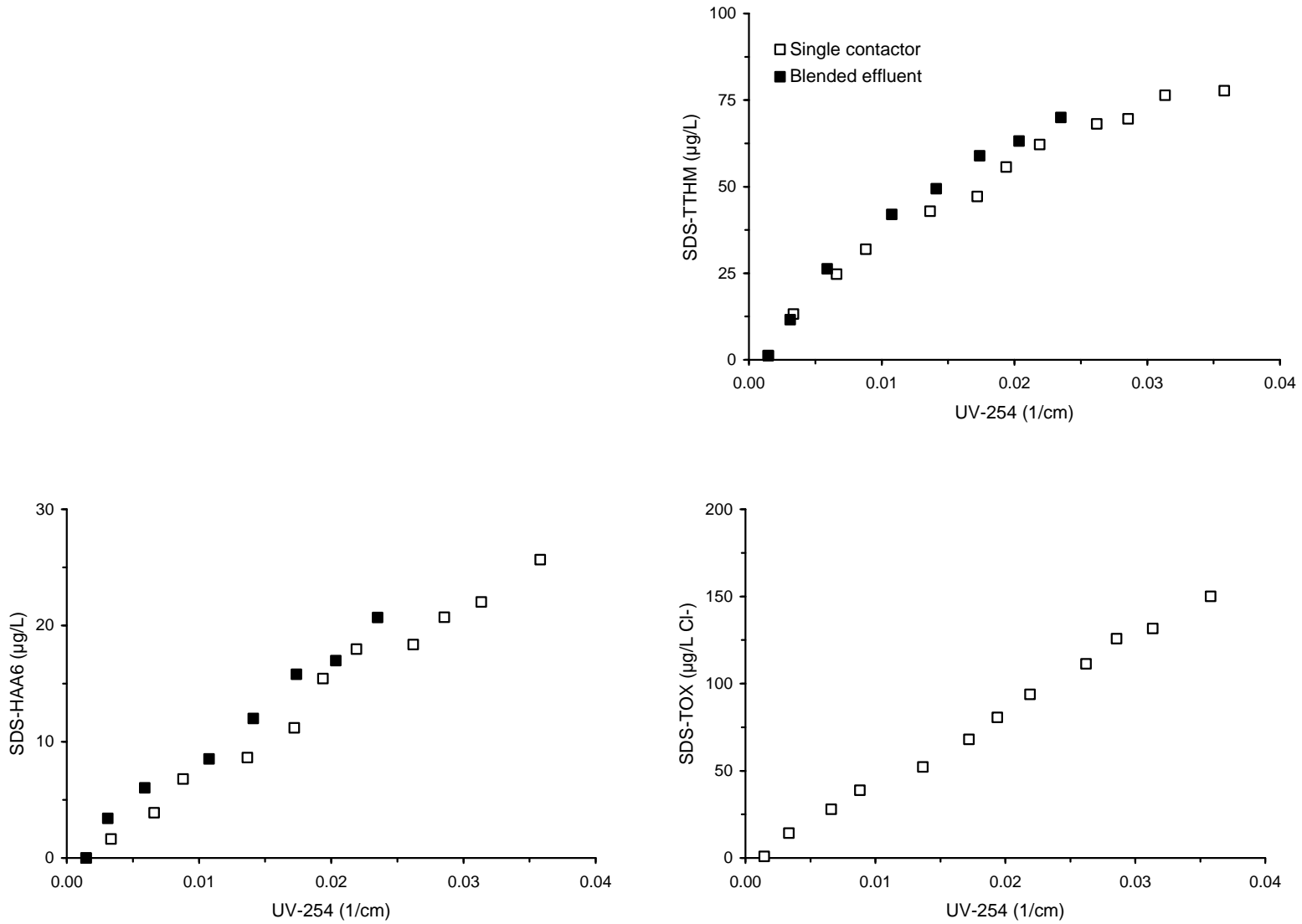


Figure D-34 Correlations based on GAC effluent UV-254 absorbance for single contactor and blended effluents for Water 2

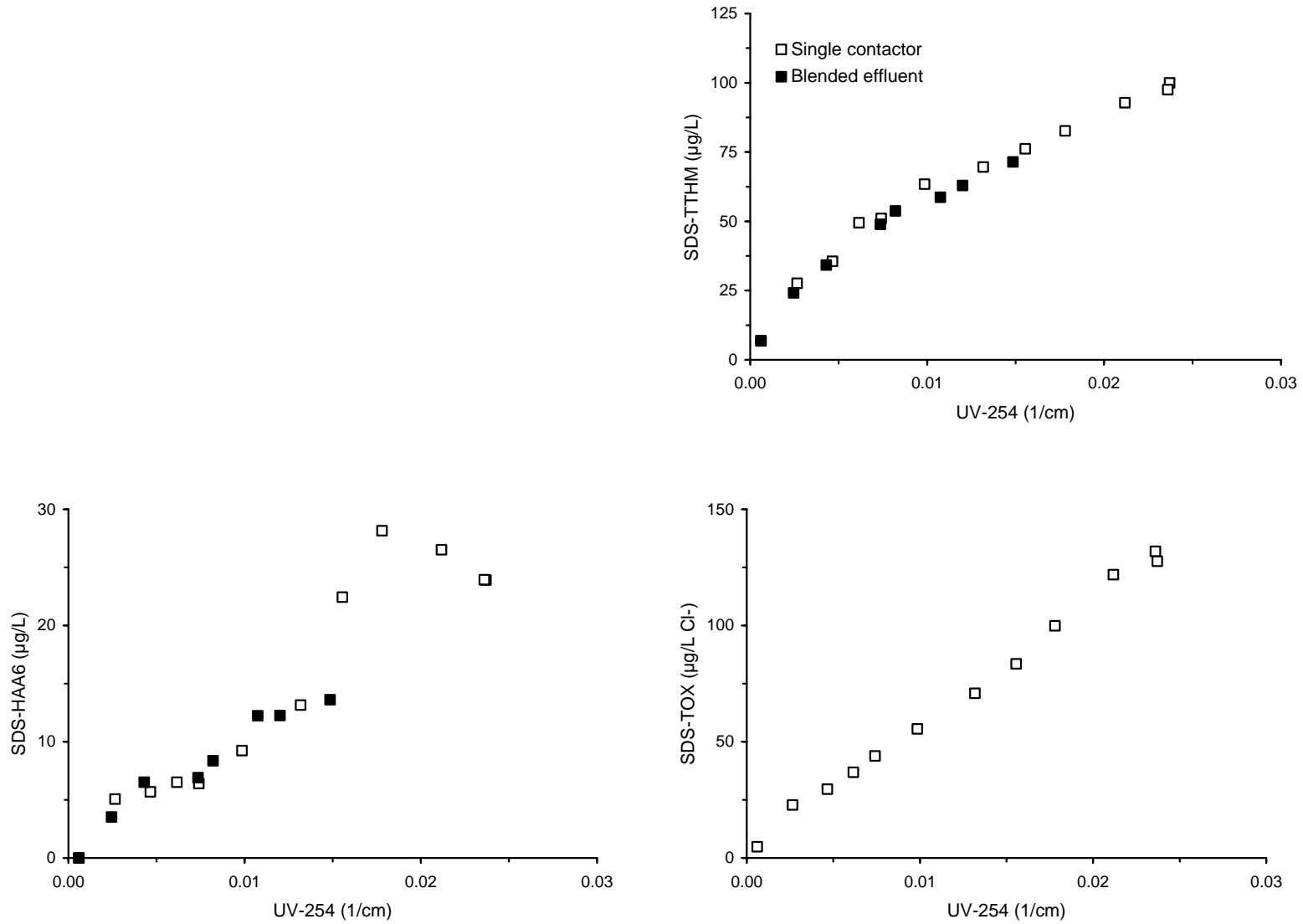


Figure D-35 Correlations based on GAC effluent UV-254 absorbance for single contactor and blended effluents for Water 3

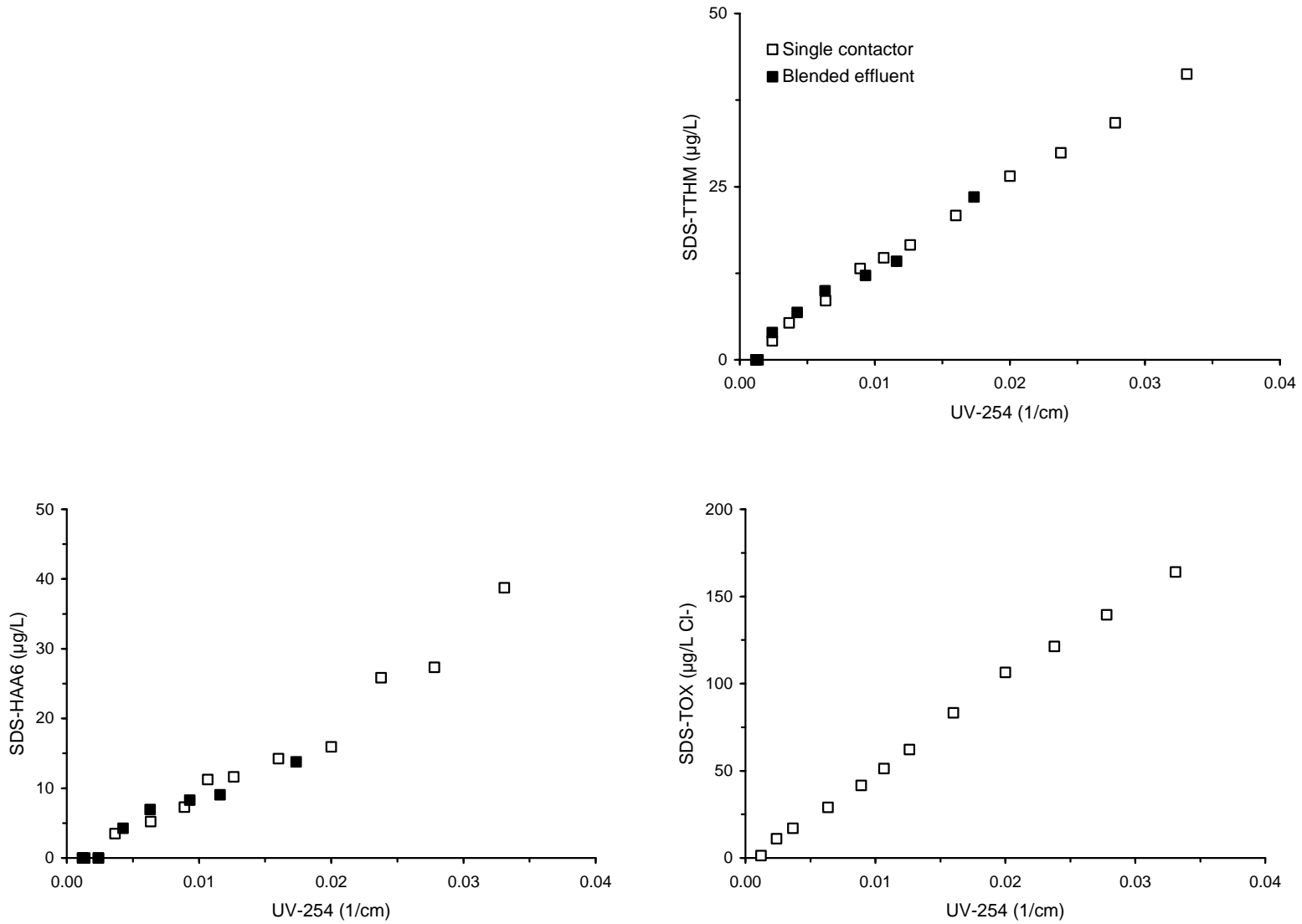


Figure D-36 Correlations based on GAC effluent UV-254 absorbance for single contactor and blended effluents for Water 4

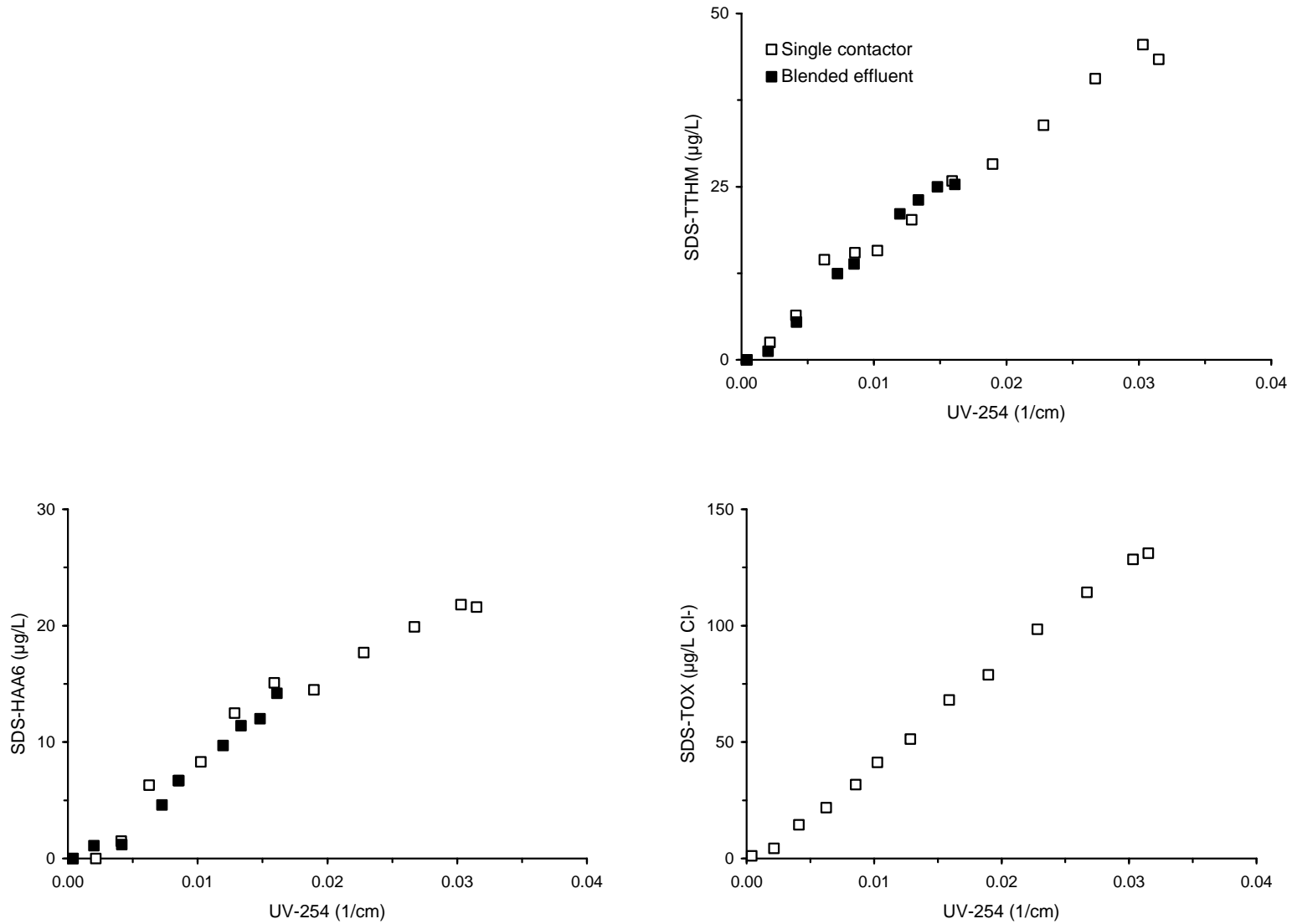


Figure D-37 Correlations based on GAC effluent UV-254 absorbance for single contactor and blended effluents for Water 5

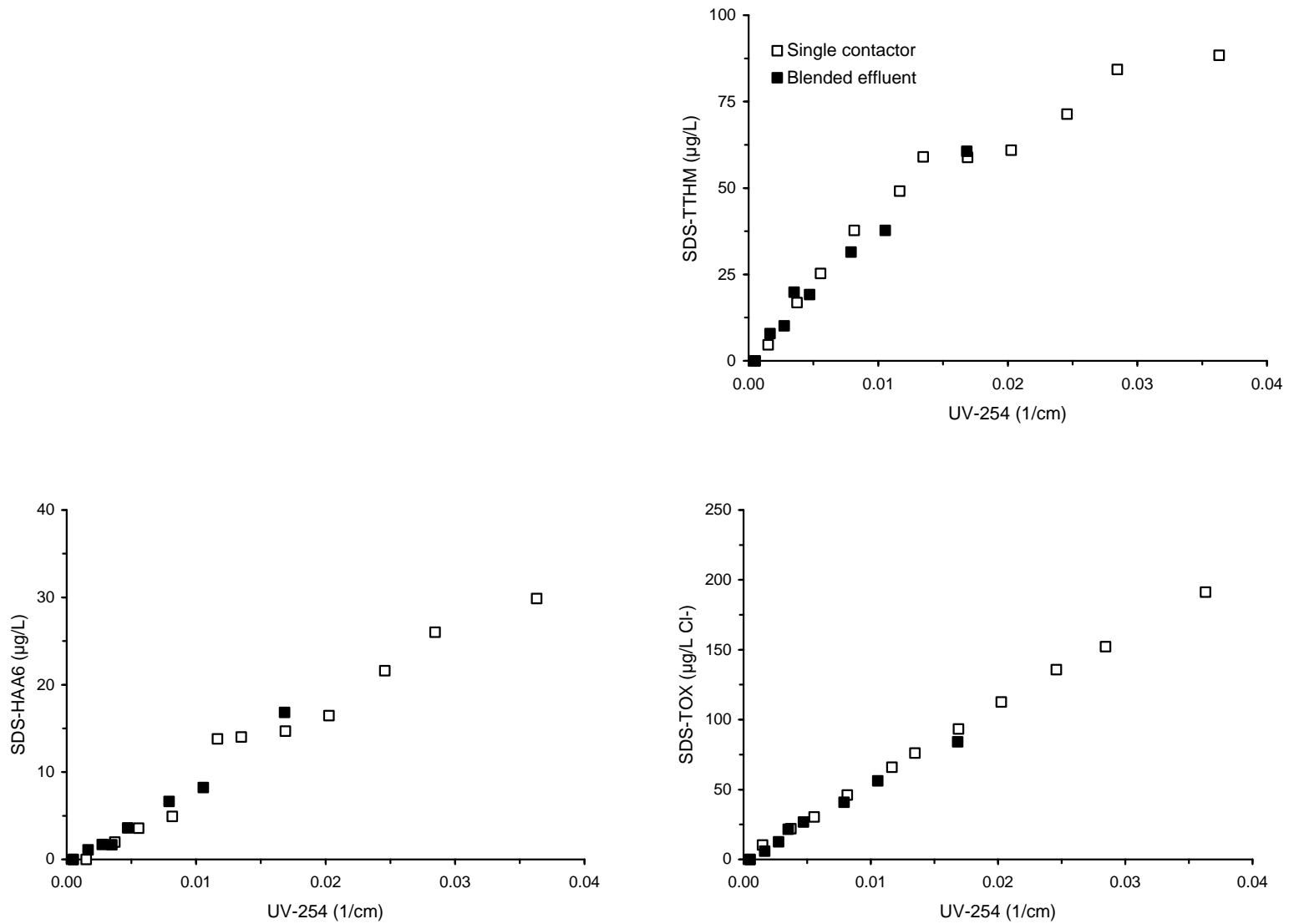


Figure D-38 Correlations based on GAC effluent UV-254 absorbance for single contactor and blended effluents for Water 6

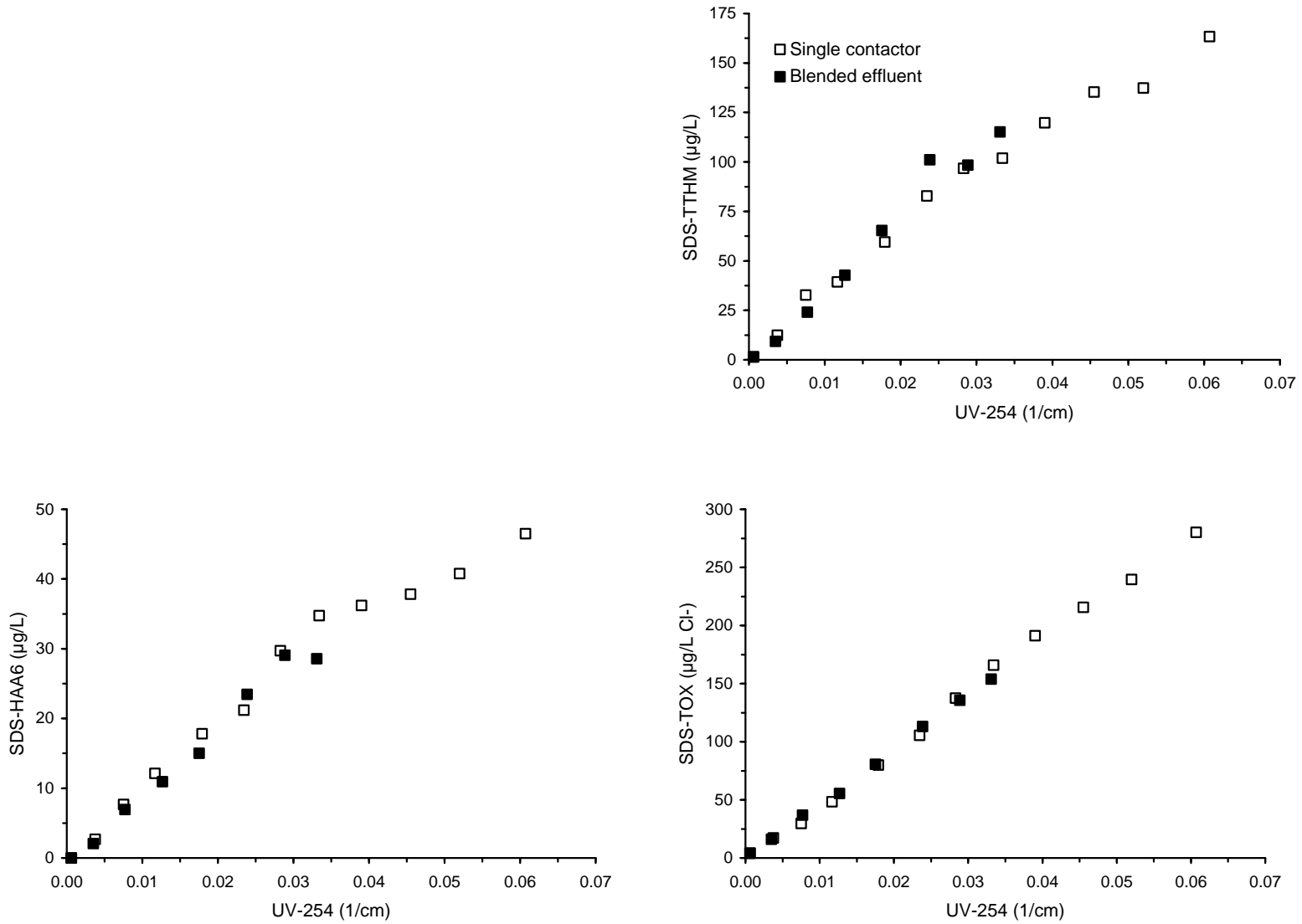


Figure D-39 Correlations based on GAC effluent UV-254 absorbance for single contactor and blended effluents for Water 7

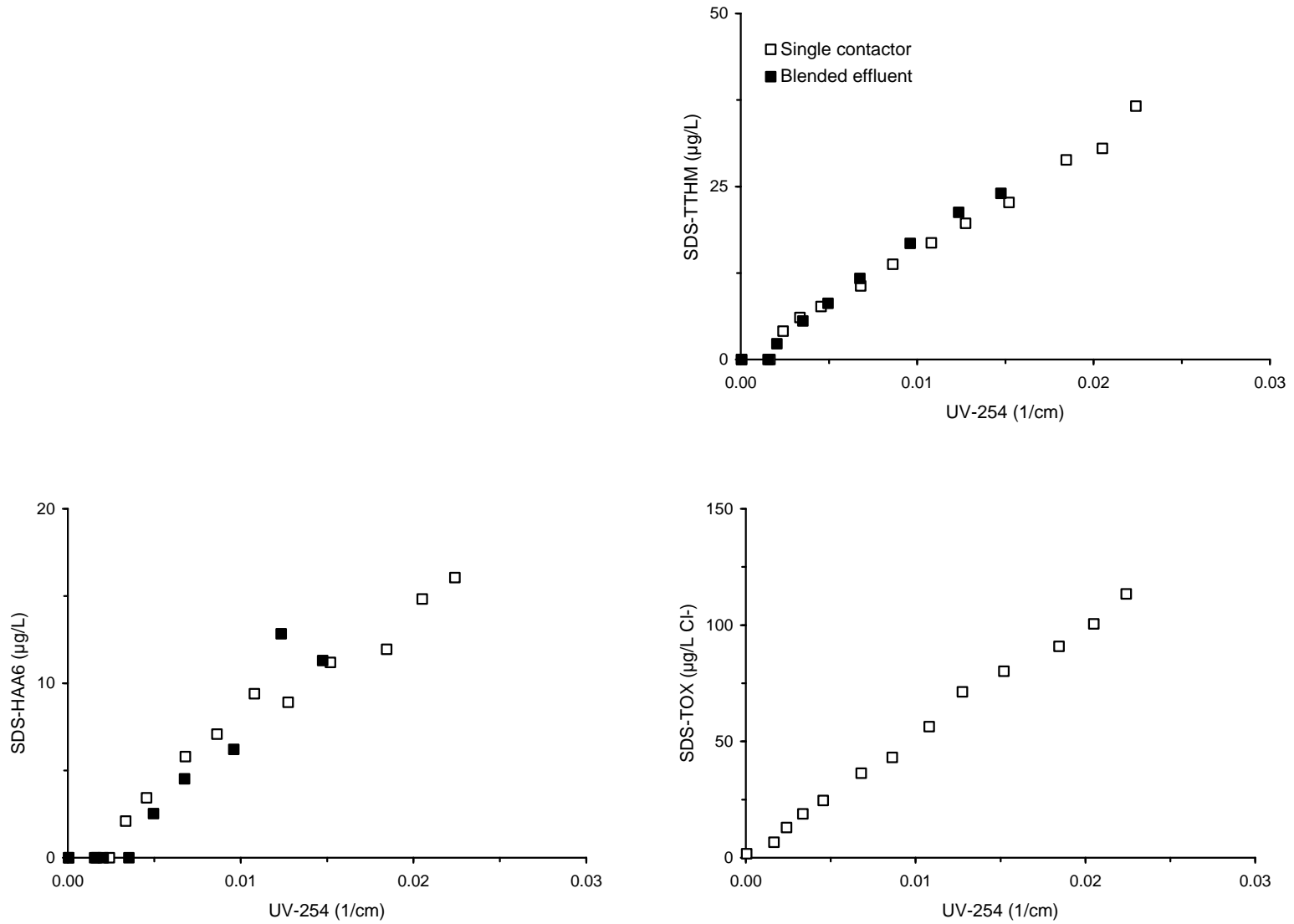


Figure D-40 Correlations based on GAC effluent UV-254 absorbance for single contactor and blended effluents for Water 8

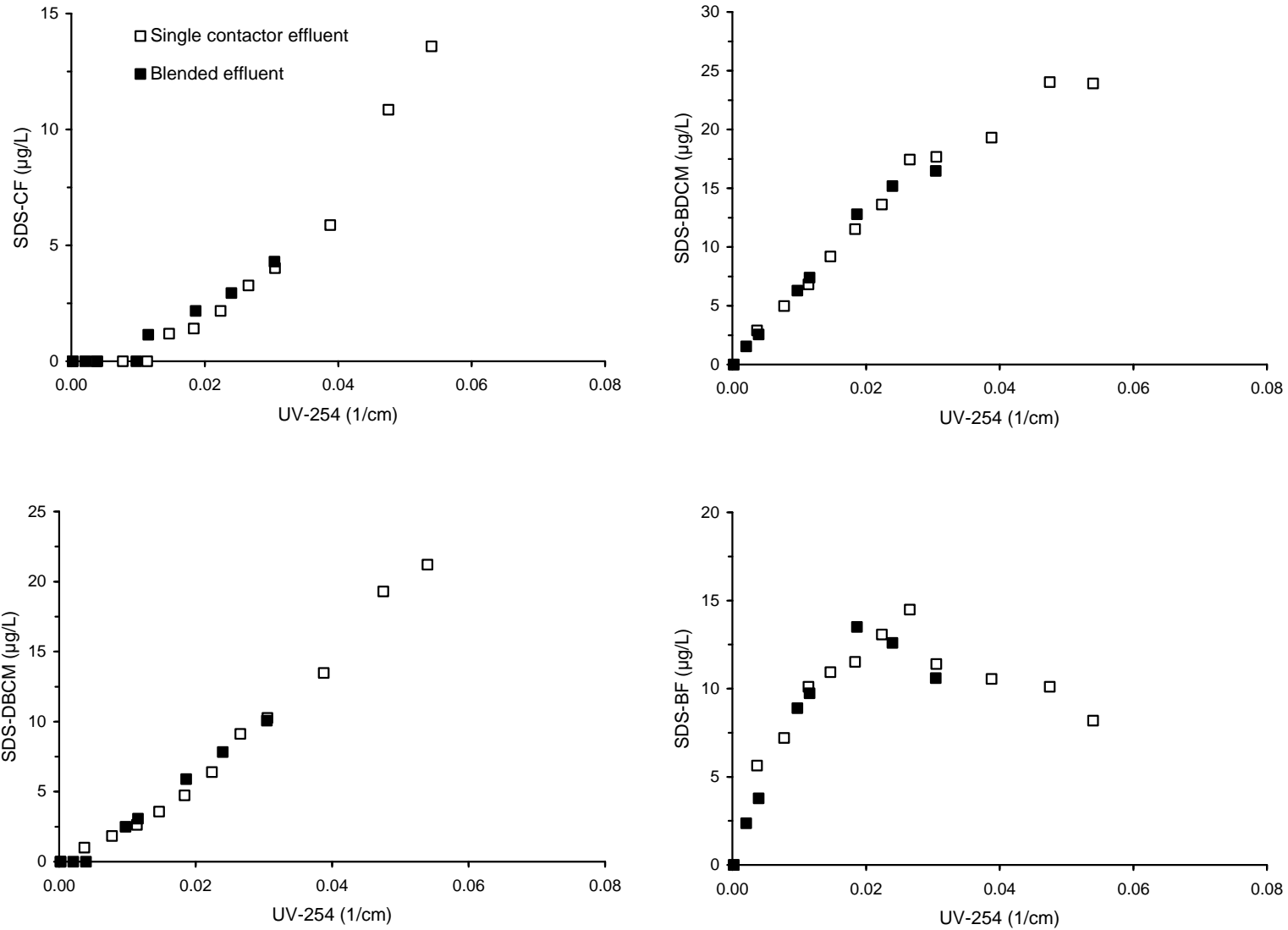


Figure D-41 THM correlations based on GAC effluent UV-254 absorbance for single contactor and blended effluents for Water 1

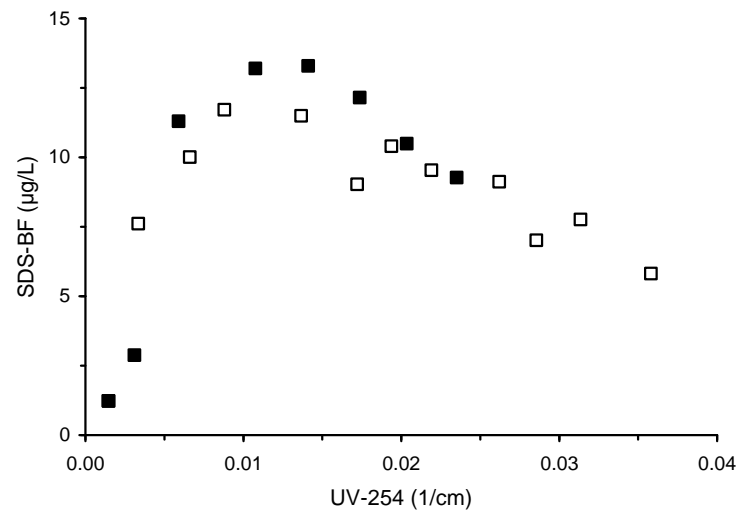
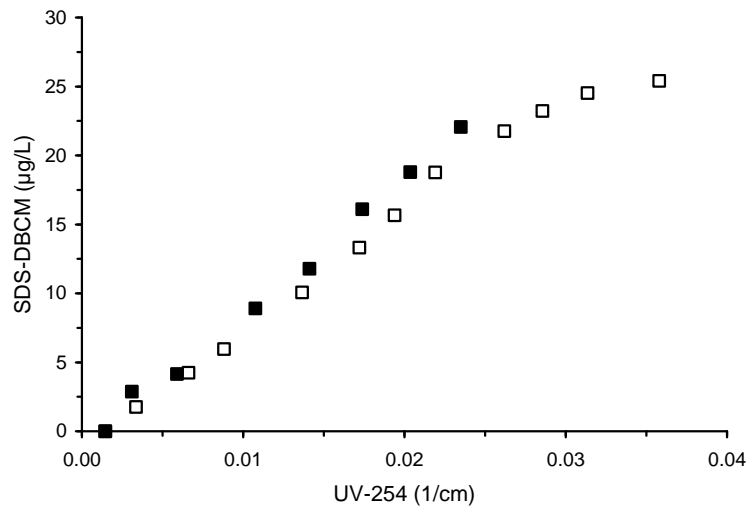
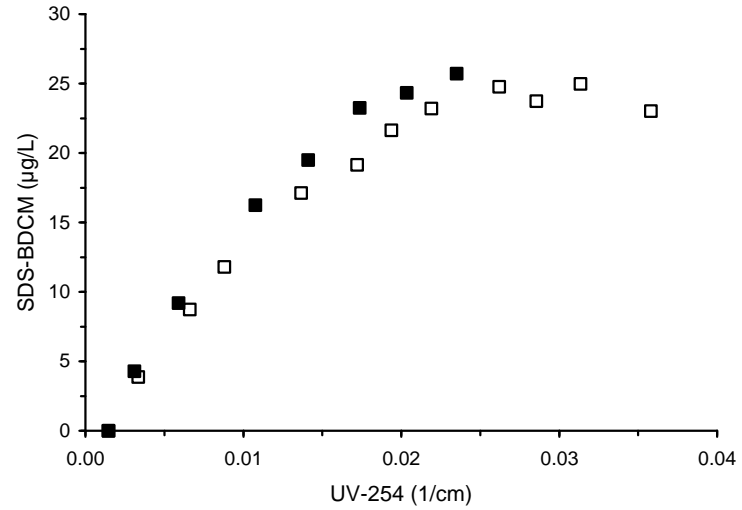
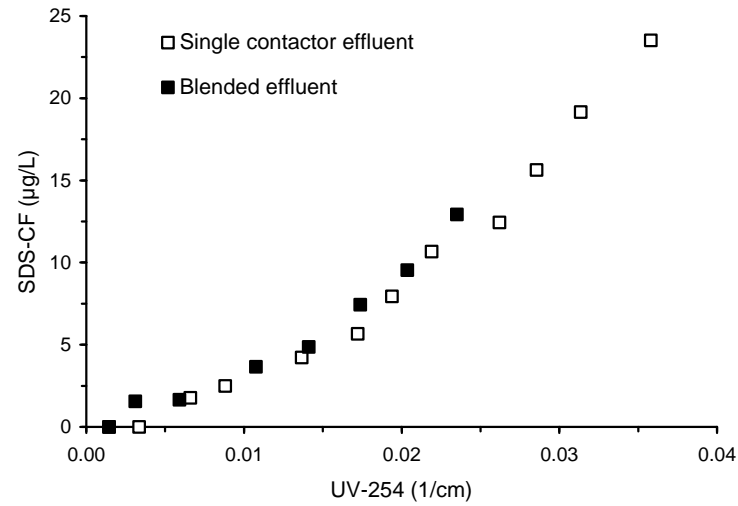


Figure D-42 THM correlations based on GAC effluent UV-254 absorbance for single contactor and blended effluents for Water 2

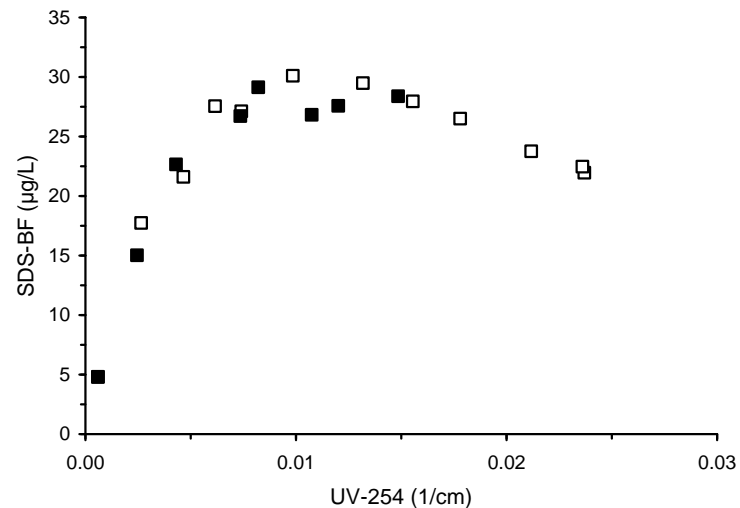
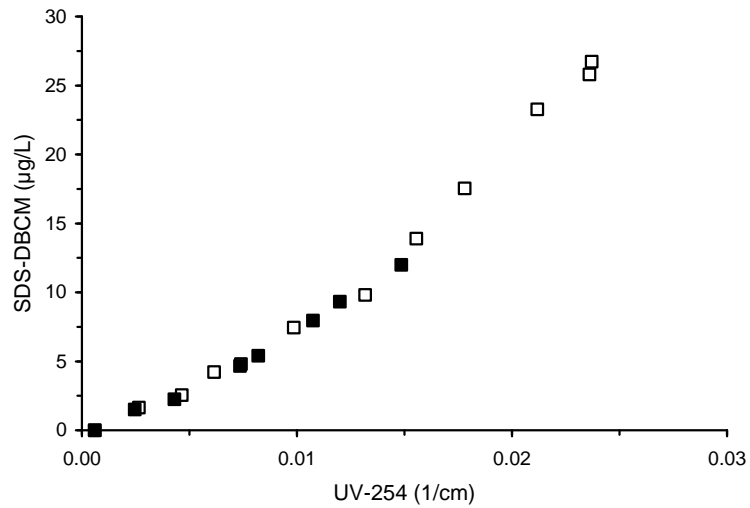
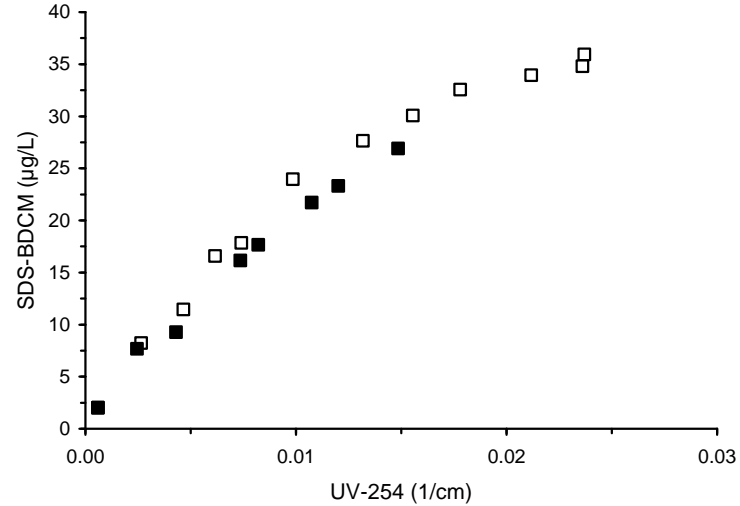
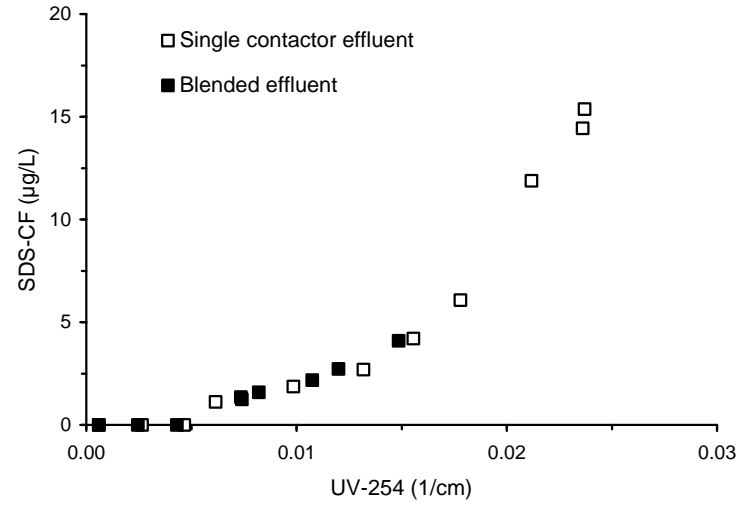


Figure D-43 THM correlations based on GAC effluent UV-254 absorbance for single contactor and blended effluents for Water 3

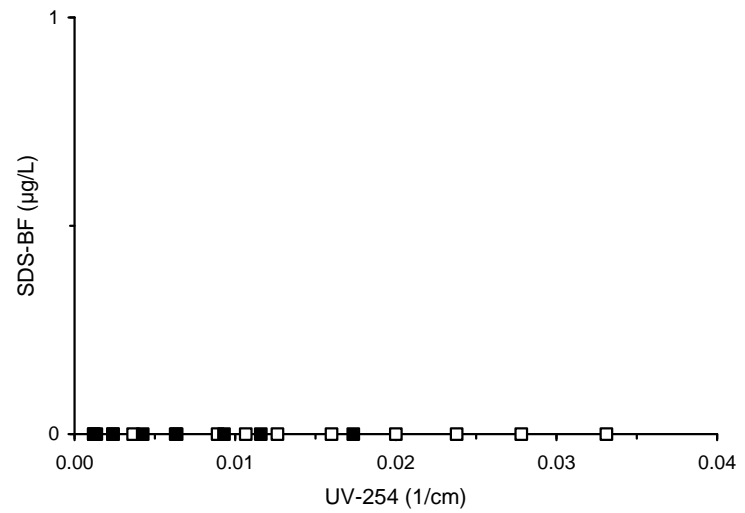
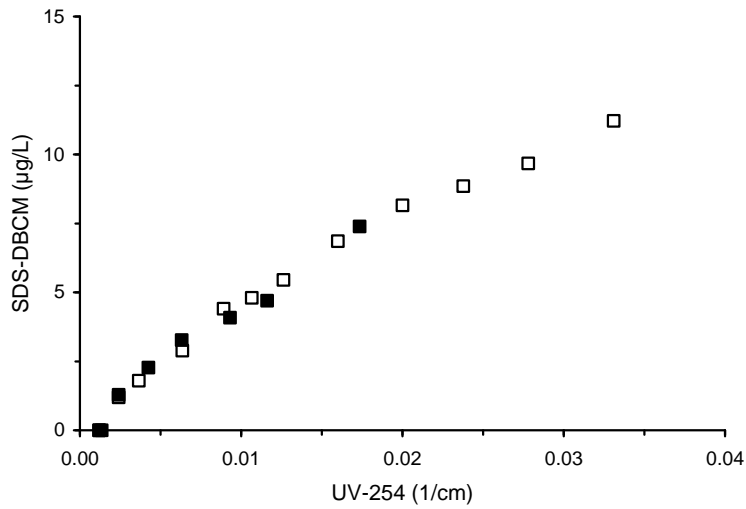
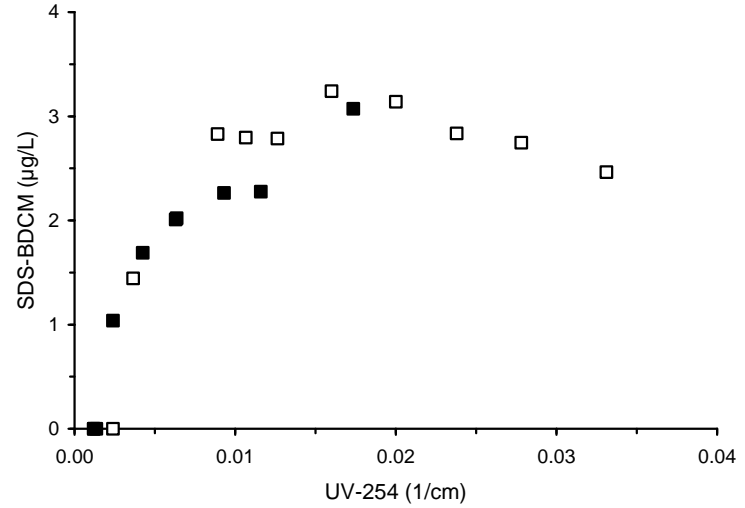
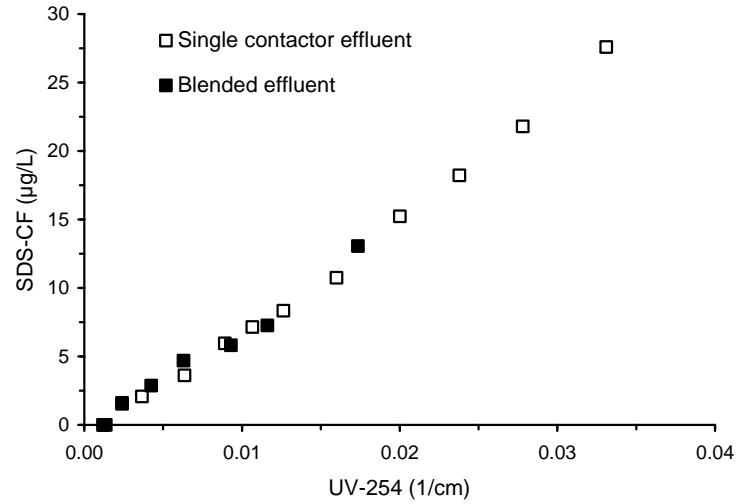


Figure D-44 THM correlations based on GAC effluent UV-254 absorbance for single contactor and blended effluents for Water 4

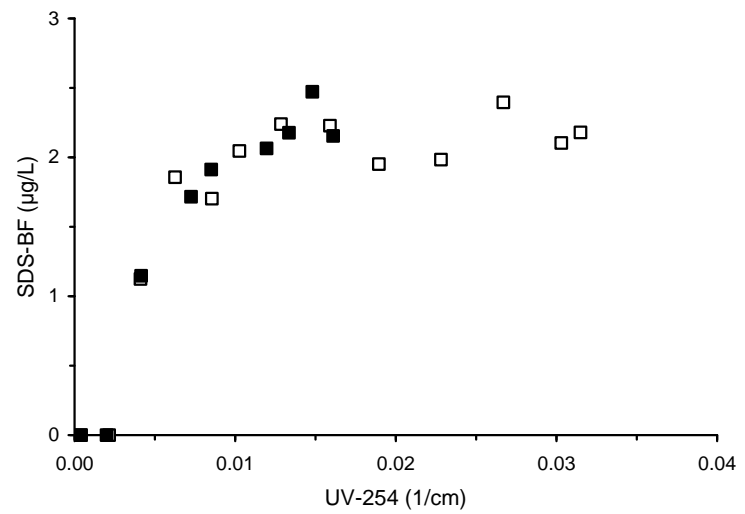
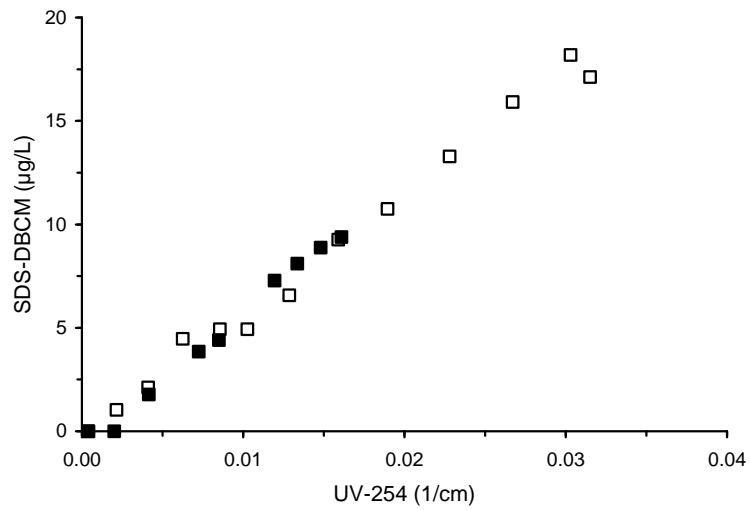
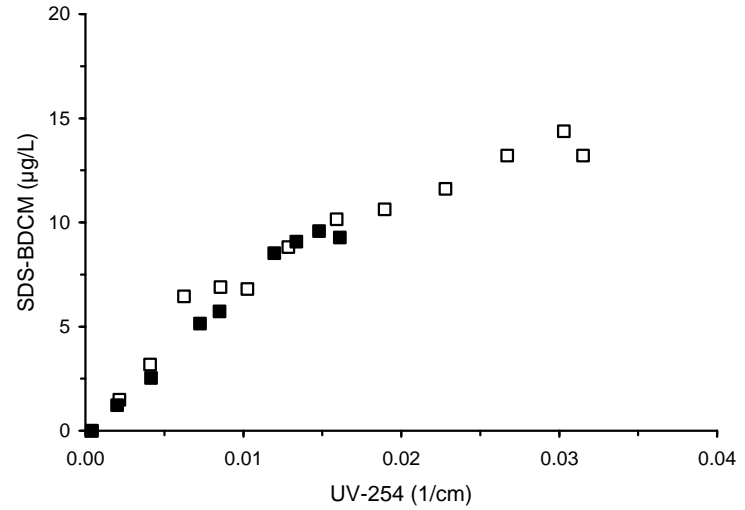
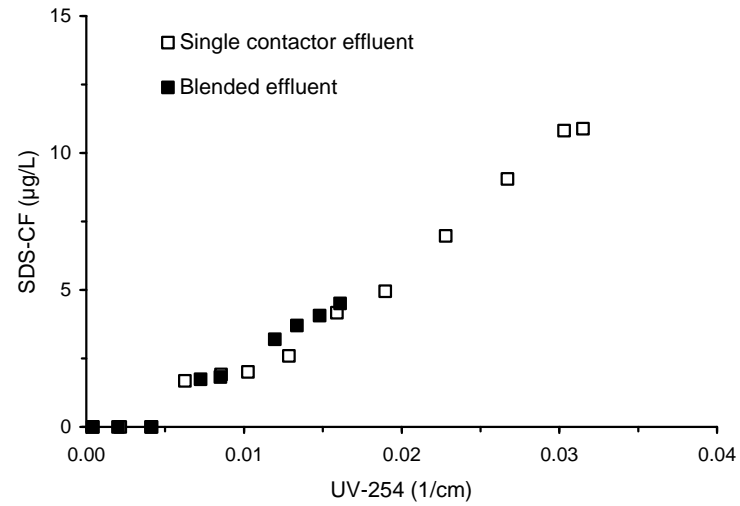


Figure D-45 THM correlations based on GAC effluent UV-254 absorbance for single contactor and blended effluents for Water 5

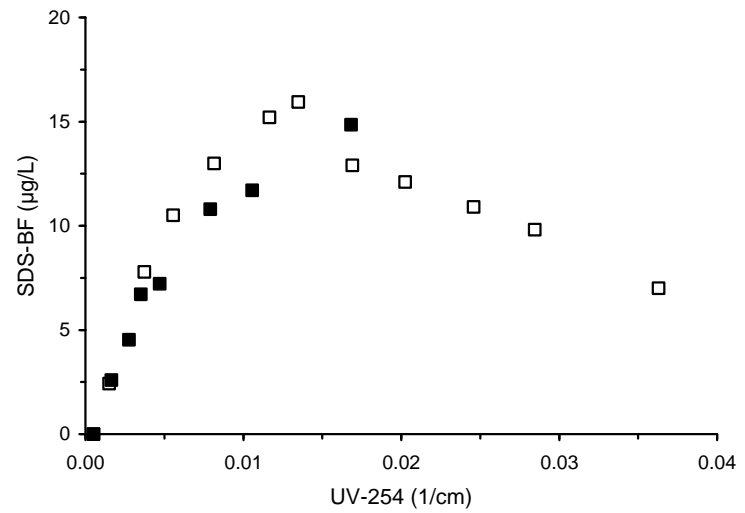
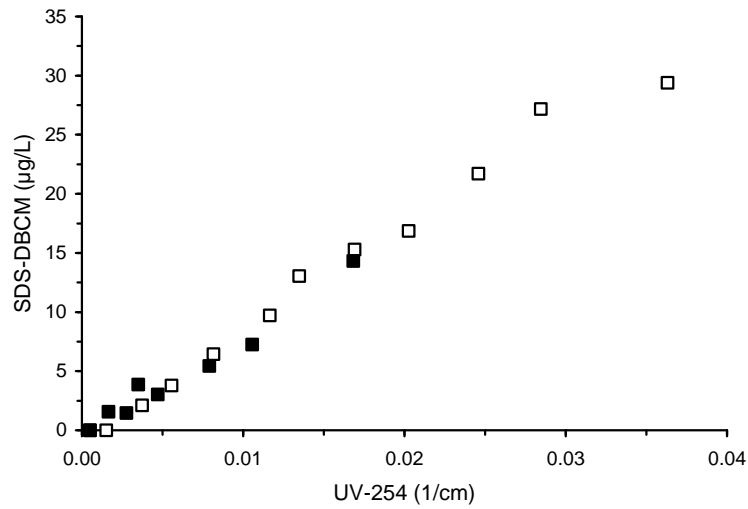
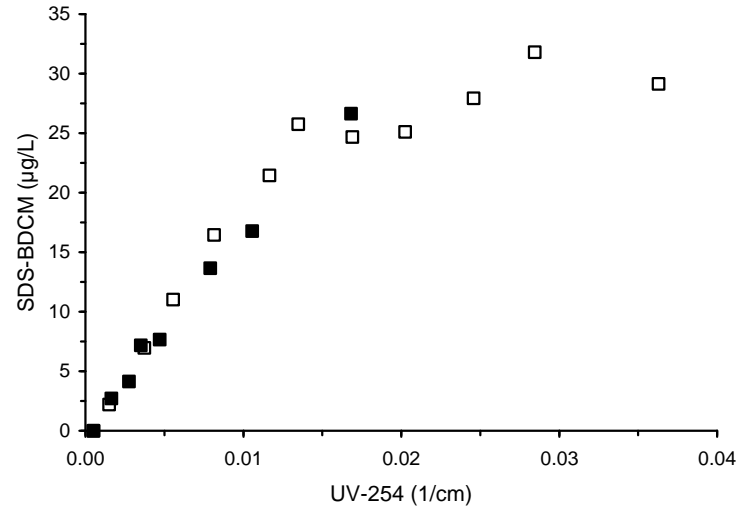
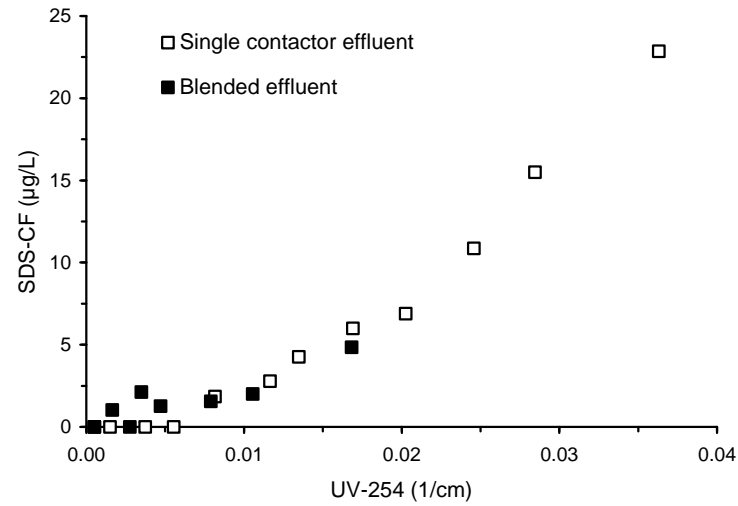


Figure D-46 THM correlations based on GAC effluent UV-254 absorbance for single contactor and blended effluents for Water 6

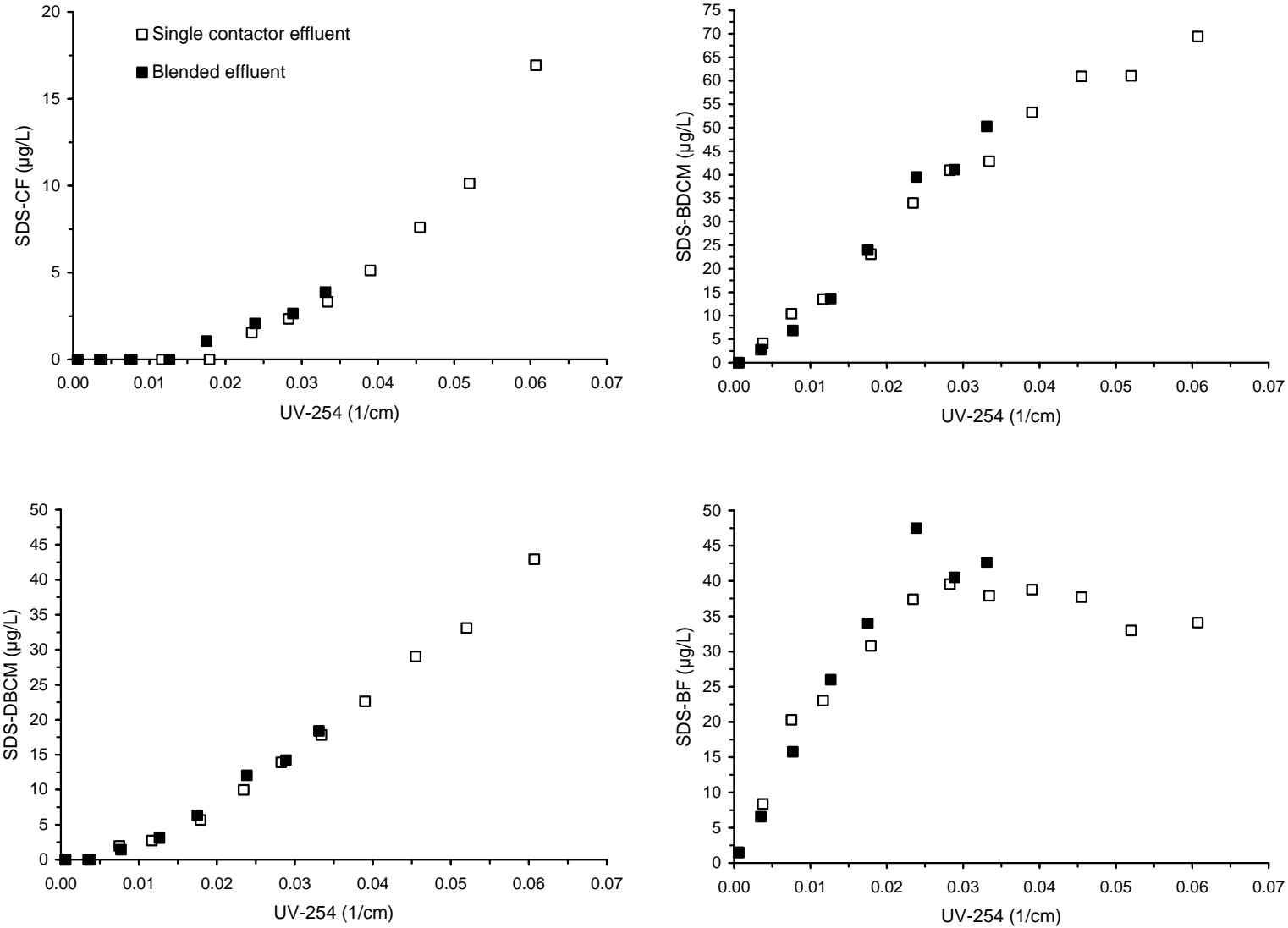


Figure D-47 THM correlations based on GAC effluent UV-254 absorbance for single contactor and blended effluents for Water 7

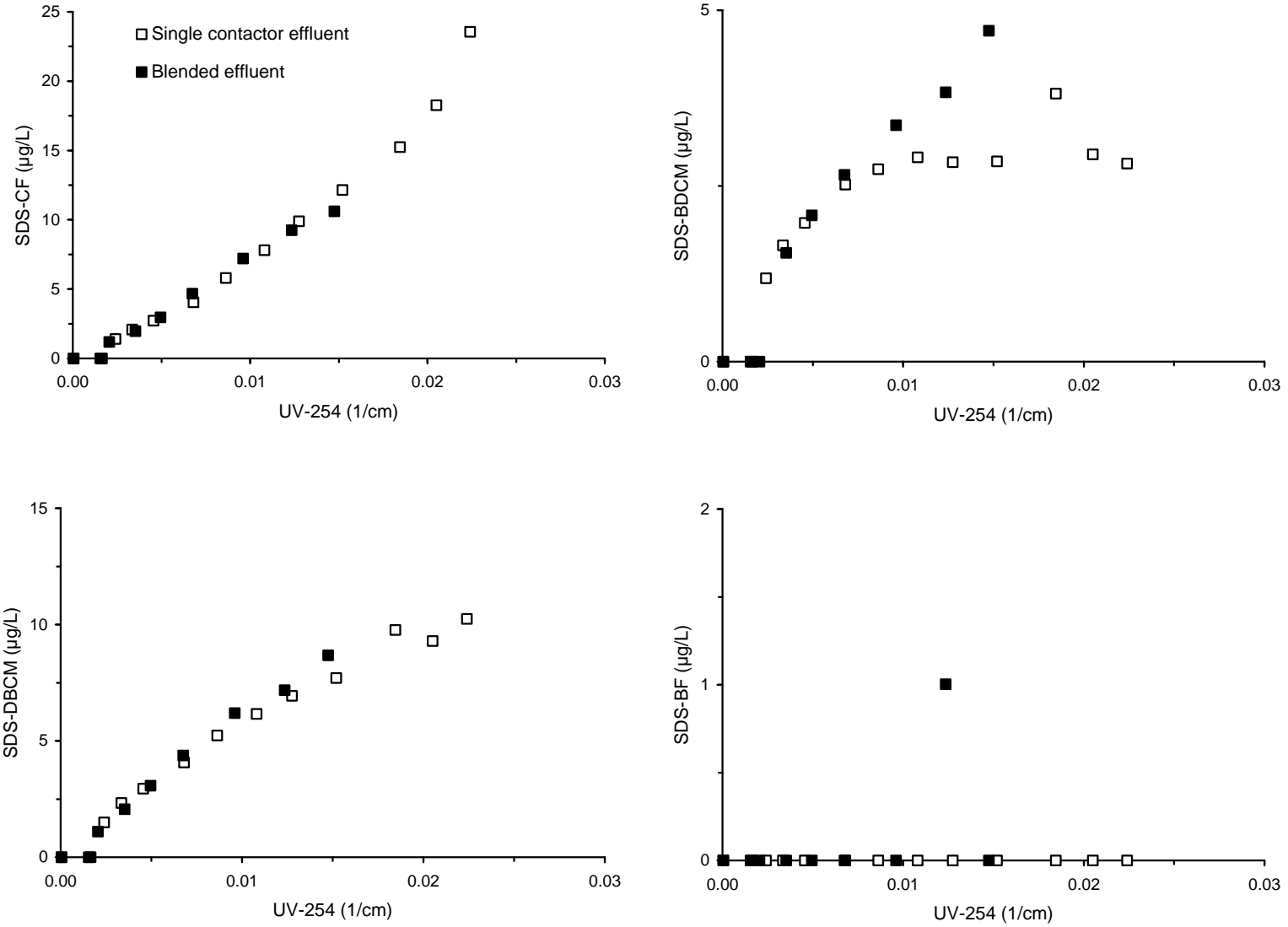


Figure D-48 THM correlations based on GAC effluent UV-254 absorbance for single contactor and blended effluents for Water 8

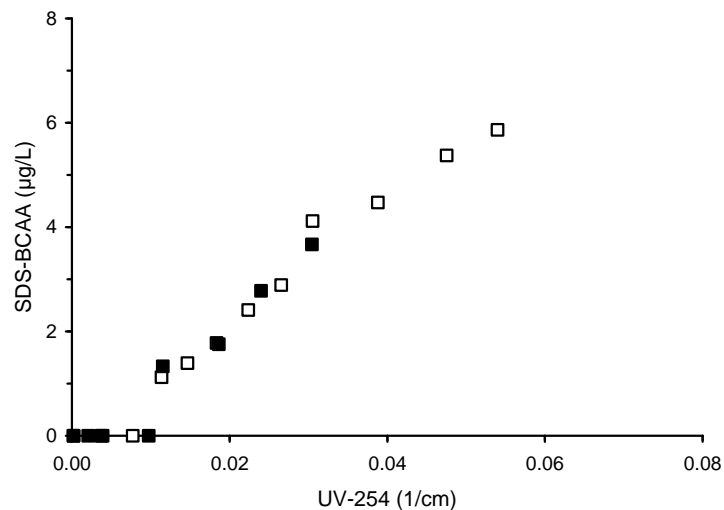
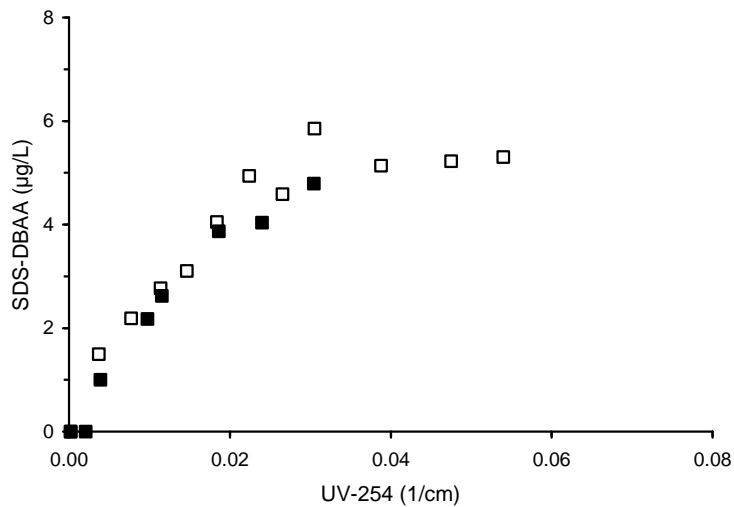
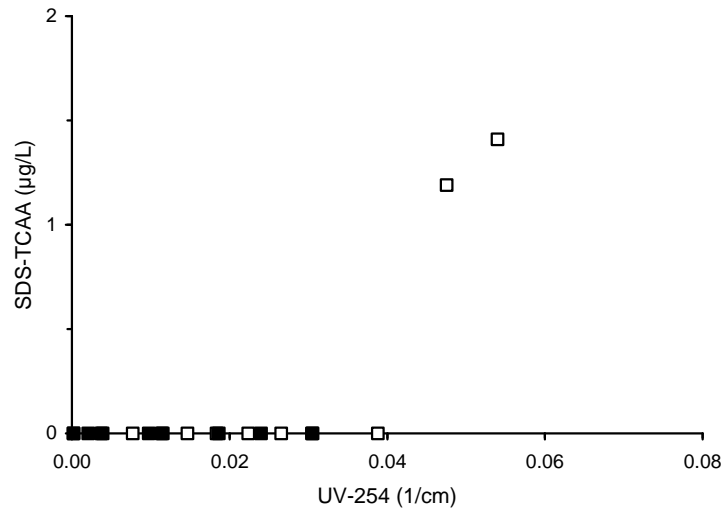
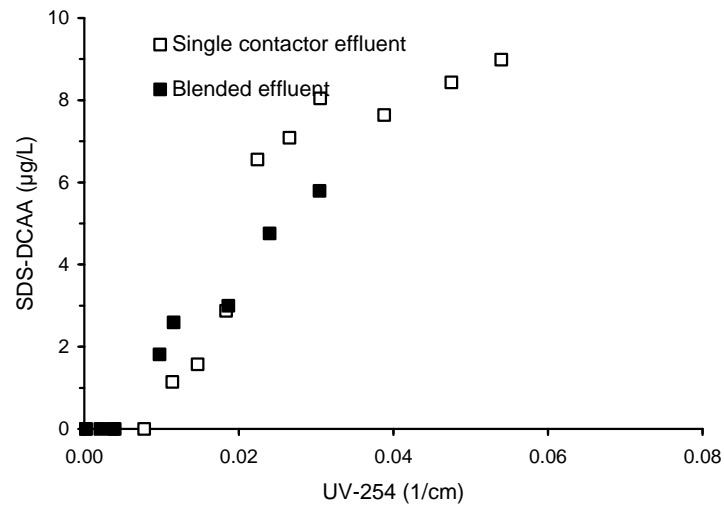


Figure D-49 HAA correlations based on GAC effluent UV-254 absorbance for single contactor and blended effluents for Water 1

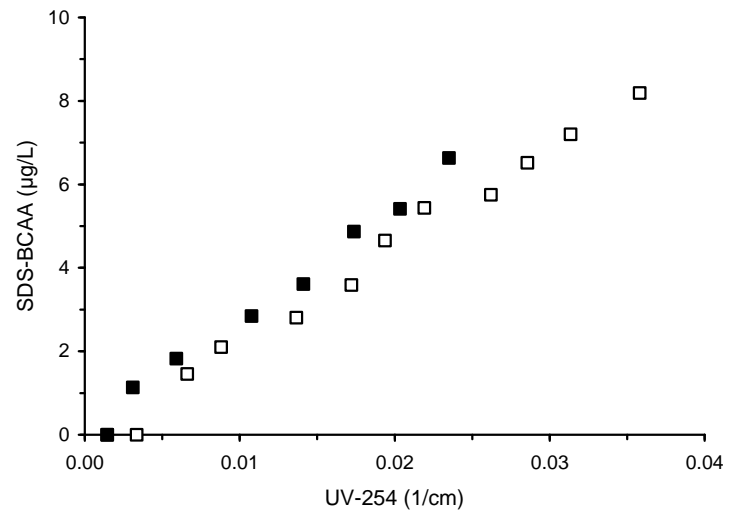
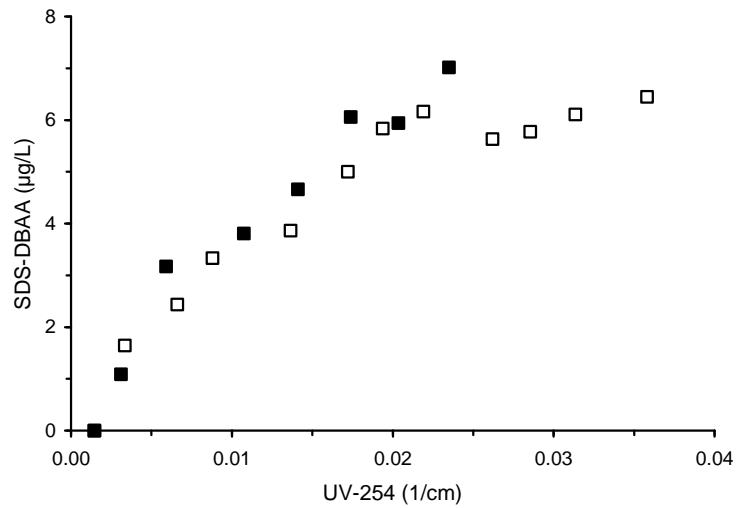
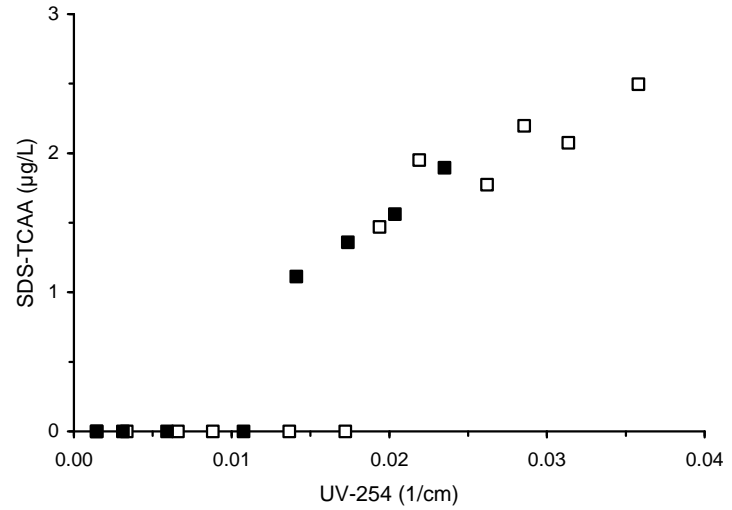
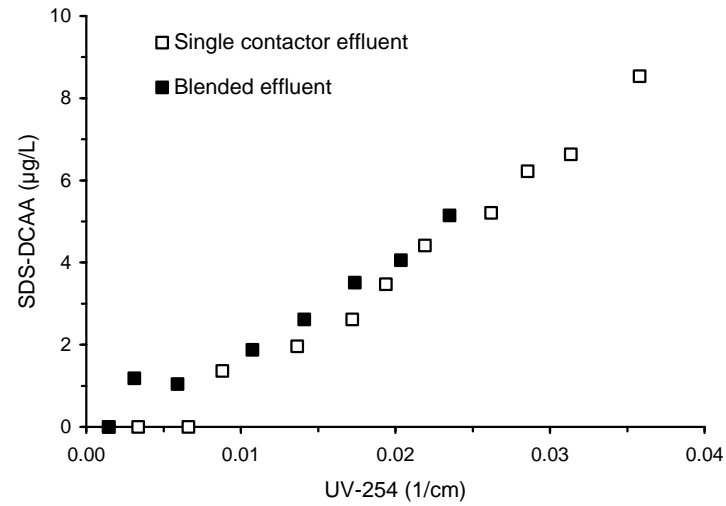


Figure D-50 HAA correlations based on GAC effluent UV-254 absorbance for single contactor and blended effluents for Water 2

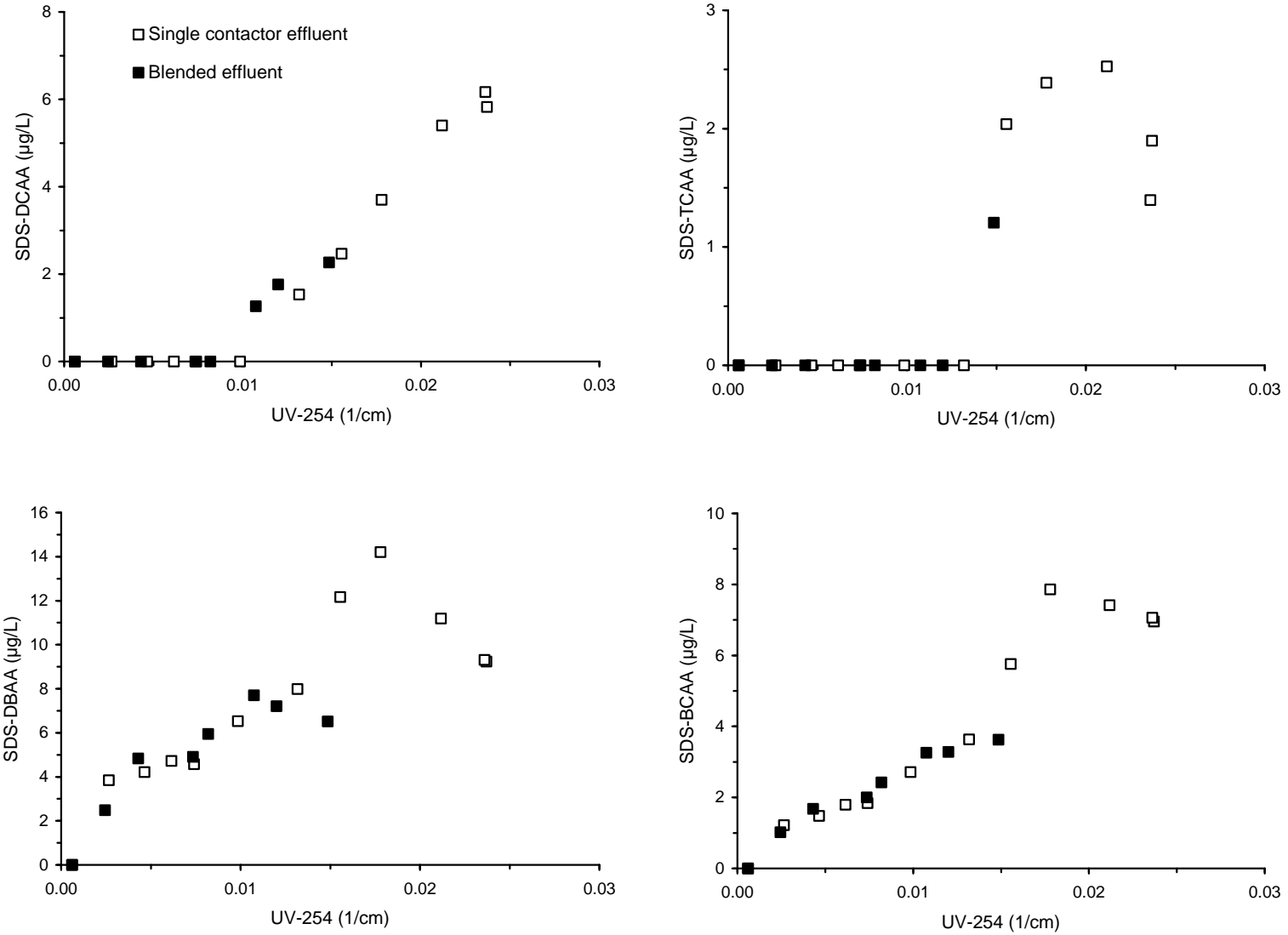


Figure D-51 HAA correlations based on GAC effluent UV-254 absorbance for single contactor and blended effluents for Water 3

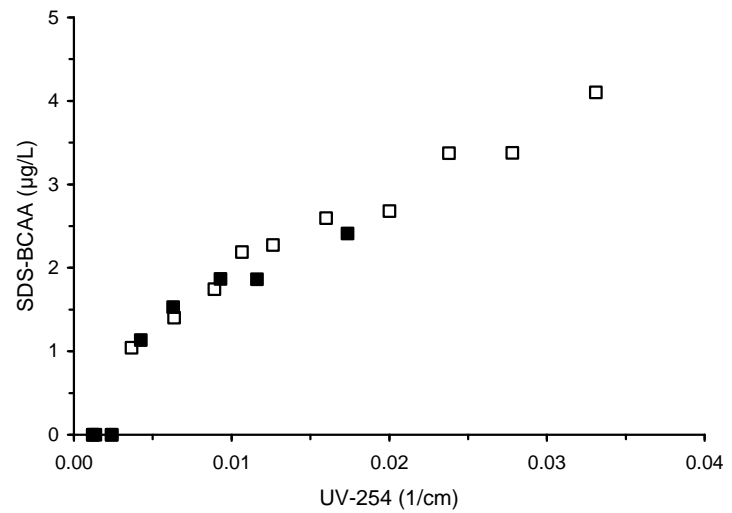
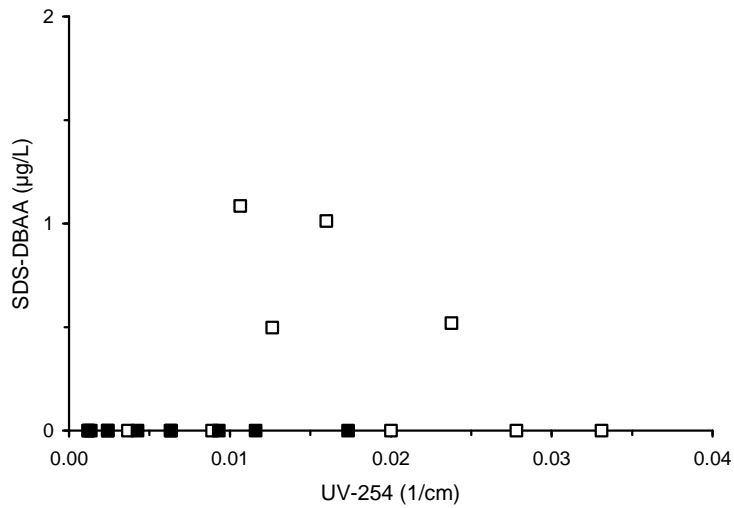
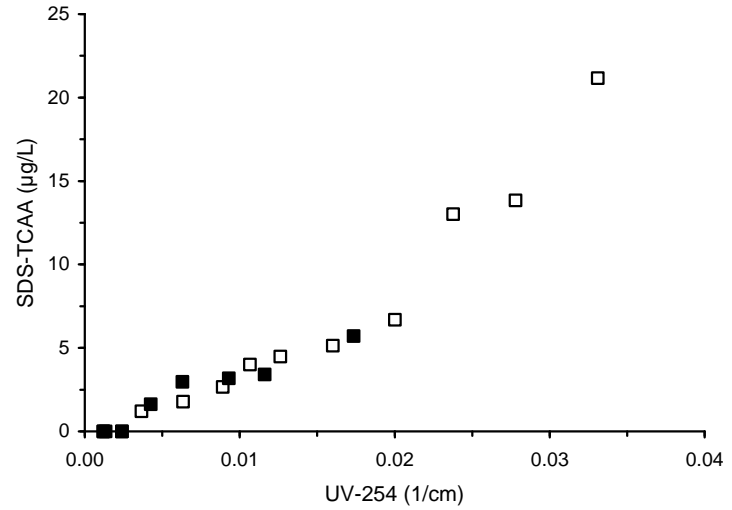
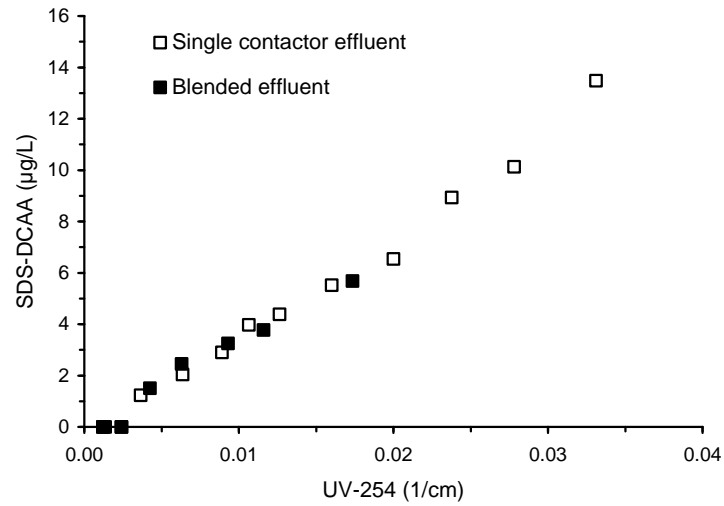


Figure D-52 HAA correlations based on GAC effluent UV-254 absorbance for single contactor and blended effluents for Water 4

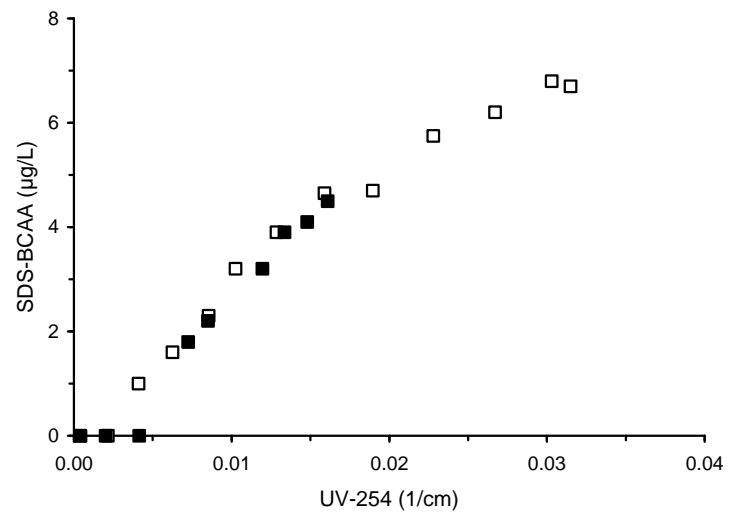
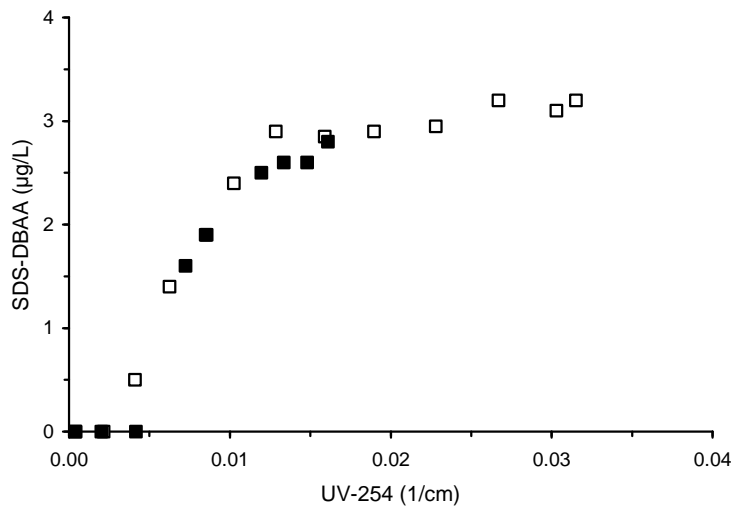
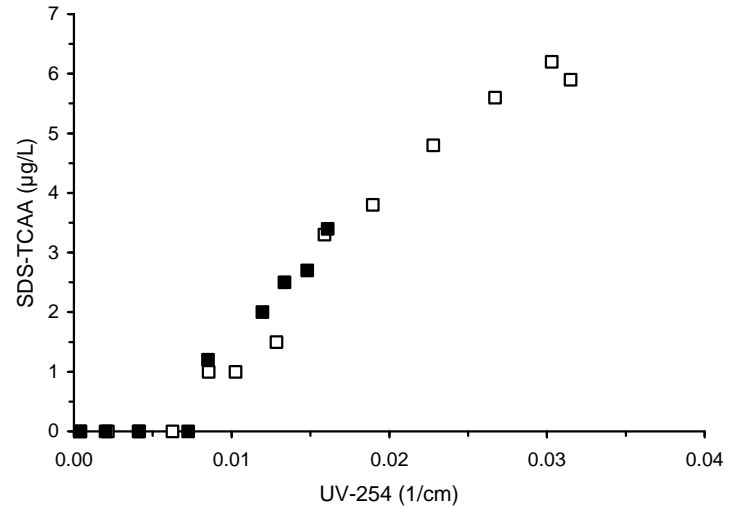
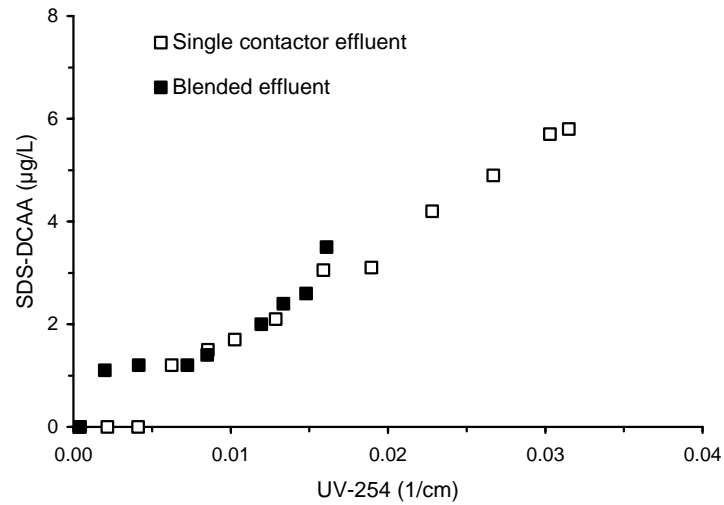


Figure D-53 HAA correlations based on GAC effluent UV-254 absorbance for single contactor and blended effluents for Water 5

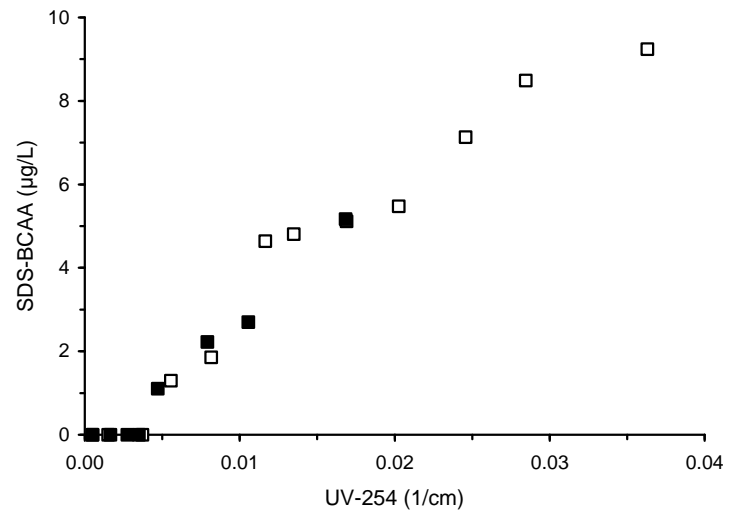
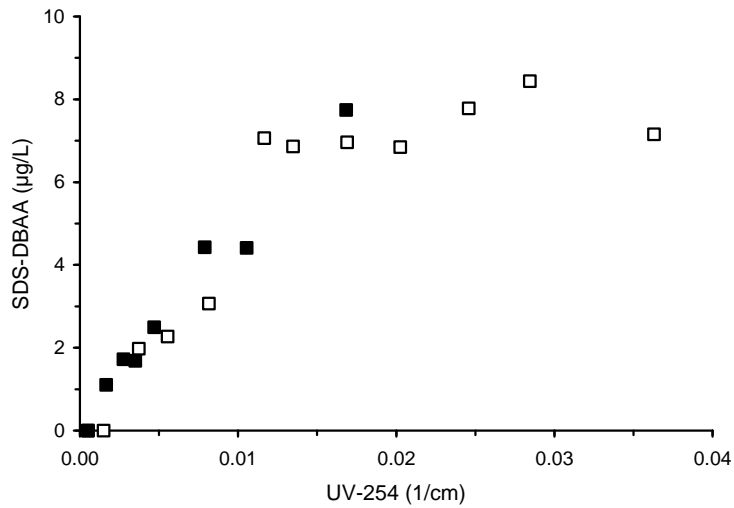
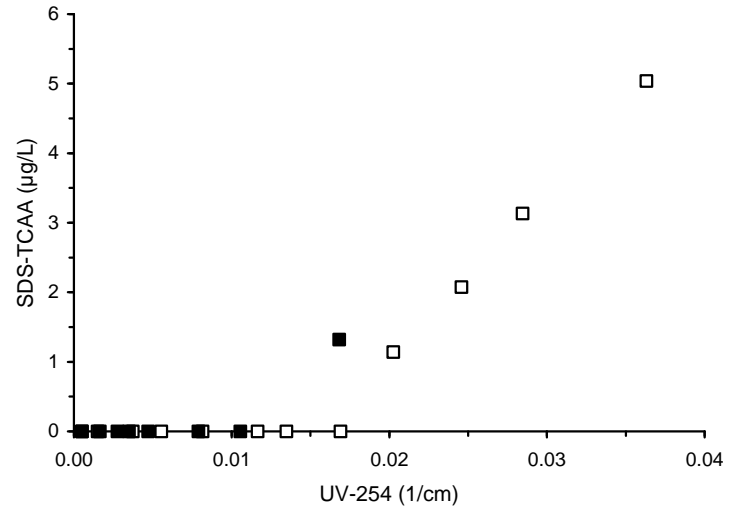
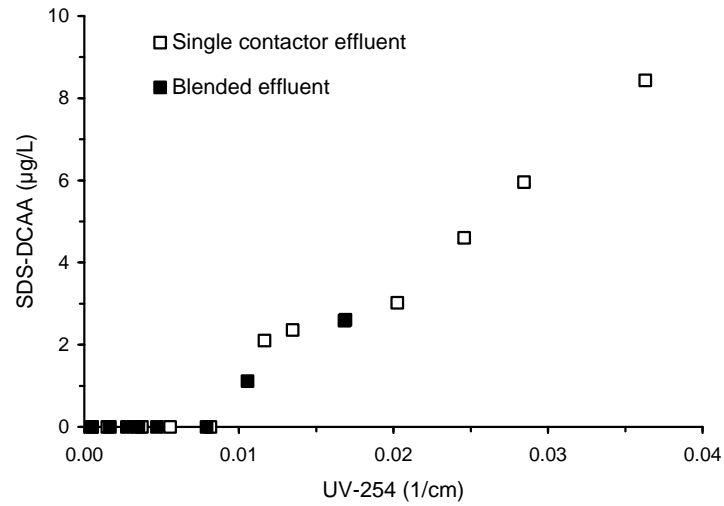


Figure D-54 HAA correlations based on GAC effluent UV-254 absorbance for single contactor and blended effluents for Water 6

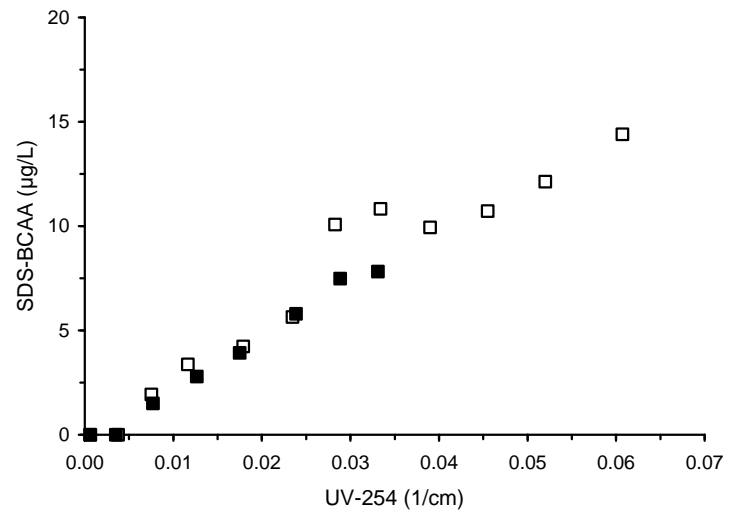
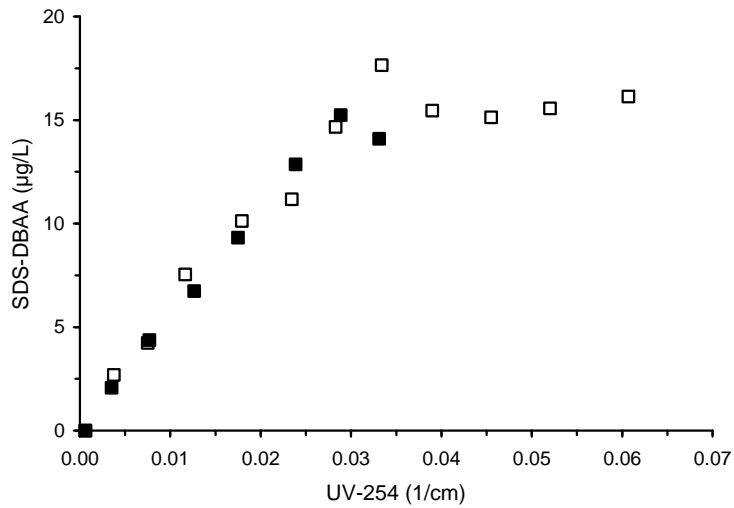
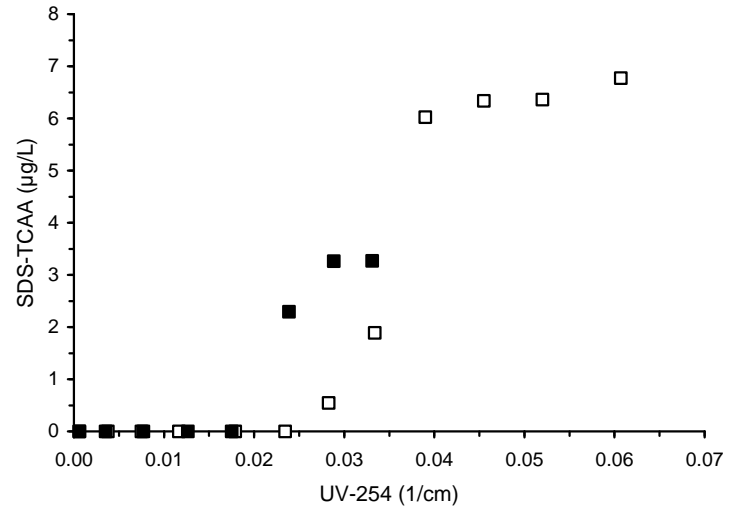
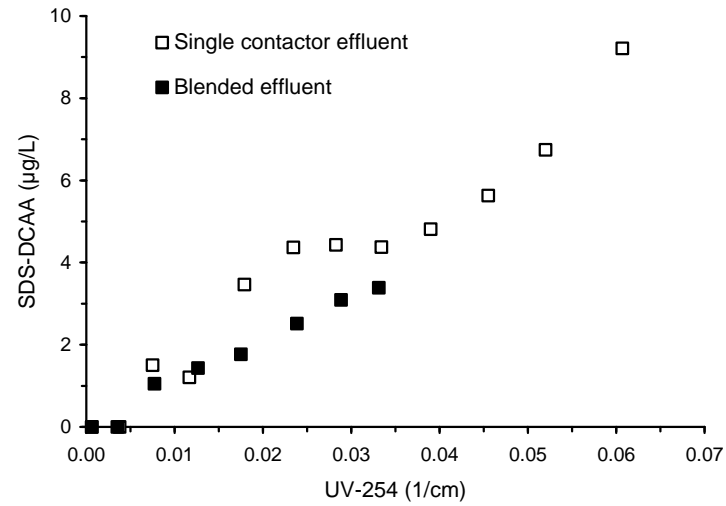


Figure D-55 HAA correlations based on GAC effluent UV-254 absorbance for single contactor and blended effluents for Water 7

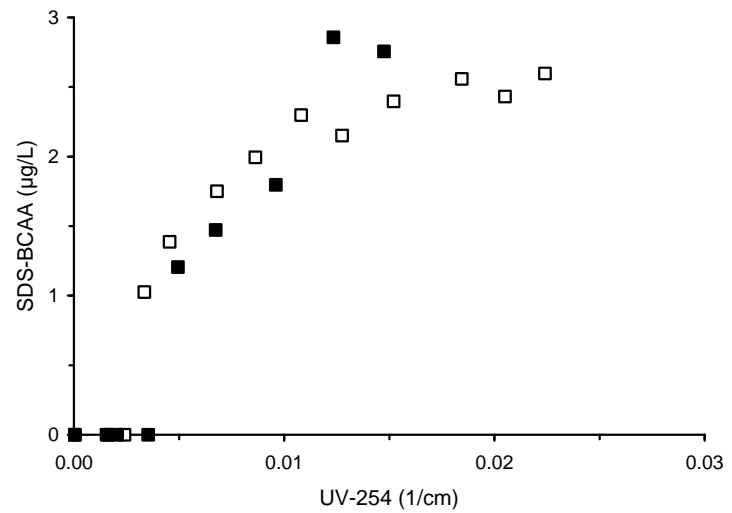
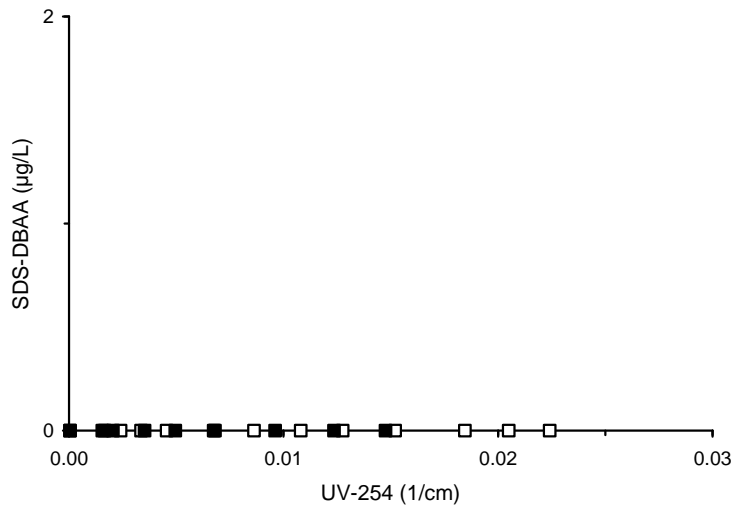
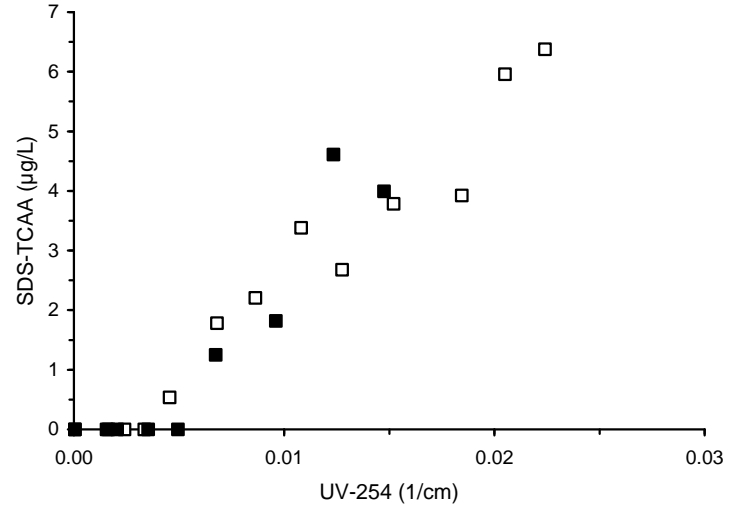
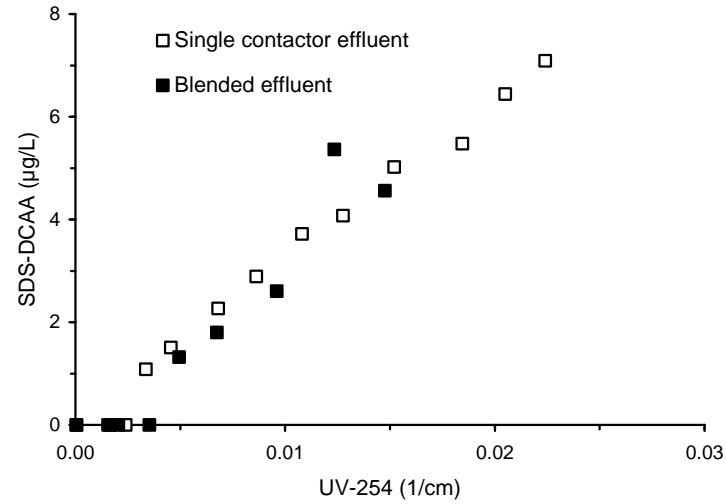


Figure D-56 HAA correlations based on GAC effluent UV-254 absorbance for single contactor and blended effluents for Water 8

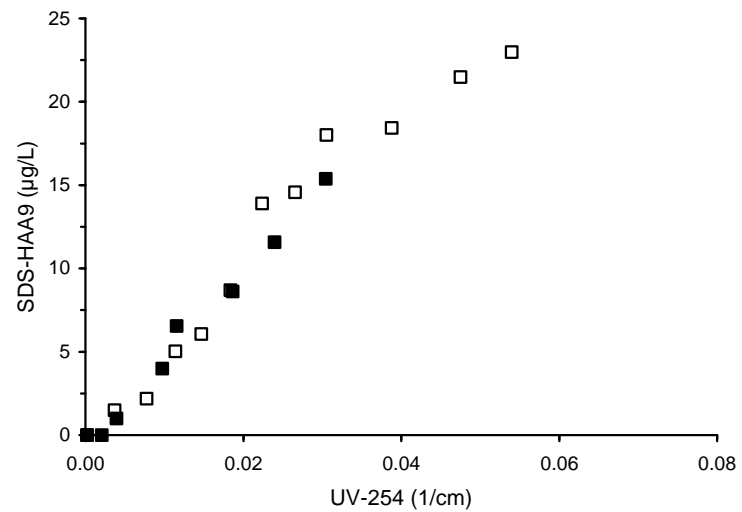
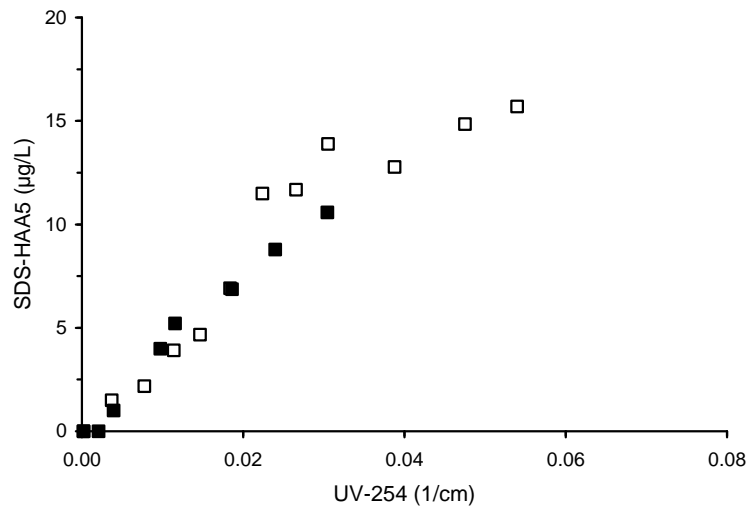
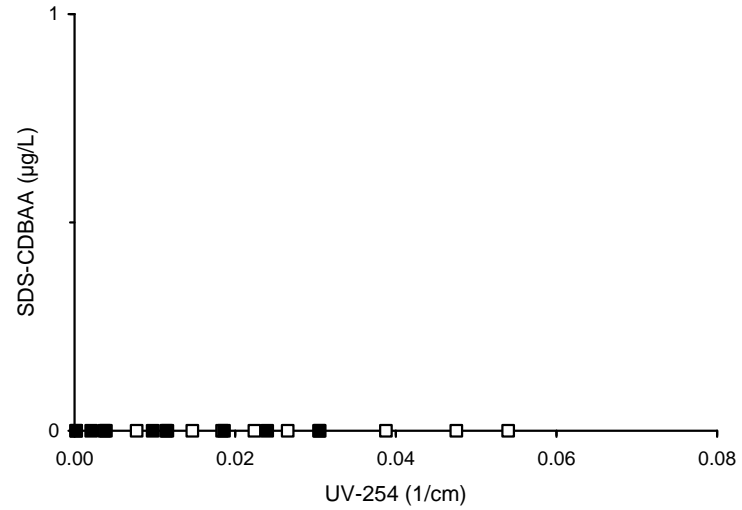
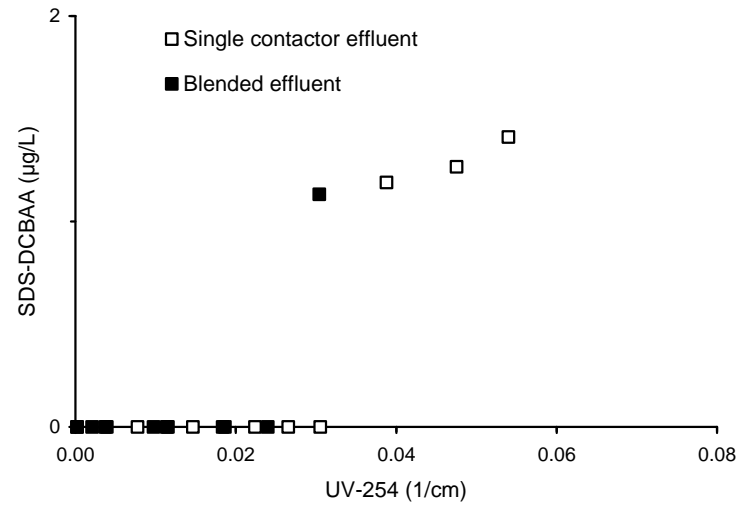


Figure D-57 HAA correlations based on GAC effluent UV-254 absorbance for single contactor and blended effluents for Water 1

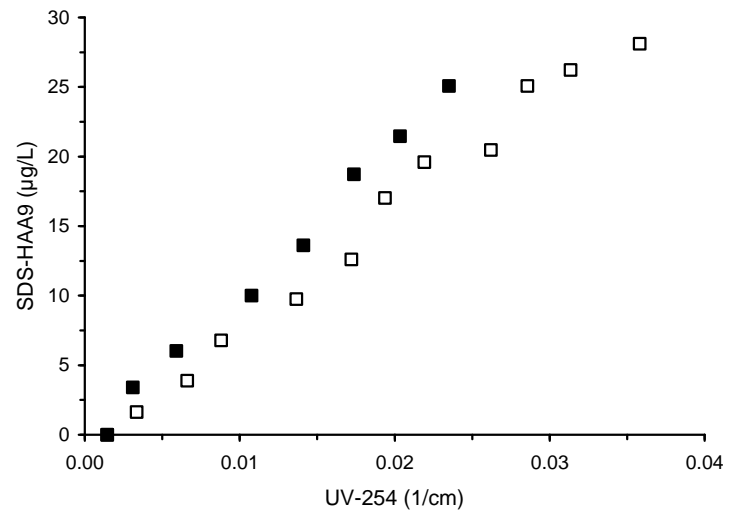
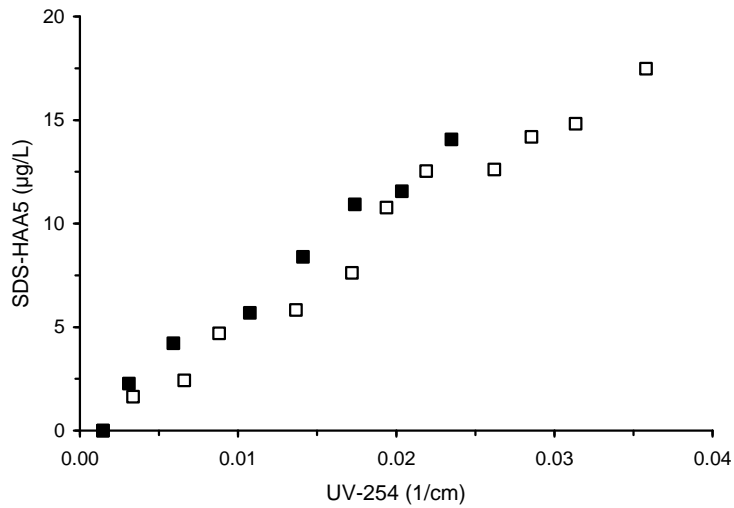
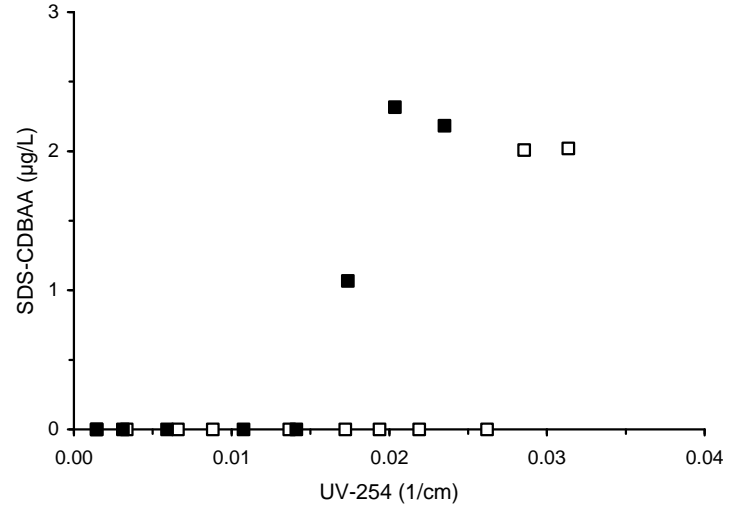
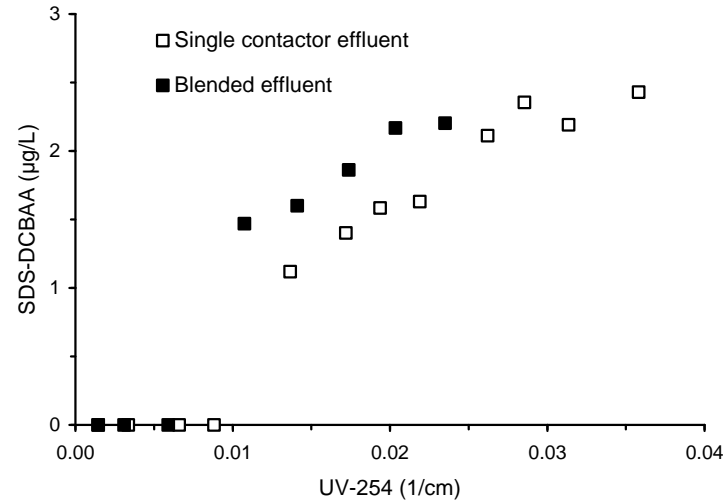


Figure D-58 HAA correlations based on GAC effluent UV-254 absorbance for single contactor and blended effluents for Water 2

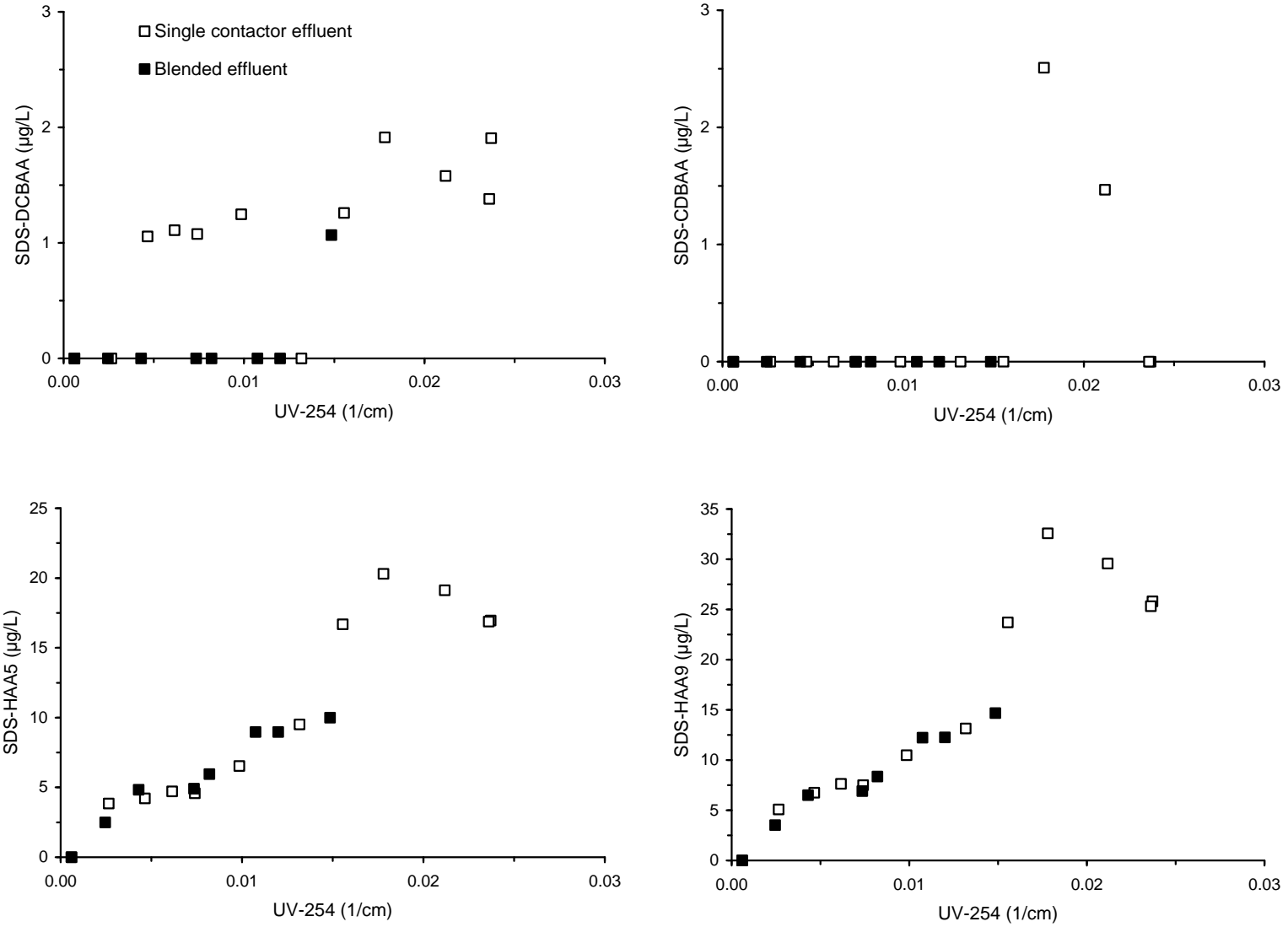


Figure D-59 HAA correlations based on GAC effluent UV-254 absorbance for single contactor and blended effluents for Water 3

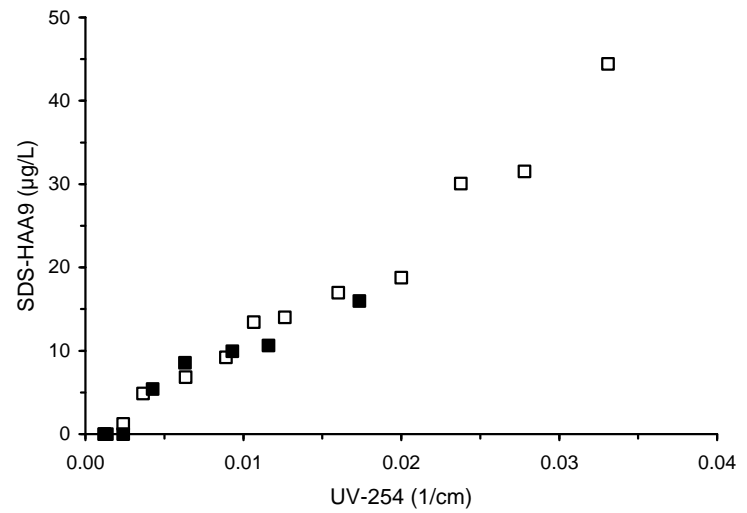
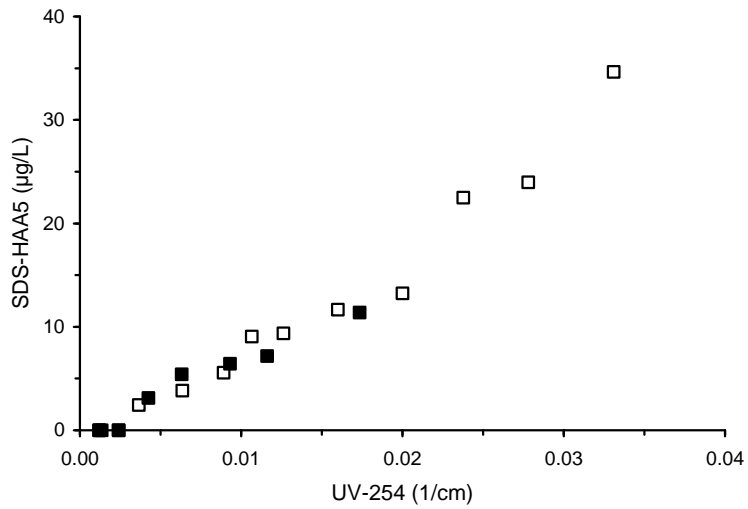
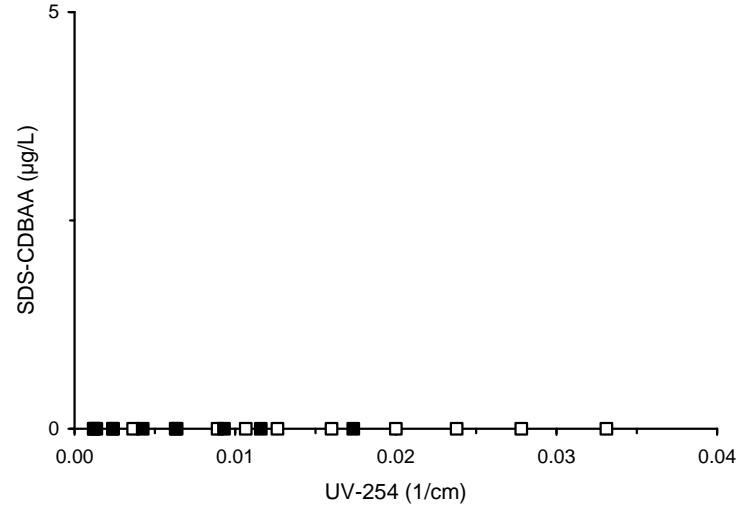
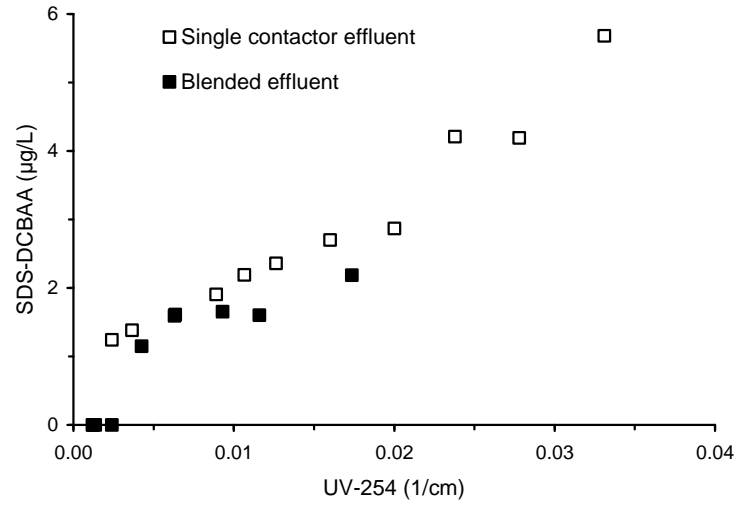


Figure D-60 HAA correlations based on GAC effluent UV-254 absorbance for single contactor and blended effluents for Water 4

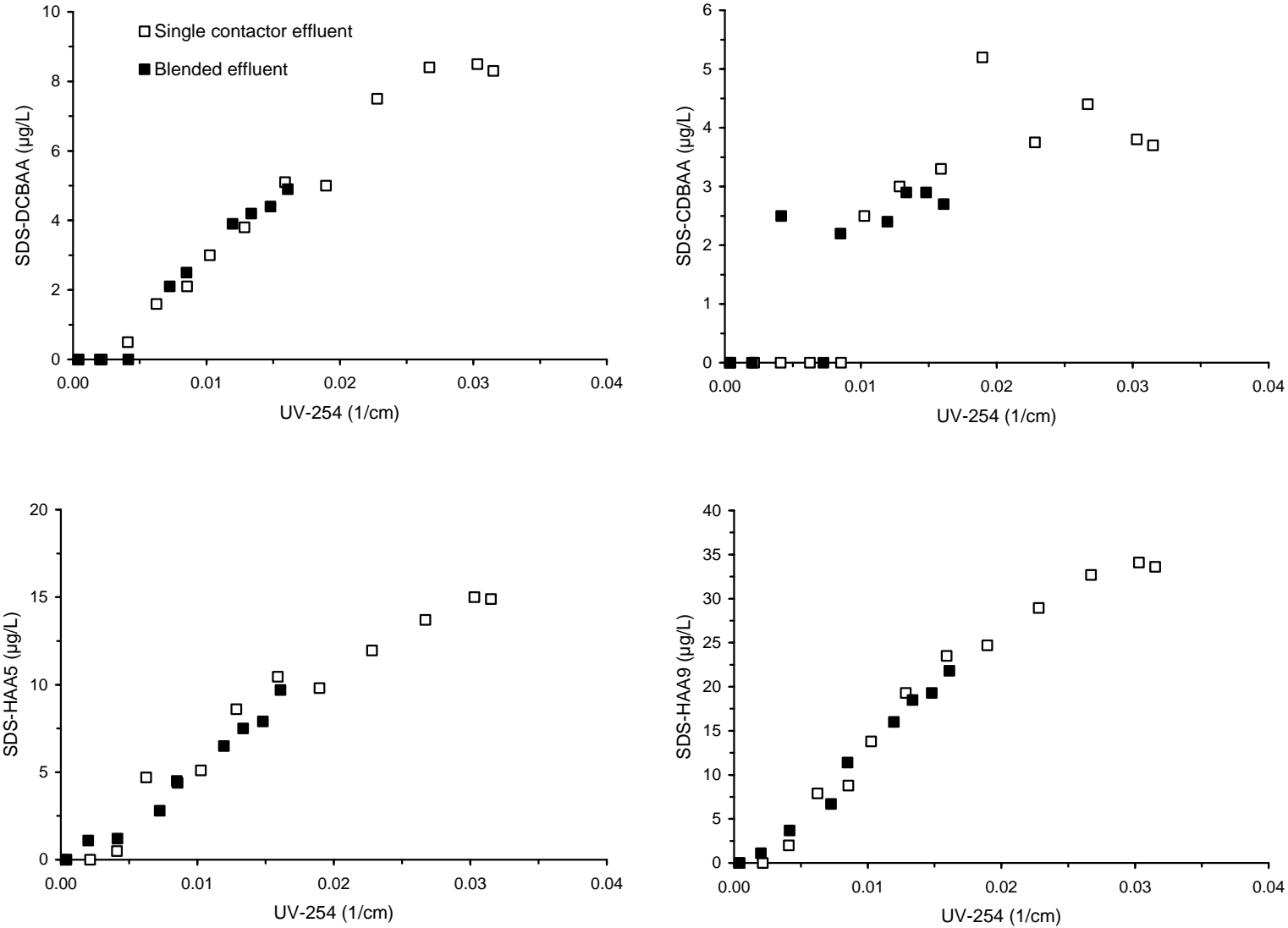


Figure D-61 HAA correlations based on GAC effluent UV-254 absorbance for single contactor and blended effluents for Water 5

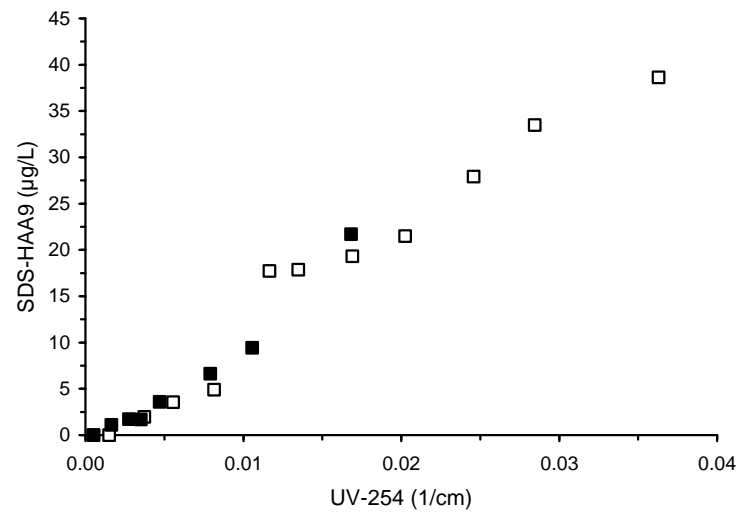
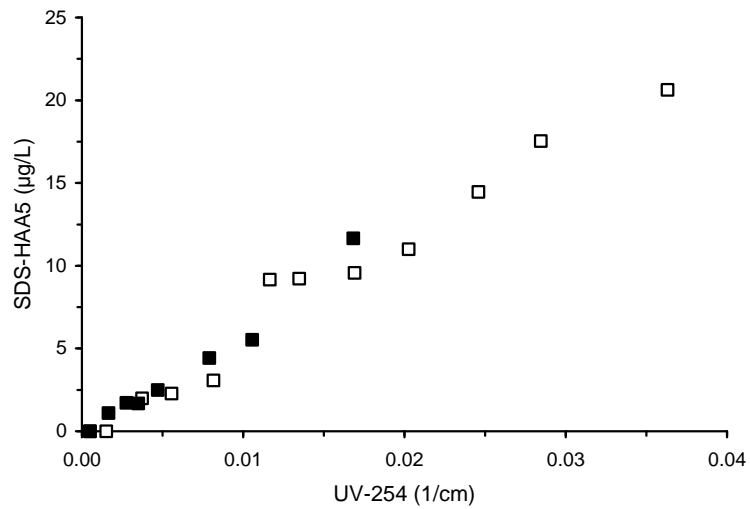
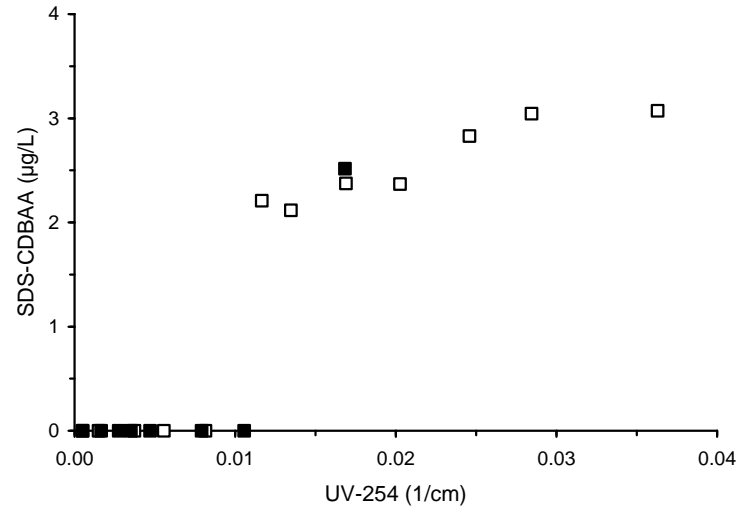
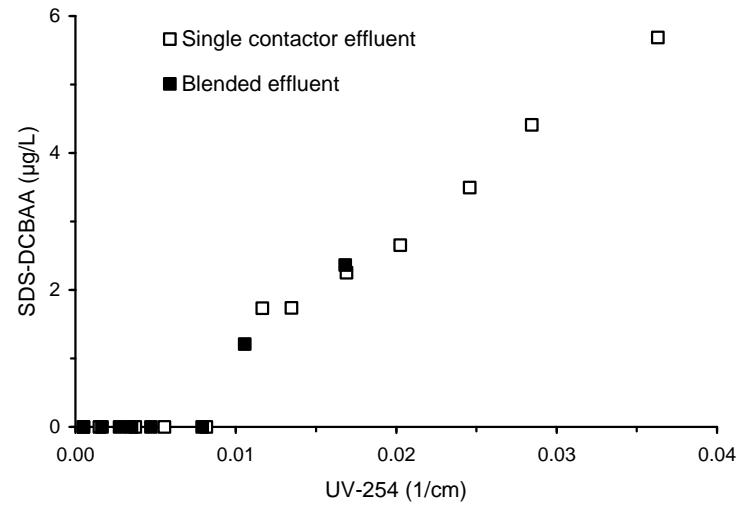


Figure D-62 HAA correlations based on GAC effluent UV-254 absorbance for single contactor and blended effluents for Water 6

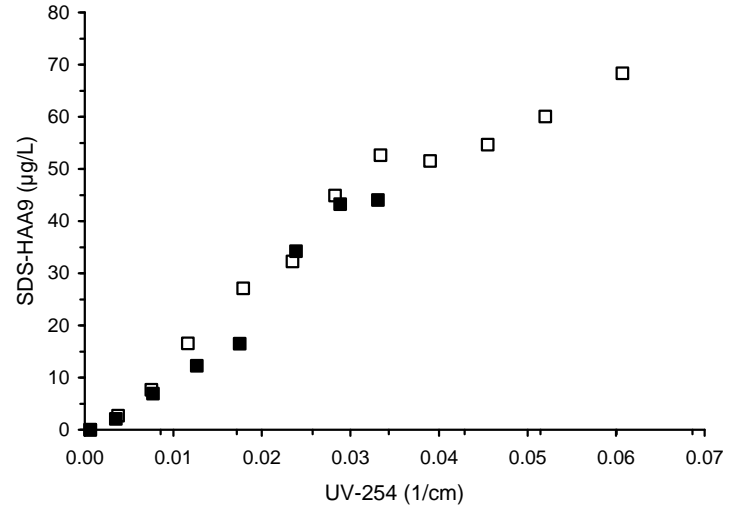
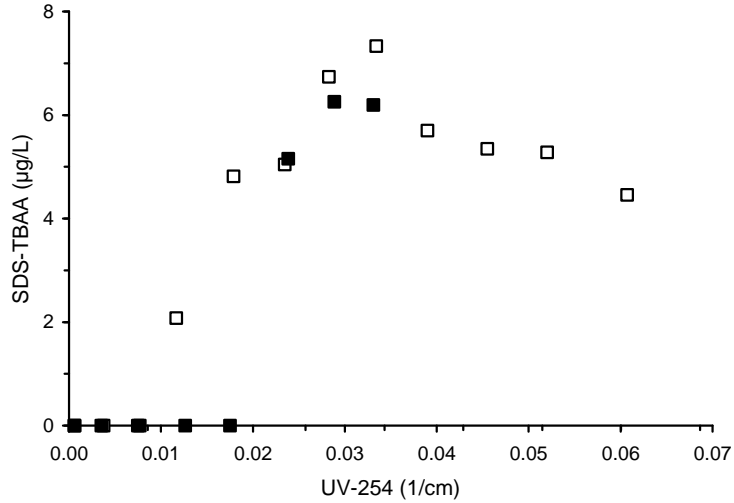
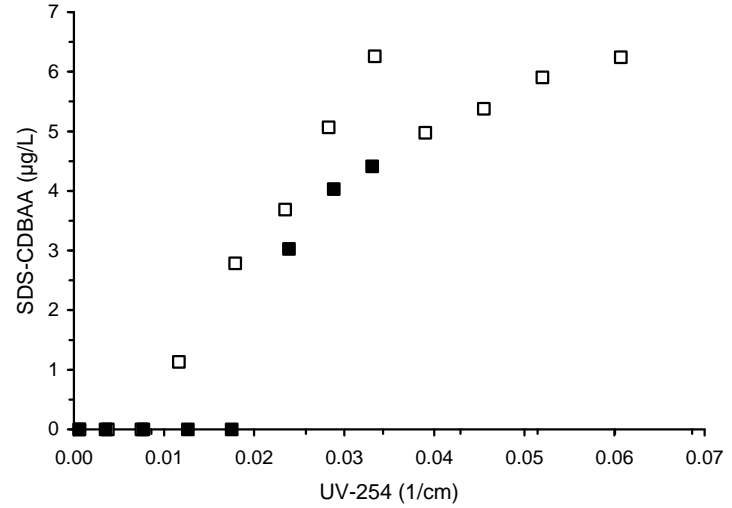
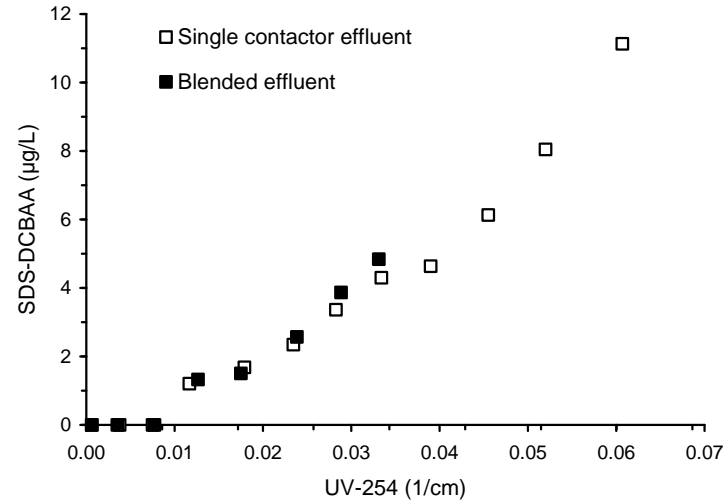


Figure D-63 HAA correlations based on GAC effluent UV-254 absorbance for single contactor and blended effluents for Water 7

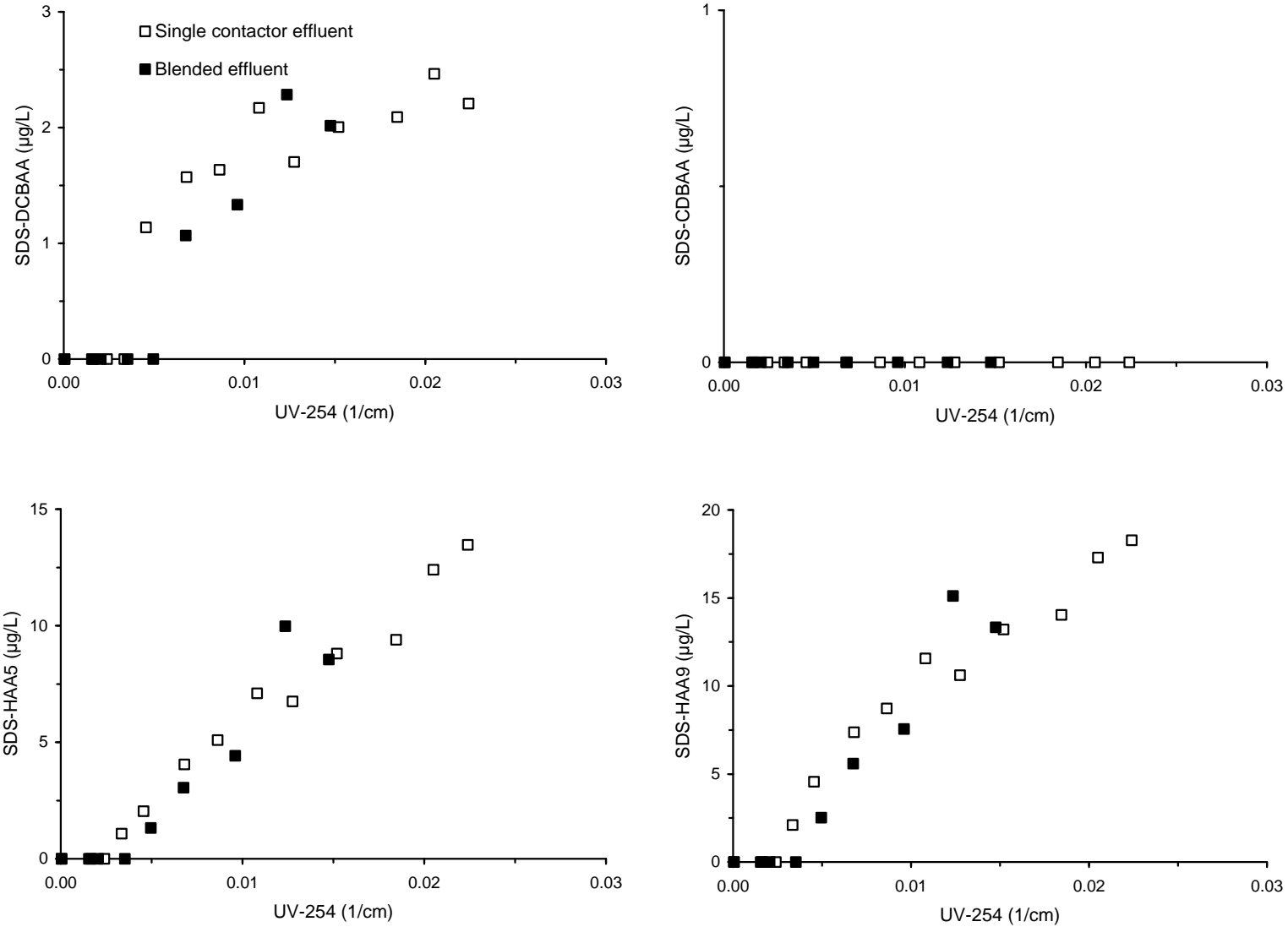
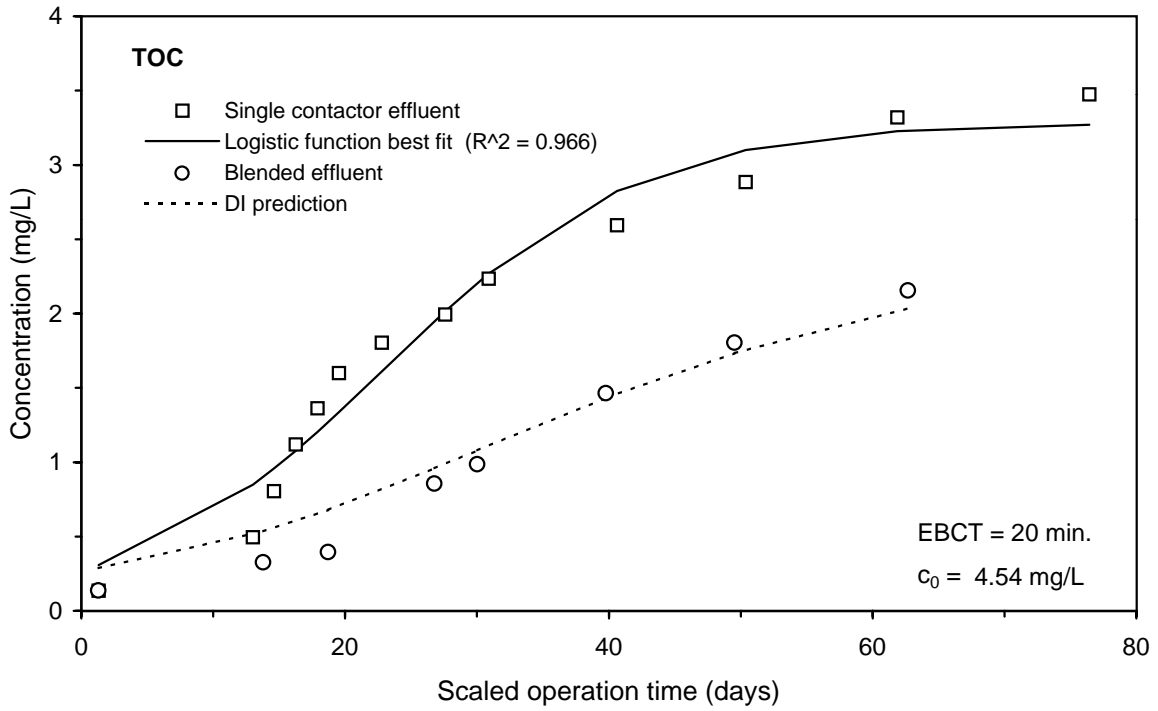


Figure D-64 HAA correlations based on GAC effluent UV-254 absorbance for single contactor and blended effluents for Water 8

This page intentionally left blank.

---

## Appendix E: Logistic Function Model Curve Fits



**Figure E-1 Single contactor and blended effluent TOC breakthrough curves for Water 1**

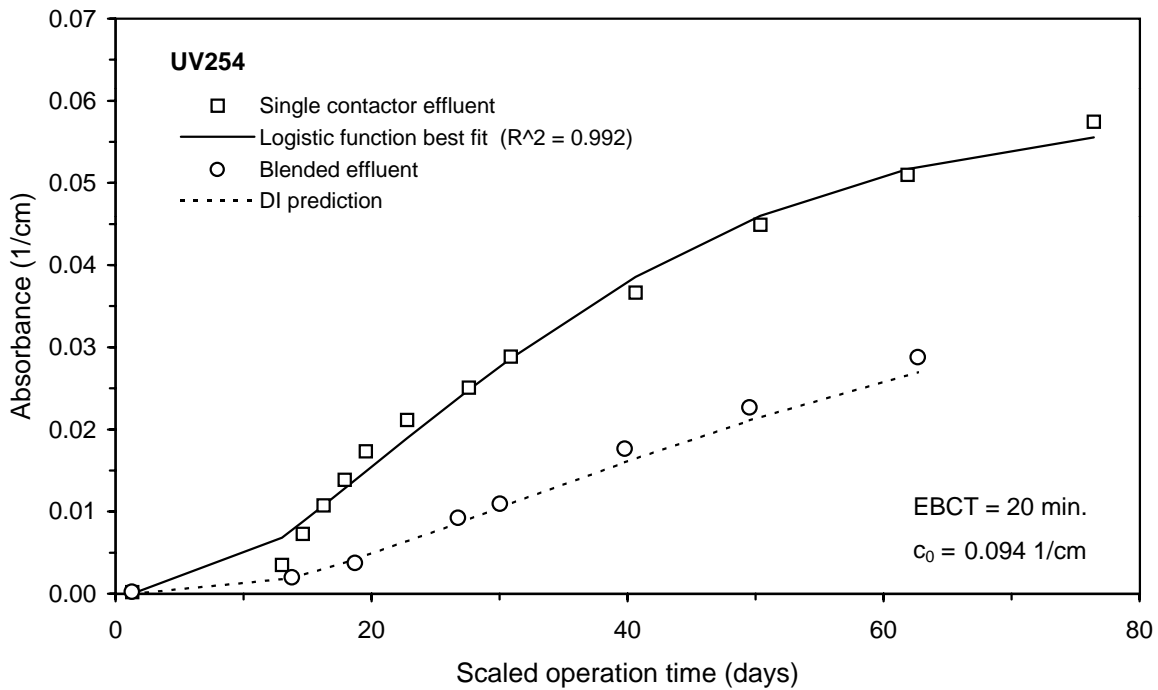


**Figure E-2 Single contactor and blended effluent UV254 breakthrough curves for Water 1**

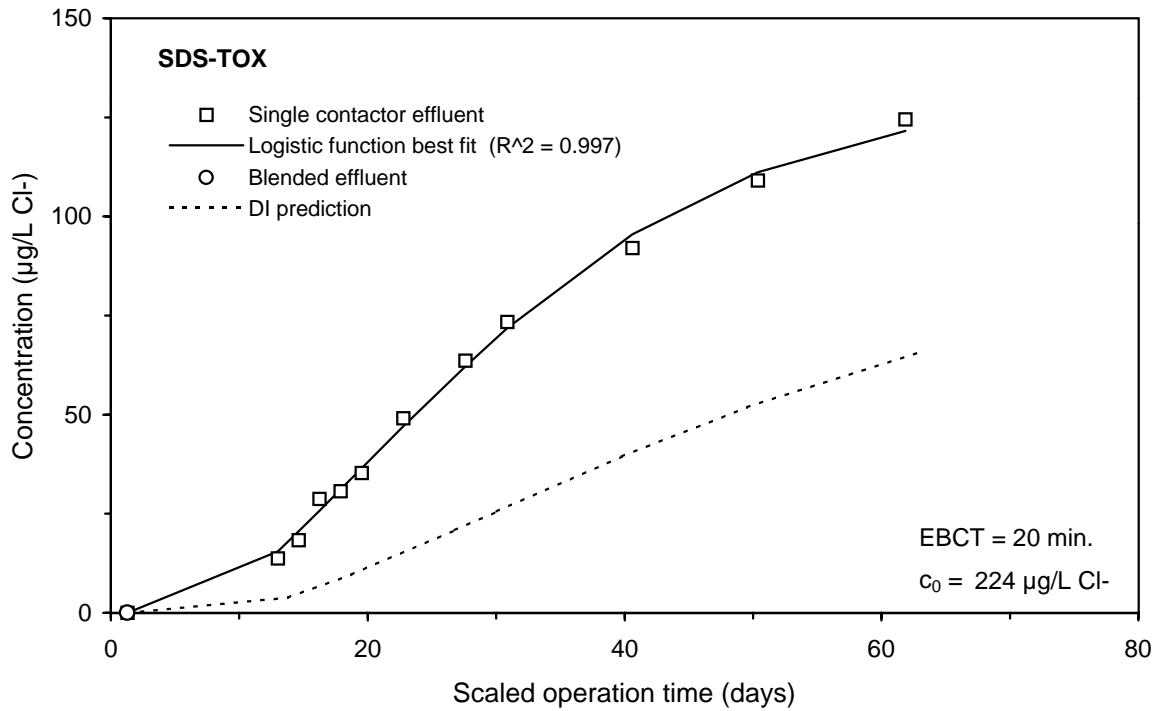


**Figure E-3 Single contactor and blended effluent SDS-TOX breakthrough curves for Water 1**

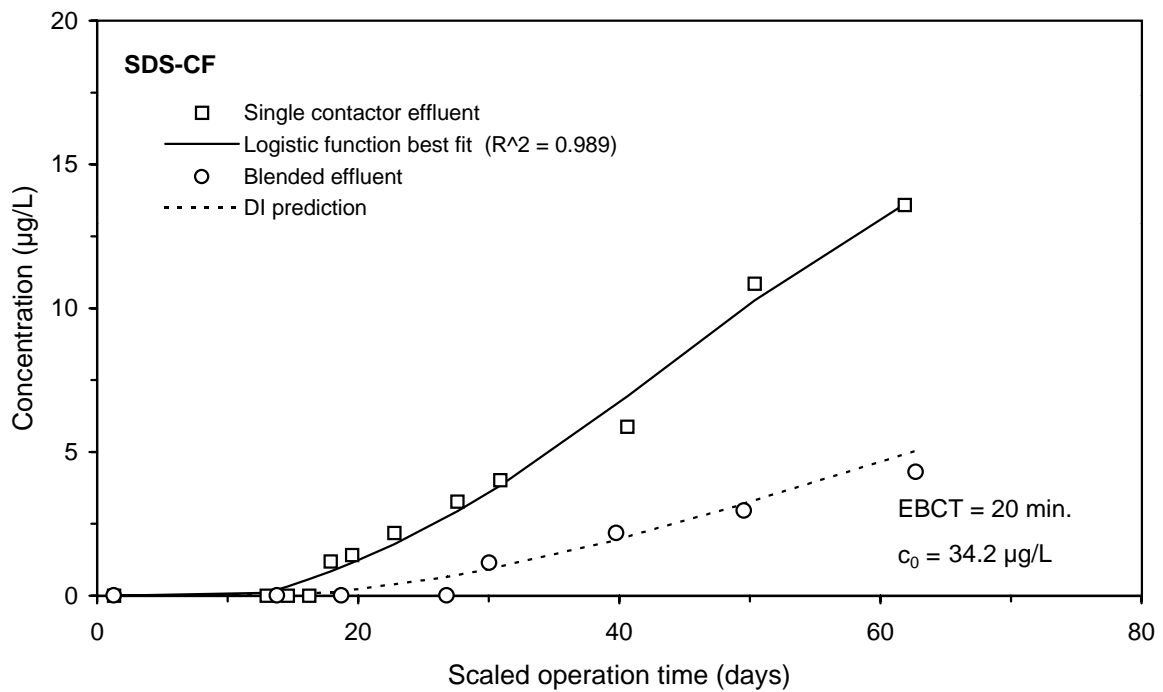


**Figure E-4 Single contactor and blended effluent SDS-CF breakthrough curves for Water 1**

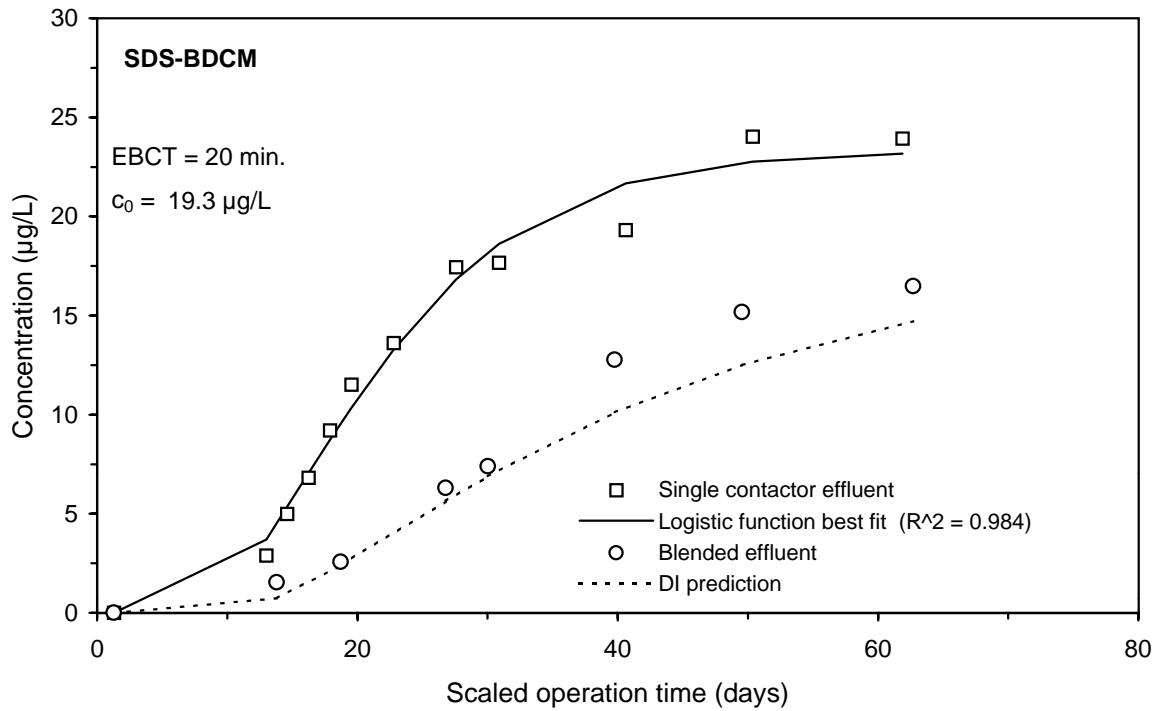


**Figure E-5 Single contactor and blended effluent SDS-BDCM breakthrough curves for Water 1**

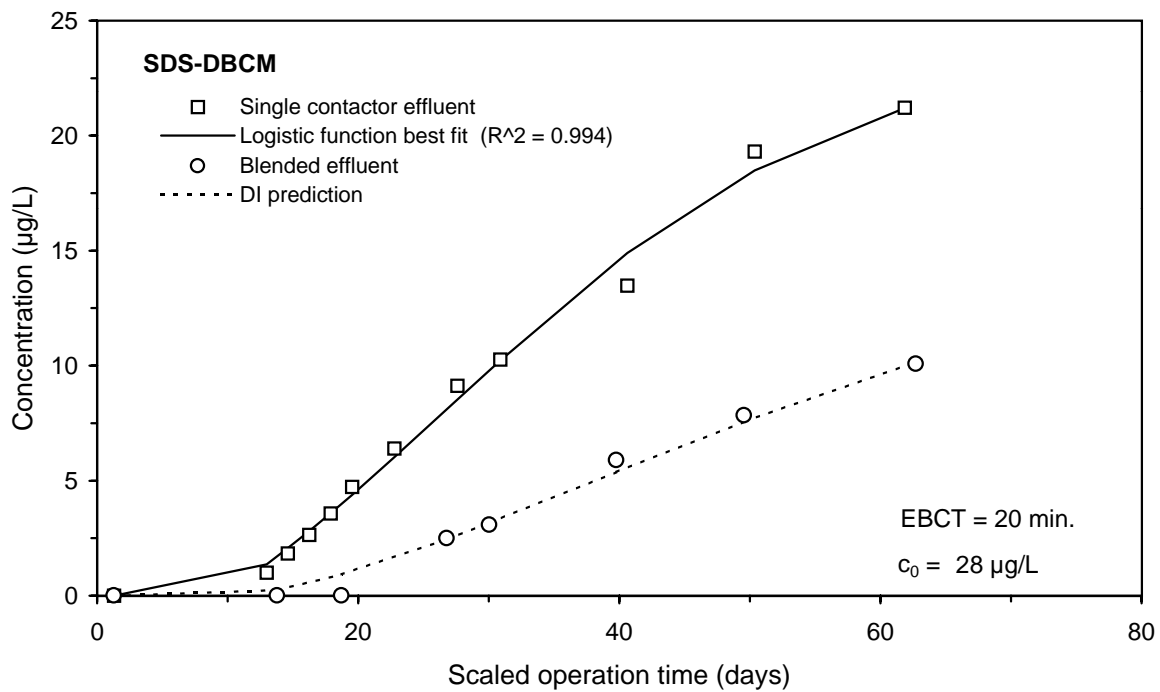


**Figure E-6 Single contactor and blended effluent SDS-DBCМ breakthrough curves for Water 1**

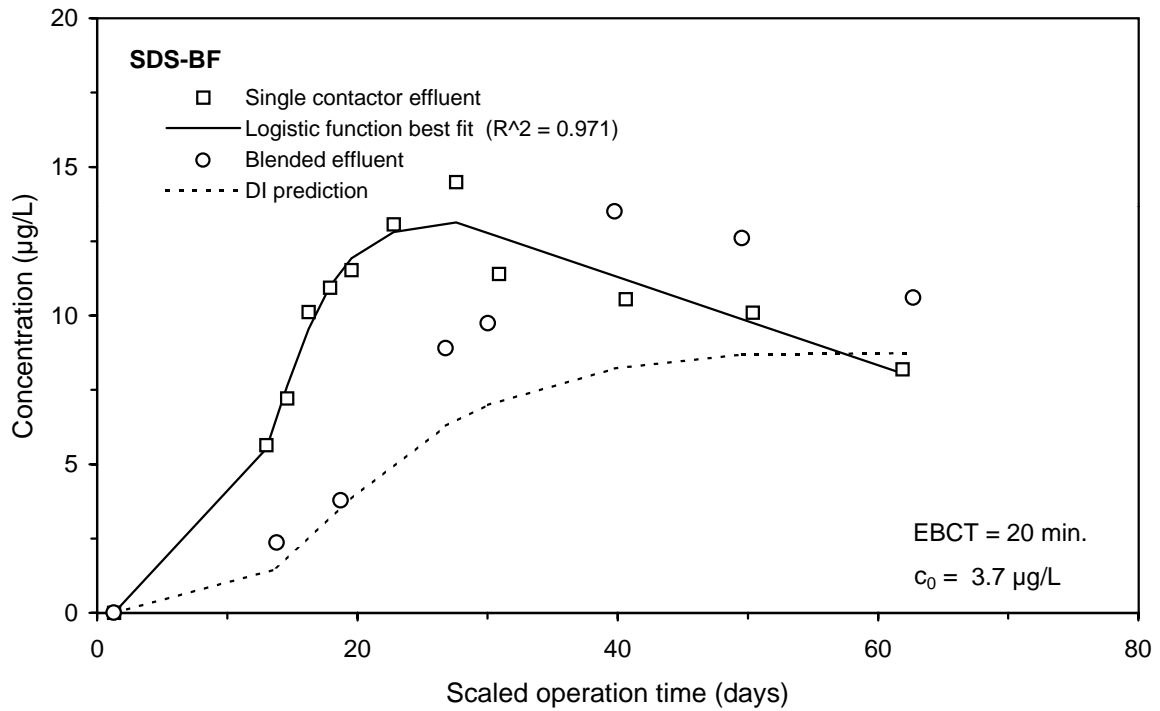


**Figure E-7 Single contactor and blended effluent SDS-BF breakthrough curves for Water 1**

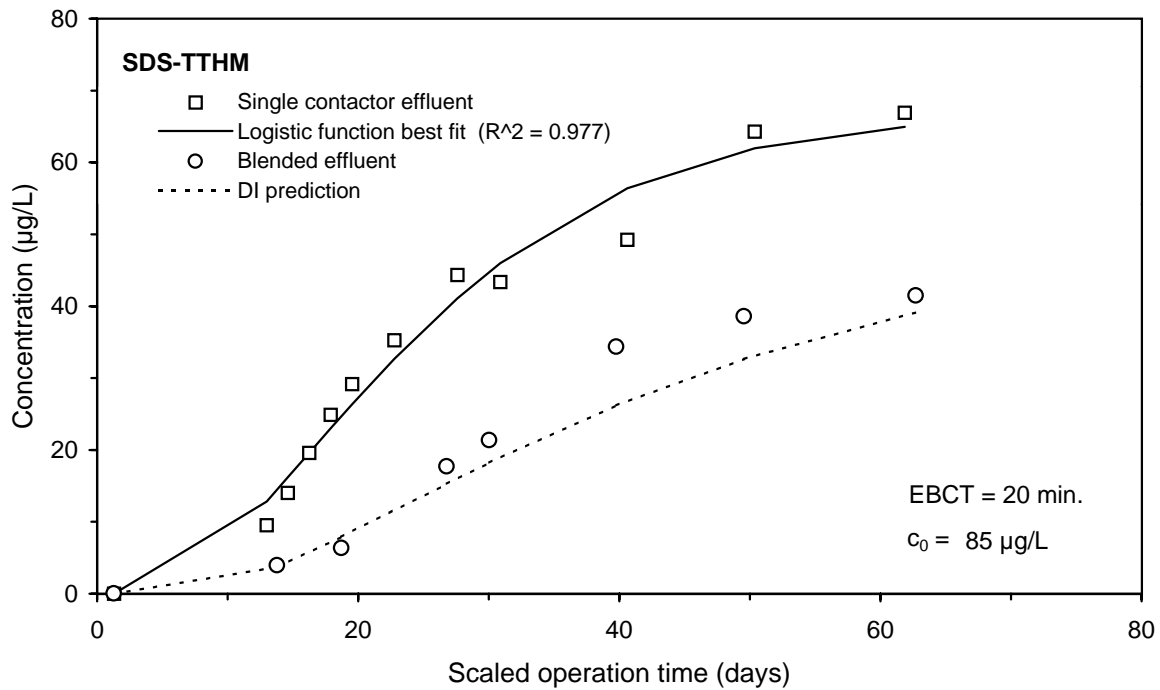


**Figure E-8 Single contactor and blended effluent SDS-TTHM breakthrough curves for Water 1**

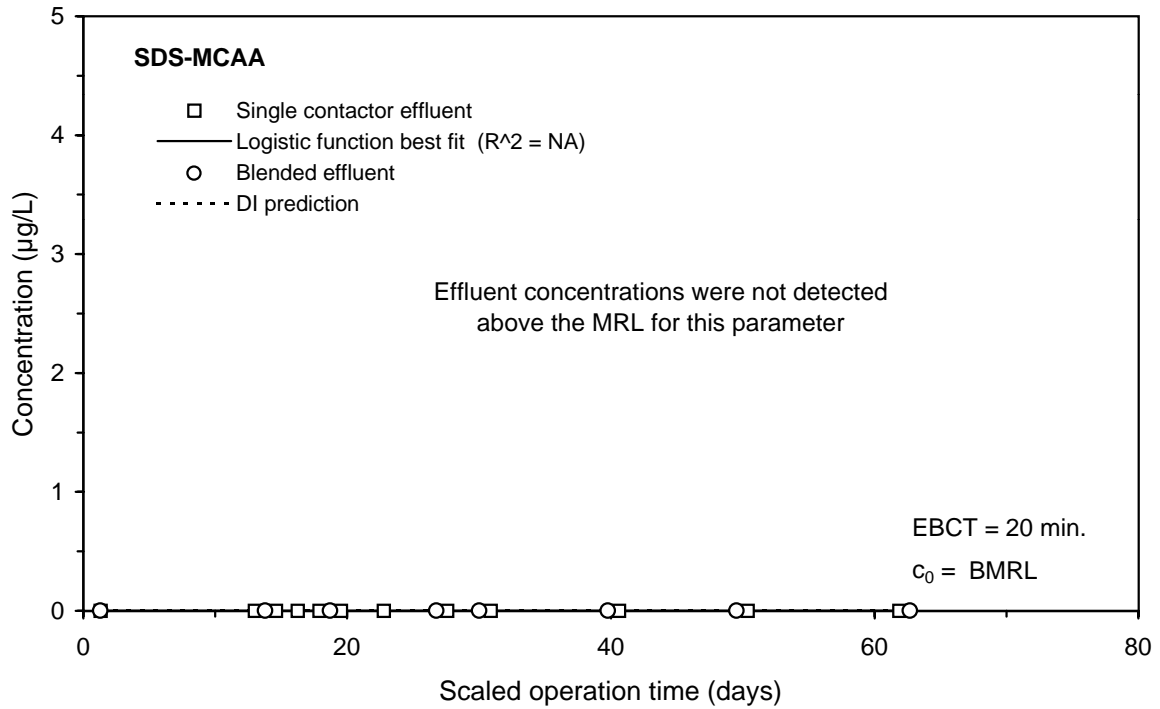


**Figure E-9 Single contactor and blended effluent SDS-MCAA breakthrough curves for Water 1**

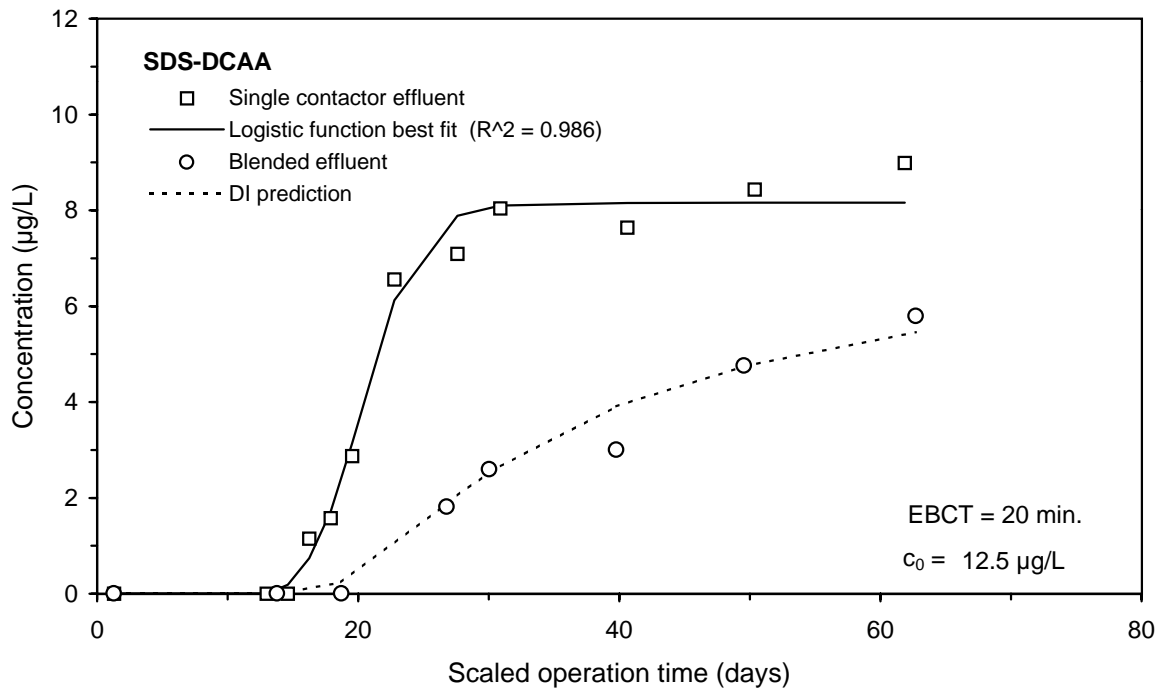


**Figure E-10 Single contactor and blended effluent SDS-DCAA breakthrough curves for Water 1**

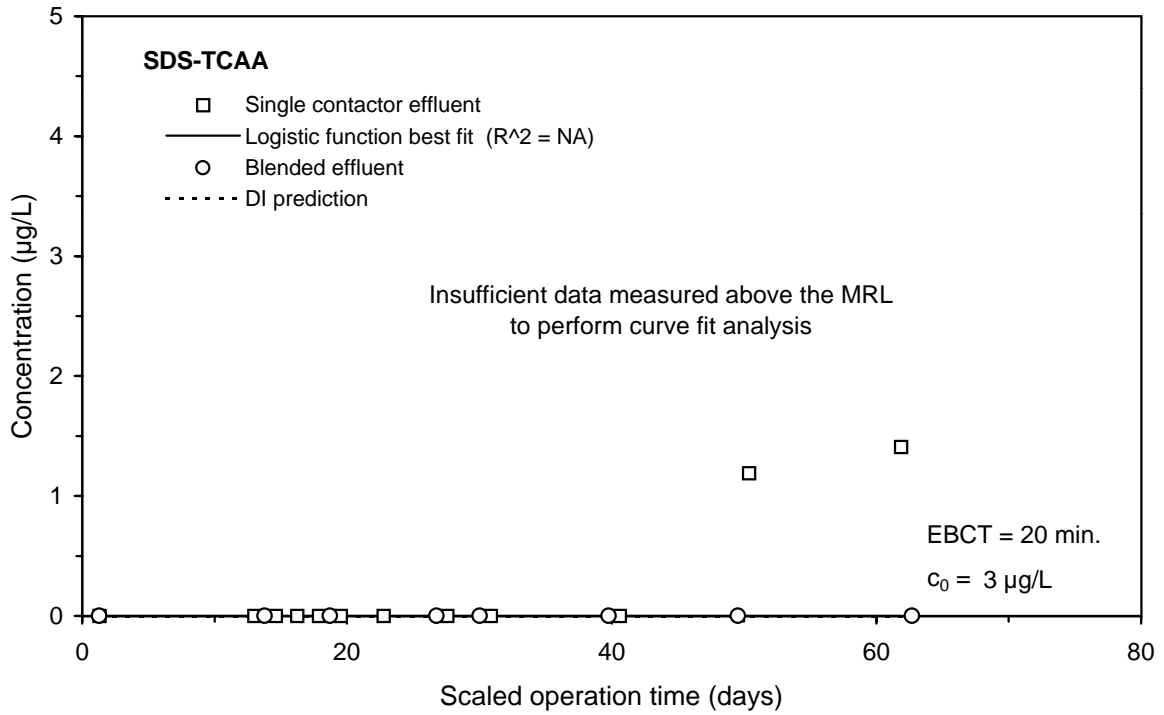


**Figure E-11 Single contactor and blended effluent SDS-TCAA breakthrough curves for Water 1**

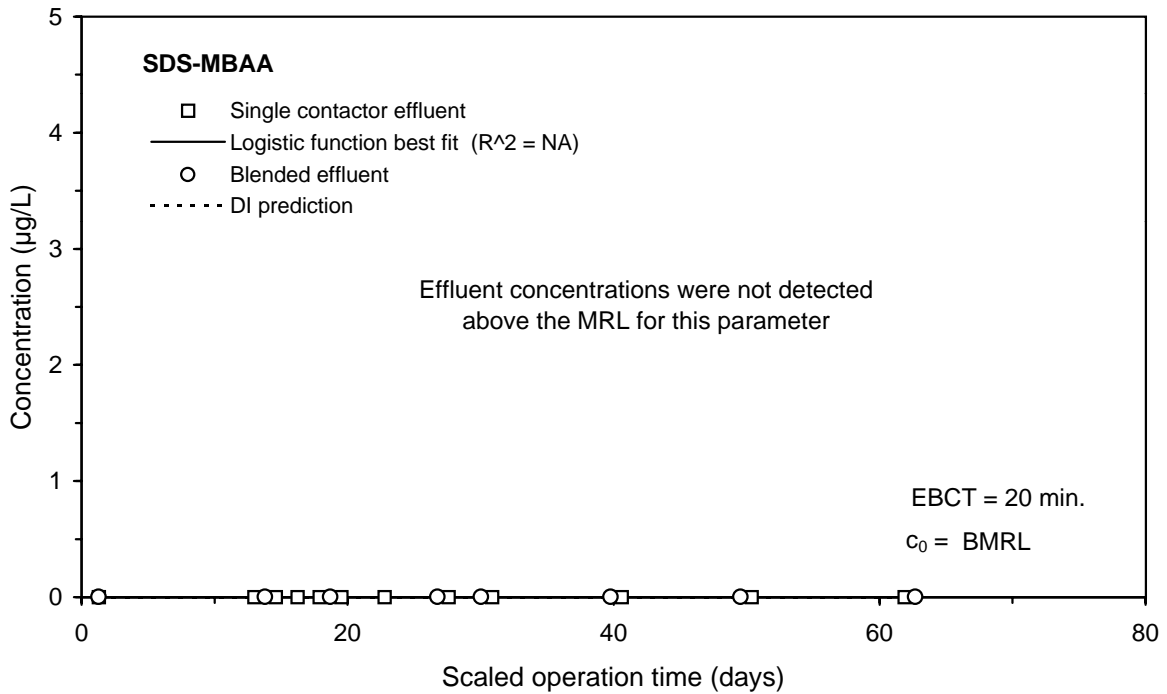


**Figure E-12 Single contactor and blended effluent SDS-MBAA breakthrough curves for Water 1**

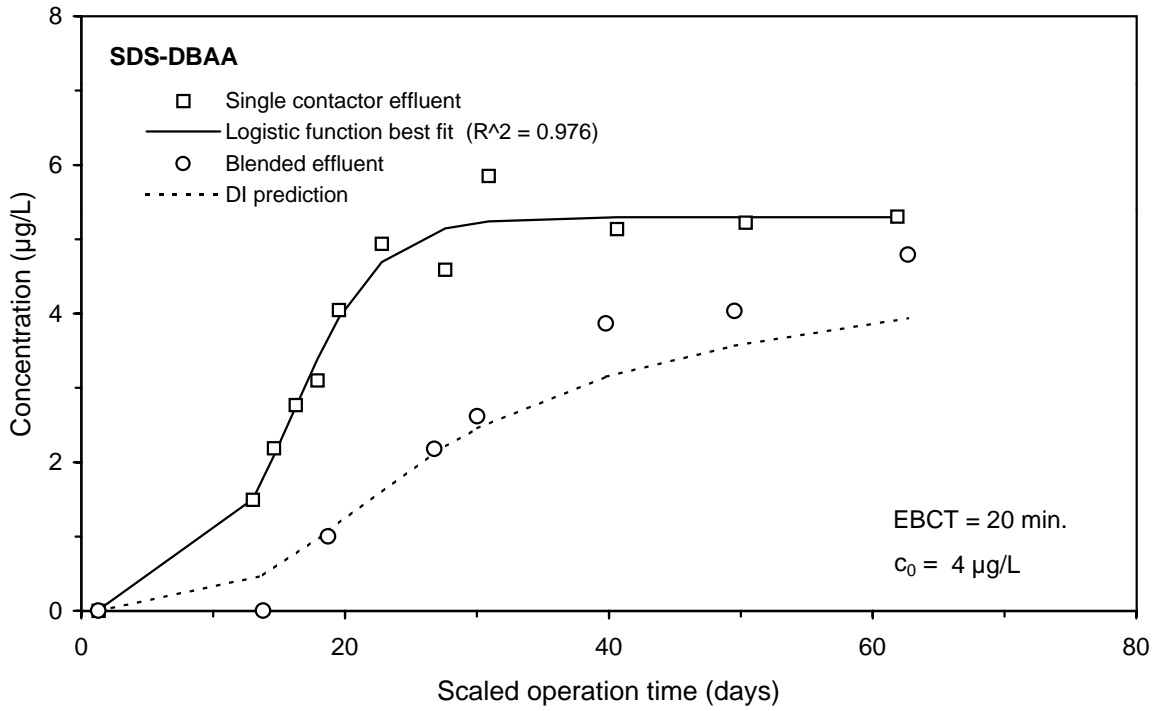


**Figure E-13 Single contactor and blended effluent SDS-DBAA breakthrough curves for Water 1**

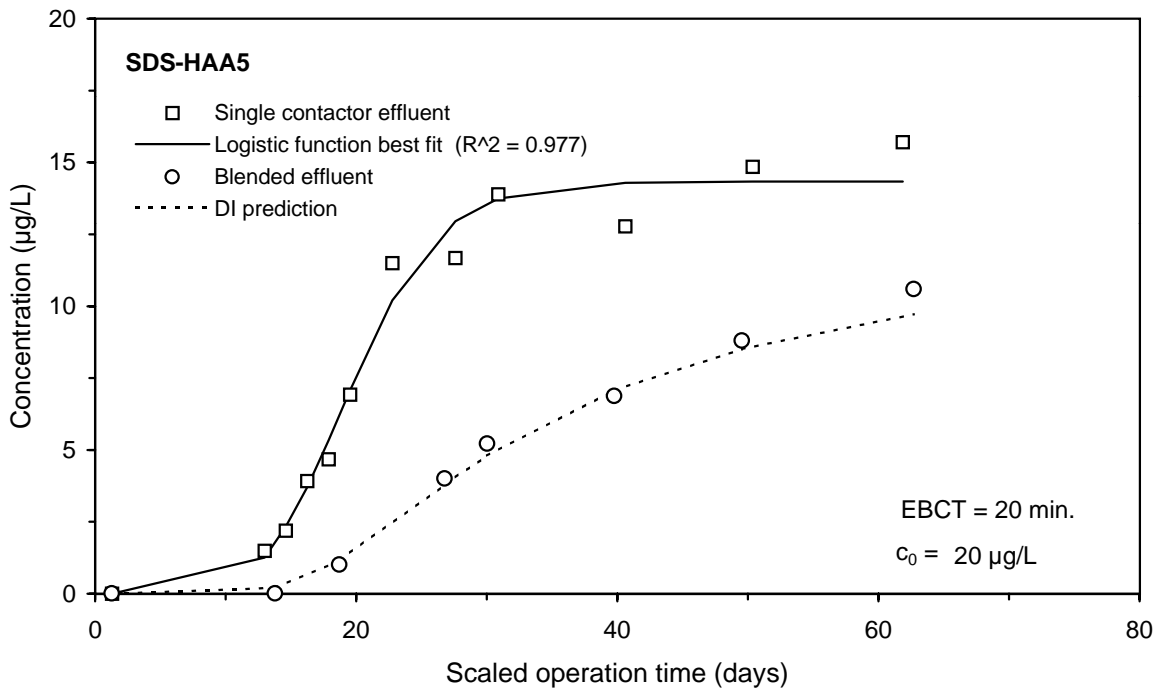


**Figure E-14 Single contactor and blended effluent SDS-HAA5 breakthrough curves for Water 1**

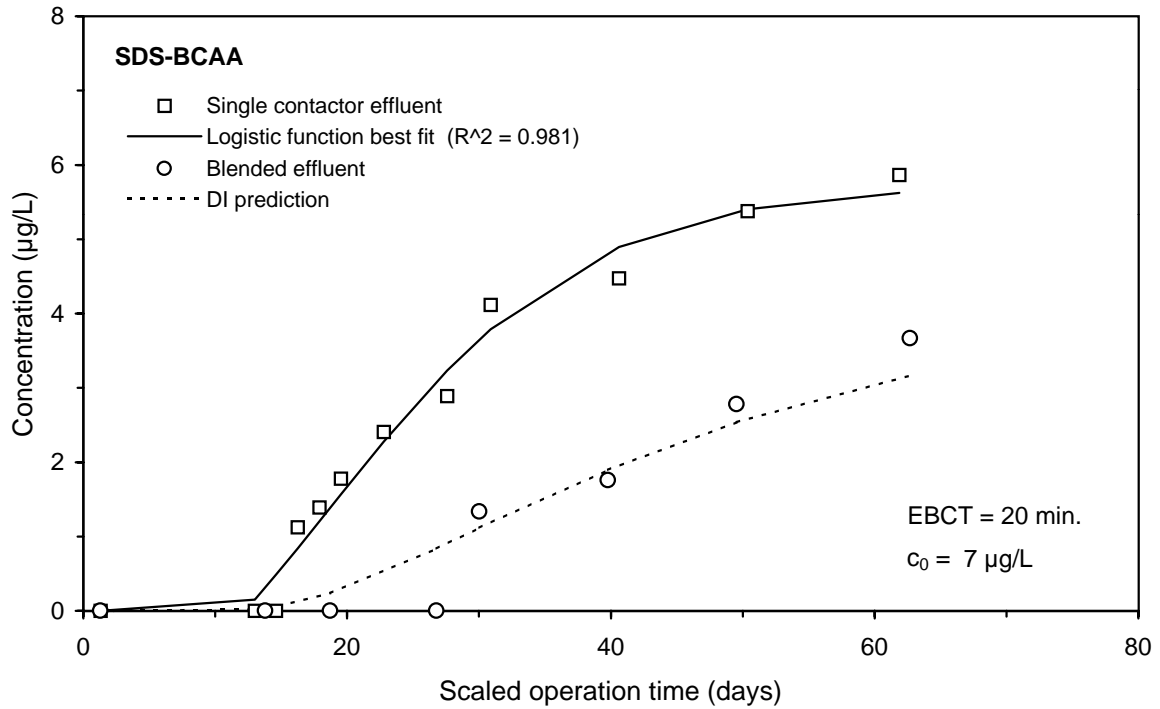


**Figure E-15 Single contactor and blended effluent SDS-BCAA breakthrough curves for Water 1**

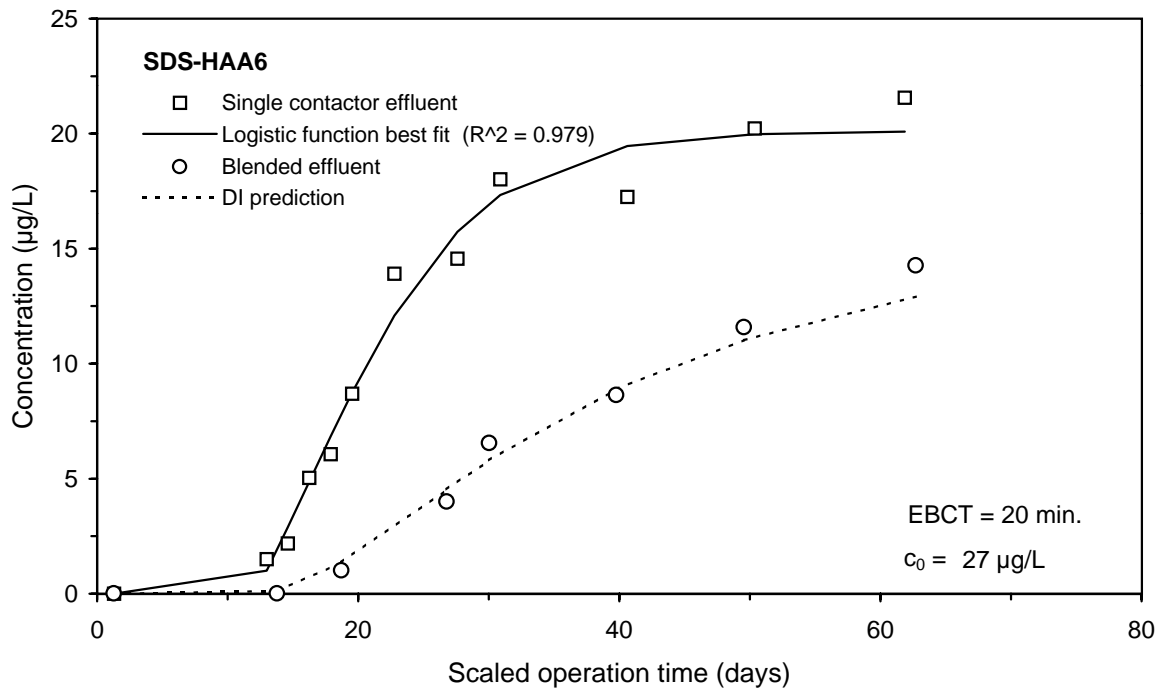


**Figure E-16 Single contactor and blended effluent SDS-HAA6 breakthrough curves for Water 1**

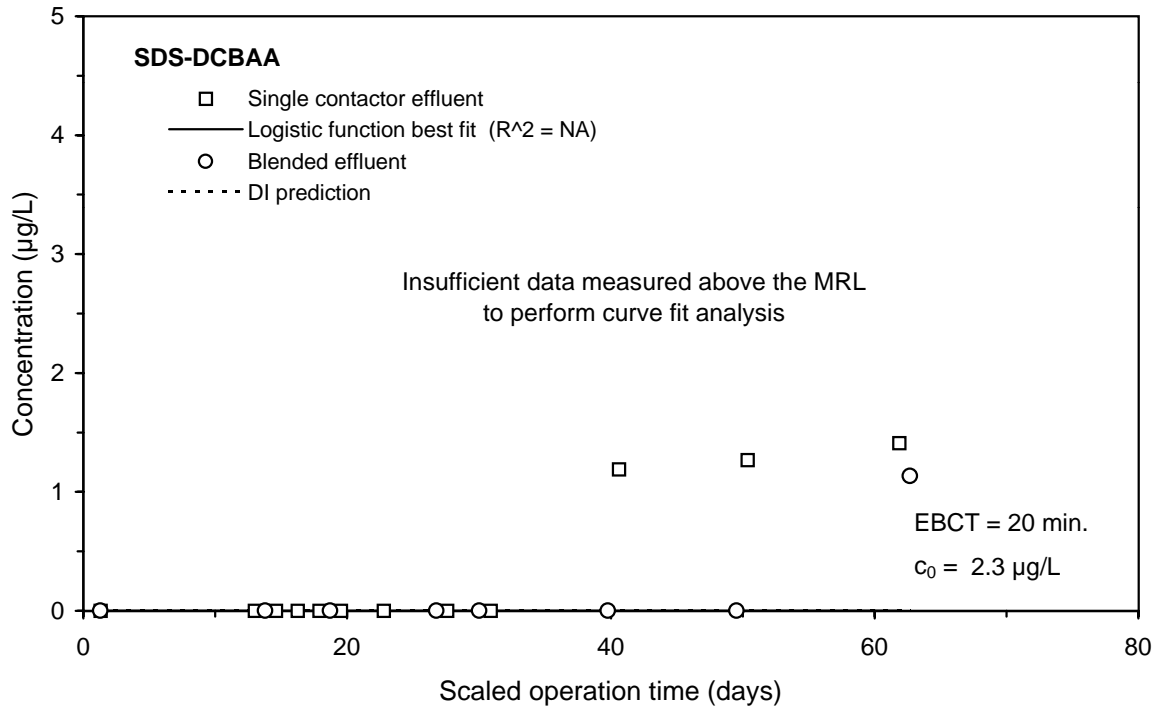


**Figure E-17 Single contactor and blended effluent SDS-DCBAA breakthrough curves for Water 1**

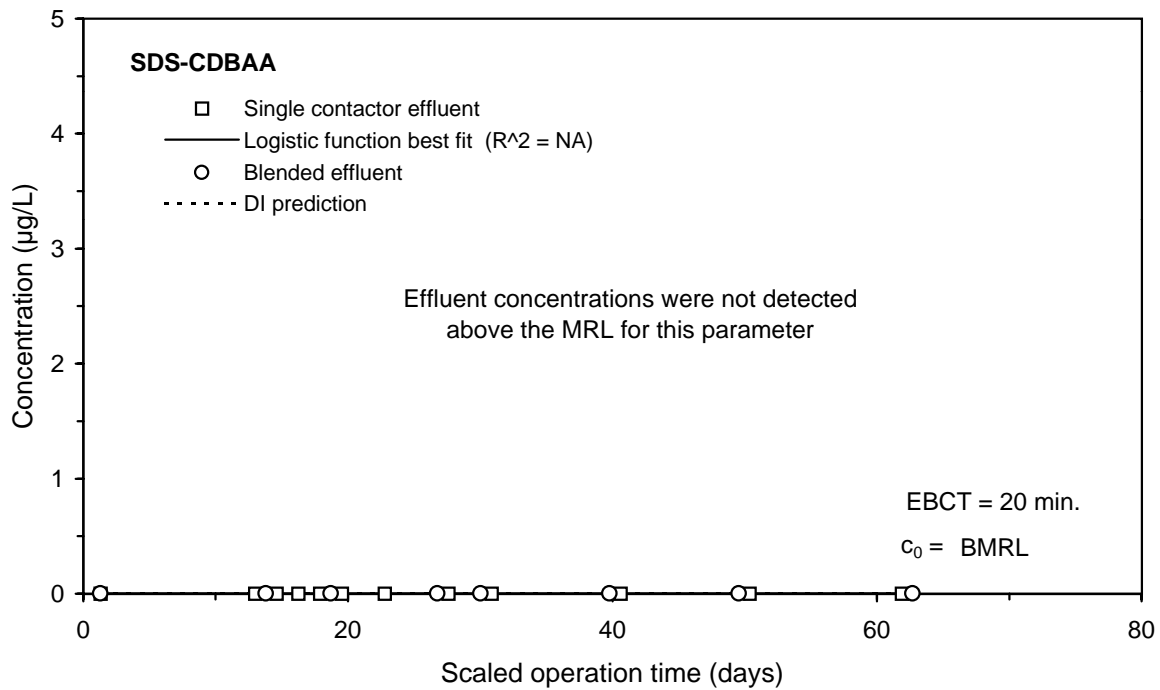


**Figure E-18 Single contactor and blended effluent SDS-CDBAA breakthrough curves for Water 1**

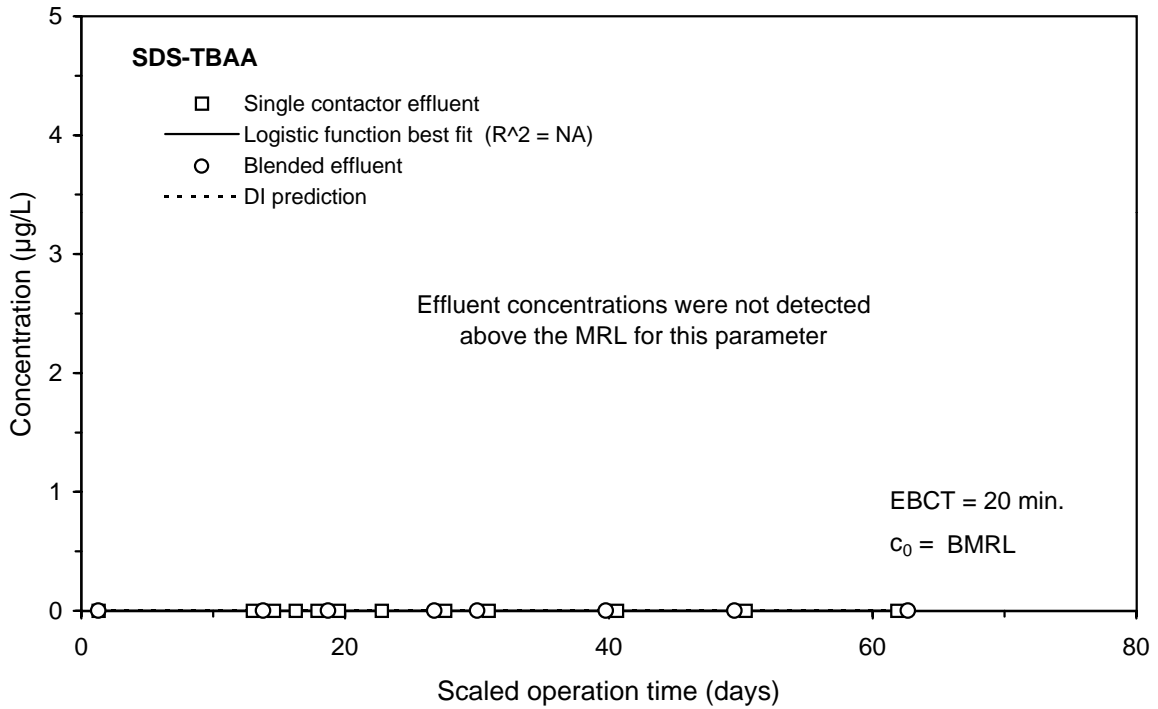


**Figure E-19 Single contactor and blended effluent SDS-TBAA breakthrough curves for Water 1**

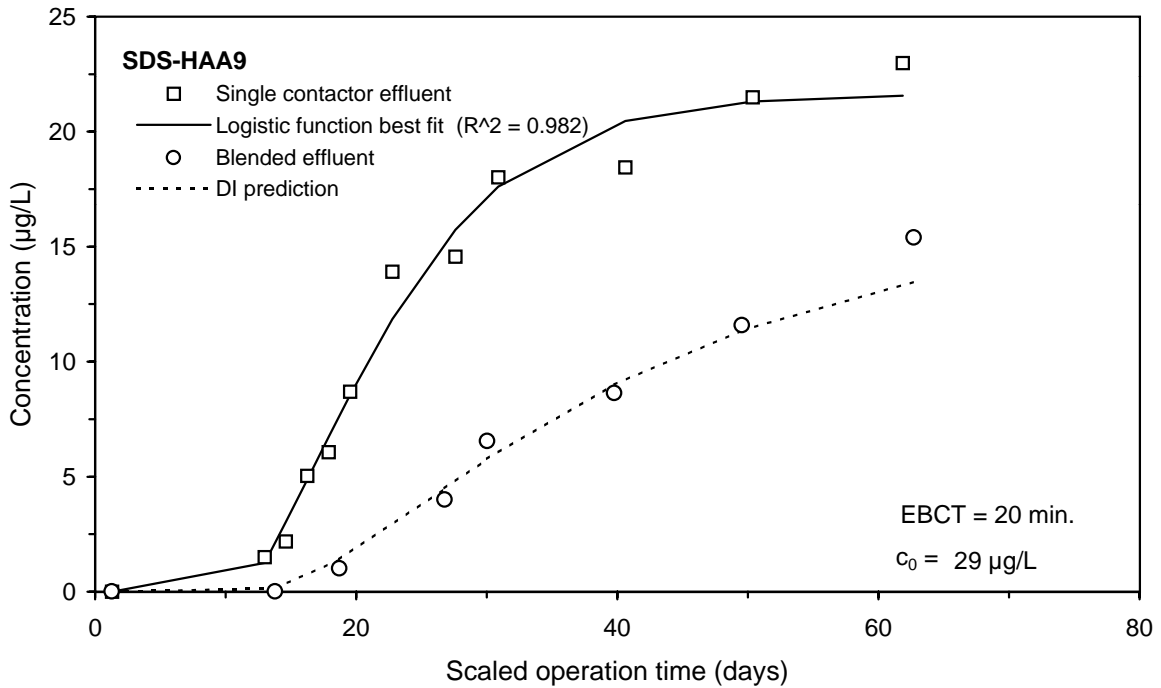


**Figure E-20 Single contactor and blended effluent SDS-HAA9 breakthrough curves for Water 1**

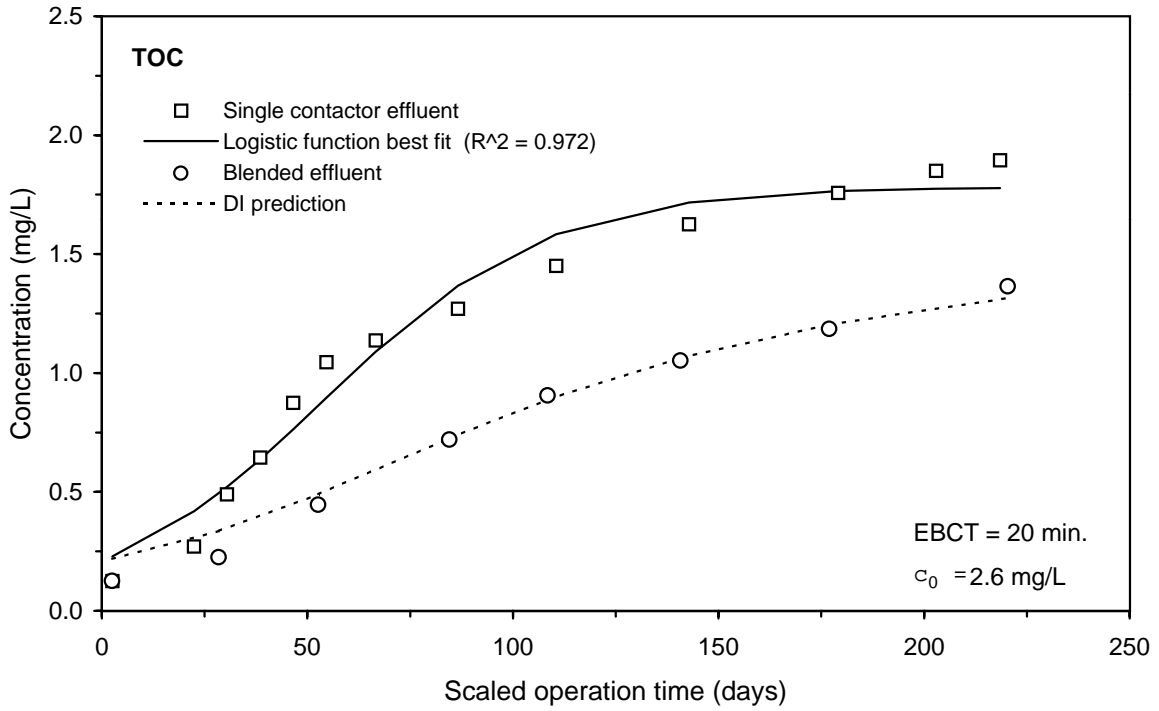


**Figure E-21 Single contactor and blended effluent TOC breakthrough curves for Water 2**

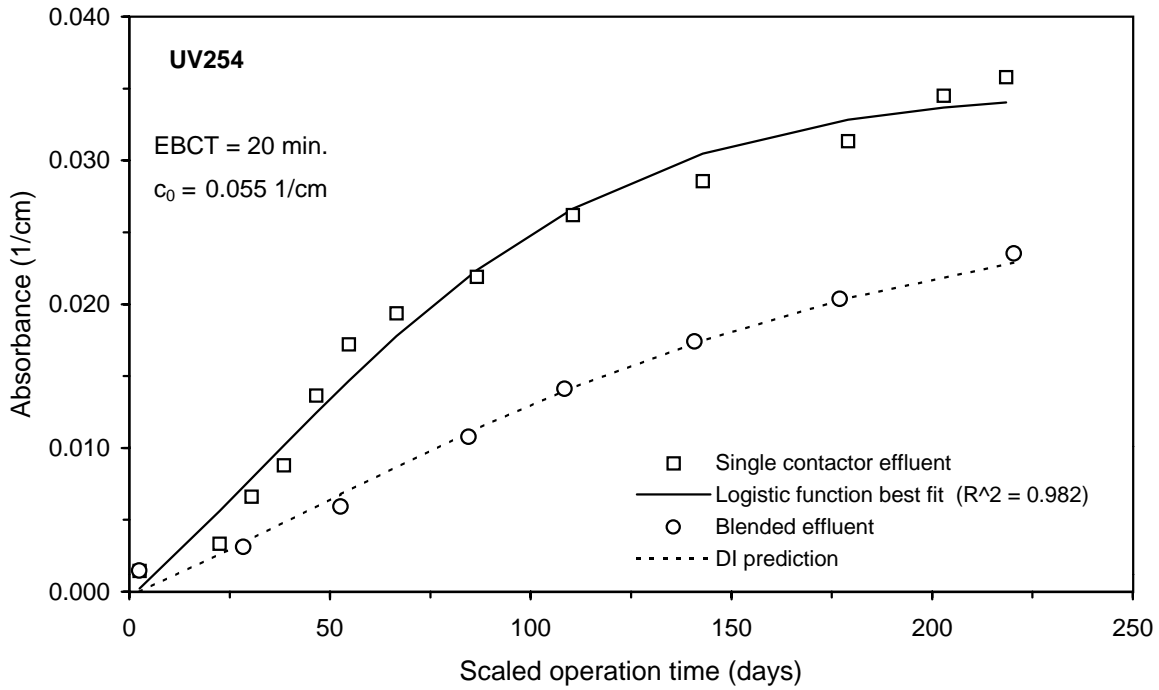


**Figure E-22 Single contactor and blended effluent UV254 breakthrough curves for Water 2**

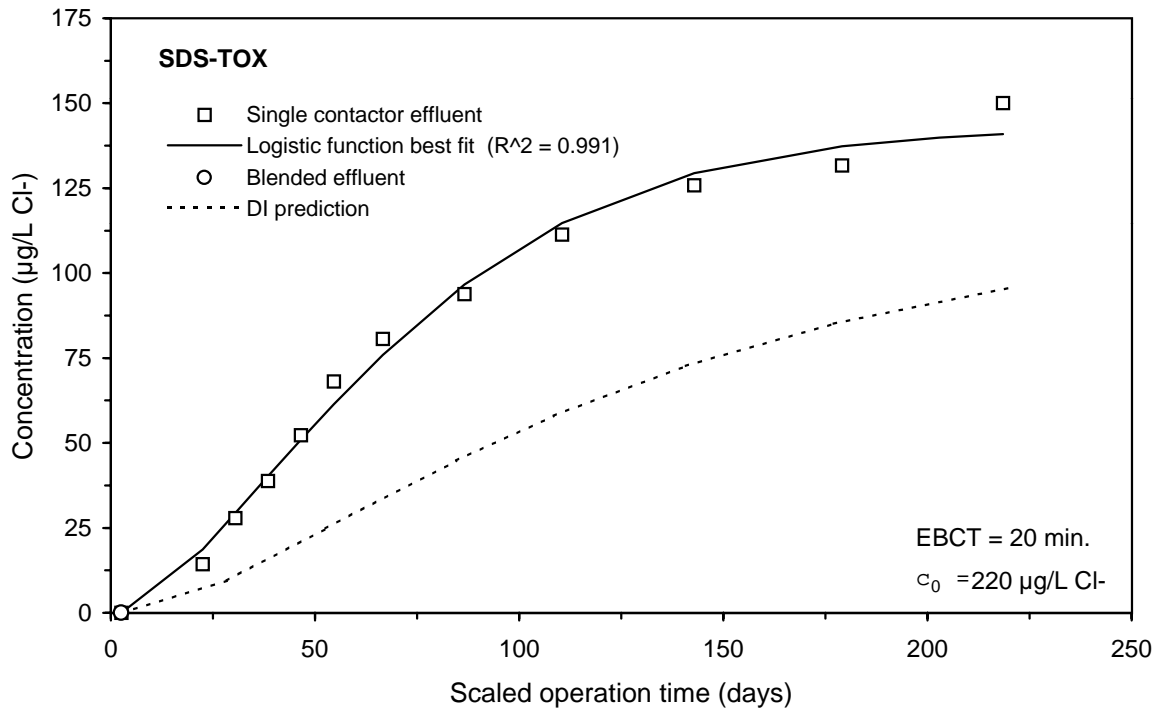


**Figure E-23 Single contactor and blended effluent SDS-TOX breakthrough curves for Water 2**

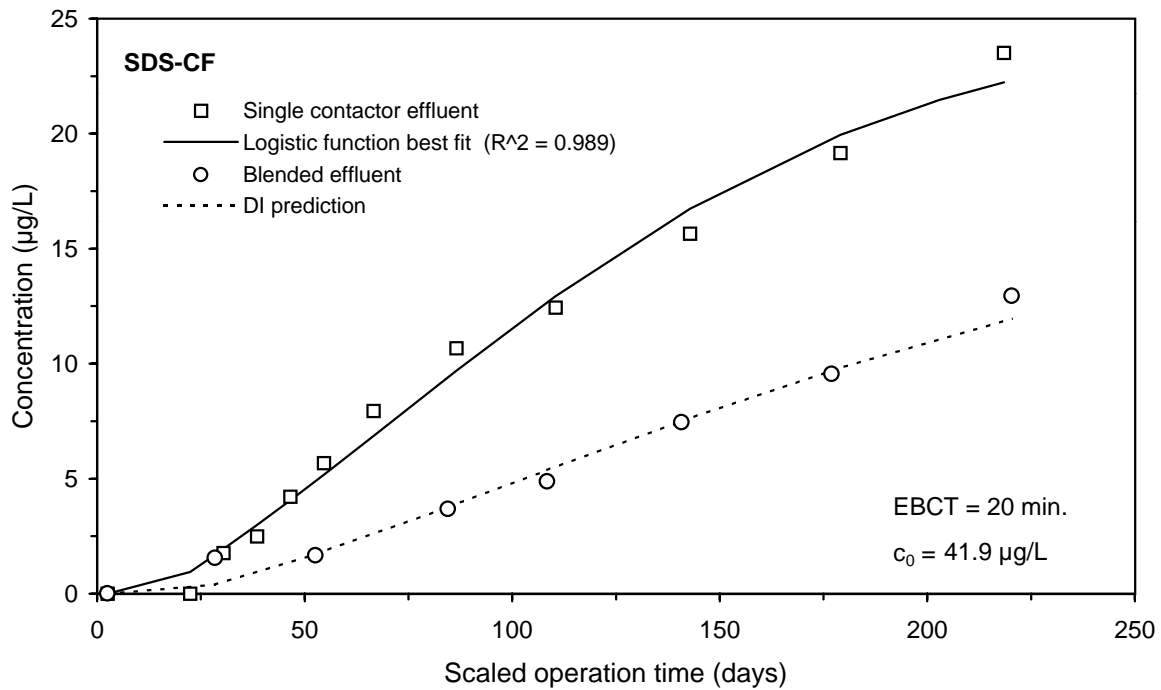


**Figure E-24 Single contactor and blended effluent SDS-CF breakthrough curves for Water 2**

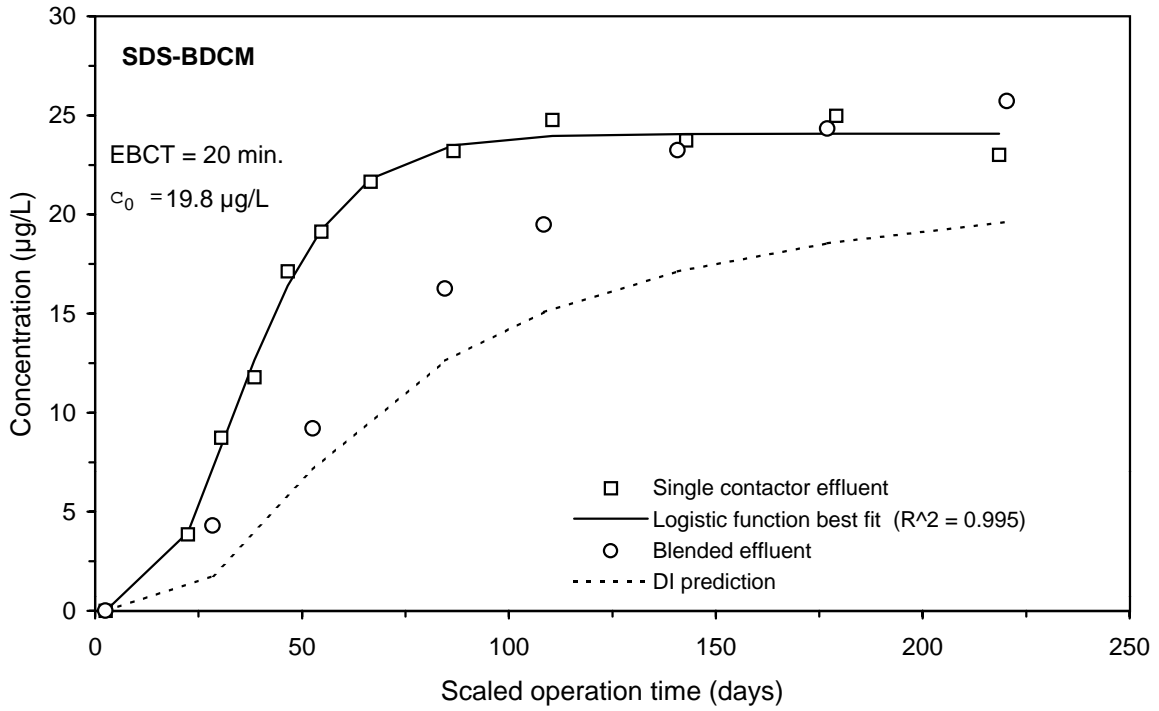


**Figure E-25 Single contactor and blended effluent SDS-BDCM breakthrough curves for Water 2**

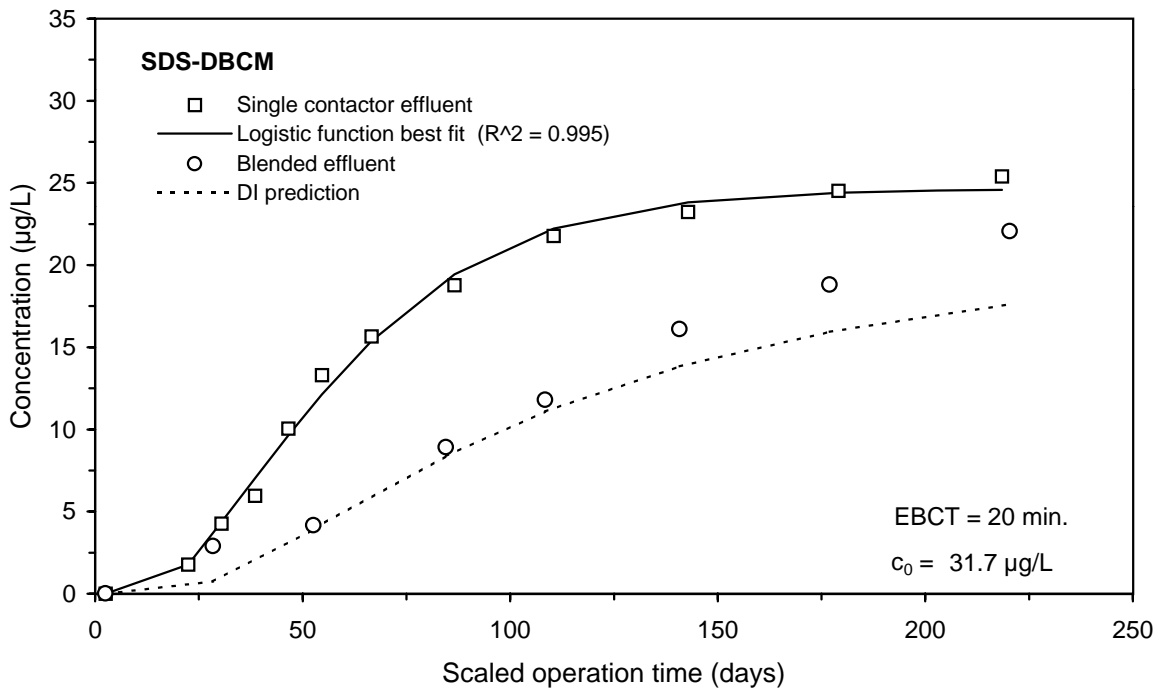


**Figure E-26 Single contactor and blended effluent SDS-DBCm breakthrough curves for Water 2**

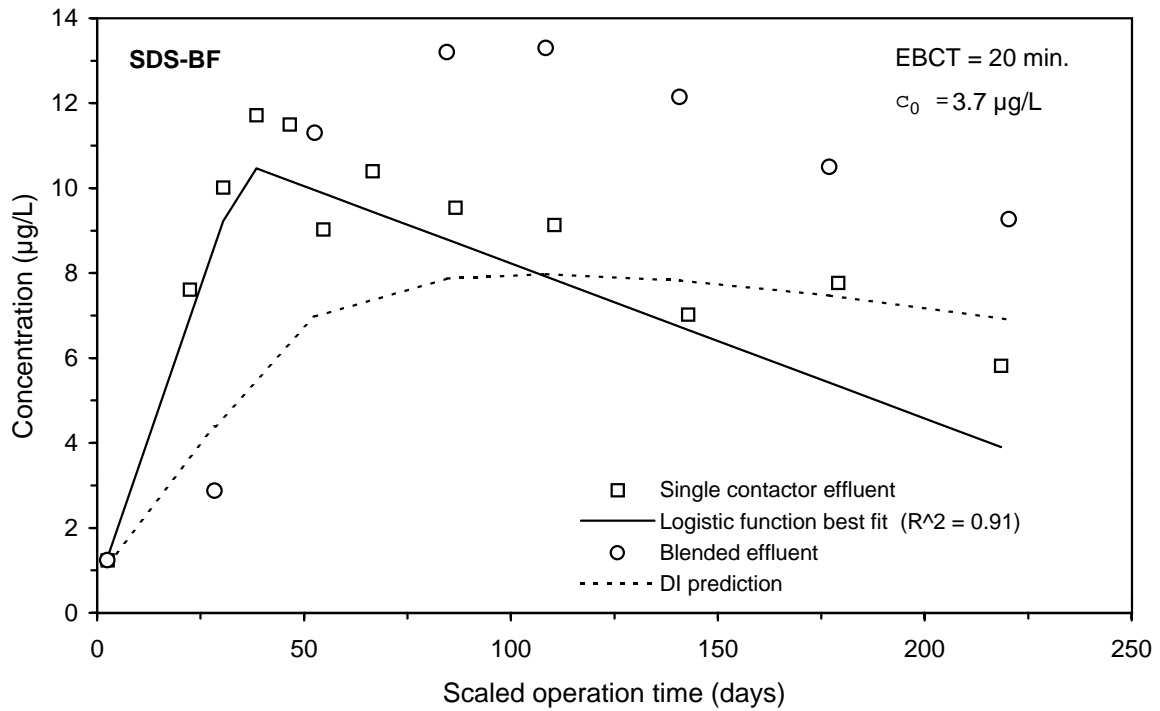


**Figure E-27 Single contactor and blended effluent SDS-BF breakthrough curves for Water 2**

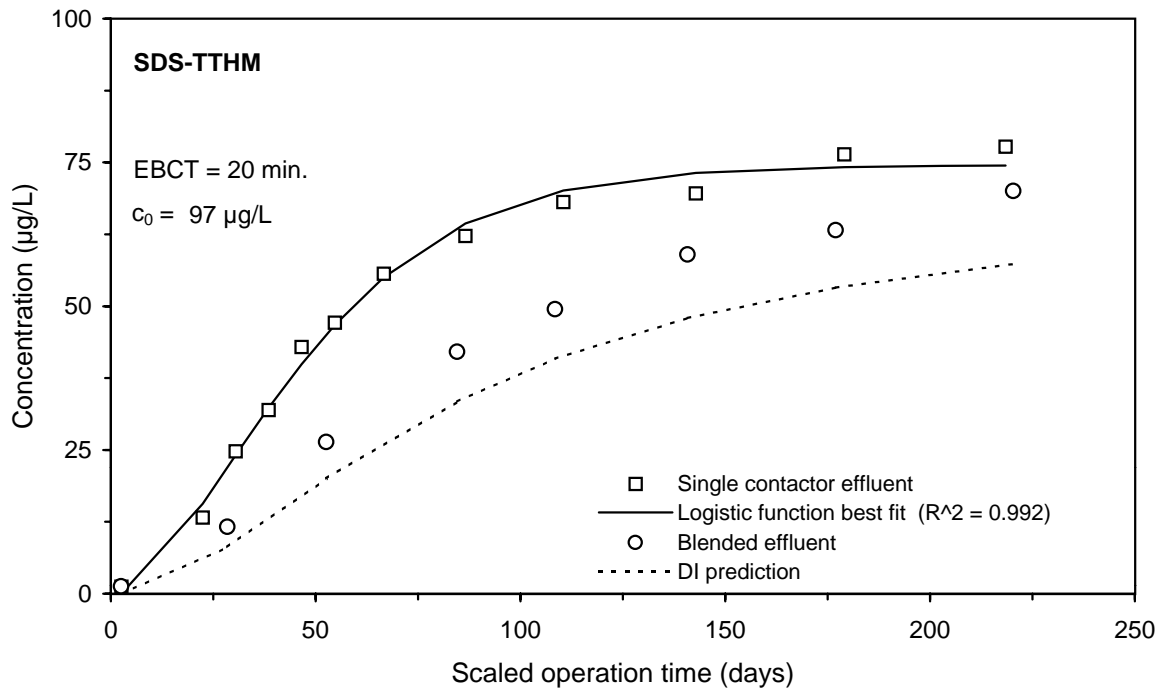


**Figure E-28 Single contactor and blended effluent SDS-TTHM breakthrough curves for Water 2**

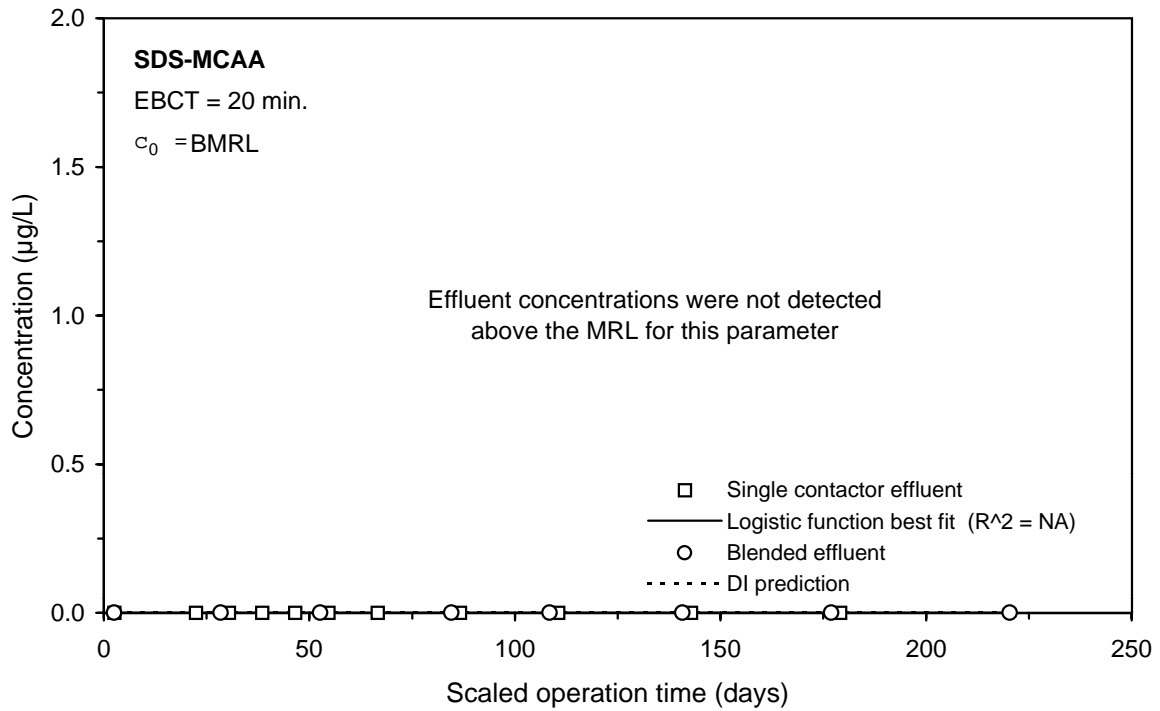


**Figure E-29 Single contactor and blended effluent SDS-MCAA breakthrough curves for Water 2**

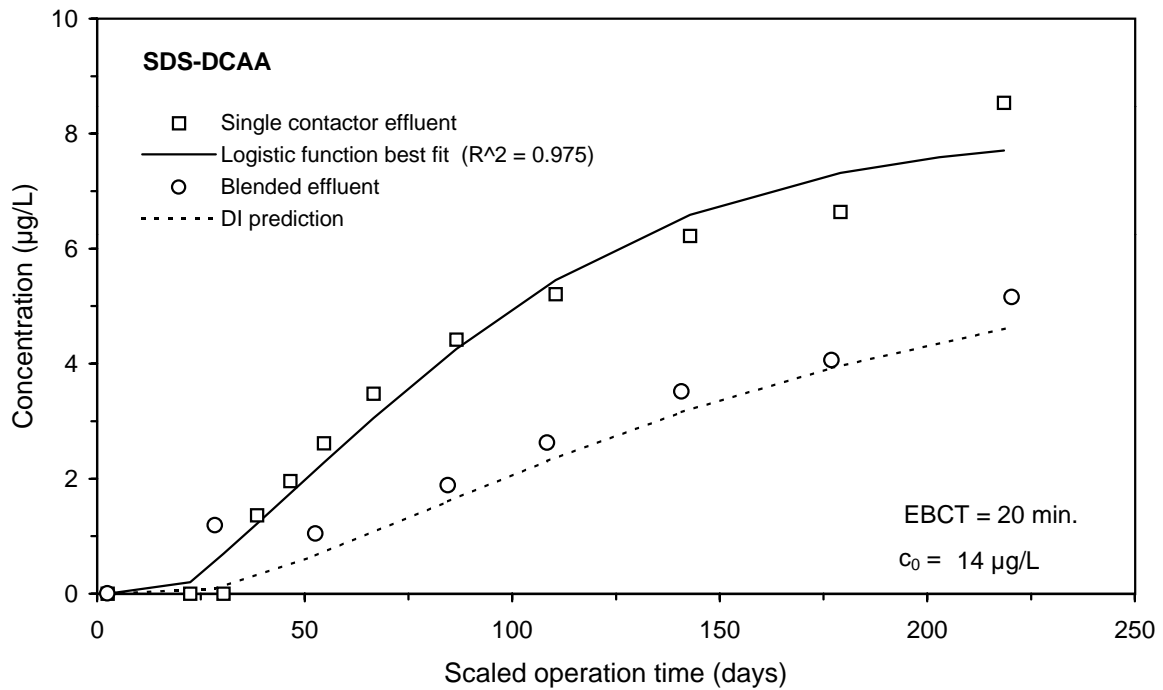


**Figure E-30 Single contactor and blended effluent SDS-DCAA breakthrough curves for Water 2**

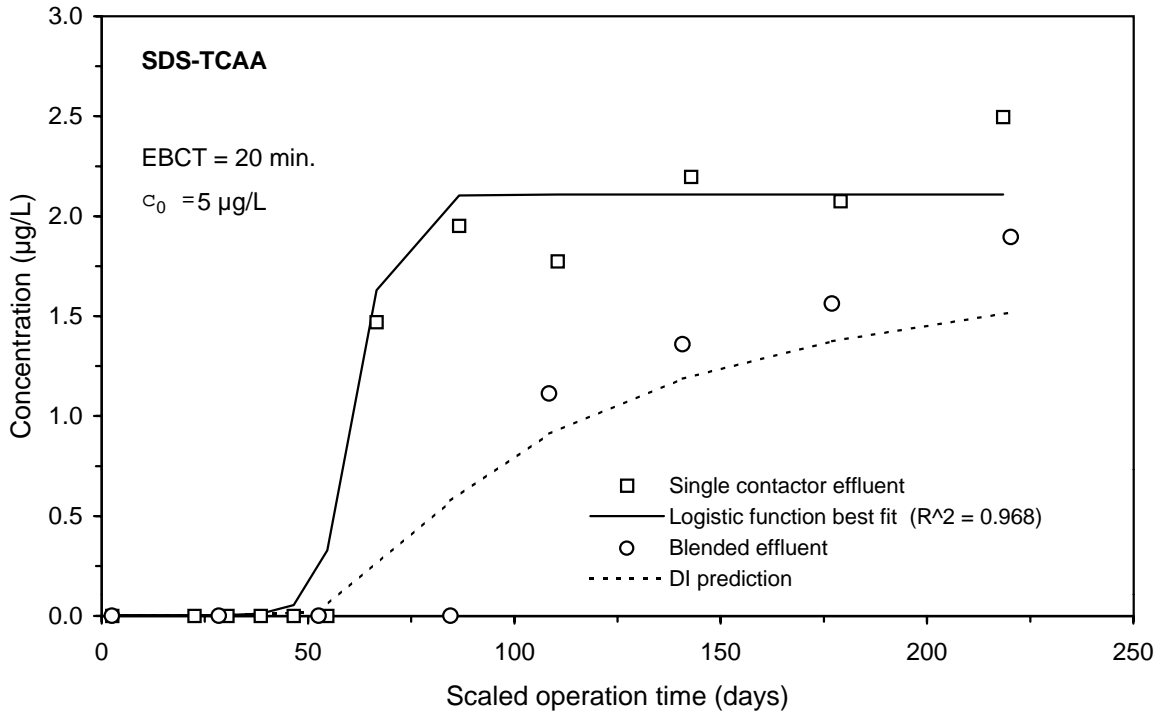


**Figure E-31 Single contactor and blended effluent SDS-TCAA breakthrough curves for Water 2**

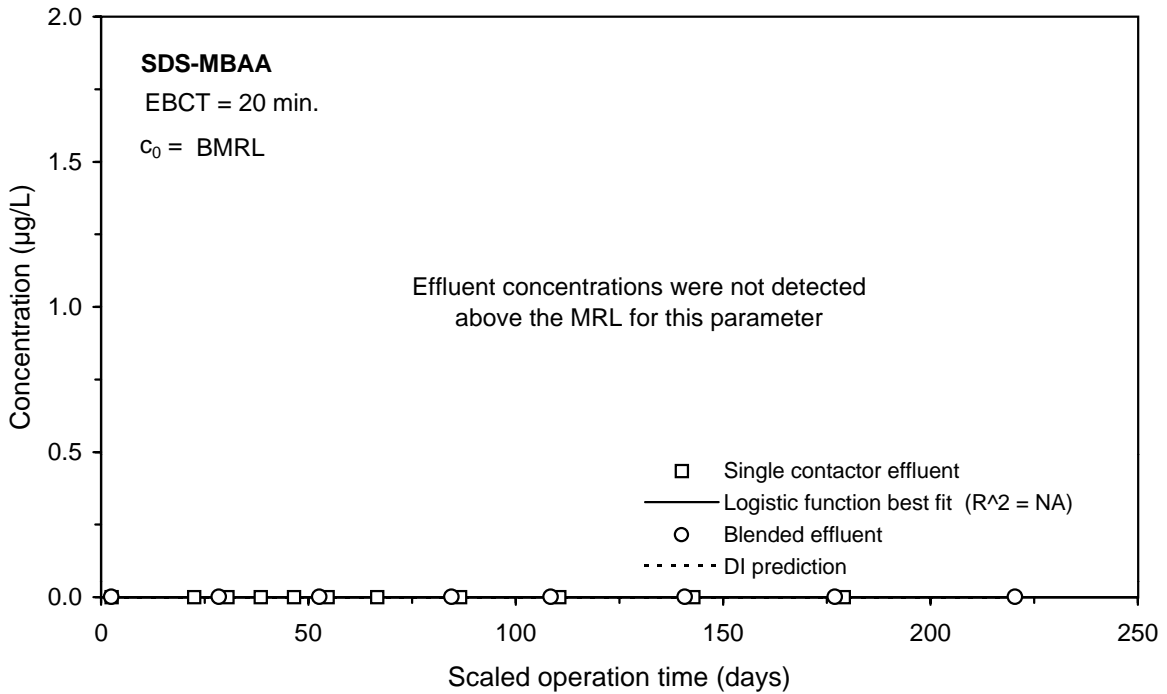


**Figure E-32 Single contactor and blended effluent SDS-MBAA breakthrough curves for Water 2**

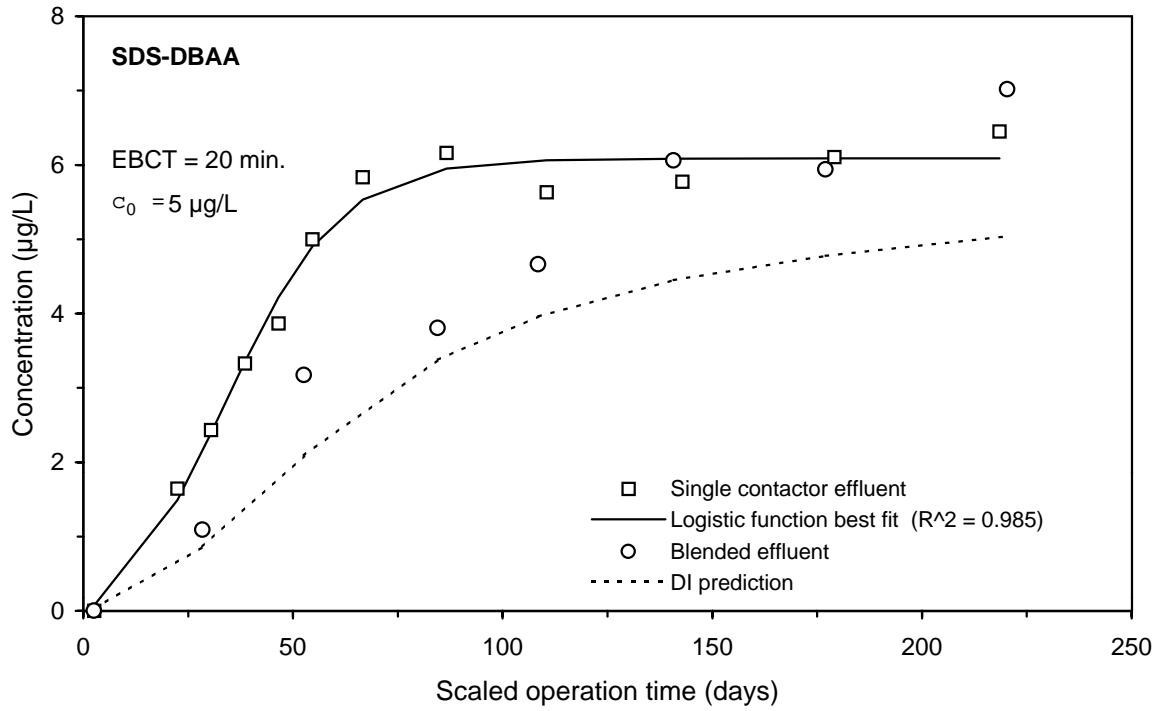


**Figure E-33 Single contactor and blended effluent SDS-DBAA breakthrough curves for Water 2**

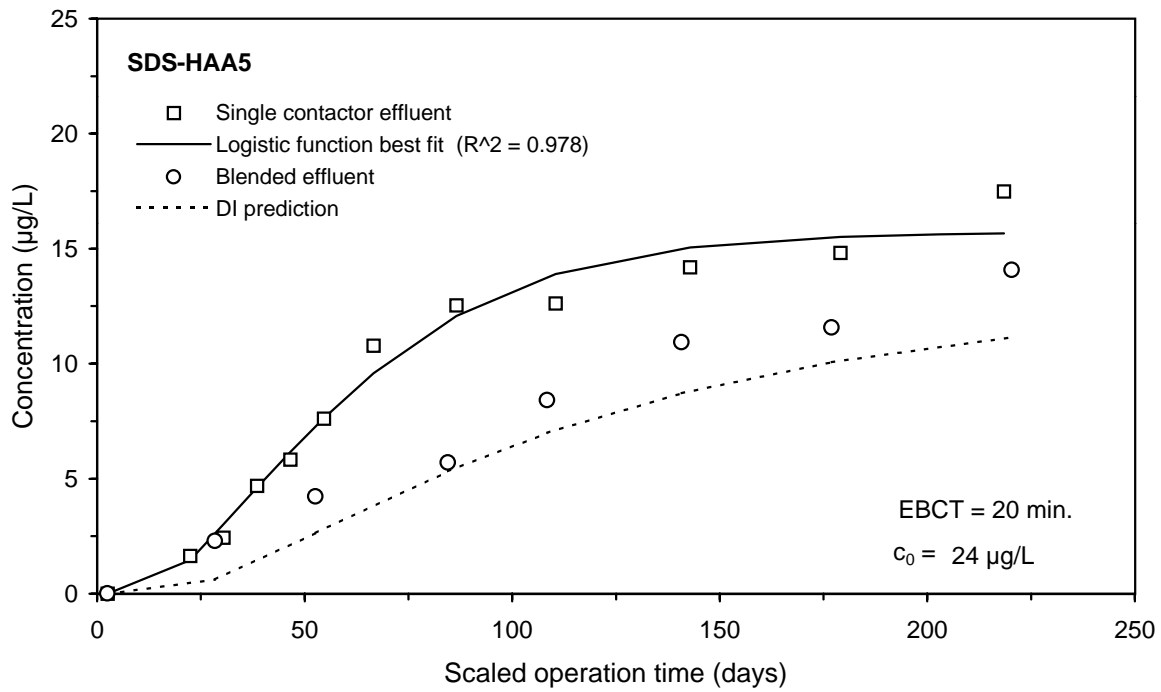


**Figure E-34 Single contactor and blended effluent SDS-HAA5 breakthrough curves for Water 2**

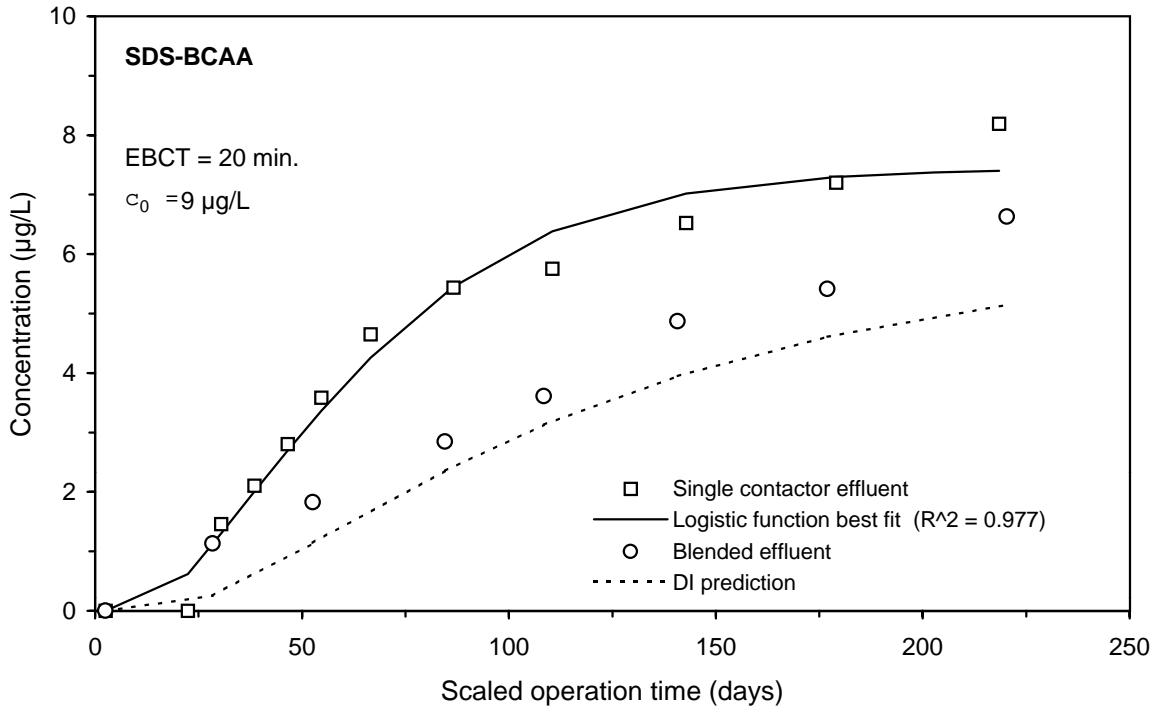


**Figure E-35 Single contactor and blended effluent SDS-BCAA breakthrough curves for Water 2**

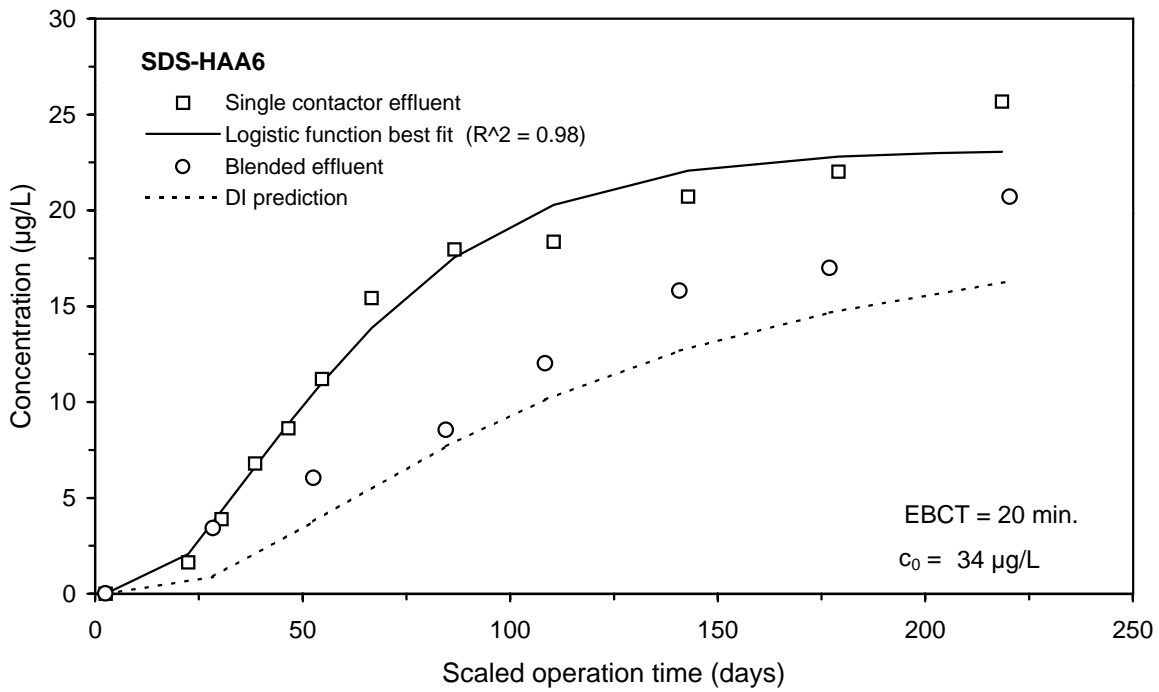


**Figure E-36 Single contactor and blended effluent SDS-HAA6 breakthrough curves for Water 2**

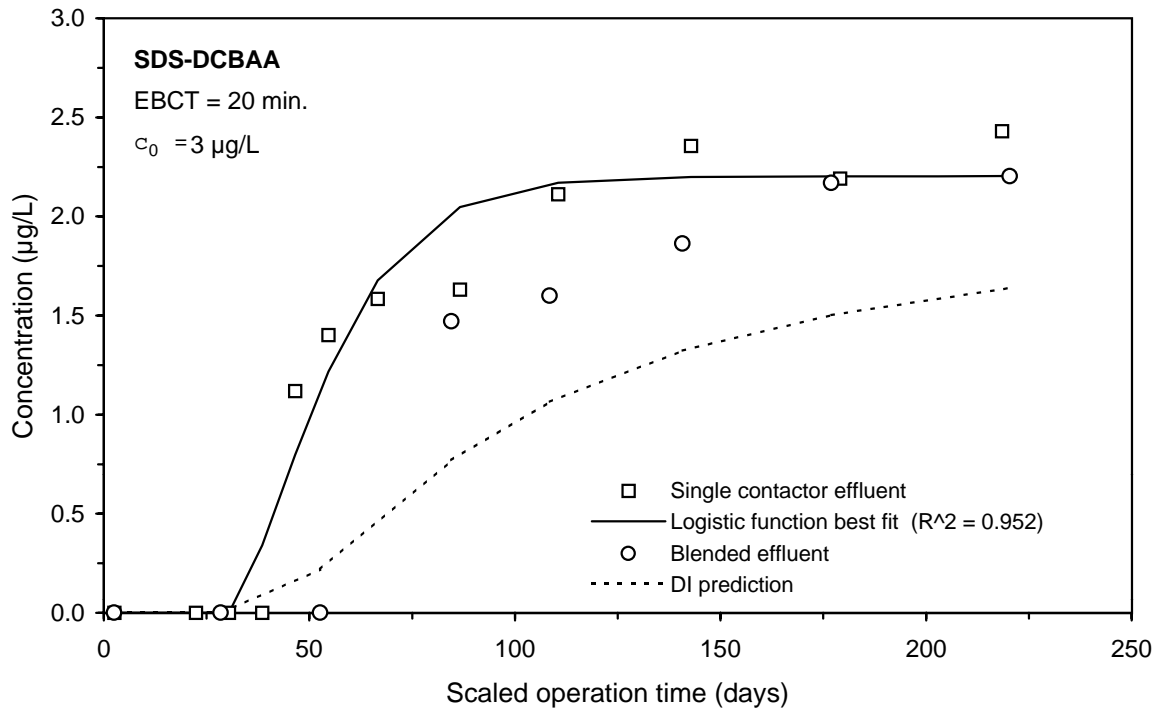


**Figure E-37 Single contactor and blended effluent SDS-DCBAA breakthrough curves for Water 2**

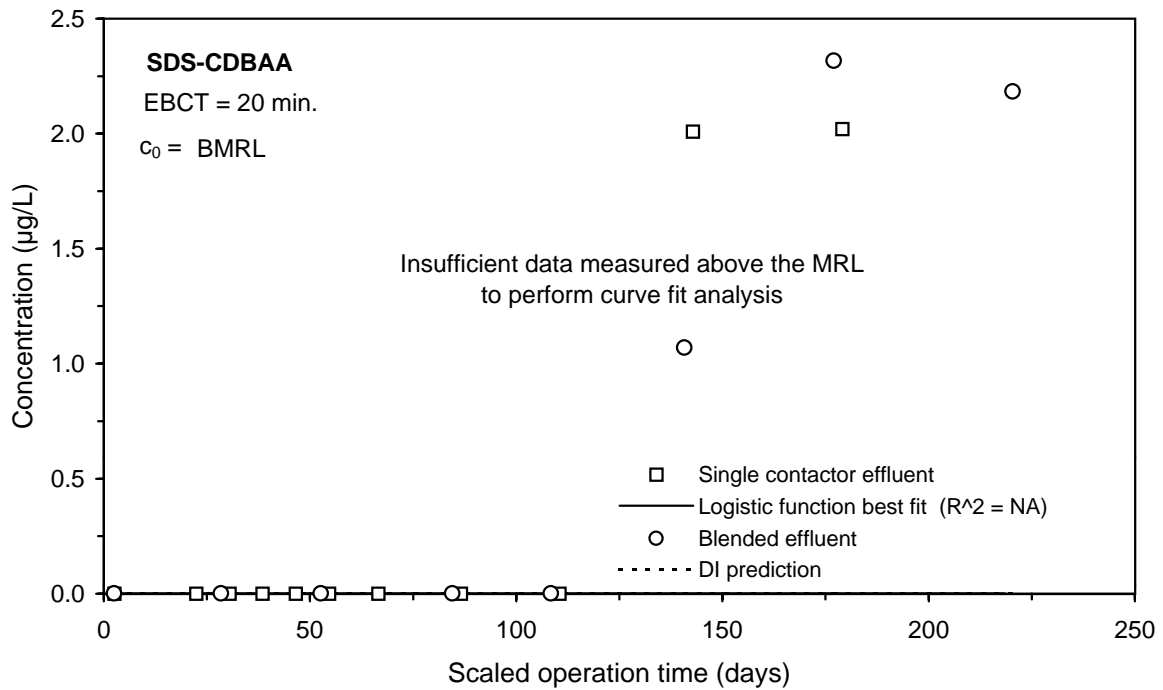


**Figure E-38 Single contactor and blended effluent SDS-CDBAA breakthrough curves for Water 2**

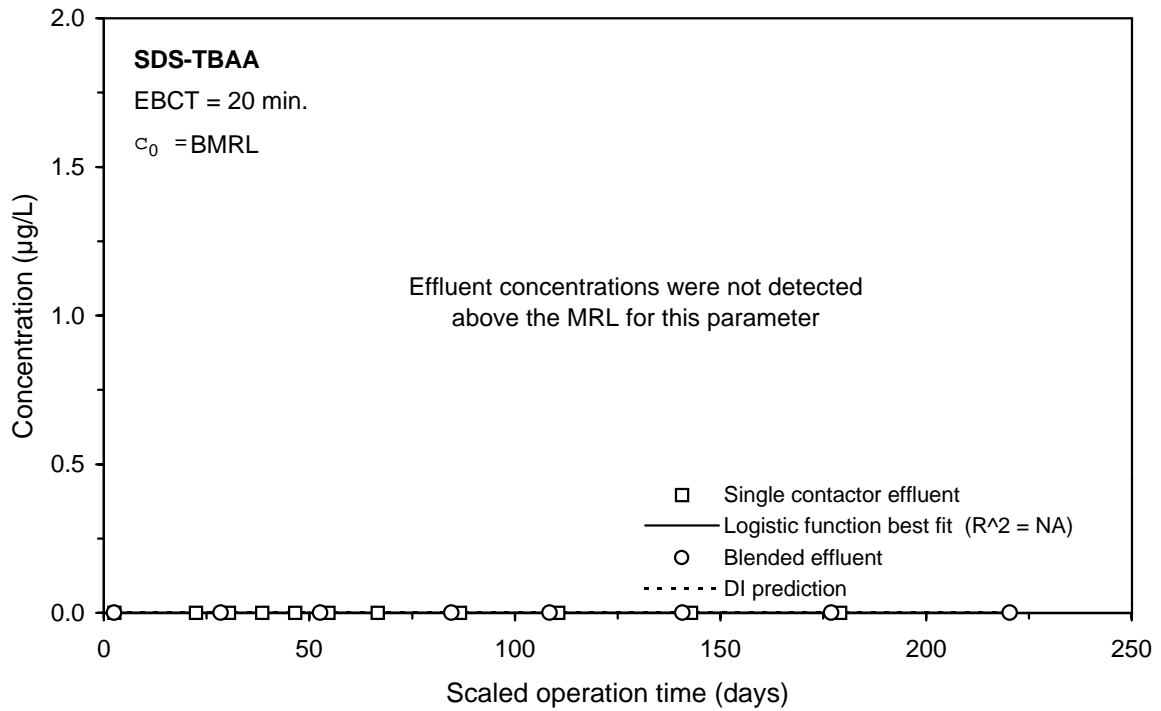


**Figure E-39 Single contactor and blended effluent SDS-TBAA breakthrough curves for Water 2**

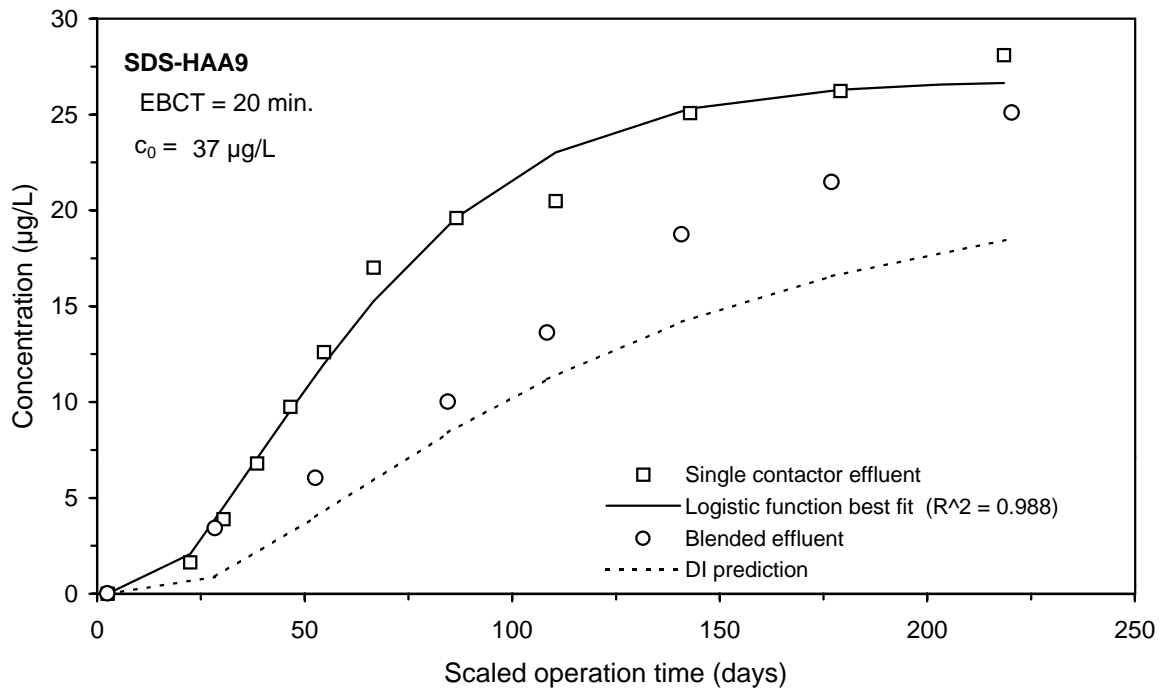


**Figure E-40 Single contactor and blended effluent SDS-HAA9 breakthrough curves for Water 2**

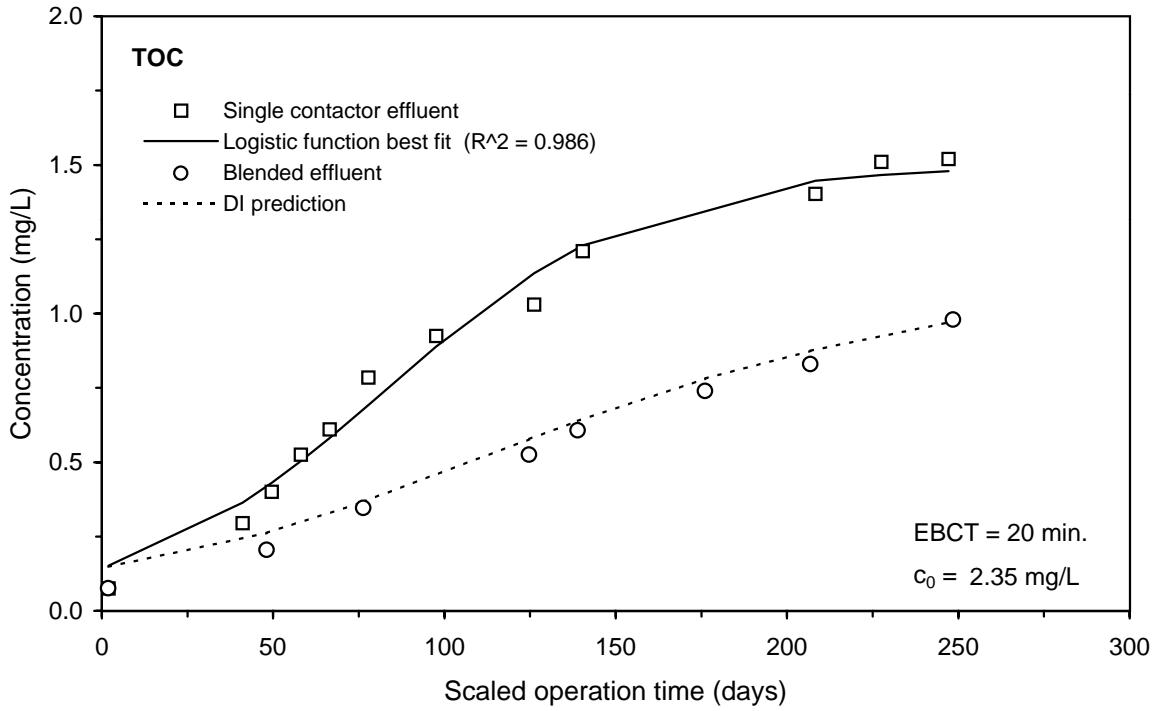


**Figure E-41 Single contactor and blended effluent TOC breakthrough curves for Water 3**

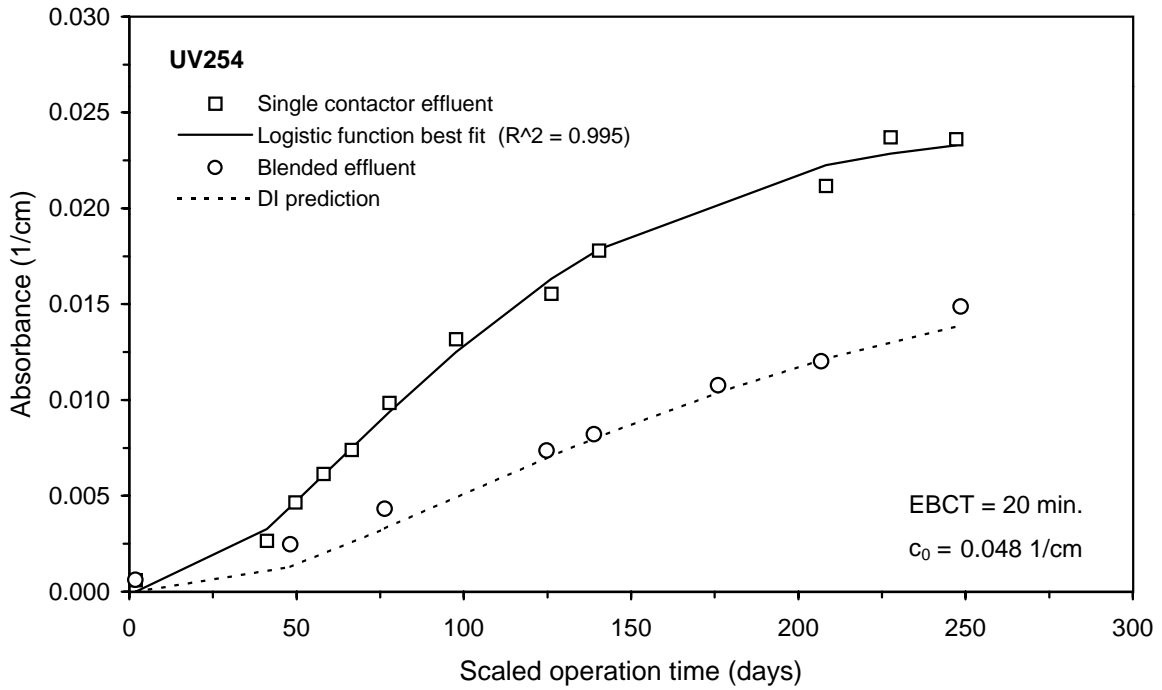


**Figure E-42 Single contactor and blended effluent UV254 breakthrough curves for Water 3**

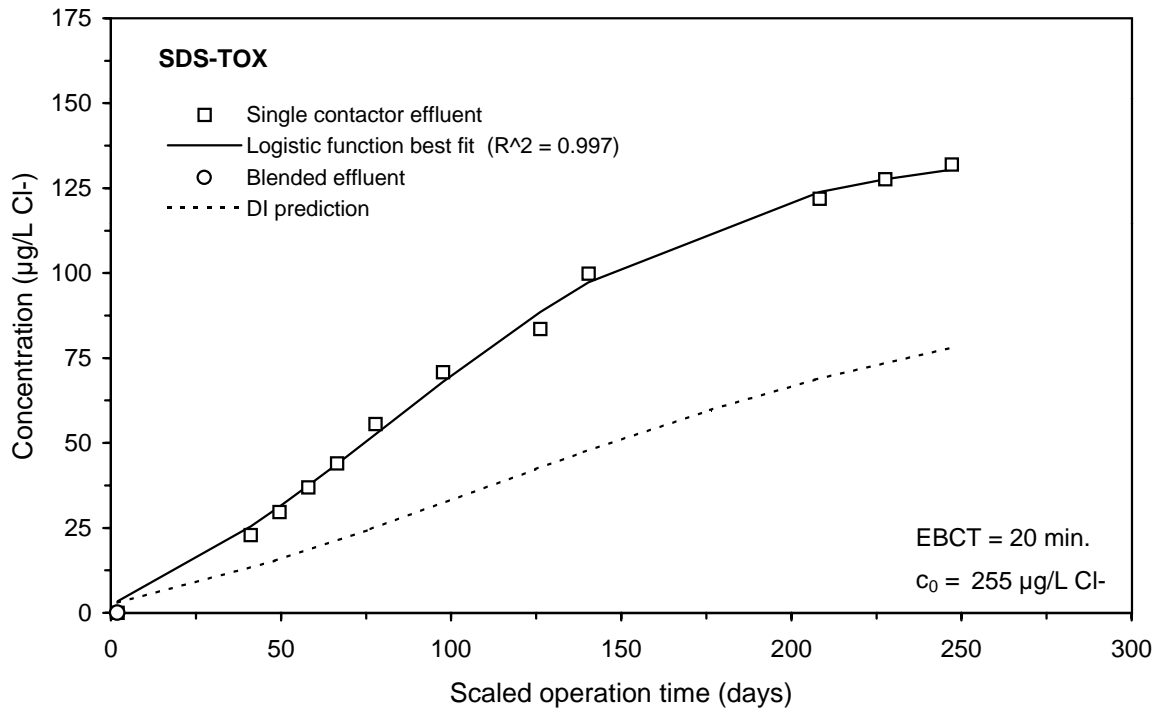


**Figure E-43 Single contactor and blended effluent SDS-TOX breakthrough curves for Water 3**

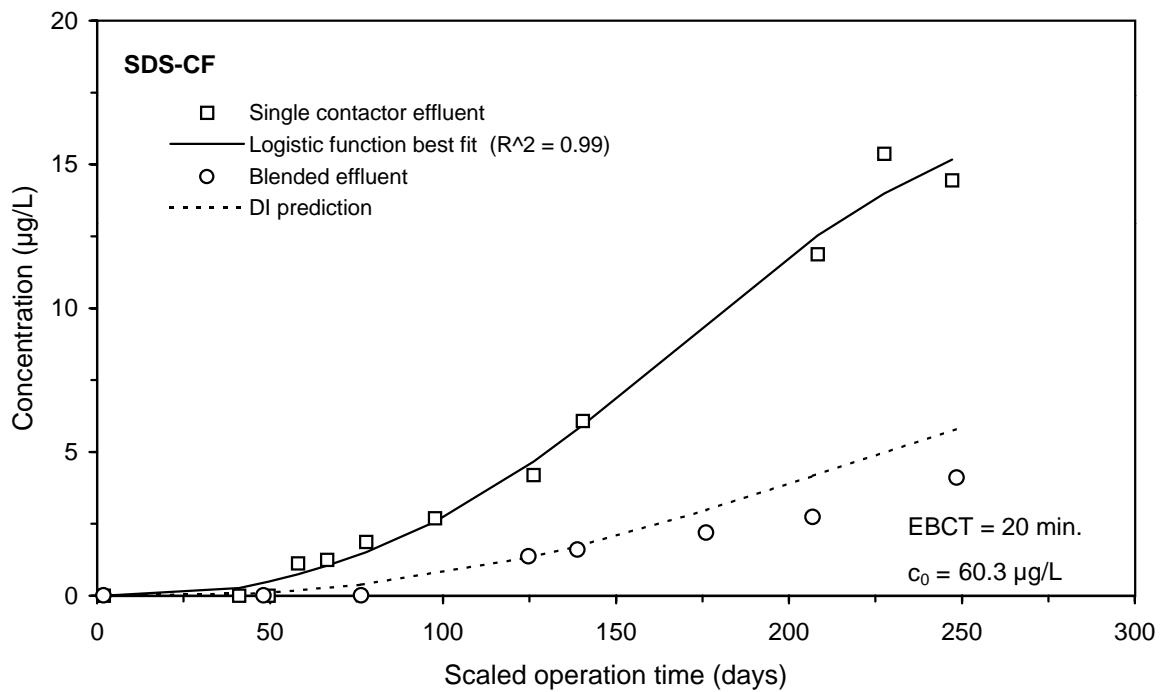


**Figure E-44 Single contactor and blended effluent SDS-CF breakthrough curves for Water 3**

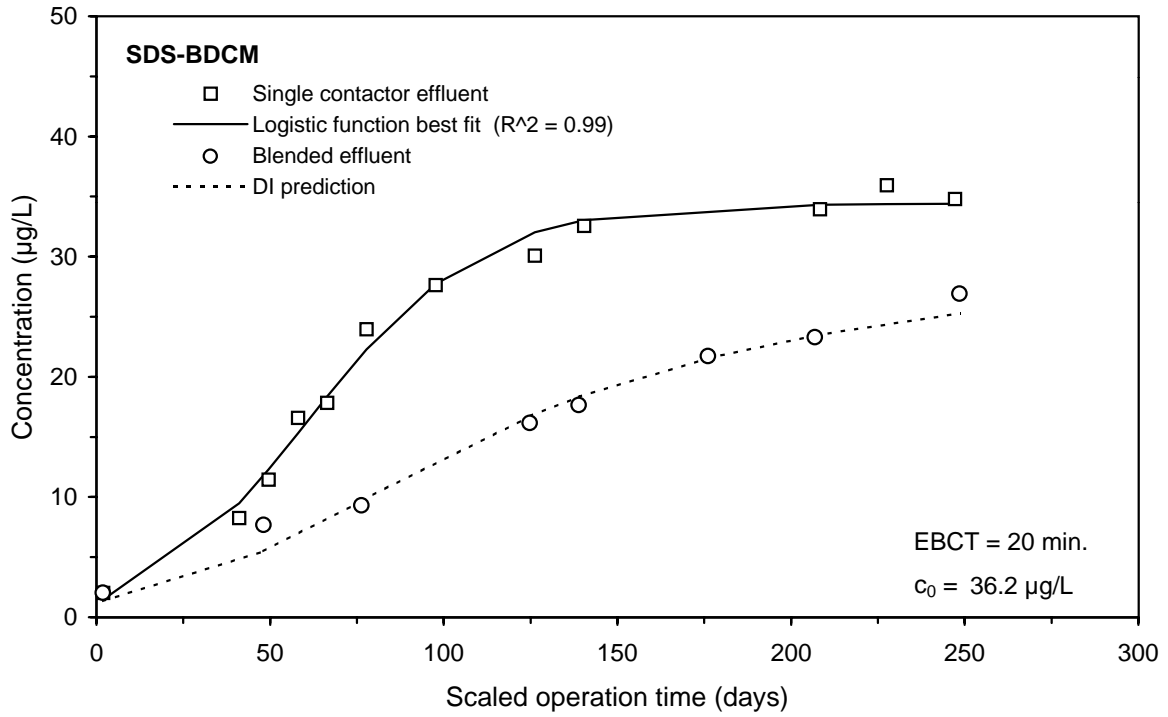


**Figure E-45 Single contactor and blended effluent SDS-BDCM breakthrough curves for Water 3**

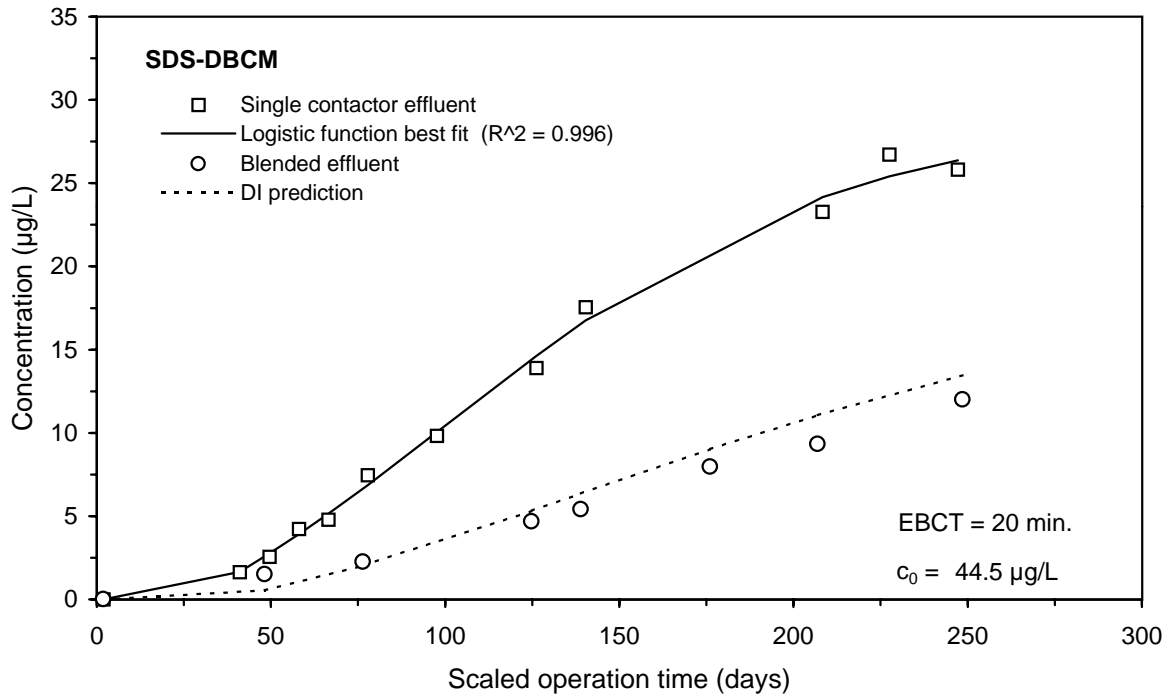


**Figure E-46 Single contactor and blended effluent SDS-DBCm breakthrough curves for Water 3**

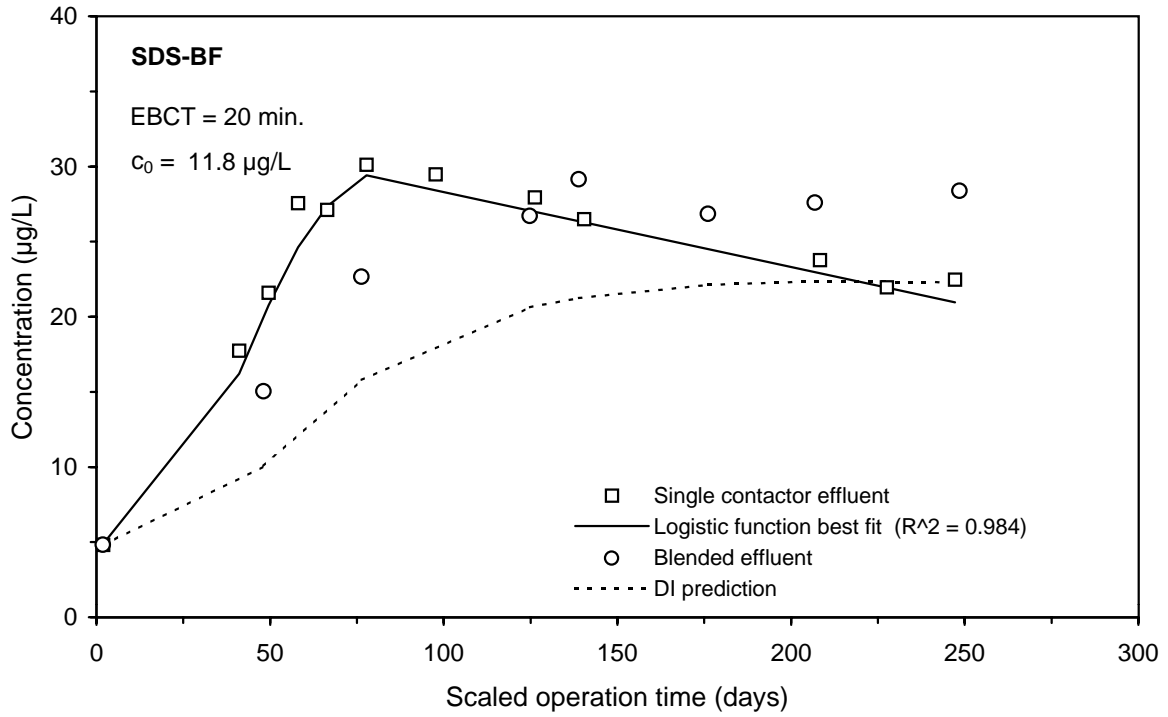


**Figure E-47 Single contactor and blended effluent SDS-BF breakthrough curves for Water 3**

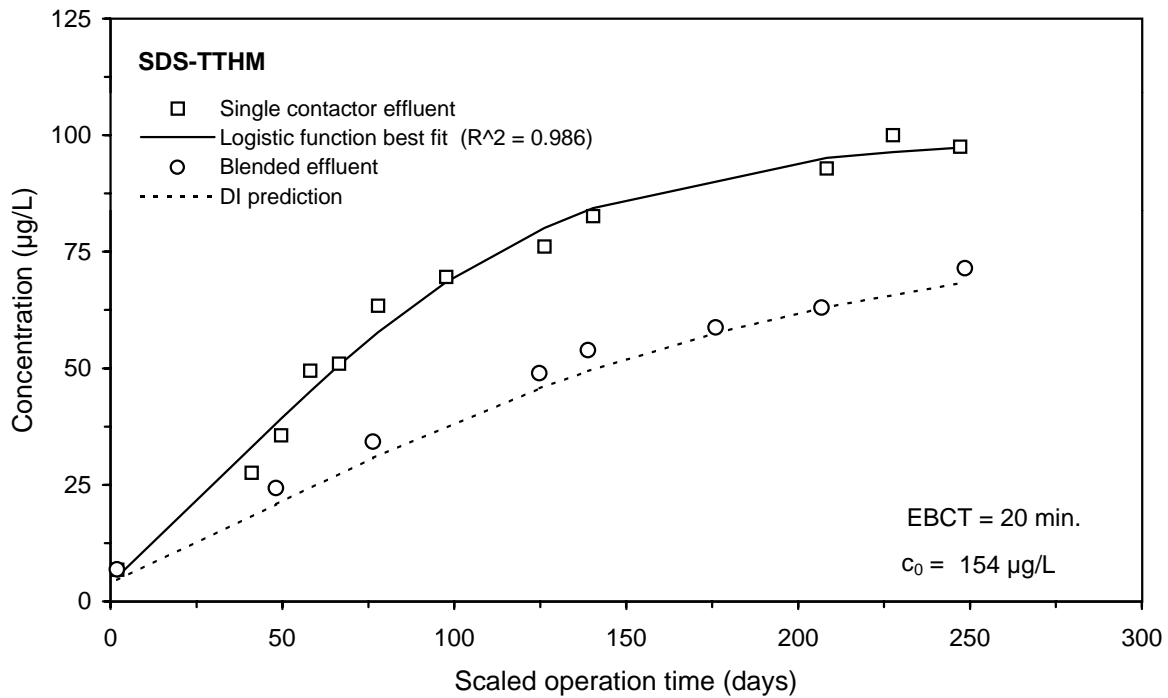


**Figure E-48 Single contactor and blended effluent SDS-TTHM breakthrough curves for Water 3**

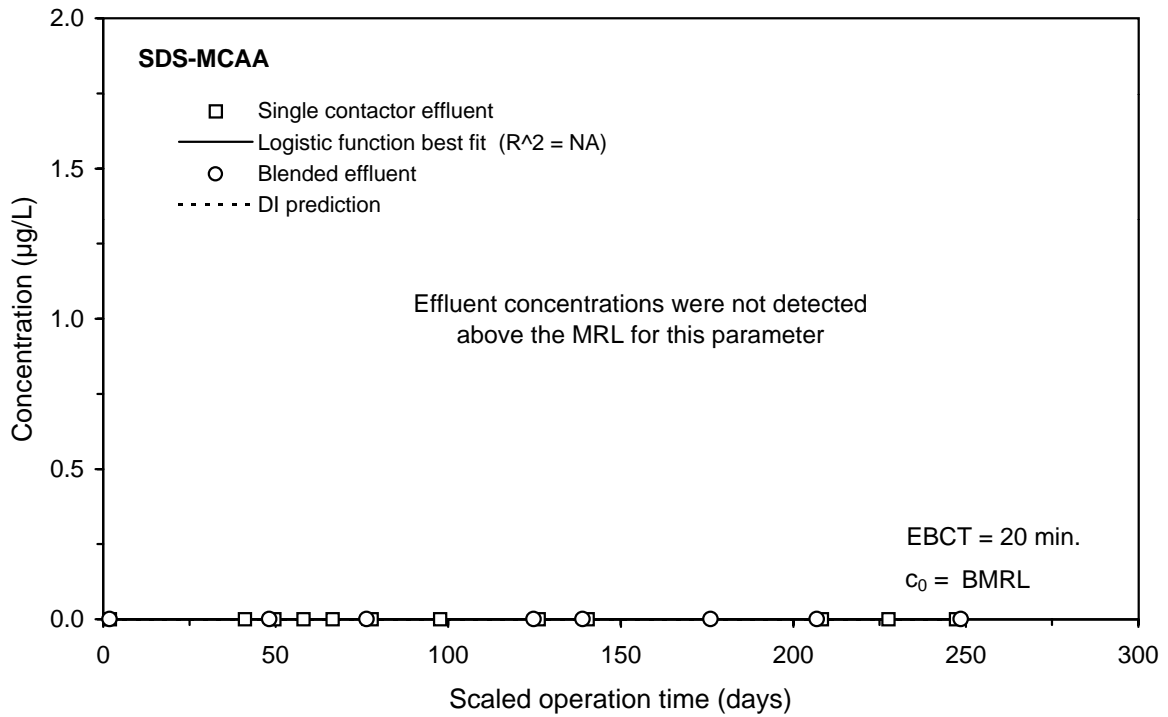


**Figure E-49 Single contactor and blended effluent SDS-MCAA breakthrough curves for Water 3**

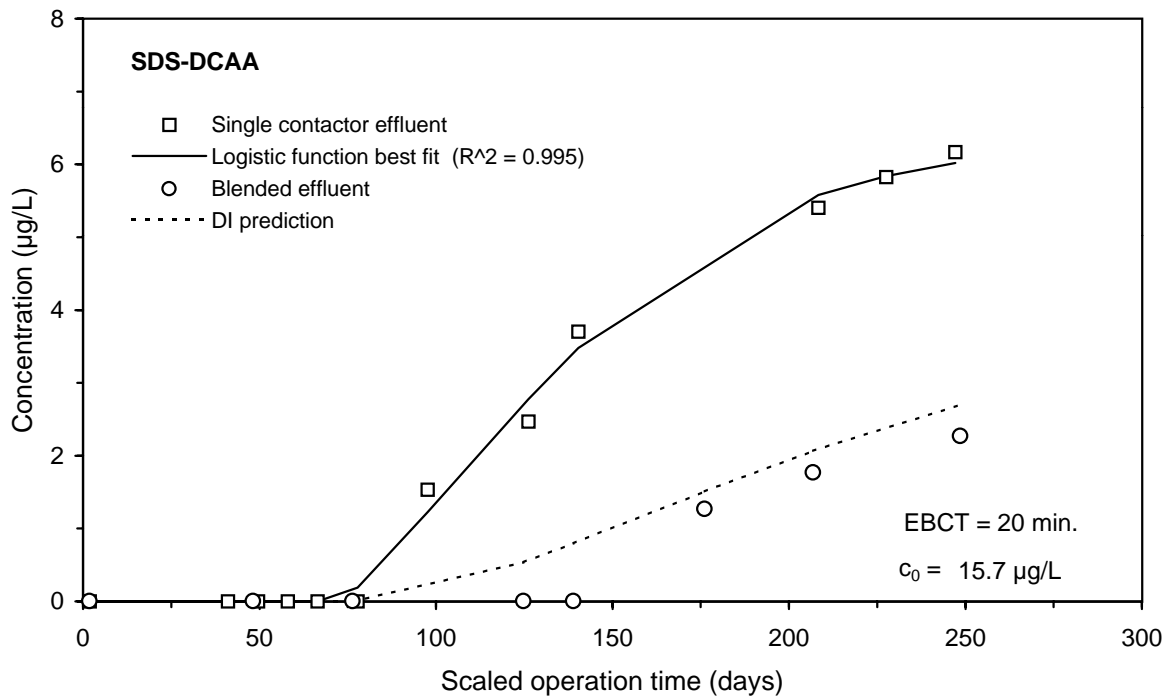


**Figure E-50 Single contactor and blended effluent SDS-DCAA breakthrough curves for Water 3**

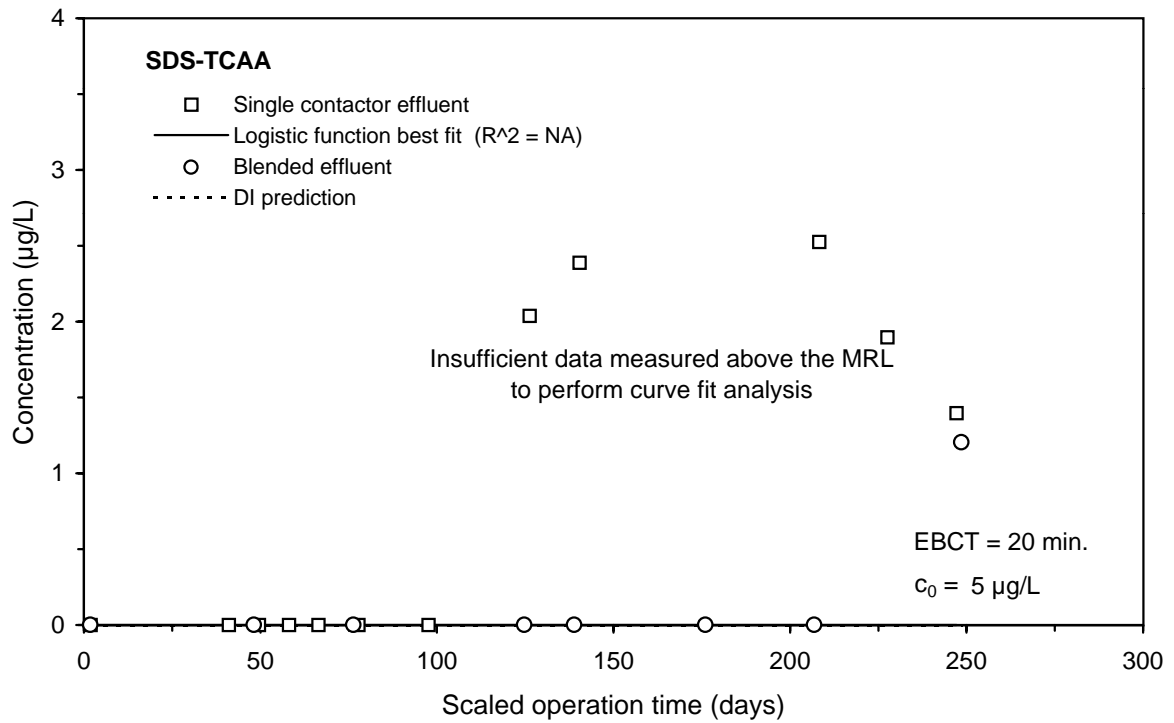


**Figure E-51 Single contactor and blended effluent SDS-TCAA breakthrough curves for Water 3**

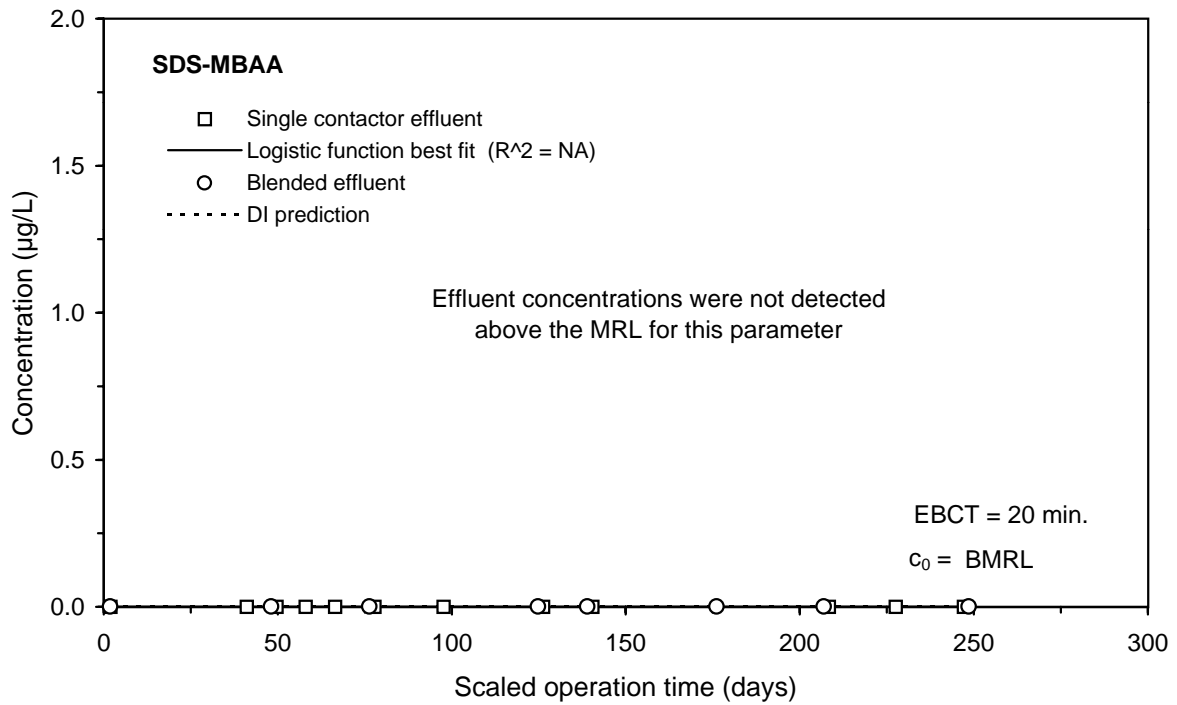


**Figure E-52 Single contactor and blended effluent SDS-MBAA breakthrough curves for Water 3**

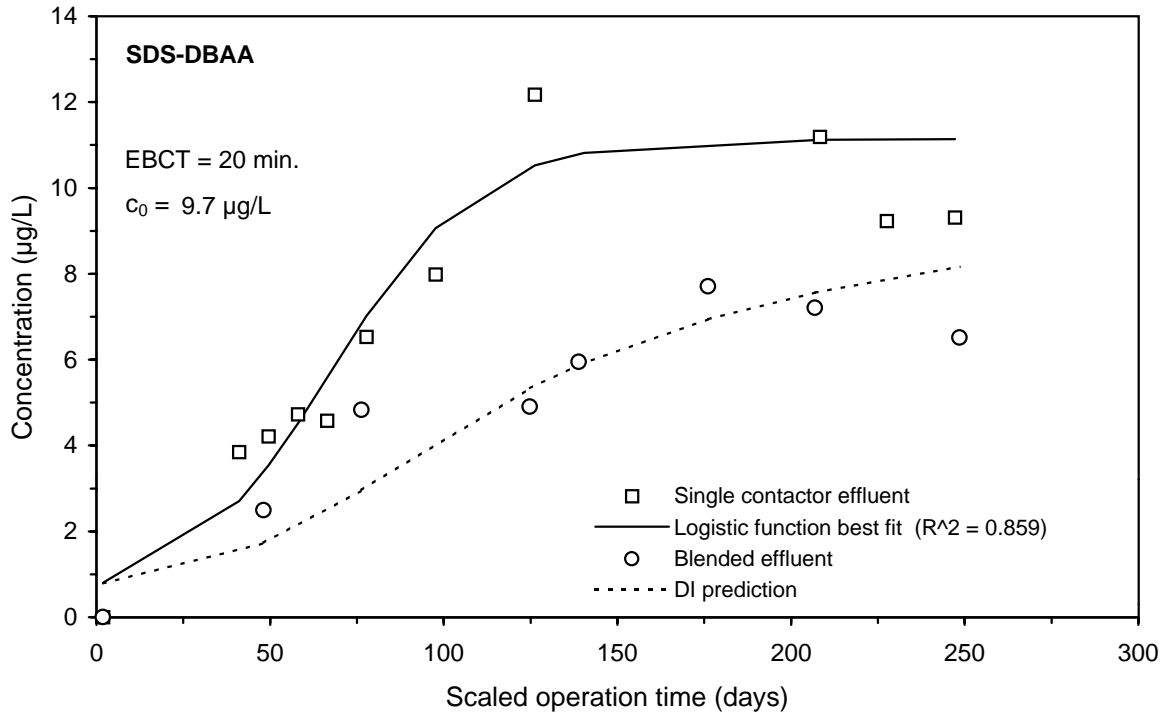


**Figure E-53 Single contactor and blended effluent SDS-DBAA breakthrough curves for Water 3**

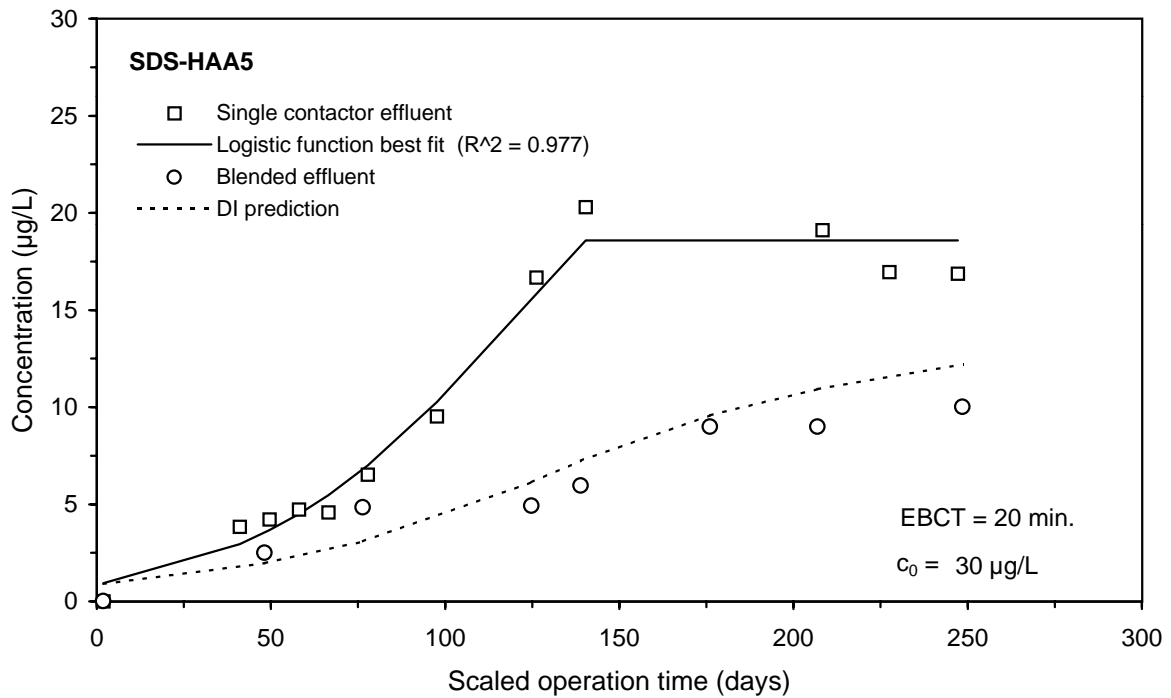


**Figure E-54 Single contactor and blended effluent SDS-HAA5 breakthrough curves for Water 3**

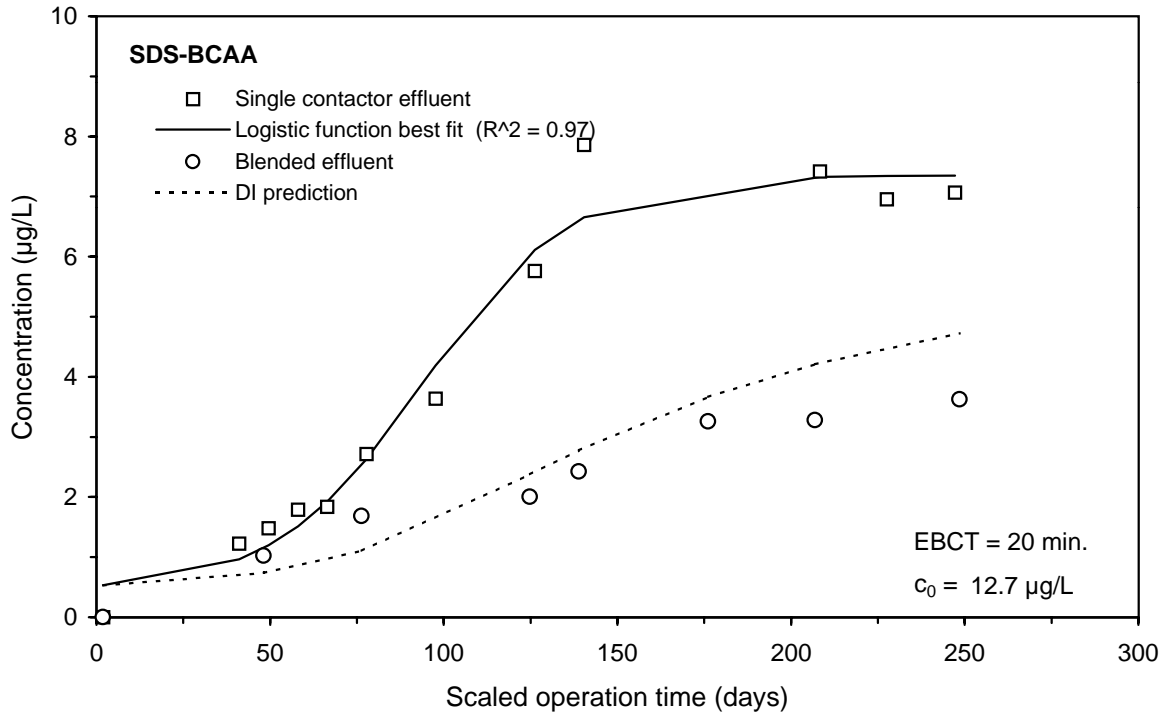


**Figure E-55 Single contactor and blended effluent SDS-BCAA breakthrough curves for Water 3**

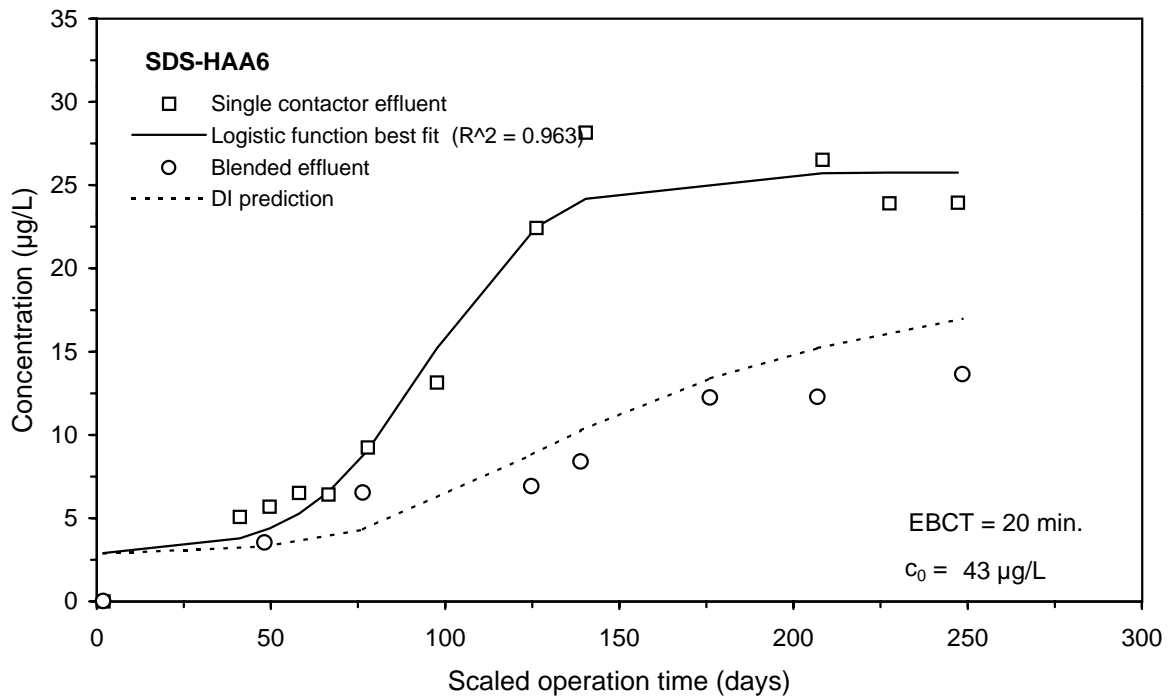


**Figure E-56 Single contactor and blended effluent SDS-HAA6 breakthrough curves for Water 3**

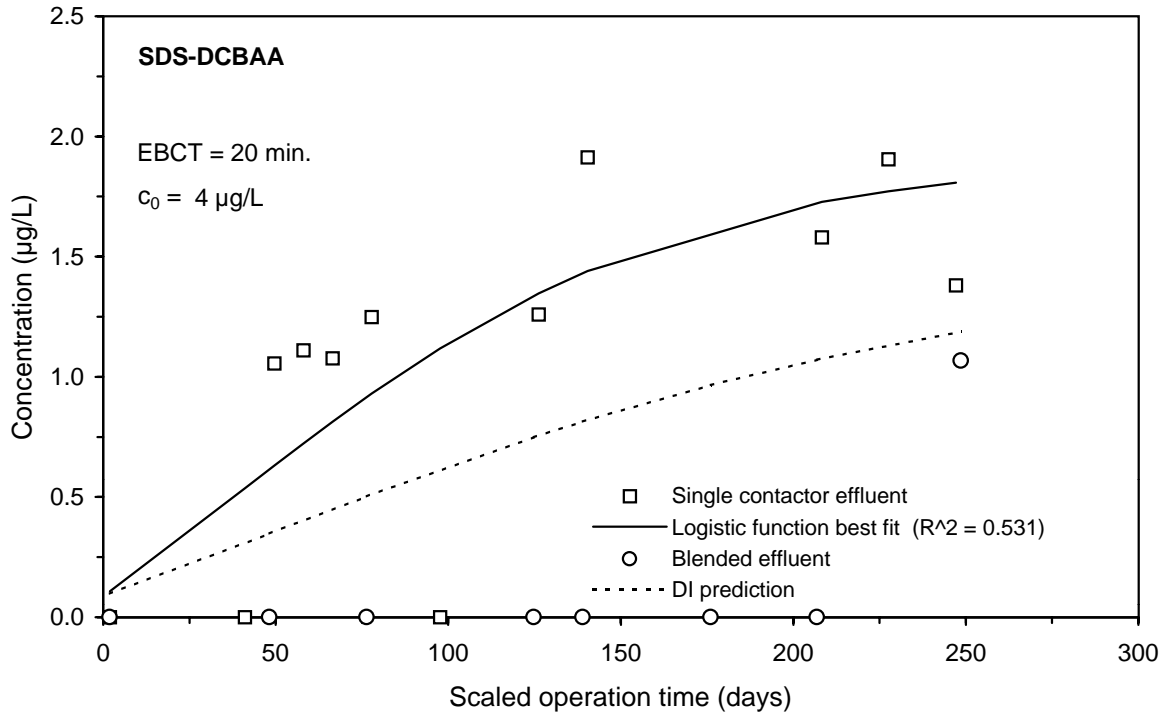


**Figure E-57 Single contactor and blended effluent SDS-DCBAA breakthrough curves for Water 3**

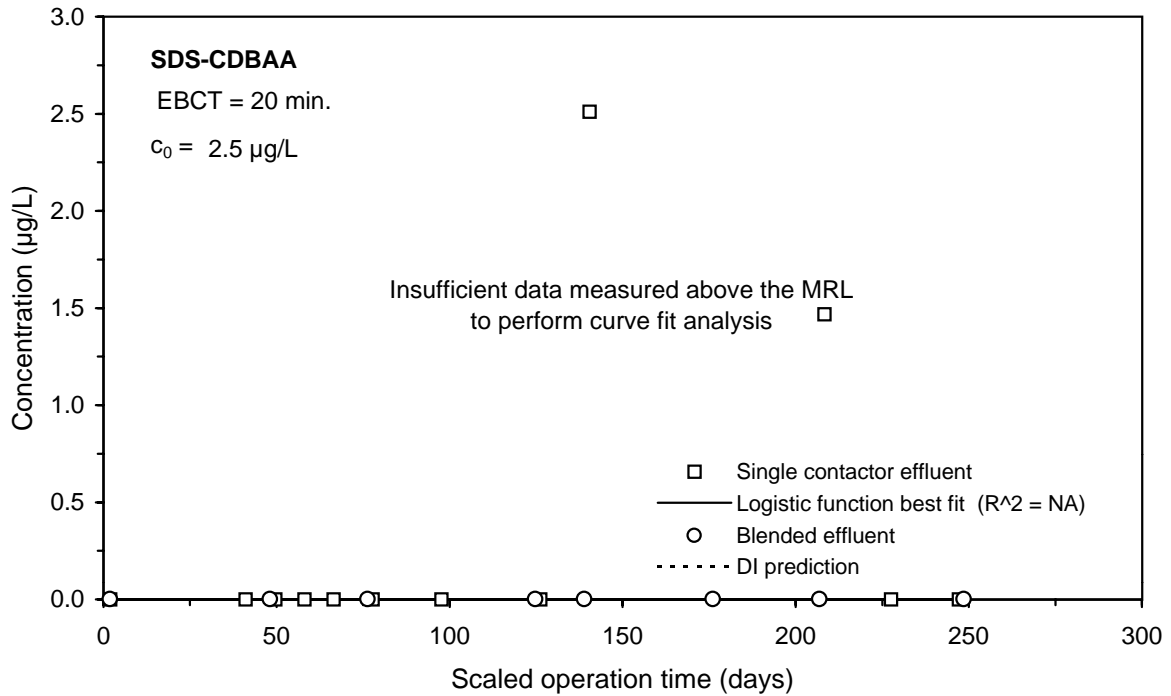


**Figure E-58 Single contactor and blended effluent SDS-CDBAA breakthrough curves for Water 3**

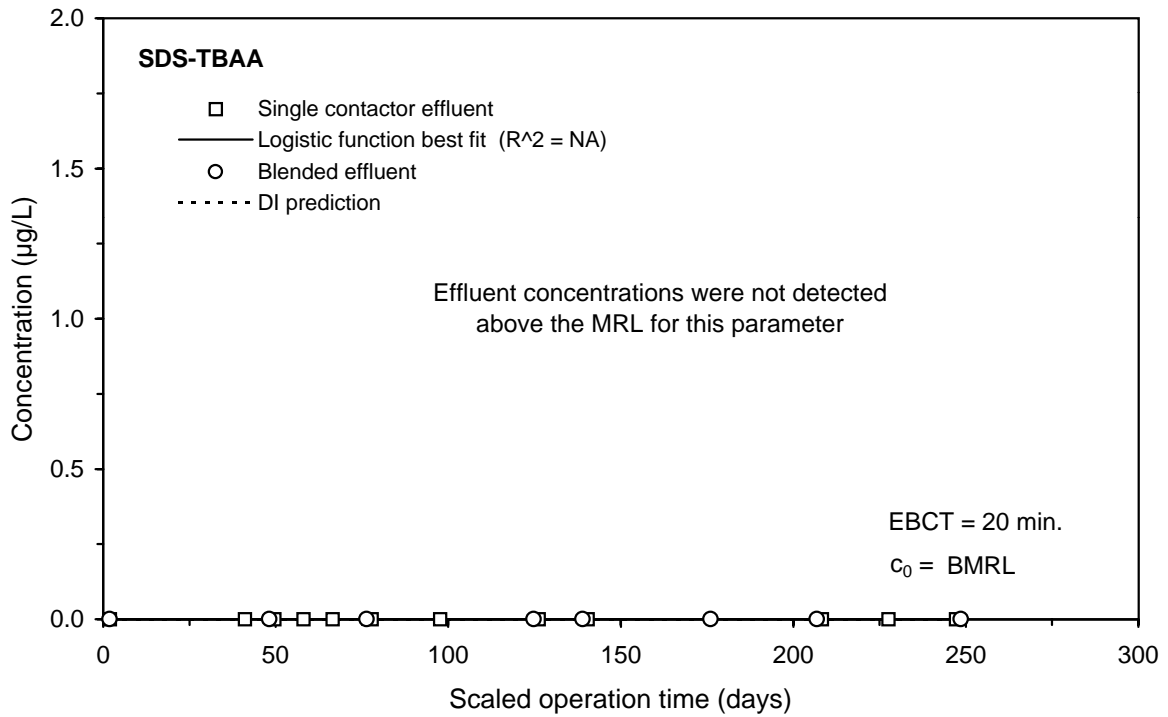


**Figure E-59 Single contactor and blended effluent SDS-TBAA breakthrough curves for Water 3**

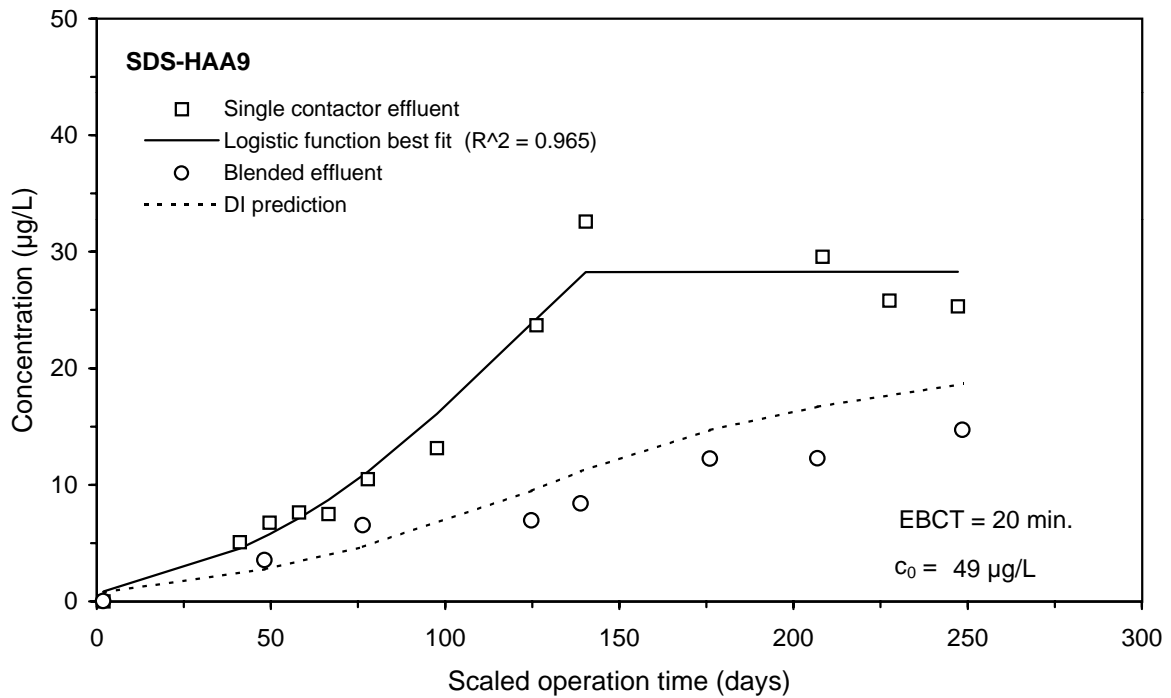


**Figure E-60 Single contactor and blended effluent SDS-HAA9 breakthrough curves for Water 3**

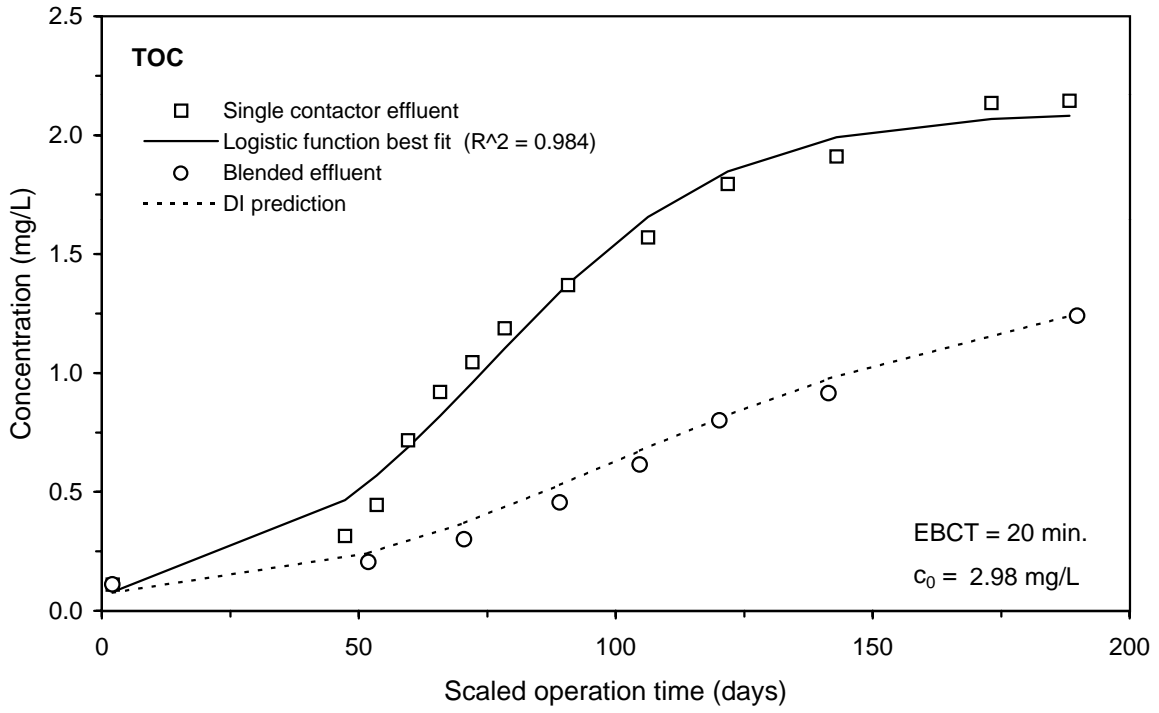


**Figure E-61 Single contactor and blended effluent TOC breakthrough curves for Water 4**

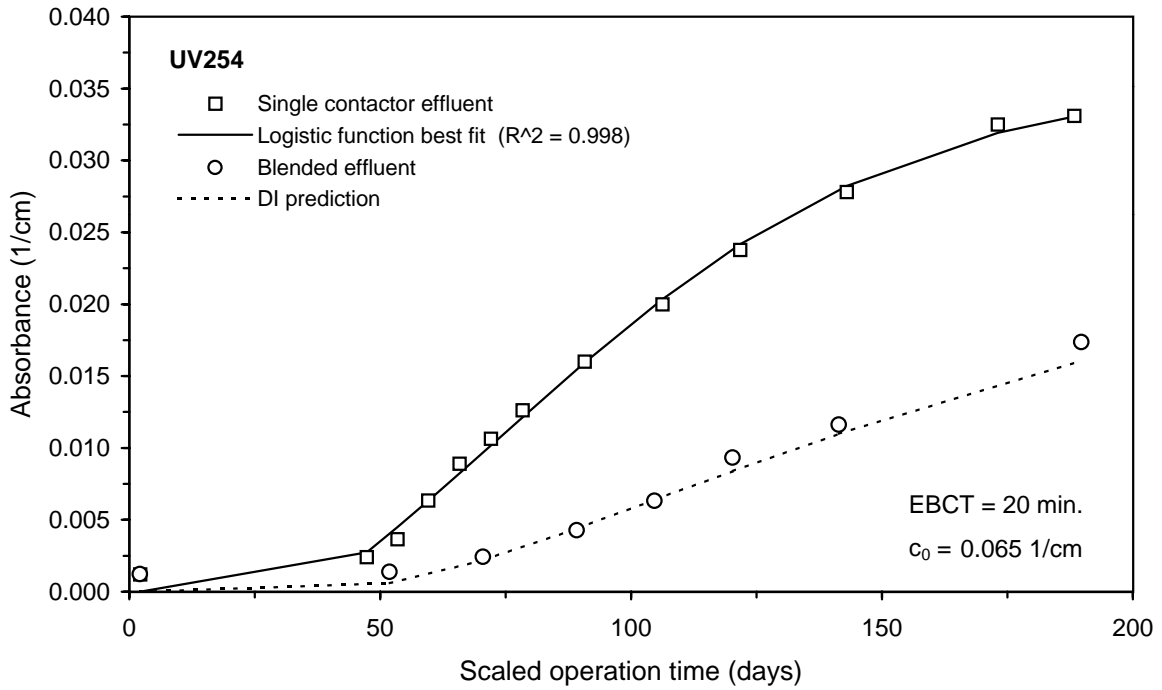


**Figure E-62 Single contactor and blended effluent UV254 breakthrough curves for Water 4**

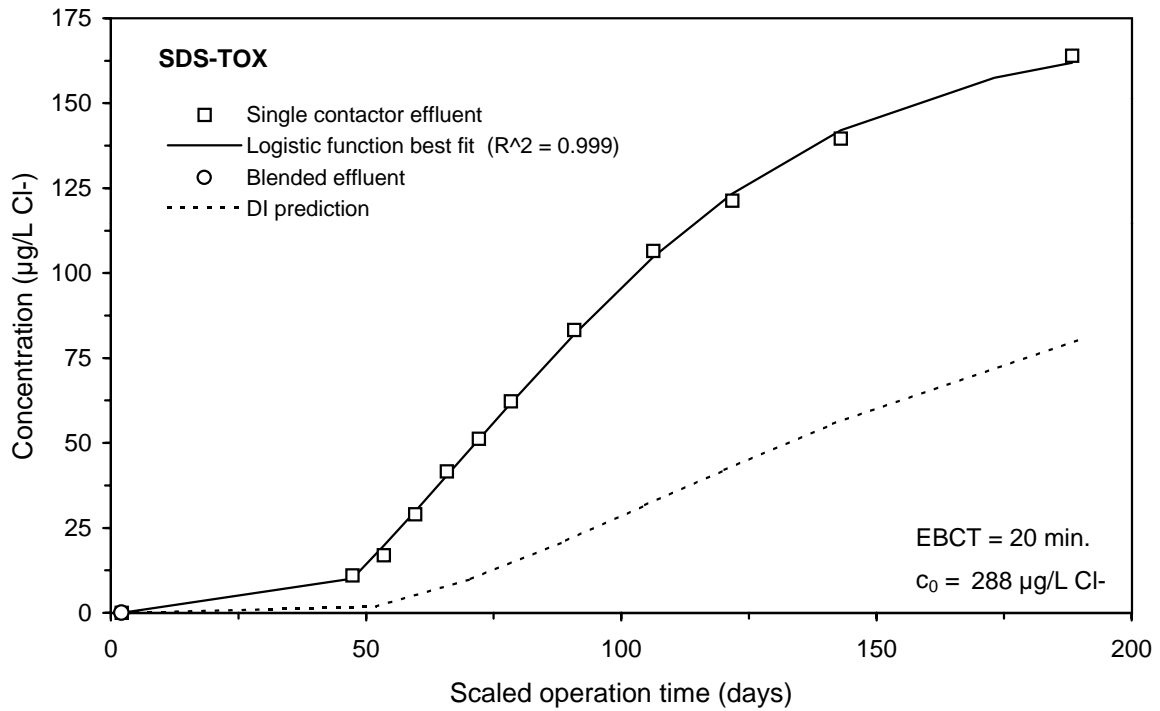


**Figure E-63 Single contactor and blended effluent SDS-TOX breakthrough curves for Water 4**

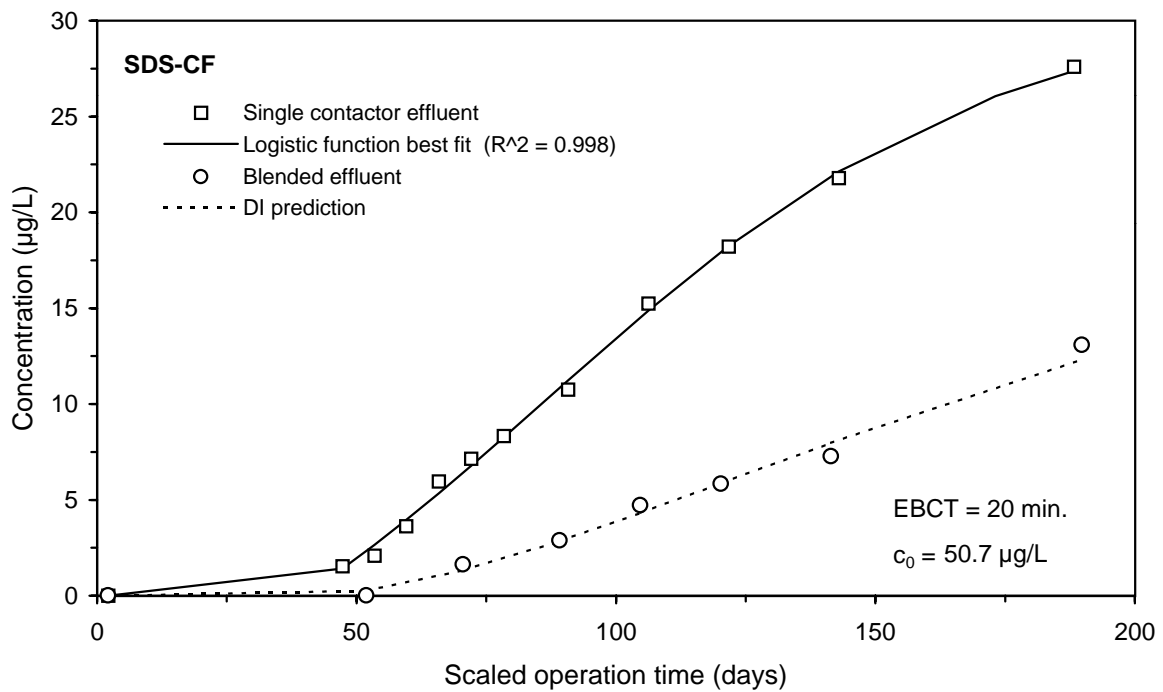


**Figure E-64 Single contactor and blended effluent SDS-CF breakthrough curves for Water 4**

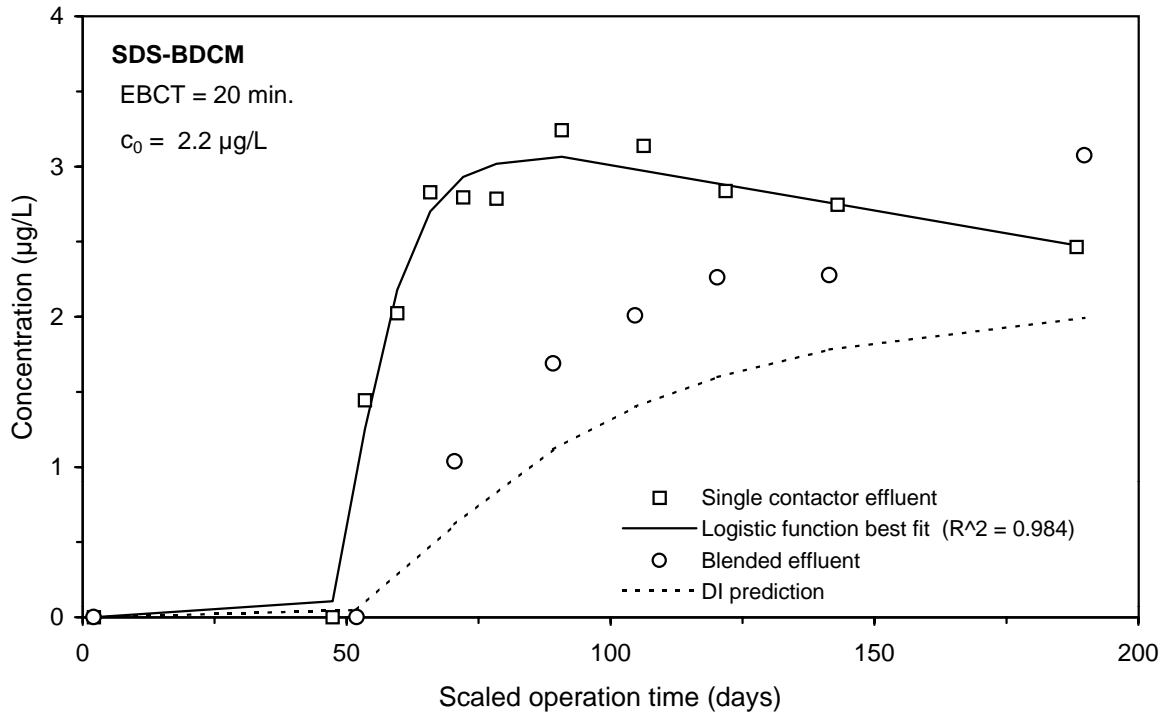


**Figure E-65 Single contactor and blended effluent SDS-BDCM breakthrough curves for Water 4**

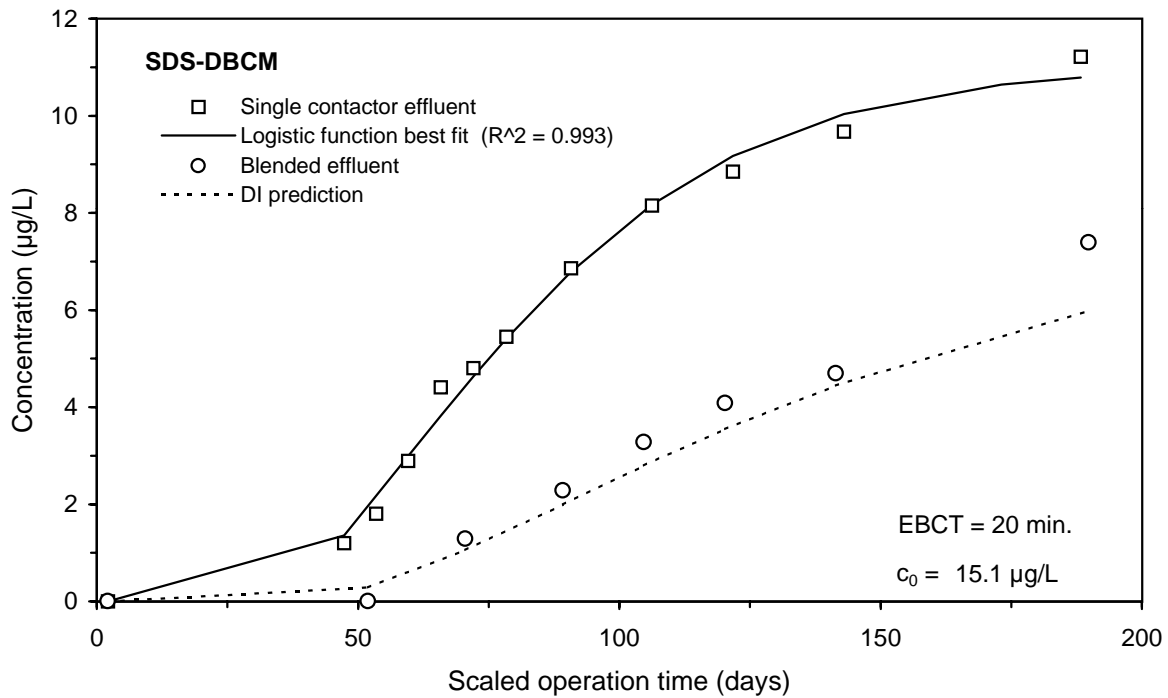


**Figure E-66 Single contactor and blended effluent SDS-DBCm breakthrough curves for Water 4**

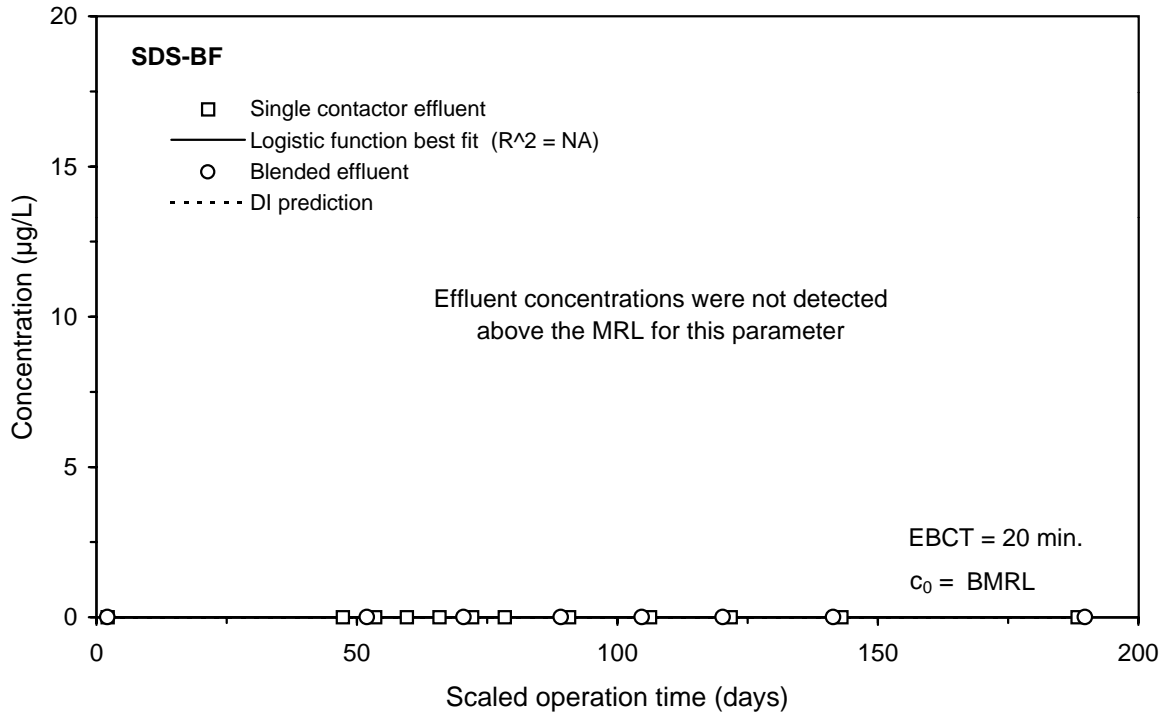


**Figure E-67 Single contactor and blended effluent SDS-BF breakthrough curves for Water 4**

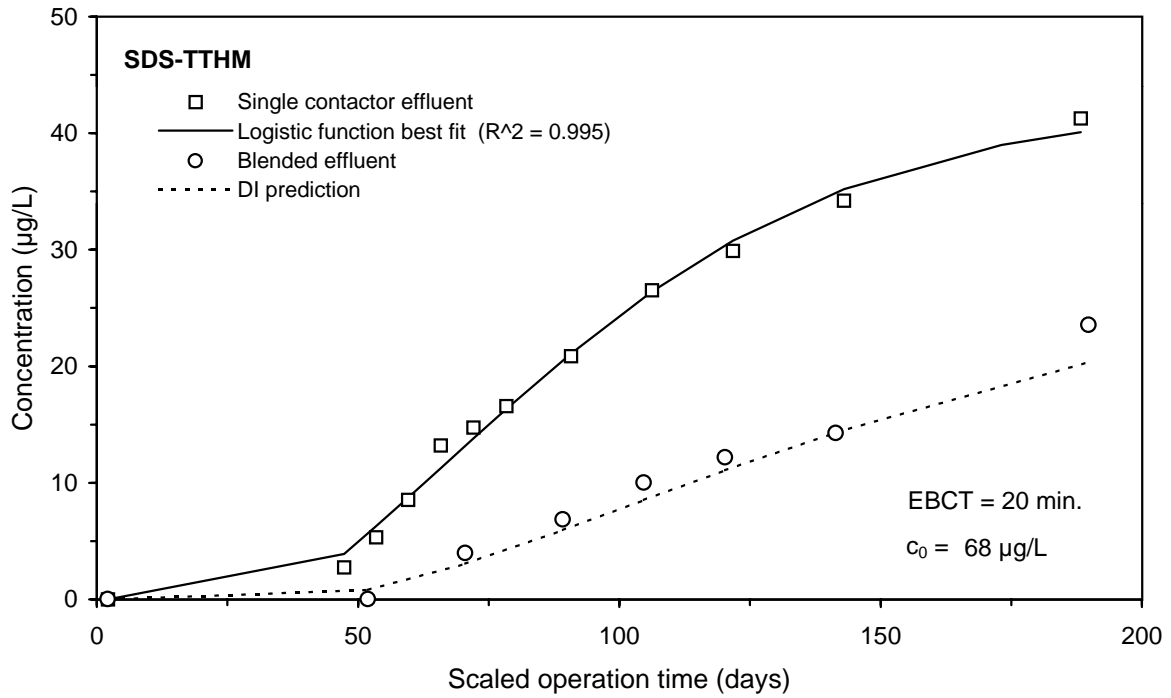


**Figure E-68 Single contactor and blended effluent SDS-TTHM breakthrough curves for Water 4**

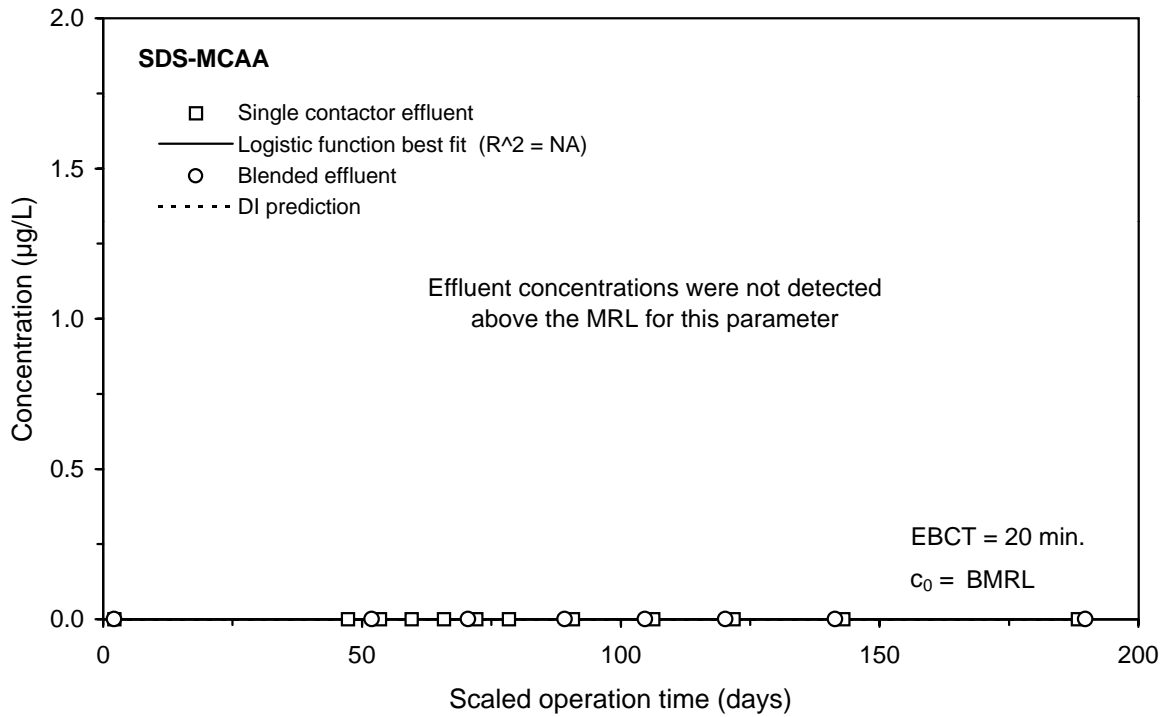


**Figure E-69 Single contactor and blended effluent SDS-MCAA breakthrough curves for Water 4**

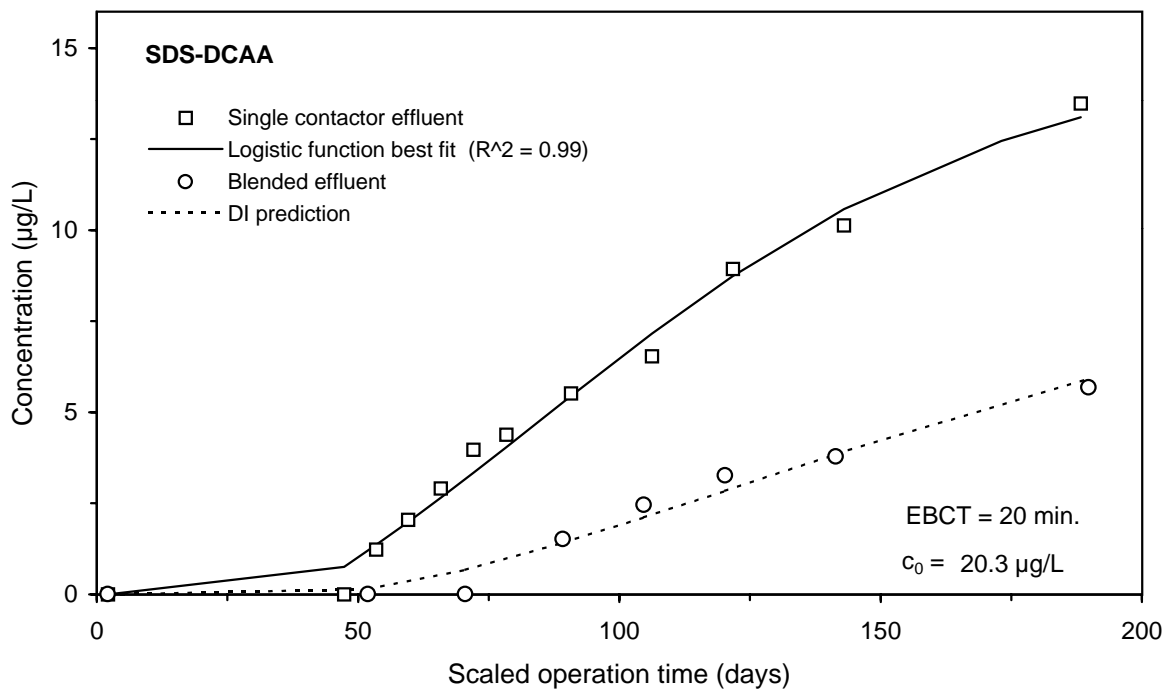


**Figure E-70 Single contactor and blended effluent SDS-DCAA breakthrough curves for Water 4**

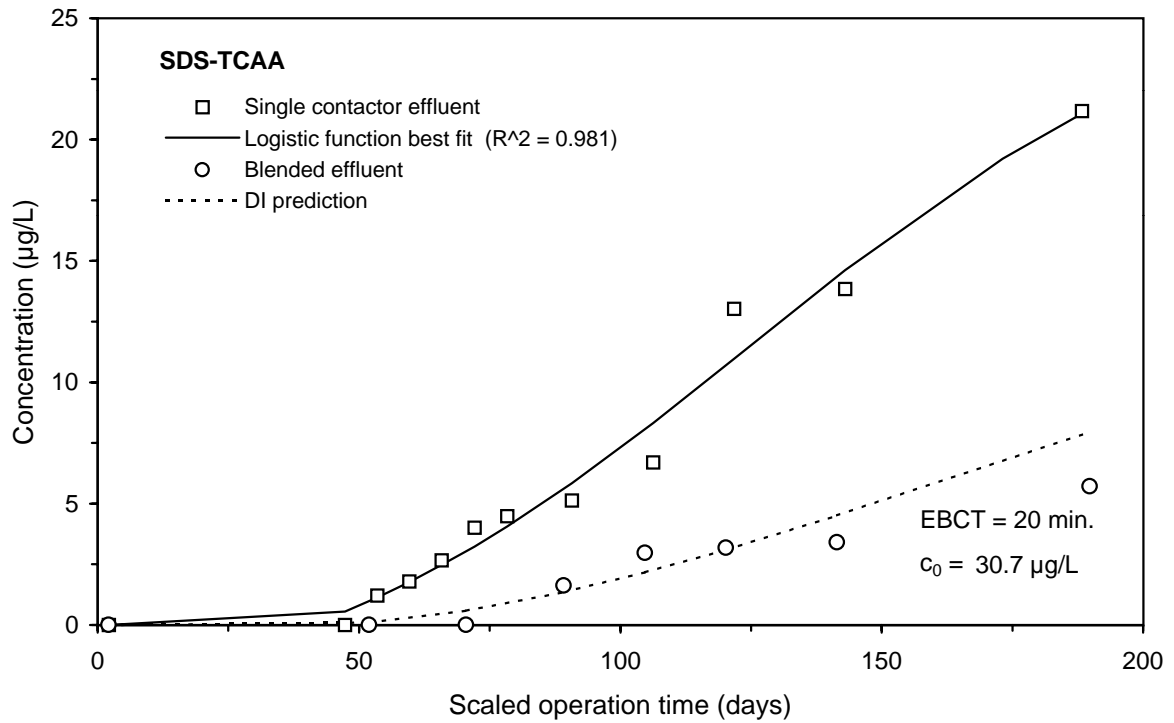


**Figure E-71 Single contactor and blended effluent SDS-TCAA breakthrough curves for Water 4**

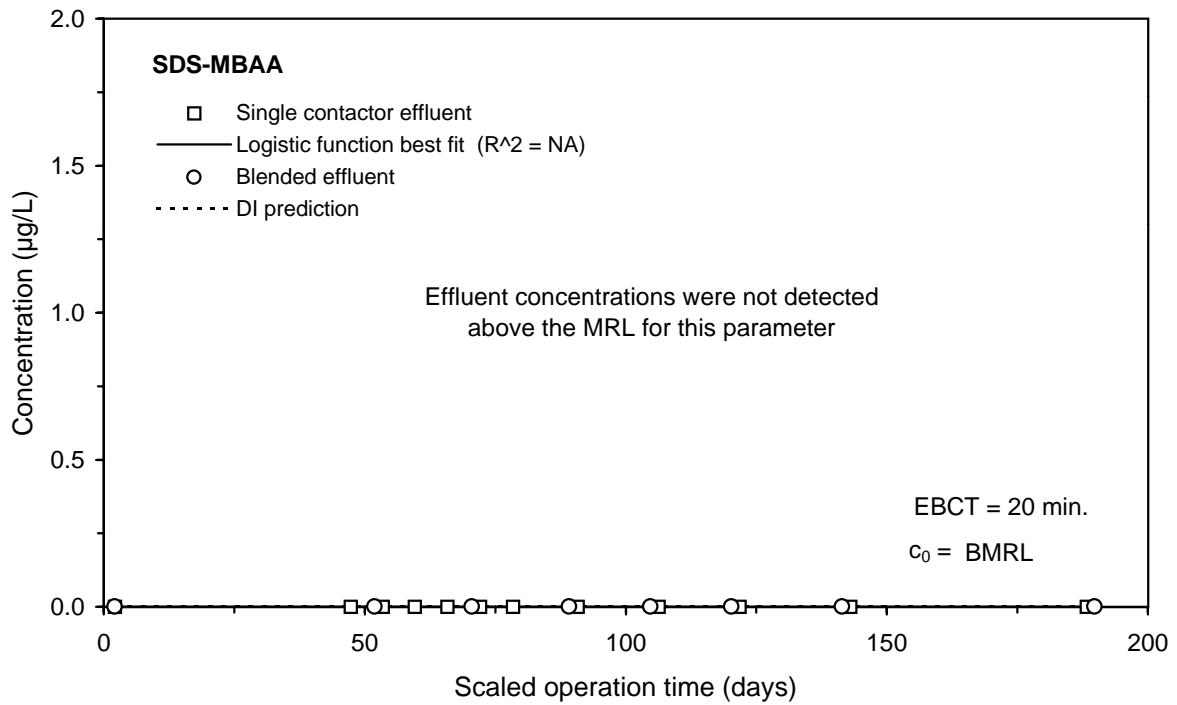


**Figure E-72 Single contactor and blended effluent SDS-MBAA breakthrough curves for Water 4**

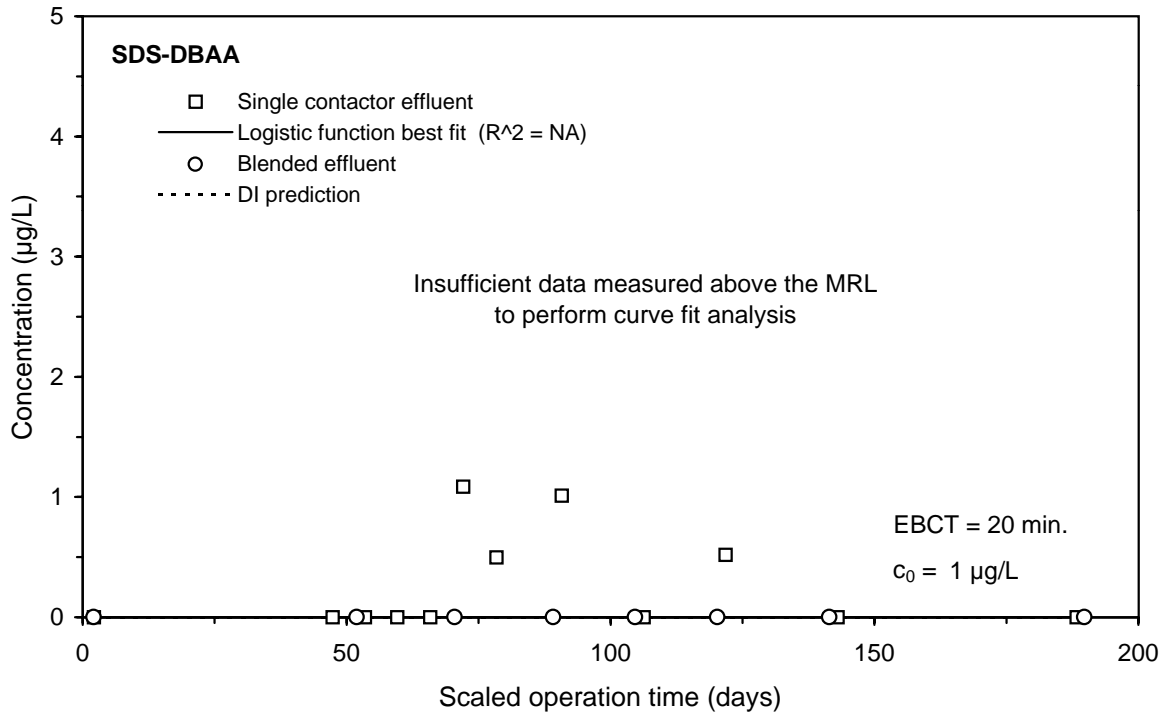


**Figure E-73 Single contactor and blended effluent SDS-DBAA breakthrough curves for Water 4**

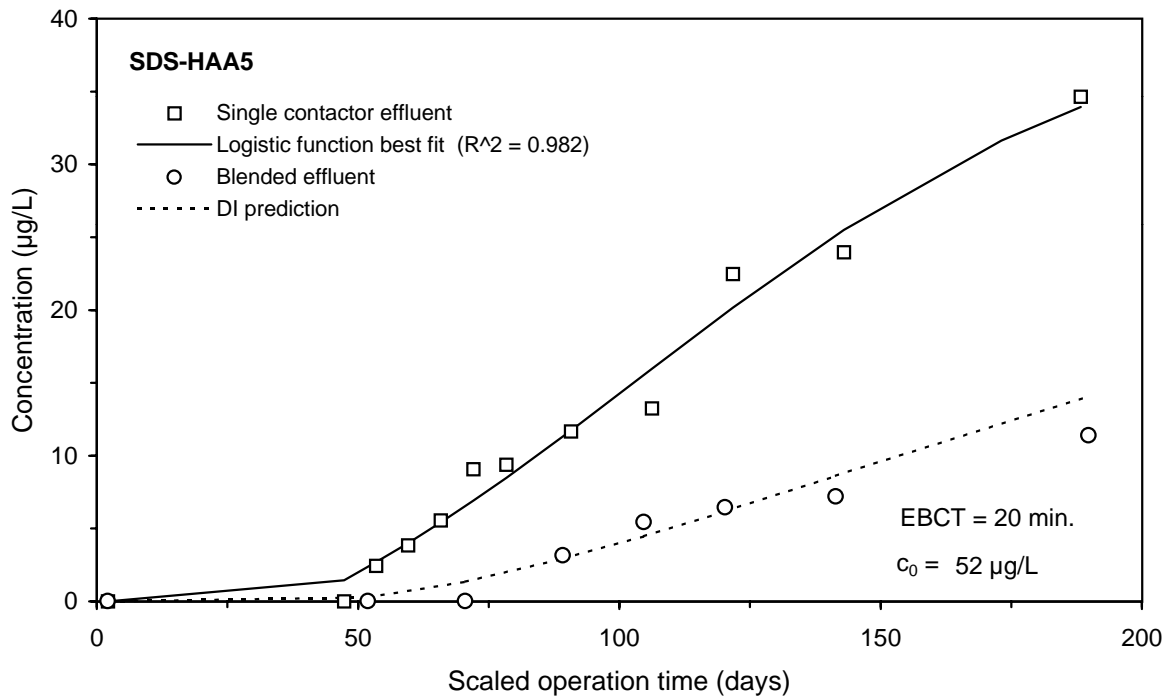


**Figure E-74 Single contactor and blended effluent SDS-HAA5 breakthrough curves for Water 4**

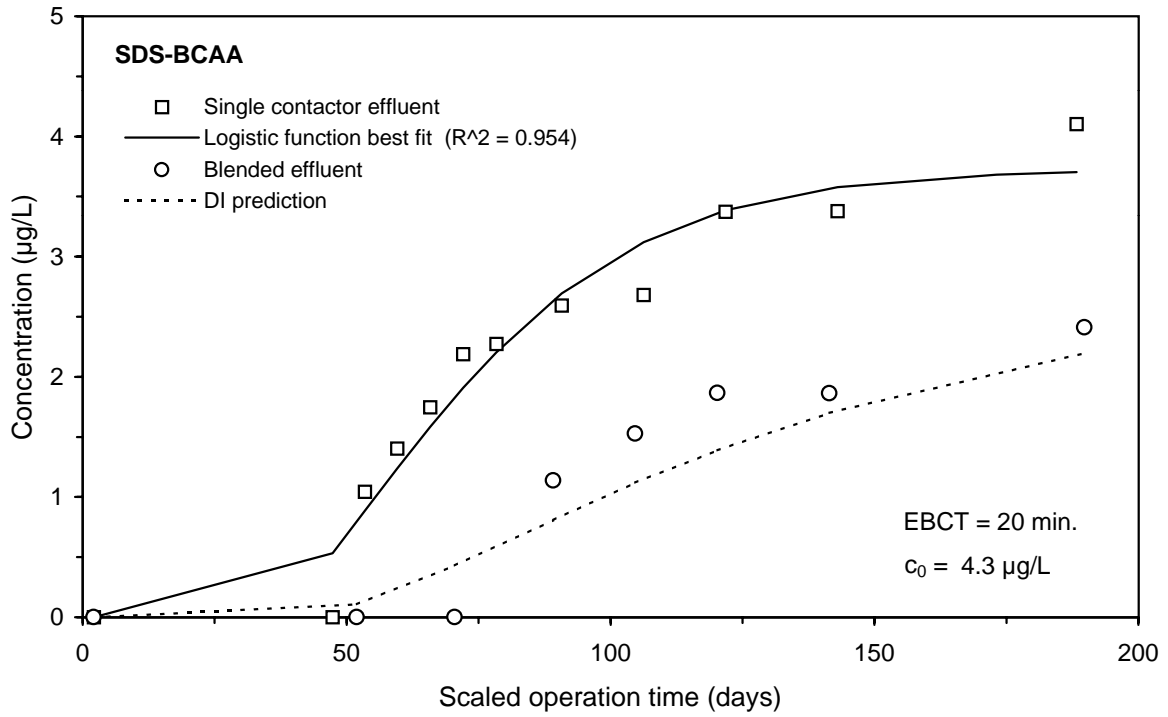


**Figure E-75 Single contactor and blended effluent SDS-BCAA breakthrough curves for Water 4**

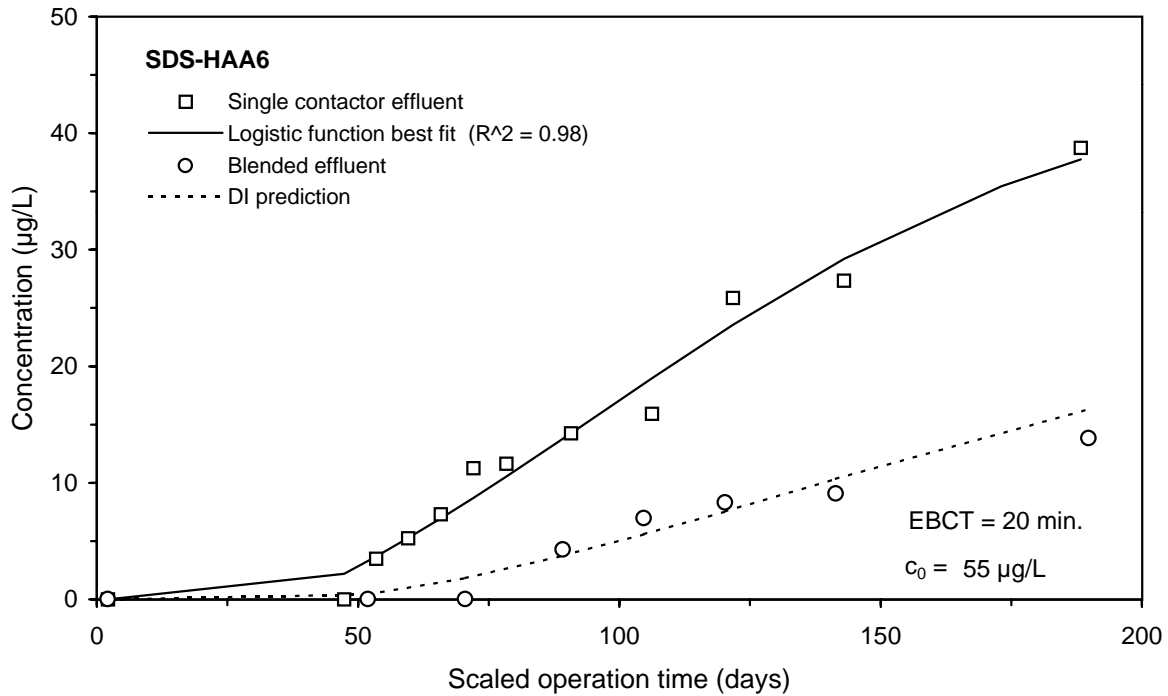


**Figure E-76 Single contactor and blended effluent SDS-HAA6 breakthrough curves for Water 4**

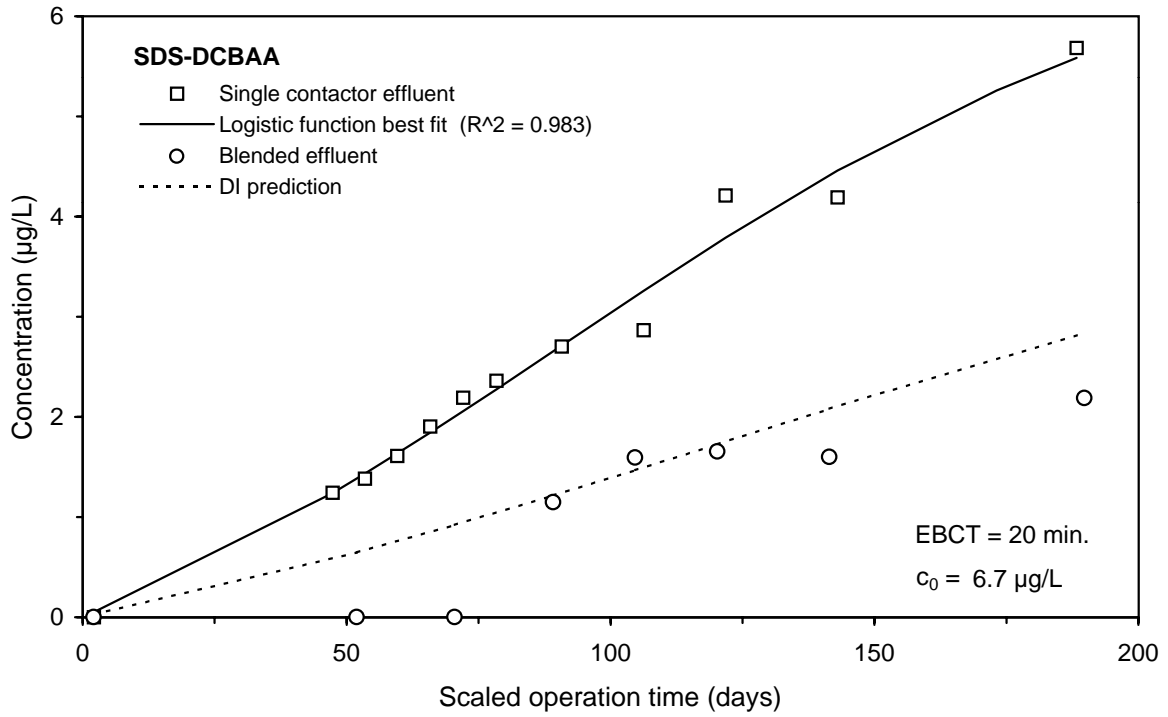


**Figure E-77 Single contactor and blended effluent SDS-DCBAA breakthrough curves for Water 4**

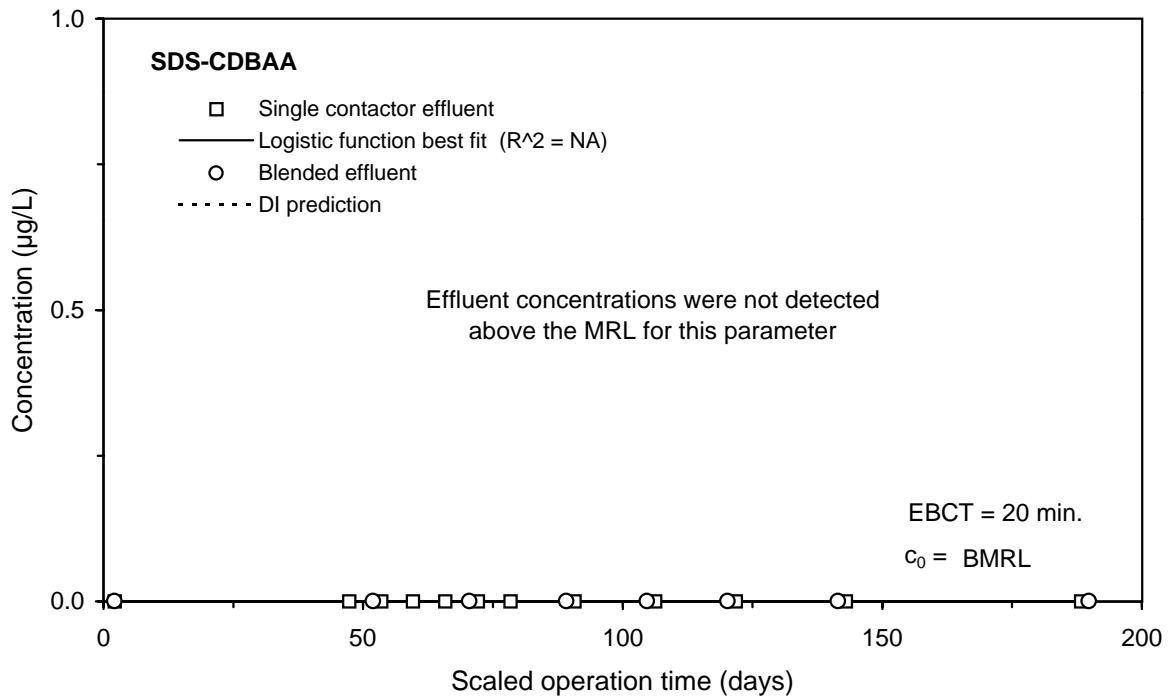


**Figure E-78 Single contactor and blended effluent SDS-CDBAA breakthrough curves for Water 4**

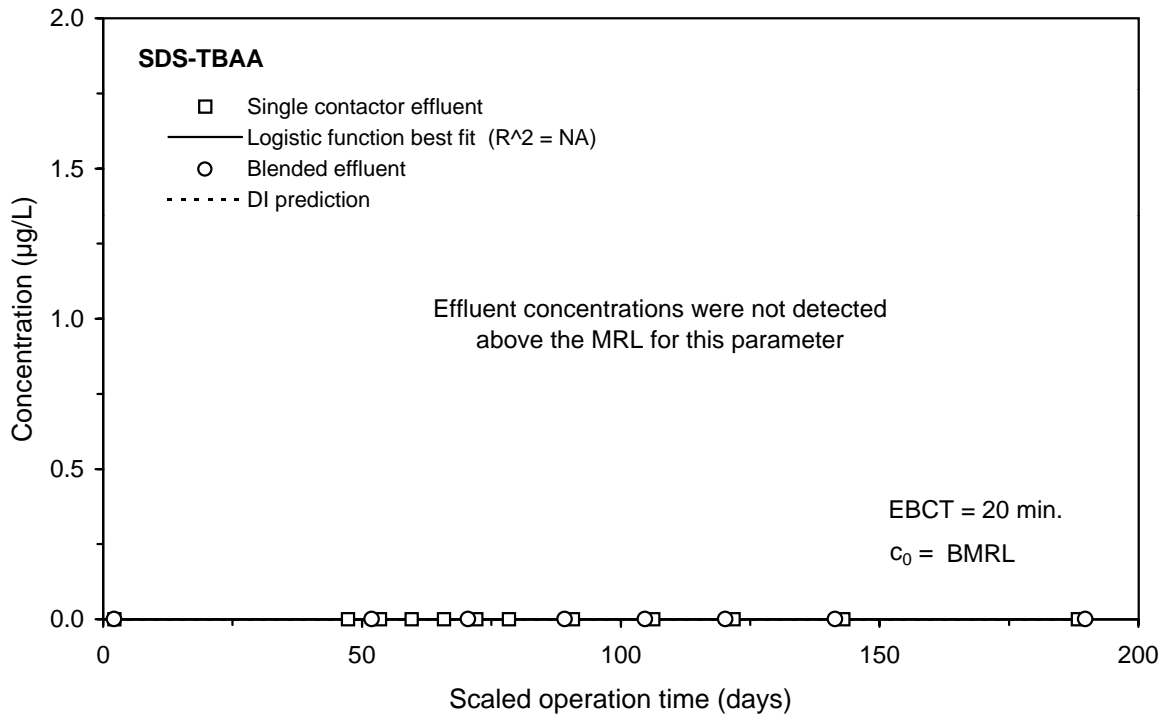


**Figure E-79 Single contactor and blended effluent SDS-TBAA breakthrough curves for Water 4**

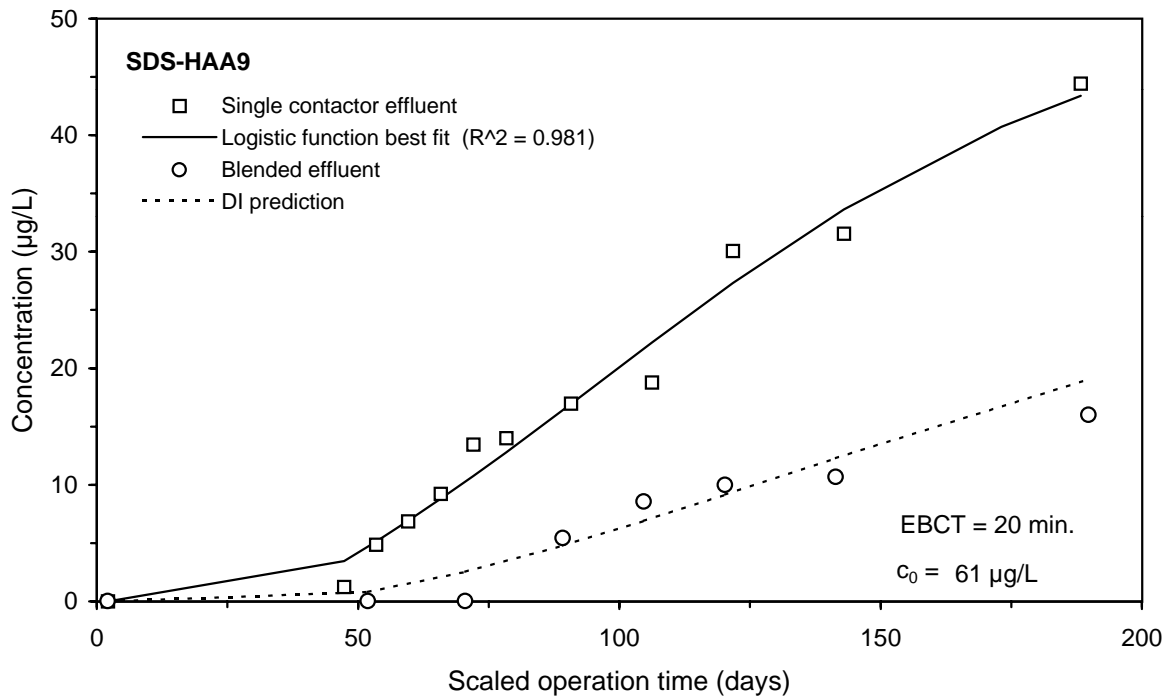


**Figure E-80 Single contactor and blended effluent SDS-HAA9 breakthrough curves for Water 4**

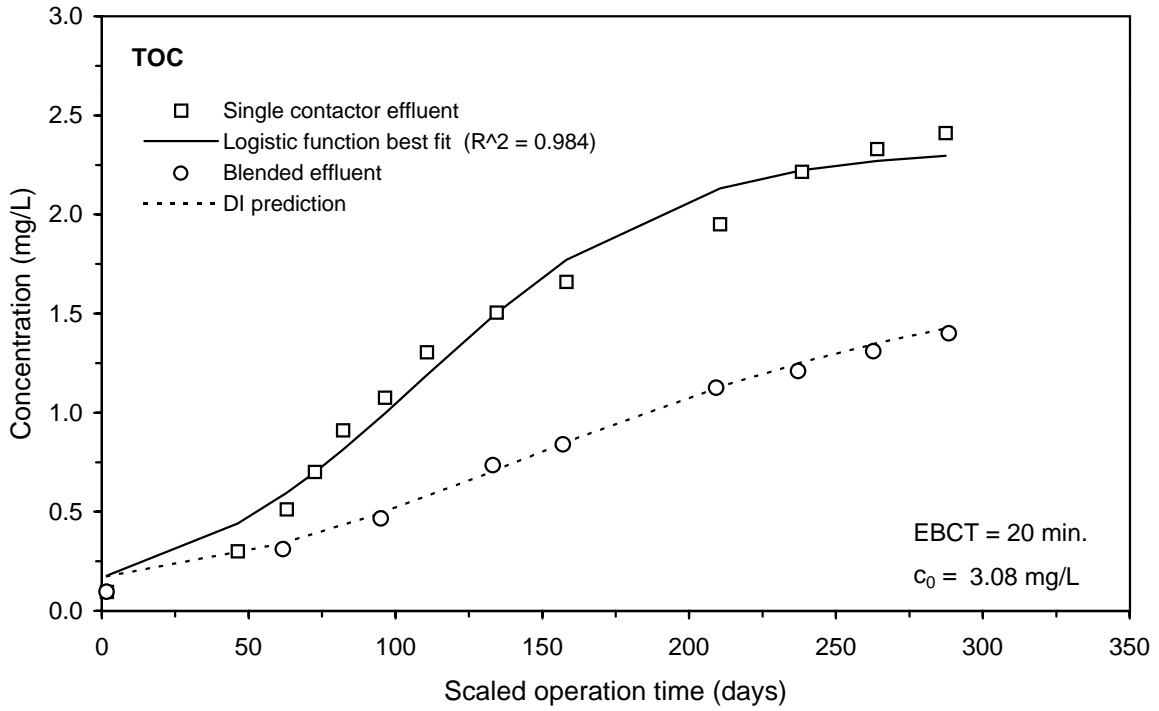


**Figure E-81 Single contactor and blended effluent TOC breakthrough curves for Water 5**

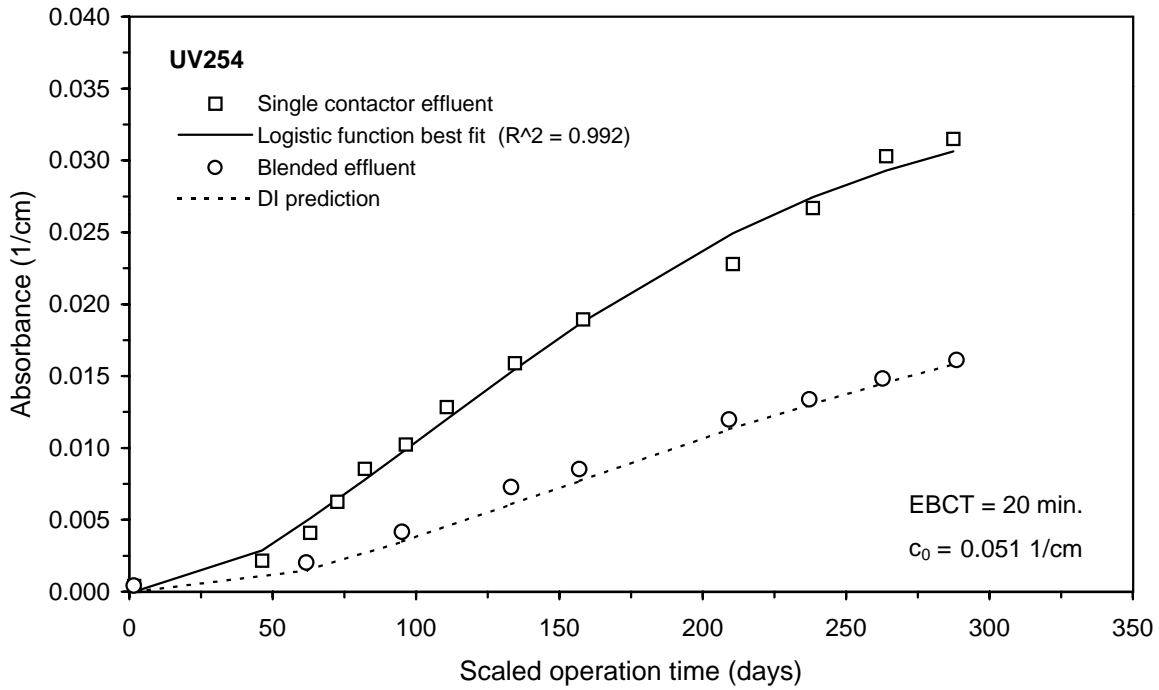


**Figure E-82 Single contactor and blended effluent UV254 breakthrough curves for Water 5**

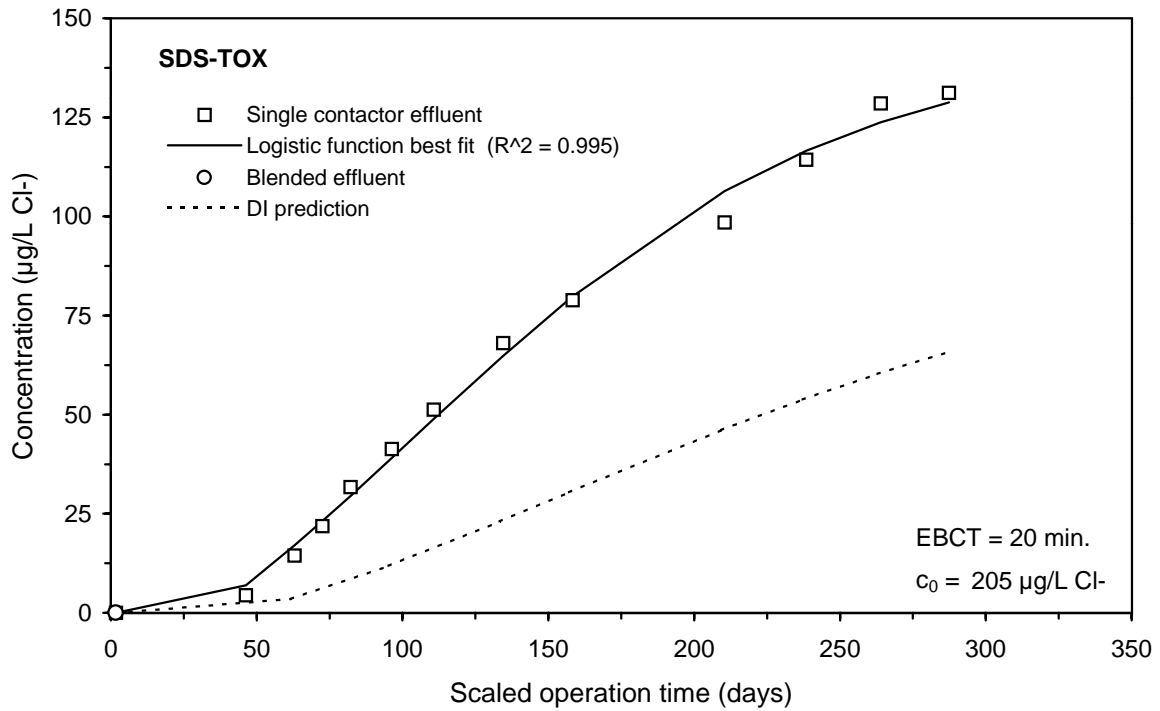


**Figure E-83 Single contactor and blended effluent SDS-TOX breakthrough curves for Water 5**

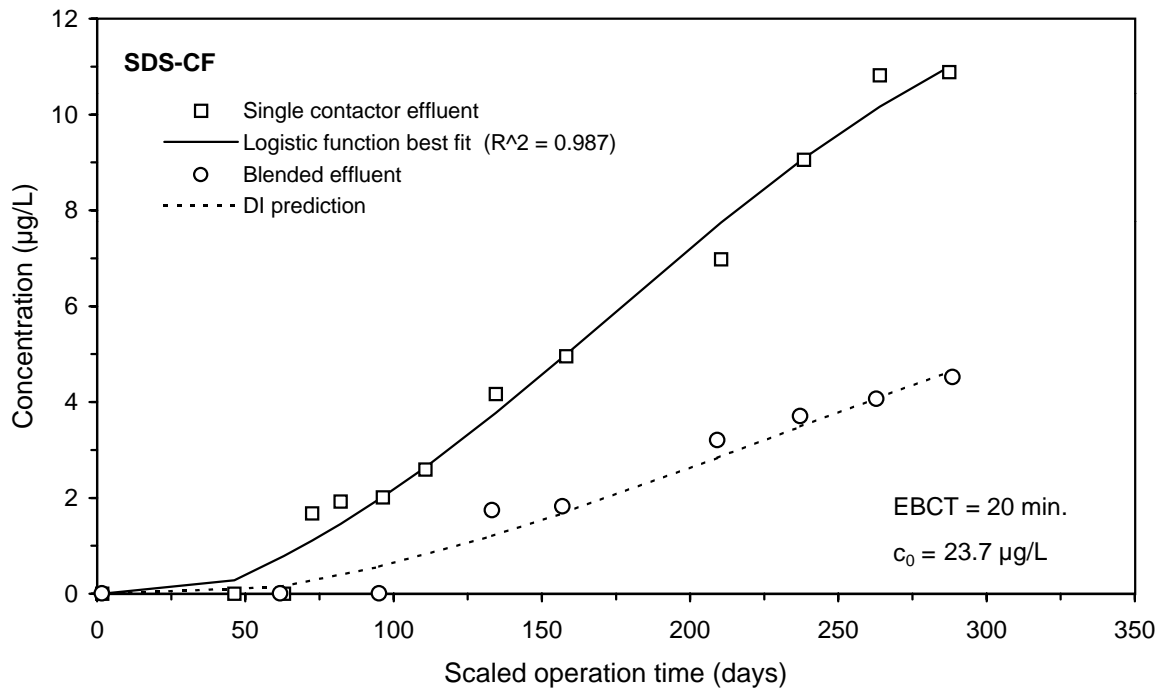


**Figure E-84 Single contactor and blended effluent SDS-CF breakthrough curves for Water 5**

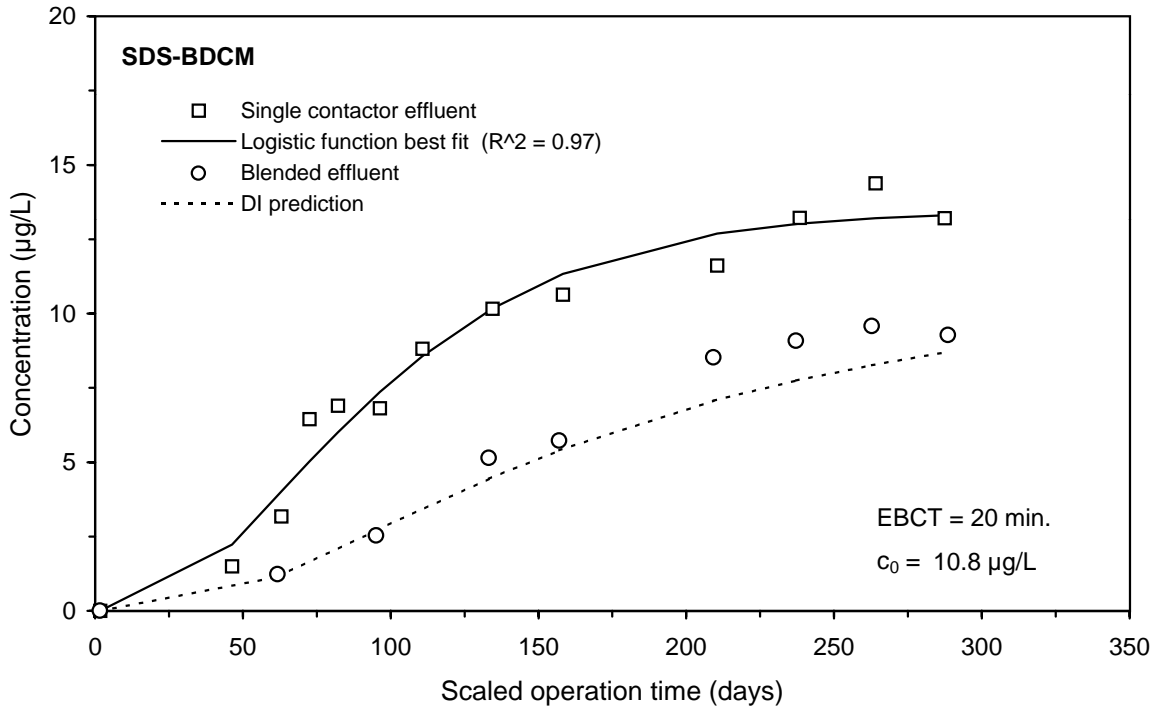


**Figure E-85 Single contactor and blended effluent SDS-BDCM breakthrough curves for Water 5**

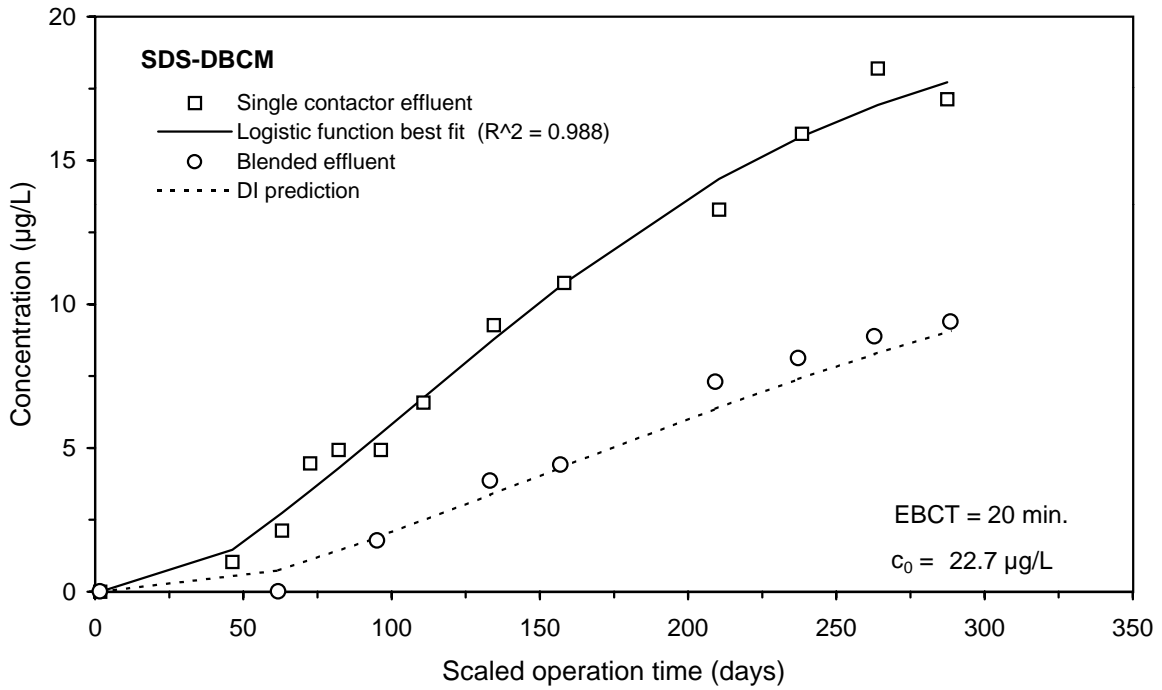


**Figure E-86 Single contactor and blended effluent SDS-DBCm breakthrough curves for Water 5**

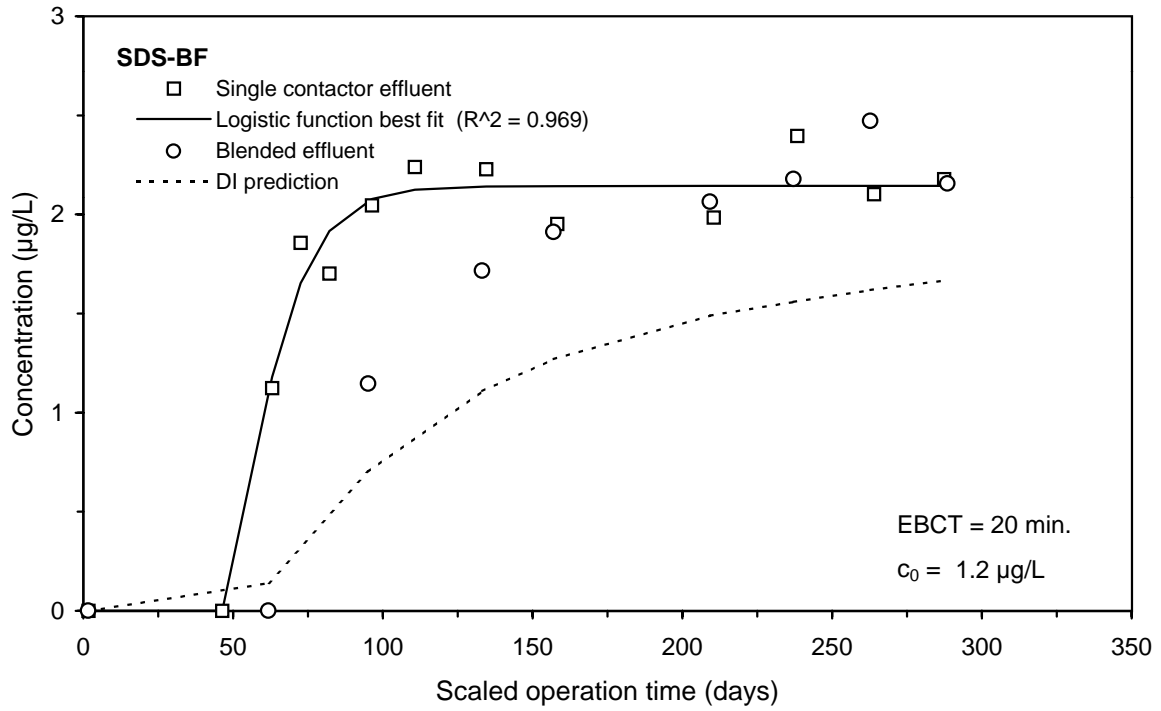


**Figure E-87 Single contactor and blended effluent SDS-BF breakthrough curves for Water 5**

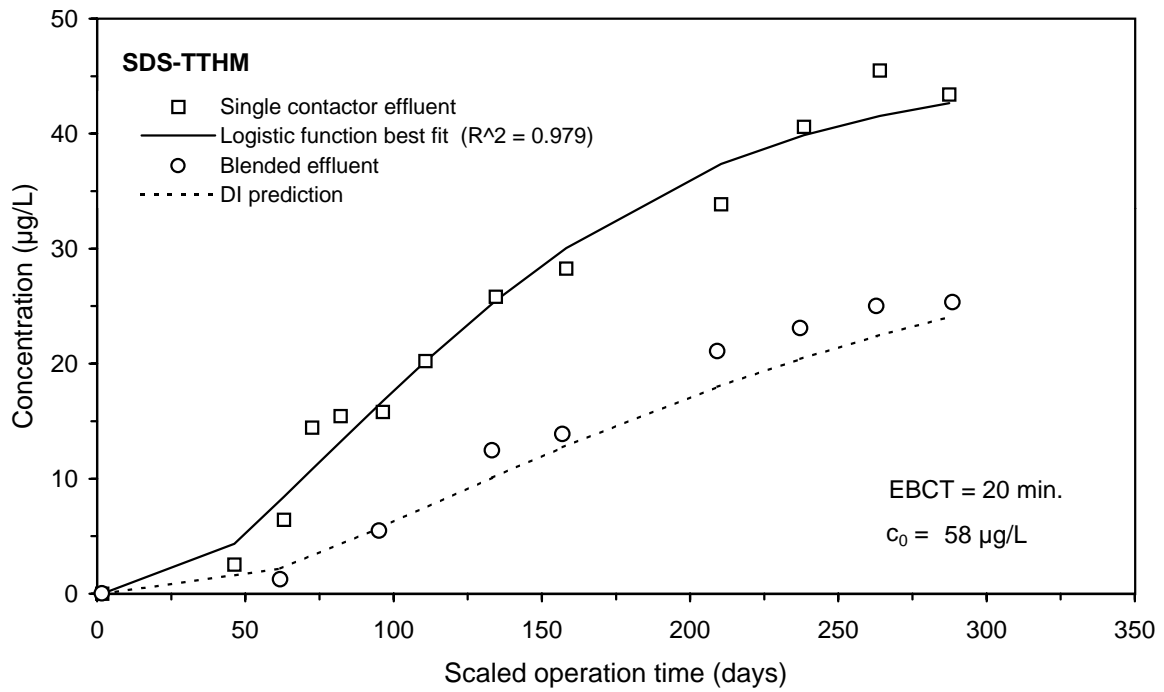


**Figure E-88 Single contactor and blended effluent SDS-TTHM breakthrough curves for Water 5**

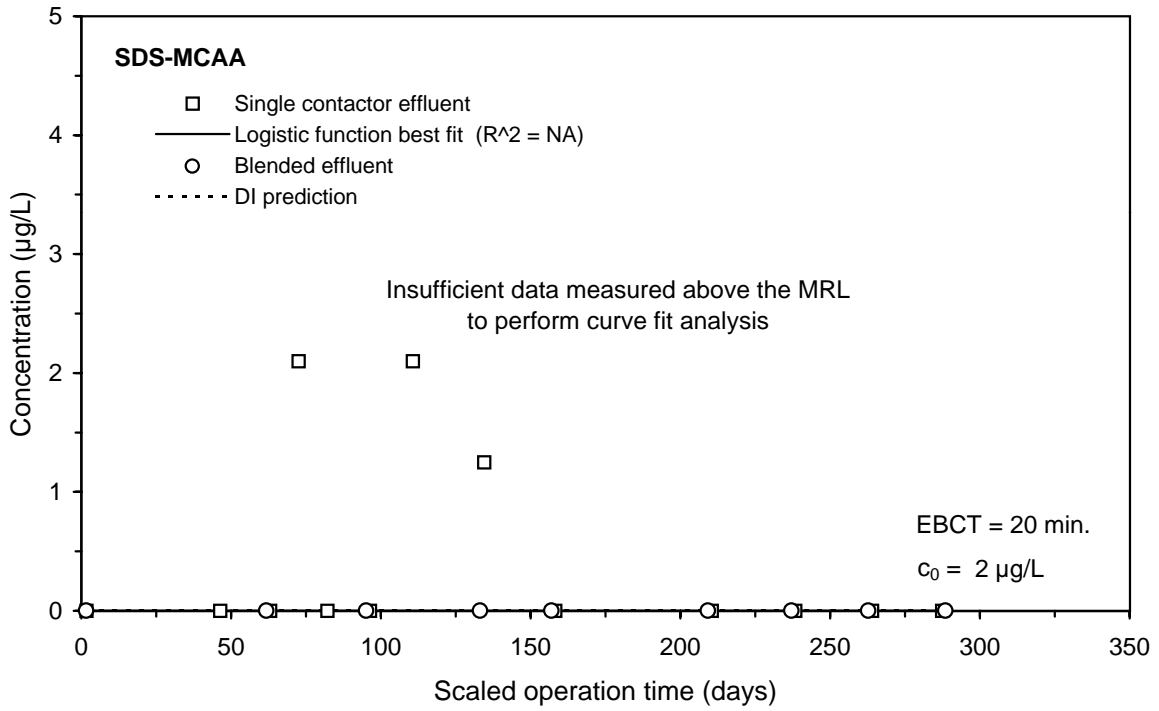


**Figure E-89 Single contactor and blended effluent SDS-MCAA breakthrough curves for Water 5**

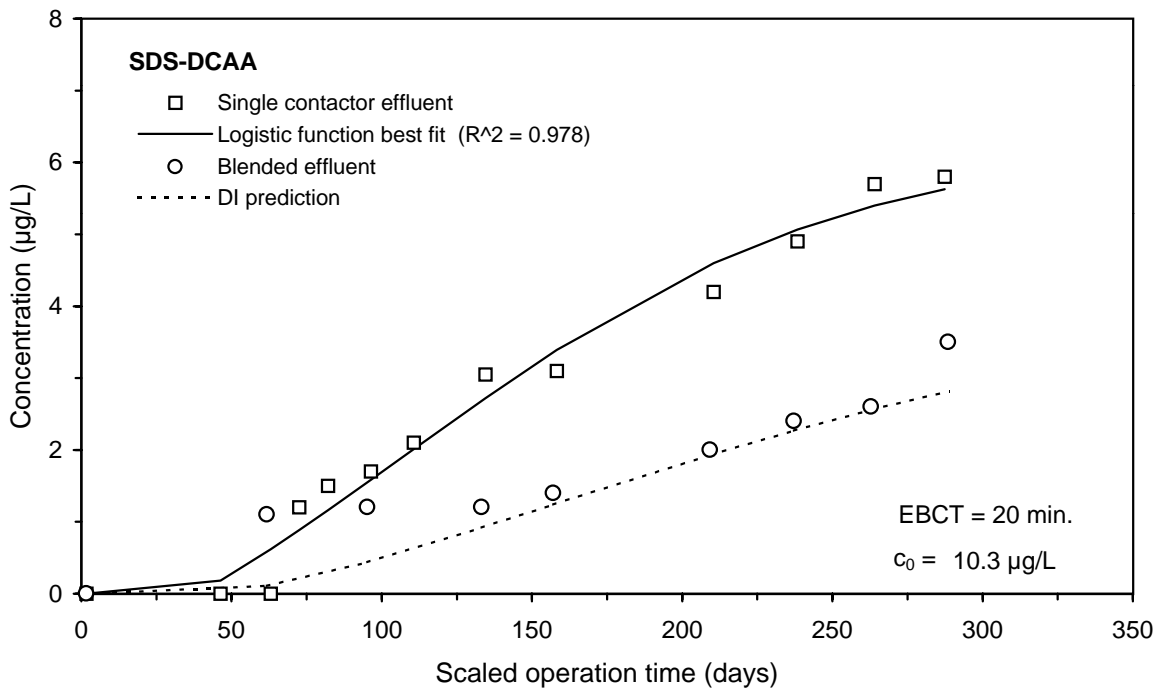


**Figure E-90 Single contactor and blended effluent SDS-DCAA breakthrough curves for Water 5**

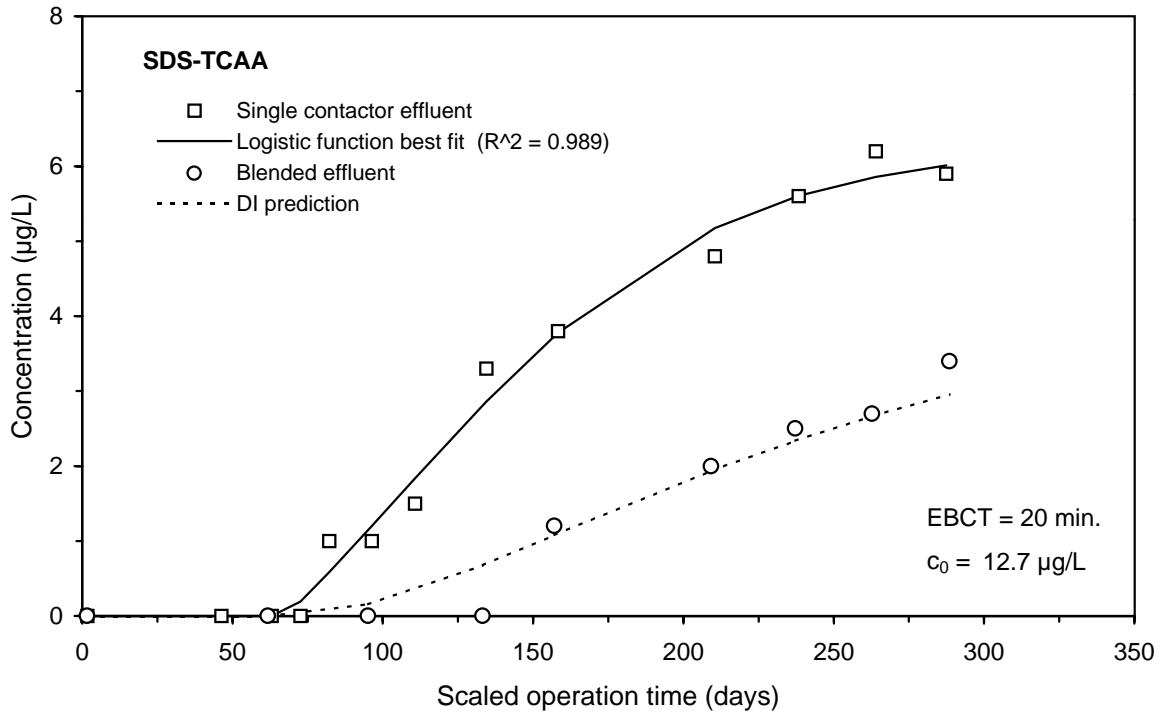


**Figure E-91 Single contactor and blended effluent SDS-TCAA breakthrough curves for Water 5**

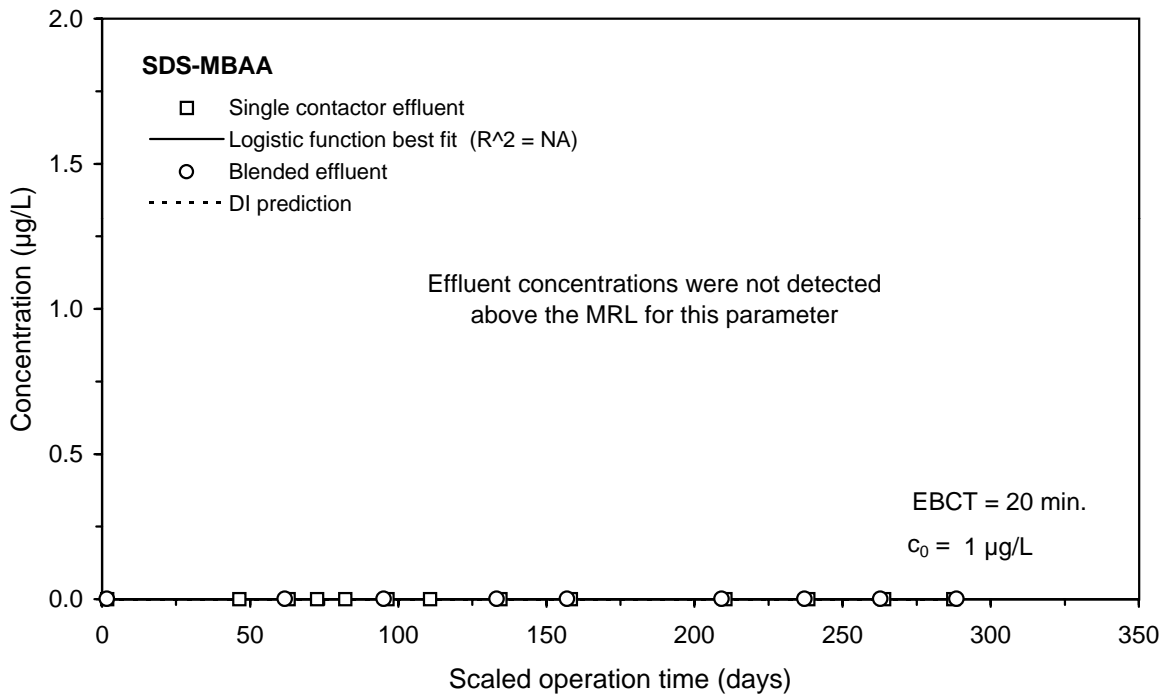


**Figure E-92 Single contactor and blended effluent SDS-MBAA breakthrough curves for Water 5**

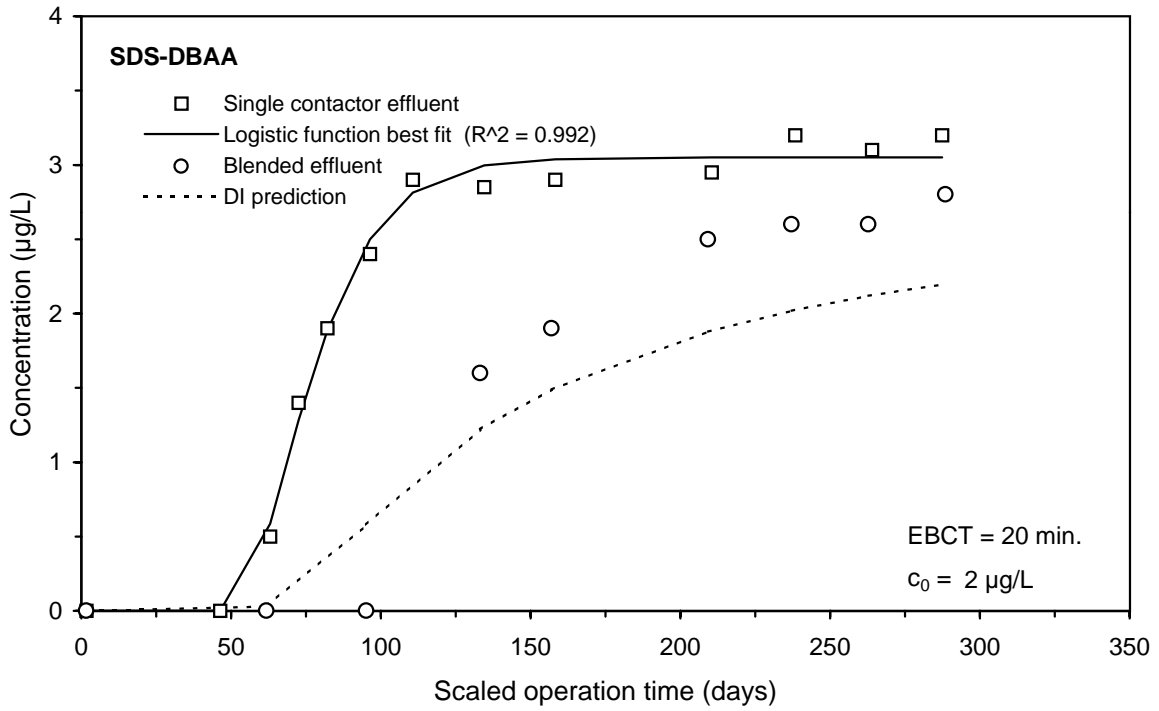


**Figure E-93 Single contactor and blended effluent SDS-DBAA breakthrough curves for Water 5**

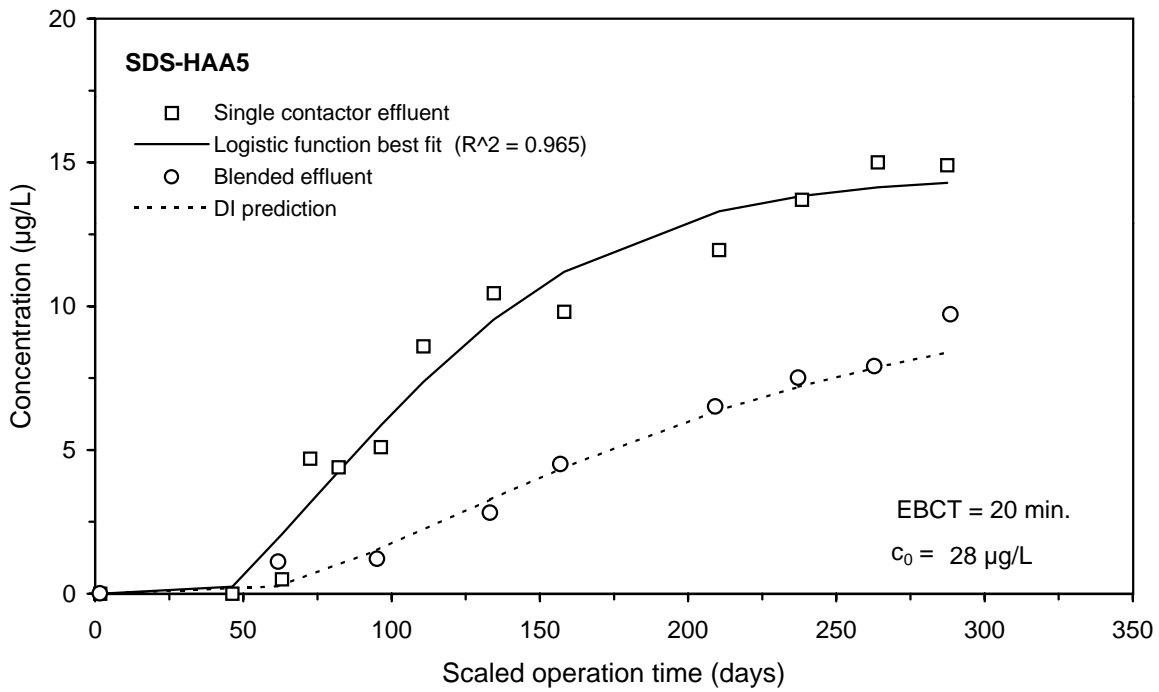


**Figure E-94 Single contactor and blended effluent SDS-HAA5 breakthrough curves for Water 5**

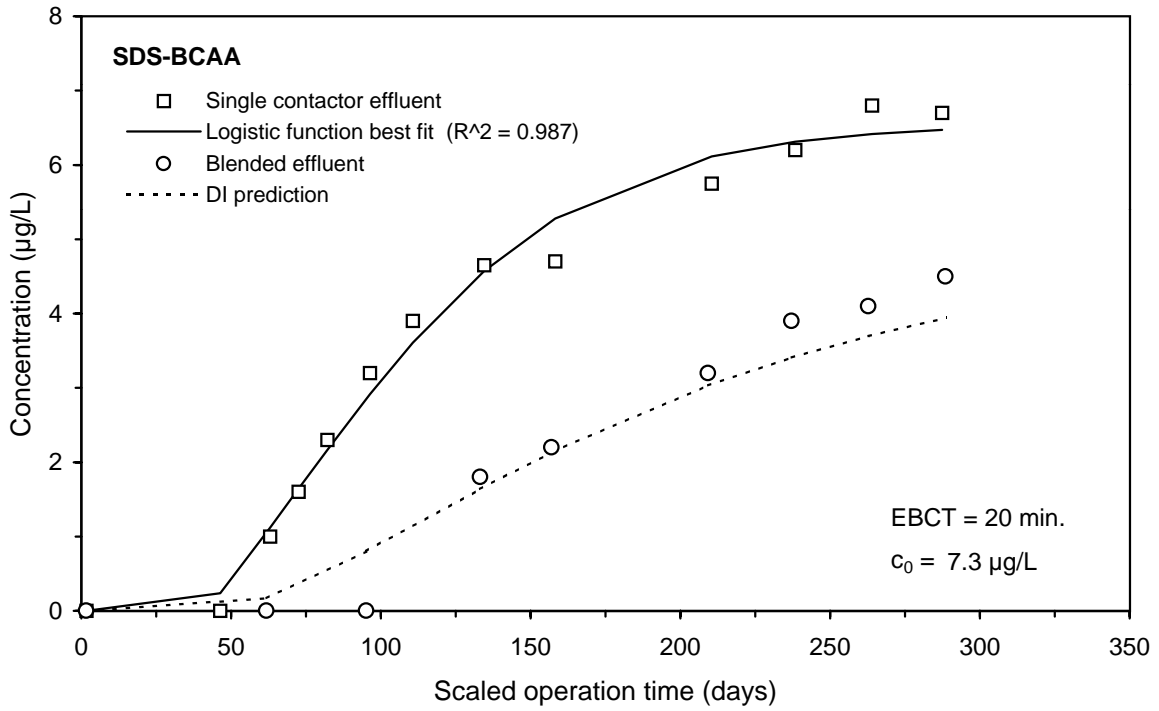


**Figure E-95 Single contactor and blended effluent SDS-BCAA breakthrough curves for Water 5**

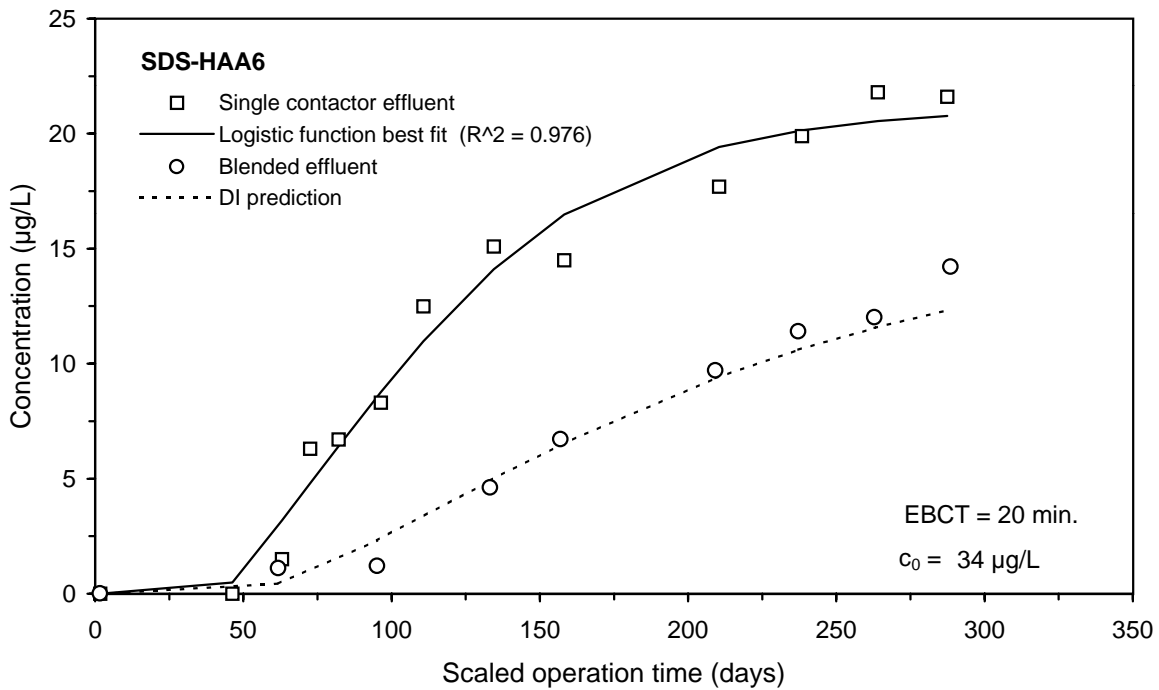


**Figure E-96 Single contactor and blended effluent SDS-HAA6 breakthrough curves for Water 5**

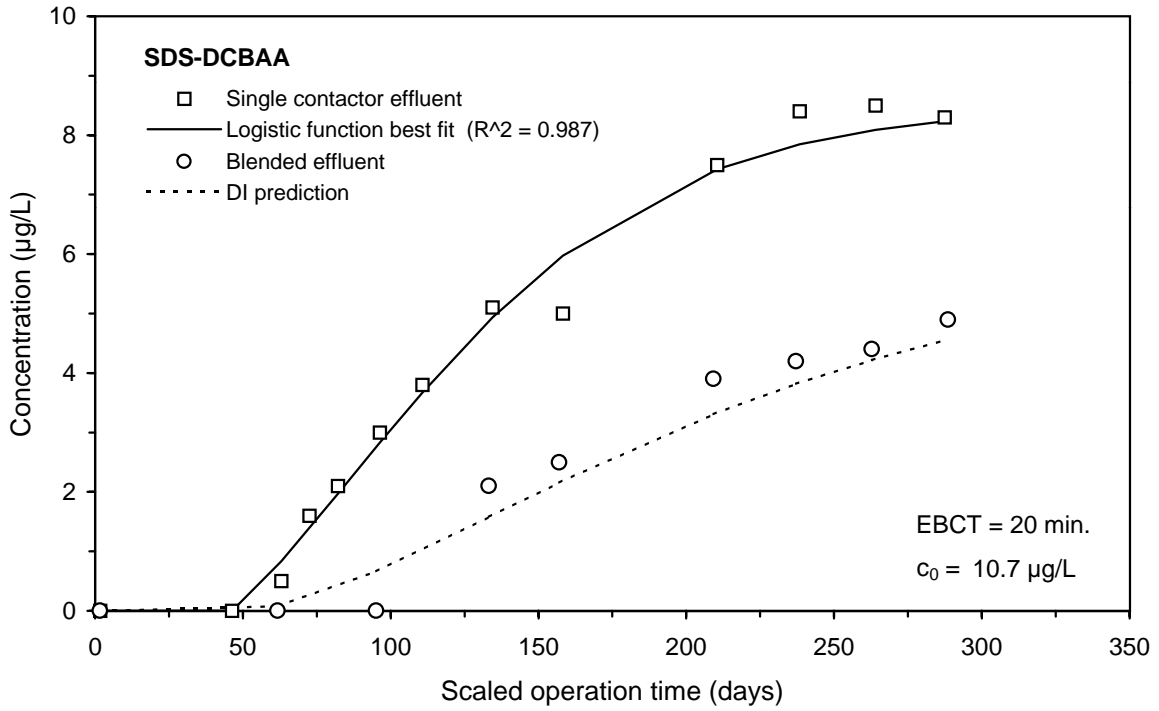


**Figure E-97 Single contactor and blended effluent SDS-DCBAA breakthrough curves for Water 5**

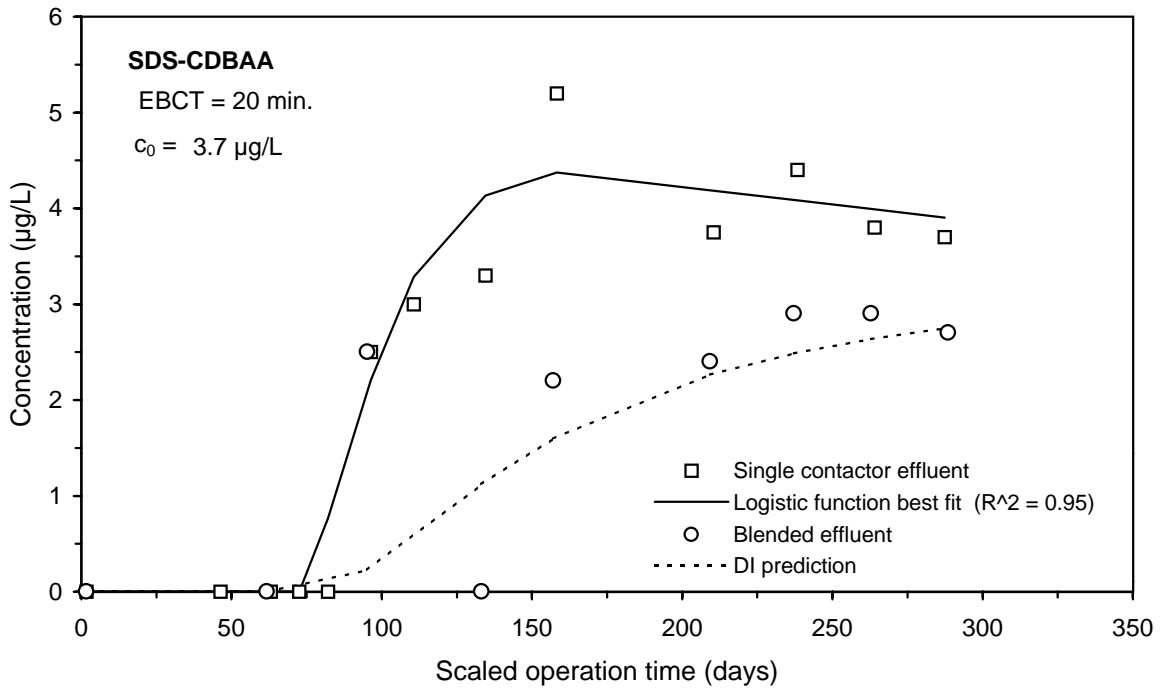


**Figure E-98 Single contactor and blended effluent SDS-CDBAA breakthrough curves for Water 5**

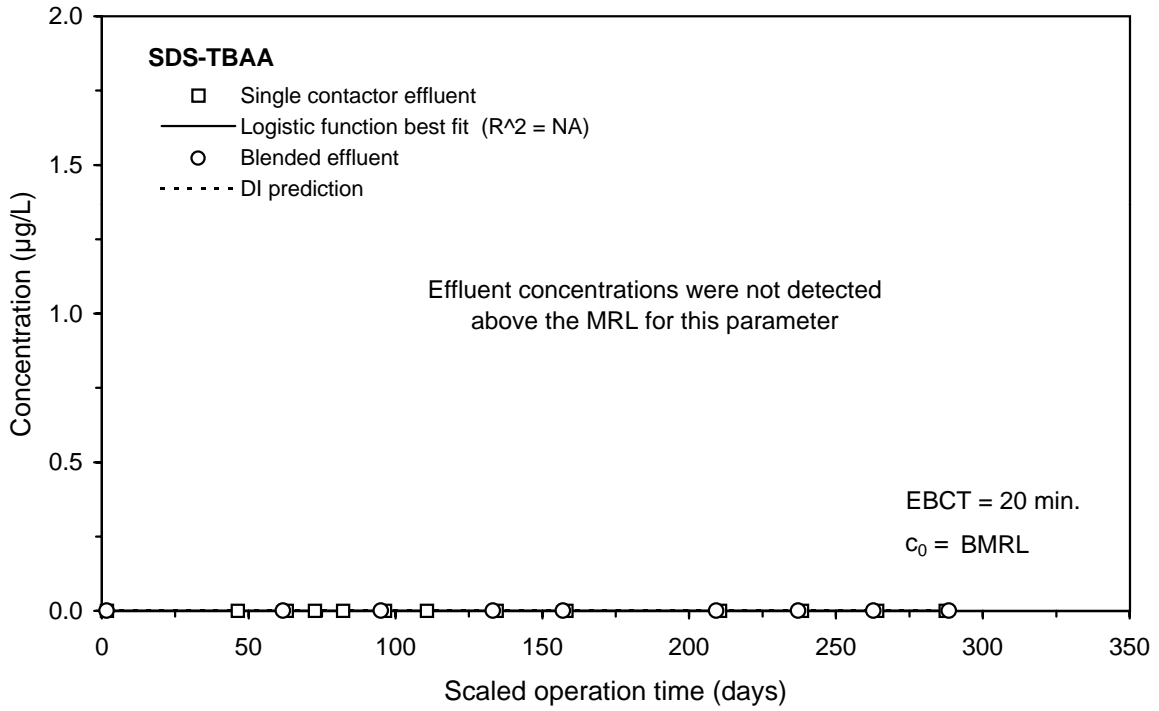


**Figure E-99 Single contactor and blended effluent SDS-TBAA breakthrough curves for Water 5**

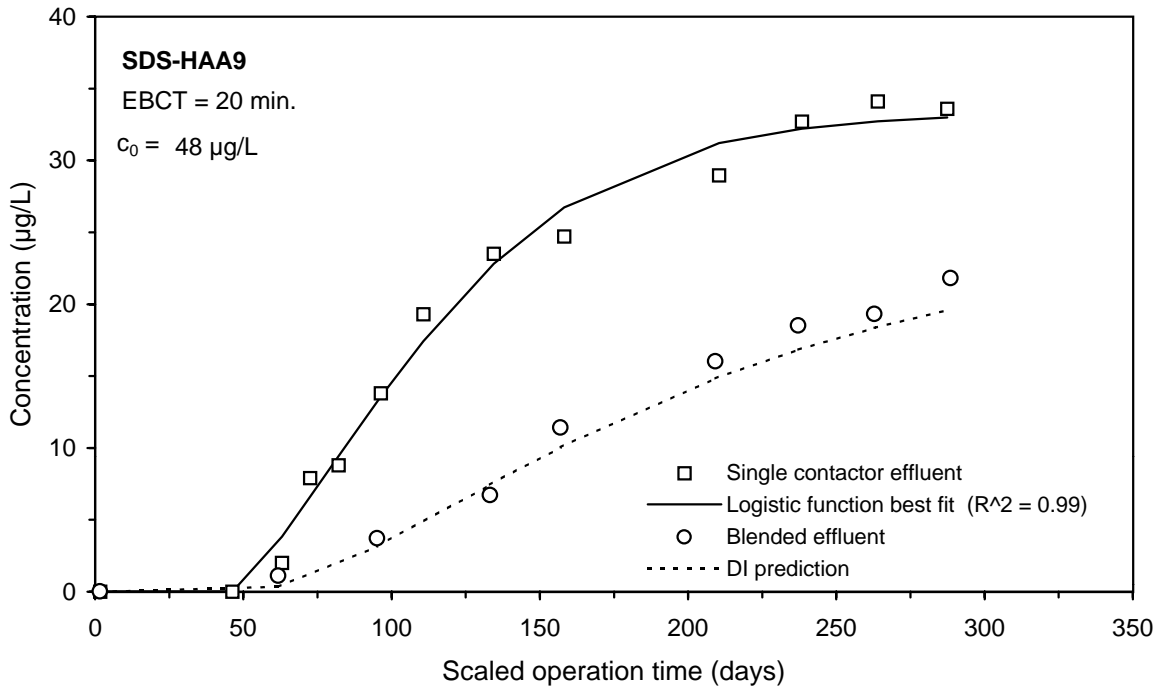


**Figure E-100 Single contactor and blended effluent SDS-HAA9 breakthrough curves for Water 5**

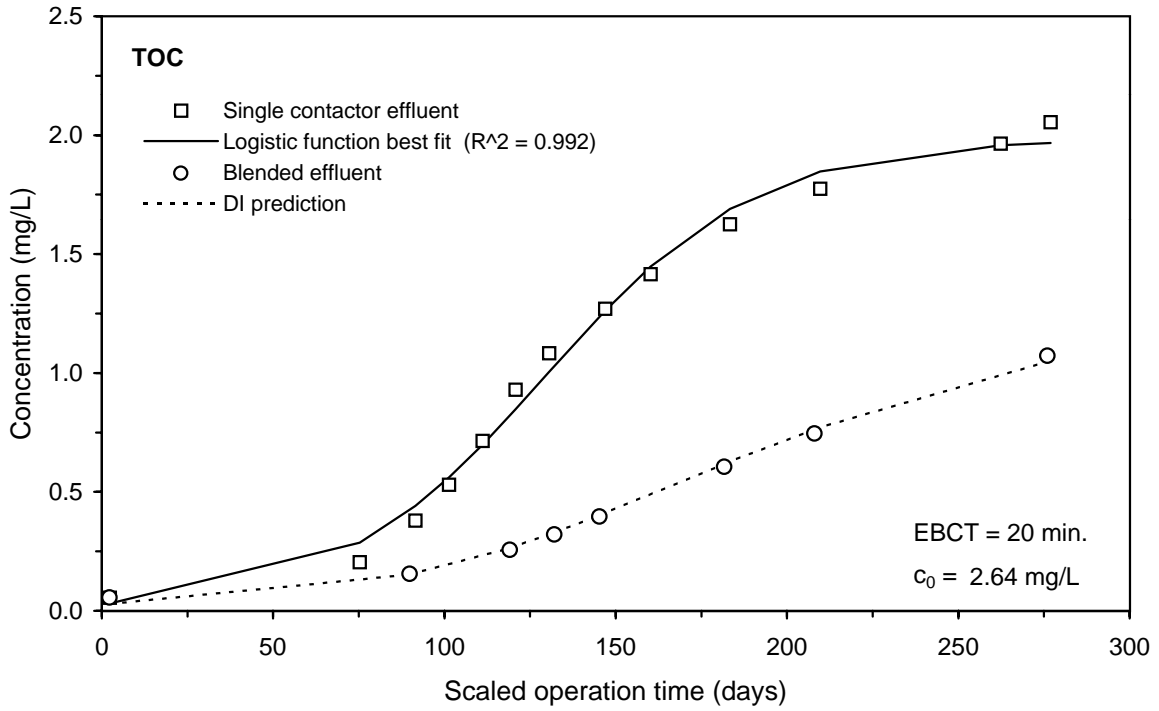


**Figure E-101 Single contactor and blended effluent TOC breakthrough curves for Water 6**

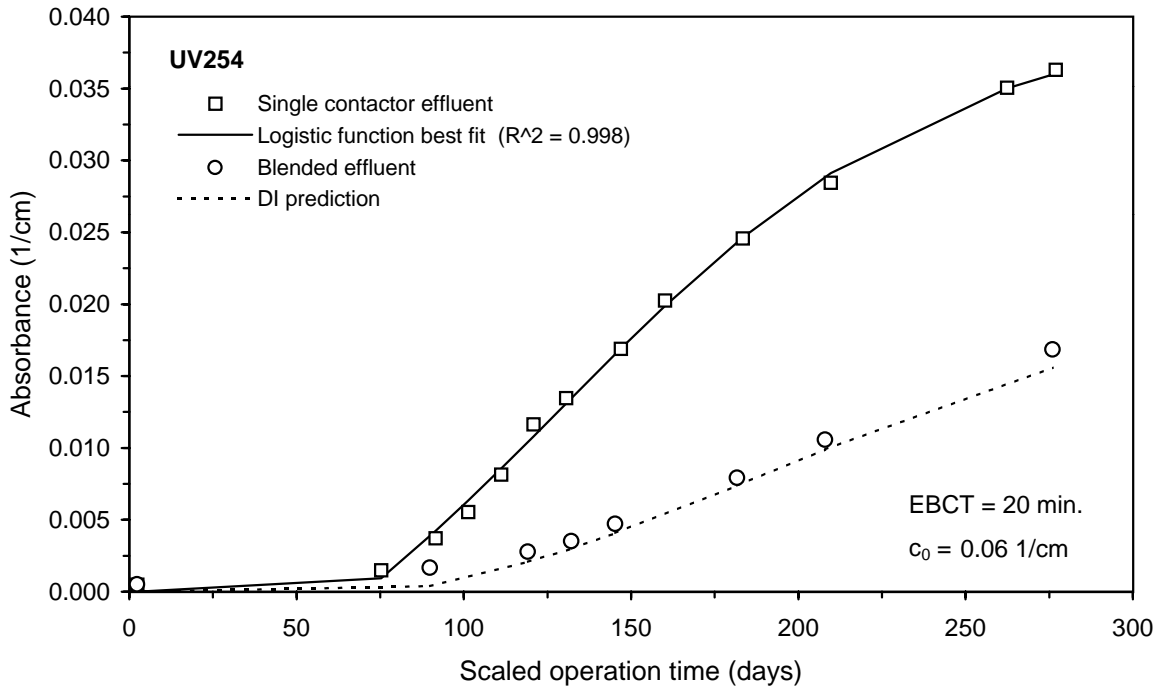


**Figure E-102 Single contactor and blended effluent UV254 breakthrough curves for Water 6**

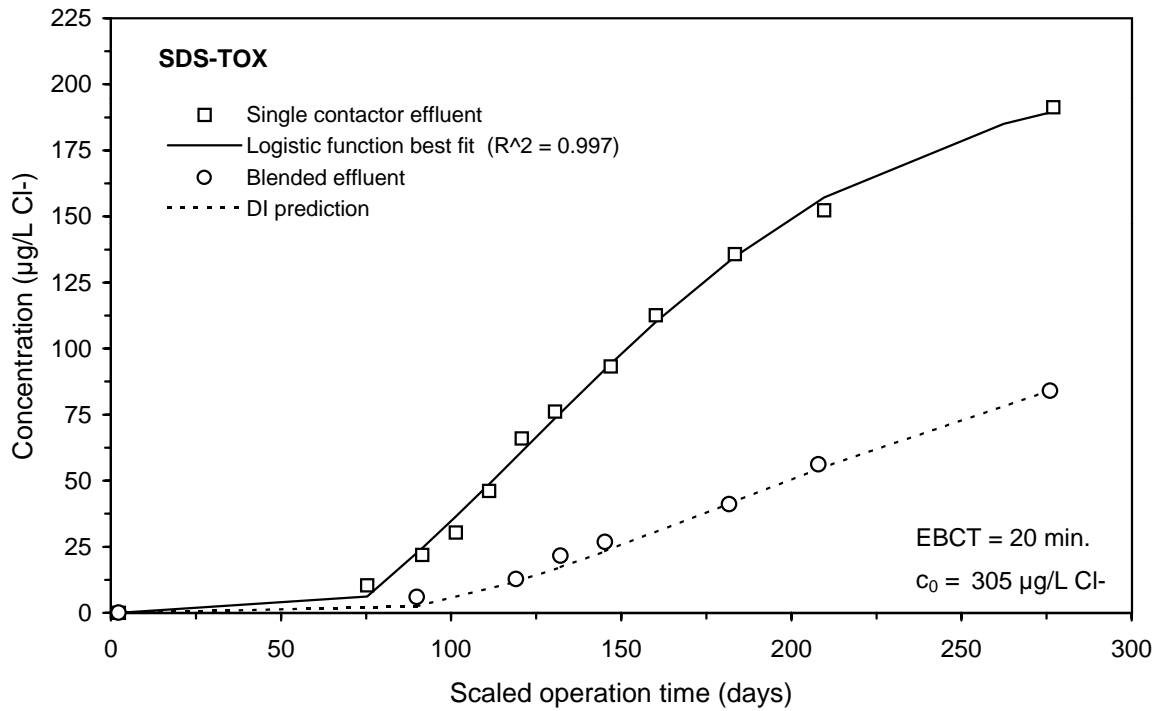


**Figure E-103 Single contactor and blended effluent SDS-TOX breakthrough curves for Water 6**

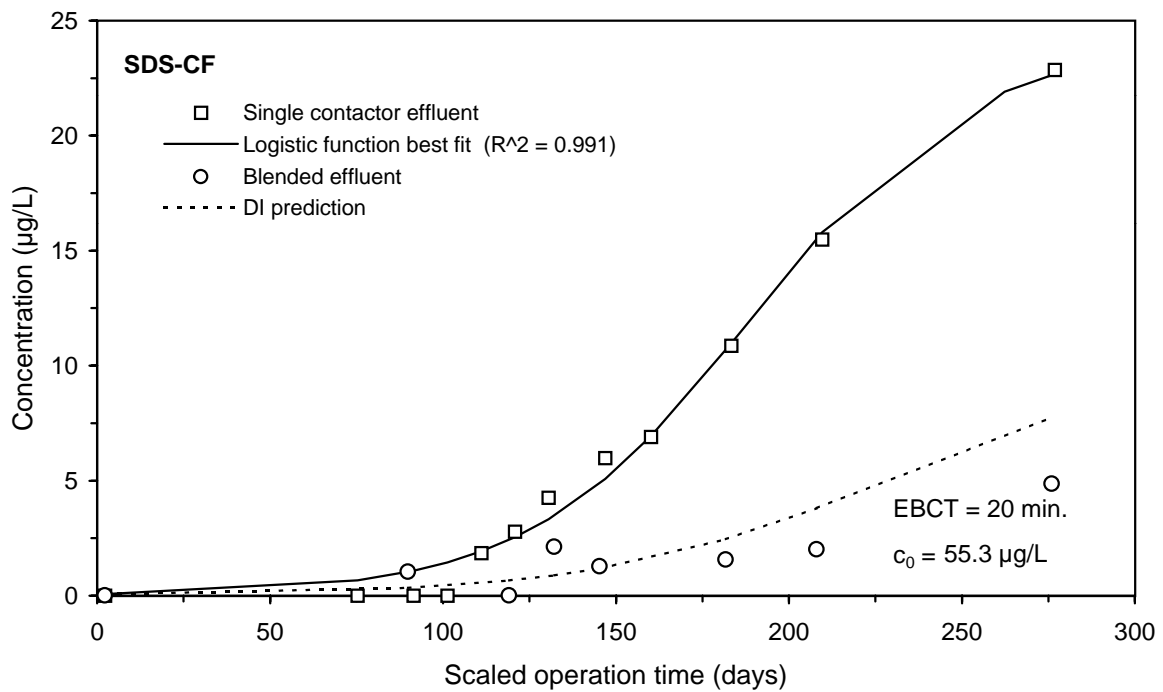


**Figure E-104 Single contactor and blended effluent SDS-CF breakthrough curves for Water 6**

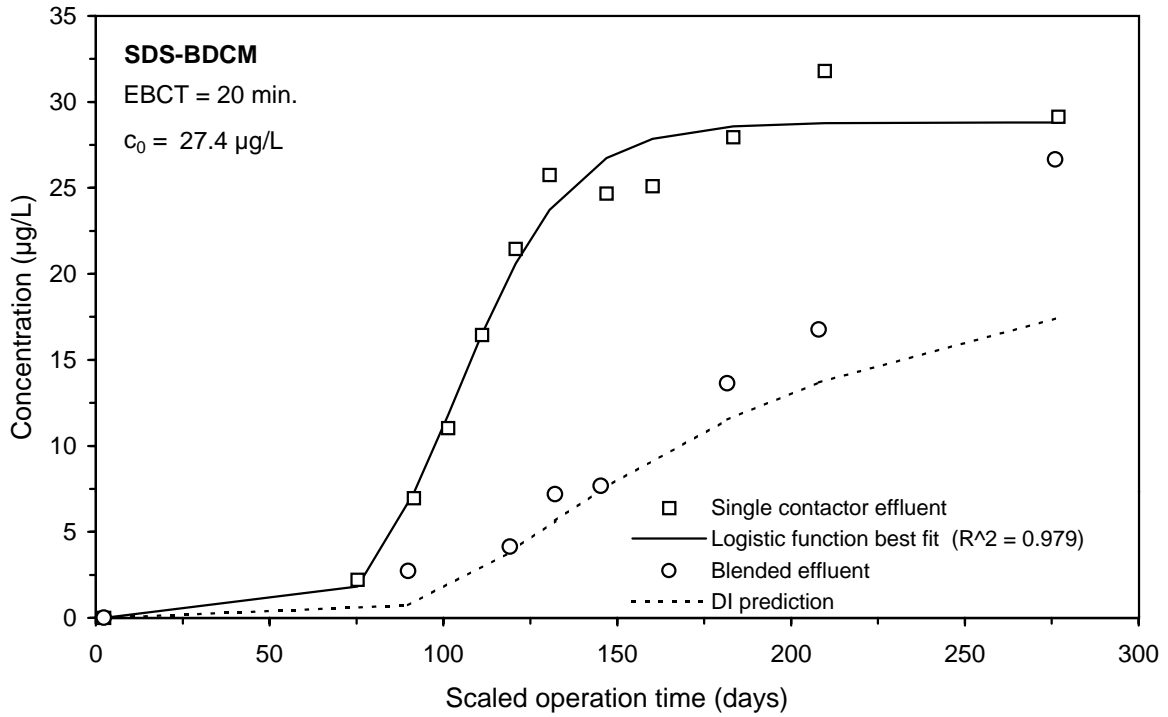


**Figure E-105 Single contactor and blended effluent SDS-BDCM breakthrough curves for Water 6**

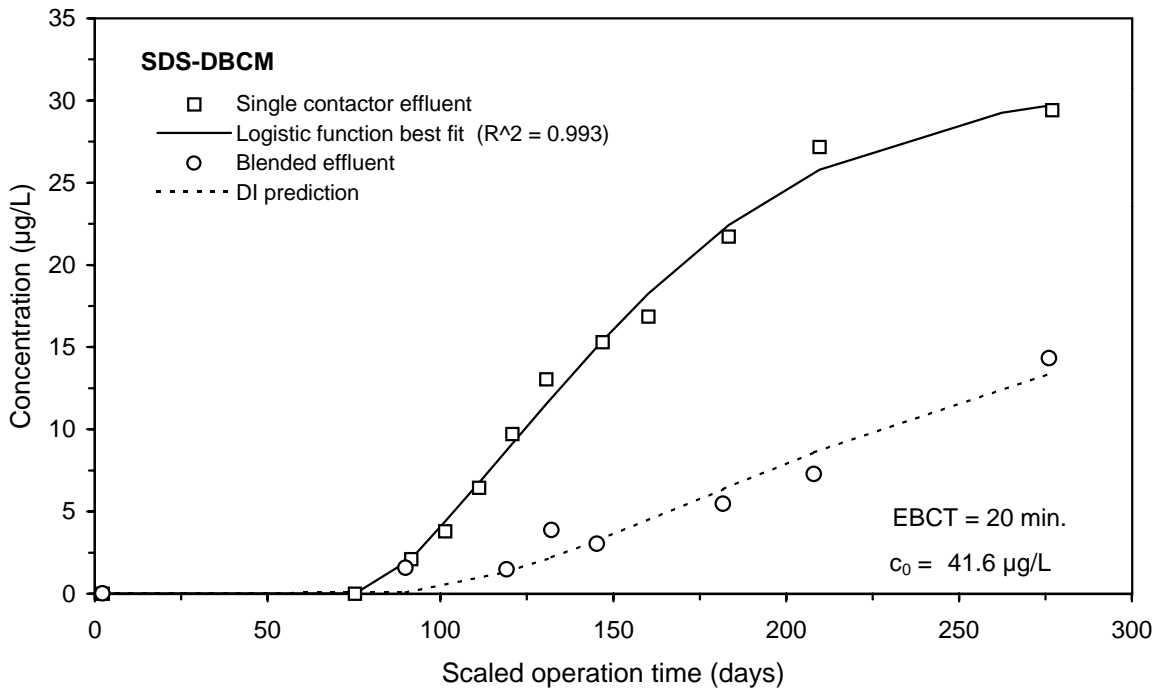


**Figure E-106 Single contactor and blended effluent SDS-DBCМ breakthrough curves for Water 6**

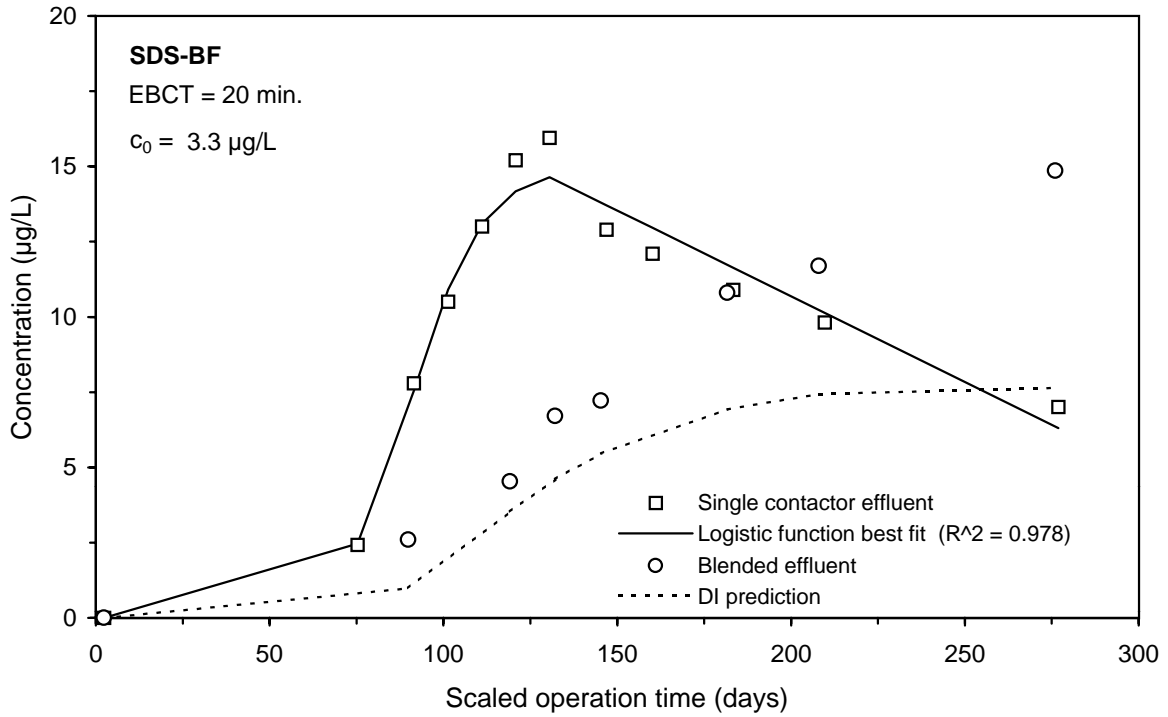


**Figure E-107 Single contactor and blended effluent SDS-BF breakthrough curves for Water 6**

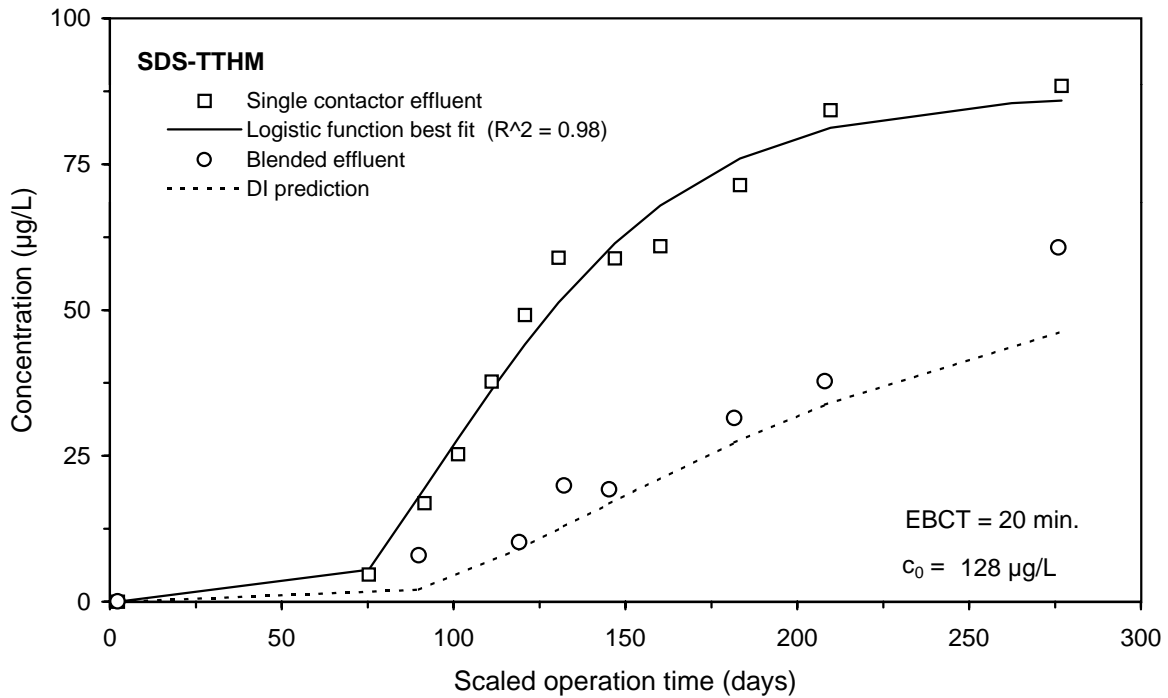


**Figure E-108 Single contactor and blended effluent SDS-TTHM breakthrough curves for Water 6**

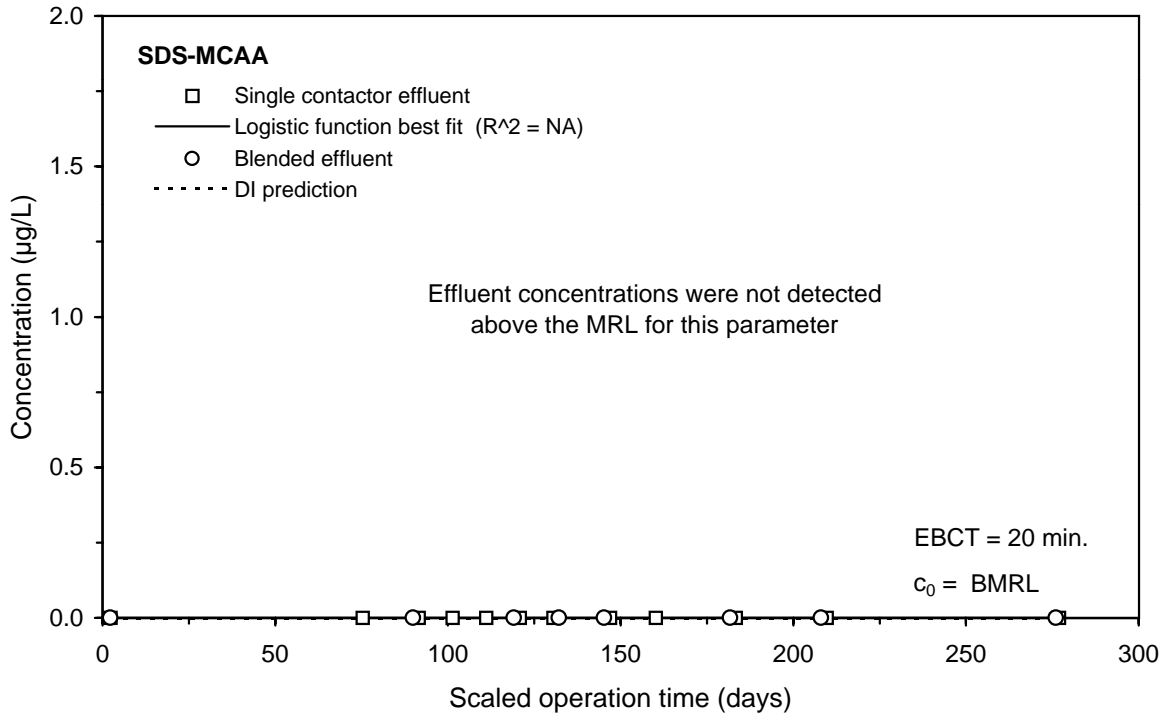


**Figure E-109 Single contactor and blended effluent SDS-MCAA breakthrough curves for Water 6**

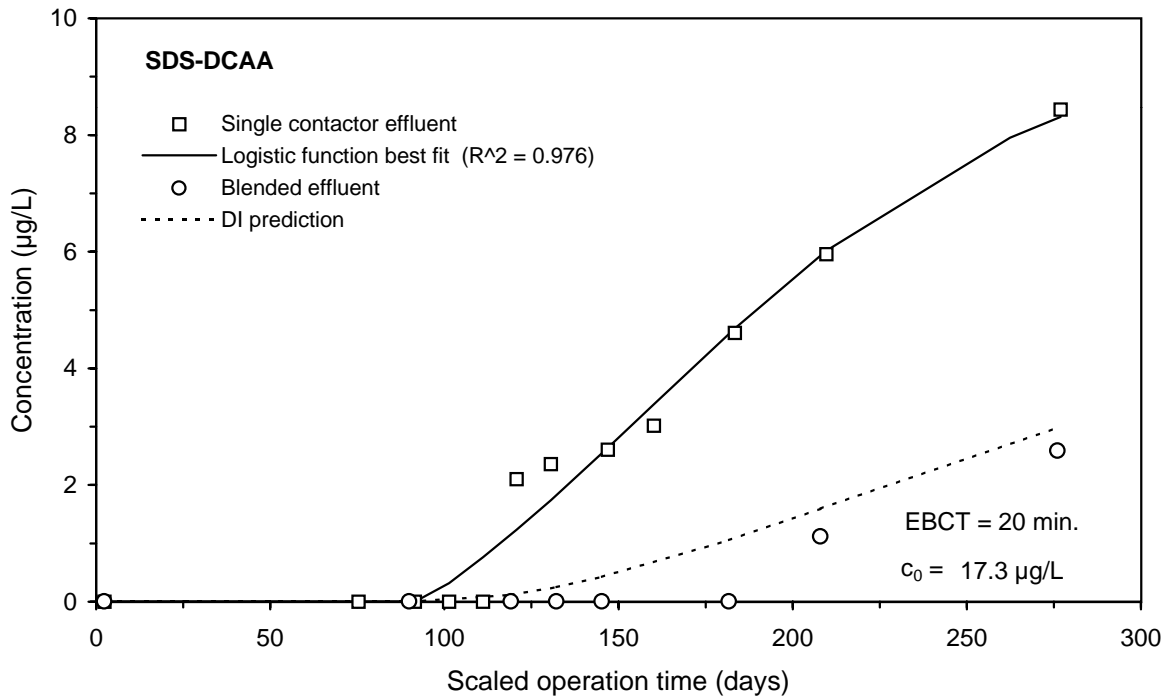


**Figure E-110 Single contactor and blended effluent SDS-DCAA breakthrough curves for Water 6**

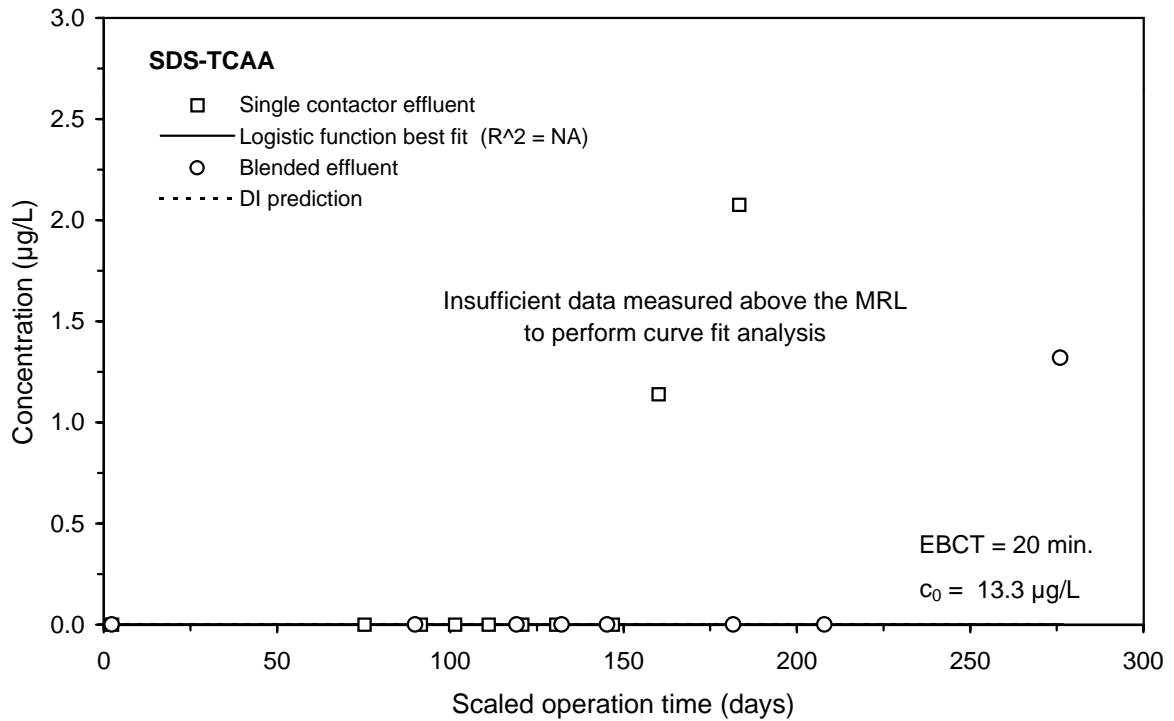


**Figure E-111 Single contactor and blended effluent SDS-TCAA breakthrough curves for Water 6**

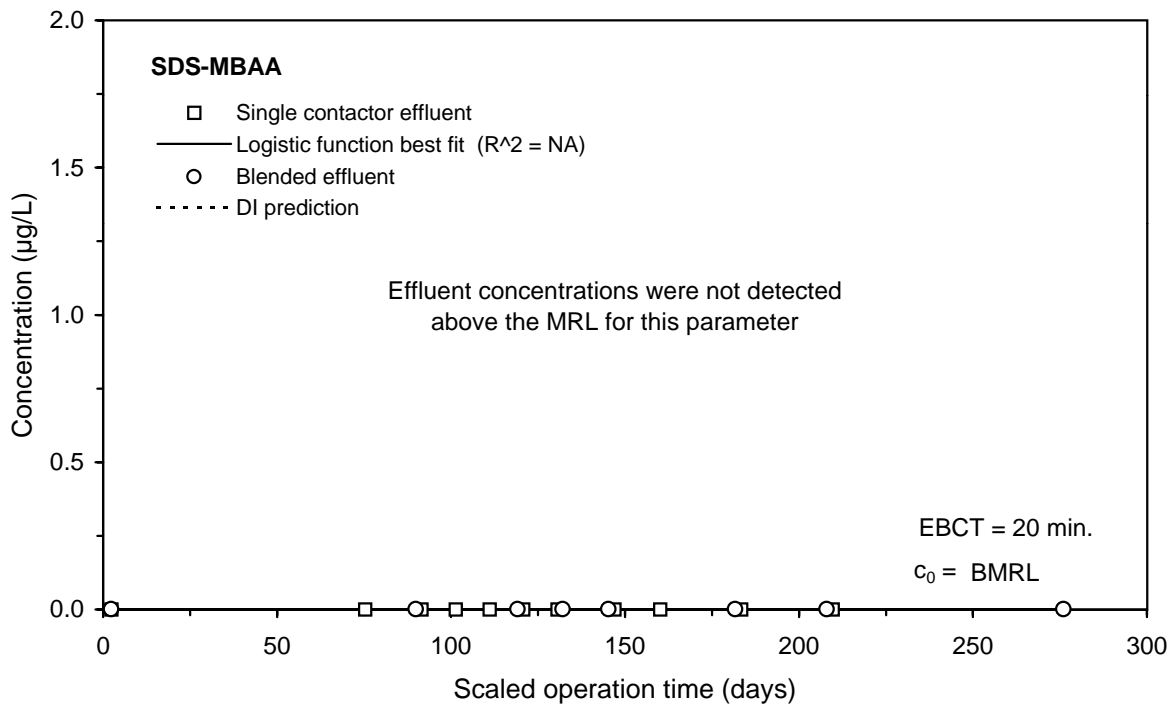


**Figure E-112 Single contactor and blended effluent SDS-MBAA breakthrough curves for Water 6**

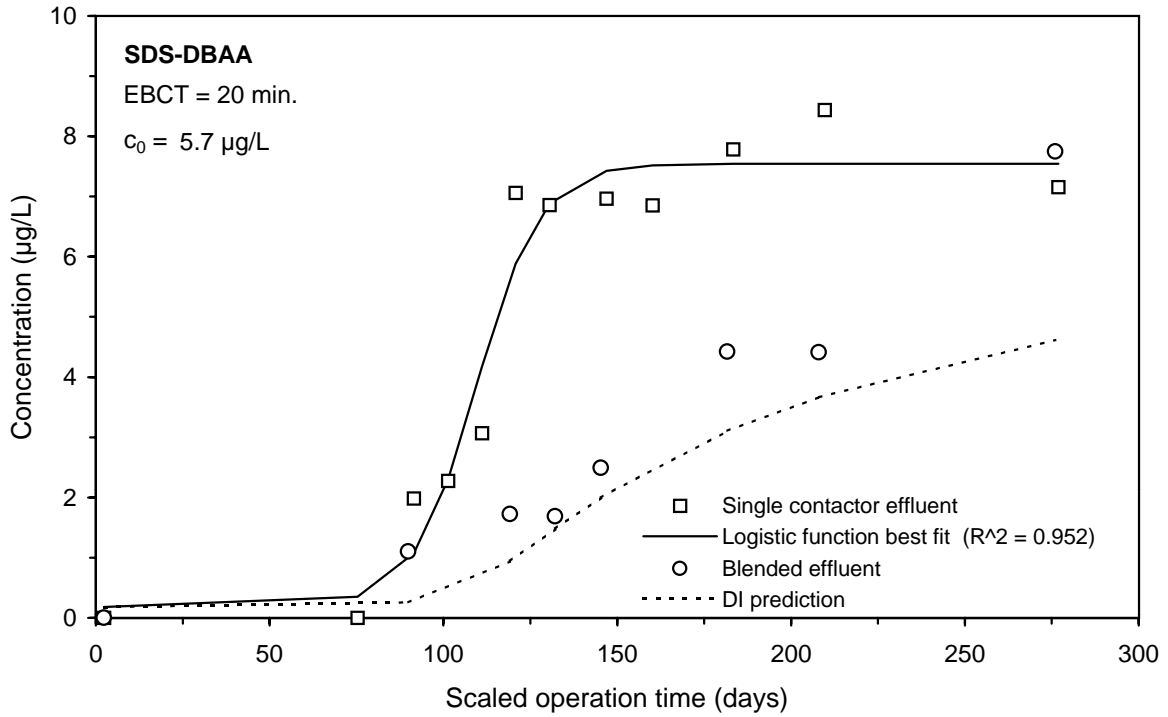


**Figure E-113 Single contactor and blended effluent SDS-DBAA breakthrough curves for Water 6**

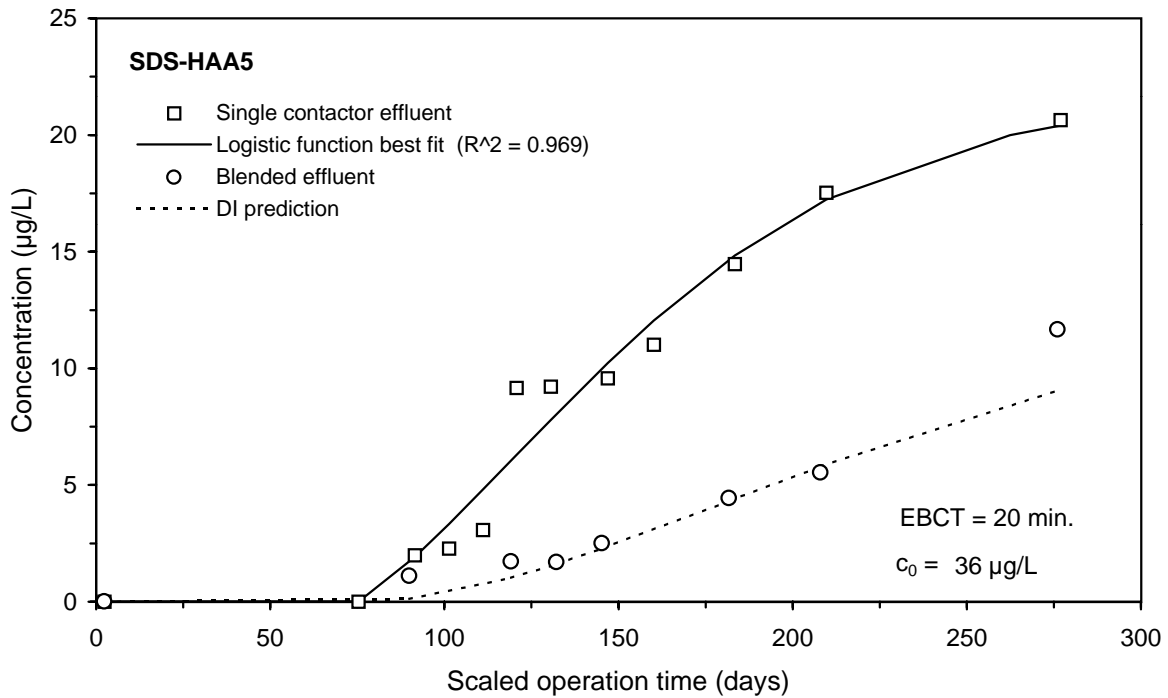


**Figure E-114 Single contactor and blended effluent SDS-HAA5 breakthrough curves for Water 6**

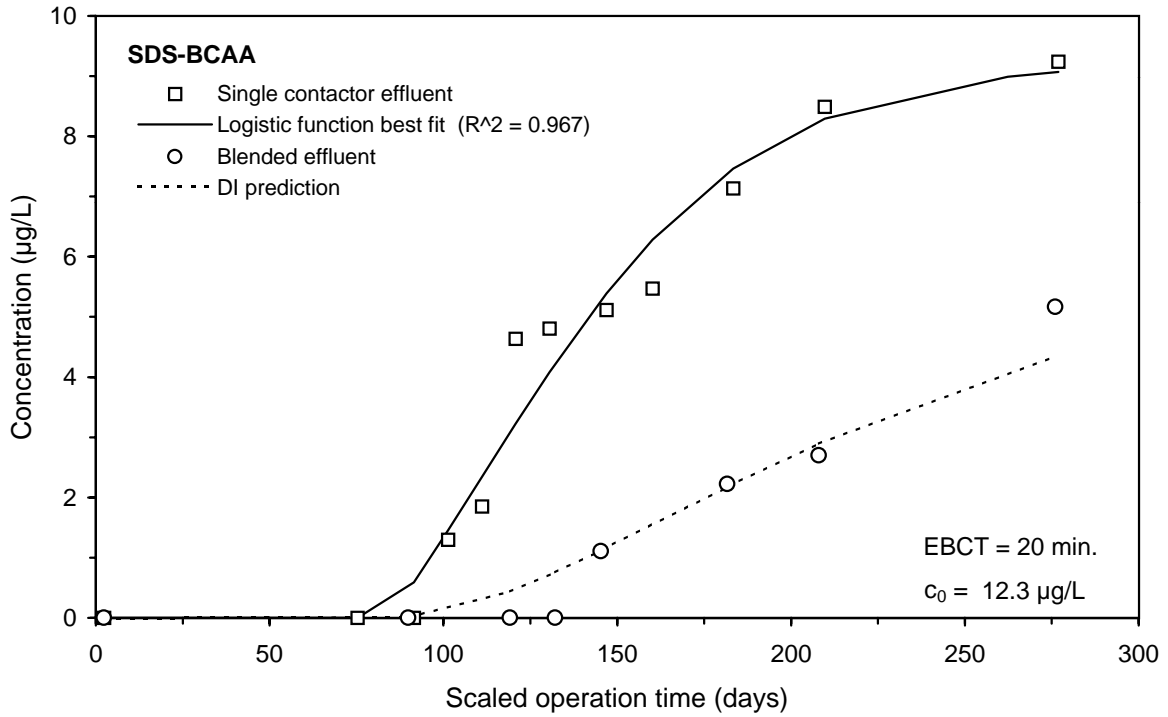


**Figure E-115 Single contactor and blended effluent SDS-BCAA breakthrough curves for Water 6**

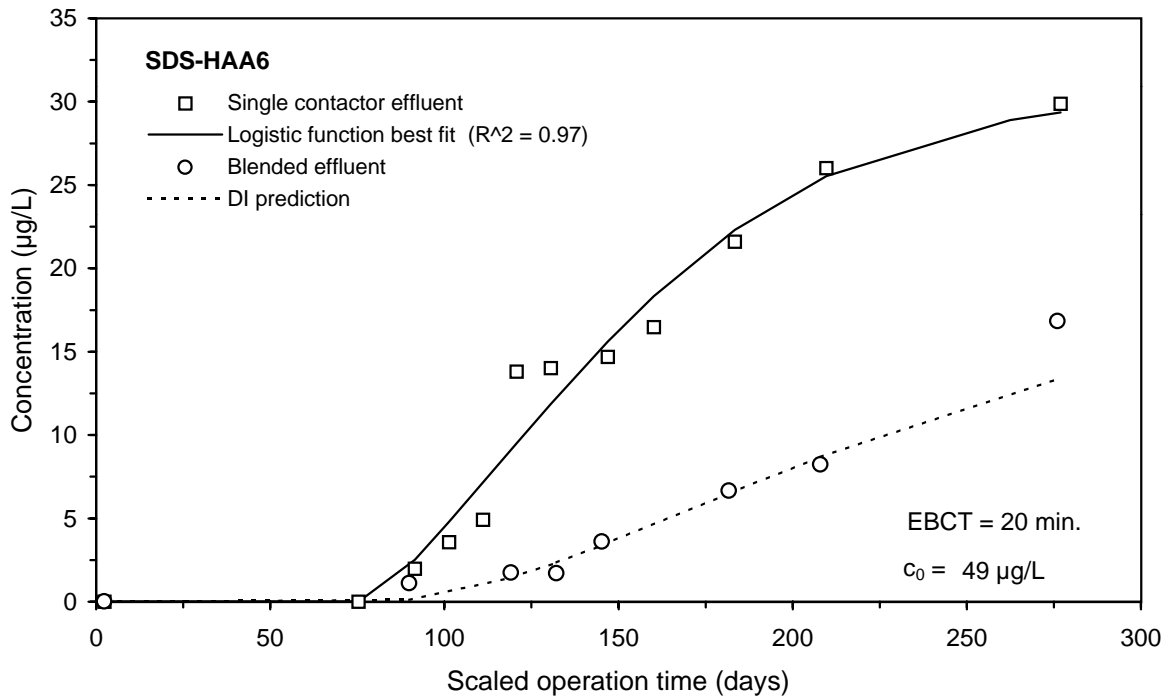


**Figure E-116 Single contactor and blended effluent SDS-HAA6 breakthrough curves for Water 6**

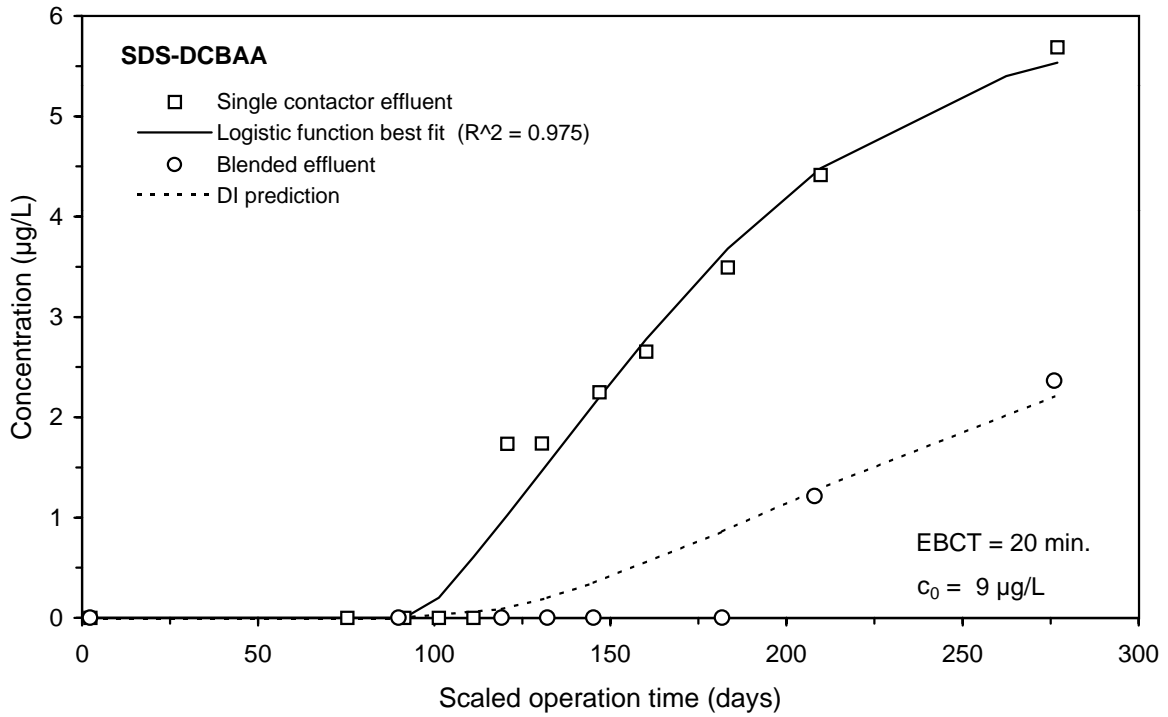


**Figure E-117 Single contactor and blended effluent SDS-DCBAA breakthrough curves for Water 6**

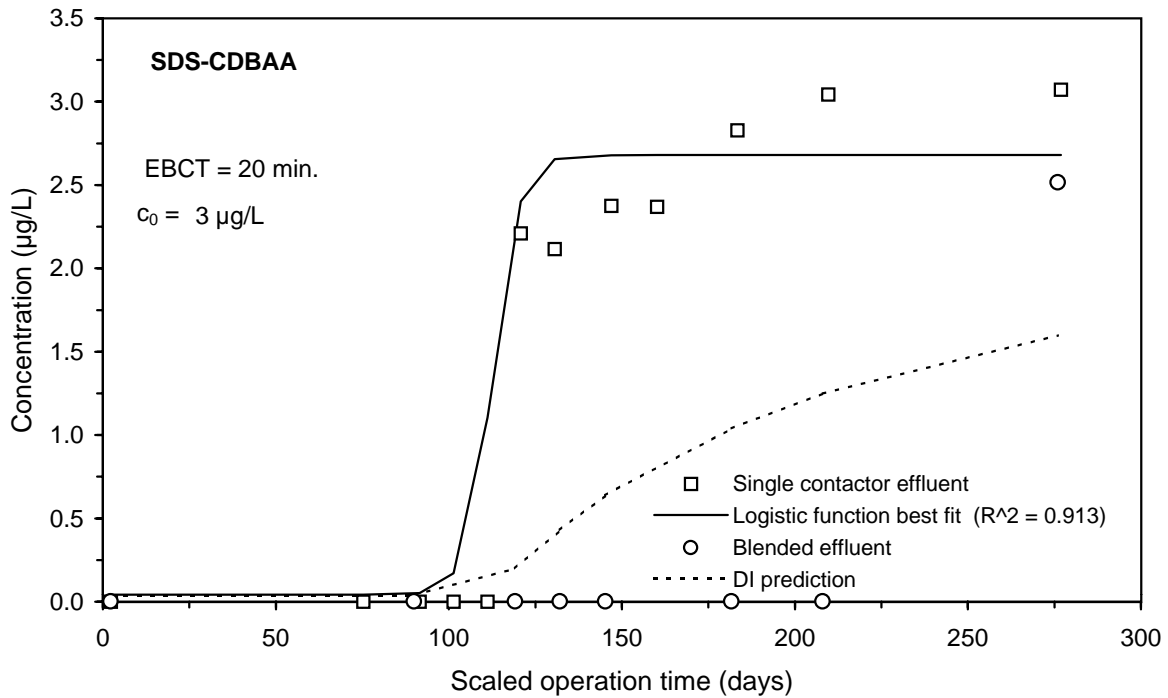


**Figure E-118 Single contactor and blended effluent SDS-CDBAA breakthrough curves for Water 6**

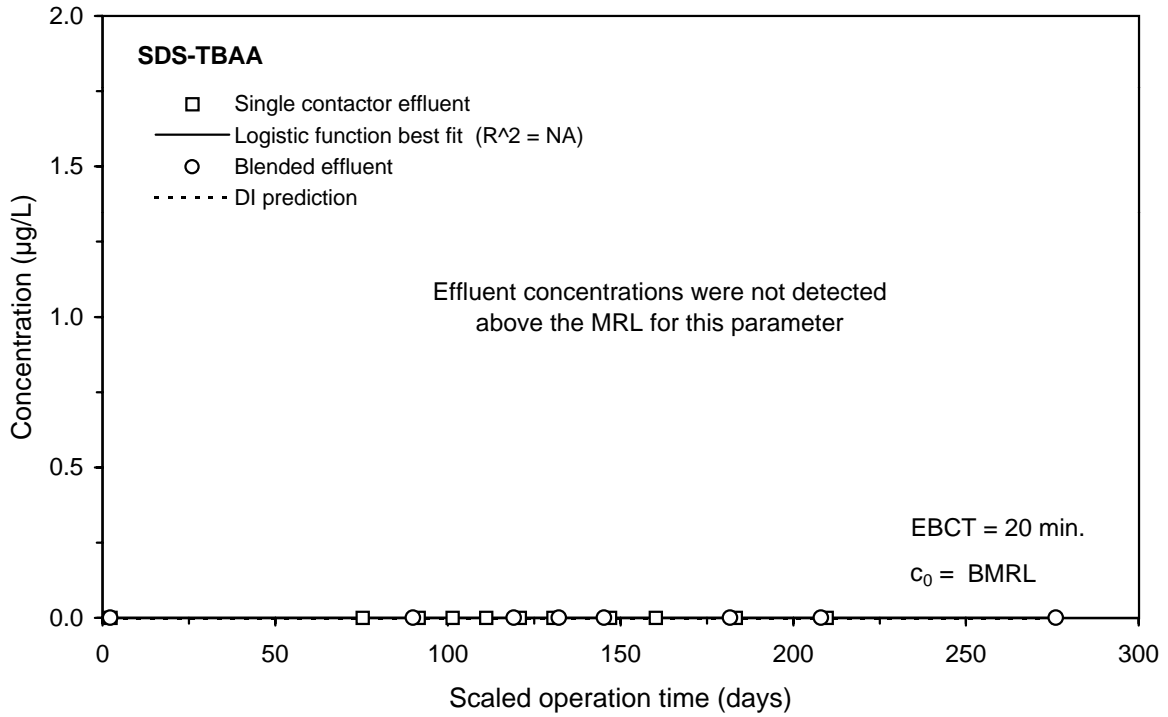


**Figure E-119 Single contactor and blended effluent SDS-TBAA breakthrough curves for Water 6**

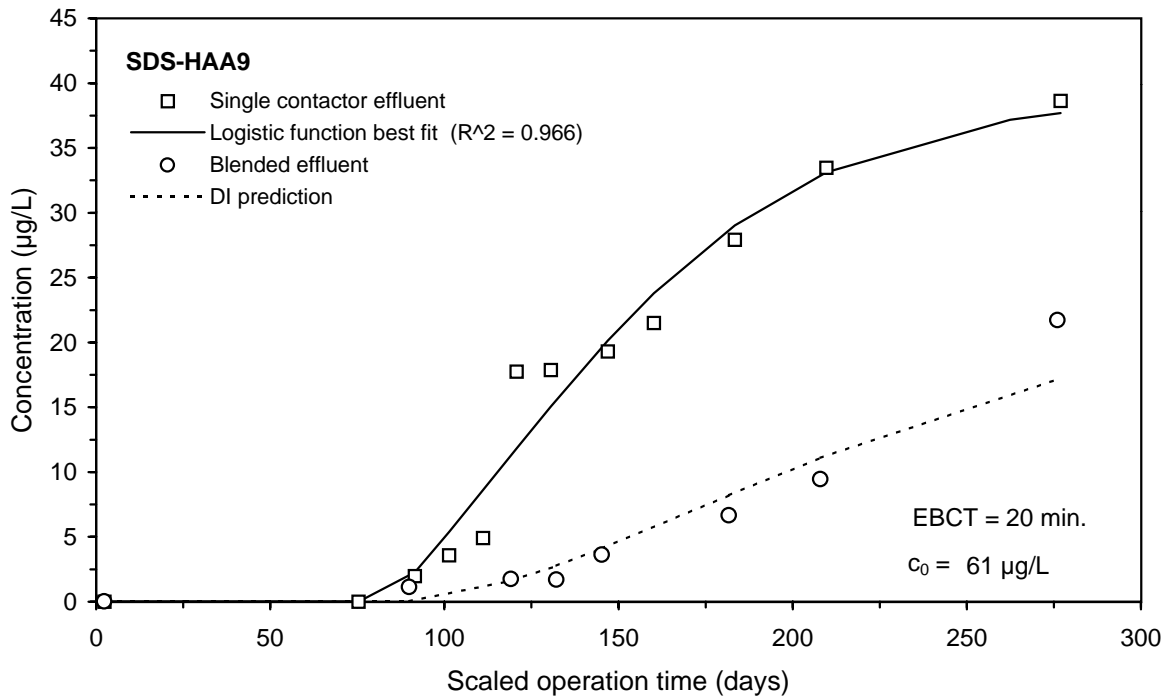


**Figure E-120 Single contactor and blended effluent SDS-HAA9 breakthrough curves for Water 6**

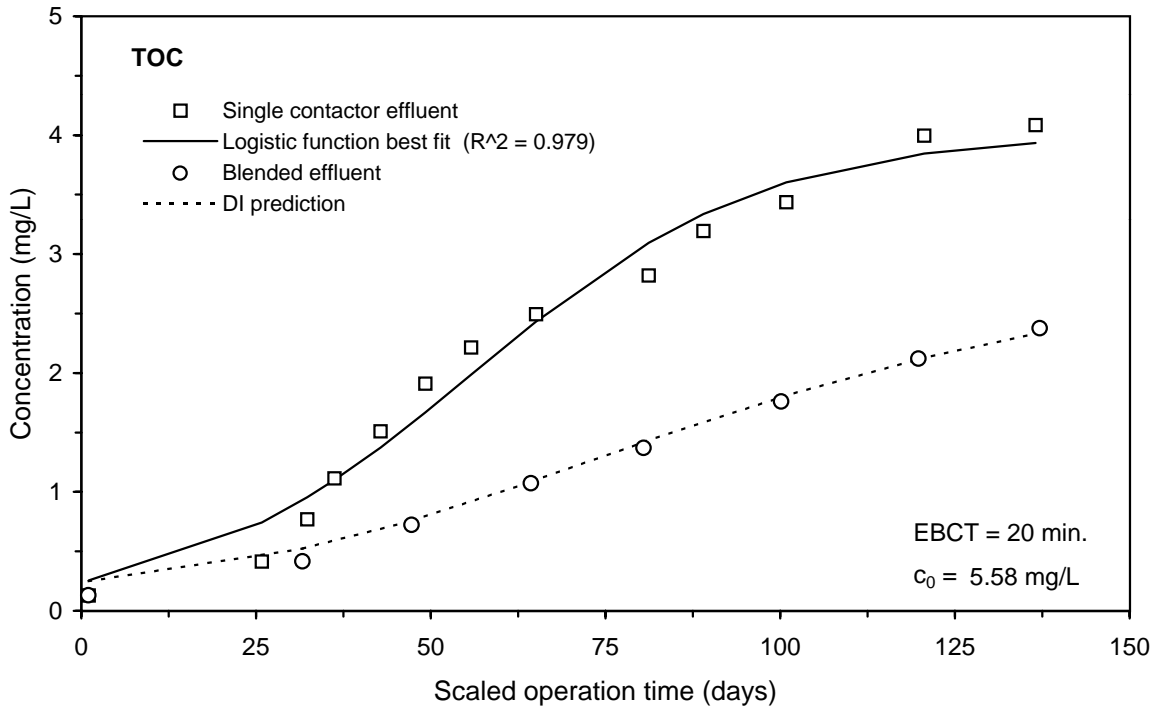


**Figure E-121 Single contactor and blended effluent TOC breakthrough curves for Water 7**

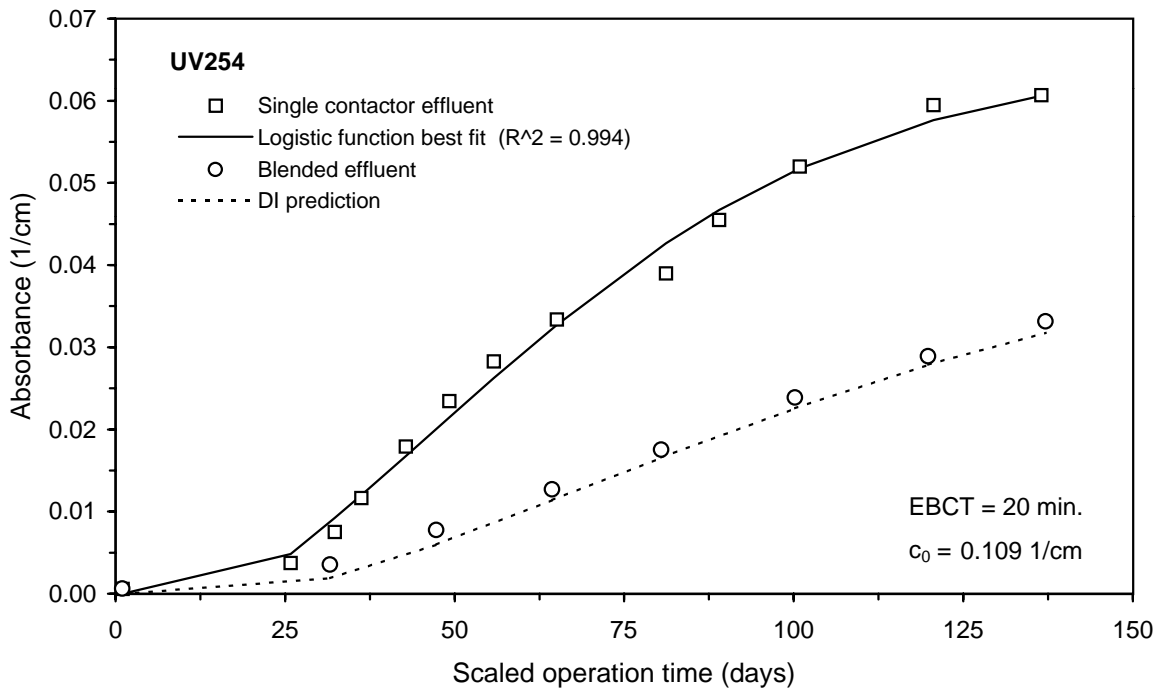


**Figure E-122 Single contactor and blended effluent UV254 breakthrough curves for Water 7**

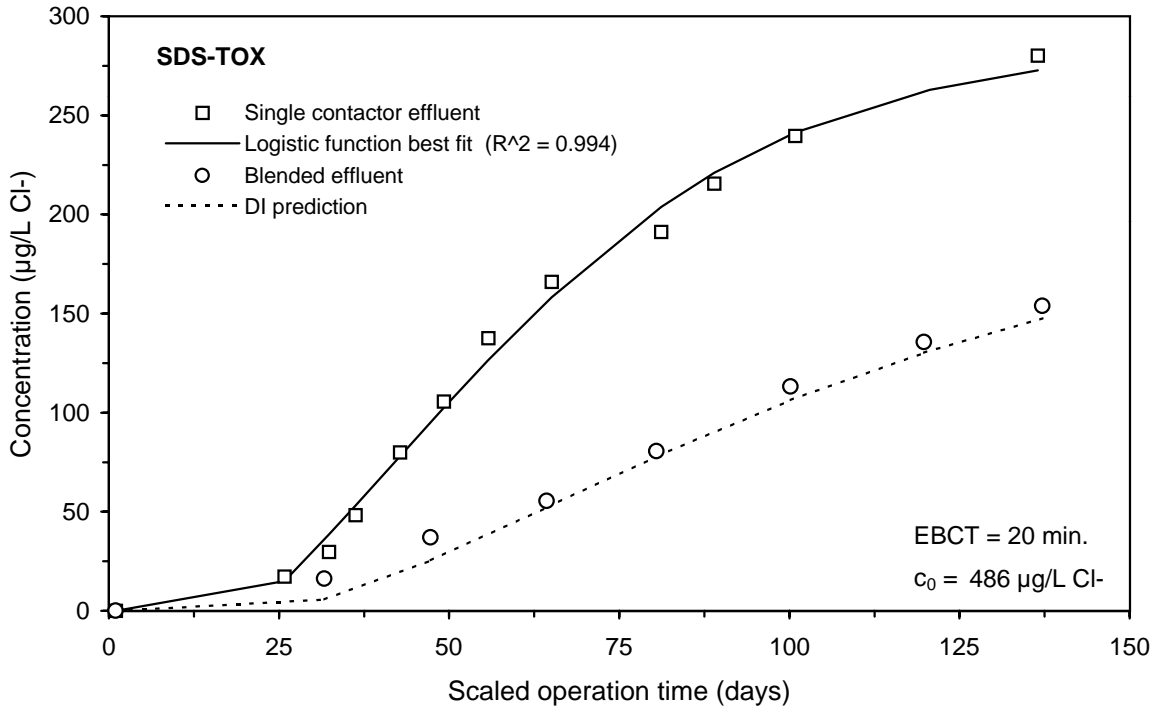


**Figure E-123 Single contactor and blended effluent SDS-TOX breakthrough curves for Water 7**

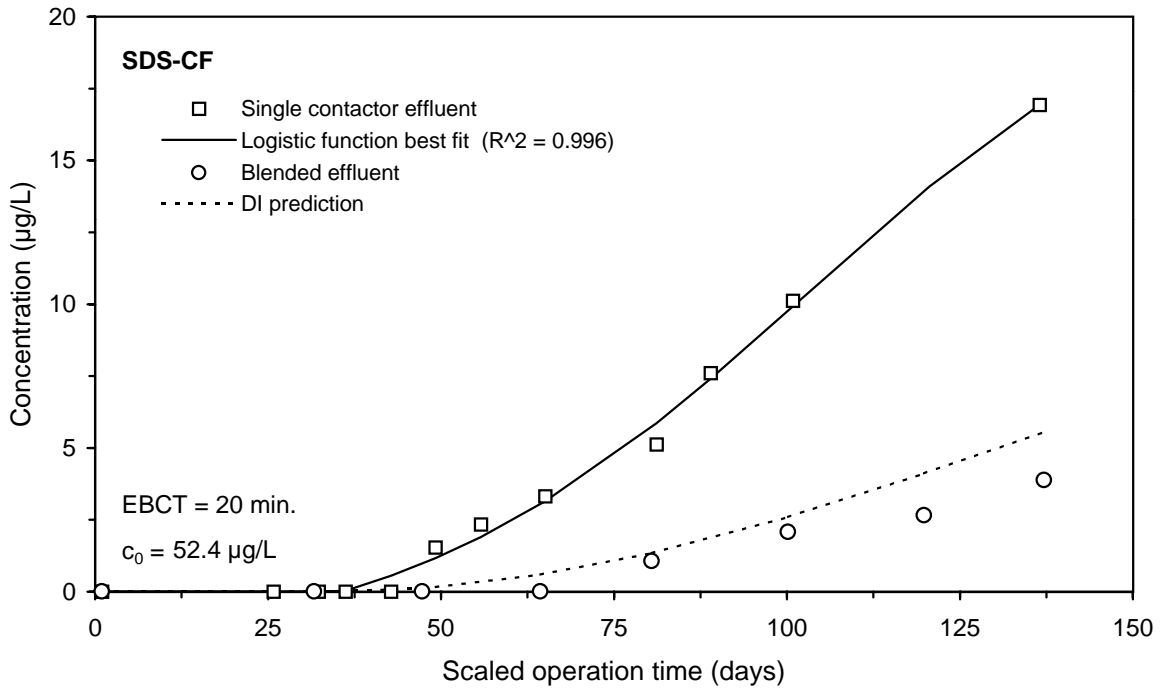


**Figure E-124 Single contactor and blended effluent SDS-CF breakthrough curves for Water 7**

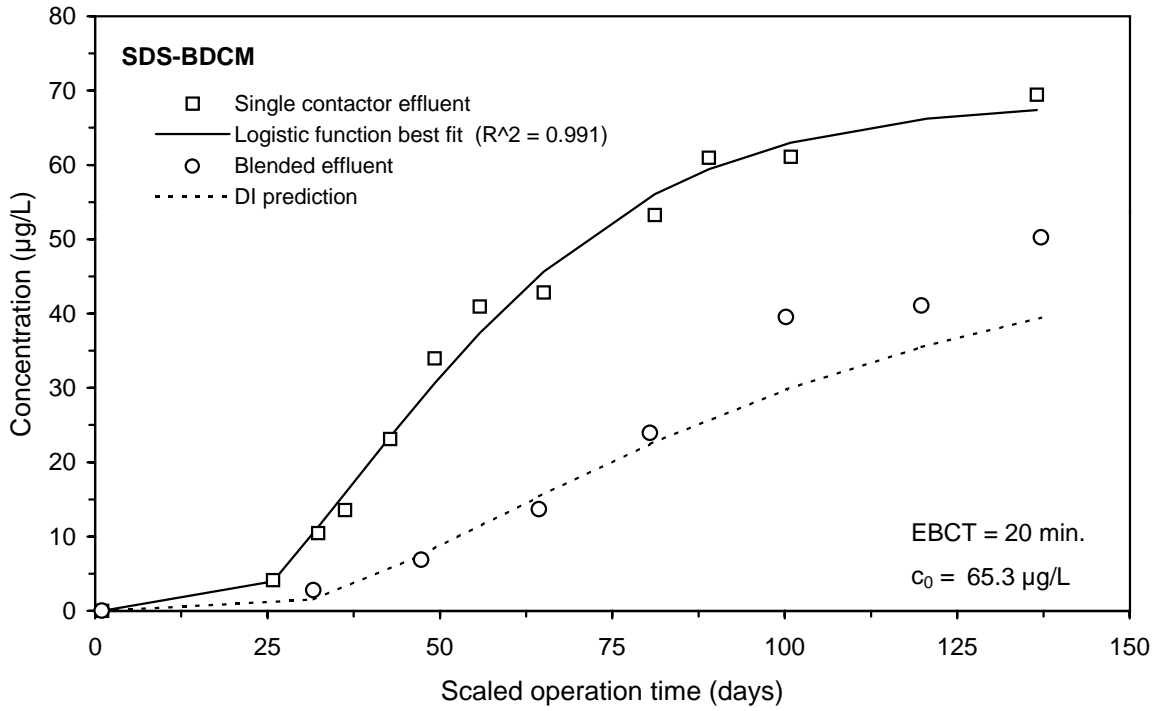


**Figure E-125 Single contactor and blended effluent SDS-BDCM breakthrough curves for Water 7**

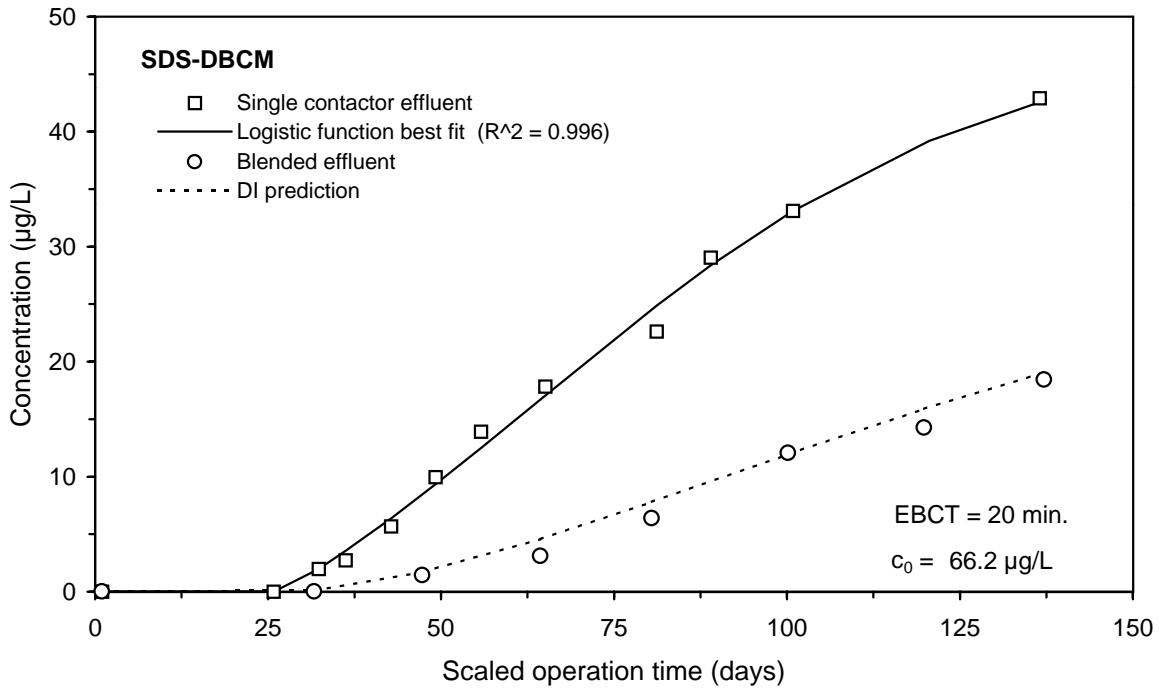


**Figure E-126 Single contactor and blended effluent SDS-DBCМ breakthrough curves for Water 7**

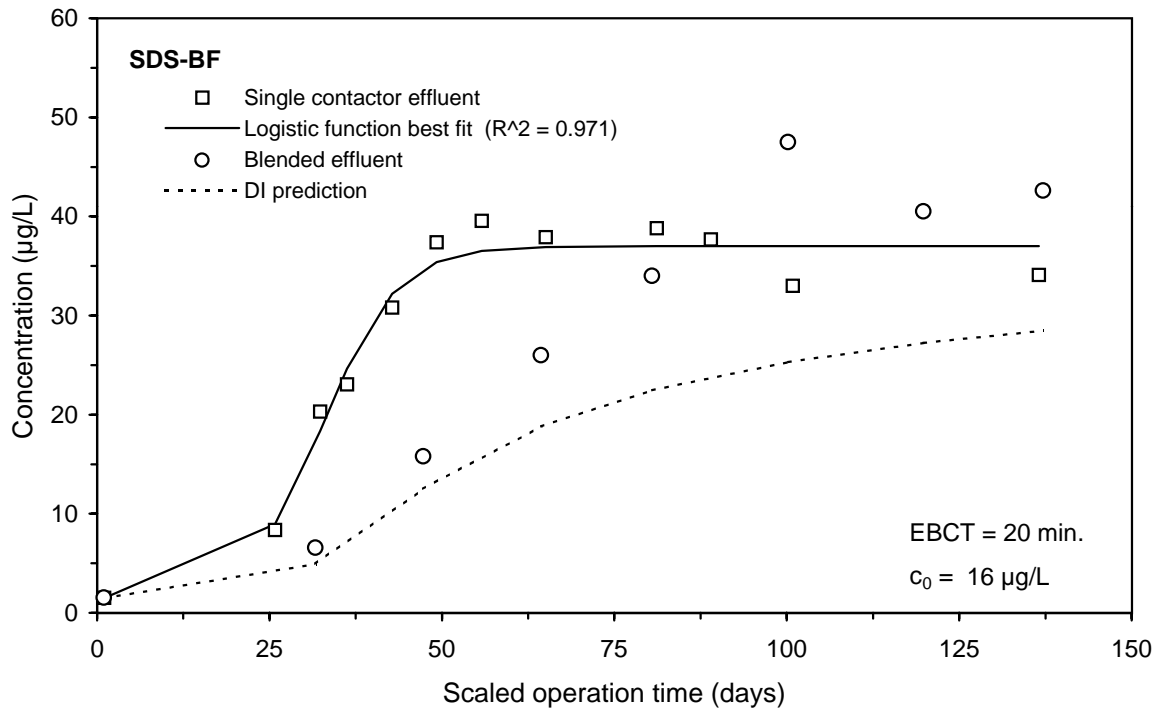


**Figure E-127 Single contactor and blended effluent SDS-BF breakthrough curves for Water 7**

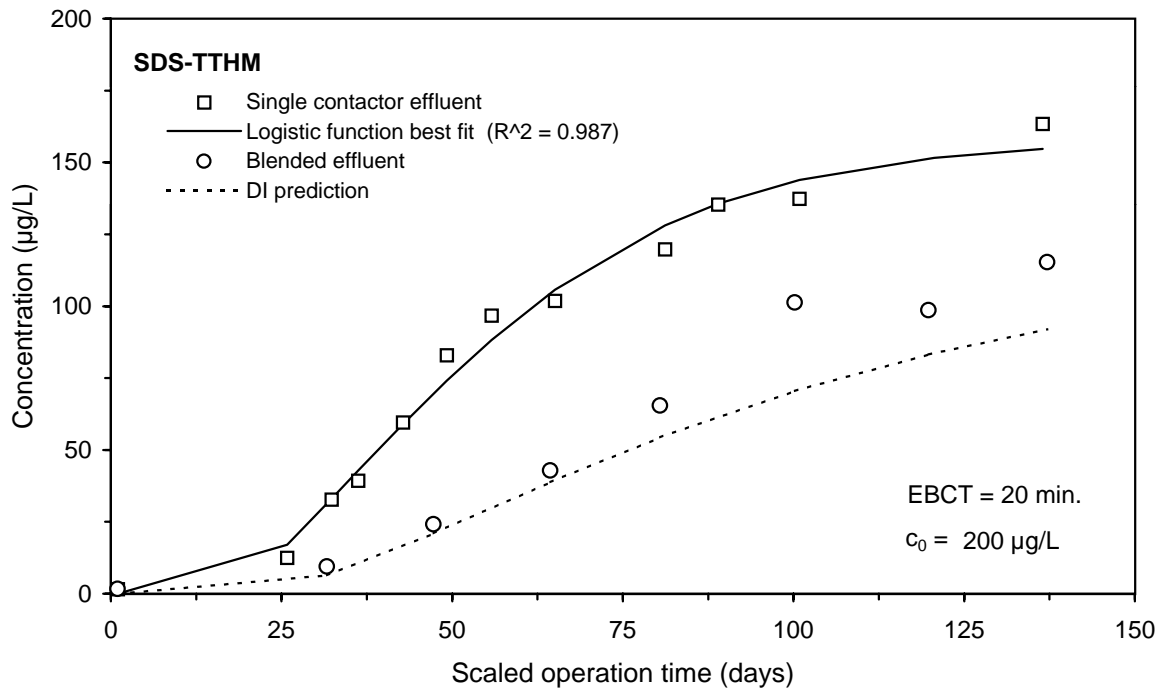


**Figure E-128 Single contactor and blended effluent SDS-TTHM breakthrough curves for Water 7**

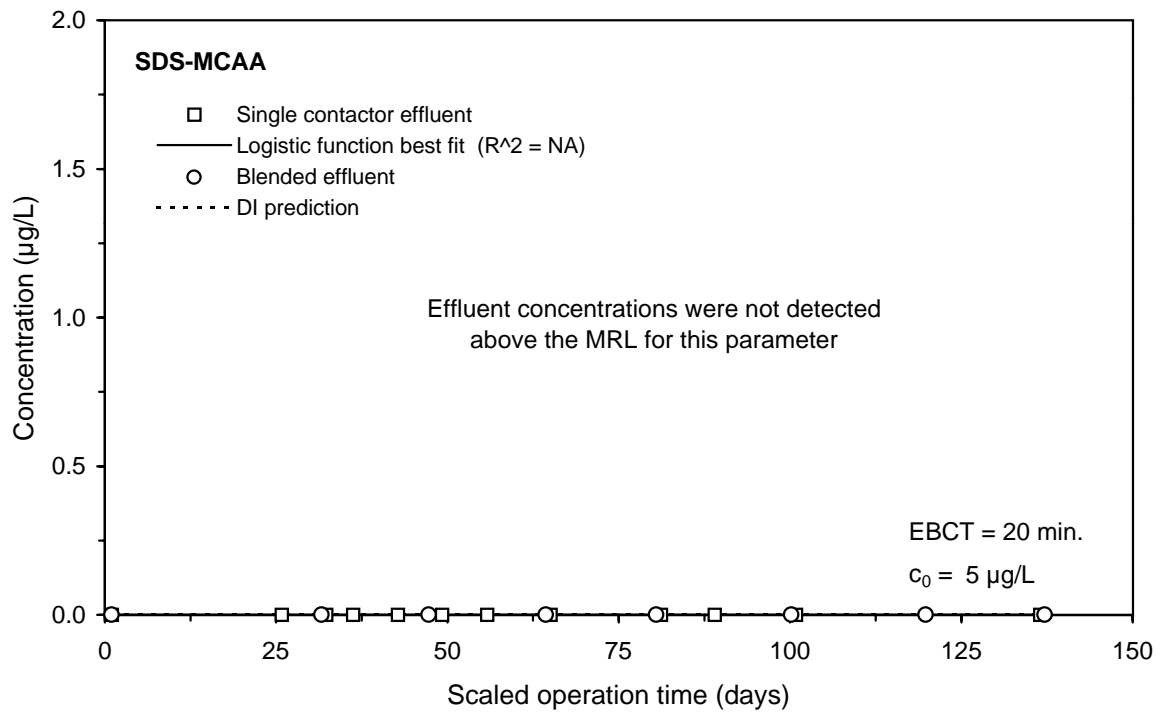


**Figure E-129 Single contactor and blended effluent SDS-MCAA breakthrough curves for Water 7**

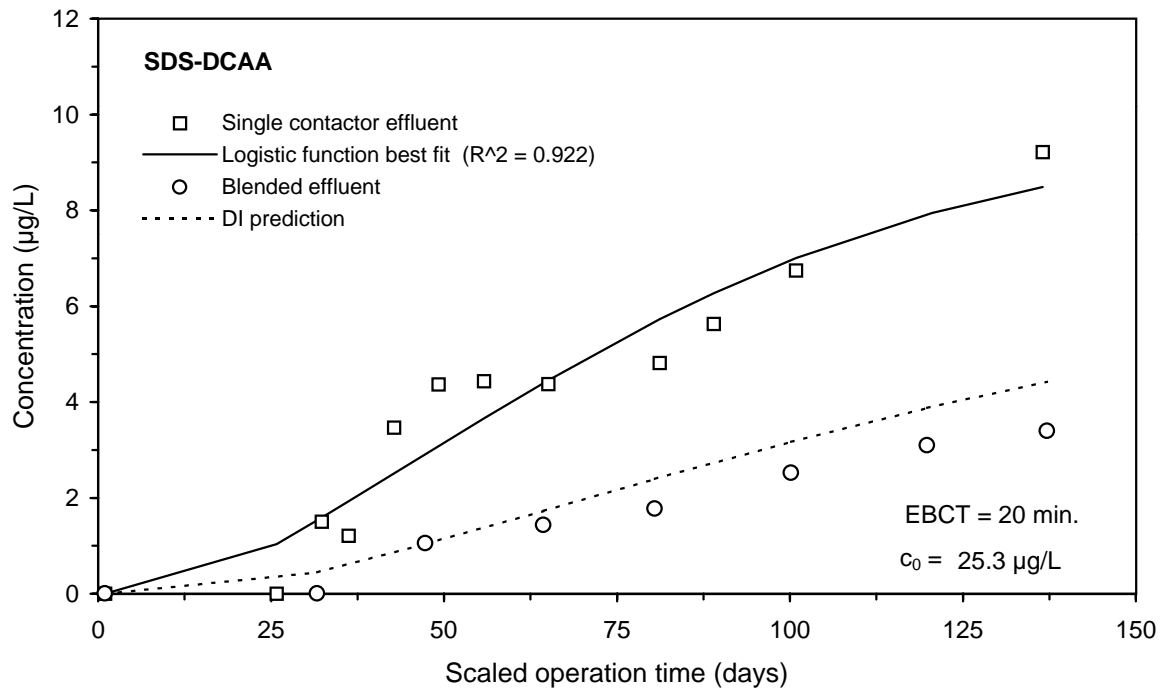


**Figure E-130 Single contactor and blended effluent SDS-DCAA breakthrough curves for Water 7**

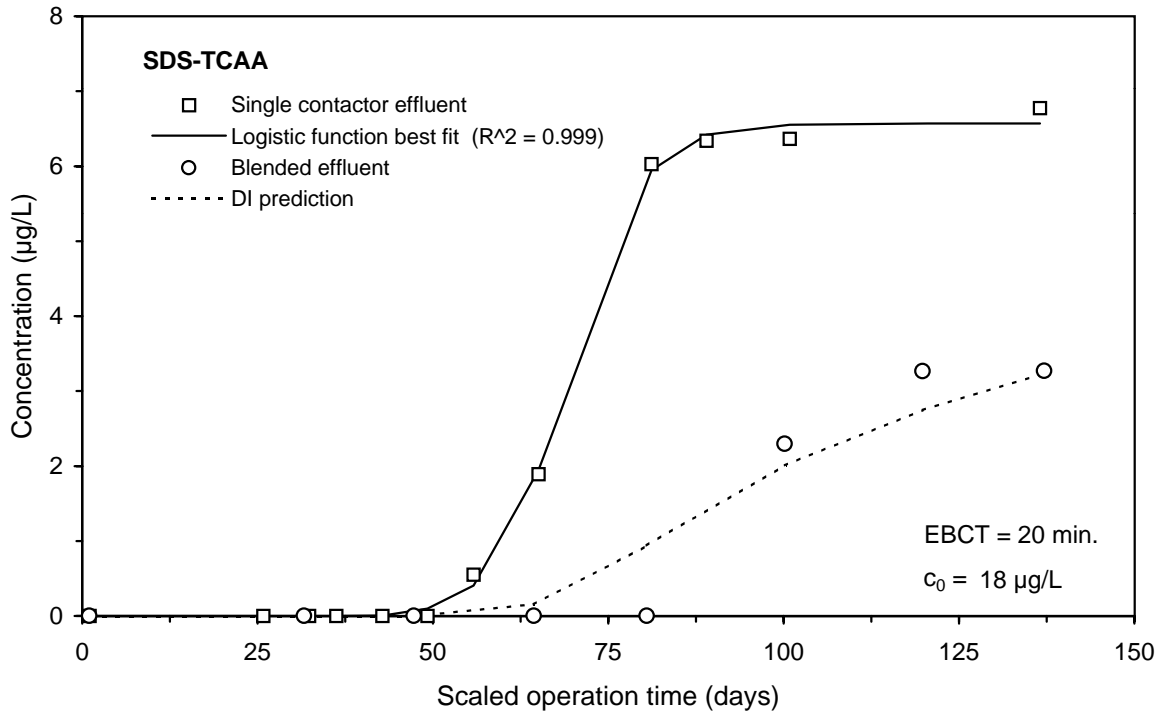


**Figure E-131 Single contactor and blended effluent SDS-TCAA breakthrough curves for Water 7**

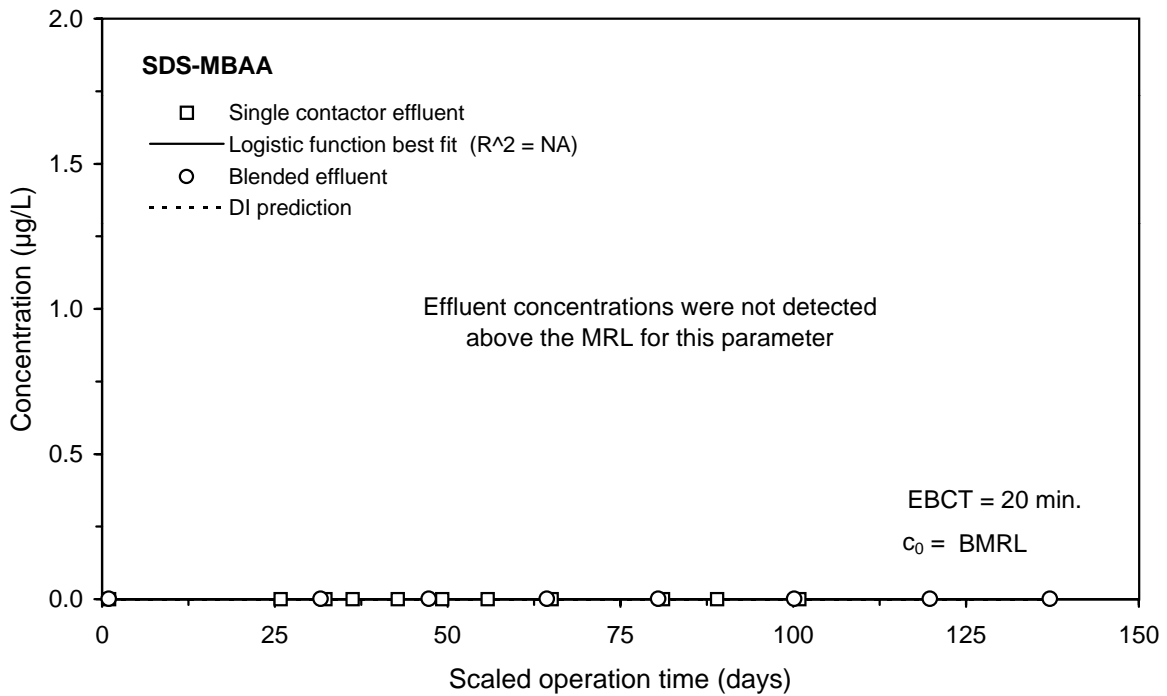


**Figure E-132 Single contactor and blended effluent SDS-MBAA breakthrough curves for Water 7**

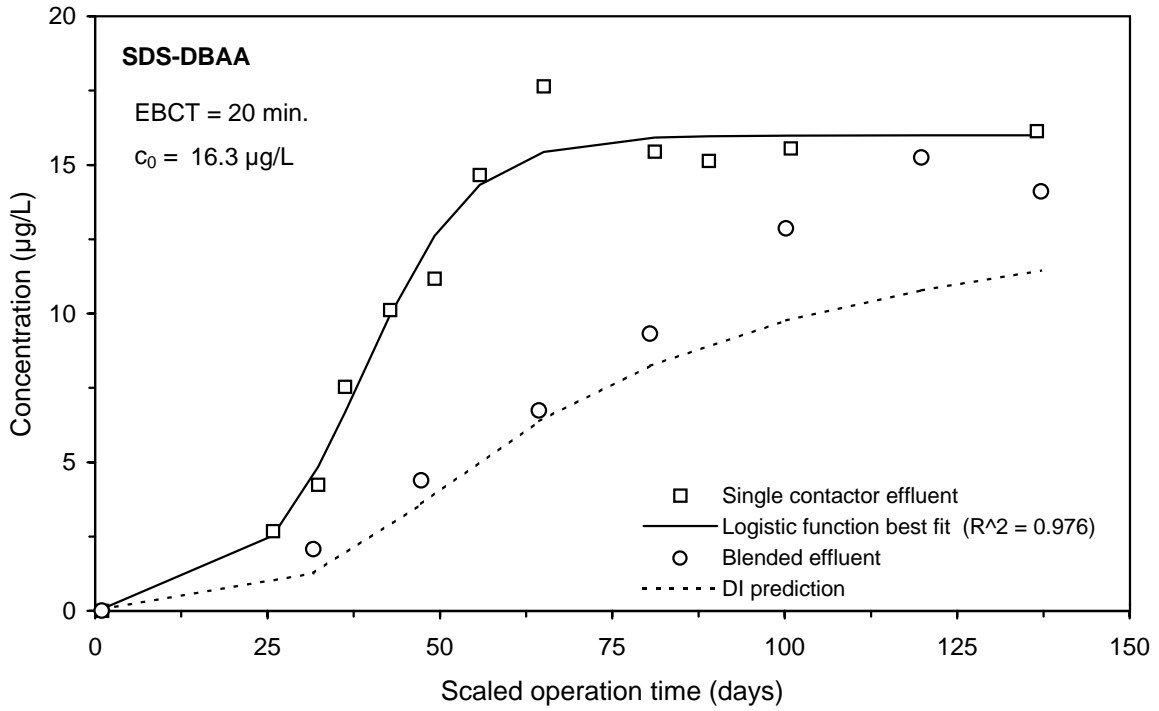


**Figure E-133 Single contactor and blended effluent SDS-DBAA breakthrough curves for Water 7**

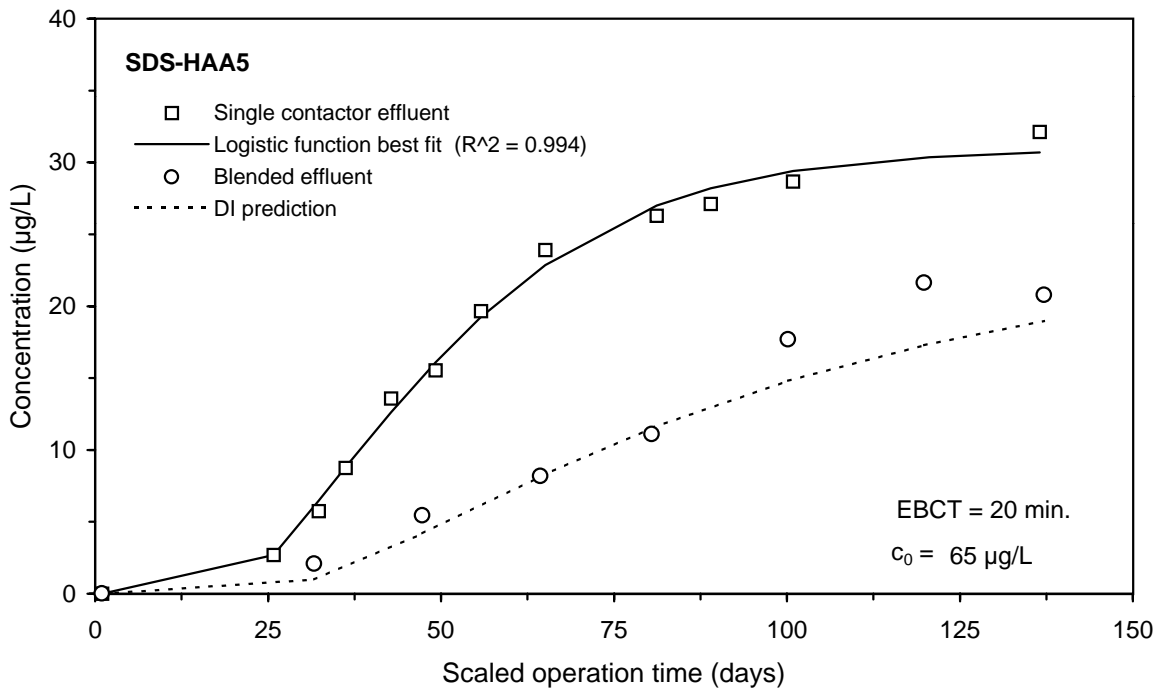


**Figure E-134 Single contactor and blended effluent SDS-HAA5 breakthrough curves for Water 7**

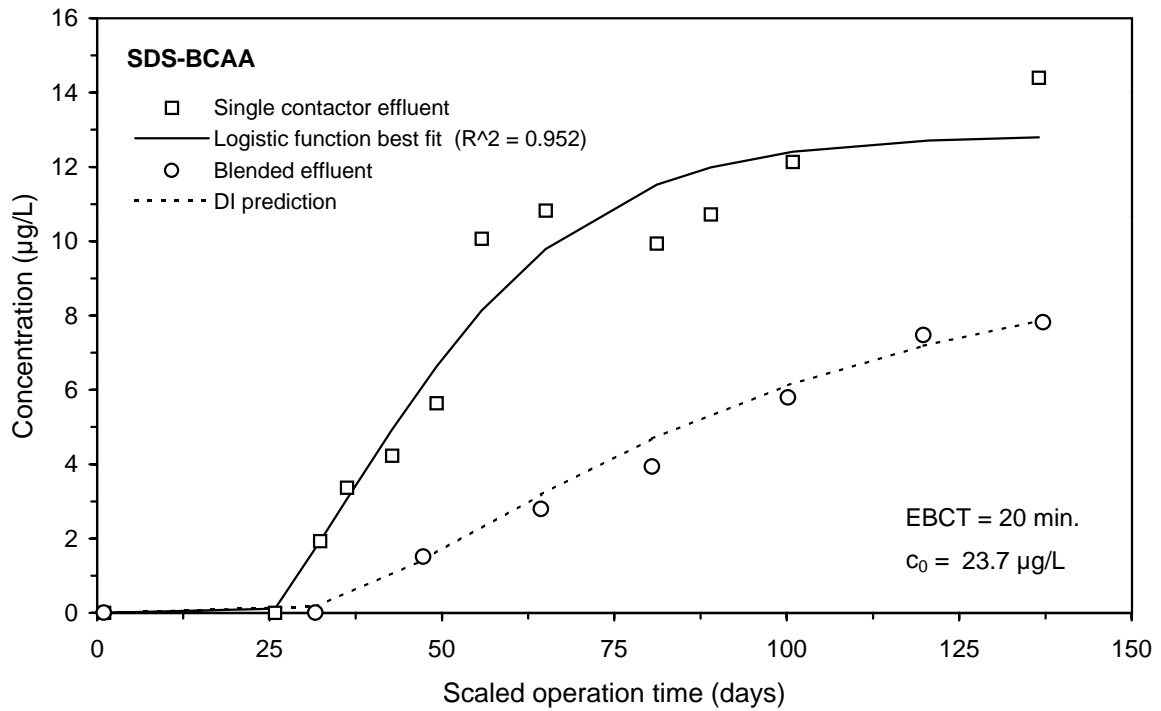


**Figure E-135 Single contactor and blended effluent SDS-BCAA breakthrough curves for Water 7**

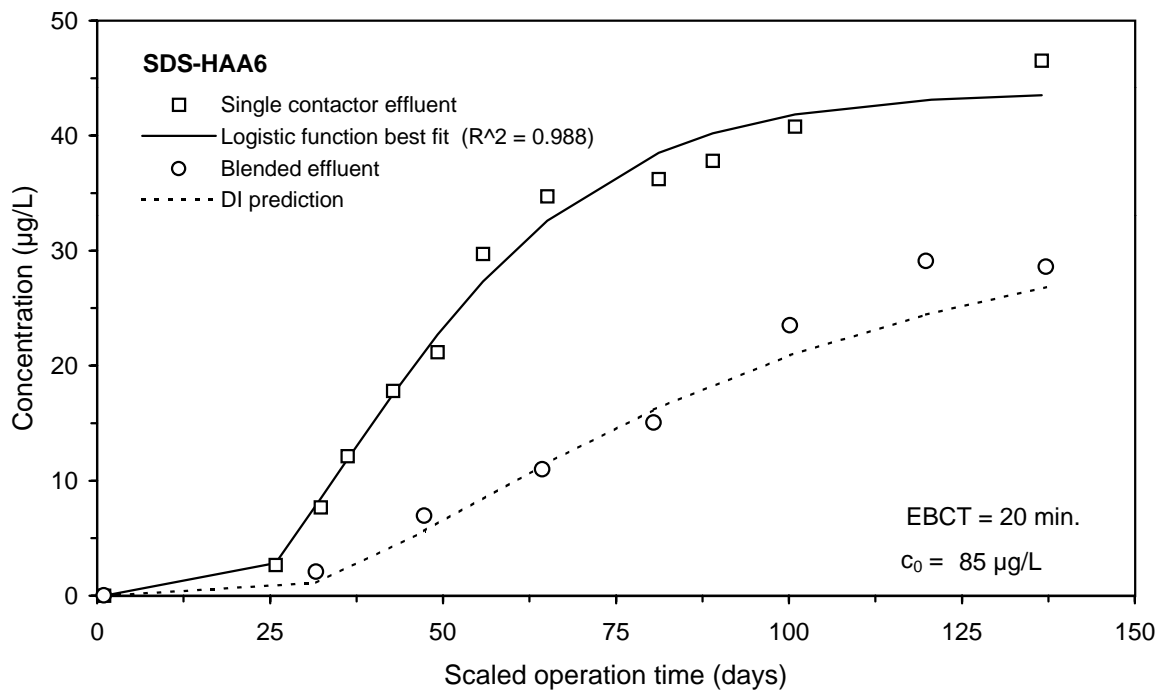


**Figure E-136 Single contactor and blended effluent SDS-HAA6 breakthrough curves for Water 7**

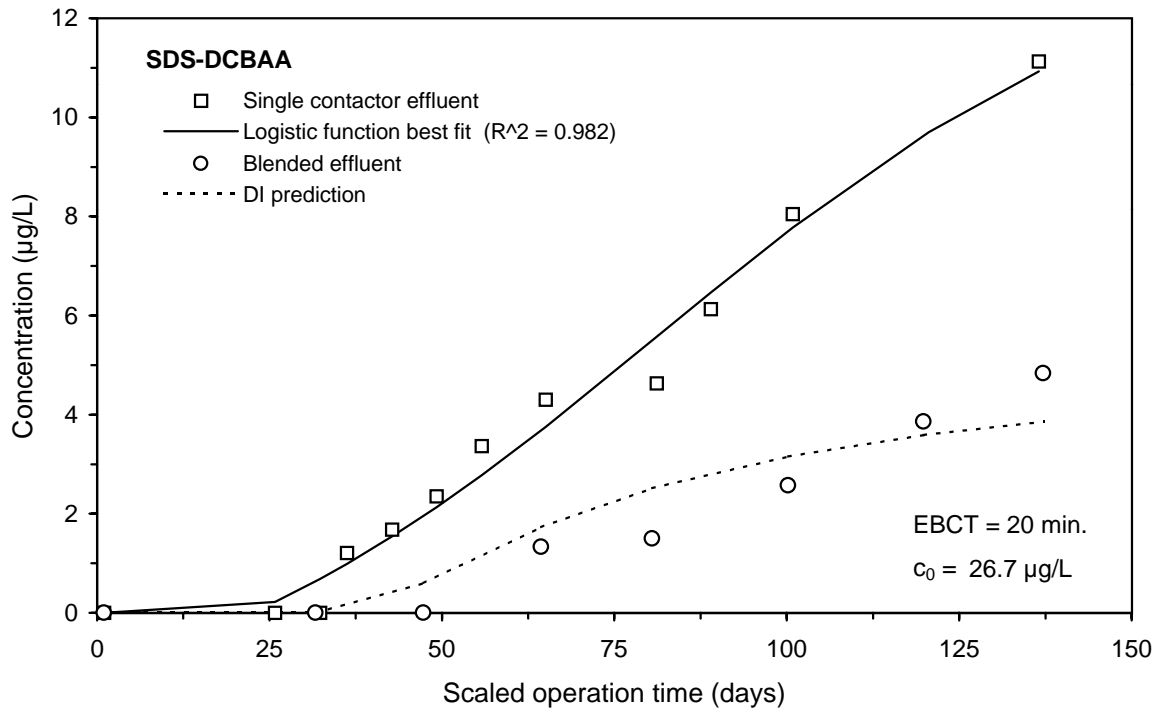


**Figure E-137 Single contactor and blended effluent SDS-DCBAA breakthrough curves for Water 7**

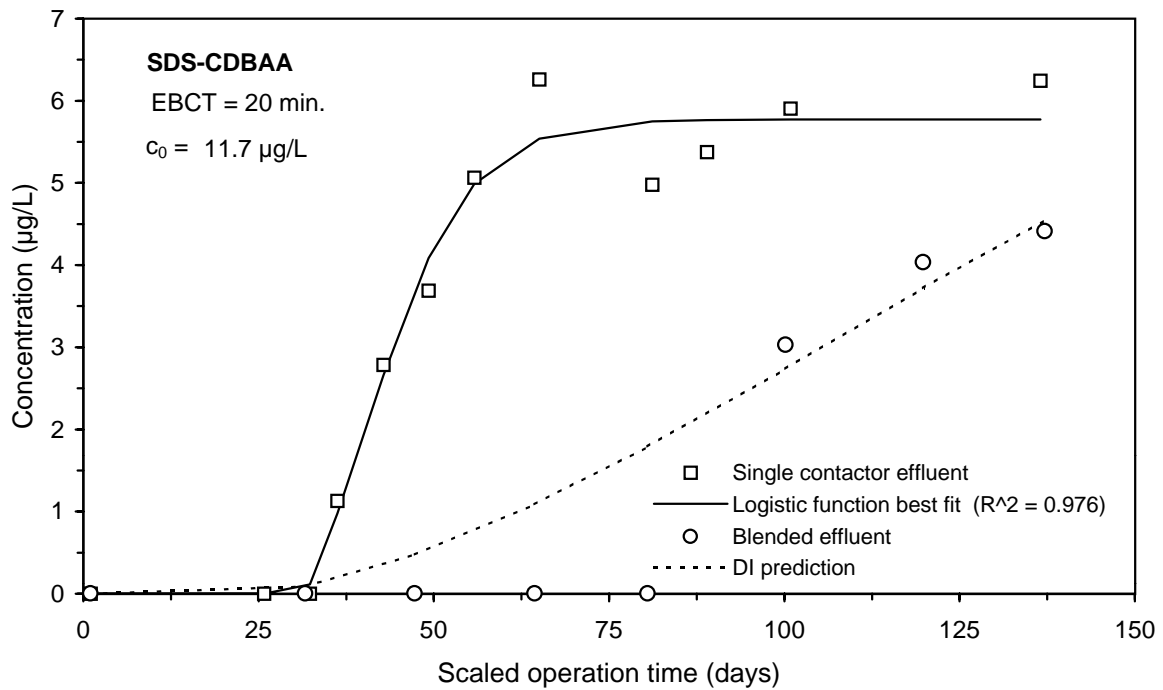


**Figure E-138 Single contactor and blended effluent SDS-CDBAA breakthrough curves for Water 7**

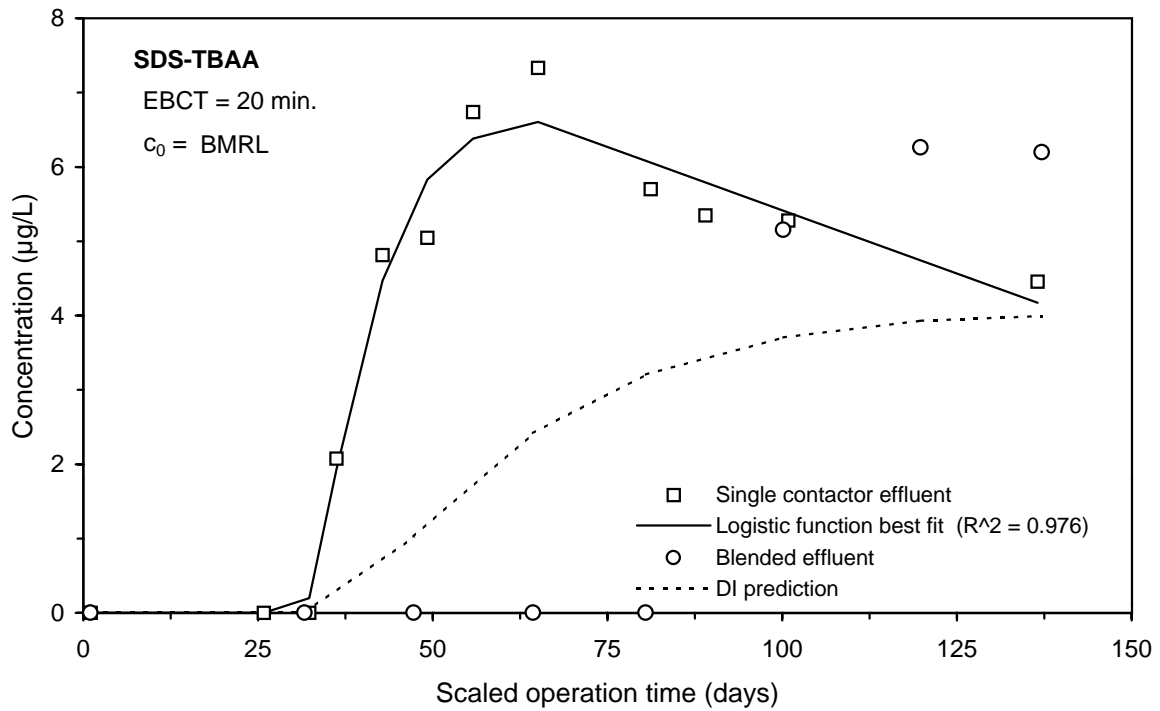


**Figure E-139 Single contactor and blended effluent SDS-TBAA breakthrough curves for Water 7**

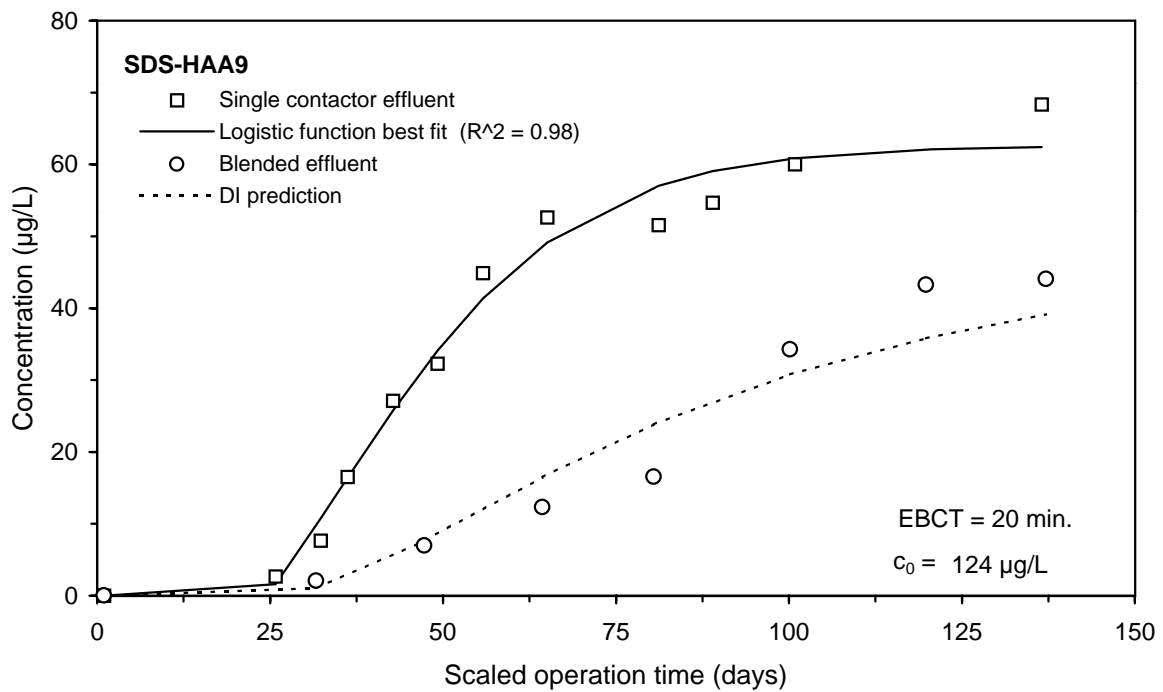


**Figure E-140 Single contactor and blended effluent SDS-HAA9 breakthrough curves for Water 7**

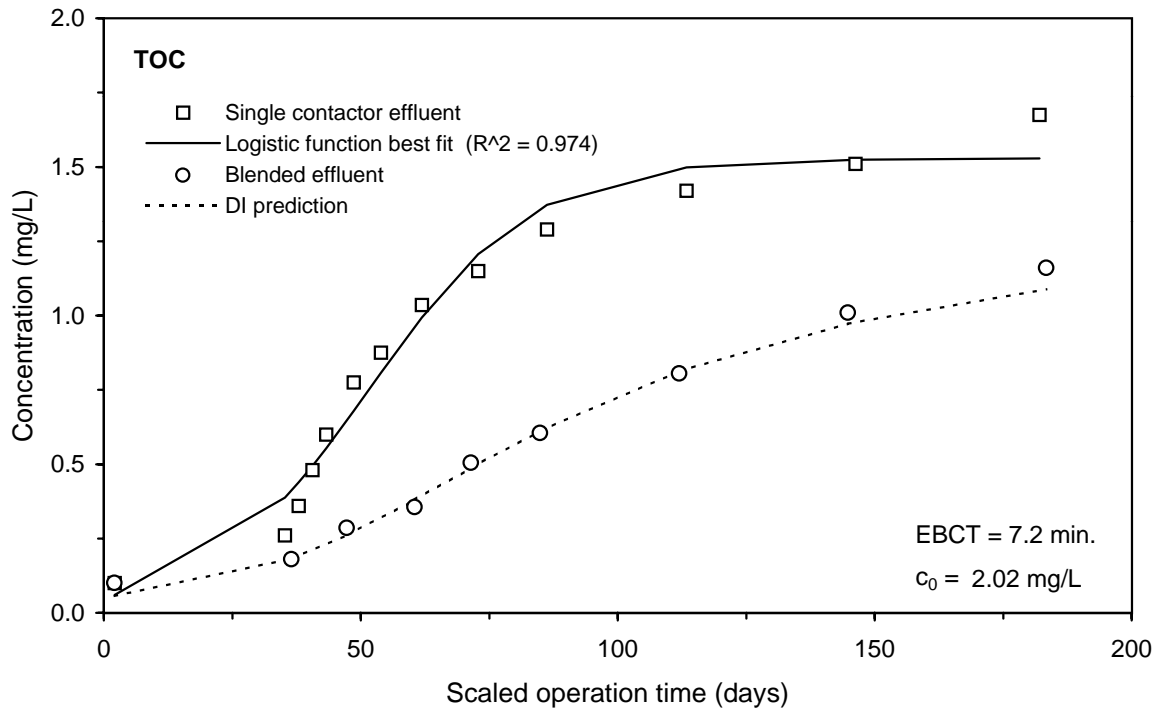


**Figure E-141 Single contactor and blended effluent TOC breakthrough curves for Water 8**

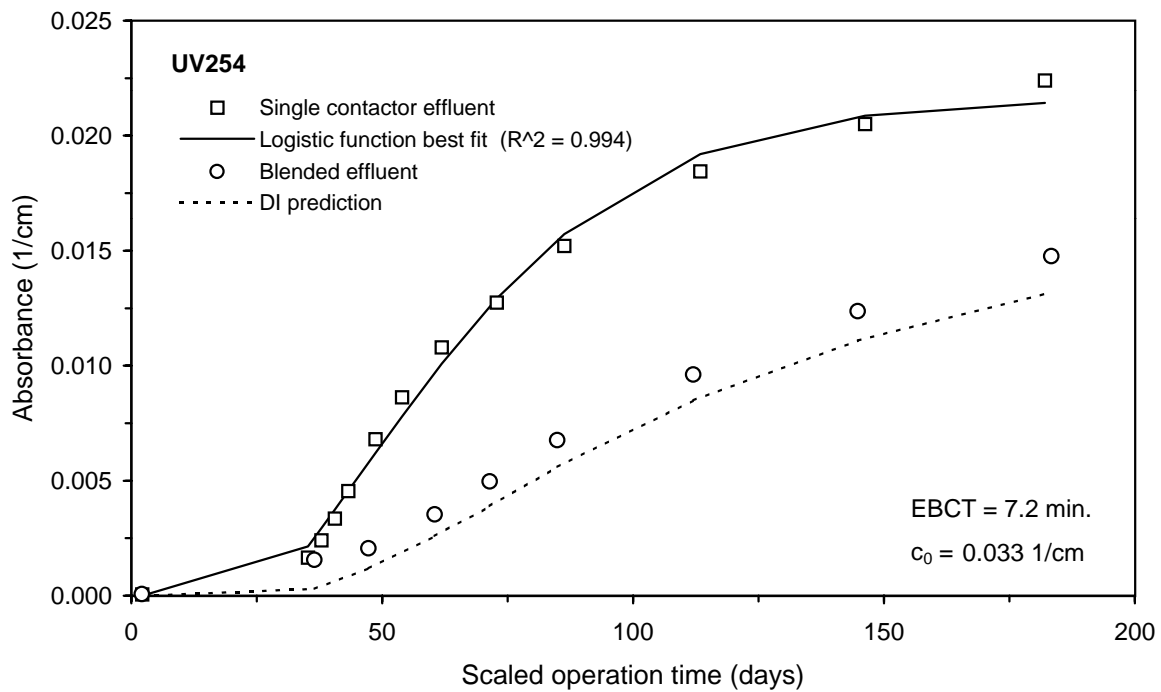


**Figure E-142 Single contactor and blended effluent UV254 breakthrough curves for Water 8**

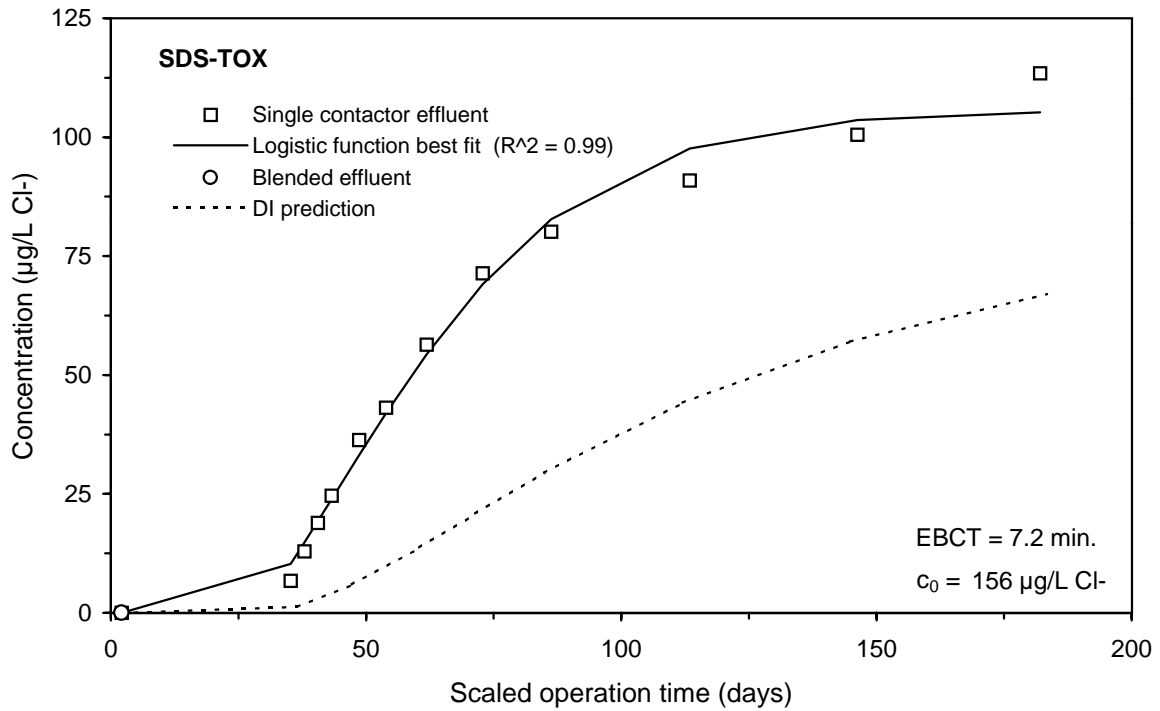


**Figure E-143 Single contactor and blended effluent SDS-TOX breakthrough curves for Water 8**

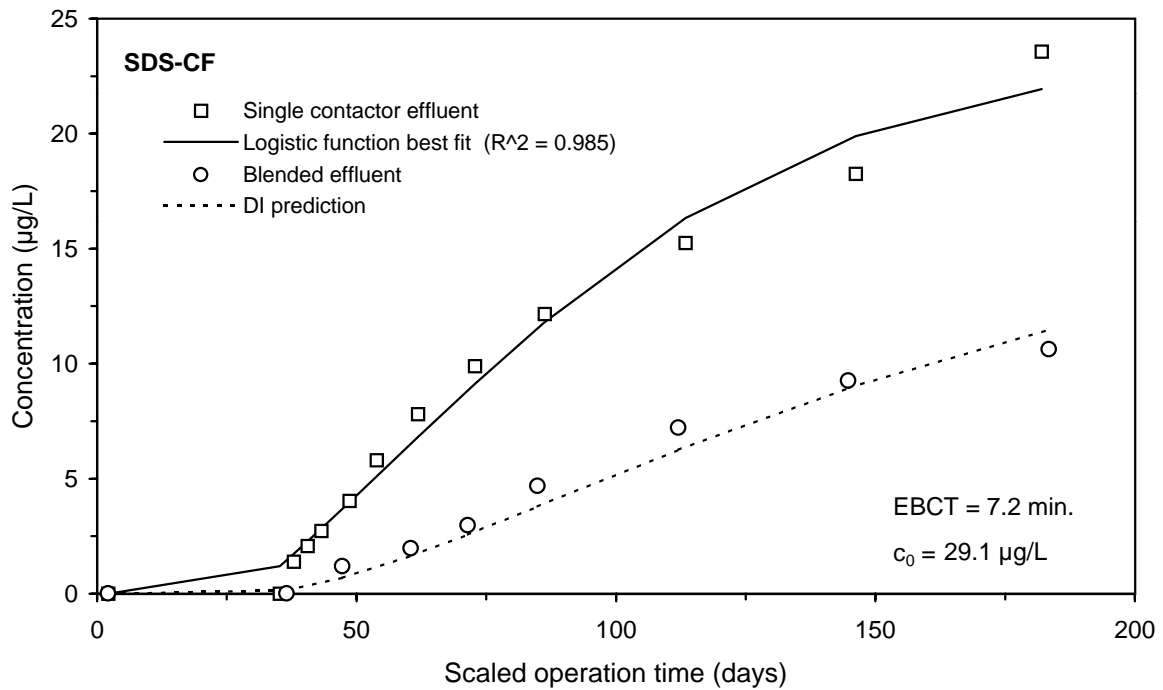


**Figure E-144 Single contactor and blended effluent SDS-CF breakthrough curves for Water 8**

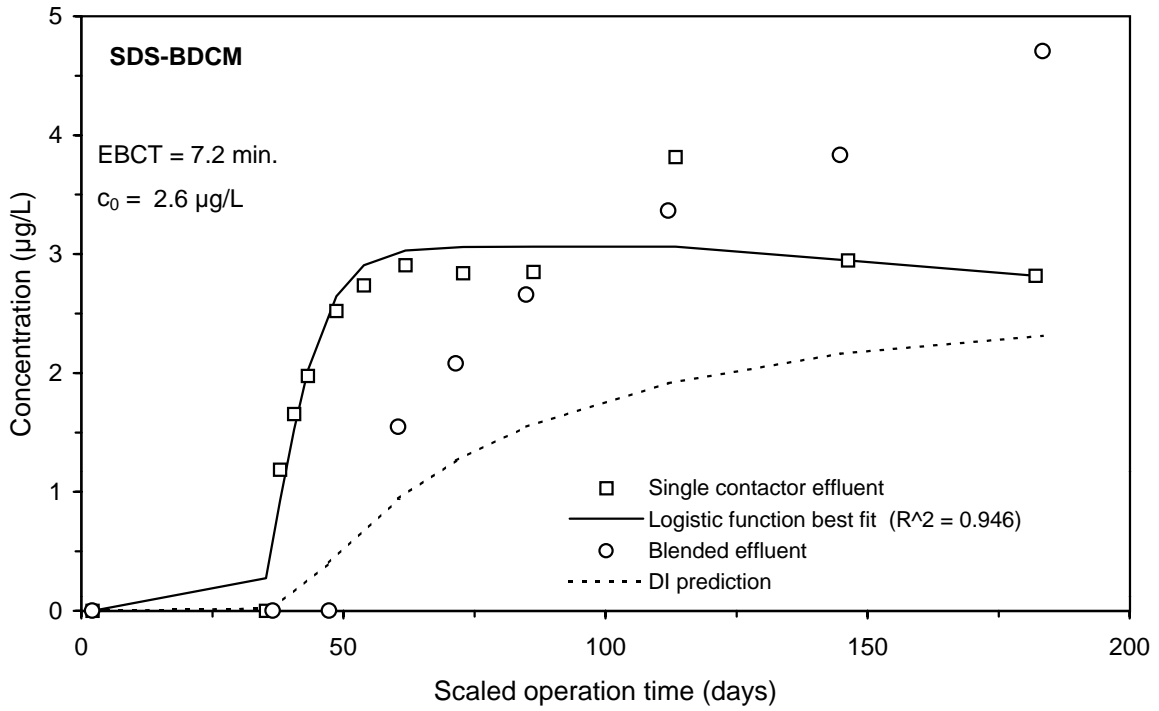


**Figure E-145 Single contactor and blended effluent SDS-BDCM breakthrough curves for Water 8**

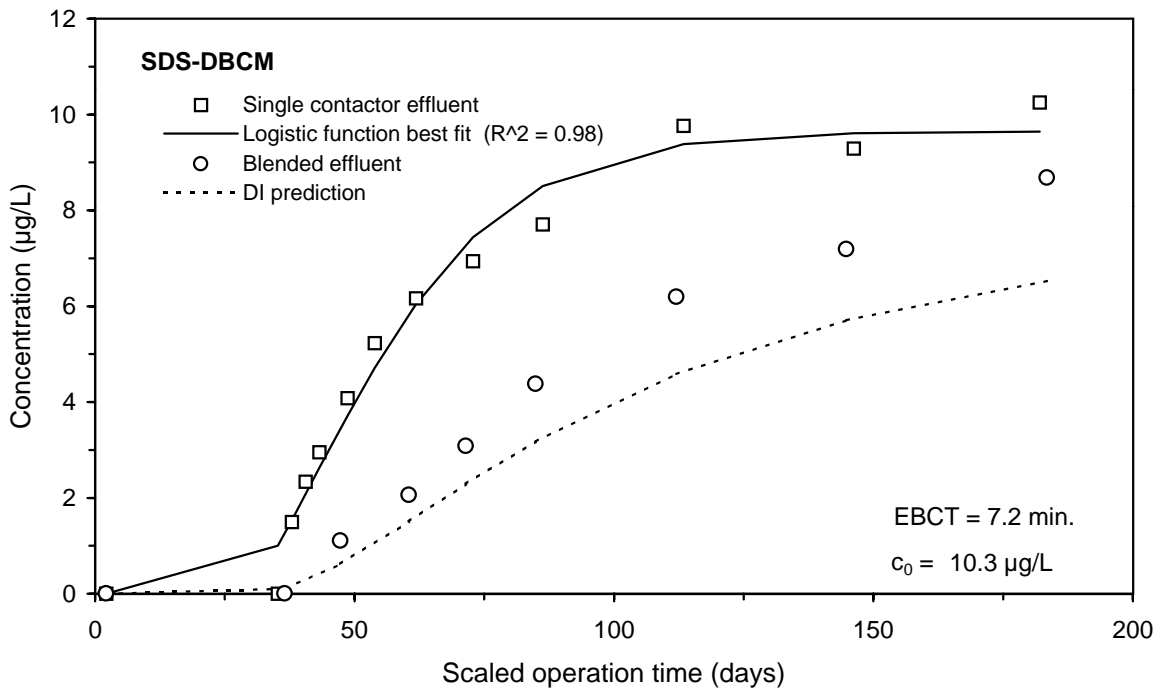


**Figure E-146 Single contactor and blended effluent SDS-DBCМ breakthrough curves for Water 8**

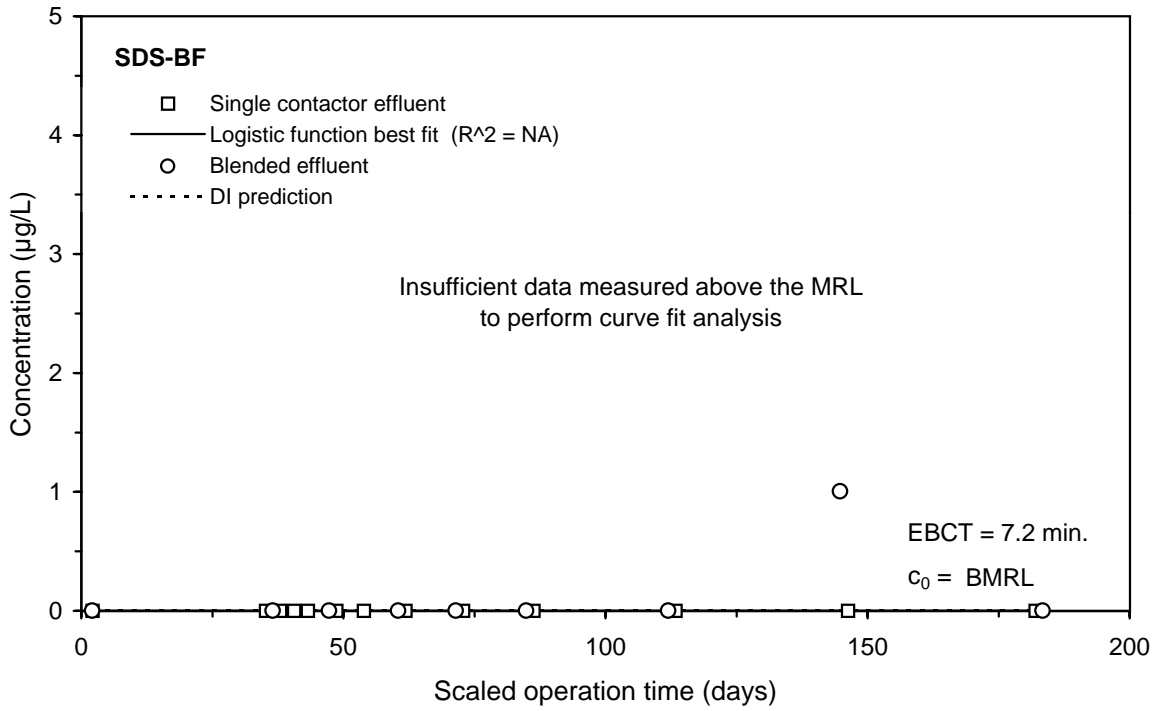


**Figure E-147 Single contactor and blended effluent SDS-BF breakthrough curves for Water 8**

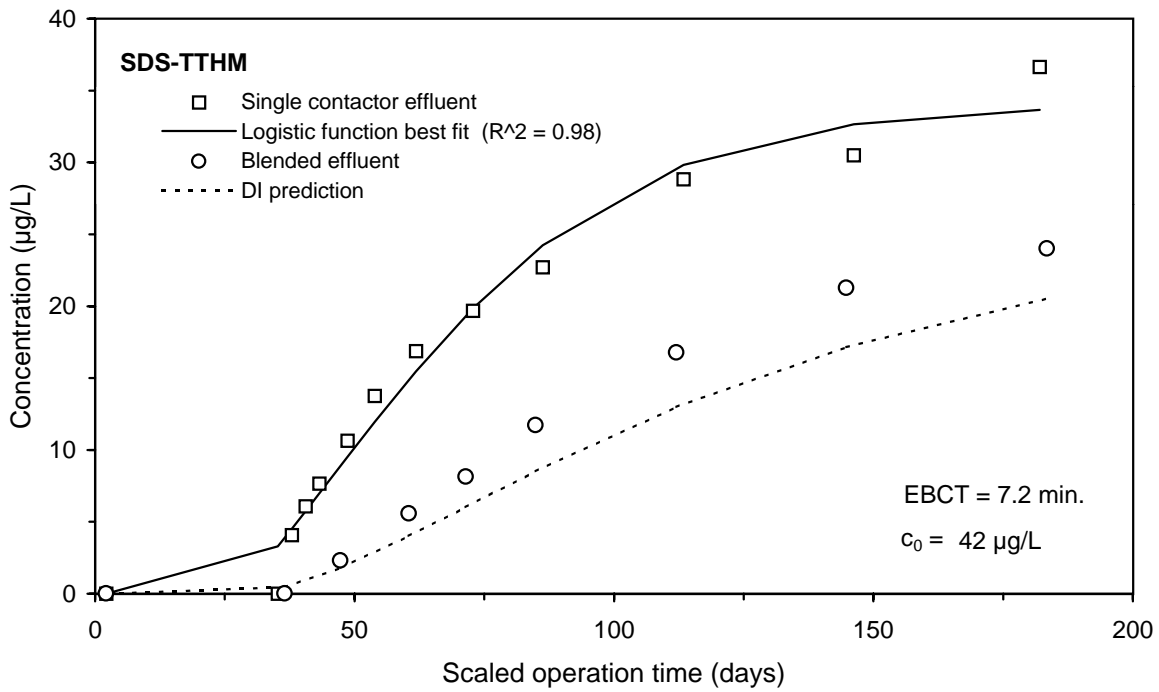


**Figure E-148 Single contactor and blended effluent SDS-TTHM breakthrough curves for Water 8**

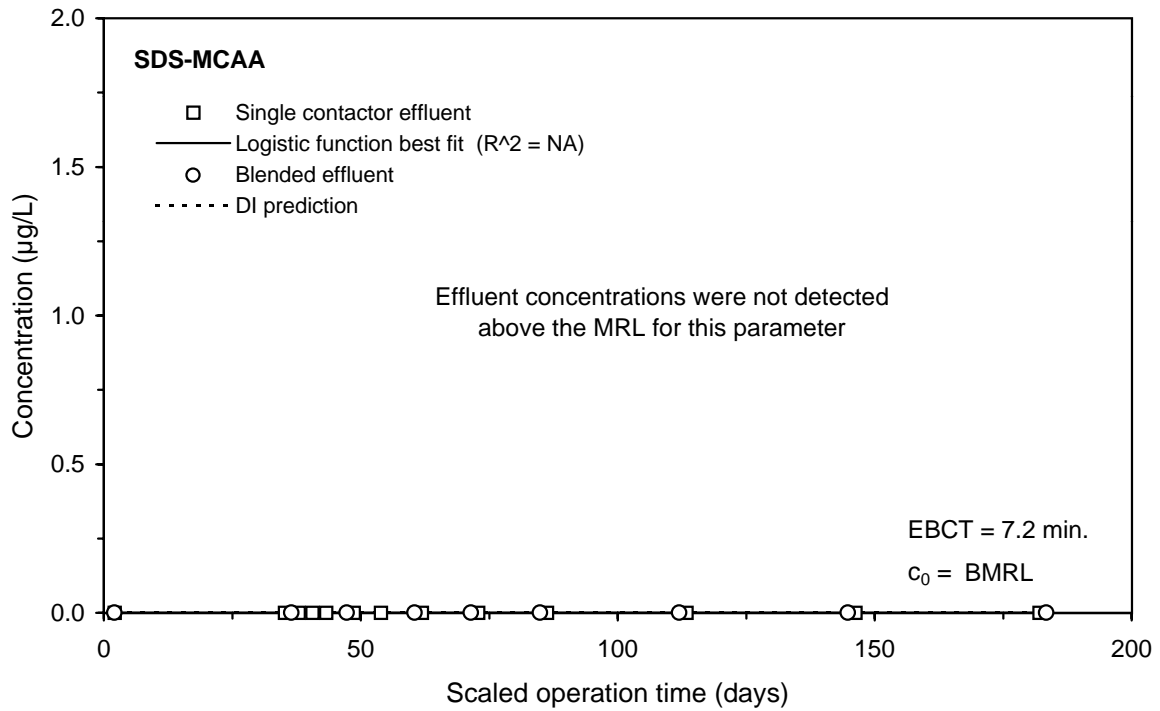


**Figure E-149 Single contactor and blended effluent SDS-MCAA breakthrough curves for Water 8**

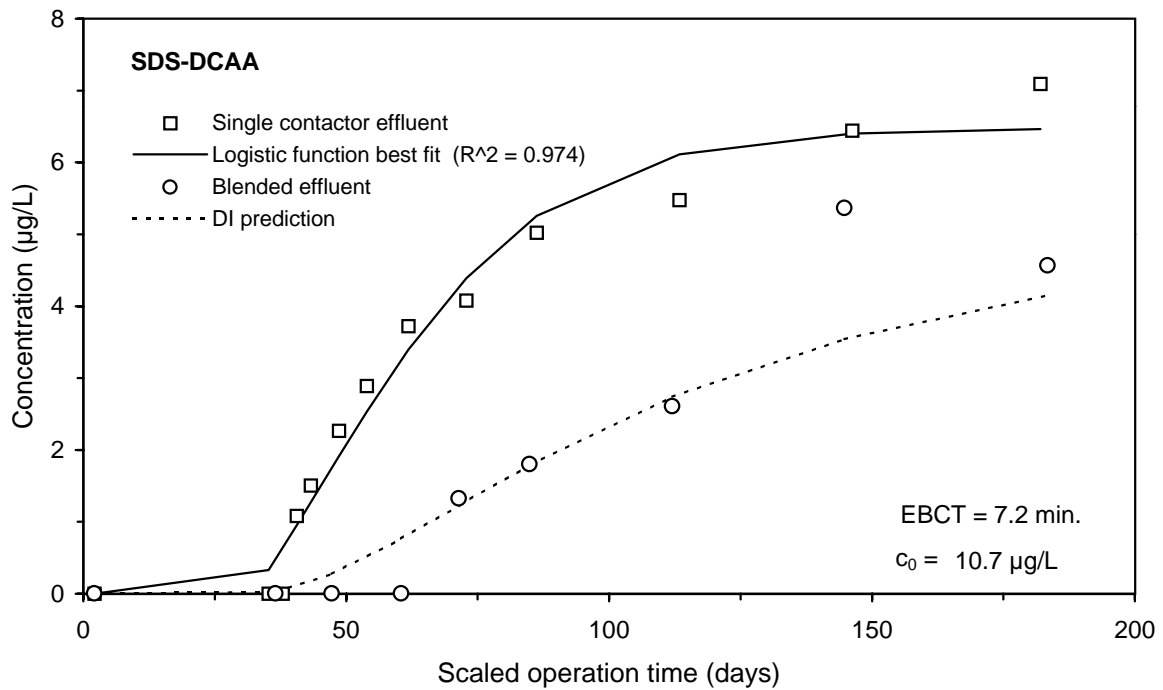


**Figure E-150 Single contactor and blended effluent SDS-DCAA breakthrough curves for Water 8**

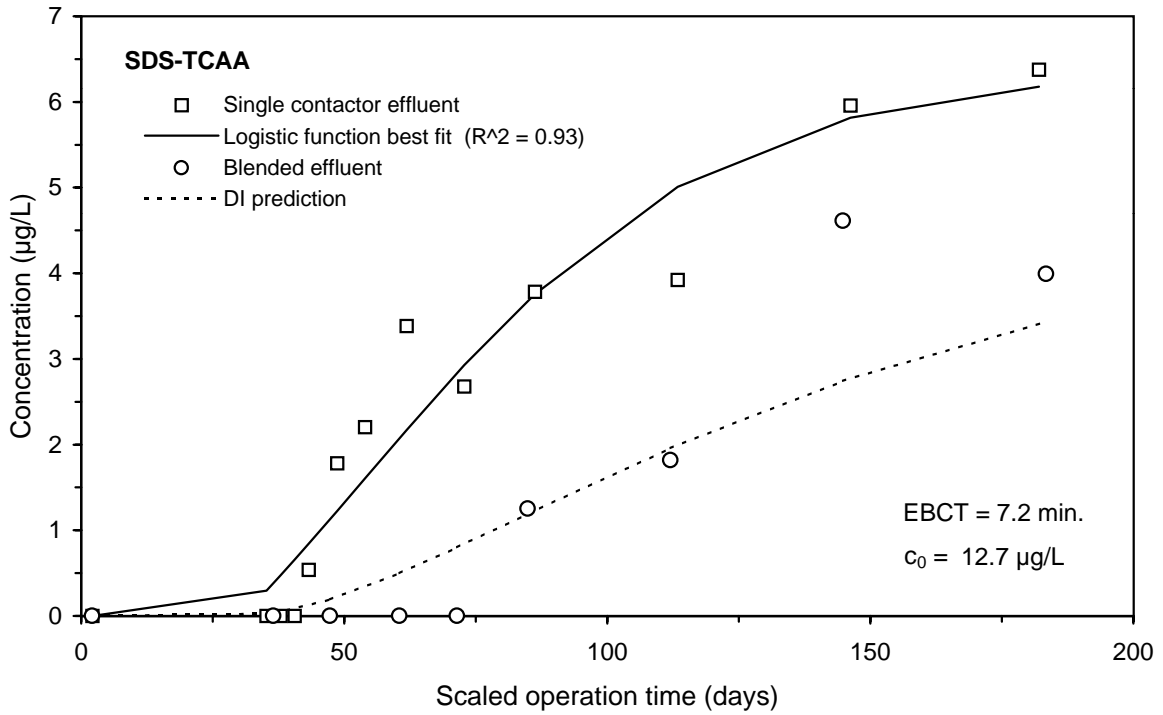


**Figure E-151 Single contactor and blended effluent SDS-TCAA breakthrough curves for Water 8**

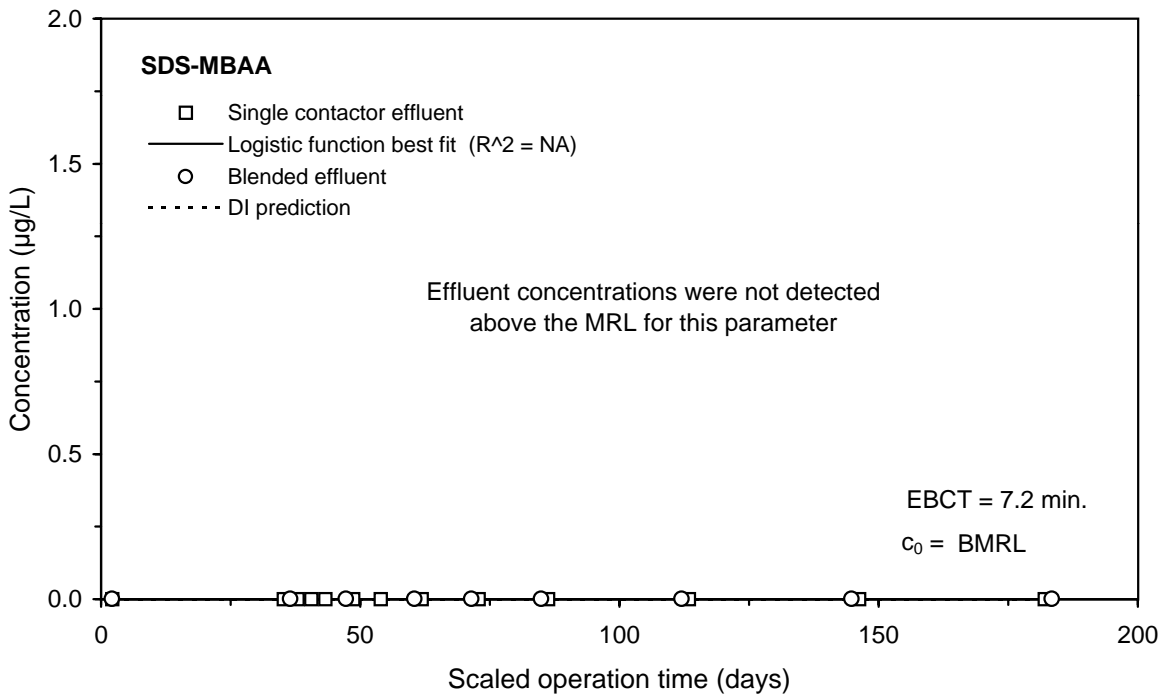


**Figure E-152 Single contactor and blended effluent SDS-MBAA breakthrough curves for Water 8**

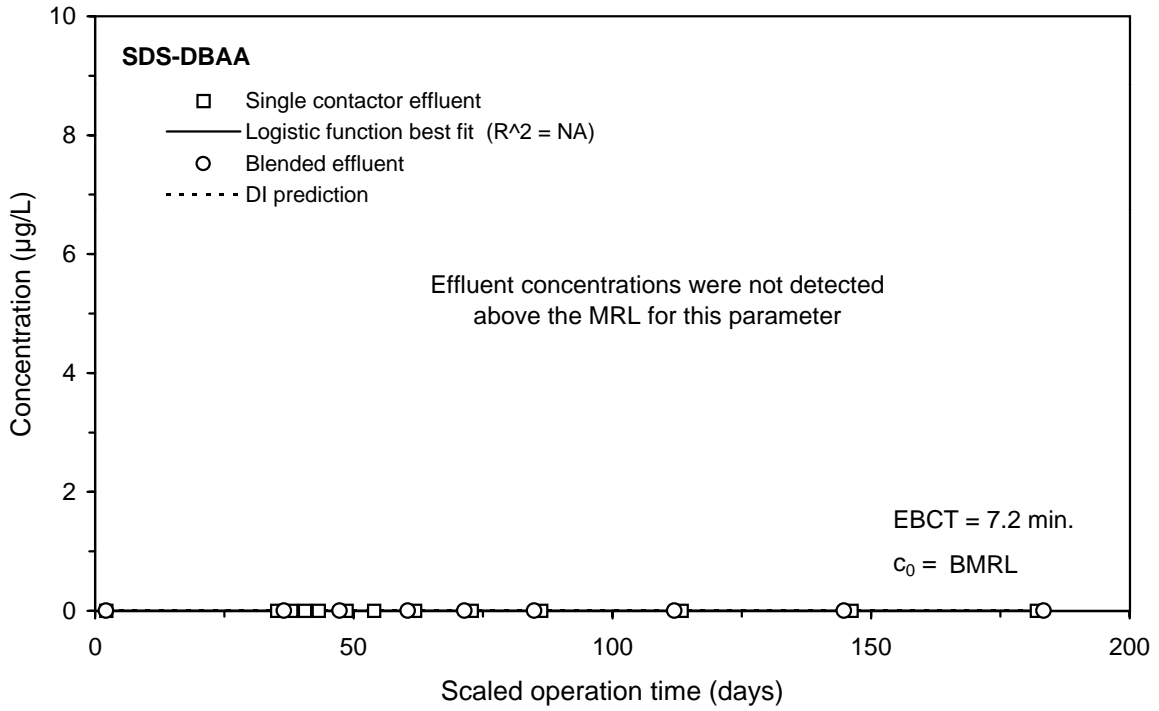


**Figure E-153 Single contactor and blended effluent SDS-DBAA breakthrough curves for Water 8**

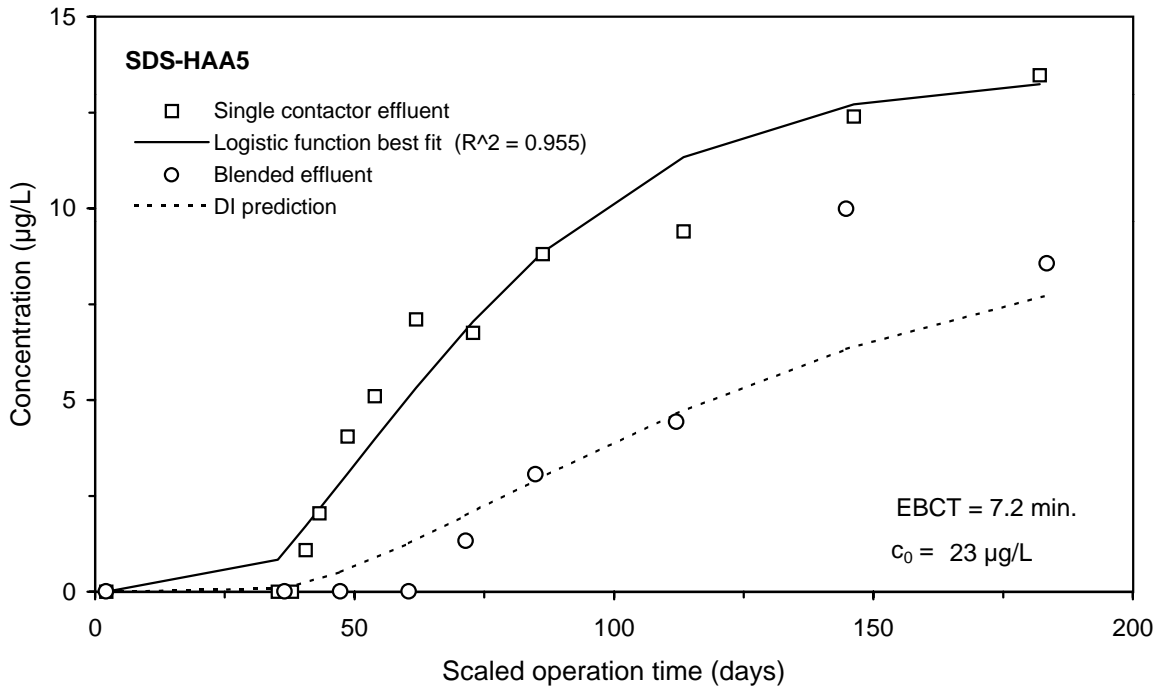


**Figure E-154 Single contactor and blended effluent SDS-HAA5 breakthrough curves for Water 8**

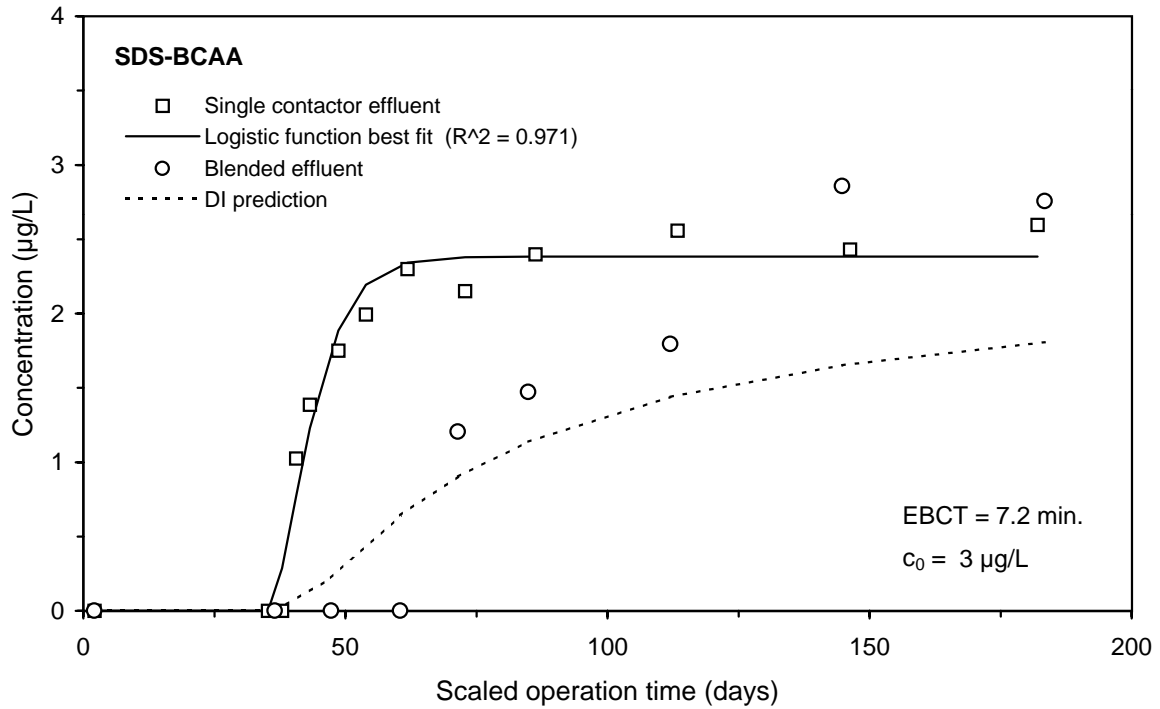


**Figure E-155 Single contactor and blended effluent SDS-BCAA breakthrough curves for Water 8**

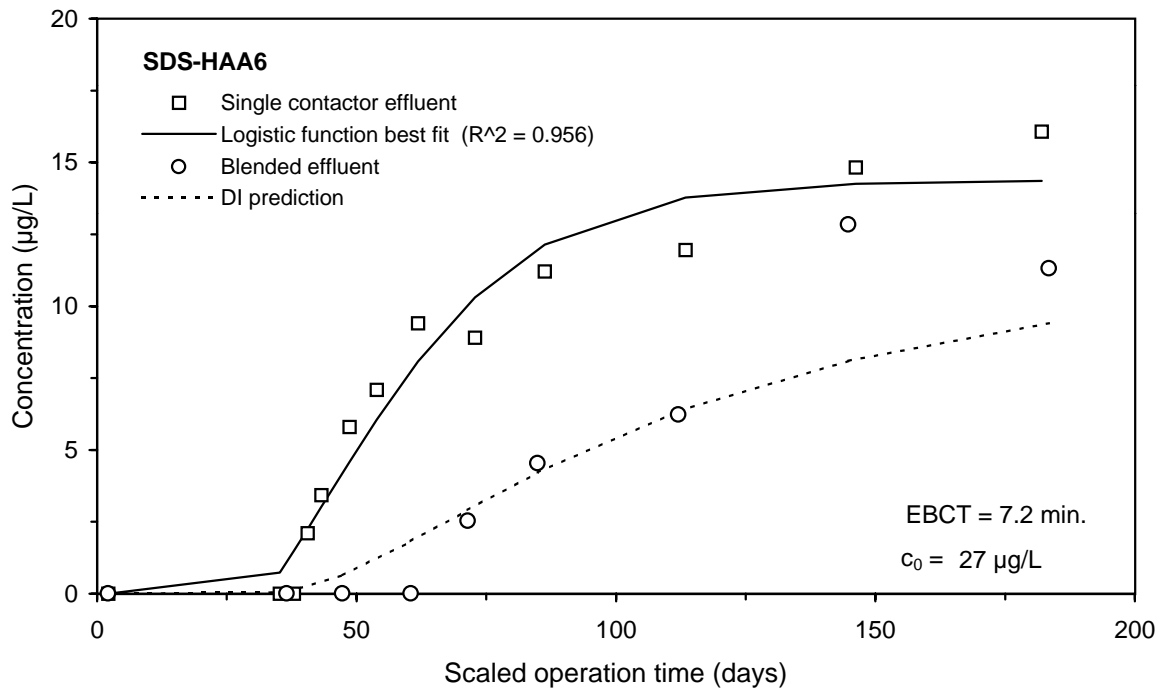


**Figure E-156 Single contactor and blended effluent SDS-HAA6 breakthrough curves for Water 8**

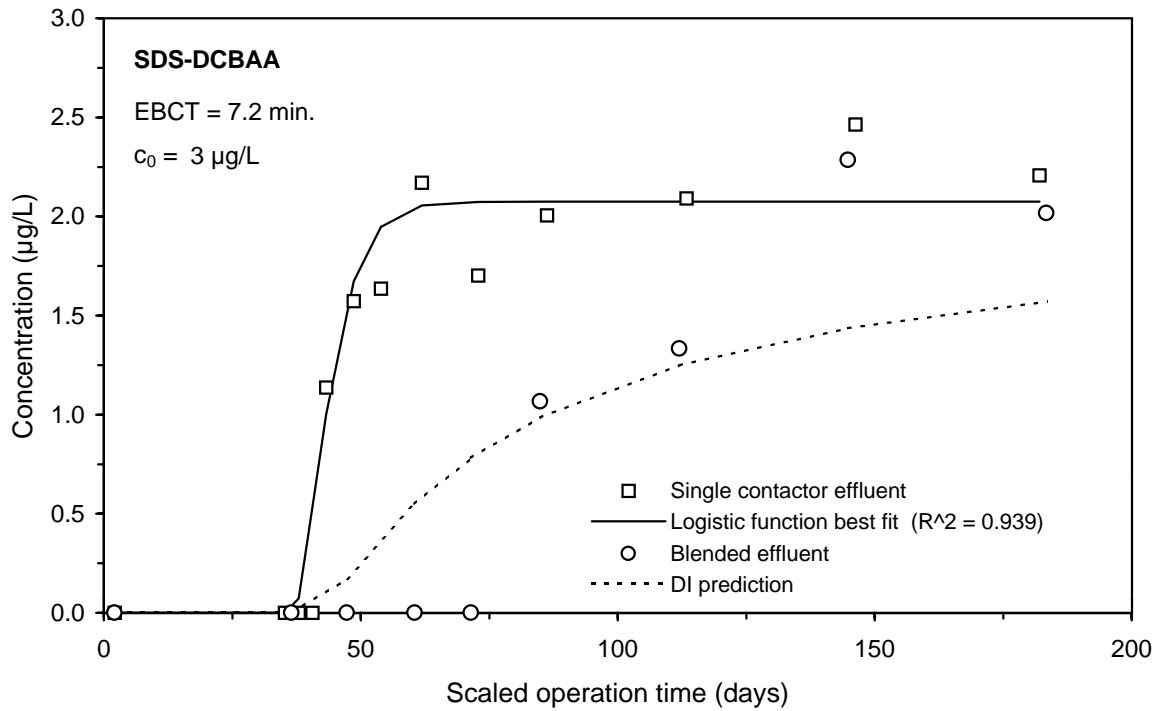


**Figure E-157 Single contactor and blended effluent SDS-DCBAA breakthrough curves for Water 8**

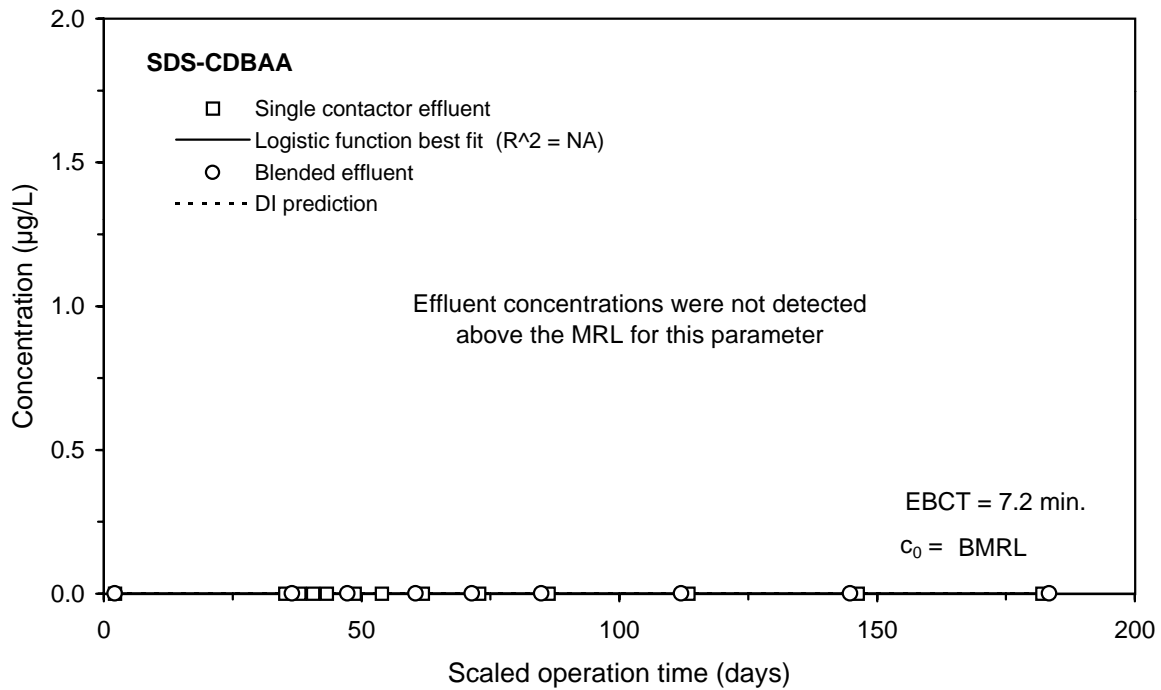


**Figure E-158 Single contactor and blended effluent SDS-CDBAA breakthrough curves for Water 8**

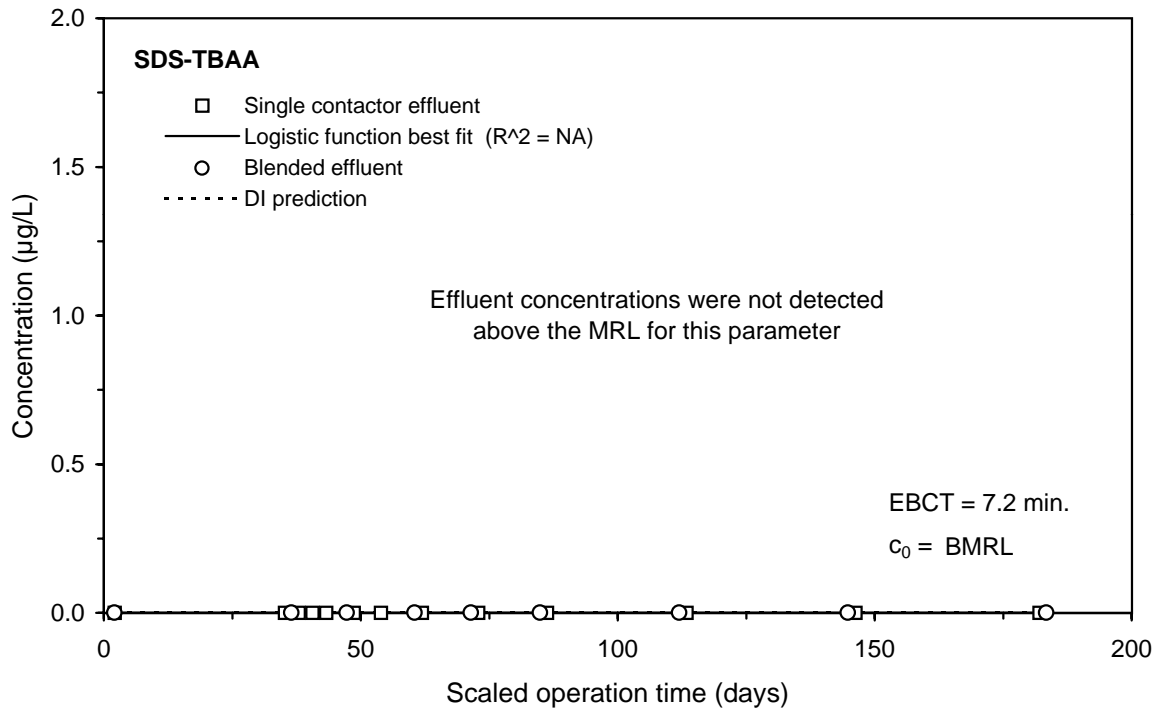


**Figure E-159 Single contactor and blended effluent SDS-TBAA breakthrough curves for Water 8**

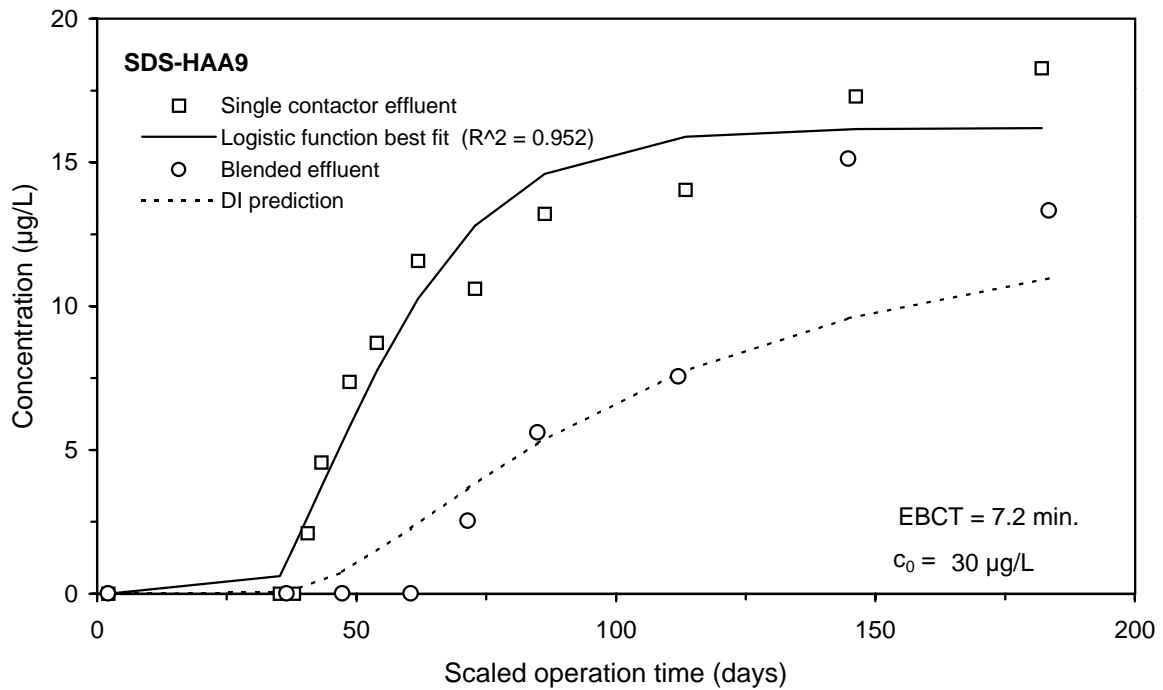


**Figure E-160 Single contactor and blended effluent SDS-HAA9 breakthrough curves for Water 8**

This page intentionally left blank.

---

**Appendix F: Comparison of SCA Method to DI Approach for Integral Breakthrough Curve Prediction**

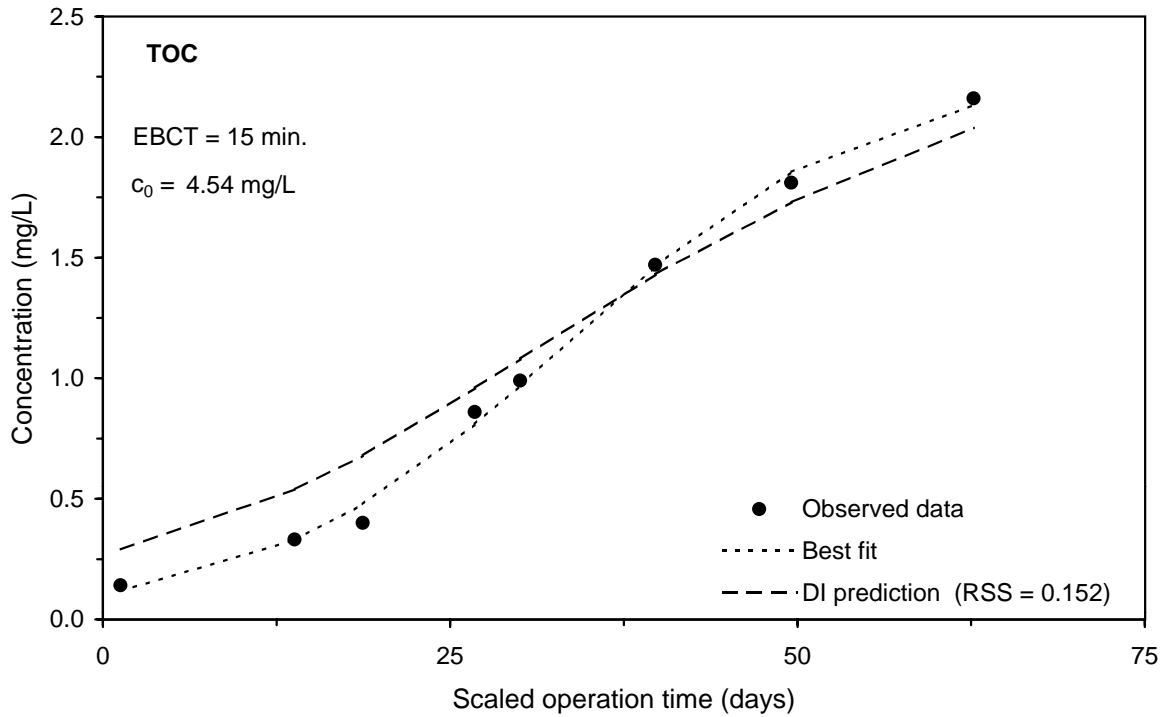


**Figure F-1 DI method prediction of the TOC integral breakthrough curve for Water 1**

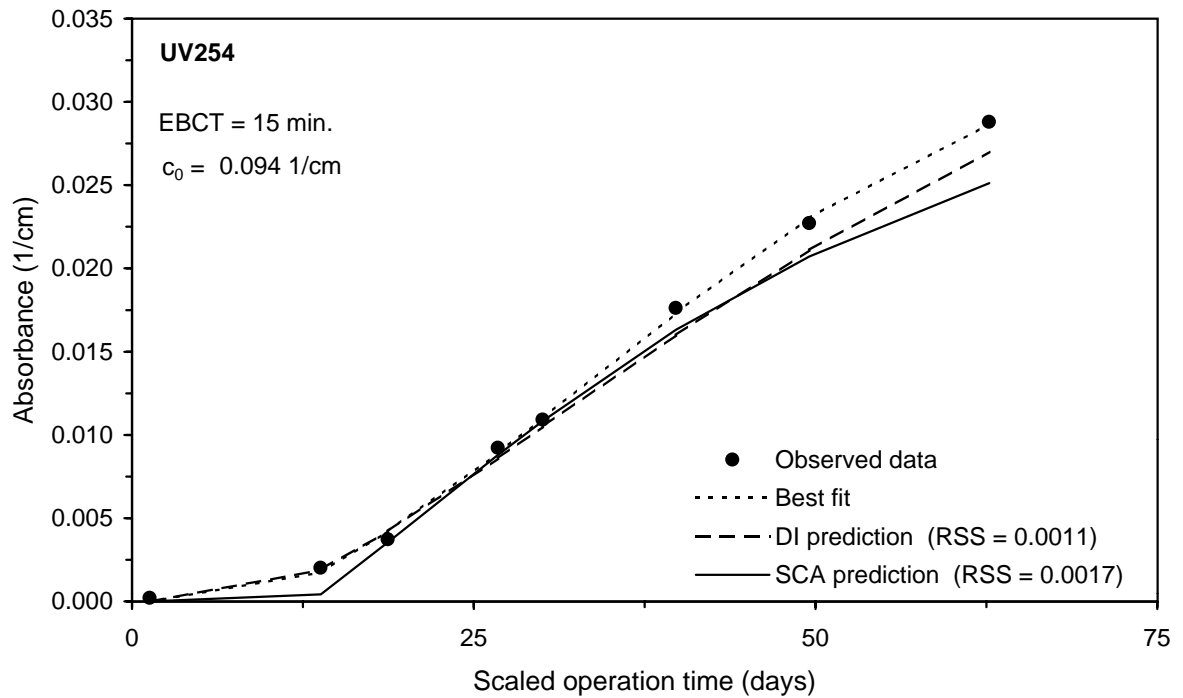


**Figure F-2 Comparison of DI and SCA methods for predicting the UV254 integral breakthrough curve for Water 1**

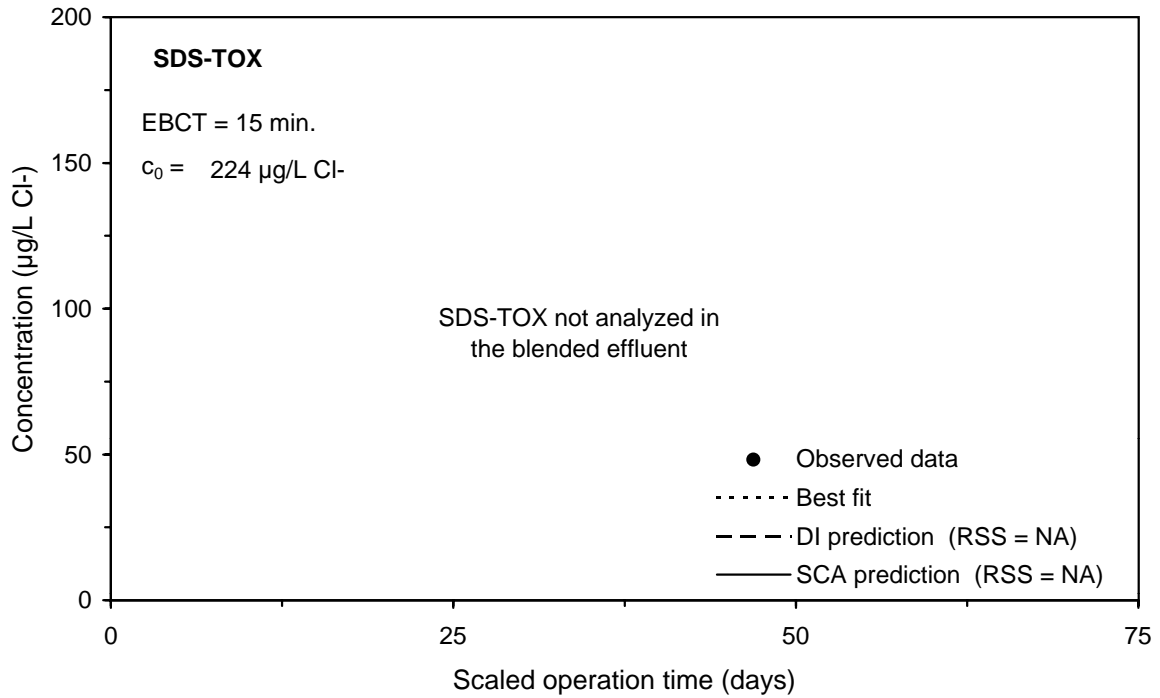


**Figure F-3 Comparison of DI and SCA methods for predicting the SDS-TOX integral breakthrough curve for Water 1**

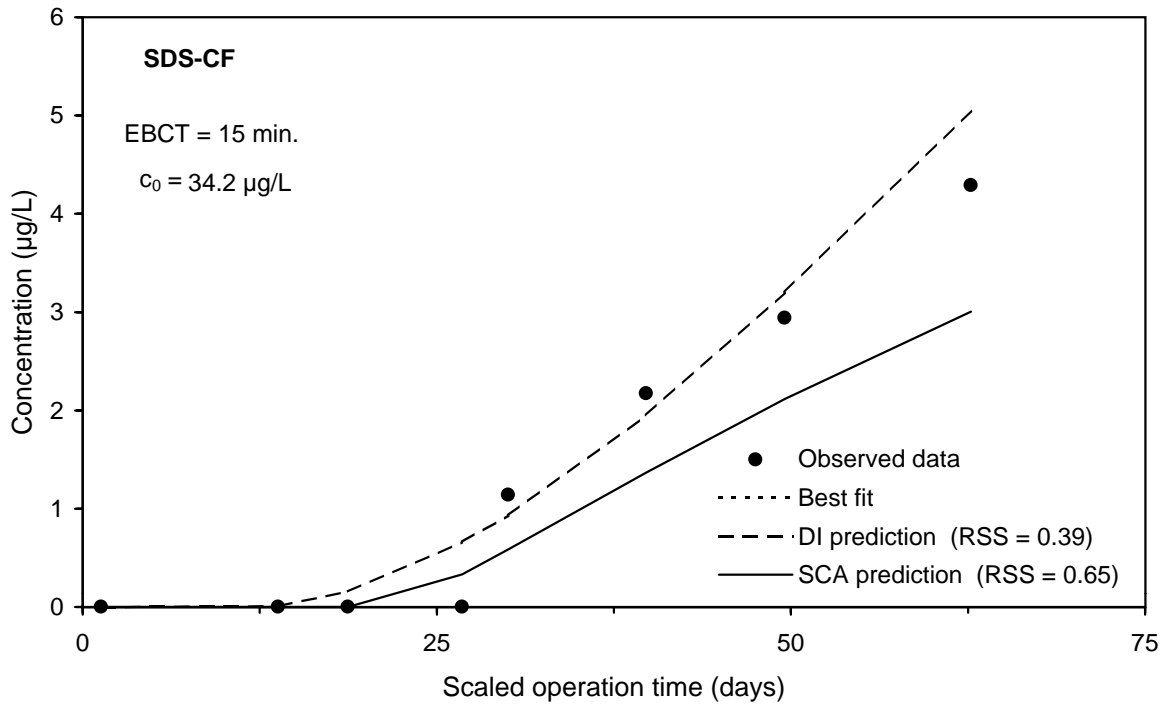


**Figure F-4 Comparison of DI and SCA methods for predicting the SDS-CF integral breakthrough curve for Water 1**

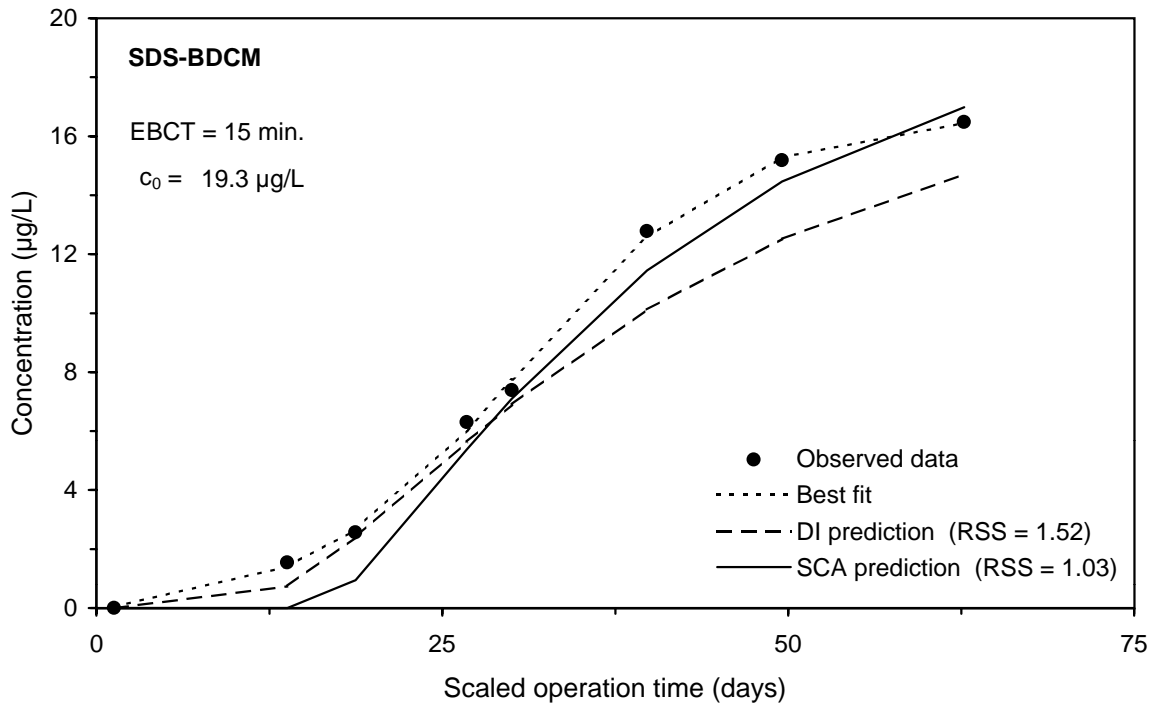


**Figure F-5 Comparison of DI and SCA methods for predicting the SDS-BDCM integral breakthrough curve for Water 1**

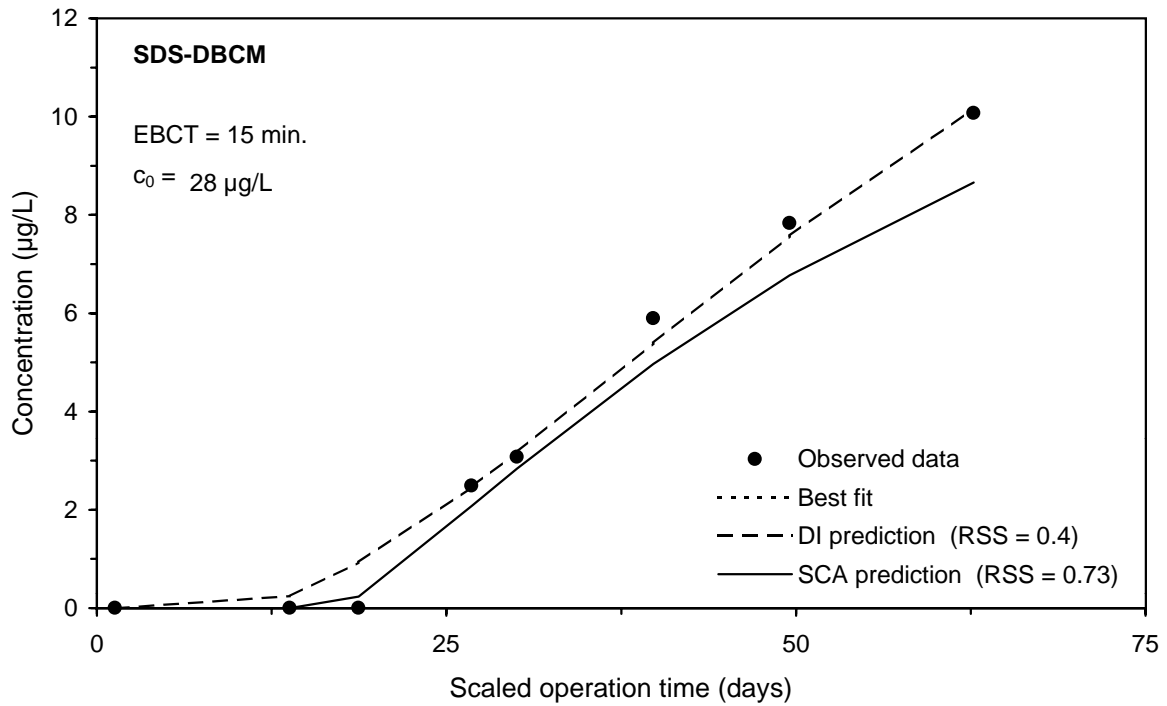


**Figure F-6 Comparison of DI and SCA methods for predicting the SDS-DBCm integral breakthrough curve for Water 1**

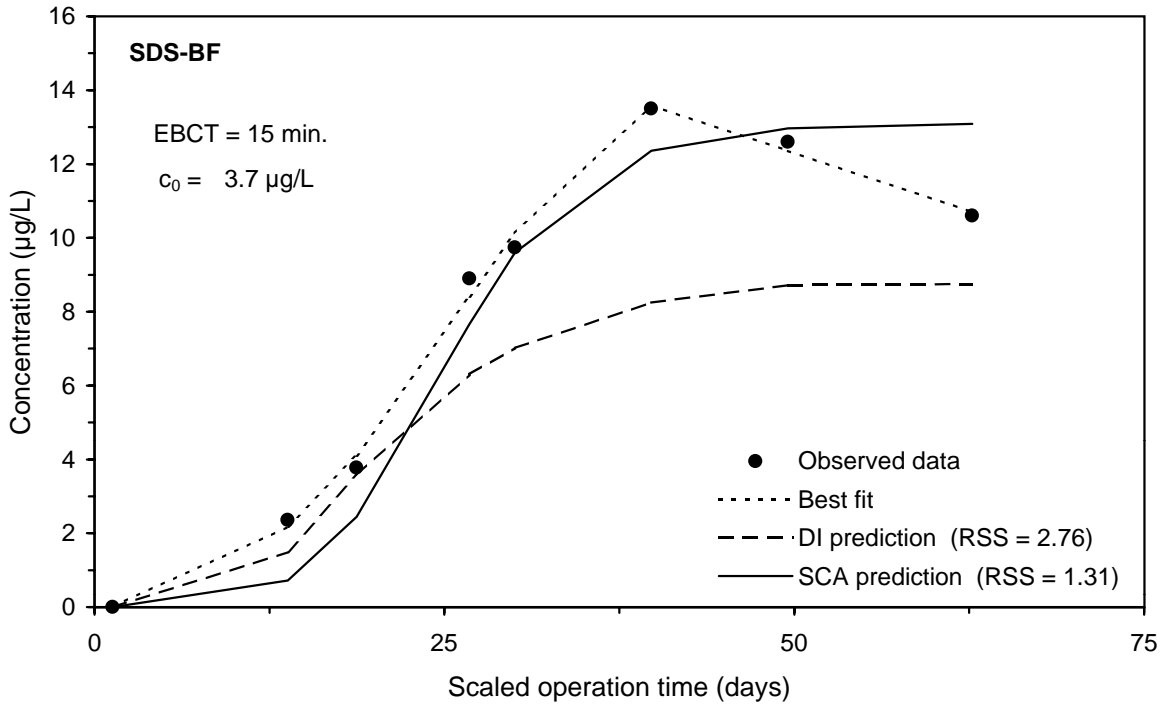


**Figure F-7 Comparison of DI and SCA methods for predicting the SDS-BF integral breakthrough curve for Water 1**

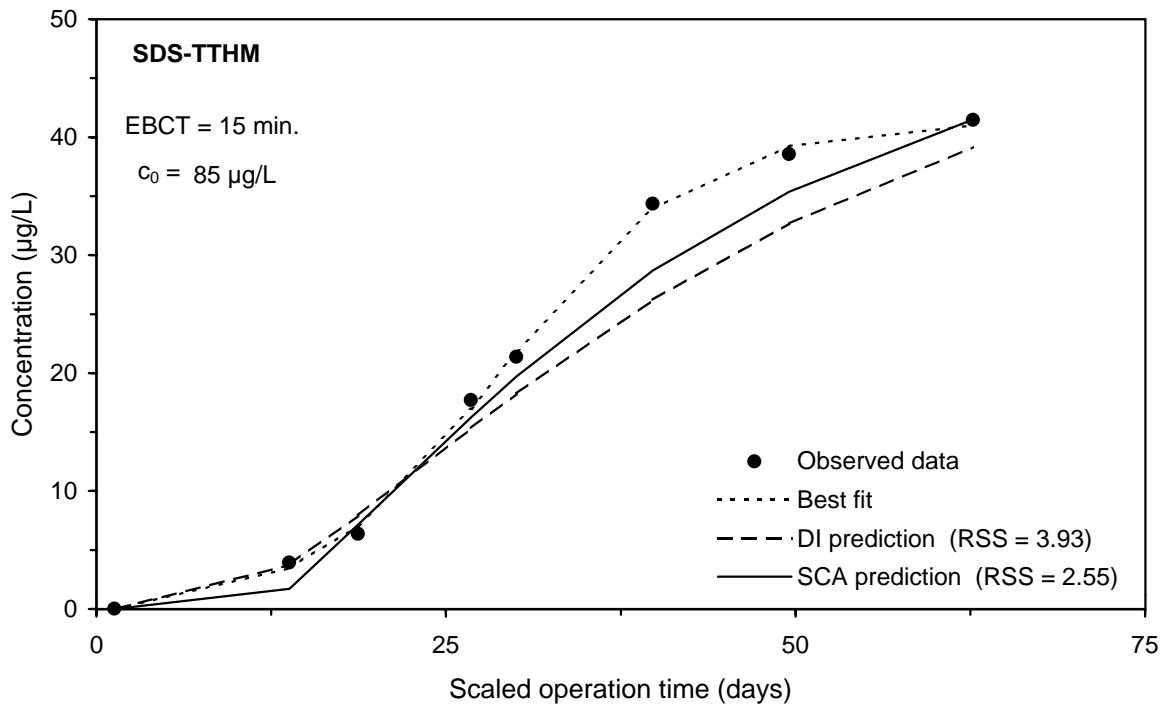


**Figure F-8 Comparison of DI and SCA methods for predicting the SDS-TTHM integral breakthrough curve for Water 1**

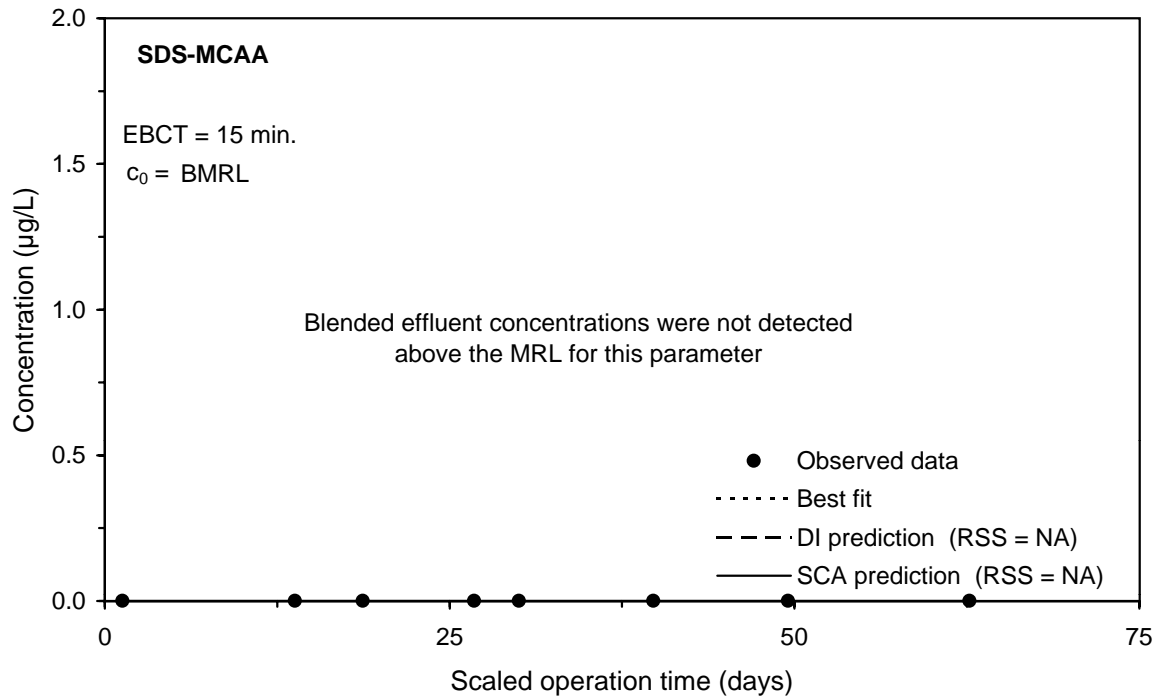


**Figure F-9 Comparison of DI and SCA methods for predicting the SDS-MCAA integral breakthrough curve for Water 1**

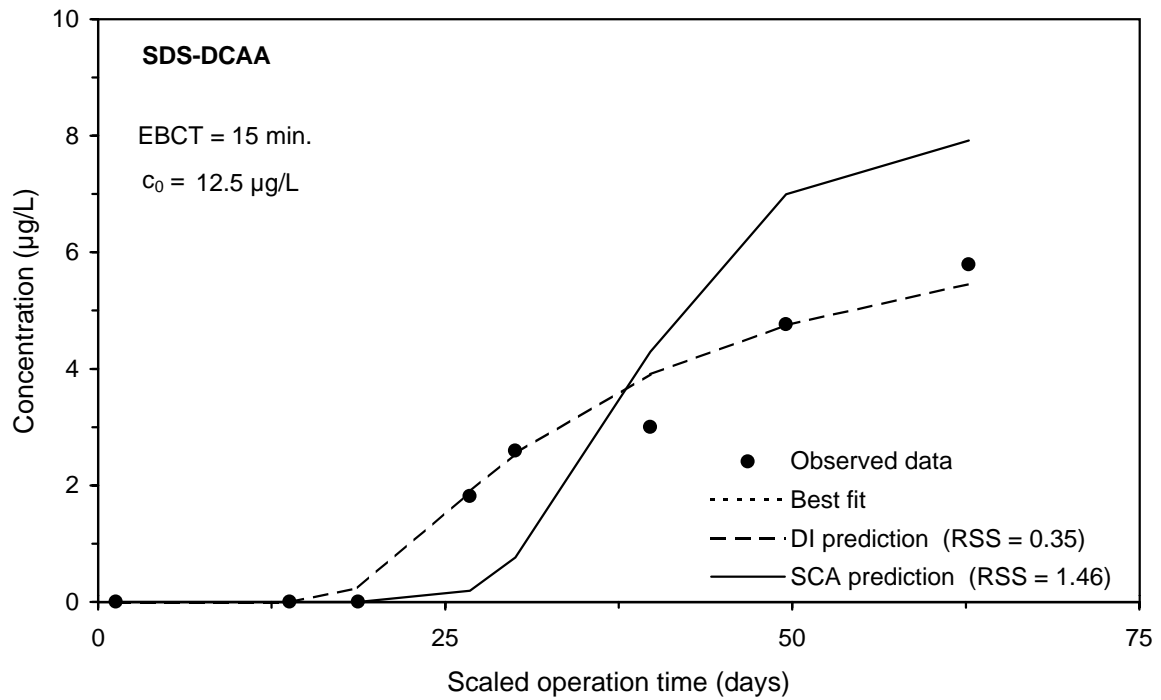


**Figure F-10 Comparison of DI and SCA methods for predicting the SDS-DCAA integral breakthrough curve for Water 1**

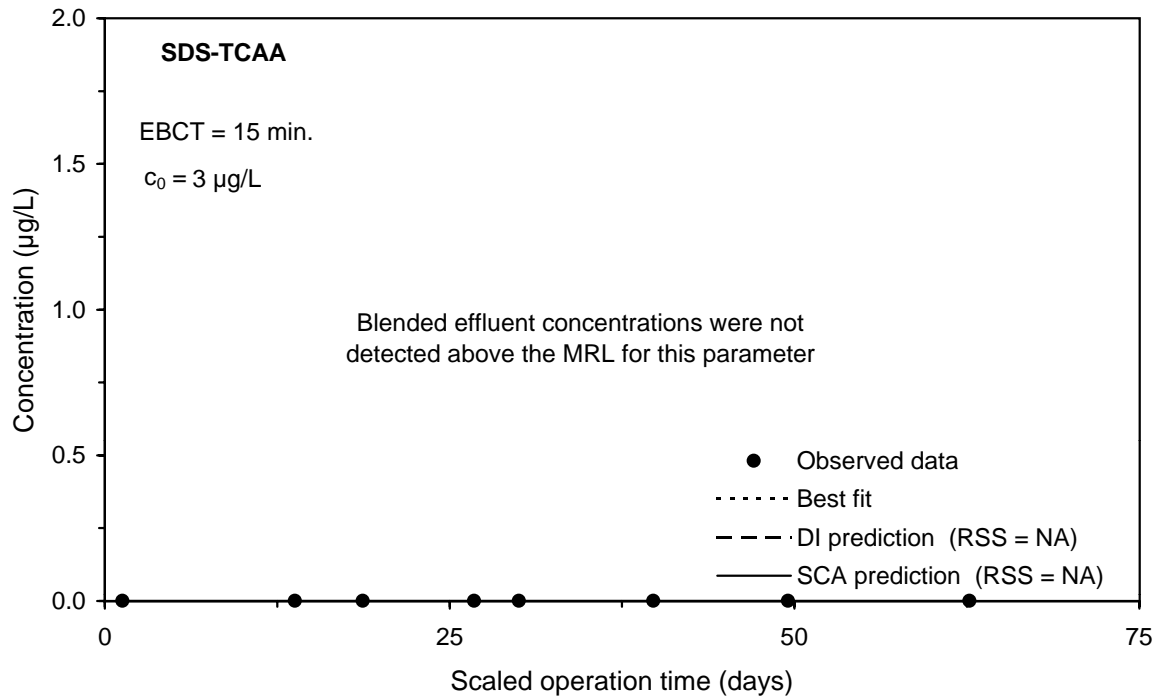


**Figure F-11 Comparison of DI and SCA methods for predicting the SDS-TCAA integral breakthrough curve for Water 1**

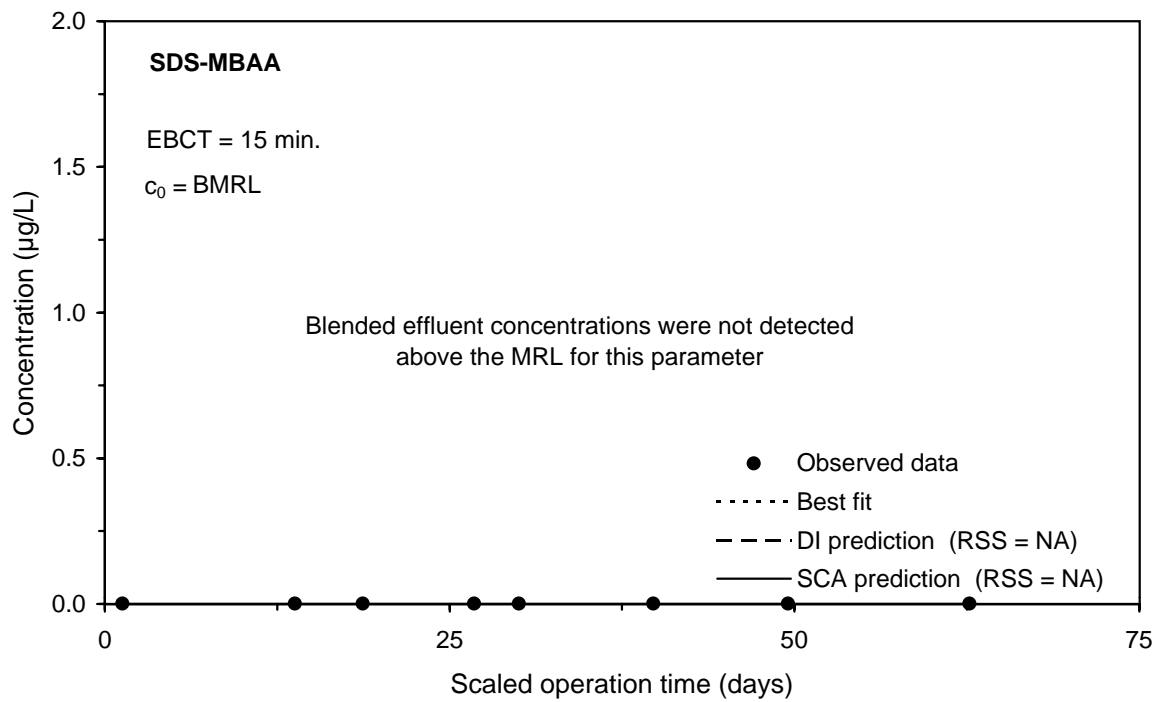


**Figure F-12 Comparison of DI and SCA methods for predicting the SDS-MBAA integral breakthrough curve for Water 1**

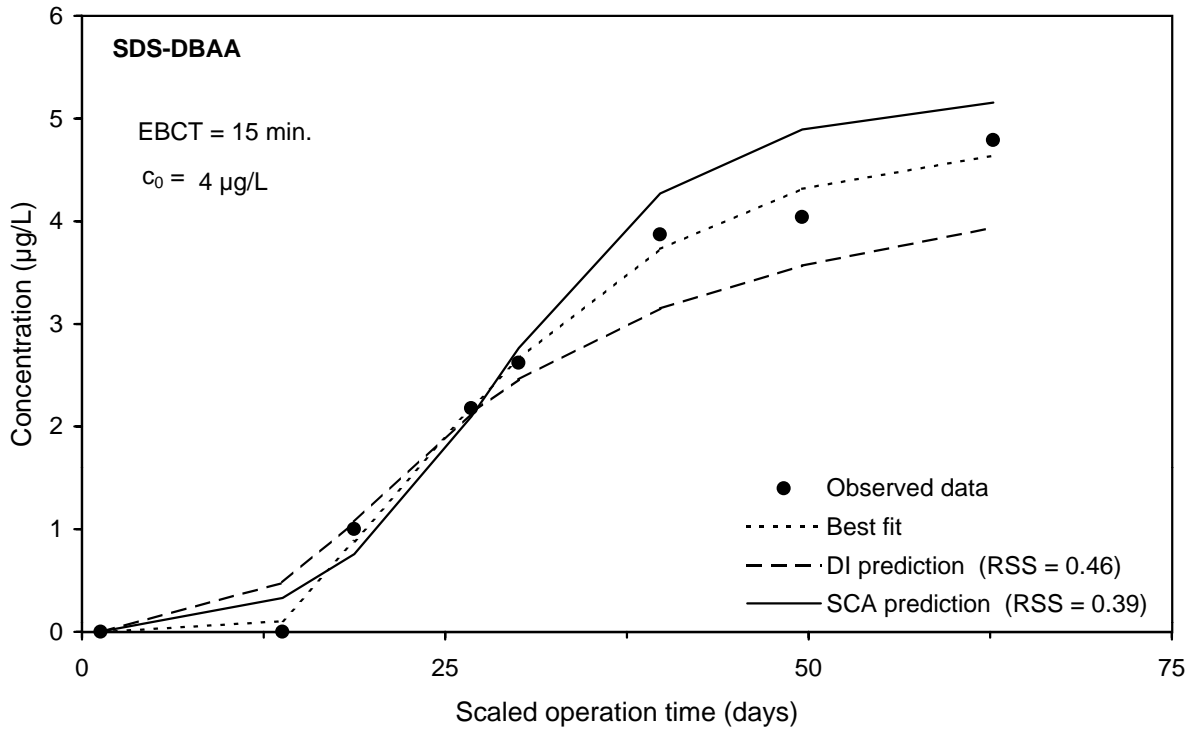


**Figure F-13 Comparison of DI and SCA methods for predicting the SDS-DBAA integral breakthrough curve for Water 1**

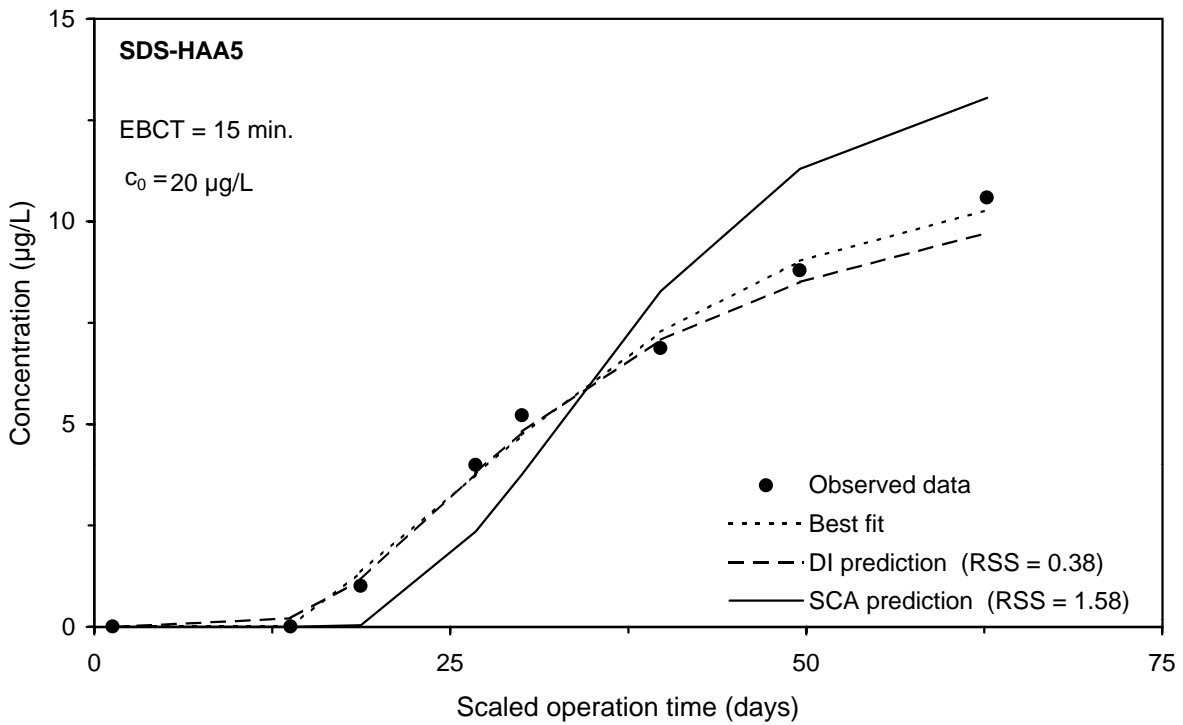


**Figure F-14 Comparison of DI and SCA methods for predicting the SDS-HAA5 integral breakthrough curve for Water 1**

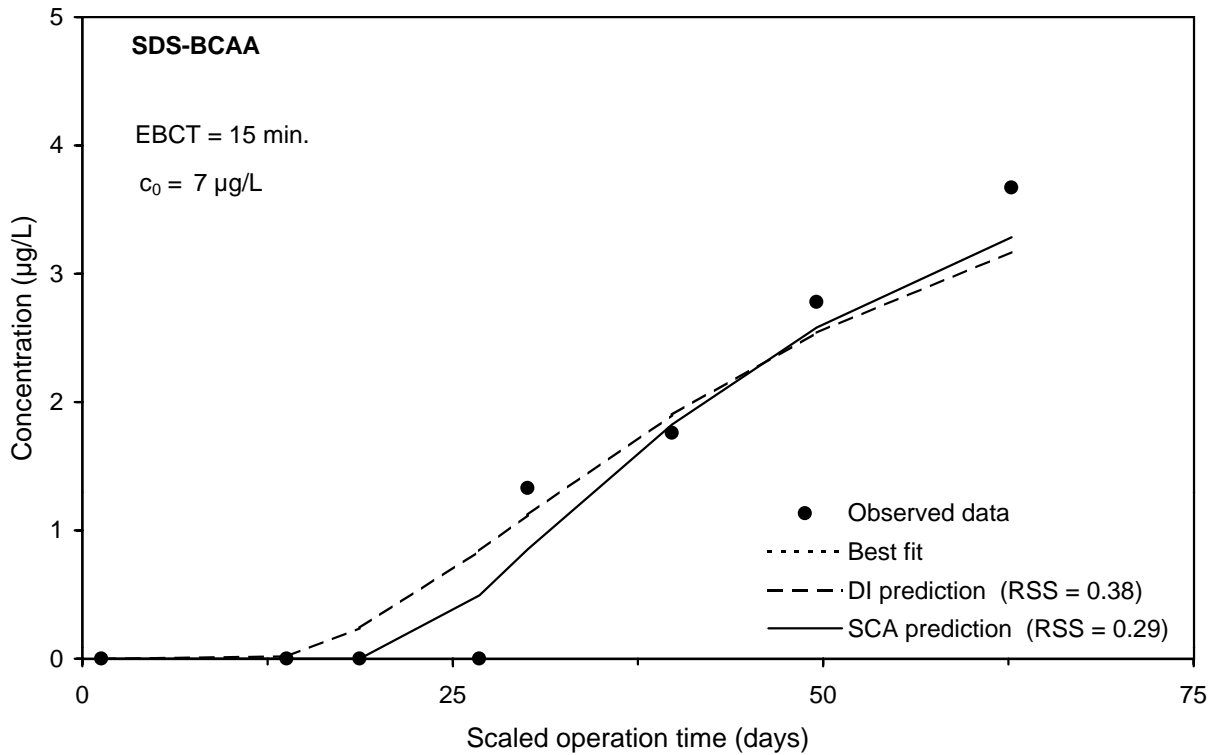


**Figure F-15 Comparison of DI and SCA methods for predicting the SDS-BCAA integral breakthrough curve for Water 1**

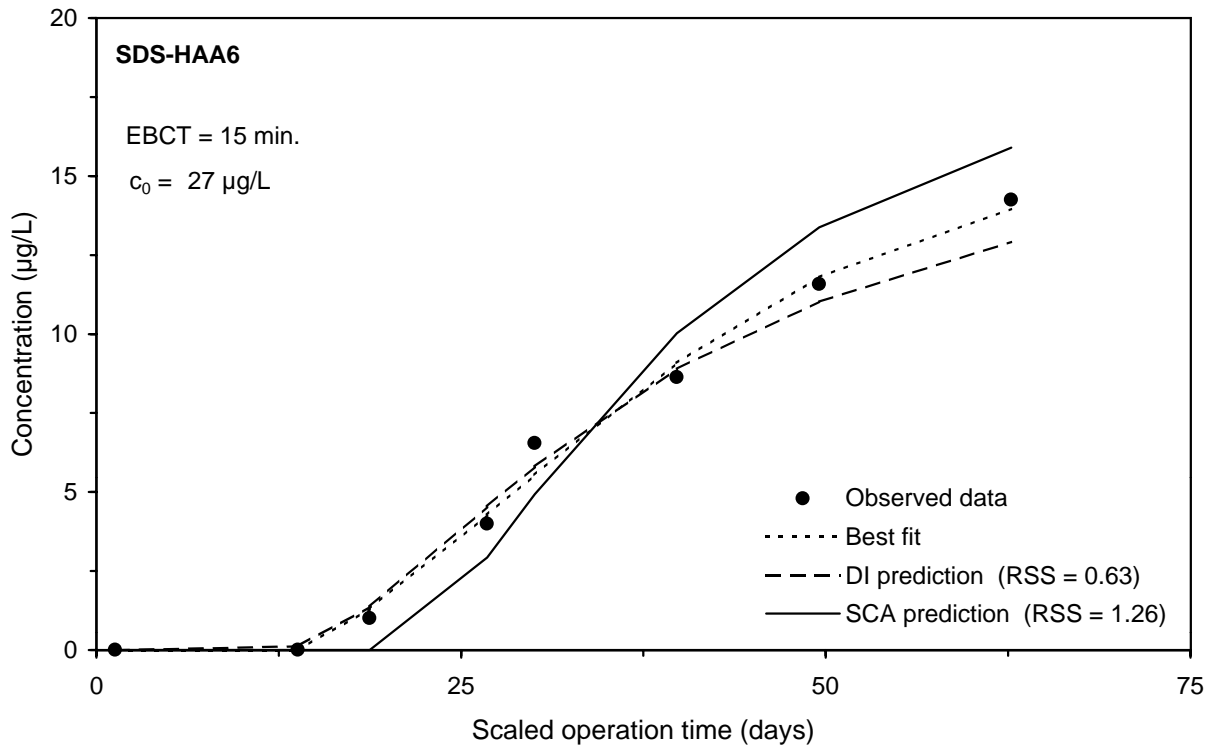


**Figure F-16 Comparison of DI and SCA methods for predicting the SDS-HAA6 integral breakthrough curve for Water 1**

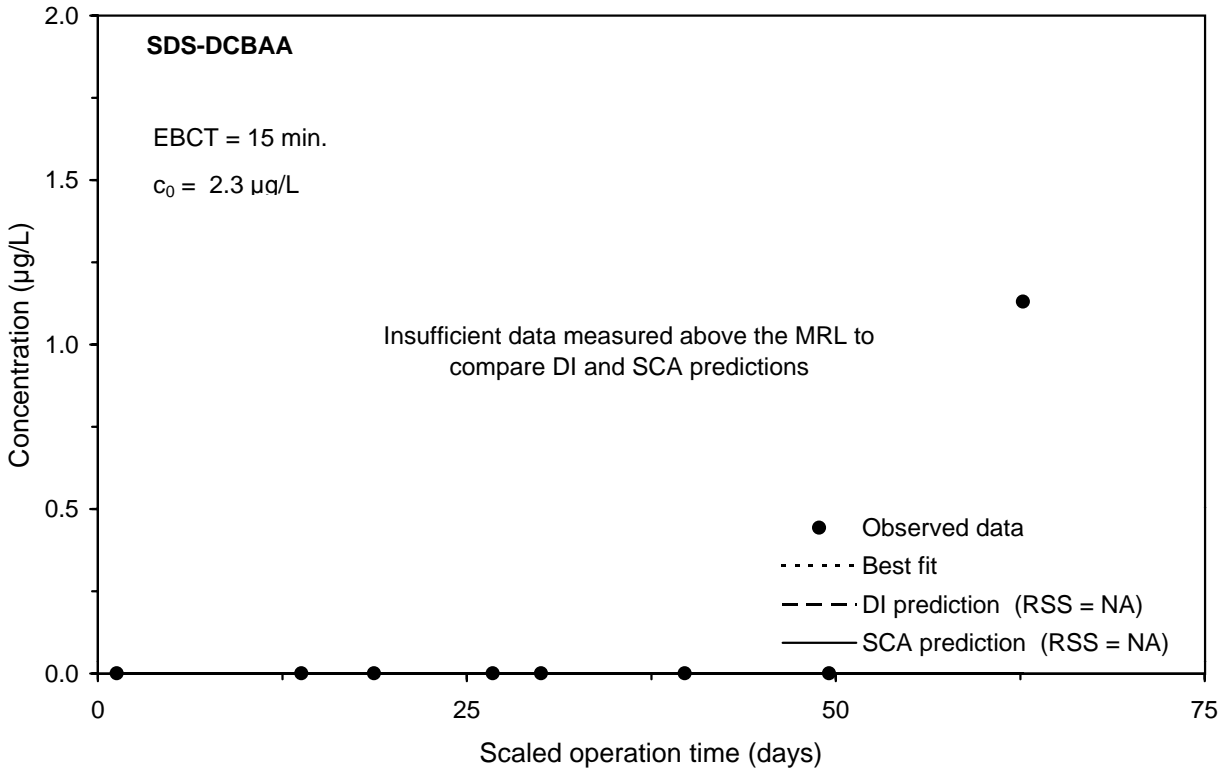


**Figure F-17 Comparison of DI and SCA methods for predicting the SDS-DCBAA integral breakthrough curve for Water 1**

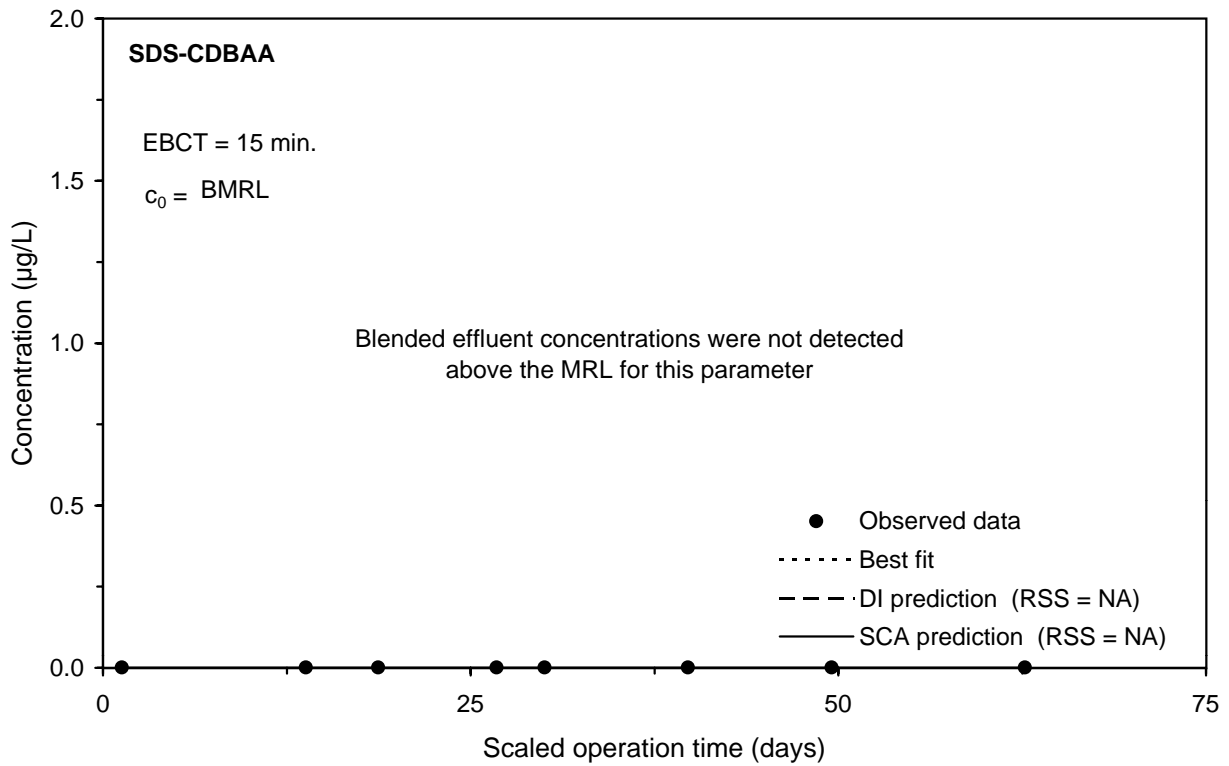


**Figure F-18 Comparison of DI and SCA methods for predicting the SDS-CDBAA integral breakthrough curve for Water 1**

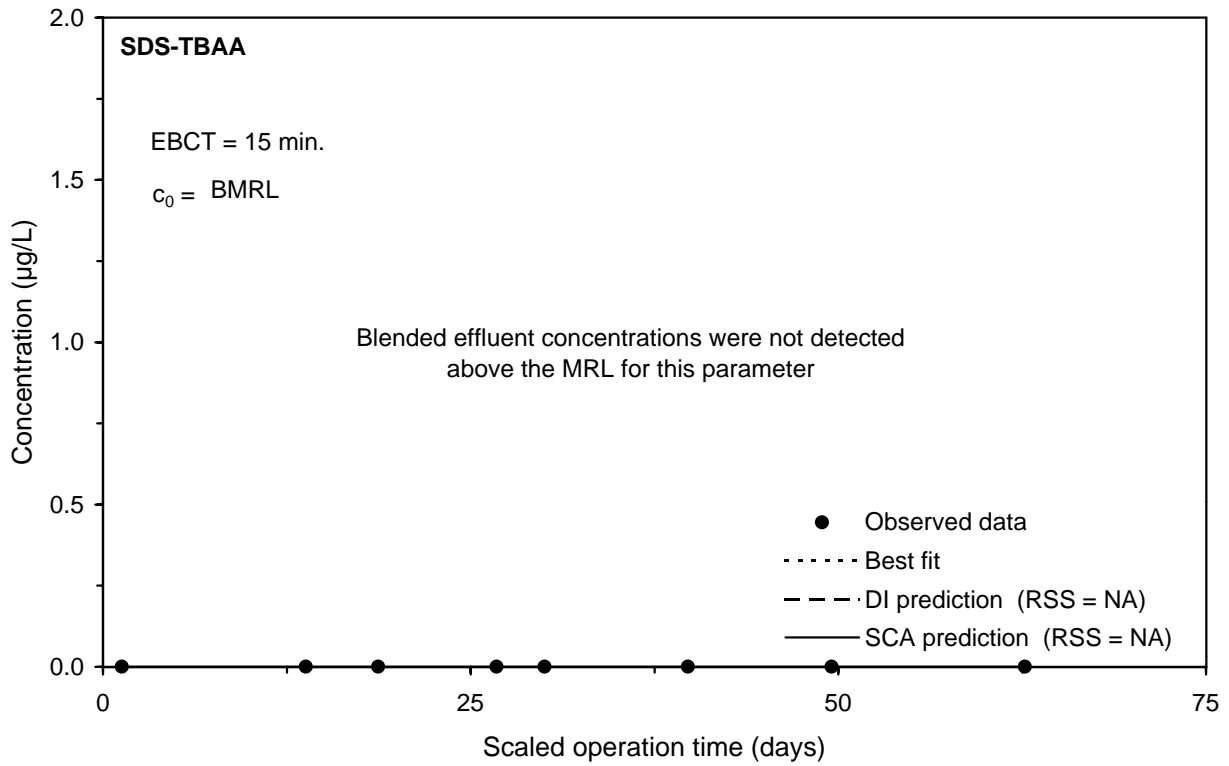


**Figure F-19 Comparison of DI and SCA methods for predicting the SDS-TBAA integral breakthrough curve for Water 1**

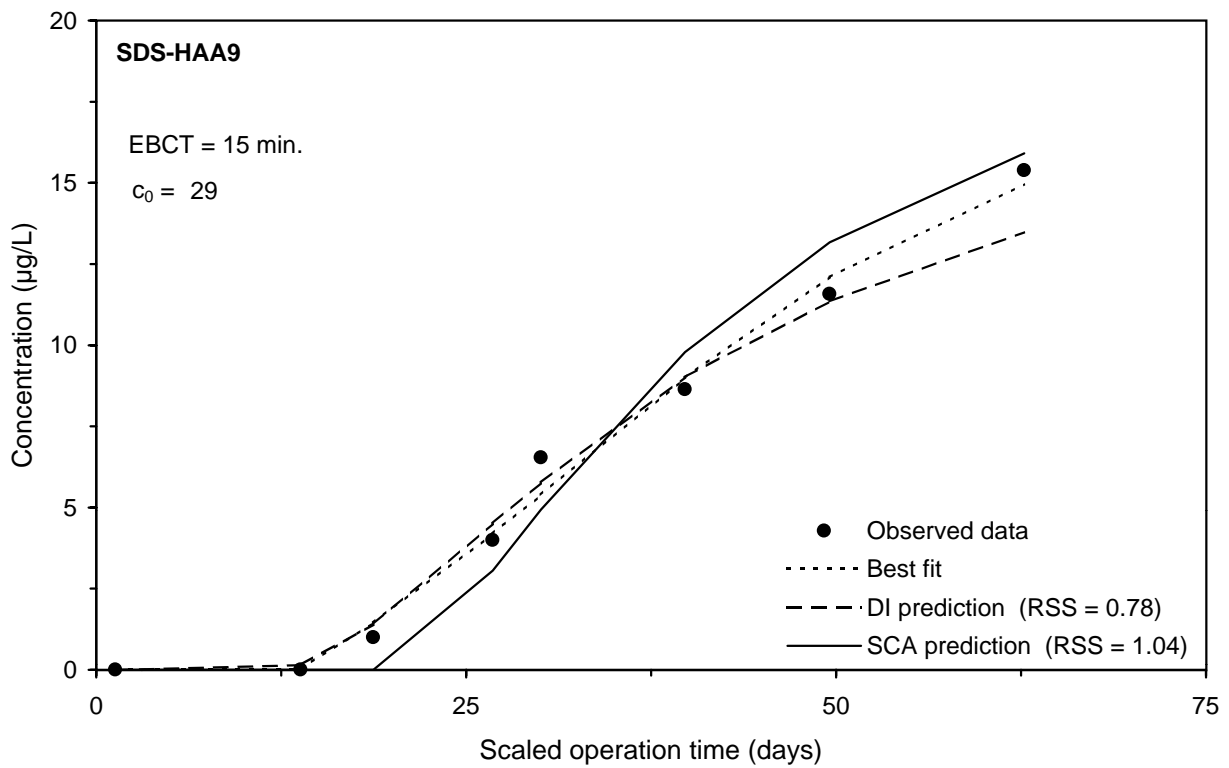


**Figure F-20 Comparison of DI and SCA methods for predicting the SDS-HAA9 integral breakthrough curve for Water 1**

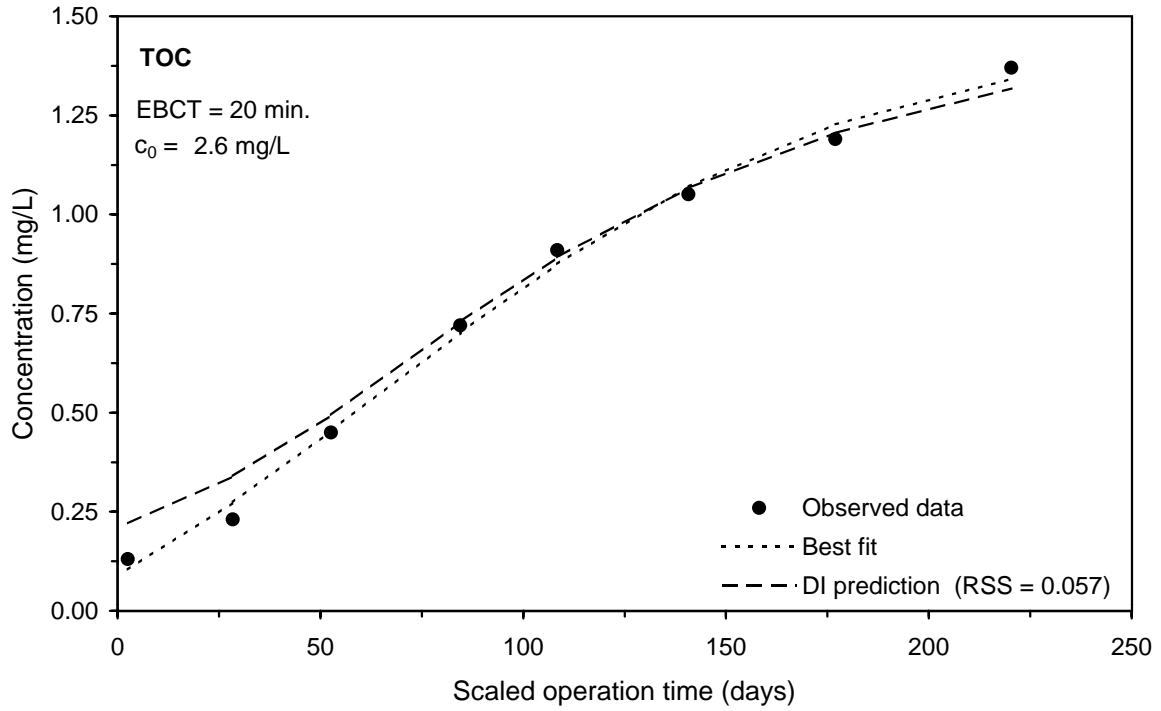


**Figure F-21 DI method prediction of the TOC integral breakthrough curve for Water 2**

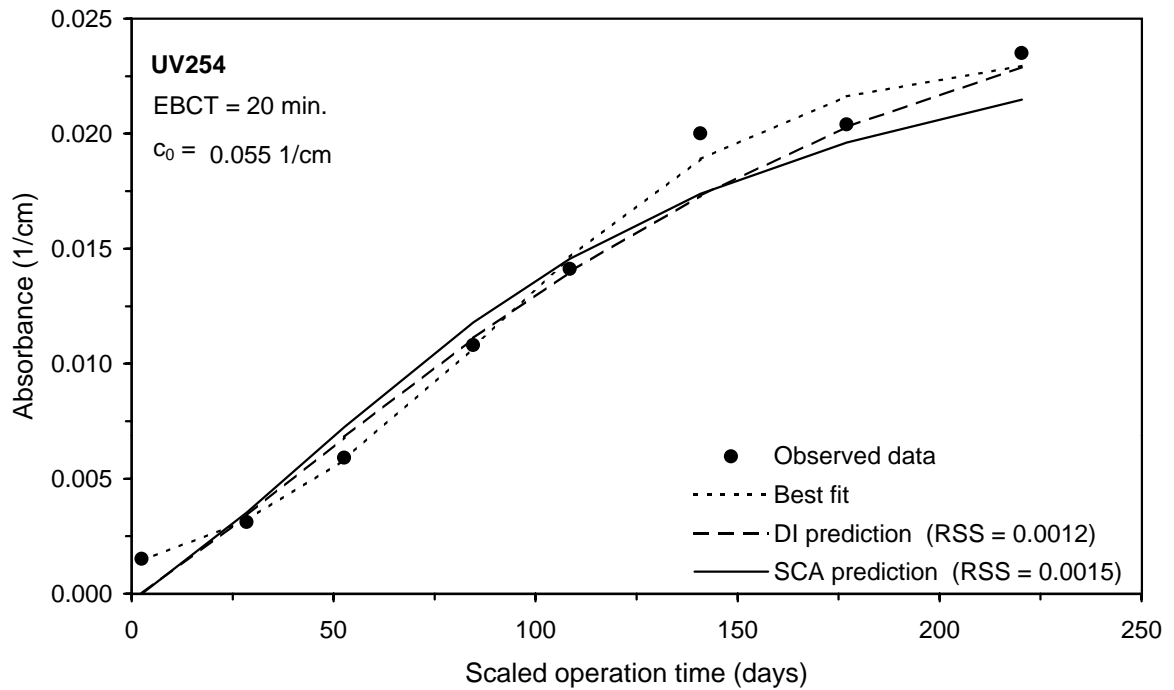


**Figure F-22 Comparison of DI and SCA methods for predicting the UV254 integral breakthrough curve for Water 2**

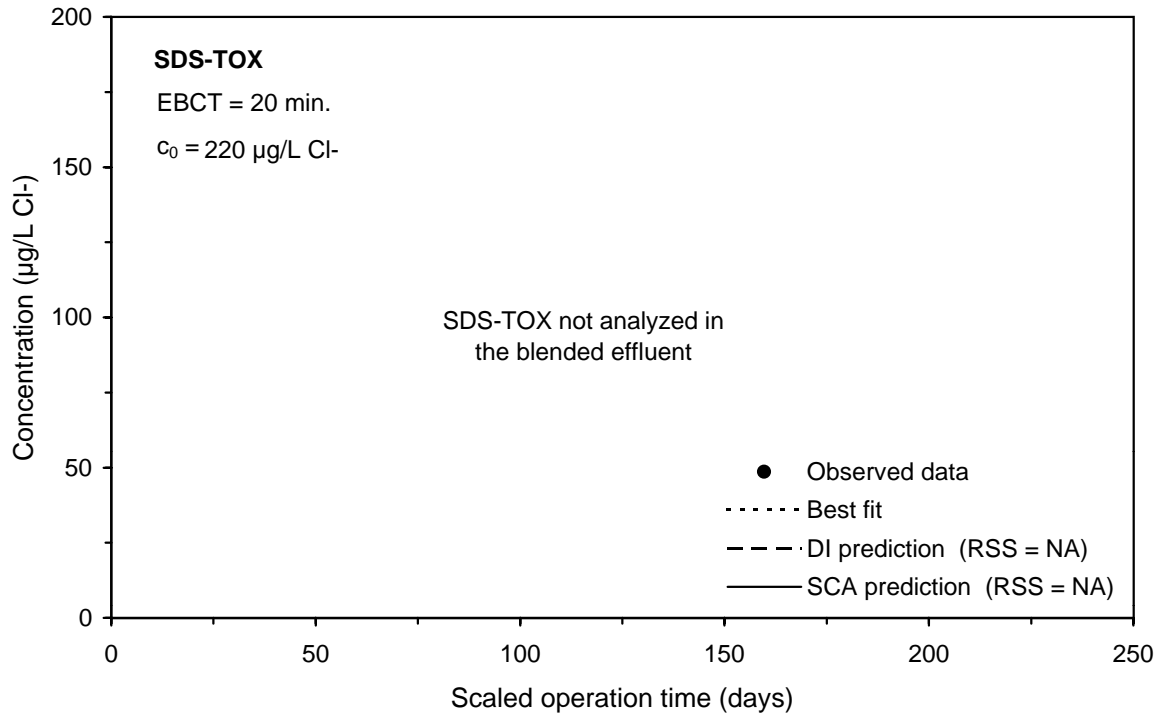


**Figure F-23 Comparison of DI and SCA methods for predicting the SDS-TOX integral breakthrough curve for Water 2**

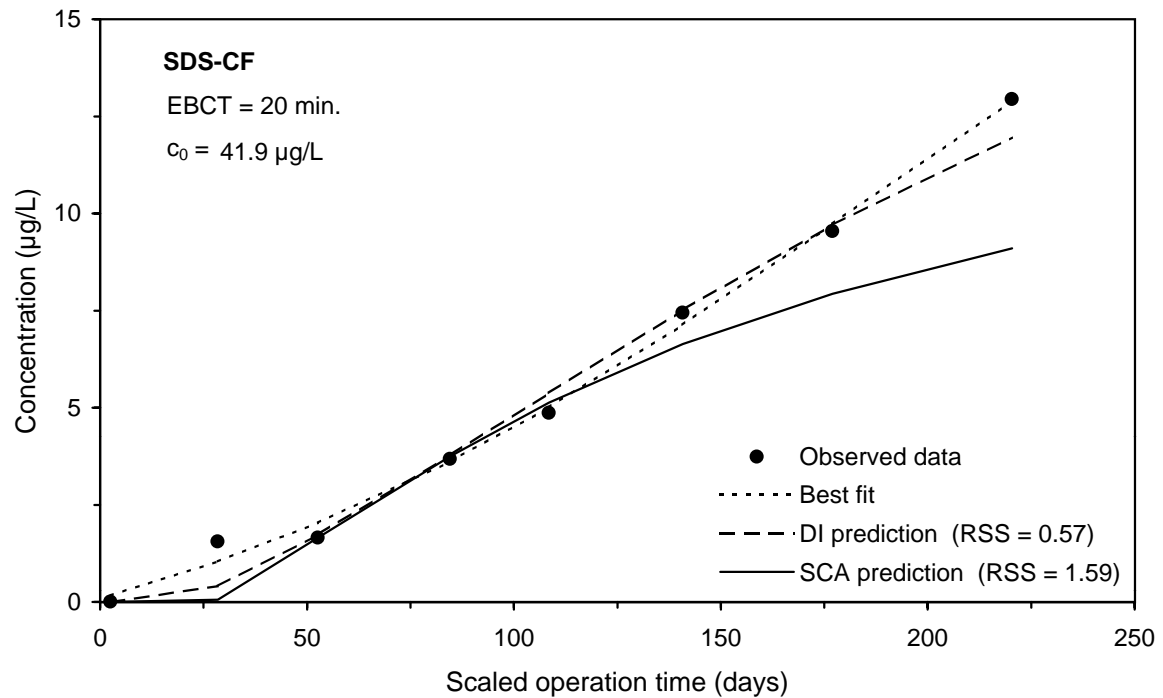


**Figure F-24 Comparison of DI and SCA methods for predicting the SDS-CF integral breakthrough curve for Water 2**

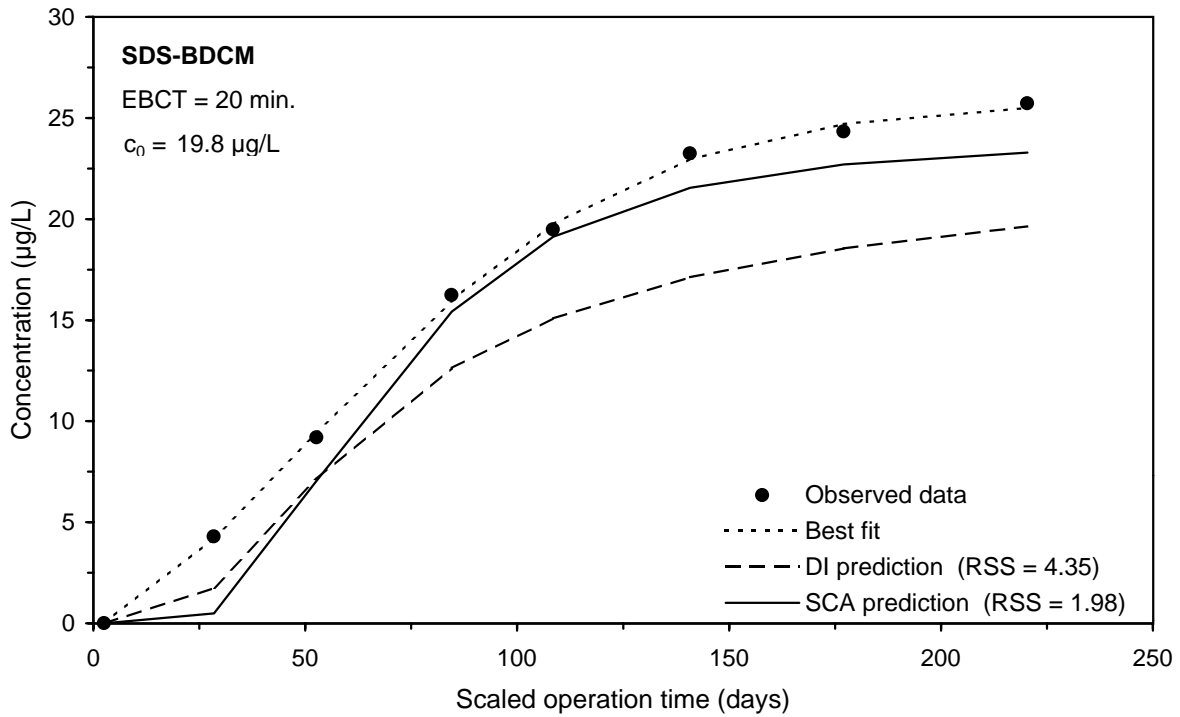


**Figure F-25 Comparison of DI and SCA methods for predicting the SDS-BDCM integral breakthrough curve for Water 2**

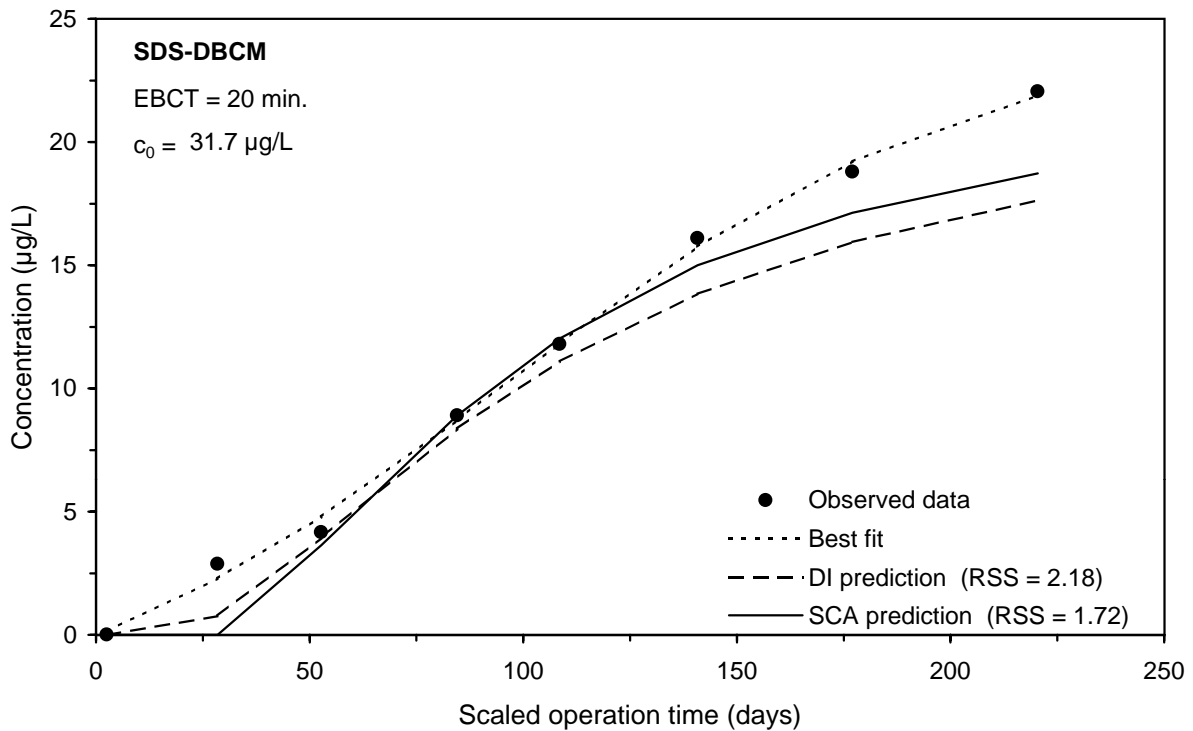


**Figure F-26 Comparison of DI and SCA methods for predicting the SDS-DBCm integral breakthrough curve for Water 2**

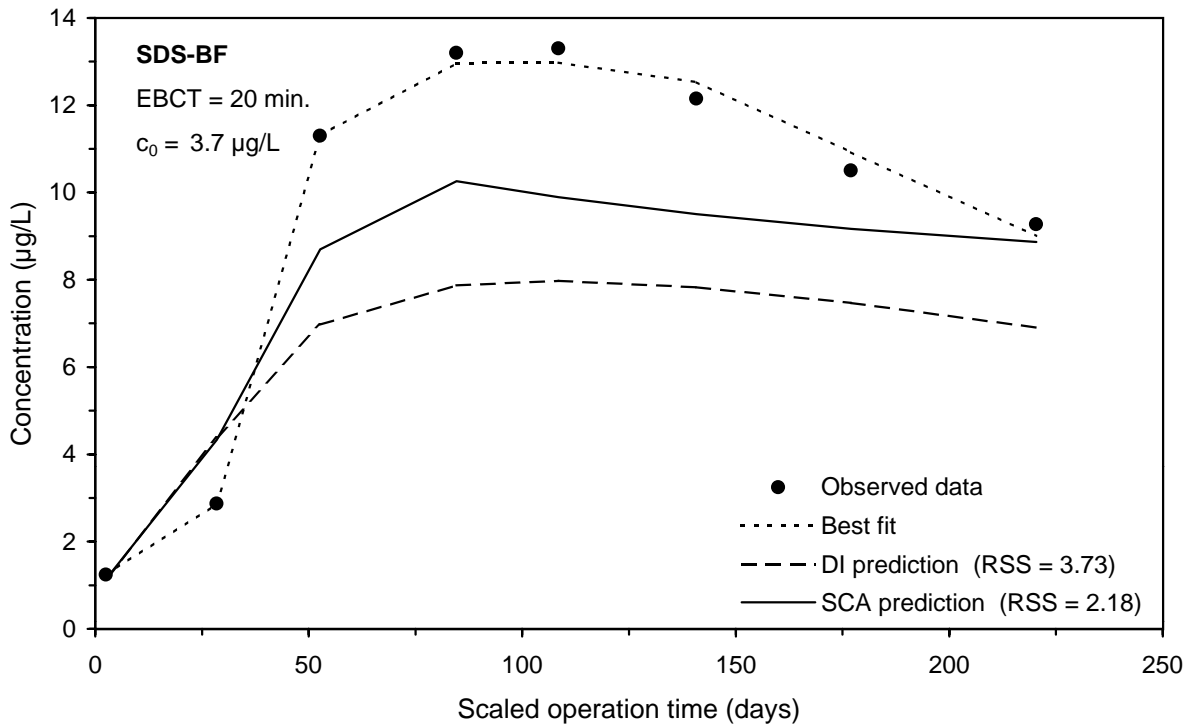


**Figure F-27 Comparison of DI and SCA methods for predicting the SDS-BF integral breakthrough curve for Water 2**

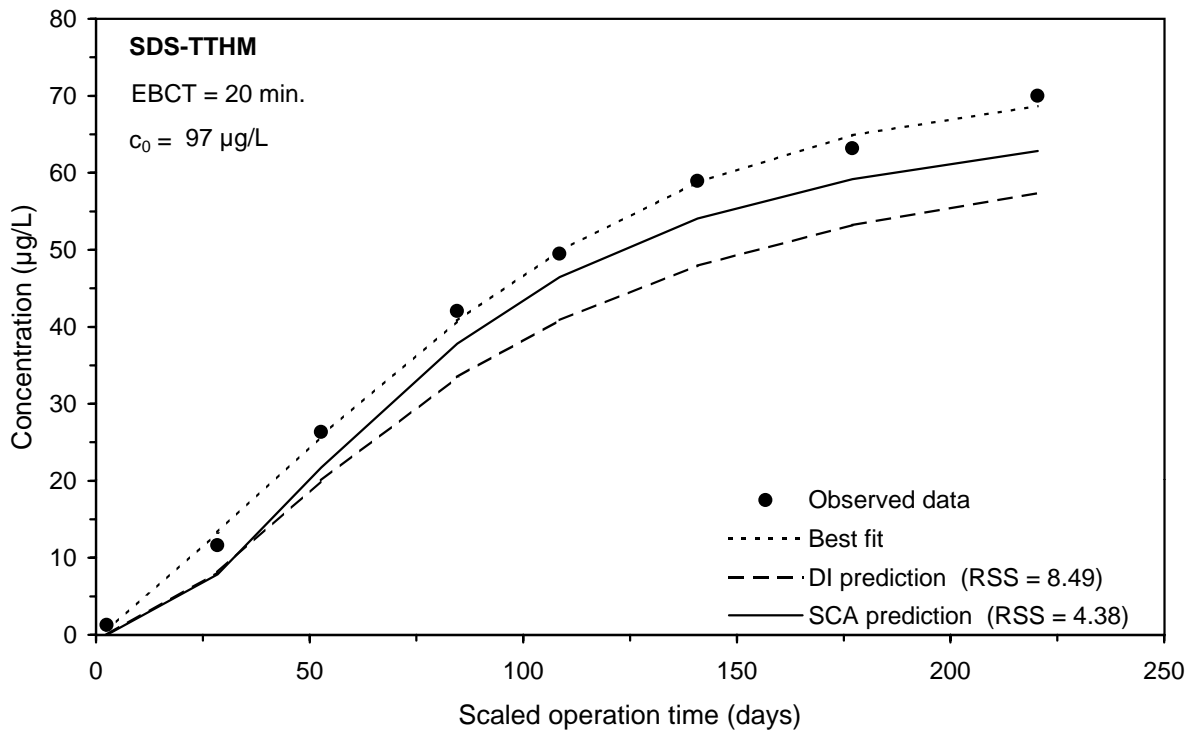


**Figure F-28 Comparison of DI and SCA methods for predicting the SDS-TTHM integral breakthrough curve for Water 2**

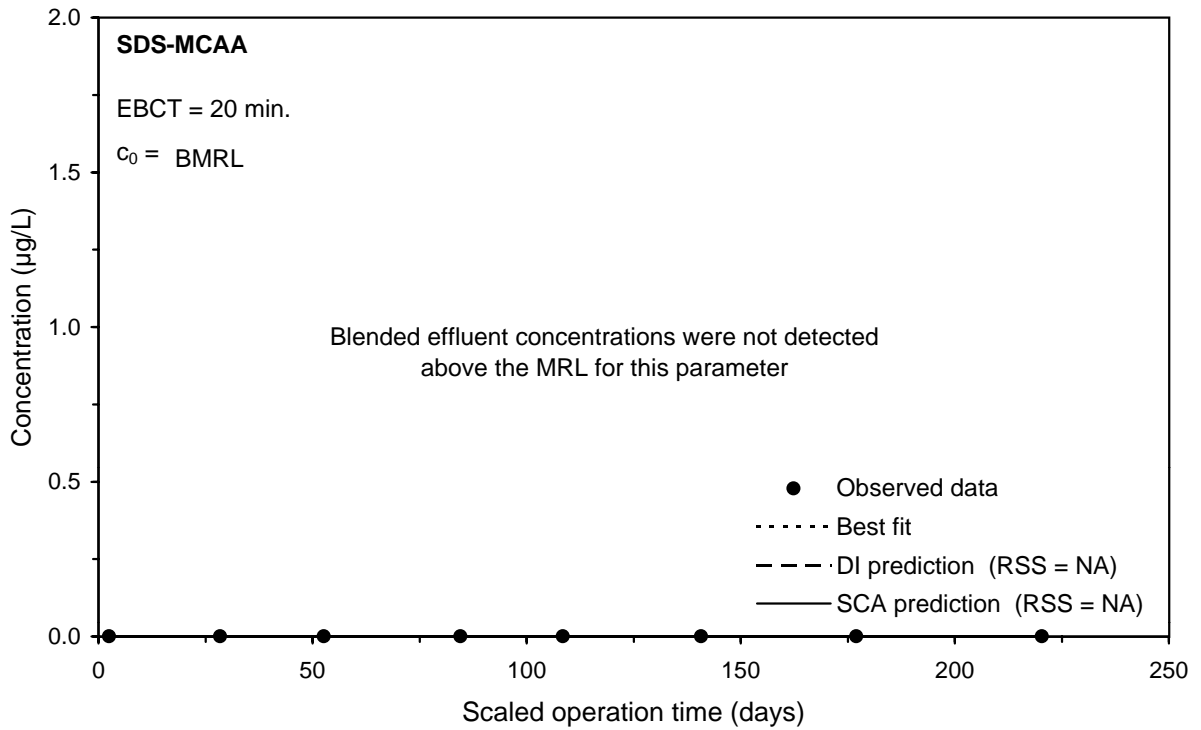


**Figure F-29 Comparison of DI and SCA methods for predicting the SDS-MCAA integral breakthrough curve for Water 2**

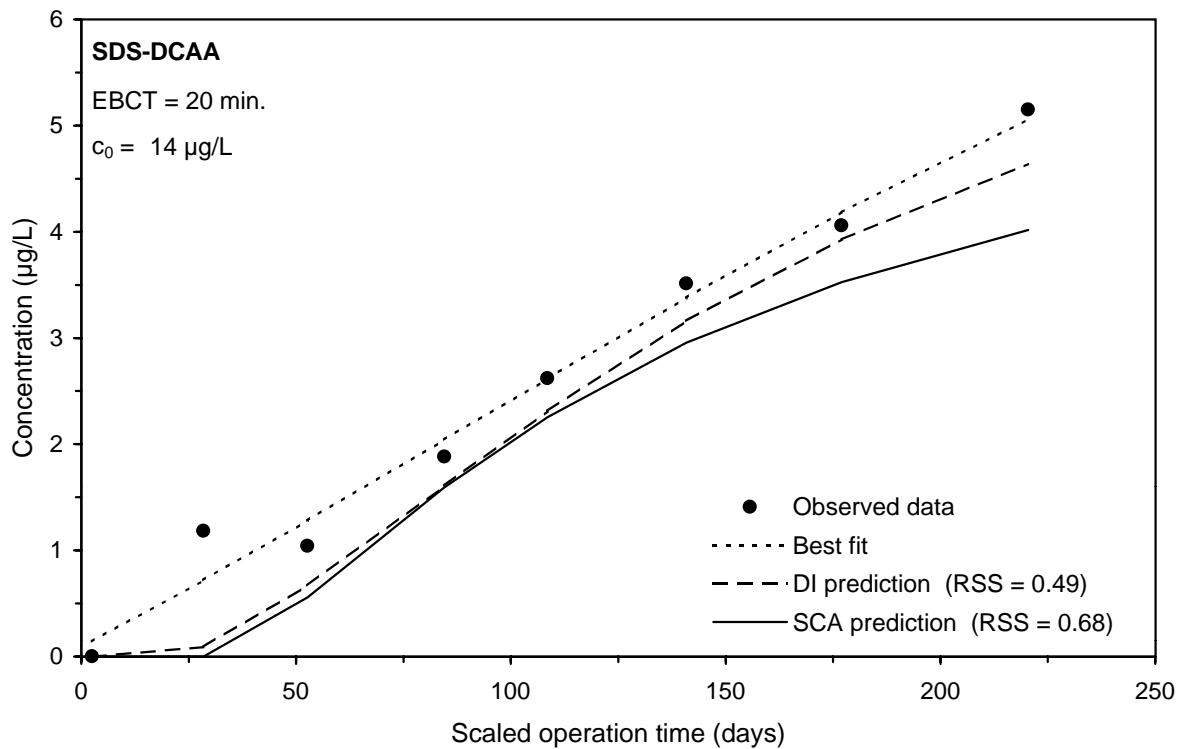


**Figure F-30 Comparison of DI and SCA methods for predicting the SDS-DCAA integral breakthrough curve for Water 2**

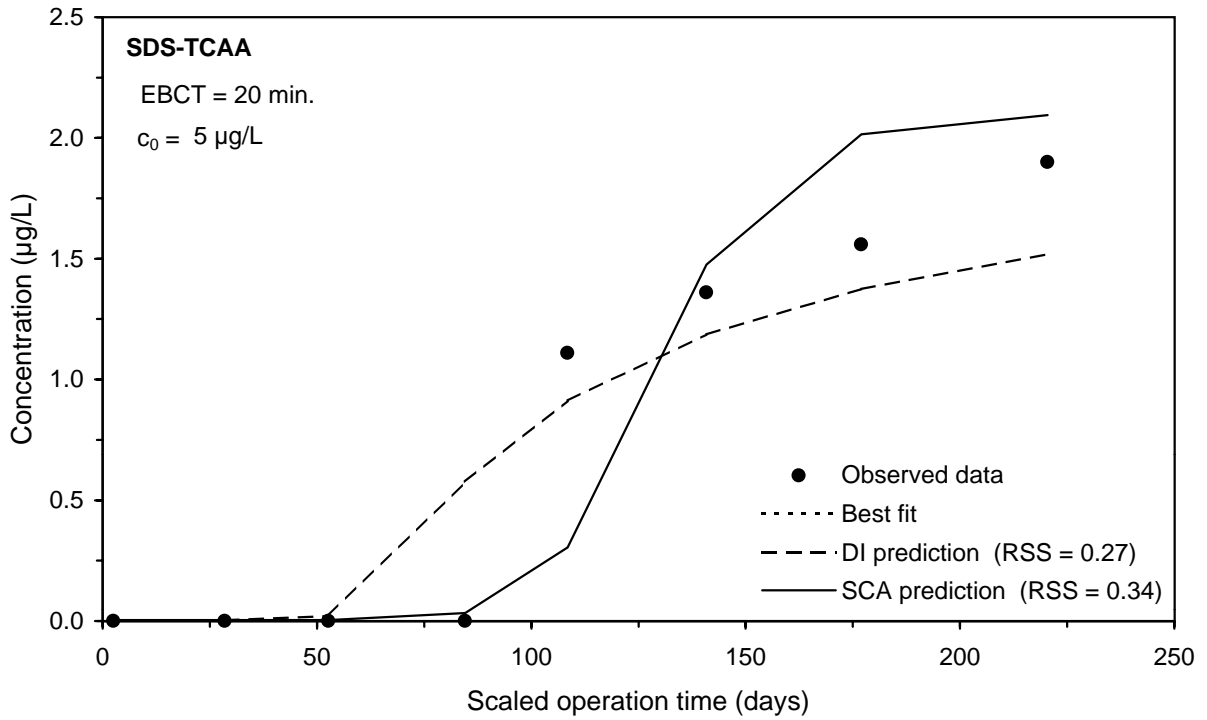


**Figure F-31 Comparison of DI and SCA methods for predicting the SDS-TCAA integral breakthrough curve for Water 2**

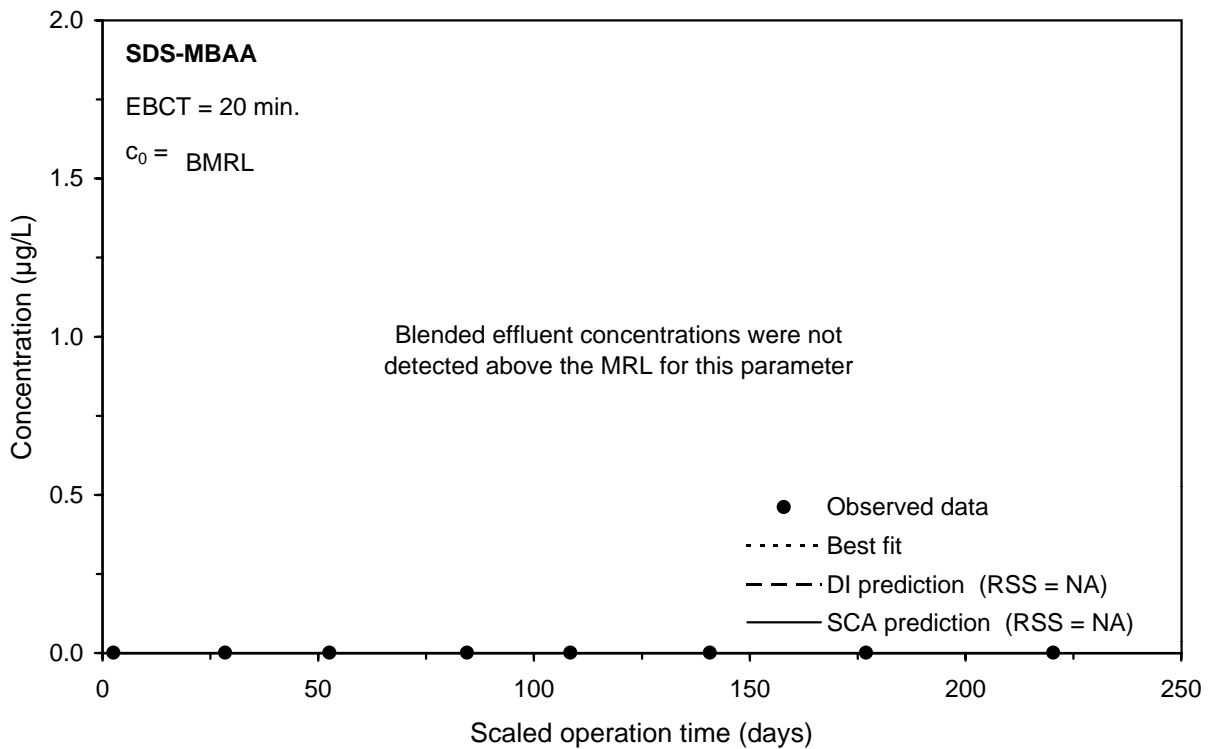


**Figure F-32 Comparison of DI and SCA methods for predicting the SDS-MBAA integral breakthrough curve for Water 2**

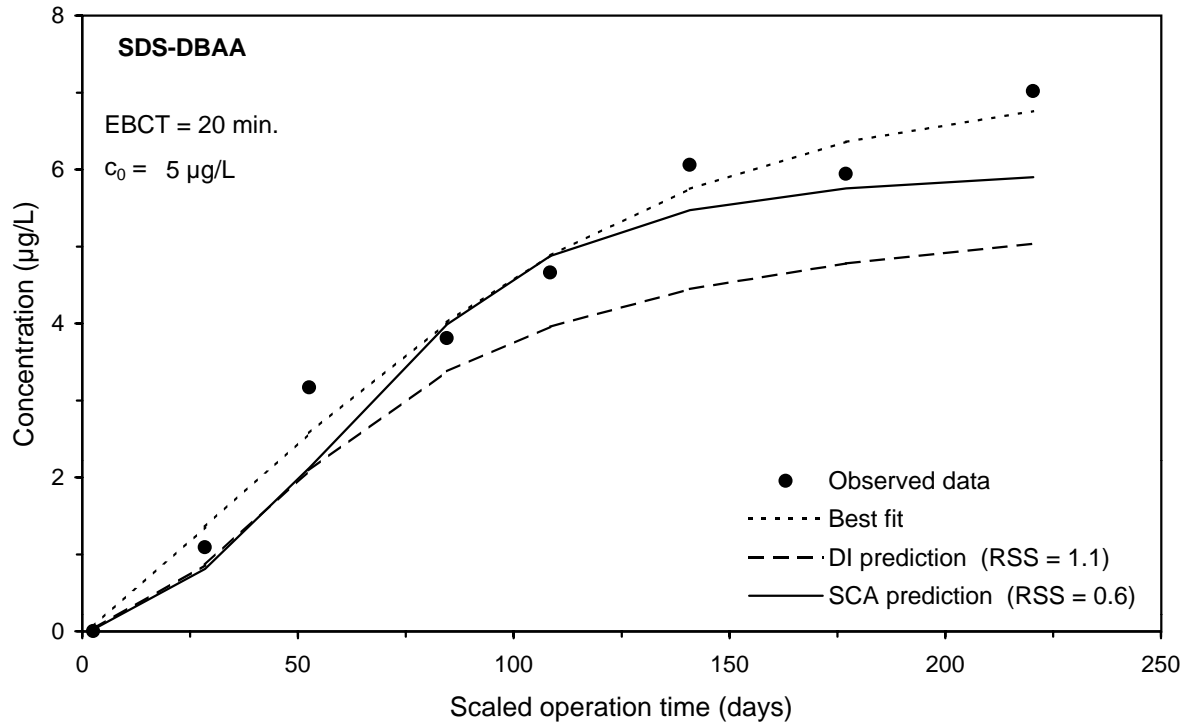


**Figure F-33 Comparison of DI and SCA methods for predicting the SDS-DBAA integral breakthrough curve for Water 2**

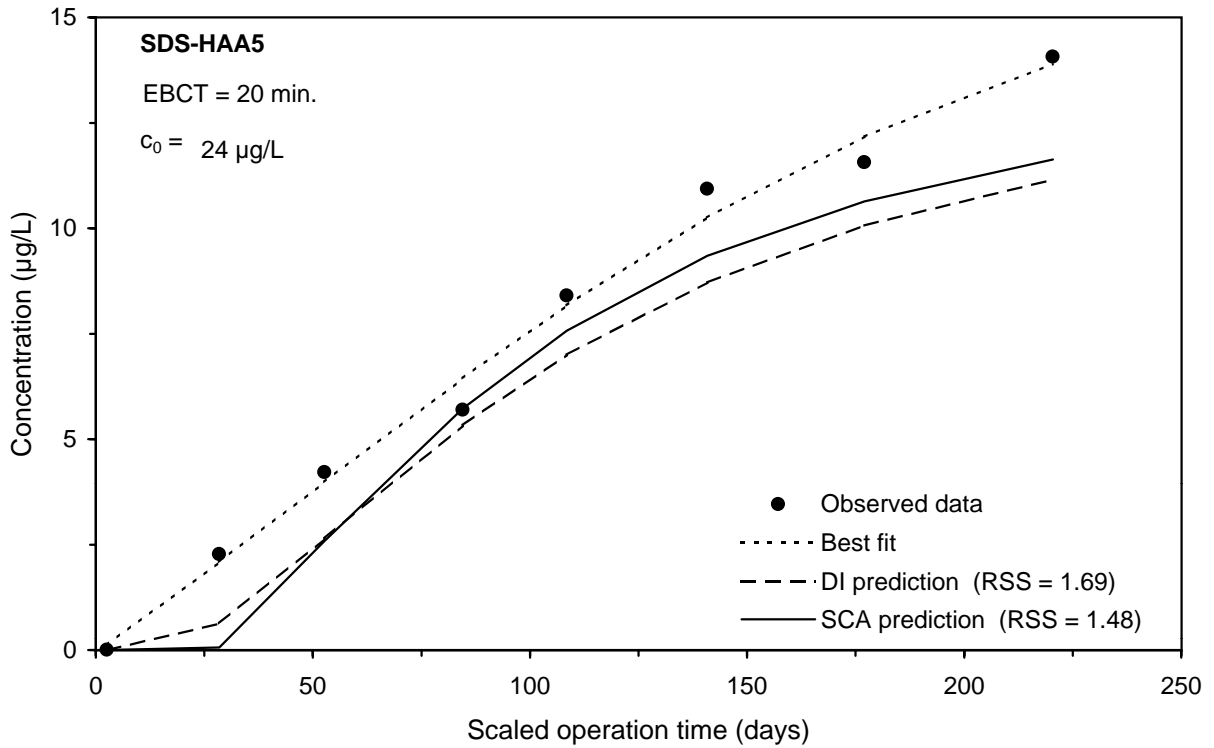


**Figure F-34 Comparison of DI and SCA methods for predicting the SDS-HAA5 integral breakthrough curve for Water 2**

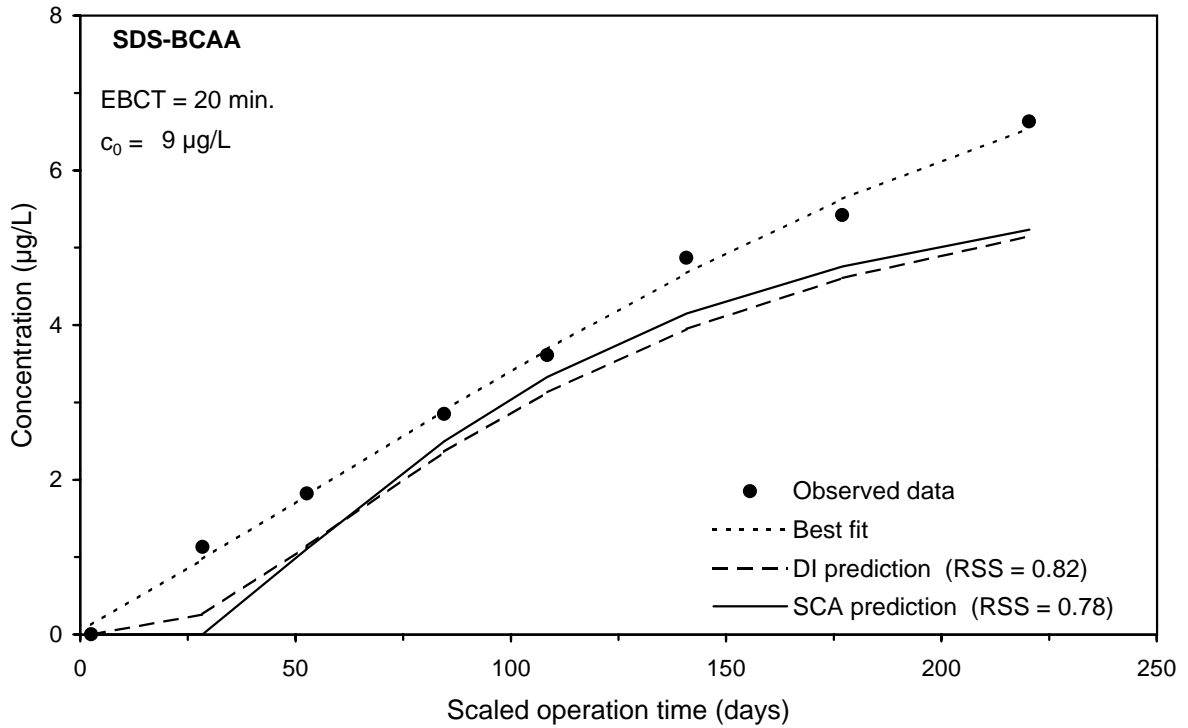


**Figure F-35 Comparison of DI and SCA methods for predicting the SDS-BCAA integral breakthrough curve for Water 2**

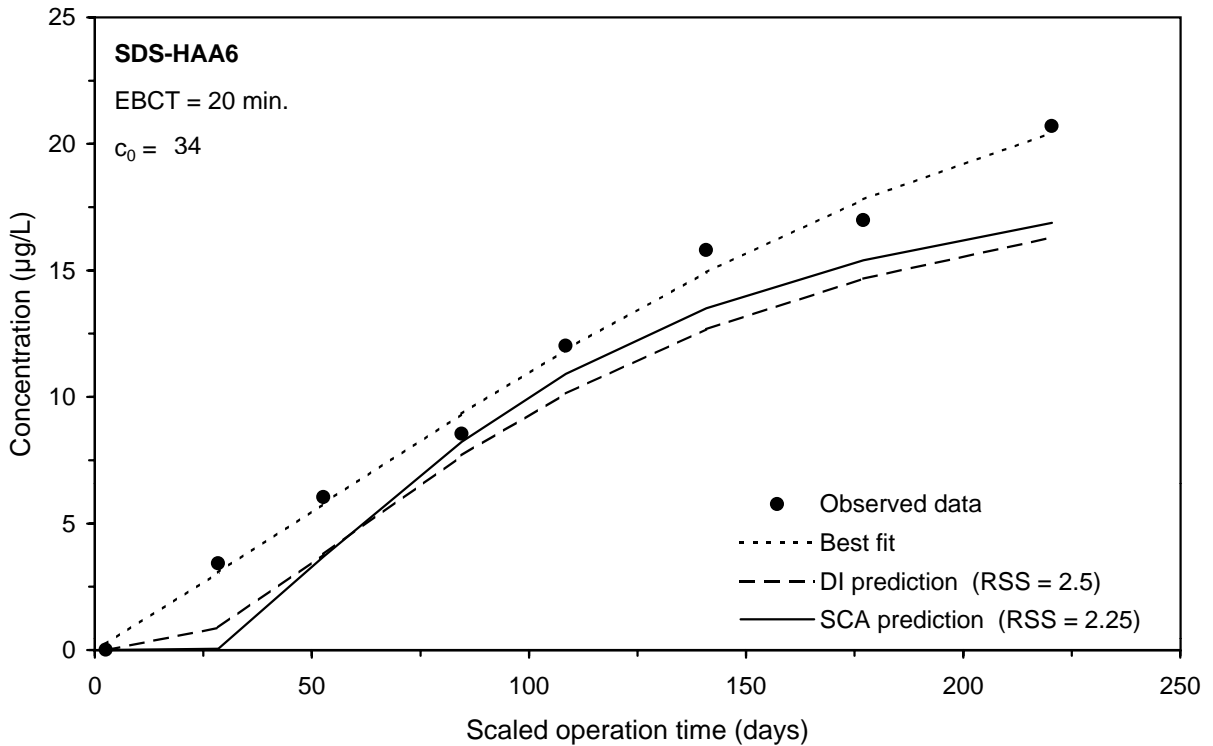


**Figure F-36 Comparison of DI and SCA methods for predicting the SDS-HAA6 integral breakthrough curve for Water 2**

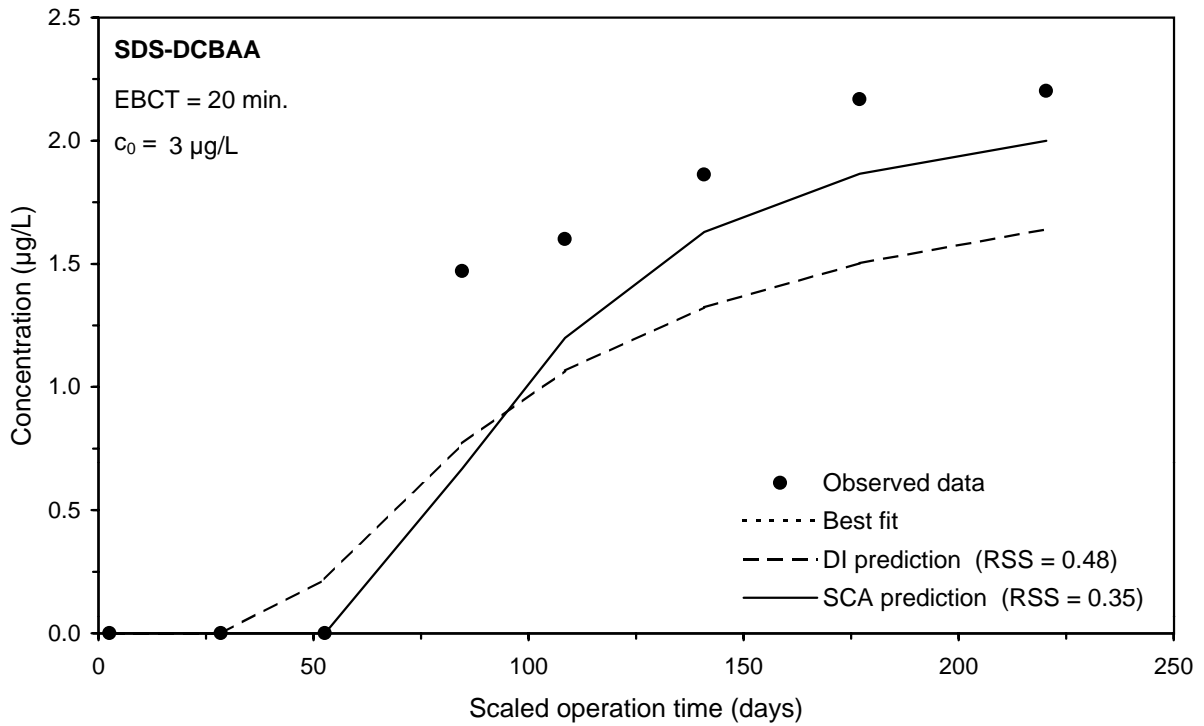


**Figure F-37 Comparison of DI and SCA methods for predicting the SDS-DCBAA integral breakthrough curve for Water 2**

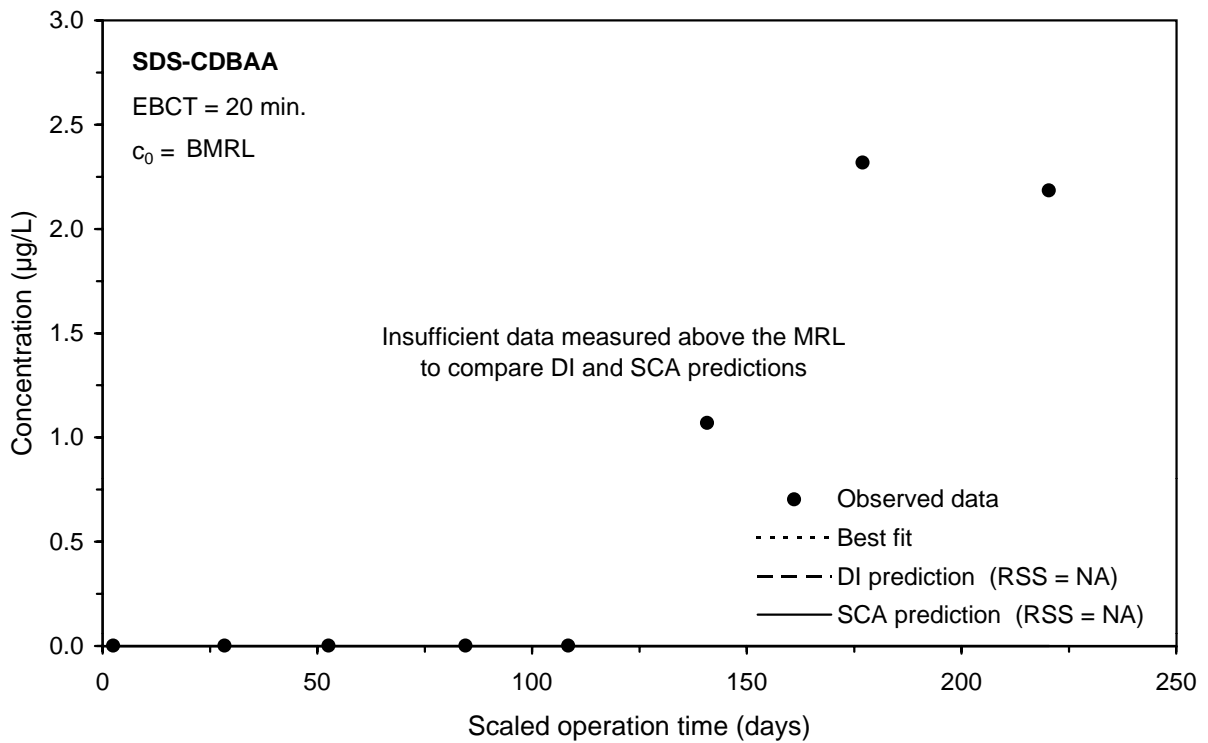


**Figure F-38 Comparison of DI and SCA methods for predicting the SDS-CDBAA integral breakthrough curve for Water 2**

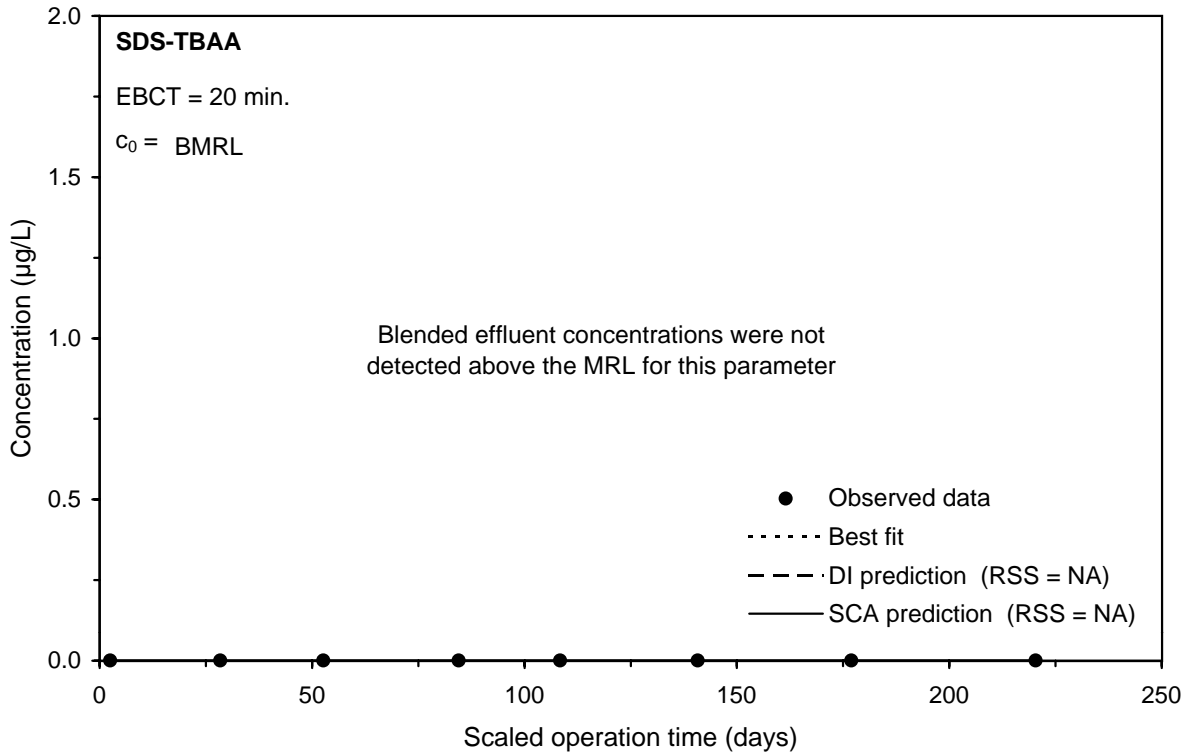


**Figure F-39 Comparison of DI and SCA methods for predicting the SDS-TBAA integral breakthrough curve for Water 2**

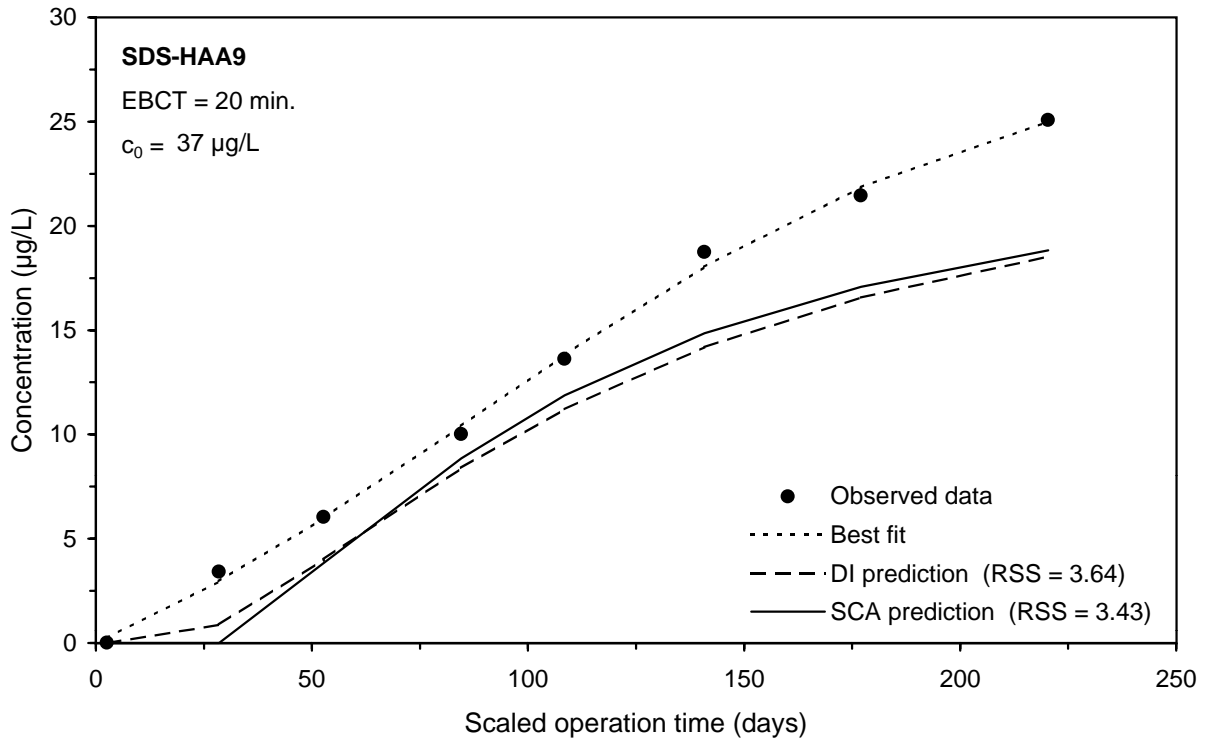


**Figure F-40 Comparison of DI and SCA methods for predicting the SDS-HAA9 integral breakthrough curve for Water 2**

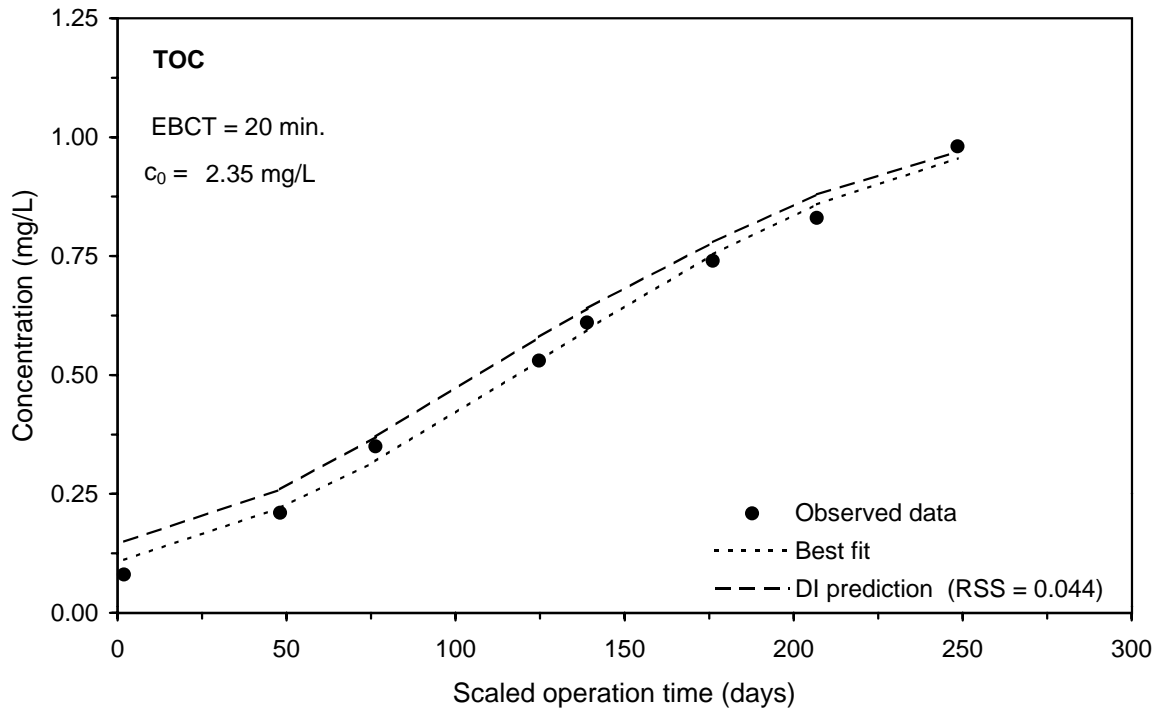


**Figure F-41 DI method prediction of the TOC integral breakthrough curve for Water 3**

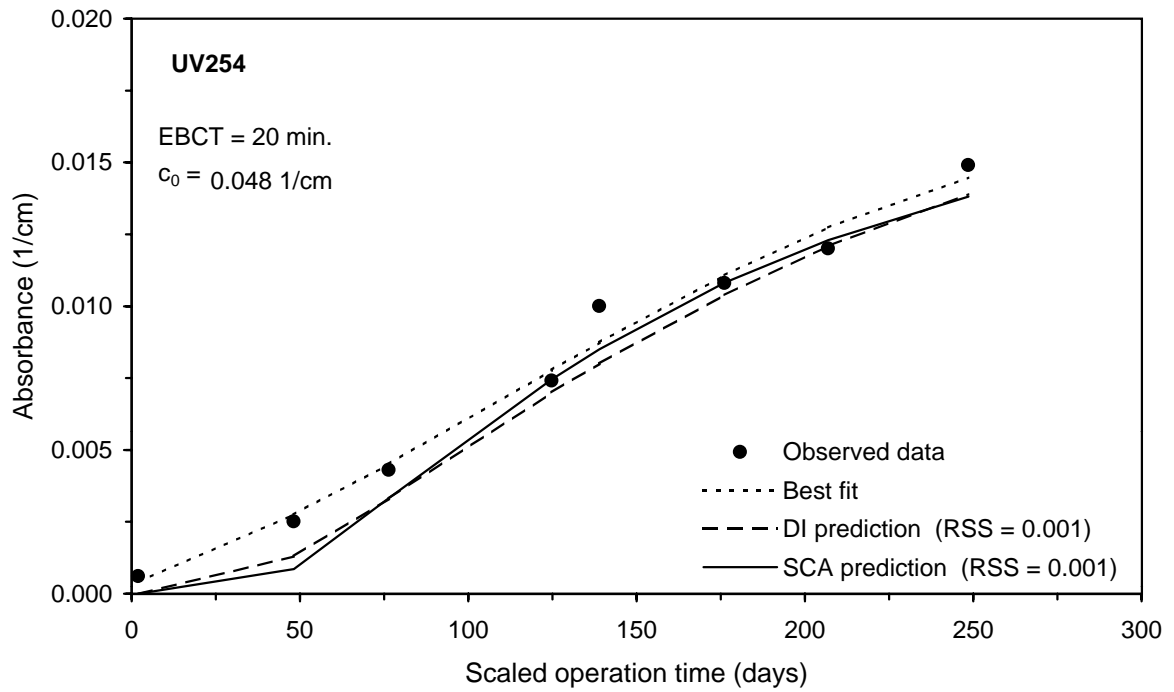


**Figure F-42 Comparison of DI and SCA methods for predicting the UV254 integral breakthrough curve for Water 3**

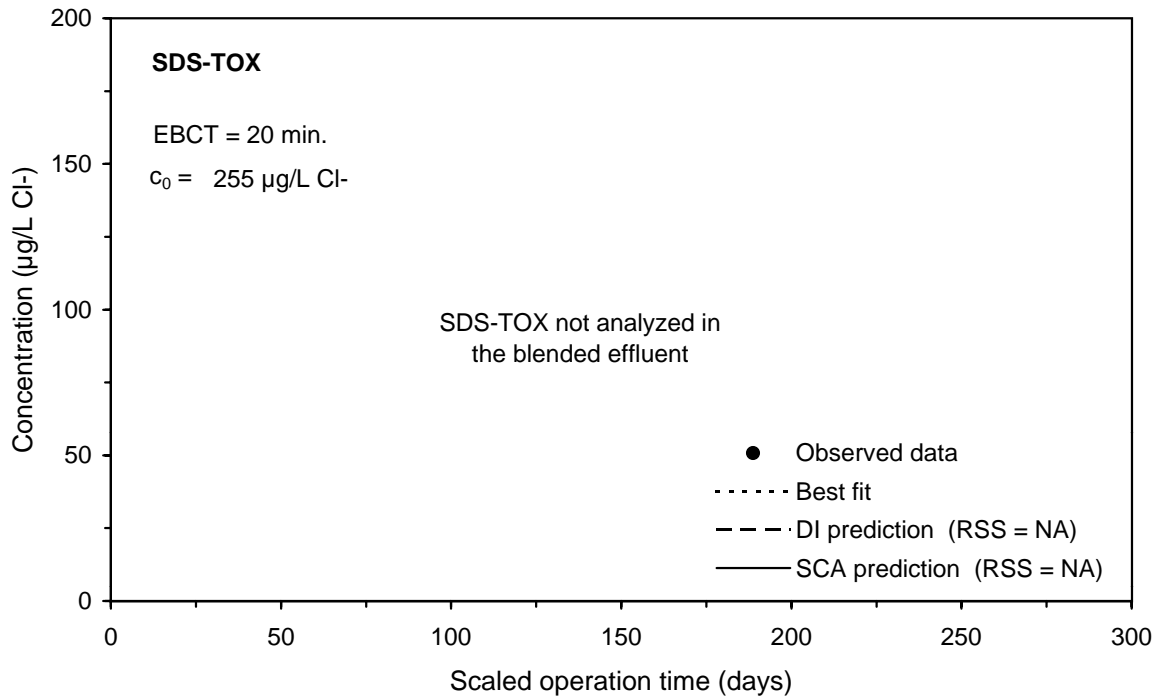


**Figure F-43 Comparison of DI and SCA methods for predicting the SDS-TOX integral breakthrough curve for Water 3**

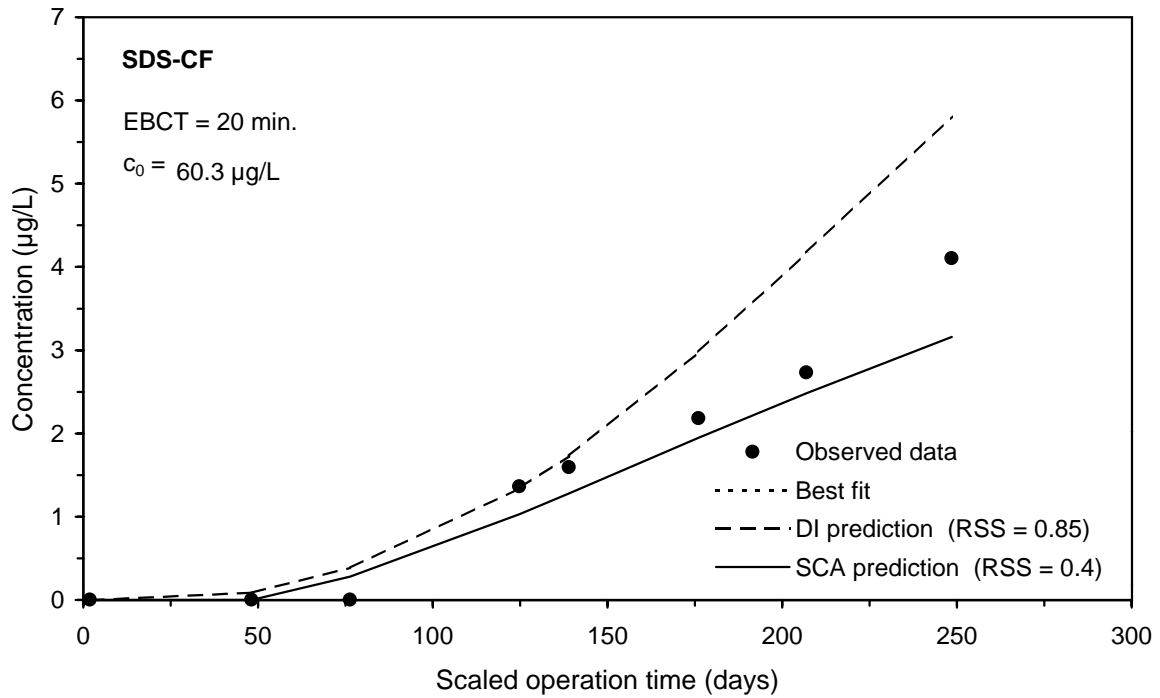


**Figure F-44 Comparison of DI and SCA methods for predicting the SDS-CF integral breakthrough curve for Water 3**

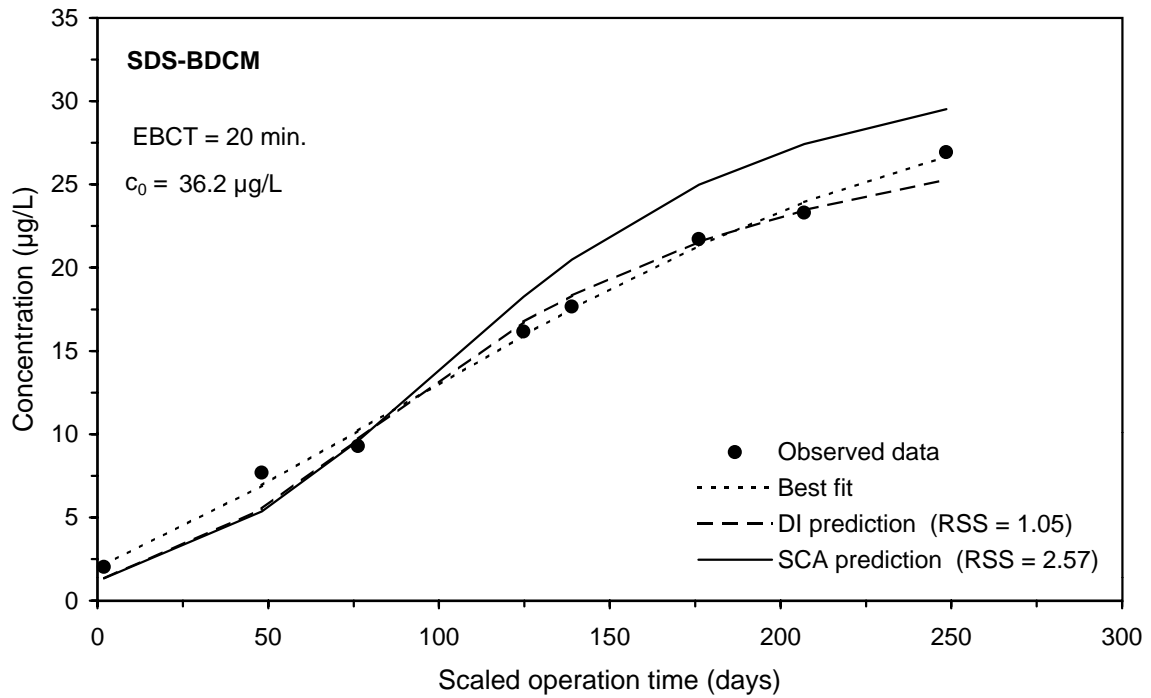


**Figure F-45 Comparison of DI and SCA methods for predicting the SDS-BDCM integral breakthrough curve for Water 3**

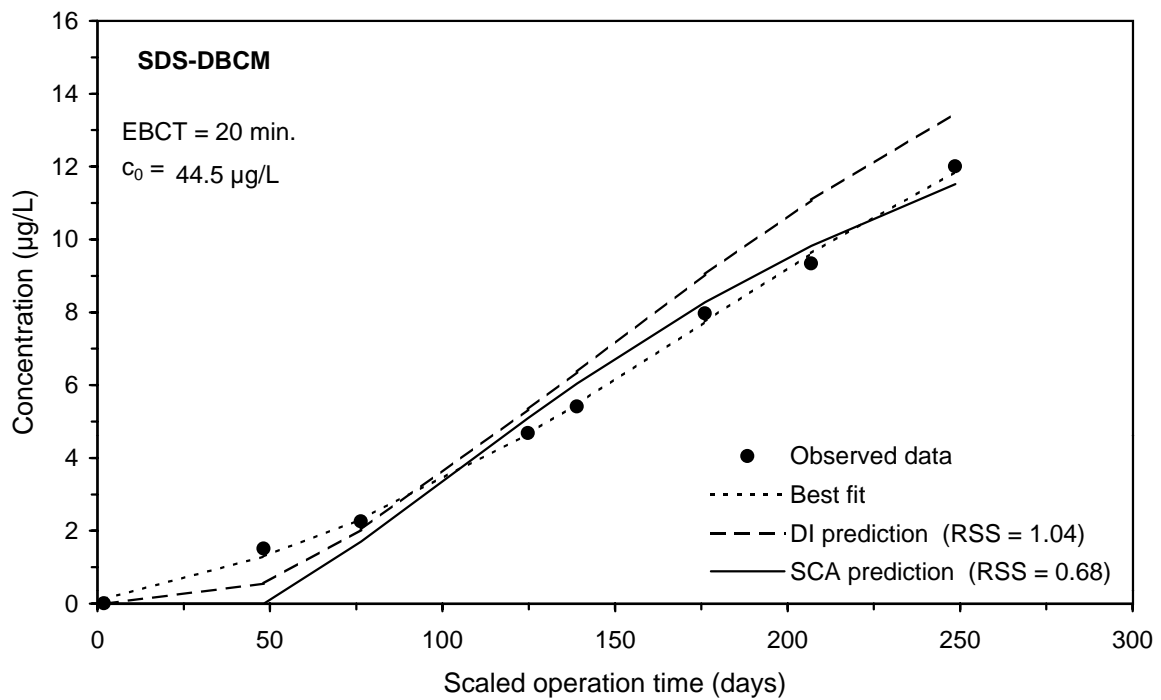


**Figure F-46 Comparison of DI and SCA methods for predicting the SDS-DBCm integral breakthrough curve for Water 3**

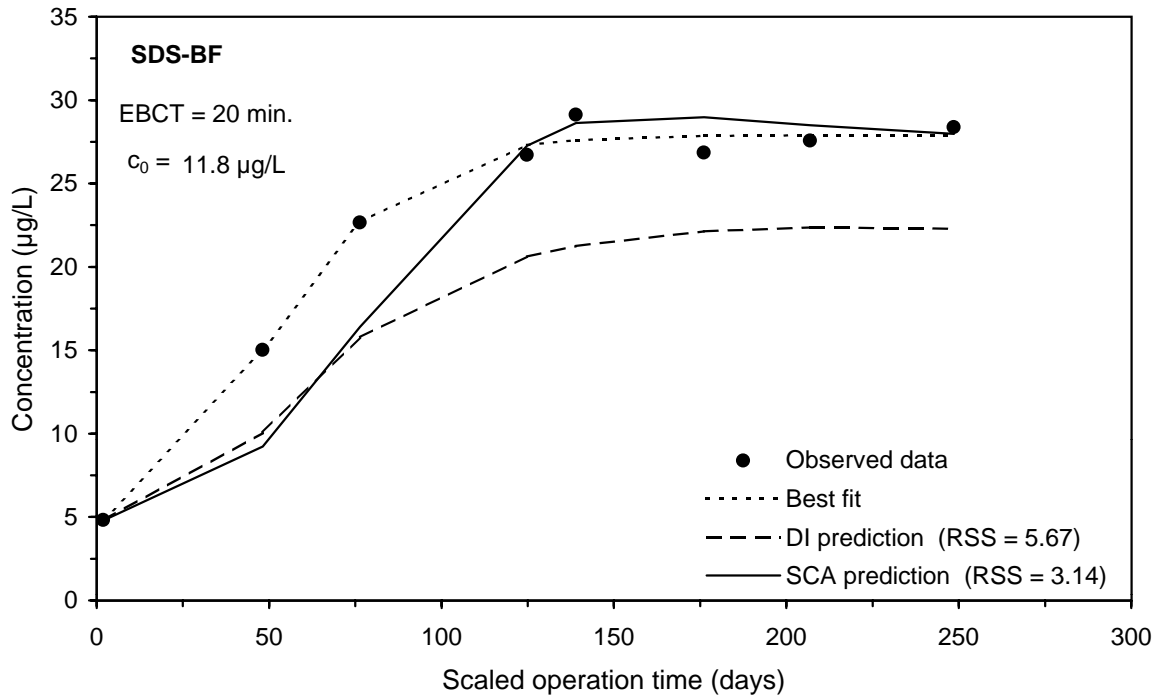


**Figure F-47 Comparison of DI and SCA methods for predicting the SDS-BF integral breakthrough curve for Water 3**

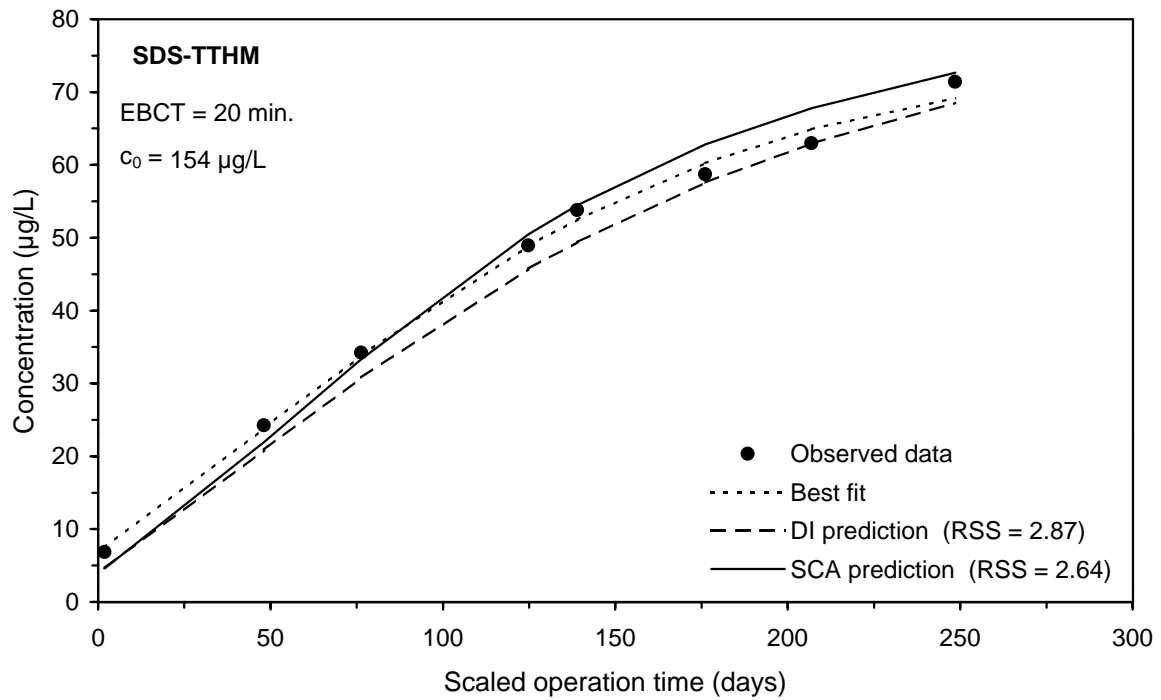


**Figure F-48 Comparison of DI and SCA methods for predicting the SDS-TTHM integral breakthrough curve for Water 3**

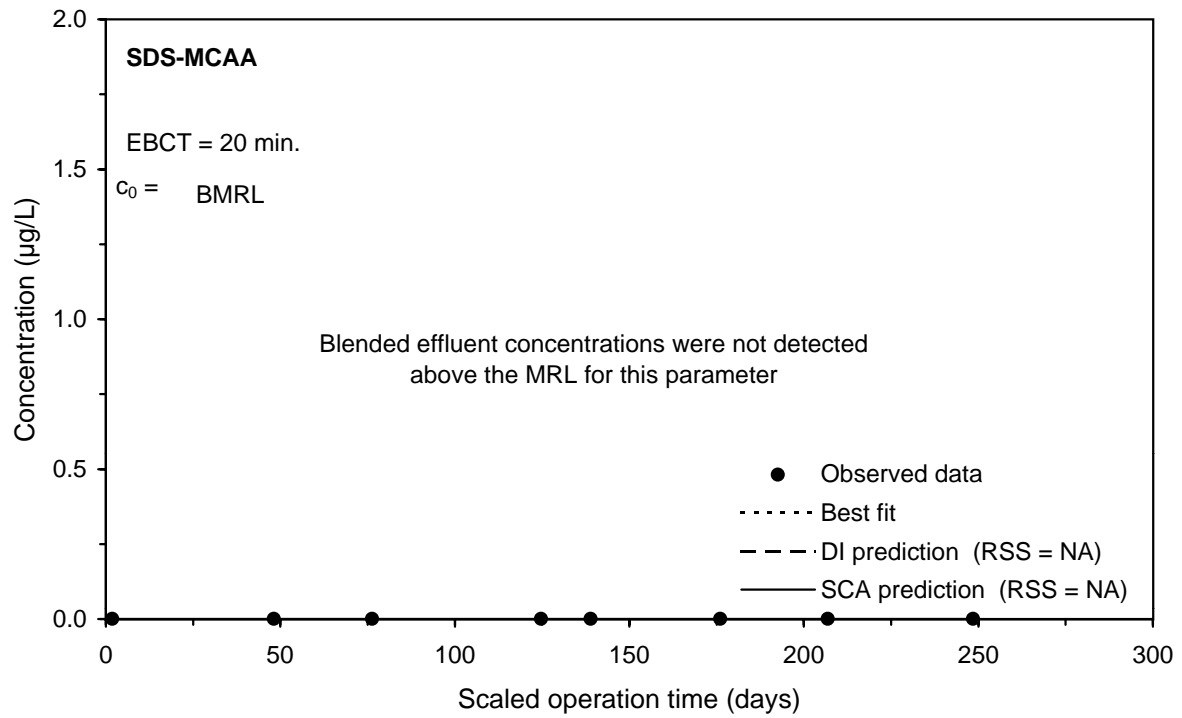


**Figure F-49 Comparison of DI and SCA methods for predicting the SDS-MCAA integral breakthrough curve for Water 3**

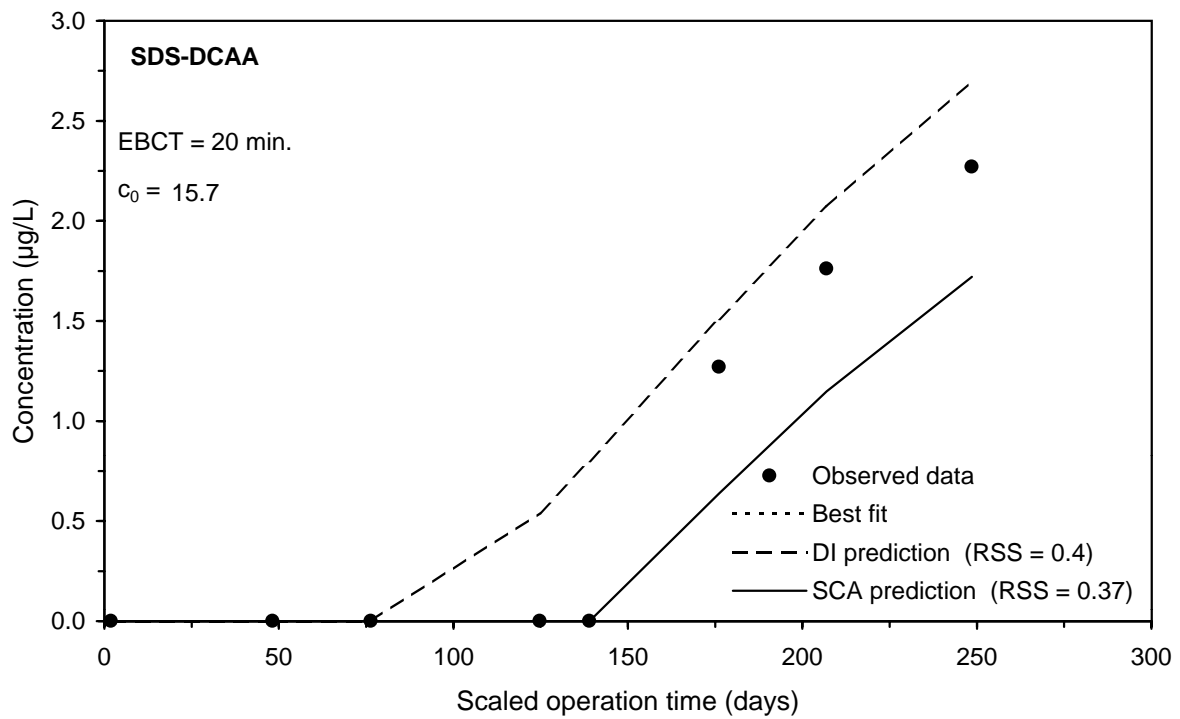


**Figure F-50 Comparison of DI and SCA methods for predicting the SDS-DCAA integral breakthrough curve for Water 3**

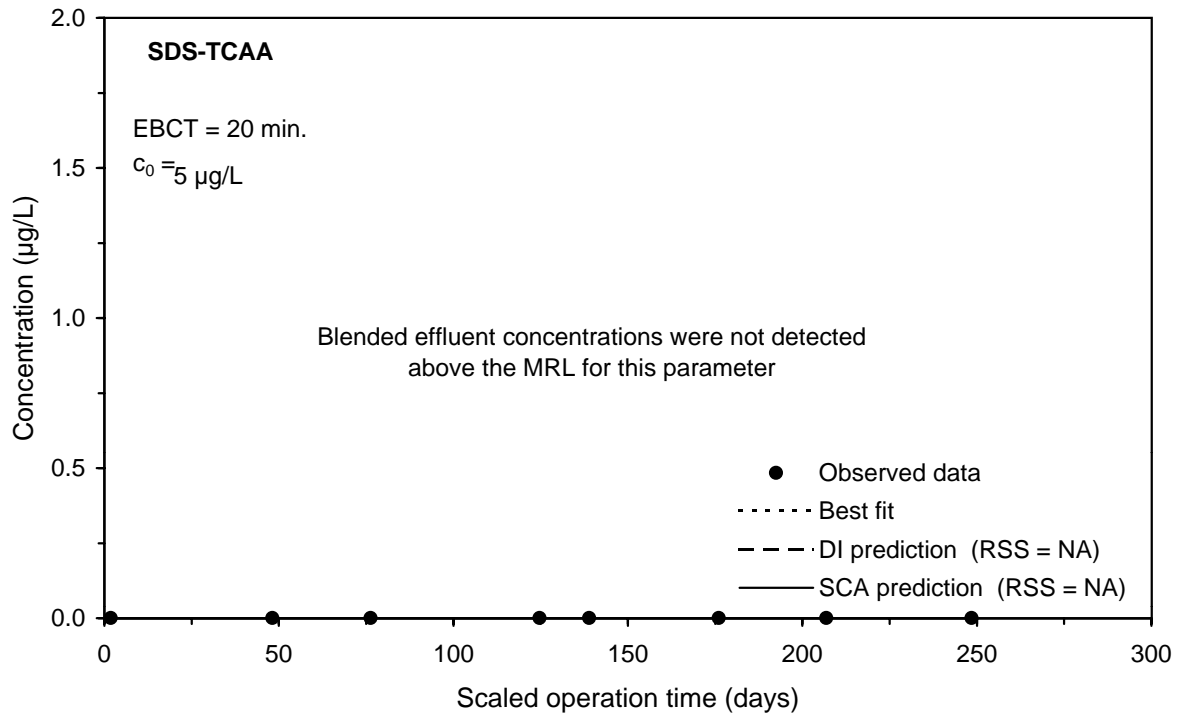


**Figure F-51 Comparison of DI and SCA methods for predicting the SDS-TCAA integral breakthrough curve for Water 3**

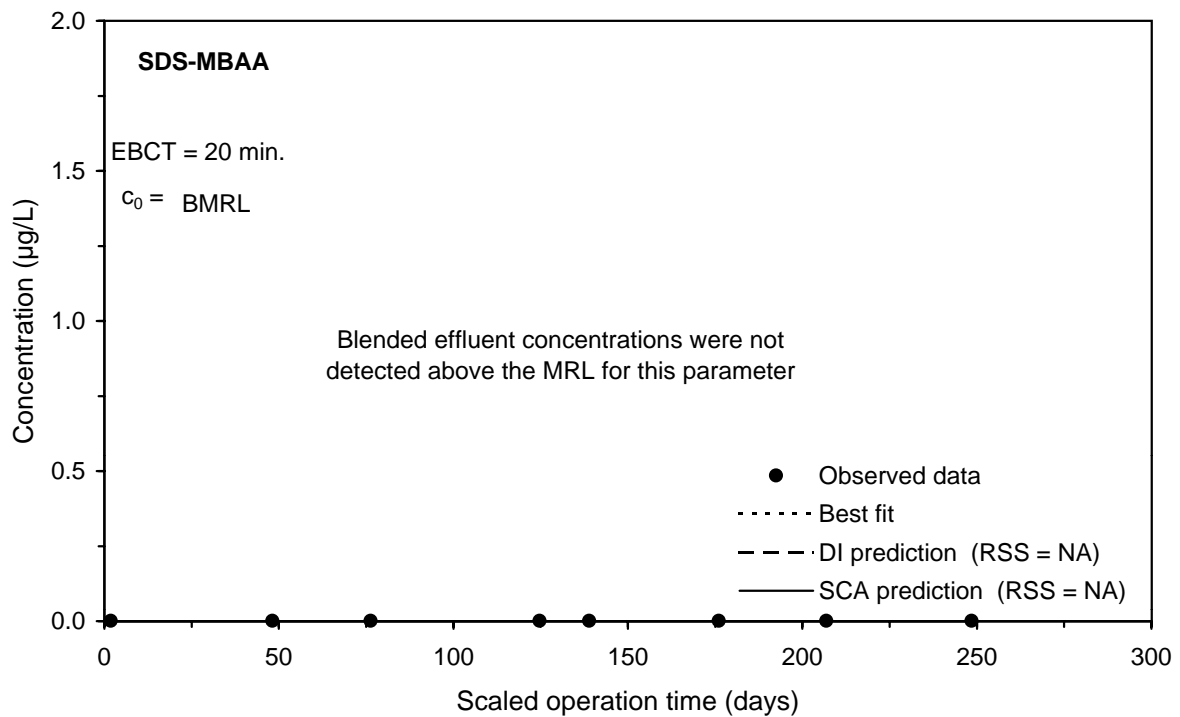


**Figure F-52 Comparison of DI and SCA methods for predicting the SDS-MBAA integral breakthrough curve for Water 3**

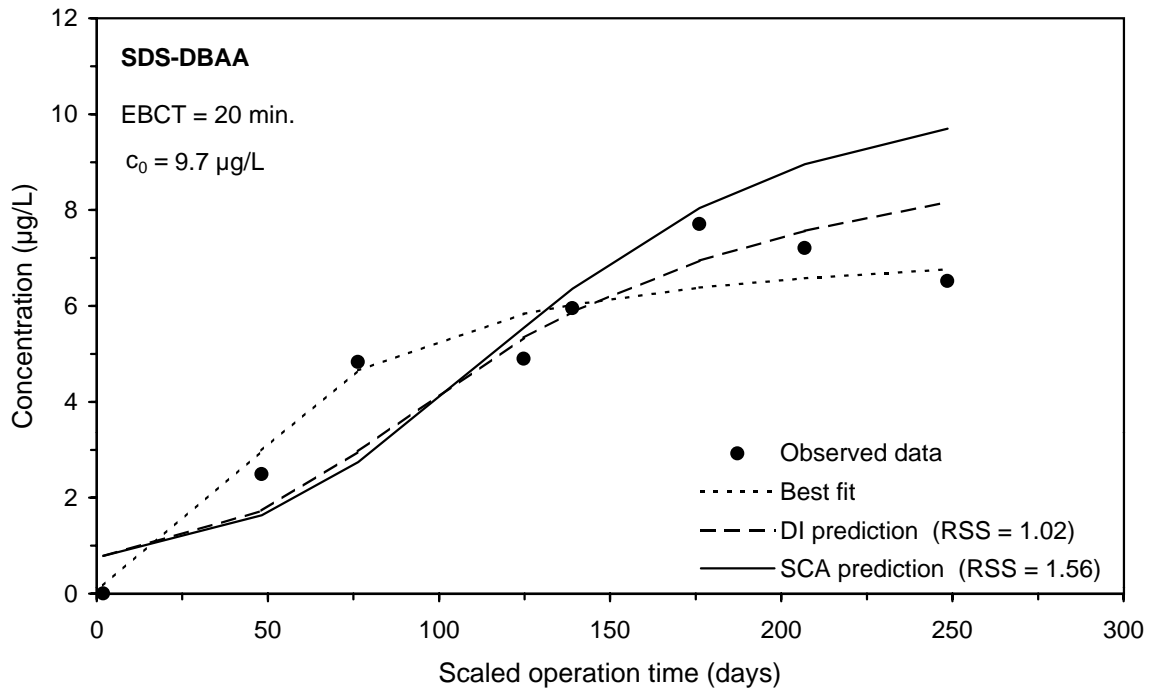


**Figure F-53 Comparison of DI and SCA methods for predicting the SDS-DBAA integral breakthrough curve for Water 3**

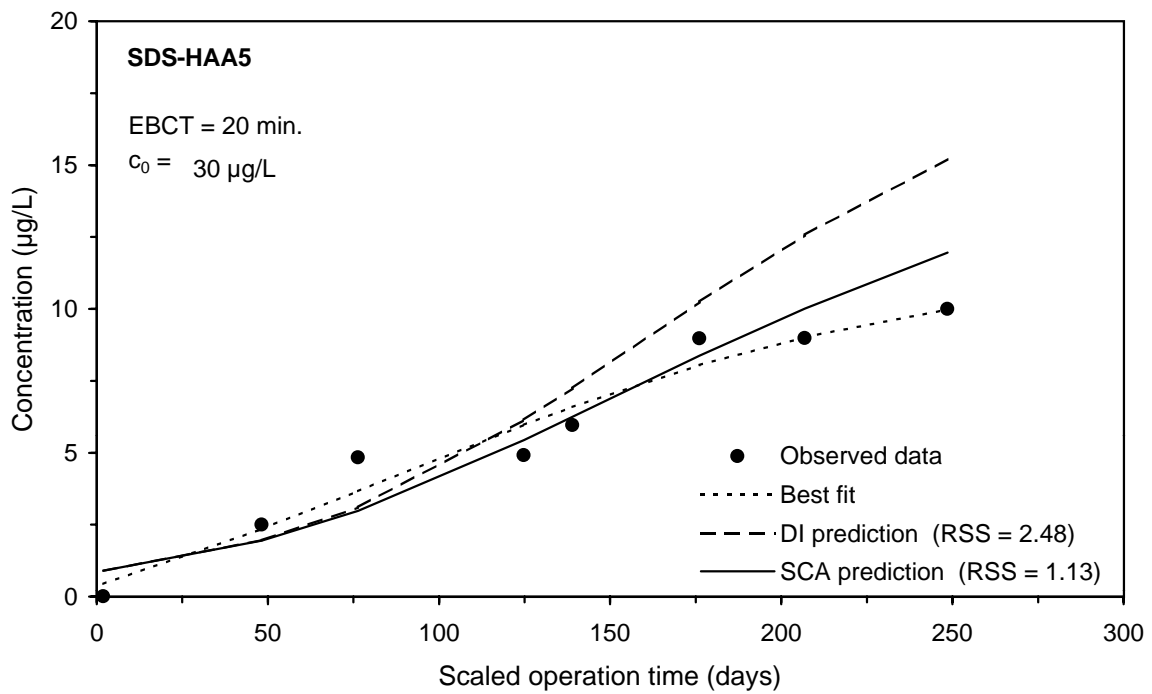


**Figure F-54 Comparison of DI and SCA methods for predicting the SDS-HAA5 integral breakthrough curve for Water 3**

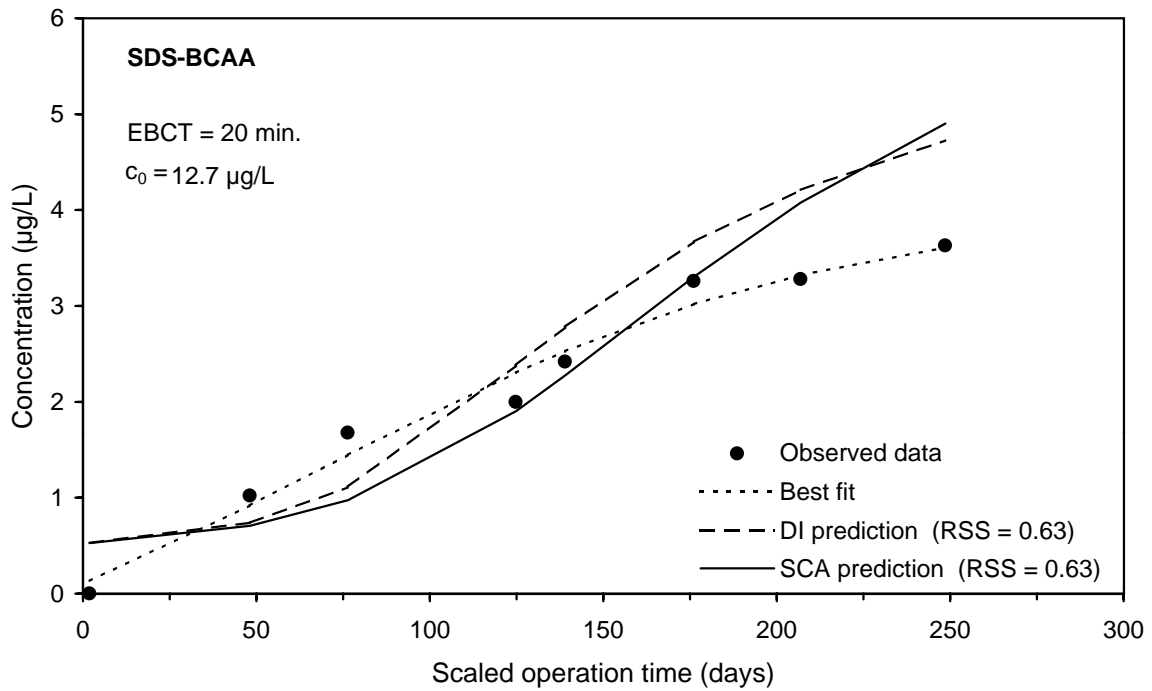


**Figure F-55 Comparison of DI and SCA methods for predicting the SDS-BCAA integral breakthrough curve for Water 3**

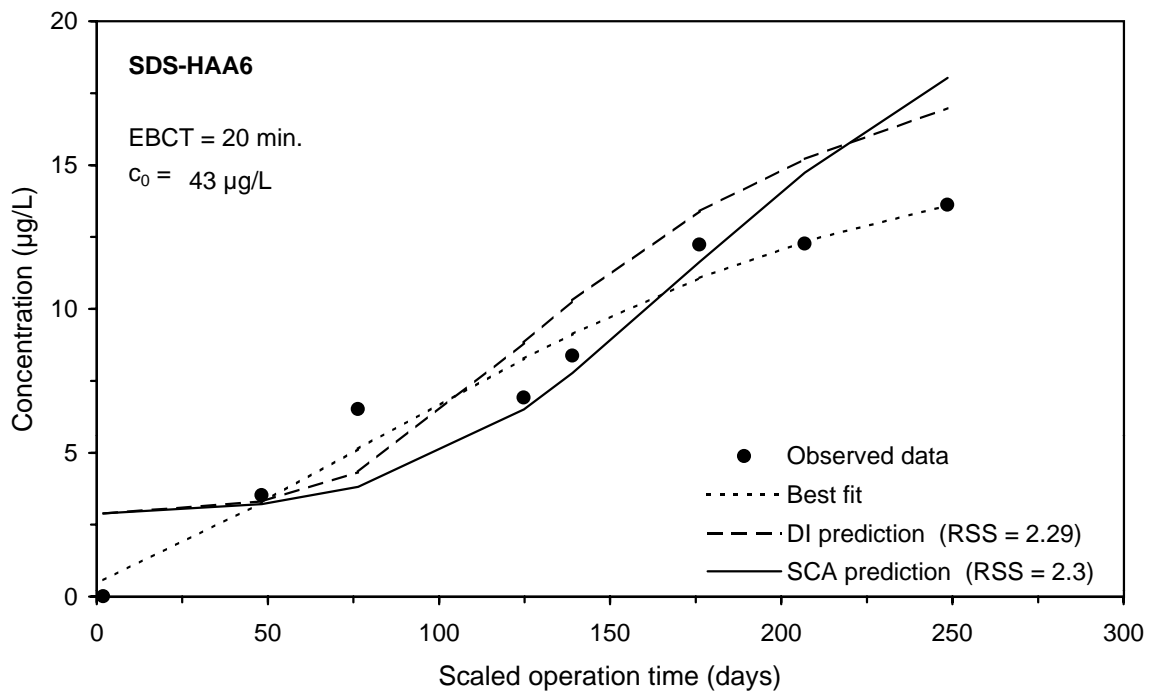


**Figure F-56 Comparison of DI and SCA methods for predicting the SDS-HAA6 integral breakthrough curve for Water 3**

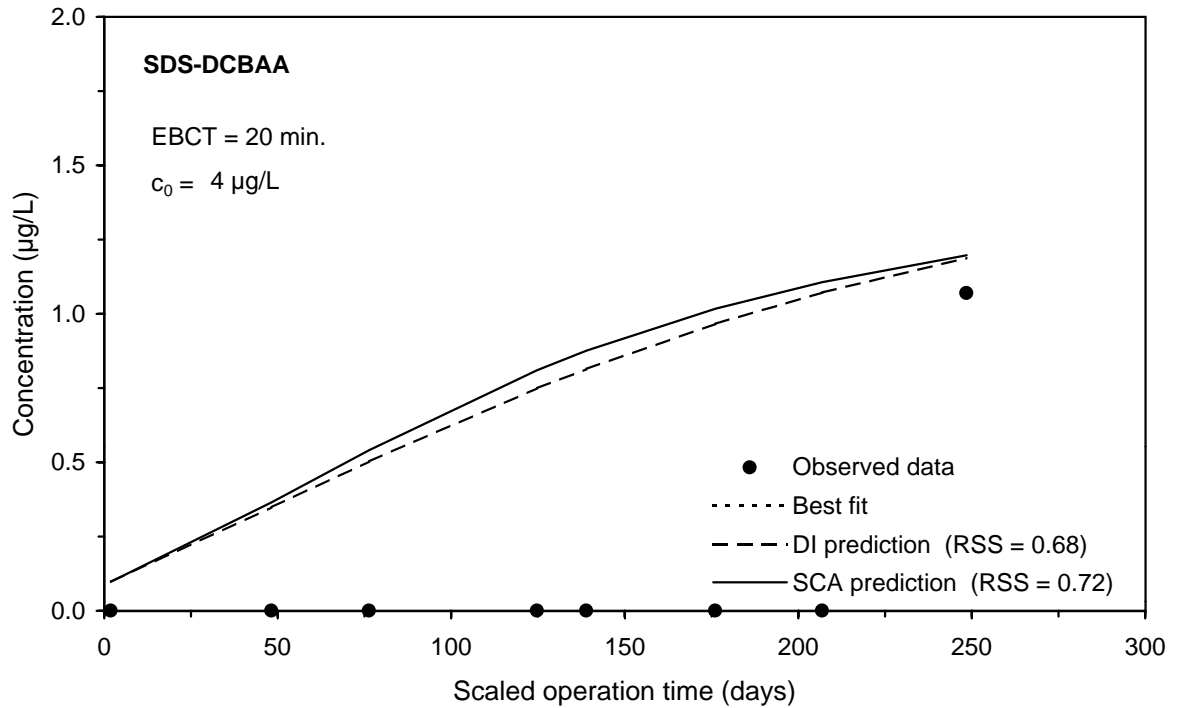


**Figure F-57 Comparison of DI and SCA methods for predicting the SDS-DCBAA integral breakthrough curve for Water 3**

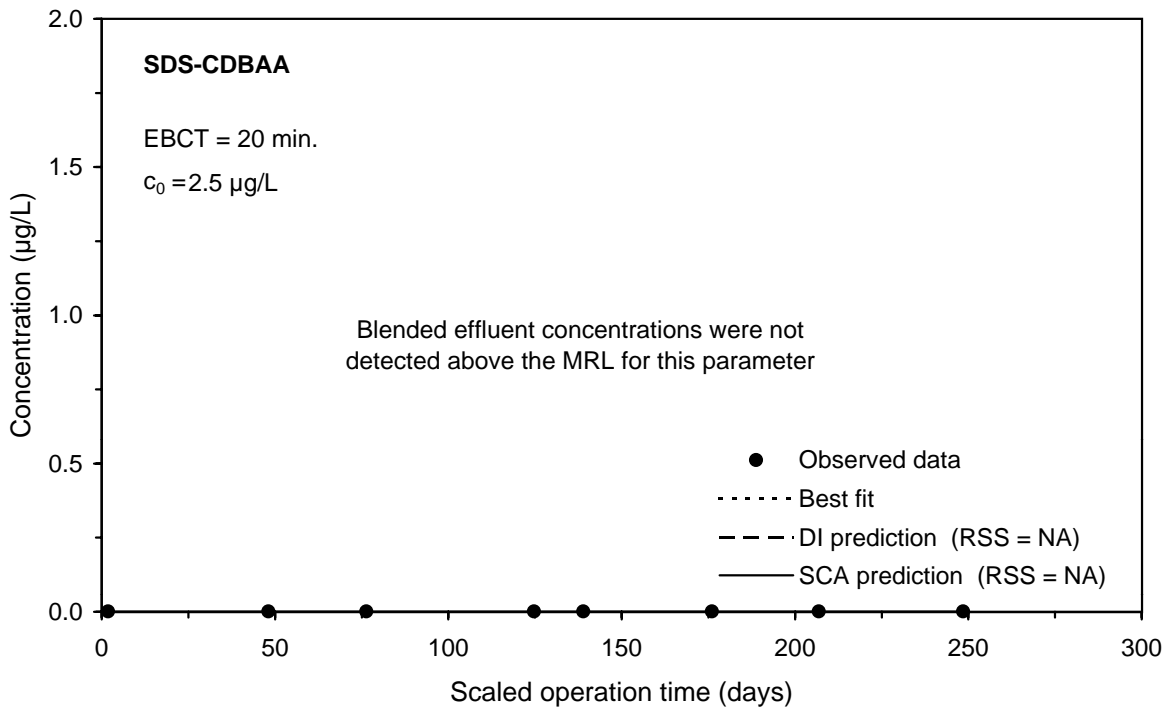


**Figure F-58 Comparison of DI and SCA methods for predicting the SDS-CDBAA integral breakthrough curve for Water 3**

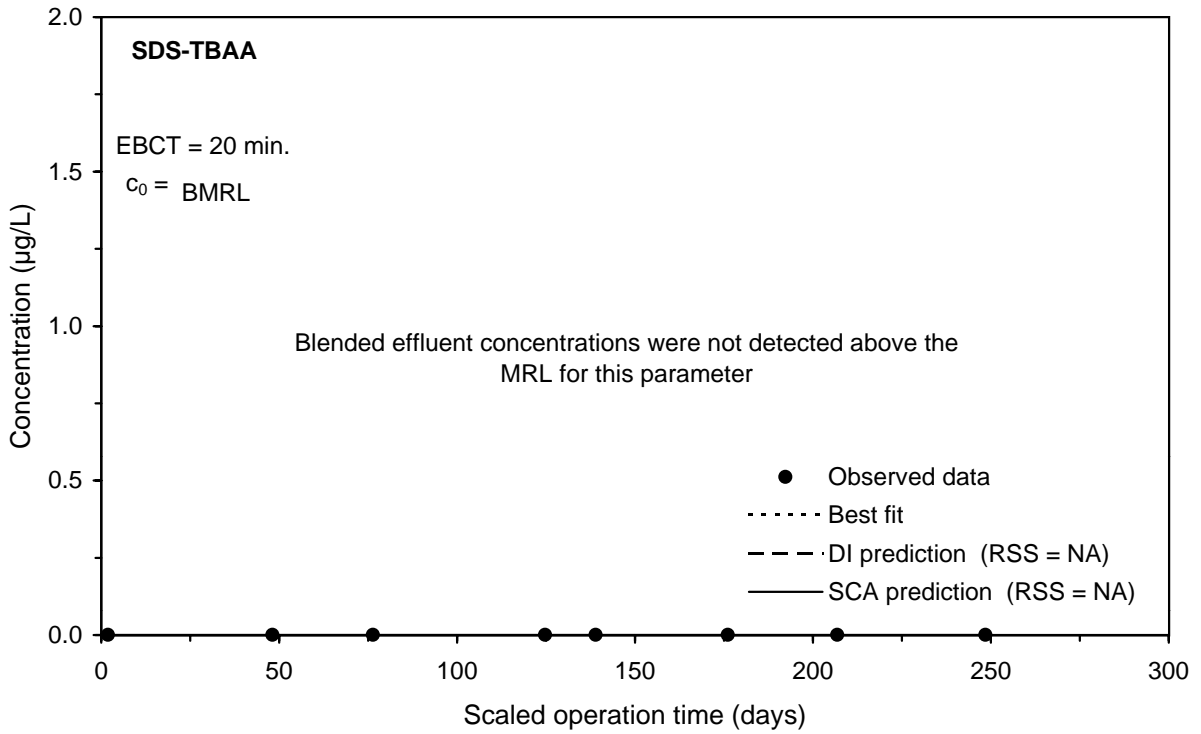


**Figure F-59 Comparison of DI and SCA methods for predicting the SDS-TBAA integral breakthrough curve for Water 3**

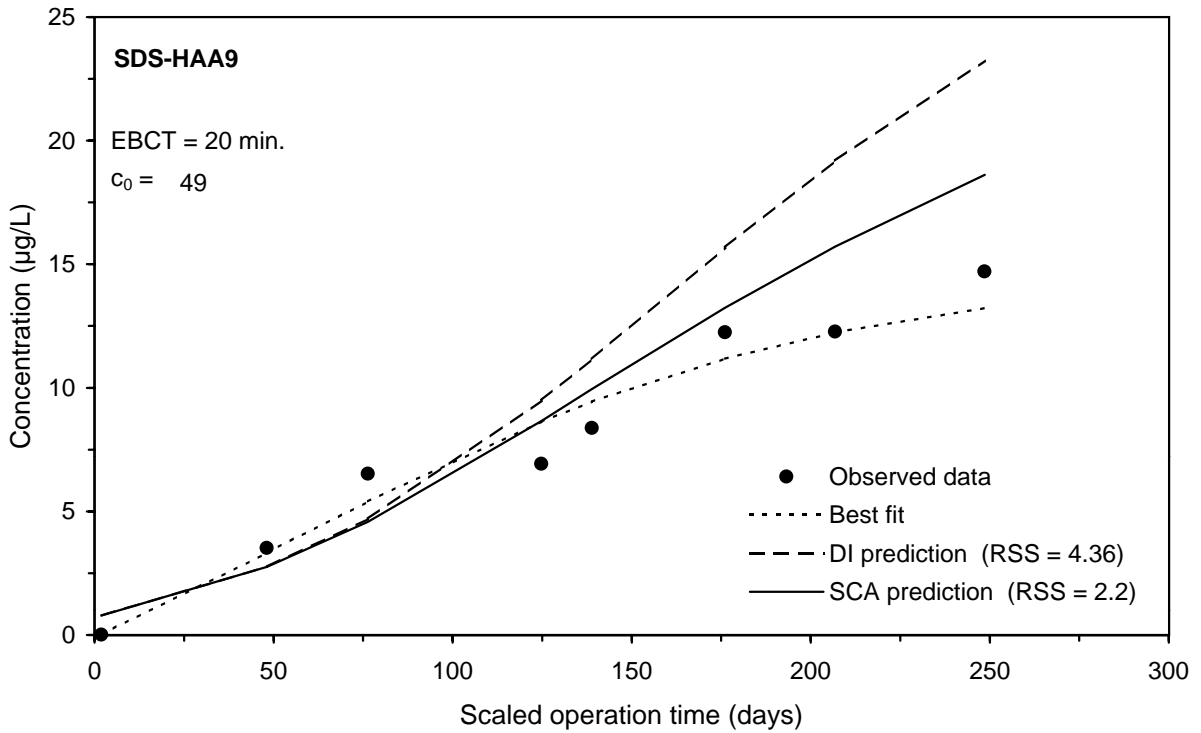


**Figure F-60 Comparison of DI and SCA methods for predicting the SDS-HAA9 integral breakthrough curve for Water 3**

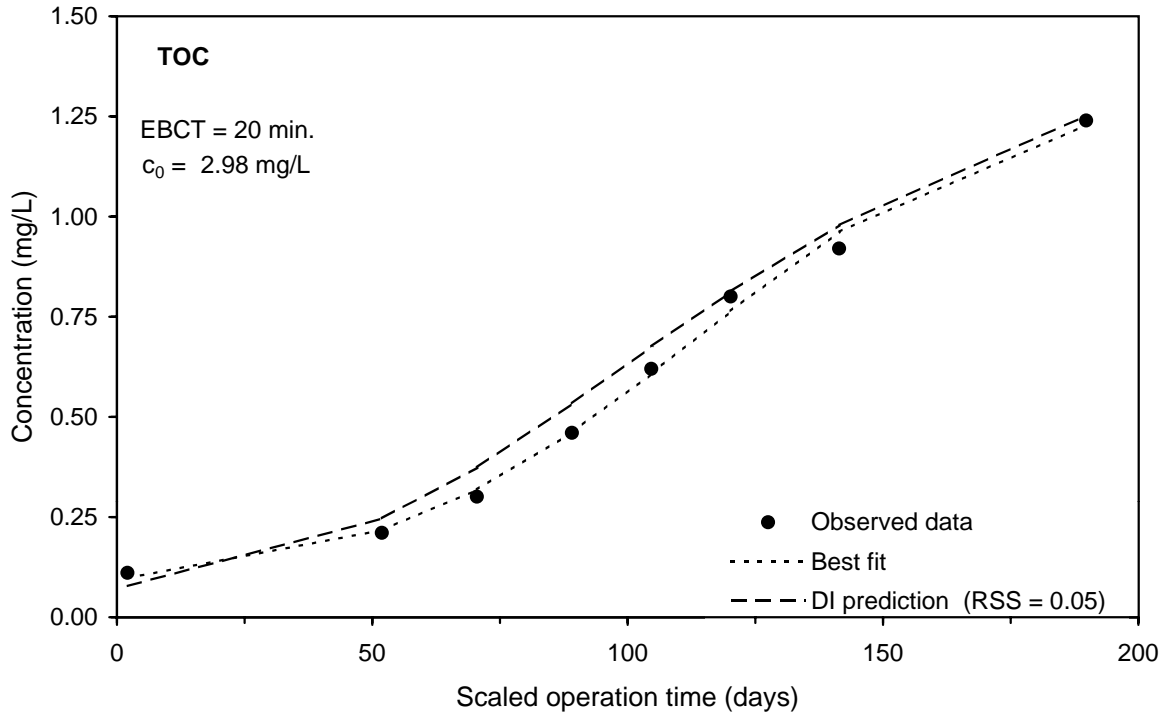


**Figure F-61 DI method prediction of the TOC integral breakthrough curve for Water 4**

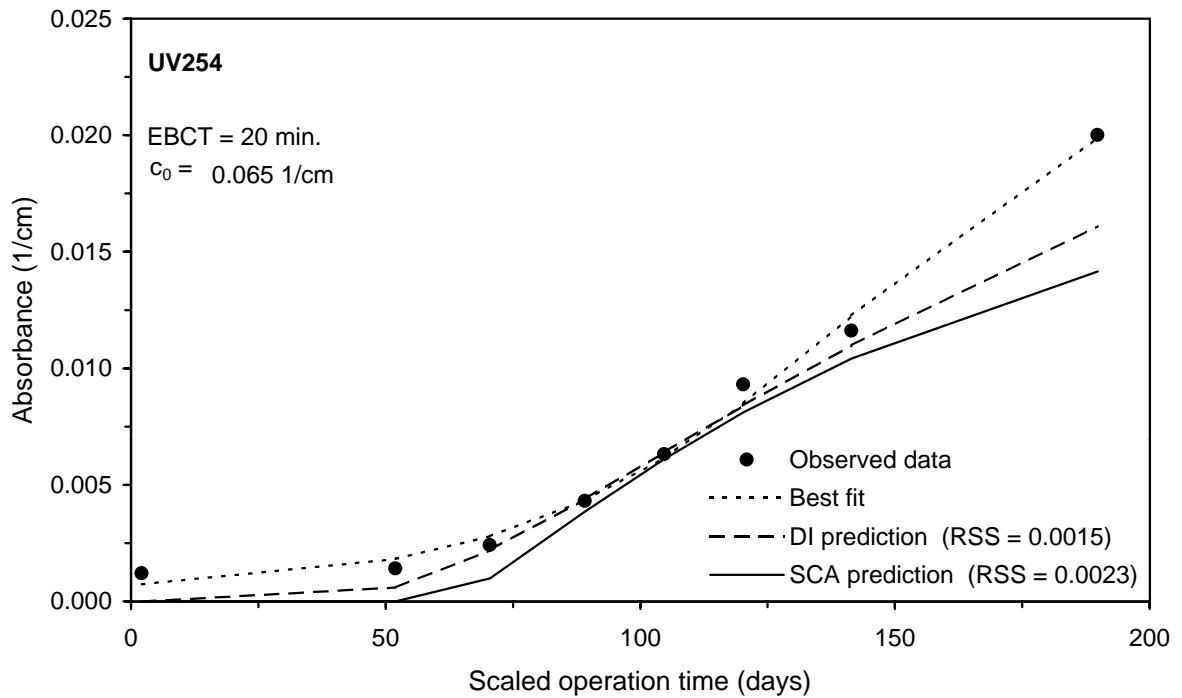


**Figure F-62 Comparison of DI and SCA methods for predicting the UV254 integral breakthrough curve for Water 4**

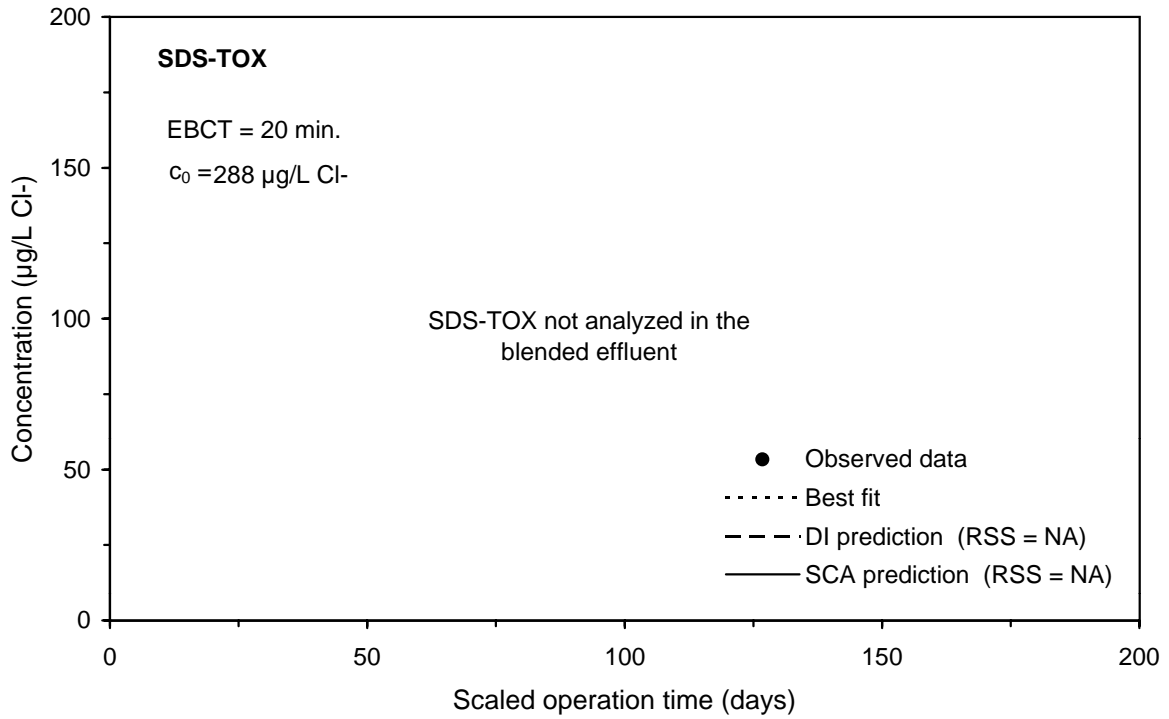


**Figure F-63 Comparison of DI and SCA methods for predicting the SDS-TOX integral breakthrough curve for Water 4**

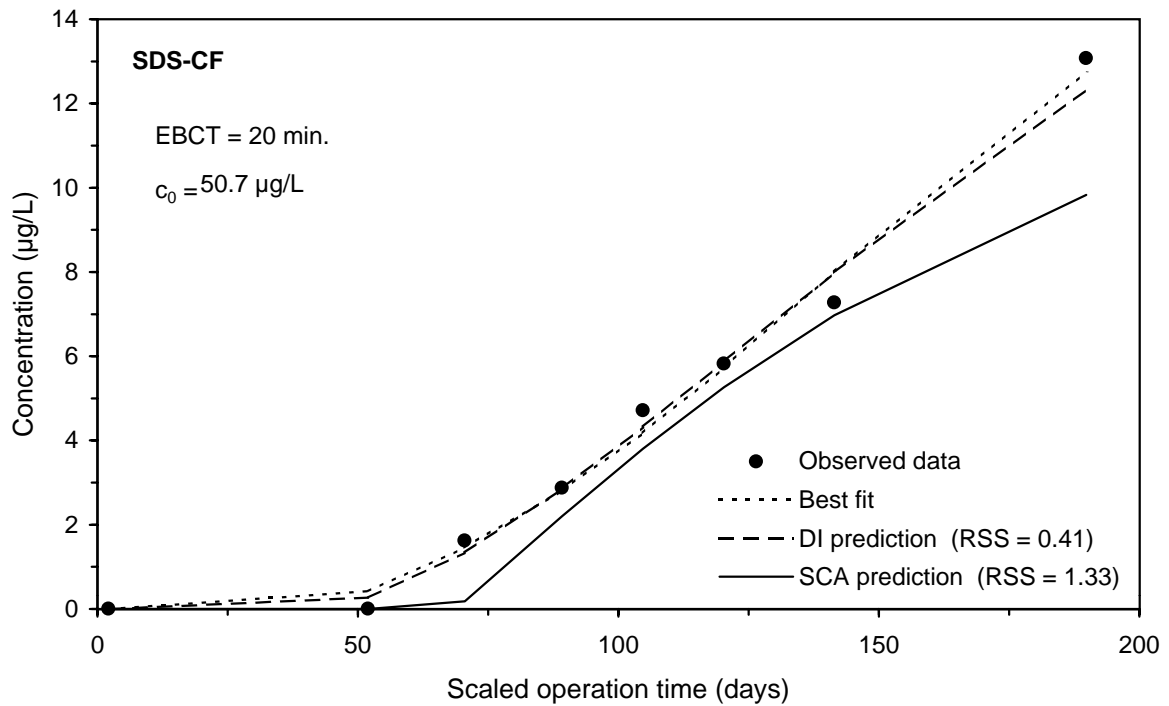


**Figure F-64 Comparison of DI and SCA methods for predicting the SDS-CF integral breakthrough curve for Water 4**

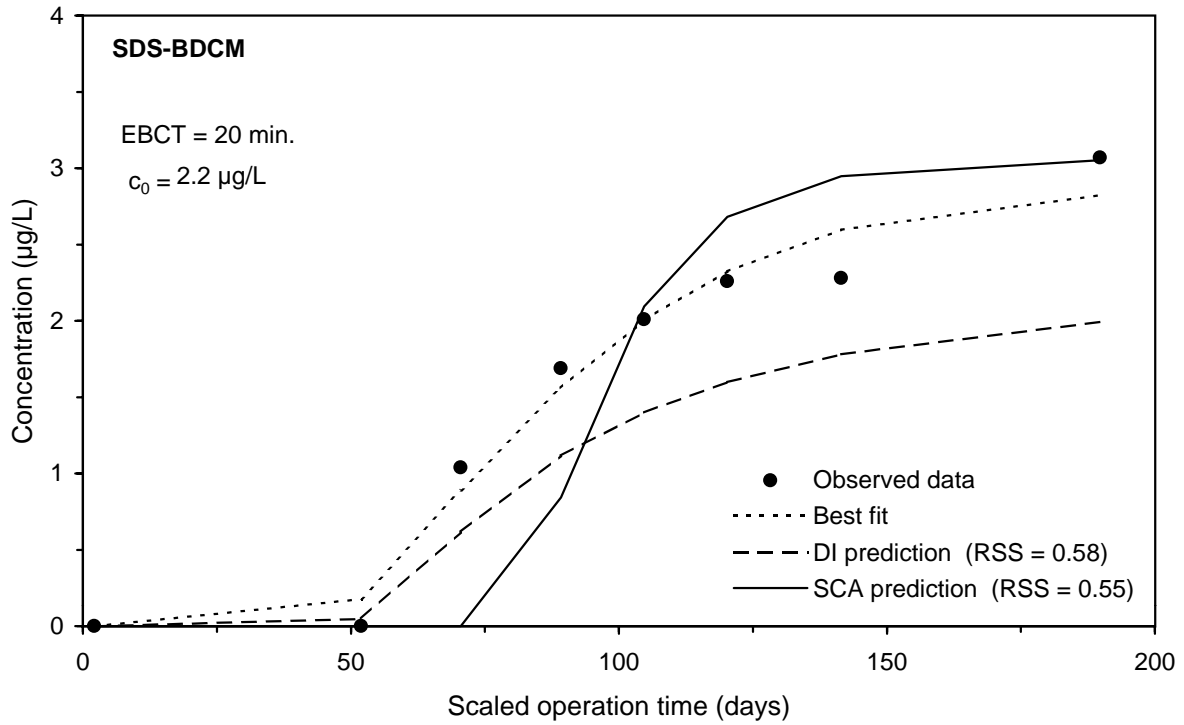


**Figure F-65 Comparison of DI and SCA methods for predicting the SDS-BDCM integral breakthrough curve for Water 4**

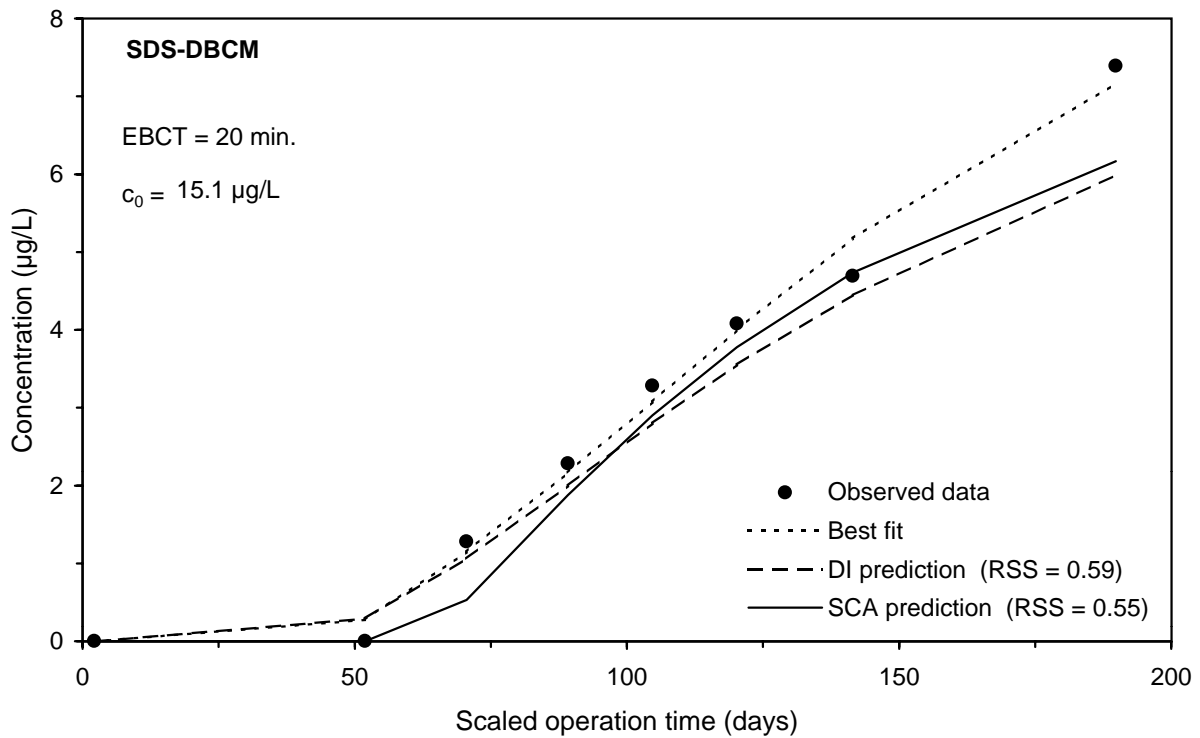


**Figure F-66 Comparison of DI and SCA methods for predicting the SDS-DBCm integral breakthrough curve for Water 4**

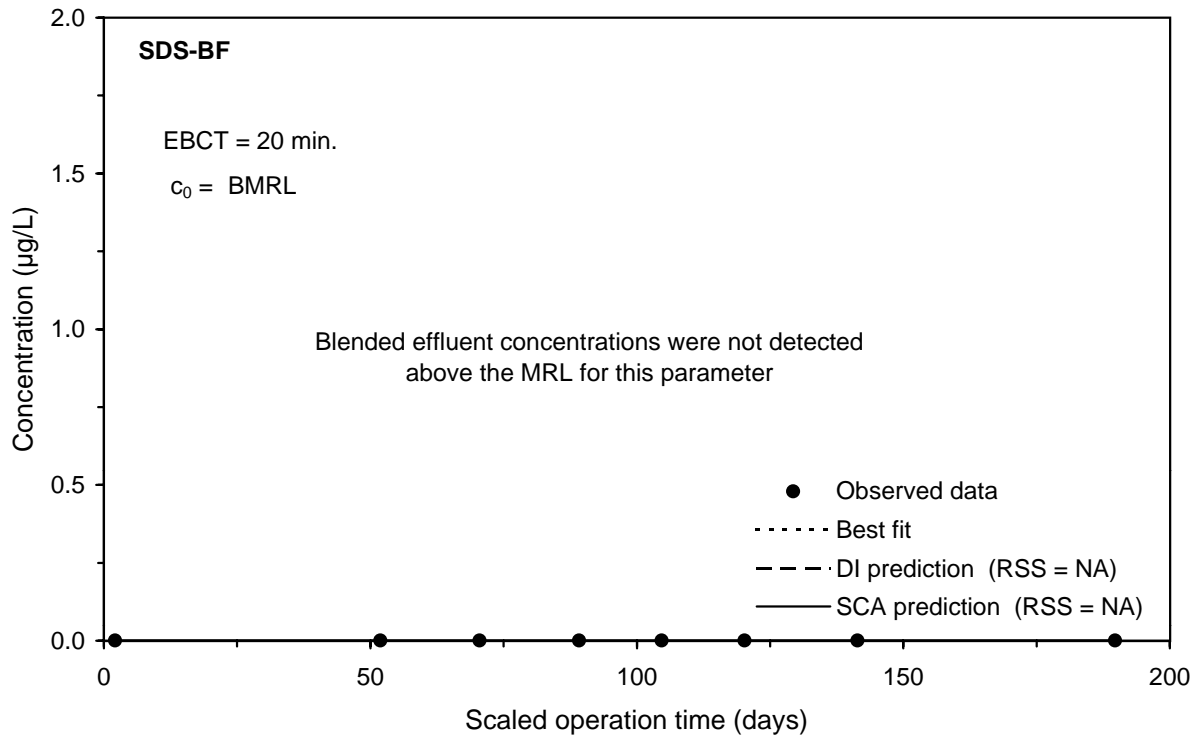


**Figure F-67 Comparison of DI and SCA methods for predicting the SDS-BF integral breakthrough curve for Water 4**

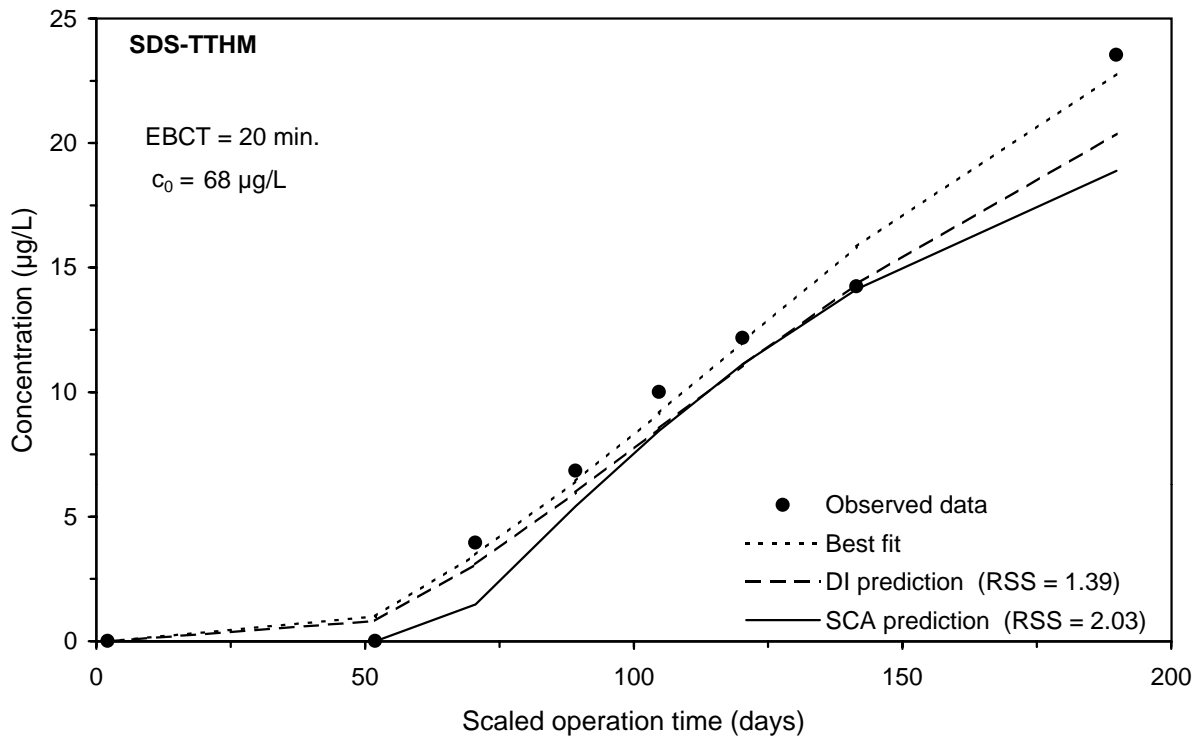


**Figure F-68 Comparison of DI and SCA methods for predicting the SDS-TTHM integral breakthrough curve for Water 4**

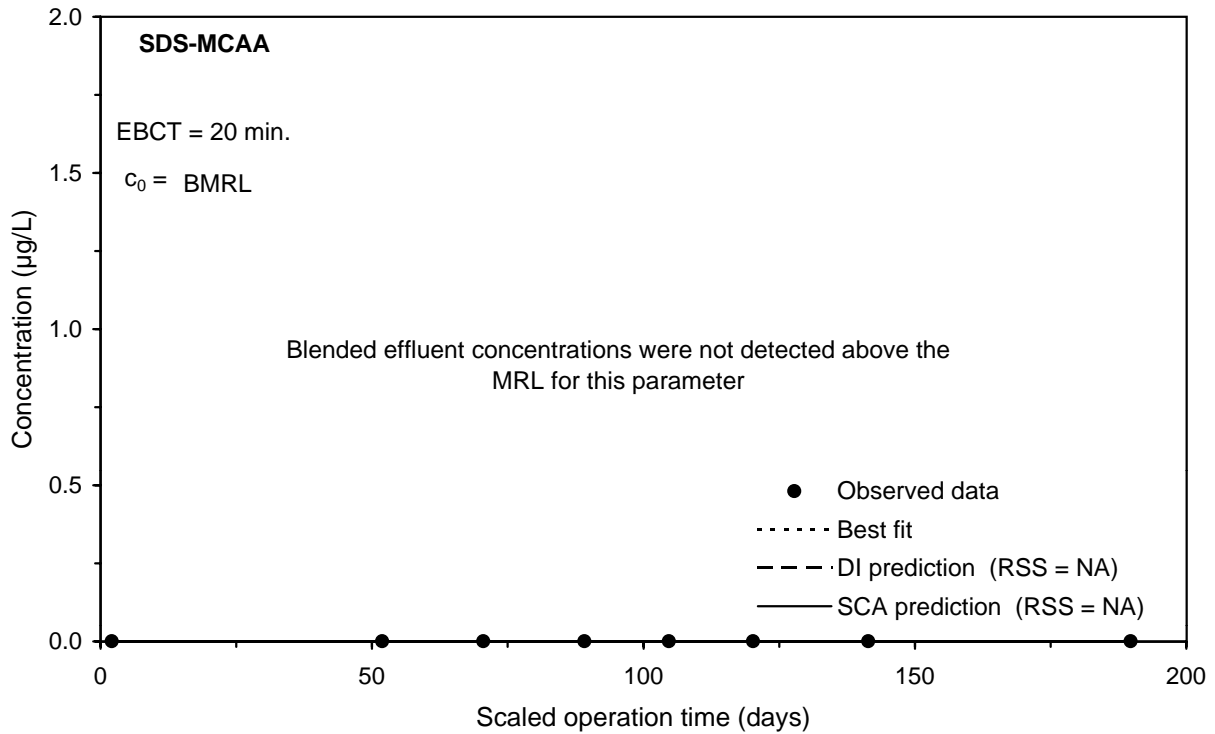


**Figure F-69 Comparison of DI and SCA methods for predicting the SDS-MCAA integral breakthrough curve for Water 4**

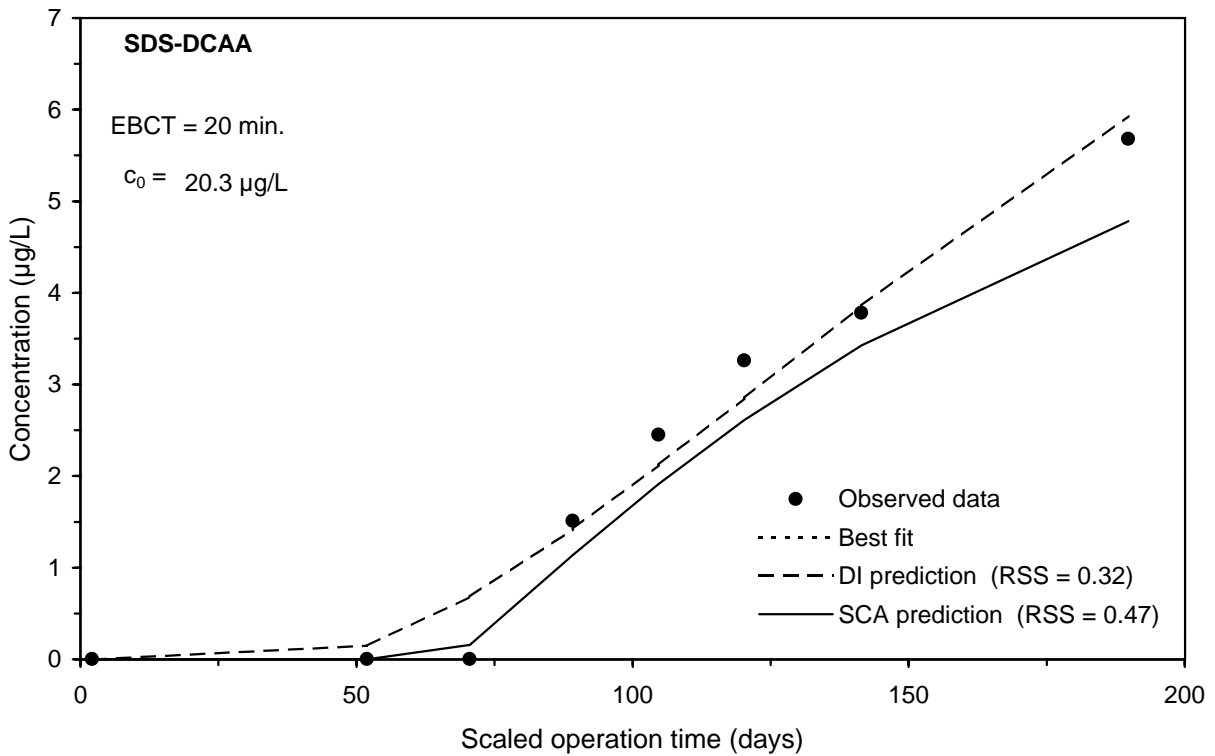


**Figure F-70 Comparison of DI and SCA methods for predicting the SDS-DCAA integral breakthrough curve for Water 4**

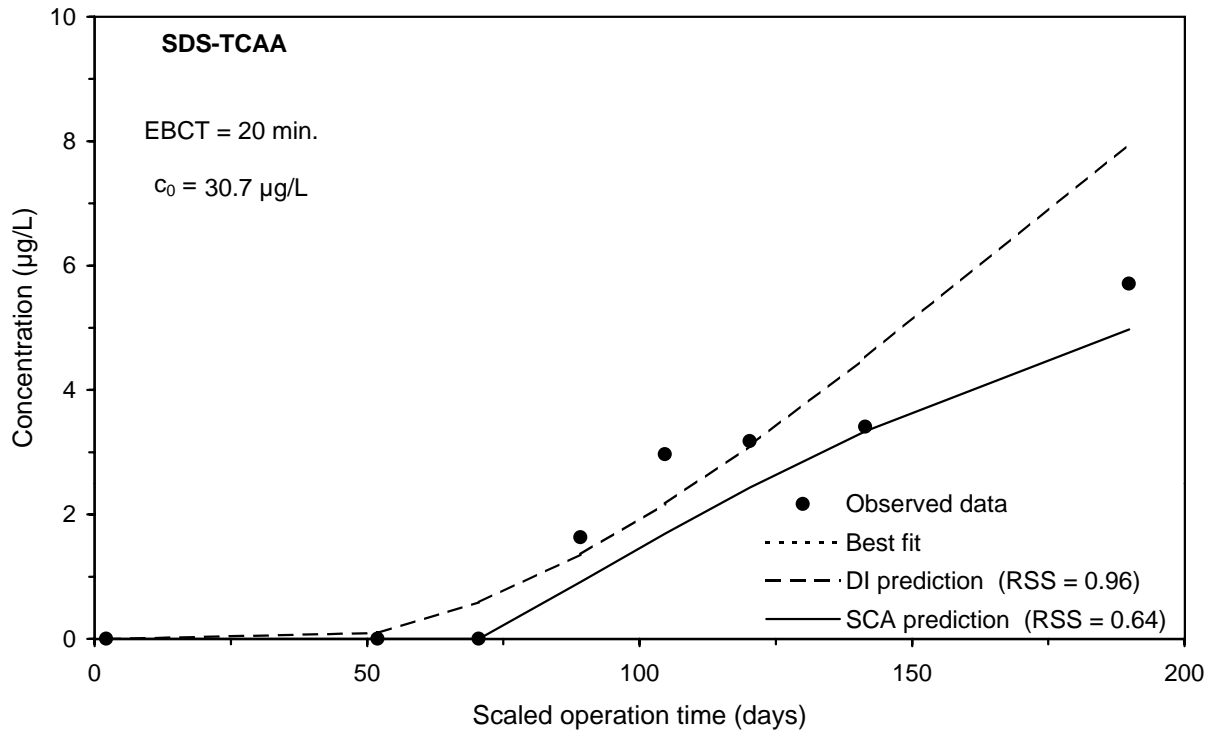


**Figure F-71 Comparison of DI and SCA methods for predicting the SDS-TCAA integral breakthrough curve for Water 4**

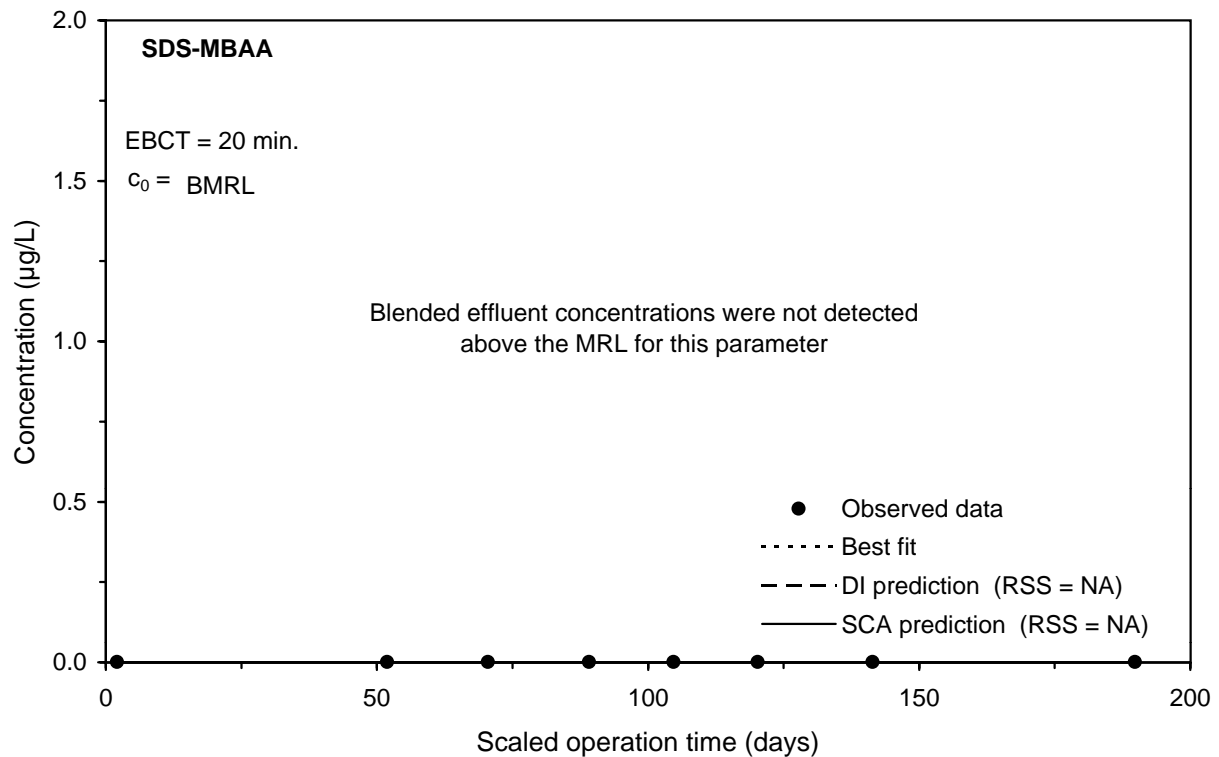


**Figure F-72 Comparison of DI and SCA methods for predicting the SDS-MBAA integral breakthrough curve for Water 4**

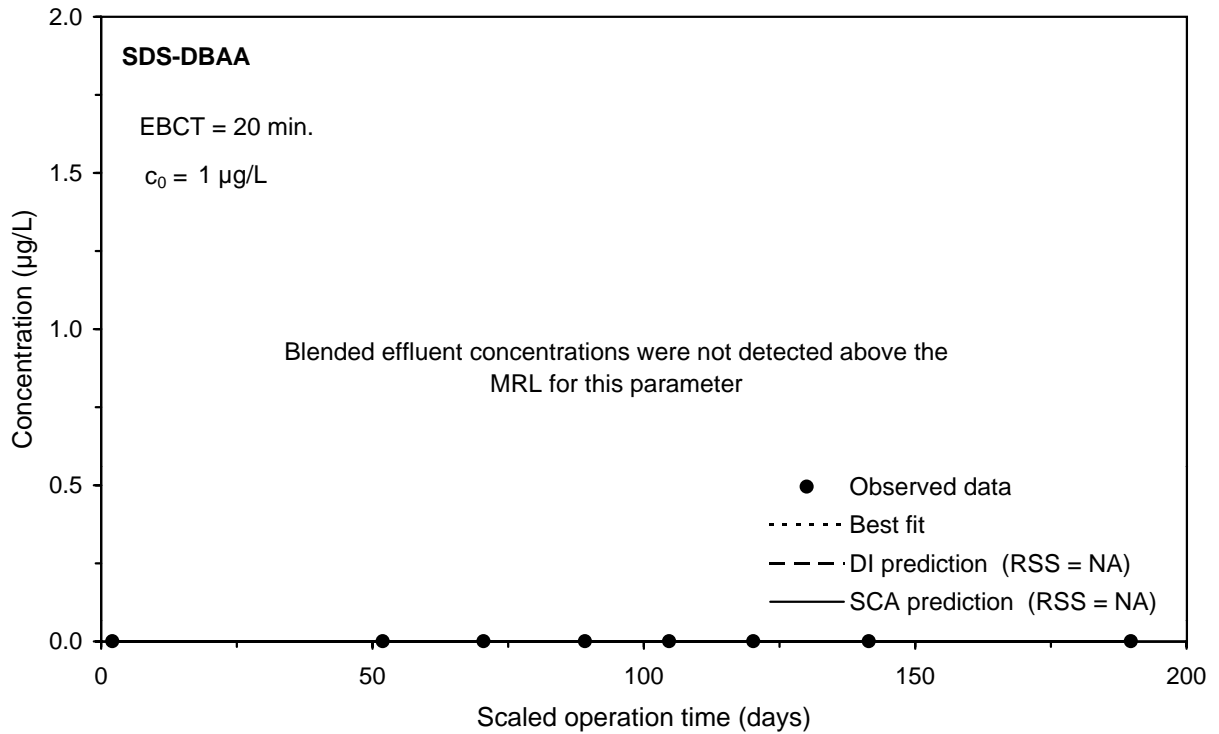


**Figure F-73 Comparison of DI and SCA methods for predicting the SDS-DBAA integral breakthrough curve for Water 4**

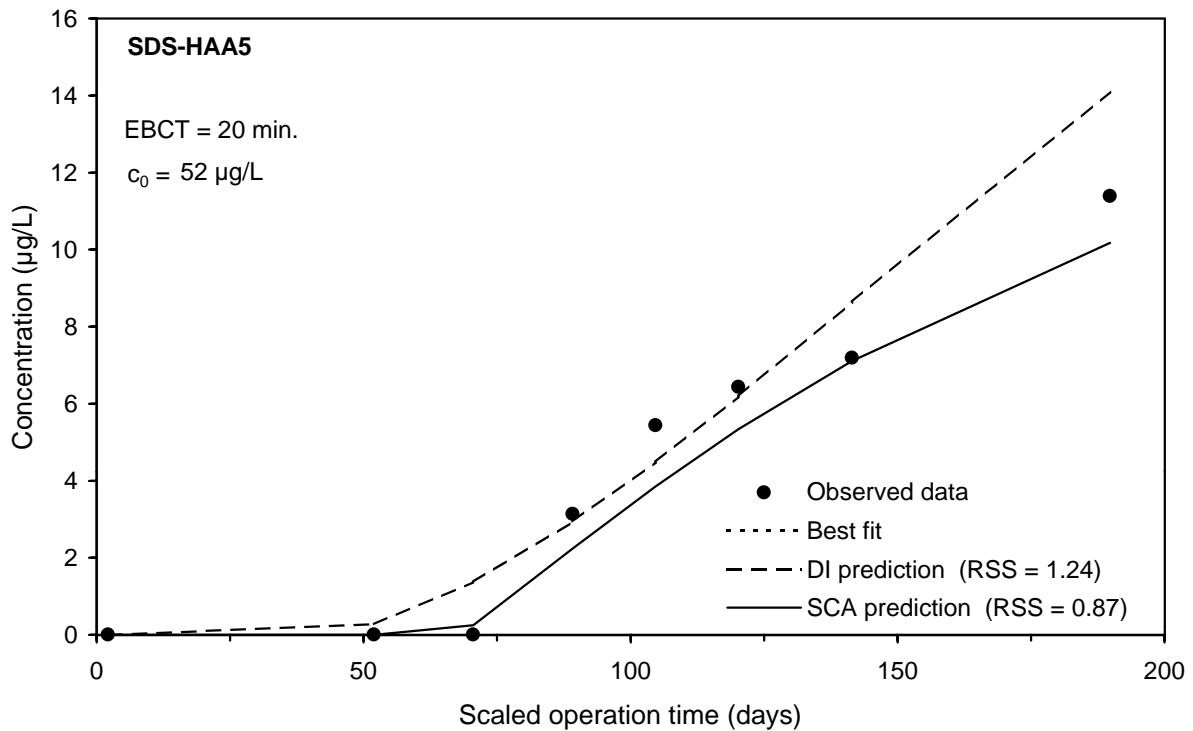


**Figure F-74 Comparison of DI and SCA methods for predicting the SDS-HAA5 integral breakthrough curve for Water 4**

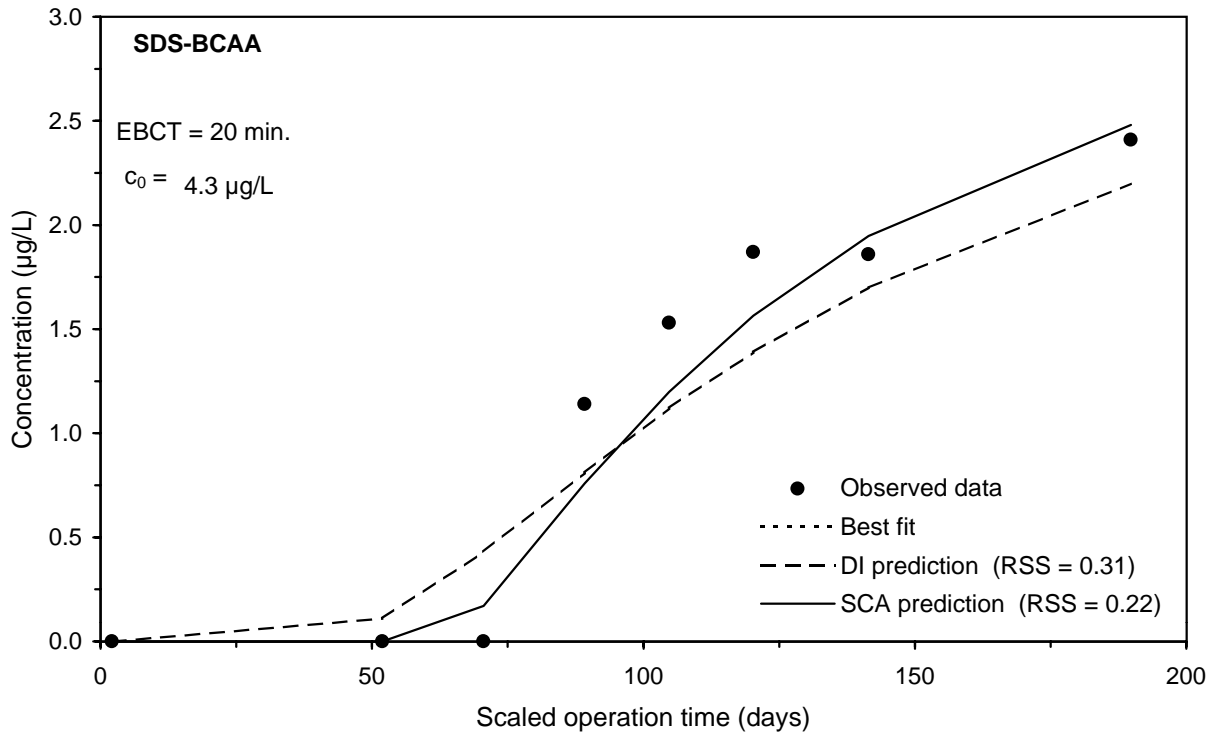


**Figure F-75 Comparison of DI and SCA methods for predicting the SDS-BCAA integral breakthrough curve for Water 4**

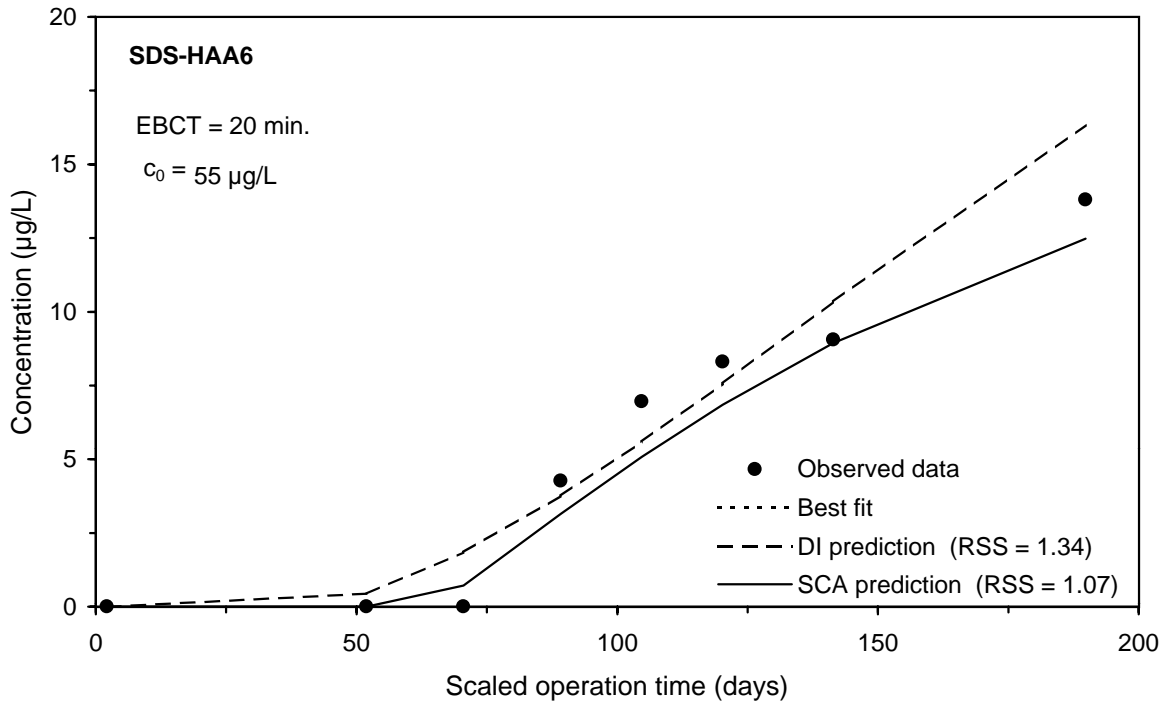


**Figure F-76 Comparison of DI and SCA methods for predicting the SDS-HAA6 integral breakthrough curve for Water 4**

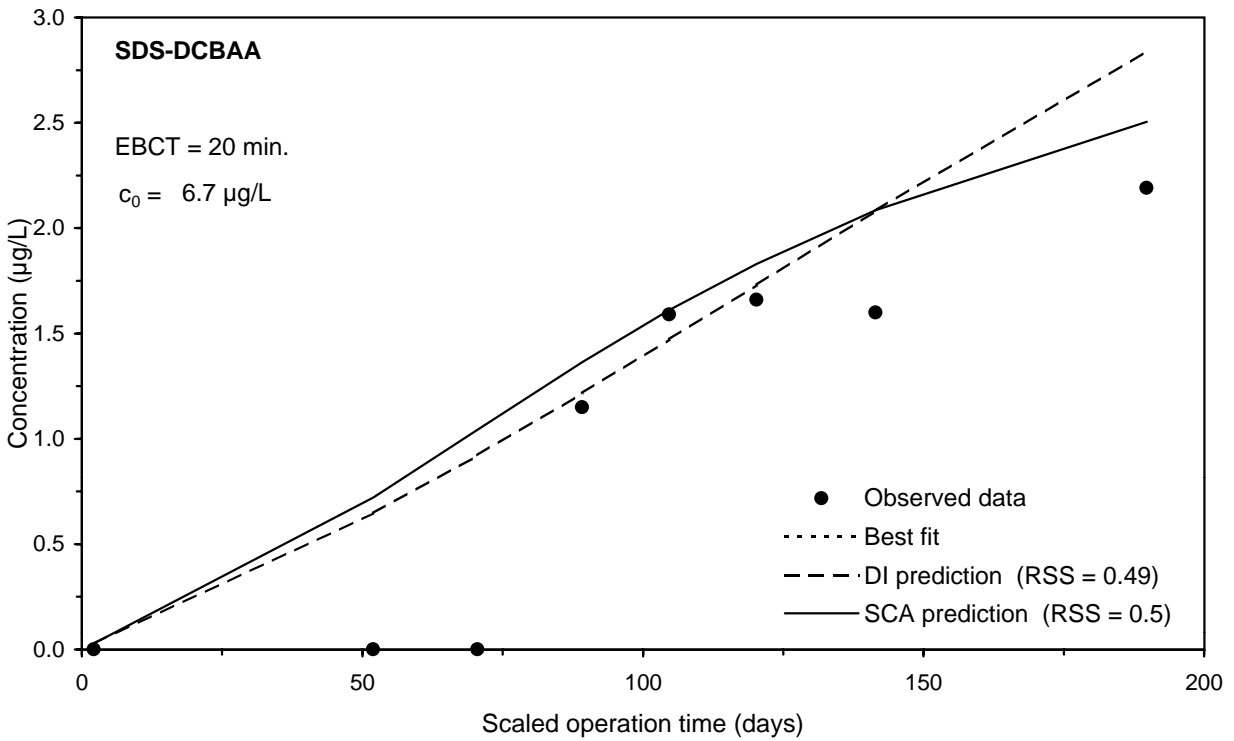


**Figure F-77 Comparison of DI and SCA methods for predicting the SDS-DCBAA integral breakthrough curve for Water 4**

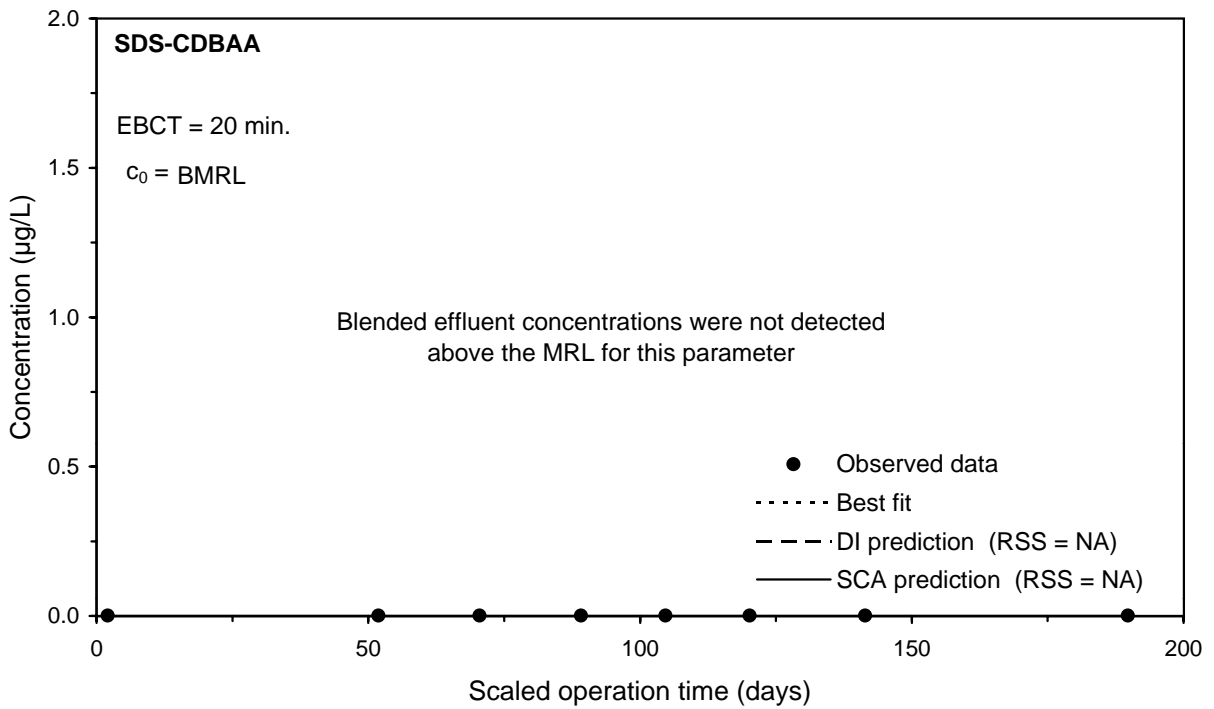


**Figure F-78 Comparison of DI and SCA methods for predicting the SDS-CDBAA integral breakthrough curve for Water 4**

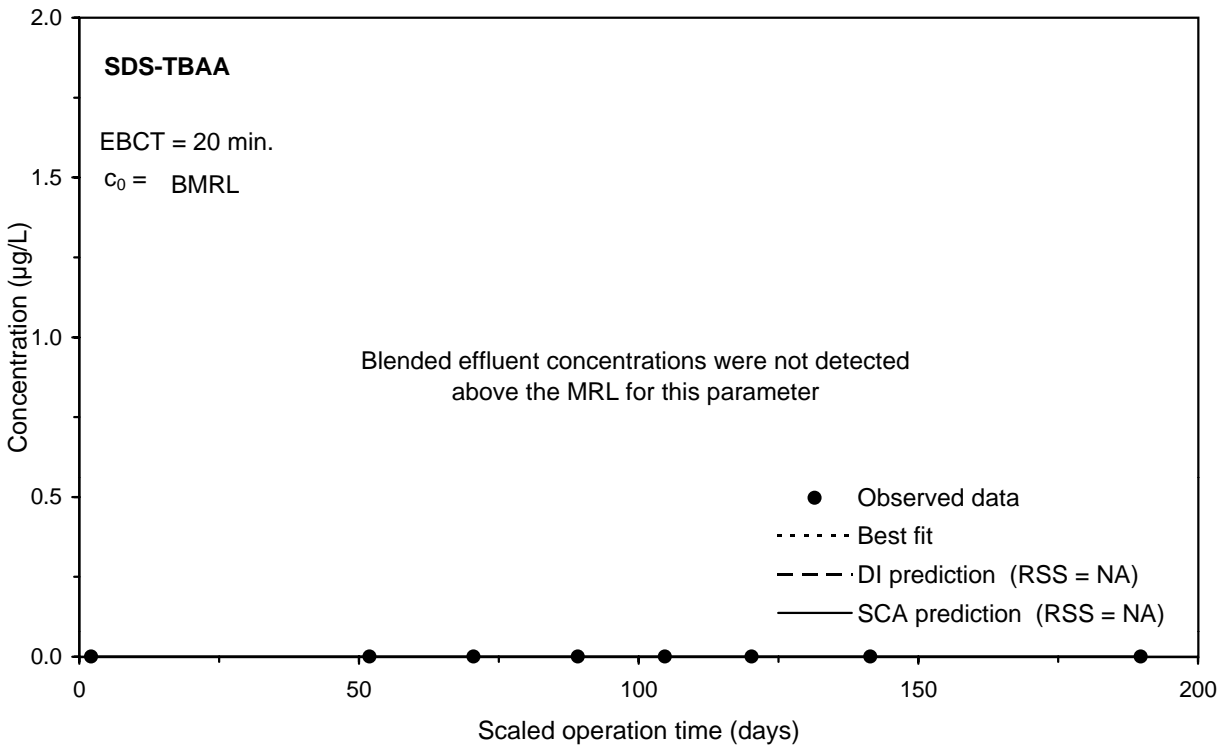


**Figure F-79 Comparison of DI and SCA methods for predicting the SDS-TBAA integral breakthrough curve for Water 4**

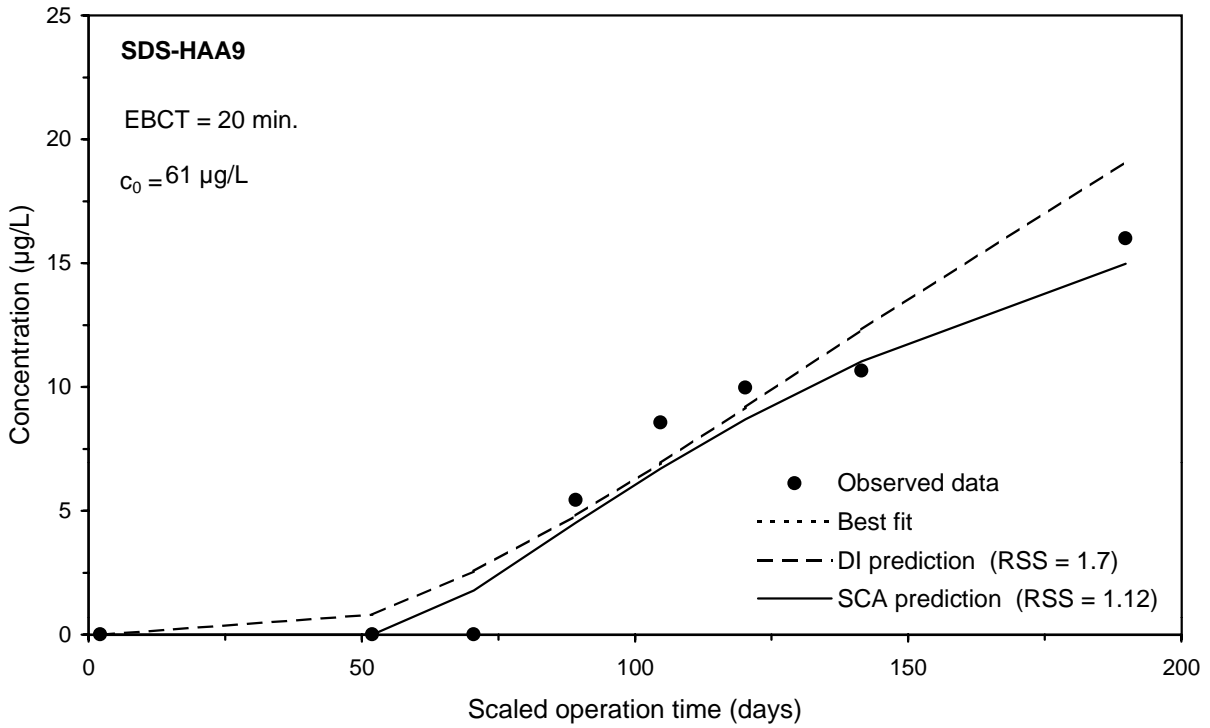


**Figure F-80 Comparison of DI and SCA methods for predicting the SDS-HAA9 integral breakthrough curve for Water 4**

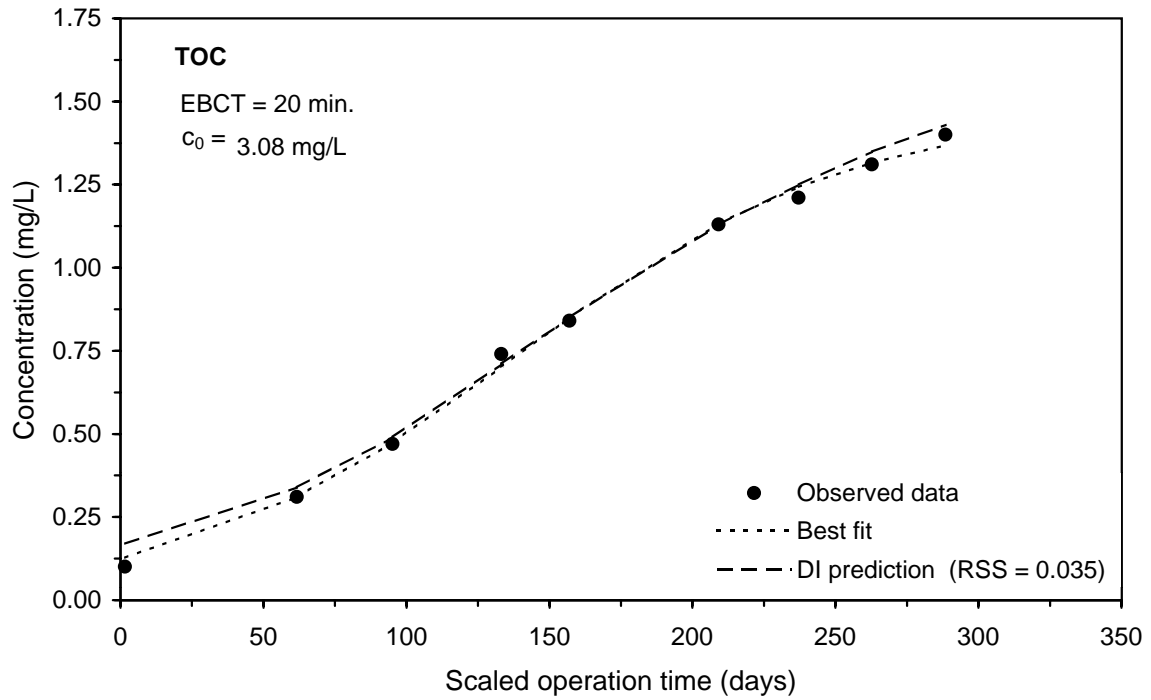


**Figure F-81 DI method prediction of the TOC integral breakthrough curve for Water 5**

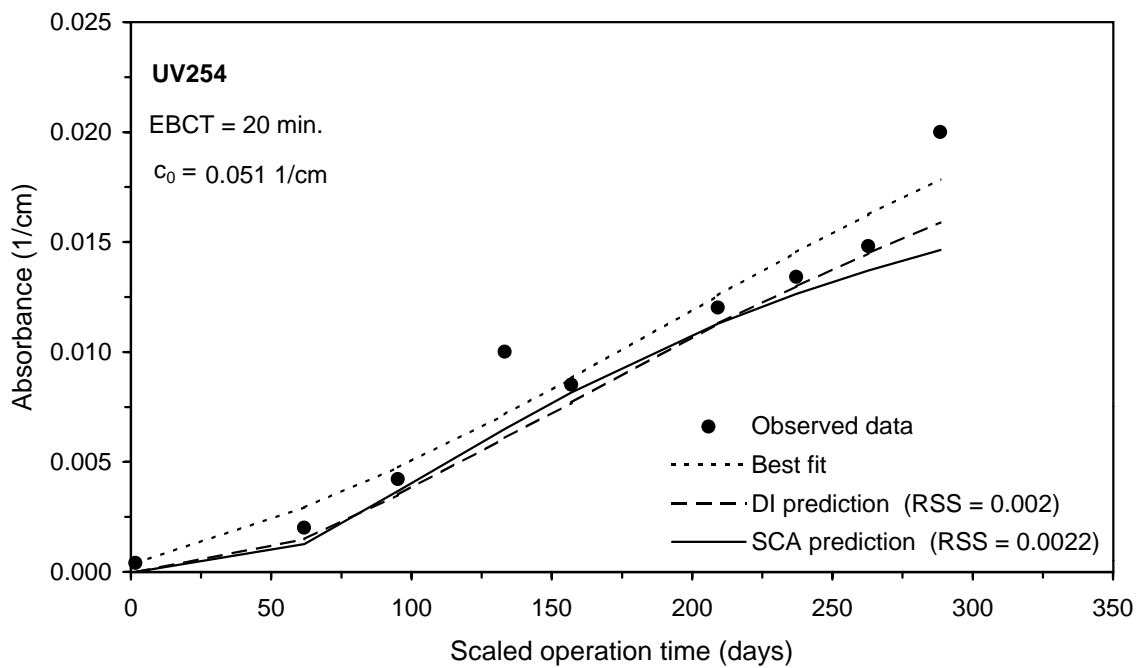


**Figure F-82 Comparison of DI and SCA methods for predicting the UV254 integral breakthrough curve for Water 5**

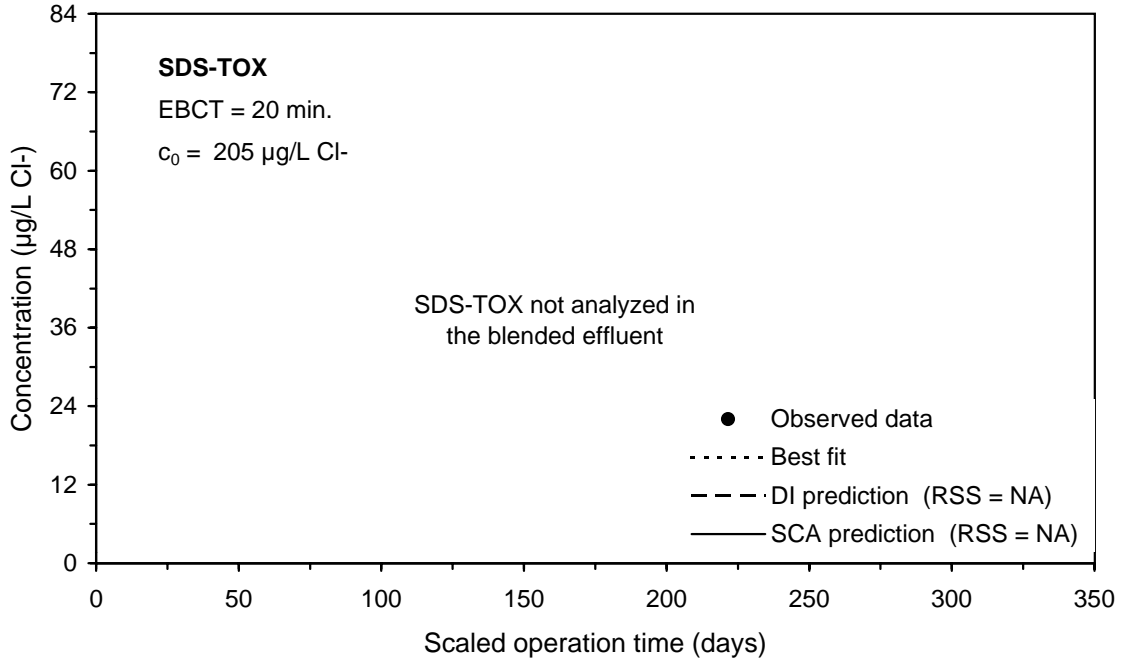


**Figure F-83 Comparison of DI and SCA methods for predicting the SDS-TOX integral breakthrough curve for Water 5**

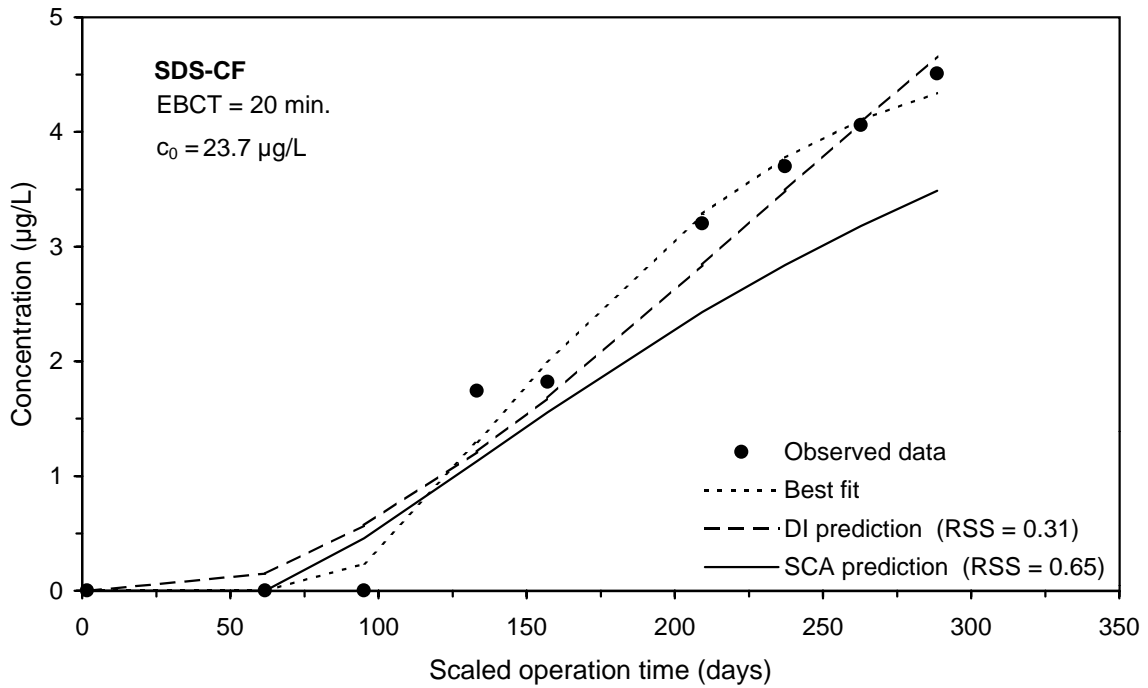


**Figure F-84 Comparison of DI and SCA methods for predicting the SDS-CF integral breakthrough curve for Water 5**

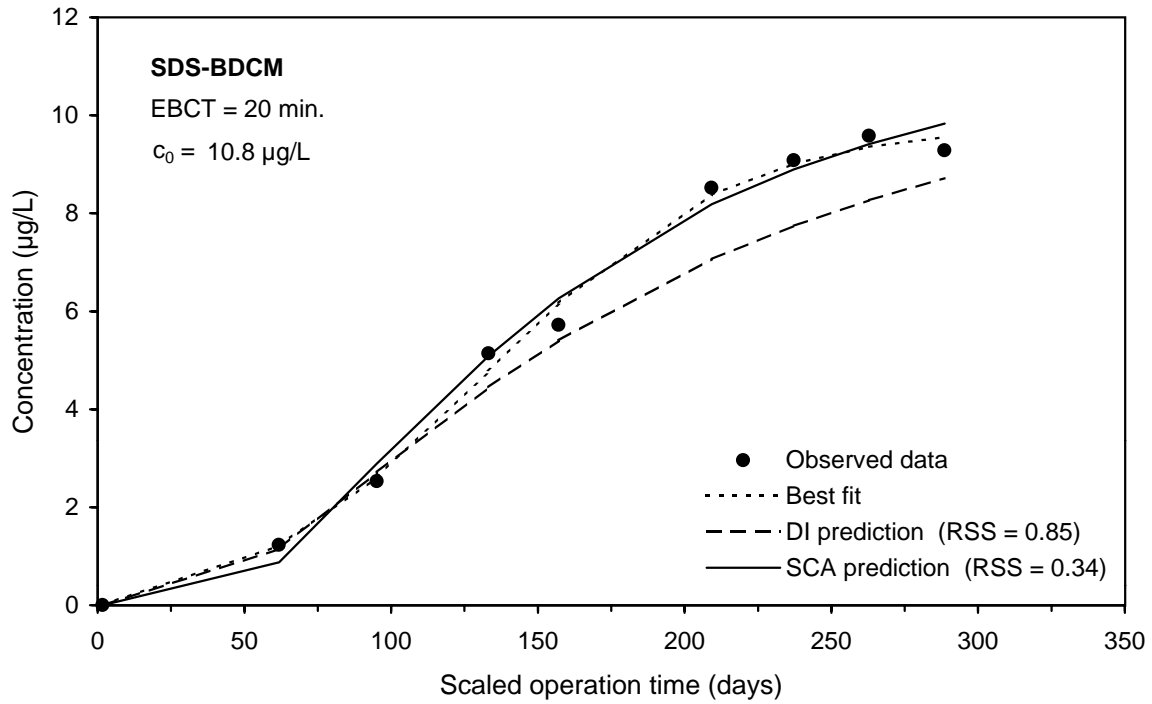


**Figure F-85 Comparison of DI and SCA methods for predicting the SDS-BDCM integral breakthrough curve for Water 5**

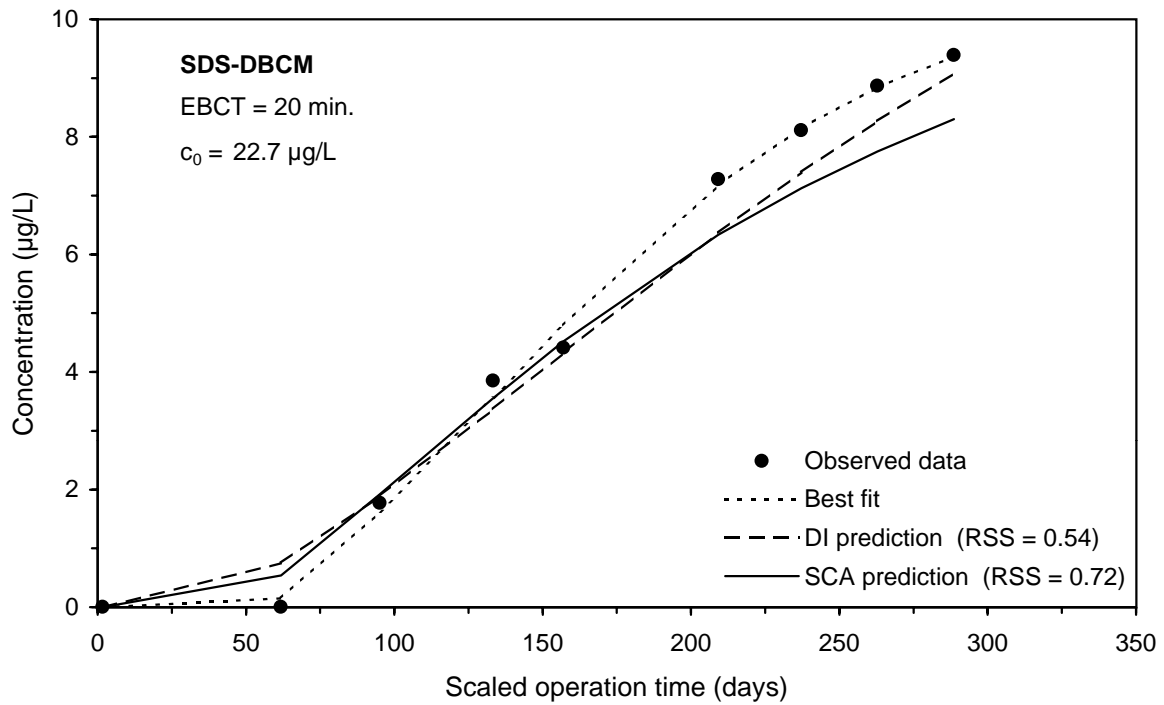


**Figure F-86 Comparison of DI and SCA methods for predicting the SDS-DBCm integral breakthrough curve for Water 5**

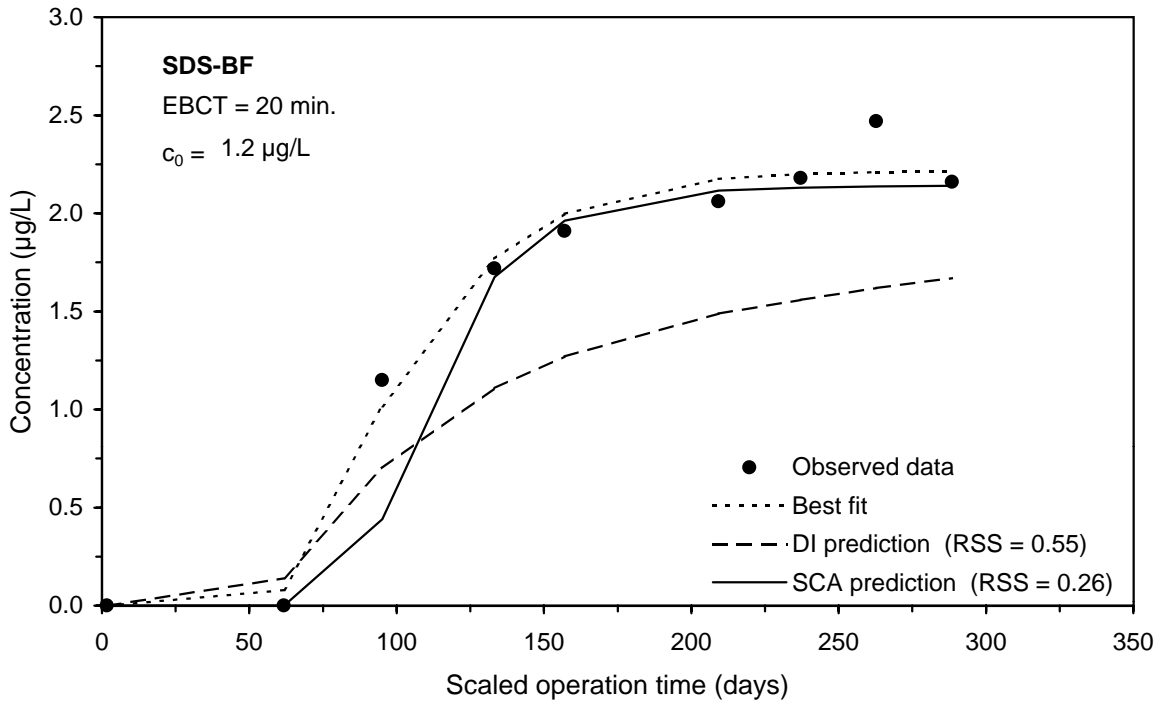


**Figure F-87 Comparison of DI and SCA methods for predicting the SDS-BF integral breakthrough curve for Water 5**

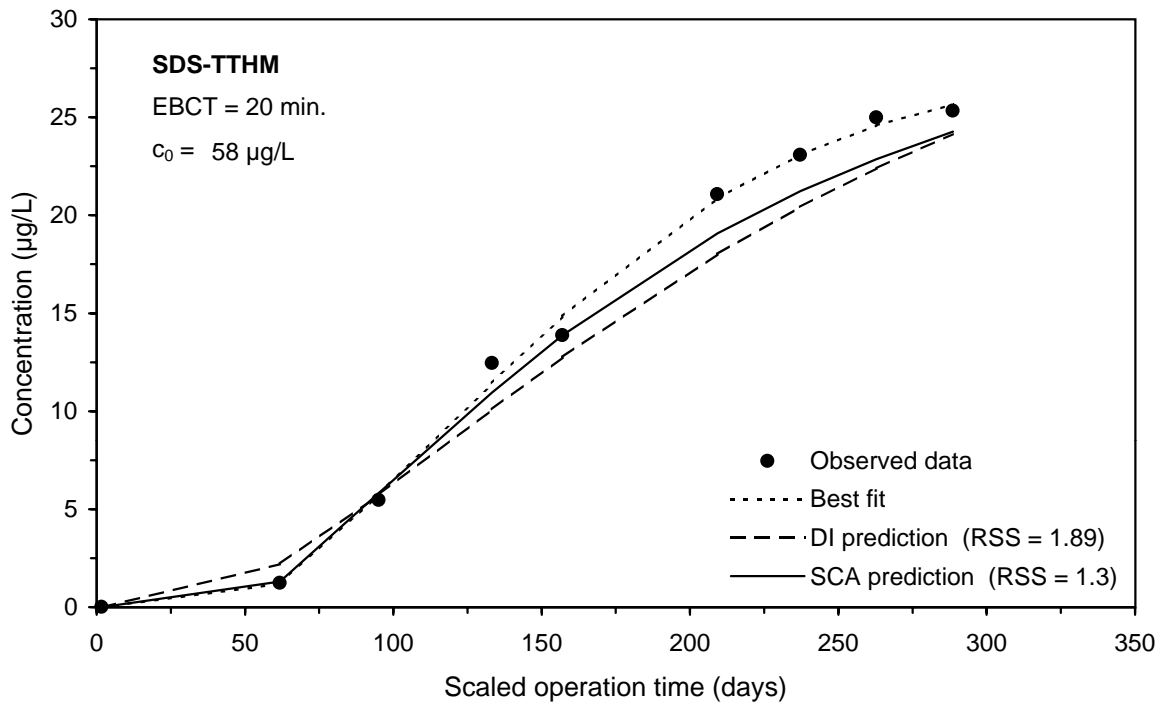


**Figure F-88 Comparison of DI and SCA methods for predicting the SDS-TTHM integral breakthrough curve for Water 5**

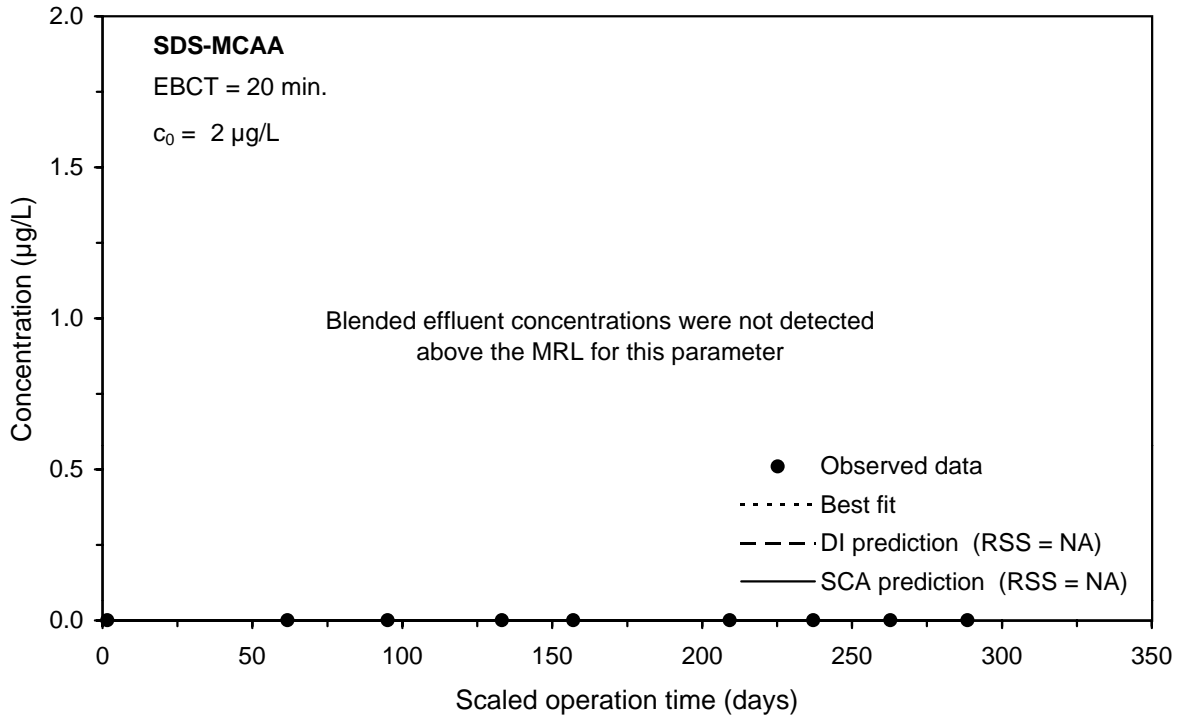


**Figure F-89 Comparison of DI and SCA methods for predicting the SDS-MCAA integral breakthrough curve for Water 5**

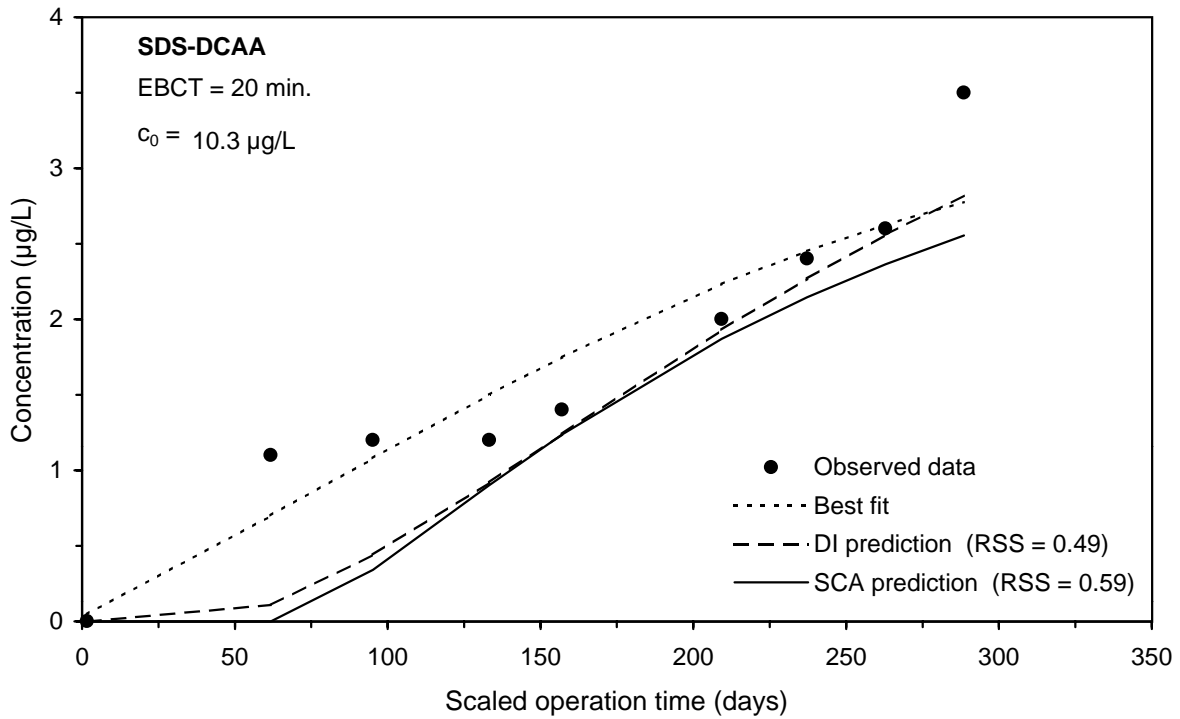


**Figure F-90 Comparison of DI and SCA methods for predicting the SDS-DCAA integral breakthrough curve for Water 5**

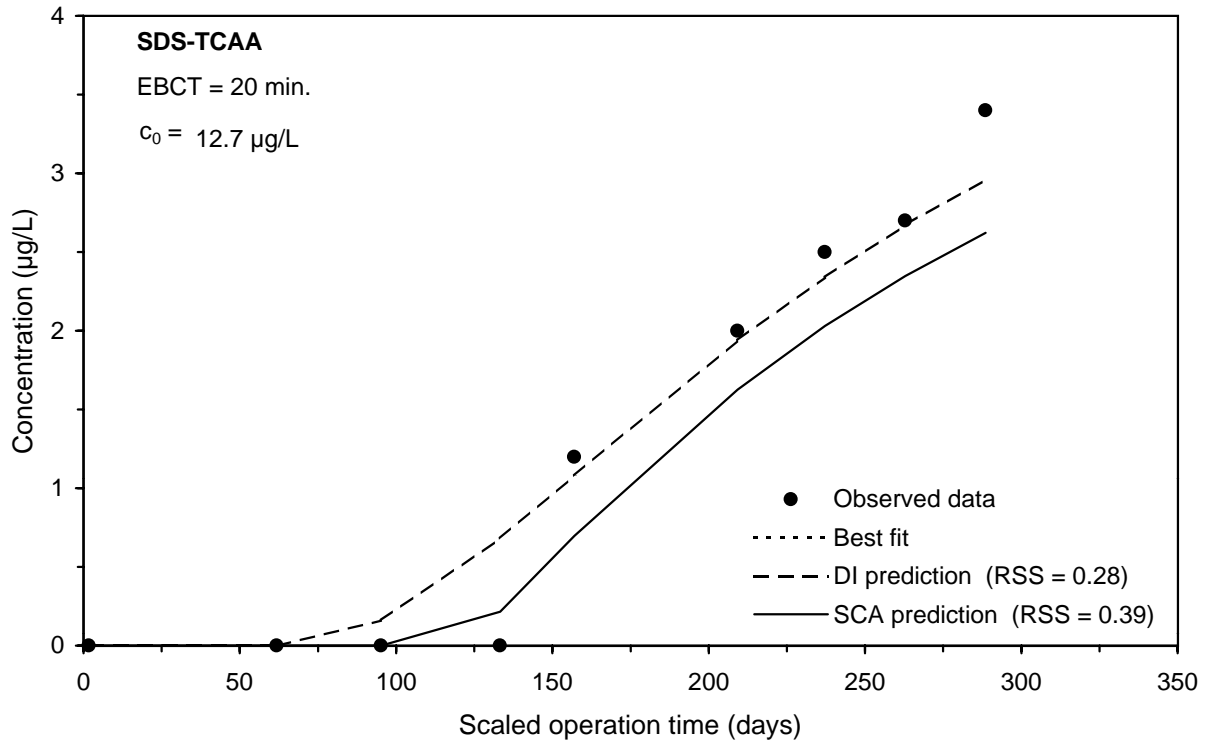


**Figure F-91 Comparison of DI and SCA methods for predicting the SDS-TCAA integral breakthrough curve for Water 5**

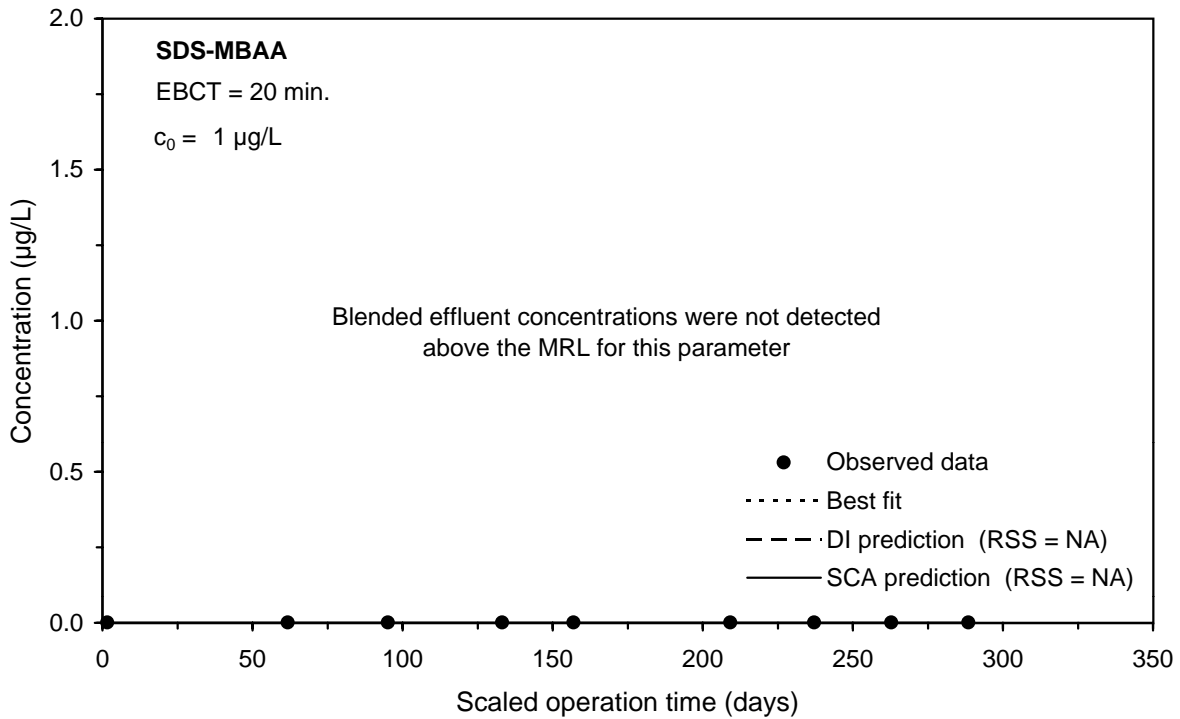


**Figure F-92 Comparison of DI and SCA methods for predicting the SDS-MBAA integral breakthrough curve for Water 5**

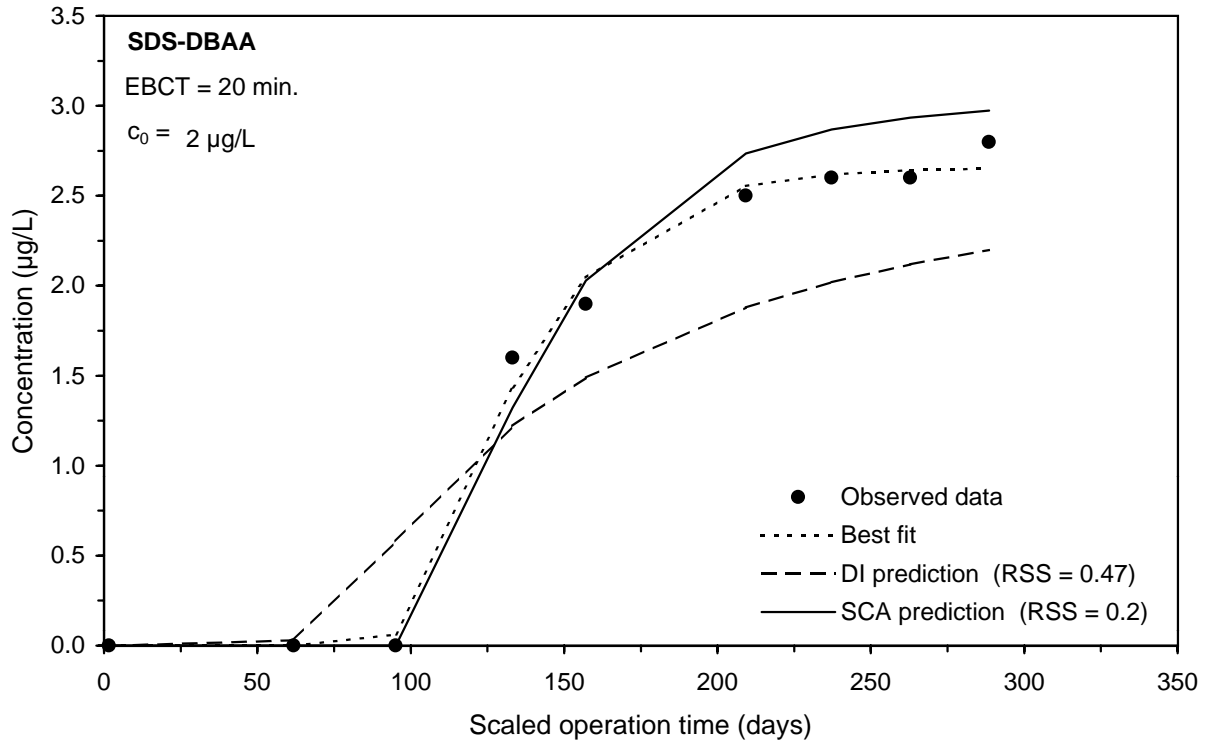


**Figure F-93 Comparison of DI and SCA methods for predicting the SDS-DBAA integral breakthrough curve for Water 5**

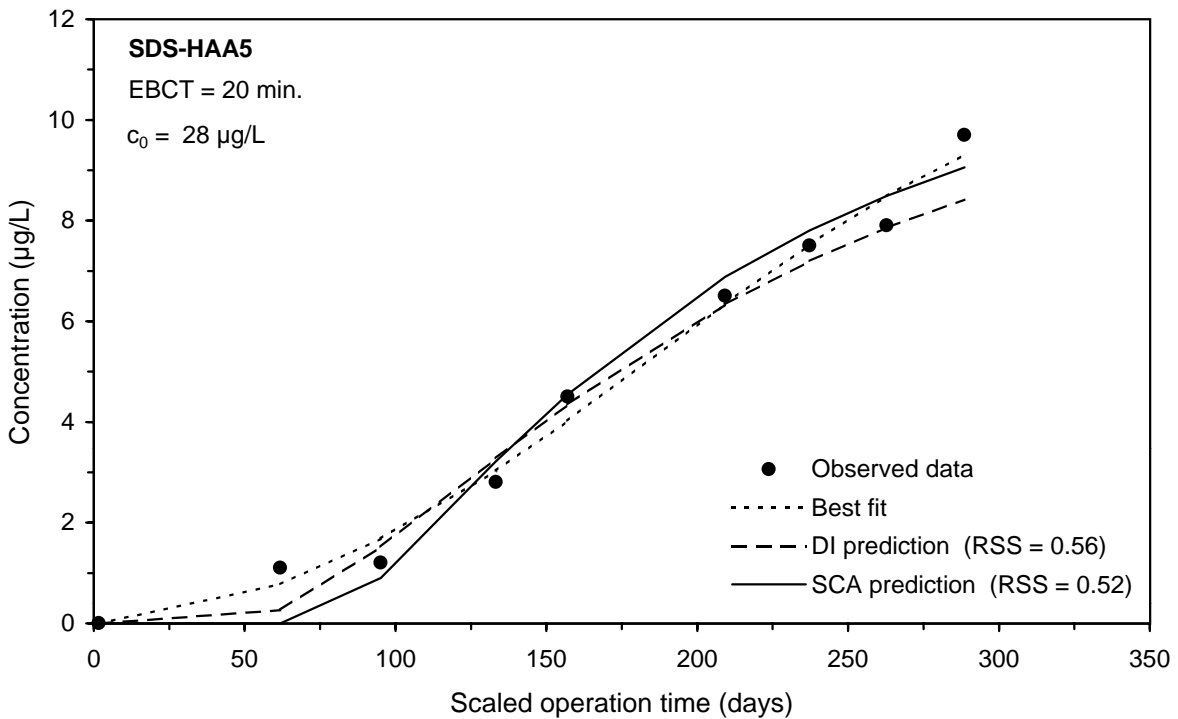


**Figure F-94 Comparison of DI and SCA methods for predicting the SDS-HAA5 integral breakthrough curve for Water 5**

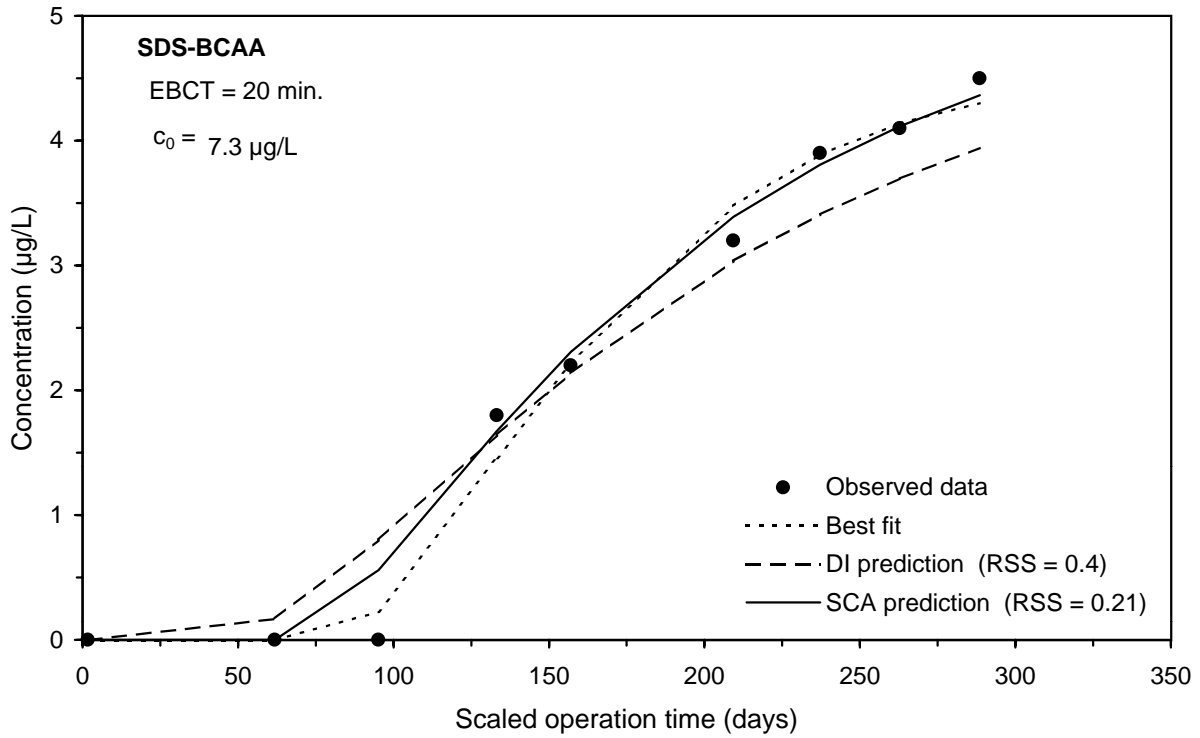


**Figure F-95 Comparison of DI and SCA methods for predicting the SDS-BCAA integral breakthrough curve for Water 5**

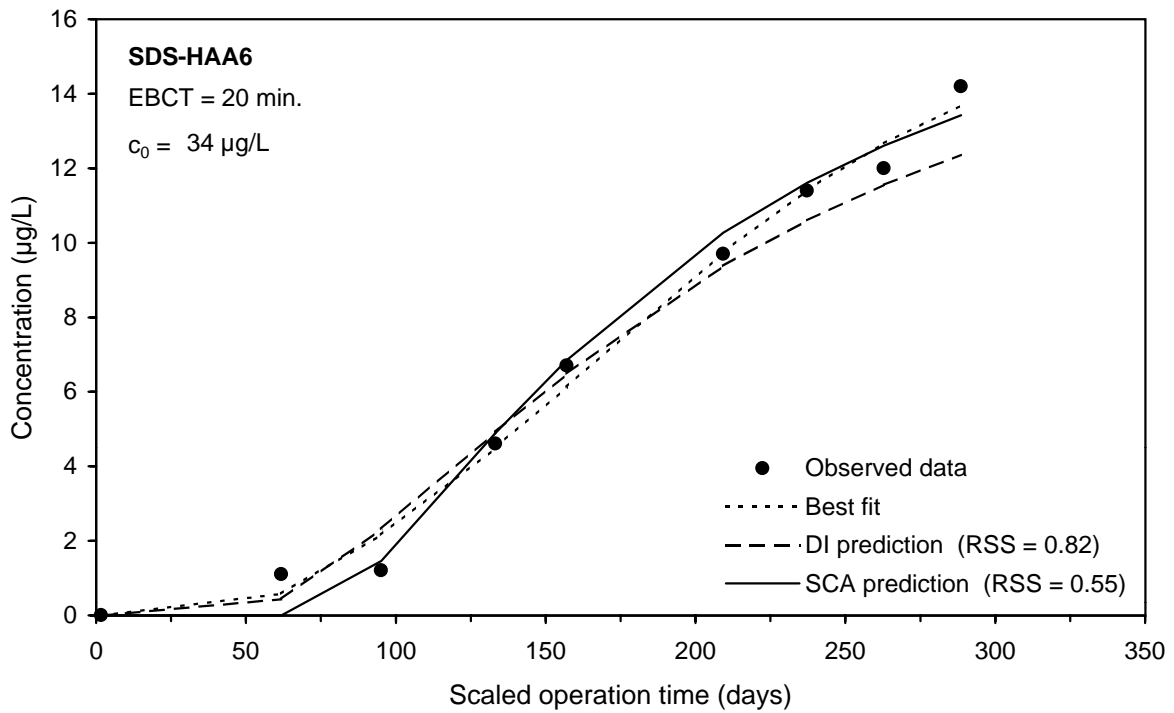


**Figure F-96 Comparison of DI and SCA methods for predicting the SDS-HAA6 integral breakthrough curve for Water 5**

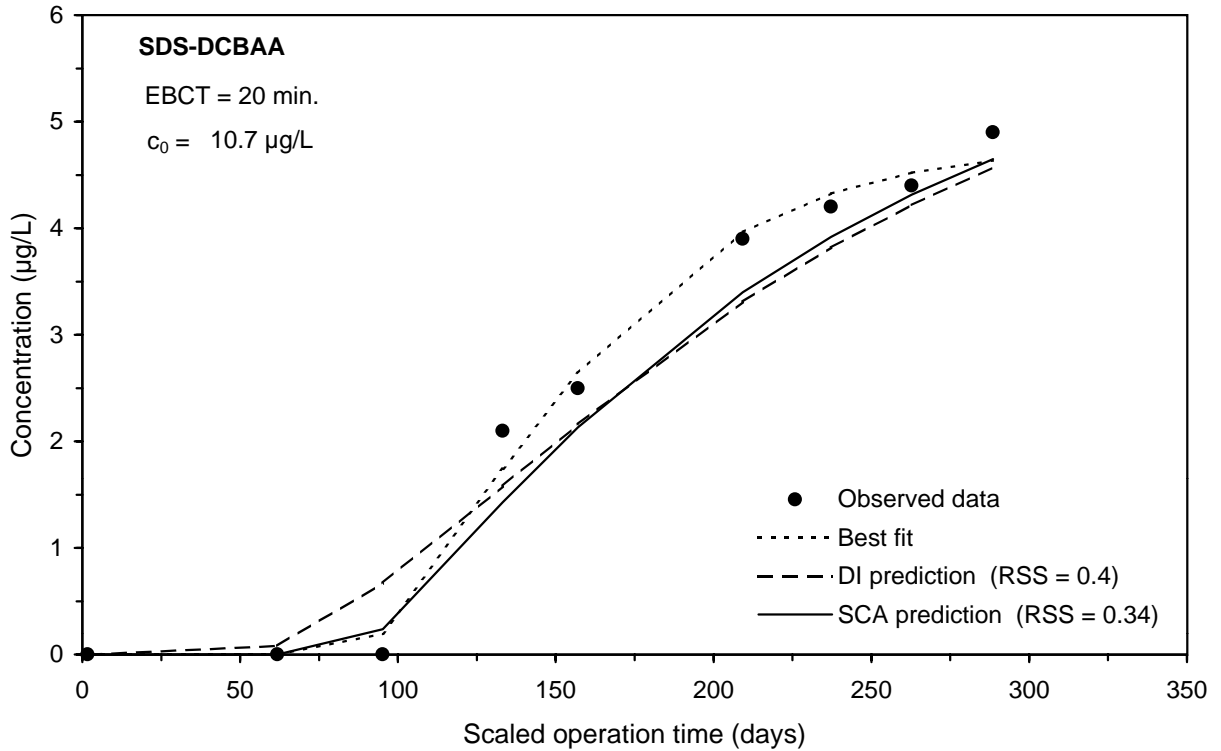


**Figure F-97 Comparison of DI and SCA methods for predicting the SDS-DCBAA integral breakthrough curve for Water 5**

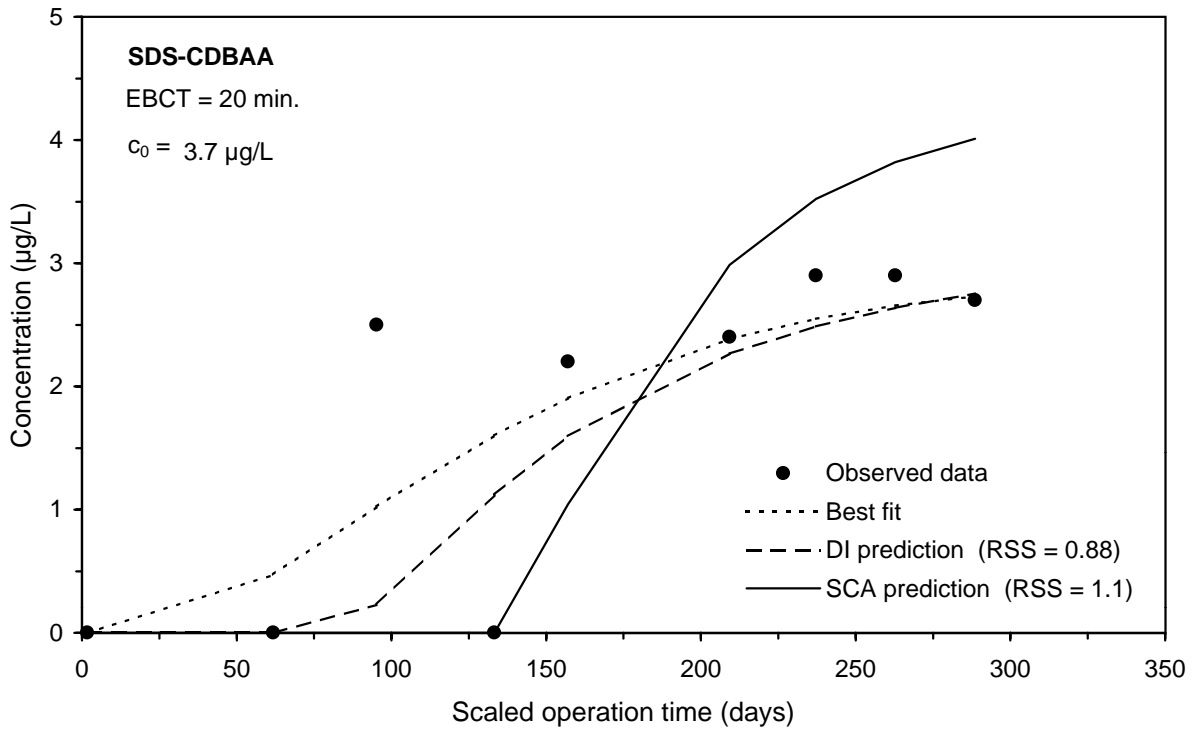


**Figure F-98 Comparison of DI and SCA methods for predicting the SDS-CDBAA integral breakthrough curve for Water 5**

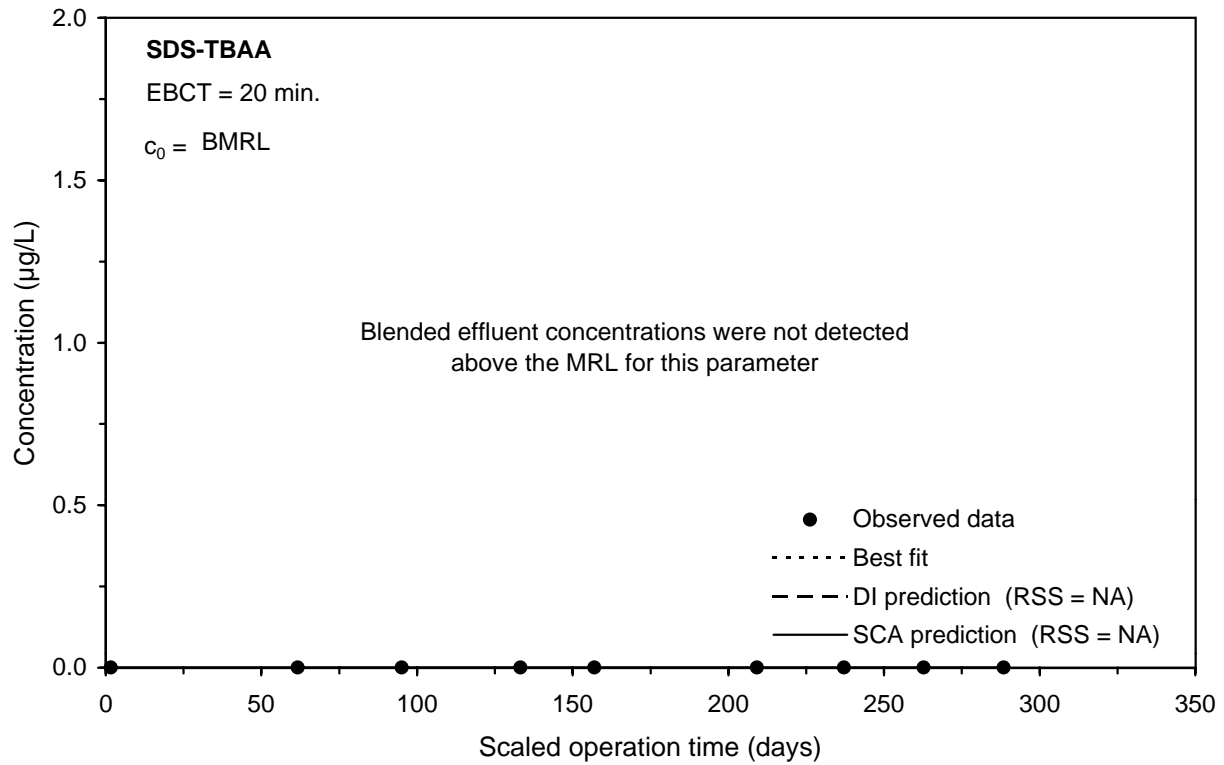


**Figure F-99 Comparison of DI and SCA methods for predicting the SDS-TBAA integral breakthrough curve for Water 5**

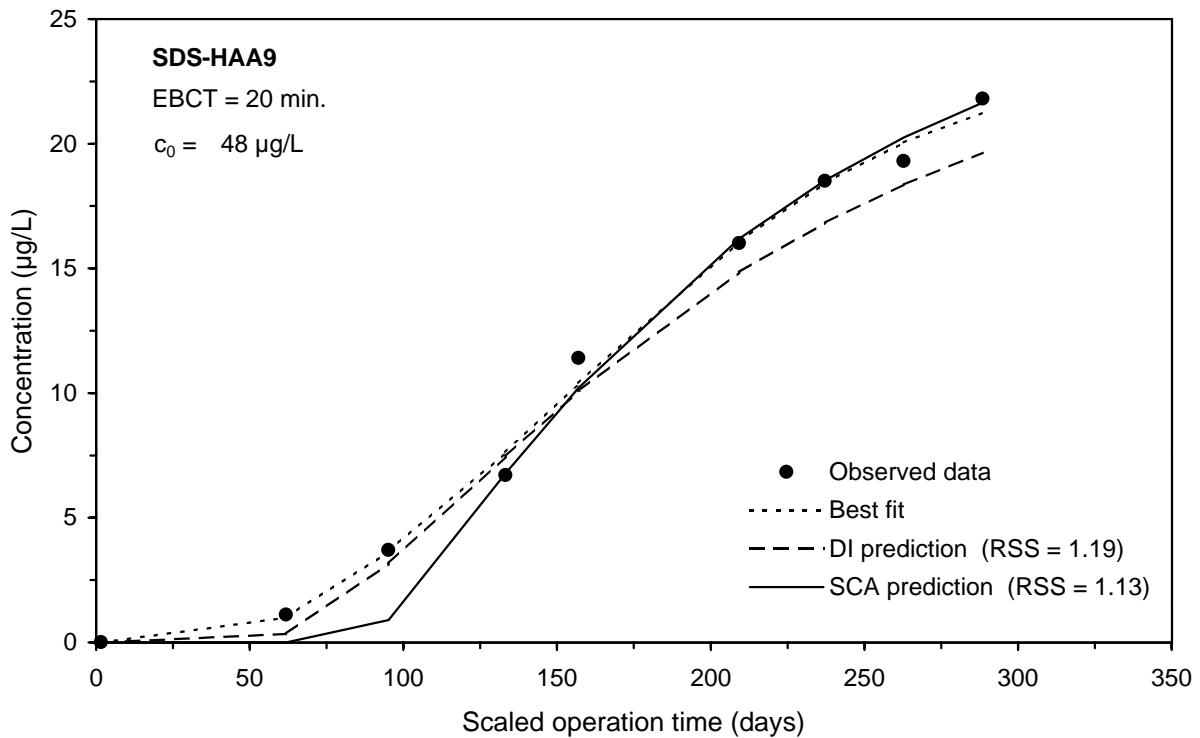


**Figure F-100 Comparison of DI and SCA methods for predicting the SDS-HAA9 integral breakthrough curve for Water 5**

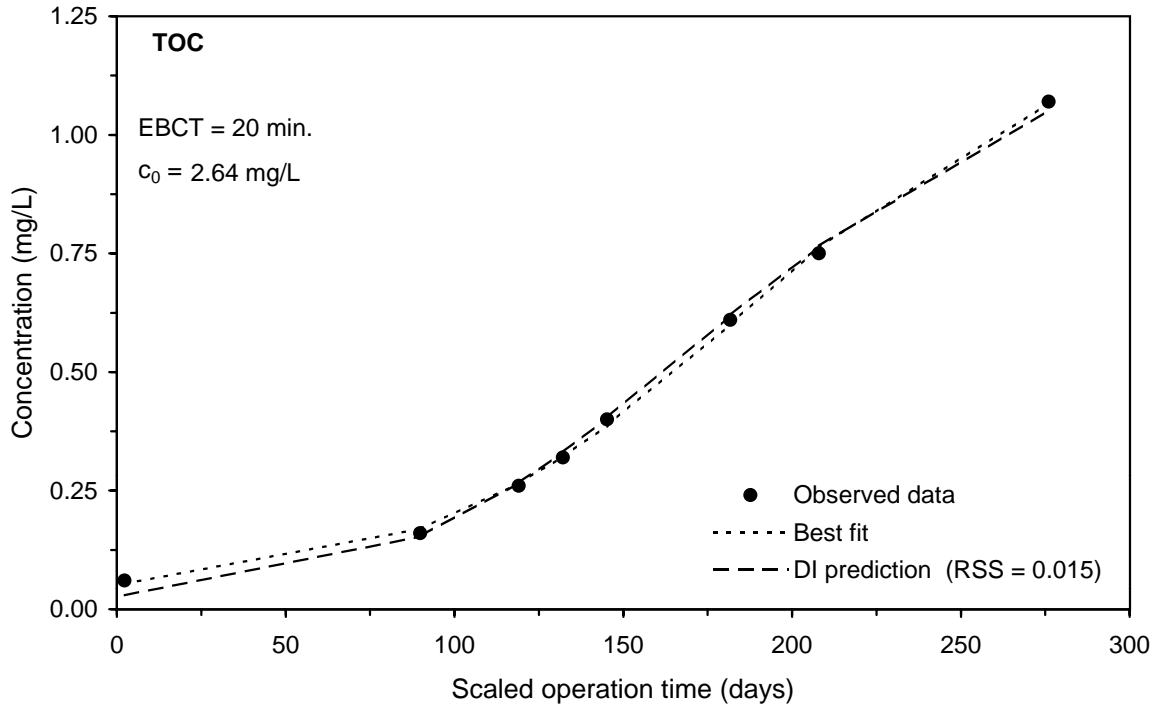


**Figure F-101** DI method prediction of the TOC integral breakthrough curve for Water 6

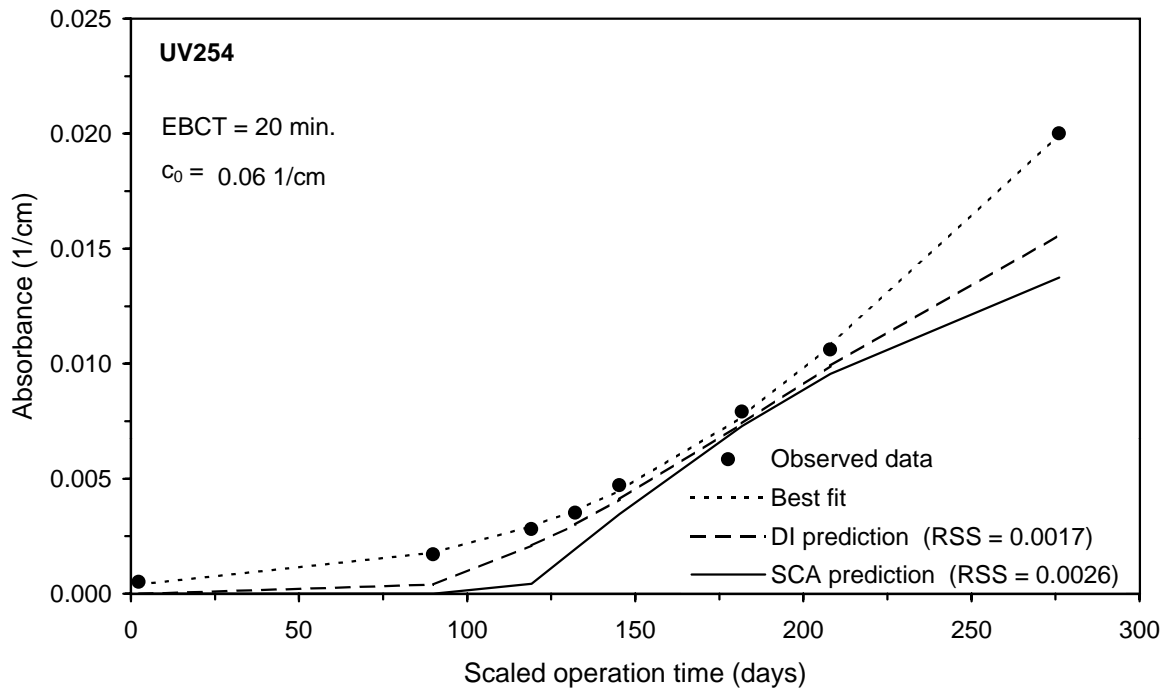


**Figure F-102** Comparison of DI and SCA methods for predicting the UV254 integral breakthrough curve for Water 6

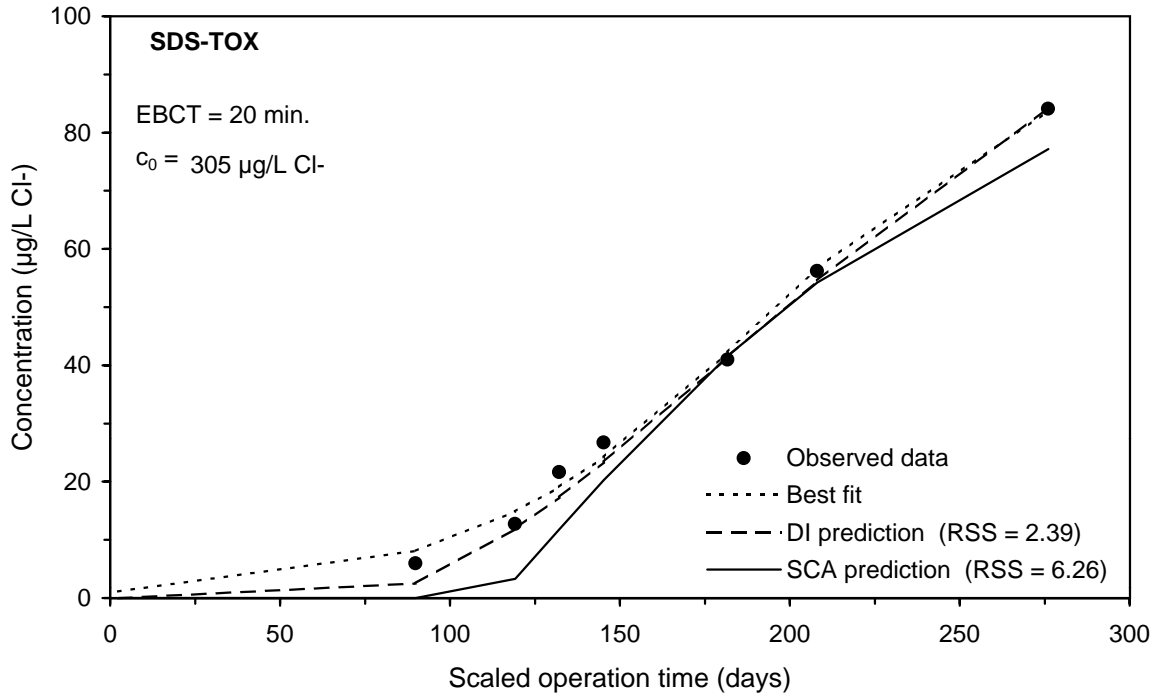


**Figure F-103 Comparison of DI and SCA methods for predicting the SDS-TOX integral breakthrough curve for Water 6**

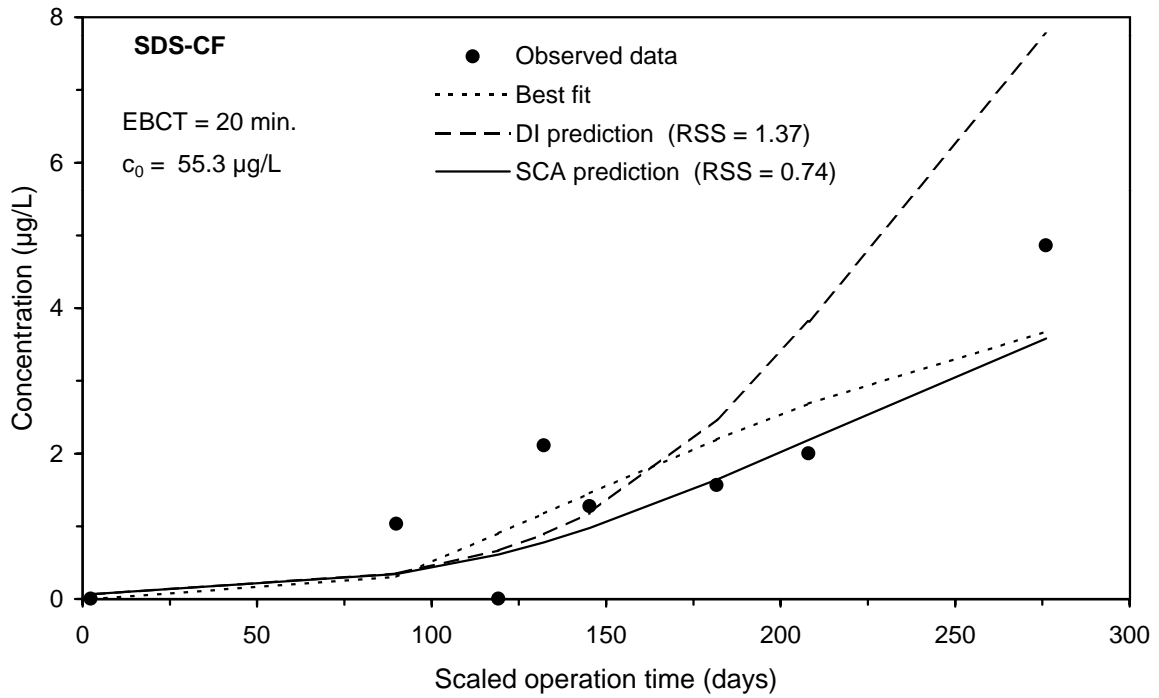


**Figure F-104 Comparison of DI and SCA methods for predicting the SDS-CF integral breakthrough curve for Water 6**

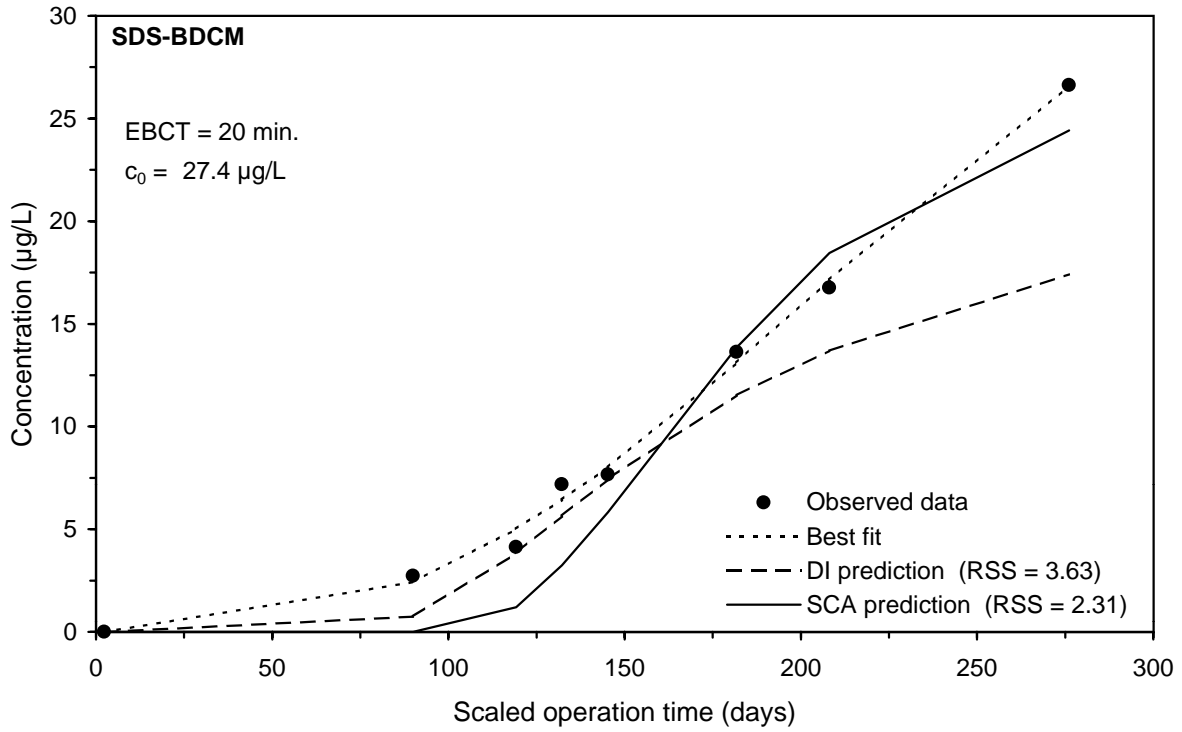


**Figure F-105 Comparison of DI and SCA methods for predicting the SDS-BDCM integral breakthrough curve for Water 6**

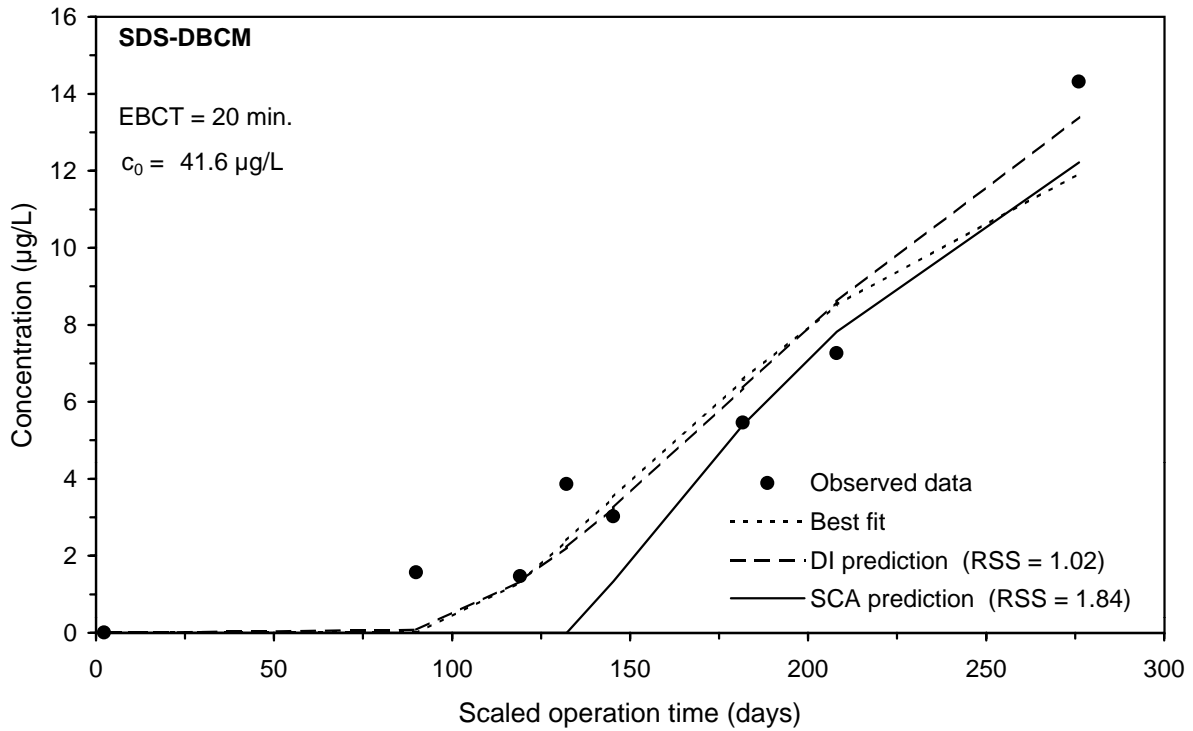


**Figure F-106 Comparison of DI and SCA methods for predicting the SDS-DBCm integral breakthrough curve for Water 6**

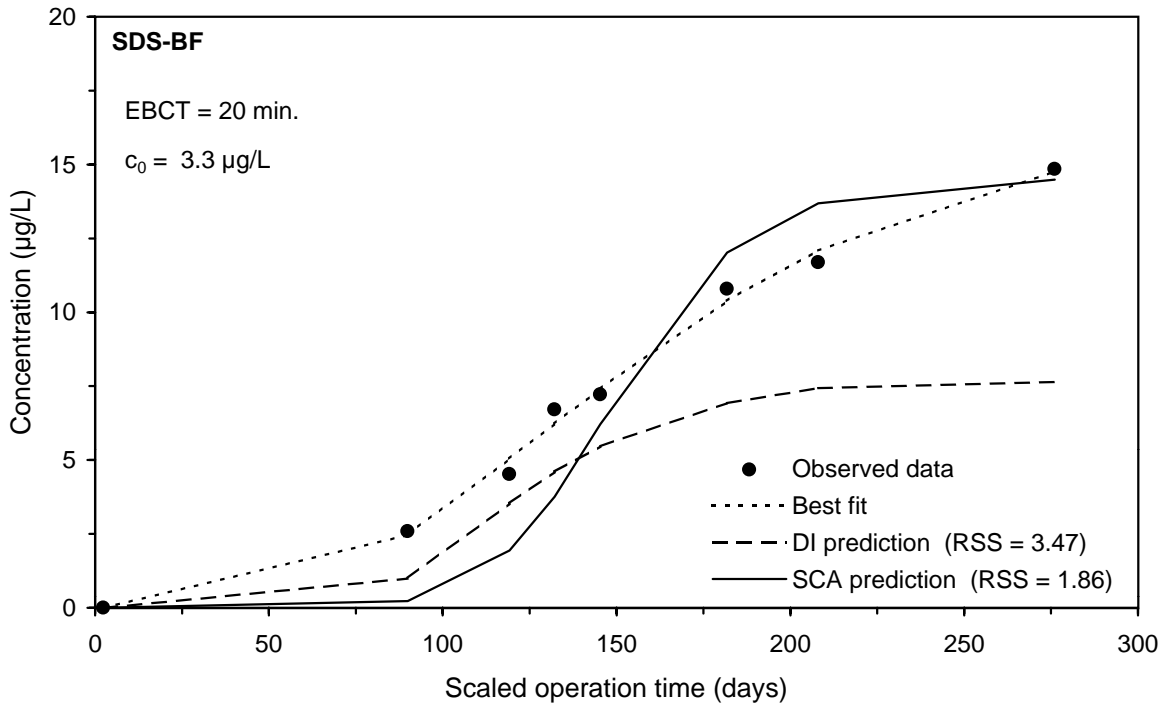


**Figure F-107 Comparison of DI and SCA methods for predicting the SDS-BF integral breakthrough curve for Water 6**

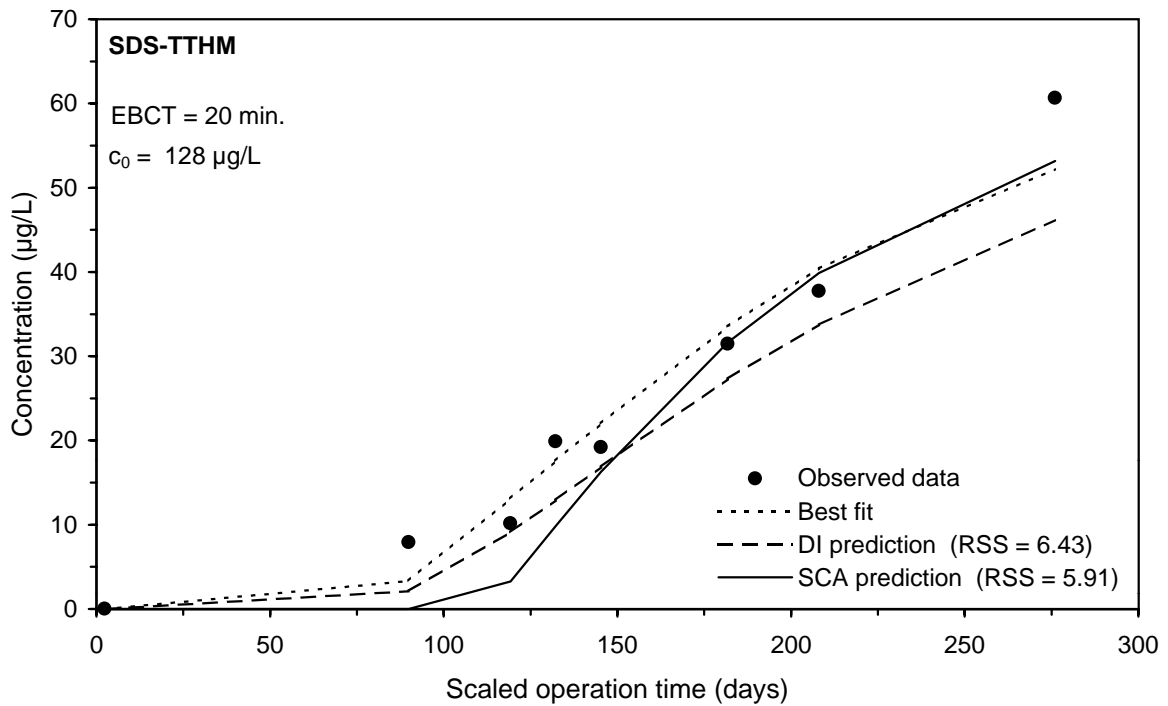


**Figure F-108 Comparison of DI and SCA methods for predicting the SDS-TTHM integral breakthrough curve for Water 6**

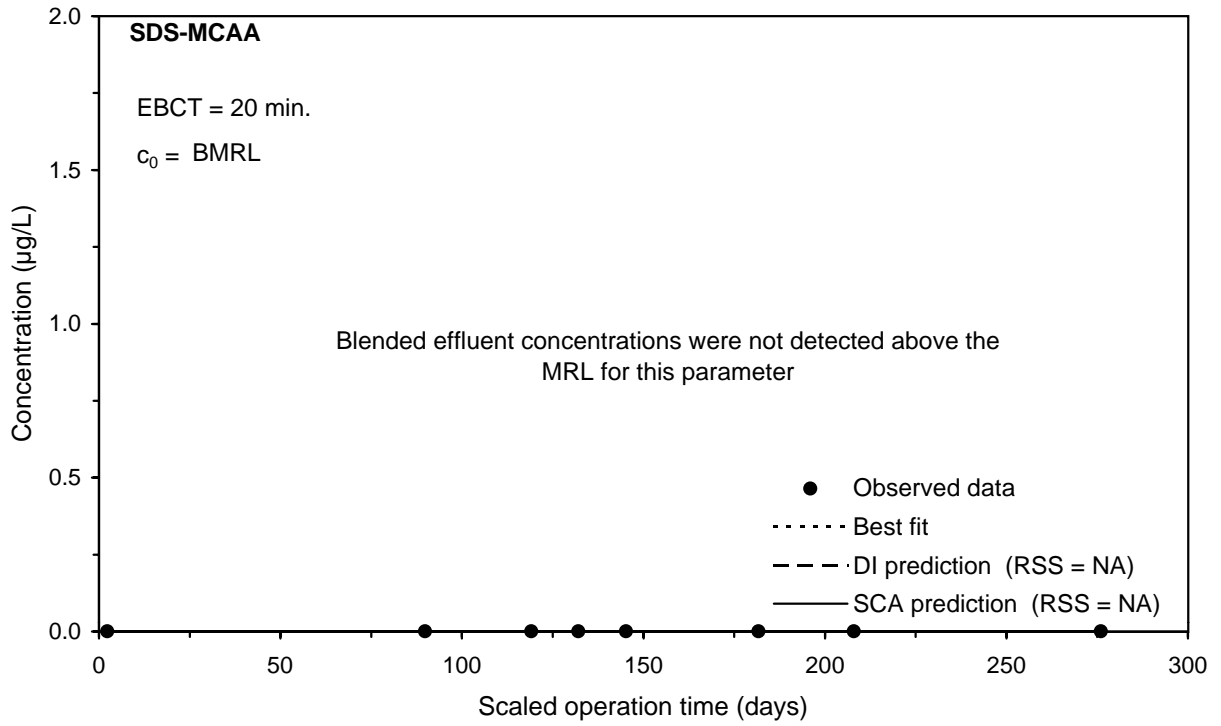


**Figure F-109 Comparison of DI and SCA methods for predicting the SDS-MCAA integral breakthrough curve for Water 6**

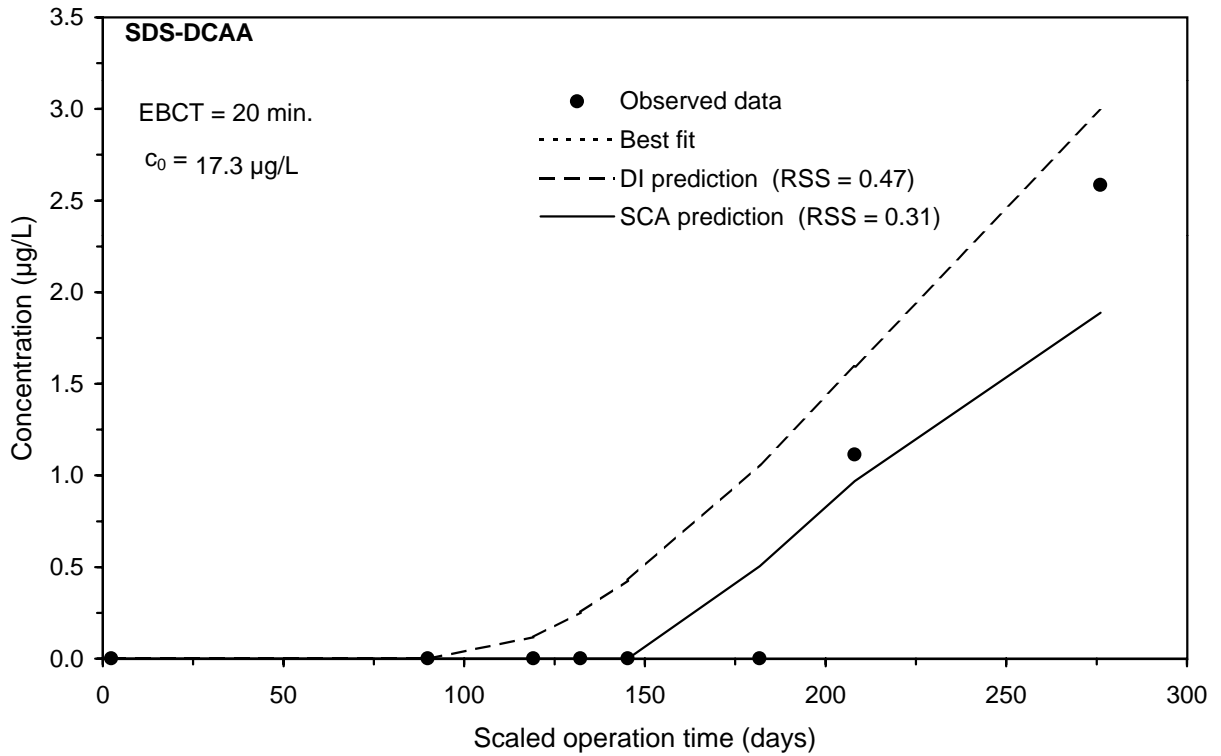


**Figure F-110 Comparison of DI and SCA methods for predicting the SDS-DCAA integral breakthrough curve for Water 6**

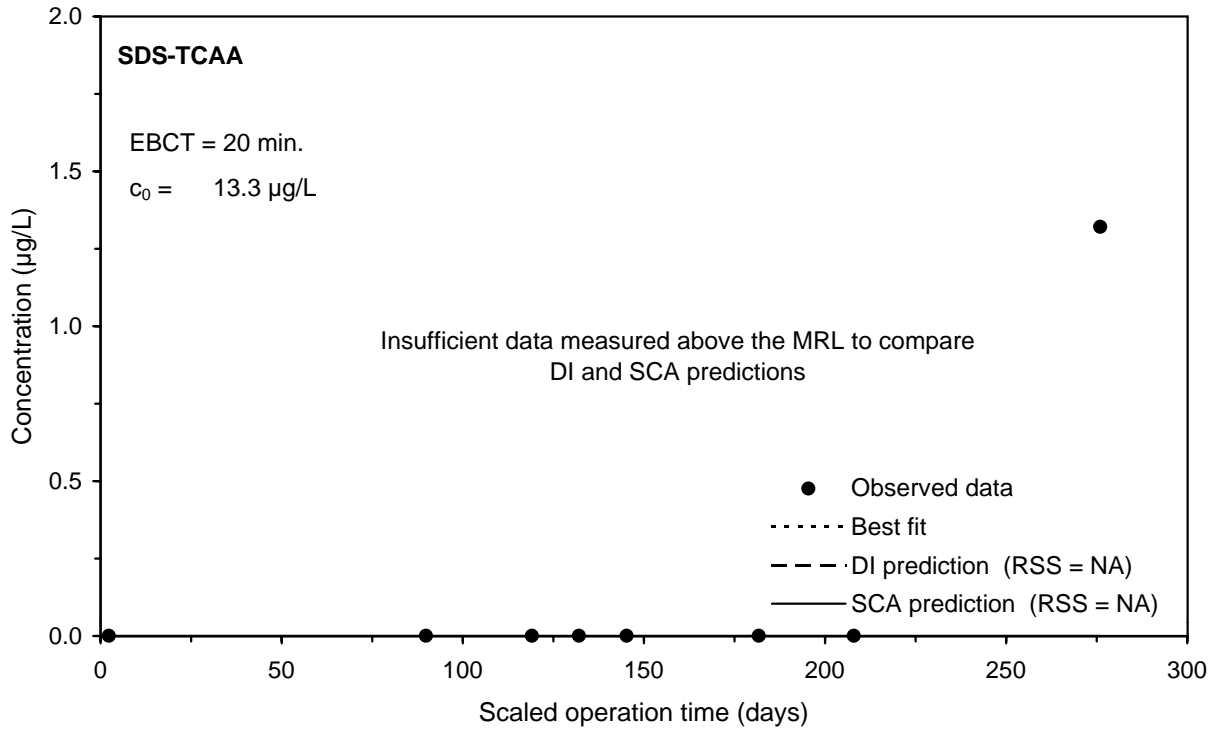


**Figure F-111 Comparison of DI and SCA methods for predicting the SDS-TCAA integral breakthrough curve for Water 6**

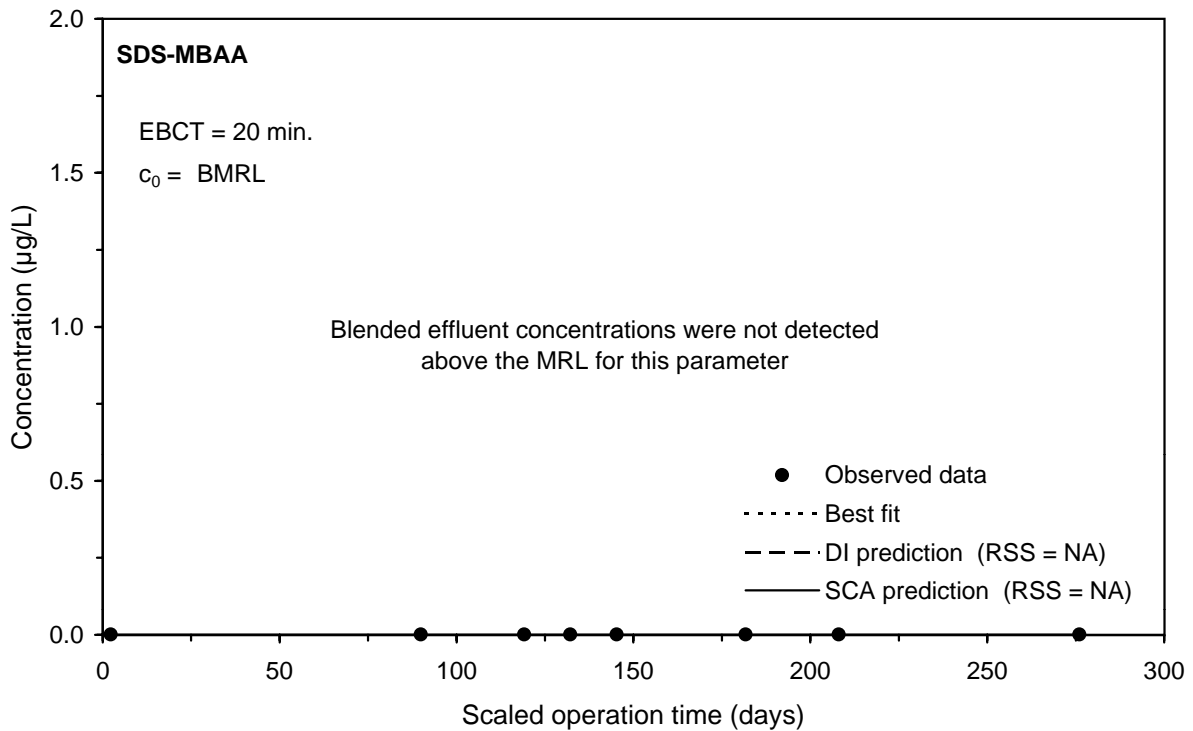


**Figure F-112 Comparison of DI and SCA methods for predicting the SDS-MBAA integral breakthrough curve for Water 6**

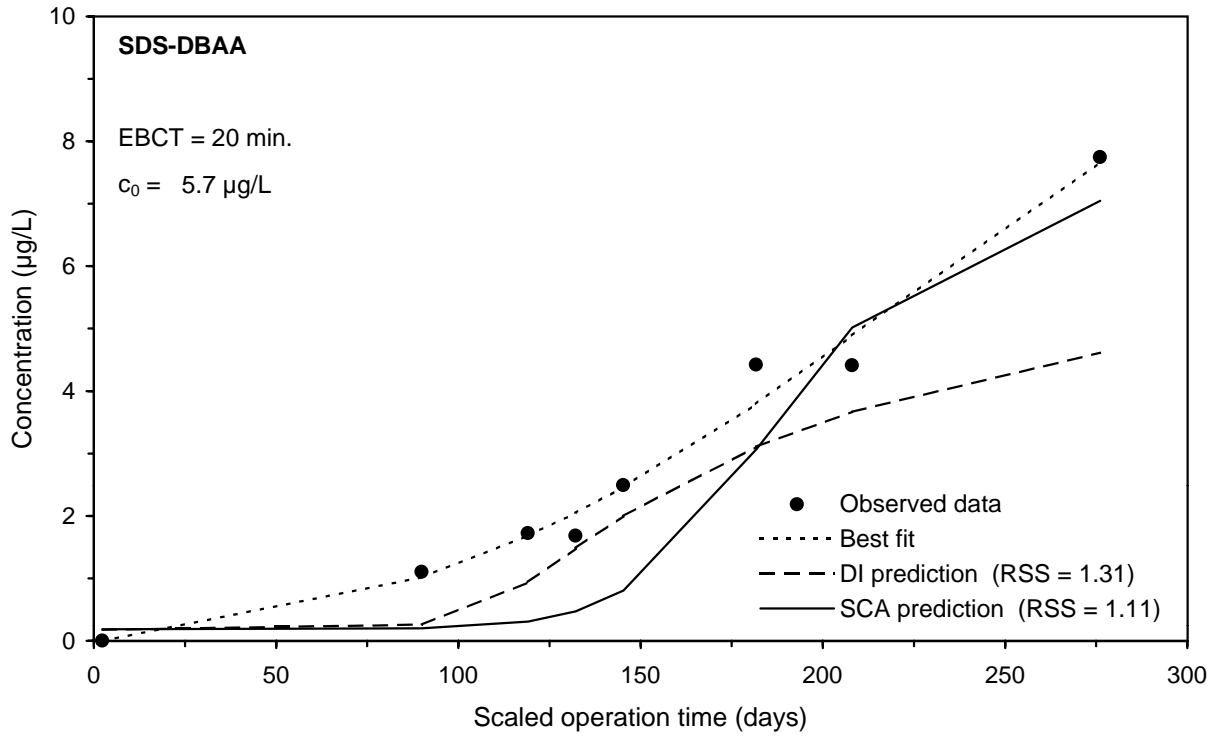


**Figure F-113 Comparison of DI and SCA methods for predicting the SDS-DBAA integral breakthrough curve for Water 6**

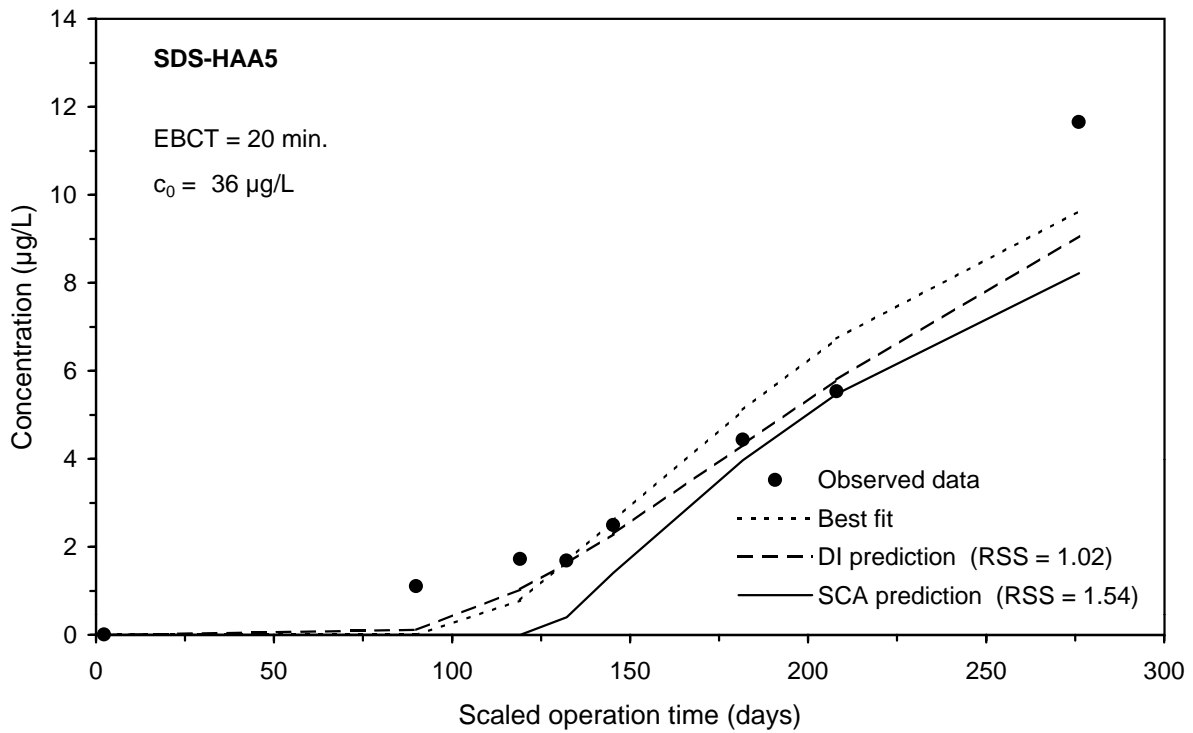


**Figure F-114 Comparison of DI and SCA methods for predicting the SDS-HAA5 integral breakthrough curve for Water 6**

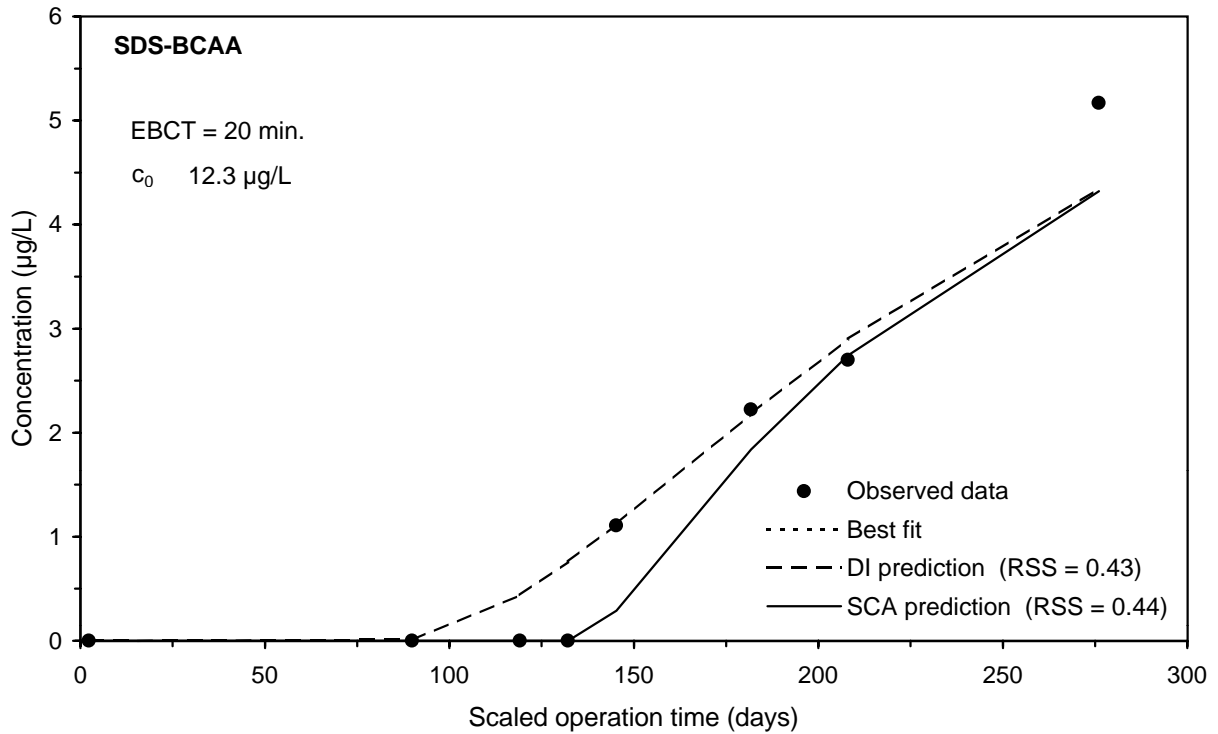


**Figure F-115 Comparison of DI and SCA methods for predicting the SDS-BCAA integral breakthrough curve for Water 6**

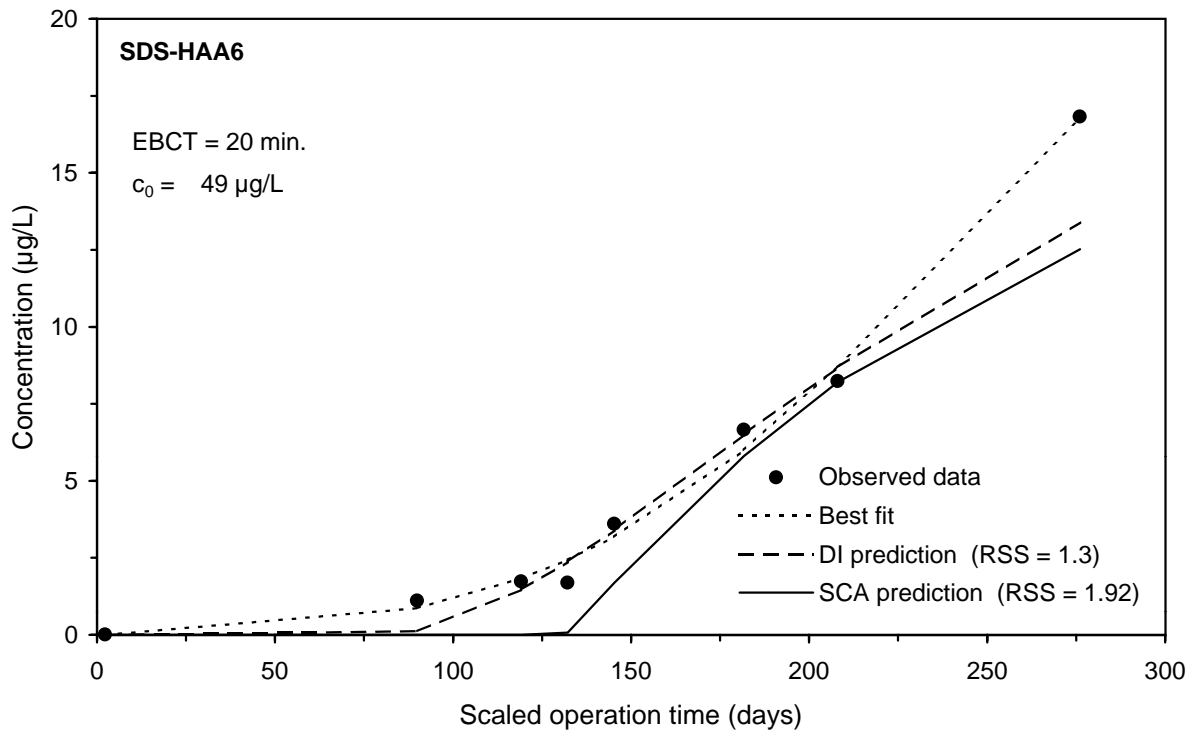


**Figure F-116 Comparison of DI and SCA methods for predicting the SDS-HAA6 integral breakthrough curve for Water 6**

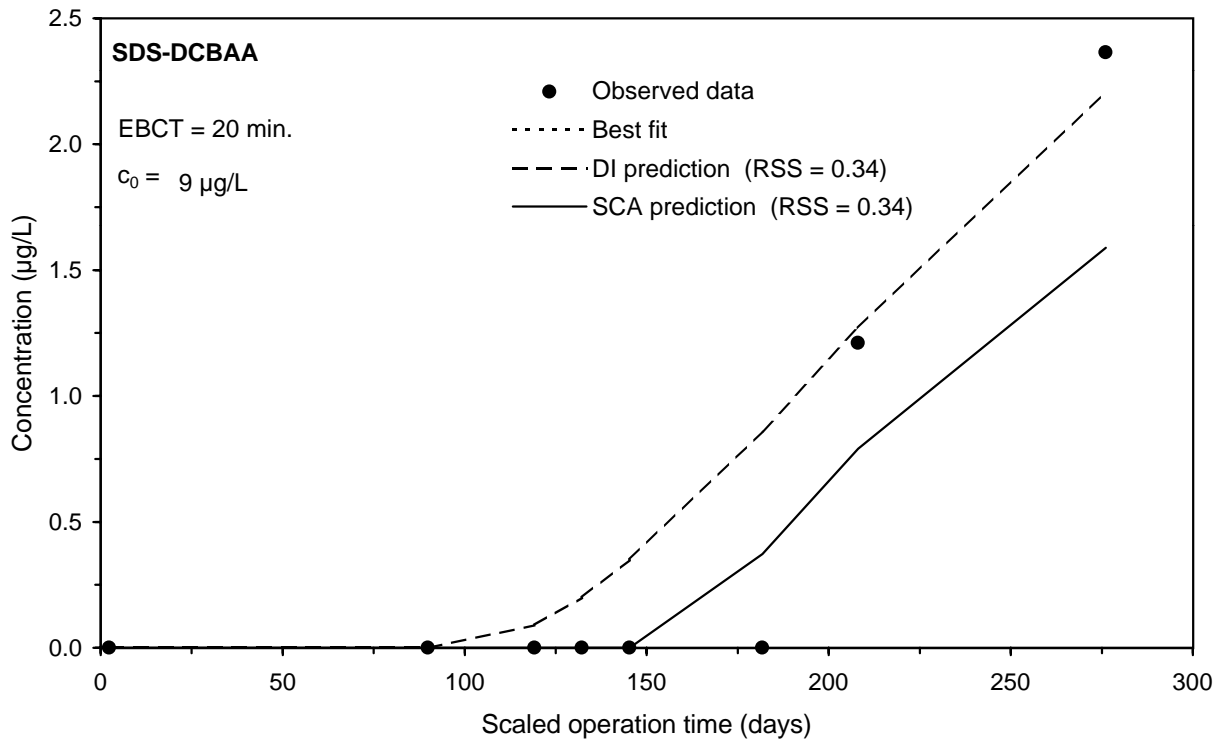


**Figure F-117 Comparison of DI and SCA methods for predicting the SDS-DCBAA integral breakthrough curve for Water 6**

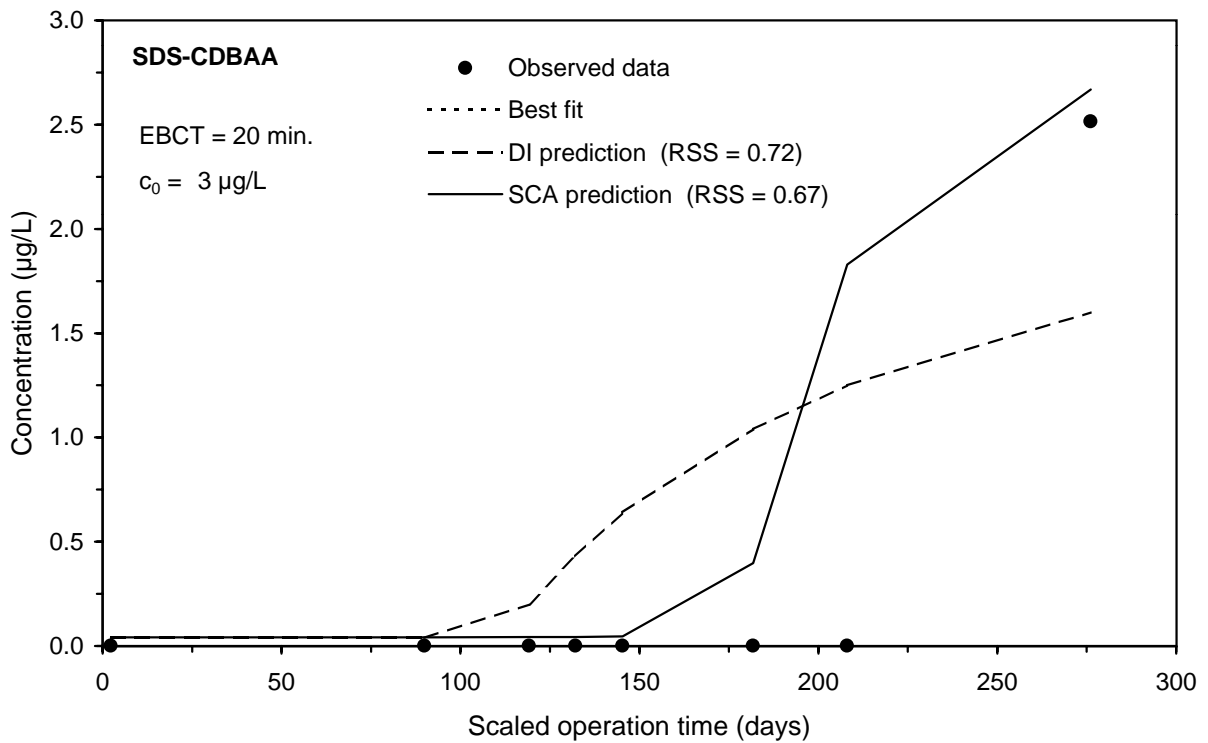


**Figure F-118 Comparison of DI and SCA methods for predicting the SDS-CDBAA integral breakthrough curve for Water 6**

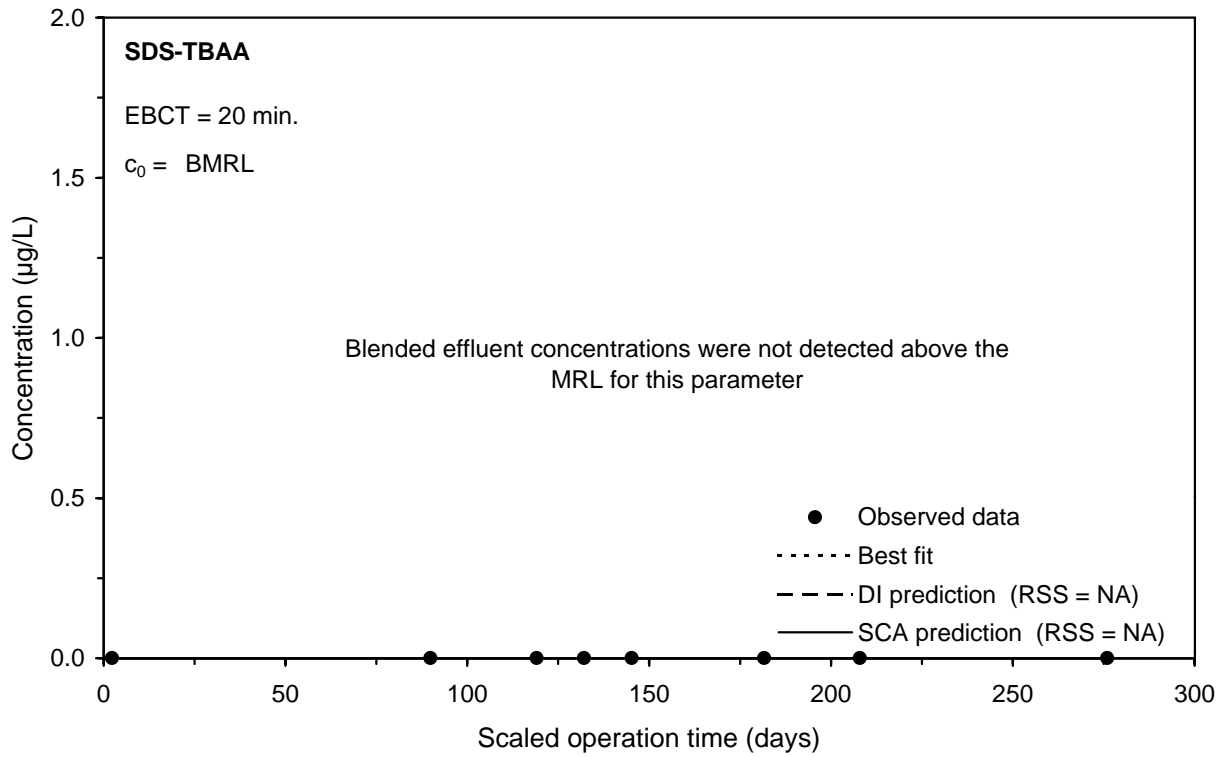


**Figure F-119 Comparison of DI and SCA methods for predicting the SDS-TBAA integral breakthrough curve for Water 6**

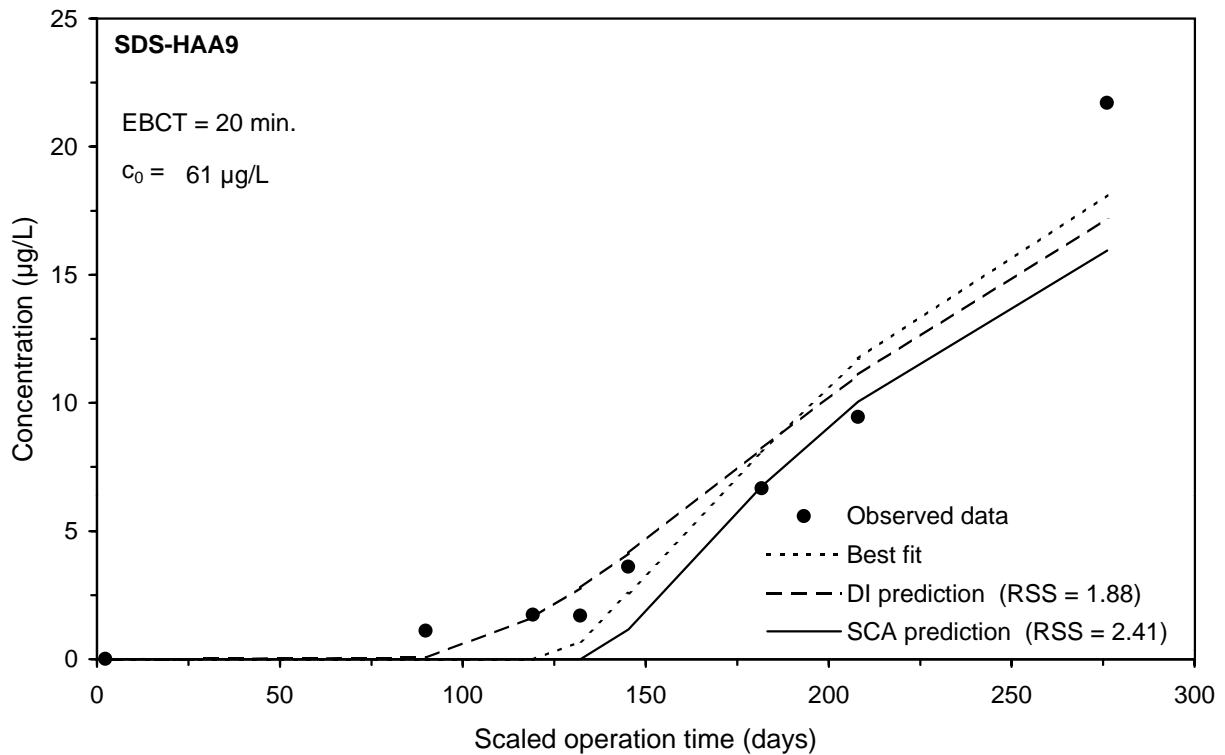


**Figure F-120 Comparison of DI and SCA methods for predicting the SDS-HAA9 integral breakthrough curve for Water 6**

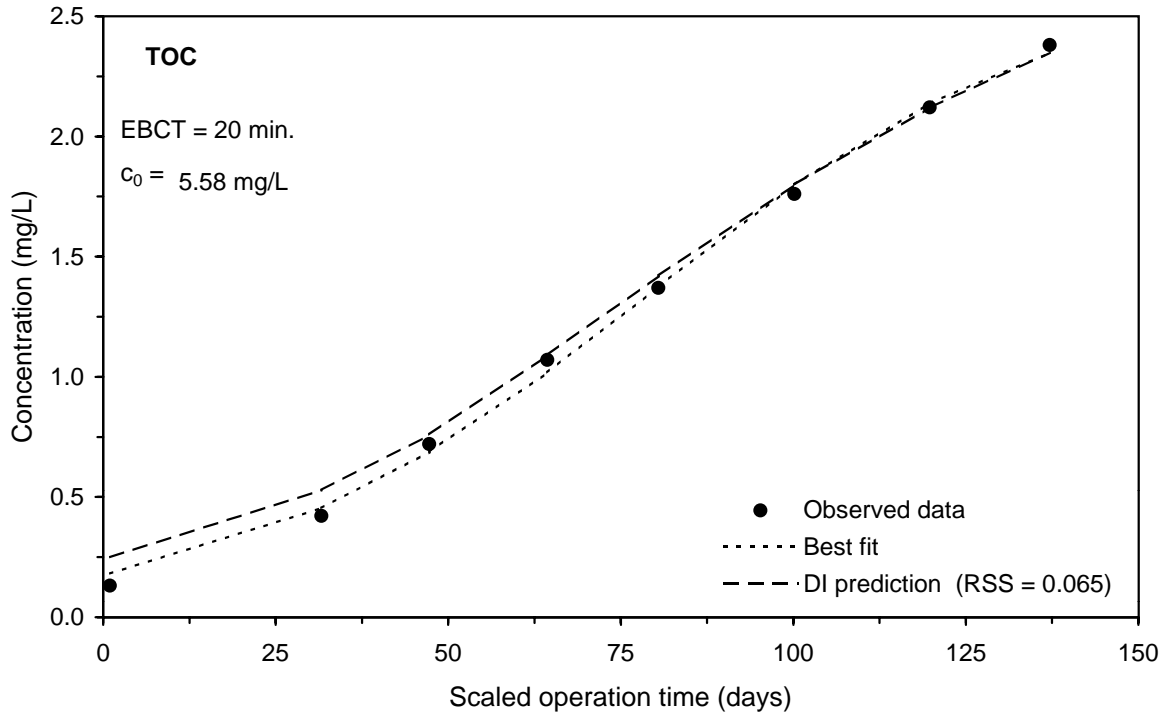


**Figure F-121 DI method prediction of the TOC integral breakthrough curve for Water 7**

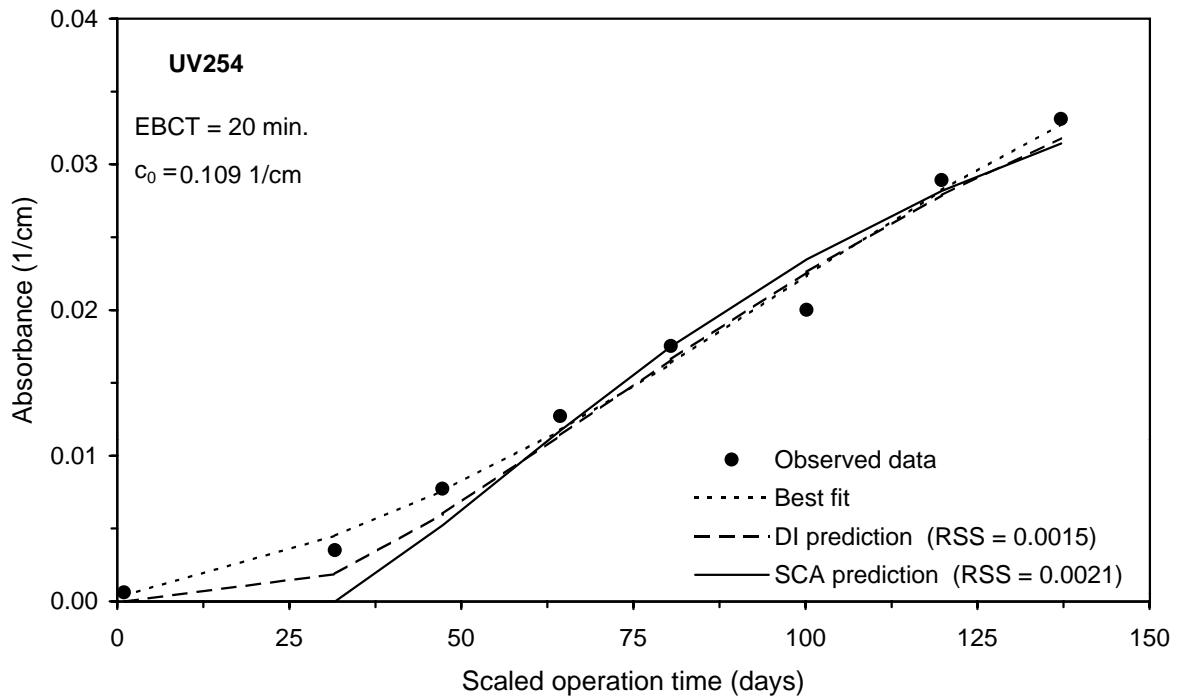


**Figure F-122 Comparison of DI and SCA methods for predicting the UV254 integral breakthrough curve for Water 7**

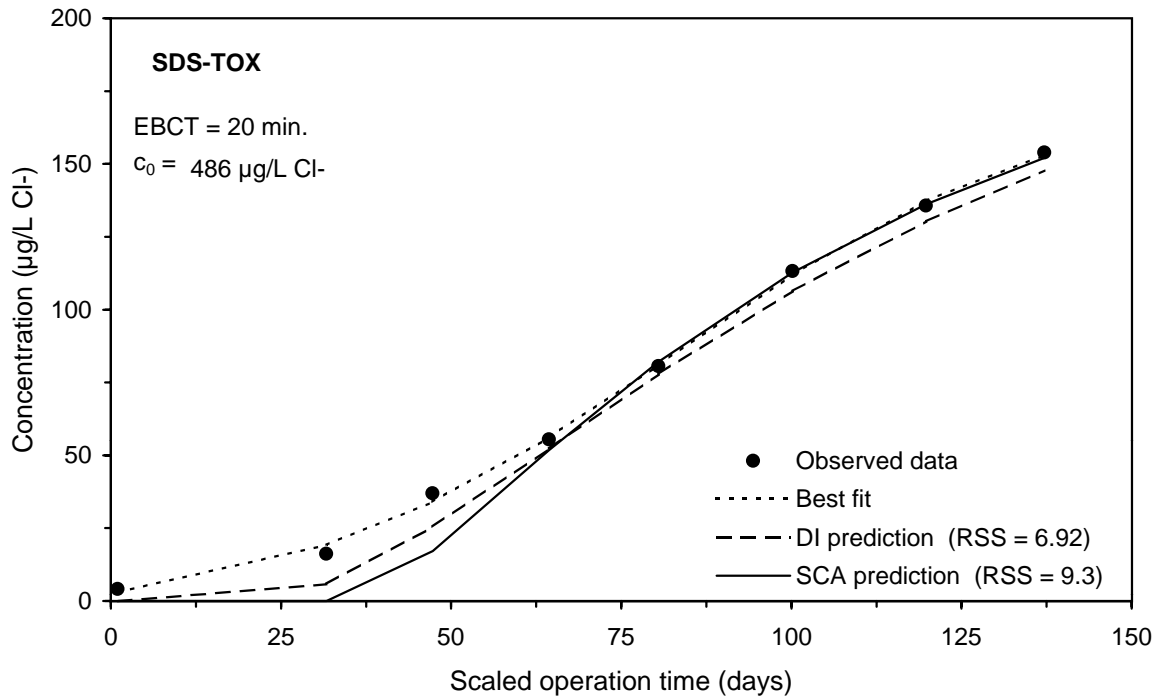


**Figure F-123 Comparison of DI and SCA methods for predicting the SDS-TOX integral breakthrough curve for Water 7**

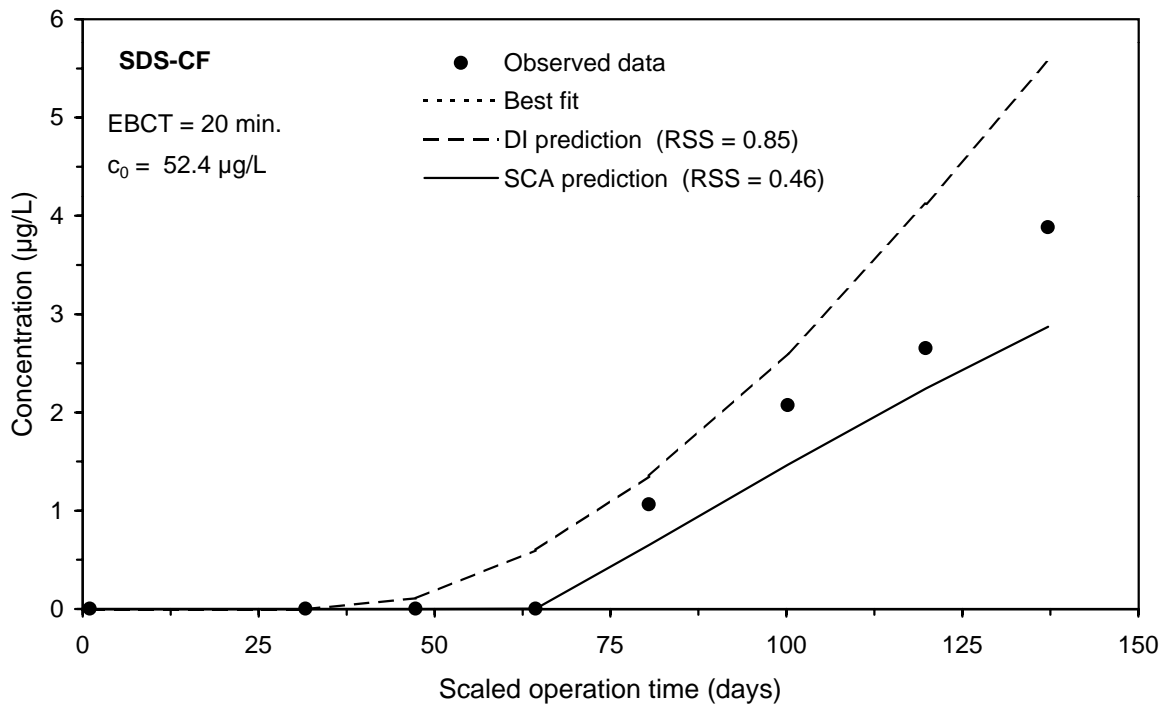


**Figure F-124 Comparison of DI and SCA methods for predicting the SDS-CF integral breakthrough curve for Water 7**

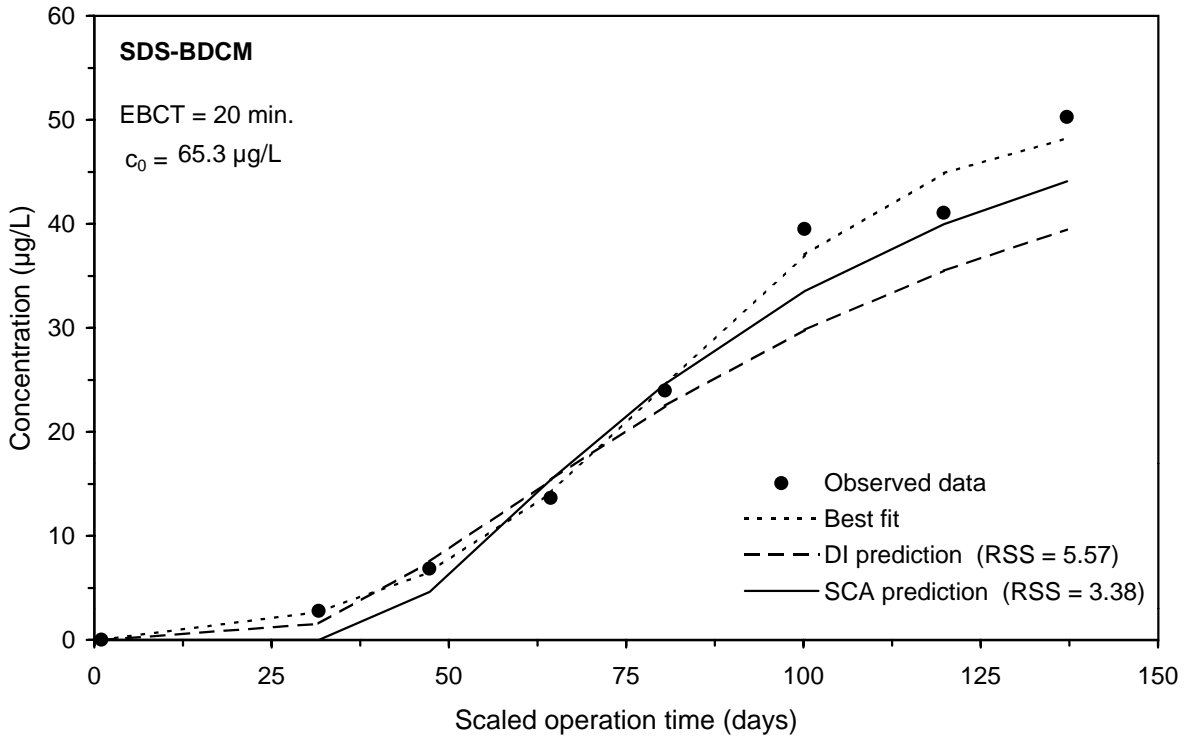


**Figure F-125 Comparison of DI and SCA methods for predicting the SDS-BDCM integral breakthrough curve for Water 7**

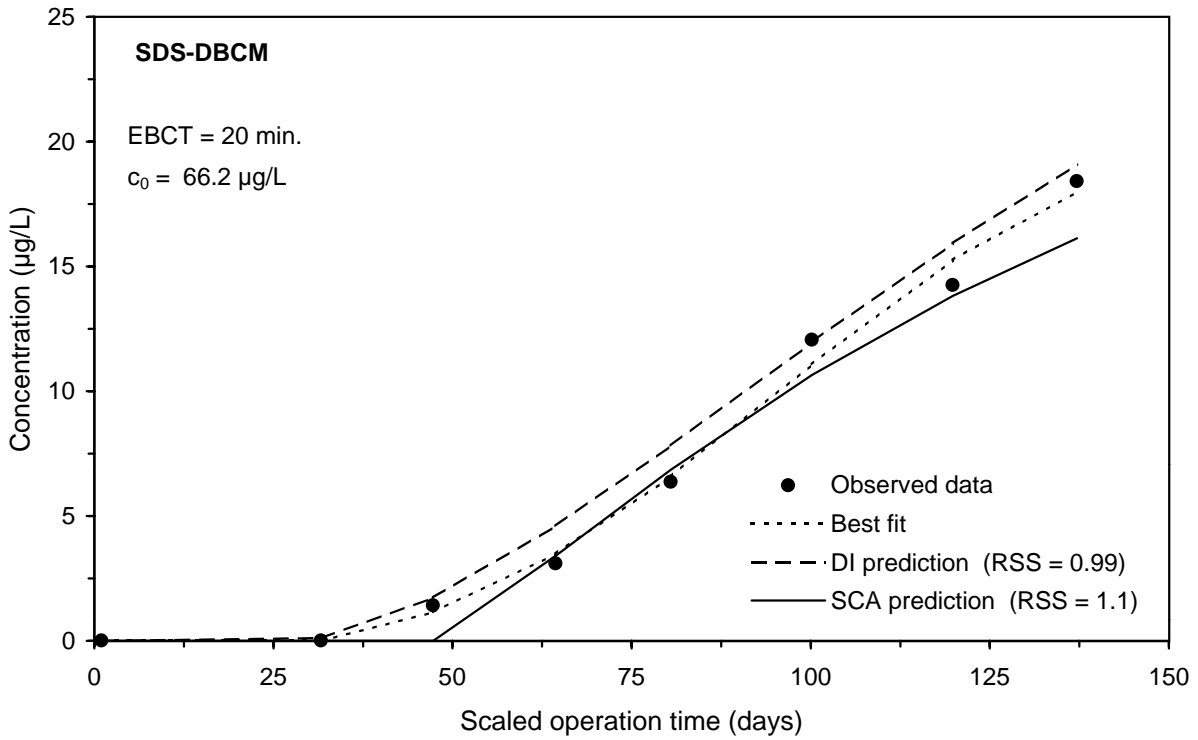


**Figure F-126 Comparison of DI and SCA methods for predicting the SDS-DBCm integral breakthrough curve for Water 7**

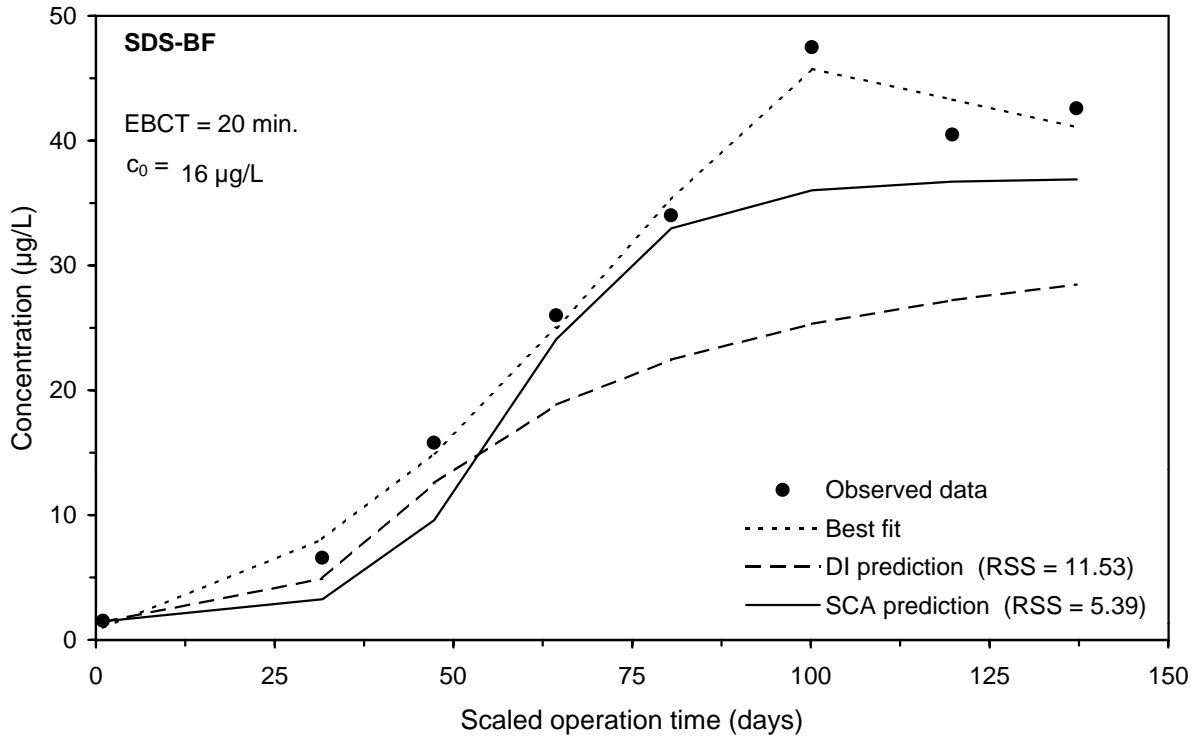


**Figure F-127 Comparison of DI and SCA methods for predicting the SDS-BF integral breakthrough curve for Water 7**

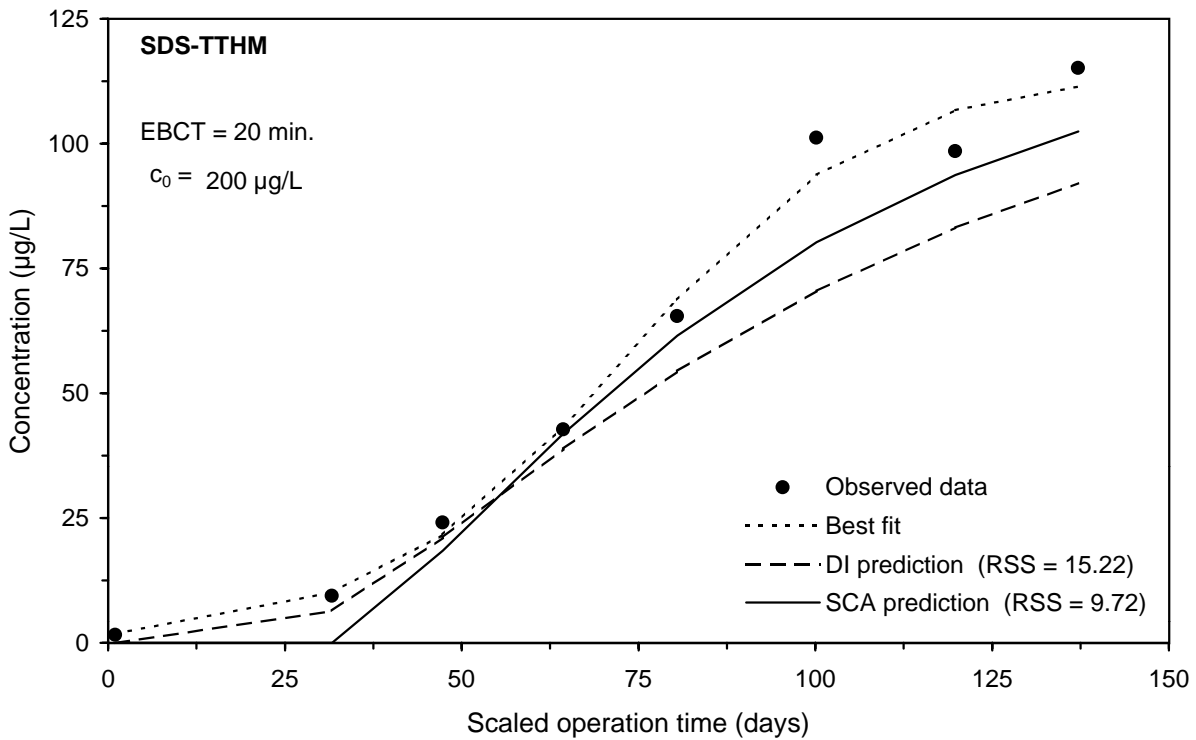


**Figure F-128 Comparison of DI and SCA methods for predicting the SDS-TTHM integral breakthrough curve for Water 7**

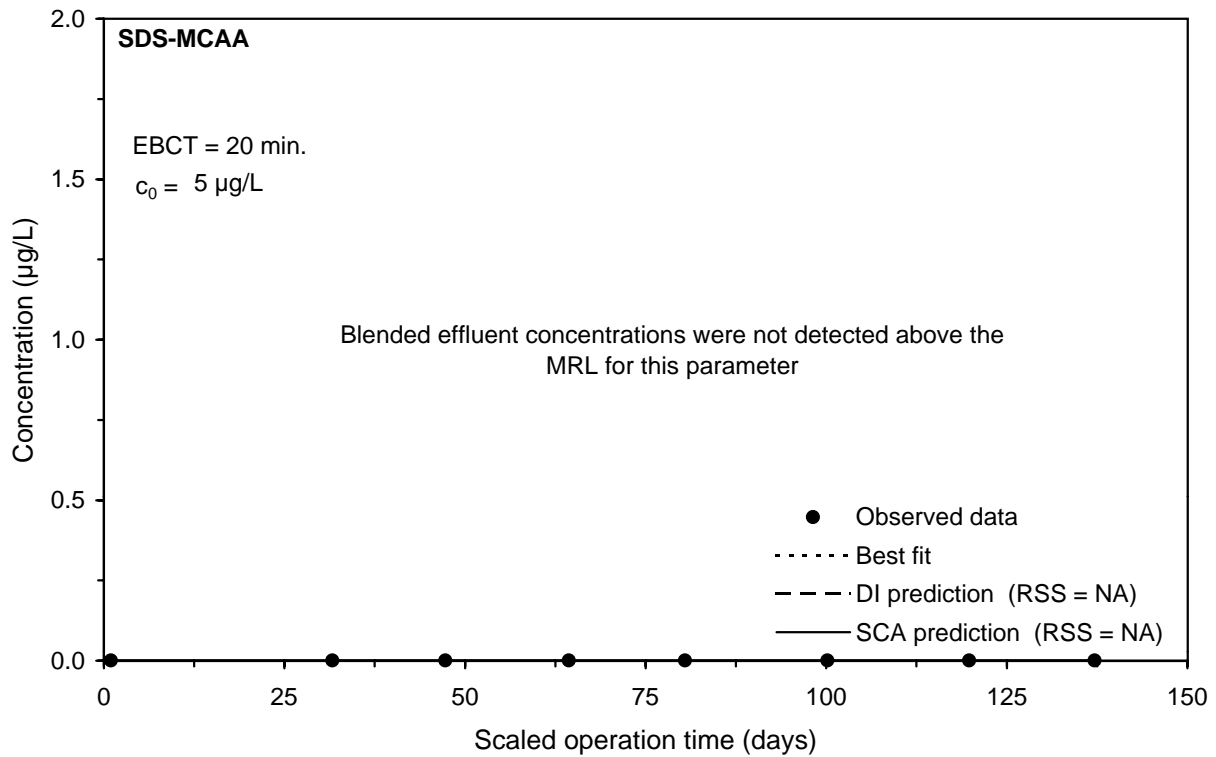


**Figure F-129 Comparison of DI and SCA methods for predicting the SDS-MCAA integral breakthrough curve for Water 7**

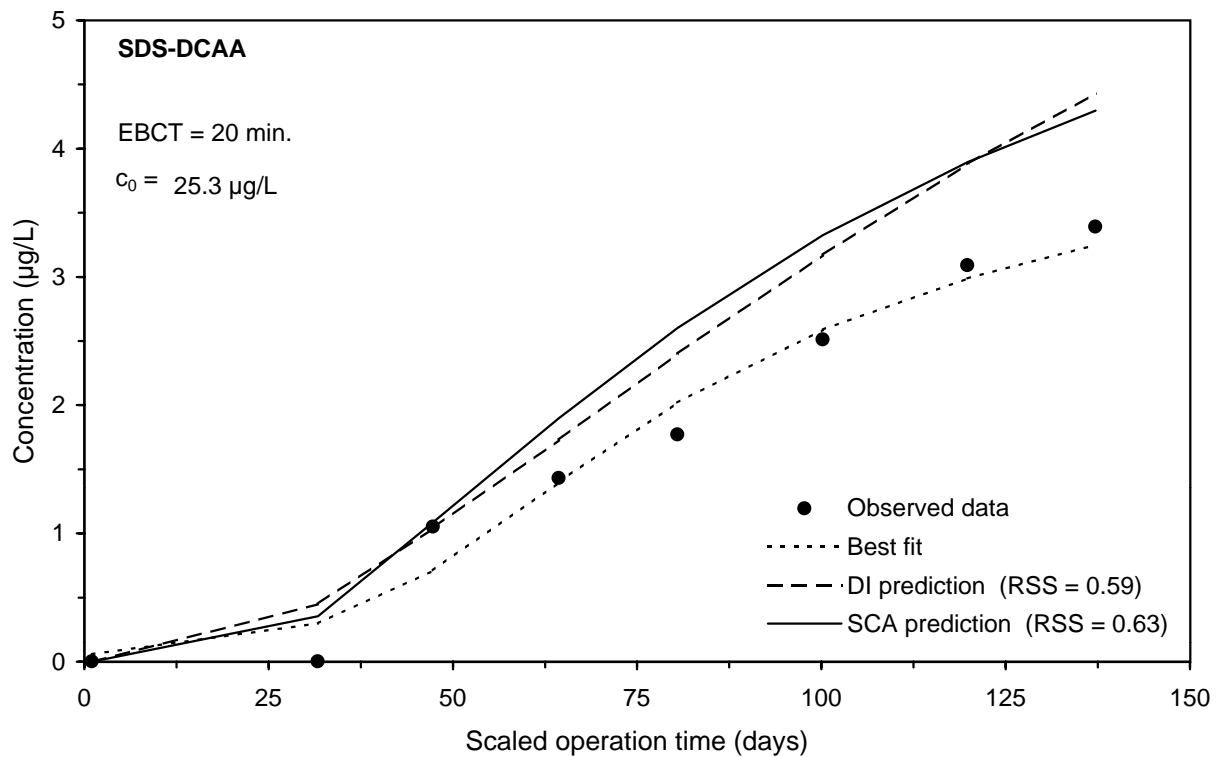


**Figure F-130 Comparison of DI and SCA methods for predicting the SDS-DCAA integral breakthrough curve for Water 7**

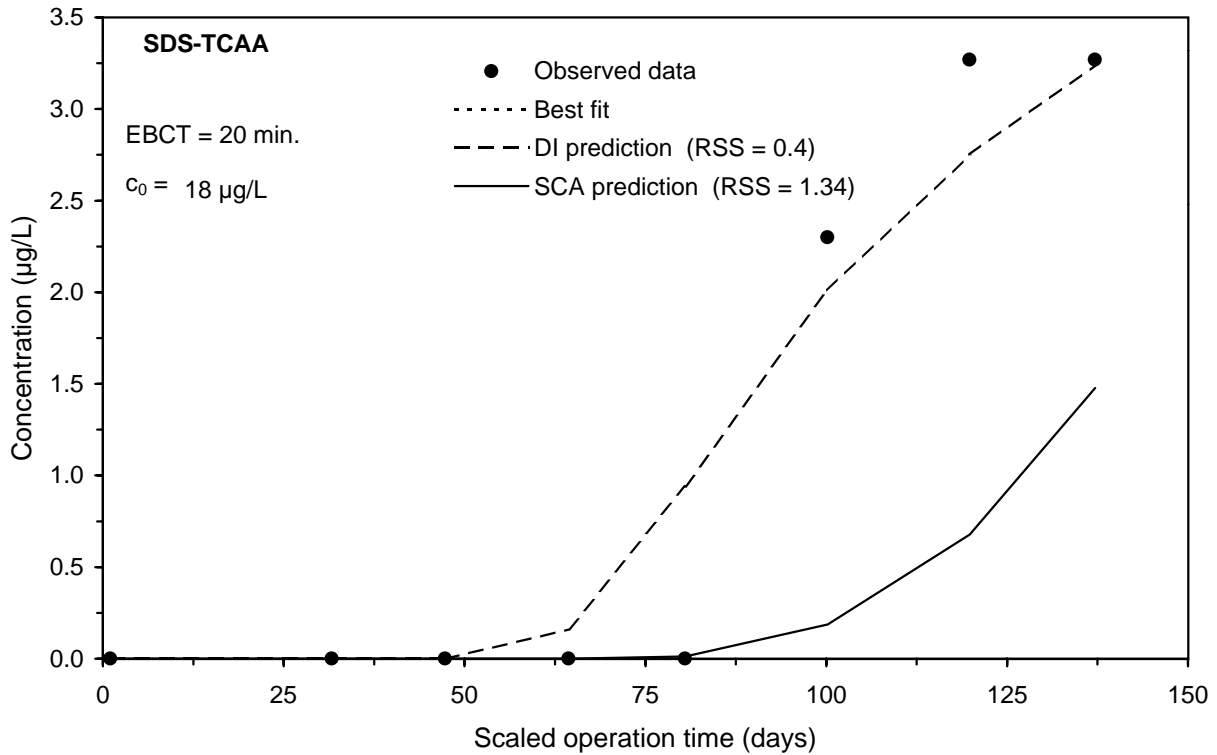


**Figure F-131 Comparison of DI and SCA methods for predicting the SDS-TCAA integral breakthrough curve for Water 7**

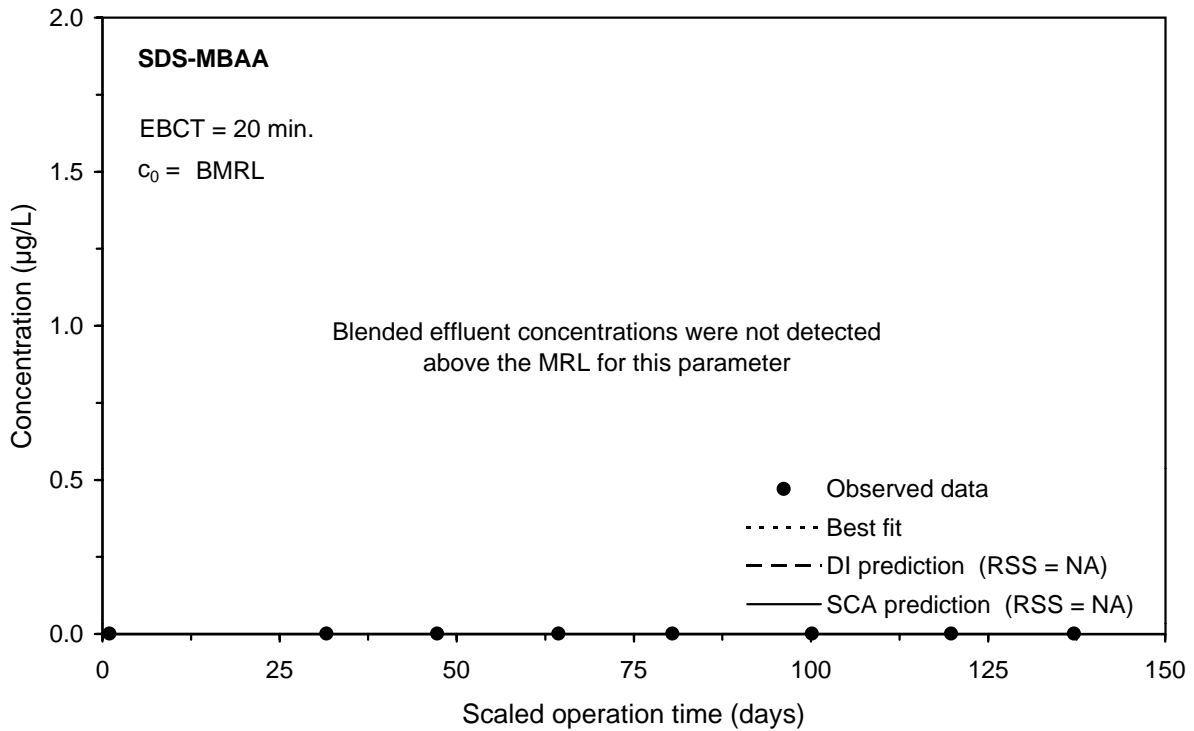


**Figure F-132 Comparison of DI and SCA methods for predicting the SDS-MBAA integral breakthrough curve for Water 7**

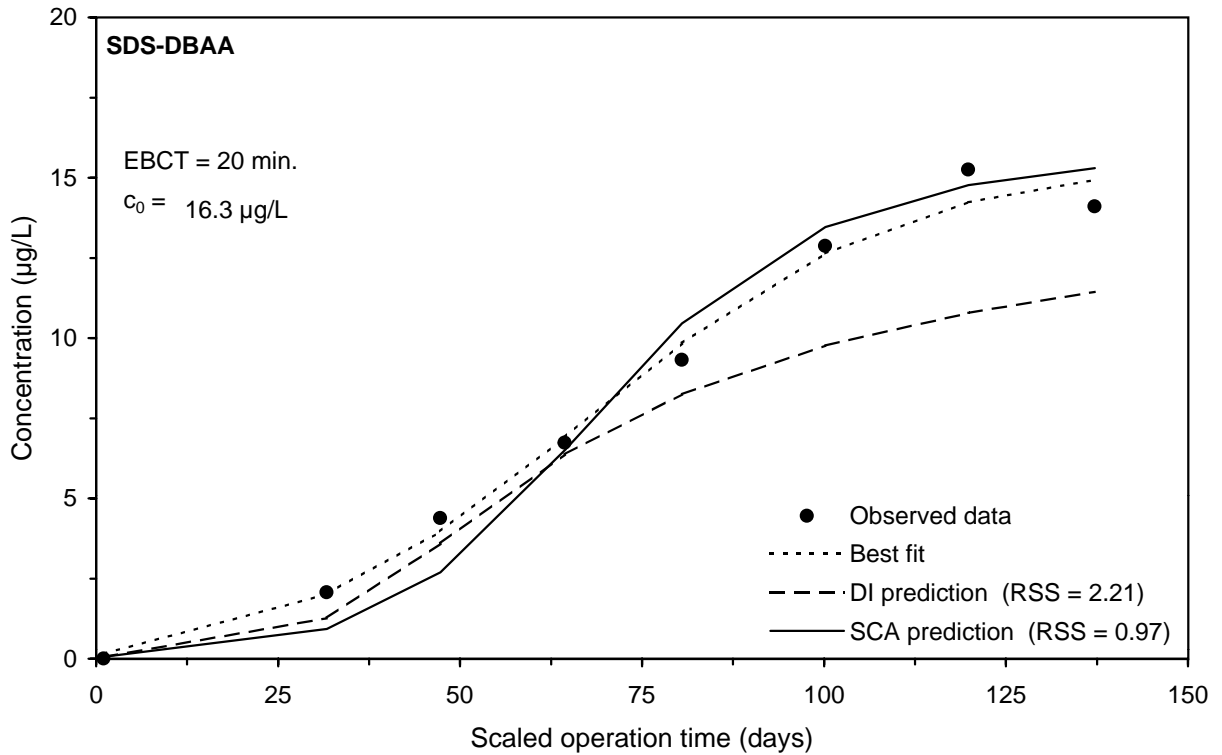


**Figure F-133 Comparison of DI and SCA methods for predicting the SDS-DBAA integral breakthrough curve for Water 7**

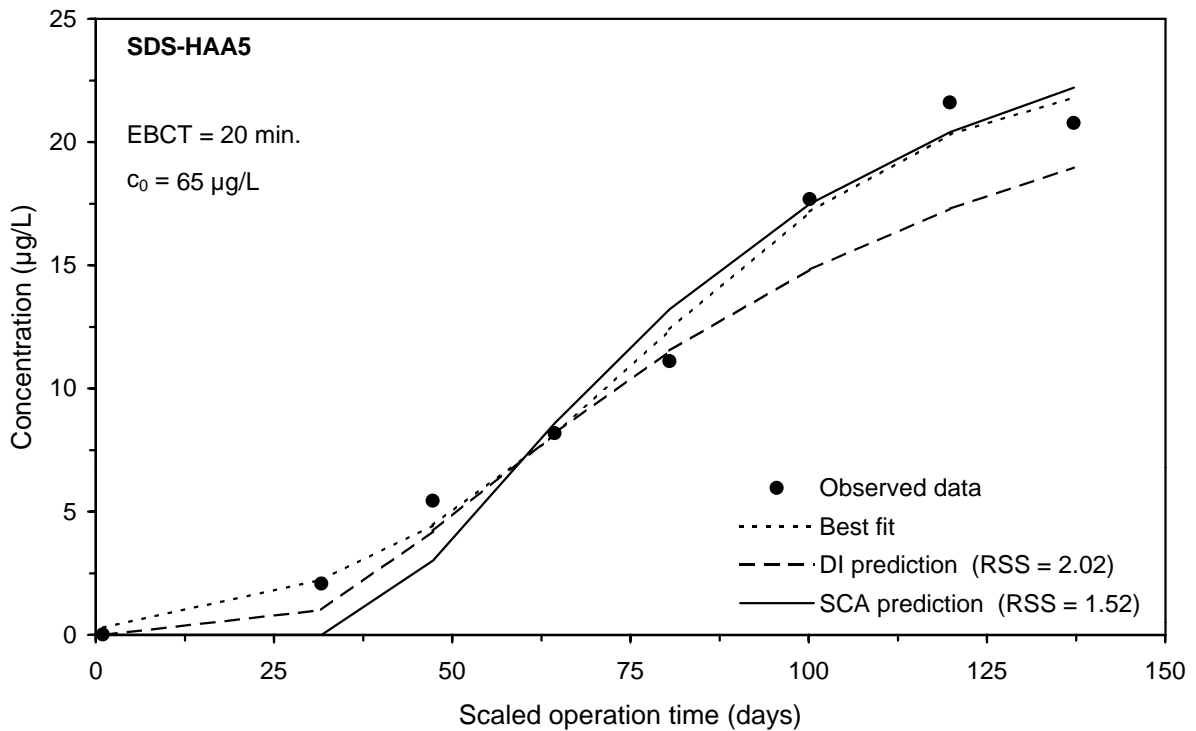


**Figure F-134 Comparison of DI and SCA methods for predicting the SDS-HAA5 integral breakthrough curve for Water 7**

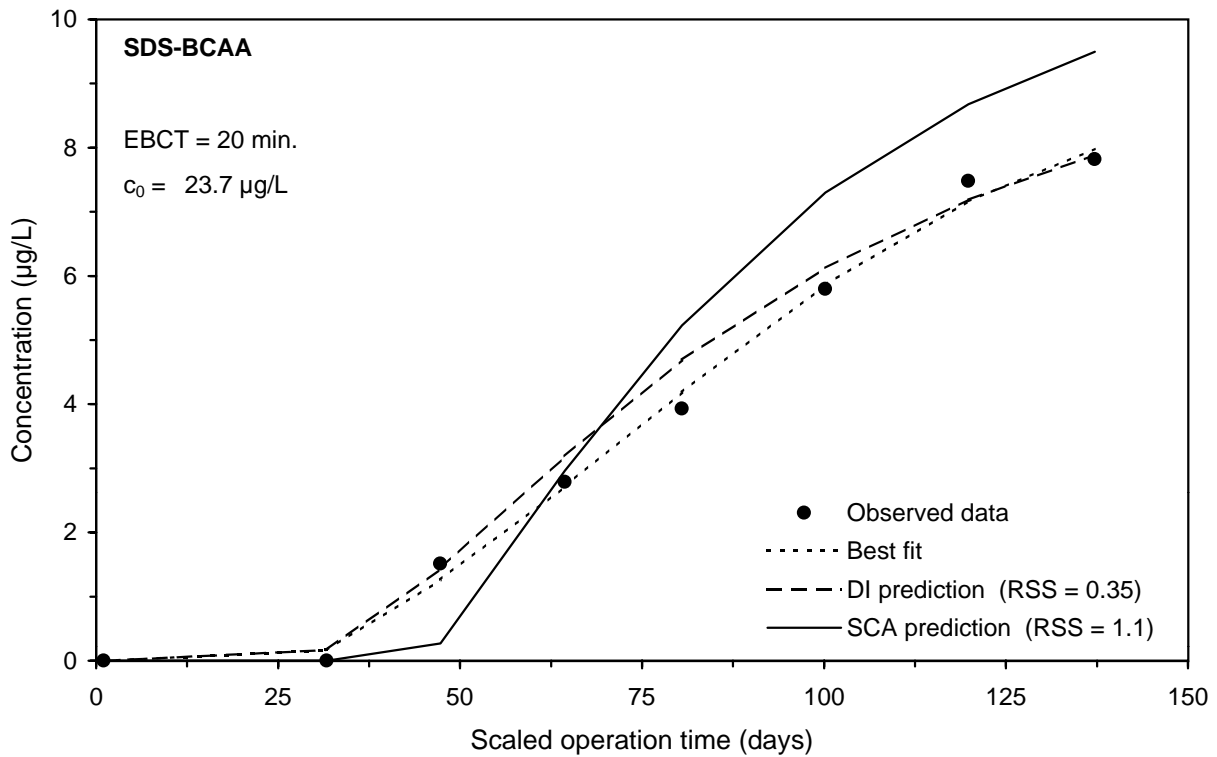


**Figure F-135 Comparison of DI and SCA methods for predicting the SDS-BCAA integral breakthrough curve for Water 7**

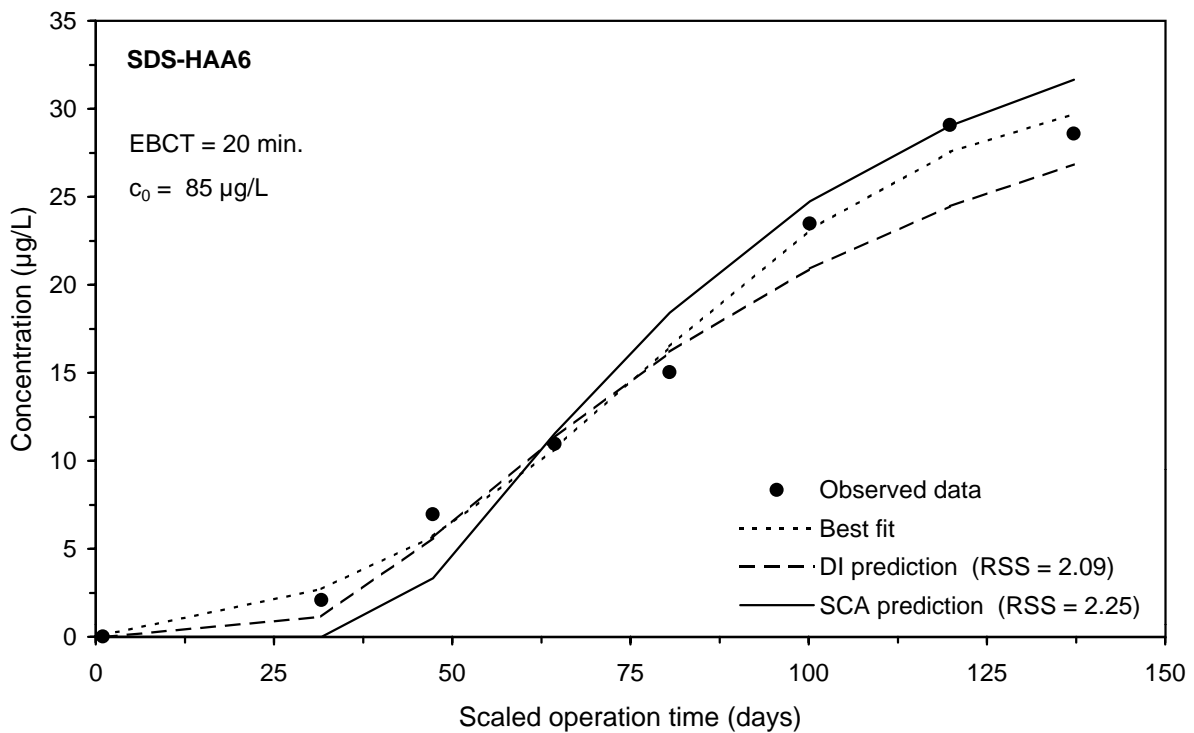


**Figure F-136 Comparison of DI and SCA methods for predicting the SDS-HAA6 integral breakthrough curve for Water 7**

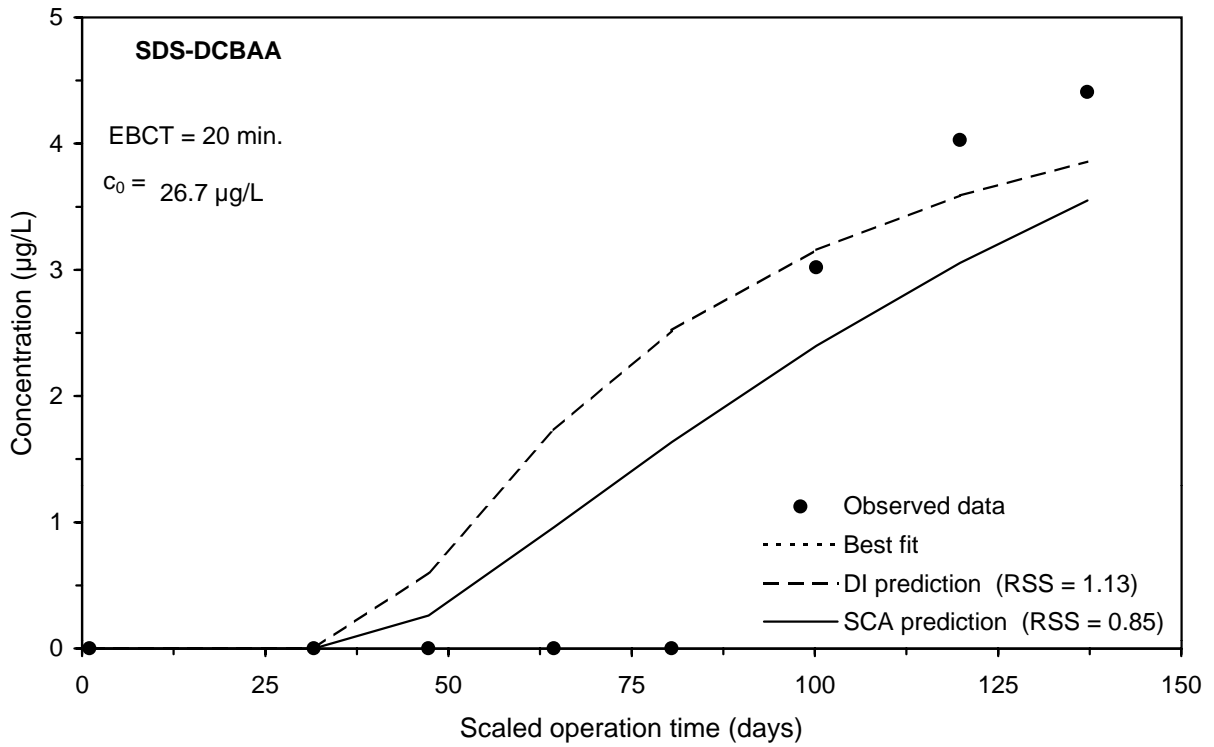


**Figure F-137 Comparison of DI and SCA methods for predicting the SDS-DCBAA integral breakthrough curve for Water 7**

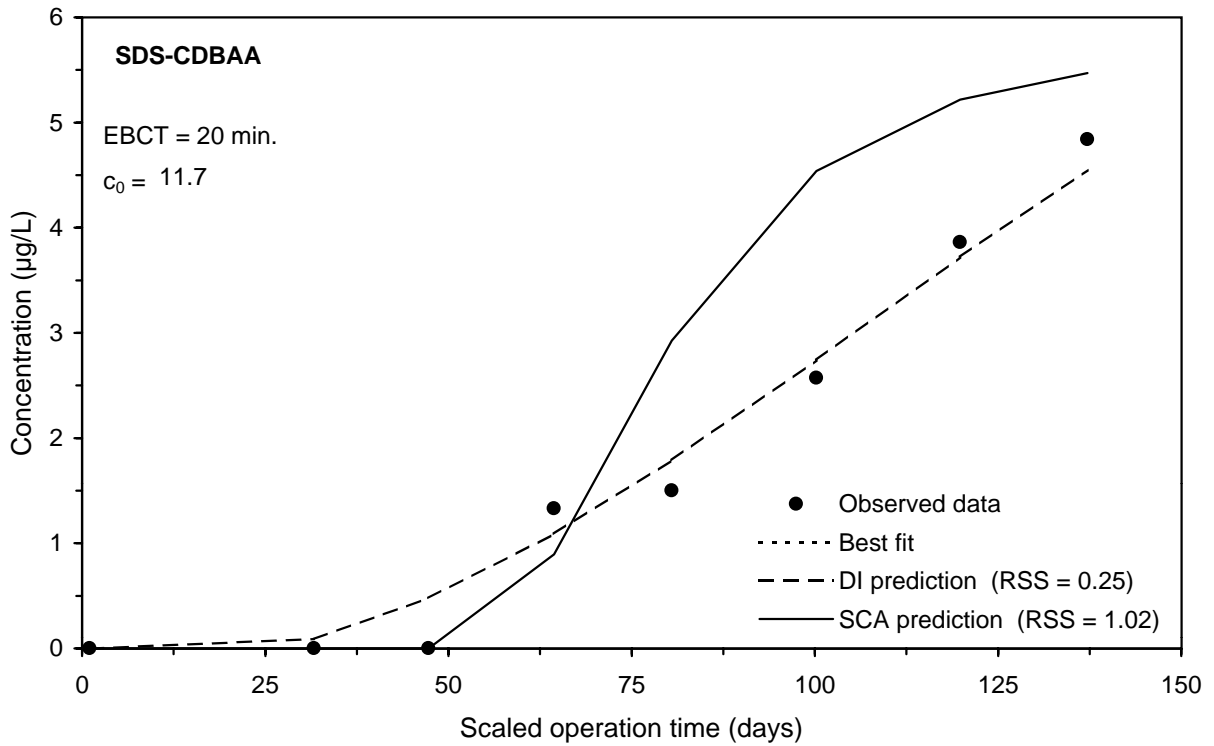


**Figure F-138 Comparison of DI and SCA methods for predicting the SDS-CDBAA integral breakthrough curve for Water 7**

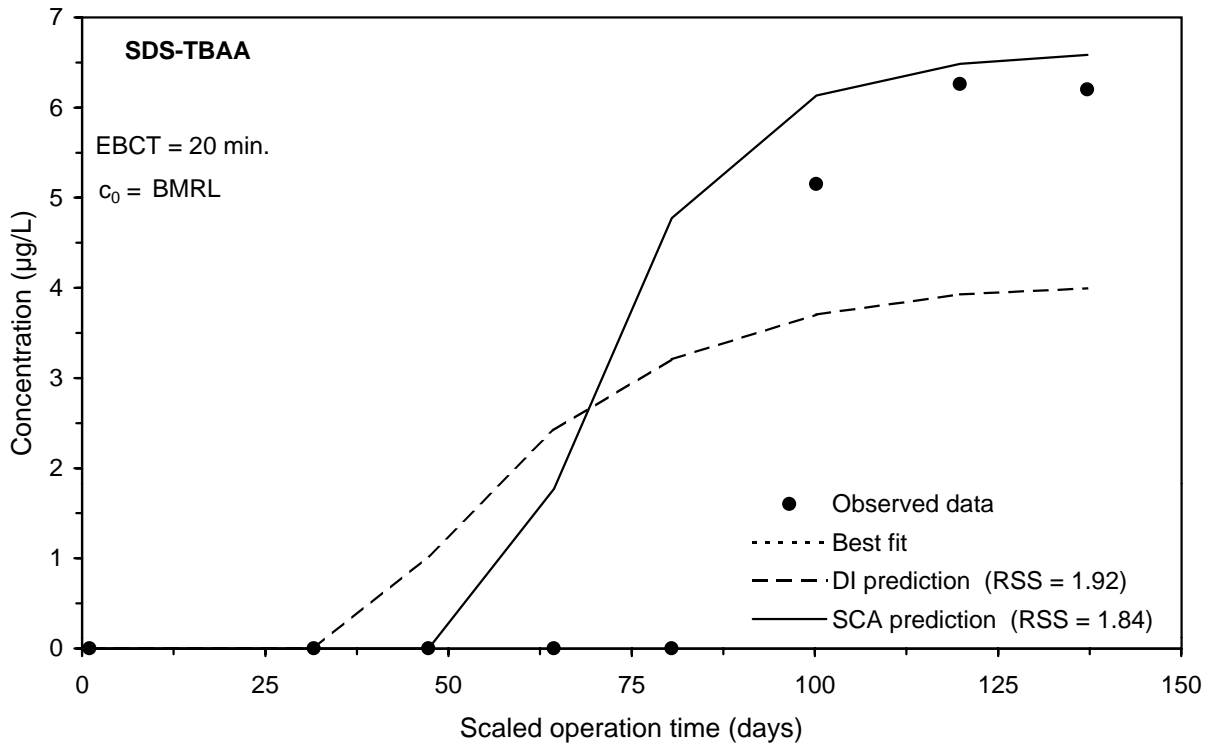


**Figure F-139 Comparison of DI and SCA methods for predicting the SDS-TBAA integral breakthrough curve for Water 7**

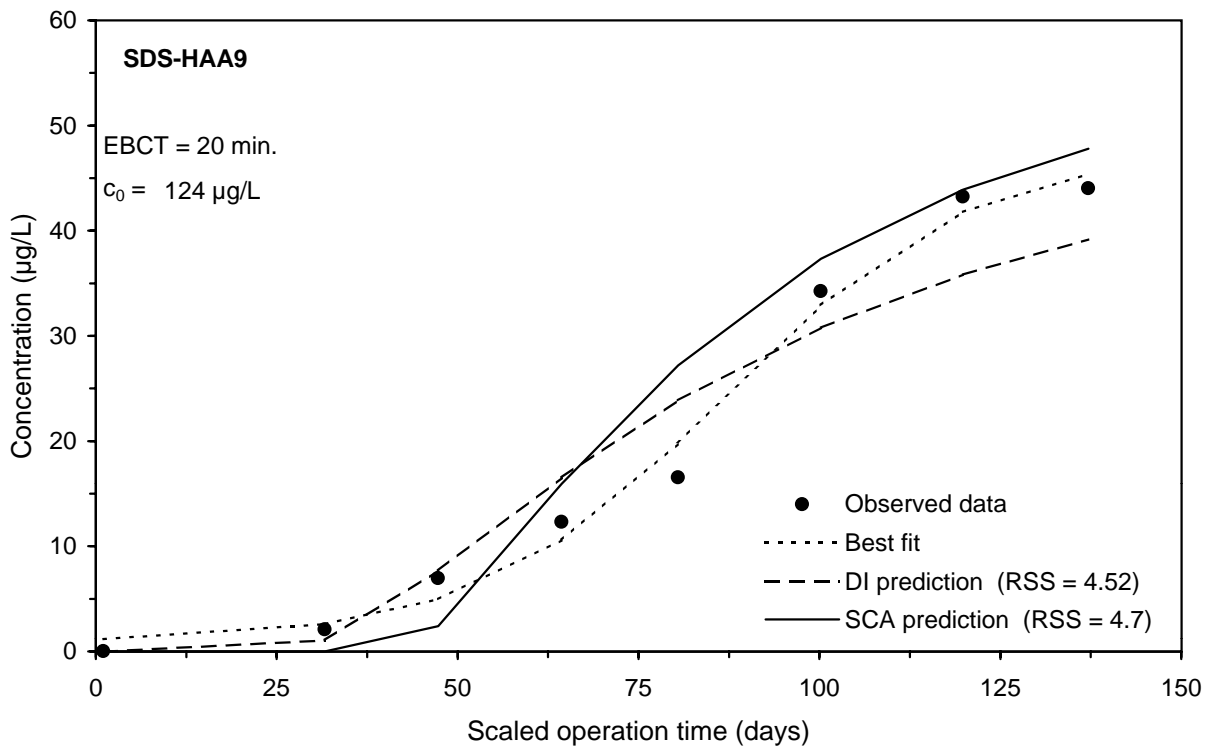


**Figure F-140 Comparison of DI and SCA methods for predicting the SDS-HAA9 integral breakthrough curve for Water 7**

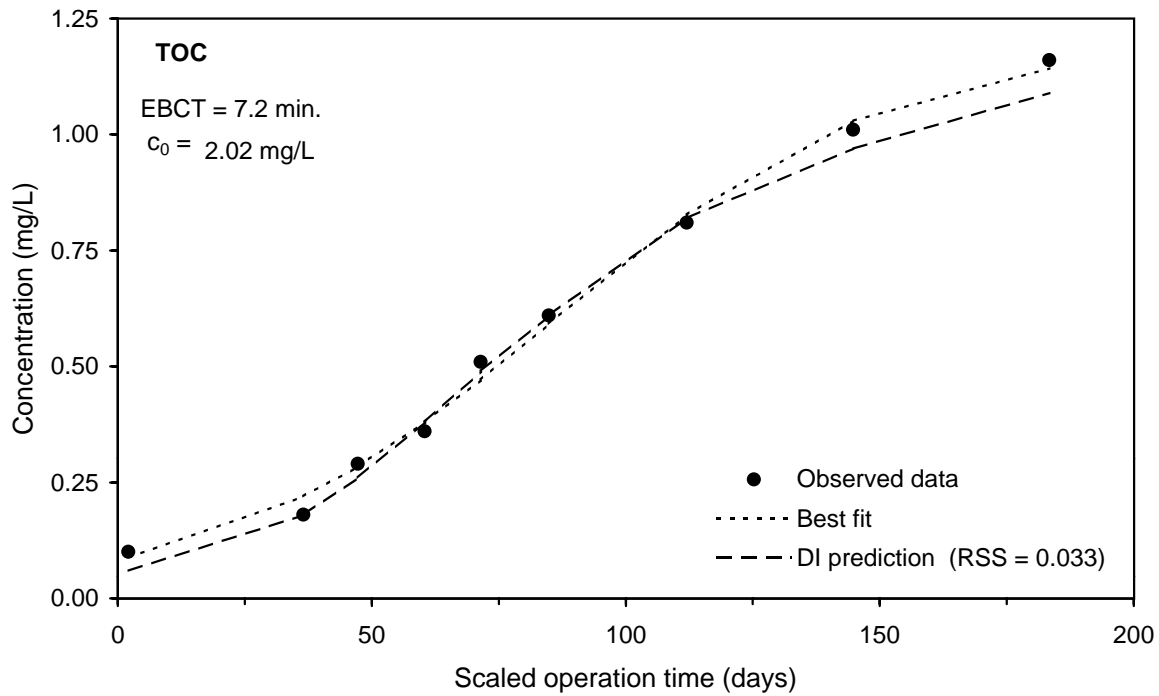


**Figure F-141 DI method prediction of the TOC integral breakthrough curve for Water 8**

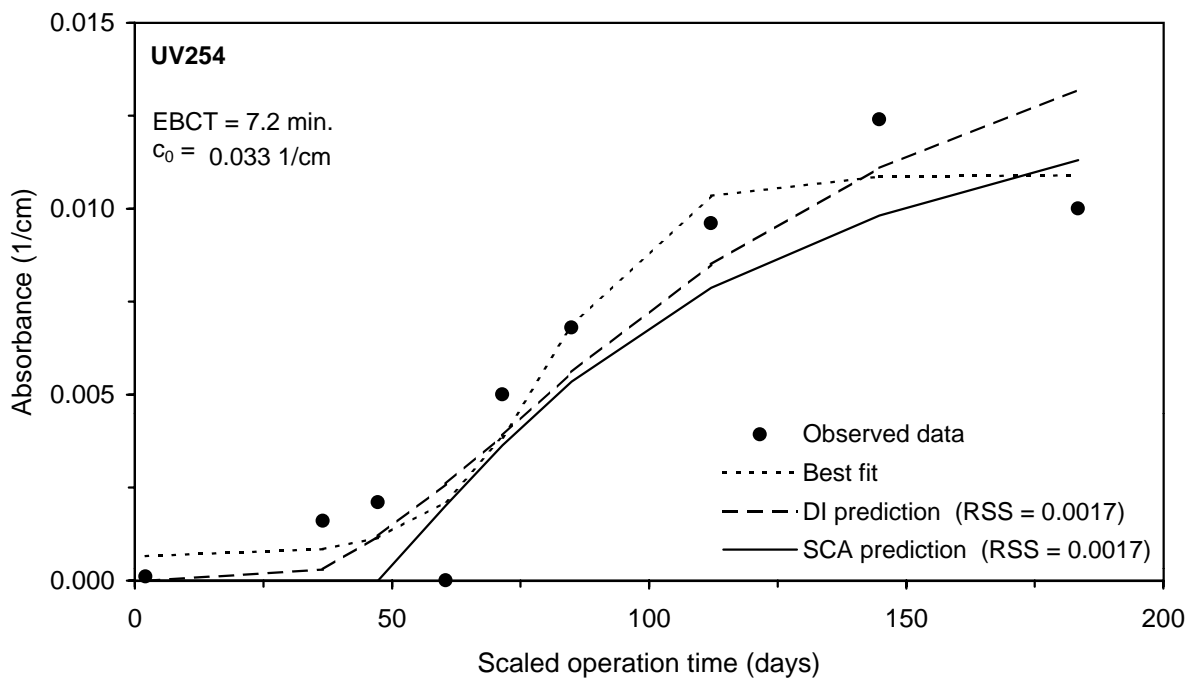


**Figure F-142 Comparison of DI and SCA methods for predicting the UV254 integral breakthrough curve for Water 8**

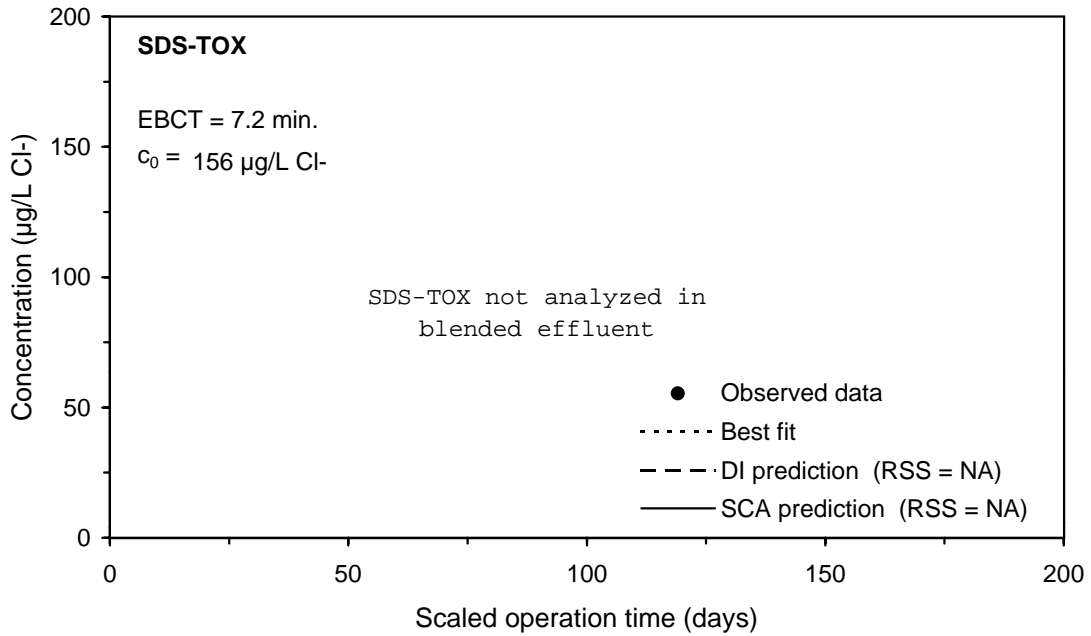


**Figure F-143 Comparison of DI and SCA methods for predicting the SDS-TOX integral breakthrough curve for Water 8**

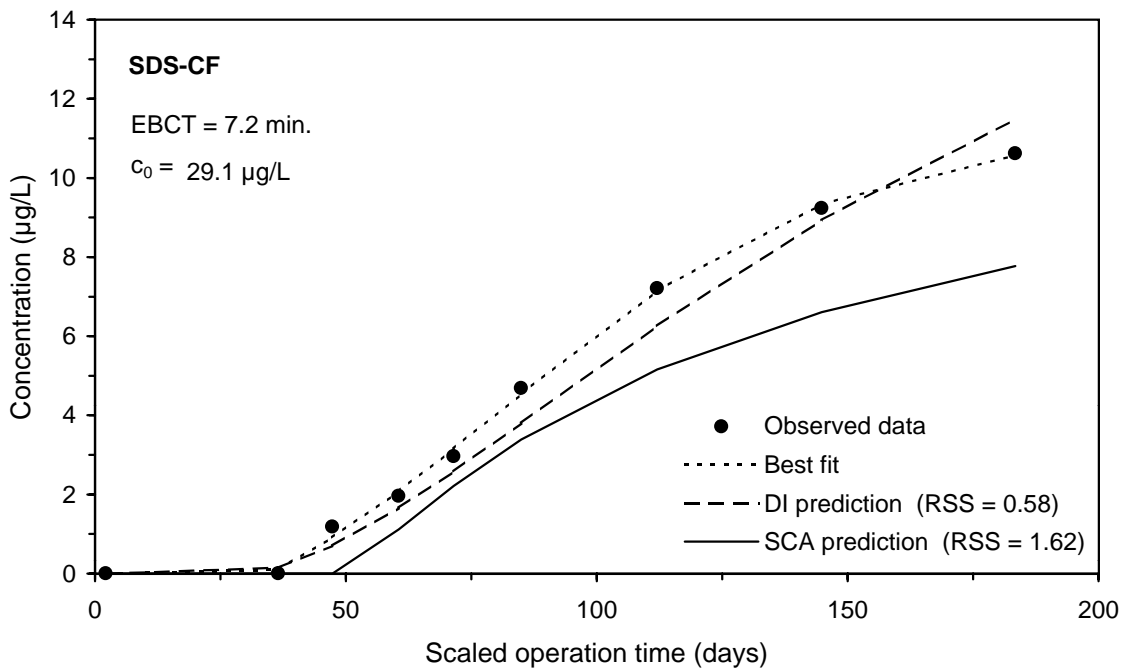


**Figure F-144 Comparison of DI and SCA methods for predicting the SDS-CF integral breakthrough curve for Water 8**

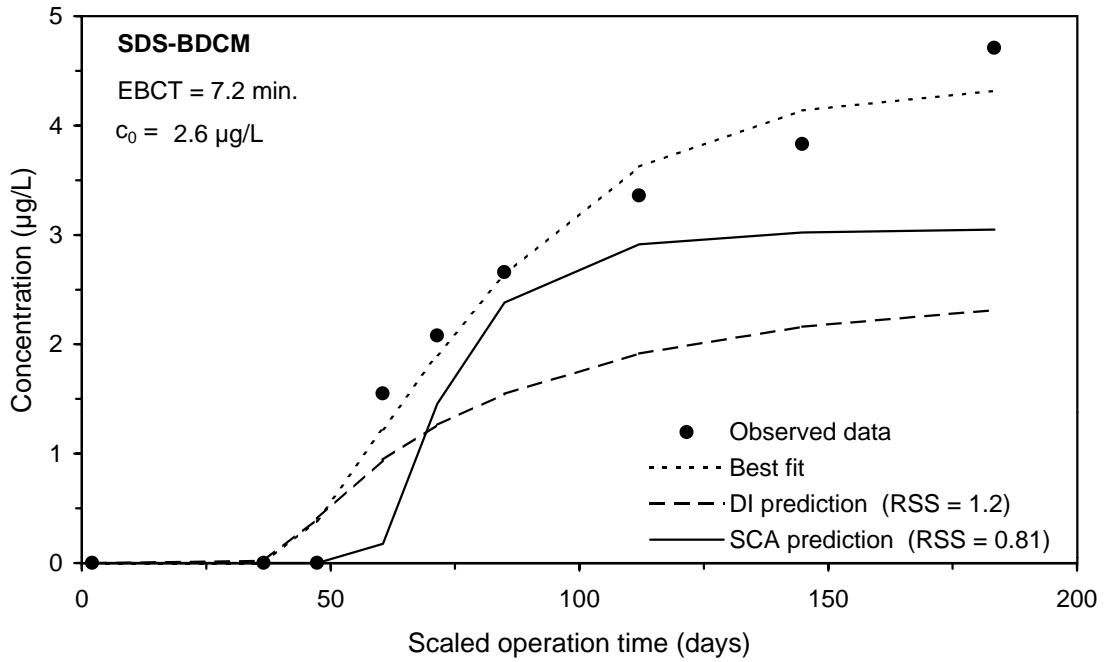


**Figure F-145 Comparison of DI and SCA methods for predicting the SDS-BDCM integral breakthrough curve for Water 8**

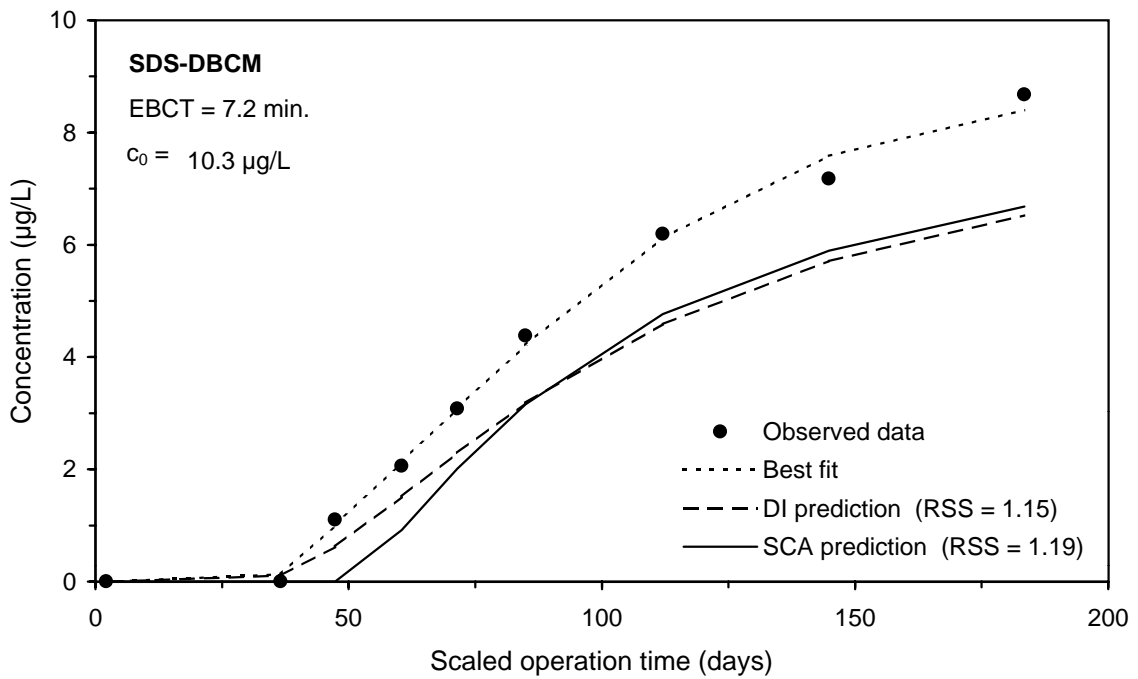


**Figure F-146 Comparison of DI and SCA methods for predicting the SDS-DBCm integral breakthrough curve for Water 8**

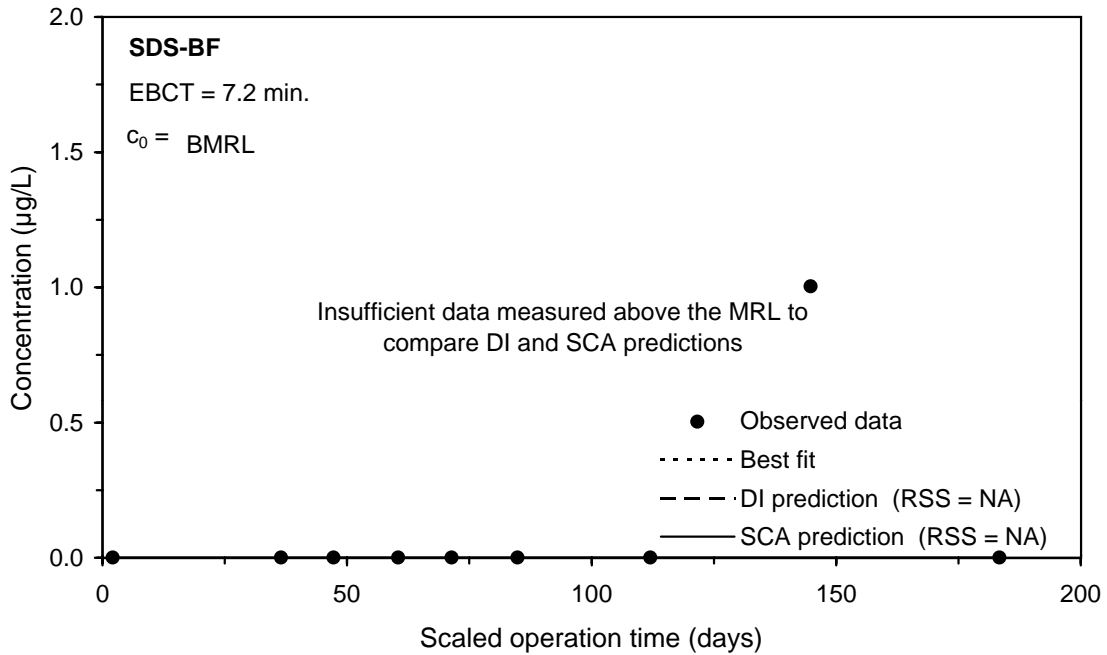


**Figure F-147 Comparison of DI and SCA methods for predicting the SDS-BF integral breakthrough curve for Water 8**

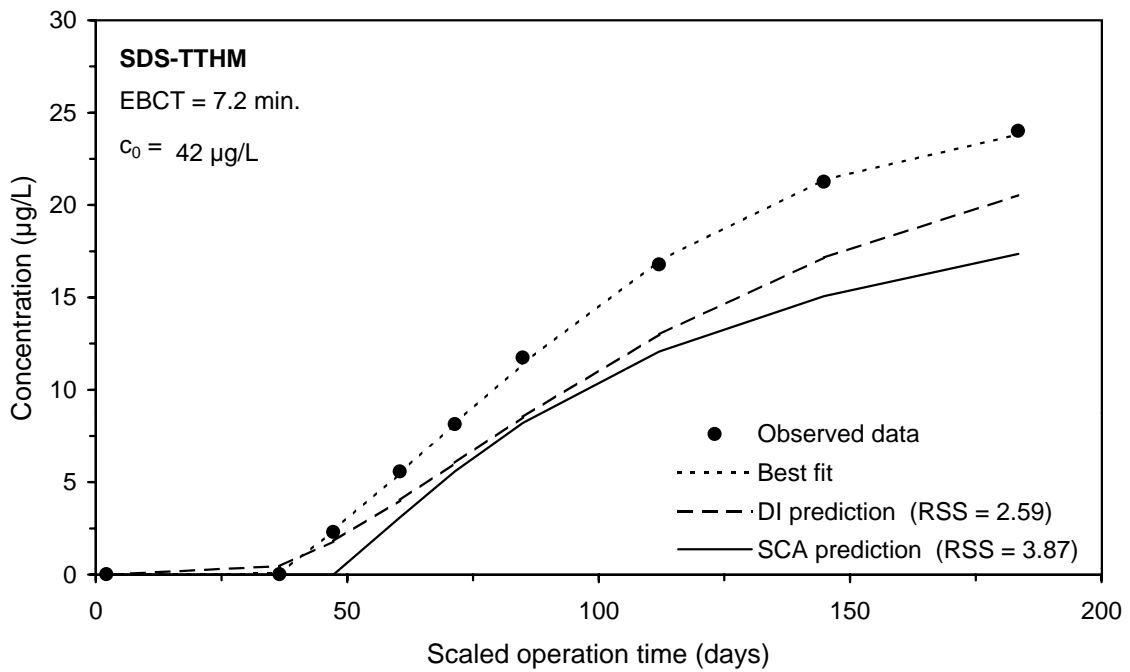


**Figure F-148 Comparison of DI and SCA methods for predicting the SDS-TTHM integral breakthrough curve for Water 8**

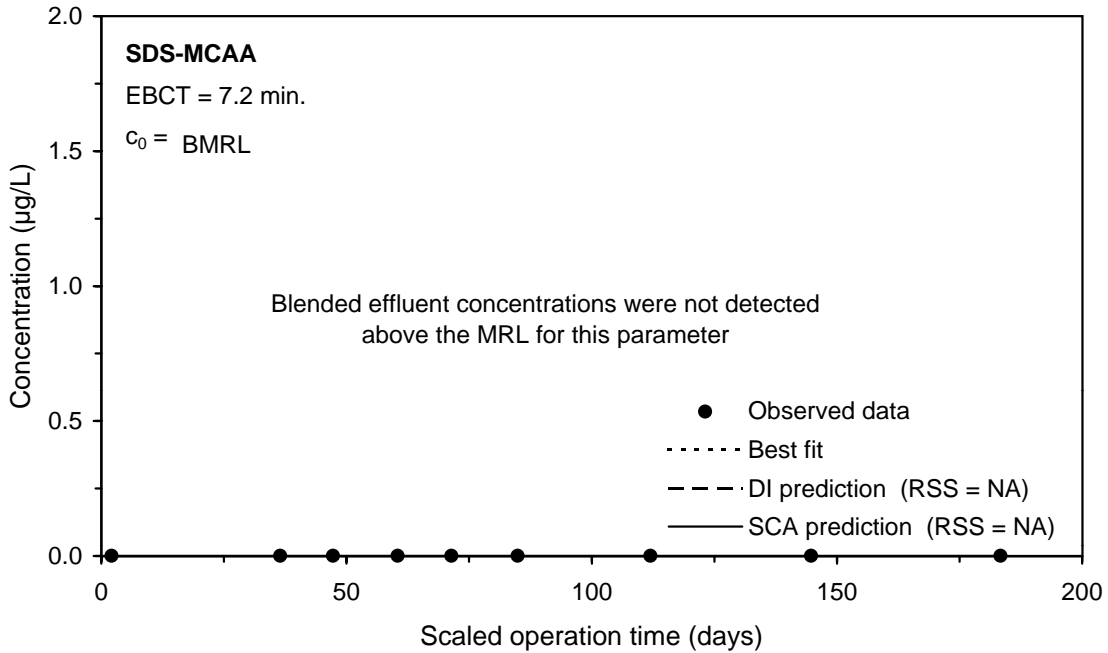


**Figure F-149 Comparison of DI and SCA methods for predicting the SDS-MCAA integral breakthrough curve for Water 8**

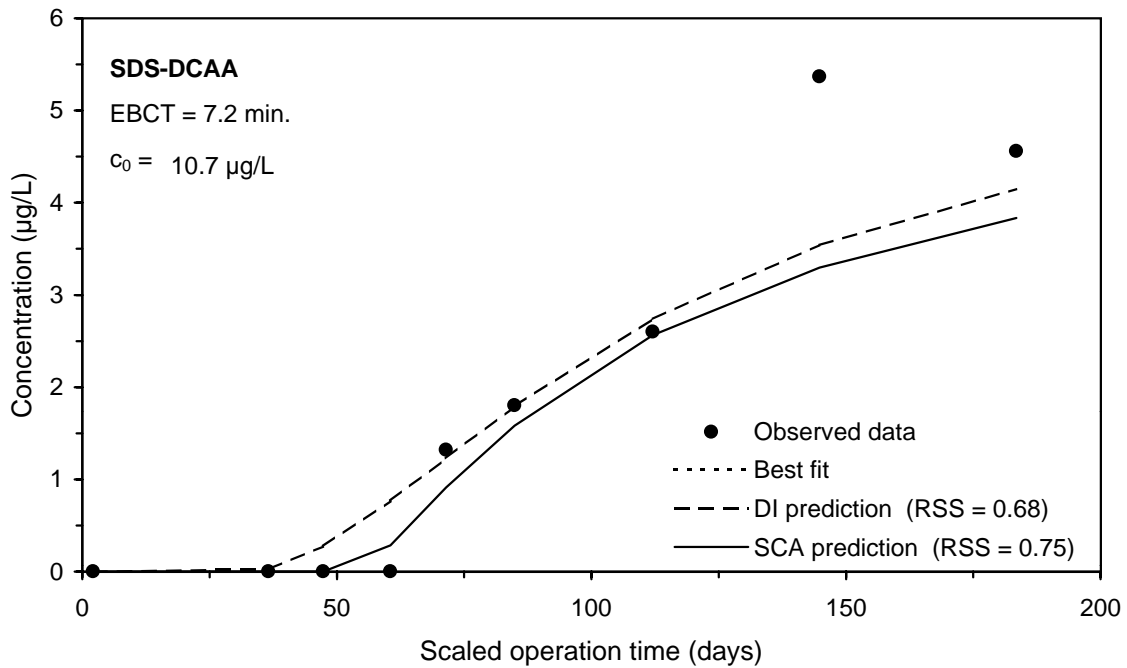


**Figure F-150 Comparison of DI and SCA methods for predicting the SDS-DCAA integral breakthrough curve for Water 8**

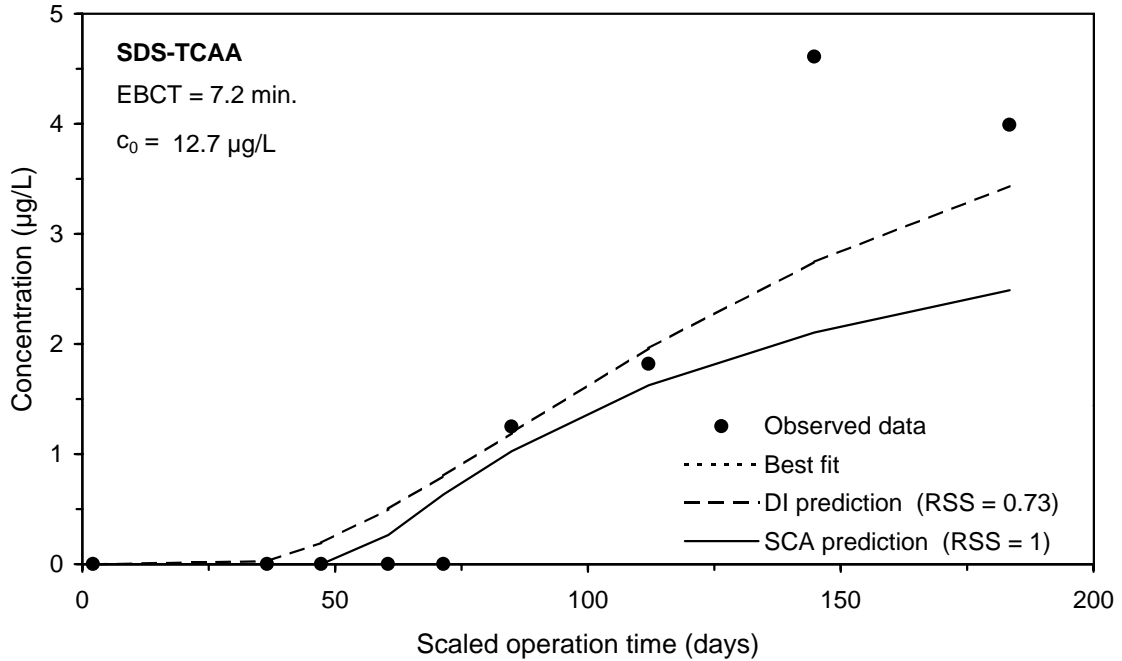


**Figure F-151 Comparison of DI and SCA methods for predicting the SDS-TCAA integral breakthrough curve for Water 8**

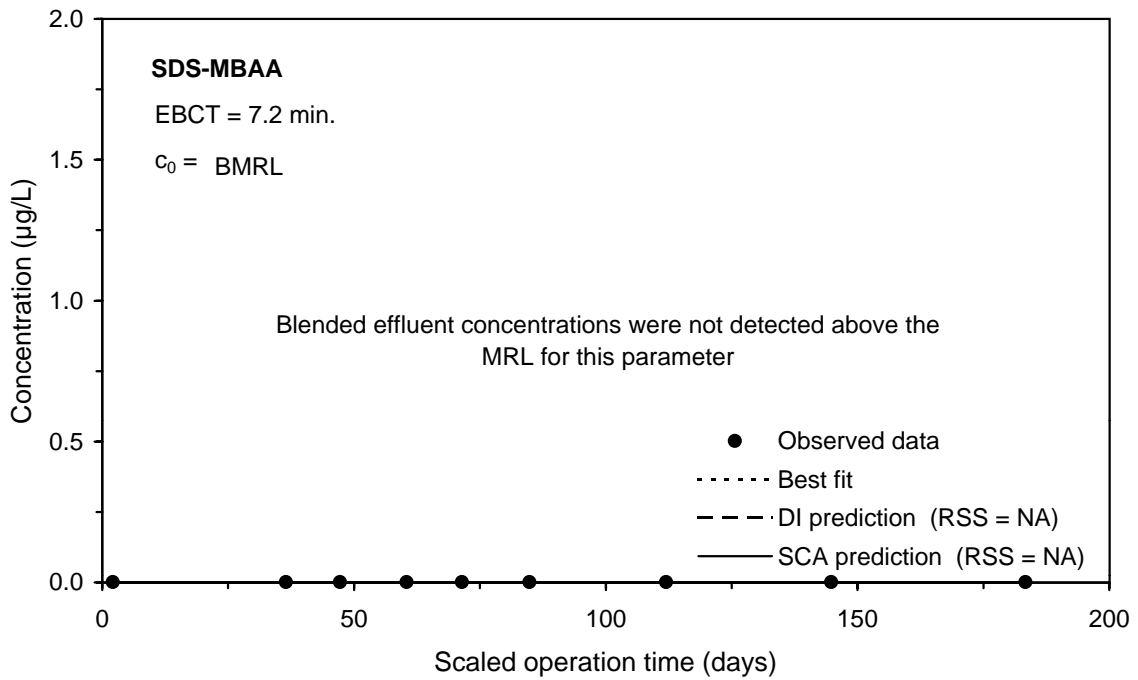


**Figure F-152 Comparison of DI and SCA methods for predicting the SDS-MBAA integral breakthrough curve for Water 8**

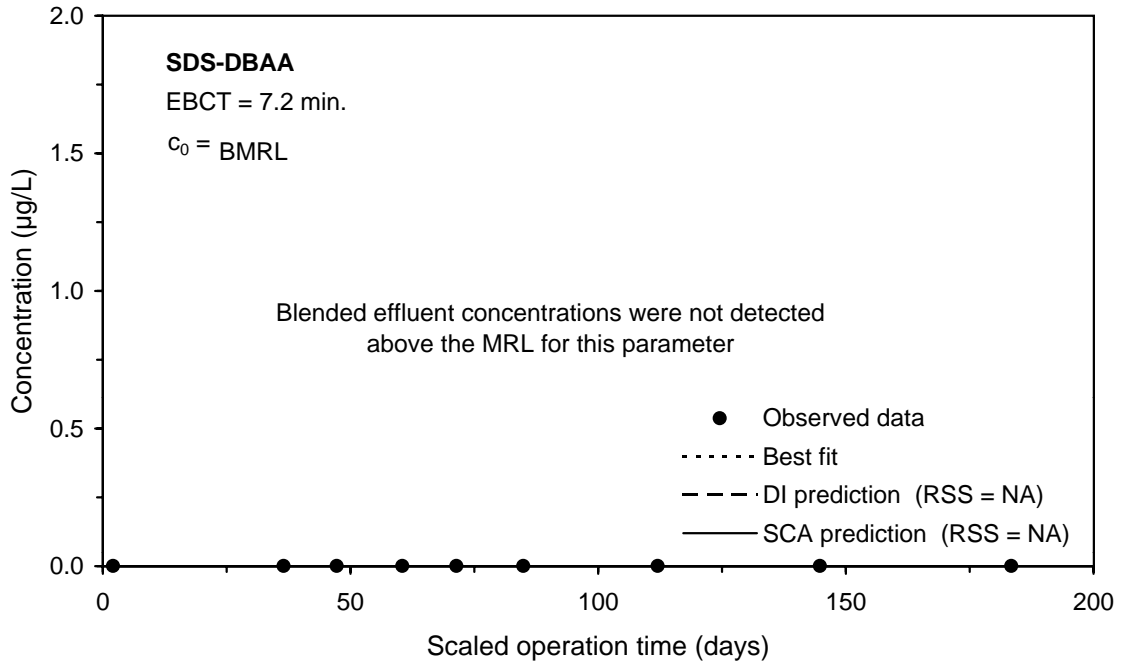


**Figure F-153 Comparison of DI and SCA methods for predicting the SDS-DBAA integral breakthrough curve for Water 8**

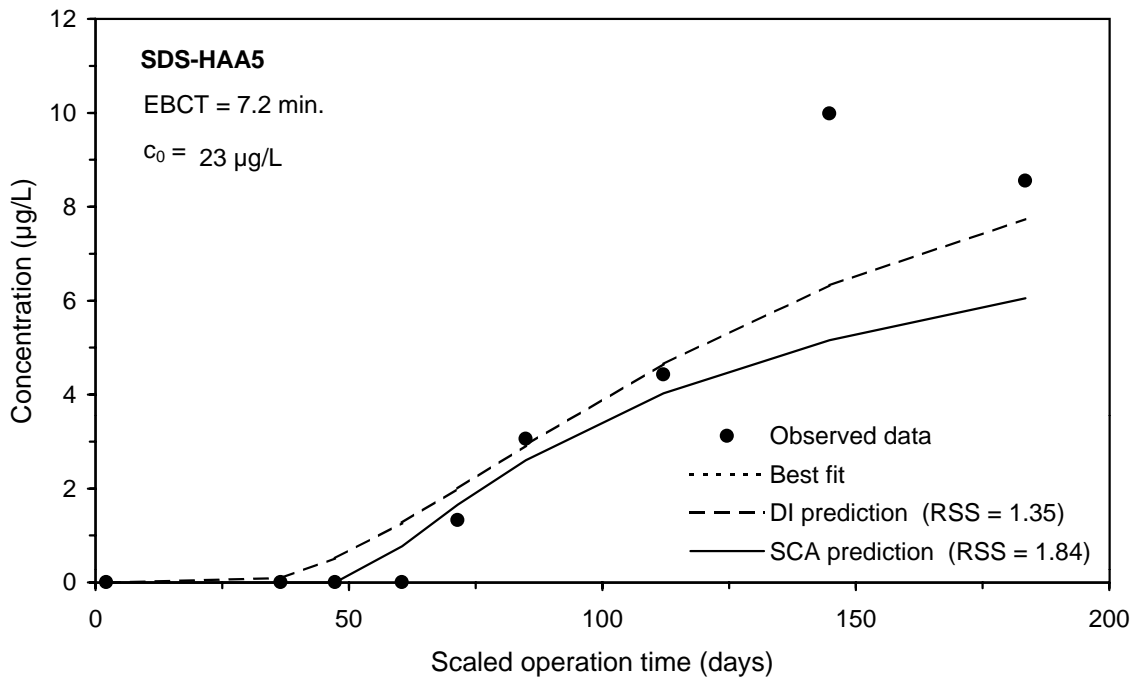


**Figure F-154 Comparison of DI and SCA methods for predicting the SDS-HAA5 integral breakthrough curve for Water 8**

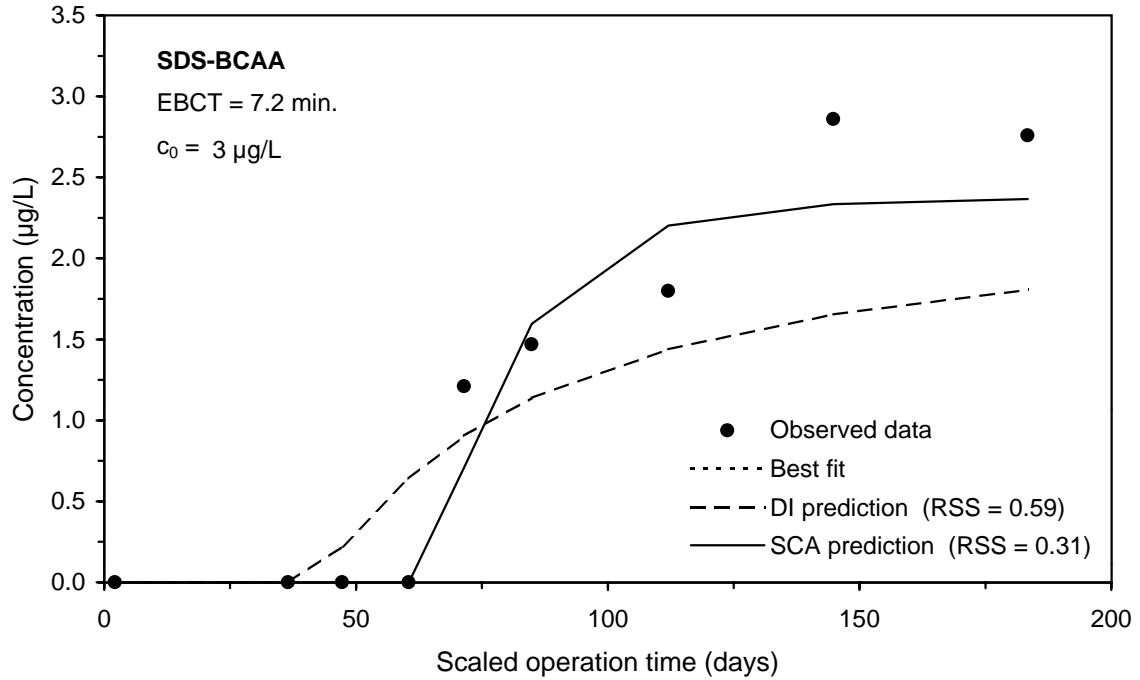


**Figure F-155 Comparison of DI and SCA methods for predicting the SDS-BCAA integral breakthrough curve for Water 8**

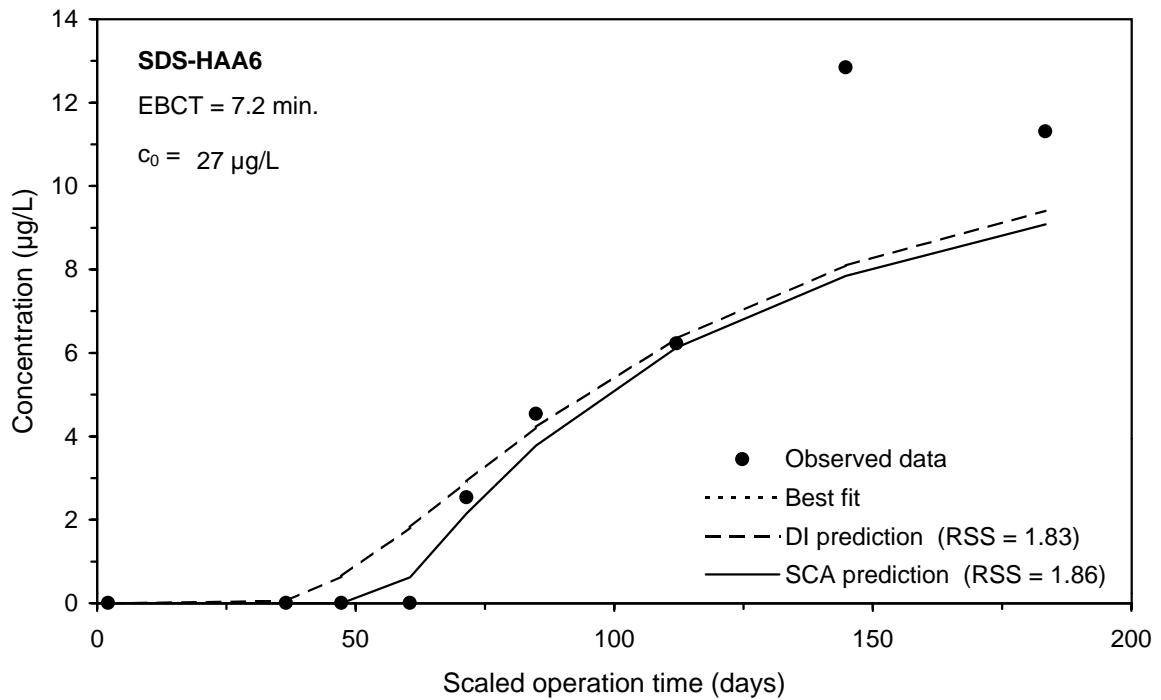


**Figure F-156 Comparison of DI and SCA methods for predicting the SDS-HAA6 integral breakthrough curve for Water 8**

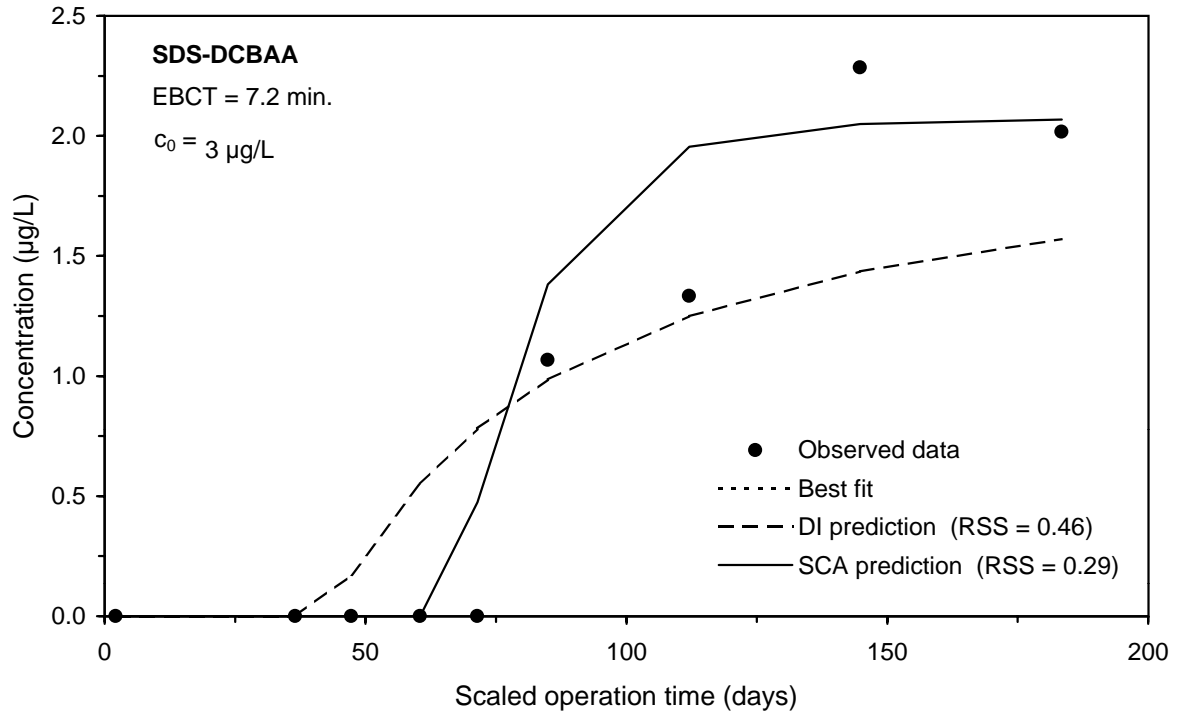


**Figure F-157 Comparison of DI and SCA methods for predicting the SDS-DCBAA integral breakthrough curve for Water 8**

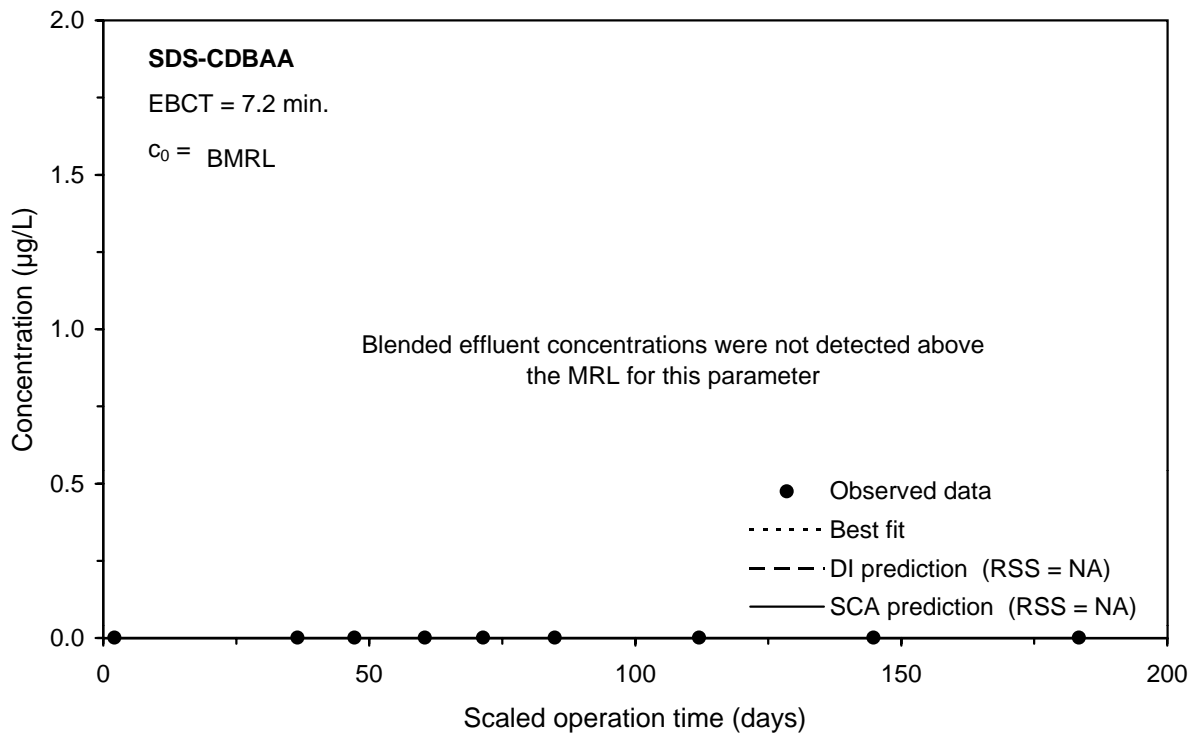


**Figure F-158 Comparison of DI and SCA methods for predicting the SDS-CDBAA integral breakthrough curve for Water 8**

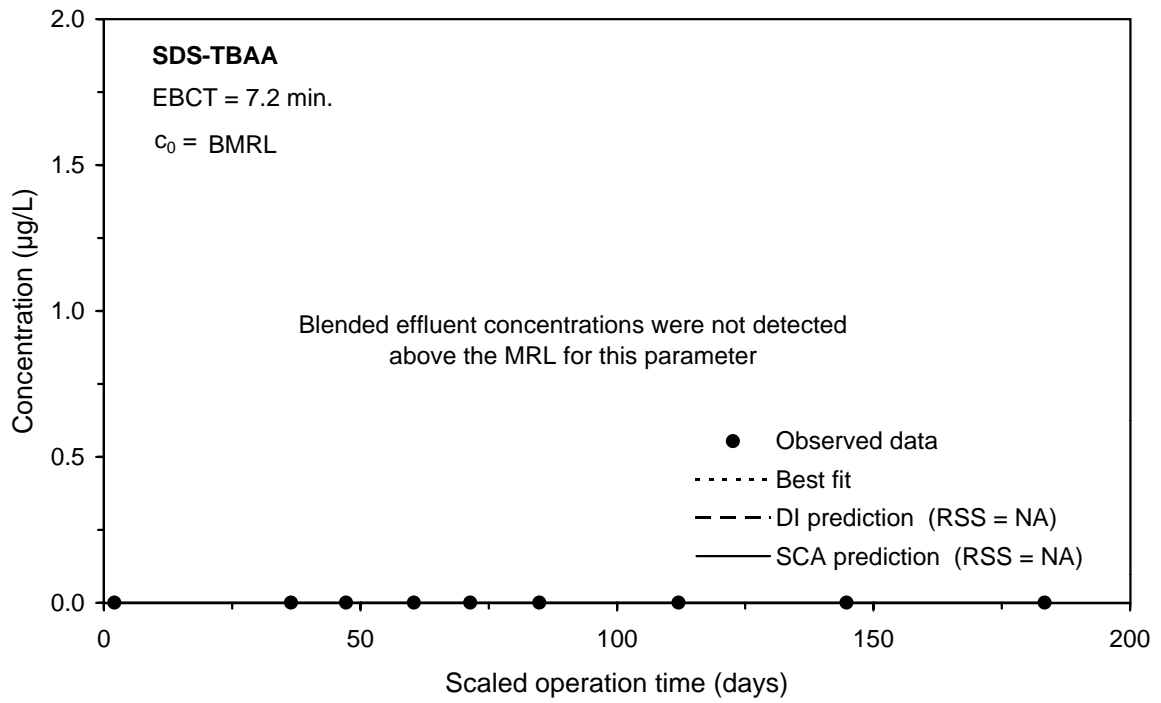


**Figure F-159 Comparison of DI and SCA methods for predicting the SDS-TBAA integral breakthrough curve for Water 8**

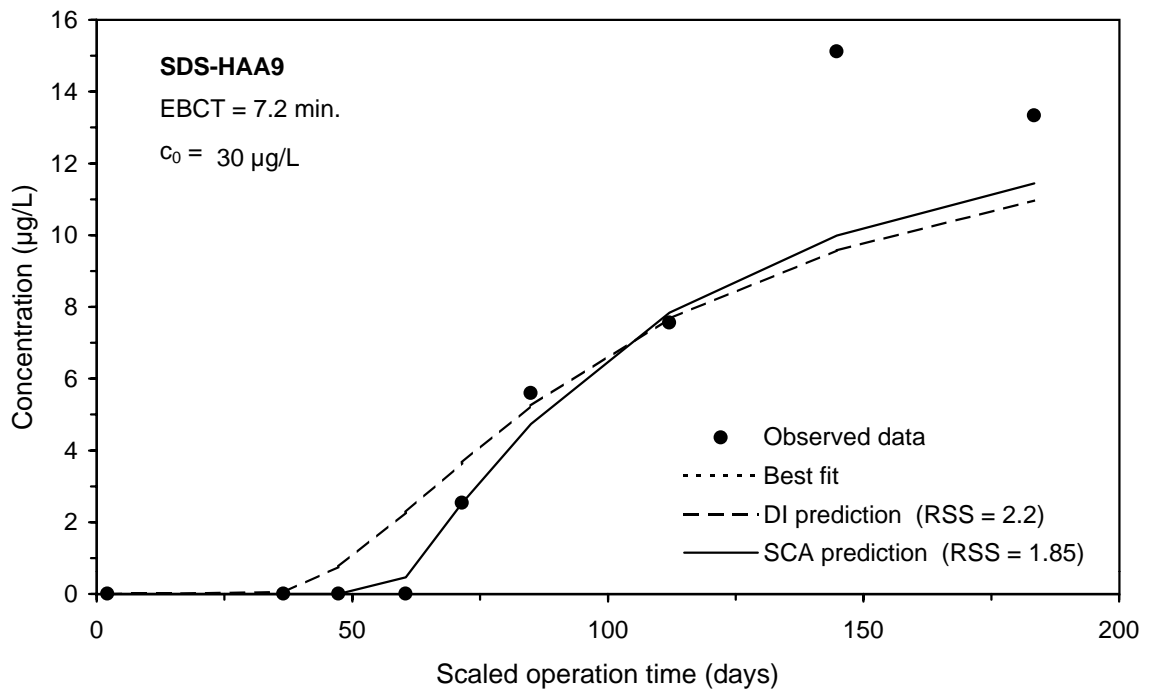


**Figure F-160 Comparison of DI and SCA methods for predicting the SDS-HAA9 integral breakthrough curve for Water 8**

This page intentionally left blank.

---

## Appendix G: Logistic Function Model Best-Fit Parameters

Analyte	Type of curve fit	$A_0$	$A$	$B$	$D$	$S$	$t_p$	$n^*$
TOC	Step	0.00	3.28	11.11	0.104	NA	NA	13
UV-254	Step-lag	-0.03	0.09	3.21	0.058	NA	NA	13
SDS-TOX	Step-lag	-55.82	186.75	4.02	0.070	NA	NA	12
SDS-TTHM	Step-lag	-33.46	100.37	3.45	0.083	NA	NA	11
SDS-HAA5	Step-lag	-1.25	15.59	180.13	0.273	NA	NA	11
SDS-HAA6	Step-lag	-10.79	30.90	12.40	0.157	NA	NA	11
SDS-HAA9	Step-lag	-11.49	33.13	9.47	0.137	NA	NA	11
SDS-CF	Step-lag	-2.12	20.37	19.81	0.068	NA	NA	8
SDS-BDCM	Step-lag	-12.01	35.33	5.74	0.117	NA	NA	11
SDS-DBCM	Step-lag	-7.70	31.82	5.91	0.066	NA	NA	11
SDS-BF	Step-lag-peak	-0.40	13.59	200.86	0.388	-0.148	28	11
SDS-MCAA	No fit	NA	NA	NA	NA	NA	NA	0
SDS-DCAA	Step-lag	-0.36	8.52	1.39E+04	0.470	NA	NA	9
SDS-TCAA	No fit	NA	NA	NA	NA	NA	NA	2
SDS-MBAA	No fit	NA	NA	NA	NA	NA	NA	0
SDS-DBAA	Step-lag	-0.05	5.35	124.71	0.302	NA	NA	11
SDS-BCAA	Step-lag	-2.94	8.66	6.86	0.103	NA	NA	9
SDS-CDBAA	No fit	NA	NA	NA	NA	NA	NA	0
SDS-DCBAA	No fit	NA	NA	NA	NA	NA	NA	3
SDS-TBAA	No fit	NA	NA	NA	NA	NA	NA	0

NA: not applicable

\*Number of observations above the MRL

**Table G-1 Summary of single contactor best-fit logistic function model parameters for Water 1**

Analyte	Type of curve fit	$A_0$	$A$	$B$	$D$	$S$	$t_p$	$n^*$
TOC	Step	0.00	1.78	7.48	0.037	NA	NA	13
UV-254	Step-lag	-0.02	0.05	2.03	0.022	NA	NA	13
SDS-TOX	Step-lag	-75.03	218.15	2.32	0.025	NA	NA	12
SDS-TTHM	Step-lag	-38.87	113.39	2.50	0.037	NA	NA	12
SDS-HAA5	Step-lag	-8.74	24.47	2.89	0.032	NA	NA	11
SDS-HAA6	Step-lag	-12.84	35.99	2.89	0.032	NA	NA	11
SDS-HAA9	Step-lag	-14.05	40.85	3.06	0.031	NA	NA	11
SDS-CF	Step-lag	-9.99	35.27	3.20	0.016	NA	NA	10
SDS-BDCM	Step-lag	-7.34	31.41	8.73	0.071	NA	NA	11
SDS-DBCM	Step-lag	-12.70	37.33	3.51	0.036	NA	NA	11
SDS-BF	Step-lag-peak	0.06	11.27	11.03	0.127	-0.036	39	12
SDS-MCAA	No fit	NA	NA	NA	NA	NA	NA	0
SDS-DCAA	Step-lag	-4.27	12.29	2.84	0.021	NA	NA	9
SDS-TCAA	Step-lag	0.00	2.10	3.51E+06	0.245	NA	NA	6
SDS-MBAA	No fit	NA	NA	NA	NA	NA	NA	0
SDS-DBAA	Step-lag	-0.56	6.65	11.45	0.073	NA	NA	11
SDS-BCAA	Step-lag	-4.10	11.54	2.86	0.030	NA	NA	10
SDS-CDBAA	No fit	NA	NA	NA	NA	NA	NA	2
SDS-DCBAA	Step-lag	-1.21	3.42	15.85	0.067	NA	NA	8
SDS-TBAA	No fit	NA	NA	NA	NA	NA	NA	0

NA: not applicable

\*Number of observations above the MRL

**Table G-2 Summary of single contactor best-fit logistic function model parameters for Water 2**

Analyte	Type of curve fit	$A_0$	$A$	$B$	$D$	$S$	$t_p$	$n^*$
TOC	Step	0.00	1.50	9.36	0.027	NA	NA	12
UV-254	Step-lag	-0.01	0.04	3.15	0.019	NA	NA	12
SDS-TOX	Step-lag	-24.55	161.23	4.95	0.019	NA	NA	12
SDS-TTHM	Step-lag	-45.77	144.99	1.92	0.020	NA	NA	12
SDS-HAA5	Step-lag-peak	-0.33	30.45	24.34	0.026	0.000	140	11
SDS-HAA6	Step-lag	2.79	22.97	228.87	0.057	NA	NA	11
SDS-HAA9	Step-lag-peak	-1.91	48.87	17.53	0.024	0.000	140	11
SDS-CF	Step-lag	-0.91	18.88	36.59	0.022	NA	NA	9
SDS-BDCM	Step-lag	-1.52	35.95	12.00	0.041	NA	NA	12
SDS-DBCM	Step-lag	-7.80	36.72	5.97	0.018	NA	NA	11
SDS-BF	Step-lag-peak	3.92	27.13	32.31	0.080	-0.050	78	12
SDS-MCAA	No fit	NA	NA	NA	NA	NA	NA	0
SDS-DCAA	Step-lag	-2.92	9.26	12.56	0.024	NA	NA	6
SDS-TCAA	No fit	NA	NA	NA	NA	NA	NA	5
SDS-MBAA	No fit	NA	NA	NA	NA	NA	NA	0
SDS-DBAA	Step-lag	0.37	10.77	25.97	0.048	NA	NA	11
SDS-BCAA	Step-lag	0.44	6.91	85.06	0.047	NA	NA	11
SDS-CDBAA	No fit	NA	NA	NA	NA	NA	NA	2
SDS-DCBAA	Step-lag	-0.96	2.87	1.75	0.016	NA	NA	9
SDS-TBAA	No fit	NA	NA	NA	NA	NA	NA	0

NA: not applicable

\*Number of observations above the MRL

**Table G-3 Summary of single contactor best-fit logistic function model parameters for Water 3**

Analyte	Type of curve fit	$A_0$	$A$	$B$	$D$	$S$	$t_p$	$n^*$
TOC	Step	0.00	2.10	27.87	0.044	NA	NA	13
UV-254	Step-lag	-0.01	0.05	6.52	0.025	NA	NA	13
SDS-TOX	Step-lag	-75.14	246.00	7.02	0.028	NA	NA	12
SDS-TTHM	Step-lag	-19.39	61.91	5.76	0.026	NA	NA	11
SDS-HAA5	Step-lag	-10.44	51.98	9.16	0.021	NA	NA	10
SDS-HAA6	Step-lag	-12.99	58.13	7.66	0.021	NA	NA	10
SDS-HAA9	Step-lag	-14.39	66.66	7.19	0.020	NA	NA	11
SDS-CF	Step-lag	-10.41	41.38	7.49	0.023	NA	NA	11
SDS-BDCM	Step-lag-peak	-1.62	4.69	3.64E+03	0.162	-0.006	91	10
SDS-DBCM	Step-lag	-5.61	16.64	6.38	0.032	NA	NA	11
SDS-BF	No fit	NA	NA	NA	NA	NA	NA	0
SDS-MCAA	No fit	NA	NA	NA	NA	NA	NA	0
SDS-DCAA	Step-lag	-5.31	20.22	6.76	0.022	NA	NA	10
SDS-TCAA	Step-lag	-4.35	31.76	15.48	0.022	NA	NA	10
SDS-MBAA	No fit	NA	NA	NA	NA	NA	NA	0
SDS-DBAA	No fit	NA	NA	NA	NA	NA	NA	4
SDS-BCAA	Step-lag	-2.05	5.78	8.18	0.040	NA	NA	10
SDS-CDBAA	No fit	NA	NA	NA	NA	NA	NA	0
SDS-DCBAA	Step-lag	-1.52	8.53	4.59	0.017	NA	NA	11
SDS-TBAA	No fit	NA	NA	NA	NA	NA	NA	0

NA: not applicable

\*Number of observations above the MRL

**Table G-4 Summary of single contactor best-fit logistic function model parameters for Water 4**

Analyte	Type of curve fit	$A_0$	$A$	$B$	$D$	$S$	$t_p$	$n^*$
TOC	Step	0.00	2.33	12.66	0.023	NA	NA	13
UV-254	Step-lag	-0.01	0.05	3.83	0.013	NA	NA	13
SDS-TOX	Step-lag	-53.67	196.80	4.28	0.014	NA	NA	13
SDS-TTHM	Step-lag	-22.75	68.25	3.01	0.015	NA	NA	12
SDS-HAA5	Step-lag	-7.50	22.06	4.85	0.021	NA	NA	11
SDS-HAA6	Step-lag	-10.90	32.01	4.84	0.021	NA	NA	11
SDS-HAA9	Step-lag	-17.05	50.40	6.20	0.023	NA	NA	11
SDS-CF	Step-lag	-2.28	16.34	9.86	0.013	NA	NA	10
SDS-BDCM	Step-lag	-7.19	20.65	3.14	0.021	NA	NA	12
SDS-DBCM	Step-lag	-6.98	27.30	4.02	0.013	NA	NA	12
SDS-BF	Step-lag	-1.20	3.34	116.01	0.090	NA	NA	11
SDS-MCAA	No fit	NA	NA	NA	NA	NA	NA	3
SDS-DCAA	Step-lag	-2.40	8.70	4.51	0.014	NA	NA	10
SDS-TCAA	Step-lag	-3.00	9.30	7.63	0.019	NA	NA	9
SDS-MBAA	No fit	NA	NA	NA	NA	NA	NA	0
SDS-DBAA	Step-lag	-1.60	4.65	62.79	0.064	NA	NA	11
SDS-BCAA	Step-lag	-3.40	9.96	4.82	0.022	NA	NA	11
SDS-CDBAA	Step-lag-peak	-2.60	7.06	148.78	0.060	-0.004	158	8
SDS-DCBAA	Step-lag	-4.25	12.75	4.99	0.019	NA	NA	11
SDS-TBAA	No fit	NA	NA	NA	NA	NA	NA	0

NA: not applicable

\*Number of observations above the MRL

**Table G-5 Summary of single contactor best-fit logistic function model parameters for Water 5**

Analyte	Type of curve fit	$A_0$	$A$	$B$	$D$	$S$	$t_p$	$n^*$
TOC	Step	0.00	1.98	69.54	0.033	NA	NA	13
UV-254	Step-lag	-0.01	0.05	9.28	0.017	NA	NA	13
SDS-TOX	Step-lag	-77.38	283.38	9.39	0.018	NA	NA	11
SDS-TTHM	Step-lag	-44.21	131.09	12.29	0.027	NA	NA	11
SDS-HAA5	Step-lag	-9.22	30.95	10.99	0.020	NA	NA	10
SDS-HAA6	Step-lag	-14.16	44.81	12.39	0.022	NA	NA	10
SDS-HAA9	Step-lag	-18.87	57.94	14.38	0.023	NA	NA	10
SDS-CF	Step	0.00	24.13	372.30	0.031	NA	NA	8
SDS-BDCM	Step-lag	-2.82	31.63	605.70	0.062	NA	NA	11
SDS-DBCM	Step-lag	-13.11	44.11	14.75	0.022	NA	NA	10
SDS-BF	Step-lag-peak	-0.13	15.07	8.23E+03	0.099	-0.057	131	11
SDS-MCAA	No fit	NA	NA	NA	NA	NA	NA	0
SDS-DCAA	Step-lag	-2.97	12.66	17.57	0.018	NA	NA	7
SDS-TCAA	No fit	NA	NA	NA	NA	NA	NA	4
SDS-MBAA	No fit	NA	NA	NA	NA	NA	NA	0
SDS-DBAA	Step-lag	0.18	7.36	1.73E+05	0.110	NA	NA	10
SDS-BCAA	Step-lag	-4.62	13.86	18.59	0.026	NA	NA	9
SDS-CDBAA	Step-lag	0.04	2.64	7.20E+12	0.263	NA	NA	7
SDS-DCBAA	Step-lag	-2.59	8.53	17.66	0.021	NA	NA	7
SDS-TBAA	No fit	NA	NA	NA	NA	NA	NA	0

NA: not applicable

\*Number of observations above the MRL

**Table G-6 Summary of single contactor best-fit logistic function model parameters for Water 6**

Analyte	Type of curve fit	$A_0$	$A$	$B$	$D$	$S$	$t_p$	$n^*$
TOC	Step	0.00	4.01	15.49	0.049	NA	NA	13
UV-254	Step-lag	-0.03	0.09	4.57	0.032	NA	NA	13
SDS-TOX	Step-lag	-134.27	420.30	4.63	0.036	NA	NA	12
SDS-TTHM	Step-lag	-81.69	239.78	4.18	0.042	NA	NA	12
SDS-HAA5	Step-lag	-16.06	47.02	5.56	0.051	NA	NA	11
SDS-HAA6	Step-lag	-23.26	67.10	6.08	0.052	NA	NA	11
SDS-HAA9	Step-lag	-34.18	96.81	8.04	0.060	NA	NA	11
SDS-CF	Step-lag	-2.35	25.39	33.37	0.034	NA	NA	7
SDS-BDCM	Step-lag	-34.72	103.28	5.34	0.045	NA	NA	11
SDS-DBCM	Step-lag	-15.55	64.36	7.25	0.031	NA	NA	10
SDS-BF	Step-lag	1.39	35.62	459.64	0.187	NA	NA	12
SDS-MCAA	No fit	NA	NA	NA	NA	NA	NA	0
SDS-DCAA	Step-lag	-4.10	13.83	3.28	0.026	NA	NA	10
SDS-TCAA	Step-lag	-0.03	6.60	6.68E+05	0.193	NA	NA	6
SDS-MBAA	No fit	NA	NA	NA	NA	NA	NA	0
SDS-DBAA	Step-lag	-0.06	16.06	136.54	0.127	NA	NA	11
SDS-BCAA	Step-lag	-7.20	20.05	7.76	0.058	NA	NA	10
SDS-CDBAA	Step-lag	-1.78	7.56	262.52	0.138	NA	NA	9
SDS-DCBAA	Step-lag	-2.77	16.70	9.30	0.027	NA	NA	9
SDS-TBAA	Step-lag-peak	-3.67	10.33	471.50	0.174	-0.034	65	9

NA: not applicable

\*Number of observations above the MRL

**Table G-7 Summary of single contactor best-fit logistic function model parameters for Water 7**

Analyte	Type of curve fit	$A_0$	$A$	$B$	$D$	$S$	$t_p$	$n^*$
TOC	Step	0.00	1.53	27.83	0.064	NA	NA	13
UV-254	Step-lag	-0.01	0.03	5.40	0.037	NA	NA	13
SDS-TOX	Step-lag	-56.70	162.37	6.31	0.042	NA	NA	13
SDS-TTHM	Step-lag	-18.32	52.36	5.00	0.036	NA	NA	11
SDS-HAA5	Step-lag	-6.73	20.20	5.50	0.034	NA	NA	10
SDS-HAA6	Step-lag	-8.03	22.41	9.66	0.052	NA	NA	10
SDS-HAA9	Step-lag	-9.14	25.34	14.18	0.062	NA	NA	10
SDS-CF	Step-lag	-11.78	35.35	4.06	0.024	NA	NA	11
SDS-BDCM	Step-lag-peak	-1.91	4.97	1.26E+03	0.196	-0.004	113	11
SDS-DBCM	Step-lag	-5.12	14.78	9.93	0.055	NA	NA	11
SDS-BF	No fit	NA	NA	NA	NA	NA	NA	0
SDS-MCAA	No fit	NA	NA	NA	NA	NA	NA	0
SDS-DCAA	Step-lag	-3.55	10.03	8.52	0.048	NA	NA	10
SDS-TCAA	Step-lag	-3.19	9.56	5.04	0.030	NA	NA	9
SDS-MBAA	No fit	NA	NA	NA	NA	NA	NA	0
SDS-DBAA	No fit	NA	NA	NA	NA	NA	NA	0
SDS-BCAA	Step-lag	-1.30	3.68	2.49E+03	0.199	NA	NA	10
SDS-CDBAA	No fit	NA	NA	NA	NA	NA	NA	0
SDS-DCBAA	Step-lag	-0.97	3.05	1.44E+04	0.236	NA	NA	9
SDS-TBAA	No fit	NA	NA	NA	NA	NA	NA	0

NA: not applicable

\*Number of observations above the MRL

**Table G-8 Summary of single contactor best-fit logistic function model parameters for Water 8**

This page intentionally left blank.

---

## **Appendix H: Impact of Extrapolation on SCA Prediction of the Integral Breakthrough Curve**

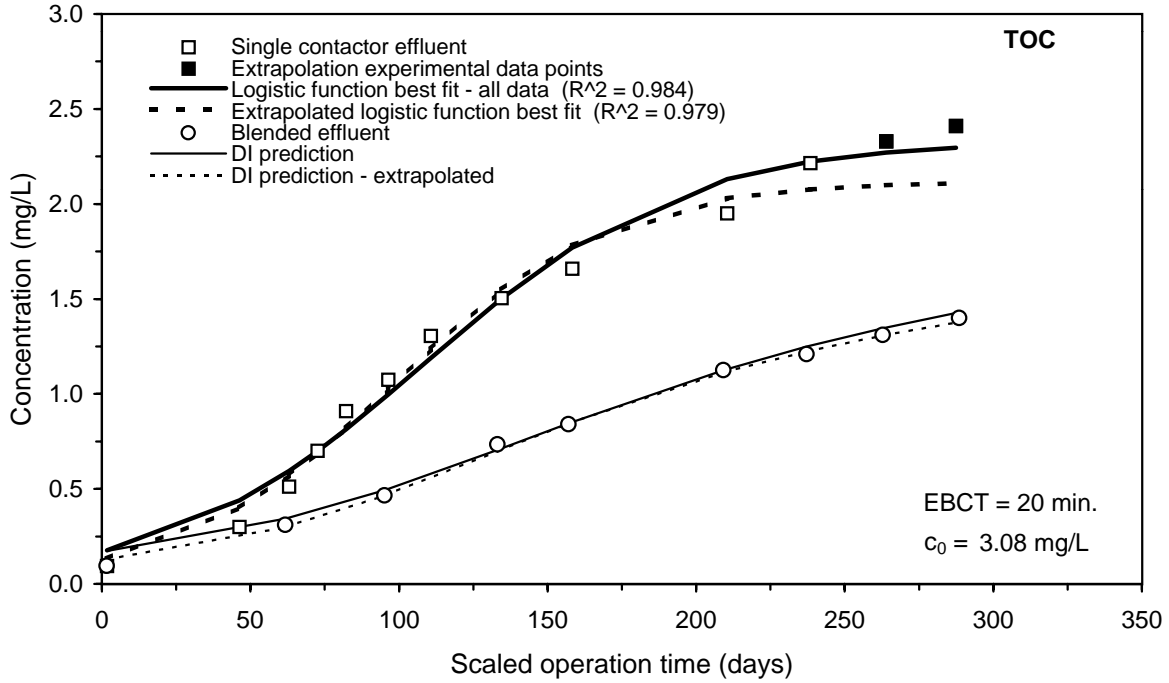


**Figure H-1 Impact of extrapolation on DI prediction of the TOC integral breakthrough curve for Water 5**

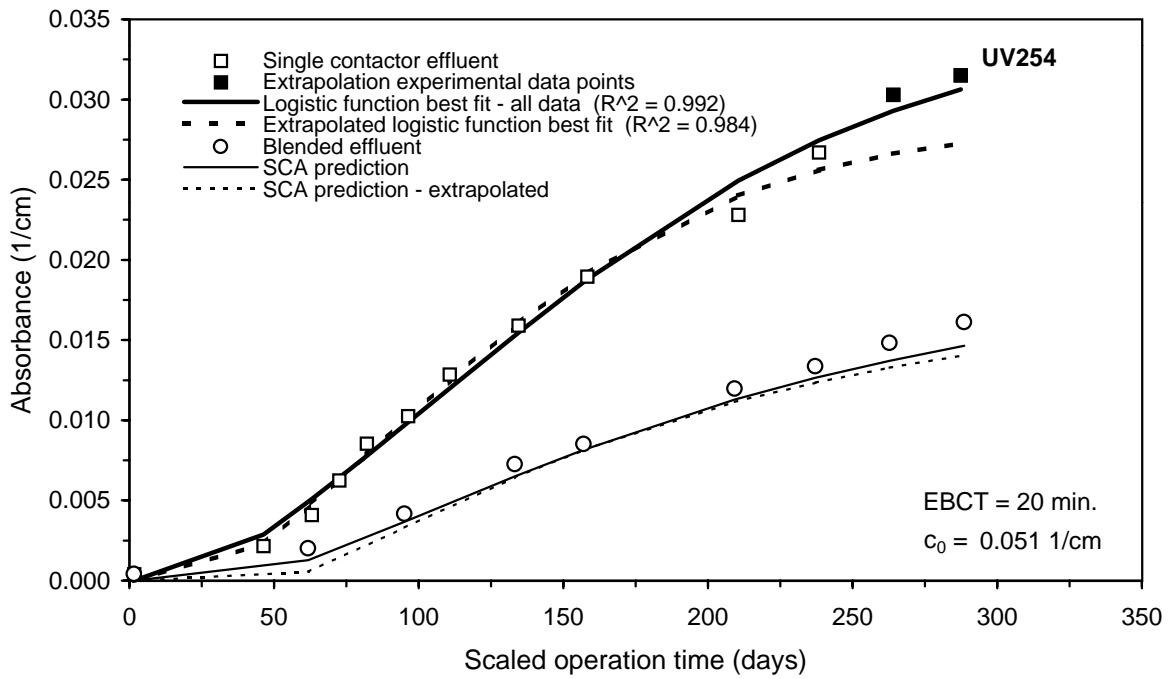


**Figure H-2 Impact of extrapolation on SCA prediction of the UV254 integral breakthrough curve for Water 5**

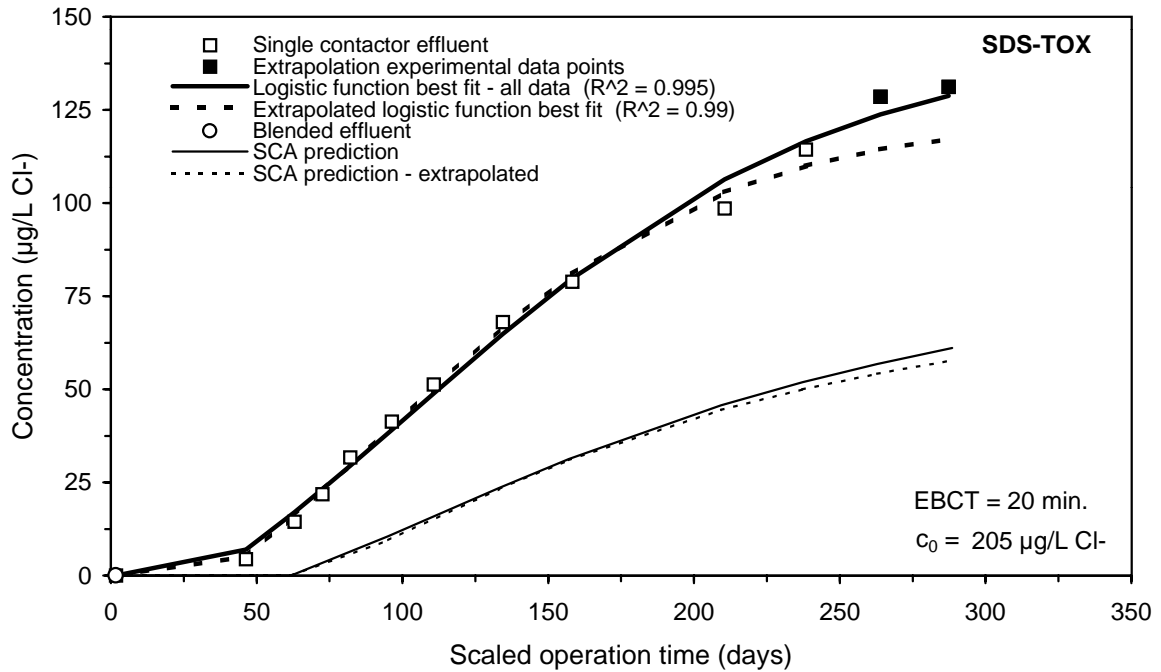


**Figure H-3 Impact of extrapolation on SCA prediction of the SDS-TOX integral breakthrough curve for Water 5**

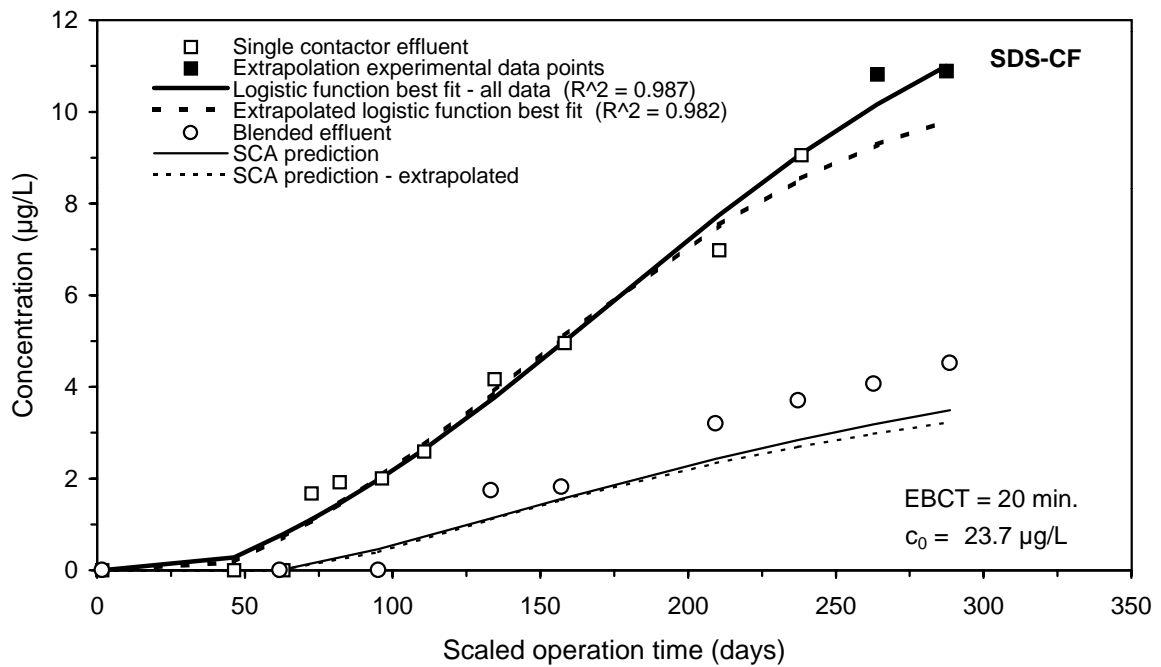


**Figure H-4 Impact of extrapolation on SCA prediction of the SDS-CF integral breakthrough curve for Water 5**

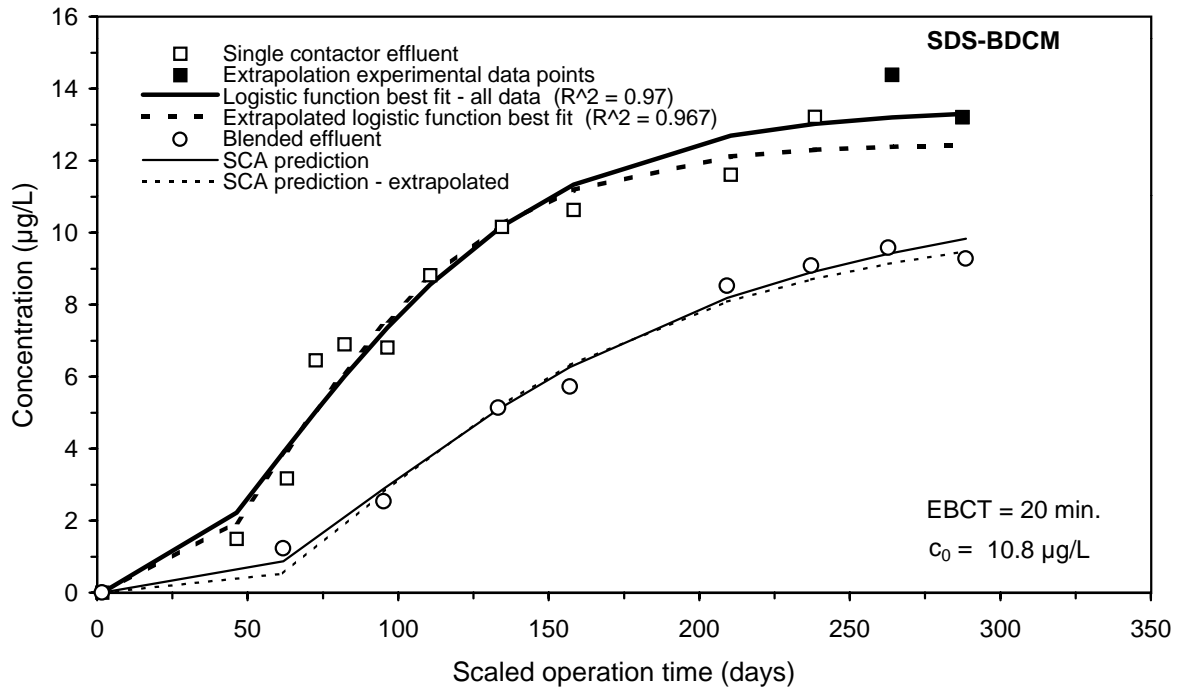


**Figure H-5 Impact of extrapolation on SCA prediction of the SDS-BDCM integral breakthrough curve for Water 5**

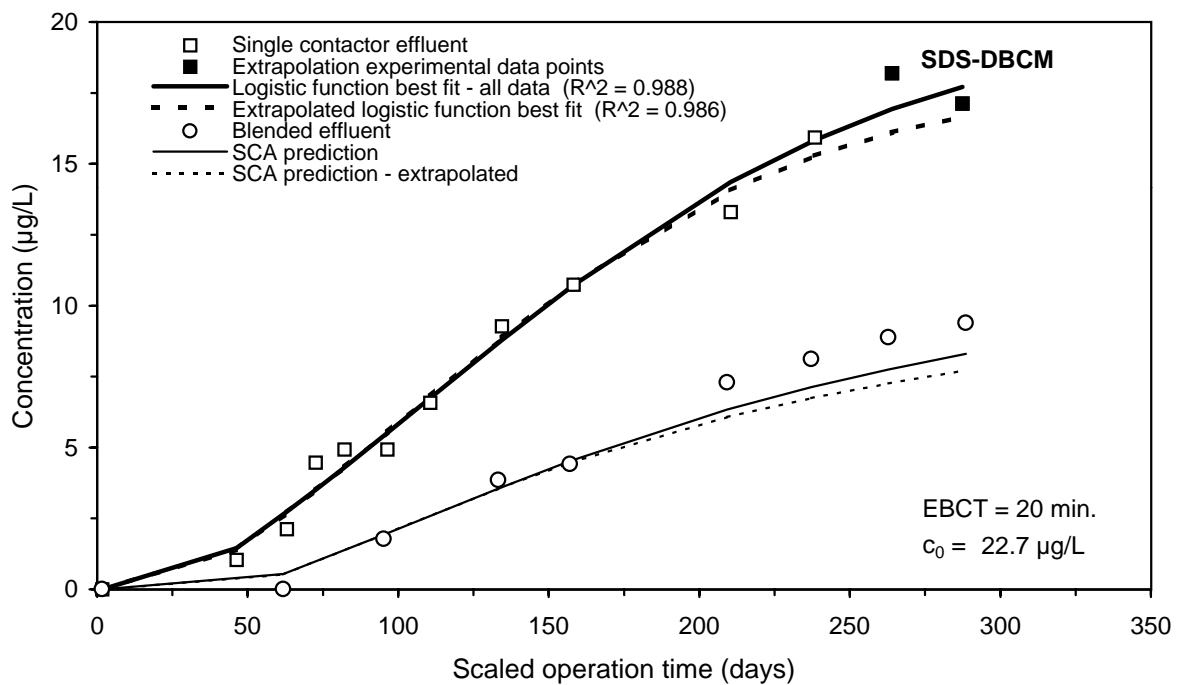


**Figure H-6 Impact of extrapolation on SCA prediction of the SDS-DBC M integral breakthrough curve for Water 5**

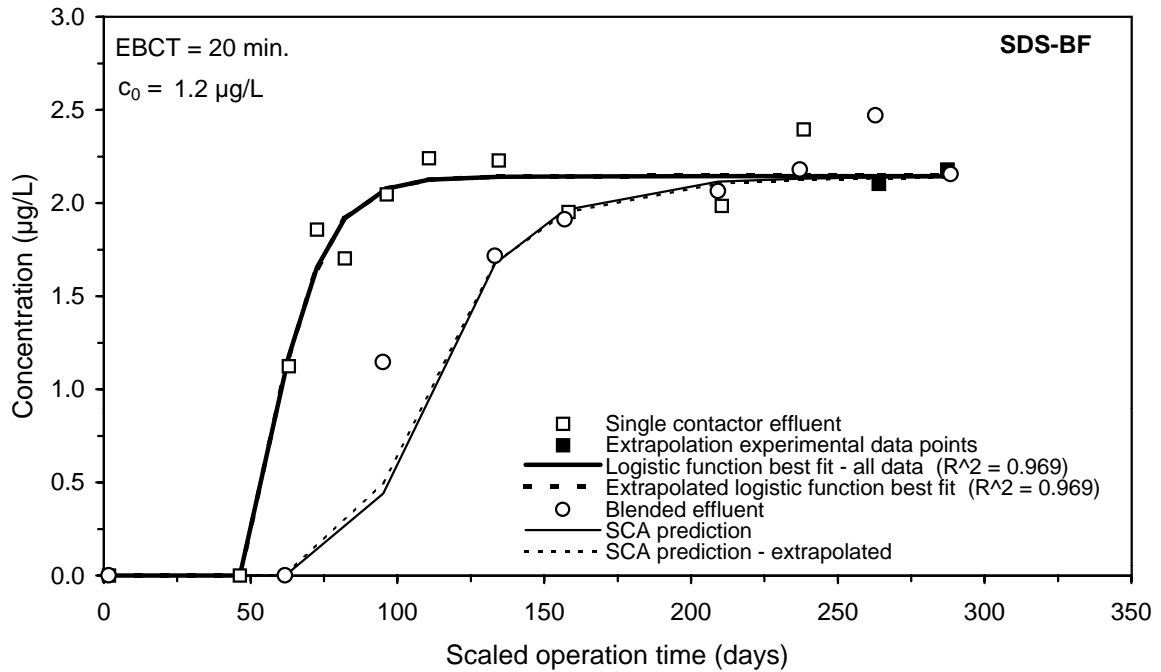


**Figure H-7 Impact of extrapolation on SCA prediction of the SDS-BF integral breakthrough curve for Water 5**

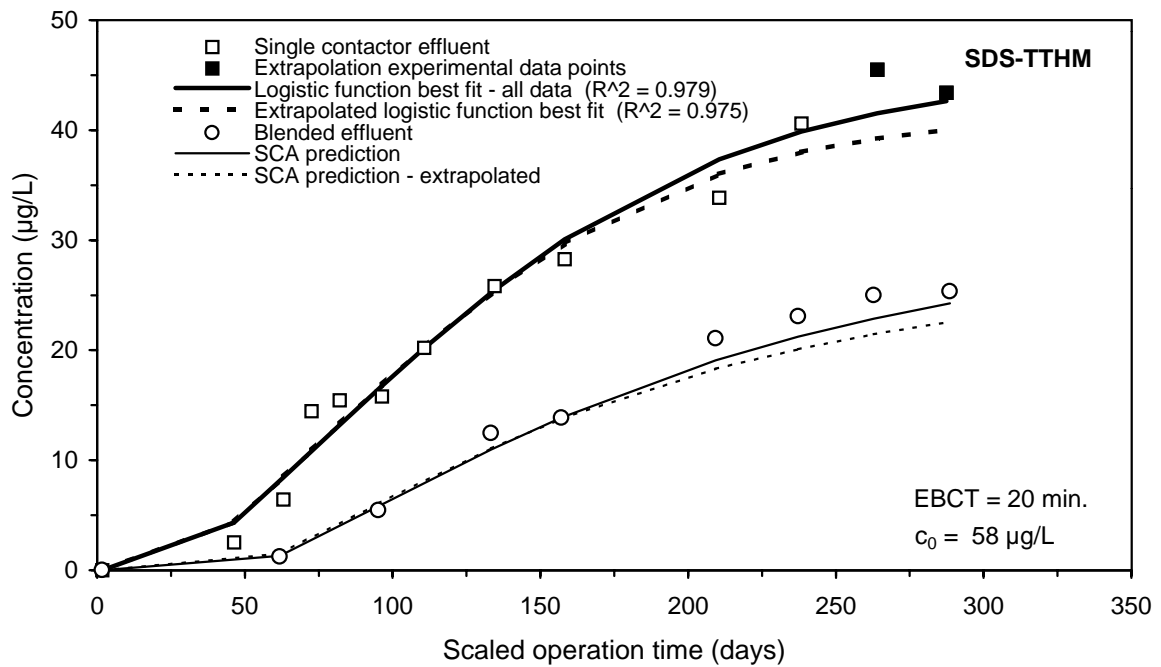


**Figure H-8 Impact of extrapolation on SCA prediction of the SDS-TTHM integral breakthrough curve for Water 5**

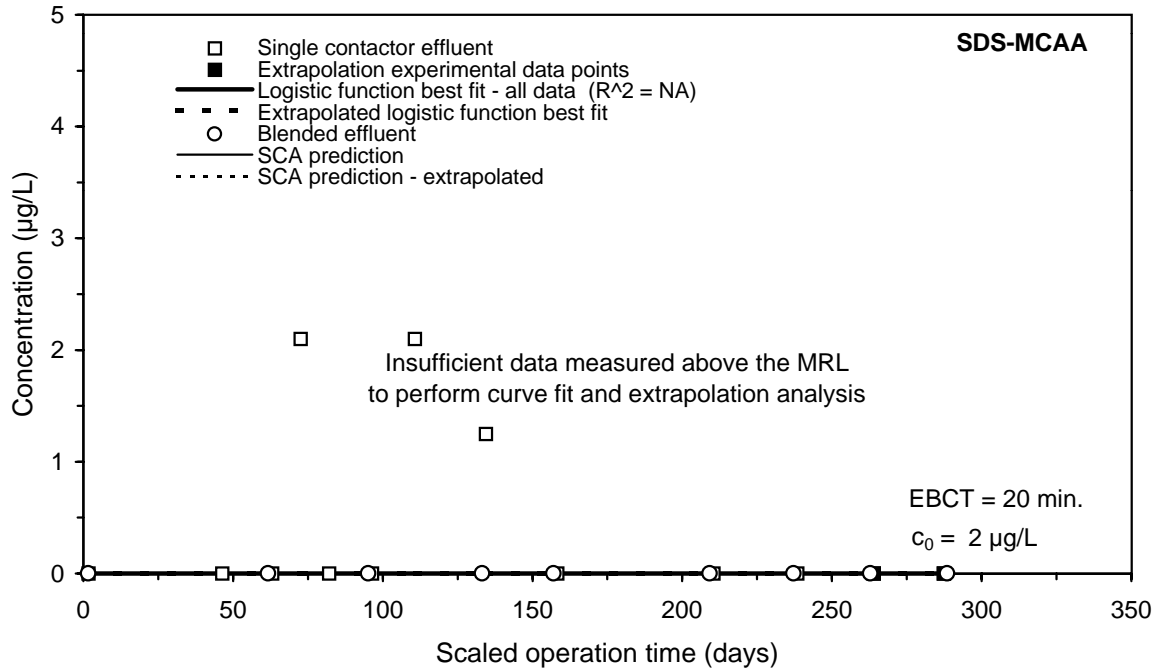


**Figure H-9 Impact of extrapolation on SCA prediction of the SDS-MCAA integral breakthrough curve for Water 5**

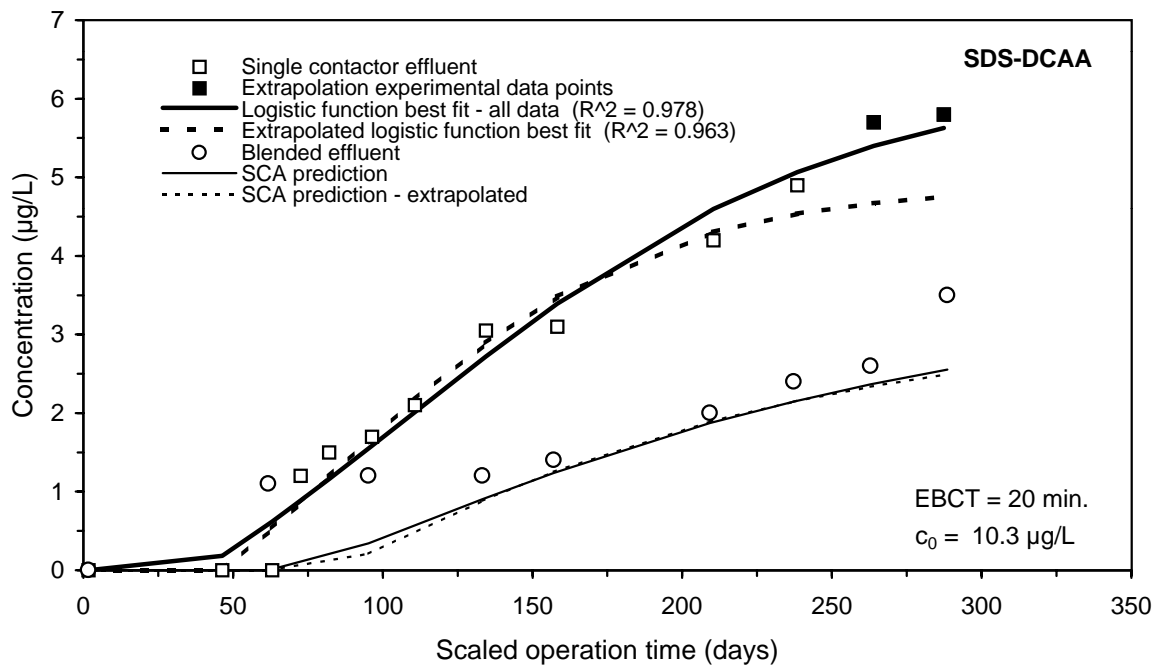


**Figure H-10 Impact of extrapolation on SCA prediction of the SDS-DCAA integral breakthrough curve for Water 5**

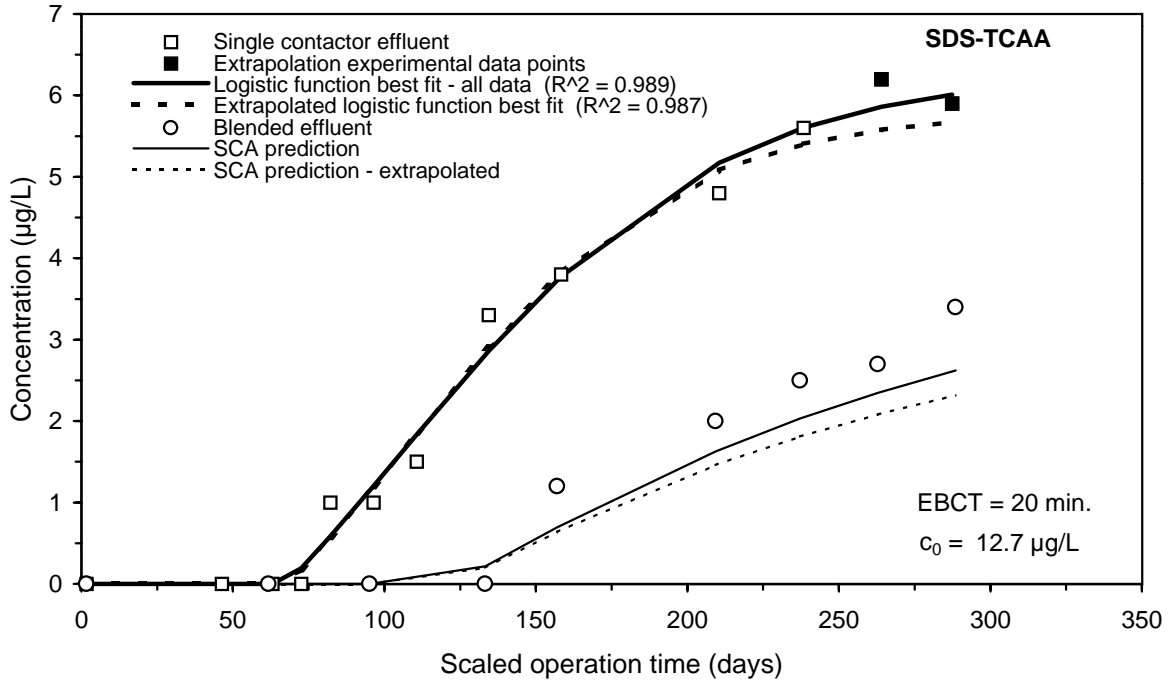


**Figure H-11 Impact of extrapolation on SCA prediction of the SDS-TCAA integral breakthrough curve for Water 5**

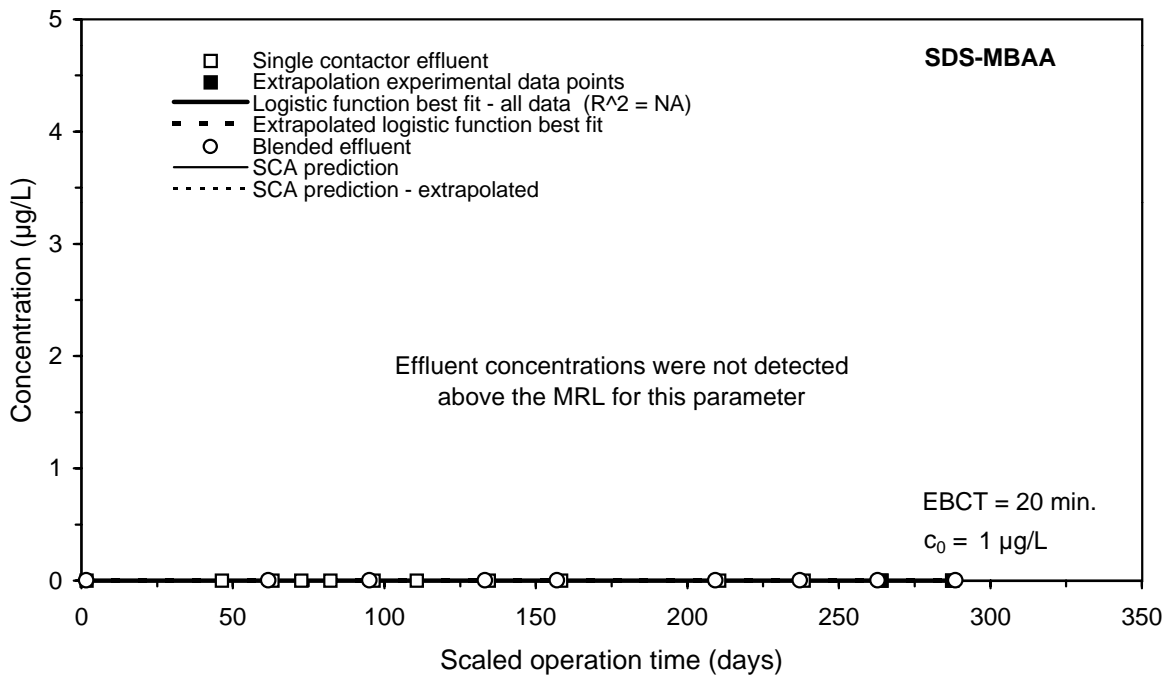


**Figure H-12 Impact of extrapolation on SCA prediction of the SDS-MBAA integral breakthrough curve for Water 5**

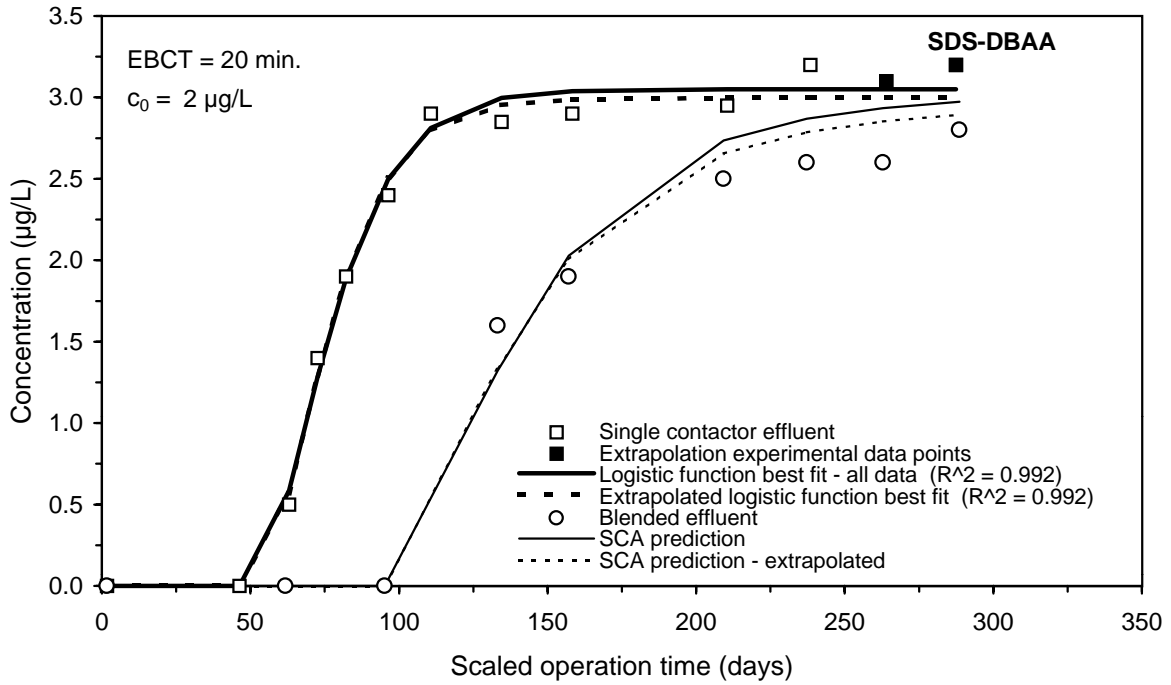


**Figure H-13 Impact of extrapolation on SCA prediction of the SDS-DBAA integral breakthrough curve for Water 5**

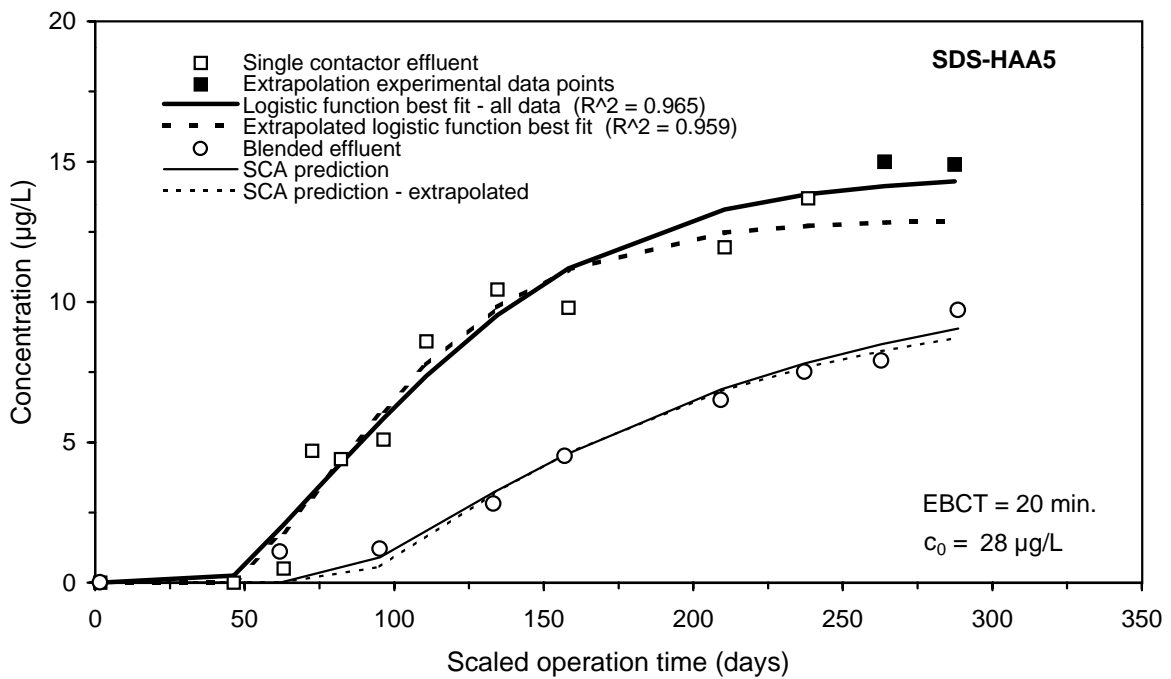


**Figure H-14 Impact of extrapolation on SCA prediction of the SDS-HAA5 integral breakthrough curve for Water 5**

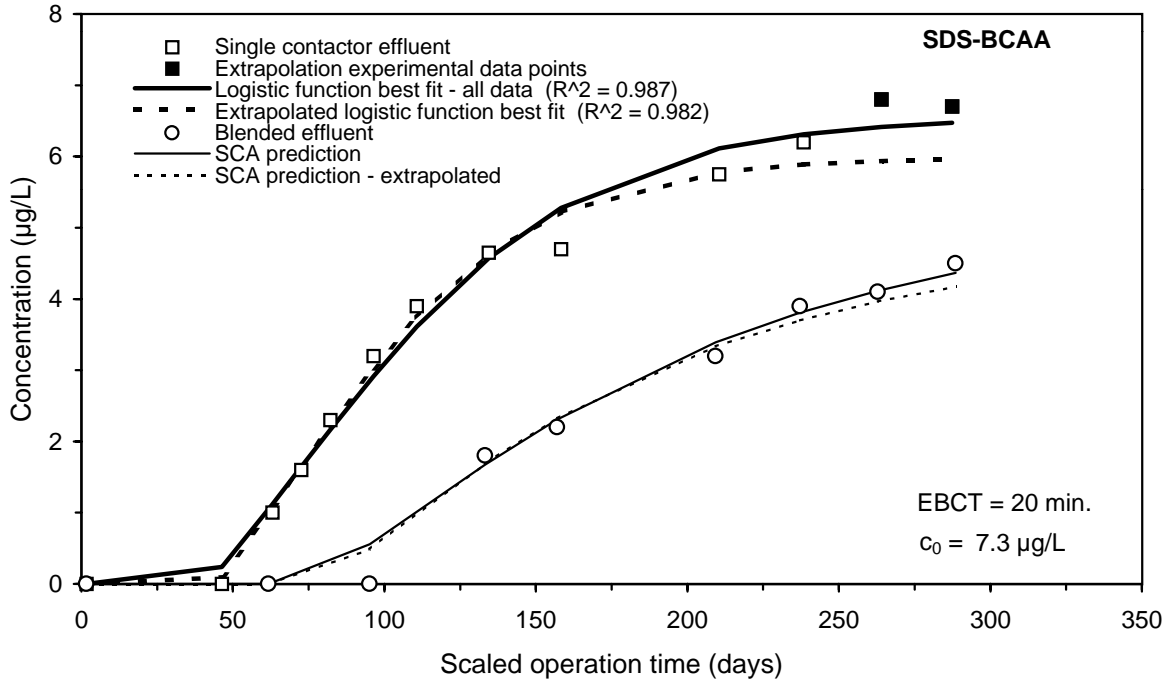


**Figure H-15 Impact of extrapolation on SCA prediction of the SDS-BCAA integral breakthrough curve for Water 5**

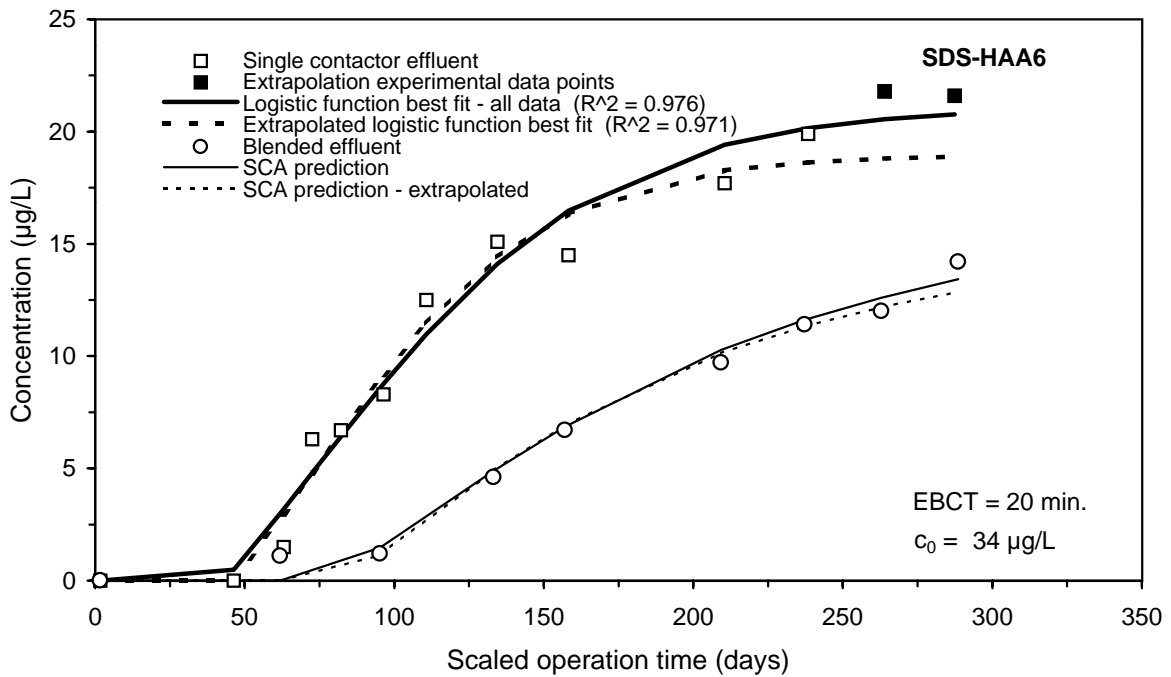


**Figure H-16 Impact of extrapolation on SCA prediction of the SDS-HAA6 integral breakthrough curve for Water 5**

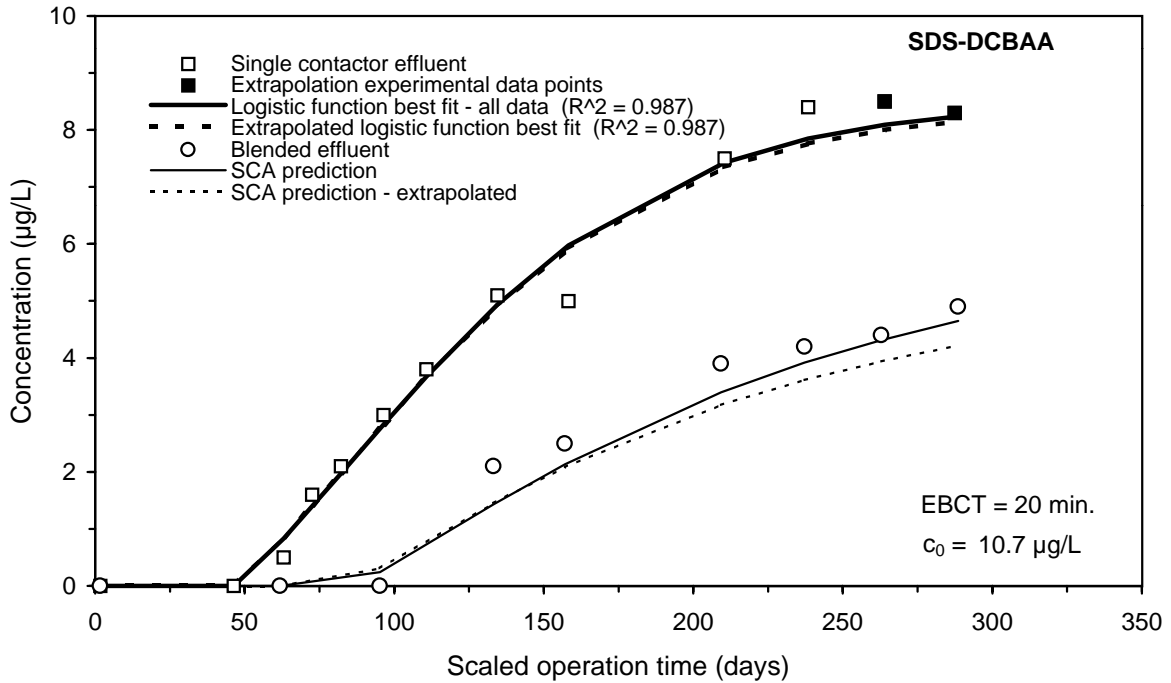


**Figure H-17 Impact of extrapolation on SCA prediction of the SDS-DCBAA integral breakthrough curve for Water 5**

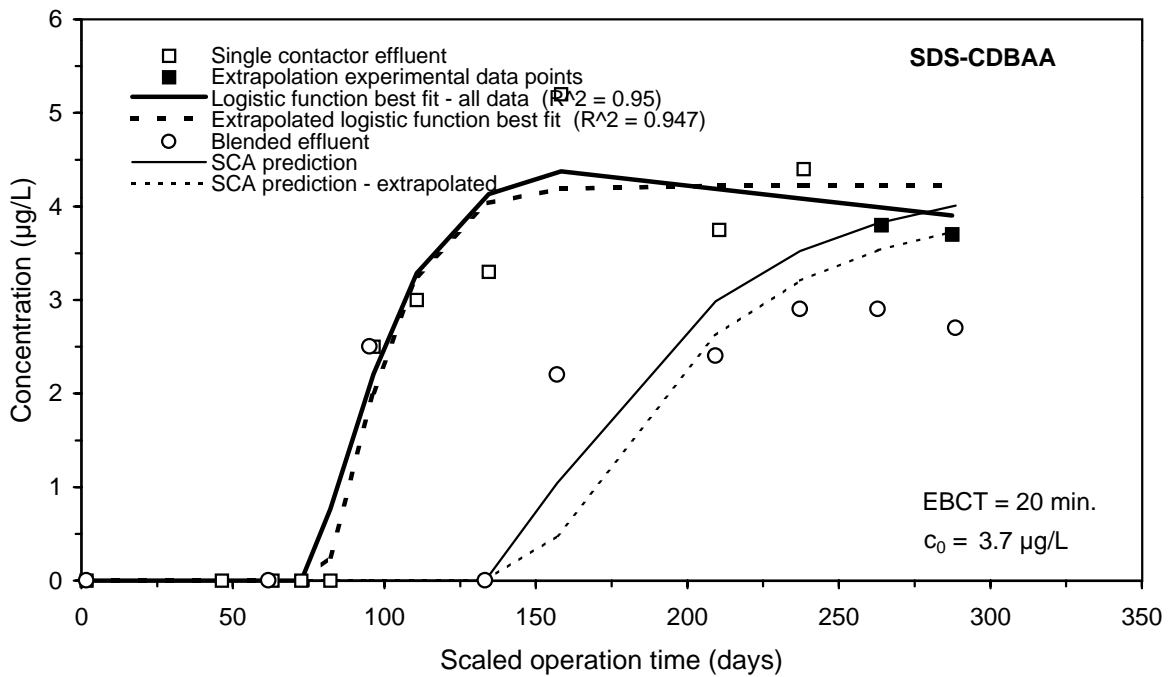


**Figure H-18 Impact of extrapolation on SCA prediction of the SDS-CDBAA integral breakthrough curve for Water 5**

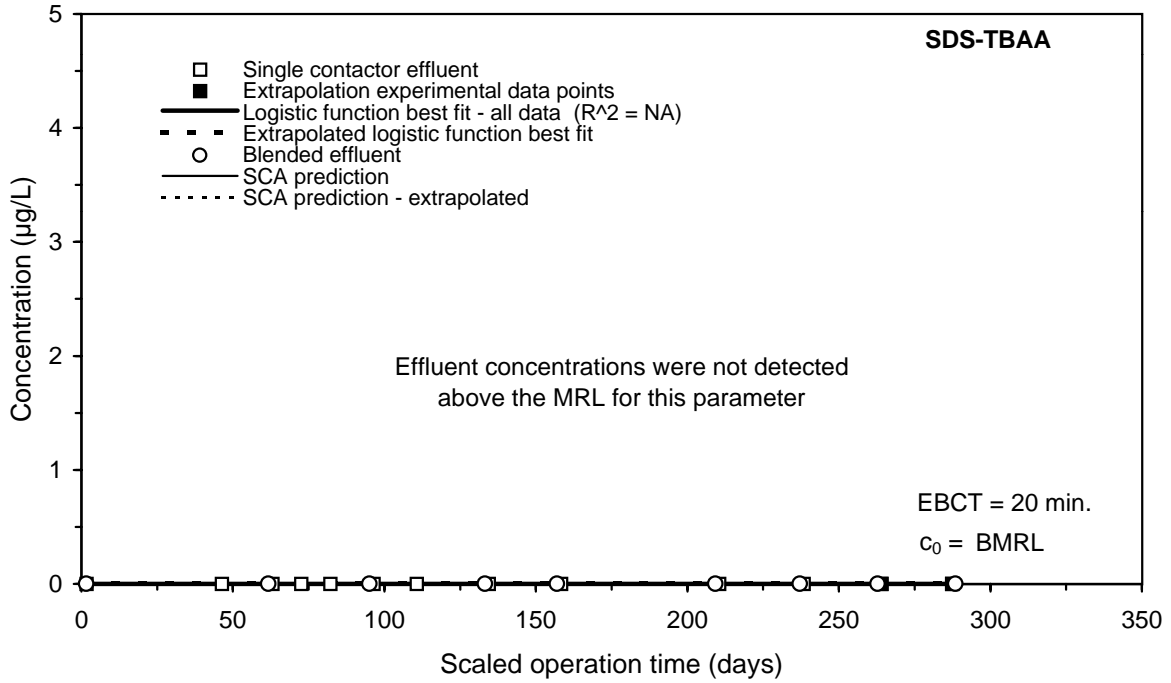


**Figure H-19 Impact of extrapolation on SCA prediction of the SDS-TBAA integral breakthrough curve for Water 5**

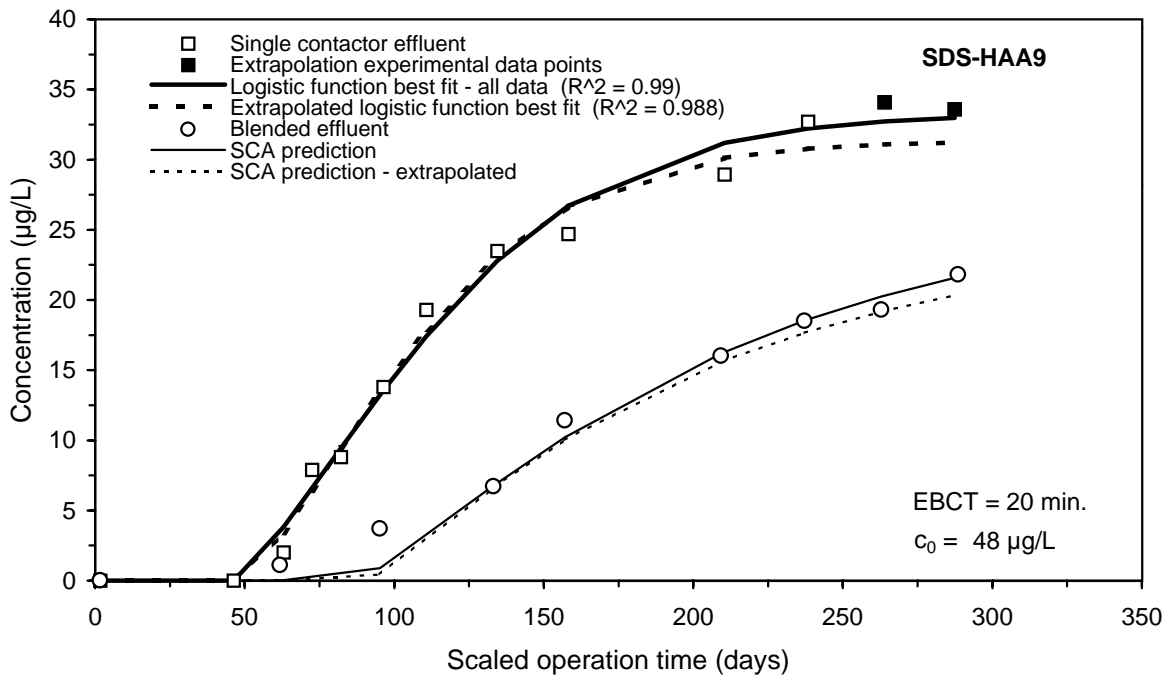


**Figure H-20 Impact of extrapolation on SCA prediction of the SDS-HAA9 integral breakthrough curve for Water 5**

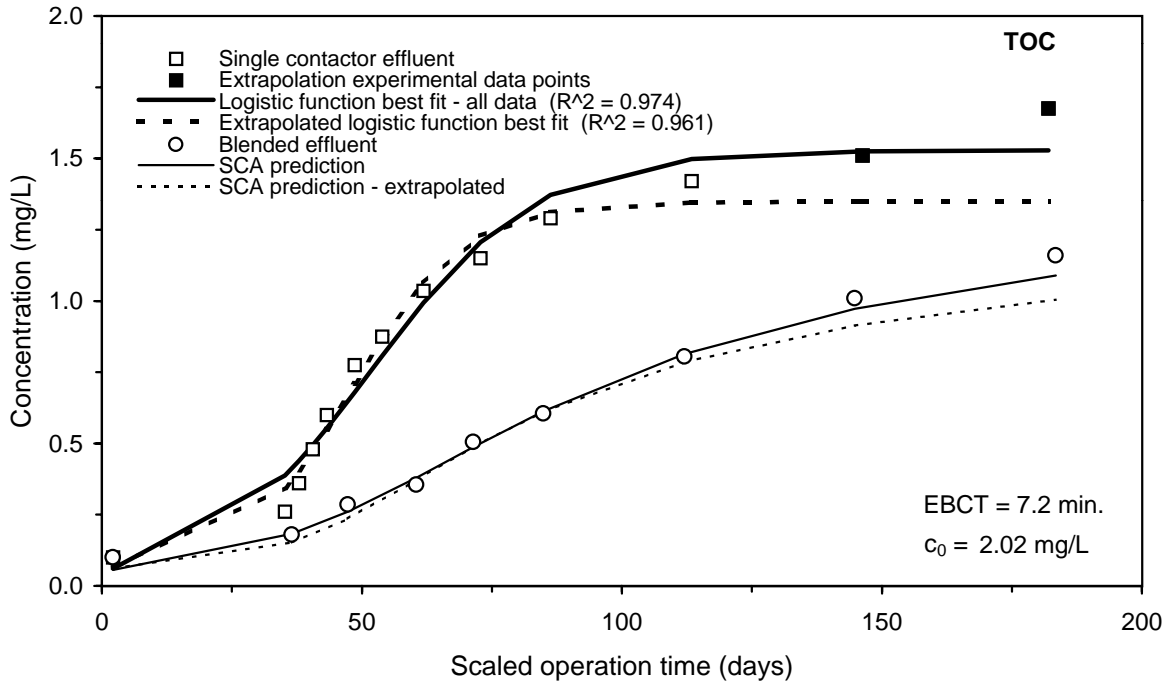


**Figure H-21 Impact of extrapolation on DI prediction of the TOC integral breakthrough curve for Water 8**

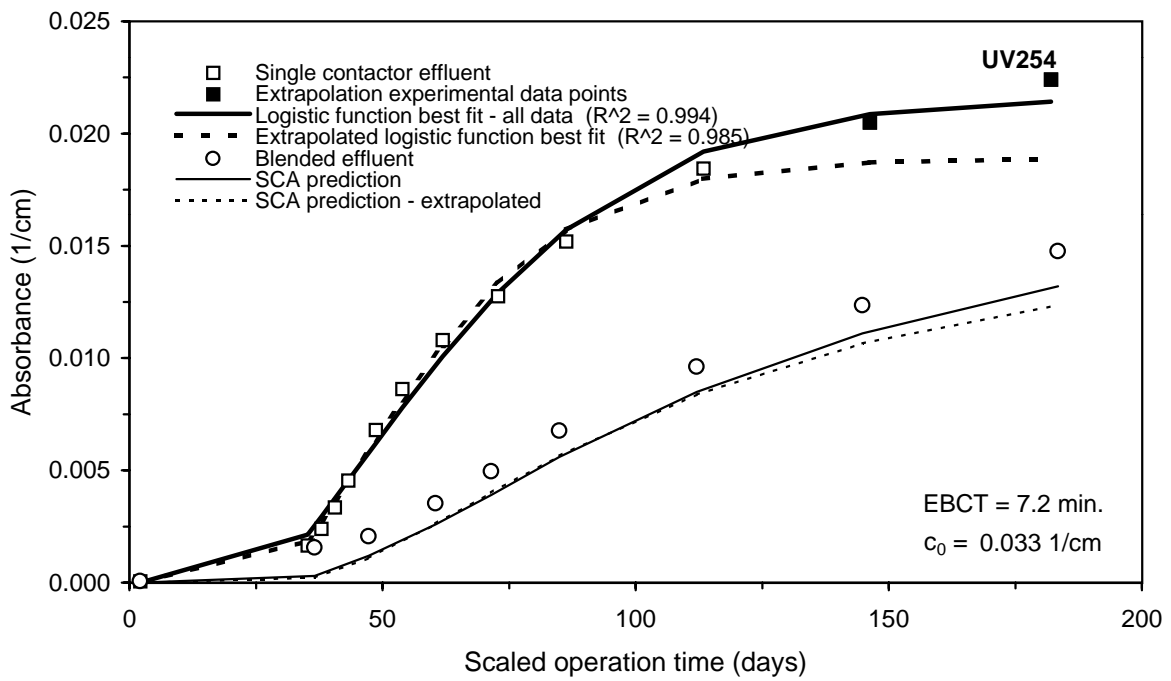


**Figure H-22 Impact of extrapolation on SCA prediction of the UV254 integral breakthrough curve for Water 8**

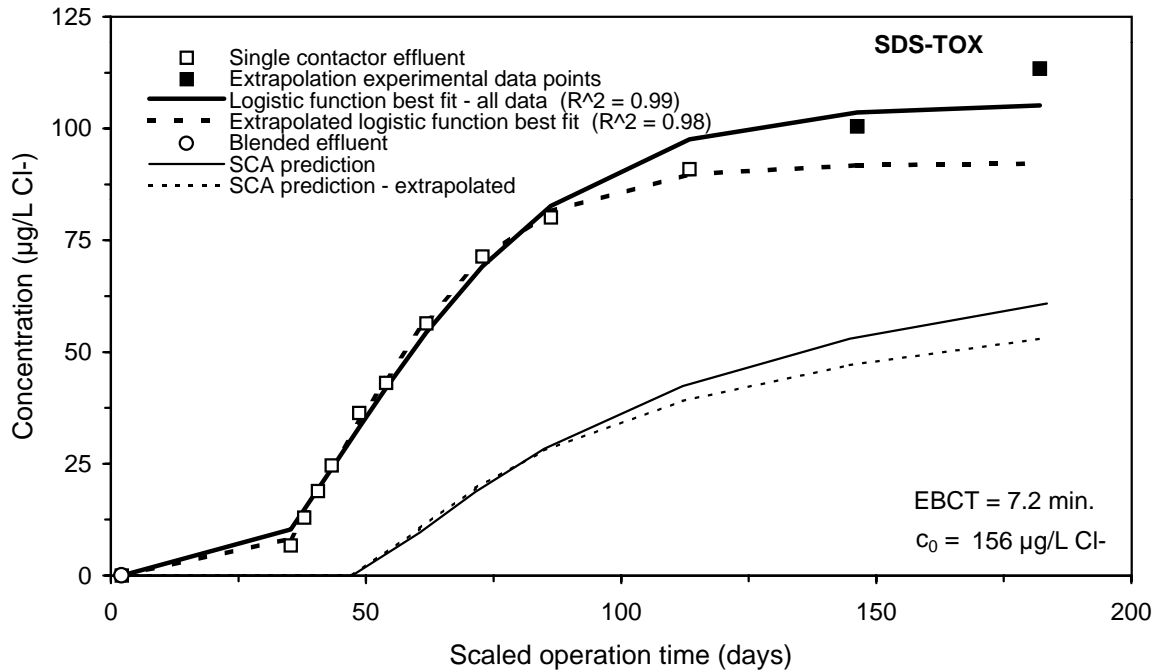


**Figure H-23 Impact of extrapolation on SCA prediction of the SDS-TOX integral breakthrough curve for Water 8**

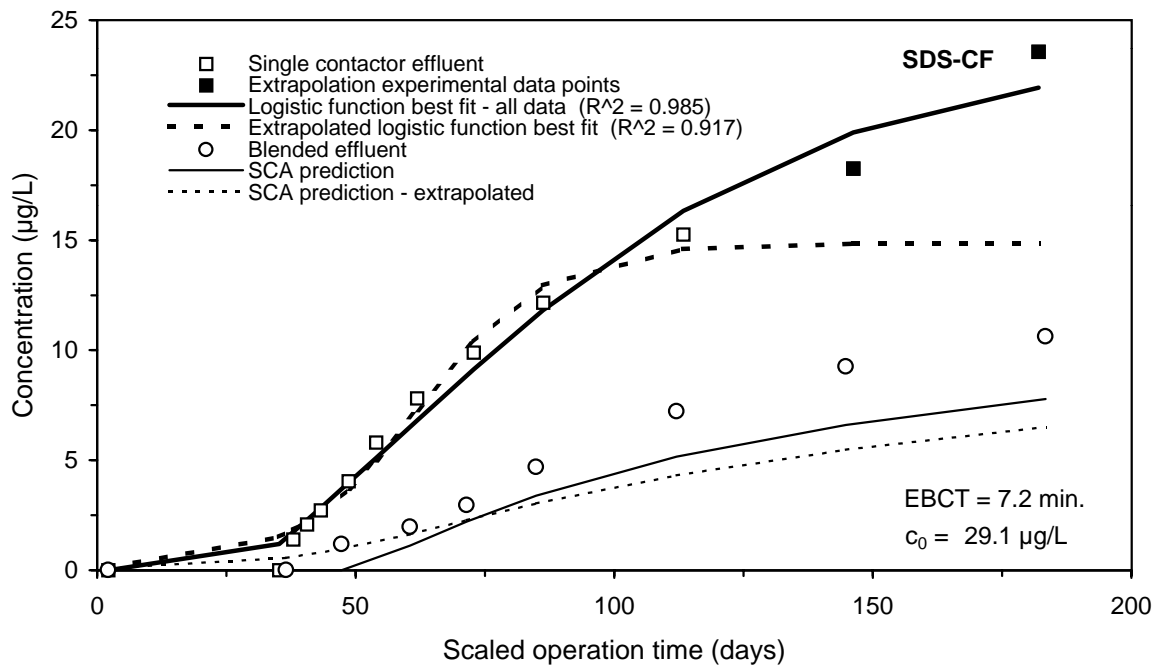


**Figure H-24 Impact of extrapolation on SCA prediction of the SDS-CF integral breakthrough curve for Water 8**

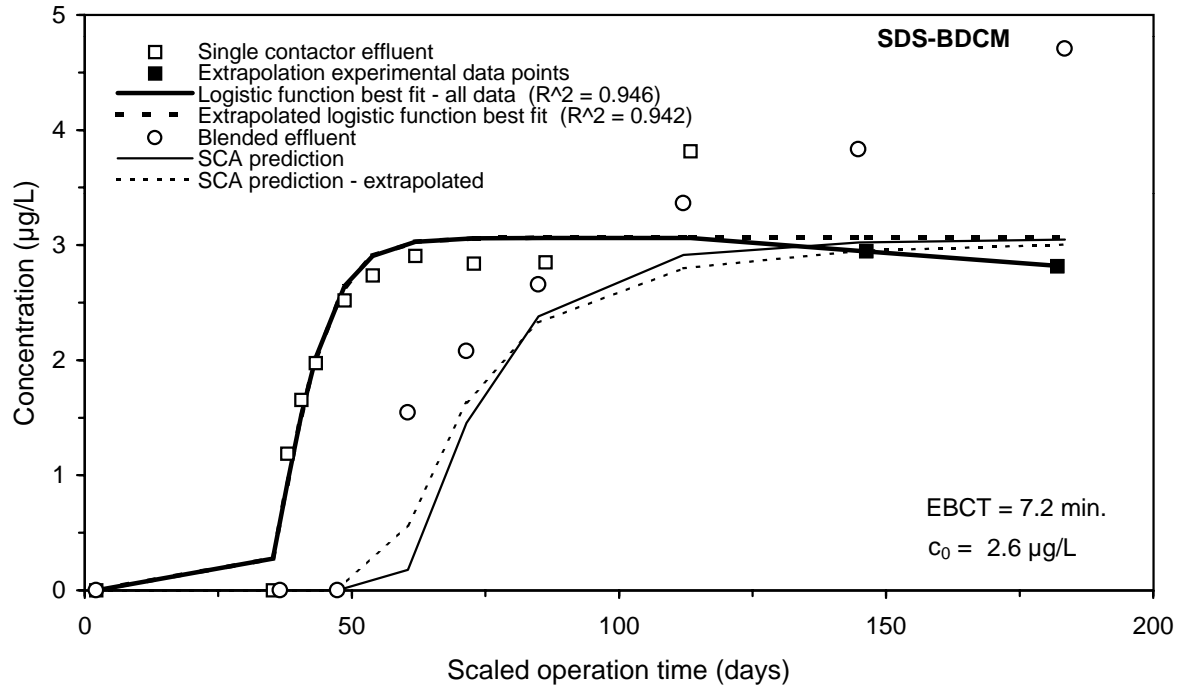


**Figure H-25 Impact of extrapolation on SCA prediction of the SDS-BDCM integral breakthrough curve for Water 8**

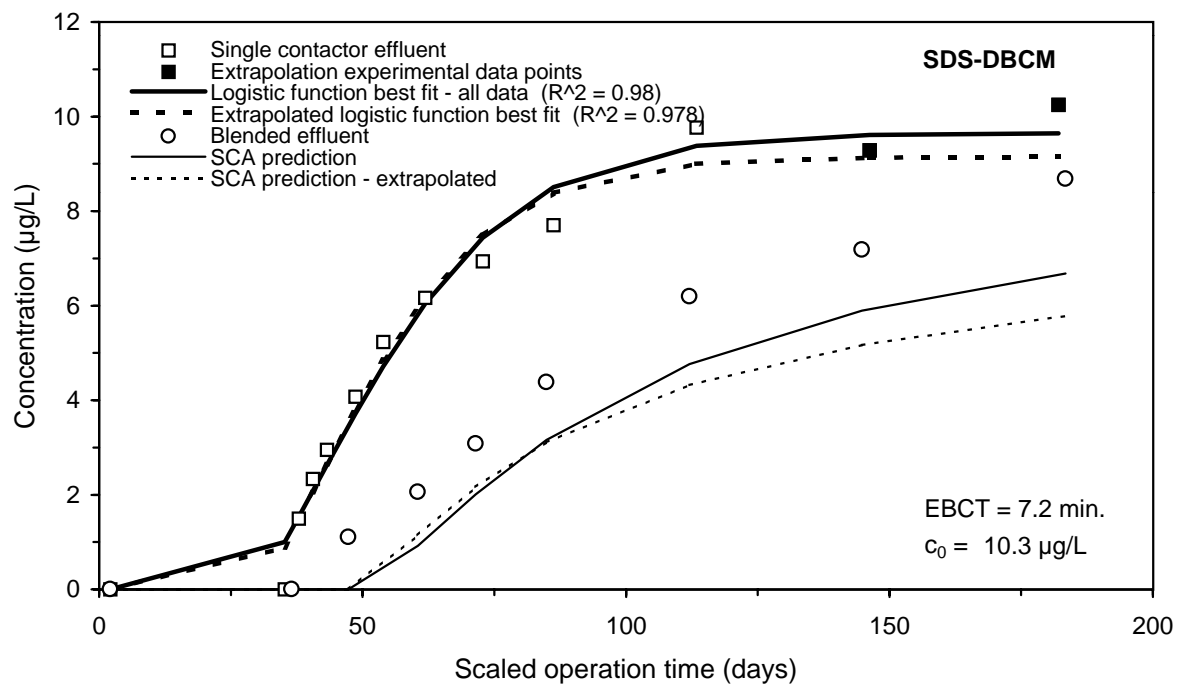


**Figure H-26 Impact of extrapolation on SCA prediction of the SDS-DBCm integral breakthrough curve for Water 8**

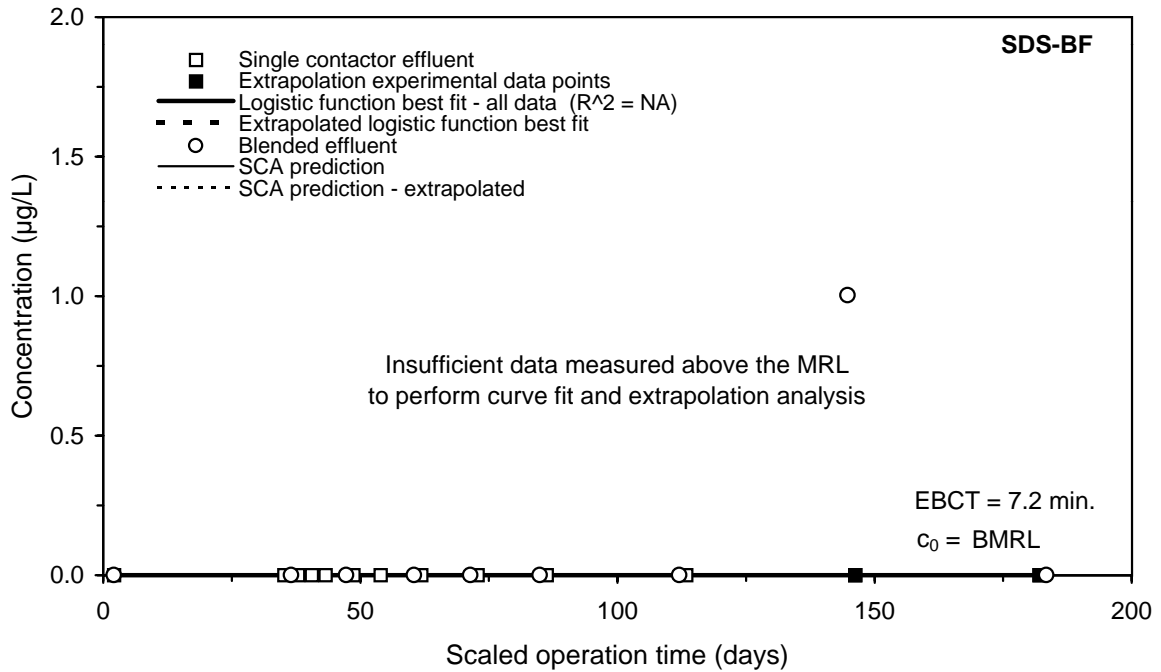


**Figure H-27 Impact of extrapolation on SCA prediction of the SDS-BF integral breakthrough curve for Water 8**

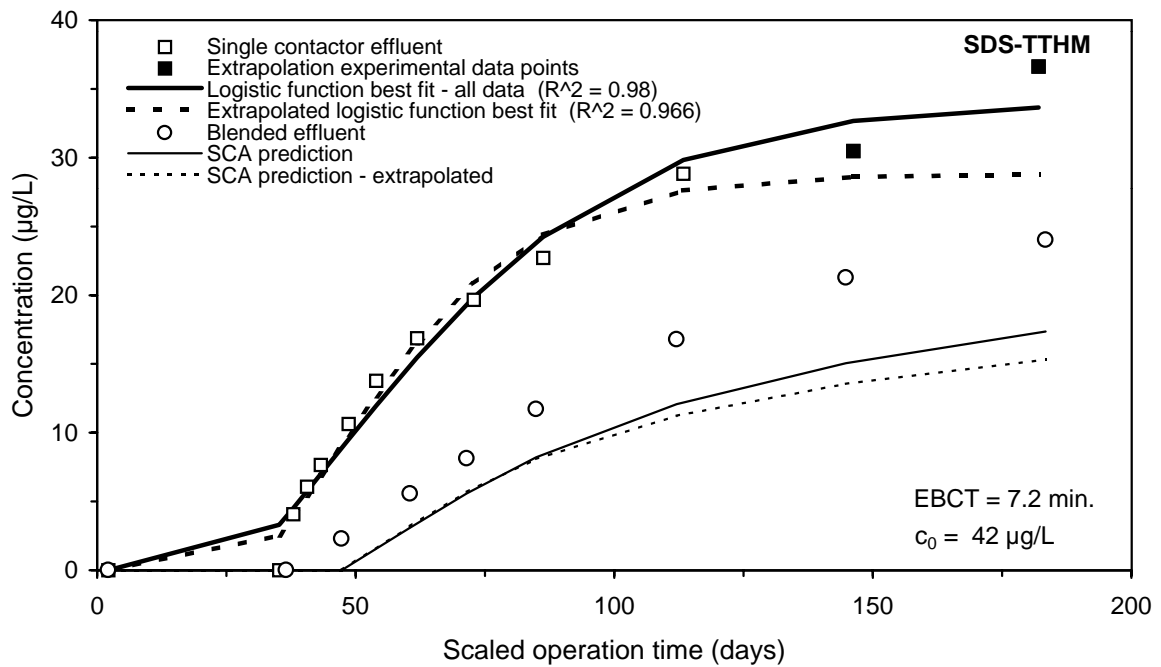


**Figure H-28 Impact of extrapolation on SCA prediction of the SDS-TTHM integral breakthrough curve for Water 8**

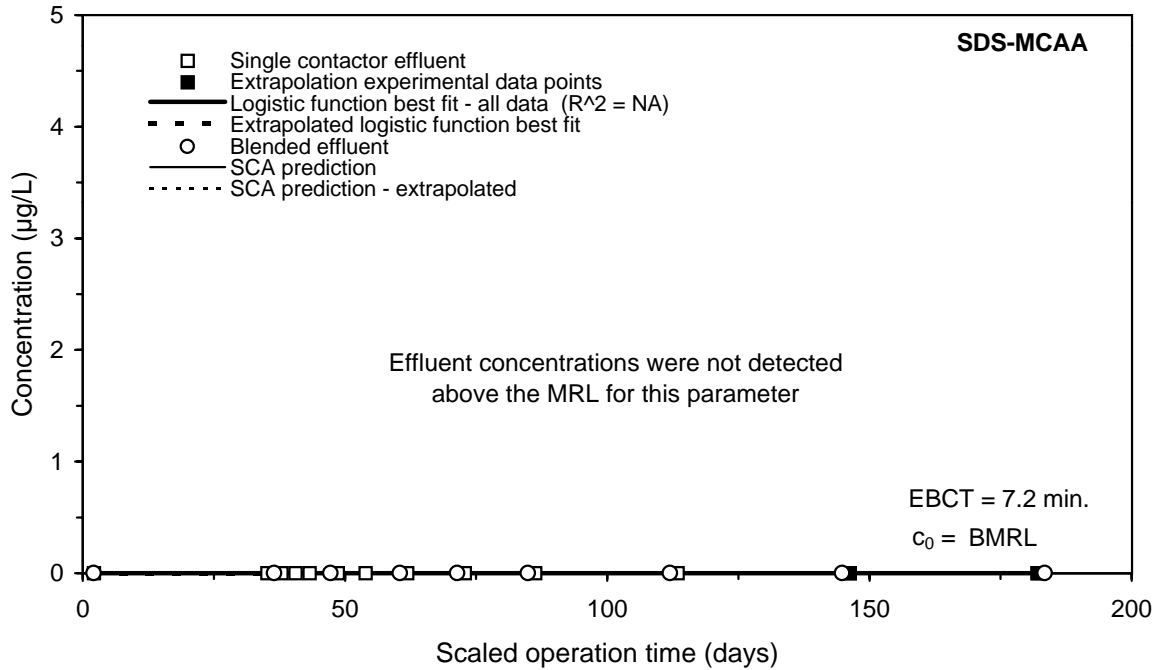


**Figure H-29 Impact of extrapolation on SCA prediction of the SDS-MCAA integral breakthrough curve for Water 8**

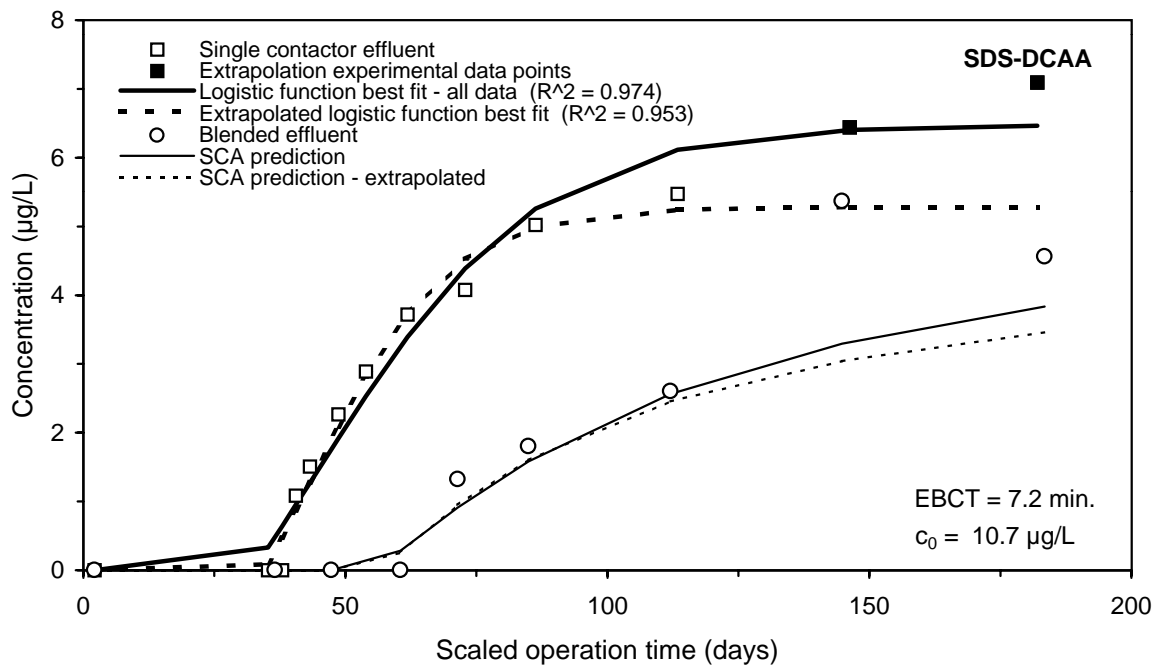


**Figure H-30 Impact of extrapolation on SCA prediction of the SDS-DCAA integral breakthrough curve for Water 8**

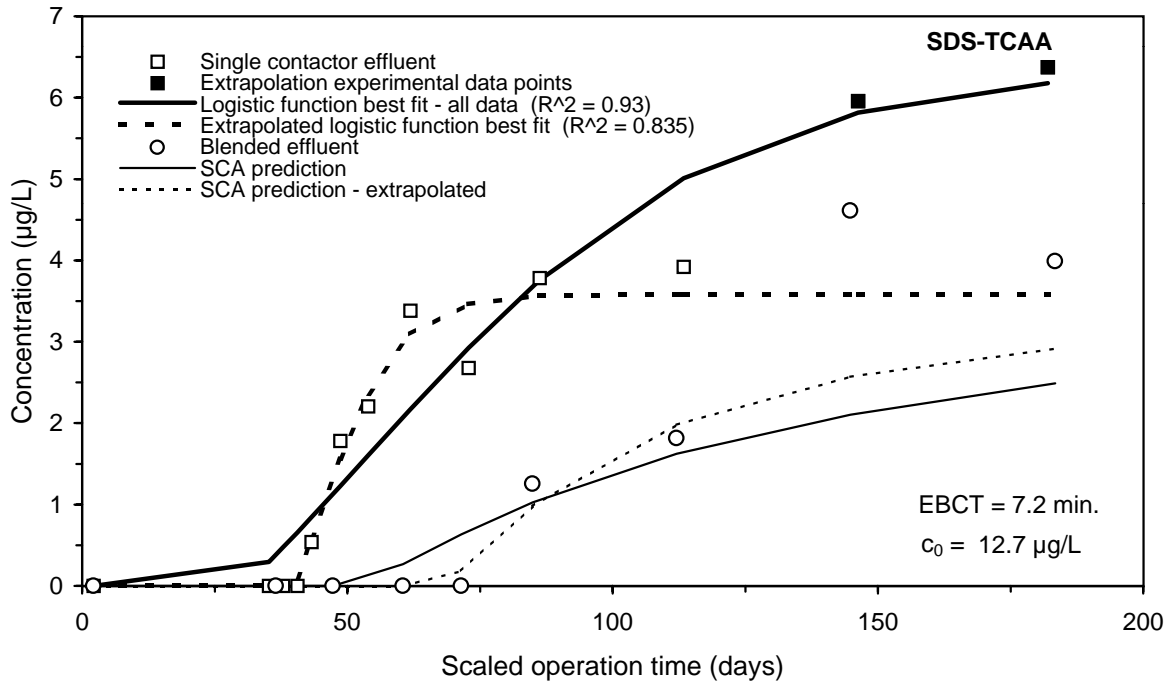


**Figure H-31 Impact of extrapolation on SCA prediction of the SDS-TCAA integral breakthrough curve for Water 8**

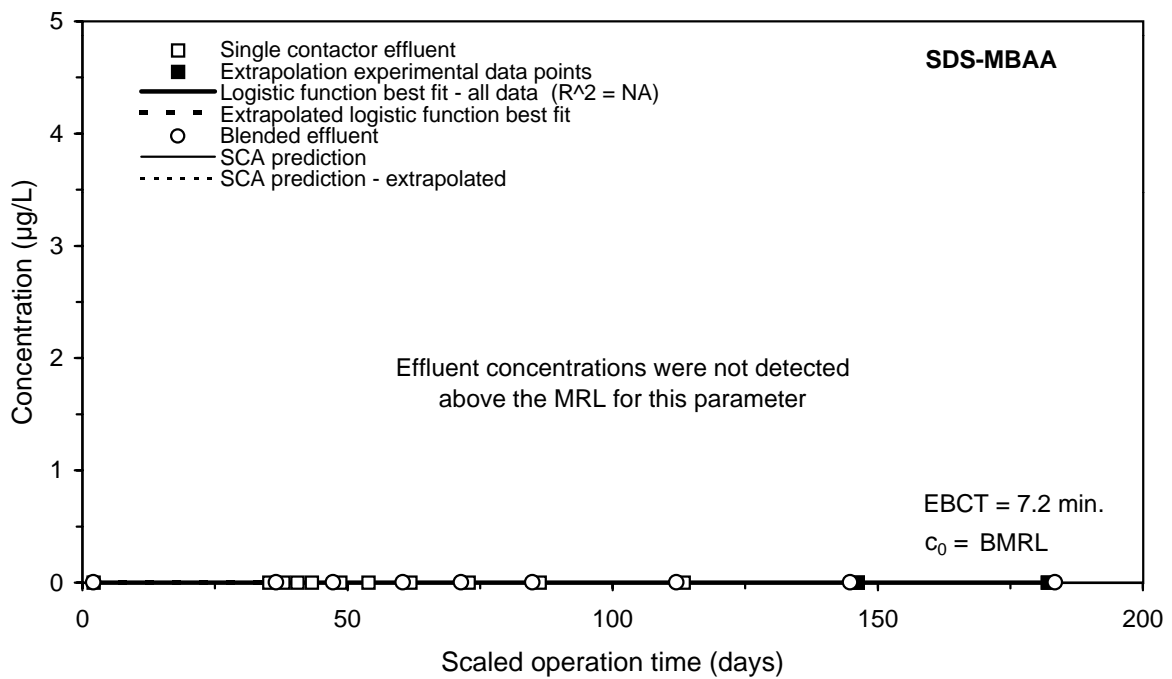


**Figure H-32 Impact of extrapolation on SCA prediction of the SDS-MBAA integral breakthrough curve for Water 8**

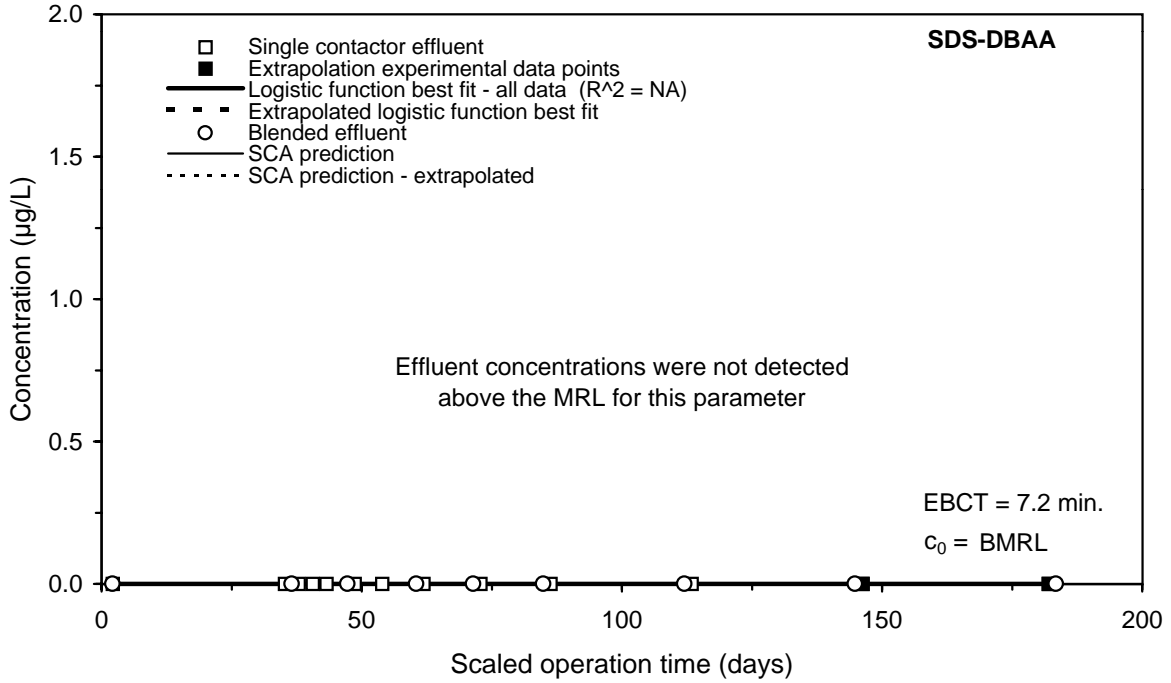


**Figure H-33 Impact of extrapolation on SCA prediction of the SDS-DBAA integral breakthrough curve for Water 8**

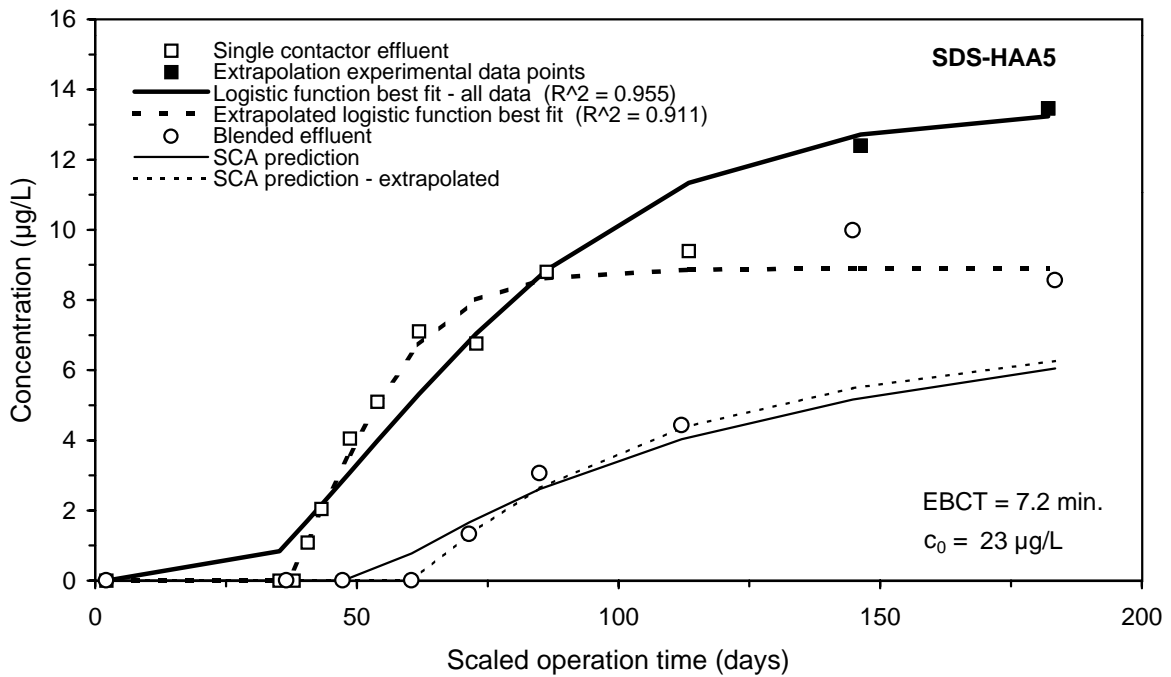


**Figure H-34 Impact of extrapolation on SCA prediction of the SDS-HAA5 integral breakthrough curve for Water 8**

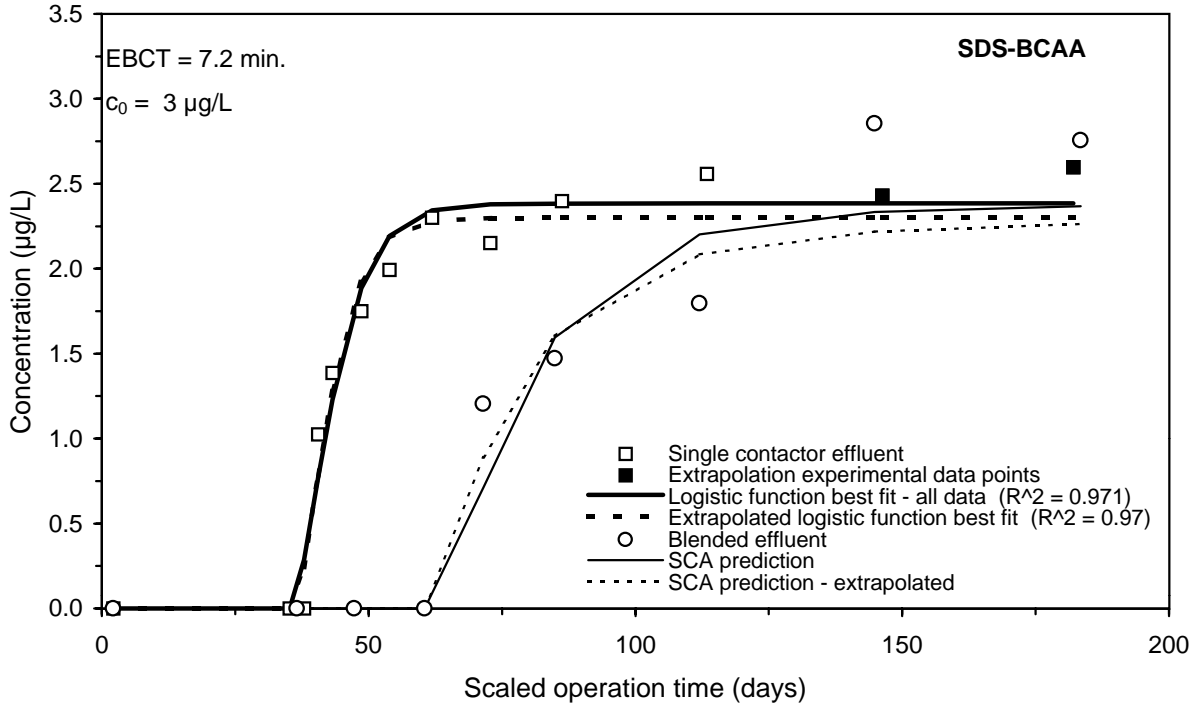


**Figure H-35 Impact of extrapolation on SCA prediction of the SDS-BCAA integral breakthrough curve for Water 8**

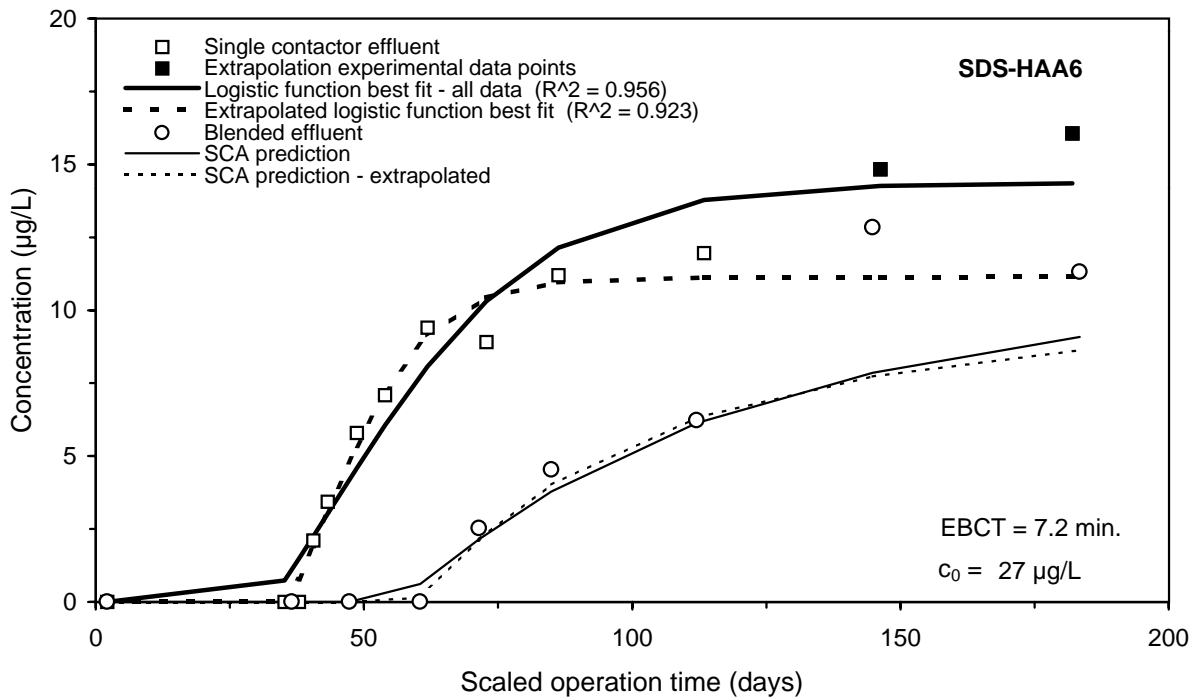


**Figure H-36 Impact of extrapolation on SCA prediction of the SDS-HAA6 integral breakthrough curve for Water 8**

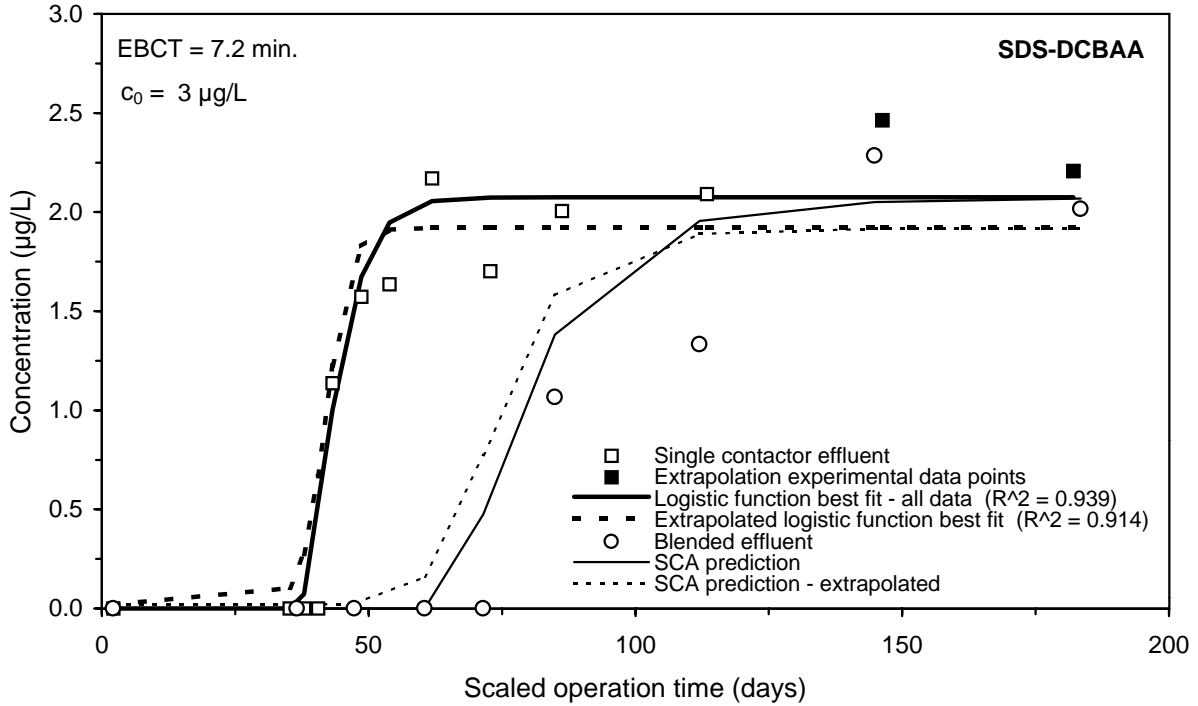


**Figure H-37 Impact of extrapolation on SCA prediction of the SDS-DCBAA integral breakthrough curve for Water 8**

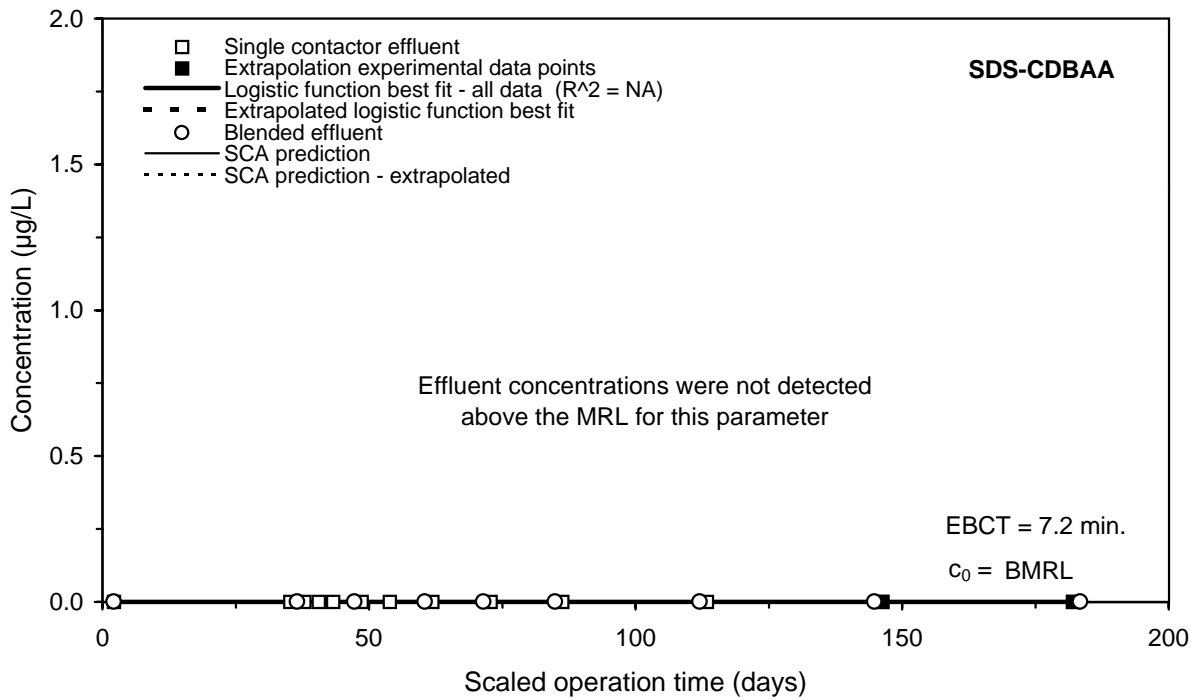


**Figure H-38 Impact of extrapolation on SCA prediction of the SDS-CDBAA integral breakthrough curve for Water 8**

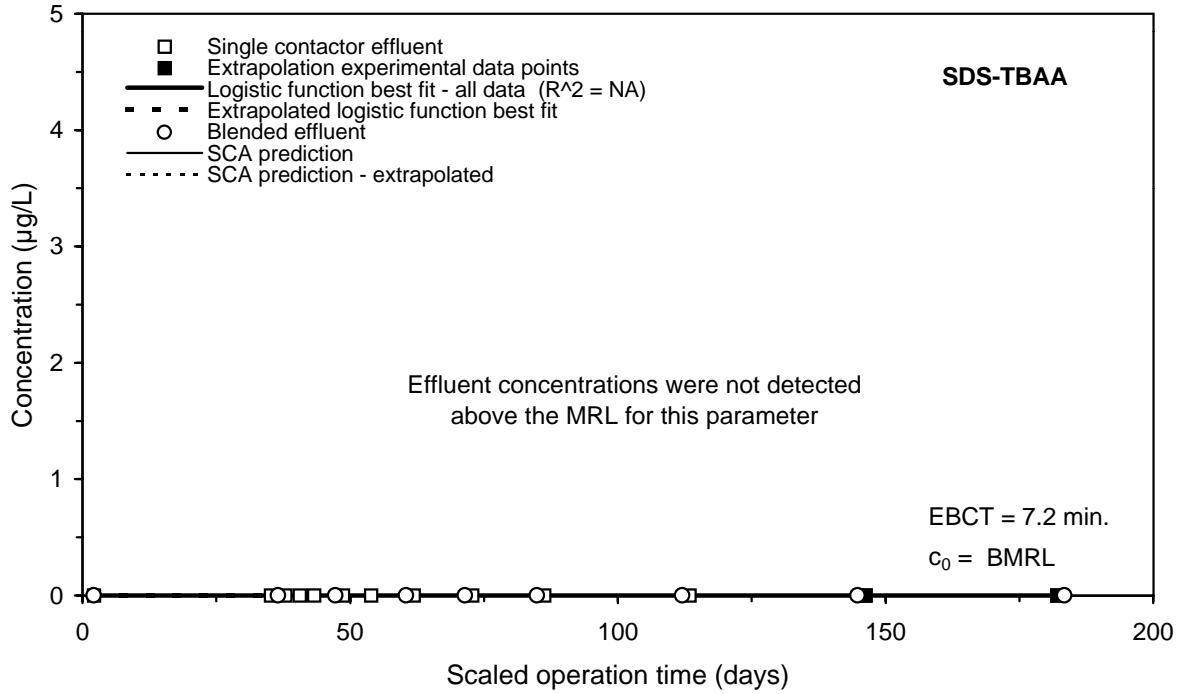


**Figure H-39 Impact of extrapolation on SCA prediction of the SDS-TBAA integral breakthrough curve for Water 8**

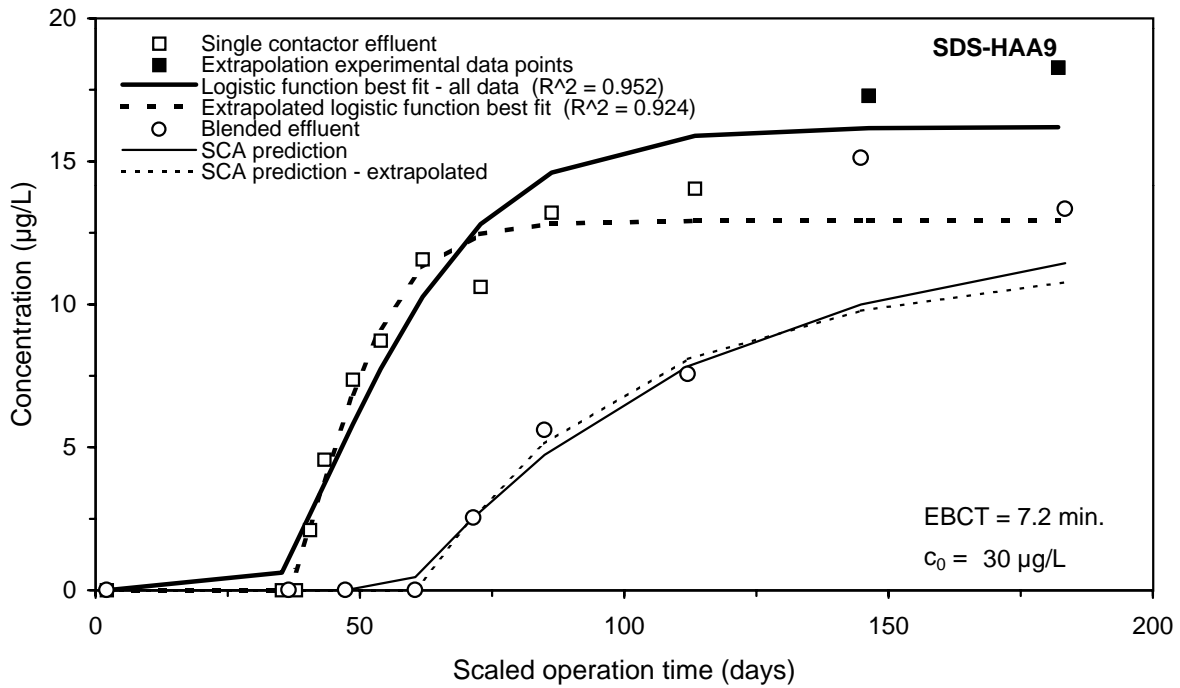


**Figure H-40 Impact of extrapolation on SCA prediction of the SDS-HAA9 integral breakthrough curve for Water 8**

This page intentionally left blank.

---

## Appendix I: Impact of Extrapolation on DI Prediction of the Integral Breakthrough Curve

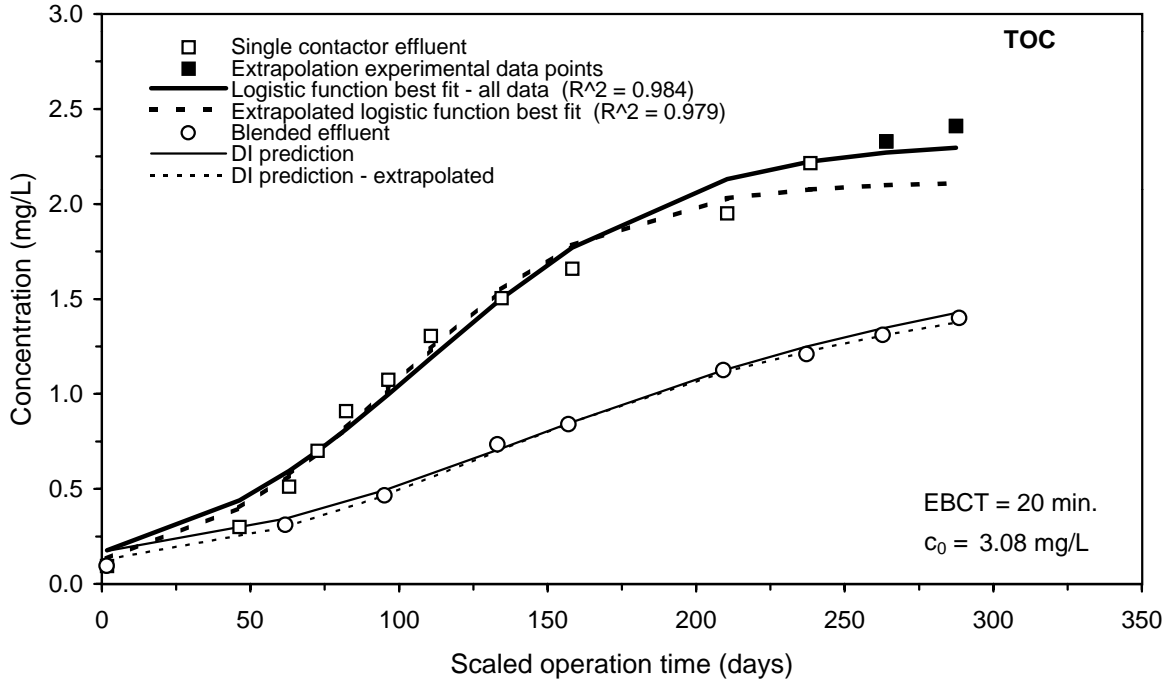


**Figure I-1 Impact of extrapolation on the DI prediction of the TOC integral breakthrough curve for Water 5**

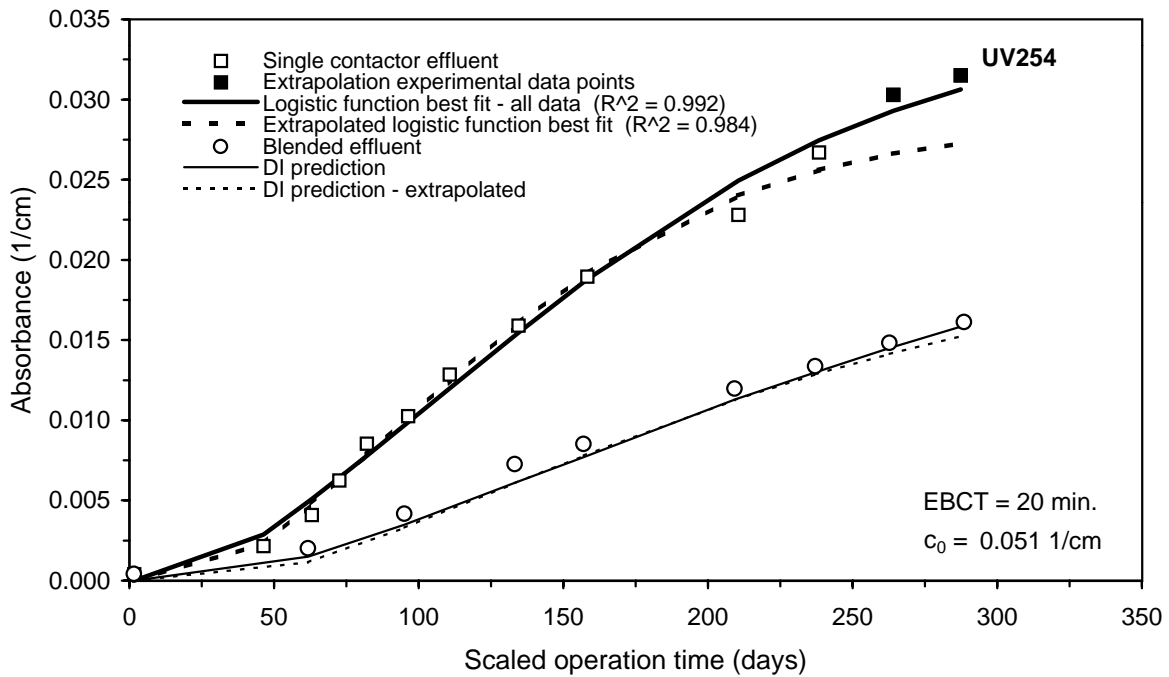


**Figure I-2 Impact of extrapolation on the DI prediction of the UV254 integral breakthrough curve for Water 5**

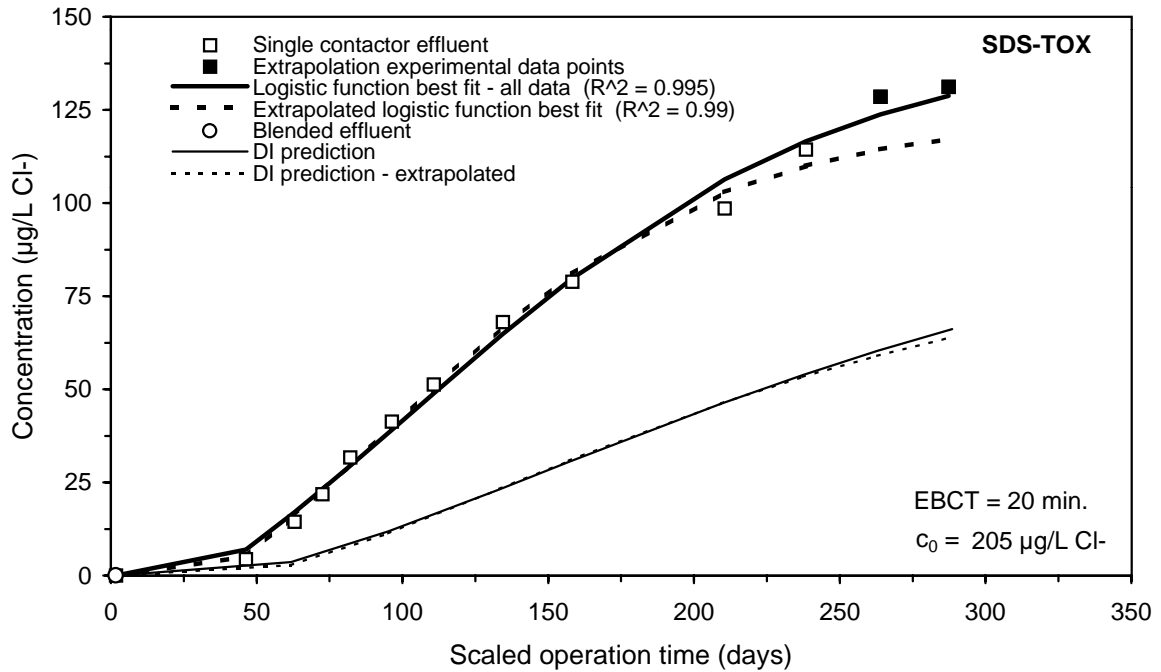


**Figure I-3 Impact of extrapolation on the DI prediction of the SDS-TOX integral breakthrough curve for Water 5**

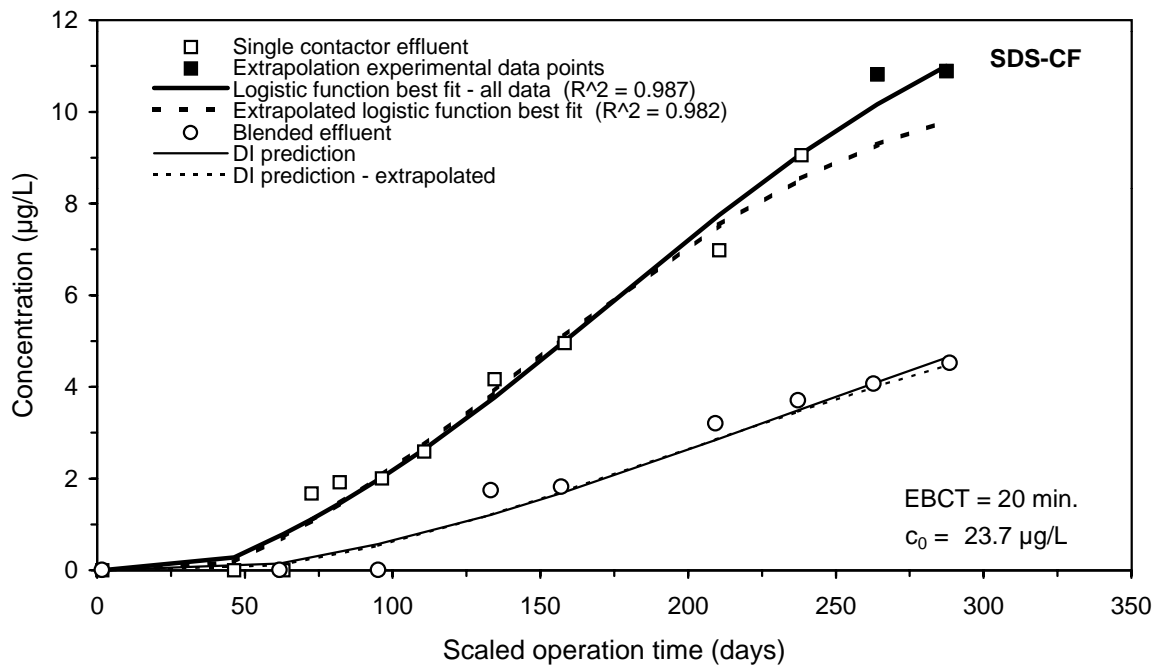


**Figure I-4 Impact of extrapolation on the DI prediction of the SDS-CF integral breakthrough curve for Water 5**

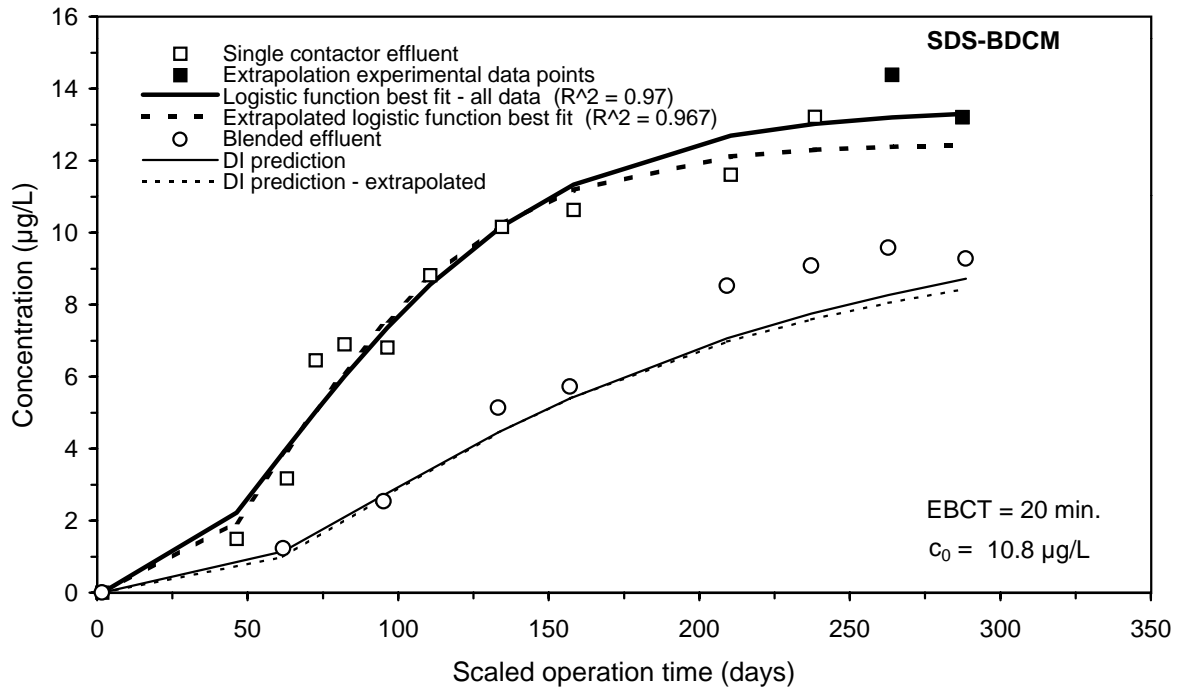


**Figure I-5 Impact of extrapolation on the DI prediction of the SDS-BDCM integral breakthrough curve for Water 5**

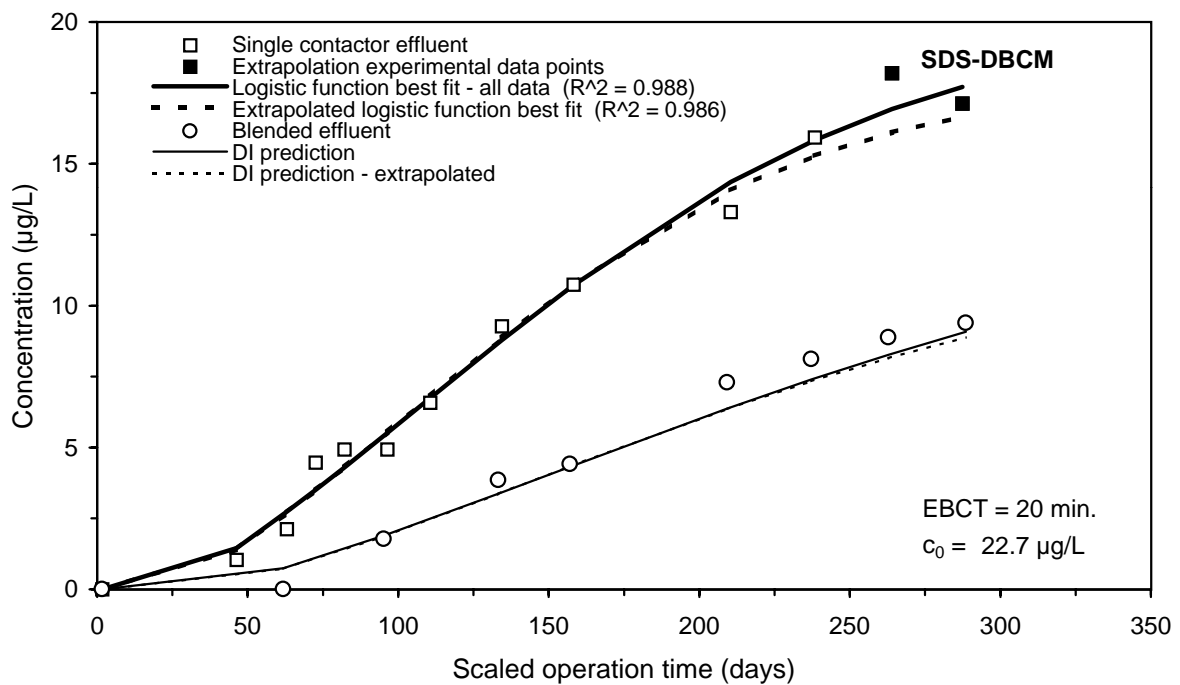


**Figure I-6 Impact of extrapolation on the DI prediction of the SDS-DBCm integral breakthrough curve for Water 5**

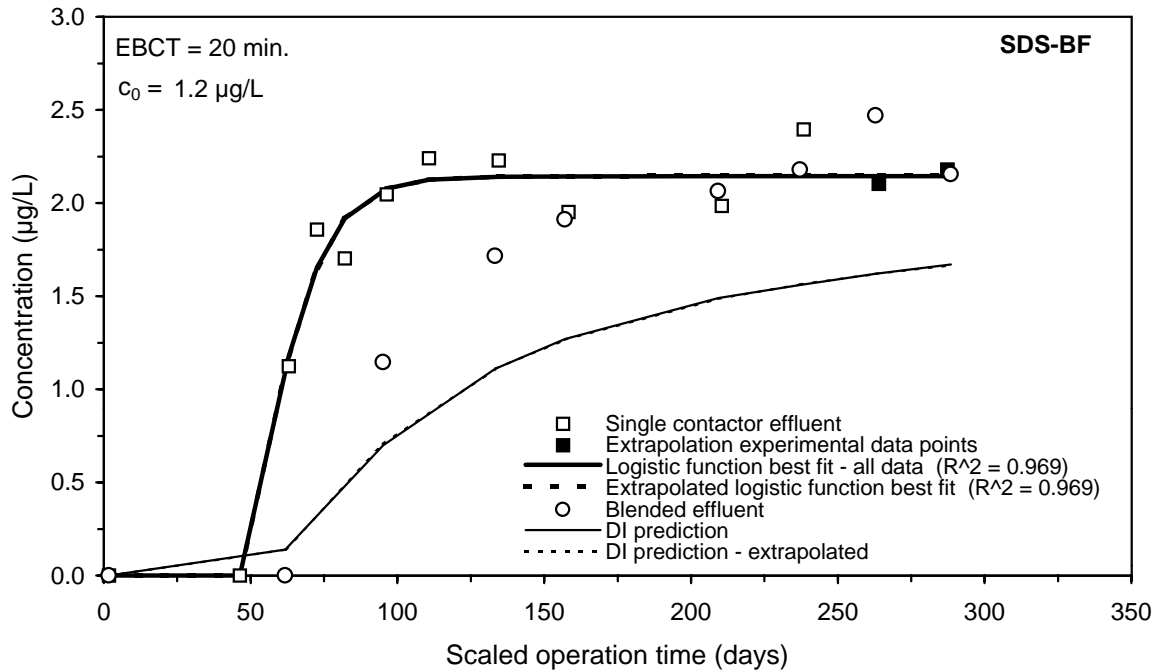


**Figure I-7 Impact of extrapolation on the DI prediction of the SDS-BF integral breakthrough curve for Water 5**

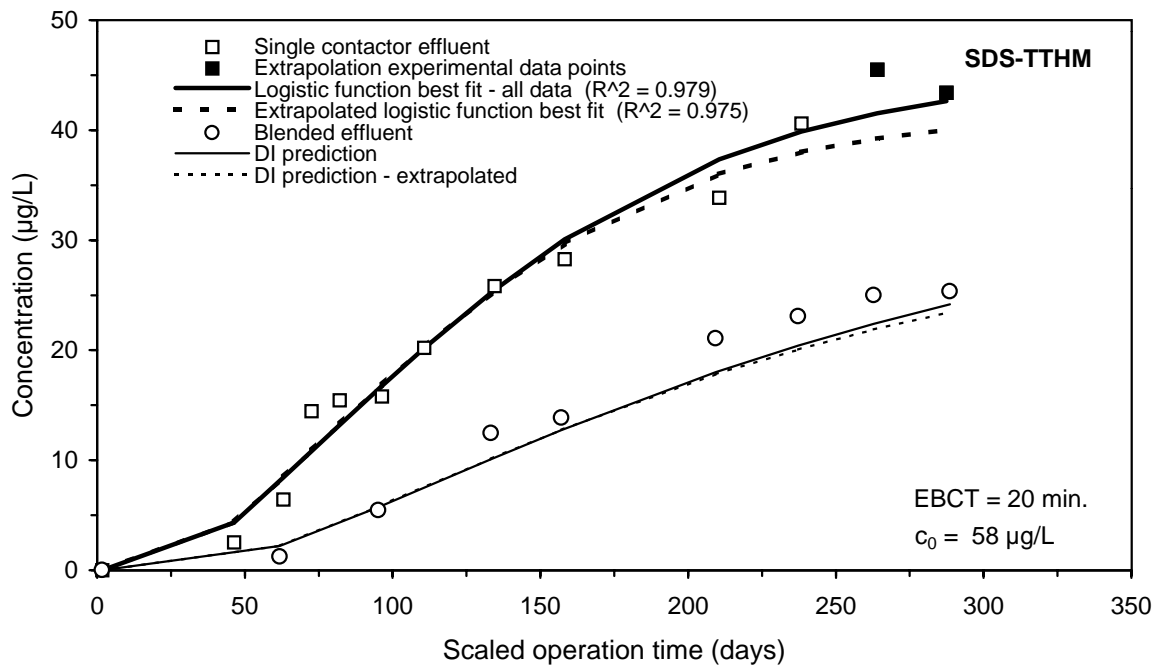


**Figure I-8 Impact of extrapolation on the DI prediction of the SDS-TTHM integral breakthrough curve for Water 5**

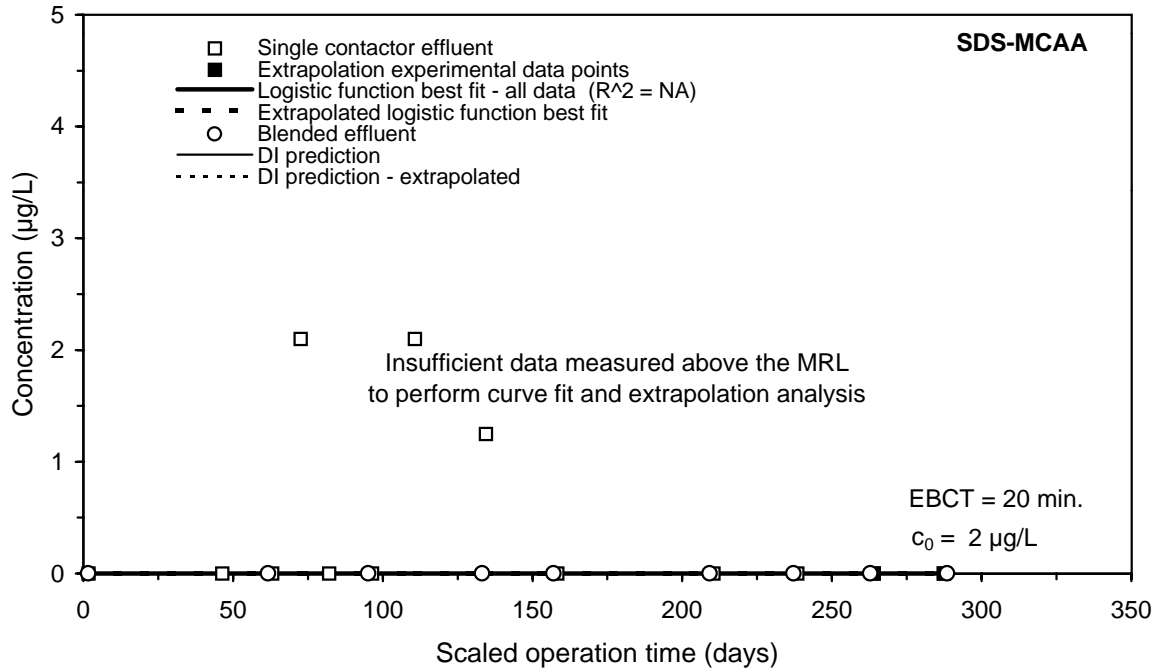


**Figure I-9 Impact of extrapolation on the DI prediction of the SDS-MCAA integral breakthrough curve for Water 5**

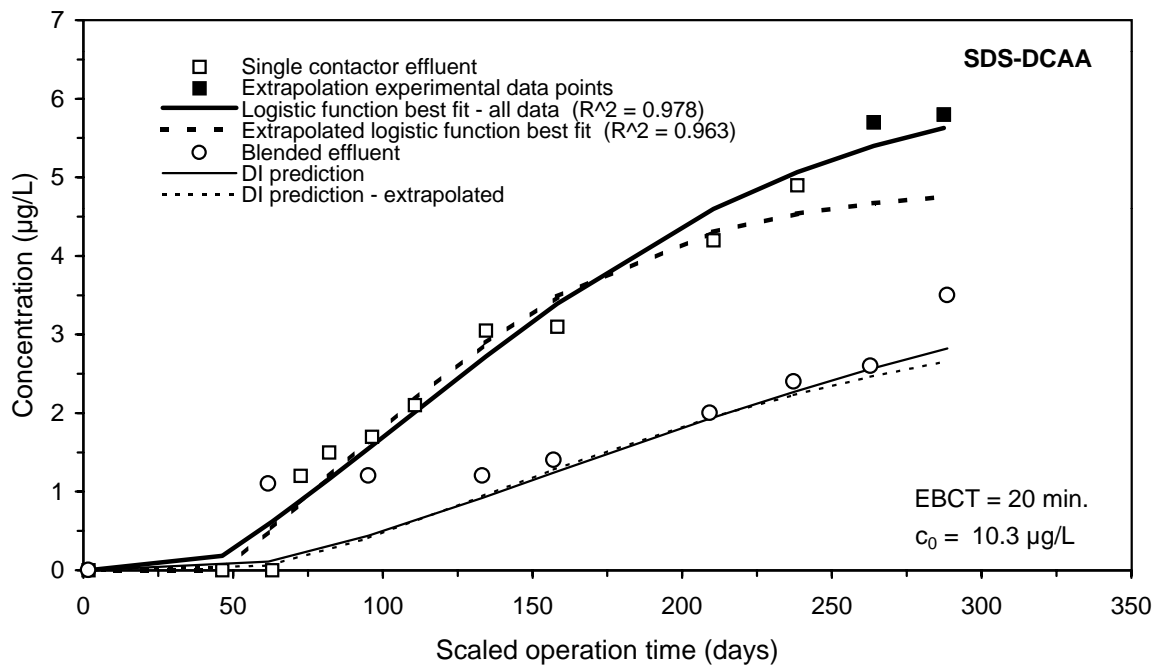


**Figure I-10 Impact of extrapolation on the DI prediction of the SDS-DCAA integral breakthrough curve for Water 5**

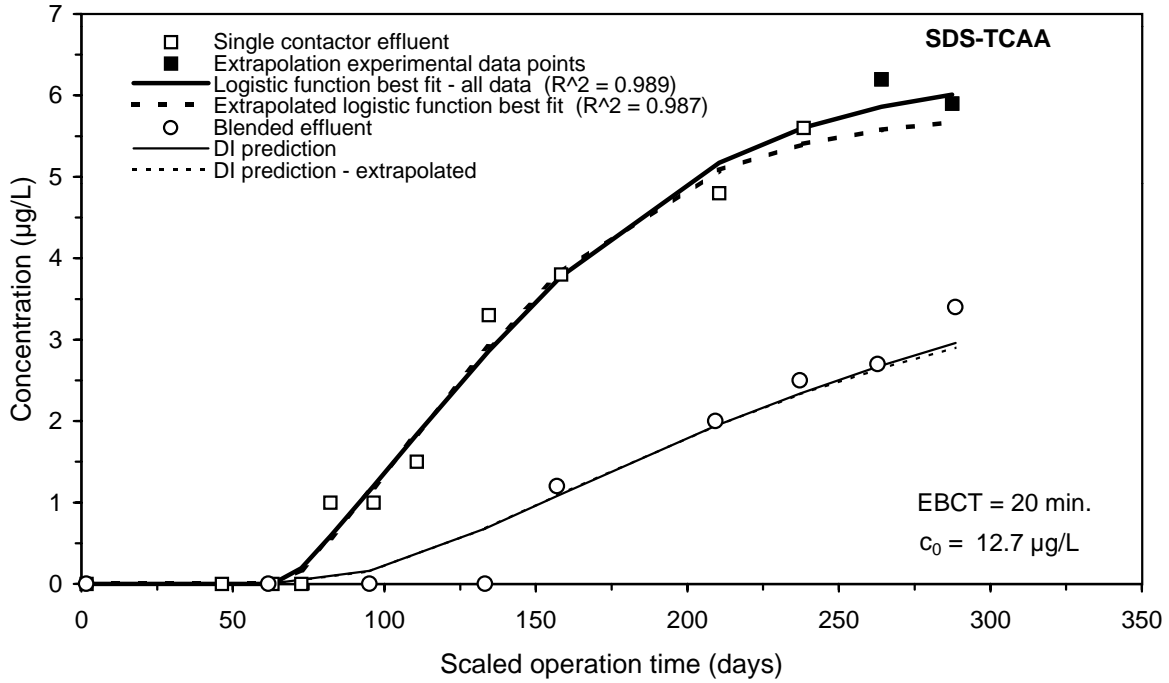


**Figure I-11 Impact of extrapolation on the DI prediction of the SDS-TCAA integral breakthrough curve for Water 5**

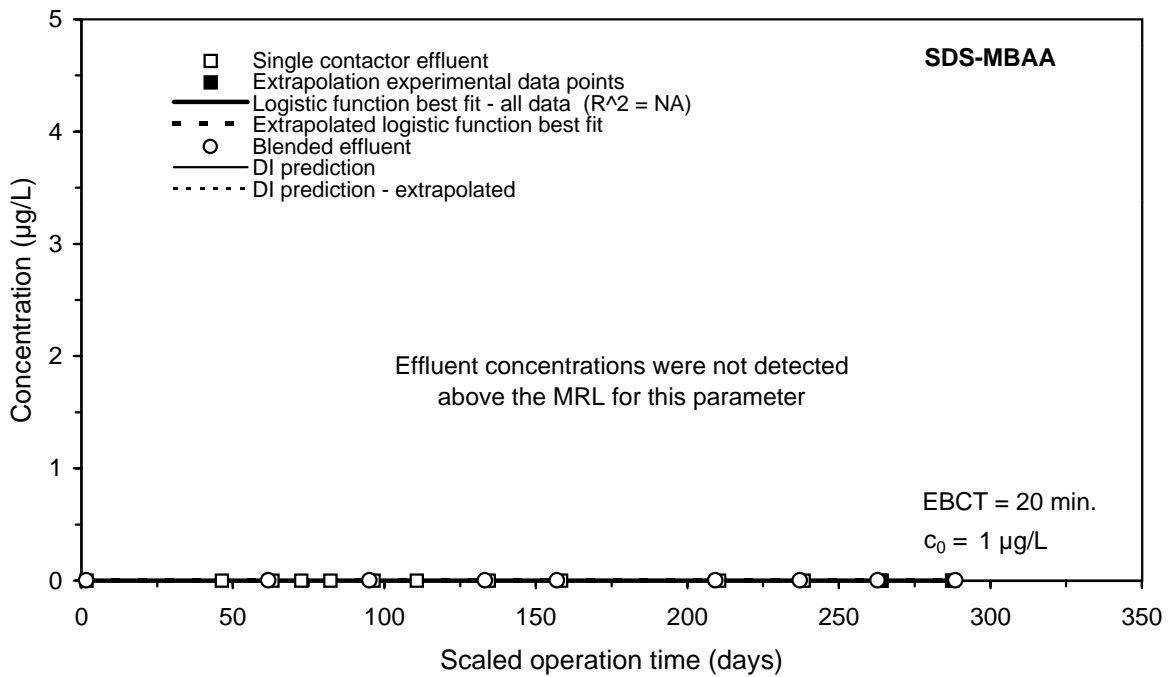


**Figure I-12 Impact of extrapolation on the DI prediction of the SDS-MBAA integral breakthrough curve for Water 5**

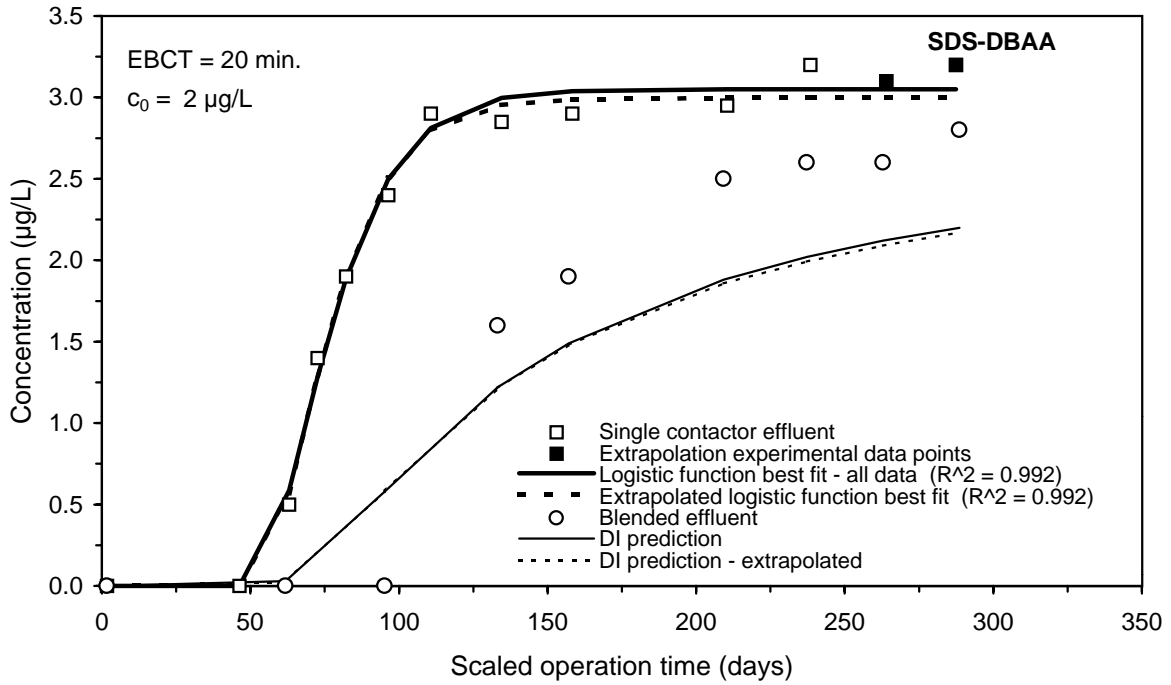


**Figure I-13 Impact of extrapolation on the DI prediction of the SDS-DBAA integral breakthrough curve for Water 5**

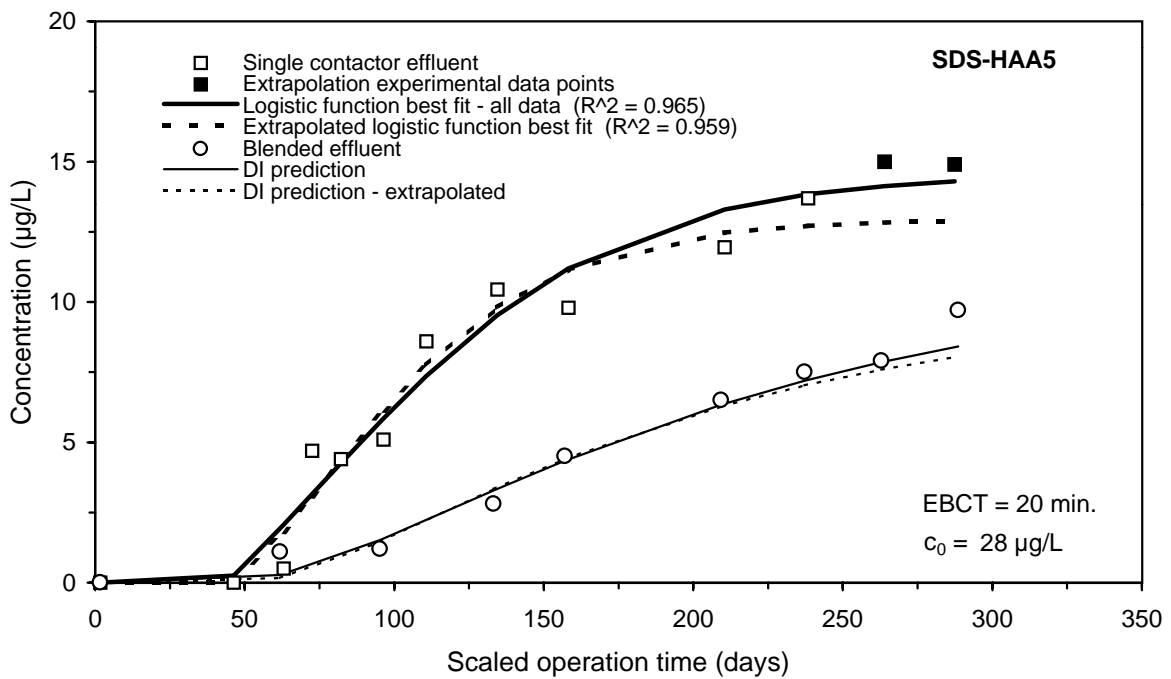


**Figure I-14 Impact of extrapolation on the DI prediction of the SDS-HAA5 integral breakthrough curve for Water 5**

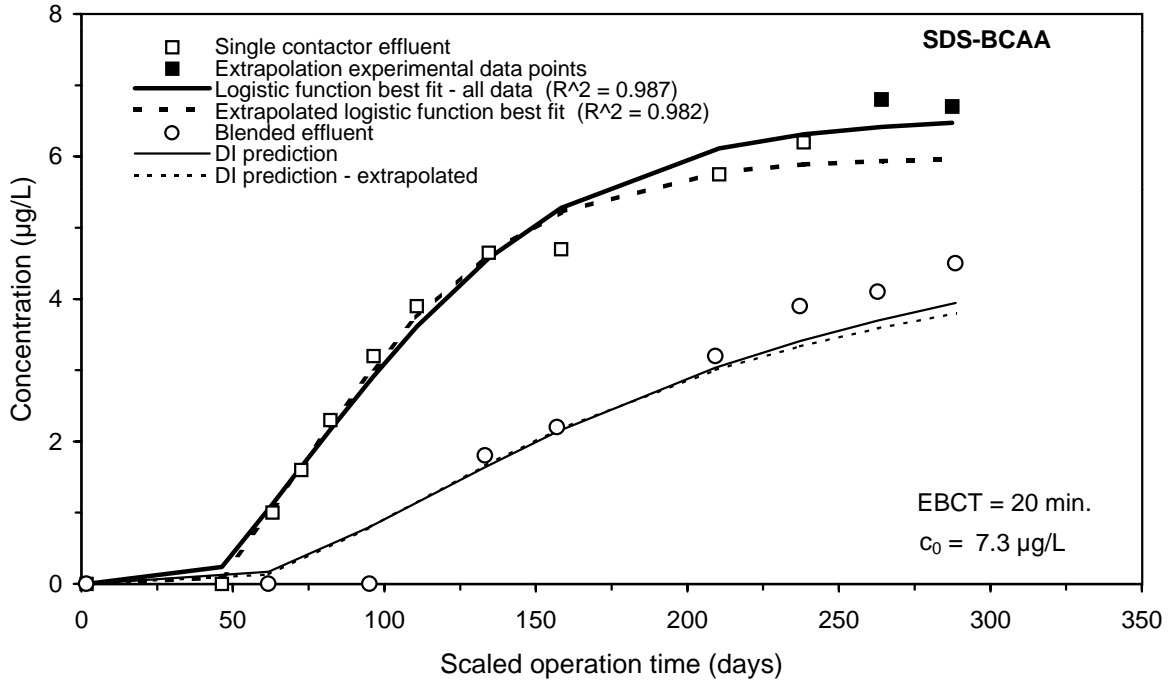


**Figure I-15 Impact of extrapolation on the DI prediction of the SDS-BCAA integral breakthrough curve for Water 5**

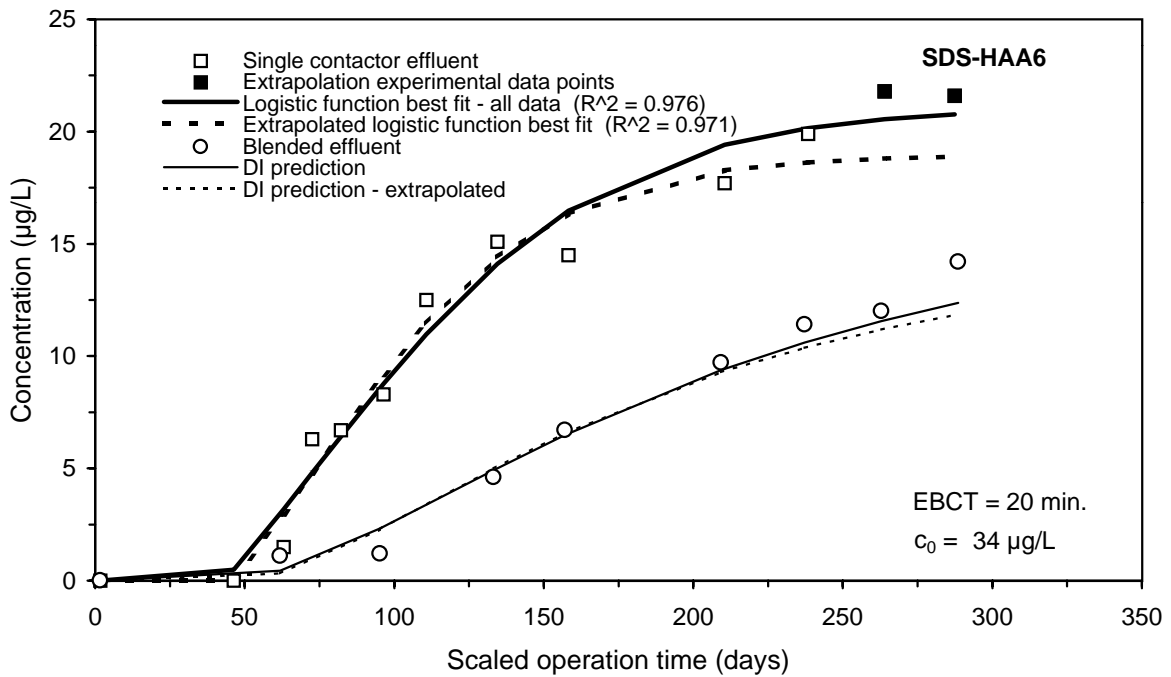


**Figure I-16 Impact of extrapolation on the DI prediction of the SDS-HAA6 integral breakthrough curve for Water 5**

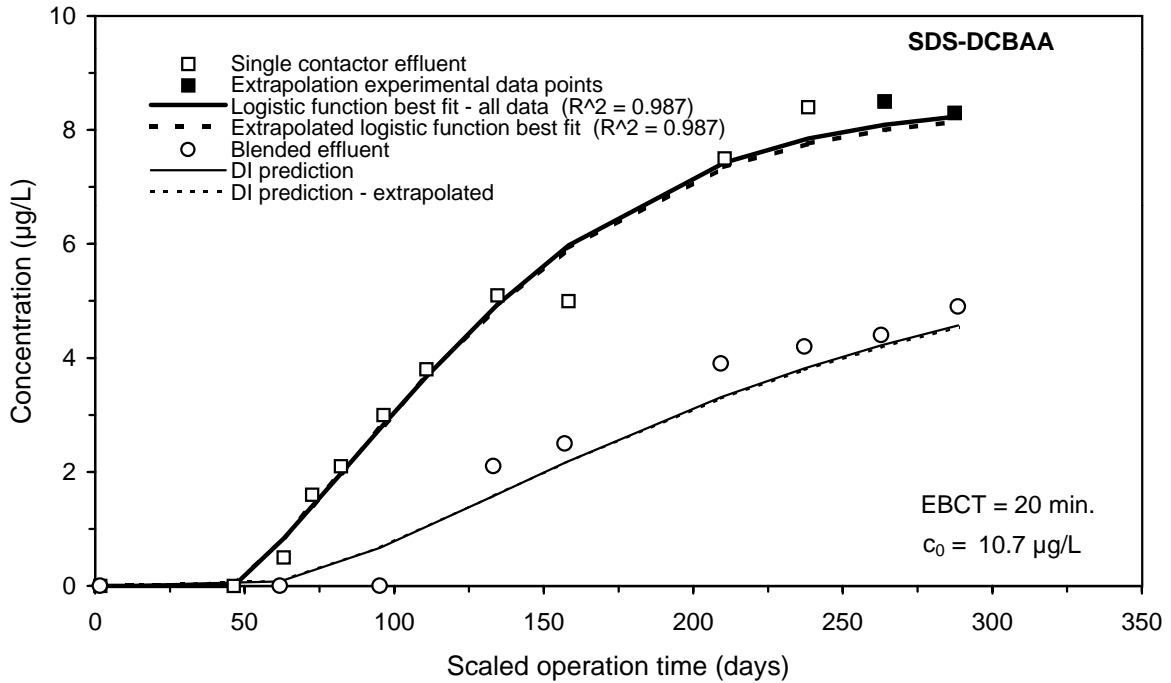


**Figure I-17 Impact of extrapolation on the DI prediction of the SDS-DCBAA integral breakthrough curve for Water 5**

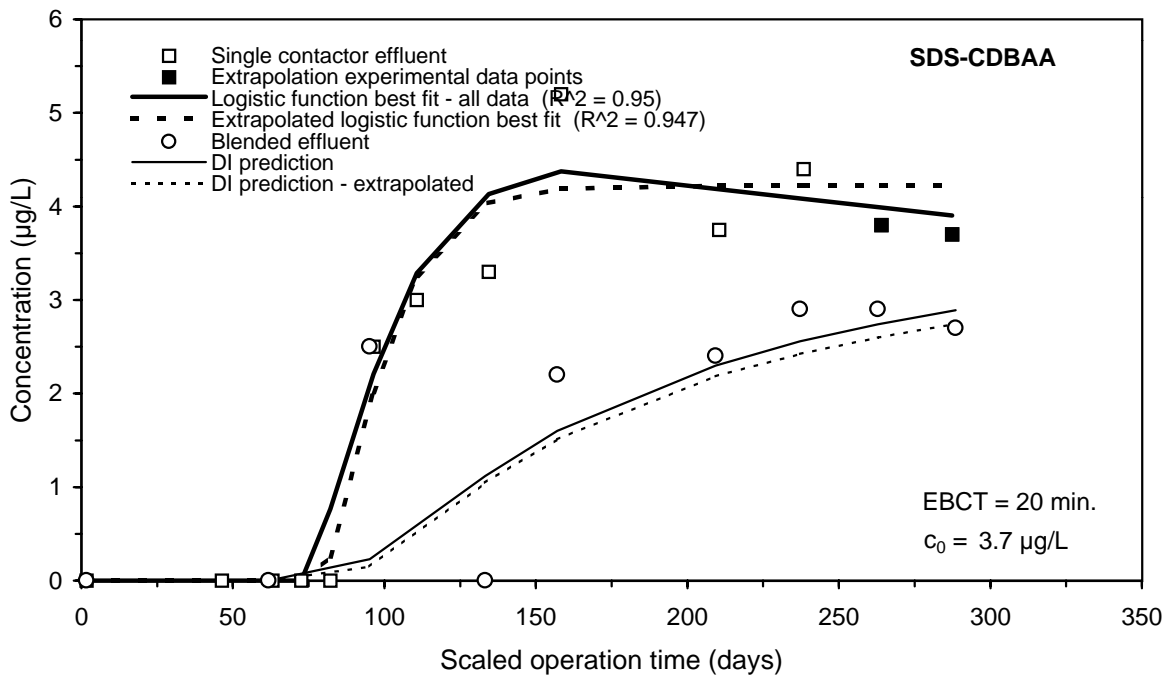


**Figure I-18 Impact of extrapolation on the DI prediction of the SDS-CDBAA integral breakthrough curve for Water 5**

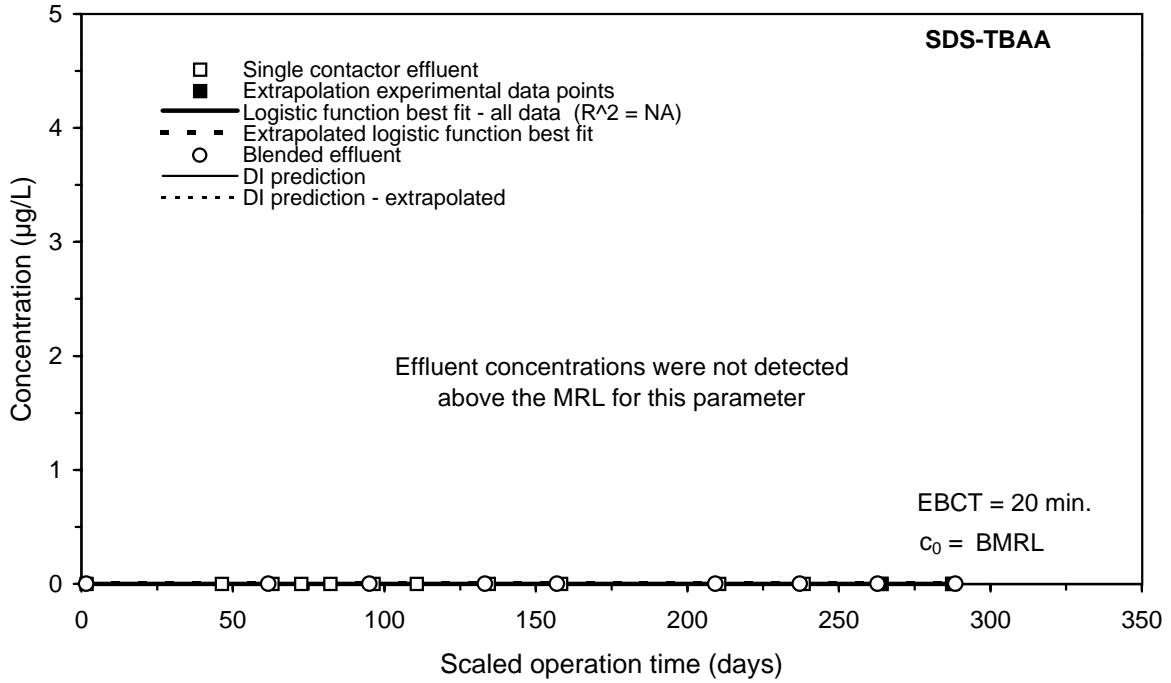


**Figure I-19 Impact of extrapolation on the DI prediction of the SDS-TBAA integral breakthrough curve for Water 5**

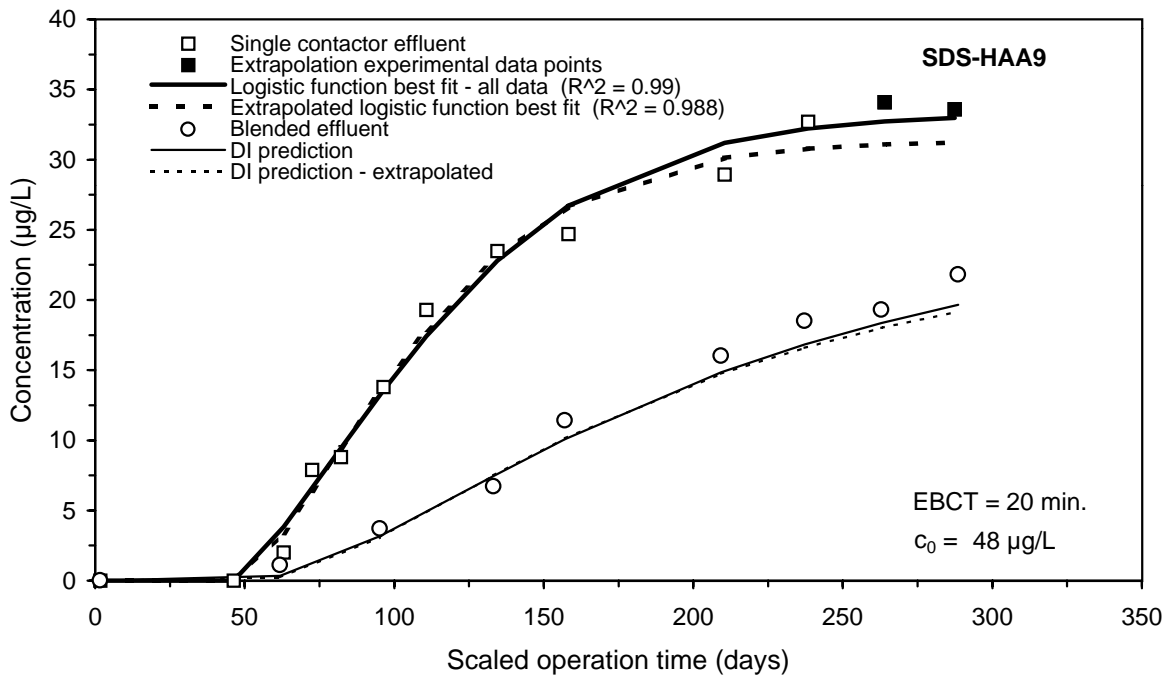


**Figure I-20 Impact of extrapolation on the DI prediction of the SDS-HAA9 integral breakthrough curve for Water 5**

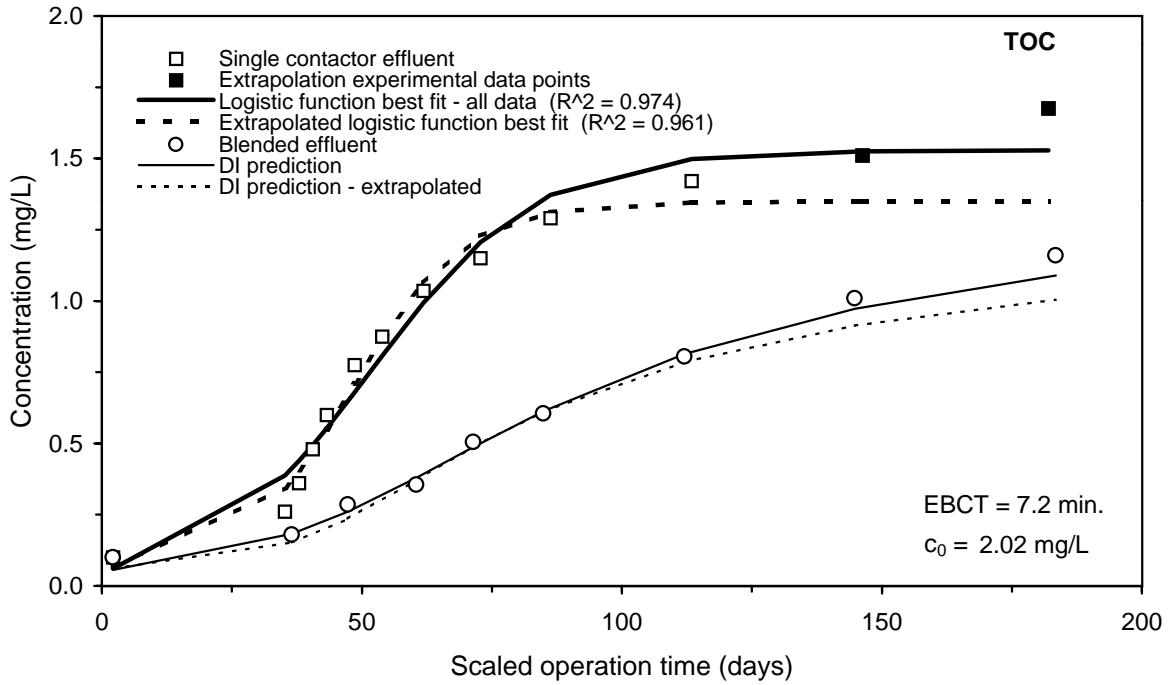


**Figure I-21 Impact of extrapolation on the DI prediction of the TOC integral breakthrough curve for Water 8**

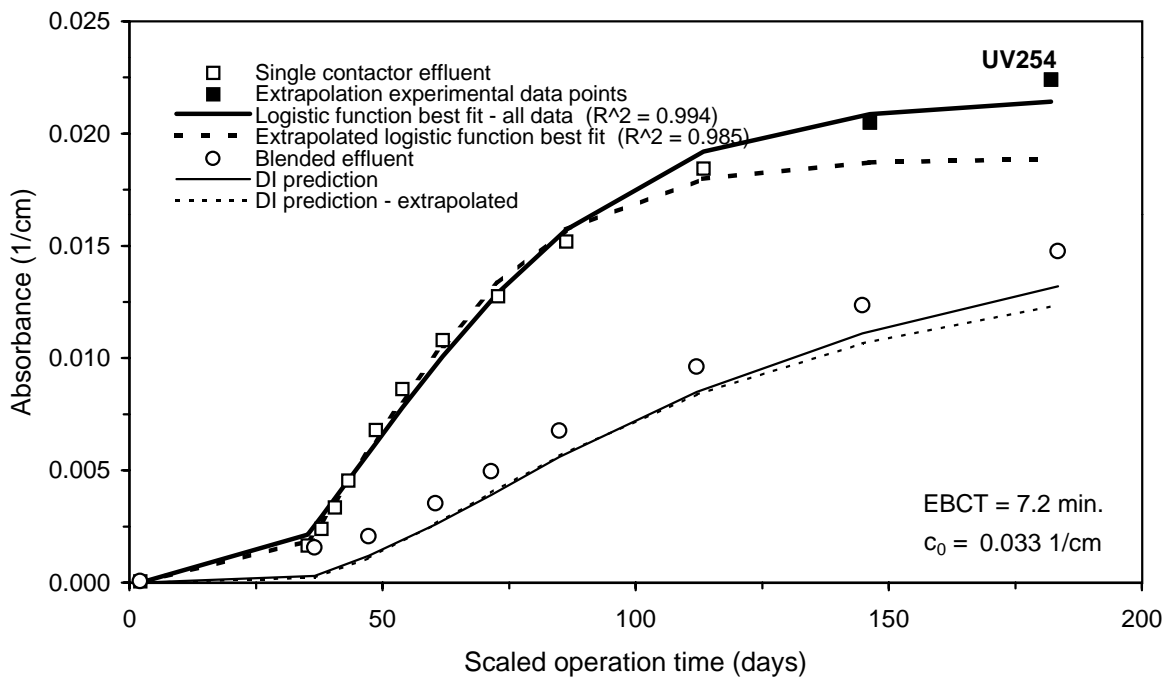


**Figure I-22 Impact of extrapolation on the DI prediction of the UV254 integral breakthrough curve for Water 8**

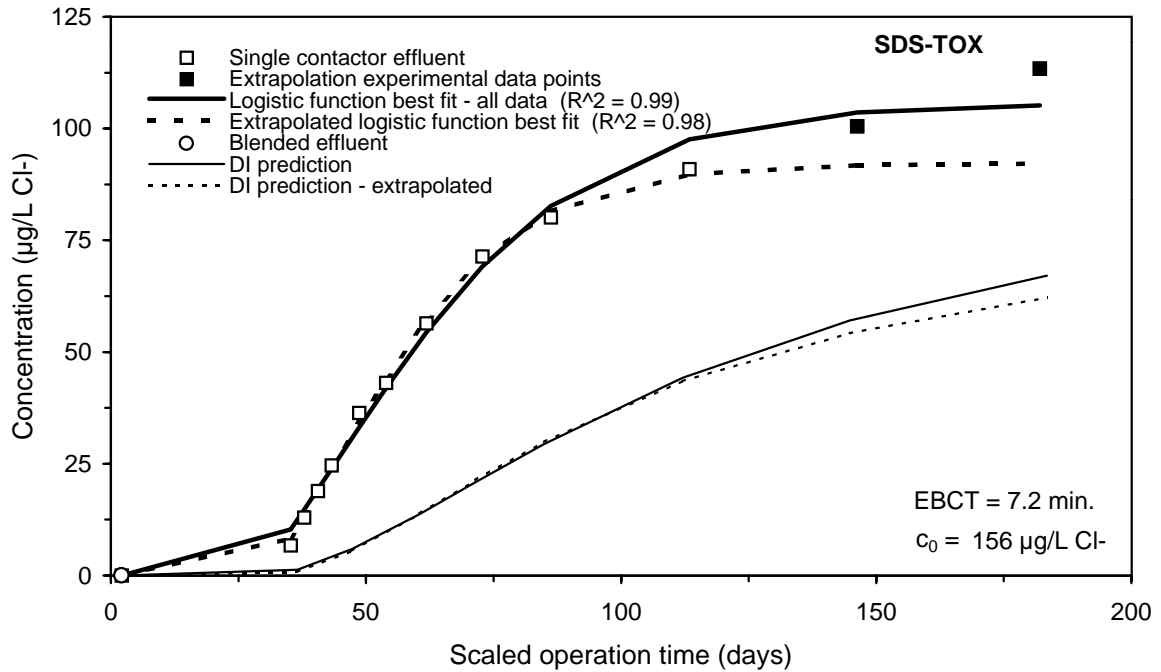


**Figure I-23 Impact of extrapolation on the DI prediction of the SDS-TOX integral breakthrough curve for Water 8**

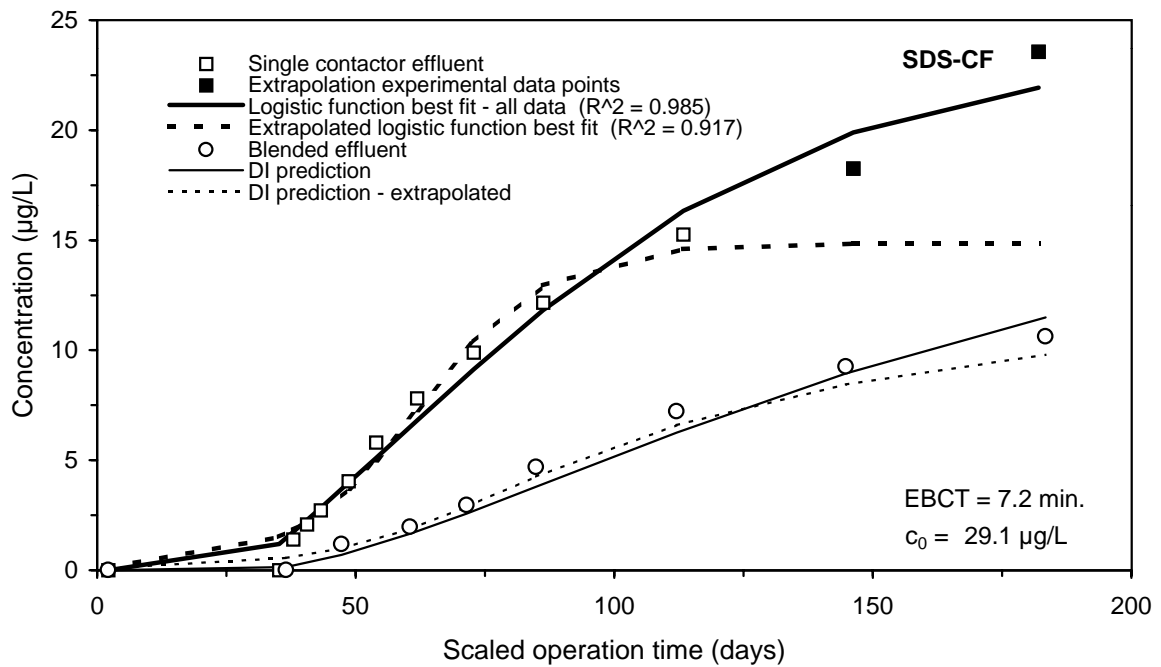


**Figure I-24 Impact of extrapolation on the DI prediction of the SDS-CF integral breakthrough curve for Water 8**

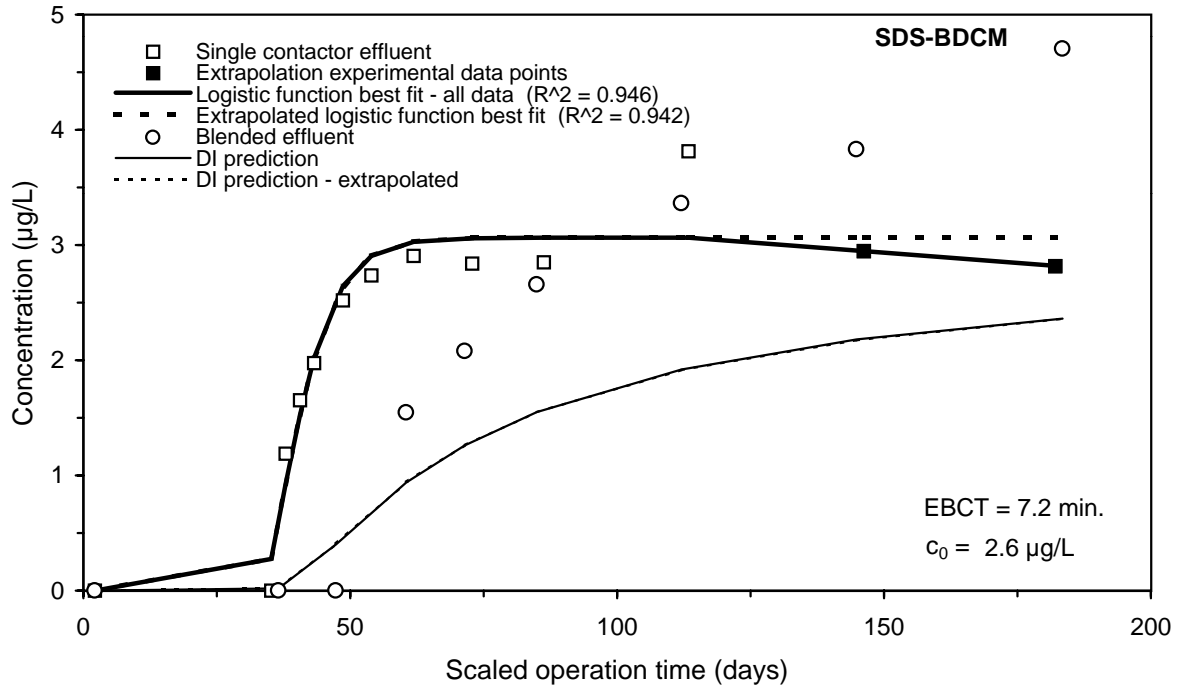


**Figure I-25 Impact of extrapolation on the DI prediction of the SDS-BDCM integral breakthrough curve for Water 8**

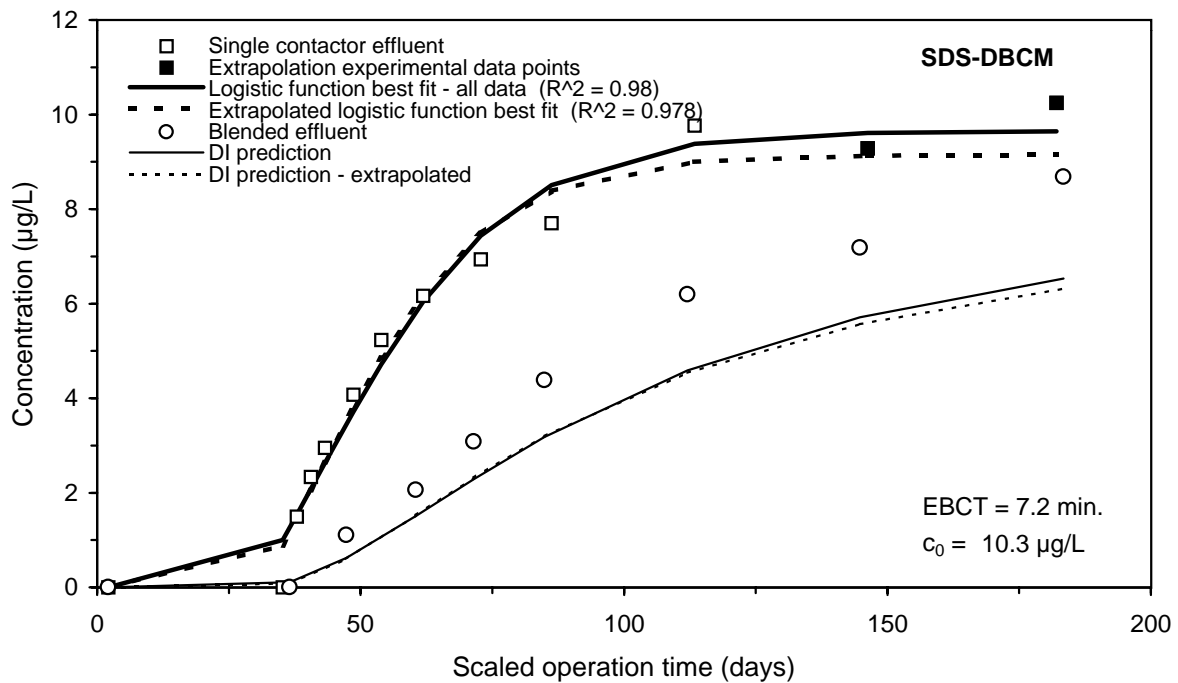


**Figure I-26 Impact of extrapolation on the DI prediction of the SDS-DBCm integral breakthrough curve for Water 8**

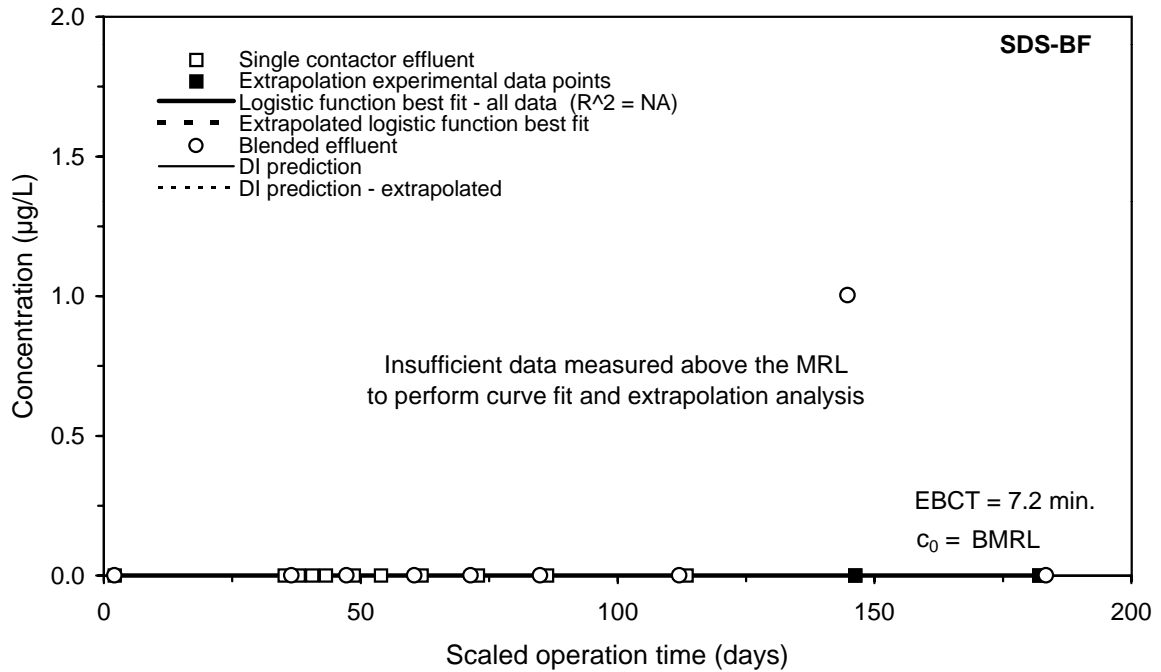


**Figure I-27 Impact of extrapolation on the DI prediction of the SDS-BF integral breakthrough curve for Water 8**

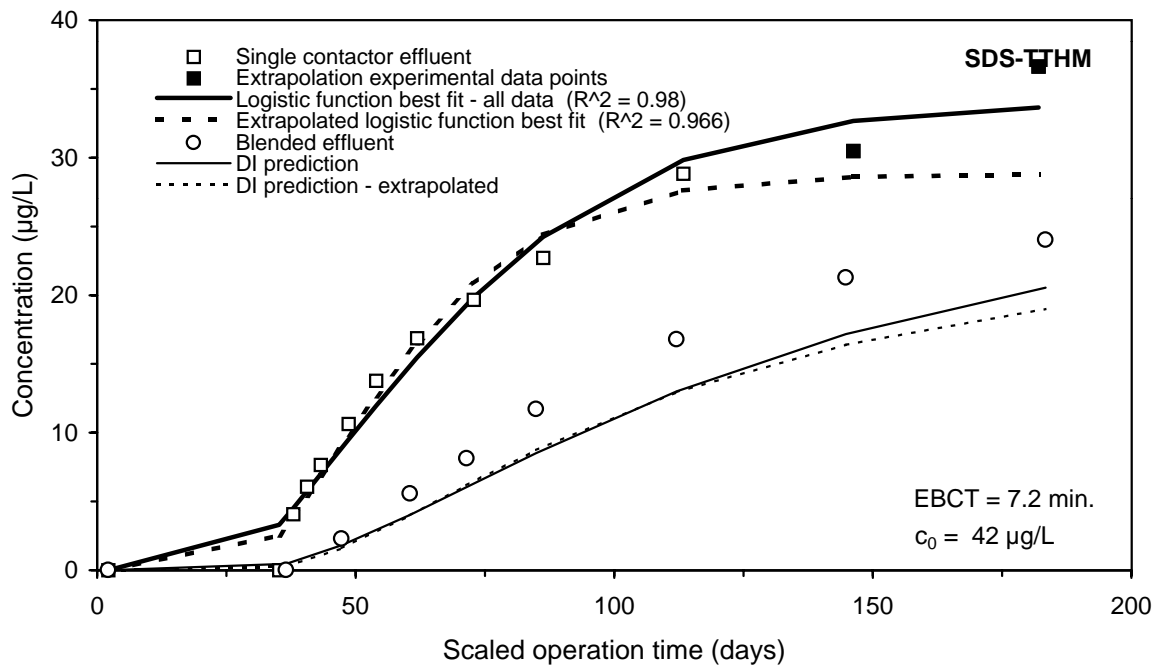


**Figure I-28 Impact of extrapolation on the DI prediction of the SDS-TTHM integral breakthrough curve for Water 8**

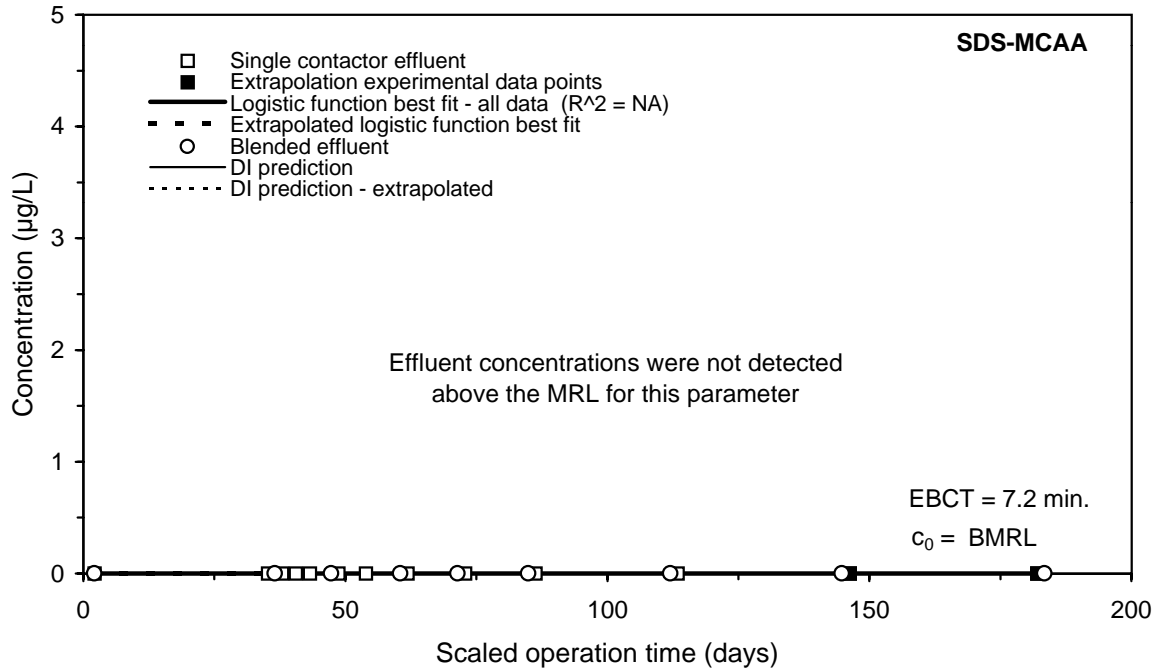


**Figure I-29 Impact of extrapolation on the DI prediction of the SDS-MCAA integral breakthrough curve for Water 8**

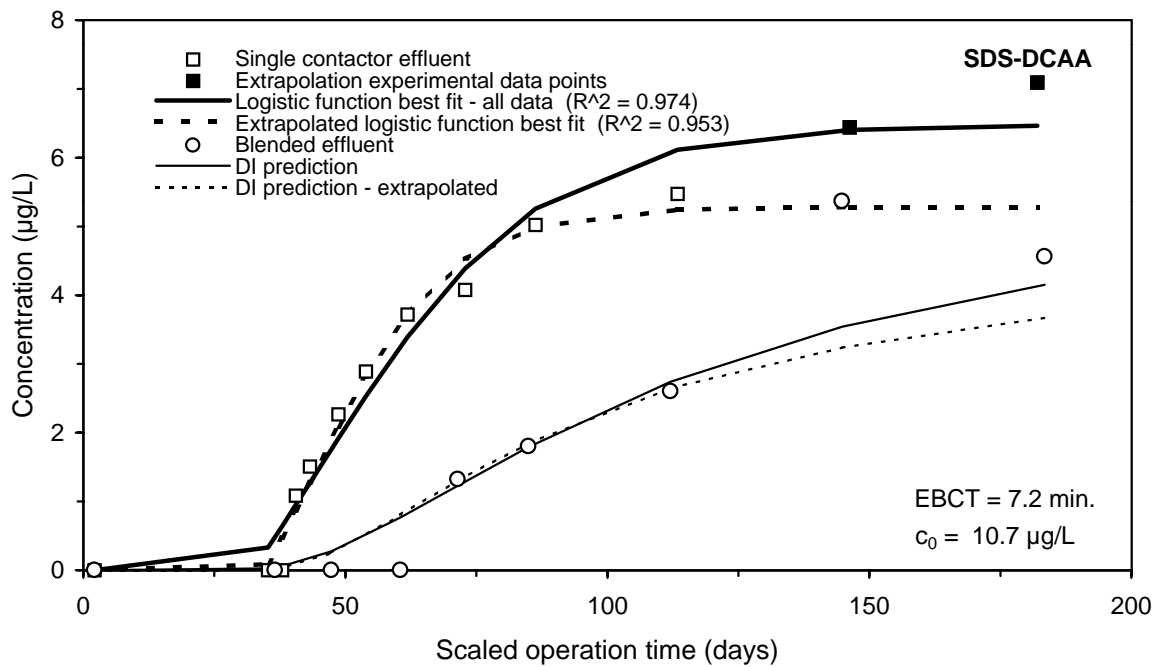


**Figure I-30 Impact of extrapolation on the DI prediction of the SDS-DCAA integral breakthrough curve for Water 8**

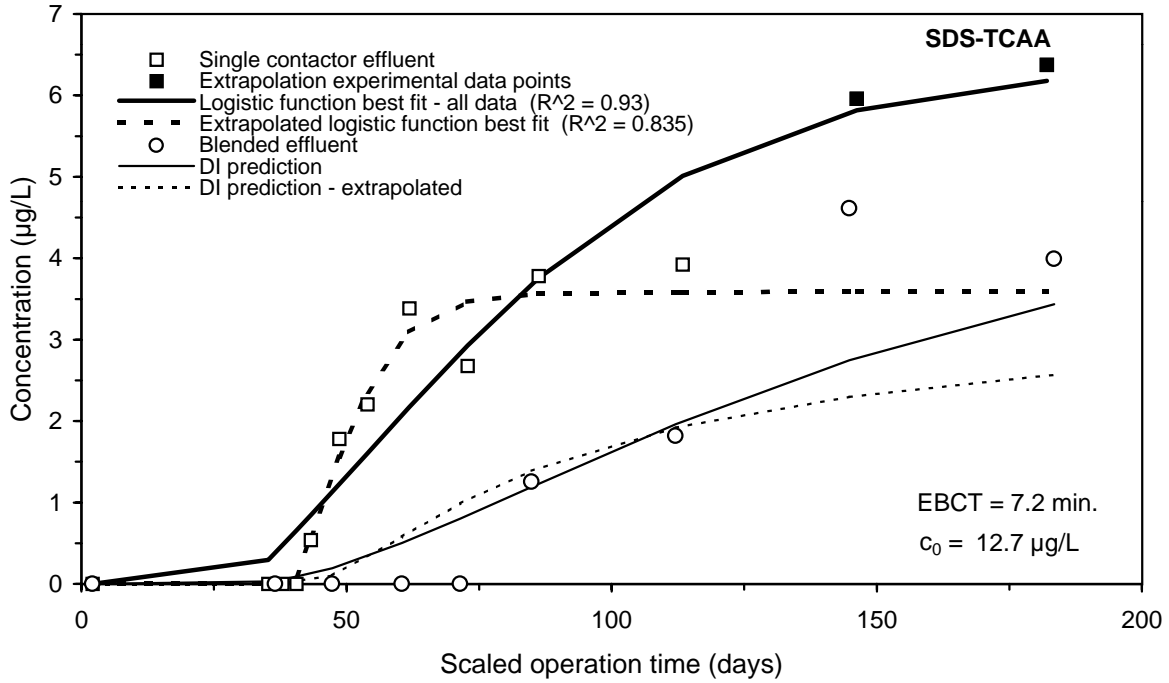


**Figure I-31 Impact of extrapolation on the DI prediction of the SDS-TCAA integral breakthrough curve for Water 8**

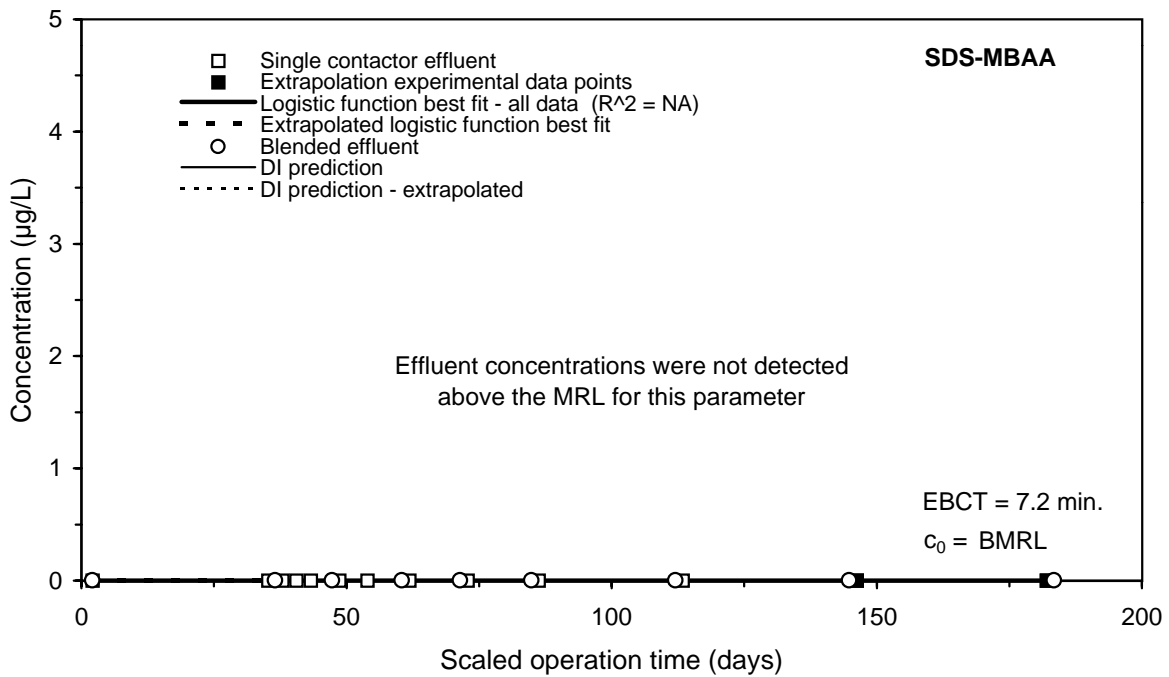


**Figure I-32 Impact of extrapolation on the DI prediction of the SDS-MBAA integral breakthrough curve for Water 8**

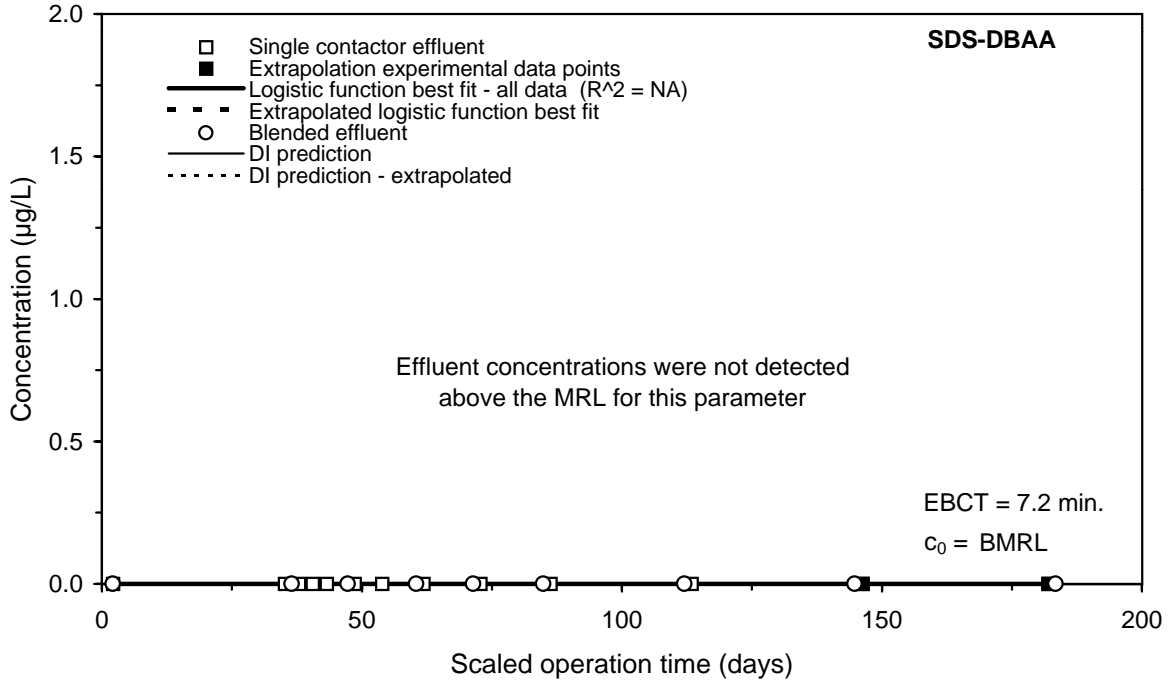


**Figure I-33 Impact of extrapolation on the DI prediction of the SDS-DBAA integral breakthrough curve for Water 8**

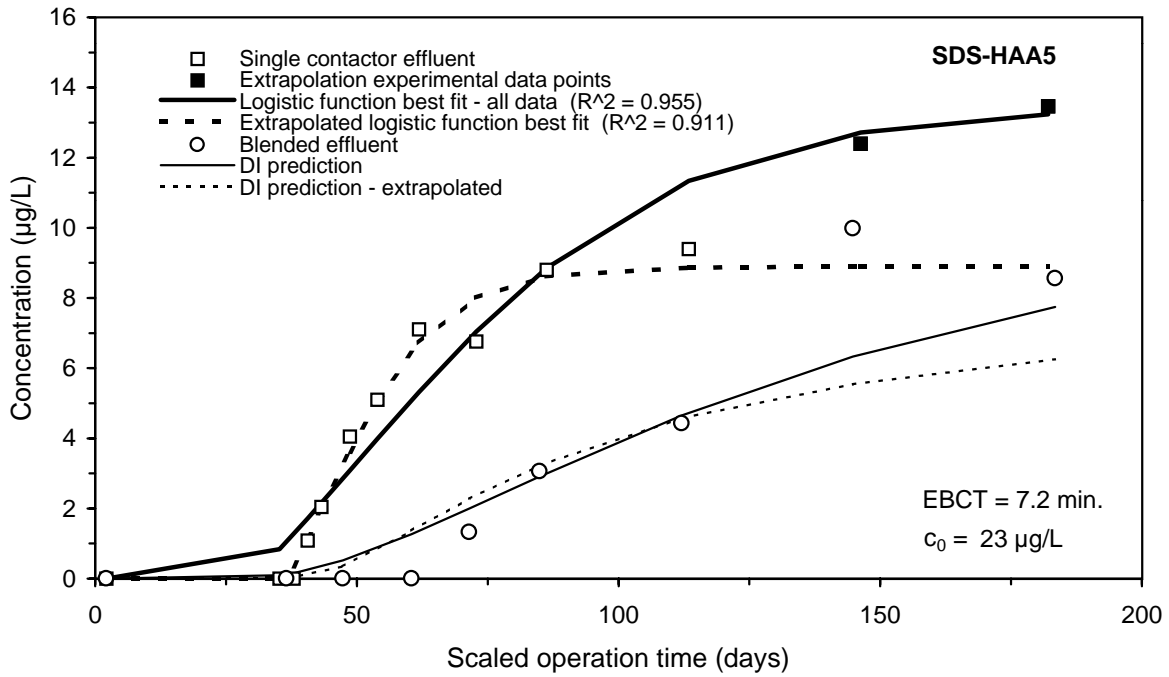


**Figure I-34 Impact of extrapolation on the DI prediction of the SDS-HAA5 integral breakthrough curve for Water 8**

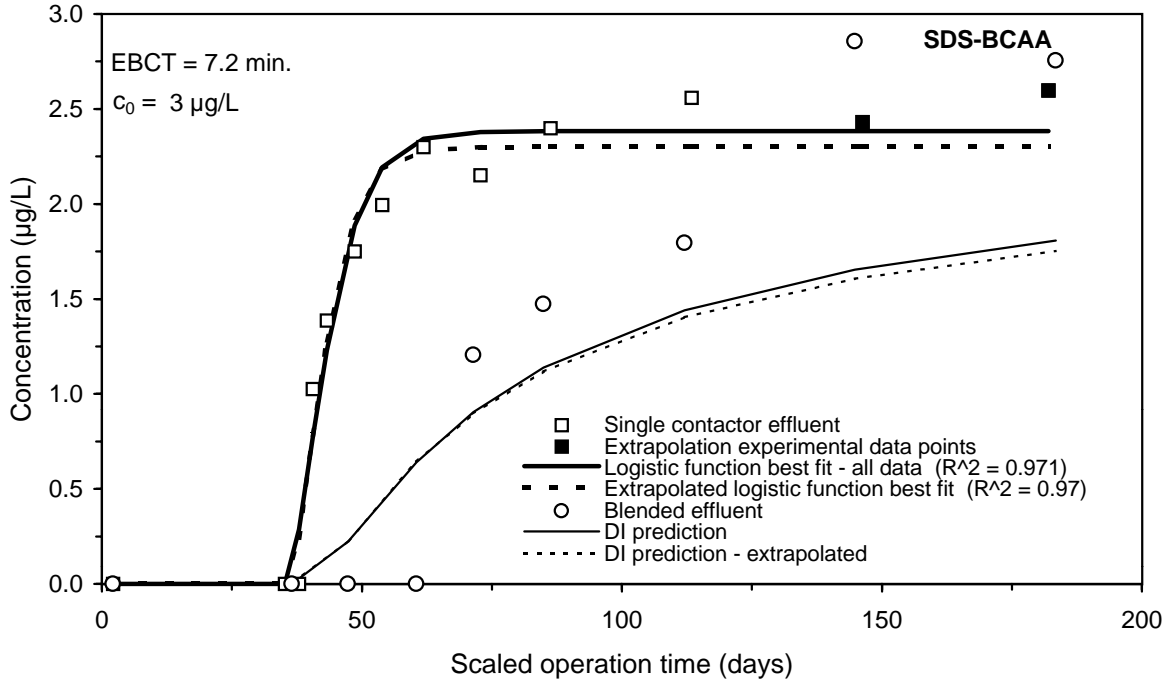


**Figure I-35 Impact of extrapolation on the DI prediction of the SDS-BCAA integral breakthrough curve for Water 8**

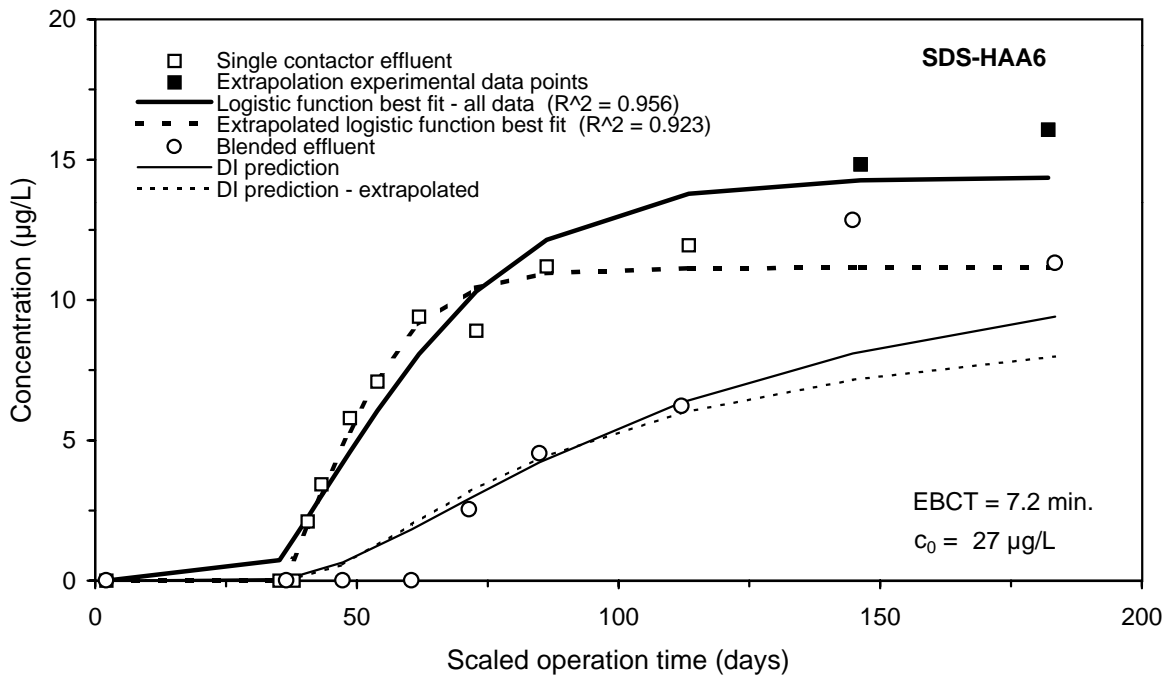


**Figure I-36 Impact of extrapolation on the DI prediction of the SDS-HAA6 integral breakthrough curve for Water 8**

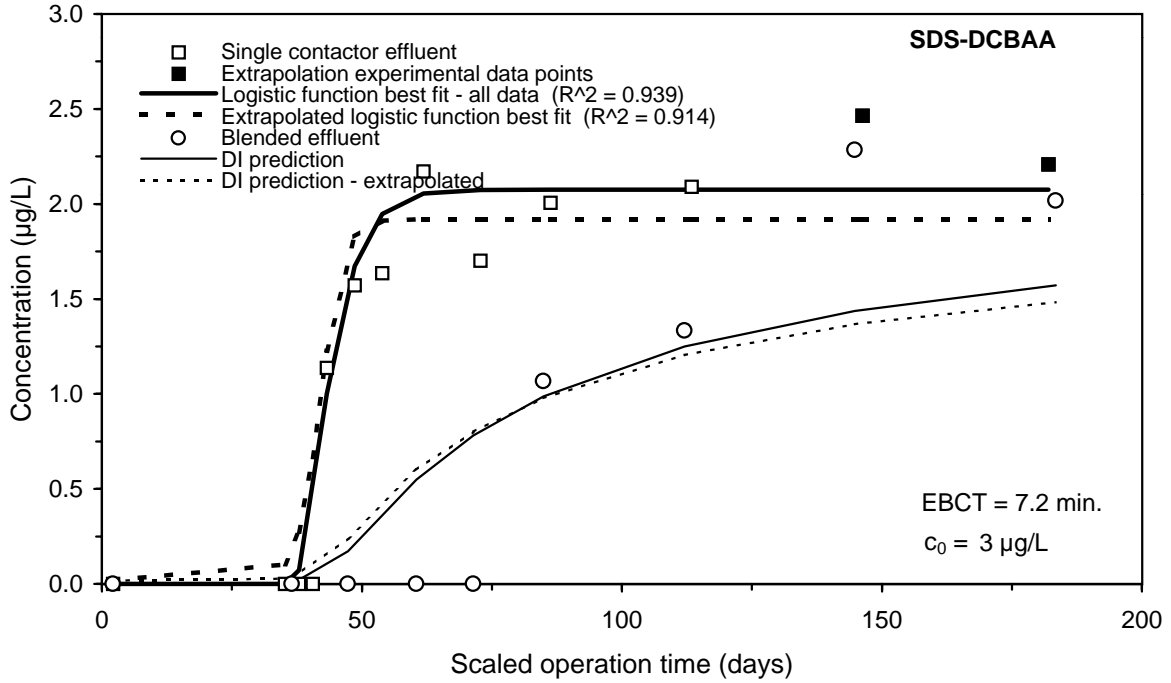


**Figure I-37 Impact of extrapolation on the DI prediction of the SDS-DCBAA integral breakthrough curve for Water 8**

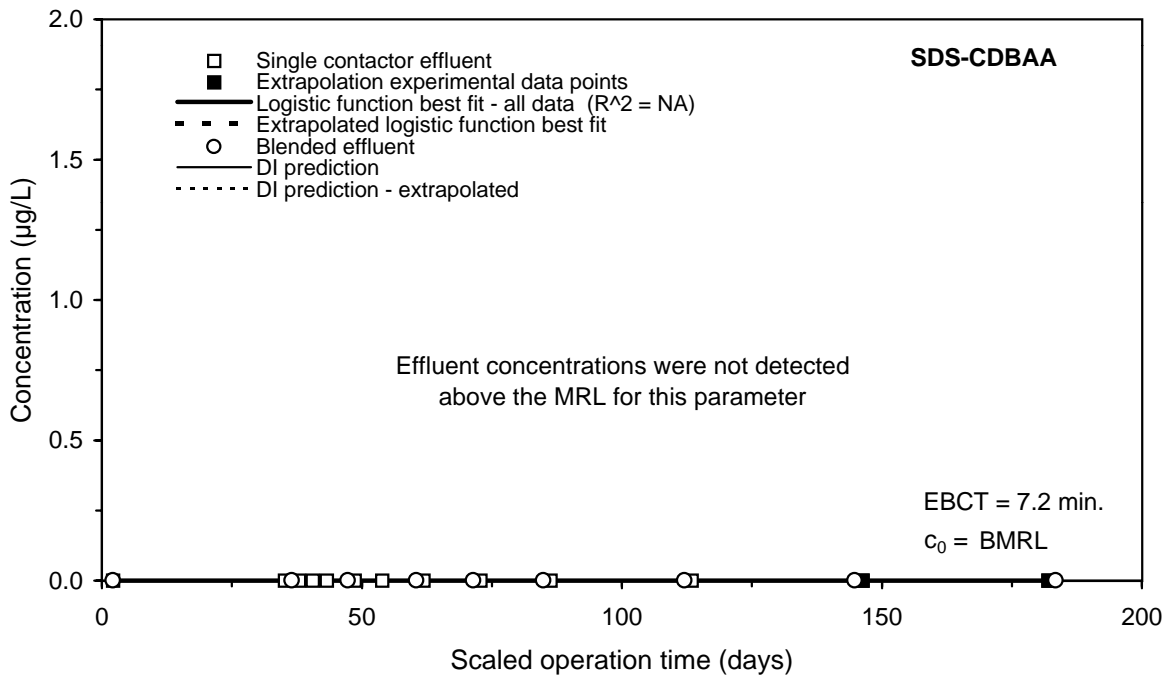


**Figure I-38 Impact of extrapolation on the DI prediction of the SDS-CDBAA integral breakthrough curve for Water 8**

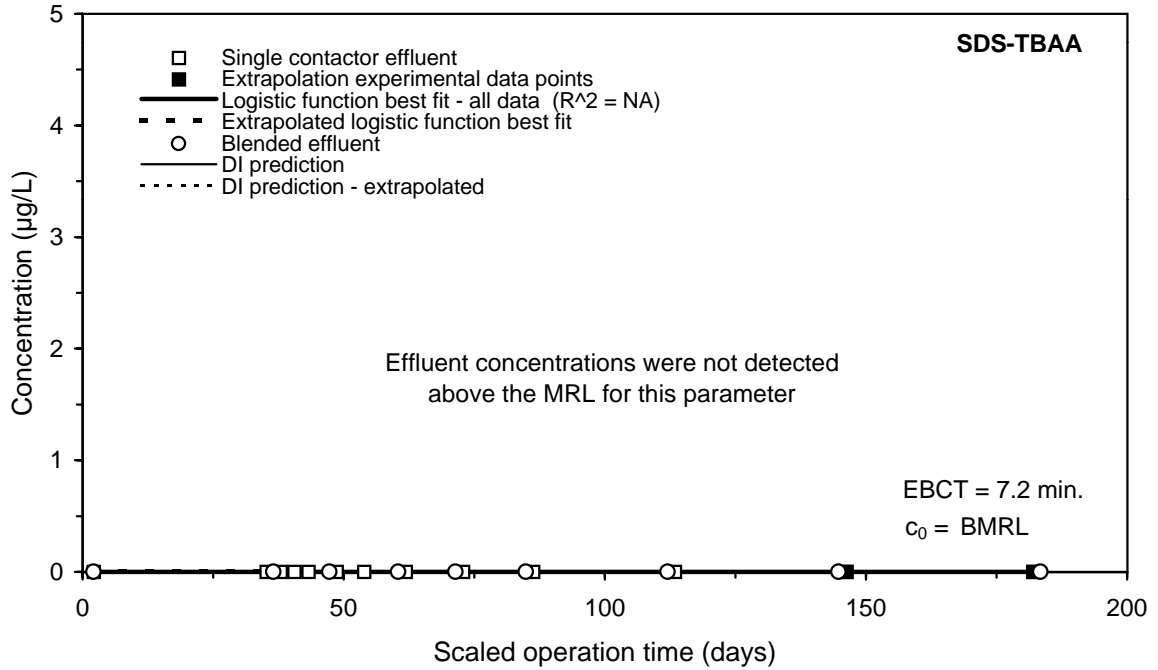


**Figure I-39 Impact of extrapolation on the DI prediction of the SDS-TBAA integral breakthrough curve for Water 8**

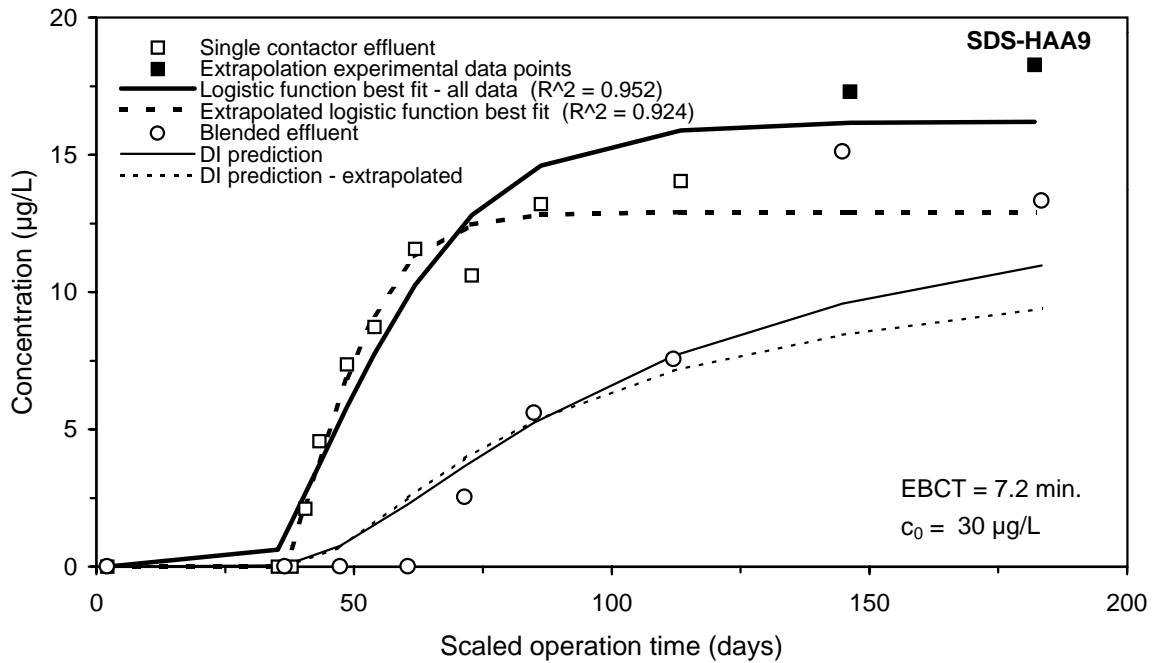


**Figure I-40 Impact of extrapolation on the DI prediction of the SDS-HAA9 integral breakthrough curve for Water 8**